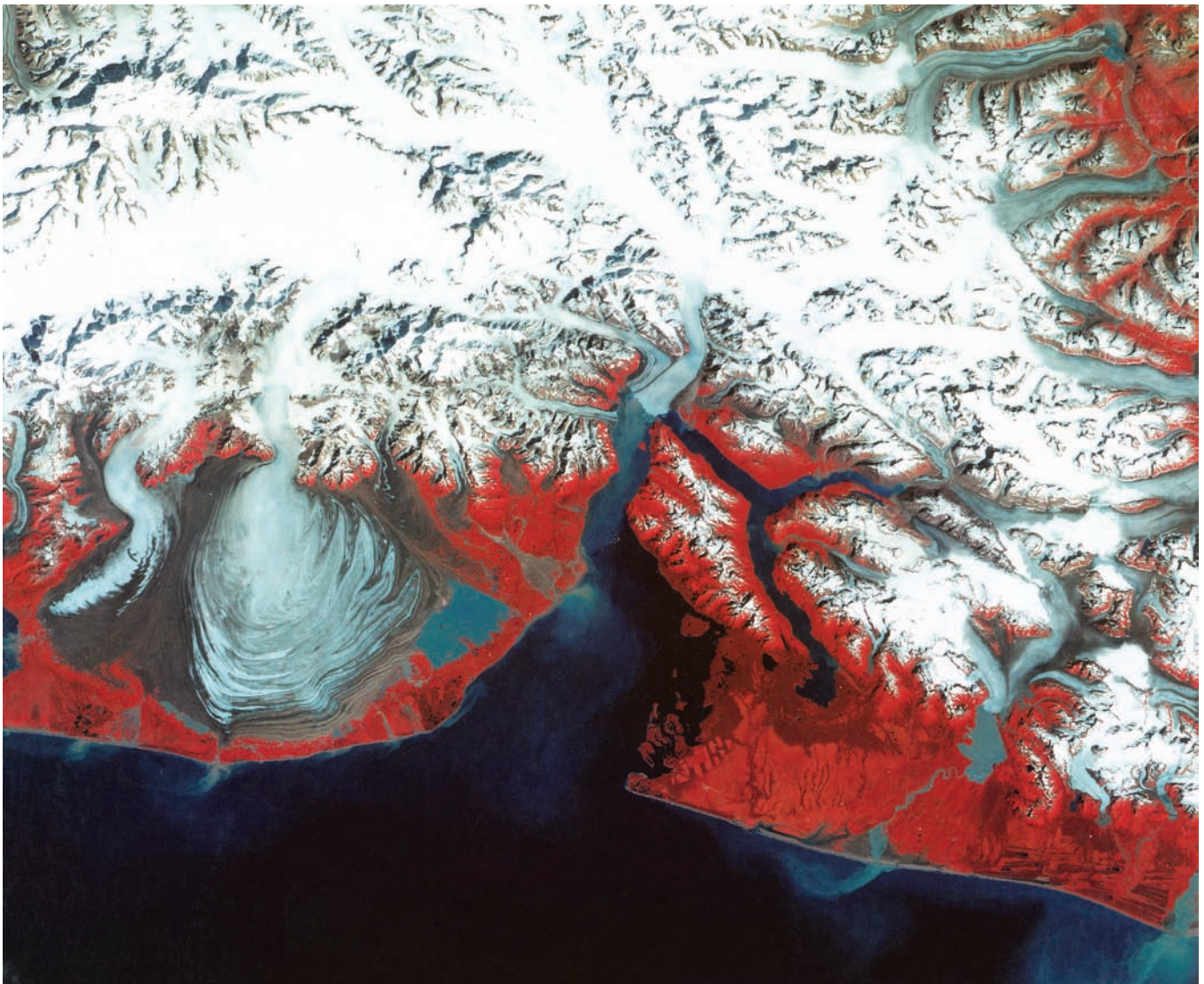


Satellite Image Atlas  
of Glaciers of the World

A L A S K A



U.S. Geological Survey  
Professional Paper 1386-K

**Cover:** *A Landsat 2 Multispectral Scanner false-color composite image of the Malaspina Glacier (piedmont outlet glacier), tidewater Hubbard Glacier, and other glaciers in the St. Elias Mountains, Alaska. (Landsat 2 MSS image 21675-19482; 24 August 1979; Path 67, Row 18 from the EROS Data Center, Sioux Falls, S. Dak.). See figure 144, p. K160, for annotated version*

Glaciers of North America—

## GLACIERS OF ALASKA

By BRUCE F. MOLNIA

*With sections on COLUMBIA AND HUBBARD TIDEWATER GLACIERS*

By ROBERT M. KRIMMEL

THE 1986 AND 2002 TEMPORARY CLOSURES OF RUSSELL FIORD BY THE HUBBARD GLACIER

By BRUCE F. MOLNIA, DENNIS C. TRABANT, ROD S. MARCH, *and* ROBERT M. KRIMMEL

GEOSPATIAL INVENTORY AND ANALYSIS OF GLACIERS: A CASE STUDY FOR THE EASTERN ALASKA RANGE

By WILLIAM F. MANLEY

## SATELLITE IMAGE ATLAS OF THE GLACIERS OF THE WORLD

*Edited by* RICHARD S. WILLIAMS, Jr., *and* JANE G. FERRIGNO

---

U.S. GEOLOGICAL SURVEY PROFESSIONAL PAPER 1386-K

*About 5 percent (about 75,000 km<sup>2</sup>) of Alaska is presently glacierized, including 11 mountain ranges, 1 large island, an island chain, and 1 archipelago. The total number of glaciers in Alaska is estimated at >100,000, including many active and former tidewater glaciers. Glaciers in every mountain range and island group are experiencing significant retreat, thinning, and (or) stagnation, especially those at lower elevations, a process that began by the middle of the 19th century. In southeastern Alaska and western Canada, 205 glaciers have a history of surging; in the same region, at least 53 present and 7 former large ice-dammed lakes have produced jökulhlaups (glacier-outburst floods). Ice-capped Alaska volcanoes also have the potential for jökulhlaups caused by subglacier volcanic and geothermal activity. Satellite remote sensing provides the only practical means of monitoring regional changes in glaciers in response to short- and long-term changes in the maritime and continental climates of Alaska. Geospatial analysis is used to define selected glaciological parameters in the eastern part of the Alaska Range.*

---

UNITED STATES GOVERNMENT PRINTING OFFICE, WASHINGTON: 2008

**U.S. DEPARTMENT OF THE INTERIOR**  
**DIRK KEMPTHORNE, Secretary**  
**U.S. GEOLOGICAL SURVEY**  
**Mark D. Myers, Director**

Any use of trade, product, or firm names in this publication is for descriptive purposes only and does not imply endorsement by the U.S. Government

Technical editing by Kathie Rankin  
Design, layout, and illustrations by Kirsten C. Healey  
Typesetting and text review by Janice G. Goodell  
Layout review by John M. Watson

---

**Library of Congress Cataloging in Publication Data**

(Revised for vol. K)

Satellite image atlas of glaciers of the world.

(U.S. Geological Survey professional paper; 1386)

Includes bibliography.

Contents:—Ch. B. Antarctica, by Charles Swithinbank; with sections on The “dry valleys” of Victoria Land, by Trevor J. Chinn, [and] Landsat images of Antarctica, by Richard S. Williams, Jr., and Jane G. Ferrigno—Ch. C. Greenland, by Anker Weidick—Ch. E. Glaciers of Europe—Ch. G. Glaciers of the Middle East and Africa—Ch. H. Glaciers of Irian Jaya, Indonesia, and New Zealand—Ch. I. Glaciers of South America—Ch. J. Glaciers of North America—Ch. K. Glaciers of Alaska.

Supt. of Docs. no.: I 19.16:1386-J

1. Glaciers—Remote sensing. I. Williams, Richard S. II. Ferrigno, Jane G. III. Series.

GB2401.72.R42S28 1988 551.3'12 87-600497

ISBN 0-607-98291-8

---

For sale by the U.S. Geological Survey, Information Services  
Box 25286, Federal Center,  
Denver, CO 80225

## Foreword

On 23 July 1972, the first Earth Resources Technology Satellite (ERTS 1 or Landsat 1) was successfully placed in orbit. The success of Landsat inaugurated a new era in satisfying mankind's desire to better understand the dynamic world upon which we live. Space-based observations have become an essential means for monitoring global environmental changes.

The short- and long-term cumulative effects of processes that cause significant changes on the Earth's surface can be documented and studied by repetitive Landsat and other satellite images. Such images provide a permanent historical record of the surface of the planet; they also make possible comparative two- and three-dimensional measurements of change over time. This Professional Paper demonstrates the importance of the application of Landsat images to global studies by using them to determine the 1970's distribution of glaciers on the planet. As images become available from future satellites, the new data will be used to document global changes in glacier extent by reference to the baseline Landsat image record of the 1970's.

Although many geological processes take centuries or even millennia to produce obvious changes on the Earth's surface, other geological phenomena, such as glaciers and volcanoes, cause noticeable changes over shorter periods. Some of these phenomena can have a worldwide impact and often are interrelated. Explosive volcanic eruptions, such as the 1991 Mount Pinatubo, Philippines, eruption, can produce dramatic effects on the global climate. Natural or culturally induced processes can cause global climatic cooling or warming. Glaciers respond to such warming or cooling periods by decreasing or increasing in size, which in turn causes sea level to rise or fall.

As our understanding of the interrelationship of global processes improves and our ability to assess changes caused by these processes develops further, we will learn how to use indicators of global change, such as glacier variation, to manage more wisely the use of our finite land and water resources. This USGS Professional Paper series is an excellent example of the way in which we can use technology to provide needed earth-science information about our planet. The international collaboration represented by this report is also an excellent model for the kind of cooperation that scientists will increasingly find necessary in the future in order to solve important earth-science problems on a global basis.



Mark D. Myers,  
Director,  
U.S. Geological Survey



## Preface

This chapter is the eighth chapter to be released in U.S. Geological Survey Professional Paper 1386, *Satellite Image Atlas of Glaciers of the World*, a series of 11 chapters. In each chapter, remotely sensed images, primarily from the Landsat 1, 2, and 3 series of spacecraft, are used to study the glacierized regions of our planet and to monitor glacier changes. Landsat images, acquired primarily during the middle to late 1970s, were used by an international team of glaciologists and other scientists to study various geographic regions or to discuss glaciological topics. In each geographic region, the present areal distribution of glaciers is compared, wherever possible, with historical information about their past extent. The atlas provides an accurate regional inventory of the areal extent of glacier ice on our planet during the 1970s as part of a growing international scientific effort to measure global environmental change on the Earth's surface.

This chapter is divided into three parts: Part I, Background and History; Part II, Glaciological Topics; and Part III, Regional Distribution of Alaska Glaciers. Glaciers in Alaska are located on 11 mountain ranges, 1 large island, an island chain, and 1 archipelago. The total number of glaciers is estimated to be >100,000, <700 of which are named.

The total glacierized area is about 75,000 km<sup>2</sup>: Coast Mountains, ~10,500 km<sup>2</sup>; Alexander Archipelago, <150 km<sup>2</sup>; St. Elias Mountains, ~11,800 km<sup>2</sup>; Chugach Mountains, ~21,600 km<sup>2</sup>; Kenai Mountains, ~4,600 km<sup>2</sup>; Kodiak Island, <15 km<sup>2</sup>; Aleutian Range, ~1,250 km<sup>2</sup>; Aleutian Islands, ~960 km<sup>2</sup>; Wrangell Mountains, ~8,300 km<sup>2</sup>; Talkeetna Mountains, ~800 km<sup>2</sup>; Alaska Range, ~13,900 km<sup>2</sup>; Wood River Mountains, <230 km<sup>2</sup>; Kigluaik Mountains, <3 km<sup>2</sup>; and Brooks Range, 723 km<sup>2</sup>.

Since the middle of the 19th century, when the "Little Ice Age" began to wane, glaciers, especially those at lower elevations, have been retreating and thinning, although each of the glacierized areas has had a different response in terms of timing, magnitude, and complexity. Most glaciers at lower elevations (<1,500 m) are retreating, except for about a dozen tidewater and valley glaciers that are advancing. The melting of glacier ice in Alaska is a regional contributor to the continuing rise in eustatic (global) sea level.

In southeastern Alaska and western Canada >200 surge-type glaciers have been documented. Ice-dammed lakes and ice-capped volcanoes have been the source of glacier-outburst floods (jökulhlaups). Satellite and aerial remote sensing and geospatial analysis of maps and remote sensing data are used in this chapter for periodic monitoring and documenting changes in the position of termini and area of glaciers in the 14 glacierized areas of Alaska.

Richard S. Williams, Jr.  
Jane G. Ferrigno  
Editors

## About this Volume

U.S. Geological Survey Professional Paper 1386, *Satellite Image Atlas of Glaciers of the World*, contains 11 chapters designated by the letters A through K. Chapter A is a general chapter containing introductory material on the Earth's cryosphere, including a discussion of the physical characteristics, classification, and global distribution of glaciers. The next 10 chapters, B through K, are arranged geographically and present glaciological information from Landsat and other sources of data on each of the geographic areas. Chapter B covers Antarctica; Chapter C, Greenland; Chapter D, Iceland; Chapter E, Continental Europe (except for the European part of the former Soviet Union), including the Alps, the Pyrenees, Norway, Sweden, Svalbard (Norway), and Jan Mayen (Norway); Chapter F, Asia, including the European part of the former Soviet Union, China (P.R.C.), India, Nepal, Bhutan, Afghanistan, and Pakistan; Chapter G, Turkey, Iran, and Africa; Chapter H, Irian Jaya (Indonesia) and New Zealand; Chapter I, South America; and Chapter J, North America (excluding Alaska); and Chapter K, Alaska.

The realization that one element of the Earth's cryosphere, its glaciers, was amenable to global inventorying and monitoring with Landsat images led to the decision, in late 1979, to prepare this Professional Paper, in which Landsat 1, 2, and 3 multispectral scanner (MSS) and Landsat 2 and 3 return beam vidicon (RBV) images would be used to inventory the areal occurrence of glacier ice on our planet within the boundaries of the spacecraft's coverage (between about 81° north and south latitudes). Through identification and analysis of optimum Landsat images of the glacierized areas of the Earth during the first decade of the Landsat era, a global benchmark or baseline could be established for determining the areal extent of glaciers during a relatively narrow time interval (1972 to 1982). This global "snapshot" of glacier extent could then be used for comparative analysis with previously published maps and aerial photographs and with new maps, satellite images, and aerial photographs in order to determine the areal fluctuation of glaciers in response to natural or culturally induced changes in the Earth's climate.

To accomplish this objective, optimum Landsat images of each of the glacierized regions of our planet were selected from the Landsat image data base at the EROS Data Center in Sioux Falls, S. Dak., although some images were also obtained from the Landsat image archives maintained by the Canada Centre for Remote Sensing, Ottawa, Ontario, Canada, and by the European Space Agency in Kiruna, Sweden, and Fucino, Italy. Between 1979 and 1981, these optimum images were distributed to an international team of more than 50 scientists who agreed to write a section of the Professional Paper concerning either a geographic area or a glaciological topic. In addition to analyzing images of a specific geographic area, each author was also asked to summarize up-to-date information about the glaciers within the area and to compare their present areal distribution with historical information (for example, from published maps, reports, and photographs) about their past extent. Completion of this atlas will provide an accurate regional inventory of the areal extent of glaciers on our planet during the 1970s.

Richard S. Williams, Jr.  
Jane G. Ferrigno  
Editors



## CONTENTS: Major Sections

	<b>Page</b>
Part 1—Background and History .....	<b>K2</b>
Part 2—Glaciological Topics.....	<b>52</b>
Part 3—Descriptions of Alaska's 14 Glacierized Geographic Regions .....	<b>84</b>
Coast Mountains.....	<b>89</b>
Alexander Archipelago.....	<b>119</b>
St. Elias Mountains.....	<b>123</b>
Chugach Mountains.....	<b>197</b>
Kenai Mountains.....	<b>314</b>
Kodiak Island .....	<b>347</b>
Aleutian Range.....	<b>349</b>
Aleutian Islands.....	<b>371</b>
Wrangell Mountains.....	<b>379</b>
Talkeetna Mountains.....	<b>401</b>
Alaska Range.....	<b>406</b>
Wood River Mountains .....	<b>457</b>
Kigluaik Mountains.....	<b>463</b>
Brooks Range.....	<b>467</b>
References Cited.....	<b>487</b>
Appendices.....	<b>505</b>

## ACRONYMS

AAAS	American Association for the Advancement of Science
AAR	accumulation area ratio
AHAP	Alaska High-Altitude Aerial Photography
AGS	American Geographical Society
amsl	above mean sea level
AMS	U.S. Army Map Service
ASTER	Advanced Spaceborne Thermal Emission and Reflection
BGN	Board on Geographic Names
BLM	U.S. Bureau of Land Management
B.P.	before present
C&GS	U.S. Coast and Geodetic Survey
CMMB	Central Medial Moraine Band
CTD	conductivity, temperature, and depth
DEM	digital elevation model
DLG	digital line graph
DMA	U.S. Defense Mapping Agency
DRG	digital raster graphic
EDC	EROS Data Center
ELA	equilibrium line altitude
ETM+	Enhanced Thematic Mapper Plus
EROS	Earth Resources Observation and Science
ERTS	Earth Resources Technology Satellite
GIS	Geographic Information System
GLIMS	Global Land Ice Measurements from Space
GNIS	Geographic Names Information System
GPS	Global Positioning System
HY	Hydrologic Year
IBC	International Boundary Commission
IGY	International Geophysical Year
IHD	International Hydrologic Decade
InSAR	Interferometric Synthetic Aperture Radar
INSTAAR	Institute of Arctic and Alpine Research
IPR	ice-penetrating radar
MODIS	Moderate Resolution Imaging Spectroradiometer
MSS	Multispectral Scanner System
NASA	National Aeronautics and Space Administration
NED	National Elevation Dataset
NGA	National Geospatial-Intelligence Agency
NGS	National Geographic Society
NIMA	National Imagery and Mapping Agency
NOAA	National Oceanic and Atmospheric Administration
NOS	National Ocean Survey
NPS	National Park Service
NSF	National Science Foundation
RBV	Return Beam Vidicon
RMSE	root mean square error
SAR	synthetic aperture radar
SLAR	side-looking airborne radar
TM	Thematic Mapper
UNESCO	United Nations Educational, Scientific and Cultural Organization
USC&GS	U.S. Coast and Geodetic Survey
USAF	United States Air Force
USFS	United States Forest Service
USGS	U.S. Geological Survey
USN	United States Navy
UTM	Universal Transverse Mercator

# CONTENTS

	<b>Page</b>
<b>Abstract</b> -----	<b>K1</b>
<b>Part 1—Background and History</b> -----	<b>2</b>
<b>Introduction</b> -----	<b>2</b>
FIGURE 1. Map of Alaska showing distribution of glaciers -----	2
2. NOAA AVHRR image mosaic of Alaska (1991)-----	2
3. Map showing the nominal scene centers of Landsat 1, 2, and 3 MSS and RBV images that include Alaskan glaciers, and Landsat MSS image mosaic of part of Alaska-----	5
4. Section of the 1982 USGS topographic map of Seward, Alaska-----	7
5. Landsat 1 MSS image of part of the Bering Glacier and Bagley Ice Valley on 26 February 1974 -----	8
TABLE 1. Optimum Landsat 1, 2, and 3 MSS and RBV images of glaciers of Alaska -----	10
FIGURE 6. Landsat ETM+ image of the terminus region of Knik Glacier and adjacent Lake George -----	18
7. Pair of Landsat 5 MSS images showing changes in the piedmont lobe of Malaspina Glacier between 1986 and 1987 -----	18
8. A Landsat MSS "temporal-change composite image" showing changes between 1985 and 1986 in the termini of Hubbard, Turner, and Valerie Glaciers-----	19
<b>Glacier Names and Place-Names in Alaska</b> -----	<b>18</b>
<b>Early Observations of Alaska and its Glaciers</b> -----	<b>20</b>
Traditional Knowledge -----	20
Limited Early Descriptions of Glaciers-----	20
<b>18th and 19th Century Explorations and Observations of Alaska and its Glaciers</b> -----	<b>20</b>
Vitus Bering-----	21
James Cook-----	21
Jean François de Galaup de La Pérouse -----	21
FIGURE 9. Three maps (1797, 1961, 1972) of Lituya Bay-----	22
Alexandro Malaspina-----	22
George Vancouver-----	22
Edward Belcher-----	24
George Simpson-----	25
Mikhail Dimitrievich Teben'kov-----	25
FIGURE 10. Two maps of the Gulf of Alaska coastal area from Yakutat Bay to Cape Suckling -----	24
William P. Blake-----	25
FIGURE 11. Part of Blake's 1868 map of the Stikine River area -----	25
William H. Dall-----	26
George Davidson-----	27
FIGURE 12. 1875 sketch map of the St. Elias Alpine Region-----	26
13. Map showing the glaciers of the Icy Strait-Cross Sound region in 1902 -----	27
Charles Erskine Scott Wood-----	27
John Muir-----	28
U.S. Military Expeditions-----	28
FIGURE 14. 1883 lithograph of an Alaskan glacier -----	28
15. 1887 lithograph of the terminus of Miles Glacier -----	29
George Frederick Wright-----	28
FIGURE 16. 1886 photograph of the terminus of Norris Glacier -----	29
17. Wright's 1889 sketch map of southeastern Alaska -----	30
<i>New York Times</i> Expedition-----	29
Israel C. Russell-----	30
FIGURE 18. I.C. Russell's 1891 "Sketch Map of the Mount St. Elias Region" -----	30
19. Photographs of USGS field party crossing the Malaspina Glacier in 1891 and Russell and field party on their survey of the St. Elias Mountains -----	31
Henry Fielding Reid-----	32
FIGURE 20. 1893 photograph of the terminus of Muir Glacier -----	32
Alaska-Canada Boundary Surveys-----	33
National Geographic Society Expeditions -----	33
Duke of Abruzzi-----	34
Figure 21. Part of a 1897 panoramic photograph of "The Chain of St. Elias and [Mount] Augusta..." -----	34

	<b>Page</b>
Postcards-----	35
FIGURE 22. Late 19th/early 20th century postcard of the terminus of Taku Glacier -----	35
Harriman Alaska Expedition -----	35
FIGURE 23. Photograph of John Muir at Cascading Glacier on 20 June 1899 -----	36
<b>Selected 20th Century Explorations and Observations of Alaska's Glaciers -----</b>	<b>36</b>
Early USGS Investigations and Photography -----	36
Ralph S. Tarr and Lawrence Martin -----	37
FIGURE 24. Tarr and Martin's 1914 graphic showing the U.S. Capitol superimposed on Child's Glacier -----	39
25. Oscar D. von Engel'n washing a strip of negatives in Yakutat Bay in 1910 -----	39
Early Aerial Photography of Glaciers by the U.S. Government -----	38
FIGURE 26. Cameras developed by James W. Bagley for use in Alaska topographic surveys -----	39
27. 1929 vertical aerial photograph of the North and South Crillon Glaciers -----	40
28. 1926 photograph of Alaska Aerial Survey Expedition operations in Juneau Harbor -----	41
29. Phototriplet obtained with the Bagley 3-lens T-1 camera in 1926 -----	41
30. 1929 oblique aerial photograph by Alaska Aerial Survey Expedition of Twin Glaciers -----	41
Later Vertical Aerial Photography Programs -----	42
FIGURE 31. Nine-lens vertical aerial photograph of Fairweather Glacier in 1959 -----	42
32. AHAP photograph of the Alsek Glacier on 21 June 1978 -----	44
William Osgood Field -----	43
FIGURE 33. American Geographical Society Glacier Studies Map 64-2-G8 compiled by W.O. Field in 1959 -----	45
34. American Geographical Society Glacier Studies Map 64-3-G7 compiled by W.O. Field in 1964 -----	46
35. Map of Little Jarvis Glacier on 18 September 1957 -----	47
Bradford Washburn -----	48
FIGURE 36. Oblique aerial photograph of the southeastern terminus of Bering Glacier in 1938 -----	48
37. Oblique aerial photograph of contorted medial moraines on Malaspina Glacier in 1938 -----	49
38. Oblique aerial photograph of an array of subparallel medial moraines on Barnard Glacier in 1938 -----	49
Austin Post -----	50
Robert M. Krimmel -----	50
Ground, Vertical, and Oblique Aerial Photographs by Other USGS Glaciologists -----	51
<b>Part 2—Glaciological Topics-----</b>	<b>52</b>
<b>Tidewater Glaciers-----</b>	<b>52</b>
FIGURE 39. Photograph on 15 July 1979 of the terminus of the tidewater Muir Glacier -----	52
40. Oblique aerial photograph of the central terminus of Bering Glacier on 16 August 1998 -----	53
TABLE 2. Glaciological characteristics of existing and former tidewater glaciers of Alaska -----	56
Columbia and Hubbard Tidewater Glaciers, by Robert M. Krimmel -----	54
Introduction -----	54
FIGURE 41. Map of active and former tidewater glaciers of Alaska -----	53
42. Diagram of tidewater glacier cycle -----	55
TABLE 3. Terminus status of major tidewater glaciers of Alaska in 1999 -----	57
Columbia Glacier -----	60
FIGURE 43. Two oblique aerial photographs of Columbia Glacier on 22 August 1979 and on 12 September 1986 -----	60
44. Oblique aerial photograph of Columbia Glacier on 10 January 1993 -----	62
45. Landsat 3 RBV image of Columbia Glacier on 7 September 1979 -----	63
46. Mosaic of five vertical aerial photographs of the lower reach of the Columbia Glacier on 2 October 1998 -----	65
Stereophotogrammetry -----	64
FIGURE 47. Graph showing changing length of Columbia Glacier between 1976 and 1999 -----	66
48. Graph showing the seasonal variation of the length of Columbia Glacier -----	67
49. Graph showing surface speed of Columbia Glacier at three locations between 1977 and 1997 -----	67
50. Graph showing average annual speed in meters per day of Columbia Glacier in 1978 and 1993 -----	67
51. Graph showing seasonal-speed deviations from the normalized speed near the terminus of Columbia Glacier -----	68
52. Graph showing the surface altitude of Columbia Glacier in 1950, 1974, 1993, and 1996 -----	69

	<b>Page</b>
<b>Hubbard Glacier</b> -----	<b>70</b>
FIGURE 53. Landsat 5 TM image of Hubbard Glacier on 7 August 1985 -----	71
54. Map showing advance of Hubbard Glacier terminus between 1965 and 1997 -----	72
55. Oblique aerial photograph of terminus of Hubbard Glacier on 29 August 1984 -----	72
56. Oblique aerial photograph of the Hubbard Glacier ice dam on 12 September 1986 -----	73
<b>Surge-Type Glaciers</b> -----	<b>74</b>
FIGURE 57. Oblique aerial photograph of the Susitna Glacier on 5 September 1966 -----	75
<b>Glacier-Dammed Lakes and Glacier-Outburst Floods (Jökulhlaups)</b> -----	<b>76</b>
Figure 58. AHAP photograph of ice-marginal lake surrounding the terminus of Sheridan Glacier and debris-covered terminus of Sherman Glacier on 13 August 1982 -----	77
59. AHAP photograph of Kenibuna Lake, Chakachamna Lake, and Shamrock Glacier on 20 July 1980 -----	78
<b>Jökulhlaups at Bering Glacier</b> -----	<b>79</b>
Figure 60. 12 September 1986 oblique aerial photograph of jökulhlaup from Berg Lake, and photograph showing the exposed lakebed on 11 August 1998 -----	80
61. Oblique aerial photograph of a channel cut through the eastern terminus of the Bering Glacier on 29 July 1994 -----	81
<b>Debris-Covered Glaciers</b> -----	<b>81</b>
<b>Part 3—Descriptions of Alaska’s 14 Glacierized Geographic Regions</b> -----	<b>84</b>
<b>Introduction</b> -----	<b>84</b>
Analysis of Glacier Activity -----	84
Evidence of Glacier Retreat Used in This Analysis -----	85
FIGURE 62. Oblique aerial photograph on 20 August 1977 of a valley glacier (informally called <i>Five Stripe Glacier</i> ) in the Chugach Mountains -----	85
63. Oblique aerial photograph on 3 October 1979 of an unnamed hanging glacier in Glacier Bay -----	85
Evidence of Glacier Advance Used in This Analysis -----	86
FIGURE 64. 15 July 1978 photograph of part of the terminus of Harriman Glacier -----	86
65. 14 July 1994 oblique aerial photograph of a lobe of Bering Glacier overriding an alder forest -----	86
66. Photograph of a late 19th century advance of La Perouse Glacier on 18 June 1899 -----	86
67. 12 July 1991 photograph of three sheared tree trunks exposed by retreat of the Bering Glacier -----	87
Evidence of Glacier Stagnation Used in This Analysis -----	86
FIGURE 68. Oblique aerial photograph of vegetation growing on the surface of Bering Glacier on 8 June 1976 -----	87
69. Photograph of a debris-covered ice-cored moraine near the retreating terminus of Herbert Glacier on 8 July 1968 -----	87
70. AHAP photograph of large thermokarst pits on Bering Glacier on 27 July 1983 -----	88
<b>Coast Mountains</b> -----	<b>89</b>
FIGURE 71. Index map and NOAA AVHRR image mosaic of the Coast Mountains -----	88
<b>Portland Canal to Burroughs Bay and the Unuk River</b> -----	<b>91</b>
FIGURE 72. Part of a Landsat 2 MSS image from the Portland Canal to Burroughs Bay and the Unuk River on 10 August 1980 -----	90
73. Part of an AHAP photograph of the unnamed, southeasternmost glacier in Alaska on 12 August 1979 -----	91
74. Part of an AHAP photograph of the retreating Soule Glacier on 14 August 1979 and part of the 1955 USGS Ketchikan 1:250,000-scale map showing Soule Glacier -----	92
75. AHAP photograph of the lower 8 km of the Chickamin Glacier and other nearby glaciers on 14 August 1979 -----	93
<b>Burroughs Bay and the Unuk River to the Stikine River</b> -----	<b>92</b>
FIGURE 76. Landsat 2 MSS image mosaic of the Coast Mountains from Burroughs Bay and the Unuk River to the Stikine River (10 and 11 August 1980) -----	93
77. Part of an AHAP photograph of Nelson Glacier on 11 August 1979 -----	94
<b>Stikine River to Taku River</b> -----	<b>94</b>
Figure 78. Landsat 2 MSS image mosaic of the Coast Mountains from Stikine River to Taku River (19 August 1979, 11 August 1980) and an August 1997 space shuttle photograph of part of the <i>Stikine Icefield</i> -----	95
79. Part of an AHAP photograph of Popof Glacier, and smaller, unnamed glaciers on 11 August 1979 -----	97
80. AHAP photograph of Shakes Glacier on 11 August 1979, and an oblique aerial photograph of the terminus of Shakes Glacier on 23 August 1990 -----	98

	<b>Page</b>
81. Map of Frederick Sound and Le Conte Bay showing bathymetry and terminus positions of Le Conte Glacier-----	99
82. AHAP photograph of the terminus of Baird Glacier and other nearby glaciers on 11 August 1979-----	100
83. Oblique aerial photograph of the terminus of South Sawyer Glacier on 26 August 1960-----	102
84. Landsat 5 TM image of the Coast Mountains from just south of Tracy Arm to the Taku River on 9 September 1984-----	103
<b>Taku River to the Canadian Border East of Gilkey Glacier-----</b>	<b>104</b>
Figure 85. Landsat 2 and 3 MSS image mosaic of the Coast Mountains from the Taku River to the Canadian border (31 August 1977, 30 July 1978, 19 August 1979)-----	104
86. Landsat 5 TM image of the Coast Mountains from east of the Taku River to west of Berners Bay on 9 September 1984-----	105
87. AHAP photograph of Taku Inlet and surrounding area on 11 August 1979-----	106
88. Oblique aerial photograph of the northeastern terminus of the advancing Taku Glacier on 14 September 1968-----	107
89. Map of the Taku Inlet and River area showing terminus positions of Taku, Norris, and Hole-in-the-Wall Glaciers-----	108
90. Oblique aerial photograph of the bulbous terminus of the advancing Hole-in-the-Wall Glacier on 28 July 1968-----	109
91. AHAP photograph of the termini of East and West Twin Glaciers on 11 August 1979-----	110
92. Bagley camera vertical and oblique aerial photographs of East and West Twin Glaciers in 1929-----	110
93. 5 July 1985, 29 May 1986, 27 June 1988, and 2 July 1989 photographs of Mendenhall Glacier and environs-----	112
94. Oblique aerial photograph of the lower reaches of the retreating Herbert Glacier on 24 August 1963-----	114
95. AHAP photographic mosaic of Gilkey Glacier and some of its principal tributaries on 11 August 1979-----	115
<b>Glaciers North of the Juneau Icefield-----</b>	<b>115</b>
FIGURE 96. Part of the 1961 USGS 1:250,000-scale Skagway, Alaska-Canada map-----	116
97. AHAP photograph of an unnamed glacier west of Chilkat Glacier on 11 August 1979-----	118
<b>Summary-----</b>	<b>118</b>
<b>Alexander Archipelago-----</b>	<b>119</b>
FIGURE 98. Index map and NOAA AVHRR image mosaic of the Alexander Archipelago-----	119
<b>Revillagigedo Island-----</b>	<b>119</b>
<b>Prince of Wales Island-----</b>	<b>120</b>
<b>Kupreanof Island-----</b>	<b>120</b>
<b>Baranof Island-----</b>	<b>120</b>
FIGURE 99. AHAP photograph of Baranof Island, north of Mount Furuhelm and east of Sitka on 11 August 1979-----	121
<b>Chichagof Island-----</b>	<b>120</b>
<b>Admiralty Island-----</b>	<b>121</b>
<b>Summary-----</b>	<b>121</b>
<b>St. Elias Mountains-----</b>	<b>123</b>
<b>Introduction-----</b>	<b>123</b>
FIGURE 100. Index map and NOAA AVHRR image mosaic of the St. Elias Mountains-----	122
101. Aerial photograph of the summit of Mount St. Elias on 28 July 2001-----	124
<b>Southeastern St. Elias Mountains Segment: From the Lynn Canal and Chilkat Inlet and River to the Eastern Side of the Alsek River-----</b>	<b>124</b>
FIGURE 102. Landsat 2 and 3 MSS image mosaic of the St. Elias Mountains from Lynn Canal to the Alsek River (31 August 1977, 30 July 1978, 28 August 1978, 19 August 1979)-----	125
103. AHAP photograph of the area around the Tsirku River on 11 August 1979-----	126
104. August 1946 and 31 August 1978 aerial photographs of Davidson Glacier-----	127
<b>Glacier Bay National Park and Preserve-----</b>	<b>128</b>
FIGURE 105. Landsat 1 MSS image of Glacier Bay and environs on 12 September 1973, and map showing contours of equal snowline altitude-----	128
106. Landsat 3 RBV image mosaic of most of Glacier Bay National Park and Preserve on 12 August 1979-----	131
TABLE 4. Accumulation area ratios for glaciers in Glacier Bay and environs-----	132

	<b>Page</b>
FIGURE 107. Map of the Glacier Bay region showing the retreat of Glacier Bay ice cover between 1750 and the 1990s, and oblique orbital view of Glacier Bay and environs (combined Landsat 7 ETM+ image and USGS NED)	133
108. Part of a Landsat 1 MSS image of the Glacier Bay region on 12 September 1973	135
<b>Muir Inlet</b>	137
Figure 109. Landsat MSS images of upper Muir Inlet on 12 September 1973 and 6 September 1986	138
<b>Adams Inlet</b>	138
FIGURE 110. AHAP photograph of central Adams Inlet and the area to the north on 11 August 1979	138
<b>Wachusett Inlet</b>	139
FIGURE 111. AHAP photograph of upper Wachusett Inlet on 11 August 1979	139
112. Oblique aerial photograph of Burroughs Glacier on 12 September 1986	140
113. Oblique aerial photograph of the rapidly retreating Plateau Glacier on 25 August 1968	140
<b>Upper Muir Inlet</b>	141
Figure 114. AHAP photographic mosaic of upper Muir Inlet on 11 August 1979	141
115. Oblique aerial photograph of the retreating terminus of McBride Glacier on 28 June 1980	142
116. Oblique aerial photograph of the terminus of Riggs Glacier on 3 October 1979	142
117. Oblique aerial photograph of Upper Muir Inlet on 24 August 1963	143
118. Oblique aerial photograph of Muir Glacier on 12 September 1986	143
<b>Queen Inlet</b>	144
<b>Rendu Inlet</b>	144
FIGURE 119. AHAP photograph of Rendu Glacier, Romer Glacier, and several unnamed retreating glaciers on 11 August 1979	144
<b>Tarr Inlet</b>	144
FIGURE 120. AHAP photograph of the termini of Margerie and Grand Pacific Glaciers on 11 August 1979	145
121. Segments of four Landsat MSS images of Margerie Glacier, between 12 September 1973 and 7 September 1986	146
<b>Johns Hopkins Inlet</b>	146
FIGURE 122. Oblique aerial photograph of Johns Hopkins Glacier on 12 September 1986	147
123. AHAP photograph of numerous glaciers at the head of Johns Hopkins Inlet on 14 August 1978	147
124. 11 August 1979 AHAP photographic mosaic of the lower reaches of Lamplugh and Reid Glaciers	148
125. Photograph of the summit of Mount Abbe on 27 July 1980	148
<b>Reid Inlet</b>	148
<b>Hugh Miller, Charpentier, and Geikie Inlets</b>	148
FIGURE 126. Photograph by G.K. Gilbert of part of the West Arm of Glacier Bay in June 1899	149
127. AHAP photographic mosaic of glaciers on the southwest side of Glacier Bay on 11 August 1979	149
<b>Glaciers of the Glacier Bay National Park and Preserve Region from West of Glacier Bay to the Alsek River</b>	149
FIGURE 128. Oblique aerial photograph of glaciers flowing into the trench of the Fairweather Fault on 24 August 1987	149
<b>Brady Glacier</b>	150
FIGURE 129. AHAP photographic mosaic of the Brady Glacier and Taylor Bay on 12 August 1979	150
130. Oblique aerial photograph of the advancing terminus of Brady Glacier on 16 September 1966	151
131. Oblique aerial photograph of a retreating and thinning unnamed glacier north of Palma Bay on 12 September 1973	151
<b>Finger and La Perouse Glaciers</b>	152
FIGURE 132. AHAP photograph of Finger Glacier and La Perouse Glacier on 12 August 1979	152
133. Oblique aerial photograph of the eastern terminus of La Perouse Glacier on 12 September 1986	153
134. Oblique aerial photograph of part of the eastern terminus of La Perouse Glacier on 18 June 1978	153
135. Two oblique aerial photographs of the eastern lobe terminus of La Perouse Glacier on 16 September 1966	153

	<b>Page</b>
Glaciers of Lituya Bay	154
FIGURE 136. AHAP photograph showing North Crillon, Lituya, and Cascade Glaciers on 12 August 1979	154
137. Aerial photograph showing the head of Lituya Bay on 2 August 1999	155
138. Photograph of the terminus of Cascade Glacier on 18 July 1979	155
139. Aerial photograph mosaic of Lituya Glacier, Desolation Glacier, and proglacial Desolation Lake on 25 June 1998	156
Fairweather and Sea Otter Glaciers	157
Figure 140. AHAP photograph of Fairweather Glacier and Sea Otter Glacier on 12 August 1979	157
Grand Plateau Glacier	157
FIGURE 141. Digital X-band radar image of the terminus of Grand Plateau Glacier in 1988	158
Alsek Glacier	157
FIGURE 142. Oblique aerial photograph of the terminus of Alsek Glacier on 25 August 1960	158
143. AHAP photograph of the retreating, thinning terminus of Alsek Glacier on 12 August 1978	159
South-central St. Elias Mountains Segment: From the Western Side of the Alsek River to the Western Side of Yakutat Bay	159
FIGURE 144. Landsat 2 MSS image of the western St. Elias Mountains, including Malaspina Glacier, Hubbard Glacier, and other nearby glaciers on 24 August 1979	160
145. Oblique aerial photograph of Harlequin Lake and the terminus of Yakutat Glacier on 12 September 1986	161
Glaciers of the Eastern Yakutat Bay Region	161
Southern Russell Fiord	161
Hidden Glacier	162
FIGURE 146. Photograph by G.K. Gilbert of the terminus of Hidden Glacier on 20 June 1899	162
147. Map showing changes in the position of the terminus of Hidden Glacier between 1905 and 1970	162
Nunatak Fiord	162
FIGURE 148. AHAP photograph of Nunatak Fiord and the termini of Art Lewis Glacier and East and West Nunatak Glaciers	162
West Nunatak Glacier	162
East Nunatak Glacier	163
Glaciers of Disenchantment Bay	163
Variegated Glacier	164
FIGURE 149. AHAP photographic mosaic of Disenchantment Bay and environs on 18 August 1978	164
150. Landsat 3 RBV image of glaciers north and east of Yakutat on 19 August 1978	165
151. Sketch map of Disenchantment Bay showing Malaspina's 1791 survey of Hubbard Glacier	166
152. Two oblique aerial photographs of the terminus of Variegated Glacier on 29 August 1964 and 22 August 1965 showing changes resulting from a surge	167
153. Two photographs of Variegated Glacier showing surge features on 4 June 1983 and on 7 July 1983	167
Hubbard Glacier	168
FIGURE 154. Photograph by I.C. Russell of the terminus of Hubbard Glacier in 1890	168
The 1986 and 2002 Temporary Closures of Russell Fiord by Hubbard Glacier, by Bruce F. Molnia, Dennis C. Trabant, Rod S. March, and Robert M. Krimmel	170
FIGURE 155. Landsat 5 TM images of the terminus of Hubbard Glacier on 7 August 1985 and 11 September 1986	170
156. Three graphs of the filling and emptying of <i>Russell Lake</i> during the 1986 and 2002 closures events	171
157. Oblique aerial photograph of the advancing terminus of Hubbard Glacier on 13 June 2002	173
Southwestern St. Elias Mountains Segment: From the Western Side of Yakutat Bay to the Western Bagley Ice Valley, the Western Robinson Mountains, and the Bering Lobe	174
FIGURE 158. Two aerial photographs of the termini of Haenke and Turner Glaciers on 25 August 1969 and 2 August 1999	175
159. Photograph by I.C. Russell of the tidewater terminus of Turner Glacier in August 1891	176
Malaspina Glacier System	176
FIGURE 160. Landsat 1 MSS image of Malaspina Glacier and environs on 12 February 1973	177
161. AHAP photograph of the southern margin of Malaspina Glacier in August 1978	178
162. Oblique aerial photograph of part of the terminus of Malaspina Glacier at Sitkagi Bluffs on 30 July 1999	178



	<b>Page</b>
163. Oblique aerial photograph of the medial moraines of the <i>Seward Lobe</i> of Malaspina Glacier on 17 September 1972	179
164. Oblique aerial photograph showing the developing Malaspina Lake on 25 August 1969	179
165. Side-looking airborne radar (SLAR) image of the piedmont lobe of the Malaspina Glacier in November 1986	181
<b>Glaciers of Icy Bay</b>	<b>183</b>
FIGURE 166. Physiographic diagram showing 1974 glacier positions and the pre-1910 position of the large terminal moraine of Guyot Glacier	184
167. Oblique aerial photograph showing the retreating glaciers at the head of Icy Bay on 24 August 1963	184
168. Oblique aerial photographs showing the retreat of Tyndall Glacier on 24 August 1963, 12 September 1986, and 13 August 1998	185
169. Oblique aerial photographs showing the slowly retreating Guyot and Yahtse Glaciers in 1938, on 25 August 1969, and on 12 September 1986	186
170. Photograph of a part of the subglacial channel under the <i>Guyot Remnant</i> on 28 July 1999	187
171. Oblique aerial photograph showing the retreating glacier margins at the head of Tsaa Fiord on 22 July 1980	187
<b>Glaciers West of Icy Bay</b>	<b>188</b>
FIGURE 172. AHAP photograph of White River, Eberly, and Yakataga Glaciers on 18 August 1978	188
173. Oblique aerial photograph of Mount Miller and numerous retreating glaciers on 12 September 1986	189
<b>Northwestern St. Elias Mountains Segment: From the Canadian Border (long 141° W.) to White River, Chitistone River, Tana River, the Eastern Wall of the Valley of Tana Glacier, and the Southern Side of the Bagley Ice Valley</b>	<b>189</b>
FIGURE 174. Oblique aerial photograph of the confluence of the Walsh and Logan Glaciers on 31 August 1984	190
175. Landsat 3 RBV image of surging glaciers in the northwestern St. Elias Mountains on 5 July 1980	191
176. AHAP photograph of the confluence of Logan and Chitina Glaciers on 9 July 1978	192
177. AHAP photograph of the northern part of the Granite Range showing many of its glaciers on 27 July 1982	192
178. Oblique aerial photographs of small valley glaciers in the Granite Range on 10 August 2001	193
179. AHAP photographic mosaic of numerous valley glaciers along Granite Creek on 18 August 1978	193
180. Photograph showing a small actively surging glacier in Goat Creek drainage south of Barnard Glacier on 14 September 1986	195
181. Oblique aerial photograph of Barnard Glacier on 31 August 1984	195
<b>Summary</b>	<b>196</b>
<b>Chugach Mountains</b>	<b>197</b>
<b>Introduction</b>	<b>197</b>
FIGURE 182. Index map and NOAA AVHRR, and Landsat MSS image mosaic of the Chugach Mountains	199
<b>Bering Glacier System Segment</b>	<b>202</b>
<b>Introduction</b>	<b>202</b>
FIGURE 183. Landsat 2 MSS image of the Bering Glacier System and Icy Bay on 23 September 1977	203
184. Map of Vitus Lake and the margin of Bering Glacier showing bathymetry of the lake	204
185. Map of the lower reaches of the Bering Glacier	204
186. Map and sketch showing the Bering Trough and glacially eroded morphology of the continental shelf in the vicinity of Bering Glacier	205
187. Photograph of the only bedrock outcrop along the perimeter of Bering Glacier on 13 August 1992	206
188. Side-looking airborne radar image of the Bering Glacier's <i>Piedmont Lobe</i> on 3 August 1990	206
189. AHAP photograph of the retreating terminus of the Bering Lobe on 18 August 1978	207
190. Two oblique aerial photographs of the Central Medial Moraine Band in 1938 and in September 1986	207
191. Three oblique aerial photographs of the northwestern terminus of the Steller Lobe of Bering Glacier in 1938, on 6 October 1974, and on 12 August 2001	208
<b>Pre-20th Century Observations of Bering Glacier</b>	<b>209</b>
FIGURE 192. Part of a late 19th century chart by the U.S. Coast and Geodetic Survey of the Gulf of Alaska	209

	<b>Page</b>
FIGURE 193. Map showing positions of the terminus of Bering Glacier between 1900 and 1993	210
194. Oblique aerial photograph of the eastern margin of the Bering Glacier on 12 August 1961	211
195. Oblique aerial photograph showing retreat of the surge-terminus region of Bering Glacier on 17 August 1979	211
20th Century Observations of Bering Glacier	211
Berg Lake	212
Surges of the Bering Glacier	213
The 1957–60, 1965–67, and 1993–95 Surges of the Bering Glacier	214
1957–60 and 1965–67 Surges	214
FIGURE 196. Oblique aerial photograph showing retreat of the <i>Piedmont Lobe</i> region of Bering Glacier on 20 July 1993	215
197. Photograph showing part of a mass of debris-covered stagnant Bering Glacier ice on 29 July 1990	215
The 1993–95 Surge	215
FIGURE 198. Oblique aerial photograph of the disintegrating terminus of the Bering Glacier on 6 October 1993	216
The 1993–94 Phase	216
FIGURE 199. Oblique aerial photograph of surge-thickened ice of the Bagley Ice Valley on 6 October 1993	217
200. Photograph of fracturing in the Central Medial Moraine Band on 24 July 1994	217
201. Map showing terminus positions of Bering Glacier between 10 July 1993 and 7 September 1994	217
202. Two aerial photographs of the Tsitus ( <i>Arrowhead</i> ) Island area on 7 October 1993 and 9 July 1995	218
Surge-Produced Changes in Vitus Lake	219
The 1995 Phase	219
FIGURE 203. Photographs showing two views of changes occurring on the southeast shoreline of Vitus Lake on 6 and 9 July 1995	220
204. Oblique aerial photographs of fracturing and crevassing that occurred during the 1993–1994 surge, on 9 May 1994 and 24 July 1994	221
The 1994–1995 Jökulhlaup	222
FIGURE 205. Oblique aerial photograph of a blue-water lake formed on the surface of Bering Glacier on 24 July 1994	222
206. Three photographs of the evolution of kettle ponds that formed during the 1994–95 jökulhlaup on 30 April 1996, 1 May 1996, and 20 July 1996	223
207. Vertical aerial photograph of Seal River on 7 September 1994	224
208. Photographs showing multiple views of the sediment plume from the Seal River in 1938, on 24 August 1978, on 12 July 1976, and on 22 August 2003	224
Post-Surge Retreat of Bering Glacier	226
FIGURE 209. Two oblique aerial photographs of the continued retreat of Bering Glacier on 6 June 1997 and 12 August 2001	227
210. Oblique aerial photograph of the post-surge retreat of Bering Glacier on 10 August 1998	227
211. Oblique aerial photograph of the post-surge retreat of Bering Glacier on 12 August 1998	228
212. Photograph of an uplifted pyramidal-shaped piece of ice in the calving embayment of Bering Glacier in Vitus Lake on 26 September 1997	228
213. Oblique aerial photograph of the terminus of Bering Glacier on 12 August 2001	229
Stellar Glacier Activity	229
FIGURE 214. Two oblique aerial photographs of the effects of the surge on the ice-cored lateral moraine of the Stellar Lobe on 12 August 2000 and 12 August 2001	229
Glaciers of Waxell Ridge	229
FIGURE 215. Photograph showing view of Mount Steller and a number of retreating, unnamed glaciers on 8 August 2001	230
Glaciers of the Southern Side of Juniper Island	230
FIGURE 216. Oblique aerial photograph of the Juniper Island area on 12 August 2001	230
Holocene History of Bering Glacier	231
FIGURE 217. Close-up photograph on 13 August 1992 of an <i>in situ</i> mollusk in the Yakataga Formation	231
218. Photograph of part of a peat deposit on the northeast side of Tashalich Arm on 13 August 1992	231
219. Five sketch maps that depict positions of the terminus of the Bering Glacier during the last half of its Holocene history	232

	<b>Page</b>
Copper River Drainage Segment (Including Glaciers That Drain Directly into the Copper River Delta) -----	233
Martin River Glacier–Martin River–Lower Copper River–Bremner River–West Fork Tana River–Tana Glacier Subdivision-----	234
Ragged Mountains-----	234
Martin River Glacier-----	234
FIGURE 220. Oblique aerial photograph on 31 July 1999 of a pair of small, retreating unnamed glaciers-----	235
Slide Glacier-----	236
FIGURE 221. Two oblique aerial photographs of Slide Glacier, with 1964 earthquake-produced rock avalanches on 6 October 1974 and 13 August 1990-----	236
Johnson Glacier-----	237
McPherson Glacier-----	237
Miles Glacier-----	237
FIGURE 222. Two photographs of the terminus area of Miles Glacier in Miles Lake on 13 August 1994 and 12 August 2001-----	238
Van Cleve Glacier-----	239
FIGURE 223. Aerial photograph of the southern part of Van Cleve Lake on 7 September 1994-----	239
Large Glaciers North of Miles Glacier-----	239
Wernicke Glacier-----	239
Fan Glacier-----	240
FIGURE 224. Two aerial photographs of Fan Glacier on 18 August 1978 (AHAP) and 16 August 2000-----	240
225. AHAP photograph mosaic of the debris-covered Bremner Glacier on 18 August 1978-----	241
Bremner Glacier-----	242
Tana Glacier-----	242
FIGURE 226. AHAP photograph of the terminus of the eastern distributary of Tana Glacier on 18 August 1978-----	243
The Bremner River–Upper Copper River–Chitina River–Tana River Subdivision (Located East of the Copper River)-----	243
FIGURE 227. Photograph by Moffitt showing early 20th century evidence of retreat of an unnamed glacier-----	243
The Western Copper River Delta–Lower Copper River–Tasnuna River Subdivision (Located on the West Side of the Copper River)-----	244
FIGURE 228. AHAP photographic mosaic of the area between Copper River and Glacier River on 13 August 1982-----	244
Saddlebag Glacier-----	244
Sherman Glacier-----	245
FIGURE 229. Three aerial photographs of Sherman Glacier on 24 August 1964, 22 August 1979, and 29 August 1984-----	246
Sheridan Glacier-----	247
FIGURE 230. Aerial photograph of the terminus of Sheridan Glacier on 22 August 1979-----	248
231. Oblique aerial photograph of the ice-marginal lakes in front of Sheridan Glacier on 17 August 2000-----	248
Scott Glacier-----	248
FIGURE 232. Two aerial photographs of Scott Glacier on 24 July 1987 and 17 August 2000-----	249
Glaciers Draining into the Tasnuna River-----	249
Woodworth Glacier-----	249
FIGURE 233. Near-vertical aerial photograph of glacial landforms in front of Woodworth Glacier in August 1938-----	249
234. AHAP photograph of Woodworth Glacier on 25 August 1978-----	250
Schwan Glacier-----	250
FIGURE 235. AHAP photograph of Schwan Glacier on 9 July 1978-----	251
Small Glaciers Between Schwan and Heney Glaciers-----	250
Heney Glacier-----	251
Allen Glacier-----	251
FIGURE 236. Two oblique aerial photographs of Allen Glacier on 17 August 2000-----	252
Grinnell Glacier-----	252
FIGURE 237. Oblique aerial photograph of Grinnell Glacier on 17 August 2000-----	253
Childs Glacier-----	253

	<b>Page</b>
FIGURE 238. Aerial photograph on 13 August 1994 and oblique aerial photographic mosaic of the terminus of Childs Glacier on 17 August 2000	254
Goodwin Glacier	254
Cleave Creek Glacier–Upper Copper River–Stephens Glacier–Tonsina Glacier	
Northwestern Subdivision	254
Cleave Creek Glacier	255
FIGURE 239. Oblique aerial photograph of the retreating terminus of Cleave Creek Glacier on 8 August 1996	255
Worthington Glacier	255
Tonsina Glacier	256
FIGURE 240. AHAP photograph of the terminus of Tonsina Glacier on 25 August 1978	257
Klutina and Stephens Glaciers	257
FIGURE 241. Oblique aerial photograph of Klutina Glacier on 30 August 2000	257
Prince William Sound Segment—Heney Range to the East Side of Valdez Arm Subdivision	258
Shephard Glacier	258
Glaciers of the Rude River Drainage	258
Cordova Glacier	258
Glaciers South of Lowe River	258
FIGURE 242. Three oblique aerial photographs of unnamed glaciers in the Rude River drainage on 8 August 2000	259
Wortmanns Glacier	259
FIGURE 243. AHAP photograph of the terminus of Wortmanns Glacier and other nearby glaciers on 25 August 1978	259
Bench Glacier	259
Heiden Glacier	260
Deserted Glacier	260
Glaciers North of Lowe River and West of Keystone Canyon	260
Valdez Glacier	260
FIGURE 244. Two photographs showing changes at Valdez and Camicia Glaciers in 1905 and on 8 August 2000	261
Prince William Sound Segment—The Northern Prince William Sound Subdivision	262
Figure 245. Landsat 3 MSS image of the western Chugach Mountains on 26 August 1978	262
Shoup Glacier	263
FIGURE 246. Two photographs of Shoup Glacier showing the position of its terminus on 13 July 1908 and 8 August 2000	263
Columbia Glacier	264
FIGURE 247. AHAP photograph of the terminus of Columbia Glacier on 24 August 1978	264
248. Photographs of the lower Columbia Glacier on 25 and 26 June 1899	266
249. Map of the lower 15 km of Columbia Glacier on 25–28 June 1899	267
250. Three photographs showing late 19th century features at the terminus of Columbia Glacier on 26 June 1899	268
251. Four oblique aerial photographs show changes in the terminus region of Columbia Glacier on 3 September 1966, 15 August 1981, 13 August 1990, and 8 August 2000	270
252. Three oblique aerial photographs of features along the margin of Columbia Glacier on 8 August 2000	271
Meares Glacier	271
FIGURE 253. Aerial photograph of the terminus of Meares Glacier on 17 August 1999	272
254. Map of the terminus of Meares Glacier showing fluctuations in its terminus from 1910 to 2000	273
Pedro and Brilliant Glaciers	273
Raney and Baby Glaciers	274
Glaciers of College Fiord	274
FIGURE 255. ASTER image of upper College Fiord on 24 June 2000	274
256. View of College Fiord shows five tidewater glaciers located on the west side on 8 August 2000	275
Cap and Tommy Glaciers	276
Crescent and Amherst Glaciers	276
FIGURE 257. Photograph of Amherst Glacier on 14 July 1978	276
Lafayette Glacier	277

	<b>Page</b>
Glaciers Draining into Coghill Lake	277
Williams Glacier	277
Muth Glacier	277
Dartmouth Glacier	277
Bathymetry of College Fiord	277
Glaciers of Yale Arm	278
Yale Glacier	278
FIGURE 258. View of the retreating Yale Glacier on 15 August 1978	280
Unnamed Glaciers of Yale Arm	280
Glaciers of Harvard Arm	280
Harvard Glacier	280
FIGURE 259. Map of Harvard Glacier showing fluctuations in the position of its terminus from 1899 to 2000	280
260. AHAP photograph of upper Harvard Arm and Harvard Glacier on 25 August 1978	282
261. Photographs showing details of the advancing Harvard Glacier on 14 August 1978 and 31 August 2000	283
Radcliffe Glacier	284
Baltimore Glacier	284
Smith Glacier	285
FIGURE 262. Two photographs show changes of Smith Glacier between 15 August 1978 and 8 August 2000	286
Bryn Mawr Glacier	285
FIGURE 263. Oblique aerial photograph of terminus of Bryn Mawr Glacier on 8 August 2000	287
Vassar Glacier	287
FIGURE 264. Photograph of the debris-covered terminus of Vassar Glacier on 15 June 1978	287
Wellesley Glacier	288
FIGURE 265. Oblique aerial photograph of the retreating terminus of Wellesley Glacier on 8 August 2000	288
Barnard Glacier	288
Holyoke Glacier	289
Barry Arm and Harriman Fiord	289
FIGURE 266. AHAP photographic mosaic of Harriman Fiord and Barry Arm on 24 August 1978	289
Glaciers of Barry Arm	290
Barry Glacier	290
FIGURE 267. Map of the lower Harriman Fiord and Barry Arm, showing Cascade, Barry, and Coxe Glaciers in 1910	291
268. Oblique aerial photographs showing changes in Cascade, Barry, and Coxe Glaciers between 8 August 1981 and 8 August 2000	292
Coxe Glacier	292
Cascade Glacier	293
Glaciers of Harriman Fiord	293
Serpentine Glacier	293
FIGURE 269. Photographs showing changes in Serpentine Glacier between 1899 and 6 September 2000	293
270. Oblique aerial photograph of Serpentine Glacier on 8 August 2000	294
Penniman Glaciers, Baker Glacier, and Detached Glacier	295
FIGURE 271. Two photographs showing changes in Baker and Detached Glaciers between 1909 and 6 September 2000	295
Surprise Glacier	296
FIGURE 272. Aerial photograph of Surprise Inlet and Surprise and Cataract Glaciers on 8 August 2000	296
Cataract Glacier	296
FIGURE 273. Two photographs showing changes at Cataract Glacier during the 91-year period from 1909 to 6 September 2000	297
Roaring Glacier	297
FIGURE 274. Photograph of the retreating terminus of Roaring Glacier on 12 July 1978	298
Harriman Glacier	297
FIGURE 275. Three photographs showing characteristics of Harriman Glacier during its advance in the late 20th century on 8 June 1976, 15 July 1978, and 6 September 2000	299
Dirty and Wedge Glaciers	300
Toboggan Glacier	300
Glaciers of Port Wells	301

	<b>Page</b>
Bettles and Pigot Glaciers	301
FIGURE 276. Oblique aerial photograph of Pigot Glacier on 8 August 2000	301
Glaciers of Passage Canal	302
Seth and Billings Glaciers	302
FIGURE 277. Oblique aerial photograph of the retreating and thinning Billings Glacier on 8 August 2000	302
<b>Northwestern Chugach Mountains Segment—North-Flowing Large Valley Glacier</b>	
Subdivision	302
FIGURE 278. Landsat 7 ETM+ image of the northwestern part of the Chugach Mountains on 1 August 2002	303
Matanuska Glacier	303
FIGURE 279. Oblique aerial photograph of the debris-covered terminus of Matanuska Glacier on 30 August 2000	304
Nelchina Glacier	304
FIGURE 280. Oblique aerial photograph of the thinning and retreating terminus of Nelchina Glacier on 30 August 2000	305
Tazlina Glacier	305
FIGURE 281. Oblique aerial photograph of Tazlina Glacier on 30 August 2000	306
<b>Northwestern Chugach Mountains Segment—The Turnagain Arm—Western Chugach</b>	
Mountains Subdivision	306
Marcus Baker Glacier	306
FIGURE 282. Oblique aerial photograph of the debris-covered terminus of Marcus Baker Glacier on 30 August 2000	306
Knik Glacier	306
FIGURE 283. Oblique aerial photograph of the northern part of the terminus of Knik Glacier on 30 August 2000	307
284. Vertical aerial photograph of the southwestern part of the terminus of Knik Glacier on 17 August 1999	307
285. Oblique aerial photograph of the westernmost part of Knik Glacier and The Gorge on 30 August 2000	308
Gannett Glacier	308
FIGURE 286. Aerial photograph of the retreating and thinning terminus of Gannett Glacier on 17 August 1999	309
Colony Glacier	308
FIGURE 287. Aerial photographs of Colony Glacier and the surrounding area on 25 August 1978 and on 15 August 2000	309
Lake George Glacier	310
Glaciers West of Knik Glacier, Upper Lake George, and Lake George Glacier	310
FIGURE 288. Oblique aerial photograph of Hunter Creek Glacier on 30 August 2000	310
Glaciers of the Eagle River and Crow Creek Drainages	311
Eagle Glacier	311
FIGURE 289. Oblique aerial photograph of Eagle Glacier on 30 August 2000	311
Eklutna Glacier	312
FIGURE 290. Oblique aerial photograph of Eklutna Glacier on 30 August 2000	312
Twentymile Glacier	312
FIGURE 291. Oblique aerial photograph of the terminus of Twentymile Glacier on 18 July 1978	313
Summary	313
<b>Kenai Mountains</b>	<b>314</b>
Introduction	314
FIGURE 292. Index map and NOAA AVHRR image mosaic of the glacierized Kenai Mountains	314
293. Landsat 1 MSS image of the Harding and Sargent Icefields on 17 August 1973, and Landsat MSS image mosaic of the Kenai Mountains	316
294. Graph showing lifespans of cross-dated, glacially overridden subfossil trees	318
Unnamed Ice Field North of the Sargent Icefield	318
Portage Glacier	318
FIGURE 295. Landsat 7 ETM+ image showing an unnamed ice field north of Sargent Icefield on 26 September 1999, and oblique aerial photograph of Portage Glacier and the lake formed by its retreat on 8 August 2000	319
Whittier Glacier	320

	<b>Page</b>
Glaciers of Blackstone Bay	320
FIGURE 296. Two aerial photographs of several glaciers in the Blackstone Bay area on 8 August 1981 and on 12 August 1984	321
297. Oblique aerial photograph of the terminus of Lawrence Glacier on 15 July 2000	322
298. Oblique aerial photograph of Tebenkof Glacier on 15 July 2000	322
Glaciers of the Western Side and South of Kings Bay	322
FIGURE 299. Oblique aerial photograph of Taylor and Cotterell Glaciers on 3 September 1966	323
300. Two aerial photographs showing changes in Claremont Glacier between 3 September 1966 and 15 July 2000	324
Glaciers of Upper Kings River	325
Wolverine Glacier	325
FIGURE 301. Oblique aerial photograph showing Wolverine Glacier on 3 September 1996 and sketch map of retreat of terminus between 1713 and 2000	325
Glaciers of Snow River	326
Trail Glacier	326
Glaciers of Placer River	326
Sargent Icefield	327
FIGURE 302. Landsat 7 ETM+ image showing the Sargent Icefield on 26 September 1999	327
Glaciers on the Eastern Side of Kings Bay	328
FIGURE 303. Three photographs showing changes in the terminus of Falling Glacier, in 1924, on 3 September 1966, and on 15 July 2000	328
304. Oblique aerial photograph of the termini of Applegate and Langdon Glaciers on 3 September 1966	329
Glaciers of Port Nellie Juan	329
FIGURE 305. Oblique aerial photograph of Nellie Juan Glacier on 3 September 1966	330
Glaciers of Icy Bay	331
FIGURE 306. Oblique aerial photograph of Chenaga and Tigertail Glaciers on 15 July 2000	331
307. Two photographs showing late 20th century changes in Nassau Fiord between 3 September 1966 and on 15 July 2000	332
308. Two photographs showing the late 20th century position of Tiger Glacier between 3 September 1966 and 15 July 2000	333
Glaciers of Port Bainbridge	333
FIGURE 309. Oblique aerial photograph of Bainbridge Glacier on 15 July 2000	333
Glaciers of the Puget Bay Region	333
Glaciers of Johnstone Bay	334
FIGURE 310. Three aerial photographs of Excelsior Glacier showing changes between 3 September 1966 and 15 July 2000	334
Glaciers of Day Harbor	336
FIGURE 311. Two aerial photographs of Ellsworth Glacier showing changes between 3 September 1966 and 15 July 2000	336
Glaciers of Nellie Juan River	337
Glaciers of Resurrection Peninsula	337
Harding Icefield	337
FIGURE 312. Landsat 7 ETM+ image showing the Harding Icefield and the unnamed ice field to the southwest on 9 August 2000	338
FIGURE 313. AHAP photograph of Bear Glacier on 14 August 1984	339
TABLE 5. Changes in outlet glaciers of the Harding Icefield: 1950s to middle 1990s	340
Glaciers of Lower Resurrection Bay	340
Glaciers of Aialik Bay	340
FIGURE 314. Oblique aerial photograph of the terminus of Aialik Glacier on 15 July 2000	341
315. Oblique aerial photograph of the terminus of Pederson Glacier on 15 July 2000	341
316. Oblique aerial photograph of the terminus of Holgate Glacier on 15 July 2000	341
Glaciers of Harris Bay	342
FIGURE 317. Part of a mosaic of 1963 and 1953 maps and a 15 July 2000 oblique aerial photograph showing changes at Northwestern Glacier during the late 20th century	342
318. Oblique aerial photograph of the terminus of <i>Ogive Glacier</i> on 15 July 2000	343
319. Oblique aerial photograph showing the terminus of <i>Anchor Glacier</i> on 15 July 2000	343

	<b>Page</b>
320. Oblique aerial photograph of <i>Southwestern Glacier</i> , a former tributary to Northwestern Glacier, on 15 July 2000	343
<b>Glaciers of Nuka Bay</b>	<b>343</b>
FIGURE 321. 1963 map and 15 July 2000 oblique aerial photograph showing changes at McCarty Glacier	344
<b>Glaciers of the Western Harding Icefield</b>	<b>344</b>
<b>Unnamed Ice Field Southwest of Harding Icefield</b>	<b>345</b>
FIGURE 322. AHAP photograph of the lower Tustumena Glacier and the terminus of Truuli Glacier on 14 August 1984	345
<b>Glaciers of the Islands of Prince William Sound</b>	<b>346</b>
FIGURE 323. AHAP photograph of central Montague Island on 13 August 1982	346
<b>Summary</b>	<b>346</b>
<b>Kodiak Island</b>	<b>347</b>
FIGURE 324. Index map and NOAA AVHRR image mosaic of Kodiak Island showing glacierized areas	347
325. Landsat 2 MSS image mosaic of the glacierized mountains on Kodiak Island on 18–19 July 1977	348
326. AHAP photograph of south-central Kodiak Island on 25 July 1979	349
<b>Summary</b>	<b>349</b>
<b>Aleutian Range</b>	<b>349</b>
<b>Introduction</b>	<b>349</b>
FIGURE 327. Index map and NOAA AVHRR image mosaic of the Aleutian Range	350
<b>Glaciers of the Neacola and Chigmit Mountains</b>	<b>351</b>
<b>Glaciers of the Neacola Mountains</b>	<b>351</b>
FIGURE 328. Part of a Landsat 7 ETM+ image mosaic of Lake Clark National Park and environs on 6 September 1999	353
329. Oblique aerial photograph of the Neacola Mountains on 4 September 1966	353
330. Oblique aerial photograph of the terminus of Shamrock Glacier on 8 September 2000	353
331. Two oblique aerial photographs of the two retreating termini of Blockade Glacier on 8 September 2000	354
332. Three oblique aerial photographs of Lake Clark Pass showing changes of Tanaina Glacier, an unnamed glacier, and Summit Lake on 25 August 1963, in August 1970, and on 8 September 2000	354
<b>Glaciers of the Chigmit Mountains</b>	<b>355</b>
FIGURE 333. Map and two oblique aerial photographs showing Double Glacier on 8 September 2000	356
<b>Glaciers of Redoubt Volcano</b>	<b>357</b>
FIGURE 334. Oblique aerial photograph of the summit and upper 1,500 m of Redoubt Volcano on 29 July 1978	357
<b>Glaciers of Iliamna Volcano</b>	<b>358</b>
FIGURE 335. Oblique aerial photograph of Iliamna Volcano on 8 August 2000	358
336. Two oblique aerial photographs of Tuxedni Glacier on 8 August 2000	358
337. Two aerial photographs of the terminus and lower reaches of Red Glacier on 26 August 1978 and on 8 August 2000	359
338. Oblique aerial photograph of the Iliamna Volcano and glaciers on its southwest side on 8 August 2000	359
339. Oblique aerial photograph of Iliamna Volcano and three glaciers on 8 August 2000	359
<b>Glaciers West and South of Redoubt and Iliamna Volcanoes</b>	<b>360</b>
FIGURE 340. Oblique aerial photograph of shrinking and disappearing cirque glaciers in the southwestern Chigmit Mountains on 8 August 2000	360
<b>Glaciers of the Kamishak Bay–Big River Area</b>	<b>360</b>
FIGURE 341. Landsat 7 ETM+ image of the Kamishak Bay–Big River area on 16 August 2000	360
342. Photograph of small cirque and cliff glaciers west of Kamishak Bay in July 1923	362
<b>Glaciers of the Ninagiak River–Puale Bay Area</b>	<b>362</b>
FIGURE 343. Landsat images of Katmai National Park and Preserve and environs on 10 October 1977 and on 16 August 2000	363
<b>Glaciers of the Icy Peak–Mount Kialagvik–Mount Chiginagak Area</b>	<b>365</b>
FIGURE 344. 1919 panorama of unnamed cirque and mountain glaciers that descend from the north side of Icy Peak	365
345. Oblique aerial photograph of the glacier-covered summit of Mount Chiginagak in August 1960	365
<b>Glaciers of the Aniakchak Crater Area</b>	<b>366</b>



	<b>Page</b>
FIGURE 346. Landsat 7 ETM+ image of the central Alaska Peninsula on 31 October 1999, and oblique aerial photograph of the Aniakchak caldera in 1977	366
<b>Glaciers of the Mount Veniaminof–Stepovak Bay Area</b>	<b>367</b>
FIGURE 347. Landsat image on 24 March 1976 and oblique aerial photograph on 23 January 1984 of Mount Veniaminof	368
<b>Glaciers of Pavlof Volcano–Frosty Peak Area</b>	<b>367</b>
FIGURE 348. Part of an annotated Landsat 2 MSS image of the southern Aleutian Range on 6 August 1979	369
<b>Summary</b>	<b>369</b>
FIGURE 349. Part of the provisional 1:63,360-scale topographic map of the Cold Bay, Alaska A-3 quadrangle	370
<b>Aleutian Islands</b>	<b>371</b>
<b>Introduction</b>	<b>371</b>
FIGURE 350. Index map and NOAA AVHRR image mosaic of the glacierized Aleutian Islands	373
<b>Unimak Island</b>	<b>373</b>
FIGURE 351. Annotated space shuttle photographs of the glacierized volcanoes of Unimak Island and environs in September 1992	374
352. Two oblique aerial photographs of Shishaldin Volcano and environs, Unimak Island, in 1932 and on 21 September 1990	375
<b>Akutan Island</b>	<b>373</b>
<b>Unalaska Island</b>	<b>373</b>
FIGURE 353. Oblique aerial photograph of the summit region of Makushin Volcano in August 1982	375
<b>Umnak Island</b>	<b>376</b>
FIGURE 354. Landsat 2 MSS image of glaciers on Umnak Island on 2 September 1977	376
<b>Herbert Island</b>	<b>377</b>
FIGURE 355. International Space Station photograph on 1 January 2001 of part of the Aleutian Islands and oblique color aerial photograph of the summit crater of Herbert Island on 27 September 1996	377
<b>Atka Island</b>	<b>378</b>
FIGURE 356. Part of a Landsat 2 MSS image of Korovin Volcano and Mount Kliuchef, Atka Island, on 23 September 1977	378
<b>Great Sitkin Island</b>	<b>378</b>
<b>Tanaga Island</b>	<b>378</b>
<b>Gareloi Island</b>	<b>378</b>
<b>Kiska Island</b>	<b>378</b>
<b>Summary</b>	<b>378</b>
<b>Wrangell Mountains</b>	<b>379</b>
<b>Introduction</b>	<b>379</b>
FIGURE 357. Index map and NOAA AVHRR image mosaic of the glacierized Wrangell Mountains	379
358. Landsat 1 MSS image of the Wrangell Mountains on 18 August 1972, and contour map of equal snowline altitude	380
TABLE 6. Wrangell Mountains accumulation area ratios	381
FIGURE 359. Part of a 1:750,000-scale map of the Mount Wrangell District, Alaska	382
360. Oblique aerial photograph of a rock glacier on the west side of Bonanza Peak in 1961	382
<b>Glaciers of the Regal Mountain – Frederika Mountain Area and the Eastern Wrangell Mountains</b>	<b>383</b>
FIGURE 361. Oblique aerial photograph of the retreating terminus of Chisana Glacier on 30 August 2000	383
362. Oblique aerial photograph of an unnamed surging glacier in the Bow Pass area on 30 August 2000	384
363. Two oblique aerial photographs of parts of Middle Fork Glacier on 30 August 2000	384
364. Two 20th century views (in 1905 and 1966) of Hole-in-the-Wall Glacier	385
365. Map, Landsat 7 ETM+ image on 10 September 2001, and oblique aerial photograph of Nizina Glacier on 30 August 2000	386
366. Oblique aerial photograph of the central Rohn Glacier adjacent to Chimney Mountain on 30 August 2000	388
<b>Glaciers of Mount Blackburn and the Southeastern Wrangell Mountains</b>	<b>388</b>
FIGURE 367. Map, Landsat image on 10 September 2001, and two oblique aerial photographs on 30 August 1999 and 30 August 2000, of the Kennicott Glacier	389
368. An early 20th century photograph of typical small cirque and mountain glaciers in 1919	391

	<b>Page</b>
<b>Kennicott Glacier</b> .....	389
FIGURE 369. Oblique aerial photograph of the northeast tributary and the main trunk of the Kuskulana Glacier on 31 August 1984 .....	392
<b>Glaciers of Mount Wrangell</b> .....	393
FIGURE 370. Radar image and oblique aerial photograph in 1981 of Mount Wrangell .....	393
<b>Glaciers Descending from Mount Wrangell's Summit Caldera</b> .....	394
FIGURE 371. Oblique aerial photograph of the pitted and hummocky terminus of Long Glacier on 30 August 2000 .....	394
372. Maps, Landsat 7 ETM+ image on 10 September 2001, and aerial photographs on 26 August 1981 and 30 August 2000 of Nabesna Glacier .....	394
<b>Mount Drum</b> .....	398
FIGURE 373. Map and oblique aerial photograph on 30 August 2000 of the glaciers of Mount Drum .....	398
<b>Mount Sanford</b> .....	398
FIGURE 374. Landsat 7 ETM+ image of Sanford Glacier on 10 September 2001 .....	400
<b>Glaciers of Mount Jarvis and Mount Gordon and the Ice Fields Plateau</b> .....	398
<b>Summary</b> .....	401
<b>Talkeetna Mountains</b> .....	<b>401</b>
FIGURE 375. Index map and NOAA AVHRR image mosaic of the Talkeetna Mountains .....	401
376. Landsat 3 MSS image mosaic showing the Talkeetna Mountains on 27 August 1978 .....	402
377. Two aerial photographs of glaciers at the head of the Sheep River on 3 August 1983 and 31 August 2000 .....	403
378. Two aerial photographs of Chickaloon Glacier and its surrounding area on 3 August 1983 and 31 August 2000 .....	404
379. Oblique aerial photograph of Talkeetna Glacier and its surrounding area on 31 August 2000 .....	405
380. Oblique aerial photograph of several large rock glaciers on 31 August 2000 .....	405
<b>Summary</b> .....	405
<b>Alaska Range</b> .....	<b>406</b>
<b>Introduction</b> .....	406
FIGURE 381. Index map of the Alaska Range showing glacierized areas .....	406
382. NOAA AVHRR image mosaic of the Alaska Range in summer 1995 .....	406
<b>The Mentasta and Nutzotin Mountains Segment between the Canadian Border and         Mentasta Pass</b> .....	408
<b>The Mount Kimball-Mount Gakona Segment between Mentasta Pass and the Delta River</b> .....	409
FIGURE 383. AHAP photograph of glaciers southeast of Needle Peak on 26 August 1981 .....	409
384. Two oblique aerial photographs of small glaciers and rock glaciers in the Nutzotin Mountains on 30 August 2000 .....	409
FIGURE 385. Oblique aerial photograph of the icefall of Gerstle Glacier on 22 August 1960 .....	410
386. AHAP photograph of the termini of Gulkana, West Gulkana, and College Glaciers on 24 August 1981 .....	411
<b>Gulkana Glacier</b> .....	412
FIGURE 387. Four photographs showing changes in Gulkana Glacier between 31 August 1967, 1975, 11 July 1993, and 18 August 1999 .....	412
<b>West Gulkana Glacier</b> .....	415
<b>Jarvis Glacier</b> .....	416
<b>The Mount Hayes-Mount Deborah Segment between Delta River and Broad Pass</b> .....	416
FIGURE 388. Landsat 3 RBV image of Black Rapids Glacier and other glaciers in the Alaska Range on 8 August 1981 .....	417
389. Three photographs of the terminus of Susitna Glacier in pre-1915, August 1941, and mid-1970s .....	418
390. Oblique aerial photograph of the terminus of an unnamed glacier on 14 September 1999 .....	419
391. Oblique aerial photograph of the terminus of an unnamed rock glacier on 14 September 1999 .....	419
<b>Black Rapids Glacier</b> .....	419
FIGURE 392. Vertical aerial photograph of part of Black Rapids Glacier on 18 August 1999 .....	421
<b>Rock Avalanches onto Glaciers Resulting from the 3 November 2002 Earthquake         (M 7.9) on the Denali Fault</b> .....	421
FIGURE 393. Map and photograph of the results of the 3 November 2002 earthquake .....	422

	<b>Page</b>
394. Oblique aerial photographs of the 3 November 2002 rock avalanches on McGinnis and Black Rapids Glaciers	423
<b>Geospatial Inventory and Analysis of Glaciers: A Case Study for the Eastern Alaska Range, by William F. Manley</b>	<b>424</b>
Abstract	424
Introduction	425
FIGURE 395. Two maps of glaciers and terrain in the eastern Alaska Range	426
<b>Methods</b>	<b>426</b>
FIGURE 396. Flow diagram for processing the original cartographic source material	428
397. Close-ups of selected GIS processing steps and results	429
TABLE 7. Results of the spatial analysis of 279 glaciers in the eastern Alaska Range	430
<b>Error Analysis</b>	<b>431</b>
FIGURE 398. Comparison of GIS results for area and length with the 19-glacier inventory	432
<b>Results</b>	<b>433</b>
FIGURE 399. Shaded-relief maps of the glaciers color-coded for selected GIS results	434
400. Frequency distribution of glaciers by area	435
401. Polar diagram of glacier area versus aspect	436
402. Plots of four geospatial measurements versus glacier area	437
403. Area-altitude distribution integrated for all glacier ice in the region compared with curves for selected glaciers	438
<b>Discussion</b>	<b>438</b>
<b>Acknowledgments</b>	<b>439</b>
<b>The Mount McKinley-Mount Foraker Segment between Broad Pass and Rainy Pass</b>	<b>440</b>
FIGURE 404. Landsat 3 and 5 MSS image mosaic of Mount McKinley area and environs, Alaska Range, between 24 August 1979 and 11 September 1984	440
405. Landsat 1 MSS image of Mount McKinley and Denali National Park and Preserve on 31 August 1977	441
406. Three views of Mount McKinley: 1923 photograph, computer-generated view using Landsat images and DEM data, and oblique aerial photograph in October 1965	443
407. Oblique aerial photograph of Muldrow Glacier on 13 September 1986	443
408. Oblique aerial photograph of Tokositna Glacier on 30 August 1984	444
409. Oblique aerial photograph of the terminus area of Straightaway Glacier on 14 September 1999	444
410. Oblique aerial photograph of the terminus area of Foraker Glacier on 14 September 1999	444
411. Oblique aerial photograph of the upper part of Yentna Glacier on 31 August 1967	445
412. Oblique aerial photograph of the upper part of Lacuna Glacier on 31 August 1967	446
413. Two 1910 photographs showing two unnamed glaciers at the head of Hidden Creek	446
414. Two oblique aerial photographs of Ruth Glacier on 4 September 1966 and on 14 September 1999	447
<b>Tokositna Glacier</b>	<b>448</b>
<b>Polychrome Glacier</b>	<b>448</b>
<b>Muldrow Glacier</b>	<b>448</b>
<b>Kichatna Mountains</b>	<b>449</b>
FIGURE 415. Two views of cirque and small valley glaciers in the Kichatna Mountains in 1902 and 24 August 1979	449
<b>The Mount Gerdine-Mount Spurr Segment between Rainy Pass and Merrill Pass</b>	<b>450</b>
FIGURE 416. Landsat 2 image of the Tordrillo Mountains, southwestern Alaska Range on 2 August 1978	450
417. AHAP photograph of the lower part and terminus of Hayes Glacier on 20 July 1982, and oblique aerial photograph of Trimble Glacier on 8 September 2000	451
418. Two oblique aerial photographs of the terminus of Triumvirate Glacier on 8 September 2000	452
419. Two oblique aerial photographs of Capps Glacier on 8 September 2000	452
420. Three oblique aerial photographs of Kidazqeni Glacier in September 1966, on 2 September 1970, and on 22 September 1992	453
421. Two oblique aerial photographs of Barrier Glacier on 4 September 1966 and 8 September 2000	454
422. Oblique aerial photograph west of the South Branch of Trimble Glacier on 8 September 2000	456
423. AHAP photograph of the lower part of an unnamed glacier on 26 August 1978	456
<b>Summary</b>	<b>457</b>

	<b>Page</b>
<b>Wood River Mountains</b> .....	<b>457</b>
FIGURE 424. Index map and NOAA AVHRR image mosaic of the Wood River Mountains.....	458
425. Landsat MSS composite image showing the northern Wood River Mountains and the adjacent Kuskokwim Mountains on 28 July 1978 .....	459
426. Map showing elevations and locations of glaciers in the central Wood River Mountains .....	460
427. AHAP photograph of Mount Waskey and environs on 15 August 1984 .....	461
428. Photograph of the glacier-covered summit of the Mount Waskey massif in July 1999 .....	462
429. Oblique aerial photograph of Chikuminuk Glacier on 6 September 1957 .....	462
Summary .....	463
<b>Kigluaik Mountains</b> .....	<b>463</b>
FIGURE 430. Index map and NOAA AVHRR image mosaic of the Kigluaik Mountains, the only glacierized part of the Seward Peninsula.....	464
431. Landsat 2 MSS image of much of the Seward Peninsula, including the Kigluaik Mountains, on 26 June 1977 .....	465
432. Photograph by A.H. Brooks of a small retreating cirque glacier in summer 1900.....	466
433. AHAP photograph of the Mount Osborn area on 1 August 1985 .....	466
434. Photograph of the Grand Union Glacier in summer 1983.....	467
Summary .....	467
<b>Brooks Range</b> .....	<b>467</b>
Introduction .....	467
FIGURE 435. Index map and NOAA AVHRR image mosaic of the Brooks Range .....	469
436. Three photographs of Okpilak Glacier, Romanzof Mountains, in June 1907 .....	469
Romanzof Mountains.....	470
FIGURE 437. Landsat 2 MSS image of the Brooks Range on 5 August 1981 .....	471
438. Landsat 3 MSS image of the Franklin and Romanzof Mountains on 29 August 1978 .....	472
439. AHAP photograph of the eastern Romanzof Mountains showing Okpilak Glacier and other glaciers on 24 August 1982.....	473
440. AHAP photograph of the eastern Romanzof Mountains showing multiple glaciers on 24 August 1982.....	474
441. Topographic map of McCall Glacier.....	475
Franklin Mountains .....	476
FIGURE 442. AHAP photographic mosaic of the central Franklin Mountains on 24 August 1982.....	477
Philip Smith and Endicott Mountains .....	478
Schwatka Mountains .....	479
Summary .....	479
<b>Summary and Conclusions</b> .....	<b>480</b>
<b>Acknowledgments</b> .....	<b>486</b>
<b>References Cited</b> .....	<b>487</b>
<b>Appendix A</b> .....	<b>505</b>
<b>Appendix B</b> .....	<b>507</b>
<b>Appendix C</b> .....	<b>508</b>
<b>Appendix D</b> .....	<b>522</b>

GLACIERS OF NORTH AMERICA—

GLACIERS OF ALASKA

By BRUCE F. MOLNIA<sup>1</sup>

**Abstract**

Glaciers cover about 75,000 km<sup>2</sup> of Alaska, about 5 percent of the State. The glaciers are situated on 11 mountain ranges, 1 large island, an island chain, and 1 archipelago and range in elevation from more than 6,000 m to below sea level. Alaska's glaciers extend geographically from the far southeast at lat 55°19'N., long 130°05'W., about 100 kilometers east of Ketchikan, to the far southwest at Kiska Island at lat 52°05'N., long 177°35'E., in the Aleutian Islands, and as far north as lat 69°20'N., long 143°45'W., in the Brooks Range.

During the "Little Ice Age," Alaska's glaciers expanded significantly. The total area and volume of glaciers in Alaska continue to decrease, as they have been doing since the 18th century.

Of the 153 1:250,000-scale topographic maps that cover the State of Alaska, 63 sheets show glaciers. Although the number of extant glaciers has never been systematically counted and is thus unknown, the total probably is greater than 100,000. Only about 600 glaciers (about 1 percent) have been officially named by the U.S. Board on Geographic Names (BGN). There are about 60 active and former tidewater glaciers in Alaska. Within the glacierized mountain ranges of southeastern Alaska and western Canada, 205 glaciers (75 percent in Alaska) have a history of surging. In the same region, at least 53 present and 7 former large ice-dammed lakes have produced jökulhlaups (glacier-outburst floods). Ice-capped volcanoes on mainland Alaska and in the Aleutian Islands have a potential for jökulhlaups caused by subglacier volcanic and geothermal activity. Because of the size of the area covered by glaciers and the lack of large-scale maps of the glacierized areas, satellite imagery and other satellite remote-sensing data are the only practical means of monitoring regional changes in the area and volume of Alaska's glaciers in response to short- and long-term changes in the maritime and continental climates of the State.

A review of the literature for each of the 11 mountain ranges, the large island, the island chain, and the archipelago was conducted to determine both the individual and the regional status of Alaskan glaciers and to characterize changes in thickness and terminus position of representative glaciers in each mountain range or island group. In many areas, observations used for determining changes date from the late 18th or early 19th century. Temperature records at all Alaskan meteorological recording stations document a 20th century warming trend. Therefore, characterizing the response of Alaska's glaciers to changing climate helps to quantify potential sea-level rise from past, present, and future melting of glacier ice (deglaciation of the 14 glacierized regions of Alaska), understand present and future hydrological changes, and define impacts on ecosystems that are responding to deglaciation.

Many different types of data were scrutinized to determine baselines and to assess the magnitude of glacier change. These data include the following: published descriptions of glaciers (1794–2000), especially the comprehensive research by Field (1975a) and his colleagues in the Alaska part of *Mountain Glaciers of the Northern Hemisphere*, aerial photography (since 1926), ground photography (since 1884), airborne radar (1981–91), satellite radar (1978–98), space photography (1984–94), multispectral satellite imagery (since 1972), aerial reconnaissance and field observations made by many scientists during the past several decades, and various types of proxy data. The published and unpublished data available for each glacierized region and individual glacier varied significantly. Geospatial analysis of digitized U.S. Geological Survey (USGS) topographic maps is used to statistically define selected glaciological parameters in the eastern part of the Alaska Range.

The analysis determined that every mountain range and island group investigated can be characterized by significant glacier retreat, thinning, and (or) stagnation, especially those glaciers that end at lower elevations. At some locations, glaciers completely disappeared during the 20th century. In other areas, retreat that started as early as the early 18th century has continued into the 21st century. Ironically, in several areas, retreat is resulting in an increase in the total number of glaciers; even though individual glaciers are separating, the volume and area of ice continue to decrease.

---

<sup>1</sup> U.S. Geological Survey, 926A National Center, Reston, VA 20192 U.S.A.

The key findings from the comprehensive analysis are the following:

- **Alexander Archipelago, Aleutian Islands, and Kodiak Island:** Every insular glacier examined showed evidence of thinning and retreat. Some glaciers have disappeared since being mapped in the middle 20th century.
- **Coast Mountains, St. Elias Mountains, Chugach Mountains, Kenai Mountains, Wrangell Mountains, Alaska Range, and the Aleutian Range:** More than 95 percent of the glaciers ending below an elevation of approximately 1,500 m are retreating and (or) thinning. Of those glaciers that are advancing, many have tidewater termini. The two largest Alaskan glaciers, Bering and Malaspina, are losing several cubic kilometers of ice each year to melting and calving.
- **Talkeetna Mountains, Wood River Mountains, Kigluaik Mountains, and the Brooks Range:** Every glacier scrutinized showed evidence of retreat. Of 109 glaciers in the Wood River Mountains, all are or were retreating; some have disappeared since they were first mapped, photographed, or imaged.

In spite of the significant changes at lower elevations, not every Alaskan glacier is thinning and retreating. In several ranges, no changes were noted in glaciers situated at higher elevations.

Glaciers that were surging or had recently advanced by surging were also noted. This type of glacier advances by redistributing existing glacier ice over a larger area rather than by increased accumulation. Consequently, following a surge, more ice surface area is exposed to ablation.

## Part 1—Background and History

### Introduction

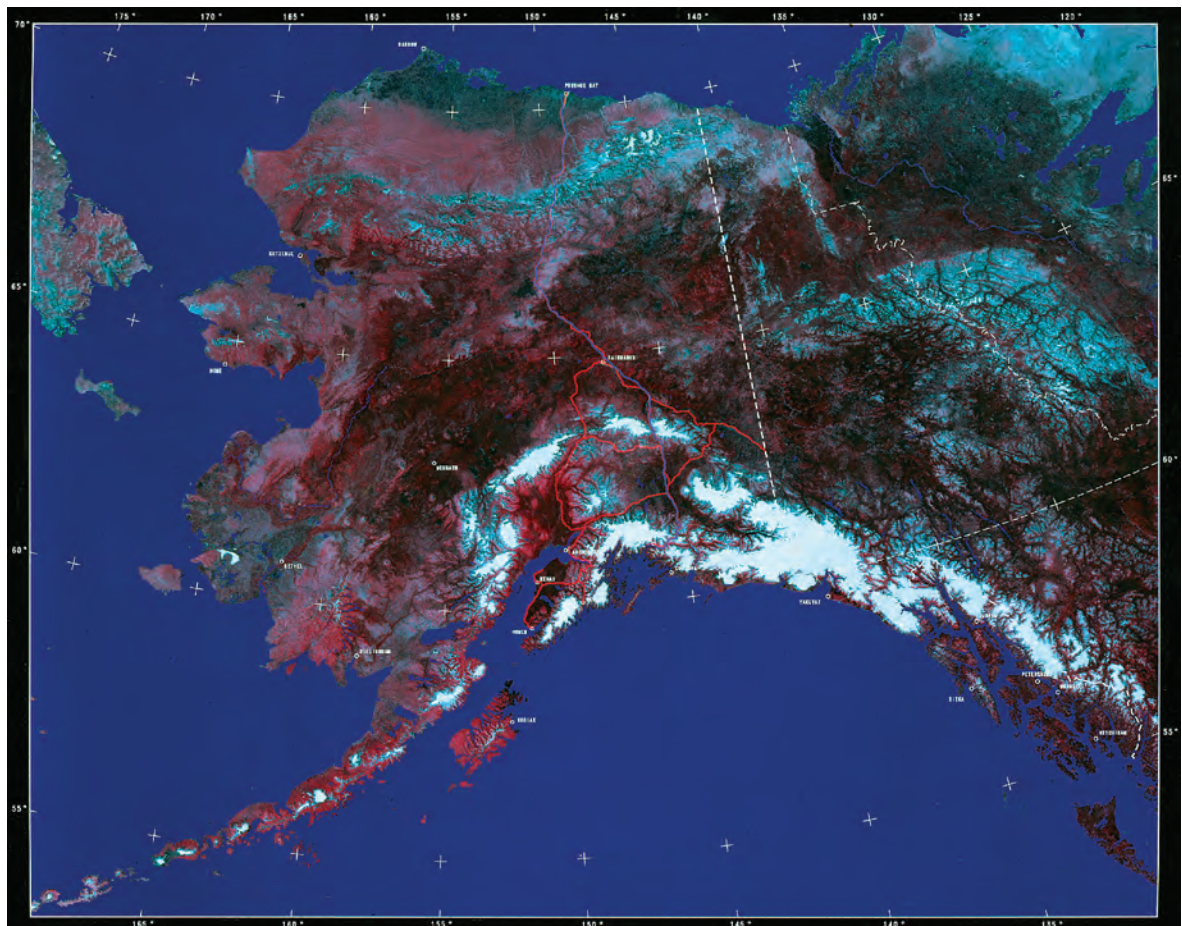
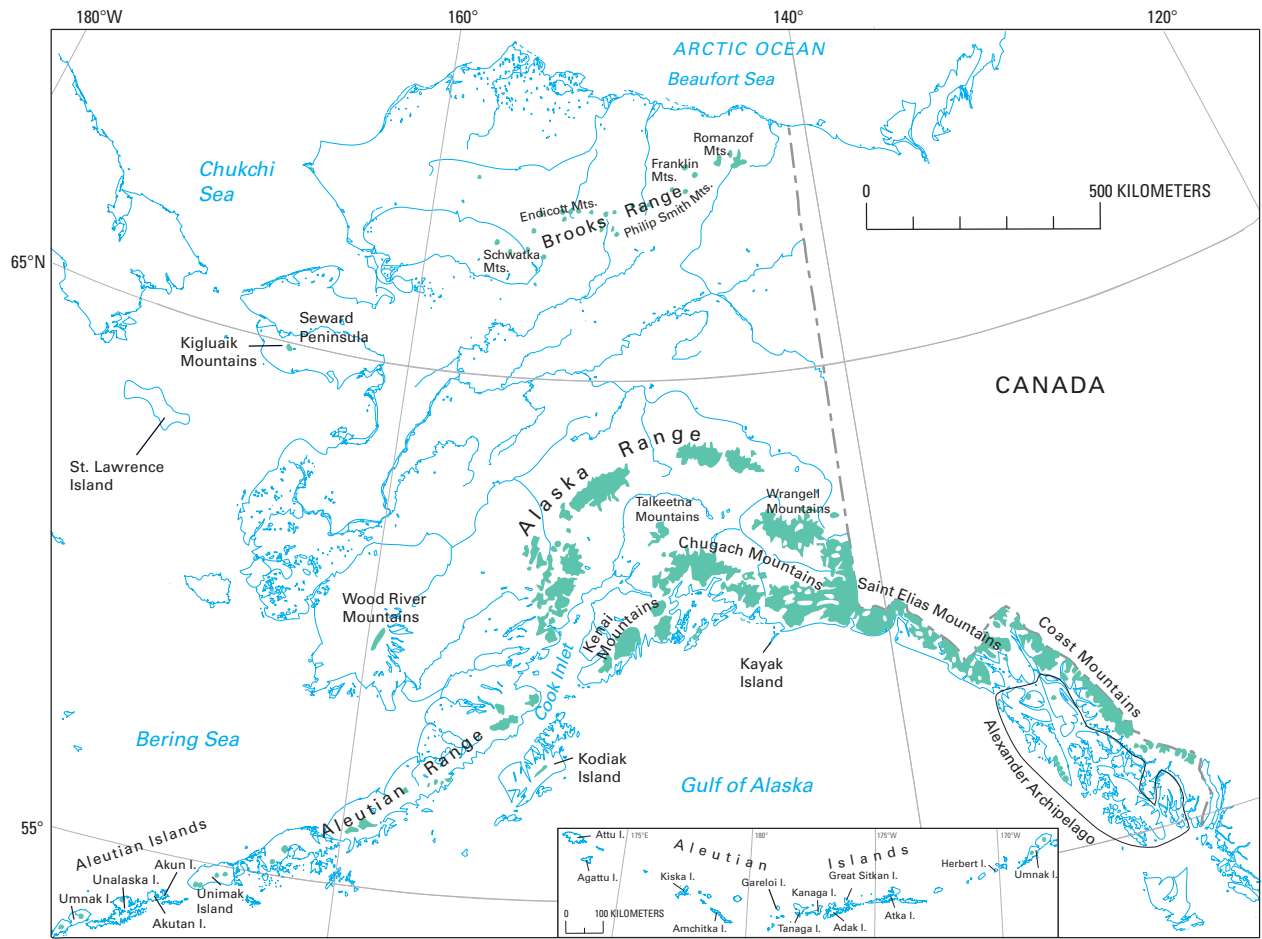
Alaska, with an area of 1,530,693 km<sup>2</sup>, is the northernmost and westernmost of the 50 United States. Because the Aleutian Islands extend across the International Date Line, it is also the easternmost State. Alaska is bounded by the Arctic Ocean and the Beaufort Sea to the north, the Pacific Ocean and the Gulf of Alaska to the south, Canada's Yukon Territory and British Columbia to the east, and the Bering Sea and the Chukchi Sea to the west. Glaciers are a major feature of much of Alaska's landscape, occurring in more than a dozen geographic regions of the State. Glaciers in Alaska extend from as far southeast as lat 55°19'N., long 130°05'W., about 100 km east of Ketchikan, to as far southwest as Kiska Island at lat 52°05'N., long 177°35'E., in the Aleutian Islands, to as far north as lat 69°20'N., long 143°45'W., in the Brooks Range. Glaciers cover about 75,000 km<sup>2</sup> (Post and Meier, 1980), or about 5 percent, of Alaska, occurring on 11 different mountain groups and several islands (figs. 1, 2). Of the 153 1:250,000-scale topographic quadrangle maps that cover the State of Alaska, glaciers are shown on 60 of the 68 topographic quadrangle maps of regions known to be glacierized (that is, to have present-day glaciers) (appendix A). In the text, where 1:63,360-scale maps of glaciers are discussed, information on these topographic quadrangle maps are given in appendix B. The total number of separate glaciers is unknown, having never been systematically counted, but probably exceeds 100,000 (Molnia, 2001, p. 5). More than 600 glaciers have been officially named by the BGN (appendix C).<sup>2</sup>

No comprehensive, detailed glacier inventory has been compiled for Alaska. Estimates of the total glacier area have been made by several scientists: Gilbert (1904) estimated an area of 52,000 km<sup>2</sup>, Post and Mayo (1971) estimated 73,800 km<sup>2</sup>, Post and Meier (1980) estimated an area of 74,700 km<sup>2</sup>, and Molnia (2001) estimated 75,110 km<sup>2</sup>. The significant retreat of Alaska glaciers during the last two decades of the 20th century would necessitate a further reduction in this estimate of glacier area. The difference between Gilbert's total and the later estimates is not owing to an expansion of glacier area in subsequent years but rather reflects an increase in geographic/cartographic knowledge and improvements in the quality of data and techniques

<sup>2</sup> Glacier place-names approved by the BGN are shown in standard font; glacier place-names not approved are shown in italicized font. Formal place-names of glaciers approved by the BGN will be used wherever possible. However, in order to provide information about unnamed glaciers, such glaciers will be described in terms of adjacent geographic features.

► **Figure 1.**—Map of Alaska showing distribution of glaciers (shown in green).

► **Figure 2.**—NOAA Advanced Very High Resolution Radiometer (AVHRR) image mosaic of Alaska in 1991; National Oceanic and Atmospheric Administration image mosaic from Michael Fleming, Alaska Science Center, U.S. Geological Survey, Anchorage, Alaska.



used to produce those estimates. In recent years, some glacier changes have been quite dramatic. Although a few glaciers are advancing, many are in retreat, especially those situated at lower elevations.

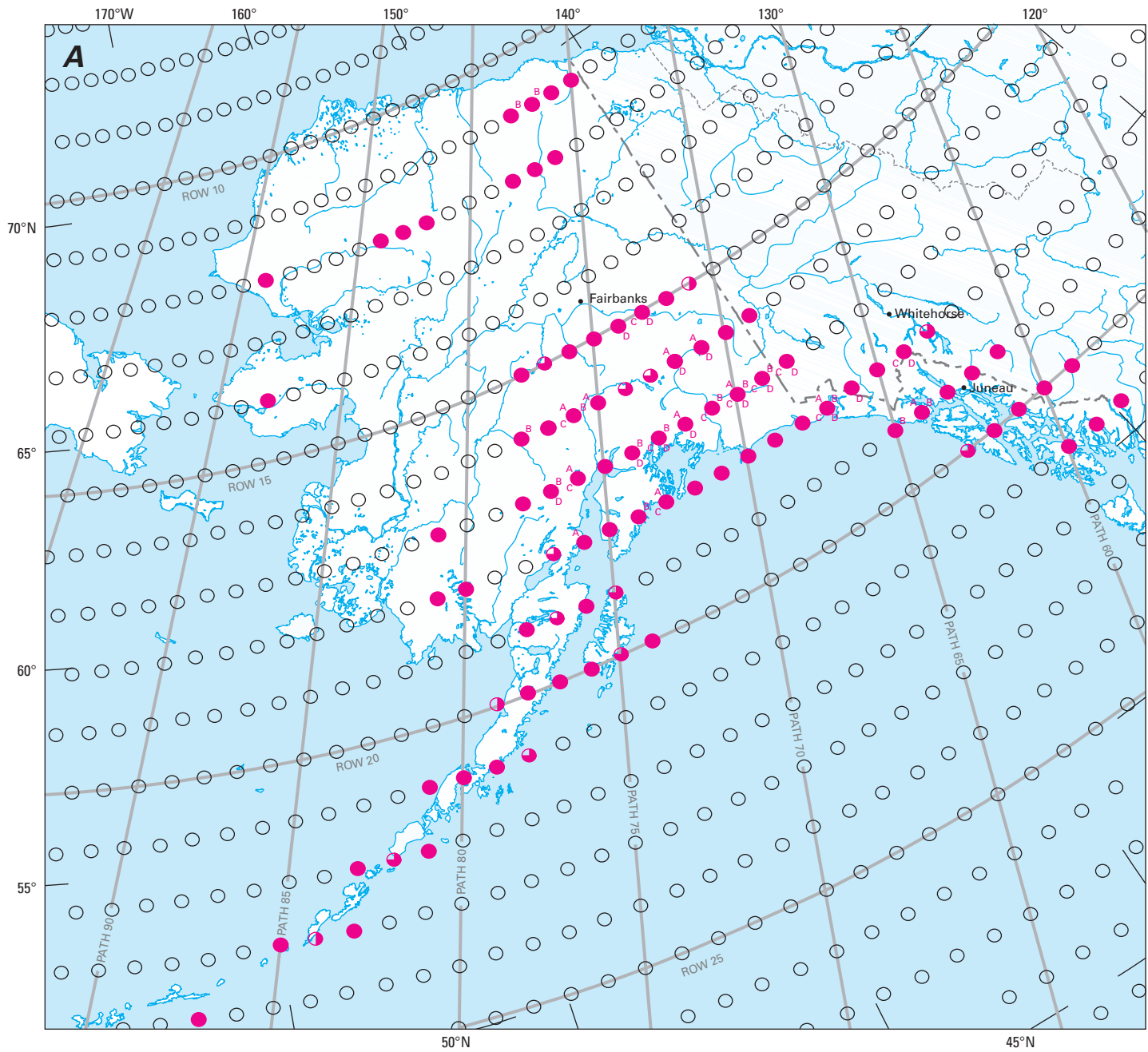
The most easily and frequently measured glacier-fluctuation parameter is the geographic position of the terminus. Modern maps, charts, satellite images, vertical and oblique aerial photographs, ground photographs, and field surveys are all used to determine terminus position. Charts from early navigators and explorers and “traditional knowledge” stories from the oral histories of Alaska’s indigenous peoples also yield information about the past extent of glaciers. Proxy methods, such as tree coring, yield approximate dates for terminus position up to several millennia ago. Together, these methods play an important role in determining the location and changes in the position of the termini of Alaskan glaciers over time.

The primary purpose of this chapter is to summarize the areal extent and distribution of Alaska’s glaciers from the 1970s to the early 1980s in order to present an improved baseline based on Landsat MSS images that can be used now and by future researchers to document change in the number, length, and area of Alaska’s glaciers. In addition, descriptions of the results of scientific investigations that provide specific information about individual glaciers and glaciers within glacierized regions are presented to improve the overall understanding of the timing and magnitude of change.

The primary image data set used for establishing a baseline is the set of 90 Landsat MSS false-color composite images compiled by the author from the Landsat image archive of the USGS Earth Resources Observation Systems (EROS) Data Center (EDC) in Sioux Falls, S. Dak. The data set consists of individual false-color composite Landsat images for each path-row nominal scene center in the glacierized regions of Alaska (fig. 3A). Each image was prepared from digital data collected by Landsat Multispectral Scanner (MSS) sensors between 23 July 1972, the launch of the first Earth Resources Technology Satellite (ERTS-1, later renamed Landsat 1), and 1981. The digital MSS data were collected by sensors on the Landsat 1, 2, and 3 satellites. An image mosaic of most of Alaska was compiled by using many of these images (fig. 3B). The data set is supplemented by additional data and information about the areal extent and distribution of Alaska’s glaciers derived from 18th- to 21st-century exploration, 19th- and 21st-century field-based scientific investigations, 19th- to 21st-century ground-based photography, and 20th-century aerial and space photography, digital satellite imagery, and airborne- and spaceborne-radar imagery to temporally extend the baseline both forward and backward in time. The work of Field (1975a) and his collaborators is the primary source for most of the quantitative area and length measurements of named and unnamed glaciers discussed in the individual glacierized geographic regions of this chapter.

In addition to all of the available imagery and photography, an important resource to develop the baseline and to assess change in Alaska’s glaciers is the 1:250,000-scale ( $1\times 3^\circ$ ) map coverage of the State (appendix A). These maps are the same ones used by Field (1975a) in his landmark study of Alaska’s glaciers. These maps, which are of variable accuracy and quality, were published between 1949 and 1979 by the USGS; they were compiled from data collected by the USGS; the U.S. Army Map Service (AMS) and its successor agency, the U.S. Defense Mapping Agency (DMA) [later the National Imagery and Mapping Agency (NIMA) and now the National Geospatial-Intelligence Agency (NGA)]; the U.S. Coast and Geodetic Survey (C&GS) [now the National Ocean Service (NOS)]; and the National Oceanic and Atmospheric Administration (NOAA). More detailed 1:63,360-scale (15-minute) maps exist for each glacierized quadrangle, although many are still provisional (appendix B). Many of the 1:250,000-scale maps have undergone limited revisions. In more than a dozen instances, these revisions have included the use of a purple pattern overprinted on glacial features to indicate glacier change, either





EXPLANATION OF SYMBOLS

Evaluation of image usability for glaciologic, geologic, and cartographic applications. Symbols defined as follows:

- Excellent image (0 to ≤5 percent cloud cover)
- Good image (>5 to ≤10 percent cloud cover)
- Fair to poor image (>10 to <100 percent cloud cover)
- Nominal scene center for a Landsat image outside the area of glaciers
- Usable Landsat 3 return beam vidicon (RBV) scenes.  
A, B, C, and D refer to usable RBV subscenes



**Figure 3.—A,** Map showing the location of nominal scene centers for optimum Landsat 1, 2, and 3 MSS and RBV images that include Alaskan glaciers.



**Figure 3. —B,** Landsat MSS false-color infrared image mosaic of part of Alaska, showing most of the glacierized areas in Alaska except for the southeastern panhandle of the state and the westernmost part of the Aleutian Islands (see fig. 2), including many of the active and former tidewater glaciers. Image mosaic compiled by the former Branch of Alaskan Geology, U.S. Geological Survey, in 1978.

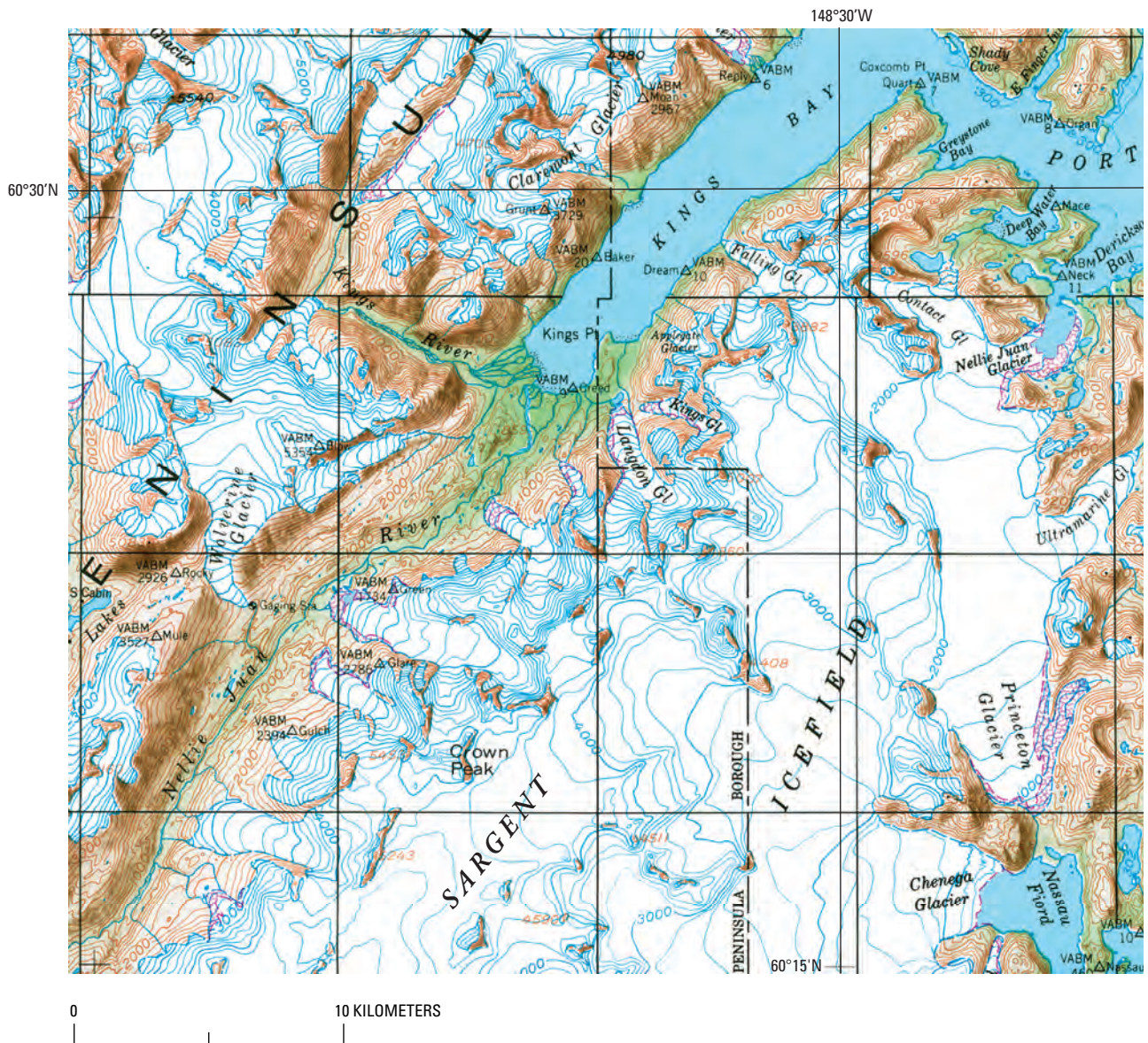


**Figure 4.**—Section of the USGS (1982) (selective revisions) 1:250,000-scale topographic map of Seward, Alaska (1951), showing the use of a purple-pattern overprint to indicate areas of selected glacier “advance or recession, visible as of the date of photography” (appendix A). The original surveys for the 1951 map (USGS, 1951) were done in 1945 and based on 1942 and 1945 vertical aerial photography. The map shown was revised in 1982 from vertical aerial photographs acquired in 1978. In this area east of Wolverine Glacier, all the outlet glaciers from the northern Sargent Icefield show recession.

advance or recession of its terminus (fig. 4, appendix A). Commercial vendors have released paper compilations (DeLorme Mapping, 1992, 1998, 2001) and CD-ROMs (Scarp Exploration, Inc., 1998–2003) of all of the USGS 1:250,000-scale topographic maps of Alaska. The DeLorme atlases are printed at a scale of 1:300,000; both commercial sources are particularly useful because of accompanying place-name indexes (lacking on USGS maps).

These abundant and diverse data clearly document the fact that the glaciers of Alaska are undergoing changes in length and area. In addition to long-term changes, calving-terminus glaciers may recede a kilometer or more in a single year; surge-type glaciers may advance several kilometers during a surge event. Such changes are of sufficient magnitude to be seen easily at the picture element (pixel) resolution (79 m) of Landsat MSS images. In many instances, Landsat may be the only permanent record of these changes.

In less than a century, major ocean inlets, such as Glacier Bay and Icy Bay, have been formed by glacier recession. The rapidly receding Columbia Glacier (and production of icebergs from its calving terminus, a recognized hazard to maritime shipping) has caused dramatic changes in this tidewater glacier (see separate sections on Columbia and Hubbard Tidewater Glaciers and the 1986 and 2002 Temporary Closures of Russell Fiord by the Hubbard Glacier in this chapter). Major lakes have formed and drained catastrophically (undergone outburst flooding [jökulhlaups]) owing to changes in their impounding ice

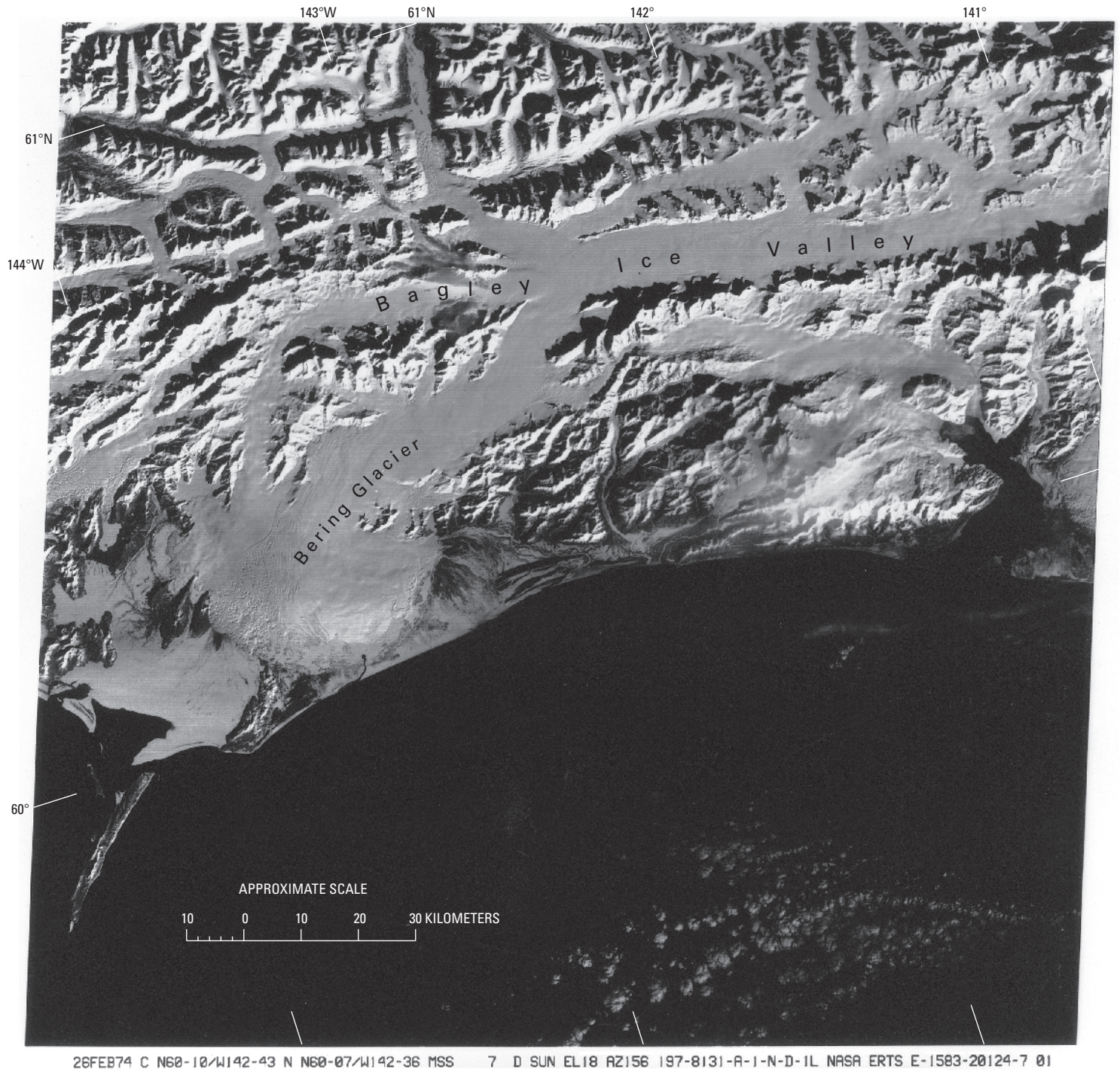


**Figure 5.** — Landsat 1 black-and-white multi-spectral scanner (MSS) image of all but the very easternmost segment of the 200-km-long Bering Glacier and Bagley Ice Valley. The Landsat image (1583-20124, band 7; 26 February 1974; Path 69, Row 18) is from the USGS, EROS Data Center, Sioux Falls, S. Dak.

dams. Glaciers, such as the Taku Glacier, have gone from being tourist attractions, accessible by oceangoing ships, to becoming impossible to reach other than in shallow-draft kayaks. Additionally, changing climate has affected the area and volume of nearly all of Alaska's glaciers, impacting the storage and release of freshwater and producing a discernible change in global eustatic sea level (Meier, 1984; National Research Council, 1984; Meier and Dyurgerov, 2002; Meier and Wahr, 2002; Arendt and others, 2002).

Today, more than two-thirds of Alaska's glaciers are located within 200 km of the shore of the Pacific Ocean in or on the Coast Mountains, the Alexander Archipelago, the St. Elias Mountains, the Chugach Mountains, the Kenai Mountains, Kodiak Island, the Aleutian Range, and the Aleutian Islands. The remaining glaciers are distributed in several interior mountain groups, including the Wrangell Mountains, the Talkeetna Mountains, the Alaska Range,

the Wood River Mountains, the Kigluaik Mountains of the Seward Peninsula, and the Brooks Range (fig. 1). The glaciers of each of these 14 glacierized geographic regions are discussed in separate sections that follow. Each section contains one or more Landsat MSS false-color composite images and an index map (Field, 1975a) selected to provide a geographic reference for detailed information about the glaciers in each region.

Other sections provide a summary of early observations of Alaska's glaciers, pre-International Geophysical Year (IGY) 20th-century investigations of Alaska's glaciers, the photographic record of Alaska's glaciers, the naming of Alaska's glaciers, tidewater and surge-type Alaskan glaciers, and glacier-outburst floods (jökulhlaups). Table 1 presents a list of the optimum Landsat 1, 2, and 3 MSS and Return Beam Vidicon (RBV) imagery of Alaska's glaciers. A map showing the location of Landsat MSS nominal scene centers for images that include Alaska's glaciers is shown in figure 3A.

Landsat images, combined with ground and aerial observations and previously published work, provide an excellent source of data and information necessary to define the geographic distribution and areal extent of and the changes occurring in the glaciers of Alaska. The synoptic scale of Landsat (generally 1:250,000 to 1:1,000,000 scale) is required to conveniently show the major glacierized regions. For example, Bering Glacier—including its source, the Bagley Ice Valley (fig. 5)—is nearly 200 km long. About 100 1:40,000-scale aerial photographs or about 50 1:63,360-scale topographic maps or two 1:250,000-scale topographic maps are necessary to portray the glacier in its entirety; it can be seen on one Landsat MSS image. Because the Landsat MSS sensor has a pixel size of 79 m (6,241 m<sup>2</sup>), an individual glacier must have an area of more than 20,000 m<sup>2</sup> to be recognized under optimum conditions (for example, minimum snowcover, not in shadow, and so on). One square kilometer in area is a more realistic minimum area for the MSS sensor. On a 1:250,000-scale Landsat image, a glacier 1 km<sup>2</sup> in area would encompass 16 mm<sup>2</sup> (4×4 mm). Glaciers of this size occur in 12 of the 14 glacierized geographic regions of Alaska listed above. One of the two exceptions is the tiny remnant glaciers in the Kigluaik Mountains. Because most of Alaska's glaciers are outlet glaciers from ice fields and ice caps that cover larger areas, these snow-covered source features are generally more easily seen, even at a scale of 1:1,000,000. For selected locations, Landsat Thematic Mapper (TM) data from Landsat 4 and 5 and Landsat Enhanced Thematic Mapper Plus (ETM+) data from Landsat 7 are also available. Landsat TM and ETM+, which have pixel sizes of about 30 m (900 m<sup>2</sup>) and 15 m (225 m<sup>2</sup>), respectively, can show glaciers and glaciological features too small to be identified on MSS images (fig. 6).

Some of Alaska's glaciers have experienced rapid changes of sufficient magnitude that they can be seen on Landsat images acquired only a few months or years apart. For instance, comparing early 1970s Landsat MSS images of the terminus of Bering Glacier with those obtained in the 1980s clearly shows significant retreat of the terminus following a 1967 surge. Between 1986 and 1987, the position of features on the Malaspina Glacier near the terminus changed by several kilometers. These changes were recorded on Landsat (fig. 7). Smaller changes can also be detected. During 1985 and 1986, changes in the terminus position of the advancing Hubbard and Turner Glaciers were monitored and measured by comparison of features on a sequential, geospatially registered, "temporal-change composite image" (composite of 1985 and 1986 Landsat MSS images) (fig. 8).

Landsat is a useful tool for glacier monitoring. Some surge-type glaciers can be identified by their distorted medial moraines, and the active phase of surge-type glaciers has been documented with Landsat. Features such as snowlines, medial and lateral moraines, ice-dammed lakes, sediment and iceberg plumes, and recent and "Little Ice Age" terminal moraines can be delineated on Landsat imagery.

TABLE 1.— *Optimum Landsat 1, 2, and 3 Multispectral scanner (MSS) and Return Beam Vidicon (RBV) images of glaciers of Alaska*  
 [USGS-GSP is the U.S. Geological Survey Glacier Studies Project; see figure 3 for explanation of symbols in the Code column]

Path-Row	Nominal scene center (lat., long)	Landsat identification number	Date	Solar elevation angle (in degrees)	Code	Cloud cover (in percent)	Remarks
58-21	55°45'N. 129°40'W.	21288-18435	2Aug78	45	●	0	Coast Mountains; Soule, Through, Chickamin, and Gracey Creek Glaciers.
58-21	55°45'N. 129°40'W.	22368-19000	17Jul81	50	●	0	Coast Mountains; Soule, Through, Chickamin, and Gracey Creek Glaciers.
59-20	57°08'N. 130°15'W.	5866-17552	01Sep77	31	●	0	Southwestern corner of image shows LeConte Glacier. Many Canadian glaciers are on this image.
59-21	55°45'N. 131°06'W.	5848-17574	14Aug77	36	●	0	Ketchikan and the southern end of southeastern Alaska; from Leconte Glacier to Through and Soule Glaciers about 100 km northwest of Ketchikan.
59-21	55°45'N. 131°06'W.	22027-19085	10Aug80	45	●	0	Coast Mountains; glaciers NNE of Bradfield Canal, Cone Mountain.
60-20	57°08'N. 131°41'W.	1772-19162	03Sep74	37	●	0	Glaciers of southeastern Alaska east and north of Petersburg; major glaciers are South Sawyer, Dawes, Baird, Patterson, and LeConte.
60-20	57°08'N. 131°41'W.	22028-19141	11Aug80	44	●	5	Coast Mountains; Shakes, LeConte, Patterson, Baird, Dawes and South Sawyer Glaciers.
60-21	55°45'N. 132°32'W.	1790-19160	21Sep74	32	●	0	Minor glaciers 50 km east of Wrangell.
60-21	55°45'N. 132°32'W.	1358-19275	16Jul73	51	●	5	Coast Mountains; glaciers east of Bradfield Canal between Burroughs Bay and Stikine River, Cone Mountain and Mount Cloud.
61-19	58°31'N. 132°13'W.	1791-19205	22Sep74	29	●	0	Glaciers 50 km east of Juneau; Wright and Sawyer Glaciers.
61-19	58°31'N. 132°13'W.	2931-18565	10Aug77	41	●	0	Coast Mountains; southeastern Juneau Icefield; Wright, Norris, Taku, Sawyer and South Sawyer Glaciers.
61-20	57°08'N. 133°07'W.	2931-18571	10Aug77	42	●	0	Southeast from Sawyer Glacier to LeConte Glacier.
61-20	57°08'N. 133°07'W.	2967-18550	15Sep77	31	◐	20	Coast Mountains; Sawyer, South Sawyer, Baird, and Dawes Glaciers.
62-19	58°31'N. 133°39'W.	1738-19284	31Jul74	46	◐	20	Glaciers north and east of Juneau.
62-19	58°31'N. 133°39'W.	21670-19195	19Aug79	40	●	5	Coast Mountains; Juneau Icefield, Taku, Mendenhall, Sawyer, and South Sawyer Glaciers.
62-19	58°31'N. 133°39'W.	20572-19180	16Aug76	41	●	0	Juneau Icefield; archived by the Canada Centre for Remote Sensing, Ottawa.
62-20	57°08'N. 134°33'W.	1738-19291	31Jul74	47	◐	10	Alexander Archipelago; small glaciers on Mount Ada and flanks of Patterson Bay.
62-20	57°08'N. 134°33'W.	22390-19221	08Aug81	44	●	0	Alexander Archipelago; small glaciers on Mount Ada and flanks of Patterson Bay.
63-18	59°54'N. 134°07'W.	1775-19324	06Sep74	34	◐	10	Glaciers near Skagway.
63-19	58°31'N. 135°05'W.	1775-19330	06Sep74	35	◐	10	Brady Glacier, eastern Glacier Bay National Park and Preserve, Juneau Icefield.
63-19	58°31'N. 135°05'W.	1667-19365	21May74	48	●	0	Coast Mountains; Juneau Icefield; Mendenhall, Herbert, Eagle, Meade, and Davidson Glaciers.
63-20	57°08'N. 135°59'W.	1775-19333	06Sep74	36	◐	10	Alexander Archipelago.
63-20	57°08'N. 135°59'W.	2897-19102	07Jul77	49	◐	10	Alexander Archipelago; glaciers on Mount Furuhelm.
64-18	59°54'N. 135°33'W.	30183-19375	04Sep78	34	●	0	Glaciers near Skagway.
64-18	59°54'N. 135°33'W.	30147-19373	30Jul78	45	●	5	Coast and St. Elias Mountains; Meade and Davidson Glaciers.
64-18	59°54'N. 135°33'W.	30525-19364-C	12Aug79	42	●	0	Landsat 3 RBV image of northeastern Glacier Bay National Park and Preserve; archived by USGS-GSP.
64-18	59°54'N. 135°33'W.	30525-19364-D	12Aug79	42	●	0	Landsat 3 RBV image of glaciers near Haines; archived by USGS-GSP.

TABLE 1.—*Optimum Landsat 1, 2, and 3 Multispectral scanner (MSS) and Return Beam Vidicon (RBV) images of glaciers of Alaska—Continued*

Path-Row	Nominal scene center (lat., long)	Landsat identification number	Date	Solar elevation angle (in degrees)	Code	Cloud cover (in percent)	Remarks
64-19	58°31'N. 136°31'W.	1416-19480	12Sep73	33	●	0	Glacier Bay National Park and Preserve; major glaciers in this image are Grand Plateau, Fairweather, La Perouse, Brady, Johns Hopkins, Margerie, Ferris, Grand Pacific, Carrol, Muir, Riggs, McBride, and Casement.
64-19	58°31'N. 136°31'W.	30147-19375	30Jul78	46	●	0	Glacier Bay National Park and Preserve.
64-19	58°31'N. 136°31'W.	1057-19542	18Sep72	31	●	0	
64-19	58°31'N. 136°31'W.	30525-19370-A	12Aug79	43	●	0	Glacier Bay National Park and Preserve; Landsat 3 RBV image; archived by USGS-GSP.
64-19	58°31'N. 136°31'W.	30525-19370-B	12Aug79	43	◐	10	Glacier Bay National Park and Preserve; Landsat 3 RBV image; archived by USGS-GSP.
65-18	59°54'N. 136°59'W.	5854-18301	20Aug77	33	●	0	Glaciers 50 km east of Yakutat.
65-19	58°31'N. 137°57'W.	1417-19534	13Sep73	33	●	0	Southeast from Yakutat Glacier to Brady Glacier.
65-19	58°31'N. 137°57'W.	2952-19124	31Aug77	35	●	5	Glacier Bay National Park and Preserve; Brady Glacier to Alosek Glacier.
65-19	58°31'N. 137°57'W.	30922-19315-B	12Sep80	32	●	5	Landsat 3 RBV image of all the major glaciers of Glacier Bay National Park and Preserve; archived by USGS-GSP.
66-18	59°54'N. 138°25'W.	21314-19297	28Aug78	36	●	0	Southeast from Hubbard Glacier to Grand Plateau Glacier.
66-18	59°54'N. 138°25'W.	30167-19491-D	19Aug78	39	●	0	Landsat 3 RBV image of glaciers east of Yakutat; Alaska glaciers: Chamberlain, Yakutat, Novatak, and Alosek Glaciers, Canada glaciers: Battle, Vern Ritchie, Tweedsmuir, Grand Pacific, and Melbern Glaciers. Archived by USGS-GSP.
67-18	59°54'N. 139°51'W.	2955-19292	03Sep77	33	●	0	Icy Bay east to Yakutat Glacier; major glaciers are Guyot, Yahtse, Tyndall, Agassiz, Seward, Malaspina, Marvine, Turner, Hubbard, Art Lewis, Nunatak, and Yakutat.
67-18	59°54'N. 139°51'W.	21675-19482	24Aug79	38	●	0	Tyndall Glacier east to Nunatak Glacier; major glaciers are Tyndall, Agassiz, Malaspina, Seward, Hubbard, Yakutat, and Novatak.
67-18	59°54'N. 139°51'W.	31194-19494-A, B, C, D	11Jun81	50	◐	0-10	Landsat 3 RBV images; archived by USGS-GSP.
68-17	61°16'N. 140°14'W.	2956-19343	04Sep77	32	●	0	Alaska glaciers: Russell, Hawkins, Barnard, Anderson, lower Chitina, Walsh, and Logan. Canada glaciers: Klutlan, Brabazon, Steel, Donjek and Kluane.
68-17	61°16'N. 140°14'W.	21676-19534	25Aug79	36	●	0	St. Elias and Chugach Mountains; Chitina, Logan, Barnard, Hawkins, and Klutlan Glaciers.
68-17	61°16'N. 140°14'W.	30853-19510-C, D	05Jul80	48	●	0	Landsat 3 RBV images of Russell, Klutlan, Hawkins, Barnard, Anderson, Walsh, Chitina, and Logan Glaciers; archived by USGS-GSP.
68-18	59°54'N. 141°17'W.	2956-19350	04Sep77	33	●	0	A major part of Bering Glacier, the Bagley Ice Valley, Tana, Jefferies, Yahtse, Guyat, Tyndall, Columbus, Seward, Agassiz, and Malaspina Glaciers.
68-18	59°54'N. 141°17'W.	1708-20035	01Jul74	50	●	0	St. Elias and Chugach Mountains; Malaspina, eastern Bering, Tana, and Logan Glaciers.
69-16	62°38'N. 140°33'W.	21677-19590	26Aug79	35	●	0	Nutzotin Mountains (southeastern part of Alaska Range); Carl and Nelson Creeks Glaciers, and glaciers on Mount Allen and northeastern part of Wrangell Mountains.
69-17	61°16'N. 141°40'W.	21677-19593	26Aug79	36	◐	10	Glaciers to the north, east, and south of McCarthy; major glaciers are Kennicott, Root, Regal, Rohn, Nizina, Chisana, Russell, Klutlan, Anderson, Walsh, Logan, Jefferies, and Barnard.
69-17	61°16'N. 141°40'W.	1709-20090	02Jul74	49	◐	10	Wrangell, St. Elias, and Nutzotin Mountains; Carl and Nelson Creeks Glaciers, Nabesna, Chisana, Kennicott, Root, Barnard, Hawkins, Chitina, and Logan Glaciers.

TABLE 1.—*Optimum Landsat 1, 2, and 3 Multispectral scanner (MSS) and Return Beam Vidicon (RBV) images of glaciers of Alaska—Continued*

Path-Row	Nominal scene center (lat., long)	Landsat identification number	Date	Solar elevation angle (in degrees)	Code	Cloud cover (in percent)	Remarks
69-17	61°16'N. 141°40'W.	30908-19542-B	29Aug80	35		15	Landsat 3 RBV image of Klutlan Glacier; archived by USGS-GSP.
69-17	61°16'N. 141°40'W.	30908-19542-C	29Aug80	35		10	Landsat 3 RBV images of Breman and Tana Glaciers; archived by USGS-GSP.
69-17	61°16'N. 141°40'W.	30908-19542-D	29Aug80	35		0	Landsat 3 RBV image of Hawkins, Barnard, Anderson, Walsh, Logan, Chitina Glaciers; archived by USGS-GSP.
69-18	59°54'N. 142°43'W.	2975-19394	23Sep77	26		0	Bagley Ice Valley, and Bering, Guyot, Yahrtse, Turner, Jefferies, Tana, Bremmer, Fan, Martin River and Steller Glaciers.
70-16	62°38'N. 141°59'W.	2958-19453	06Sep77	30		0	Glaciers 100 km southwest and south of Northway.
70-16	62°38'N. 141°59'W.	21624-20035	04Jul79	47		10	Wrangell Mountains; Nabesna, Chisana, and Copper Glaciers.
70-17	61°16'N. 143°06'W.	1422-20212	18Sep73	29		0	Glaciers of Mount Wrangell; Cooper, Nebesna, Chisana, Russell, Rohn, Regal, Root, Kennicott, Kaskulana, Long, Tana, Bremmer, Fan, and Wernicke Glaciers.
70-17	61°16'N. 143°06'W.	1692-20152	15Jun74	49		10	St. Elias, Wrangell, and Chugach Mountains; Kennicott, Root, Copper, Nabesna, and Chisana Glaciers.
70-17	61°16'N. 143°06'W.	30309-20001-A	30Aug80	34		0	Landsat 3 RBV image of Mount Wrangell; archived by USGS-GSP.
70-17	61°16'N. 143°06'W.	30309-20001-B	30Aug80	34		0	Landsat 3 RBV image of Kennicott, Root, Rega, Rohn, Russell, Barnard, and Hawkins Glaciers; archived by USGS-GSP.
70-17	61°16'N. 143°06'W.	30309-20001-C	30Aug80	34		20	Landsat 3 RBV image of Wernicke, Miles, Allen, and Schwan Glaciers; archived by USGS-GSP.
70-17	61°16'N. 143°06'W.	30309-20001-D	30Aug80	34		0	Landsat 3 RBV image of Bremmer and Tana Glaciers and Bagley Ice Valley; archived by USGS-GSP.
70-18	59°54'N. 144°09'W.	2976-19452	24Sep77	25		5	Sherman, Sheridan, Scott, Woodworth, Schwan, Allen, Childs, Miles, Wernicke, Fan, Bering, Steller, and Martin River Glaciers.
71-15	63°59'N. 142°11'W.	22399-20114	17Aug81	37		50	Alaska Range, Mount Kimball area.
71-16	62°38'N. 143°25'W.	2941-19521	20Aug77	36		0	Glaciers of the eastern Alaska Range and northern Wrangell Mountains.
71-16	62°38'N. 143°25'W.	30532-20155	19Aug79	38		35	Metasta and northeastern Wrangell Mountains; Chisana, Nabesna, and Copper Glaciers.
71-16	62°38'N. 143°25'W.	31270-20135-A	26Aug81	35		0	Landsat 3 RBV image of glaciers of the eastern Alaska Range; archived by USGS-GSP.
71-16	62°38'N. 143°25'W.	31270-20135-D	26Aug81	35		0	Landsat 3 RBV image of glaciers on the northern side of Mount Wrangell, Nabesna Glacier; archived by USGS-GSP.
71-17	61°16'N. 144°32'W.	2941-19524	20Aug77	37		0	Mount Wrangell and the Copper and Chitina Rivers. Major glaciers are Long, Kaskulana, Kennecott, Root, Fan, Wernicke, Miles, Allen, Schwan, Woodworth, Valdez, and Tonsina.
71-17	61°16'N. 144°32'W.	31270-20141-B	26Aug81	36		0	Landsat 3 RBV image of glaciers on the southern side of Mount Wrangell; archived by USGS-GSP.
71-17	61°16'N. 144°32'W.	31270-20141-C	26Aug81	36		0	Landsat 3 RBV image of glaciers to the north, east, and south of Valdez; archived by USGS-GSP.
71-18	59°54'N. 145°35'W.	2941-19530	20Aug77	37		0	Glaciers east and west of the Copper River delta.
71-18	59°54'N. 145°35'W.	1387-20281	14Aug73	42		0	Chugach Mountains; Scott and Sheridan Glaciers, Steller Lobe; Copper River and Bering Glacier sediment plumes.
72-15	63°59'N. 143°37'W.	2942-19573	21Aug77	34		15	Glaciers on the northern side of the eastern Alaska Range.
72-15	63°59'N. 143°37'W.	2582-20131	26Aug76	33		5	Glaciers on the northern side of the eastern Alaska Range.



TABLE 1.—*Optimum Landsat 1, 2, and 3 Multispectral scanner (MSS) and Return Beam Vidicon (RBV) images of glaciers of Alaska—Continued*






















Path-Row	Nominal scene center (lat., long)	Landsat identification number	Date	Solar elevation angle (in degrees)	Code	Cloud cover (in percent)	Remarks
72-15	63°59'N. 143°37'W.	2202-22020	5Aug80	40		10	Northeastern Alaska Range, Mount Gakona area.
72-16	62°38'N. 144°51'W.	2942-19575	21Aug77	35		0	Southeastern Alaska Range and western portion of Mount Wrangell; Canwell, Castner, Gerstle, Johnson, Robertson, and Gakona Glaciers.
72-16	62°38'N. 144°51'W.	2510-20154	15Jun76	48		5	Southeastern Alaska Range, western Wrangell Mountains; Long, Kluvesna, Sanford, and Copper Glaciers.
72-16	62°38'N. 144°51'W.	30551-20212-A	07Sep79	31		0	Landsat 3 RBV image of eastern Alaska Range; archived by USGS-GSP.
72-16	62°38'N. 144°51'W.	30173-20225-D	25Aug78	35		0	Landsat 3 RBV image of Mounts Drum, Stanford, and Wrangell; archived by USGS-GSP.
72-17	61°16'N. 145°59'W.	30109-20233	30Sep78	24		10	Chugach Mountains; glaciers from College Fiord to the Copper River; Columbia, Yale, Harvard, Nelchina, Tazlina, Valdez, Tonsina, Wortman, Woodworth, Schwan, Allen, Childs, Sheridan, and Scott Glaciers.
72-17	61°16'N. 145°59'W.	30551-20215	07Aug79	32		5	Chugach Mountains; glaciers from College Fiord to the Copper River; Columbia, Yale, Harvard, Nelchina, Tazlina, Valdez, Tonsina, Wortman, Woodworth, Schwan, Allen, Childs, Sheridan, and Scott Glaciers.
72-17	61°16'N. 145°59'W.	30551-20215-A	07Sep79	32		0	Landsat 3 RBV image of Nelchina and Tuzlina Glaciers; archived by USGS-GSP.
72-17	61°16'N. 145°59'W.	30551-20215-D	07Sep79	32		10	Landsat 3 RBV image of Valdez, Tonsina, Wortmanns, Woodworth, Schwan, Sheridan, and Scott Glaciers; archived by USGS-GSP.
72-18	59°54'N. 147°02'W.	1406-20334	02Sep73	35		5	Eastern Sargent Icefield.
73-15	63°59'N. 145°03'W.	2925-20041	04Aug77	39		10	Glaciers of the central and eastern Alaska Range; Hayes, Trident, Black Rapids, Susitna, Canwell, Johnson, and Gakona Glaciers.
73-15	63°59'N. 145°03'W.	2583-20190	27Aug76	33		0	Northeastern Alaska Range; Hayes, Trident, and Gerstle Glaciers.
73-15	63°59'N. 145°03'W.	31200-20230-C	17Jun81	47		0	Landsat 3 RBV image of central Alaska Range; Susitna, Hayes, Trident and Black Rapids Glaciers; archived by USGS-GSP.
73-15	63°59'N. 145°03'W.	31200-20230-D	17Jun81	47		0	Landsat 3 RBV image of eastern Alaska Range; Canwell, Fels, Castner, Gerstle, Johnson, Robertson, Chistochina, and Gakona Glaciers; archived by USGS-GSP.
73-16	62°38'N. 146°17'W.	2169-20275	10Jul75	47		10	Central and eastern Alaska Range; West Fork, Hayes, Susitna, Black Rapids, and Gakona Glaciers.
73-16	62°38'N. 146°17'W.	2943-20033	22Aug77	35		50	Talkeetna Mountains and Alaska Range; Susitna, West Fork, Maclaren, and Eureka Glaciers.
73-17	61°16'N. 147°25'W.	31074-20290	26Aug78	36		5	Chugach Mountains and Prince William Sound; Spencer, Twentymile, Harriman, Surprise, Lake George, Colony, Knik, Marcus Baker, Matanuska, Nelchina, Tazlina, Valdez, Shoup, Columbia, Meares, Yale, and Harvard Glaciers.
73-17	61°16'N. 147°25'W.	31272-20254-B	28Aug81	36		0	Landsat 3 RBV image of Nelchina, Tazlina, Stephens, Klutina, Tonsima, Valdez, Shoup, and Columbia Glaciers; archived by USGS-GSP.
73-17	61°16'N. 147°25'W.	30912-20171-C	02Sep80	33		0	Landsat 3 RBV image of Twentymile, Lake George, Colony, Knik, Marcus Baker, Harvard, Yak, Barry, Surprise, and Harriman Glaciers; archived by USGS-GSP.
73-17	61°16'N. 147°25'W.	30552-20273-D	08Sep79	32		5	Landsat 3 RBV image of Meares, Columbia, Shoup, and Valdez Glaciers; archived by USGS-GSP.
73-18	59°54'N. 148°28'W.	1389-20394	16Aug73	41		10	Harding and Sargent Icefields, Skelak, Bear, Ellsworth, Excelsior, Chenega, Princeton, and Spencer Glaciers.

TABLE 1.—*Optimum Landsat 1, 2, and 3 Multispectral scanner (MSS) and Return Beam Vidicon (RBV) images of glaciers of Alaska—Continued*

Path-Row	Nominal scene center (lat., long)	Landsat identification number	Date	Solar elevation angle (in degrees)	Code	Cloud cover (in percent)	Remarks
73-18	59°54'N. 148°28'W.	2907-20062	17Jul77	46	●	0	Chugach and Kenai Mountains; Exit Glacier to McCarty, Holgate, Aialik, Northwest, and Bear Glaciers.
73-18	59°54'N. 148°28'W.	30912-20174-A	02Sep80	34	●	0	Landsat 3 RBV image of glaciers north and south of Kings Bay, Sargent Icefield; archived by USGS-GSP.
73-18	59°54'N. 148°28'W.	30912-20174-C	02Sep80	34	●	0	Landsat 3 RBV image of eastern Harding Icefield; archived by USGS-GSP.
74-15	63°59'N. 146°29'W.	2944-20085	23Aug77	34	●	0	Central Alaska Range; Yanert, Gillam, Hayes, Trident, Black Rapids, Maclaren, Susitna, and West Fork Glaciers.
74-15	63°59'N. 146°29'W.	21286-20130	31Jul78	41	●	5	Alaska Range; Black Rapids, Susitna, West Fork, Gillam and Yanert Glaciers.
74-15	63°59'N. 146°29'W.	31273-20304-D	29Aug81	33	●	0	Landsat 3 RBV image of central Alaska Range; archived by USGS-GSP.
74-16	62°38'N. 143°43'W.	30175-20342	27Aug78	35	◐	10	Glaciers of the Talkeetna Mountains.
74-17	61°16'N. 148°51'W.	30175-20345	27Aug78	36	●	0	Glaciers of the northern Kenai Peninsula and western Chugach Mountains; Spencer, Lake George, Colony, Knik, Marcus Baker, Matanuska, Nelchina, Tazlina, Yale, and Harvard Glaciers.
74-17	61°16'N. 148°51'W.	30553-20331	09Sep79	32	●	0	Chugach Mountains; Knik Arm, Turnagain Arm and College Fiord; Knik, Lake George, Portage, Spencer, and Meares Glaciers.
74-17	61°16'N. 148°51'W.	30553-20331-B	09Sep79	31	●	10	Landsat 3 RBV image of glaciers of the northwestern Chugach Mountains; archived by USGS-GSP.
74-17	61°16'N. 148°51'W.	30553-20331-D	09Sep79	31	●	0	Landsat 3 RBV image of glaciers north and south of Whittier; archived by USGS-GSP.
74-18	59°54'N. 149°54'W.	1390-20452	17Aug73	41	●	0	Glaciers of the southern Kenai Peninsula and the Harding and Sargent Icefields; Yalik, Grewingk, Portlack, Dixon, Dinglestadt, Chernof, Tustumena, Skilak, Bear, Ellsworth, and Excelsior Glaciers.
74-18	59°54'N. 149°54'W.	30553-20334-B	09Sep79	33	●	0	Landsat 3 RBV image of glaciers of the Sargent Icefield; archived by USGS-GSP.
74-20	57°08'N. 151°46'W.	2908-20125	18Jul77	47	●	0	Northeastern end of Kodiak Island with Mount Glotoff and Koniag Peak and Koniag Glacier.
75-11	69°17'N. 141°38'W.	2927-20135	06Aug77	35	●	0	Eastern Brooks Range, Romanzof Mountains.
75-12	67°59'N. 143°28'W.	30158-20387	10Aug78		◐	15	Brooks Range.
75-15	63°59'N. 147°55'W.	2945-20143	24Aug77	34	●	0	Alaska Range; Susitna, West Fork, Yanert, and Gillam Glaciers.
75-16	62°38'N. 149°09'W.	5864-19254	30Aug77	29	●	0	Eastern Denali National Park and Preserve, Talkeetna Mountains, Kahiltna, Tokositna, Ruth, Eldridge, and Muldrow Glaciers.
75-16	62°38'N. 149°09'W.	2531-20322	06Jul76	47	●	5	Alaska Range and Talkeetna Mountains; Ruth, Tokositna, Kahiltna, Muldrow and West Fork Glaciers.
75-16	62°38'N. 149°09'W.	30554-20383-A	10Sep79	30	◐	20	Landsat 3 RBV image of eastern Denali National Park and Preserve; archived by USGS-GSP.
75-17	61°16'N. 150°17'W.	1049-20505	10Sep72	31	◐	20	Parts of glaciers east and west of Anchorage.
75-17	61°16'N. 150°17'W.	22043-20390	26Aug80	36	●	5	Chugach Mountains; Knik and Turnagain Arms; Knik, Lake George, Capps, Triumvirate and Blockade Glaciers.
75-18	59°54'N. 151°20'W.	21323-20215	06Sep78	33	◐	10	Glaciers of southern Kenai Peninsula; Yulik, Grewingk, Portlock, Dixon, Dinglestadt, Chernof, Fustumena, Skilak, and Bear Glaciers.
75-18	59°54'N. 151°20'W.	22043-20393	26Aug80	37	●	0	Kenai Mountains and Aleutian Range; Harding Icefield, Tustumena, Dinglestadt, McCarty, Double, Lateral and Red Glaciers.

TABLE 1.—*Optimum Landsat 1, 2, and 3 Multispectral scanner (MSS) and Return Beam Vidicon (RBV) images of glaciers of Alaska—Continued*



























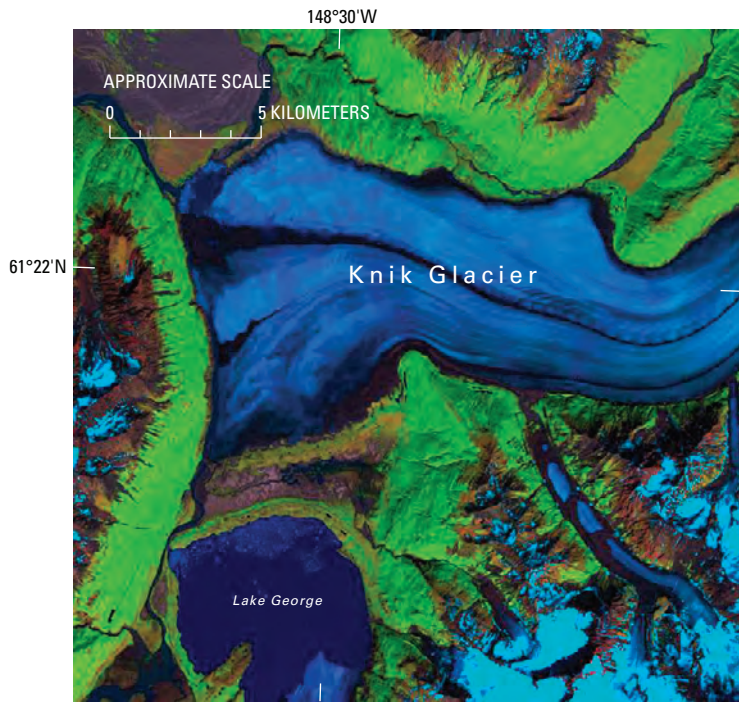
Path-Row	Nominal scene center (lat., long)	Landsat identification number	Date	Solar elevation angle (in degrees)	Code	Cloud cover (in percent)	Remarks
75-19	58°31'N. 152°18'W.	2891-20190	01Jul77	49		10	Kodiak Island and Aleutian Range; Spotted and Fourpeaked Glaciers.
75-20	57°08'N. 155°12'W.	2909-20183	19Jul77	47		10	Kodiak Island; Koniag Glacier.
76-11	69°17'N. 143°04'W.	30177-20435	29Aug78	29		0	Glaciers of the Romanzof Mountains of the Brooks Range; McCall Glacier.
76-11	69°17'N. 143°04'W.	22386-20384	04Aug81	36		0	Brooks Range, Romanzof Mountains.
76-12	67°59'N. 144°54'W.	22386-20391	04Aug81	37		5	Brooks Range, Phillip Smith Mountains.
76-15	63°59'N. 149°21'W.	5865-19305	31Aug77	28		80	Central part of Alaska Range.
76-15	63°59'N. 149°21'W.	30537-20441	24Aug79	35		0	Alaska Range; small glaciers on Mount Pendleton that drain to form the Toklat River.
76-16	62E38'N.	30537-	24Aug79			0	Alaska Range.
76-16	62°38'N. 150°35'W.	30555-20442	11Sep79	30		0	Alaska Range; Eldridge, Ruth, Tokositna, Kahiltna, Yentna, and Dall Glaciers.
76-16	62°38'N. 150°35'W.	30555-20441-A	11Sep79	30		0	Landsat 3 RBV image of Denali National Park and Preserve; Heron, Foraker, Straightaway, Peters, and Muldrow Glaciers; archived by USGS-GSP.
76-16	62°38'N. 150°35'W.	30555-20441-B	11Sep79	30		0	Landsat 3 RBV image of Denali National Park and Preserve; Eldridge Glacier; archived by USGS-GSP.
76-16	62°38'N. 150°35'W.	30555-20441-C	11Sep79	30		0	Landst 3 RBV image of Denali National Park and Preserve; Chedotlothna, Surprise, Dall, Yentna, Lacuna, Kahiltna, and Tokositna Glaciers; archived by USGS-GSP.
76-17	61°16'N. 151°43'W.	21288-20253	02Aug78	42		0	Tordrilla and Chigmit Mountains; Double, Blockade, Capps, Triumvirate, Trimble, Hayes, North Twin, and Barrier Glaciers.
76-17	61°16'N. 151°43'W.	2586-20365	30Aug76	34		20	Alaska Range; Hayes, Trimble, Triumvirate, Capps, Shamrock, Blockade, and Tanaina Glaciers.
76-17	61°16'N. 151°43'W.	30555-20444-A	11Sep79	31		0	Landsat 3 RBV image of Triumvirate, Trimble, and Hayes Glaciers; archived by USGS-GSP.
76-17	61°16'N. 151°43'W.	30915-20342-C	05Sep80	32		10	Landsat 3 RBV image of Double, Blockade, and Shamrock Glaciers; archived by USGS-GSP.
76-18	59°54'N. 152°46'W.	21288-20255	02Aug78	43		0	Illiamna and Redoubt Volcanoes; Red, Lateral, and Tuxedni Glaciers.
76-18	59°54'N. 152°46'W.	1734-20485	27Jul74	46		10	Alaska and Aleutian Ranges; Double and Tuxedni Glaciers.
76-18	59°54'N. 152°46'W.	30915-20345-A	05Sep80	33		10	Landsat 3 RBV image of Illiamna and Redoubt Volcanoes; archived by USGS-GSP.
76-19	58°31'N. 153°44'W.	1428-20563	24Sep73	29		0	Katmai National Park and Preserve; Serpent Tongue, Hook, Hallo, and Spotted Glaciers.
76-19	58°31'N. 153°44'W.	1734-20491	27Jul74	47		5	Katmai National Park and Preserve; Fourpeaked, Spotted, Hallo, Hook, and Serpent Tongue Glaciers.
76-20	57°08'N. 154°38'W.	1734-20494	27Jul74	48		0	Katmai National Park and Preserve.
77-11	69°17'N. 144°30'W.	5848-19364	14Aug77			0	Brooks Range, Romanzof Mountains.
77-11	69°17'N. 144°30'W.	22387-20443	05Aug81	36		0	Brooks Range, Romanzof Mountains.
77-11	69°17'N. 144°30'W.	30502-20481-B	20Jul79	40		10	Landsat 3 RBV image of Romanzof Mountains, Brooks Range, McCall Glacier; archived by USGS-GSP.
77-12	67°59'N. 146°20'W.	22387-2044X	05Aug81	37		0	Brooks Range, Phillip Smith Mountains.
77-12	67°59'N. 146°20'W.	2605-20400	18Sep76	22		5	Brooks Range, Phillip Smith Mountains.

TABLE 1.—*Optimum Landsat 1, 2, and 3 Multispectral scanner (MSS) and Return Beam Vidicon (RBV) images of glaciers of Alaska—Continued*

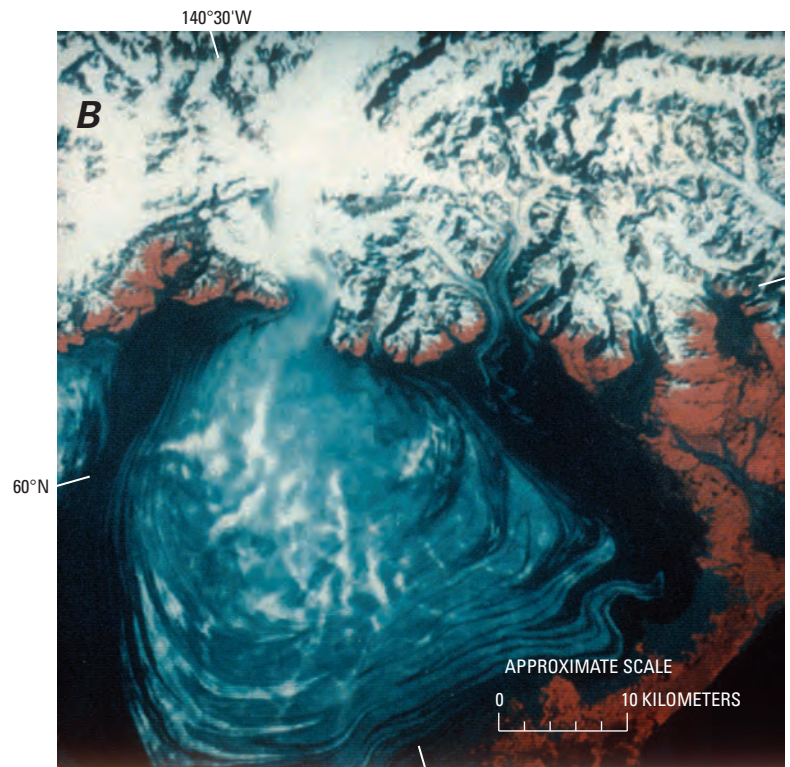
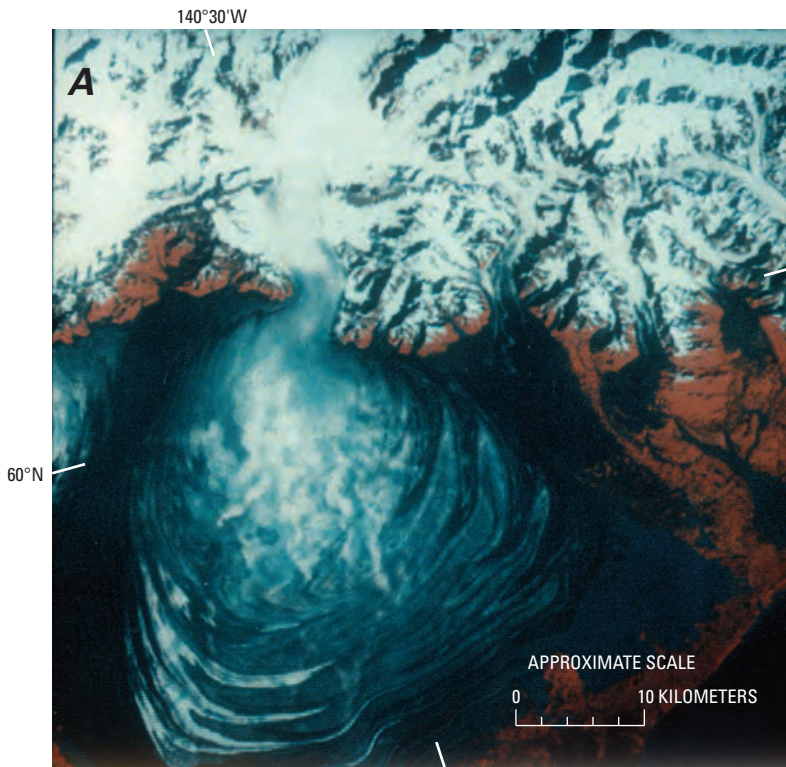
Path-Row	Nominal scene center (lat., long)	Landsat identification number	Date	Solar elevation angle (in degrees)	Code	Cloud cover (in percent)	Remarks
77-15	63°59'N. 150°47'W.	21289-20303	03Aug78	40		10	Denali National Park and Preserve; Muldrow Glacier.
77-15	63°59'N. 150°47'W.	22405-20460	23Aug81	35		60	Denali National Park and Preserve; Muldrow Glacier.
77-16	62°38'N. 152°01'W.	5865-19312	31Aug77	29		10	Denali National Park and Preserve; Dall, Yentna, Lacuna, Kahiltna, Tokositna, Ruth, Muldrow, and Peters Glaciers.
77-16	62°38'N. 152°01'W.	21487-20392	17Feb79	12		0	Denali National Park and Preserve; Ruth, Tokositna, and Kahiltna Glaciers.
77-16	62°38'N. 152°01'W.	30556-20500-B	12Sep79	29		5	Denali National Park and Preserve; Ruth, Eldridge, and Muldrow Glaciers.
77-17	61°16'N. 153°09'W.	1033-21022	25Aug75	37		10	Double, Blockade, Capps, Triumvirate, Trimble, and Hayes Glaciers.
77-17	61°16'N. 153°09'W.	21613-20441	23Jun79	49		5	Alaska and Aleutian Ranges; Hayes, Trimble, Triumvirate, Capps, Shamrock, Blockade, and Tanaina Glaciers.
77-17	61°16'N. 153°09'W.	30880-20413-B	01Aug80	43		0	Landsat 3 RBV image of Capps, Triumvirate, Trimble, and Hayes Glaciers; archived by USGS-GSP.
77-17	61°16'N. 153°09'W.	30880-20413-D	01Aug80	43		10	Landsat 3 RBV image of Double, Blockade, and Shamrock Glaciers; archived by USGS-GSP.
77-18	59°54'N. 154°12'W.	21289-20314	03Aug78	43		20	Laterol and Tuxedni Glaciers.
77-18	59°54'N. 154°12'W.	21613-20443	23Jun79	50		5	Aleutian Range; Tuxedni Glacier.
77-19	58°31'N. 155°10'W.	2983-20253	01Oct77	24		10	Katmai National Park and Preserve; Hallo, Hook, and Serpent Tongue Glaciers.
77-19	58°31'N. 155°10'W.	2533-20450	8Jul76	49		10	Katmai National Park and Preserve; Hallo, Hook, and Serpent Tongue Glaciers.
77-20	57°08'N. 156°04'W.	30448-20525	27May79	50		0	Aleutian Range; Alaska Peninsula.
78-11	69°17'N. 145°56'W.	5848-19364	14Aug77	31		0	Brooks Range, Romanzof Mountains; McCall Glacier.
78-11	69°17'N. 145°56'W.	2570-20462	14Aug76	33		10	Brooks Range, Romanzof Mountains; McCall Glacier.
78-11	69°17'N. 145°56'W.	30485-20540-B	03Jul79	43		10	Landsat 3 RBV image of Romanzof Mountains; McCall Glacier; archived by USGS-GSP.
78-12	67°59'N. 147°46'W.	5848-19371	14Aug77	31		0	Brooks Range, Phillip Smith Mountains.
78-12	67°59'N. 147°46'W.	22028-20541	11Aug80	36		5	Brooks Range, Phillip Smith Mountains.
78-15	63°59'N. 152°13'W.	1882-20574	03Sep74	32		5	Denali National Park and Preserve; Heron, Foraker, and Straightaway Glaciers.
78-16	62°38'N. 153°27'W.	1772-20580	03Sep74	33		0	Western Denali National Park and Preserve; Kichatna Mountains.
78-16	62°38'N. 153°27'W.	30557-20554-B	13Sep79	29		10	Landsat 3 RBV image of western Denali National Park and Preserve; archived by USGS-GSP.
78-17	61°16'N. 154°35'W.	1772-20583	03Sep74	34		0	Glacier northeast of Lake Clark.
78-19	58°31'N. 156°36'W.	1772-20592	03Sep74	36		30	Katmai National Park and Preserve; McNeal River glaciers.
78-19	58°31'N. 156°36'W.	21488-20462	18Feb79	16		0	Katmai National Park and Preserve; McNeal River glaciers.
78-20	57°08'N. 157°30'W.	2534-20511	09Jul76	50		0	Alaska Peninsula, Aniakchak Crater, Mount Chiginagak.
78-21	55°45'N. 158°21'W.	2192-20581	02Aug75	47		10	Alaska Peninsula, Mount Veniaminof.
79-11	69°17'N. 147°23'W.	1773-21014	4Sep74	27		0	Brooks Range.
79-12	67°59'N. 149°12'W.	1773-21020	4Sep74	28		0	Brooks Range.

TABLE 1.—*Optimum Landsat 1, 2, and 3 Multispectral scanner (MSS) and Return Beam Vidicon (RBV) images of glaciers of Alaska—Continued*

Path-Row	Nominal scene center (lat., long)	Landsat identification number	Date	Solar elevation angle (in degrees)	Code	Cloud cover (in percent)	Remarks
79-20	57°08'N. 158°56'W.	1449-21133	15Oct73	22		20	Alaska Peninsula, Aniakchak Crater.
79-21	55°45'N. 159°47'W.	2427-21091	24Mar76	31		10	Alaska Peninsula, Mount Veniaminof, winter snow obscures the glaciers.
79-21	55°45'N. 159°47'W.	22191-21025	21Jan81	11		5	Alaska Peninsula, Mount Veniaminof.
80-11	69°17'N. 148°49'W.	1774-21072	5Sep74	26		0	Brooks Range.
80-12	67°59'N. 150°38'W.	1774-21074	5Sep74	28		0	Brooks Range.
80-18	59°54'N. 158°30'W.	2950-20441	29Aug77	35		0	Wood River Mountains.
80-18	59°54'N. 158°30'W.	30145-21091	28Jul78	45		5	Wood River Mountains.
80-21	55°45'N. 161°13'W.	21688-21044	06Sep79	37		0	Alaska Peninsula, Povlof Volcano.
81-12	67°59'N. 151°37'W.	1775-21133	6Sep74	27		0	Brooks Range.
81-17	61°16'N. 158°26'W.	21347-20570	30Sep78	23		0	Wood River Mountains.
81-17	61°16'N. 158°26'W.	30146-21143	29Jul78	—	—	—	Wood River Mountains.
81-18	59°54'N. 159°29'W.	2591-21055	04Sep76	33		10	Wood River Mountains.
81-18	59°54'N. 159°29'W.	2285-21130	03Nov75	13		0	Wood River Mountains.
81-21	55°45'N. 162°13'W.	2825-20574	26Apr77	42		0	Alaska Peninsula, Povlof Volcano.
81-22	54°22'N. 163°01'W.	2591-21073	04Sep76	37		50	Unimak Island, Shishaldin Volcano.
81-22	54°22'N. 163°01'W.	2825-20581	26Apr77	43		5	Unimak Island, Shishaldin Volcano.
82-22	67°59'N. 153°29'W.	22410-21133	20Aug81	30		0	Brooks Range, Endicott Mountains.
82-22	54°22'N. 164°53'W.	1056-21331	17Sep72	35		10	Unimak Island, Pogromni and Shishaldin Volcanoes.
83-12	67°59'N. 154°55'W.	2557-21155	01Aug76	38		0	Brooks Range, Endicott Mountains.
83-12	67°59'N. 154°55'W.	22015-21224	29Jul80	39		75	Brooks Range, Endicott Mountains.
83-22	54°22'N. 166°19'W.	2413-21240	10Mar76	27		0	Northern part of Unalaska Island; Makushin Volcano, winter snow obscures glaciers.
83-23	52°58'N. 167°04'W.	2413-21243	10Mar76	28		0	Southern part of Unalaska Island and Umnak Island, Umnak Volcano, winter snow obscures glaciers.
84-12	67°59'N. 156°22'W.	22412-21245	30Aug81	29		0	Brooks Range, Phillip Smith Mountains.
84-23	52°58'N. 168°30'W.	2954-21090	02Sep77	38		30	Southern part of Unalaska Island and Umnak Island; glaciers on Okmok Volcano and Mounts Recheshnoi and Vsevidof.
85-23	52°58'N. 169°56'W.	2307-21374	25Nov75	13		0	Southwestern part of Umnak Island with glaciers on Mounts Recheshnoi and Vsevidof.
87-24	51°34'N. 173°21'W.	2975-21252	23Sep77	32		5	Atka Island; glacier on Kovin Volcano.
88-14	65°20'N. 165°13'W.	1710-21565	03Jul74	46		0	Seward Peninsula.
88-14	65°20'N. 165°13'W.	2886-21315	26Jun77	45		0	Seward Peninsula.
89-12	67°59'N. 163°32'W.	22417-21533	04Sep81	28		0	Brooks Range.
89-12	67°59'N. 163°32'W.	1387-22090	14Aug73	—	—	—	Brooks Range.



**Figure 6.**—Landsat 7 Enhanced Thematic Mapper Plus (ETM+) false-color composite image of the terminus region of Knik Glacier and adjacent Lake George, east of Anchorage in the Chugach Mountains. With this band combination, snow appears light blue, glaciers appear darker blue, and healthy vegetation is bright green. The Landsat image (L7068017009921250; bands 5, 4, 2) is from the USGS, EROS Data Center, Sioux Falls, S. Dak.

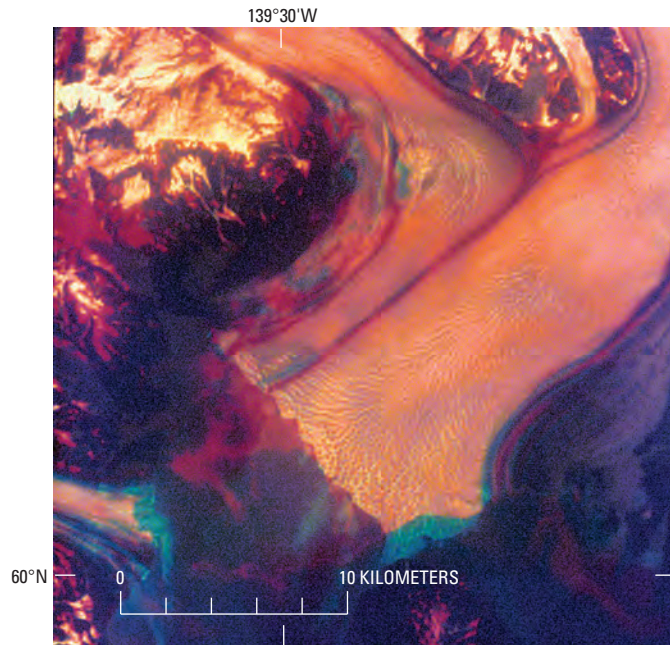


**Figure 7.**—Pair of Landsat 5 MSS subscene false-color composite images showing changes in the piedmont lobe of Malaspina Glacier resulting from a 1986 surge of the eastern side of the glacier. The images were acquired on 11 September 1986 (A) and 29 August 1987 (B). Between the dates of the two images, folded loop moraines on the eastern side of the glacier were displaced as much as 5 km. The Landsat images (50924–19513; 11 September 1986; Path 62, Row 18; and 51276–19572; 29 August 1987; Path 62, Row 18) are from the USGS, EROS Data Center, Sioux Falls, S. Dak.

## Glacier Names and Place-Names in Alaska

The names of Alaska's glaciers and other place-names have diverse origins (appendix C), including at least four European languages and numerous dialects of the languages of the indigenous peoples of Alaska. Beginning in the 18th century, when Russian, English, Spanish, and French explorers and merchants began interacting with the indigenous peoples, they recorded many of the names of geographic features, frequently transliterating or translating them into European languages. Additionally, the Europeans provided new place-names for many geographic features, many of which are still in use.

**Figure 8.**—A Landsat MSS “temporal-change composite image” showing differences occurring between 1985 and 1986 in the termini of Hubbard (center) and Turner (lower left) Glaciers and the Valerie Glacier, a tributary to the Hubbard Glacier. All are located in the upper end of Disenchantment Bay. This image was produced by digital addition of two geographically registered Landsat MSS images and determination of differences in brightness values for individual pixels. Differences, including the 1986 advance of the terminus to block Russell Fiord (lower right), are shown in green. Unpublished 1986 analysis by Bruce F. Molnia and Matthew Schwaller.



U.S. involvement in the naming of Alaska’s geographic features predates its purchase of Alaska in 1867 from Russia. U.S. whalers hunting in the Arctic Ocean applied names to many northern geographic features. Additionally, official pre-purchase expeditions, such as the 1854–55 U.S. Navy (USN) North Pacific Exploring Expedition, provided new geographic-feature names. In order to track and authenticate Alaskan place-names, a formal system of legitimizing named features evolved in the 19th century, leading to Marcus Baker’s *Geographic Dictionary of Alaska* (Baker, 1902), which contained 2,000 identified names. A second edition four years later contained about 9,300 names and 3,300 cross references and was released as USGS Bulletin 299 (Baker, 1906).

In 1967, the most recent version of a USGS Alaskan geographic dictionary—*Dictionary of Alaska Place Names*—was released as USGS Professional Paper 567 (Orth, 1967). Containing more than 20,000 names, it was reprinted with minor revisions in 1971 (Orth, 1971). In 1991, The Denali Press (Schorr, 1991) released a compendium of about 1,300 additional place names—*Alaska Place Names*—based on BGN decisions made between January 1966 and December 1990. More than 25 new glacier names were included.

Today, most BGN databases have been computerized. The *Alaska Dictionary Database* and the USGS *Geographic Names Information System* (GNIS) serve as the central repositories for approved Alaskan place-names. “The Geographic Names Information System (GNIS) is the Federal standard for geographic nomenclature. The U.S. Geological Survey developed the GNIS for the U.S. Board on Geographic Names as the official repository of domestic geographic names data.” The USGS GNIS is available on the Internet at the following URL: <http://geonames.usgs.gov/>. The *Alaska Dictionary Database* is currently available to the general public only through Orth (1967). Even though more than 600 glacier names have been officially approved as of March 1998 (appendix C), the great majority of Alaska’s glaciers, perhaps as many as 99 percent of extant glaciers, are still unnamed.

Many names that were given to glaciers by early expeditions and USGS field parties were never formally adopted. Neither of the glacier names that Schwatka uses for the two glaciers depicted in his 1885 book, *Baird Glacier* and *Saussure Glacier* (Schwatka, 1885, p. 73, 77), for example, were adopted as official names. Both are shown without names on the latest USGS map of the area. Similarly, the names of some glaciers have changed several

times. For instance, the LeConte Glacier, named in 1887 by the U.S. Navy for University of California geologist Joseph LeConte, was previously called *Hutli Glacier* and *Thunder Glacier*. Similarly, Taku Glacier originally was called *Schulze Glacier* and *Foster Glacier*.

## **Early Observations of Alaska and its Glaciers**

### **Traditional Knowledge**

Alaska's indigenous peoples were cognizant of the presence of glaciers. In many areas, local peoples, such as the Tlingit, lived near glaciers and developed a history and culture that took into account the influence that glaciers played in their daily activities. For example, the famous anthropologist de Laguna (1972) gives several accounts of native villages being destroyed by the advance of glaciers. Similarly, after John Muir visited Glacier Bay in 1879, he wrote that the Indians who guided him during his exploration would not go near the face of the tidewater glaciers. They told him that ice rising out of the water had capsized canoes and drowned their occupants. This account is the earliest reported description of submarine calving from the termini of glaciers by a scientist (Muir, 1895) (see also Vancouver, 1798).

### **Limited Early Descriptions of Glaciers**

Only a very few early explorers, mostly from expeditions carried out during the second half of the 19th century, mentioned glaciers in their reports or provided technical information about the extent and distribution of Alaska's glaciers. Several factors can be offered to explain this situation: (1) most of the early explorers had no personal knowledge or understanding of glaciers or the concept of glacierization, and (2) most were searching for a "Northwest Passage" or for expanding economic trading spheres for their countries and were not focused on descriptions of geographical features.

An additional factor may be the vocabulary commonly used in Europe during the period of early exploration. An 1855 discussion of glaciers by Wilhelm Wittich states that "The term glacier is frequently considered as being synonymous with that of snow-mountain, and both terms are sometimes used without discrimination" (Wittich, 1869). However, even without using the correct terminology, explorers did describe glaciers. For example, although Vancouver (1798) never used the word glacier, he did use phrases such as "an immense body of compact perpendicular ice, extending from shore to shore..." to describe Brady Glacier in Taylor Bay and "From the shores of this basin a compact body of ice extending some distance nearly all round" (Vancouver, 1798, p. 416–417) to describe Taku Glacier. Obviously, Vancouver had an understanding of glaciers, even if not of modern glaciological terminology.

What follows is a summary of the accomplishments of selected explorers who conducted 18th through 20th century sea and land expeditions that provided descriptions of the glaciers of Alaska or contributed to Alaska's geographic information. Qualitative information provided by these explorers can be used to extend the record of historic changes in Alaska's glaciers.

## **18th and 19th Century Explorations and Observations of Alaska and its Glaciers**

The 18th and 19th centuries saw a number of European expeditions to Alaska. Some were focused on exploration, some on exploitation, some on adventure, and some on scientific investigation. Together, these explorers, scientists, and adventurers provided descriptions of glaciers or contributed to Alaska's geographic information. Appendix D provides a chronological list of many of those explorers and expeditions, their nationality, and date(s) of exploration. For a number of locations, this mostly qualitative informa-



tion can be used to draw conclusions about the location and size and even the processes active at selected Alaska glaciers. Much of the information for appendix D was compiled from Davidson (1901, 1904), Baker (1902, 1906), Hulley (1953), Sherwood (1965), Orth (1967), Henry (1984), and Molnia and Post (1995). Following is a brief summary of selected explorers/expeditions who visited Alaska during the 18th, 19th, and early 20th centuries and their contributions to our earliest knowledge of glaciers in Alaska.

### **Vitus Bering**

The first documented European expedition to explore Alaska, conducted in 1741 for Russia, consisted of two ships, the *St. Peter*, captained by Vitus Bering, with Sven Waxell as second-in-command and Georg W. Steller as naturalist, and the *St. Paul*, captained by Alexie Chirikof. Soon after leaving Kamchatka, the ships lost contact with each other and remained separated for the remainder of their respective voyages. The *St. Peter* sailed as far east as the vicinity of the St. Elias Mountains, sighting land on the western side of Yakutat Bay and Mount St. Elias in mid-July 1741. Although the *St. Peter* sailed within a few kilometers of the largest glaciers in continental North America, no written information exists about any glaciers from any of the expedition's members.

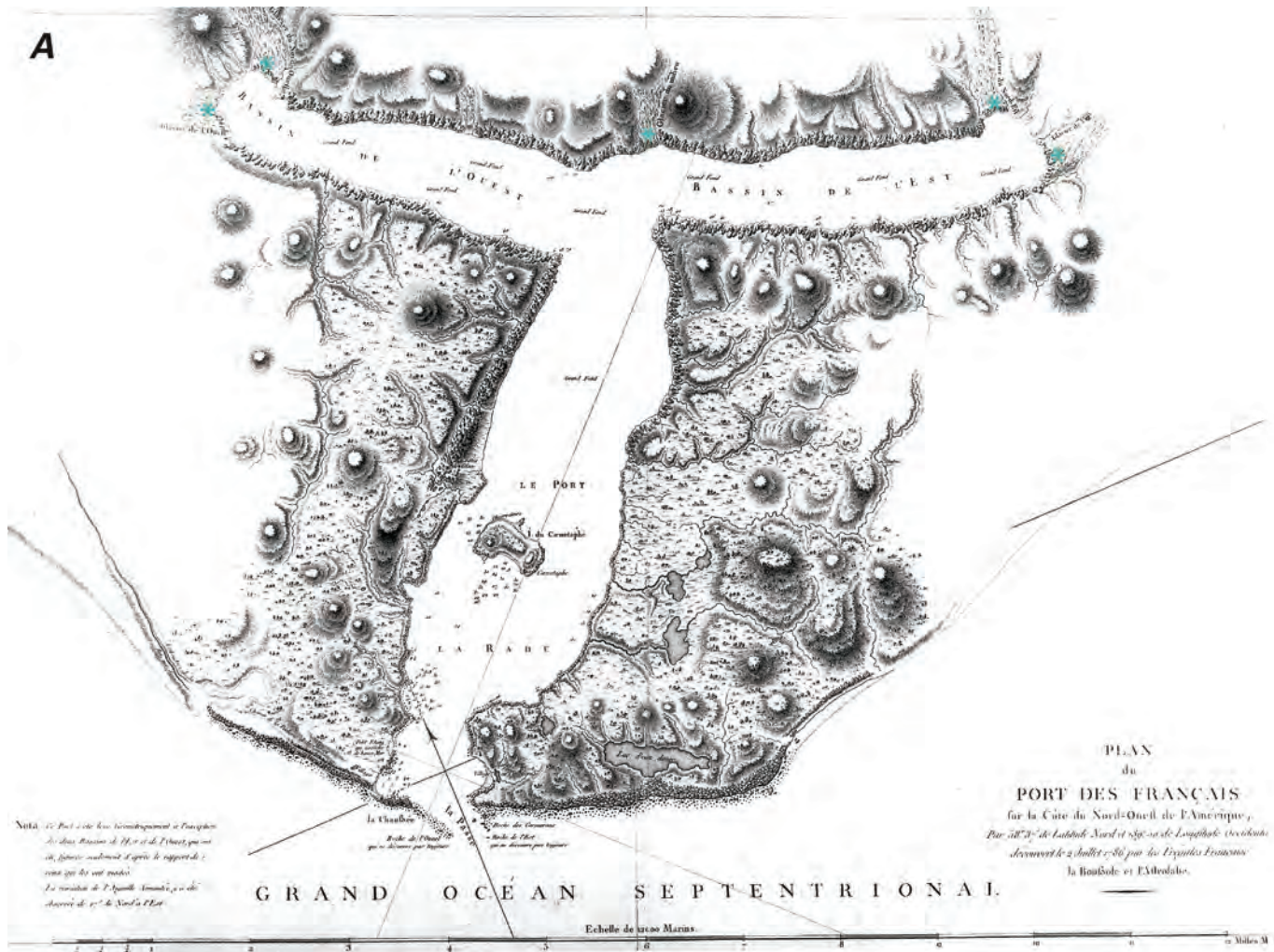
On 20 July 1741, Steller and members of the crew landed on Kayak Island (Waxell, 1952). Attempting to return to Kamchatka, Captain Bering sailed along the Aleutian Islands before most of the crew fell ill with scurvy, and the ship suffered permanent damage. On 5 November 1741, to prevent its sinking, the *St. Peter* was run aground on an island off the coast of Russia, now called Bering Island. Although Captain Bering died without reaching home, his expedition produced the first information and descriptions of the Pacific Ocean coast of Alaska. Captain Chirikof sailed as far east as the Alexander Archipelago, perhaps to what is now known as Sitka on the western coast of Baranov Island, before safely returning to Russia.

### **James Cook**

Beginning in May 1778, Captain James Cook, in command of the HMS *Resolution*, and Captain Charles Clerke, in command of the HMS *Discovery*, sailed westward along the North American shoreline of the Pacific Ocean looking for a passage to the Atlantic Ocean. After naming Mount Edgecumbe (on Baranof Island), Cook observed snow-covered Mount Fairweather (in Glacier Bay National Park and Preserve). Cook later explored Prince William Sound and Cook Inlet from 12 May through 25 June 1778. The expedition then proceeded through the Bering Strait into the Arctic Ocean, where it was turned back by pack ice on 28 August 1778. Many sketches of coastal features, including the St. Elias Mountains and the Chugach Mountains, were made by William Bligh, sailing master of HMS *Resolution*, but there are no known descriptions of glaciers from that voyage.

### **Jean François de Galaup de La Pérouse**

In July 1786, Jean François de Galaup de La Pérouse led two ships, the *Boussole* and the *Astrolabe*, in an expedition to the coast of the St. Elias Mountains. In Lituya Bay, a T-shaped fiord with numerous glaciers at its head, he set up a scientific observatory on Cenotaph Island. He clearly had knowledge of glaciers because his log describes their locations and characteristics (La Pérouse, 1798–99). His map of Lituya Bay (fig. 9A) accurately depicts water depths within the bay and the location of five glaciers at the upper ends of the bay. La Pérouse's narrative describes how several members of the expedition attempted to climb one of the glaciers at the head of the western arm of the bay. He stated that "With unspeakable fatigue they advanced 2 leagues, being obliged at extreme risk of life to leap over clefts of great depth; but they could only perceive one continued mass of ice and snow, of



which the summit of Mount Fairweather must have been the termination” (La Pérouse, 1798–99, p. 374). Drawings by expedition members Lieutenant de frégate Blondela and Gaspard Duché de Vancy show Cascade Glacier at the head of Lituya Bay. The details of La Pérouse’s descriptions and map provide a qualitative source of data to estimate changes in the positions of glacier termini in Lituya Bay (figs. 9B, 9C) and sediment accumulation for a period that now exceeds 200 years (Jordan, 1962; Molnia, 1979).

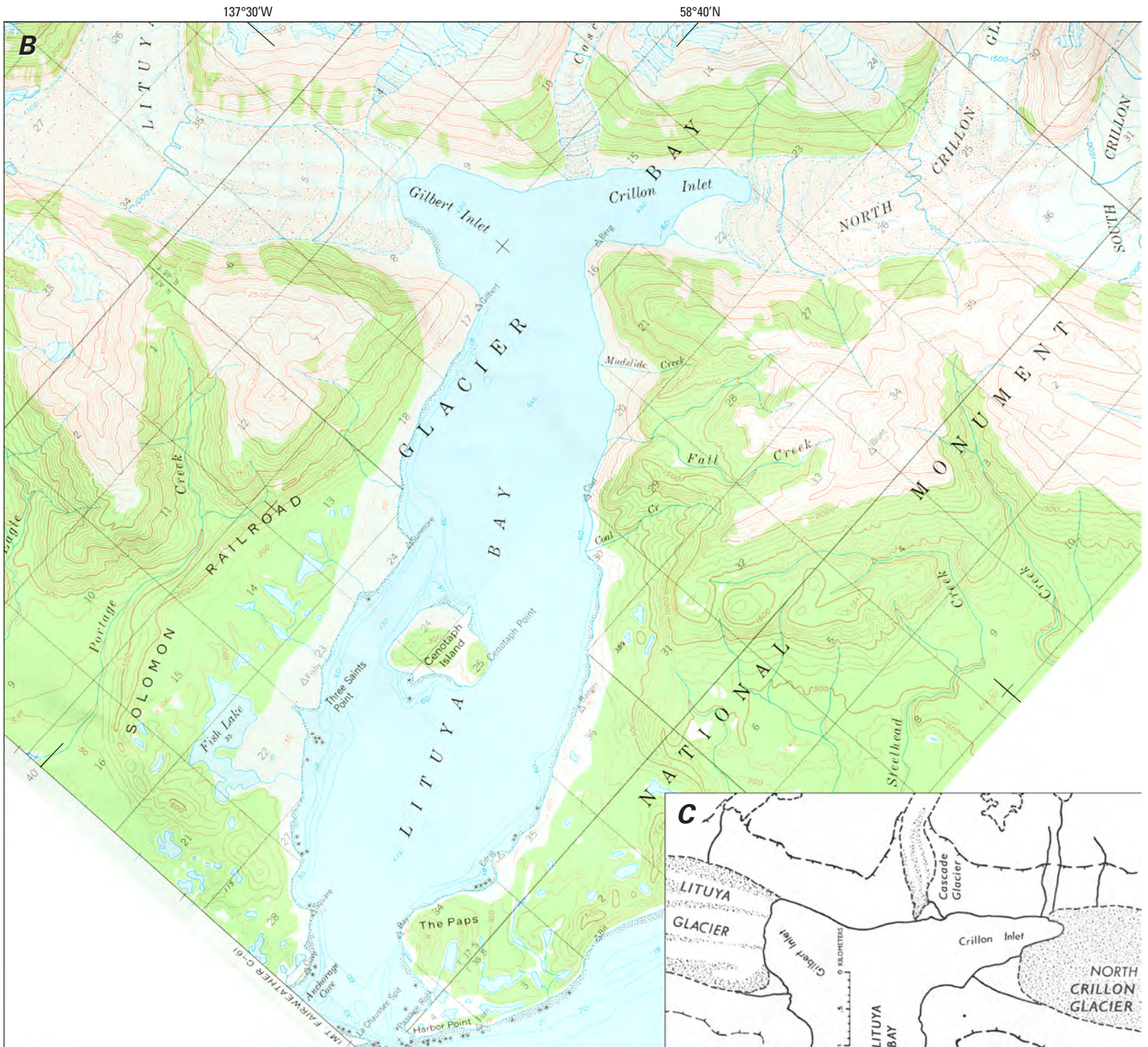
### Alexandro Malaspina

In 1791, a Spanish scientific expedition reached Alaska with the purpose of collecting natural history materials and information, preparing maps, and investigating the political state of Spanish possessions in the New World (Beddall, 1979). The expedition, which carried three naturalists, consisted of two ships, the *Descubierta* and the *Atrevida*, under the leadership of Alexandro Malaspina. On 2 June 1791, they reached Sitka and then proceeded north to Yakutat Bay which they explored in detail and named Disenchantment Bay (Bahia del Desengano). While they were in Yakutat Bay, a description of a glacier, now known as the Malaspina Glacier, was prepared. The expedition also studied Icy Bay and Prince William Sound.

### George Vancouver

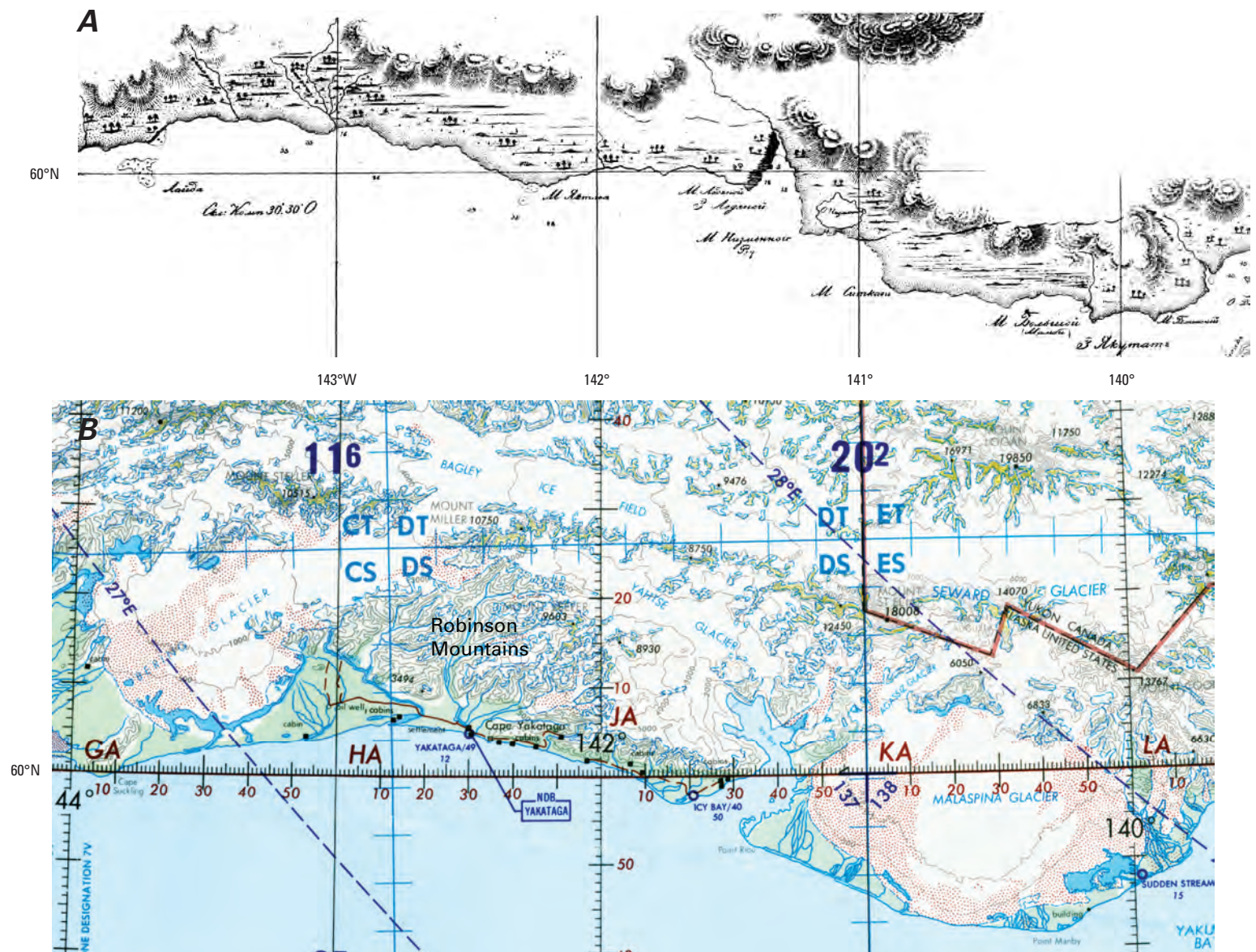
In 1793, Captain George Vancouver of the British Navy, commanding the sloop *HMS Discovery*, explored the southeastern corner of Alaska from the vicinity of Portland Inlet north to the vicinity of Cape Caamano at the northern end of Clarence and Sumner Straits. Captain Vancouver named the cape

▲ **Figure 9.**—Three maps of Lituya Bay: 1797, 1961, and 1972. **A**, La Pérouse’s 1797 map; **B**, Part of the USGS (1961) 1:63,360-scale topographic map (appendix B) of the same area. (Mt. Fairweather, C-5, Alaska; compiled photogrammetrically from vertical aerial photographs acquired in 1948 and 1958, field annotated in 1961). **C**, 1972 sketch map by Austin Post, U.S. Geological Survey. The La Pérouse map shows the presence of five named glaciers (green asterisks) at the head of the bay. The USGS and Post maps show only three. In the interval of time between the three maps, the pairs of glaciers at the heads of each arm of the bay have coalesced and each has advanced more than 3 km. By 1972, however, Cascade Glacier had retreated to a stable position on the beach (table 3). Compare with figures 136 and 137 to see continuing changes.



after Don Jacinto Caamano, a Spaniard commissioned by the Viceroy of Mexico in 1792 to explore the southeastern Alaskan coast. In 1794, Vancouver returned to Alaska, exploring the coast from Chirikof Island, west of Kodiak, to Kodiak, to Cook Inlet, to Prince William Sound, to the mouth of Glacier Bay, and south to Port Conclusion on the east coast of Baranof Island. During this expedition, Lieutenant James Whitbey frequently went ashore in a small launch and made detailed investigations of many coastal features.

During Captain Vancouver's 1794 exploration of College Fjord in Prince William Sound, a correlation was made between the frightening thunderous roars that were frequently heard and the falling of blocks of frozen snow off the faces of "snow cliffs." This instance is the first recorded observation of glacier calving in Alaska. Captain Vancouver described Icy Bay (Vancouver,



1798). Many sketches of coastal features, including Mount St. Elias and Icy Bay, were made by Thomas Heddington, a midshipman.

### Edward Belcher

In 1837, Sir Edward Belcher, aboard HMS *Sulphur*, journeyed to Alaska in order to fix the geographic coordinates and determine the height of Mount St. Elias (Belcher, 1843). In the vicinity of Cape Suckling, the expedition made what is probably the first observation of the surge of an Alaskan glacier. Belcher described a surface composed of rectangular prisms of severely shattered ice lightly mantled with morainic debris in the area of Bering Glacier's present terminus. Years later, Belcher (1862) had become more familiar with glaciers and icebergs but still did not understand what he had observed in 1837 or its dynamics. After severe thought over a period of many years, he presented an explanation for and a description of the icebergs that he saw near Icy Bay and tried to relate them to the pyramids observed in 1837. He stated that "the apparently descending ice, from the mountains to the base, was in irregular broken masses, which tumbled in confusion. The motion was clearly continuous" (Belcher, 1862, p. 186–187).

**Figure 10.**—Maps of the Gulf of Alaska coastal area from Yakutat Bay on the east to the Cape Suckling area on the west. **A**, Teben'kov's 1849 map shows the margin of the Malaspina Glacier as a snow-covered plateau surrounded by forest and marsh. The "Icy Bay" shown west of long 141°W. is not the present Icy Bay. In the intervening years the embayment was filled. To the west of Icy Bay, the Robinson Mountains are shown as snow-covered. **B**, The same area portrayed on the 1975 U.S. Air Force Operational Navigation Chart (ONC) D-11.

## George Simpson

In 1841, George Simpson, Governor of the Hudson Bay Company, visited many of the settlements in Russian America, observing the local geography as well as their economic situations. In September 1841, he sailed through Stephens Passage, where he observed “The valleys were lined with glaciers down to the water’s edge; and the pieces that had broken off during the season had filled the channels and straits with fields and masses of ice, through which the vessel could scarcely force her way” (Simpson, 1847, v. 1, p. 213).

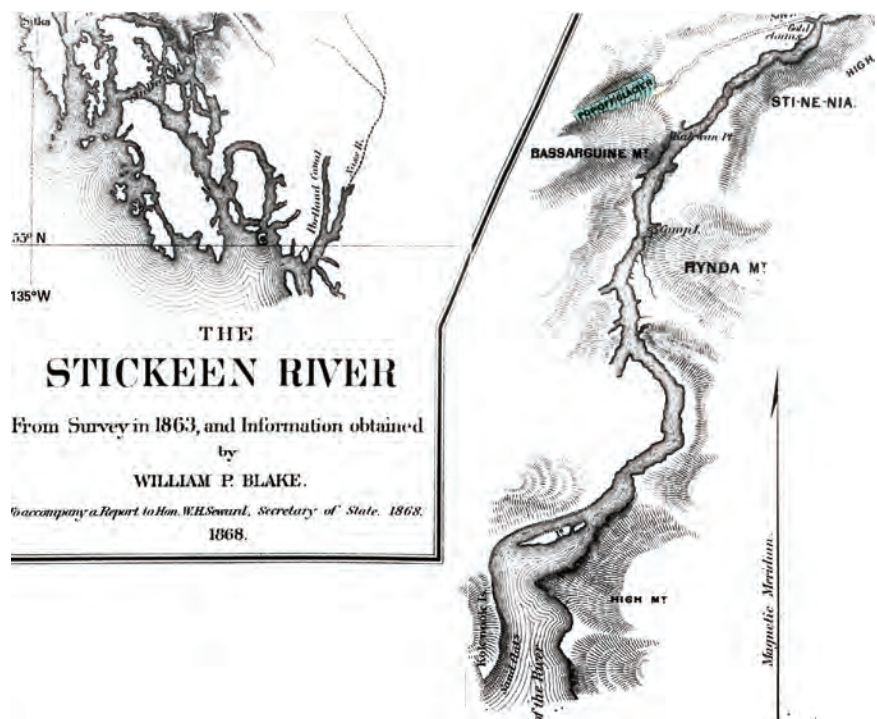
## Mikhail Dimitrievich Teben’kov

Between 1848 and 1850, a series of charts and maps appeared that were prepared by cartographers Kosima Trentiev and M.M. Kadin for Admiral Mikhail Dimitrievich Teben’kov, Director of the Russian American Company and Governor of the Russian American colonies. These charts and maps, published as the *Atlas of the Northwest Coast of America* (Teben’kov, 1852), clearly show the location of many coastal features, including glaciers. The observations of more than 50 pilots and Russian explorers (appendix D) were consolidated into these charts and maps (fig. 10).

## William P. Blake

In 1863, the Russian Navy invited Professor William P. Blake of Yale University to accompany Commander Vladimir Bassarguine on the corvette *Rynda* on an exploration expedition to Russian America. After arriving at Sitka, Blake accompanied a party for the first exploration of the Stikine River valley. Blake described “four large glaciers and several smaller ones” (Blake, 1867, p. 96) within 60 to 70 miles of the mouth of the river. His observations were published as early as July 1863 in California newspapers and, in 1867, as *Glaciers of Alaska, Russian America* (Blake, 1867), the first summary of Alaska’s glaciers. His 1868 map and report to Secretary of State William Seward (Blake, 1868) includes several sketches of glacier terminus morphology and descriptions of individual glacial moraines. The map shows the terminus position of four glaciers, including Popof Glacier (fig. 11).

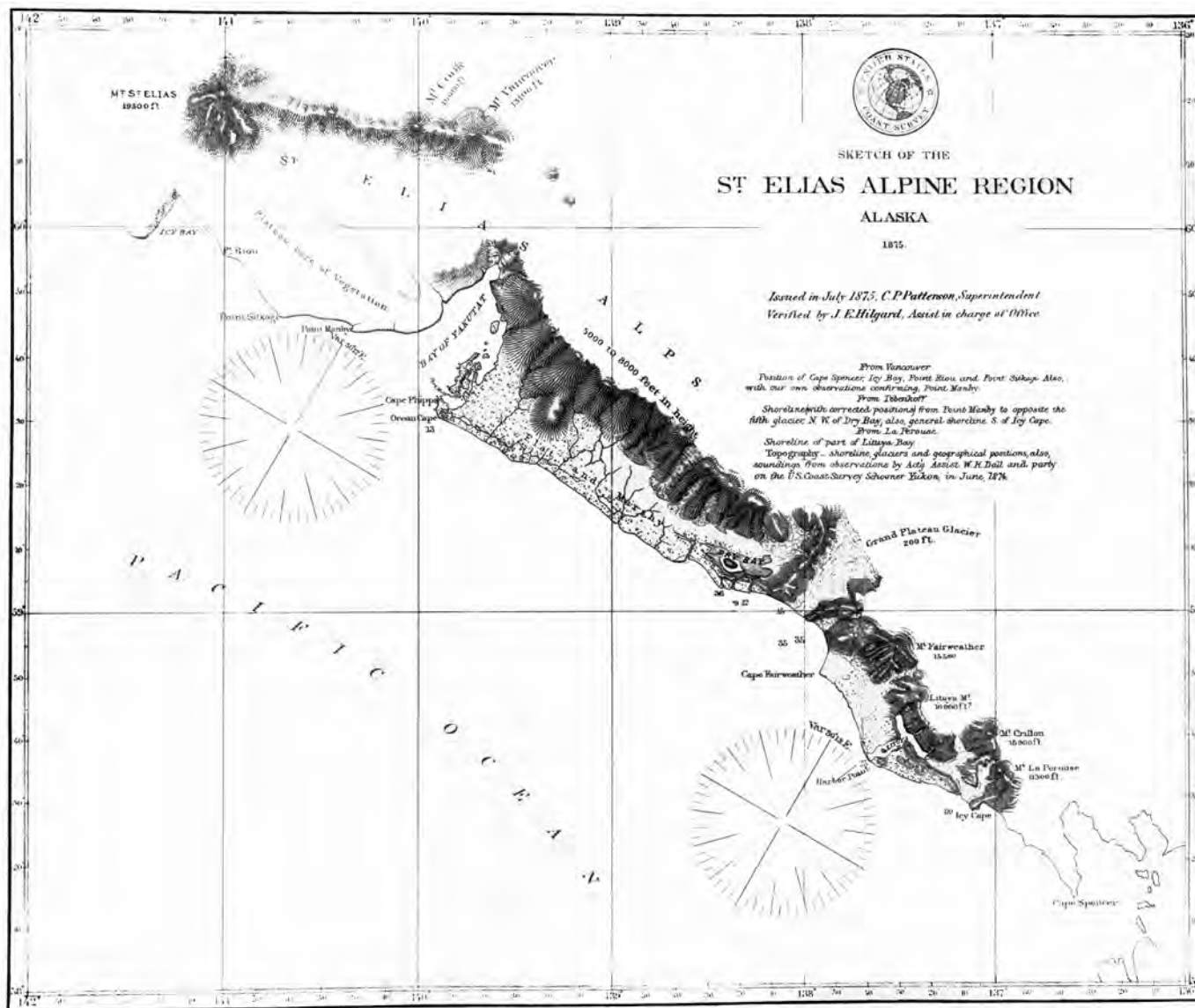
**Figure 11.**—Part of Blake’s 1868 map of the Stikine (Stickeen) River area showing the terminus of Popoff [Popof] Glacier. Farther upstream, off this section of the map, three other glaciers are depicted, all located on what is now the Canadian side of the border. Blake uses the terms “moraine” and “old moraine” to describe sedimentary deposits in front of two of the Canadian glaciers.



## William H. Dall

Beginning in 1865, William H. Dall began a lifelong investigation of the resources of Alaska, including its glaciers. His reports mention the effects of past and present glaciation and the geology of the region. In his 1870 description of the resources and geography of Alaska, Dall (1870), notes several glaciers of the Coast Mountains, including the Davidson Glacier and those near the Taku River, and mentions Icy Bay, named “for the glaciers which surround it” (Dall, 1870, p. 252). On 21 April 1883, Dall presented a summary of his observations about the glaciation of Alaska to the Philosophical Society of Washington (Dall, 1884). In the interior of Alaska, he observed ice lenses in permafrost and took time to clearly differentiate between ice of glacial origin and permafrost ice. Dall described the distribution of glaciers as “confined to the region of the Alaska range and the ranges parallel with it south of the Yukon Valley, but particularly to the coast mountains bordering on the Gulf of Alaska and the Alexander Archipelago, of which the St. Elias Alps form the most conspicuous uplift” (Dall, 1884, p. 35). Dall recognized “that the extent of Alaskan glaciers is generally diminished from its former state, and is probably still diminishing” (Dall, 1884, p. 35).

**Figure 12.**—Sketch map of the Saint Elias Alpine Region [sic, mountains] produced by the U.S. Coast Survey in 1875. Shown and named is Grand Plateau Glacier. Shown but not named are La Perouse and the Crillon Glaciers north of Dry Bay. The Malaspina Glacier is shown as a flat area in front of a mountain chain that includes Mount Saint Elias, Mount Cook, and Mount Vancouver. In front of the Malaspina Glacier is a “Plateau bare of Vegetation.”



## George Davidson

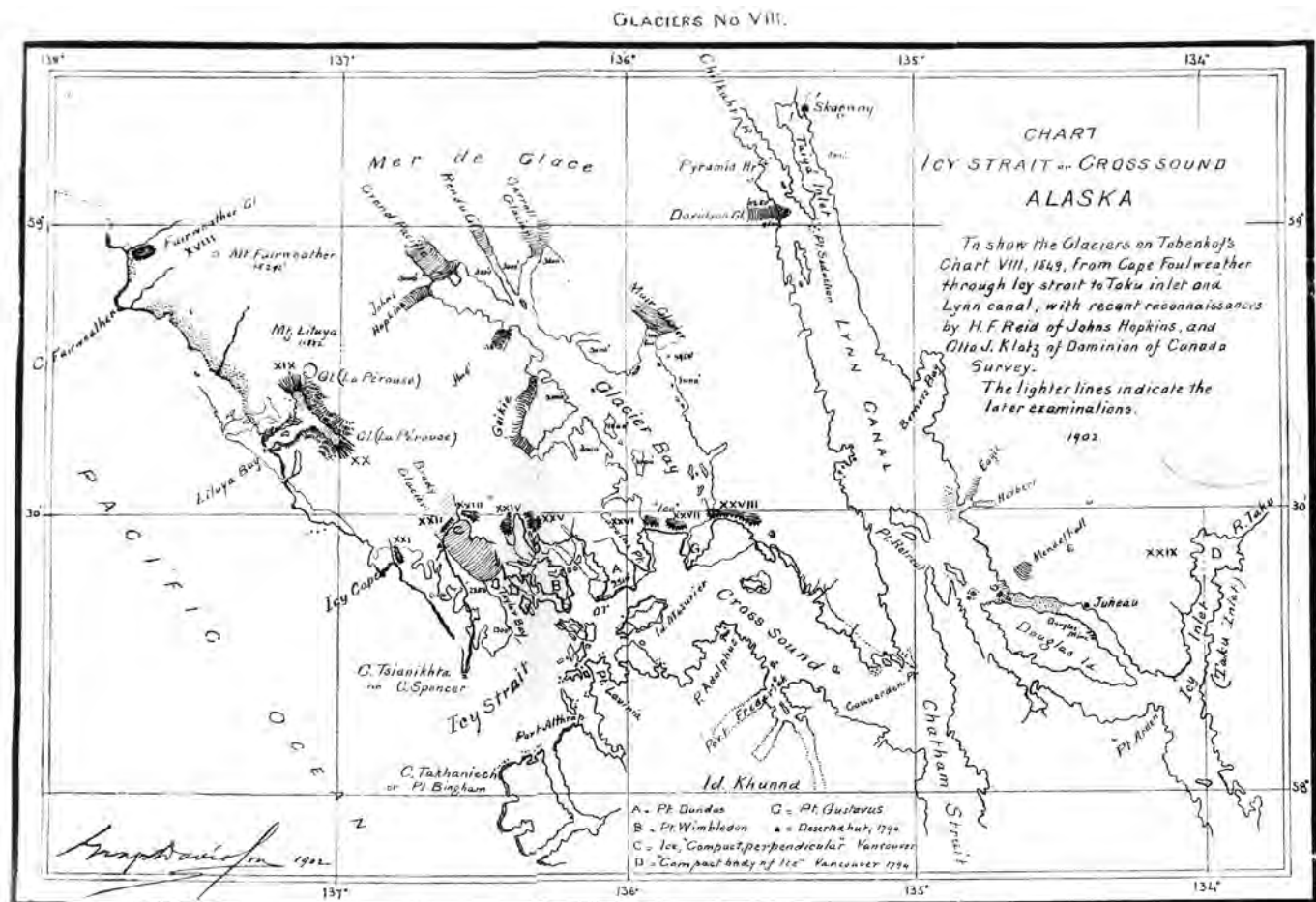
Following the purchase of Alaska from Russia in 1867, George Davidson was directed by the Superintendent of the United States Coast Survey [USCS, later the U.S. Coast and Geodetic Survey (USC&GS), and now the National Ocean Survey (NOS)] to “gather whatever information I could of the resources of that terra incognita” (Lewis, 1954, p. 42). This directive began investigations of the coastline and continental margin of Alaska that continue to the present. These types of investigations produced figure 12, an 1875 *Sketch of the St. Elias Alpine Region* (United States Coast Survey, 1878), combining topography and shoreline glacier positions compiled during an 1874 survey directed by Dall with data and observations from the charts of Vancouver, La Pérouse, and Teben'kov. The sketch map shows the La Perouse and Grand Plateau Glaciers and describes the area covered by the Malaspina Glacier as a “plateau bare of vegetation” (United States Coast Survey, 1878, pl. 22).

Davidson maintained a keen and continuing interest in Alaska into the 20th century. In 1901, he published a detailed examination of Bering's 1741 voyage (Davidson, 1901). More importantly, in 1904, Davidson completed his summary of *The Glaciers of Alaska That Are Shown on Russian Charts or Mentioned in Older Narratives* (Davidson, 1904). This summary contains 11 plates depicting the early mapped glacier positions, one of which is shown in figure 13.

**Figure 13.**—Map showing the glaciers of the Icy Strait-Cross Sound region compiled in 1902 by George Davidson from data published by the Russian-American Company and other 19th century sources (Davidson, 1904, Plate VIII). Comparing this map to earlier maps, shows very clearly that the delineation of landforms in general and glaciers in particular was becoming much more accurate.

## Charles Erskine Scott Wood

In 1877, Lieutenant Charles Erskine Scott Wood journeyed to Alaska in an attempt to climb Mount St. Elias. His indigenous guides refused to undertake



an ocean canoe trip and led him to the Mount Fairweather area instead. From there, Wood saw Glacier Bay in the distance from the divide (Wood, 1882).

## John Muir

In 1879, John Muir, a naturalist and travel writer, visited Alaska for the first time. He was accompanied by Samuel Hall Young, a Presbyterian missionary. Together, they performed the first detailed investigation of Glacier Bay and Muir Glacier. Muir returned in 1881 (Muir, 1893, 1895) and 1899 (Muir, 1902) and noted many changes in the bay and its glaciers. He also explored numerous glaciers in other parts of southern Alaska.

## U.S. Military Expeditions

In 1883, a U. S. Army expedition led by Lieutenant Frederick Schwatka (1885) explored the northern part of the Alaska panhandle in the vicinity of the Chilkoot Pass while on its way north to the headwaters of the Yukon River. The expedition transported a camera and exposed glass photographic plates, capturing images of several glaciers north of Skagway. These photographs are likely the earliest of Alaskan glaciers. Schwatka described and mapped an “immense glacier” at the head of the Nourse River and “the southern terminal spur of a large glacier” between the Nourse and the Dayay Rivers. He named these the Baird and Saussure Glaciers (fig. 14) and prepared lithographs of each (Schwatka, 1885).

In 1885, Lieutenant Henry T. Allen of the Second U. S. Cavalry led a 1,500-mile (2,414-km) expedition to the Copper, Tanana, Koyukuk, and Yukon Rivers to make a reconnaissance of the Copper and Tanana River valleys of Alaska (Allen, 1887). His report contains lithographs of the termini of the Childs and Miles Glaciers (fig. 15) based on his photographs and narrative, which describe Childs and Miles Glaciers and several other glaciers in the Copper River Valley.

## George Frederick Wright

In 1886, G. Frederick Wright, a professor at Oberlin Theological Seminary and an Assistant of the USGS, conducted a month-long investigation of Muir Glacier and Glacier Bay (Wright, 1887, 1889). Among his findings is an estimate of the annual sediment budget of the Muir Glacier. Wright also made observations on the glaciers of the Stikine River and many other parts of the Coast Mountains (fig. 16). Wright’s *The Ice Age in North America and its Bearings upon the Antiquity of Man* (Wright, 1889) contains a map



**Figure 14.**—1883 lithograph produced from one of the first photographs taken of an Alaskan glacier. Although it is labeled “Finger of Saussure Glaciers,” this name was never adopted. The glacier, which is underfit in its valley, appears to have a retreating terminus. It is probably an unnamed glacier on the east side of Mount Hoffman, Coast Mountains. Lithograph from Schwatka (1885). Photograph by Charles A. Homan, U.S. Engineers.



of southeastern Alaska that systematically depicts the location of known Alaskan glaciers between Dixon Entrance [54°30'N.] and Mount St. Elias [60°20'N.] (fig. 17). Wright quoted H.W. Elliot as stating that “counting great and small, there can not be less than five thousand glaciers between Dixon’s Entrance and the extremity of the Alaskan Peninsula” (Wright, 1889, p. 30).

### ***New York Times Expedition***

In 1886, a *New York Times* expedition led by Frederick Schwatka attempted to reach Mount St. Elias. Schwatka was accompanied by William Libbey, Jr., of the College of New Jersey and Lieutenant Heywood W. Seton Karr, a former British Army officer and mountaineer. Seton Karr applied the name “Bering Glacier” to an “ice-plain” that he observed west of Icy Bay (Seton Karr, 1887). Libbey (1886) named the Guyot and Aggasiz Glaciers and also recognized that the majority of the glaciers that he saw were retreating. “Today we find in the glaciers which gleam on the mountain sides of these channels only the relics of their former greatness. The history of the great Muir Glacier at the head of Glacier Bay is but silent witness of the fact that these ice masses are rapidly retreating to their mountain fastnesses, for it has retreated many miles towards its sources since it was first discovered” (Libbey, 1886, p. 281–282). This expedition was responsible for providing the first written description of the complex glacier systems now known as the Bering, Guyot, and Malaspina Glaciers.

**Figure 15.**—1887 lithograph produced from one of the few surviving photographs taken by Lt. Allen’s Copper River Expedition of 1885 (Allen, 1887). Shown is the terminus of Miles Glacier.

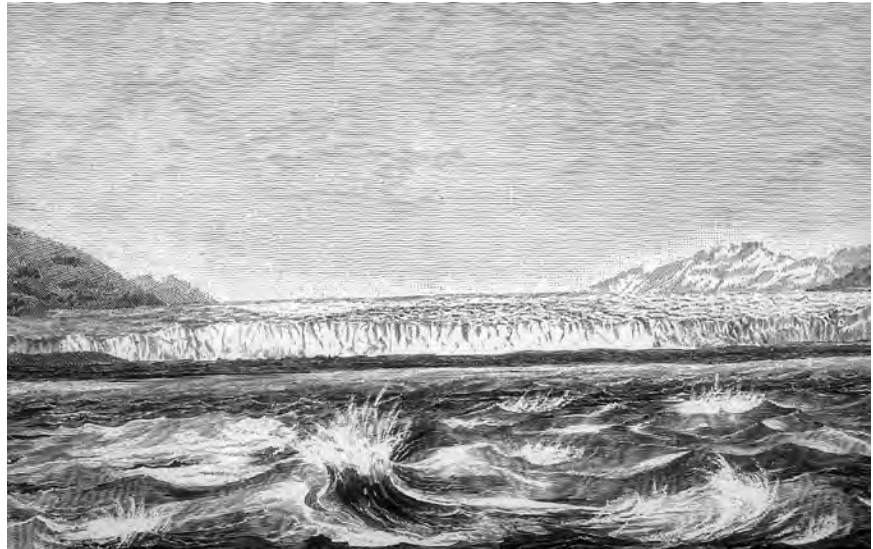


**Figure 16.**—1886 photograph by W.H. Partridge of the terminus of Norris Glacier, Coast Mountains. This image was published in Wright (1889).





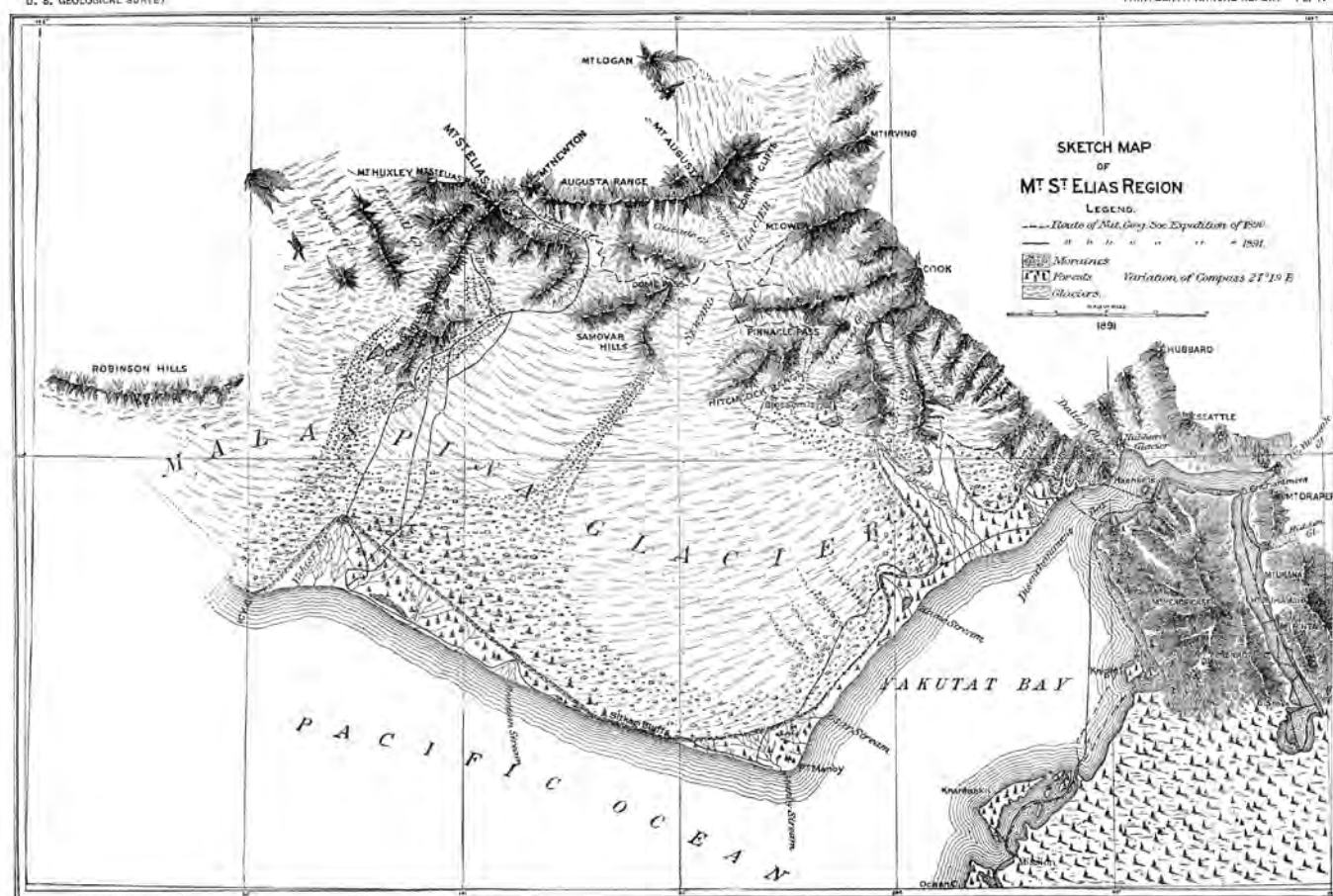


**Figure 19.**—**A**, 1891 Israel C. Russell photograph of a USGS field party crossing the Malaspina Glacier, St. Elias Mountains, during their unsuccessful attempt to climb Mount St. Elias. Samovar Hills is in the middle background. Photograph Russell 520 from the USGS Photographic Library, Denver, Colo. **B**, Israel C. Russell and members of his survey team in the St. Elias Mountains. Israel C. Russell was the first recipient of a field-research grant from the National Geographic Society in 1890 (USGS Photographic Library photograph Russell 568).

height of Mount St. Elias, thought to be 18,008 ft, was calculated to be  $18,100 \pm 100$  ft. The ascent failed owing to severe weather. Russell Fiord, later named for him, was also explored in detail. Russell's expeditions produced more than 150 photographs (fig. 19), including the earliest photographs of the positions of the termini of the Turner and Hubbard Glaciers. Many of these photographs were published in 1892 and in 1893 (Russell, 1892, 1893), and some were used by other investigators, such as Tarr and Martin (1914), to assist them in determining change in glaciers.

## Henry Fielding Reid

Henry Fielding Reid was affiliated with the Case School of Applied Science in Cleveland (now Case Western Reserve University) and with Johns Hopkins University in Baltimore. In 1890 and 1892, he conducted two expeditions to Glacier Bay to study Muir Glacier. He made numerous photographs and described how to document the location of a glacier's terminus:

(1) All photographs at the end of a glacier are useful; particularly if the magnetic bearings of the camera, and the approximate distance from the glacier are given.

(2) Select two stations, one on each side of the valley, commanding a view of the glacier's end. Photograph the end from these two stations... Mark the station, describe them carefully... so that they can easily be found by later observers... This will be the beginning of a systematic record of the glacier. From these photographs it will be possible to make a map of the glacier's end if we know: the distance between the stations; the angle at each station between the other and some points in the photograph and the focal length of the lens (Reid, 1895, p. 286–287).

In a pair of publications (Reid 1892, 1896), he described the morphology of the bay, its geology, glaciers, and glacial deposits, changes between his two visits, moulins, Glacier Bay's tides, and its water chemistry. H.P. Cushing of Western Reserve University (Cleveland), a member of the first Reid expedition, published the first geological map of the region in 1895 (Cushing, 1896). A preliminary version showing the geology of the Muir Glacier Basin was included in Reid (1892). During the same time period, other photographers came to Glacier Bay and also recorded the position of the terminus of Muir Glacier (fig. 20).

Starting in 1895, Reid began to compile summaries of the global variations of glaciers, including glaciers of Alaska.

The great interest which the physical study of living glaciers has to the geologist is the light it may throw on the causes producing, and the conditions prevailing during the Ice Age. One of the habits of living glaciers bearing most directly on the Ice Age is the variation continually occurring in their length, thickness, and velocity of motion... but it is only within about twenty years that anything like systematic work has been done in getting together records which enable us, in some cases, to exhibit roughly the variations in the extent of certain glaciers for three hundred years, during which period there has been quite a number of advances and retreats... (Reid, 1895, p. 278).

On an almost annual basis, he continued to compile and report these changes in a series of articles, frequently titled *Variations in Glaciers*, until the advent of World War I (for example, Reid, 1897, 1898, 1899, 1900, 1904, 1909, 1913a, 1913b, 1915). He last visited Glacier Bay in 1931.

[Editors' note: According to Mark F. Meier (written commun., 2004), Reid was the first scientist to carry out true glaciological studies in Alaska. One of his many significant achievements was the mapping, using planetable-mapping techniques, of the large, heavily crevassed Muir Glacier from its terminus to its head. He also published many "cutting-edge" scientific papers, including an exposition on the "kinematic theory" of glacier flow. Reid



**Figure 20.**—1893 photograph by Frank LaRoche (standing) (T.J. Richardson, sitting) of the terminus of Muir Glacier, Saint Elias Mountains. Morse Glacier can be seen in the left background. The photograph is from the National Snow and Ice Data Center (NSIDC), Boulder, Colo.

was the U.S. representative on the International Commission on Glaciers. He clearly was the most prominent U.S. glaciologist until the emergence of a new generation of glaciologists, such as Robert P. Sharp and others in the post-World War II years. Unfortunately for the science of glaciology, the 1906 Earthquake in San Francisco diverted his attention to the science of seismology, where he published a seminal paper on the “elastic-rebound theory” of earthquakes.]

### **Alaska-Canada Boundary Surveys**

The boundary survey work done by the Americans and Canadians from approximately 1893 to 1920 to delineate the boundary between Canada and Alaska is an invaluable source of glacier photographs.<sup>3</sup> The settlement of the border involved a tremendous amount of hard work and sacrifice on the part of the boundary survey parties. The Anglo-Russian Treaty of 1825 fixed the boundary between British and Russian possessions in 1867; after Canada took over the British possessions in 1870 and 1871, the boundary description given in the treaty continued unchanged. The vague language of the 1825 treaty with regard to the Alaska panhandle led to U.S.–Canadian disagreement over the boundary description in that area. In 1892, the parties agreed to a joint survey of the disputed area by the Alaska Boundary Commission, which was made up of both Americans and Canadians. An unproductive field season in 1893 caused by poor weather was followed by a very successful season in 1894 and then a wrap-up of the work in 1895. In 1899, a Joint High Commission was still unable to settle the boundary dispute, and the differences culminated in the 1903 Alaska Boundary Tribunal. The six-member tribunal voted in favor of the United States, resulting in the *Atlas of Award*, which was published in 1904. Joint surveys by the United States and Canada, under the auspices of the International Boundary Commission, then followed from 1904 through 1928 to demarcate the boundary as indicated in the *Atlas*.

The surveys were performed by using a 5-year-old photo-topographic method developed for mountain work. A series of photographs were taken from a triangulated camera station covering a full 360 degrees. Camera stations established high in the Coast Mountains afforded clear views of the mountains, valleys, and glaciers farther inland. The result was a superb set of photographs of glaciers in the Coast Mountains dating from the 1890s. Several people are credited with much of the glacier photography: A.J. Brabazon, J.A. Flemer, James L. Gibbons, James G. Gibbons, Otto Klotz, William Ogilvie, J.J. McArthur, and A.C. Talbot. Otto Klotz, a Canadian, was one of the first to recognize that photography could be a useful tool for surveying and documenting the position of glaciers and for determining changes in glacier position with time. In 1894, he conducted a photo-topographic survey of the terminus of Baird Glacier (Klotz, 1895). He also realized that “Probably nowhere on the earth are better opportunities afforded for the study of living and dead glaciers than on the north-west continental shore of America” (Klotz, 1899, p. 534). He instructed future investigators to leave “readily recognizable marks near the ice-front...for the determination of smaller fluctuations of the glaciers” and to develop consistency in future photographic surveys so that the “study of the motion of glaciers will then be reduced to an exact science” (Klotz, 1899, p. 534).

### **National Geographic Society Expeditions**

Starting in the 1890s, the NGS served as a focal point both for organizing and funding studies of Alaskan glaciers and for reporting their results in its magazine. In addition to Russell’s descriptions of Mount St. Elias, the

---

<sup>3</sup> The editors appreciate the scholarly contribution to this section by C Suzanne Brown, formerly with the USGS, in using her extensive knowledge of the history of these surveys.

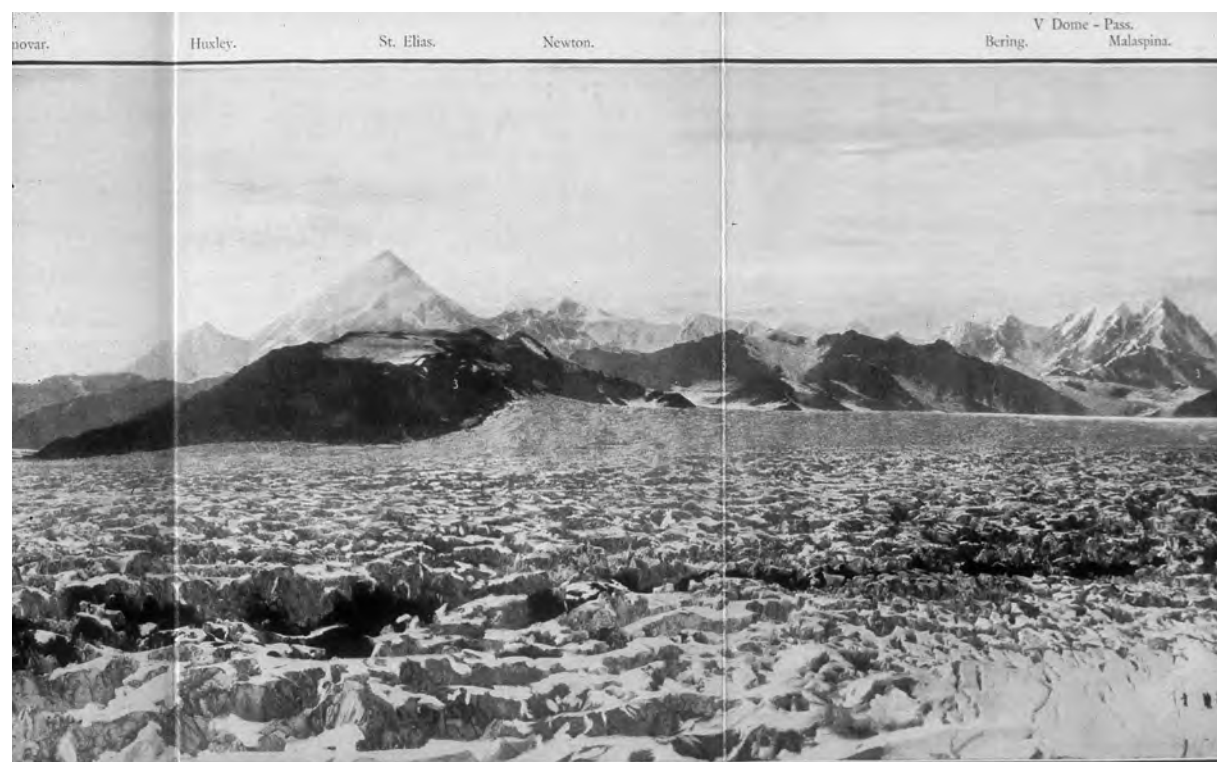
Malaspina Glacier, and Yakutat Bay (Russell, 1891, 1892, 1893), the NGS presented the results of the Frederick Swatka and C.W. Hayes explorations of the Copper River and the area north of the St. Elias Mountains (Hayes, 1892; Swatka, 1885); H.F. Reid's descriptions of Glacier Bay and Muir Glacier (Reid, 1892); G.K. Gilbert's summary of the glaciers of Alaska (Gilbert, 1903); Henry Gannett's description of Alaskan glaciers, including those in Prince William Sound (Gannett, 1899); E.R. Skidmore's descriptions of the glaciers of the Stikine River area and the exploration of Alaska and its glaciers (Skidmore, 1894, 1896, 1899); C.L. Andrews, Fremont Morse, and G.K. Gilbert's studies of Muir Glacier during the first decade of the 20th century (Andrews and Gilbert, 1903; Morse, 1908); W. C. Mendenhall's exploration of the glaciers of the Wrangell Mountains (Mendenhall, 1903a, b); studies of the glaciers of the Mount McKinley region by W.A. Dickey, A.H. Brooks, and Robert Muldrow (Dickey, 1897; Brooks and Reaburn, 1903; Muldrow, 1901); W.H. Osgood's descriptions of the glaciers of the Lake Clark region (Osgood, 1904); and Ferdinand Westdahl's photographs of glaciers in the Aleutian Islands (Westdahl, 1903); A.H. Brooks' studies of the geography of Alaska (Brooks, 1902, 1904, 1906a, b, 1911, 1914); and the work by Ralph Tarr and Lawrence Martin for the NGS (Martin, 1911; Tarr and Martin, 1910, 1914).

### Duke of Abruzzi

In 1897, Prince Luigi Amedeo Di Savoia, Duke of Abruzzi, successfully led an expedition to the summit of Mount St. Elias and named many of the glacial features that were seen during the ascent. His narrator, Filippo de Filippi (1899), provided a description of a "huge glacier" observable from the summit. Not realizing that this glacier was part of the already named Bering Glacier, the Duke named the new discovery Columbus Glacier after Christopher Columbus: "This glacier, of even greater extent than the Seward, forms a vast snow-level showing no fissures on its surface" (de Filippi, 1899, p. 158).

One of the most significant products of the expedition were a number of foldout panoramic photographs of the surrounding region (fig. 21). Aside from those made by Israel C. Russell, these photographs were among the

**Figure 21.**—Part of a 1897 panoramic photograph of "The Chain of Saint Elias and [Mount] Augusta seen from the Eastern Side of Seward Glacier, near its Outflow into Malaspina Glacier," made by members of the first successful expedition to the summit of Mount St. Elias led by the Prince Luigi Amedeo Di Savoia, Duke of Abruzzi. Photograph from de Filippi (1899).



first photographs of the St. Elias Mountains ever made and the first of the large valley glaciers located at the base of Mount Logan.

## Postcards

Toward the end of the 19th century and the early years of the 20th, a new industry developed: printing picture postcards of Alaska, many of which featured glacier termini. Many postcard photographs included enough of the geography around the glacier termini to qualitatively determine the location of the glacier at the time the photograph was exposed. Copyright dates in the captions and postmarks on the cards permit some accuracy in determining the date of the photograph. The glaciers of Glacier Bay, and Miles, Childs, Hubbard, Mendenhall, and Taku Glaciers (fig. 22) were frequently depicted.

## Harriman Alaska Expedition

The Harriman Alaska Expedition of 1899, privately funded by Edward Henry Harriman, a wealthy financier and railroad executive, “was originally planned as a summer cruise for the pleasure and recreation of my family and a few friends. ...Our comfort and safety required a large vessel and crew. ...We decided, therefore, ...to include some guests who...would gather useful information and distribute it for the benefit of others” (Harriman, 1902, p. xxi-xxiii). So was born one of the most prolific multidisciplinary scientific explorations of Alaska. Twelve separate volumes of scientific observations were published as a result of the Harriman-funded investigations. Harriman chartered the steamer *George W. Elder* and invited about two dozen distinguished scientists to participate. Scientific disciplines covered by the expedition included ethnology, zoology, botany, geography, and geology. The expedition sailed from Seattle on 31 May 1899, covered more than 9,000 miles (14,500 km), and visited more than 50 locations. Glacierized areas studied included Lynn Canal, Davidson Glacier, Glacier Bay, La Perouse Glacier, Lituya Bay, Yakutat Bay (fig. 23), and Prince William Sound. The expedition returned to Seattle on 30 July 1899. The five geologists aboard the *George W. Elder* were William H. Dall, John Muir, Benjamin K. Emerson of Amherst College, Charles Palache of Harvard University, and Grove Karl Gilbert of the USGS. Edward S. Curtis, the expedition’s official photographer, (who was later known for his photographs of Native Americans), took 1,000 photographs. Volumes 1 and 3 of the Harriman Alaska Expedition, which summarize the geological, glaciological, and glacial findings of the expedition, were published by Burroughs and others (1902) and Gilbert



**Figure 22.**—Late 19th/early 20th century postcard of the terminus of Taku Glacier, Coast Mountains. This photograph of the Taku Glacier is one of the earliest in existence.



**Figure 23.**—20 June 1899 photograph of Cascading Glacier, descending from Mount Draper on the south wall of Nunatak Fiord, Saint Elias Mountains. John Muir is pictured at left. Photograph by USGS geologist Grove Karl Gilbert while he was a participant on the Harriman Expedition. Photograph Gilbert 303 from the USGS Photographic Library, Denver, Colo.

(1904), respectively. As noted by Meier and Post (1980), Gilbert's contributions to the science of glaciology were significant.

## **Selected 20th Century Explorations and Observations of Alaska's Glaciers**

### **Early USGS Investigations and Photography**

Many late 19th and early 20th century USGS geologists carried cameras as a standard part of their field equipment. Although many studies were not primarily focused on glaciers, many of the photographs serve to provide a 50- to 75-yr extension back in time from the Landsat baseline period (1972–81). Between 1898 and 1924, for example, Alfred H. Brooks took more than 1,300 photographs: Tanana Glacier in 1899, the Kigluaik Mountains in 1900, the Tordrillo, Kichatna, and Talkeetna Mountains in 1902, Miles and Childs Glaciers in the Chugach Mountains in 1909 and 1910, Davidson Glacier in 1912, and the glaciers of Glacier Bay and Prince William Sound in 1924.

Similarly, in an Alaska career that spanned more than 35 years (1903–39), Fred H. Moffit took nearly 2,000 photographs: Resurrection Bay and its glaciers and Turnagain Arm with Portage and Twentymile Glaciers in 1904; the glaciers of the Wrangell, Skolai, and Chugach Mountains, including Kluvesna, Kennicott, Childs, Miles, Russell, Frederica, and Valdez Glaciers in 1905; Gulkana Glacier in 1910; Kuskulana, Kennicott, and Chitina Glaciers in 1919; Kennicott Glacier in 1922; the glaciers of Prince William Sound, including McCarty, Chenega, and Columbia Glaciers in 1924; the glaciers of Prince William Sound, including Port Nellie Juan, Taylor, Cottrell, Columbia, Kings, Falling, and Contact Glaciers in 1925; Chitistone, Russell, Frederica, Nizina, and Rohn Glaciers in 1927; Kennicott Glacier in 1928, Muldrow Glacier in



1930; Black Rapids Glacier in 1937; and Black Rapids, Jarvis, and Gerstle Glaciers in 1939. Other USGS geologists who took photographs of glaciers in Alaska included Stephen Capps (1908–36), Ernest Leffingwell (1906–14), Alfred G. Maddren (1906–17), Walter C. Mendenhall (1898–1902), John B. Mertie (1911–42), and Sidney Paige (1905 to about 1908). Many of these photographs, a good number of which are archived in the USGS Photographic Library in Denver, Colo., are used in later sections of this report to visually document historic glacier changes throughout the State of Alaska.

In 1905, 1908, and 1909, the USGS investigated the glaciers of Prince William Sound and the southern part of the Kenai Peninsula. Valdez, Shoup, Columbia, and Meares Glaciers were investigated by U.S. Grant and Sidney Paige in 1905. In 1908, Valdez, Shoup, Columbia, and Barry Glaciers, as well as the glaciers of Port Nellie Juan, Icy Bay, Port Bainbridge, and Thumb Cove of Resurrection Bay were investigated by U.S. Grant and D. F. Higgins. In 1909, Grant and Higgins visited and mapped all of the glaciers of the northern shore of Prince William Sound from Port Valdez westward to and including Blackstone Bay and most of the glaciers of the southern shore of the Kenai Peninsula (Grant and Higgins, 1911a, b, 1913). As a result, “All of the tidewater glaciers and many near tidewater were seen and some notes, photographs, and maps were made of all of the tidewater glaciers and many of the others” (Grant and Higgins, 1913, p. 7). The results contain many maps and plates that can be compared with later USGS and American Geographical Society (AGS) maps to document changes in the position of glacier termini.

Of the more than 235 photographs they took, many were published in the 1913 summary of their observations (Grant and Higgins, 1913). Like so many other of their contemporaries, Grant and Higgins realized the significance of systematic, sequential photography of glaciers. “In any study of the positions of glacier fronts, dated photographs are of prime importance, for they furnish accurate records and can be obtained when there is no time for detailed observation. If the photographs are taken from easily recognized stations which can be occupied in later years their value is still greater” (Grant and Higgins, 1913, p. 10). Realizing that documented photographs “will be of so great value in the study of future fluctuations of these ice streams” (Grant and Higgins, 1913, p. 10), they presented systematic lists of photographs available for each glacier studied. In addition to their photographs made in 1908–09, they included photographs by F.C. Schrader in 1898, G.K. Gilbert and W.C. Mendenhall in 1899, A.C. Spencer in 1900, and Sidney Paige in 1905 (Grant and Higgins, 1913).

### **Ralph S. Tarr and Lawrence Martin**

Ralph S. Tarr of Cornell University and Lawrence Martin of the University of Wisconsin were involved in more than half a dozen expeditions to study the glaciers of southeastern and south-central Alaska, concentrating on the areas of Yakutat Bay, Malaspina Glacier, the Copper River, Cook Inlet, the Alaska Peninsula, Controller Bay, and Prince William Sound. Before his death in 1912, Tarr conducted investigations in 1905 and 1906 for the USGS and in 1909 and 1911 for the NGS. In 1904, Martin also worked with the USGS. His 1905 investigations were funded by the AGS. In 1909, 1910 (Martin, 1911), and 1913, his studies were funded by the NGS. Investigations in 1905, 1909 (Tarr and Martin, 1910), and 1911 were performed together.

The rationale they presented for studying Alaska glaciers is still relevant nearly 100 years later: “Alaska offered the best field in the world for these investigations, its glaciers being the largest in the world except those of the polar regions. There are thousands of them and only a few of them even have been named” (Tarr and Martin, 1914, p. vii).

*Alaskan Glacier Studies*, completed by Martin after Tarr’s death in 1912 and published in 1914 (Tarr and Martin, 1914) by the NGS, is their *magnum opus*. The 498-page volume is the most comprehensive treatment of Alaska’s glaciers released before the comprehensive research by William O. Field and

his colleagues in the 1970s (Field, 1975a). Containing 172 numbered plates, many with multiple photographs, 72 text illustrations, a frontispiece, and 10 folded maps in a rear pocket, *Alaskan Glacier Studies* is among the best illustrated glacier books ever produced. A number of other scientific publications (for example, Bean, 1911) and a unique 1:80,000-scale relief model of the Malaspina Glacier region (Martin, 1909) also resulted from their work.

Tarr and Martin (1914) used several innovative graphic approaches to illustrate the physical appearance and size of many Alaskan glaciers, such as superimposing a map of the greater Boston area on a map of the Malaspina Glacier to show the large area that the glacier covered; superimposing the street plan of the greater Washington, D.C. area on a map of the Columbia Glacier to show the area covered by the glacier; combining a scaled image of the U.S. Capitol (fig. 24) and other well-known buildings with the vertical front of a glacier to show the height of the ice terminus, and showing the Hubbard Glacier with three European Alps glaciers superimposed to document its great area and length (Tarr and Martin, 1914, p. 102).

Several thousand photographs resulted from the expeditions. During expeditions after the 1905 expedition, many of the photographs were made by Oscar D. von Engeln, a professional photographer who became a geologist as a result of his involvement in these expeditions (fig. 25). Later, following Tarr's death, von Engeln became Professor of Geomorphology at Cornell University. In 1910, von Engeln published an article in *National Geographic Magazine* providing tips to maximize success in obtaining photographs in Alaska's glacier-covered areas (von Engeln, 1910).

### **Early Aerial Photography of Glaciers by the U.S. Government**

Between 1907 and 1916, James W. Bagley, a USGS topographer, experimented with the use of panoramic cameras for mapping large areas (Bagley, 1917). He used several such cameras in his topographic surveys of Alaska (fig. 26A). Before World War I, Bagley was commissioned by the U.S. Army and assigned the task of developing a multiple-lens camera for mapping surveys from aircraft. This type of multiple-lens camera "is regarded primarily as an instrument which makes use of the principles of plane-table surveying for constructing a map rather than an instrument for picturing the surface of the earth" (Sargent and Moffit, 1929, p. 144). It was this type of camera, referred to as a Bagley T-1 Camera, that would be used for the first systematic aerial photographic survey of Alaska (fig. 26B).

Two U.S. Government aerial photographic expeditions in 1926 and 1929 produced the first vertical aerial photographs of Alaska glaciers (fig. 27). According to R.H. Sargent, Chief Topographer for the Alaska Branch of the USGS and the USGS representative on both expeditions, "It is doubtful whether many exploratory expeditions of late years have contributed so much of financial and scientific value as these two aerial surveys" (Sargent, 1930, p. 145). During the fiscal year 1924–25, funds were identified to pay for a 1926 effort to obtain aerial photographs of 10,000 square miles of Alaska. This survey would "test this new method in regions where large areas are particularly adapted to its success and the common methods are difficult to apply because the country is remote and many parts of it are, at present almost inaccessible" (Sargent and Moffit, 1929, p. 144).

In response to a request from the USGS, the Department of the Navy organized the Alaskan Aerial Survey Expedition in 1926. Under the command of Lt. Ben Wyatt, USN, the 112-man expedition consisted of the tender *Gannet*, four open-cockpit Loening Amphibian biplanes, and a 140-ft-[43-m-] long barge completely equipped to perform all necessary photographic and film-processing operations (fig. 28). Sargent was responsible for selecting the specific areas to be flown, preparing flight lines, and inspecting and transmitting film to the USGS in Washington, D.C. Photographs at a scale of approximately



**Figure 24.**—An example of Tarr and Martin's innovative approach to making information about glaciers understandable to the lay public by depicting part of the terminus of the Childs Glacier with the U.S. Capitol superimposed for scale (Tarr and Martin, 1914, Plate CXLVIII, p. 416).

**Figure 25.**—Oscar D. von Engeln, photographer on the 1910 NGS Alaska Expedition led by Lawrence Martin, washing a strip of negatives in Yakutat Bay sea water, surrounded by icebergs. Photograph from Cornell University archives. Original photograph in National Geographic Society archives, Washington, D.C. (Bendavid-Val and others, 1999).

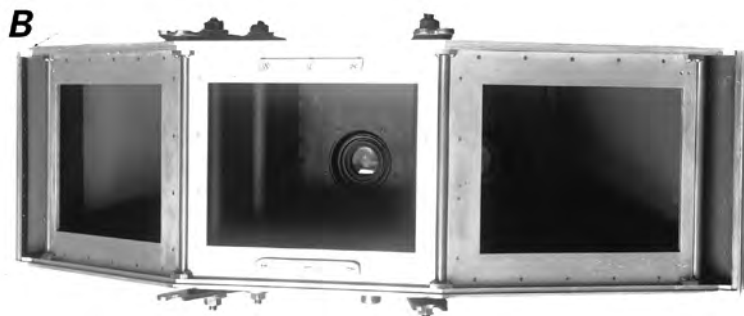
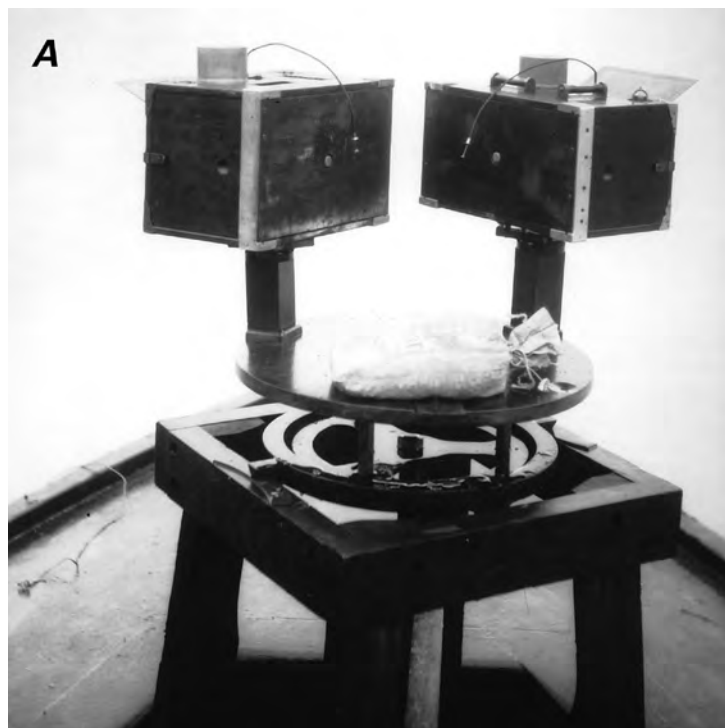


**Figure 26.**—Cameras developed by James W. Bagley, a USGS topographer, for use in Alaskan topographic surveys. **A**, Bagley panoramic camera used by USGS topographers in many Alaskan surveys prior to the First World War. 1926 photograph by R.H. Sargent (see USGS, 1929) from USGS Photographic Library, Denver, Colo.; **B**, Bagley 3-lens T-1 camera used in systematic Alaskan aerial photographic surveys in 1926 and 1929 by the USGS-U.S. Navy Alaska Aerial Survey Expedition. Photograph Moffitt 729 from the USGS Photographic Library, Denver, Colo.



1:20,000 were obtained from an altitude of 10,000 ft [3,050 m] [Editors' note: 6-in (15 cm) focal-length lens] on flight lines of 3.5 miles (5.6 km). In all, 5,760 three-image aerial photographs (a total of 17,280 negatives) were exposed with the Bagley T-1 cameras during the expedition. According to Sargent and Moffit (1929), each triplet includes "a central picture which represents the ground directly under the airplane and two side pictures which represent adjoining areas on each side of the central picture. A set of three pictures thus taken represents an area of about 11 square miles when the plane flies at the preferred elevation of 10,000 ft (3,050 m)" (Sargent and Moffit, 1929, p. 160) (fig. 29). The Bagley T-1 camera was the forerunner of the Trimetrogon camera that was used extensively by the USN in support of the USGS mapping program in Antarctica in 1946–47 (USN *Operation Highjump*) and by the U.S. Air Force in the late 1940s for the USGS mapping program in Alaska.

Among the areas photographed were Admiralty, Annette, Dall, Duke, Etolin, Gravina, Heceta, Kosciusko, Kuiu, Kupreanof, Long, Mitkof, Prince of Wales, Revillagigedo, Sikkwan, Tuxekan, Woronkofski, Wrangell and Zarembo Islands; the Cleveland and Lindenberg Peninsulas; and the area of the Chickamin River. Glaciers are present on Admiralty and Kupreanof Islands and in the headwaters of the Chickamin River.

The 1926 expedition was considered to be so successful that a similar mission was conducted in 1929. Photographing glaciers was one of the highest priorities of this expedition. "It was my purpose to have the fronts of all large glaciers in the region photographed, both by the mapping and the oblique cameras, so as to record the positions of the fronts of the glaciers in 1929. These vertical photographs reveal the phenomenon of glacier flow in a manner never before recorded in the United States. It is believed that there is a wealth of scientific information for the glaciologists in these pictures" (Sargent, 1930, p. 145). The 1929 expedition (fig. 30) produced approximately 7,600 three-image photographs, covering approximately 12,750 mi<sup>2</sup> (33,023 km<sup>2</sup>) of Alaska.

An additional 692 oblique aerial photographs were also taken. Film was exposed at an altitude of 10,900 ft (3,325 m) producing a picture of an area more than 6 mi (9.7 km) wide and about 2½ miles [4 km] in the direction of the flight. Additional Alaskan Aerial Survey Expedition missions by the Navy Department acquired photographs of Alaskan glaciers in 1932 and 1934. The 1934 missions photographed Finger Glacier, La Perouse Glacier, Malaspina Glacier, Icy Bay, and Bering Glacier.

**Figure 27.**—Vertical aerial photograph of North Crillon Glacier (darker surface) flowing into an arm of Lituya Bay and South Crillon Glacier (lighter surface) flowing into both Lituya Bay and Crillon Lake, Fairweather Range, Saint Elias Mountains. It is an example of the type of aerial photography produced by the 1926 and 1929 USGS-US Navy Alaska Aerial Survey Expedition using the Bagley T-1 camera. This photograph was taken in 1929 and is Alaska 177 from the USGS Photographic Library, Denver, Colo.

**Figure 28.**—1926 photograph of Alaska Aerial Survey Expedition operations in Juneau Harbor, showing the stern of the tender Gannet; one of the open-cockpit Loening Amphibian biplanes used to obtain aerial photography; and the stern of the 140-ft-long barge used for photographic and film-processing operations. Photograph Alaska 363 from the USGS Photographic Library, Denver, Colo.



**Figure 29.**—Phototriplet obtained with the Bagley 3-lens T-1 camera on the 1926 Alaska Aerial Survey Expedition (USGS, 1929). This triplet shows a recently deglaciated cirque and valley in the Alexander Archipelago. Photograph Alaska 175 is from the USGS Photographic Library, Denver, Colo.

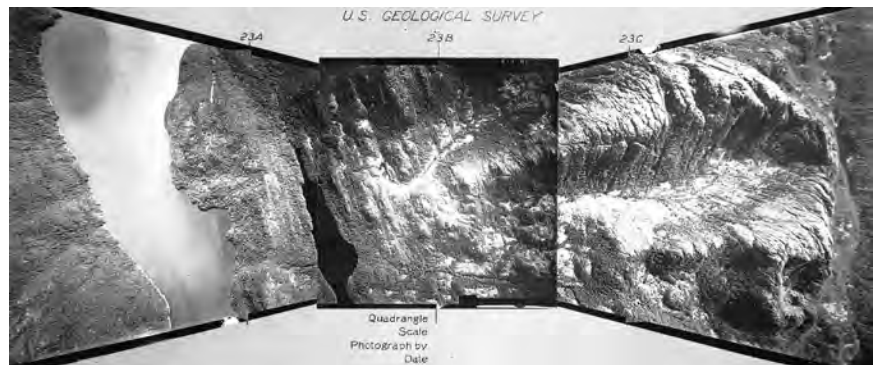


**Figure 30.**—1929 oblique aerial photograph by the Alaska Aerial Survey Expedition of Twin Glaciers, Coast Mountains, northeast of Juneau. The photograph was made from the oblique camera in plane 3. Photograph Alaska 188 is from the USGS Photographic Library, Denver, Colo.



## Later Vertical Aerial Photography Programs

Between 1941 and the late 1950s, several U.S. Government aerial photographic programs produced systematic vertical aerial coverage of many parts of Alaska. Glaciers of the Gulf of Alaska region were photographed with a 9-lens mapping camera (fig. 31) in 1941 and again in 1959 and with the Trimetrogon camera system in 1948. Glaciers in much of the southeastern part of Alaska were photographed with a single-lens vertical camera in a series of U.S. Air Force photographic missions between 1948 and the middle 1950s, all designated by the prefix "SEA." Since the early 1950s, Federal, State of Alaska agencies, and private companies have conducted many vertical photographic missions of Alaska that included glacierized areas. For example, during the 1993–95 surge of Bering Glacier, the USGS, the Bureau of Land Management, and the Department of the Interior's

**Figure 31.**—1959 nine-lens vertical aerial photograph of Fairweather Glacier, St. Elias Mountains. The nine-lens camera, designed by Oliver Reading in the early 1930s, was a state-of-the-art aerial camera used by the U.S. Coast and Geodetic Survey for three decades. The nine-lens system was used to minimize internal distortion in the photography. This camera system was used several other times to photograph the glaciers in southern Alaska. Looking closely at the photograph, it is possible to see the central octagon-shaped image, surrounded by eight joined polygons.



Office of Aircraft Services flew nearly a dozen individual missions to monitor the changes in the terminus region and lower reaches of the glacier.

The most significant aerial photographic program for Alaska began in 1978, when a number of Federal and State of Alaska agencies pooled their resources and initiated an integrated and standardized program, the Alaska High-Altitude Aerial Photography (AHAP) Program to develop a uniform aerial photographic database of Alaska. The purpose of the program was to cover the entire State of Alaska with “a set of unified and coordinated photographs” (Brooks, 1988). By 1986, the last year of data acquisition, 90 percent of Alaska was imaged with both black-and-white and color-infrared vertical aerial photography. The aerial photographs were acquired by a NASA U-2C high-altitude aircraft from 65,000 ft. Black-and-white aerial photography is at a scale of approximately 1:120,000; color-infrared aerial photography is at a scale of approximately 1:65,000. A black-and-white aerial photograph covers an area of about 250 mi<sup>2</sup> (648 km<sup>2</sup>); a color-infrared aerial photograph covers an area of about 64 mi<sup>2</sup> (166 km<sup>2</sup>) (fig. 32). Many of these photographs are used in the later sections of this report to document glaciers throughout Alaska.<sup>4</sup>

### **William Osgood Field**

William O. Field<sup>5</sup> made his first visit to Glacier Bay in 1926. It was the first of many scientific visits to Alaska that would continue for the next six decades. The primary purpose of the 1926 trip was to see how the glaciers in Glacier Bay had changed since last reported by H.F. Reid in 1890 and 1892, H.P. Cushing in 1891, and G.K. Gilbert in 1899 (Field, 1926). Field recorded the glacier terminus positions throughout Glacier Bay, including the spectacular find that Johns Hopkins Glacier had retreated 6 to 7 miles from where it had last been seen in 1912. In 1931, Field visited glaciers in Prince William Sound to reoccupy photo-survey stations established by Lawrence Martin in 1909, 1910, and 1911, by Grant and Higgins in 1905, 1909, and 1910, and by Gilbert and Gannett during the 1899 Harriman Expedition. In 1935, Field returned to both Glacier Bay and Prince William Sound, the beginning of systematic repeated measurements and photographs of glacier termini in both places. His last field trip to Glacier Bay was in 1982 and to Prince William Sound in 1976, but his son J.O. Field and C.S. Brown reoccupied his photo stations in Glacier Bay in 1989, 1994, 1997, and 2000 to continue his legacy. Many of Field’s photo stations were revisited in 2003 and 2004 by a joint USGS-U.S. National Park Service (NPS) expedition led by the author. His photographs and observations comprise the largest ground-based photographic data base on the changes in Alaska glaciers in existence. Field also established numerous survey/photographic stations that were reoccupied, often in successive years. The result was numerous publications documenting glacier variations (for example, Field, 1942, 1948; for a complete list, see Field’s (2004) appendix B) and a series of maps that systematically depicts changes in the positions of individual glaciers (figs. 33, 34). Field was unique in that he personally knew many of the pioneer scientists/explorers who visited Alaska around the turn of the 20th century. A link to these pioneers and to their early work in glaciology (Field, 2004), Field collected many of their photographs, which, together with all of his photographs and other materials, are housed in the Archives of the Alaska and Polar Regions Department in the Elmer E. Rasmuson

---

<sup>4</sup> The AHAP aerial photographs are archived at the USGS EDC in Sioux Falls, SD and at the GeoData Center, Geophysical Institute, University of Alaska, Fairbanks, AK (<http://www.gi.alaska.edu/services/geodata/>). AHAP photographs are archived at the GeoData Center by flight line and frame number (for example, L185F4825). The 3-digit L number could not be found for a few photographs; LXXX is used to indicate missing data.

<sup>5</sup> The editors appreciate the contribution to this section by C Suzanne Brown, formerly with the USGS. Her long professional association with William O. Field, her extensive knowledge of his published and unpublished work on Alaska’s glaciers, and her recently published, richly illustrated, oral biography of him (Field, 2004) have been of enormous help.

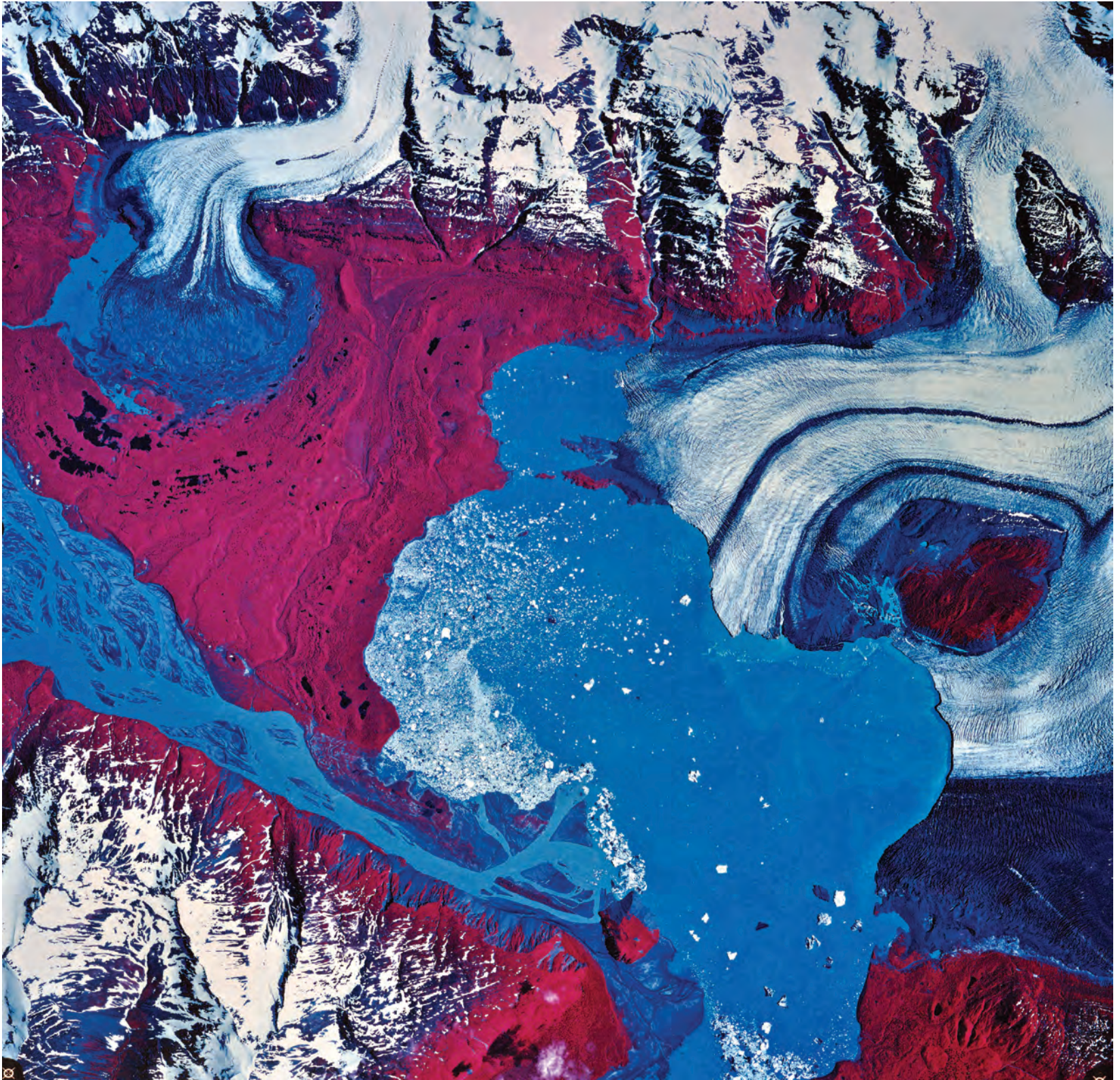


**Figure 32.**—NASA high-altitude, false-color infrared vertical aerial photograph (Kodak SO-193 film with a Wratten 12 filter) of Alsek River and part of the terminus of Alsek Glacier, southeast of Yakutat, Alaska. The photograph (1:65,000-scale) was acquired by a National Aeronautics and Space Administration Ames U-2C aircraft on 21 June 1978 from an altitude of 19,800 m, with an RC-10 camera having a 305-mm

(12 in) focal length, in support of the interagency Alaska High-Altitude Aerial Photograph Program (AHAP). The spectral range of the film-filter combination is 0.51 to 0.90  $\mu\text{m}$ . Aerial photograph is from the USGS EROS Data Center, Accession No. 578002618 ROLL, frame 4898; or AHAP photograph no. L170F4898 from the GeoData Center, Geophysical Institute, University of Alaska, Fairbanks, Alaska.



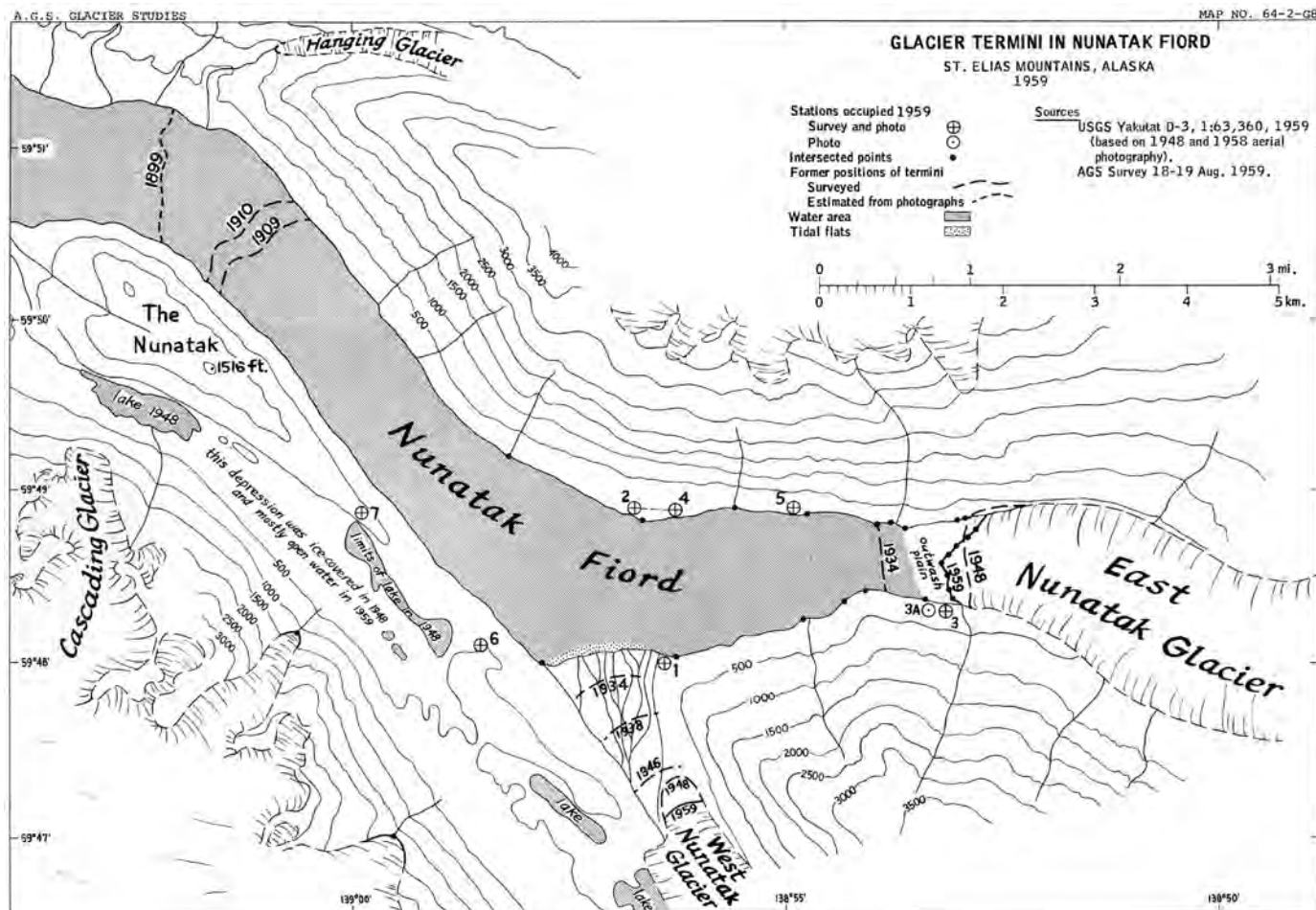
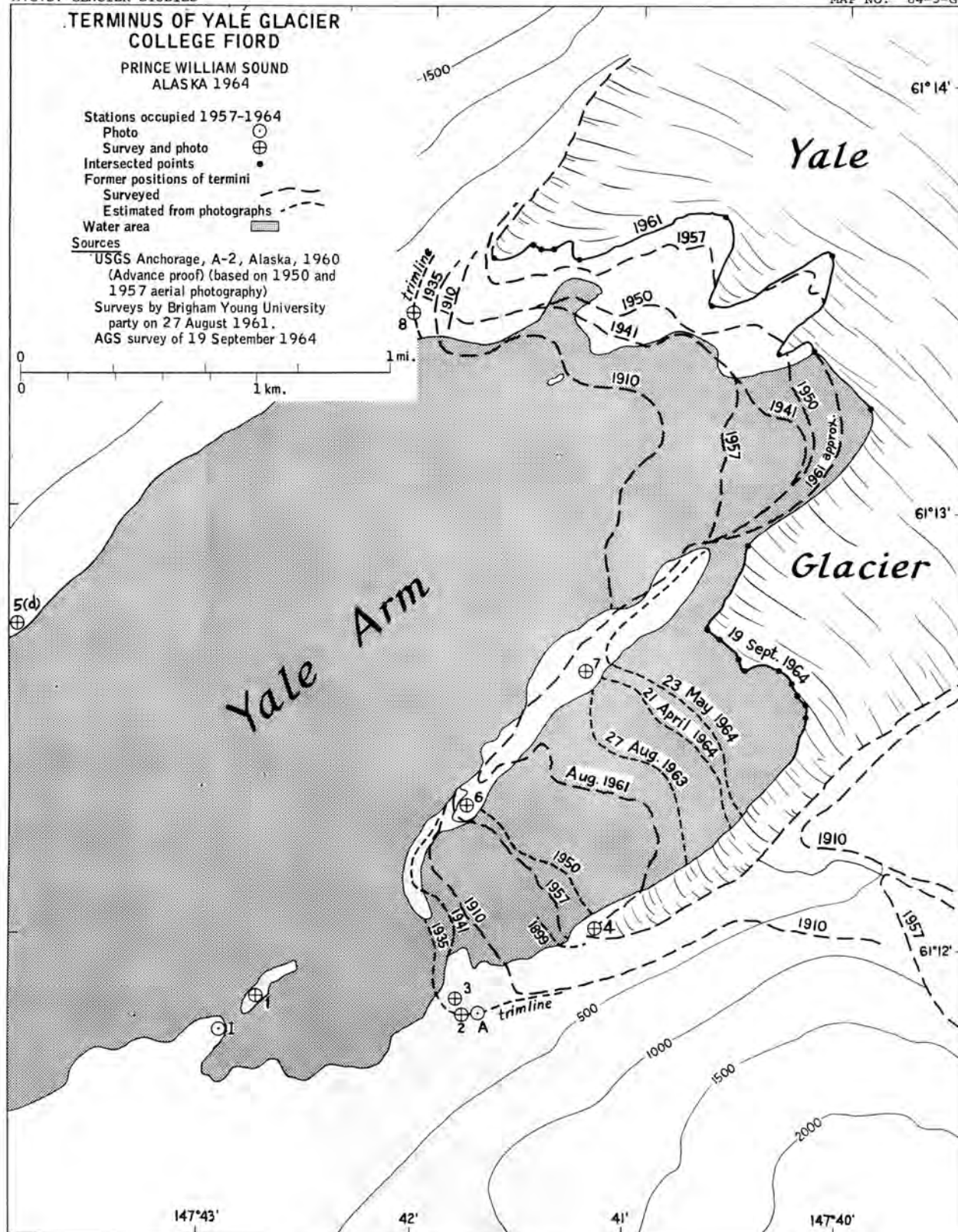


**Figure 33.**—American Geographic Society Glacier Studies Map 64-2-G8 compiled by W.O. Field in 1959, showing the chronology of changes in the position of glacier termini in Nunatak Fiord, St. Elias Mountains, between 1899 and 1959.

Library at the University of Alaska Fairbanks. He also bequeathed funds to the University of Alaska: (1) to fund the cataloging of his extensive archive of photographs (more than 100,000) and (2) to establish an endowment to support continued research on changes in the glaciers of Glacier Bay National Park and Preserve.

In 1940, Field began working for the American Geographical Society (AGS) in New York City (Morrison, 1995). According to Mel Marcus, “As glaciology developed [in America] in the 1950s culminating in the International Geophysical Year (IGY) in 1957–58, Field’s office was an informal, de facto headquarters for the discipline” (Field, 2004). In 1956, the Technical Panel on Glaciology of the International Geophysical Year (IGY), chaired by Field, recommended that “one of the most useful contributions of the IGY to glaciology would be the preparation of precise maps, on large scales, of selected small glaciers” (American Geographical Society, 1960). The rationale for the project was that “the maps would form a permanent record of the condition of these glaciers so that at a future date they could be resurveyed and compared” (American Geographical Society, 1960). With funding from the National Science Foundation (NSF), Field selected a number of “simple unbranched” valley glaciers ranging from 5 to 8 km in length. Logistical planning was provided by Austin Post. The AGS Glacier Mapping Project ultimately produced 1:10,000-scale maps using photogrammetric and field methods for Lemon Creek, Polychrome, West Gulkana, Worthington, Little Jarvis (fig. 35), Salmon Creek (given the official name of Bear Lake Glacier in 1959), Kilbuck (now known as Chikuminuk Glacier, although Kilbuck Glacier is still recognized as an official variation), and McCall Glaciers in Alaska and Blue Glacier in Washington. The map of Little Jarvis Glacier (fig. 35) is an example of an AGS map produced during the IGY. In the 1980s, Lemon Creek and West Gulkana



Glaciers were resurveyed by teams led by Mel Marcus (Marcus and Reynolds, 1988; Marcus and others, 1995). Between 1993 and 1996, all eight Alaska glaciers mapped by the AGS were remapped by Sapiano and others (1998) using airborne surface-elevation, laser-altimeter profiling augmented with global-positioning system (GPS) methods. Elevation, volume, and terminus changes were determined for each glacier. The results of this remapping are presented in later sections of this report. In 1975, Field published *Mountain*

**Figure 34.**—American Geographical Society Glacier Studies Map 64-3-G7 compiled by W.O. Field in 1964, showing the chronology of changes in the position of glacier termini in Yale Arm, Prince William Sound, between 1910 and 1964.

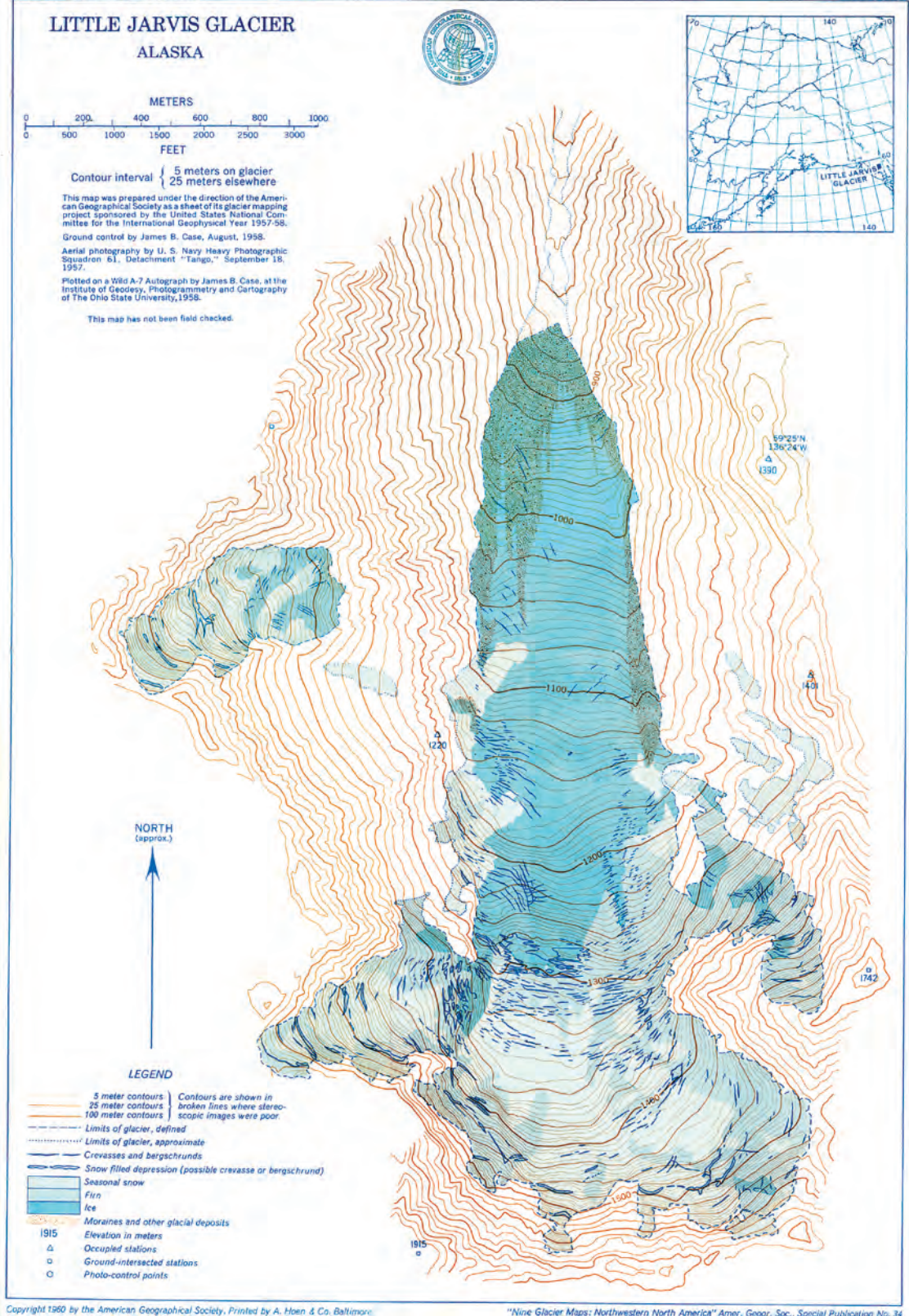


**Figure 35.**—Copyrighted map of Little Jarvis Glacier, Alaska, produced by the American Geographical Society (1960) as part of its Glacier Mapping Project 1960, as a contribution to the International Geophysical Year 1957–58. It is based on 18 September 1957 vertical aerial photographs. Used

with permission. In addition to the Little Jarvis Glacier, seven other glaciers in Alaska—Lemon Creek, Polychrome, West Gulkana, Worthington, Bear Lake, Chikuminuk, and McCall Glaciers—were mapped as well as Blue Glacier in Washington. All maps were produced at 1:10,000 scale.

*Glaciers of the Northern Hemisphere*, a three-volume set complete with an atlas of maps (Field, 1975a). This work is the most comprehensive summary of the glaciers of Alaska and other glaciers of the Northern Hemisphere; the regional maps in the atlas by Field (1975a) are reproduced in each geographic section of this chapter.

### **Bradford Washburn**

In the early 1930s, Bradford Washburn began photographic reconnaissances of Alaska mountains as a prelude to many of his climbing expeditions. His black-and-white photographs are famous for their artistic quality, documentation of glacial and fluvio-glacial processes, and historic record of the position of termini and margins of many Alaskan glaciers. Washburn's negatives and prints are archived at the Elmer E. Rasmuson Library, University of Alaska (Fairbanks), and at the Museum of Science (Boston). Many of his photographs are included in this chapter. A comparison of his large-format (23×23 cm) oblique aerial photographs with those taken later by Austin Post and Robert M. Krimmel, two other superb aerial photographers of Alaska's glaciers, visually document many changes. Many of his photographs include some of the earliest aerial observations of glaciers in the Fairweather Range, St. Elias Mountains, Chugach Mountains, and Alaska Range. In 1933 and 1934, Washburn photographed the glaciers of the Fairweather Range between Finger Glacier and Malaspina Glacier. In 1937, he photographed Lituya Bay and Fairweather Glacier; in 1938, he photographed the area between Yakutat Bay and Bering Glacier (fig. 36), including the Malaspina Glacier (fig. 37) and the Barnard Glacier (fig. 38) north of the Chitina River. In 1935, much of his aerial photography was north of the Alaskan border in Canada's Yukon Territory, but he did conduct a dog-team survey of Alaska's Art Lewis and Nunatak Glaciers. In 1941, he photographed the Susitna Glacier. Support for these photographic expeditions was provided by the NGS. Washburn returned to Alaska many times thereafter, continuing to photograph glaciers at a number of locations. In 1966, he rephotographed the Malaspina Glacier and conducted a photographic survey of the Mount Hubbard-Mount Kennedy area for the NGS (Washburn, 1971a, b) that was the basis for a superb

**Figure 36.**—1938 oblique aerial photograph of the southeastern terminus of Bering Glacier, Chugach Mountains, looking west-northwest. Photograph courtesy of Bradford Washburn, Museum of Science (Boston, Mass.). This image is the earliest known aerial photograph of the Bering Glacier.



**Figure 37.**—Oblique aerial photograph of contorted medial moraines (“marble-cake”) of Malaspina Glacier, Saint Elias Mountains, taken in August 1938. Photograph (negative no. 5742) courtesy of Bradford Washburn, Museum of Science (Boston, Mass.).



**Figure 38.**—Oblique aerial photograph of an array of subparallel medial moraines on the Barnard Glacier and tributary glaciers, Saint Elias Mountains, taken in August 1938. Photograph (negative no. 1355) courtesy of Bradford Washburn, Museum of Science (Boston, Mass.). Compare also with figure 181.

map (Williams and Ferrigno, 2002, fig. 5). A recently published biography of Washburn documents his extensive use of photography in his Alaskan expeditions (Sfraga, 2004).

## **Austin Post**

From 1960 through 1983, Austin Post, first with the University of Washington and later with the USGS, conducted annual photographic missions to document changes in glaciers. Post received his introduction to “organized aerial photography of glaciers in western North America” (Post and LaChapelle, 1971, p. i; 2000, p. xii), from Richard C. Hubley of the University of Washington. In 1955, Hubley conducted a photo reconnaissance of the North Cascade Mountains. During the IGY, Post was involved in planning the logistics of the *AGS Glacier Mapping Project*, which included obtaining black-and-white aerial photography of the glaciers to be mapped.

Beginning in 1960, Post began a systematic aerial photographic effort, the *Program for Aerial Photographic Surveying of Glaciers in Western North America*. The first 3 years of the program were funded by the NSF and administered by the Department of Meteorology and Climatology, University of Washington. The primary focus of the program was the glaciers of southeastern and south-central Alaska. However, glaciers in the Alaska Range, the Alaska Peninsula, and the Wrangell Mountains, as well as glacierized mountain ranges of the Western United States and Canada, were also photographed. After the end of the 1963 collection year, the program was nearly terminated. However, the value of photographing Alaskan glaciers annually was confirmed by the numerous photographs (see fig. 229C) made in the years immediately following the Great Alaska Earthquake of [27 March] 1964. Post writes that “After the quake, Mark F. Meier, Director of the U.S. Geological Survey’s Glaciology Project Office in Tacoma, Washington wanted me to continue the photography and record changes resulting from the shaking. Again, so many interesting things were observed that Mark continued this program the next year, and two years later, after a monumental effort, actually obtained for me a professional position with the Survey” (Post, 1995, p. 19).

During the first decade of the program, Post used aircraft of opportunity, flying with William R. Fairchild and many well-known Alaskan bush pilots. Beginning in the early 1970s, many photo missions were conducted in cooperation with Robert M. Krimmel, USGS glaciologist and pilot; Krimmel frequently piloted the aircraft. Typically, both vertical and oblique photographs were made on each flight. In all, about 100,000 negatives were exposed. Many of these aerial photographs are used in the geographic-area sections of this report to document glacier changes throughout the State of Alaska. Post’s aerial photographs are archived at the GeoData Center, Geophysical Institute, University of Alaska, Fairbanks [<http://www.gi.alaska.edu/>]. The reader is also referred to Post and LaChapelle’s (1971, 2000) superbly illustrated book on *Glacier Ice*, an excellent compilation of large-format black-and-white photographs of glaciers in Alaska and other glacierized regions on Earth.

## **Robert M. Krimmel**

Robert M. Krimmel, who has already been mentioned in the previous section as one of the pilots of aircraft used by Austin Post to acquire aerial photographs of glaciers in Alaska, the western United States and western Canada, also has a distinguished two-decade record (1984–90) of acquiring large-format (23×23 cm) black-and-white oblique aerial photographs of glaciers in Alaska, the United States, and Canada. Many of his superb photographs, which he took in 1984, 1986, 1988, and 1990, are reproduced in this chapter.

## Ground, Vertical, and Oblique Aerial Photographs by Other USGS Glaciologists

Three other USGS glaciologists have also been active in long-term photographic documentation of Alaska's glaciers: Lawrence C. Mayo (Fairbanks, Alaska), Dennis C. Trabant (Fairbanks, Alaska), and Bruce F. Molnia (Reston, Va). Mayo and Trabant have extensive archives of ground photographs of Alaskan glaciers from several decades of field work in Alaska, especially annual mass-balance studies of Wolverine, Black Rapids, and Gulkana Glaciers, and rapid recession of the Columbia Glacier. In addition, Molnia's multiyear investigations of Bering Glacier have produced a large volume of ground and oblique aerial photography.

For 36 years (beginning in 1968), Molnia photographed and imaged, on the ground and from the air, glaciers of the Coast, St. Elias, and Chugach Mountains (initially using a 35-mm single-lens, reflex camera and later a digital camera). Beginning in 1974, as part of a U.S. Government assessment of the impact of oil and gas activities in the Gulf of Alaska region, he began aerial and ground-based glacier photography that has produced more than 15,000 small-format (35-mm) color photographs. Areas of geographic emphasis include Bering and Malaspina Glaciers, Icy and Glacier Bays, and the Juneau Ice Field. Many of these small-format color, oblique aerial photographs are used in the geographic-area sections of this report. *Alaska's Glaciers* (Molnia, 1982, 1993, 2001), a summary of the distribution and history of investigation of many of Alaska's glaciers, contains small-format color photographs of about 100 Alaskan glaciers. In the late 20th century and early part of the 21st century, Molnia added digital imagery to the documentation of Alaska's glaciers. In 2003, in a partnership between the USGS, Alpha DVD, and the Alaska Geographic Society, *Glaciers: Alaska's Rivers of Ice*, a DVD about glaciers and glacier terminology, was published (Alpha DVD, 2003).

## Part 2—Glaciological Topics

### Tidewater Glaciers

Of the tens of thousands of glaciers in Alaska, only about 0.1 percent end in the ocean, in the glacial-marine environment (Molnia, 1983a). These glaciers are known as tidewater glaciers, a term introduced by Russell (1893) and defined as “glaciers which enter the ocean and calve off to form bergs.” A similar definition, a “glacier that terminates in the sea, where it usually ends in an ice cliff from which icebergs are discharged,” is given in the *Glossary of Geology* (Jackson, 1997, p. 665). According to Mark F. Meier (written commun., 2004) all of Alaska’s tidewater glaciers are grounded at their beds (a criterion included in the Meier and Post, 1987, definition of a tidewater glacier). Meier also noted that tidewater glaciers are not to be confused with “floating glaciers,” such as ice tongues and ice shelves. A discussion of “ice walls” (grounded glacier ice) and “ice fronts” (floating glacier ice) is given by Swithinbank (1988, p. B4, <http://pubs.usgs.gov/prof/p1386b/>). Today the ocean-terminating tidewater glaciers are termed marine tidewater glaciers to distinguish them from an even larger group of lacustrine-terminating calving glaciers.

Calving is defined as the “breaking away of a mass or block of ice from a glacier” (Jackson, 1997, p. 92). In tidewater glaciers, the rate of calving controls the glacier’s length much more than climate. “Calving glaciers” lose most of their mass by calving rather than by surface melting. Typically, the terminus of a marine tidewater calving glacier has a steep, near-vertical to vertical face characterized by significant fracturing and the presence of seracs (fig. 39). Rapid calving often produces amphitheater-shaped embayments, some many hundreds of meters in diameter in the face (fig. 40). In some glaciers, the rate of calving and the volume of ice calved are so great, that no open water can be seen in front of the glacier margin.

Tidewater glaciers can exhibit rapid changes in terms of the speed of advance and retreat of their termini and the flow of glacier ice. Hubbard Glacier, which retreated through much of the “Little Ice Age,” has been advancing for more than 100 years. Molnia and Post (1995) reported that, between 1967 and 1993, Bering Glacier had retreated as much as 10.7 km (an average of approximately 450 m a<sup>-1</sup>, with a maximum retreat of 2,600 m between 1977 and 1978).

From a detailed analysis of topographic maps and aerial photography, Viens (1995) determined that there were 51 Alaskan tidewater glaciers and 9 former tidewater glaciers (fig. 41). Some of the tidewater glaciers, like the Columbia Glacier, produce large quantities of icebergs. Some, like Muir Glacier, no longer make contact with the sea at present. The 60 present and former tidewater glaciers have a combined area of about 27,000 km<sup>2</sup>, approximately 36 percent of the glacierized area of Alaska. Table 2 is a compilation of information presented by Viens (1995) on the length, total area, accumulation area, ablation area, and accumulation area ratio (the accumulation area divided by the total area of the glacier at the end of the balance year or AAR) of each of the 60 tidewater glaciers that he characterized. Even though some tidewater glaciers may have AARs (see tables 2 and 3) of greater than 0.93, they still are retreating because of calving. Details about the behavior of individual tidewater glaciers will be described by geographic region in the sections that follow.

**Figure 39.**—15 July 1979 photograph of the 60-m-high terminus of Muir Glacier, St. Elias Mountains, which was a calving tide-water glacier at that time. The steep vertical face characterized by significant fracturing and the presence of seracs is typical of tidewater calving glaciers. Photograph by Bruce F. Molnia, U.S. Geological Survey.





**Figure 40.**—Oblique aerial photograph of the central terminus of Bering Glacier in Vitus Lake, Chugach Mountains, on 16 August 1998. The amphitheater-shaped embayment produced by the rapid calving retreat of the terminus is about 2 km in diameter. Photograph by Bruce F. Molnia, U.S. Geological Survey.

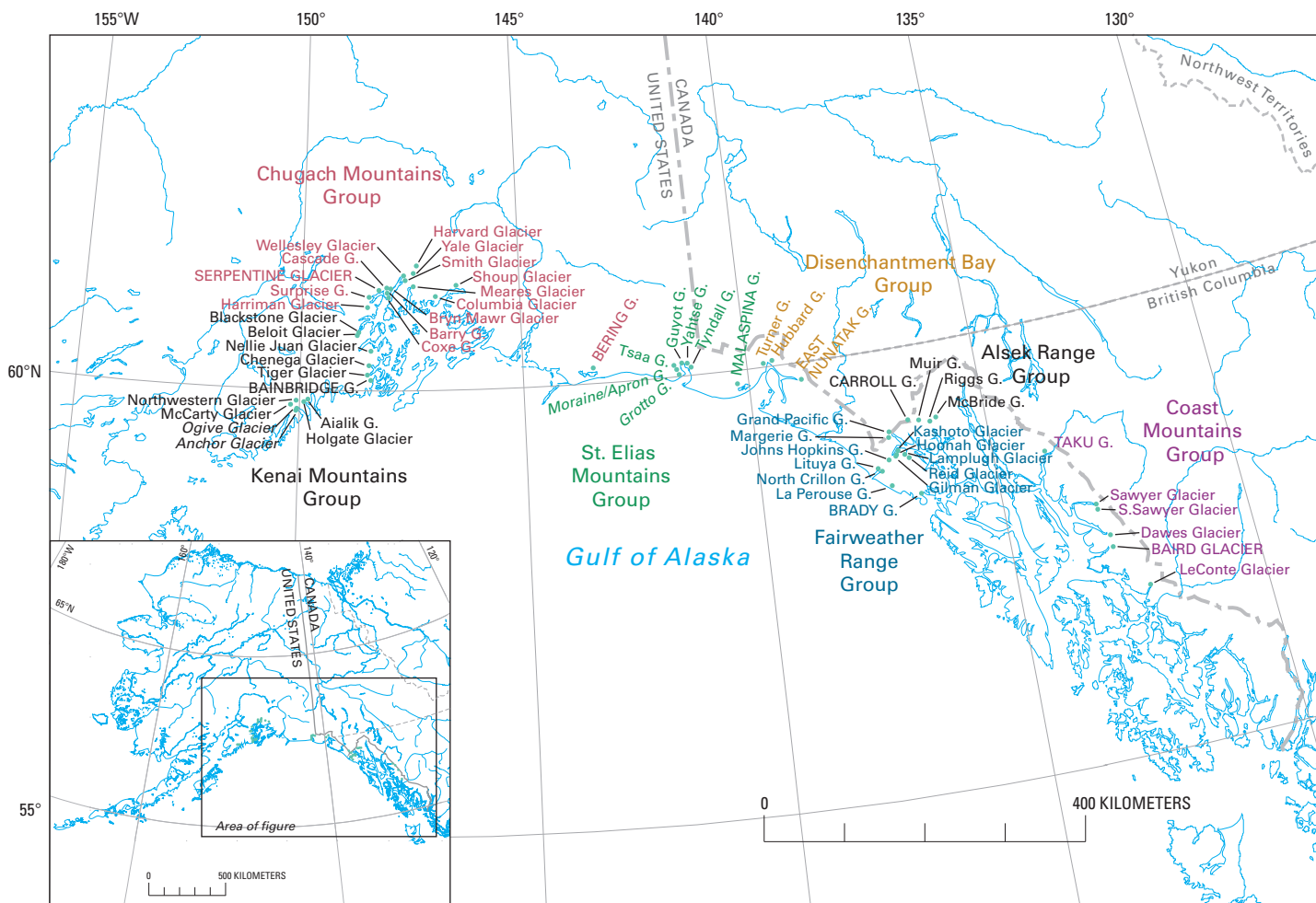


**Figure 41.**—Map of active and former tidewater glaciers of Alaska compiled by the editors using glaciers selected by Viens (1995). G indicates glacier. Glacier names in italics have not been approved by the U.S. Board on Geographic Names. Glaciers shown in capital letters were previously classified as tidewater glaciers (tables 2, 3).

## Columbia and Hubbard Tidewater Glaciers

By ROBERT M. KRIMMEL<sup>6</sup>

### Introduction

Glaciers that flow into the ocean are known as tidewater glaciers. Figure 41 shows the active and former tidewater glaciers found in Alaska, according to Viens (1995) and Krimmel (tables 2, 3). Some tidewater glaciers, including Columbia Glacier, produce large numbers of icebergs by calving; others barely reach the sea. In Alaska, all tidewater glaciers are grounded on their beds. Loss of mass by calving may exceed the loss of mass by melting by several orders of magnitude in some of the larger and more active tidewater glaciers. Nearly all tidewater glaciers in Alaska have undergone large-scale asynchronous advance and retreat (fig. 42A–D). Apparently, this behavior is not related directly to climatic variations.

The primary influence on the stability of tidewater glaciers was first suggested by Post (1975) as the water depth at the calving face; calving speed is related directly to water depth—slow in shallow water and faster in deep water. According to Mark F. Meier (written commun., 2004), the validity of this relatively simple concept has been questioned by Van der Veen (1996, 1997b) who suggests that the relationship is more complex. Advancing tidewater glaciers end on a terminal-moraine shoal consisting of unconsolidated material that nearly fills the fjord at the glacier front. Measured water depths near the calving faces of stable and advancing glaciers have been found to be generally less than about 80 m, in comparison with several hundred meters of water in the fjord beyond the shoal (Brown and others, 1982).

On a time scale of hundreds of years, tidewater glaciers advance by moving their submarine terminal moraines down the fjord (fig. 42B). The moraine is not simply pushed. The moraine is advanced by glacial erosion of material on the upstream side and redeposition on the downstream side. The deposition produces a series of foreset beds. Foreset bedding has been observed by subbottom sounder profiling (Meier and others, 1978), which supports this theory of moraine advance. The rate of advance of the terminal moraine is slow (rarely more than a few tens of meters per year) in deep fjords and is controlled by the amount of morainal material that must be moved to maintain relatively shallow water at the calving face. An advance generally continues until the glacier becomes increasingly sensitive to external influences, including climate variations, that may cause it to retreat from its moraine shoal (fig. 42C).

Drastic retreat of a tidewater glacier normally begins when a small recession from the shoal causes its terminus to recede into deeper water behind the crest of the terminal moraine (fig. 42D) (Meier and Post, 1987). Because calving speed may be directly related to the water depth at the terminus (Brown and others, 1982), a retreat into deeper water stimulates an increase in calving speed. Instability develops when the calving speed becomes greater than the ice speed and the retreating calving front moves into even deeper water. Drastic retreat ends when the terminus recedes into shallow water, normally at the head of the fjord (fig. 42A). The rate of retreat can be a kilometer or more per year—many times faster than the rate of advance. In most cases, as tidewater glaciers drastically retreat, the AAR increases as the ice in the ablation area is discharged as icebergs. Thus, tidewater glaciers ending near the heads of fjords frequently have high AAR's, whether they are advancing or retreating. Readvance, following a drastic retreat, begins when there is enough morainal material at the calving face to maintain a terminal moraine shoal as the calving face advances into the fjord (fig. 42B, C). Calving speed is then less than the ice-flow speed.

---

<sup>6</sup>U.S. Geological Survey, 1201 Pacific Avenue–Suite 600, Tacoma, WA 98402

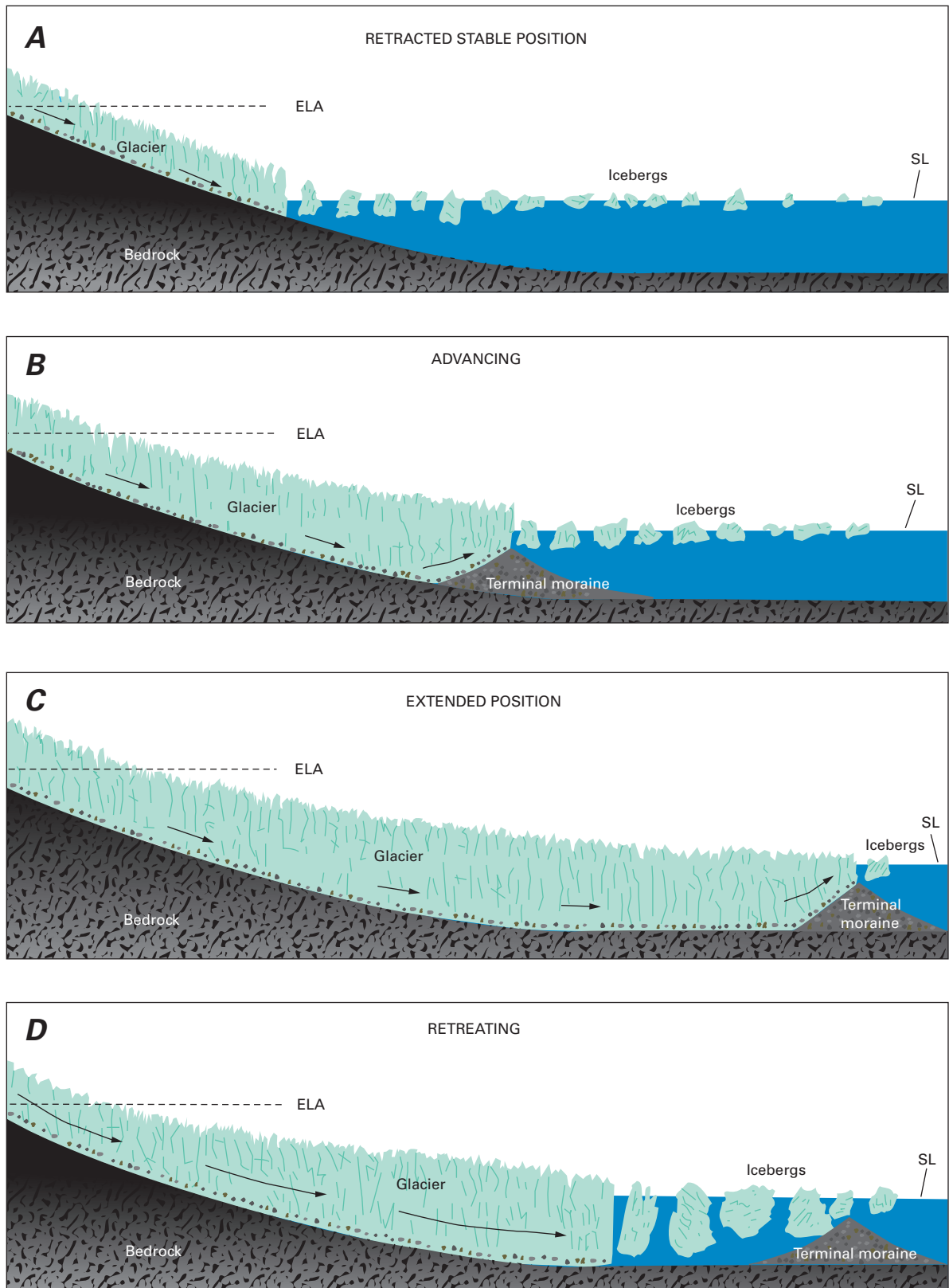


**Figure 42.**—Tidewater-glacier cycle (from Trabant and others, 1990). Cross sections in A through D show four phases in the cycle. **A** shows the beginning and end of the cycle, when the glacier is located at the head of the fjord. **B** illustrates the advancing glacier moving the terminal moraine down fjord; and **C** the fully extended phase. **D** shows the retreat-

ing phase of the cycle, in which icebergs are much larger than those calved in the other three phases. The stable equilibrium line altitude (ELA) indicates that the tidewater-glacier cycle is relatively independent of climate change. Eustatic sea level (SL) is also stable.

TABLE 2.—*Glaciological characteristics of existing (1–51) and former (52–60) tidewater glaciers of Alaska*  
 [Data in this table are from Viens (1995); \* informal name proposed by Viens (1995). AAR, Accumulation area ratio.]

	Glacier name	length (km)	Total area <sup>2</sup> (km <sup>2</sup> )	Accumulation area <sup>3</sup> (km <sup>2</sup> )	Ablation area (km <sup>2</sup> )	AAR
1.	McCarty	19.3	111	88	23	0.79
2.	Northwestern	12.1	60	54	6	0.89
3.	<i>Anchor*</i>	4.8	7	5	2	0.77
4.	<i>Ogive*</i>	6.8	9	6	2	0.73
5.	Holgate	12.9	69	63	6	0.92
6.	Aialik	12.9	70	62	8	0.88
7.	Chenega	24.1	369	346	23	0.94
8.	Tiger	11.3	56	50	6	0.89
9.	Nellie Juan	14.5	56	51	5	0.91
10.	Blackstone	12.1	32	29	2	0.92
11.	Beloit	10.1	25	24	1	0.95
12.	Harriman	12.9	60	48	13	0.79
13.	Surprise	12.1	80	64	16	0.80
14.	Barry	26.5	95	70	25	0.74
15.	Cascade	8.0	15	14	2	0.89
16.	Coxe	11.3	20	15	5	0.74
17.	Smith	9.7	20	16	4	0.81
18.	Bryn Mawr	7.6	26	22	4	0.84
19.	Wellesley	7.2	16	12	4	0.78
20.	Harvard	39.4	524	423	101	0.81
21.	Yale	32.2	194	153	41	0.79
22.	Mearns	25.7	142	121	20	0.86
23.	Columbia	59.5	1,121	753	368	0.67
24.	Shoup	29.0	156	95	62	0.61
25.	Grotto-Moraine Apron	9.7	42	33	9	0.78
26.	Grotto-Moraine Apron		included in 25			
27.	Grotto-Moraine Apron		included in 25			
28.	Tsaa	20.9	150	144	70	0.96
29.	Guyot-Yahtse	64.4	1,432	1,368	64	0.96
30.	Guyot-Yahtse		included in 29			
31.	Tyndall	23.3	154	129	25	0.84
32.	Turner	31.8	186	150	36	0.81
33.	Hubbard	114.2	3,865	3,699	166	0.96
34.	Lituya	20.9	103	78	25	0.76
35.	North Crillon	20.1	71	57	13	0.81
36.	La Perouse	25.7	147	98	49	0.67
37.	Margerie	33.8	174	143	31	0.82
38.	Grand Pacific	60.3	654	459	195	0.70
39.	Reid	16.9	49	31	18	0.64
40.	Lamplugh	32.2	171	145	25	0.85
41.	Gilman	12.1	35	31	4	0.88
42.	Johns Hopkins	22.5	316	283	33	0.90
43.	Kashoto	4.7	5	5	<1	0.94
44.	Hoonah	6.9	12	10	1	0.88

TABLE 2.—*Glaciological characteristics of existing (1–51) and former (52–60) tidewater glaciers of Alaska*

Glacier name	length (km)	Total area <sup>2</sup> (km <sup>2</sup> )	Accumulation area <sup>3</sup> (km <sup>2</sup> )	Ablation area (km <sup>2</sup> )	AAR
45. Muir	26.5	148	112	37	0.75
46. Riggs	24.9	126	91	35	0.72
47. McBride	24.1	143	84	59	0.59
48. Sawyer	37.4	399	289	110	0.72
49. South Sawyer	49.9	683	530	153	0.78
50. Dawes	37.0	653	450	203	0.69
51. LeConte	36.2	472	438	34	0.93
52. Bainbridge	16.0	56	39	17	0.70
53. Serpentine	10.0	30	21	9	0.70
54. Bering	191.0	5,173	3,213	1,961	0.62
55. Malaspina	108.0	5,008	2,575	2,433	0.51
56. Nunatak	34.0	312	182	131	0.58
57. Brady	51.0	590	382	208	0.65
58. Carroll	49.0	527	387	140	0.73
59. Taku	60.0	831	728	102	0.88
60. Baird	50.0	784	527	257	0.67

<sup>1</sup> Multiple appearances of the same name (that is, Grotto-Moraine Apron and Guyot-Yahrtse) indicate a single glacier with more than one tidewater face.

<sup>2</sup> Total area of the 60 tidewater glaciers is 26,834 km<sup>2</sup> or approximately 35 percent of the glacierized area of Alaska

<sup>3</sup> Total accumulation area of the 60 tidewater glaciers is 19,821 km<sup>2</sup>.

<sup>4</sup> The average AAR for these 60 glaciers is 0.74.

TABLE 3.—*Terminus status of major tidewater glaciers of Alaska in 1999 (with status in 2004 added for selected glaciers)*

[See figure 41, this volume. na, not available.]

Glacier	Lat. (N) <sup>1</sup>	Long. (W) <sup>1</sup>	Area (km <sup>2</sup> ) <sup>1</sup>	Median ELA (m amsl) <sup>1,2</sup>	Terminus position <sup>1,3</sup>	Status of terminus in 1999 (from Robert M. Kimmel, except where noted)	Terminus status in 2004 <sup>3,6</sup>
<b>Kenai Mountains Group</b>							
McCarty	59°50'	150°13'	111	991	Advance rate decreased between 1985 and 1995	Very slow advance since 1960 in shallow water at head of McCarty Fiord	Ret.
Northwestern	59°52'	150°5'	60	976	R	Stable at head of Northwestern Fiord	Ret.
Anchor <sup>1</sup>	59°46'	150°5'	7	991	na	Stable <sup>1</sup>	Slowly Ret.
Ogive <sup>1</sup>	59°47'	150°5'	9	1,204	na	Stable <sup>1</sup>	Slowly Ret.
Holgate	59°52'	149°54'	69	610	R	Stable at head of Holgate Arm	Slowly Ret.
Aialik	59°53'	149°49'	70	732	R	Stable at head of Aialik Bay	–
Bainbridge <sup>5</sup>	60°7'	148°27'	565	5645	R <sup>4</sup> , FTW <sup>5</sup>	Stable <sup>5</sup>	–
Tiger	60°11'	148°30'	56	518	R	Stable at head of Icy Fiord	–
Chenega	60°17'	148°28'	369	534	R	Stable at head of Nassau Fiord	Slowly Ret.
Nellie Juan	60°26'	148°25'	56	396	I	Drastic retreat in narrow inlet, Derickson Bay	–
Blackstone	60°39'	148°44'	32	503	R	Stable at head of Blackstone Bay	Slowly Ret.
Beloit	60°38'	148°43'	25	473	R	Stable at head of Blackstone Bay	Slowly Ret.
<b>Chugach Mountains Group</b>							
Harriman	60°56'	148°31'	60	427	I	Extended position on moraine exposed at low tide in Harriman Fiord	Slowly Adv.
Surprise	61°3'	148°29'	80	854	R	Stable at head of Surprise Inlet	Slowly Ret.
Cascade	61°8'	148°12'	15	945	I	Stable on beach, Harriman Fiord	Slowly Ret.
Coxe <sup>1</sup>	61°8'	148°3'	20	1,006	R	Stable <sup>1</sup>	Slowly Ret.

TABLE 3.—Terminus status of major tidewater glaciers of Alaska in 1999 (with status in 2004 added for selected glaciers)

Glacier	Lat. (N) <sup>1</sup>	Long. (W) <sup>1</sup>	Area (km <sup>2</sup> ) <sup>1</sup>	Median ELA (m amsl) <sup>1,2</sup>	Terminus position <sup>1,3</sup>	Status of terminus in 1999 (from Robert M. Kimmel, except where noted)	Terminus status in 2004 <sup>4,6</sup>
Serpentine <sup>5</sup>	61°7'	148°17'	305	8545	R <sup>4</sup> , FTW <sup>5</sup>	Slow retreat <sup>5</sup>	–
Barry	61°12'	148°2'	95	1,021	R	Stable at head of Barry Arm	–
Wellesley	61°7'	147°56'	16	1,037	na	Stable on beach, College Fiord	Rapidly Ret.
Bryn Mawr	61°17'	147°48'	26	1,006	na	Stable on beach, College Fiord	Slowly Ret.
Smith	61°15'	147°50'	20	976	na	Stable on beach, College Fiord	Slowly Ret.
Harvard	61°23'	147°23'	524	1,098	I	Slow advance on terminal moraine shoal, College Fiord	–
Yale	61°18'	147°27'	194	1,098	R	Drastic retreat, or stable at head of Yale Arm	Slowly Ret.
Meares	61°13'	147°27'	142	1,052	I	Slow advance on terminal moraine shoal at head of Unakwik Inlet	Same as 1999
Columbia	61°15'	146°54'	1,121	899	I	Drastic retreat, fore bay, Columbia Bay	Same as 1999
Shoup	61°14'	146°28'	156	1,037	I	Drastic retreat in tidal basin, Shoup Bay	Same as 1999
Bering <sup>5</sup>	60°30'	142°24'	5,1735	1,0375	R <sup>4</sup> , FTW <sup>5</sup>	Drastic retreat <sup>5</sup>	Same as 1999
<b>St. Elias Mountains Group</b>							
<i>Grotto</i>	60°3'	141°33'	42	701	R	Stable on beach, Tsaa Fiord	Slowly Ret.
<i>Moraine/Apron</i>					R	Stable on beach, Tsaa Fiord	Slowly Ret.
Tsaa	60°7'	141°37'	150	625	R	Stable at head of Tsaa Fiord	Slowly Ret.
Guyot	60°13'	141°22'	1,432	747	R	Stable at head of Icy Bay	Ret.
Yahrtse					R	Stable at head of Icy Bay	Ret.
Tyndall	60°13'	141°5'	154	915	R	Stable at head of Taan Fiord	–
Malaspina <sup>5</sup>	60°6'	140°30'	5,0085	8235	R <sup>4</sup> , FTW <sup>5</sup>	Stable <sup>5</sup>	Rapidly Ret.
<b>Disenchantment Bay Group</b>							
Turner	60°5'	139°45'	186	854	na	Advances to terminal moraine shoal during surges	At shoal
Hubbard	60°10'	139°30'	3,865	915	I	Slow advance on terminal moraine shoal, Disenchantment Bay	Same as 1999
East Nunatak <sup>4</sup> (Nunatak <sup>5</sup> )	59°42'	138°3'	3125	1,0525	R <sup>4</sup> , FTW <sup>5</sup>	Stable at head of Nunatak Fiord, no longer calves icebergs	Ret.
<b>Fairweather Range Group</b>							
Lituya	58°44'	137°26'	103	1,052	I	Stable on terminal moraine shoal, Lituya Bay	Adv.
North Crillon	58°40'	137°19'	71	991	I	Stable on terminal moraine shoal, Lituya Bay	Adv.
La Perouse	58°32'	137°13'	147	960	na	Stable on open beach in Gulf of Alaska	Same as 1999
Reid	58°46'	136°48'	49	732	R	Stable at head of fiord, Reid Inlet	Slowly Ret.
Lamplugh	58°48'	136°52'	171	701	R	Stable on beach, Johns Hopkins Inlet	Same as 1999
Gilman	58°48'	137°3'	35	838	na	Stable on beach, Johns Hopkins Inlet	Adv.
Johns Hopkins	58°47'	137°12'	316	747	I	Advancing on terminal moraine shoal, Johns Hopkins Inlet	Same as 1999
Margerie	58°58'	137°14'	174	1,067	na	Stable on beach, Tarr Inlet	Same as 1999
Grand Pacific	59°6'	137°27'	654	1,189	I	Slow advance on terminal moraine shoal at head of Tarr Inlet	Rapidly Ret., stagnant ice
Kashoto <sup>1</sup>	58°52'	137°2'	5	762	na	Stable <sup>1</sup>	Ret.
Hoonah <sup>1</sup>	58°50'	137°4'	12	793	na	Stable <sup>1</sup>	Ret.
Brady <sup>5</sup>	58°33'	137°45'	5905	6105	R <sup>4</sup> , FTW <sup>5</sup>	Stable <sup>1</sup>	Ret.

TABLE 3.—Terminus status of major tidewater glaciers of Alaska in 1999 (with status in 2004 added for selected glaciers)

Glacier	Lat. (N) <sup>1</sup>	Long. (W) <sup>1</sup>	Area (km <sup>2</sup> ) <sup>1</sup>	Median ELA (m amsl) <sup>1,2</sup>	Terminus position <sup>1,3</sup>	Status of terminus in 1999 (from Robert M. Krimmel, except where noted)	Terminus status in 2004 <sup>3,6</sup>
<b>Alsek Range Group</b>							
Muir	59°10'	136°28'	148	960	R	Stable at head of fiord, Muir Inlet, no longer calves icebergs	400 m inland from shoreline, stagnant ice
Riggs	59°8'	136°14'	126	960	R	Stable on beach, Muir Inlet	Ret.
McBride	59°10'	136°5'	143	1,189	I	Stable at head of tidal inlet, Muir Inlet	Rapidly Ret.
Carroll <sup>5</sup>	59°11'	136°40'	5275	9915	R <sup>4</sup> , FTW <sup>5</sup>	Stable <sup>5</sup>	Debris-covered, stagnant ice
<b>Coast Mountains Group</b>							
Taku <sup>4,5</sup>	58°36'	134°9'	8315	8995	R <sup>4</sup> , FTW <sup>5</sup>	Stable on river bar/terminal moraine, Taku Inlet, no longer calves icebergs. Viens <sup>5</sup> indicated that it had been advancing at a decreased rate	Same as 1999
Sawyer	57°53'	132°55'	399	1,372	R	Retreat in narrow inlet, Tracy Arm	Same as 1999
South Sawyer	57°45'	132°43'	683	1,372	I	Stable in narrow inlet, sharp bend, Tracy Arm	Same as 1999
Dawes	57°27'	132°30'	653	1,402	I	Drastic retreat in narrow, deep inlet, Endicott Arm	Same as 1999
LeConte	56°54'	132°22'	472	915	R	Drastic retreat in narrow, deep inlet, LeConte Bay	Same as 1999
Baird <sup>5</sup>	57°15'	132°21'	7845	1,2345	R <sup>4</sup> , FTW <sup>5</sup>	Stable <sup>5</sup>	Same as 1999

<sup>1</sup> Viens (1995, table A1).

<sup>2</sup> Meters above mean sea level.

<sup>3</sup> R, Retracted; I, Intermediate; Ret., Retreating; Adv., Advancing.

<sup>4</sup> From Robert M. Krimmel (written commun., 1999).

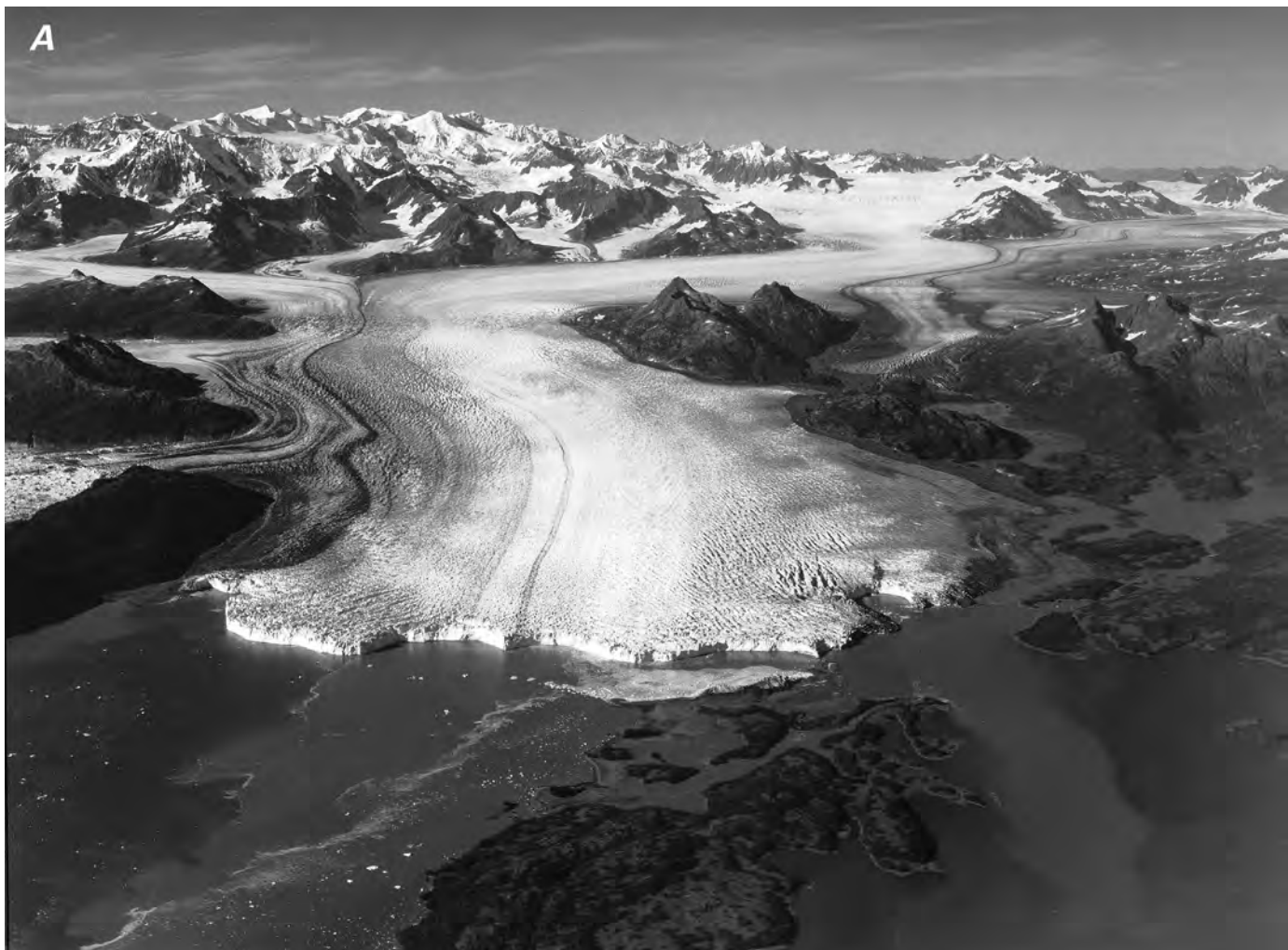
<sup>5</sup> Classified by Viens (1995, table A2) as a former tidewater (FTW) calving glacier.

Examples of tidewater glacier instability abound in Alaska. During the 20th century, most of the glaciers in Glacier Bay ended a drastic retreat of nearly 100 km that began about 200 years ago. Johns Hopkins Glacier, in western Glacier Bay, began a slow readvance early in the 20th century, while Muir Glacier in eastern Glacier Bay continued its retreat through the present. Glaciers in Icy Bay began a retreat from an extended position early in the 20th century and had retreated 30 km by late in the century. Hubbard Glacier has generally advanced during the 20th century; it advanced rapidly across a major fjord in May 1986 and created an ice-dammed lake that drained catastrophically (jökulhlaup), but harmlessly, in October 1986. A similar event occurred in the summer of 2002 (see section on “The 1986 and 2002 Temporary Closures of Russell Fjord by the Hubbard Glacier” in this chapter). Columbia Glacier began a rapid retreat during 1982 that continued into the 21st century. Columbia Glacier, the most intensively studied tidewater glacier in the world, is of particular interest because its discharge of icebergs into shipping lanes of Prince William Sound constitutes a hazard to navigation.

### Columbia Glacier

The Columbia Glacier (about lat 61°N., long 147°W.) (figs. 43–46) is a calving glacier that terminates in an embayment (forebay) of Prince William Sound, near Valdez, Alaska; it has an area of about 1,000 km<sup>2</sup>. The glacier is currently undergoing a rapid retreat from what had been a stable position for more than two centuries prior to 1980 (Vancouver, 1798). Ice mass is lost from the Columbia Glacier predominately through the calving of icebergs from its tidewater terminus. Some of the icebergs float into the shipping lanes that are used by oil tankers traveling to or from the port of Valdez, the

**Figure 43.**—Two oblique aerial photographs of the Columbia Glacier, Chugach Mountains. **A**, By 22 August 1979, large embayments formed in the terminus, and the glacier had receded from Heather Island (foreground), where a stagnant ice mass still remained. **B**, By 12 September 1986 there had been more than 2 km of retreat. The moraine shoal, where the water was no deeper than 21 m, is marked by stranded icebergs, which tend to keep the concentrated brash ice contained in the forebay between the terminus and moraine. Water depth in the forebay is 200 to 300 m. The rapid retreat will continue for several decades and will not end until the fjord head is reached in the east branch (right side). Photograph Nos. 79-L2-028 and 86-R2-256 by Austin Post, and Robert M. Krimmel, respectively, U.S. Geological Survey. Caption courtesy of Robert M. Krimmel, U.S. Geological Survey.





southern terminus of the Trans-Alaska [oil] Pipeline. Although the glacier terminates in tidewater, Columbia Glacier is grounded on its bed because the ice thickness overcomes buoyancy. In places, the glacier bed lies as much as 550 m below sea level (Meier and others, 1994). Flotation of the glacier may take place for brief periods in localized areas near the calving face.

The retreat of Columbia Glacier is interesting because it provides an opportunity for glaciologists to study the processes involved in iceberg calving and movement (Meier, 1994, 1997; Kamb and others, 1994), the ice dynamics of a rapidly changing system, a modern-day analog of suspected past rapid glacier retreats, and the processes associated with marine-based ice-sheet disintegration (for example, the marine-based part of the Antarctic ice sheet in West Antarctica) (see Swithinbank, 1988). Iceberg production during this retreat is important to shipping interests because icebergs are a navigation hazard. The tourist industry is interested because calving glaciers and icebergs are natural attractions in Prince William Sound.

A large part of the scientific studies of Columbia Glacier has been documenting the changes associated with its retreat (Rasmussen and Meier, 1982, 1985; Sikonja, 1982; Bindschadler and Rasmussen, 1983; Brown and others, 1982, 1986; Meier and others, 1985, 1994; Walters and Dunlap, 1987;



Rasmussen, 1989). This documentation has been done at a variety of temporal and spatial scales. For instance, ice displacement at a few places has been measured by using automated, laser-ranging devices with centimeter accuracy at a 10-minute frequency (Walters and Dunlap, 1987; Meier and others, 1994). [Editors' note: According to Mark F. Meier (written commun., 2004), the results of these studies showed the short-term response of the glacier to daily melt cycles, precipitation events, and even the changing pressure on the subglacier water system caused by ocean tides and thereby defined glacier-sliding processes.] At the synoptic scale, Landsat imagery has been used to observe the extent of iceberg plumes emanating from the glacier (fig. 45). Geodetic surveying is labor intensive and focuses on very specific

**Figure 44.**—Oblique aerial photograph of Columbia Glacier on 10 January 1993, from about 7,000 m in altitude, looking approximately north, with the iceberg-filled forebay in the foreground. At the time of the photograph, the glacier was undergoing a rapid retreat; the accelerated retreat produced the large number of icebergs (see fig. 42D). Photograph No. 93-V1-39 by Robert M. Krimmel, U.S. Geological Survey.



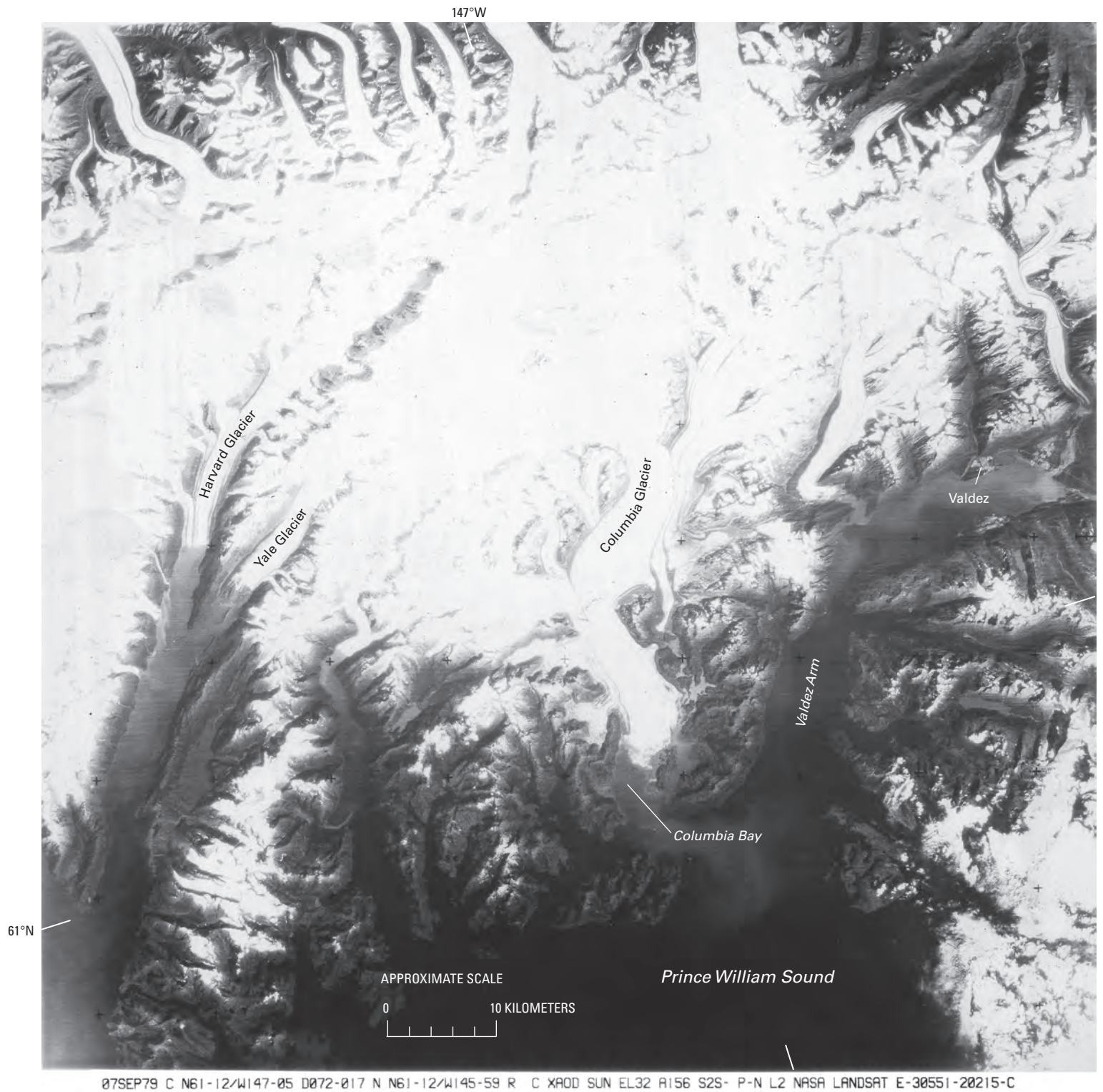


**Figure 45.**—Landsat 3 RBV image of Columbia Glacier and a part of Prince William Sound. The plume of icebergs caused by calving can be seen extending from Columbia Bay into Valdez Arm and Prince William Sound. Landsat 3 RBV image (30551-20215-C; 7 September 1979; Path 72, Row 17), originally published by Krimmel and Meier (1989), is from the USGS, EROS Data Center, Sioux Falls, S. Dak.

goals. Satellite images do not offer sufficient detail for many purposes and are dependent on weather (cloud cover) and orbit (frequency of imaging). The most practical method for documenting the changes at Columbia Glacier has proven to be repetitive aerial photography (Meier and others, 1985).

Oblique and vertical aerial photography has been used routinely to study Columbia Glacier since 1960, when Austin Post (USGS) began near-annual observations of Columbia Glacier as part of broad-coverage aerial surveys of Alaskan glaciers. Post documented glacier conditions with a large-format (9-in [23-cm] film) metric camera that could be mounted to acquire either oblique or vertical aerial photography. By the early 1970s, Post had become aware that Columbia Glacier was the only major tidewater glacier in Alaska that was neither retreating nor advancing. As mentioned previously, the tidewater glaciers of Glacier Bay had been undergoing a major retreat during the last two centuries; Hubbard Glacier was advancing slowly, and the glaciers in Icy Bay had retreated rapidly since about 1930. Post (1975) published a report that described changes in the terminus of Columbia Glacier and suggested that the increasing size and frequency of seasonal embayments in the terminus might be a precursor to a more rapid retreat. Summer and fall retreats of the terminus from a terminal-moraine shoal, where the water was mostly less than about 20 m deep, were normally offset by the subsequent winter and spring advances. But what if the winter and spring readvances did not occur? In 1976, the USGS systematically began to obtain aerial photographs of the lower reach of Columbia Glacier to document the changes. This photography enabled accurate monitoring and mapping of the retreat (fig. 46) (Krimmel, 1987, 2001).

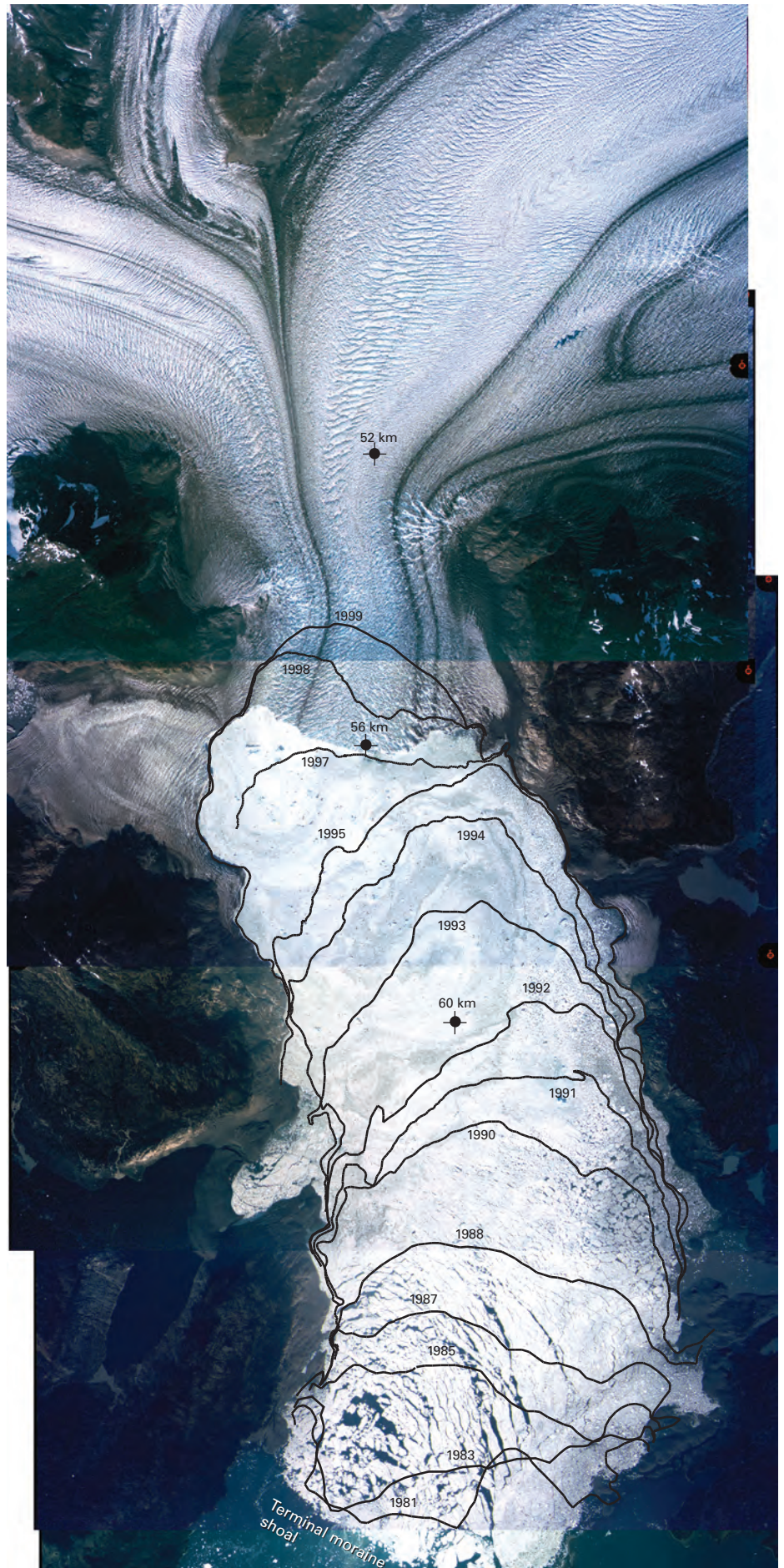
Repeated stereo aerial photography covered the lowest 20 km of the glacier at a spatial scale that allowed a single frame to span the entire width of the glacier and include off-glacier geodetic ground-control points along both edges of the flight line (fig. 46). A 6-in (15.3 cm) focal-length lens, metric camera, with 9-in (23 cm) film, flown at 7,000 m in altitude yielded the required coverage with six overlapping frames. (The overlap was at least 60 percent to achieve stereoscopy.) The temporal scale was designed so that ice features were preserved from one survey flight to the next. Thus, seasonal changes of the terminus position and ice speed were documented. By 2000, photography of the lower reach had been acquired 120 times. Flight frequency was controlled by scientific requirements, weather, logistics, and project funding. The shortest interval between flights was 3 days; the longest was 330 days. On 20 flights, coverage was extended to include areas beyond the lower reach of the glacier.

### **Stereophotogrammetry**

Analytical stereophotogrammetric techniques were used to analyze the vertical aerial photographs of Columbia Glacier.

*Terminus position.* Normally a well-defined ice cliff is formed where glacier ice calves into a lake or the ocean, and the terminus can be identified easily at many points along the ice-water contact. At times, the Columbia Glacier ice cliff is so low that it is difficult to define the contact between water and glacier; in those areas the position was estimated.

**Figure 46.**—Reduced-scale mosaic of five vertical aerial photographs of the lower reach of the Columbia Glacier on 2 October 1998 from an altitude of about 7,000 m. North is approximately at the top; the terminus of the glacier is about 4 km wide. Superimposed on the mosaic are plots of selected terminus positions from 1981 to 1999. Also shown by symbol are three locations where the velocity of the glacier surface was determined. Glacier surface speeds are shown in figure 49. The scale of the original U.S. Geological Survey (USGS) aerial photographs is about 1:46,000 at sea level. The current scale is approximately 1:100,000. USGS Columbia Glacier aerial photographs are referenced as: 10–2–98; 23,000 feet; Frames 1–3 through 1–7.



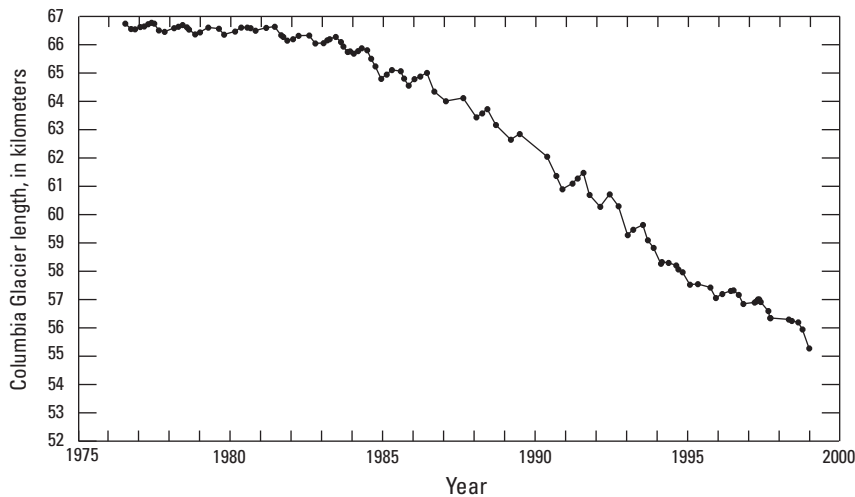


**Figure 47.**—The changing length of Columbia Glacier between 1976 and 1999. Each dot represents an aerial survey. When the recessional trend is removed, the seasonal variations shown in figure 48 become evident.

The width-averaged (one-dimensional) terminus position in terms of glacier length is plotted in figure 47. The glacier length plot shows that the major recession began about 1982 (slowly at first) and then increased to a rate of about  $0.7 \text{ km a}^{-1}$  until 1995, when the recession rate decreased until 1998. In the last years of the 20th century, there was a marked increase in the rate of retreat (Pfeffer and others, 2000). During the end of 1998, the retreat rate increased to nearly  $1.0 \text{ km a}^{-1}$ , and in 2004 it had decreased to  $0.6\text{--}0.7 \text{ km a}^{-1}$  (Mark F. Meier, written commun., 2004).

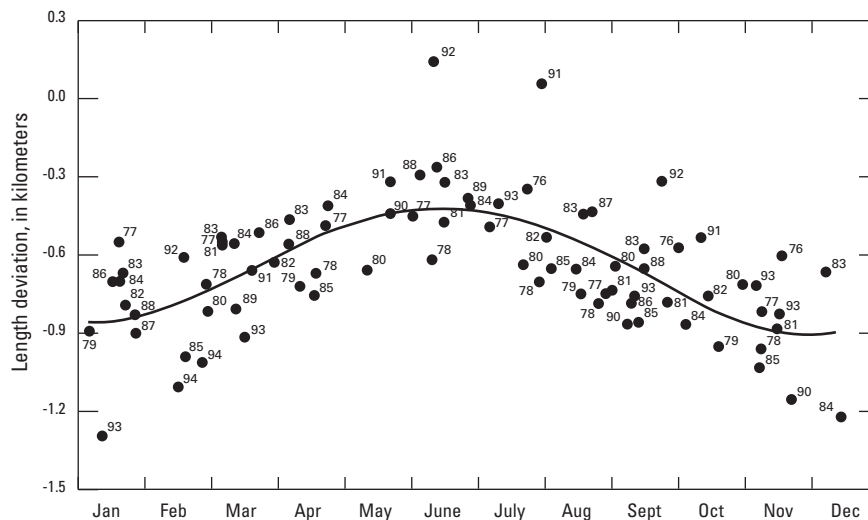
The persistent change in the terminus position is seasonal. The glacier terminus is extended during the winter and spring, and the terminus retreats in summer and fall. This seasonal cycle of change in glacier length is shown in figure 48.

*Ice speed.* The highly crevassed lower reach of Columbia Glacier lends itself to measurements by aerial-stereophotogrammetric methods (fig. 49). An individual crevasse or local pattern of crevasses retains its unique geometric identity for days, in some cases for months, and in some rare areas for several years. These intervals allow sufficient time for photographic-identification of features and measurement by means of stereophotogrammetric methods. Displacements of these features can be converted to speeds by dividing the displacement by the time interval. Such measurements can be made over the entire lower reach of Columbia Glacier if the time interval between survey flights is short enough that the features or crevasse patterns on the aerial photographs remain identifiable.

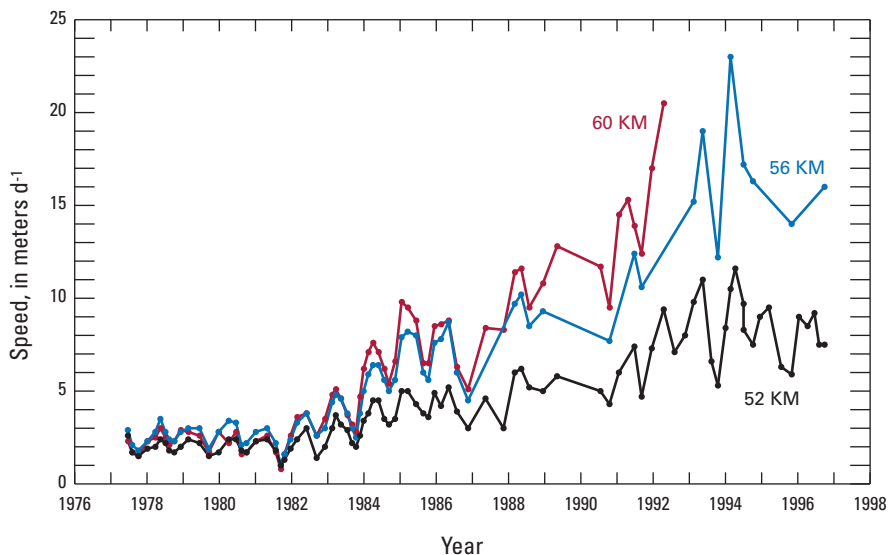
Before the Columbia Glacier began to retreat, features or crevasse patterns could be followed over the entire lower reach for periods of up to 4 months. By the middle 1980s, the ice speed and rate of deformation had increased to such an extent that features within a few kilometers of the terminus could be reidentified only within intervals of a few weeks or less. In the spring of 1997, five aerial photography sets obtained at intervals of 10 to 20 days allowed detailed spatial and temporal speed measurements to be made.

The glacier speed has increased severalfold since the retreat began. Before the retreat, the maximum annual ice speed averaged about  $5 \text{ m d}^{-1}$ , the seasonal maximum speed being about  $7 \text{ m d}^{-1}$ . The speed increased differentially in the lower reaches of the glacier, the greatest increase occurring near the terminus (fig. 49). As the retreat progressed, speed near the terminus increased to more than  $20 \text{ m d}^{-1}$  averaged annually (fig. 50) and reached  $30 \text{ m d}^{-1}$  during the seasonal speed maximum. The seasonal speed variation

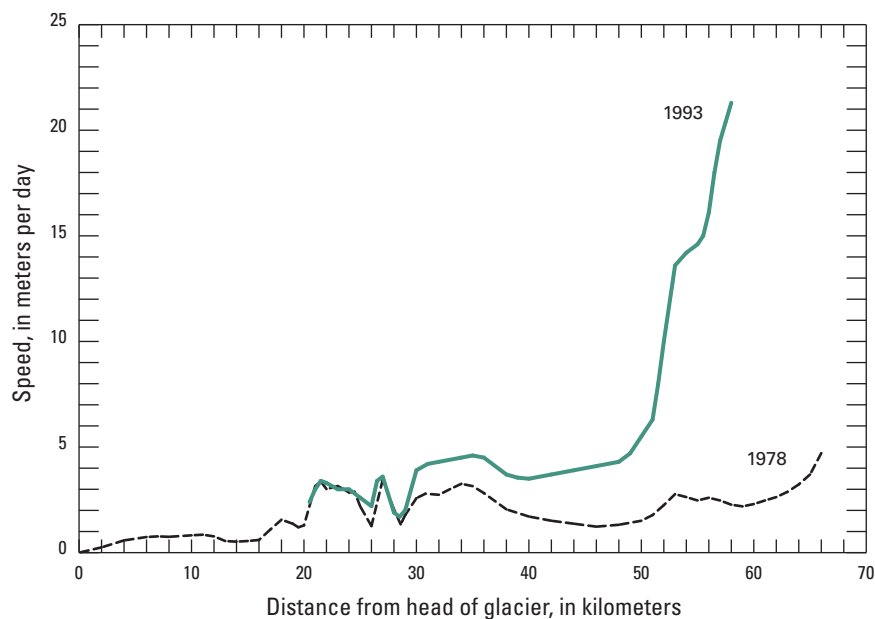
**Figure 48.**—The seasonal variation of the length of Columbia Glacier. Deviations from the normalized length (best fit curve) are plotted against the time of year. The numerals indicate the survey year (76=1976).



**Figure 49.**—Surface speed of Columbia Glacier at three locations, 52 km (black), 56 km (blue), and 60 km (red), from the origin (head) of the glacier on different aerial survey dates from 1977 to 1997. The location where the velocities were determined is shown on figure 46.



**Figure 50.**—Average annual speed in meters per day along the length of Columbia Glacier in 1978 and 1993. The fourfold increase in speed near the terminus is evident.



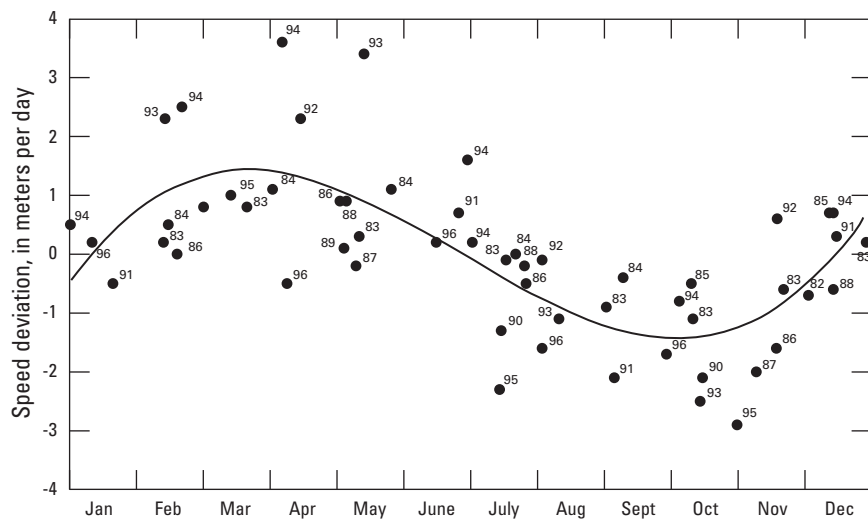


**Figure 51.**— The seasonal-speed deviations from the normalized speed (best fit curve) near the terminus of Columbia Glacier. Speed is highest in early spring and lowest in early fall. The numerals indicate the year (84=1984).

near the terminus is shown in figure 51, where deviations from the normalized speed (the long-term trend removed) are plotted against the time of year. Speed is highest in early spring and lowest in early fall.

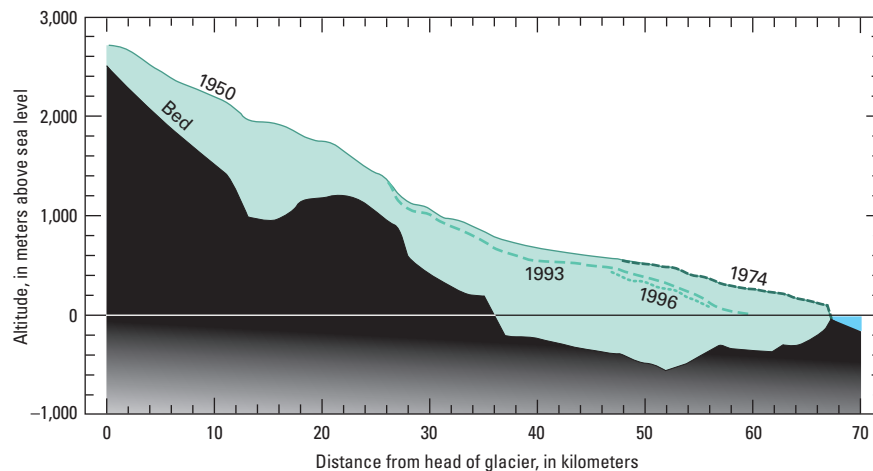
Ice displacement also has been measured very precisely, with a temporal resolution of less than 1 hour for several multiple-week periods at a few locations. Ice speed fluctuated daily, the highest speed occurring about 8:00 p.m. and the lowest at about 8:00 a.m. In addition, speed reached high extremes near the end of rain or wind storms. High glacier speed seemed to correlate with measured or assumed high basal-water pressure or volume of water in storage at the bed, depending on the time scales of the fluctuations (Meier and others, 1994; Kamb and others, 1994). Within 1.5 km of the terminus, the stage of the tide also affected ice speed. When there was little or no surface water input by melt or precipitation, glacier speed had an inverse relation to tide stage. The increased pressure of high tide against the ice cliff slowed the glacier slightly (Krimmel and Vaughn, 1987; Walters and Dunlap, 1987) and overwhelmed any speed increase that may have occurred because of a local increase in basal pressure owing to high tide.

*Forebay of Columbia Glacier.* As Columbia Glacier has retreated, the fjord has lengthened. Except for a narrow band along each side of the glacier, the glacier bed has been below sea level throughout the area of the retreat. Thus, fjord expansion is nearly equal in area to glacier retreat. As the glacier has retreated, the surface of the newly opened fjord, presently known as the forebay, usually has been covered with a floating mass of icebergs, brash ice, and frozen fresh-water ice. This “freeze-welded” sheet has covered almost all of the forebay most of the time during the retreat (fig. 44). The southern limit of the forebay is the terminal moraine shoal, which was the stable position of the terminus of Columbia Glacier before the beginning of the retreat. Maximum water depth over the moraine was 27 m at high tide in the middle 1980s. The northern end of the forebay is the glacier terminus. The forebay ice mass is continuously replenished by newly calved ice and moves toward the terminal moraine at a rate of about 100 m d<sup>-1</sup>. The ice mass in the forebay undergoes little transverse mixing. As a result, the relatively debris-laden icebergs calved from the medial moraine retain their transverse position as they move through the forebay (fig. 44).

Beginning in late 1995, the floating ice mass in the forebay occasionally thinned enough so that boats could approach the glacier terminus. Shipborne bathymetric measurements indicate that the maximum fjord water depth was about 360 m and that submarine topographic features were up to 100 m in relief (Post, 1997).



**Figure 52.**—Surface altitude of Columbia Glacier in 1950, 1974, 1993, and 1996, with an estimated width-averaged bed. The lower part of the glacier has thinned at a rate of about  $20 \text{ m a}^{-1}$ .



*Ice-surface altitude.* The surface altitude of points on stereophotogrammetric models is measured easily. It is more difficult to obtain a consistent area-averaged ice-surface altitude. Ice surface relief is typically 20 to 30 m. This roughness must be smoothed to give meaningful measurements of changes in ice-surface altitude. The surface altitude has been reduced during retreat.

The lower part of Columbia Glacier has thinned at a rate of about  $20 \text{ m a}^{-1}$ . The magnitude of thinning decreases up glacier, reaching approximately zero about 26 km from the head of the glacier (fig. 52).

*Calving.* Calving is the breaking off of ice from the terminus of a glacier. If the terminus position of a calving glacier is stable, the calving rate is equal to the ice speed. If the terminus is retreating, the calving rate is equal to the ice speed plus the retreat rate. Calving is rarely observed directly on aerial photographs. It is normally measured by the difference between the observed glacier speed and the change in terminus position. Calving can also be measured directly between two observation dates by delineating the area of ice that is present near the terminus on the first date but is missing on the second date. By measuring the area of “ice to be-calved” and the average altitude of its top surface, and by estimating the ice thickness, one can determine a calving volume. Applying this analysis to Columbia Glacier indicates that the calving rate has increased by a factor of 5 or more since the retreat began and that, during the retreat, it has often been as high as  $5 \text{ km}^3 \text{ a}^{-1}$ . During the years 2001–03, the calving discharge approached  $10 \text{ km}^3 \text{ a}^{-1}$  (O’Neel and others, 2005).

*Discussion.* The high ice-surface velocities measured at Columbia Glacier rival those measured at glaciers during surges (Kamb and others, 1985). However, the condition of Columbia Glacier is unlike that of a typical surging glacier in two ways. First, high ice speed at a surging glacier occurs during a shorter period; a typical large surging glacier has one or more short periods of high speed lasting a few months and a period of several decades when speeds are “normal” ( $50\text{--}200 \text{ m a}^{-1}$ ). The high ice speed of Columbia Glacier has been sustained for more than a decade. Second, a surge usually begins upglacier, well above the terminus (often in the accumulation zone), and it propagates downglacier. No propagation of a speed pulse downglacier has occurred at Columbia Glacier. The only longitudinal effect is that ice drawdown and ice speedup are progressing upglacier (Meier and others, 1985; Pfeffer, 2007). Thus, the term “surge” should not be applied to the flow regime of Columbia Glacier.

The seasonal velocity variations of Columbia Glacier—fast in the early spring and slow in the fall—are consistent with those of many other glaciers and can be explained as seasonal variations in the basal-water pressure at the glacier-bed interface (Kamb and others, 1994). The dominant mechanism of movement of Columbia Glacier must be basal sliding (Rasmussen, 1989; Kamb and others, 1994), for which Bindschadler (1978) has devised a general

ice-flow law, although some of its parameters remain in doubt. A qualitative description of the basal-sliding process depends on basal-water pressure and storage of water. Basal-water pressure is controlled by a channel network at the bed, which may be opened (allowing for water passage) or closed (resulting in water storage). During the summer, sufficient water is available from ice melt and rain to keep many basal channels open despite their tendency to be closed by ice deformation. Basal-water pressure in the summer is therefore low. In the fall, surface melting is reduced, and precipitation is increasingly dominated by snow; basal-water pressure is at an annual minimum as the water input diminishes. Basal sliding and deformation gradually disrupt the channel system. Once the channels are disrupted, no more water can pass under the glacier, and residual water draining from the glacier surface, intraglaciar conduits, and the surrounding subglacier basin is stored. Basal-water pressure increases throughout the winter and well into the spring. Ultimately, however, water pressure becomes high enough to force channels to open and remain open owing to the high volume of water moving through and under the glacier. Glacier speed is a direct function of basal-water thickness and pressure. Consistent with this explanation, short-term measurements show that speed has a strong diurnal variation that is directly related to diurnal water input (Kamb and others, 1994) and summer precipitation events.

Although the cause of seasonal ice-speed variations is agreed upon generally, the cause of decadal-scale increases in speed is not understood. One hypothesis is that a feedback exists, in which decreasing ice thickness causes reduced effective pressure at the bed, which in turn allows increased sliding; this process reduces the ice thickness, and further reduces effective pressure (Meier and Post, 1987; Meier, 1994). Another hypothesis is that a change in the bulk characteristics of the glacier ice results in lower tensional strength and increased speed. How the process of calving works, how it is related to changes in speed, and, perhaps, how calving influences speed are open questions (van der Veen, 1995, 1996, 1997b) and were discussed in a workshop focusing on these questions (Van der Veen, 1997a).

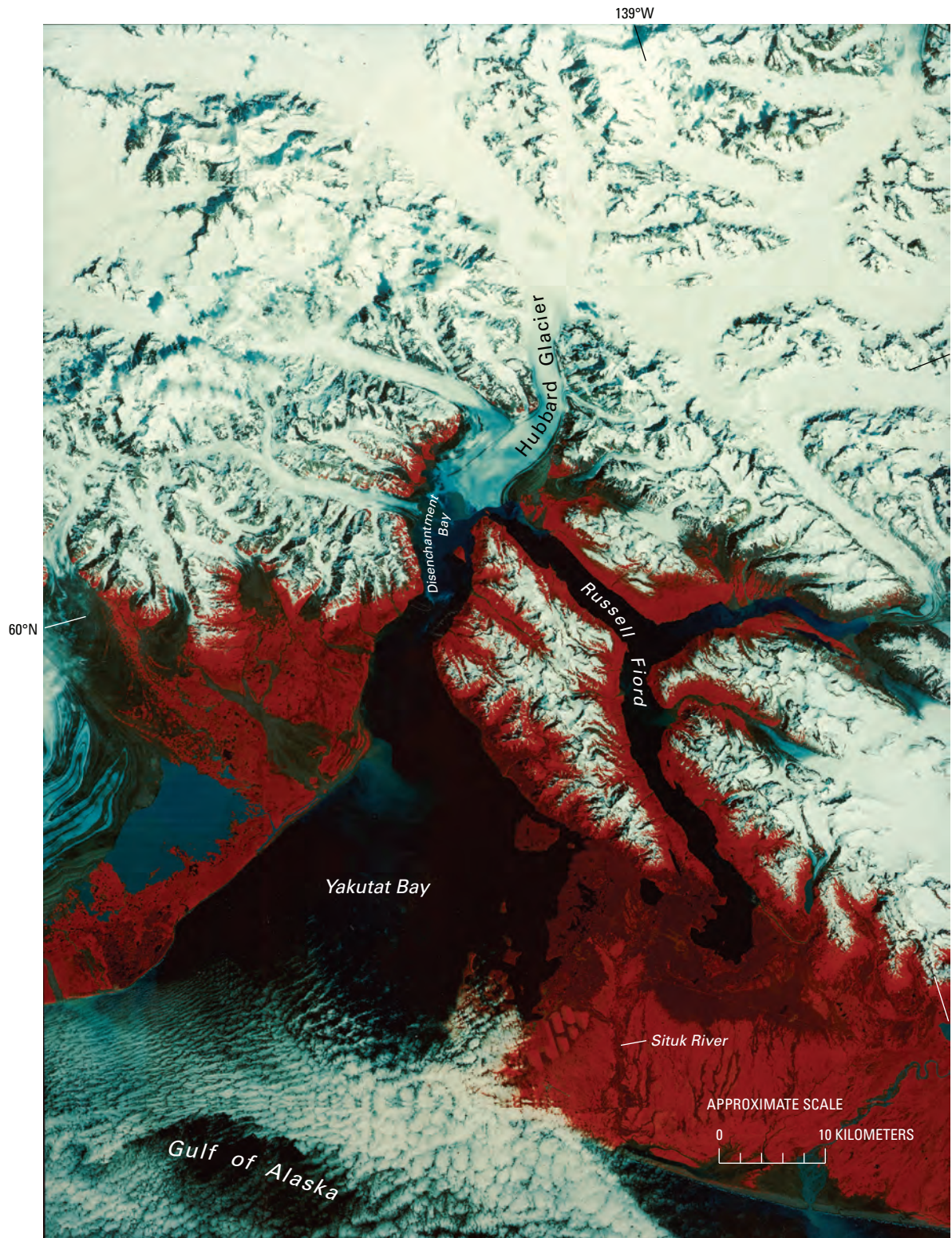
### **Hubbard Glacier**

Hubbard Glacier (about lat 60°N., long 139°30'W.) (fig. 53) is the largest tidewater glacier in Alaska and has been generally advancing (figs. 54, 55, 56) since it was first mapped by the International Boundary Commission (IBC) in 1895 (Davidson, 1903). The advance has accelerated during the 20th century at the following average advance rates: 1895–1948, 16 m a<sup>-1</sup>; 1948–62, 18 m a<sup>-1</sup>; 1962–72, 30 m a<sup>-1</sup>; 1972–83, 38 m a<sup>-1</sup>; and 1983–88, 47 m a<sup>-1</sup> (Trabant and others, 1990). This slow advance led Post and Mayo (1971) to predict that Hubbard Glacier would dam Russell Fiord by 1990. The overall advance is persistent but varies locally over the 10-km width of the terminal ice cliff. Hubbard Glacier often exhibits short-lived pulses characterized by much higher advance rates. Although these pulses usually occur in the spring, it is not known whether they occur every spring or how much of the terminus they affect. In 1986, one such pulse was directed across the mouth of Russell Fiord and resulted in a temporary closure. The advancing ice was protected by a ridge of moraine material that the glacier pushed ahead of itself, and calving was thus effectively reduced. By the end of May, the entrance to the fjord was closed (fig. 56). When the closure (fig. 56) was completed, the level of the “lake” in Russell Fiord began rising from spring snowmelt and precipitation runoff. A far-reaching concern was the possible overflow from the south end of *Russell Lake* and the effect that such an overflow would have on the productive fishery in the Situk River basin. Overflow would have occurred when the lake level reached 40 m, but, on 7 October 1986, at a water level of 25 m, the ice dam failed, and *Russell Lake* drained catastrophically (jökulhlaup) but harmlessly into Disenchantment Bay (Mayo, 1988b). Temporary closure occurred again in 2002. For a further

**Figure 53.**—Digitally enhanced Landsat 5 TM image of Hubbard Glacier. Hubbard Glacier has been generally advancing since 1895. The Landsat 5 TM image (50620–18008; bands 2, 3, 4; 7 August 1985; Path 62, Row 18) is from the USGS, EROS Data Center, Sioux Falls, S. Dak. (Also available in EROS Data Center Image Gallery: No. E-564-99CT.)

discussion of the closures, see the section on “The 1986 and 2002 Temporary Closures of Russell Fjord by the Hubbard Glacier” in the following discussion of the St. Elias Mountains.

Although the closure of Russell Fjord is unique to present-day inhabitants of the area, it is known to have occurred in the past. Native legends refer to events that may have been the result of closure. The channel of the Situk River on the southern end of Russell Fjord is larger than necessary, so that it can handle the discharge when the fjord is not open to Disenchantment Bay.



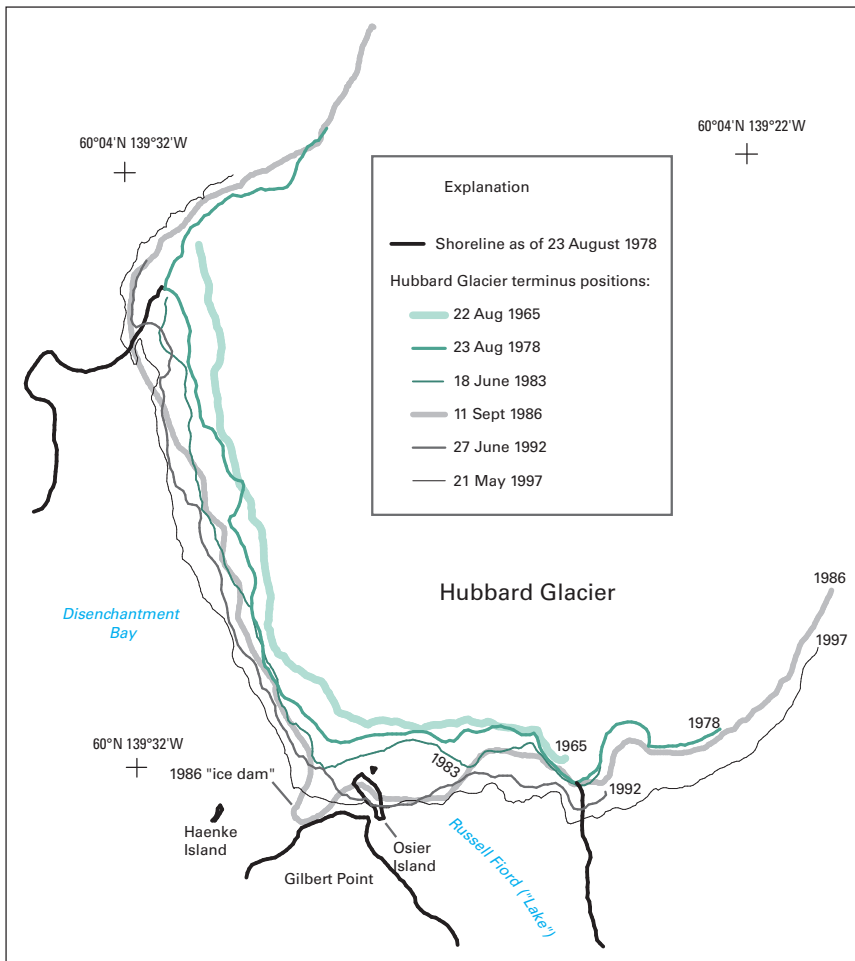


**Figure 54.**—Advance of Hubbard Glacier terminus between 1965 and 1997. (Modified from Trabant and others, 2003.)



**Figure 55.**—29 August 1984 oblique aerial photograph of the terminus of the 112-km-long Hubbard Glacier, North America's largest tidewater glacier. This slowly advancing glacier closed the entrance to Russell Fjord in the spring of 1986 (see fig. 56) and again in 2002 (see fig. 157). On the date of this aerial photograph, the entrance to Russell Fjord (lower right) was about 500 m wide. Osier Island, in the entrance to the fjord, is about 500 m long. The Hubbard Glacier flows down the valley on the right from the St. Elias Mountains into Disenchantment Bay; the Valerie Glacier tributary merges into it from the left. Photograph No. 84-R1-082 by Robert M. Krimmel, U.S. Geological Survey.

Under those conditions, *Russell Lake*, when full, drains via the Situk River to the south directly into the Gulf of Alaska. Moraines of Hubbard Glacier exist far beyond the position required for closure.

The general flow of Hubbard Glacier is regulated by its mass balance, which is largely controlled by the local climate and calving losses. Year-to-year



**Figure 56.**—Oblique aerial photograph of the Hubbard Glacier ice dam on 12 September 1986, as it blocked the entrance to Russell Fiord (middle right center) at Gilbert Point (lower center). Osier Island is almost completely covered. A push moraine that formed as the glacier approached Gilbert Point reduced calving. The dam width is about 0.5 km. The ice dam, which formed in May 1986, created “Russell Lake.” The ice dam failed because of calving and increased water pressure in Russell Fiord on 8 October 1986, releasing 5.3 km<sup>3</sup> of water in less than 1 day. The maximum water discharge was estimated by Mayo (1988b) to be 104,500 m<sup>3</sup> s<sup>-1</sup>. Variegated Glacier (upper right) underwent a major surge in 1983. Photograph No. 86-R2-124 by Robert M. Krimmel, U.S. Geological Survey.

changes of the AAR are an index to the climatically controlled accumulation and ablation components of mass balance. In many years since 1963, observations of the glacier near the end of the melt season have shown that the line separating the accumulation area from the ablation area (the equilibrium line) is normally at about 1,000 m in altitude. This equilibrium line altitude (ELA) gives Hubbard Glacier the extremely high AAR of 0.95, which demonstrates that the glacier’s mass balance is very positive. As a result, Hubbard Glacier can easily sustain its calving and melt losses and increase its thickness while the terminus and its submarine terminal moraine advance farther into Disenchantment Bay. Furthermore, Hubbard Glacier is not currently sensitive to small climate changes. The equilibrium line lies on a steep, narrow part of the outlet glacier, where a 200-m increase in the ELA changes the AAR to 0.91 and a 200-m decrease in the ELA changes the AAR to 0.96. Changes in the ELA likely have been smaller than  $\pm 200$  m for decades. For instance, the 1987–88 balance year resulted in a 50-m lowering of the ELA. This relatively small change was the response to winter precipitation that was about twice the 1951–80 normal amount, followed by a summer of near-normal temperatures, both of which suggest near-normal ablation (Trabant and others, 1990).

The accumulated ice mass must go somewhere. It is estimated that there is an ice flux of 6.8 km<sup>3</sup> a<sup>-1</sup> through the cross section at the equilibrium line of Hubbard Glacier. This ice either is melted in the ablation zone (0.3 km<sup>3</sup> a<sup>-1</sup>),

increases the volume of the lower glacier by advance and increased thickness ( $0.05 \text{ km}^3 \text{ a}^{-1}$ ), or calves ( $6.45 \text{ km}^3 \text{ a}^{-1}$ ).

Surface-ice speeds of Hubbard Glacier measured in the ablation zone and near the equilibrium line are about  $8 \text{ m d}^{-1}$  near the terminus,  $5 \text{ m d}^{-1}$  in the central ablation area, and  $12 \text{ m d}^{-1}$  near the equilibrium line (Krimmel and Sikonia, 1986). Ice thickness also has been measured; the maximum thickness is about 700 m in the central ablation zone. The bed of the glacier is about 400 m below sea level at that location (Mayo, 1988a).

Hubbard Glacier also exhibits seasonal terminus changes. The glacier tends to advance in the winter and spring and retreat in the summer and fall (Krimmel and Trabant, 1992). These fluctuations may be caused by seasonal changes in calving rate or speed or by a combination of the two.

Alaska's tidewater glaciers (tables 2, 3; fig. 41), although large for North America, are relatively small in comparison with the large outlet glaciers from the ice sheets in the Antarctic and Greenland (Swithinbank, 1988; Weidick, 1995). Research on the Alaska glaciers is important, however, because the results of frequent and detailed observations on smaller glacier systems can be applied to the larger systems. Tidewater glaciers are unique in that the cycle of changing glacier size is indirectly related to climate (Post, 1975). The cycle for a specific tidewater glacier may be radically different from the cycle of land-terminating glaciers in the same region that is caused by climate change.

---

## Surge-Type Glaciers

Most glaciers have relatively constant average annual flow rates. A small percentage exhibit substantial variations and major flow irregularities. When the average annual flow is relatively constant, variations that occur are generally predictable on a seasonal basis; longer period changes occur as the glacier responds to changes in mass balance. When the average annual flow is variable, some glaciers have dramatic annual velocity changes, often characterized by brief velocity increases of at least an order of magnitude. These glaciers are called surge-type glaciers. Surges involve large volumes of ice displacement and often are characterized by rapid advance of the glacier terminus. The first observed surge to be widely reported by the media in the United States occurred in 1937. The terminus of Black Rapids Glacier in the eastern Alaska Range advanced more than 5 km in less than a year (Time Magazine, 1937; Moffit, 1942). The terms "galloping glacier" and "runaway glacier" were widely used by the media to report this occurrence.

The first, and seminal treatise on surge-type glaciers was by Post (1960), followed by Meier and Post (1969) and Raymond (1987). Post (1969, p. 229) offered the following definition for a surge-type glacier: "one which periodically (15–100+ years) discharges an ice reservoir by means of a sudden, brief, large-scale ice displacement, which moves 10 to 100 or more times faster than the glacier's normal flow rate between surges." He continued "Glacier surges are not unique events which might result from exceptional conditions such as earthquakes, avalanches, or local increases in snow accumulation. These movements apparently are due to some remarkable instability which occurs at periodic intervals in certain glaciers." This comment about earthquakes and avalanches was in response to a theory of earthquake-induced glacier advance proposed by Tarr and Martin (1910) to explain changes that they observed in glaciers of the Yakutat Bay Region following the 1899 Yakutat Earthquake. Post (1965) concluded that the Great Alaska Earthquake of 1964 had not produced snow-and-ice avalanches or short-lived glacier advances in the Coast, St. Elias, Chugach, and Wrangell Mountains or in the

Alaska Range. Post (1965) coined the term “surge” because “advance” is frequently technically incorrect in that affected glaciers do not always advance beyond their former limits. The term “surge” is here used to describe sudden, large-scale, short-lived glacier movements that may or may not be associated with a terminal advance. Surge-type glaciers typically undergo alternating phases of short periods of active rapid flow, usually lasting from less than 1 to 3 years (surge), followed by much longer periods of slow flow lasting from 10 to 100 years (quiescence). The quiescent stage of a surge-type glacier may have seasonal velocity variations. Some glaciers, called “pulsing glaciers” (Mayo, 1978), exhibit frequent weak surges.

Surge-type glaciers have been observed in many parts of the world (for example, in the Pamirs, Tajikistan (Krimmel and others, 1976); and Svalbard (Liestøl, 1993, p. E127–E151), but one of the greatest concentrations of surge-type glaciers occurs in western North America, especially in the St. Elias, eastern Chugach, and eastern Wrangell Mountains, in parts of the Alaska Range, and in the Icefield Ranges adjacent to the U.S.- Canadian border (Post, 1969). In the regions that support surge-type glaciers, most glaciers do not surge. Post (1969) noted only 204 surge-type glaciers out of the several thousand western North American glaciers that he examined. About 75 percent of these surge-type glaciers were in Alaska. Clarke and others (1986) noted that only 6.4 percent (151 of 2,356) glaciers they examined in the St. Elias Mountains of Canada were of the surge type. However, more recent information has indicated that there are only 136 surge-type glaciers in the St. Elias Mountains of Canada (see also Clarke and Holdsworth, 2002b).

Most of the surge-type glaciers included in these studies were recognized from the air or from aerial photographs on the basis of their contorted medial moraines (Post, 1972) (fig. 57). Differential flow velocities and irregular flow conditions contort medial moraines and thus produce easily identifiable



**Figure 57.**—Oblique aerial photograph of the Susitna Glacier, Alaska Range, showing contorted medial moraines indicative of a surging glacier. The glacier is approximately 3.5 km wide in the foreground. The 5 September 1966 photograph no. 667–40 is by Austin Post, U.S. Geological Survey.

evidence of surging. Surge-type glaciers can also be recognized on Landsat images by their contorted medial moraines (see fig. 404).

Meier and Post (1969) identified 12 characteristics of surge-type glaciers:

(1) All surge-type glaciers surge repeatedly, (2) Most surges are uniformly periodic, and the length of a surge cycle appears to be constant for a single glacier, (3) All surges take place in a relatively short period of time and are followed by a longer quiescent phase, (4) The time required for a complete surge cycle has no relation to the length, area, or speed of the glacier, (5) Total horizontal displacements of ice during the active phase are typically only a few kilometers but can be less than 1 km, (6) Most surges do not result in advance of the terminus, (7) An ice reservoir and an ice receiving area can be defined for all surges, (8) No abrupt bedrock sills, depressions, or ice dams are evident in most surging glaciers, (9) All sizes and kinds of glaciers surge, including glaciers in almost all climatic zones, (10) In western North America, surge-type glaciers occur only in certain restricted areas, (11) Western North American surge-type glaciers can be divided into three categories: type I, large to moderate length valley glaciers with very high speeds, large resulting displacements, and large-scale lowering of the ice reservoir; type II, large to moderate length valley glaciers with much smaller displacements and moderate lowering of the ice reservoir; and type III, small, steep glaciers with moderate lowering of the ice reservoir, (12) Whether there is a complete transition of glacier behavior from surge to normal is not known.

From the analysis of the characteristics of the 2,356 glaciers that they examined, Clarke and others (1986) determined that (1) long glaciers have a higher probability of being surge type than short glaciers do; (2) surge-type glaciers tend to have a higher overall elevation than normal glaciers do; and (3) surge-type glaciers have greater slopes in the accumulation zone and lesser slopes in the ablation zone. Later, Clarke (1991) concluded that surge-type glaciers tend to be longer and wider and to have lower overall slope than normal glaciers.

Water plays an important role in surging. Kamb and others (1985) found that high subglacial water pressures occur during rapid surge displacement. Variegated Glacier, a surge-type glacier, has been studied by many scientists (Balise and Raymond, 1985; Harrison and others, 1986; Humphrey and others, 1986; McMeeking and Johnson, 1986; Raymond and Malone, 1986; Raymond and others, 1987; Raymond and Harrison, 1987, 1988), who examined various aspects of basal-water pressure and storage of water. Kamb (1987) proposed that the mechanism for surge onset was based on the blockage of the linked-cavity network configuration of a glacier's basal water conduit system. Harrison and Post (2003) summarized the current state of knowledge about surge-type glaciers, with specific reference to Alaskan glaciers.

Sturm (1987) called the dry or water-filled depressions on glaciers that measure from a few meters to 100 m in diameter "potholes," Post and LaChapelle (1971, figs. 77, 78) called such depressions "lacunas." Sturm (1987) determined that fields of "potholes" usually are found on the surfaces of surge-type glaciers rather than on those of non-surge-type glaciers. After examining photographs of several thousand glaciers, Sturm determined that 21 of the 26 glaciers observed to have "potholes" were surge-type glaciers and that most "pothole" fields were found near the equilibrium line.

## **Glacier-Dammed Lakes and Glacier-Outburst Floods (Jökulhlaups)**

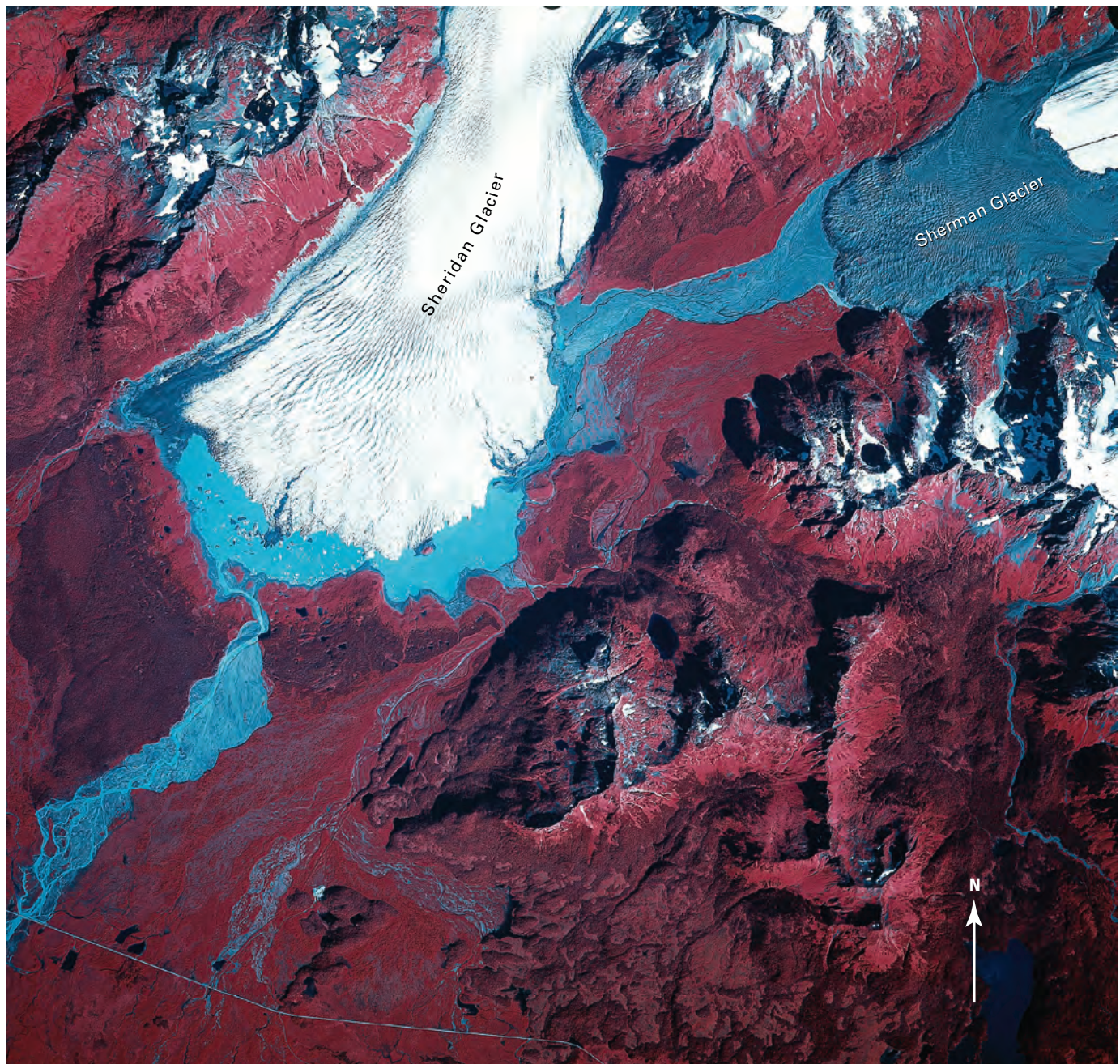
Many Alaskan glaciers end in ice-marginal lakes formed by terminal or recessional moraines (fig. 58). Other glaciers form lakes by blocking or having distributaries that extend into adjacent valleys (fig. 59). (see also section on Columbia and Hubbard Tidewater Glaciers by Robert M. Krimmel in this volume.) Many Alaskan communities are located on rivers fed by glacial meltwater. Catastrophic flooding (jökulhlaups) caused by (1) drainage of ice-dammed lakes, (2) drainage of ice-marginal lakes, (3) release of water stored subglacially, englacially, or supraglacially, sometimes through surge-related processes, or (4) melting glaciers located around the summit craters of erupting volcanoes are a significant hazard. Annually, floods in Alaska cause many millions of dollars of damages (Lamke, 1991). Information about



**Figure 58.** — 13 August 1982 AHAP false-color or infrared vertical aerial photograph of the ice-marginal lake surrounding the terminus of Sheridan Glacier, Chugach Mountains, formed by the 20th century retreat of the glacier's terminus. The boundary between the darker red and lighter red vegetation surrounding the southern side of the lake marks the location of Sheridan Glacier's "Little Ice Age" end moraine. Note the icebergs in the ice-marginal lake. The debris-covered terminus of the Sherman Glacier is visible on the upper right of the photograph. Photograph No. L115F1516 from GeoData Center, Geophysical Institute, University of Alaska, Fairbanks, Alaska.

the flooding history of Alaskan glaciers is presented in some of the sections that follow.

Stone (1963a) summarized the characteristics of 53 present and 7 former large ice-dammed lakes in an 1,285×160-km area of south-central and south-eastern Alaska and adjacent Canada. His purpose was to call attention to "one of the world's greatest concentrations of lakes dammed by glacial [glacier] ice" (Stone, 1963a, p. 332). He defined these lakes as "impounded by glacial [glacier] ice touching the water, a minimum of ¼ to ½ mile [0.4–0.8 km] wide and ½ to 1½ mile [0.8–1.6 km] long, and with water supplied from one or two streams or glaciers in addition to the water from the damming glacier," (Stone, 1963a, p. 332). He noted that 11 of the 16 larger lakes have histories of regular or irregular emptying and that at least 6 ice-dammed lakes threaten transportation routes in Alaska. Three of the six lakes are located in Canada, but their floodwaters flow into the Pacific Ocean through Alaska via the Taku and Stikine Rivers. These six are (1) Lake George (Knik Glacier) (Stone, 1963a); (2) Hidden Creek Lake (Kennicott Glacier) (Anderson and

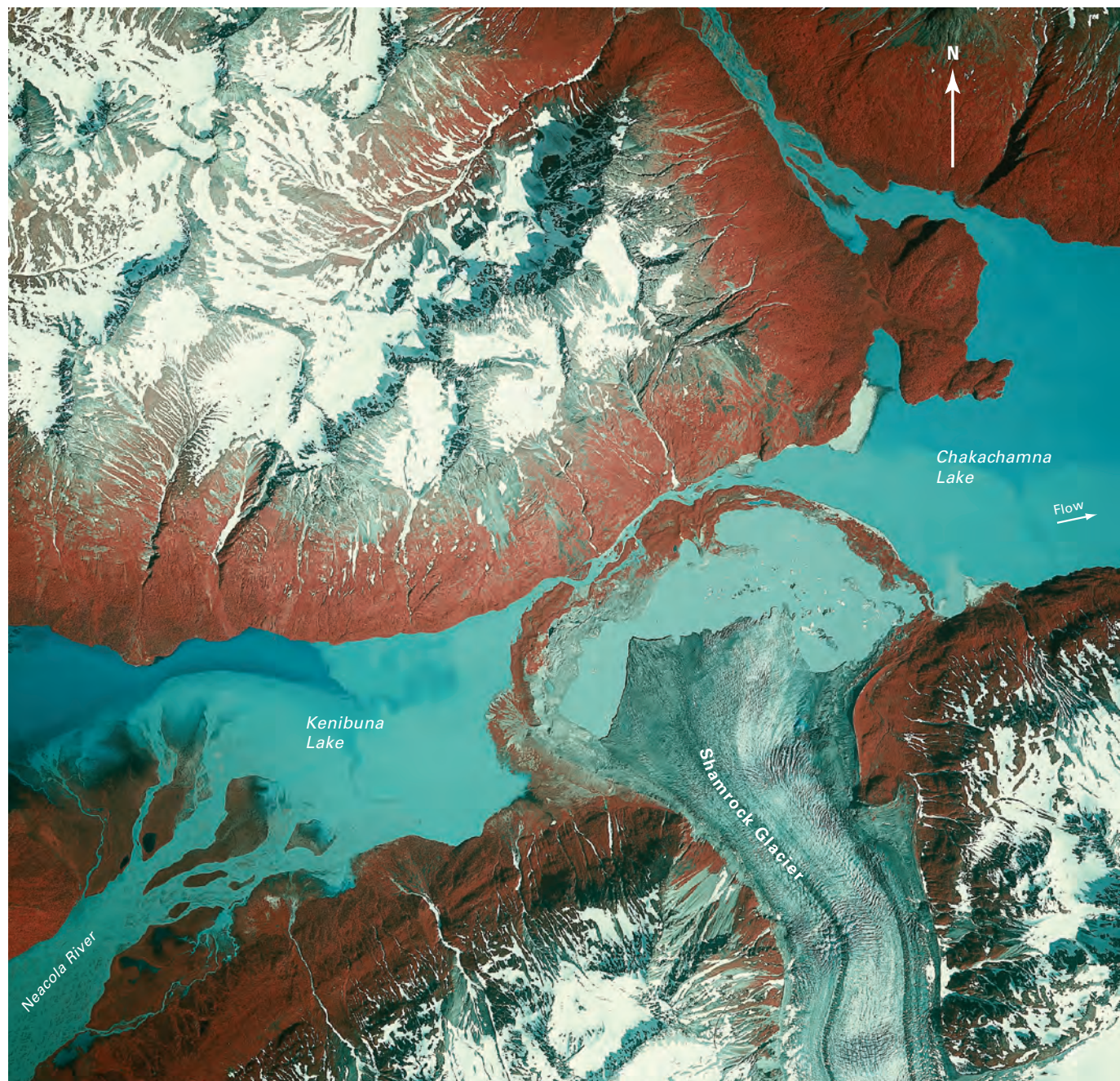


others, 2003); (3) Lower Skolai Lake (Nizina Glacier); (4) Tulsequah Lake (Tulsequah Glacier, Canada); (5) Flood Lake (Flood Glacier, Canada) (Omanney, 2002a, fig. 21, p. J54); and (6) Great Lake (Great Glacier, Canada).

From an analysis of topographic maps and aerial photographs, Post and Mayo (1971) determined that there were 750 glacier-dammed lakes larger than 0.1 km<sup>2</sup> in south-central Alaska, southeastern Alaska, and adjacent Canada. They noted that additional glacier-dammed lakes are located in the Aleutian Islands, the Alaska Peninsula, Kodiak Island, and the Brooks Range. However, they did not include these lakes in their total. They presented maps showing the location of glacier-dammed lakes, glacier-clad volcanoes, and other areas subject to jökulhlaups and also gave information on the location and area of the lakes, the areas impacted, the type of hazards involved, individual histories of flooding for specific glacier-dammed lakes, and other available data about the glacier-dammed lakes.

Post and Mayo (1971) presented seven mechanisms through which glacier-dammed lakes form subglacial, englacial, or supraglacial channels that

**Figure 59.**—20 July 1980 AHAP false-color infrared vertical aerial photograph of Kenibuna Lake, west of Shamrock Glacier, Chigmit Mountains, Aleutian Range, formed by damming of the Neacola River's valley. Chakachamna Lake, located to the east of Shamrock Glacier, is formed by the blockage of the eastern extension of this valley by Barrier Glacier. Recent retreat of Shamrock Glacier has resulted in the formation of an ice-marginal lake behind the glacier's "Little Ice Age" end moraine. Note the icebergs in the ice-marginal lake. Photograph No. L108F6633 is from GeoData Center, Geophysical Institute, University of Alaska, Fairbanks, Alaska.



facilitate the release of water: (1) slow plastic yielding of the ice owing to hydrostatic pressure differences between the lake and the less dense ice (Glen, 1954); (2) raising of the ice dam by floating (Thorarinnsson, 1939); (3) crack progression under combined shear stress owing to glacier flow and high hydrostatic pressure (Nichols and Miller, 1952); (4) drainage through small, preexisting channels at the ice-rock interface or between crystals in the ice; (5) water overflowing the ice dam, generally along the margin (Liestøl, 1956); (6) subglacial melting by volcanic heat (Tryggvason, 1960); and (7) weakening of the dam by earthquakes (Tryggvason, 1960). All of these mechanisms are applicable to Alaskan glacier-dammed lakes. [Editors' note: Other related research on the physics of the failure of ice-dammed lakes and associated jökulhlaups include work on Lake Donjek (Donjek Glacier) (Collins and Clarke, 1977; Clarke and Mathews, 1981), work on ice-dammed lakes in Iceland (Björnsson, 1976, 1977), and theoretical work by Nye (1976) on Flood Lake in the Coast Mountains of British Columbia, Canada (Clarke and Waldron, 1984) (see also Clarke and Holdsworth, 2002a).]

## Jökulhlaups at Bering Glacier

In the latter part of the 20th century (1981–84), jökulhlaups occurred from Berg Lakes on the western margin of the Steller Glacier in the Chugach Mountains. A second major outburst flood took place in 1986. The flooding of the river drainage west of the Bering Glacier was recorded on 12 September 1986 (fig. 60). In 1994, Bering Glacier in the Chugach Mountains experienced two jökulhlaups that significantly impacted local fauna and flora and modified the topography of adjacent land surfaces and the bathymetry of ice-marginal lakes. The glacier-outburst floods, both ice-margin, were of two different types: the catastrophic draining of an ice-dammed lake in May 1994 and the draining of surge-trapped water and sediment from an ice-margin outburst flood in July 1994 (Molnia, 1998).

The May 1994 flood resulted from the development of an approximately 500-m-long subglacial channel through and the subsequent failure of an ice dam at the northwestern margin of the Bering Glacier. The breaching of this tongue of ice lowered the surface level of 9×6-km Berg Lakes by more than 100 m (fig. 60B). An estimated 5.5 billion cubic meters of water escaped Berg Lakes and drained through Bering River during the ensuing 72-hour flood, completely inundating the Bering River valley from wall to wall. Because May is the time of moose calving and significant avian nesting activity—especially Dusky Canada Geese (*Branta canadensis occidentalis*) and Trumpeter Swans (*Olor buccinator*)—the outburst flood had a major impact on the local ecosystem. Post and Mayo (1971) previously stated that “lowering of the ice dam if continued will almost certainly lead to the release of immense floods in the near future. The Bering River flood plain and area surrounding Bering Lake are endangered by this increasingly critical situation” (cf. Post and Mayo, 1971, Sheet 3).

The July 1994 flood (fig. 61), which occurred on the southeastern margin of Bering Glacier approximately 45 km east of the May 1994 event, continued intermittently for more than a year. This flood event had estimated peak discharges in excess of 100,000 m<sup>3</sup> s<sup>-1</sup>; it deposited about 0.3 km<sup>3</sup> of sediment and ice into the ice-margin lake system on the southeastern side of Bering Glacier. Buried ice-blocks continue to melt, initiating the formation of kettle-holes and changing the surface morphology.

The 1994 floods were not unique. Bering Glacier has experienced similar flooding several times this century. Ice-dam failures at Berg Lakes have produced at least two similar floods in the last three decades. A 1967 aerial photograph taken by Post shows that a surge-terminating flood was occurring at about the same location that the 1994 eastern margin flood occurred. Bering Glacier floods have caused significant changes to the local environment.



**Figure 60.**—Photographs of jökulhlaups at Bering Glacier. **A**, 12 September 1986 oblique aerial photograph showing inundation of the Bering River and environs caused by a jökulhlaup from Berg Lakes. Photograph No. 86-R2-236 by Robert M. Krimmel, U.S. Geological Survey. **B**, Photograph looking across the basin of Berg Lakes, Bering Glacier, on 11 August 1998 showing the exposed lakebed produced by the catastrophic drainage of the lake in May 1994. The lake level was lowered by more than 100 m, and the jökulhlaup consisted of an estimated 5.5 billion m<sup>3</sup> of water. Photograph by Bruce F. Molnia, U.S. Geological Survey.



Jaeger and Nittrouer (1999a) examined Gulf of Alaska marine sediments looking for evidence of jökulhlaups from Bering Glacier. In a 250-cm-long core collected at the head of Bering Trough, they identified six laminated, high-porosity beds from 1994, 1953( $\pm 4$ ), 1938( $\pm 6$ ), 1917( $\pm 8$ ), 1899( $\pm 10$ ), and 1874( $\pm 13$ ). They correlated five of these beds with 20th century floods associated with surges reported by Molnia and Post (1995) that occurred in 1994, 1957–60, 1938–40, 1920, and 1900. No bed was identified that correlated with an observed jökulhlaup in 1967 that marked the end of the 1965–67 surge. Their 1874 bed probably correlates with a surge that has no remaining surficial evidence.

**Figure 61.**—Oblique color aerial photograph of the channel cut through the eastern terminus of the Bering Glacier by a jökulhlaup that initially discharged at the face of the glacier (the point marked by the “X” on the photograph). At the time this 29 July 1994 photograph was taken, less than 24 hours after the start of the jökulhlaup, the point of discharge had retreated nearly 0.8 km. Photograph by Bruce F. Molnia, U.S. Geological Survey.



## Debris-Covered Glaciers

Hundreds—probably thousands(?)—of Alaskan glaciers are partially, if not completely, covered by supraglacial sediment ranging in thickness from a few millimeters to many meters. Glaciers with large concentrations of supraglacial sediment are called “debris-covered glaciers.” Debris on glaciers is the result of a variety of mass-wasting, ice-transport, hydrologic, and eolian (including tephra) sediment-transport processes. The debris often has a significant influence on the rate of ablation of the ice located underneath, and most debris-covered glaciers have their greatest amount of debris, in area and (or) in thickness, in their ablation areas. However, some glaciers, especially those where the debris cover is the result of mass-wasting processes, may have their debris cover on either the accumulation areas or the ablation areas of the glacier (or both). On some glaciers, the thickness of supraglacial debris can exceed 15 m. Mature forests, often with trees more than 50 cm in breast-height diameter (BHD), grow on the debris-covered termini of more than a dozen glaciers in south-central Alaska, including Bering, Malaspina, Fairweather, and Yakataga Glaciers.

The origin of glacier debris varies from glacier to glacier and from geographic region to geographic region. With respect to mass-wasting processes, supraglacial debris on Alaskan glaciers can result from avalanching of snow, ice, and rock from adjacent valley walls; from rock avalanches caused by earthquakes, high-precipitation rainfall events, and other triggering processes; from solifluction from adjacent surfaces; and from frost wedging. The March 1964 *Good Friday* earthquake caused more than 100 rock avalanches onto glaciers in the Chugach and St. Elias Mountains (Post, 1967a) (see also figs. 58, 228, 229). Similarly, the 2 November 2002 M7.9 earthquake along the Denali Fault generated several large rock avalanches on a number of glaciers in the Alaska Range (see fig. 394). Typically, debris formed by mass-wasting processes is distinguishable by its angular character. Often, however, supraglacial debris transported by mass-wasting processes is reworked by glaciological and fluvio-glacial processes.

With respect to ice-transport processes, most debris on Alaskan glaciers results from concentration in the ablation area of sediment transported downglacier as englacial debris or as medial and lateral moraines. Debris produced in this fashion is also often reworked by aeolian and fluvial processes.

With respect to sedimentological processes, debris on Alaskan glaciers can also result from transport of sediment onto the glacier's surface by glacier-outburst floods (jökulhlaups) resulting from the failure of ice-dammed lakes in tributary valleys and from upglacier, ice-marginal lakes; from subglacial geothermal and (or) volcanic activity; from eolian transport of adjacent sand, silt, and clay, especially from the outwash plain; from the fall of volcanic tephra; and from lahar-type deposits originating from the summits or along drainage systems of glacier-covered volcanoes.

At many glaciers, ablation moraine produced by a combination of processes is reworked by meltwater and results in both winnowing and stratification of the deposits. Following initial deposition, much of a glacier's supraglacial debris is subject to secondary reworking.

Many Alaskan glaciers include a stagnant-ice zone characterized by thick accumulations of surface debris. One of the first of these glaciers to be studied in detail was the Martin River Glacier, located in the Chugach Mountains east of the Copper River. There, the evolution of a sequence of thermokarst landforms, including water-filled, sinkhole-like lakes, was documented by Reid and Clayton (1963) and Clayton (1964). Many glaciers with thermokarst lakes are the sites of high-discharge jökulhlaups. The evolution and growth of these lakes during the melting of the ice beneath the sediment are the focus of much recent research (Nakawo and others, 2000).

Stagnant, debris-covered ice goes through a geomorphological process that results in the final melting of buried ice, generally during a period of several decades to centuries, and the formation of a hummocky topography frequently referred to as "kame-and-kettle" topography. During the ablation process, local differences in the thickness of the insulating debris cover, combined with redistribution of sediment, result in differential ablation of the underlying ice and the formation of thermokarst pits, many of which support supraglacial lakes and ponds. As these lakes and ponds evolve, they frequently drain and cause flooding downstream from the glacier's terminus.

Richardson and Reynolds (2000) studied processes leading to ice-cored moraine degradation for three natural dams in Perú and Nepal. They noted that potentially hazardous lakes form on the snouts of debris-covered glaciers and that this occurrence may separate a stagnant-ice body from the upper reaches of the glacier to form an ice-cored, end-moraine complex. They described a process that ultimately results in a jökulhlaup. Degradation through ablation beneath the debris cover by localized thermokarst development and by associated loss of ice mass leads to lake expansion, typically along glacier crevasses and other internal glacier structures. Once exposed, the ice undergoes accelerated wastage through the combined effects of solar radiation and mechanical failure caused by the rheological response of the ice to deepening ice depressions. Continuing degradation reduces the lake "freeboard" and weakens the moraine dam, thereby setting the stage for catastrophic failure of the dam.

Debris-covered ice melts at a slower rate than bare glacier ice under similar conditions. If the protective debris cover is sufficiently thick, the ablation rate approaches zero, as it does at the terminus region of Sherman Glacier (see figs. 58, 229). On the other hand, a thin debris cover may act as a heat sink and cause the rate of the melting of the ice to increase immediately below. Although no studies of Alaskan glaciers were found comparing ablation rates for adjacent bare and debris-covered ice, investigations have been conducted on temperate glaciers at several locations. [Editors' note: According to Mark F. Meier (written commun., 2004), Driedger's (1981) research on the effect of tephra fall on the melting of ice and snow on Mount St. Helens, Wash., concluded that the "breakeven point" between accelerated melting and insulation occurred at a thickness of 2.5 cm.]

Kayastha and others (2000) studied the ablation of bare and debris-covered ice on Khumbu Glacier, Nepal, from 21 May to 1 June 1999 to determine

how the sediment cover affected the relationship between the positive degree-day factor and the ablation rate. They found that, with a debris cover ranging in thickness from 0 to 5 cm, ice ablation was at its maximum with a debris cover of 0.3 cm and that debris thicker than 5 cm retarded ablation. Ice ablation from net solar radiation was measured at several depths on the glacier. On a bare ice surface, ablation was  $16.9 \text{ mm d}^{-1}$ . Under 10- and 40-cm-thick debris layers, ablation was  $11.1$  and  $5.3 \text{ mm d}^{-1}$ , respectively. Similarly, Takeuchi and others (2000) measured ablation and heat balance in debris-covered and debris-free areas of the ablation zone at Khumbu Glacier during the same period of time. They found that ablation rates on the debris-free ice ranged from  $1.4$  to  $4.7 \text{ cm d}^{-1}$  and were inversely correlated with the albedo. Melting of debris-covered ice decreased sharply with increasing thickness. Debris with a thickness of 10 cm slowed melting to about 40 percent of the rate of bare ice at the same low albedo. The primary cause of melt reduction was the insulating effect of the debris cover. Interestingly, they also found that the heat stored in the debris layer during daytime was released to the atmosphere during nighttime and warmed the air rather than being conducted downward to melt ice.

As part of ongoing annual mass balance measurements on Lyman Glacier and Columbia Glacier, North Cascades, Wash., Pelto (2000) measured ablation of ice on adjacent clean and debris-covered sections of each glacier. For Columbia Glacier, between 1986 and 1998, the annual ice ablation was 3.3 m water equivalent for clean glacier ice and 2.3 m water equivalent for debris-covered areas. For Lyman Glacier from 1986 to 1999, the average annual ablation on the clean glacier ice was 3.4 m; under the debris cover, average annual ablation was 2.6 m water equivalent.

Finally, debris-covered glaciers pose a problem for monitoring glacier change by means of remote sensing techniques, especially those using medium- to low-resolution multispectral instruments. A debris-covered surface of a glacier has a spectral reflectance similar to that of adjacent bedrock or sediment bodies. Often, the glacier's debris cover and the adjacent ice-marginal sediment are derived from the same bedrock and therefore have the same composition. Given the lower spatial resolution of large picture elements (pixels), the ability to discriminate between supraglacial, moraine, and outwash deposits on the basis of morphological characteristics is also greatly diminished.

# Part 3—Descriptions of Alaska's 14 Glacierized Geographic Regions

## Introduction

As stated in the introduction to this volume, the primary purpose of this compilation is to provide a baseline that summarizes the areal extent and geographic distribution of Alaskan glaciers during the decade marking the advent of the Landsat series of satellites. The first satellite in the series, ERTS-1 (later renamed Landsat 1), was launched on 23 July 1972. By 2004, there had been seven satellites in the series; six successfully reached orbit and became operational for varying lengths of time. It is hoped that this baseline will be used now and by future researchers to document change in the number, length, and area of Alaska's glaciers. Because of the large geographic area involved, Alaska has been divided into 14 glacierized regions:

- Coast Mountains
- Alexander Archipelago
- St. Elias Mountains
- Chugach Mountains
- Kenai Mountains
- Kodiak Island
- Aleutian Range
- Aleutian Islands
- Wrangell Mountains
- Talkeetna Mountains
- Alaska Range
- Wood River Mountains
- Kigluaik Mountains
- Brooks Range

Landsat MSS imagery collected between 1972 and 1983 has been used to define 14 glacierized geographic regions in Alaska. Each geographic region is treated separately. Oblique and vertical aerial and ground photographs acquired during the period of the baseline and baseline-contemporary field observations are used to supplement the information derived from analysis of remotely sensed data. Of particular value are the high-altitude false-color infrared vertical aerial photographs of Alaska's glaciers acquired by a NASA U-2 aircraft between 1978 and 1986. Many of the AHAP photographs are used as figures throughout or cited in the text.

Pre-baseline ancillary information, such as historic ground and aerial photography and maps, and descriptive narratives of early explorers are included wherever possible to extend the baseline back to the 18th and 19th centuries or earlier if possible. These pre-baseline qualitative and quantitative data are used to characterize the activity of Alaskan glaciers before the acquisition of Landsat MSS images and to extend the documentation of long-term trends and changes.

Recent information about changes that have occurred in Alaska's glaciers after the period of the baseline is also presented if it is available. Many of these later data were acquired by increased picture element (pixel) resolution satellite sensors that did not exist at the time of the Landsat MSS image baseline—for example, Landsat Thematic Mapper (TM), Landsat 7 Enhanced Thematic Mapper (ETM+), Advanced Spaceborne Thermal Emission and Reflection (ASTER), and satellite Synthetic Aperture Radar (SAR) imagery.

## Analysis of Glacier Activity

Wherever possible, information used to produce and enhance the baseline is also used to determine the activity of individual glaciers and is included





**Figure 62.**—Oblique color aerial photograph on 20 August 1977 of a valley glacier in the Chugach Mountains, informally called Five Stripe Glacier. The well-defined trimlines on the valley walls on both sides of the terminus, a layer of lateral moraine paralleling the left margin of the glacier and extending both above and downvalley of the terminus, and several exposed medial moraines elevated above the ice surface and extending beyond the ice margin are all evidence of recent thinning and retreat. As most of these sedimentary features are ephemeral, these changes have had to occur in a very short period of time. Photograph by Bruce F. Molnia, U.S. Geological Survey.

in the description of each of the 14 glacierized geographic regions and sub-regions. The terminus of a glacier may be advancing, retreating, or stationary. A stationary terminus generally represents a glacier that is in dynamic equilibrium, where the rate of glacier flow equals the rate of melting (that is, the glacier has a mass balance that is in equilibrium; accumulation is equal to ablation). Thus, the position of the terminus does not change. A stationary terminus may also be stagnant. In a stagnant state, glacier ice is typically detached from its source area and is no longer in motion. Frequently, stagnant ice develops a thick cover of glacial debris that insulates it from significant melting. In many such cases, the glacier-ice surface is subsequently covered by vegetation.

### Evidence of Glacier Retreat Used in This Analysis

A number of glacial-geology criteria are used to determine recent glacier activity. Indicators of retreat usually involve exposure of deglaciated terrain, often with specific sedimentary and geomorphic features. Among the most common indicators are trimlines, abandoned lateral moraines, and abandoned medial moraines, although the latter are very rarely preserved. Figure 62 shows a number of retreat characteristics displayed by a valley glacier in the Chugach Mountains, informally known as *Five Stripe Glacier*. In addition to the characteristics already mentioned, vegetation-free bedrock surrounding an ice-margin is another criterion useful to document recent retreat. Figure 63 shows additional criteria such as vegetation along the break-in-slope at the lower end of the central U-shaped valley, which suggests that the glacier has not recently extended beyond that point. The absence of vegetation on the floor or walls of the hanging valley indicates that the entire surface was covered by glacier ice not too long ago and has only recently been deglaciated. A distinctive trimline on the right side of the valley and the color change near the top on the left side of the valley offer additional evidence of recent retreat.

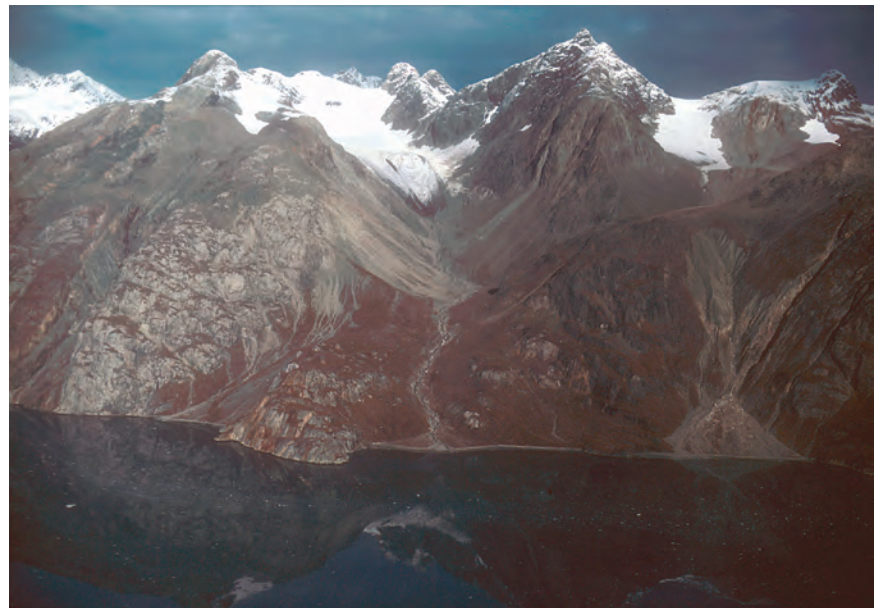


**Figure 63.**—Oblique color aerial photograph on 3 October 1979 of an unnamed hanging glacier in Glacier Bay, Saint Elias Mountains, which displays additional criteria that can be used to document recent glacier recession. Vegetation along the break in slope at the lower end of the central “U”-shaped valley suggests that the glacier has not extended beyond that point recently. The absence of vegetation on the floor or walls of the hanging valley suggests that the entire surface was recently covered by glacier ice. The distinctive trimline on the right side of the valley and the color change on the left side of the valley near the top are additional evidence of recent, rapid retreat. Photograph by Bruce F. Molnia, U.S. Geological Survey.

### Evidence of Glacier Advance Used in This Analysis

The formation of push moraines (fig. 64) and the overriding of vegetation by advancing ice (fig. 65) are two primary indicators of glacier advance. As a glacier advances, it generally displaces, flows over, or flows around anything in its path. As it advances over unconsolidated sediment, it may push both forward and upward to form a push moraine. Generally, push moraines are from 1 to 2 m high. However, they may reach a height of 5 m or more. During the 1993–95 surge of Bering Glacier, numerous push moraines developed along more than 15 km of the margin of the glacier. Many were spatulate in shape and showed evidence of an upward thrusting of the advancing terminus. If an advancing glacier encounters a forest, it sometimes uproots or shears off the trees and then overrides them (fig. 66). Glaciers that produce large quantities of fluvio-glacial sediment may bury vegetation in outwash deposits to a uniform height and then override this sediment and shear trees at the top of the sediment. Subsequent erosion may expose the trunks in their *in situ* growth position (fig. 67).

### Evidence of Glacier Stagnation Used in This Analysis

Sediment-covered stagnant ice may persist for decades or even several hundred years. Many of Alaska's glaciers, such as Bering, Yakataga, Fairweather, Malaspina, and Muldrow Glaciers, have vegetation, including trees more than 100 years old growing on their debris-covered stagnant ice sur-



▲ **Figure 64.**—15 July 1978 photograph of part of the terminus of Harriman Glacier, Chugach Mountains, showing a recently formed 1-m-high push moraine. Photograph by Bruce F. Molnia, U.S. Geological Survey.

◀ **Figure 65.**—14 July 1994 oblique aerial photograph of a lobe of Bering Glacier, Chugach Mountains, which was overriding an alder (*Alnus* sp.) forest as it advanced during the 1993–95 surge. The trimline above the advancing terminus and the very young vegetation suggest that a thicker ice mass recently existed in this area. Photograph by Bruce F. Molnia, U.S. Geological Survey.



**Figure 66.**—Photograph of the results of late 19th century advance of La Perouse Glacier that sheared and overrode the trees located along its western margin. Subsequent retreat left the vegetation as an integral part of the push moraine. 18 June 1899 photograph by Grove Karl Gilbert, USGS. Photograph Gilbert 333 from the USGS Photographic Library, Denver, Colo.

faces (fig. 68). Others, such as Herbert Glacier, have large debris-covered ice-cored moraines (fig. 69). Typically, large circular depressions known as thermokarst pits will form on these sediment-covered stagnant bodies of ice.

**Figure 67.**—12 July 1991 photograph of three sheared tree trunks exposed by erosion following the recent retreat of the margin of Bering Glacier. These trunks are in growth position. Photograph by Bruce F. Molnia, U.S. Geological Survey.



**Figure 68.**—Oblique color aerial photograph of vegetation growing on the surface of sediment-covered stagnant ice, Bering Glacier, Chugach Mountains, on 8 June 1976. The height of the ice face is about 15 m. On the Malaspina Glacier, mature spruce trees more than 100 years old, exist in a similar setting. Photograph by Bruce F. Molnia, U.S. Geological Survey.



**Figure 69.**—8 July 1968 photograph of a debris-covered, ice-cored moraine that lies adjacent to the retreating terminus of the Herbert Glacier, Coast Mountains. This ice-cored moraine was emplaced about 40 years prior to the time of the photograph. Photograph by Bruce F. Molnia, U.S. Geological Survey.



As the pits expand by melting, vegetation will be displaced from the surface and fall into the thermokarst pits (fig. 70).

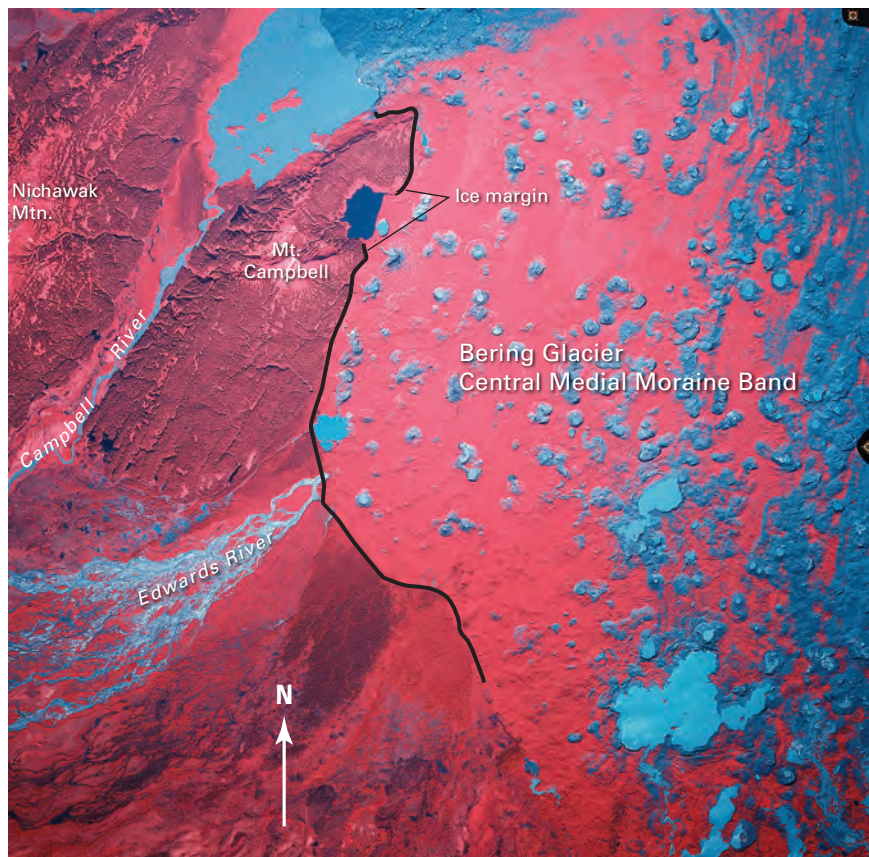


**Figure 70.**—27 July 1983 AHAP false-color infrared vertical aerial photograph of large circular depressions, termed thermokarst pits, that are developing on the sediment-covered stagnant ice surface of Bering Glacier's Central Medial Moraine Band. The Central Medial Moraine Band separates the active Bering Lobe from the active Steller Lobe. Vegetation-covered ice is red in color, whereas debris-covered ice is blue gray. The largest depressions are more than 400 m in diameter. AHAP photograph no. L118F4494 from the GeoData Center, Geophysical Institute, University of Alaska, Fairbanks, Alaska.

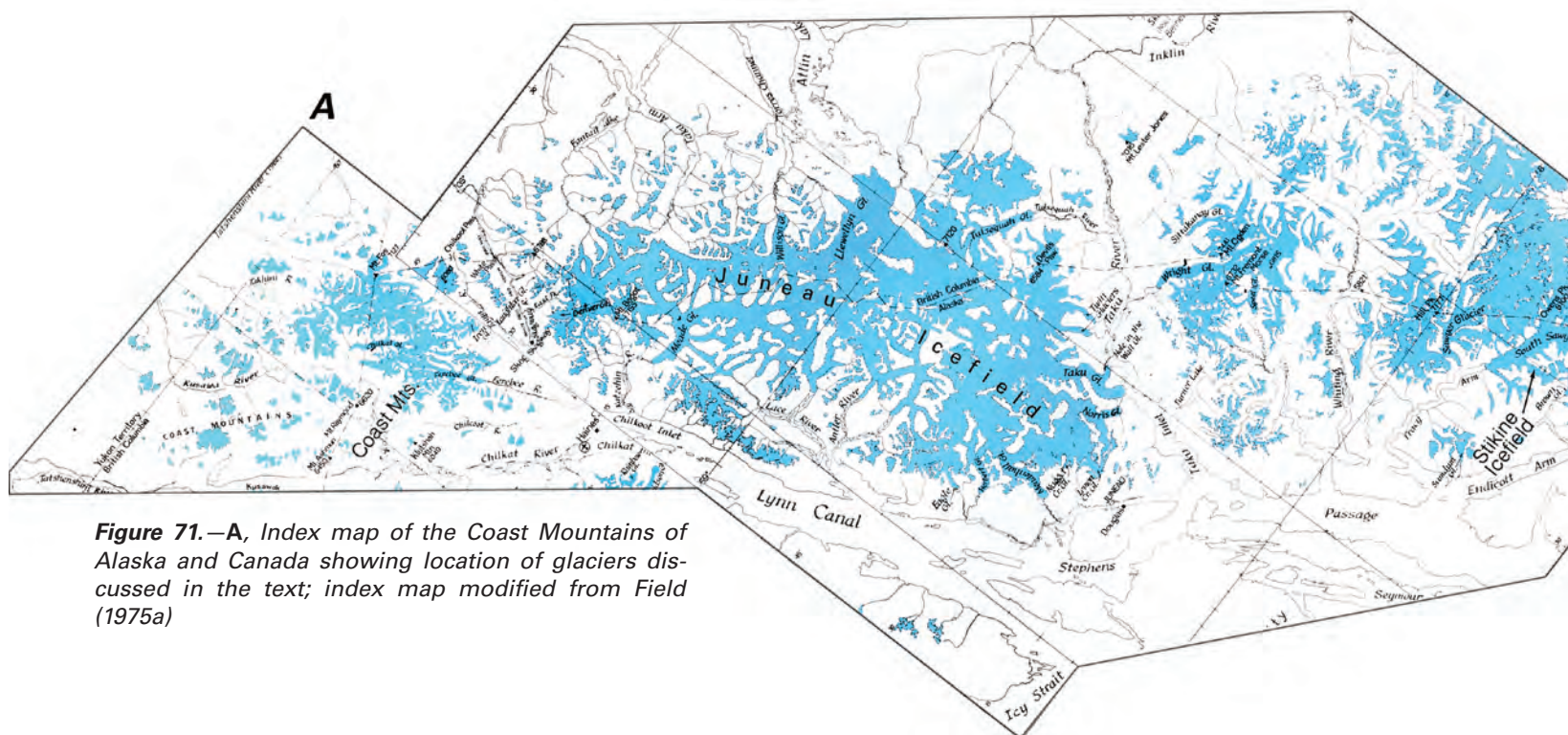
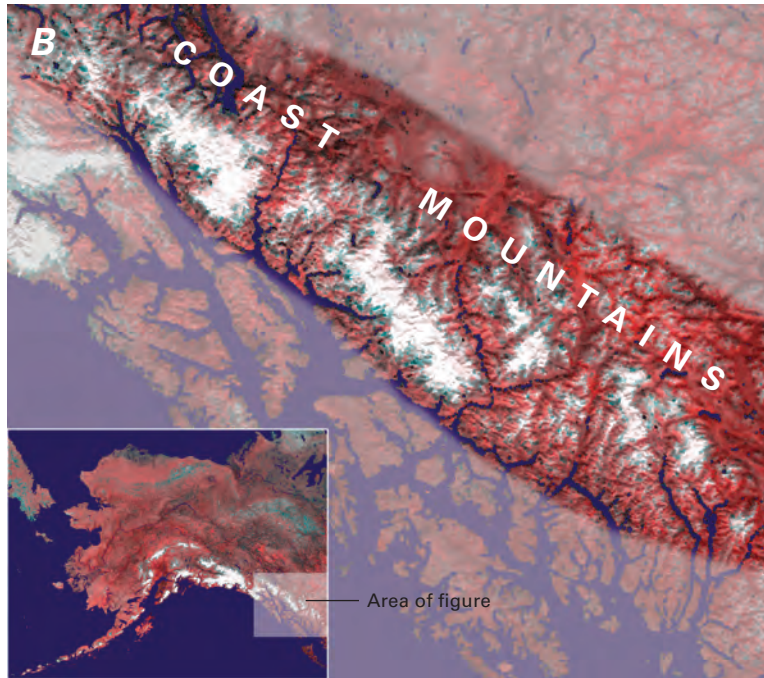


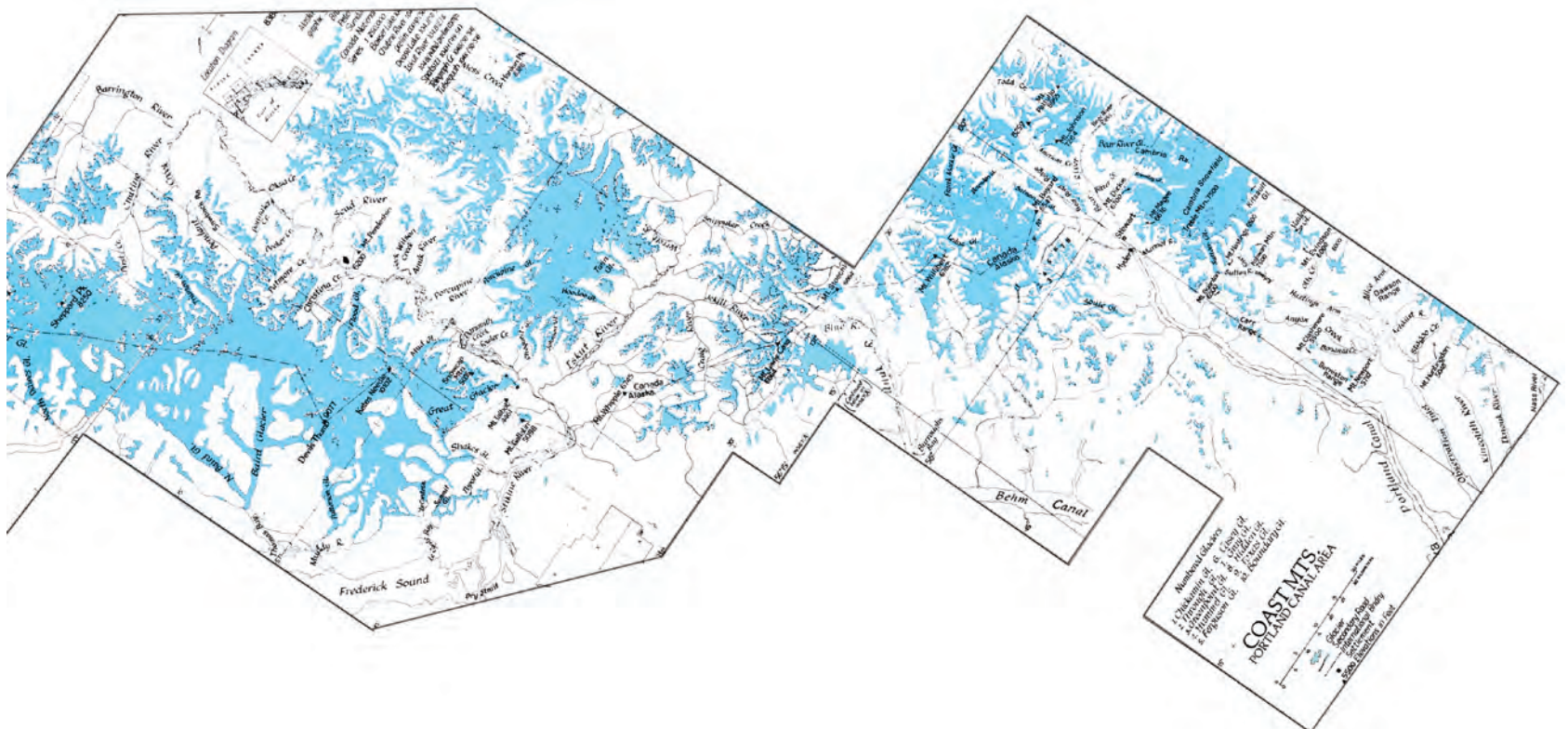
**Figure 71.**—A, Index map of the Coast Mountains of Alaska and Canada showing location of glaciers discussed in the text; index map modified from Field (1975a)

## Coast Mountains

**Figure 71.—B,** Enlargement of NOAA Advanced Very High Resolution Radiometer (AVHRR) image mosaic of the Coast Mountains in summer 1995. National Oceanic and Atmospheric Administration image mosaic from Mike Fleming, USGS, EROS Data Center, Alaska Science Center, Anchorage, Alaska.



The Coast Mountains, which form the mainland portion of southeastern Alaska, extend for about 700 km from Portland Canal in the south to Mount Foster north-northwest of Skagway. From east to west, the glacierized area of the Coast Mountains is as much as 130 km wide (fig. 71). Included in the Coast Mountains are a number of individual ranges: Peabody Mountains, Rousseau Range, Halleck Range, Seward Mountains, Lincoln Mountains, Buddington Range, Kakuhan Range, Chilkoot Range, Sawtooth Range, and Takshanuk Mountains, all of which support glaciers. To the south, the glaciers are small and sparsely distributed. They increase in area and number to the north. The greatest concentration of Coast Mountain glaciers are in two ice fields, the *Stikine Icefield* and the Juneau Icefield. [Editors' note: Ice field is used throughout the text in its glaciological sense with reference to "an extensive mass of land ice covering a mountain region consisting of many interconnected alpine and other types of glaciers, covering all but the highest peaks and ridges" (Jackson, 1997, p. 316). The UNESCO (1970) definition is slightly different. "Ice masses of sheet or blanket type of a thickness not sufficient to obscure the subsurface topography." In this volume, icefield is standardized and used as a compound word in formal geographic place-names, that is, approved by BGN—(for example, Sargent Icefield). Most Alaskan "icefields" and associated outlet glaciers are true ice fields.] The total area of glaciers in the Coast Mountains is 10,500 km<sup>2</sup> (Post and Meier, 1980, p. 45). Unless otherwise noted, lengths and areas presented here are those given by Field (1975c), who used primarily



USGS 1:250,000-scale topographic maps (appendix A) for his quantitative measurements. These maps were generally compiled from aerial photography acquired and ground surveys performed between 1948 and 1964 and vary in the accuracy of the cartographic representation of the glaciers.

Much diverse information is available to monitor changes in the glaciers of this area. Baird Glacier (in the central Coast Mountains at lat 57°13'N., long 132°26'W.) is typical of the area. It was covered by early (1977, 1979, 1980) and later (post-1980) Landsat imagery and aerial photography (1929, 1948, 1967, 1979) and has also been surveyed and mapped many times. It was first surveyed by the United States Coast and Geodetic Survey in 1887 (USC&GS, 1891). It was then mapped by the IBC in 1894, during which time O.J. Klotz (1895, 1899) performed “a photo-topographic survey of the front of the glacier for the study of its motion,” (Klotz, 1899, p. 523). It was visited by USGS field parties in 1904, 1922, 1923, and 1924, mapped again by the USC&GS in 1924, visited by an AGS field party in 1941 (Field, 1942), and then topographically mapped by the USGS between 1948 and 1961.

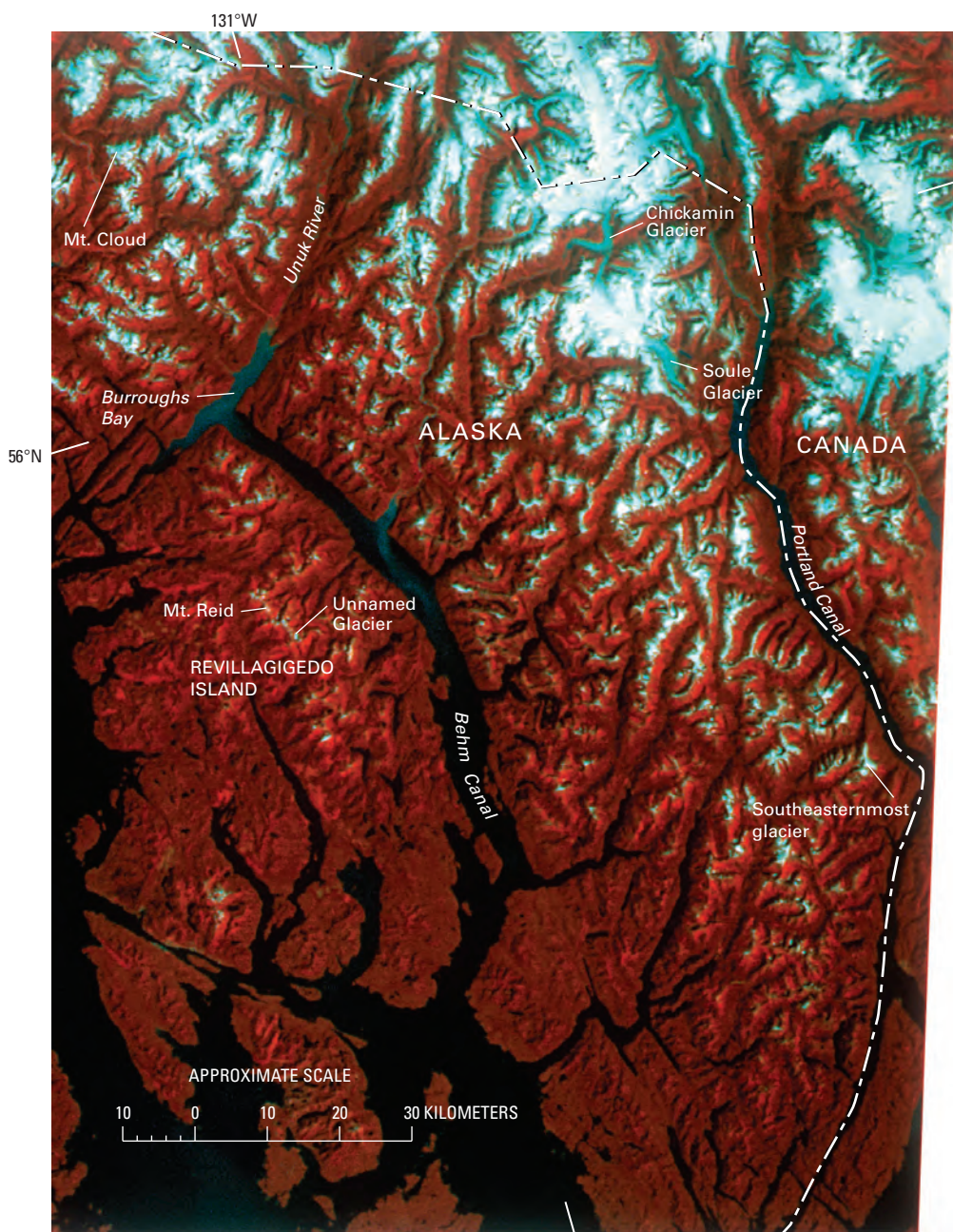


**Figure 72.**—Part of an annotated Landsat 2 MSS false-color composite image showing the Portland Canal to Burroughs Bay and Unuk River segment of the Coast Mountains and Revillagigedo Island. The locations of numerous Coast Mountain glaciers, up to 22 km in length, and the only glacier on Revillagigedo Island are shown. Landsat image (22027–19085; 10 Aug 1980; Path 59, Row 21) is from the USGS, EROS Data Center, Sioux Falls, S. Dak.

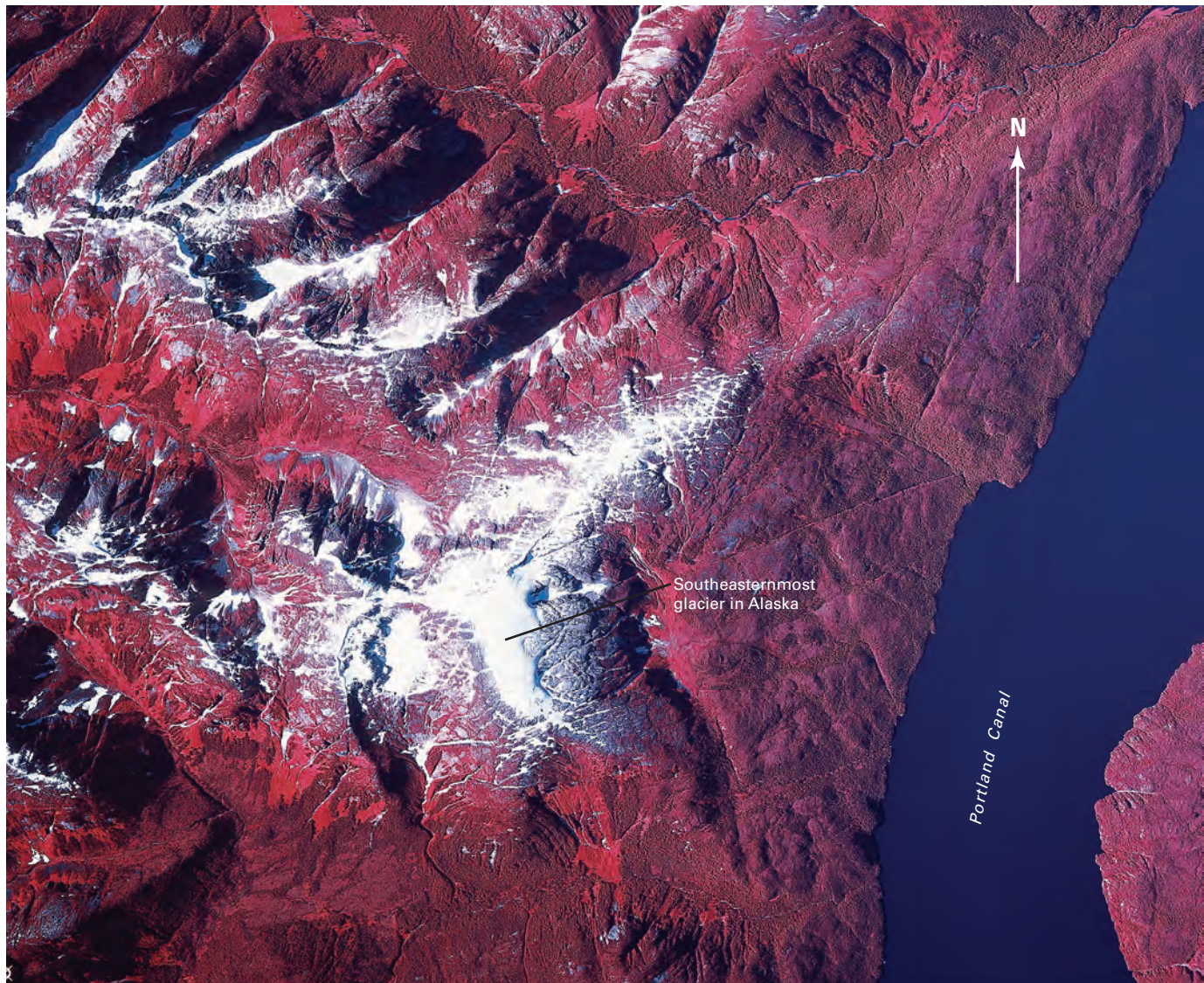
Additional studies, such as tree-ring investigations, were carried out by Donald Lawrence (Lawrence, 1950).

### Portland Canal to Burroughs Bay and the Unuk River

Landsat MSS images that cover the Coast Mountains from Portland Canal to Burroughs Bay and the Unuk River have the following Path/Row coordinates: 58/21 and 59/21 (fig. 3A, table 1). This region contains several hundred glaciers, including the southeasternmost glaciers in Alaska (figs. 72, 73). Only about a dozen glaciers are named. Most glaciers are small (generally less than 2 km long) and show evidence of recent retreat (fig. 73). Soule Glacier, one of the larger glaciers in the region, has an area of about 66 km<sup>2</sup> (Field, 1975c, p. 99). Its terminus retreated about a kilometer in the 31 years between 1948, when aerial photography was acquired for mapping, and 14 August 1979, when it was photographed by the AHAP program (figs. 74A, B). It was still retreating when it was photographed from the space shuttle in August 1989 (see NASA Space Shuttle photograph no. STS028-073-039 acquired in August 1989).

Similarly, 26-km-long Chickamin Glacier, the largest glacier in the region, has an area of about 140 km<sup>2</sup> (Field, 1975c, p. 99). It retreated about 1 km and formed an ice-marginal lake in the 24 years between 1955, when it was mapped (USGS Bradfield Canal 1:250,000-scale map, appendix A), and 14 August 1979, when an AHAP false-color infrared vertical aerial photograph

**Figure 73.**—Part of a 12 August 1979 AHAP false-color vertical aerial photograph of the unnamed southeasternmost glacier in Alaska. This 1.5-km-long glacier shows evidence of recent retreat and is fringed by vegetation-free exposed bedrock that appears grey. AHAP photograph no. L185F4825 from the GeoData Center, Geophysical Institute, University of Alaska, Fairbanks, Alaska.





was acquired (fig. 75). Field (1975a) reported that, during the first two-thirds of the 20th century (1902–1964), Chickamin Glacier retreated more than 2.7 km, an annual rate of approximately  $44 \text{ m a}^{-1}$ . Elsewhere in this region, Through Glacier (approximately 8 km) and Gracey Creek Glacier (approximately 5.25 km) exceed 5 km in length. All of the larger glaciers are located in the northern part of this region in the higher elevations, and all show evidence of recent retreat. Texas Glacier (8 km long in Alaska, with an area of about  $12 \text{ km}^2$ ) (Field, 1975c, p. 99) and Hummel, Ferguson, Casey, and Hidden Glaciers, all located east and southeast of Chickamin Glacier, are mapped with vegetation-free zones around their perimeters.

### Burroughs Bay and the Unuk River to the Stikine River

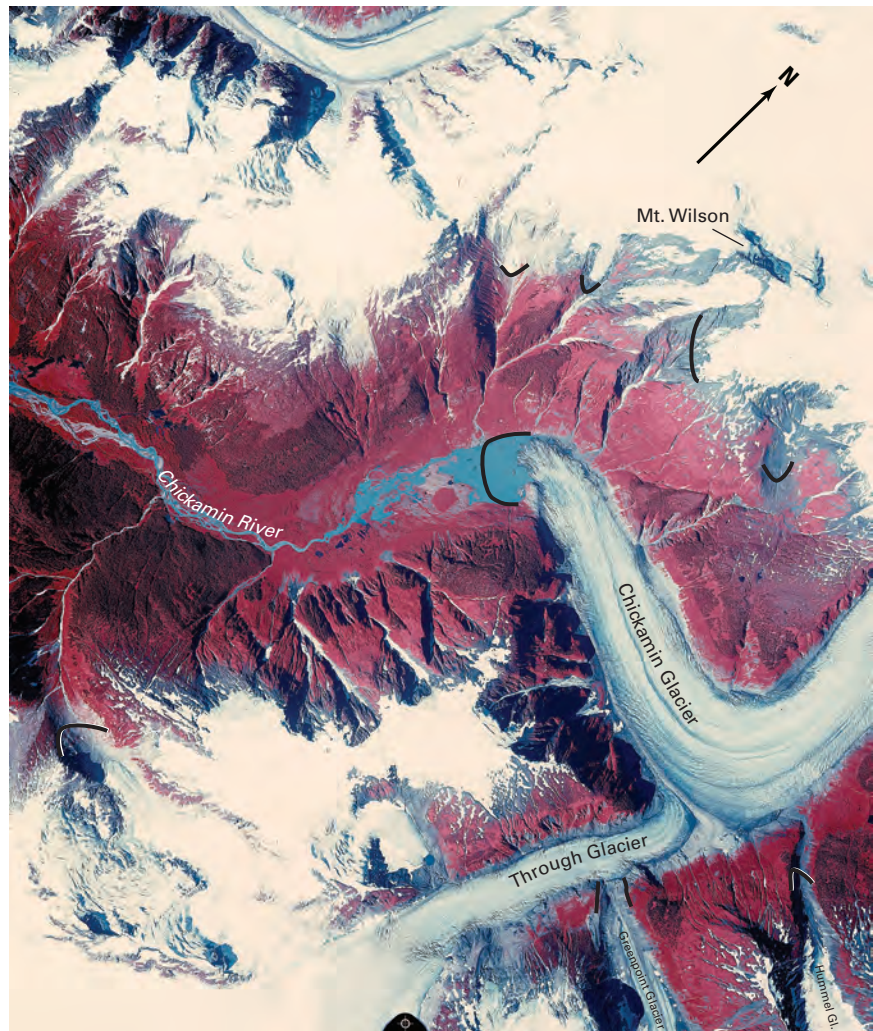
Landsat MSS images that cover the Coast Mountains from Burroughs Bay and the Unuk River to the Stikine River have the following Path/Row coordinates: 58/21, 59/21, and 60/20 (fig. 3A, table 1). This region contains several hundred glaciers, only one of which (Nelson Glacier) is named (figs. 76, 77). Most are small (generally less than 2 km long) and show evidence of recent retreat. Several areas between Bradfield River and Cone Mountain, generally above 1,500 m in elevation, host significant accumulations of glacier ice. The largest of these accumulations is a small ice field centered about 11 km southeast of Cone Mountain. About a dozen individual distributary glaciers descend from the ice field, some to elevations as low as approximately 500 m. A similar accumulation of ice occurs east of Mount Cloud.

Five-kilometer-long Nelson Glacier, located about 25 km east of Wrangell, heads between Marsha Peak (1,380 m) and Mount Waters (1,330 m). It and the many smaller unnamed glaciers adjacent to it show significant evidence of recent retreat. Nelson Glacier retreated about 1 km and formed an ice-marginal lake in the 31 years between 1948 and 14 August 1979, the dates that aerial photography was acquired (fig. 77).

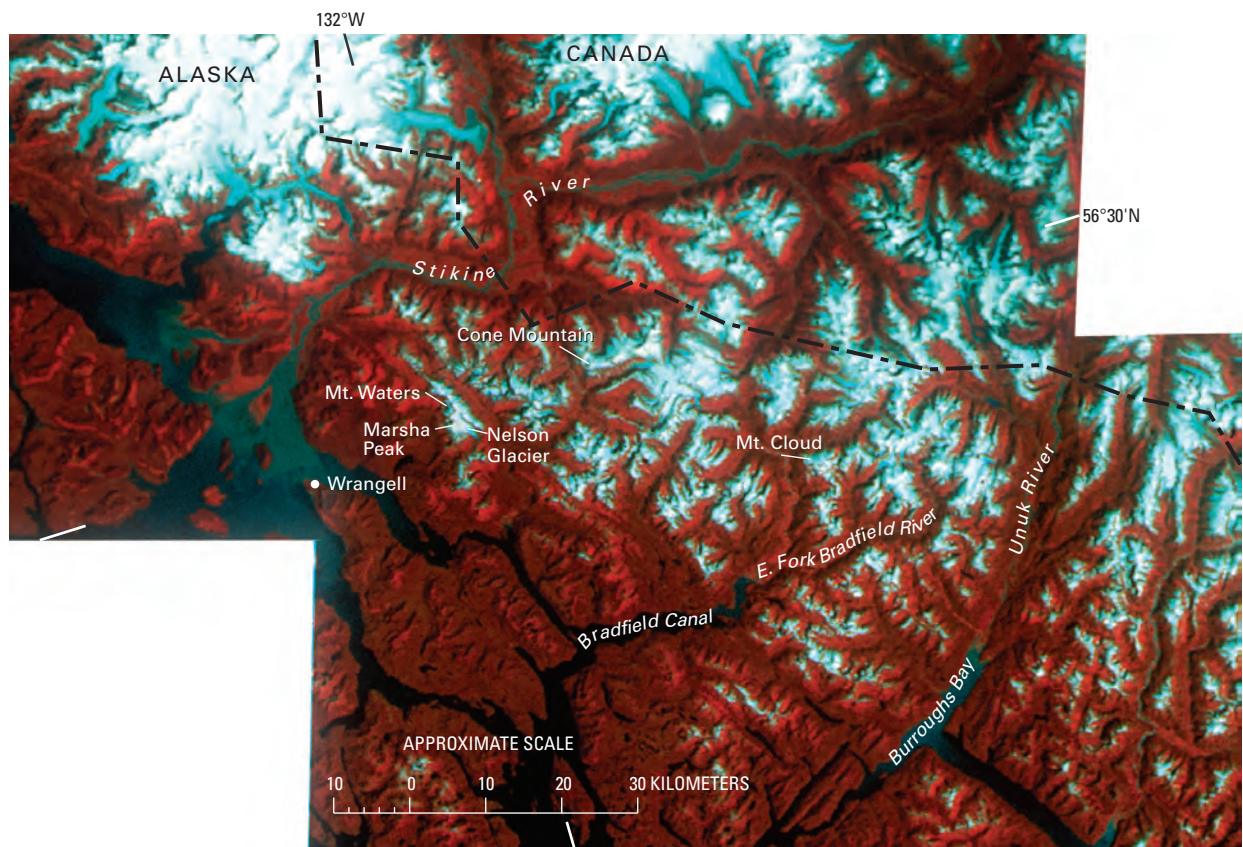
**Figure 74.**—**A**, Part of a 14 August 1979 AHAP false-color vertical aerial photograph of the lower 7 km of the retreating Soule Glacier, located between the Lincoln Mountains to the northeast and the Seward Mountains to the west. Trimline development and the formation of two small ice-marginal lakes indicate recent downwasting. Tributary hanging glaciers that previously descended from the Seward Mountains have also recently retreated. AHAP photograph no. L183F5093 from the GeoData Center, Geophysical Institute, University of Alaska, Fairbanks, Alaska. **B**, Part of USGS Ketchikan map (1955) showing the Soule Glacier and environs. On the 1948 aerial photographs used for the map, Soule Glacier was nearly a kilometer longer than shown on the 1979 AHAP photograph. USGS Alaska Topographic Series, 1:250,000-scale, Ketchikan, Alaska-Canada (appendix A).



► **Figure 75.**—14 August 1979 AHAP false-color vertical aerial photograph of the lower 8 km of the Chickamin Glacier and adjacent Through, Greenpoint, and Hummel Glaciers. Many other small unnamed glaciers occur on the flanks of Mount Wilson. Exposed bedrock around many of the smaller glaciers documents recent retreat. All of the named glaciers and most of the unnamed glaciers are retreating. When photographed in 1948, Greenpoint Glacier made contact with Through Glacier and Through Glacier made contact with Chickamin Glacier. The heavy black lines show the approximate extent of glacier termini in 1948. AHAP photograph no. L183F5097 from the GeoData Center, Geophysical Institute, University of Alaska, Fairbanks, Alaska.



▼ **Figure 76.**—Annotated Landsat 2 MSS false-color composite image mosaic showing the Coast Mountains from Burroughs Bay and Unuk River to the Stikine River. The image mosaic depicts Nelson Glacier, a small icefield southeast of Cone Mountain, and another concentration of ice east of Mount Cloud. Landsat images 22028–19141; 11 August 1980; Path 60, Row 20 (north) and 22027–19085; 10 August 1980; Path 59, Row 21 (south) are from the USGS, EROS Data Center, Sioux Falls, S. Dak.



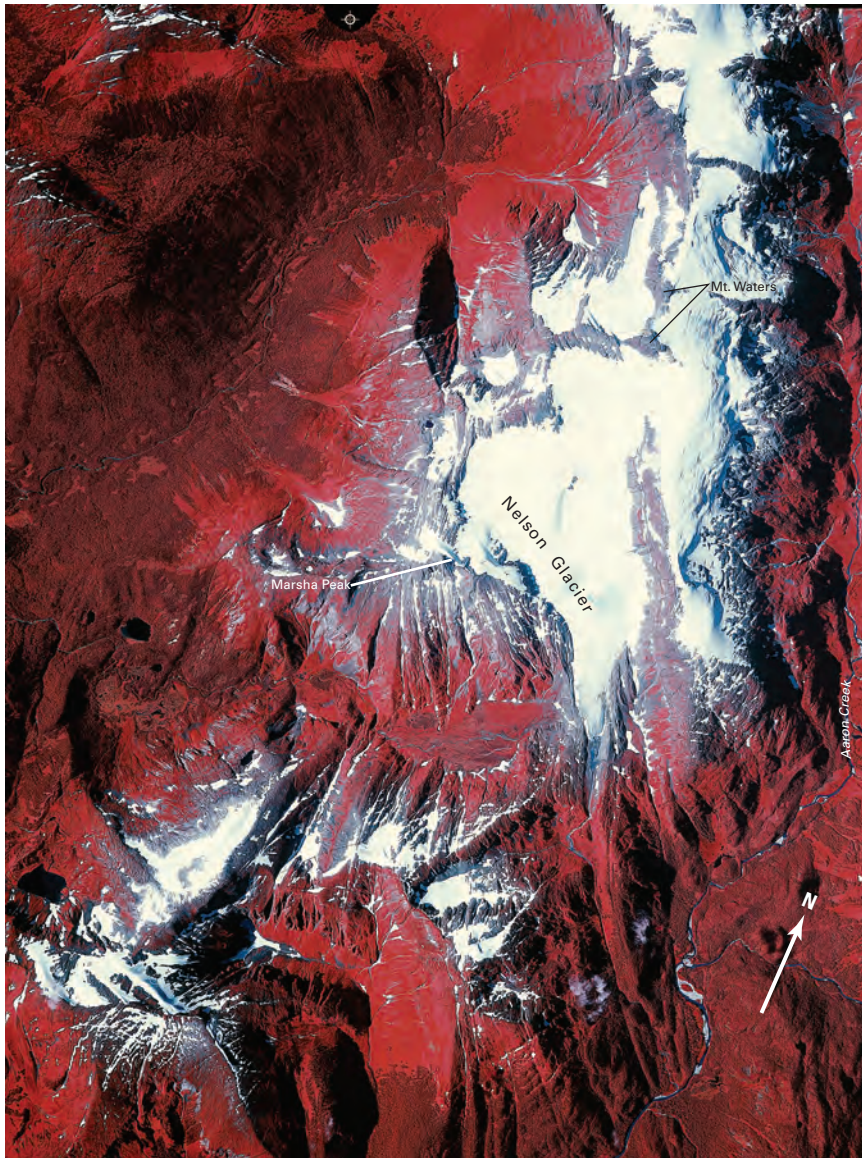


**Figure 77.**—Part of an 11 August 1979 AHAP false-color vertical aerial photograph of 5-km-long Nelson Glacier and adjacent smaller, unnamed glaciers, many snow covered. Vegetation-free, recently exposed bedrock around Nelson Glacier and many of the smaller glaciers documents recent retreat. AHAP photograph no. L189F4363 from the GeoData Center, Geophysical Institute, University of Alaska, Fairbanks, Alaska.

## Stikine River to Taku River

Landsat MSS images that cover the Coast Mountains from the Stikine River to the Taku River have the following Path/Row coordinates: 59/20, 60/20, 61/19, 61/20, and 62/19 (fig. 3A, table 1). Between the Stikine River and the Whiting River, the glaciers increase in number, size, and organization (fig. 78A). The southernmost tidewater glaciers in Alaska are found here (fig. 41). Most glaciers in this region are distributaries of the *Stikine Icefield*, which extends from north of the Stikine River to south of the Taku River. The *Stikine Icefield* straddles the crest of the Coast Mountains along the U.S.-Canadian Border and has a length of approximately 190 km. This region contains several hundred glaciers, about a dozen of which are named. More than a dozen glaciers are 15 km in length or longer. Several of the larger glaciers originate in Canada at elevations above 2,000 m and flow westward to sea level. The word “Stikine” is the Tlingit name for Great River. Much of the southern *Stikine Icefield* is shown in an August 1997 photograph taken from the space shuttle (fig. 78B).

The southernmost glaciers in this region—Popof, Summit, and Shakes Glaciers—occur just north of the Stikine River. Nine-kilometer-long Popof Glacier, which has an area of about 18 km<sup>2</sup> (Field, 1975c, p. 108) and is located near the mouth of the Stikine River, was one of the first named glaciers

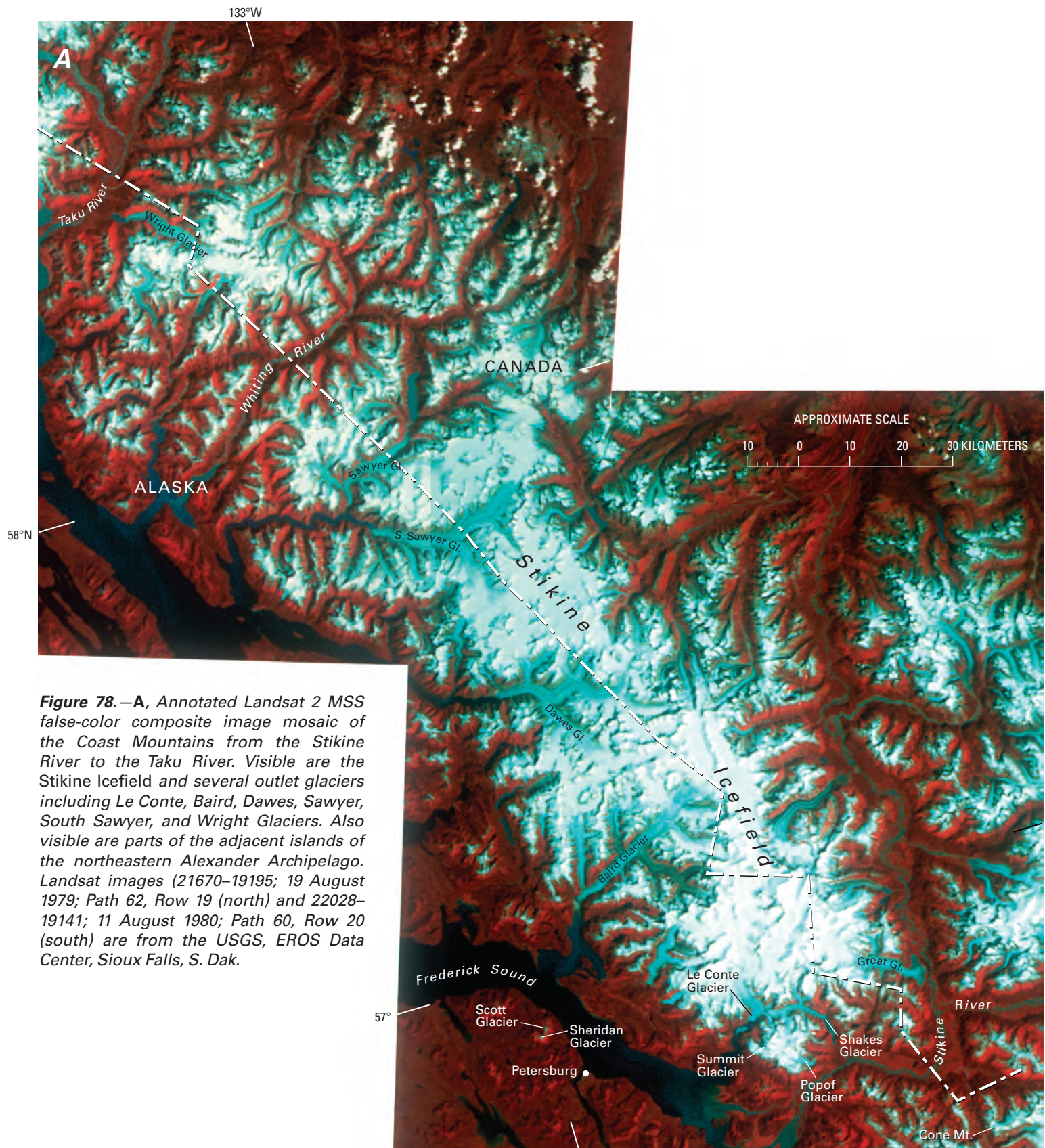
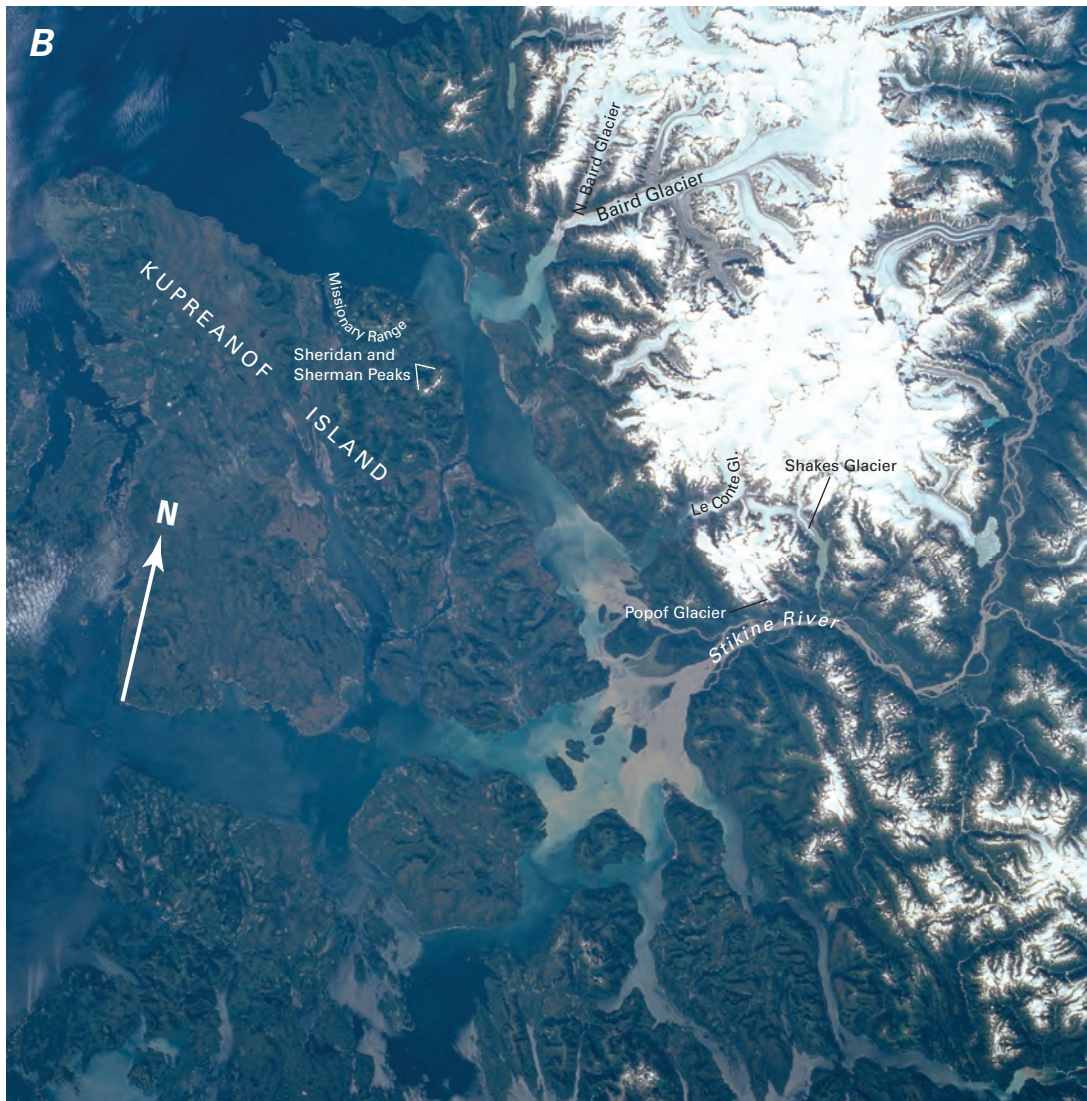


**Figure 78.—A,** Annotated Landsat 2 MSS false-color composite image mosaic of the Coast Mountains from the Stikine River to the Taku River. Visible are the Stikine Icefield and several outlet glaciers including Le Conte, Baird, Dawes, Sawyer, South Sawyer, and Wright Glaciers. Also visible are parts of the adjacent islands of the northeastern Alexander Archipelago. Landsat images (21670–19195; 19 August 1979; Path 62, Row 19 (north) and 22028–19141; 11 August 1980; Path 60, Row 20 (south) are from the USGS, EROS Data Center, Sioux Falls, S. Dak.



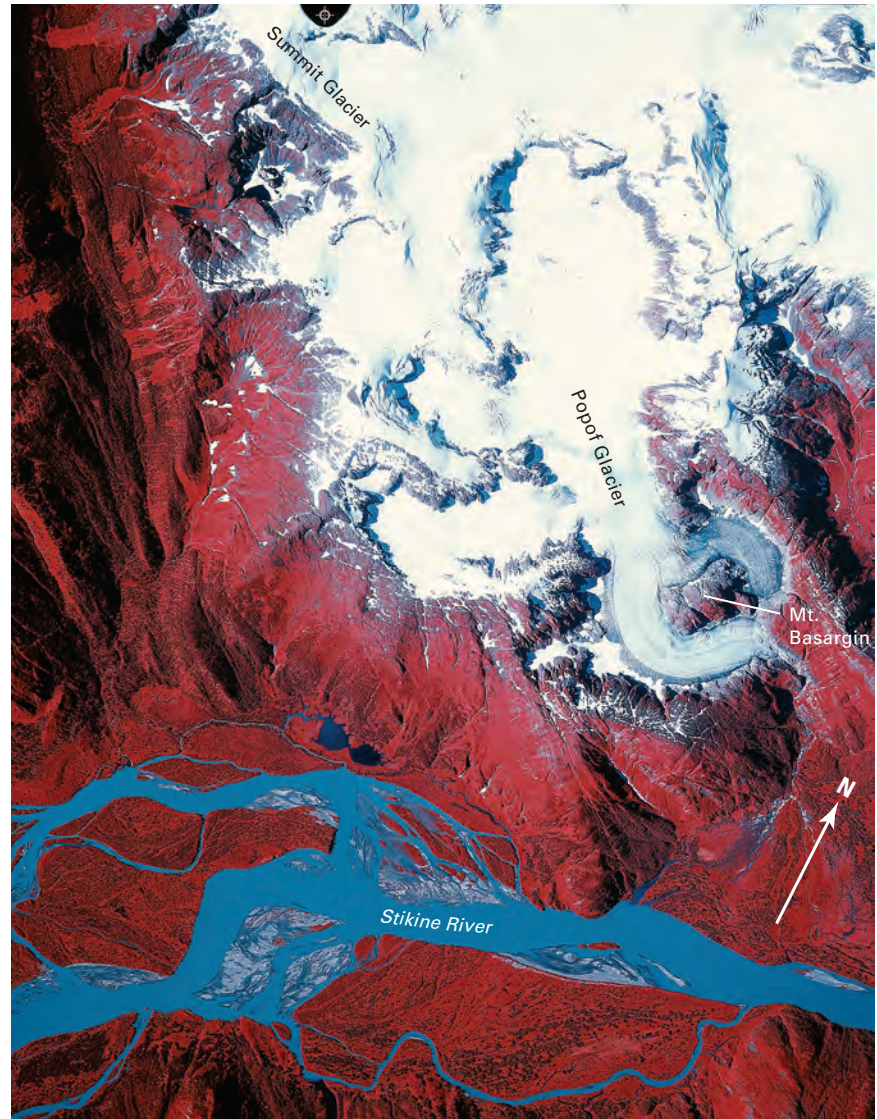
in Alaska. The name first appeared on the Russian Rynda Survey in 1863, although, at that time, it was spelled with two “f”s (fig. 11). Thirteen years later, Canadian surveyor Joseph Hunter called it *First Glacier*. Since it was first surveyed more than 125 years ago, its terminus has retreated about 3 km. In the 31 years between 1948 and 11 August 1979, the dates when aerial photography was acquired (fig. 79), the two lobes of ice that joined to form the glacier’s 1948 terminus separated and the northern lobe retreated approximately 0.5 km.

Eighteen-kilometer-long Shakes Glacier, with an area of about 56 km<sup>2</sup> (Field, 1975c, p. 109), is another glacier that shows significant change in the 31 years between aerial photographic flights. When it was photographed in 1948, its terminus dammed the northern end of Shakes Lake and created a small impoundment. When it was photographed on 11 August 1979 by the AHAP Program (fig. 80A), the terminus was calving large icebergs and had retreated about 0.7 km. In the 11 years that followed, the glacier retreated another 0.7 km, according to a 23 August 1990 oblique aerial photograph (fig. 80B).

Le Conte Glacier, “long known to the Indians as Hutli or the Thunderer, because of the noise produced by ice falling from its face” (Russell, 1897, p.78), has a length of 36 km, an area of 472 km<sup>2</sup> (Viens, 1995; tables 2, 3), ice speeds near the terminus of up to 23 m d<sup>-1</sup>, and an AAR of 0.93. Le Conte Glacier was photographed on 11 August 1979 by the AHAP Program (L189F4355). It is the southernmost tidewater glacier in North America and probably in the

**Figure 78.—B,** August 1997 Space Shuttle photograph of the southern part of the Stikine Icefield, including Popof, Shakes, LeConte, Baird, and North Baird Glaciers, some of the largest in the southern Coast Mountains. Also shown is the south-central part of Alexander Archipelago including Missionary Range and Sherman and Sheridan Peaks, the sites of the only reported glaciers on Kupreanof Island. Space shuttle photograph No. STS085–709–028 is from the National Aeronautics and Space Administration.

**Figure 79.**—Part of an 11 August 1979 AHAP false-color vertical aerial photograph of 8-km-long Popof Glacier, the upper reaches of Summit Glacier, and about a half-dozen smaller unnamed glaciers, many snow covered. Popof Glacier and almost all of the unnamed glaciers show evidence of recent retreat documented by trimline and vegetation-free, recently exposed bedrock. When photographed in 1948, the two lobes of Popof Glacier, which flow around Mount Basargin, were joined. AHAP photograph no. L189F4358 from the GeoData Center, Geophysical Institute, University of Alaska, Fairbanks, Alaska.



entire Northern Hemisphere. Its 1.5-km-wide terminus sits at the head of Le Conte Bay in water depths of about 260 m. At the end of the 20th century, Le Conte Glacier had an extremely active calving terminus, producing large quantities of icebergs from a 50-m-high face. Between 1887, when it was first charted, and 1963, Le Conte Glacier retreated 3.7 km (Post and Motyka, 1995). This retreat was followed by a period of terminus stability from 1963 to 1994 (fig. 81). In the later years of the 20th century, the terminus began to actively retreat. Between 1994 and 1998, the glacier retreated 2 km, much of it by submarine calving (Echelmeyer and Motyka, 1997; Hunter and others, 2001; Connor and others, 1999; White and others, 1999).

Hunter and others (2001) reported that, since 1998, the glacier has entered a phase of temporary stability at a constriction in the fjord. They concluded that surface-ice speeds indicate that sliding dominates ice flow in the glacier's lower reaches. Between 1998 and 2000, they performed oceanographic monitoring in the ice-proximal basin at the glacier's stable face, including repeat bathymetric surveys, conductivity, temperature, and depth (CTD) casts, and near-surface velocity measurements. They measured suspended sediment concentrations near the ice margin of up to 55 mg l<sup>-1</sup>. At a distance of 10.5 km from the terminus, these concentrations decline to 20 mg l<sup>-1</sup>. Near-surface water-column velocity measurements range from 12 to 52 cm s<sup>-1</sup> within 0.25 to 0.5 km of the ice margin, where flow was generally away from the ice margin in a radial pattern. They estimated discharge to

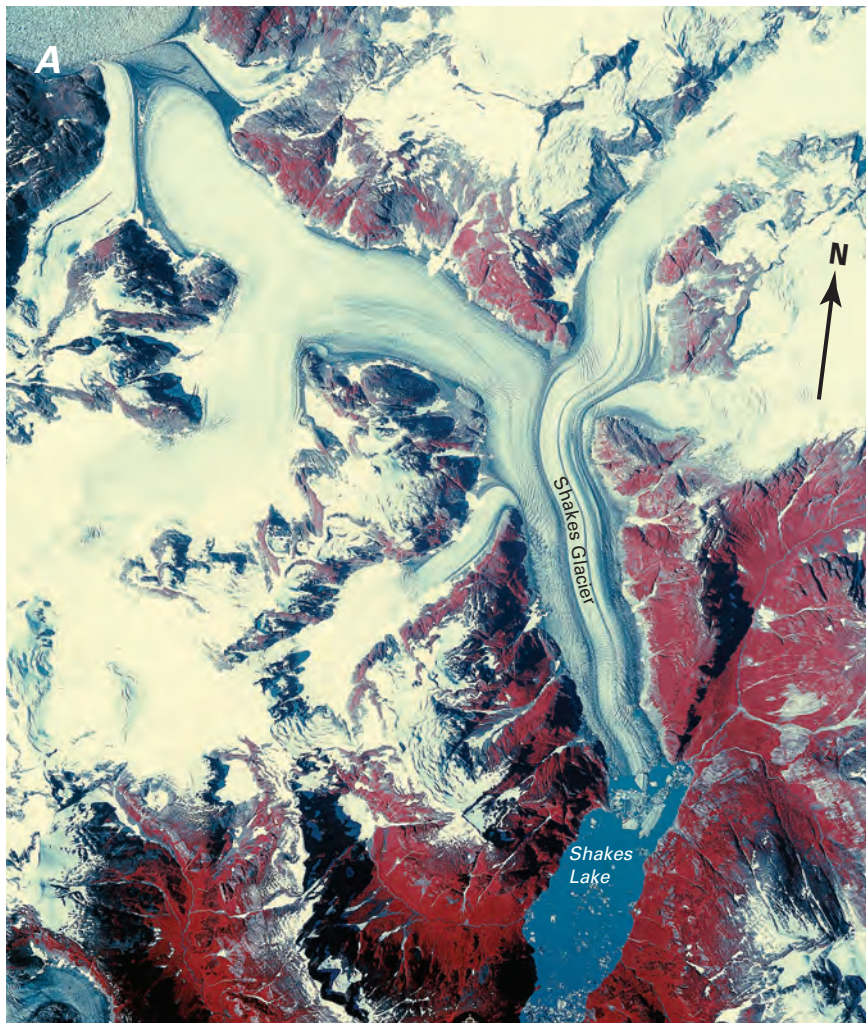


**Figure 80.**—**A**, An 11 August 1979 AHAP false-color vertical aerial photograph of 11-km-long Shakes Glacier and about a dozen smaller unnamed glaciers, many snow covered. Shakes Glacier and all of the unnamed glaciers are retreating. Icebergs as large as 0.7 km across have recently calved. The trimline on the east side of Shakes Glacier and the empty hanging valleys on the west side of the lower part of the glacier document recent retreat and thinning. AHAP photograph no. L188F4225 from the GeoData Center, Geophysical Institute, University of Alaska, Fairbanks, Alaska. **B**, 23 August 1990 annotated USGS oblique aerial photograph of the terminus of Shakes Glacier. The right side of the glacier has a conspicuous trimline, indicative of recent rapid thinning. Many of the tributary glacier termini also show evidence of recent retreat. The heavy black lines show the approximate locations of the terminus in 1948 and 1979. There was about 0.7 km of retreat during each time interval. Photograph no. 90-R1-8 by Robert M. Krimmel, U.S. Geological Survey.



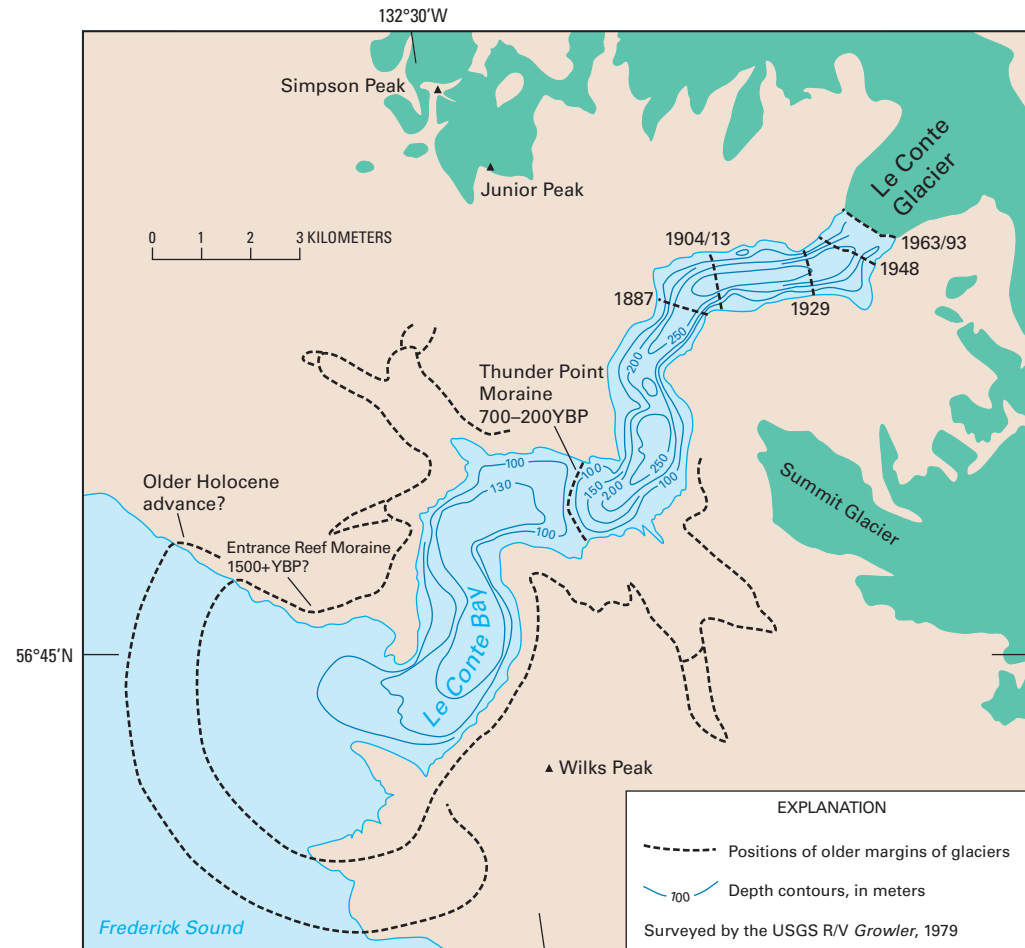


**Figure 81.**—Map of Frederick Sound and Le Conte Bay showing bathymetry and terminus positions of Le Conte Glacier for the past several thousand years. Water depths shown for Le Conte Bay are as of 1979. By the end of the 20th century, the glacier retreated nearly an additional 2 km. Map is adapted from Post and Motyka (1995).

be  $6,088 \text{ m}^3 \text{ s}^{-1}$ . Depths in the Le Conte Bay exceed 260 m along the 1.4-km-wide terminus. Sediment accumulation is restricted to a small basin near the ice margin where approximately  $7 \times 10^6 \text{ m}^3$  of sediment has accumulated between the end of 1998 and 2000. Extrapolated across the entire glacier, this amount equates to approximately  $5 \text{ mm a}^{-1}$  of denudation.

Patterson Glacier, with an area of about  $104 \text{ km}^2$  (Field, 1975c, p. 109), has been observed since 1879, the year that William Dall named this 23-km-long glacier (Field, 1975c, p. 109) for the then Superintendent of the Coast Survey. Patterson Glacier was photographed on 11 August 1979 by the AHAP Program (L189F4353). Near the end of the 19th century, the terminus bifurcated, flowing to both the east and the west, and was slowly advancing and knocking down trees (USC&GS, 1891). Klotz (1899) visited it in 1894 and documented that the slope of the first 16 km of the glacier was  $4^\circ 25'$ . When Field next reported on the glacier, nearly 50 years later in 1941 (Field, 1942), it had retreated about 600 m. In the 7 years that followed, it retreated another 600 m (Field, 1975a); another 700 m of retreat occurred between 1948 and 1964 and another 200 m through 1968. In the 31 years between 1948 and 1979, the dates when aerial photography was acquired, the glacier retreated about 1 km. The photography displays several indicators of recent thinning such as trimlines, ice-marginal lakes, and vegetation-free bedrock near the terminus. In all, Patterson Glacier retreated more than 3 km during the 20th century, forming an ice-dammed lake to the east. Continued retreat has resulted in the draining of the basin.

Baird Glacier is unique in the Coast Mountains because it had been advancing at least since the late 19th century. The 50-km-long glacier (fig. 82) has an area of about  $784 \text{ km}^2$  (Viens, 1995) (tables 2, 3) and terminates at an outwash plain-delta that it built into the head of Thomas Bay. Since it was



**Figure 82.** — 11 August 1979 AHAP false-color vertical aerial photograph of the terminus of 35-km-long Baird Glacier, its primary tributary North Baird Glacier, and a number of smaller unnamed glaciers, many snow covered. Although Baird Glacier displays several indicators of recent thinning, especially the beginning of trimline development, the terminus was slowly advancing. Many of the small tributary glaciers, adjacent to both Baird and North Baird Glacier, are characterized by the appearance of vegetation-free bedrock. AHAP photograph no. L189F4349 from the GeoData Center, Geophysical Institute, University of Alaska, Fairbanks, Alaska.

first mapped in 1887, the glacier had been slowly advancing, but it is now slowly retreating. From 1887 to 1941, the advance totaled about 1 km (Field, 1942). From 1941 through the end of the 20th century, the glacier also advanced about 1 km. The recent advance was accompanied by a gradual thinning. Between 1887 and 1948, the outwash plain-delta at the head of Thomas Bay has lengthened by more than 2 km. As late as the 18th century and early 19th century, descriptions of Baird Glacier mention icebergs in Thomas Bay (Field, 1975a). It is likely that Baird Glacier had a tidewater terminus before 1887. Rapid accumulation of sediment built a sedimentary apron in front of the glacier margin, infilling the head of the bay. Lengthening of the sedimentary apron into Thomas Bay at a rate that exceeded the rate of advance of the glacier margin would explain the transition from a tidewater calving margin to a terrestrial terminus.

While the terminus of Baird was advancing, several of its tributaries were significantly downwasting. Two glaciers, Oasis Glacier and Witches Cauldron, have retreated and thinned to the point that ice from the trunk of Baird Glacier flows into both valleys; the ice extends about 8 km into the Witches Cauldron valley. Oasis Glacier and Witches Cauldron were photographed on 11 August 1979 by the AHAP Program (L188F4232). Most of the unnamed valley glaciers located north and west of Baird Glacier are also retreating and thinning. These glaciers were also photographed on 11 August 1979 by the AHAP Program (L188F4237).

Endicott Arm is a 48-km-long southeast-trending fjord that penetrates the Coast Mountains from Stephens Passage. Dawes and North Dawes Glaciers are located in two arms at its head. The glaciers were photographed on 11 August 1979 by the AHAP Program (L188F4240). Dawes Glacier was originally named *Young Glacier* by John Muir, who visited it in 1880 (Muir, 1915). It has an area of about 653 km<sup>2</sup>, is 37 km long, and has a rapidly



retreating tidewater calving terminus (Viens, 1995) (tables, 2, 3). In the 78 years between 1889, when it was mapped by the USC&GS (1891), and 1967, when it was photographed by the USGS, the terminus retreated about 6.8 km, an average of almost  $90 \text{ m a}^{-1}$ .

North Dawes Glacier, with a length of about 16 km and an area of about  $50 \text{ km}^2$  (Field, 1975c, p. 111), was a tidewater calving glacier when Muir observed it in 1890. By 1923, its terminus had retreated about 525 m and was located on land (Buddington and Chapin, 1929). Between 1929 and 1961, another 1.8 km of terminus retreat occurred. D.B. Lawrence (reported by Field, 1975a) suggested that, before about 1790, the termini of Dawes and North Dawes Glaciers combined to form a single large glacier at the head of Endicott Arm, at least 10 km more advanced than their 1979 positions as shown on a 11 August 1979 AHAP photograph (L188F4240).

Fords Terror, a T-shaped 12-km-long tributary fjord of Endicott Arm, was so named by an 1889 USN surveying party because it was “very narrow at one point. Floating ice from glaciers, with falling tide, jamming in this contracted throat makes it a dangerous place” (reported by Orth, 1967). Several kilometers up valley from the head of the eastern end of the T are two glaciers—Brown and South Brown Glaciers—that have a history of very rapid retreat in the late 19th and 20th centuries. When Muir visited them in 1880, the two glaciers were joined and their combined terminus, called Brown Glacier, was a tidewater calving glacier. Thirteen years later, in 1893, the terminus was first mapped by the Boundary Survey. By 1909, when the Boundary Survey resurveyed the terminus, the terminus had moved onto land and had retreated about 2.5 km from its 1893 position. In 1923, when USGS geologist A.F. Buddington examined Brown Glacier, he called its retreat “the most conspicuous case of glacial retreat seen by the writer on the mainland” (Buddington and Chapin, 1929, p. 31–32).

In 1935, Field (1937) photographed the glacier and documented that the terminus was about 3 km from the shoreline and about 5.5 km from its 1890s position. In the 75 years between 1893 and 1968, the date of the latest position determined by Field (1975a), the glacier had retreated nearly 10 km, an average retreat rate of  $125 \text{ m a}^{-1}$ . In 1948, it had a length of about 9 km and an area of about  $18 \text{ km}^2$  (Field, 1975c, p. 111). Today, only debris-covered remnants remain. South Brown Glacier separated from Brown Glacier between 1923 and 1929. It, too, retreated rapidly, losing about 2 km of length between 1929 and 1948. By 2000, only a small debris-covered mass remained. Retreat since 1948 approached 10 km.

Four-kilometer-long Sumdum Glacier is the largest and only named glacier between Endicott Arm and Tracy Arm. When it was first photographed by the Boundary Commission in 1893, it was a land-terminating glacier located at the forest edge but near sea level. It was little changed when Buddington observed it in 1923. However, by 1948, it had retreated nearly a kilometer and had a terminus elevation of about 335 m (Field, 1975a). The name “Sumdum” which is derived from the Tlingit word for the booming sound made when icebergs calve from the glacier, suggests that, at some time before 1893, Sumdum Glacier was an active tidewater calving glacier.

Named for former Secretary of the Navy Benjamin Tracy (1889–93), 45-km-long Tracy Arm has two tidewater glaciers at its head. The two—South Sawyer Glacier (fig. 83) and Sawyer Glacier (fig. 84), both of which arise in Canada—may have been joined as recently as about 1880. At the end of the 20th century, their termini were about 7.5 km apart. Sawyer Glacier has a length of 37 km and an area of 399 km<sup>2</sup> (Viens, 1995) (tables 2, 3). South Sawyer Glacier has a length of 50 km and an area of 683 km<sup>2</sup> (Viens, 1995) (tables 2, 3). In the 68 years between 1899 and 1967, South Sawyer Glacier retreated about 3.5 km, and Sawyer Glacier lost nearly 1 km. This retreat was interrupted by long periods of stability. In 2001, the terminus positions of both Sawyer Glacier and South Sawyer Glacier showed evidence of thinning and retreat. All of the other cirque and former valley glaciers in Tracy Arm showed significant evidence of retreat.

North of Tracy Arm and south of Whiting River are a number of unnamed glaciers, most of which are generally less than 5 km in length and drain into the Whiting River. No information is available about the recent status of these glaciers.

Between the Whiting and Taku Rivers, Speel Glacier, with a length of 15 km and an area of 42 km<sup>2</sup> (Field, 1975c, p. 113), and Wright Glacier are the only two named glaciers. Field (1975a) stated that Speel Glacier retreated about 3 km from its recent “Little Ice Age” maximum position and that a little more than 1 km of retreat occurred in the 20 years between 1948 and 1968. Wright Glacier has a length of 33 km and an area of 148 km<sup>2</sup> (Field, 1975c, p. 113). Between 1891 and the early 1960s, it retreated more than 4 km, forming an ice-marginal lake. A comparison of the positions of both glaciers on the Taku River map (USGS, 1960; appendix A) and a 9 September 1984 Landsat TM image of the northern part of the Stikine River to the Taku River region (fig. 84) shows that both glaciers have undergone significant retreat during the baseline period.



**Figure 83.**—26 August 1960 oblique aerial photograph of the terminus of South Sawyer Glacier, showing evidence of recent calving and the development of a calving embayment on the right (east) side of the terminus. The left (west) side of the glacier has a conspicuous trimline, indicative of recent rapid thinning. Many of the tributary glacier termini also show evidence of recent retreat. Photograph no. R18 by Austin Post, U.S. Geological Survey.

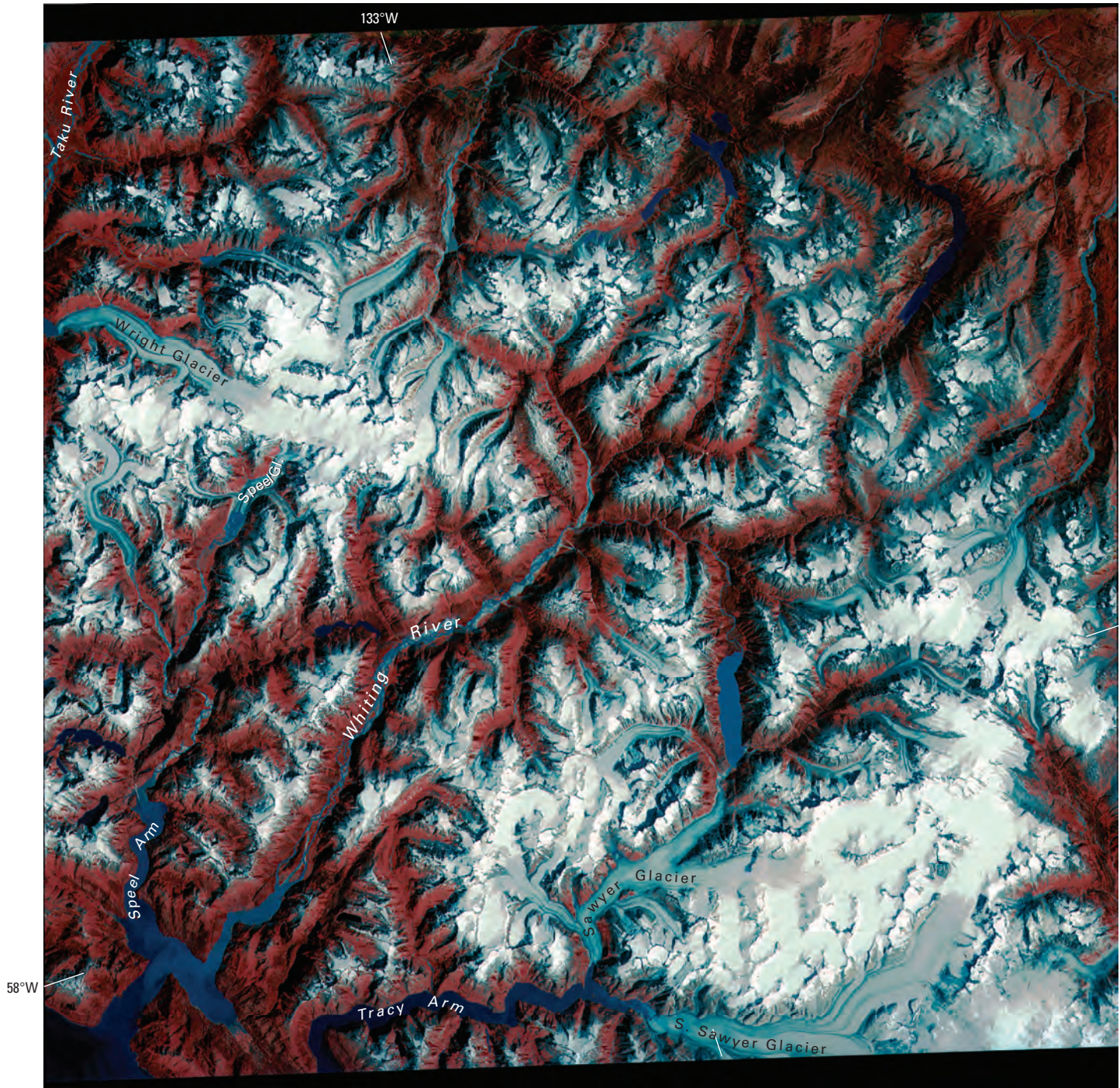
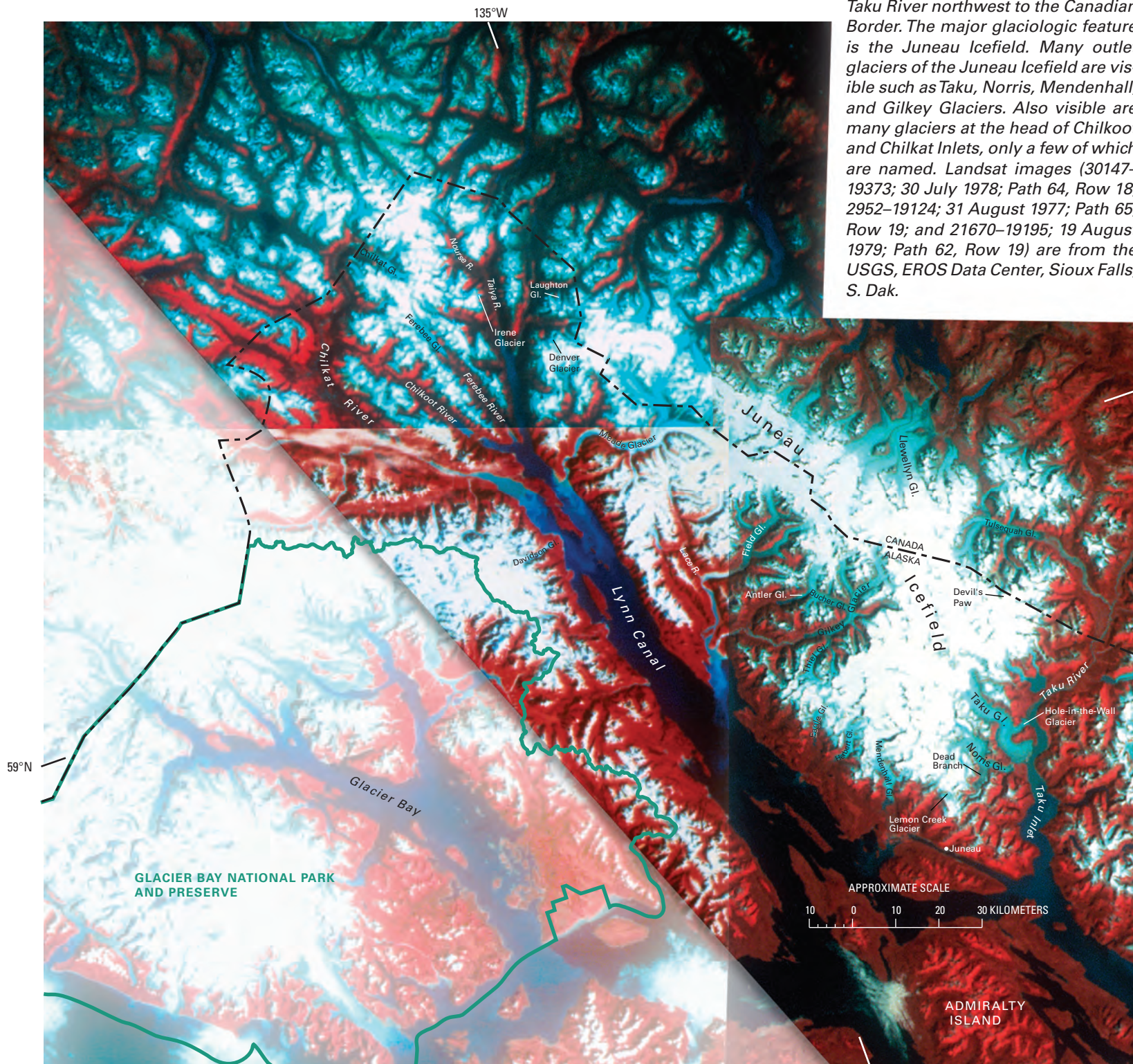


**Figure 84.**—Annotated Landsat 5 TM quarter-scene, false-color composite image acquired on 9 September 1984 of the Coast Mountains from just south of Tracy Arm to the Taku River, including the Sawyer, South Sawyer, Speel, and Wright Glaciers. Approximate scale 1:500,000. Non-standard Landsat image by the USGS, EROS Data Center, Sioux Falls, S. Dak.

## Taku River to the Canadian Border East of Gilkey Glacier

Landsat MSS images that cover the Coast Mountains region from the Taku River to the Canadian border have the following Path/Row coordinates: 61/19, 62/19, 63/18, 63/19, 64/18, 64/19, 65/18, and 65/19 (fig. 3A, table 1). A mosaic of three of these scenes covers the entire area (fig. 85). For comparison, a 9 September 1984 Landsat TM image of the southern part of the Taku River to the Canadian border region (fig. 86) is also presented. The dominant glacier feature in this region is the Juneau Icefield, one of the largest ice fields

**Figure 85.**—Annotated Landsat 2 and 3 MSS false-color composite image mosaic of the Coast Mountains from the Taku River northwest to the Canadian Border. The major glaciologic feature is the Juneau Icefield. Many outlet glaciers of the Juneau Icefield are visible such as Taku, Norris, Mendenhall, and Gilkey Glaciers. Also visible are many glaciers at the head of Chilkoot and Chilkat Inlets, only a few of which are named. Landsat images (30147–19373; 30 July 1978; Path 64, Row 18; 2952–19124; 31 August 1977; Path 65, Row 19; and 21670–19195; 19 August 1979; Path 62, Row 19) are from the USGS, EROS Data Center, Sioux Falls, S. Dak.



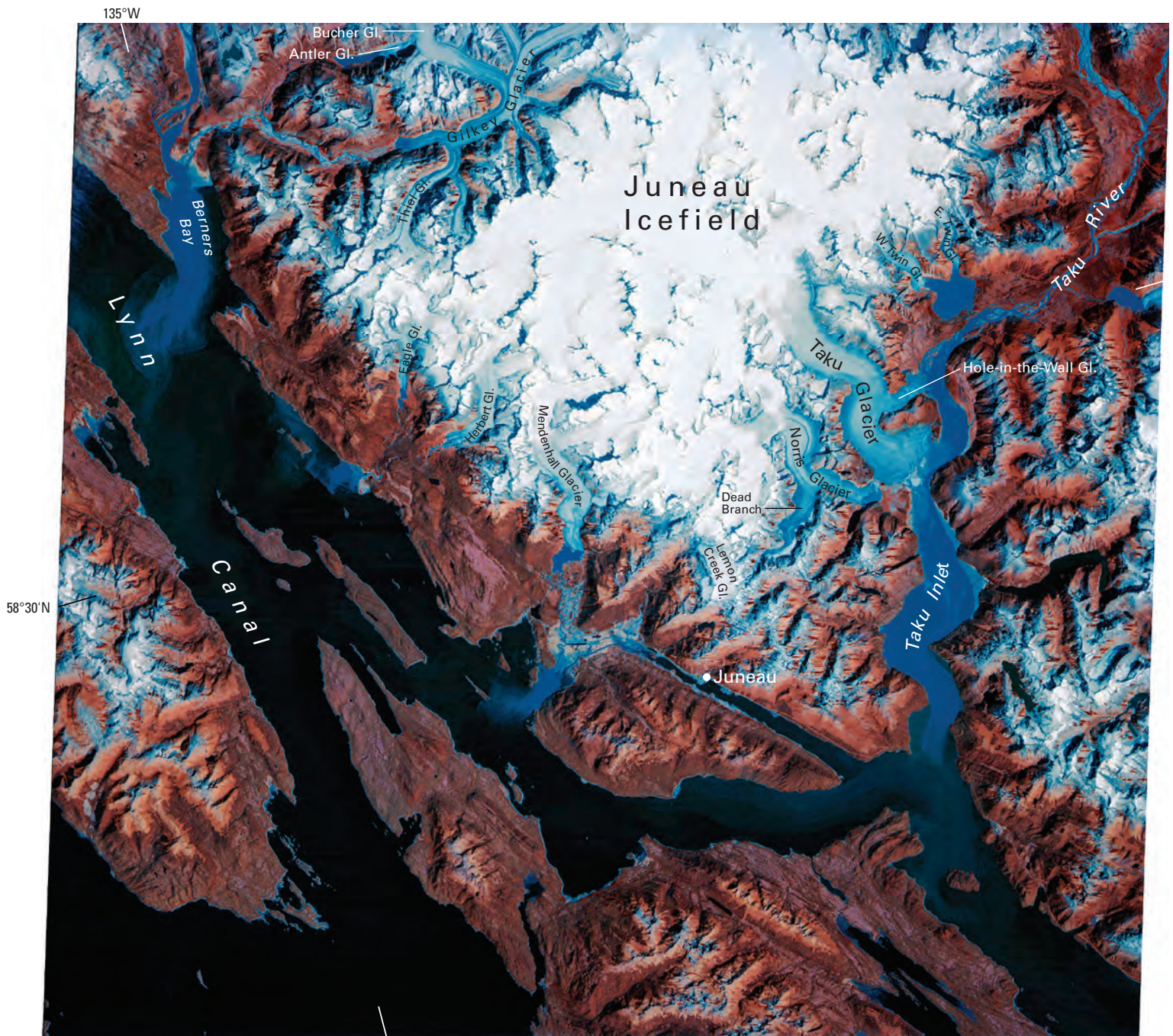


**Figure 86.**—Annotated Landsat 5 TM quarter-scene, false-color composite image acquired on 9 September 1984 of the Coast Mountains from east of the Taku River to west of Berners Bay. Outlet glaciers from the Juneau Icefield include the Twin, Hole-in-the-Wall, Taku, Norris, Lemon Creek, Mendenhall, Herbert, Eagle, Gilkey, and Bucher Glaciers. According to Robert M. Krimmel (written commun.) "All of the various tidewater and non-tidewater glaciers that flow from the ice field, except the Taku Glacier, have been in a general recession since before 1900." Miller (1963) attributes this difference in activity to the relative greater area of the Taku Glacier that is above the snowline (larger accumulation area); thus, it has maintained a positive mass balance and advanced. The other glaciers in the area, at lower altitudes and with smaller accumulation areas, have negative mass balances. Approximate scale 1:500,000. Landsat image L5057019008425350 is courtesy of Robert M. Krimmel, U.S. Geological Survey, and is from the USGS, EROS Data Center, Sioux Falls, S. Dak.

in Alaska. It is located along the crest of the Coast Mountains between the Taku River and Devil's Paw to the south, Lynn Canal to the west, and the Antler-Gilkey River drainages to the north. Like the *Stikine Icefield*, a portion of the Juneau Icefield is located in British Columbia, but most of the 1,215-mi<sup>2</sup> (1,955 km<sup>2</sup>) ice field is located in Alaska (Molnia, 2001, p. 62). Large glaciers that drain the Juneau Icefield are the Taku, Norris, Hole-in-the-Wall, Mendenhall, Herbert, Eagle, Gilkey, and Antler Glaciers on the Alaskan side of the ice field and the Llewellyn and Tulsequah Glaciers on the Canadian side. The ice field, which was known as the “home of the spirits” to the Tlingits, has about 40 major and 100 minor glaciers (Miller and others, 1987).

East of Lynn Canal and north of the Gilkey River, a significant number of large glaciers—including the Field, Meade, Laughton, and Denver Glaciers—drain the central névé or interconnected outlying névés on the crest of the Coast Mountains. Field (1975a, p. 85), however, classified these areas as being separate from the limits of the Juneau Icefield. Coast Mountains glaciers also exist west of Lynn Canal in the mountains that are drained by the Taiya, Ferebee, and Chilkat Rivers. Ferebee, Chilkat, and Irene Glaciers are the only named glaciers, but several large unnamed glaciers exist along the Nourse River and in the Chilkat and Chilkoot River drainages.

Most of the glaciers on the Alaskan side of the Juneau Icefield are retreating. One major exception is 60-km-long Taku Glacier, which has an area of about 831 km<sup>2</sup> (Viens, 1995) (tables 2, 3) (figs. 87, 88). It was advancing during the Landsat baseline period, was stable for about a decade, and, at the beginning of the 21st century, began to readvance. Taku Glacier is the primary outlet glacier from the Juneau Icefield. Taku Glacier was known by the Tlingits as “Klumma Klutt or Klumu Gutta,” a Tlingit name meaning “Spirits House.” It was also previously named *Schulze Glacier* and *Foster Glacier*. Muir (1893) said of Taku Glacier: “To see this one glacier is well worth a trip to Alaska.” During much of the 20th century, Taku Glacier was advancing across Taku Inlet at a rate of nearly 100 m a<sup>-1</sup> and knocking down trees in forests along both of its margins (fig. 88). It also was overriding moraines



**Figure 87.**—11 August 1979 AHAP false color vertical aerial photograph of Taku Inlet and the lower portions of Taku and Norris Glaciers. Also shown is Hole-in-the-Wall Glacier. As recently as about 1750, Taku Glacier was more than 3.5 km beyond its late 20th century position. At that time, it dammed Taku River at Taku Point. A large ice-dammed lake extended northeast into Canada. Many ice-free cirques and areas of vegetation-free bedrock southeast of the Taku Inlet show that many small glaciers in this area are actively thinning and retreating. AHAP photograph no. L188F4260 from the GeoData Center, Geophysical Institute, University of Alaska, Fairbanks, Alaska.

**Figure 88.**—14 September 1968 oblique aerial photograph of the northeastern terminus of the then-rapidly advancing Taku Glacier as it advanced into the adjacent spruce forest and bulldozed trees. Photograph by Austin Post, U.S. Geological Survey.



and outwash of Norris Glacier located to its southwest. At the end of the 19th century, when the recent advance of Taku Glacier began, it was a tidewater calving glacier with depths in its fjord exceeding 100 m. When the terminus was photographed by the Alaska Aerial Survey Expedition in the late 1920s, it was still tidewater. Sediment produced by the advancing glacier began filling upper Taku Inlet, so that, by the mid-1930s, ships that previously had had access to the terminus of the glacier could not enter the inlet. About 1937, Taku Glacier's advancing terminus began forming a push moraine that protected the terminus and restricted calving. Advance continued until about 1988. During the last few years of the 20th century, the terminus position appeared to be stable. A map prepared by Post and Motyka (1995) showing the location of the terminus of Taku Glacier for the previous 250 years is presented as figure 89.

Nolan and others (1995) used radio-echosounding and seismic-reflection techniques to measure Taku Glacier's ice thickness and bed morphology. Maximum ice thickness was about 1,477 m, and minimum bed elevation was about 600 m below sea level. They determined that the sub-sea-level basin that underlies the glacier extends about 50 km up-glacier. Future retreat of the glacier would expose a deep fjord basin extending well into the Coast Mountains. Along one transect near the Brassiere Hills, 5.5 km up-glacier from the terminus, the maximum ice thickness was 558 m, and the maximum depth of the bed was 212 m below sea level. Even more importantly, Nolan and others (1995) compared the surface elevation in 1989, the date of the survey, with the 1948 surface elevation determined from photogrammetry. They stated that the glacier had thickened by "10–25 m over the past 40 years," but measurement of the differences between the 1948 and 1989 surface elevations (Nolan and others, 1995, fig. 4) showed thickening of more than 100 m on the northeastern side of the transect. Regardless of the actual amount of thickening, a positive mass balance so close to the glacier's terminus is significant. Geodetic airborne laser altimetry studies performed by K.A. Echelmeyer in 1999 indicated that Taku Glacier was thickening (Shad



**Figure 89.** — Map of the Taku Inlet and River area showing terminus positions of Taku, Norris, and Hole-in-the-Wall Glaciers for 1750 and the past hundred years or so. Map is adapted from Post and Motyka (1995).

O'Neel, Geophysical Institute, University of Alaska Fairbanks, personal commun., 7 January 2000).

Motyka and others (2001) reported that, between late 2000 and the summer of 2001, Taku Glacier has begun to readvance at a rate of  $30 \text{ cm d}^{-1}$ . The advance has caused striking deformation of adjacent proglacial sediments. Compression by the advancing ice has caused the outward propagation of at least two prominent bulges: the more distal (width 35 m, height 3 m) at a rate of about  $10 \text{ cm d}^{-1}$  and the more proximal (width 80 m, height 4.5 m) at a rate of  $15 \text{ cm d}^{-1}$ . There are no visible thrust faults in the sediments, but shear must be occurring as part of bulge propagation. Although the glacier's terminus region remained stationary during the 1990s, it continued to thicken, with surface elevation rising at an average rate of  $1.4 \text{ m a}^{-1}$ . Previous work showed that Taku Glacier is actively excavating soft sediments and entrenching itself into these sediments as its terminus continues to grow and advance.

Twenty-seven-kilometer-long Norris Glacier, with an area of about  $183 \text{ km}^2$  (Field, 1975c, p. 116) (fig. 89), located in a parallel drainage immediately west of the Taku Glacier, is proof that adjacent glaciers do not always act in a similar fashion. While Taku Glacier had retreated up its valley during the second half of the 19th century, Norris Glacier was actively advancing and reached its most recent maximum position between 1911 and 1917. Through the remainder of the 20th century, when Taku Glacier was advancing as much as  $100 \text{ m a}^{-1}$ , Norris Glacier retreated about 2 km and thinned by many tens of meters. At the start of the 20th century, the southwestern limb of the Norris



Glacier, known as the “Dead Branch,” was an active ice-supplying tributary with a gradient sloping to the northwest. The glacier was photographed on 11 August 1979 by the AHAP Program (L189F4321). During the early 20th century, its upper reaches thinned so significantly that a reversal of drainage occurred. At the end of the 20th century, most of the “Dead Branch” was stagnant, wasting away in place, with only minimal ice flow from the main trunk of Norris Glacier into the thinning distributary arm. Several ice-free cirques and areas of vegetation-free bedrock around the “Dead Branch” and on the western side of Norris Glacier indicate that many small glaciers in this area are actively retreating and thinning.

Hole-in-the-Wall Glacier, a distributary lobe of Taku Glacier (figs. 89, 90), has also experienced a major retreat and readvance since the “Little Ice Age.” In about 1750, the glacier extended to its “Little Ice Age” maximum position, nearly 1 km beyond its 20th century maximum position. By 1890, Hole-in-the-Wall Glacier had retreated nearly 4.5 km. The current glacier formed when an arm of Taku Glacier thickened during the first half of the 20th century and overtopped the divide between Goat Ridge and the Brassiere Hills in about 1940 (fig. 89). During much of the second half of the 20th century, its continued advance formed a bulbous terminus that extended to near the Taku River (fig. 90). At the end of the 20th century, the terminus of Hole-in-the-Wall Glacier was stable.

East and West Twin Glaciers, formerly Twin Glacier (fig. 91), are also distributaries of Taku Glacier and drain Hades Highway, the eastern branch of Taku Glacier. Before the late 1920s, the two glaciers were joined and filled much of the present Twin Glacier Lake basin, separating just before 1929 (fig. 92). Lawrence (1950) determined that the combined glacier began to retreat from its “Little Ice Age” maximum terminal moraine position between 1775 and 1777. He also determined from other dated moraines that the retreating glacier did not expose any of the ice-marginal lake basin until about 1880. Through 1948, D.B. Lawrence (1950) determined that the West Twin Glacier (1948 length of about 7 km) had retreated 5.2 km; the East Twin Glacier (1948 length of about 10 km) retreated 4 km. The retreat of both glaciers has continued for the remainder of the 20th century; each glacier has lost more than 1 km.

Field (1975a) described 6-km-long Lemon Creek Glacier (fig. 86) (see AHAP false-color infrared vertical aerial photograph no. L190F0390 acquired on 11 August 1979) as being an extension of the Juneau Icefield rather than an ice-field-outlet glacier. Lemon Creek Glacier has been the site of many detailed studies since the early 1950s and, beginning in 1957, was one of the

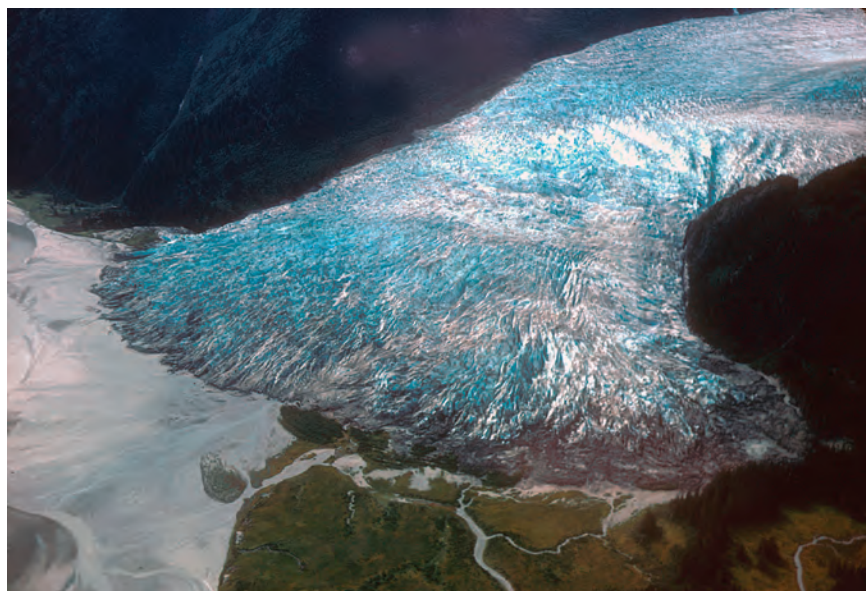


**Figure 90.**—28 July 1968 oblique aerial photograph of the bulbous terminus of the then-advancing Hole-in-the-Wall Glacier, Coast Mountains. Photograph by Bruce F. Molnia, U.S. Geological Survey.



**Figure 91.**—11 August 1979 AHAP false-color vertical aerial photograph of the termini of East and West Twin Glaciers, Coast Mountains. The arcuate latest "Little Ice Age" terminal moraine complex south of Twin Glacier Lake is clearly seen. AHAP photograph no. L189F4406 from the GeoData Center, Geophysical Institute, University of Alaska, Fairbanks, Alaska.

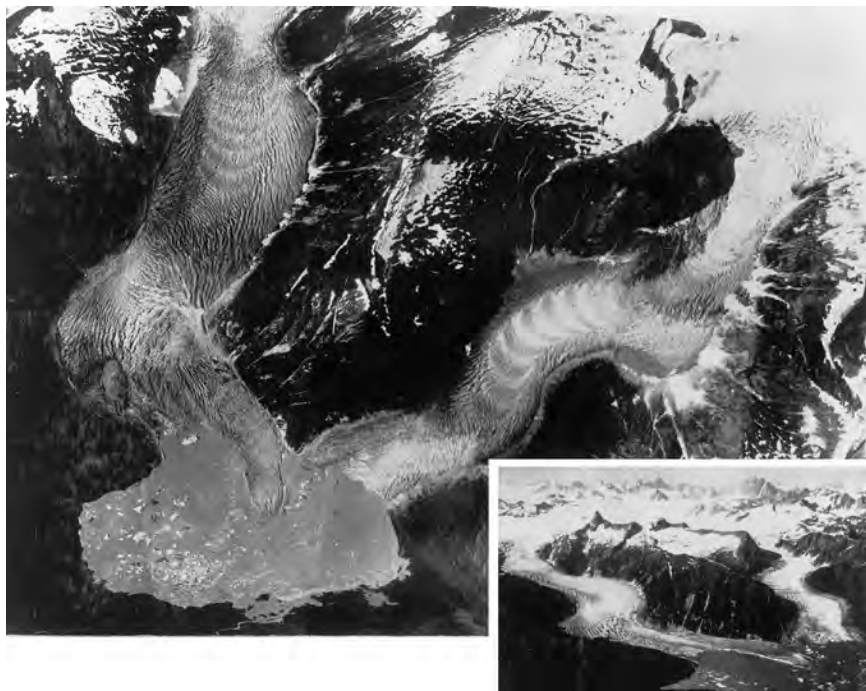


**Figure 92.**—Bagley camera vertical and high-angle oblique (inset) 1929 aerial photographs of East and West Twin Glaciers, Coast Mountains. Photograph Alaska 185 from the USGS Photographic Library, Denver, Colo. (See also fig. 30.)

glaciers mapped by the AGS, as part of its IGY mapping project (American Geographical Society, 1960). It was remapped by Marcus and others (1995) and surveyed by using geodetic airborne laser altimeter (surface-elevation) profiling by Sapiano and others (1998). Its post-“Little Ice Age” history has been documented by Heusser and Marcus (1964). About 1759, Lemon Creek Glacier began to retreat from its “Little Ice Age” maximum moraine. By 1958, retreat totaled 2.5 km. Maximum retreat rates were 37.5 m a<sup>-1</sup> during the period 1948 to 1958. Sapiano and others (1998) updated these observations through 1995. They found that, between 1957 and 1989, the glacier retreated another 700 m and an additional 100 m between 1989 and 1995. Through 1995, Lemon Creek Glacier had retreated about 3.3 km, an average retreat rate of about 14 m a<sup>-1</sup>.

Mendenhall Glacier was visited by John Muir in 1879. Muir (1915, p. 219) described it as “one of the most beautiful of all the coast glaciers that are in the first stage of decadence.” Originally known as *Auk Glacier* after the Auks, a Tlingit tribe, Mendenhall Glacier is 21 km long and 100 km<sup>2</sup> in area (Field, 1975c, p. 116) (figs. 85, 86). Its “decadence” has amounted to more than 5 km of retreat from its “Little Ice Age” maximum position. Lawrence (1950) determined that retreat began between 1767 and 1769; by 1910, the terminus had retreated about 1.5 km, an average retreat rate of about 10 m a<sup>-1</sup>. This period of retreat included a readvance that tilted trees in the mid-1800s. Between 1910 and 1949, the last year of Lawrence’s field investigation, the glacier had retreated another 1.5 km, an average rate of nearly 40 m a<sup>-1</sup>. Near the beginning of the 20th century, the continuing retreat began to expose a bedrock basin that became the location of an ice-marginal lake that fronted the central portion of the glacier’s terminus. Through the early 20th century, ongoing retreat exposed more of the basin and enlarged the lake. One reason for the significant difference in pre-1910 versus post-1910 retreat rates is the addition of calving as a means of ice loss. Previously, when the terminus was land based and sublimation was not included, only melting was responsible for ice loss. With the development of the ice-marginal lake, a single calving event could remove a volume of ice from the glacier’s terminus equal to what otherwise would take weeks or months to lose by melting. However, the shrinking of Mendenhall Glacier is caused primarily by surface melting throughout the entire length of the glacier and secondarily by calving of its terminus into a proglacial lake (Motyka and others, 2003). The glacier continued to retreat through the start of the 21st century.

During much of the 1990s, the southeastern margin of the glacier retreated more rapidly than it had during the previous four decades. This rapid retreat and other recent changes at the margin were not entirely related to changing climate, but were instead the result of an unusual sequence of events triggered by a small advance of the glacier during the winter of 1984–85 (Molnia, 1989a, 1991). Like the mid-19th century readvance described by D.B. Lawrence, minor short-lived readvances are not uncommon. The author observed evidence of such advances in 1974 and 1977.

Before the winter 1984–85 advance, the eastern edge of Mendenhall Glacier's margin was separated from its valley wall by the channel and outwash plain of Nugget Creek, a stream that flowed into the Mendenhall Valley along the eastern valley wall adjacent to the glacier terminus. The 1984–85 advance, which occurred while Nugget Creek's discharge was near zero, pushed a mass of basal ice and moraine across the valley, covering the outwash plain and blocking the course of Nugget Creek (figs. 93A, B). In the spring of 1985, as Nugget Creek's flow increased, water pooled on the glacier's surface and eventually overtopped the low point of the push moraine dam. The result was a flood, which perpetuated itself by partially melting and eroding the dam. In time, Nugget Creek's water melted a lake-basin depression into the glacier. By the summer of 1985, the expanding ice-surface lake continued to melt downward, finally reaching the level of adjacent Mendenhall Lake. Water entering the new lake from Nugget Creek drained subglacially into Mendenhall Lake and resulted in Nugget Creek's abandonment of its outwash plain. Between 1986 and 1988, the ice-bound lake, located within the glacier a few hundred meters behind the terminus, continued to expand, essentially consuming the glacier from within. Iceberg production from the walls of the ice-bound lake further accelerated its growth. During the period of expansion, iceberg calving was more of a growth factor than melting (fig. 93B). During the summer of 1988, the expanding lake grew in size to the point where it breached the remaining glacier ice at the terminus of Mendenhall Glacier, merging with Mendenhall Lake (fig. 93C). The entire southeastern terminus of the glacier thus was fronted by the deep waters of Mendenhall Lake, as shown in a 2 July 1989 photograph (fig. 93D). During the 4-year duration of this event, the eastern margin of the glacier retreated nearly 0.5 km. Loss of ice through iceberg production is responsible for this exceptionally rapid retreat. Its continuation will ultimately result in Mendenhall Glacier's retreat out of its lake basin. When the glacier was observed in 2004, it had retreated more than 600 m from Nugget Creek and thinned significantly.

In 1998, Shad O'Neel of the Geophysical Institute, University of Alaska Fairbanks, performed mass-balance studies on Mendenhall Glacier. He measured 12.75 m of ablation at the Mendenhall Glacier terminus (O'Neel, written commun., 7 January 2000).



**Figure 93.**—A, 5 July 1985 photograph of the eastern terminus of the Mendenhall Glacier, Coast Mountains, taken from the location of the glacier's terminus at the end of the 1930s. The ridge of sediment in contact with the glacier at the right center of the photograph is part of the push moraine formed by the 1984–85 advance of the glacier.

**Figure 93.**—**B**, 29 May 1986 north-looking, ground-based photograph of the easternmost part of the terminus of Mendenhall Glacier in Mendenhall Lake. The icebergs adjacent to the glacier margin have recently separated from the terminus, partly because of subglacial erosion by water seeping from the ice-bound lake. The terminus and the push moraine in the center of the photograph form the dam. Nugget Creek, descending from the valley wall to the right, is the source of most of the water in the ice-bound lake. Note the person for scale. **C**, 27 June 1988 photograph of the location of Mendenhall Glacier's former ice-bound lake. Breaching of the ice-marginal dam resulted in the joining of the lake with Mendenhall Lake. **D**, 2 July 1989 photograph of the eastern terminus of the Mendenhall Glacier, Coast Mountains, taken from near the same location as figure 93A. The push moraine is essentially gone, and the glacier has lost nearly 500 m of its terminus in 4 years. Photographs by Bruce F. Molnia, U.S. Geological Survey.



Herbert Glacier, northwest of Mendenhall Glacier, has a length of 17 km and an area of 68 km<sup>2</sup> (Field, 1975c, p. 116) (figs. 69, 86, 94). It was examined by Knopf (1912) in 1909 and 1910 and by Wentworth and Ray (1936) in 1931. However, work by Lawrence (1950) was instrumental in documenting changes in its position since the “Little Ice Age.” Herbert Glacier reached its maximum about 1700 and remained at or near this position for about the next 65 years. Retreat began about 1766 and was continuing when Lawrence performed his fieldwork in 1949. During this 183-year period, retreat totaled 3.29 km, yielding an average retreat rate of 18 m a<sup>-1</sup>. Field (1975a), on the basis of aerial photographs taken by Post through 1969, reported that, between 1949 and 1969, the glacier retreated about another 0.55 km, yielding an average retreat rate of 27.5 m a<sup>-1</sup>. Retreat continues through the early 21st century.

Eagle Glacier, having a length of 13 km and an area of 50 km<sup>2</sup> (Field, 1975c, p. 116), is less well known than adjacent Herbert Glacier. Work by Lawrence (1950) documented that “one of the oldest of the recessional moraines has been ice free since about 1785–1787.” Through 1949, retreat was about 2 km, about half occurring during the period 1900–49. Field (1975a) reported that, during the 1950s, the terminus became stagnant and “virtually detached” from the retreating glacier. Between 1958 and 1967, the glacier retreated about 700 m, an average annual retreat rate of 37 m a<sup>-1</sup>.

Gilkey Glacier, in a remote location more than 15 km east of Lynn Canal, is the northwesternmost outlet glacier of the Juneau Icefield. It is 32 km long and has an area of about 245 km<sup>2</sup> (Field 1975c, p. 116) (figs. 86, 95). It was virtually unknown until it was observed from the air in 1942 by the U.S. Army Air Corps. During the more than 60 years since it was first photographed, it has been retreating. Field (1975a) reported that, between 1948 and 1967, the terminus retreated about 600 m, a retreat rate of about 31 m a<sup>-1</sup>. By 1961, an ice-marginal lake had begun to develop. As was the case with Twin and



**Figure 94.**—Oblique aerial photograph of the lower reaches of the retreating Herbert Glacier and its valley, Coast Mountains, on 24 August 1963. The arcuate recessional moraines in the foreground date from the late 18th and 19th centuries. Photograph by Austin Post, U.S. Geological Survey.

**Figure 95.** — 11 August 1979 AHAP false-color vertical aerial photographic mosaic of Gilkey Glacier and a number of its named and unnamed principal tributaries. Named tributaries include Thiel, Battle, Bucher, and Echo Glaciers. All show evidence of recent retreat and thinning. Retreat and thinning of the terminus of the Gilkey Glacier have resulted in the formation of an ice-marginal lake at the terminus and the development of a well-defined trimline along its north side. Thiel and Battle Glaciers no longer flow into the Gilkey Glacier, nor do they join each other. A small lake is developing along the east side of the Thiel/Battle Glaciers margin. A distinct trimline has formed along the north margin of the Bucher Glacier and along both margins of the unnamed tributary glacier (labeled "A") that joins the Gilkey Glacier from the north. Echo Glacier barely reaches the floor of Avalanche Canyon. The tongue of Gilkey Glacier ice that Echo Glacier previously joined on the floor of Avalanche Canyon has retreated, resulting in the formation of an ice-marginal lake. A similar but significantly larger lake has formed in the valley to the west. Most of the small unnamed glaciers in the photograph also show evidence of active thinning and retreating. AHAP photograph nos. L188F4268 and L189F4314 from the GeoData Center, Geophysical Institute, University of Alaska, Fairbanks, Alaska.

Mendenhall Glaciers, iceberg calving further enhanced the rate of retreat. In each illustration of the ice-marginal lake (figs. 86, 95), recently calved large icebergs can be seen near the head of the lake. By 1984, the lake was about 1.5 km long. The principal named tributaries to the Gilkey Glacier—Thiel, Battle, Bucher, and Echo Glaciers—all show evidence of recent retreat and thinning. By 11 August 1979 (fig. 95), former tributary glaciers that flowed from Avalanche Canyon and the unnamed valley to its west had retreated so far that Gilkey Glacier was entering both valleys and forming ice-marginal lakes. In the late 1960s, up-glacier at elevations above 1,000 m, many tributary glaciers to the Gilkey were also showing evidence of thinning and retreat.

### Glaciers North of the Juneau Icefield

On the eastern side of Lynn Canal from north of Juneau Icefield to the head of Taiya Inlet, the principal named glaciers include Antler, Field, Mead, Schubee, Laughton, and Denver Glaciers. A significant accumulation of glacier ice, spanning more than 35 km, also occurs in the Kakuhan Range parallel to Lynn Canal and northwest of Berners Bay, continuing along the ridge capped by Sinclair Mountain to the southern edge of Mead Glacier.

In the mid-18th century, Antler Glacier had a length exceeding 9 km (Miller, 1964). Antler Glacier retreated through the beginning of the 20th century and then, like Taku Glacier, began to readvance. By 1925, the end of this period of advance, its terminus had moved down valley nearly 1.5 km, and the glacier reoccupied much of the area exposed during the 19th century. By 1948, the position of the retreating terminus was about 2.4 km from the mid-18th century maximum and a 1700-m-long ice-marginal lake fronted the terminus. By 1984, Antler Glacier (fig. 86) had a length of less than 3 km, and the enlarging lake was nearly 5 km long. Retreat continues through the early 21st century.

By 1979, 30-km-long Field Glacier had retreated less than 1 km from its "Little Ice Age" maximum position. The glacier was photographed on 11 August 1979 by the AHAP Program (L188F4272). Since then it has retreated about 2.3 km and an ice-marginal lake is located at the terminus. Large



trimlines along both sides of its margin document that a significant thinning has occurred. Similar thinning is exhibited by its two principal tributaries. The surface elevation of the tributaries appears to be lower than that of the main glacier, and no flow into the main glacier can be seen. Named Field Glacier in 1995 by Austin Post in honor of the late William O. Field, the glacier had an area of more than 250 km<sup>2</sup> and is located at the head of the eastern branch of the Lacey River.

Meade Glacier has a length of 37 km and an area of about 400 km<sup>2</sup> (Field, 1975c, p. 118). The glacier was photographed on 11 August 1979 by the AHAP Program (L188F4277). It is located about 25 km southeast of Skagway and is another glacier with little history of scientific investigation. Field (1975a, p. 87) stated that it had “receded very little since its last maximum,” which he described as being 400 to 800 m down valley from its 1948 terminus position. Field also stated that, in the 21 years between 1948 and 1969, the terminus retreated an additional 400 m and an ice-marginal lake that existed in 1948 was filled with sediment (Field, 1975a). This information indicates that Meade Glacier retreated at a rate of about 20 m a<sup>-1</sup> between 1948 and 1969. The terminus position measured by the author from 1979 AHAP photography is only about 300 m upstream of the position mapped from 1948 aerial photography. If Field’s statement about the glacier retreating in 1969 is correct, then the terminus would have had to advance about 100 m in the decade between 1969 and 1979. The 11 August 1979 AHAP photograph (L188F4277) shows that two unnamed tributaries have well-developed trimlines along their margins. One tributary does not appear to flow into the main trunk; the other clearly does. Down-valley vegetation indicates that most of the small unnamed glaciers in the photograph, have been separated from the main trunk for many years. All of the small glaciers show evidence of active thinning and retreat. Since 1979, Meade Glacier has retreated and thinned by more than 1 km and thinned by more than 100 m.

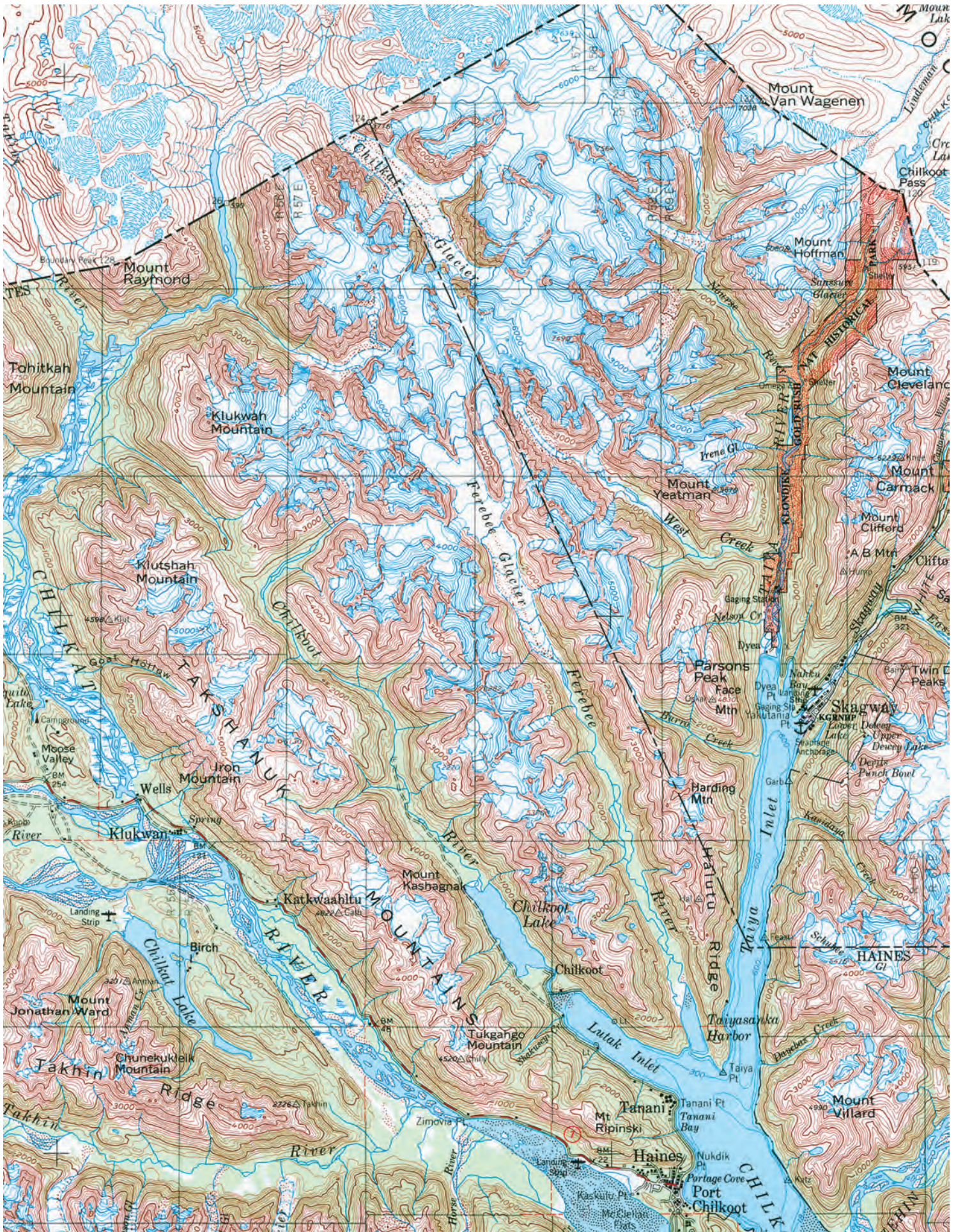
At the beginning of the 20th century, Denver Glacier, located about 7 km east of Skagway, was a popular destination and one of the most visited glaciers in Alaska. Field (1975a) stated that its terminus was photographed by C.L. Andrews in at least three different years: 1903, about 1912, and 1938. During the summer of 1903, Andrews observed that the glacier had retreated 12 m in just two months along an extensive barren zone fronting the terminus (Reid, 1904). Andrews’ 1912 photographs show that the glacier had advanced across the barren zone and had reached a vegetated area (Field, 1975a). The 1938 photographs show that the glacier was once again retreating. Trimetrogon aerial photographs taken in 1941 and 1942 depict an older terminal moraine down valley from the 1903 location. As mapped in 1948, the glacier terminus was about 1.5 km up valley from this moraine. By 1958, the glacier had retreated another 900 m. Field (1975a) reported that, by 1964, “the terminus had receded considerably since 1958.” When observed by the author in 2004, it had retreated about an additional 2 km.

In the Coast Mountains north of Lynn Canal and east of Chilkat River, a number of small and medium-sized glaciers exist (fig. 96). Only three—Ferebee, Irene, and Chilkat Glaciers—are named. No information about scientific investigations on any of these three glaciers or any others in this area could be found. Chilkat Glacier, formerly named *Leslie Glacier* in the 1890s, is the largest, with a length of about 23 km and an area of about 107 km<sup>2</sup> (Field, 1975a, p. 121). An unnamed glacier located immediately to its west (fig. 97) typifies the response of glaciers in this region. Since this north-flowing glacier was photographed in 1948, its terminus has thinned and retreated until it barely extends across the border into Canada.

Ferebee Glacier has a length of 20 km and an area of 55 km<sup>2</sup> (Field, 1975c, p. 121). The glacier was photographed on 11 August 1979 by the AHAP Program (L189F4298). An examination of the 1979 AHAP aerial photography of Ferebee Glacier and adjacent glaciers showed, in each

► **Figure 96.**—Part of the USGS (1961) 1:250,000-scale map of Skagway, Alaska-Canada, showing the occurrence of glaciers north of the Lynn Canal, west of Taiya Inlet, and east of the Chilkat River. Only three glaciers are named—the Chilkat, the Ferebee, and the Irene Glaciers. All glaciers in the area show evidence of retreat.





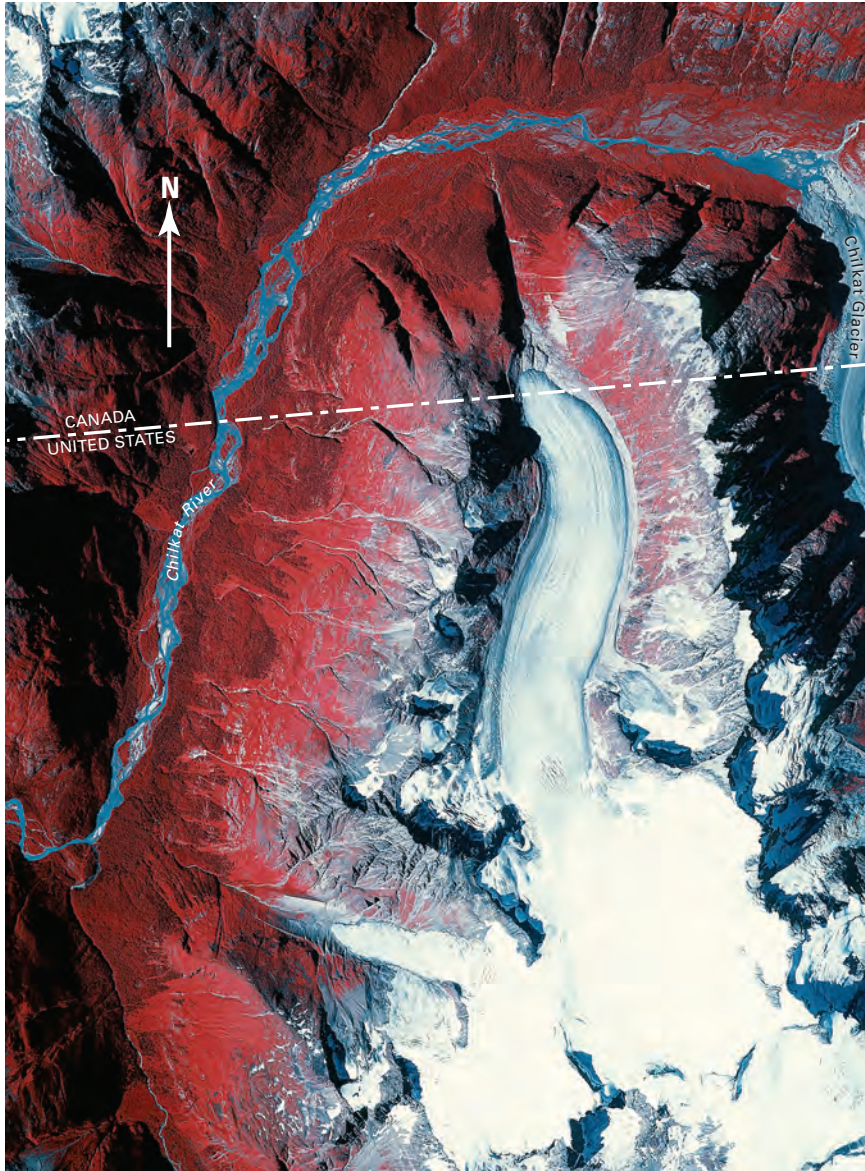


**Figure 97.**—11 August 1979 AHAP false-color vertical aerial photograph of an unnamed 4-km-long glacier to the west of Chilkat Glacier. The unnamed glacier retreated south across the border into the United States in the 1980s. The terminus of Chilkat Glacier can be seen in the upper right of the photograph. AHAP photograph no. L189F4294 from the GeoData Center, Geophysical Institute, University of Alaska, Fairbanks, Alaska.

instance, conspicuous evidence of recent retreat. The retreat of the tributaries and the thinning of Ferebee Glacier have caused every one of the former tributaries to lose contact with the glacier. In the eastern part of this area adjacent to Irene Glacier, examination of a 11 August 1979 aerial photograph taken by the AHAP Program (L188F4285) failed to identify any glaciers that were advancing, and few that appeared to be stable. All the glaciers show either vegetation-free bedrock or outwash deposits, exposed lateral moraines, well-developed trimlines, ice-marginal lakes, or other evidence of active thinning and retreat. All of the glaciers in the Takshanuk Mountains east of the Chilkat River (fig. 96) showed evidence of recent retreat.

### Summary

During the period of the Landsat baseline (1972–81), Baird, Taku, Hole-in-the-Wall, and Mead Glaciers were advancing. Available evidence suggests that all other valley and outlet glaciers in the Coast Mountains were thinning and retreating. At the end of the 20th century, Baird and Taku Glaciers were advancing, and Hole-in-the-Wall Glacier was stable. No new information was available about Mead Glacier. All other observed valley and outlet glaciers in the Coast Mountains continued to thin and retreat.

## Alexander Archipelago

The Alexander Archipelago is a group of about 1,100 islands in southeastern Alaska that extends 450 km from south to north, from the Canadian border at Dixon Entrance to Cross Sound and Icy Strait (fig. 98). Examination of topographic maps and aerial photography indicated that, in the middle of the 20th century, glaciers existed on these islands. Most, if not all, of these glaciers were retreating at the time of observation. Glaciers may presently exist in mountainous areas on the six main islands of the archipelago: Revillagigedo, Prince of Wales, Kupreanof, Baranof, Chichagof, and Admiralty. None of the glaciers on any of these islands has been studied in detail. The total area of glaciers in the Alexander Archipelago is estimated by the author at less than 150 km<sup>2</sup>.

### Revillagigedo Island

Located between the Alaska mainland and Prince of Wales Island, 90×55-km Revillagigedo Island has elevations that reach 1,400 m. A single 0.8×0.4-km unnamed glacier is located about 3.5 km south of 1,225-m-high Mount Reid, the highest point on the island (fig. 72) (see NASA space shuttle photograph no. STS028-073-039 acquired in August 1989). This glacier is also shown on the USGS (1955) Ketchikan C-4, Alaska, 1:63,360-scale topographic map (appendix B), which is based on 1948 aerial photography. It heads at an elevation of about 915 m. The 1995 revision of the map indicates no change in the glacier, although it does show a new snowfield on the eastern flank of Mount Reid. The snowfield was probably present earlier but not mapped. Landsat MSS images that cover the location of the glacier on Revillagigedo Island have the following Path/Row coordinates: 58/21 and 59/21 (fig. 3A, table 1). No other information about this glacier could be located.

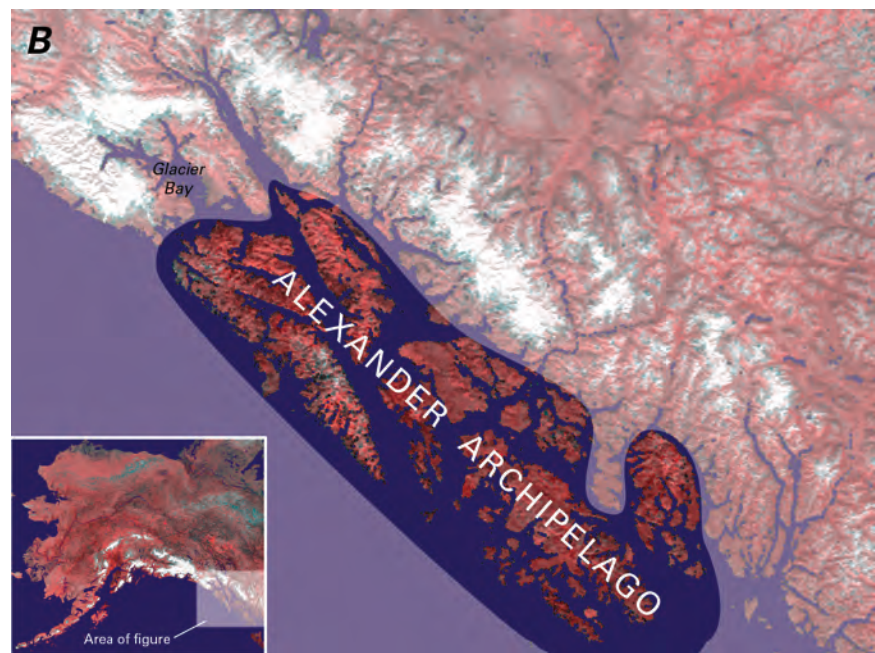
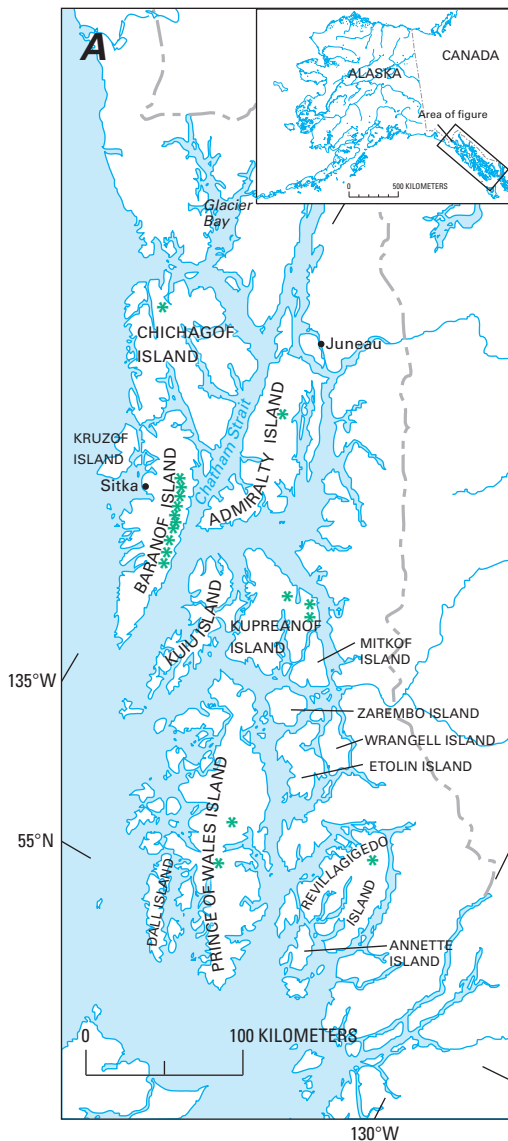


**Figure 98.**—**A**, Index map of the Alexander Archipelago showing the six main islands where glaciers are located. The green asterisks indicate the approximate location of mapped glaciers. **B**, Enlargement of NOAA Advanced Very High Resolution Radiometer (AVHRR) image mosaic of the Alexander Archipelago in summer 1995. National Oceanic and Atmospheric Administration image mosaic from Michael Fleming, Alaska Science Center, U.S. Geological Survey, Anchorage, Alaska.

## Prince of Wales Island

At 212×72 km, Prince of Wales Island is the largest of the islands of the Alexander Archipelago. The USGS (1975) Craig, Alaska, 1:250,000-scale topographic map, which is based on 1950–56 aerial photography, shows one small unnamed southeast-facing glacier on the southern face of 1,160-m Pin Peak, south of Black Bear Lake. Its length is less than 1.0 km. Its runoff drains into the Harris River and finally enters Twelvemile Arm. The Landsat 1–3 MSS image that covers this area has the following Path/Row coordinates: 60/21 (fig. 3A, table 1). The most recent 1:63,360-scale maps of the area do not show any glaciers (Craig, B2, 1997; C3, 1994; appendix B). No other information about this glacier could be located.

## Kupreanof Island

Separated from the Alaska mainland by Frederick Sound, 90×45-km Kupreanof Island has elevations that approach 1,200 m. Field (1975a) reported that several small unnamed glaciers are located on the eastern side of the island. All are 10 to 15 km north of Petersburg and less than a kilometer in length. They exist on peaks near Frederick Sound: one on 1,190-m-high Sherman Peak, one on 1,100-m-high Sheridan Peak, and one in the Missionary Range. Their location is shown on figure 78A, the Landsat MSS image that covers the eastern part of Kupreanof Island, and on an August 1997 space shuttle photograph (fig. 78B). The Landsat 1–3 images that cover the area have the following Path/Row coordinates: 60/20 and 61/20 (fig. 3A, table 1).

## Baranof Island

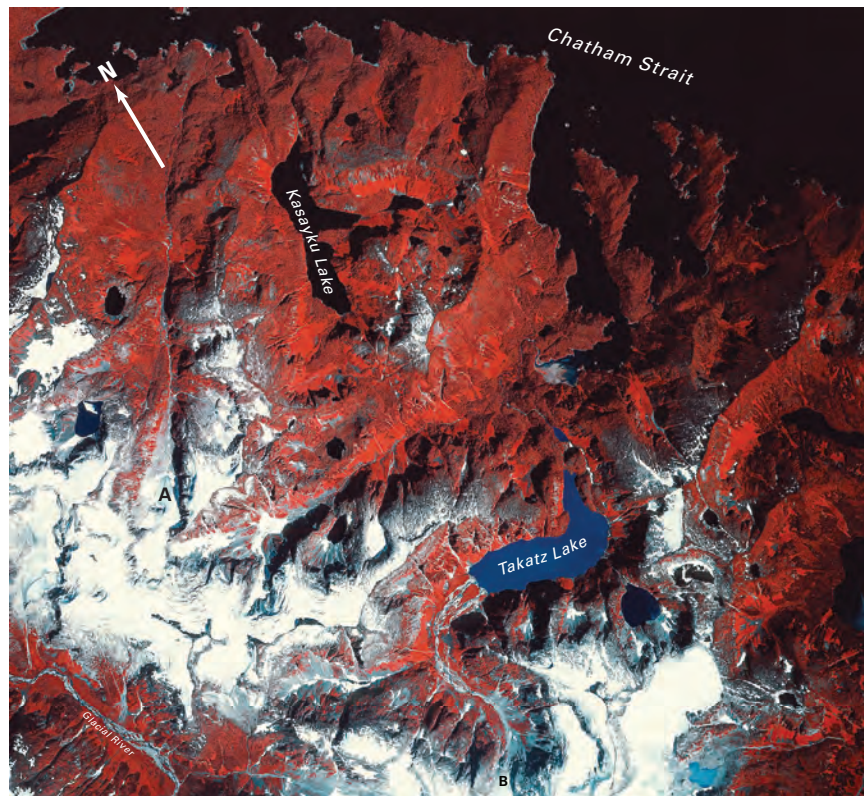
Along the crest of 170-km-long Baranof Island, more than 50 unnamed glaciers extend for approximately 90 km from west of Patterson Bay to the northern side of an unnamed 1,430-m peak 4.6 km north of Annahootz Mountain. These glaciers were photographed in 1926 by the USGS-USN Aerial Photographic Expedition. Their location is shown on a Landsat 2 MSS image and on a space shuttle photograph (see NASA space shuttle photograph no. STS028–083–057 acquired in August 1989) that cover the eastern part of Baranof Island. The Landsat images that cover the area have the following Path/Row coordinates: 61/20, 62/20, and 63/20 (fig. 3A, table 1). An examination of the photographs and images showed much evidence of thinning and retreat.

The largest of these glaciers extends for about 5 km on a ridge between 1,100-m-high Mount Furuhelm and an unnamed 1,624-m peak. Numerous parallel and subparallel fjords, some as long as 65 km, cut through Baranof Island. The fjords are evidence of the area's extensive past history of glaciation. Snow-covered glaciers both north and south of Mount Furuhelm show vegetation-free exposed bedrock, evidence of recent retreat on a photograph taken 11 August 1979 (fig. 99) (see also AHAP false-color infrared vertical aerial photograph no. L200F4540 acquired on 12 August 1979). Many of the glaciers in the vicinity of Mount Furuhelm were photographed in 1926 with a three-lens Bagley aerial camera (figs. 26, 29).

## Chichagof Island

The northwesternmost island of the Alexander Archipelago, 116-km-long Chichagof Island, has more than a dozen small unnamed glaciers near its northern end. Each is less than one kilometer in length. Their location is imaged by Landsat 1–3 MSS scenes with the following Path/Row coordinates: 63/19, 64/19 and 65/19 (fig. 3A, table 1). One glacier flows northwest from the summit of Pegmatite Mountain down to an elevation of about 350 m (see AHAP false-color infrared vertical aerial photograph no. L199F190 acquired on 12 August 1979). Vegetation-free bedrock around the margins of many of the glaciers in this area indicate recent retreat.

**Figure 99.**—11 August 1979 AHAP false-color vertical aerial photograph of Baranof Island showing the area north of Mount Furuhelm and east of Sitka. Here many of the glaciers east of Glacial River are fringed by vegetation-free bedrock. Two in particular, unnamed glaciers labeled A and B, each show about 0.5 km of recent retreat. AHAP photograph no. L199F211 from the GeoData Center, Geophysical Institute, University of Alaska, Fairbanks, Alaska.



### Admiralty Island

On central Admiralty Island, two glaciers are shown on the USGS (1951) Sitka, Alaska, 1:250,000-scale topographic map (appendix A), which is based on 1949 and 1951 aerial photography. They are located on an unnamed 1,000 to 1,200-m-high mountain ridge between Hasselborg Lake and Lake Florence. The larger is about 2 km in length; the smaller is only about 0.8 km in length. Their location is shown on Landsat MSS images with the following Path/Row coordinates: 61/20 and 62/19 (fig. 3A, table 1). No other information about these glaciers could be located.

### Summary

During the period of the Landsat baseline (1972–81), all available evidence suggests that the glaciers in the Alexander Archipelago were thinning and retreating. No information is available about the status of these glaciers through the early 21st century. However, their small size, low elevation, and southerly location in an area with significant late 20th century temperature increases suggests that they have probably continued to thin and retreat.

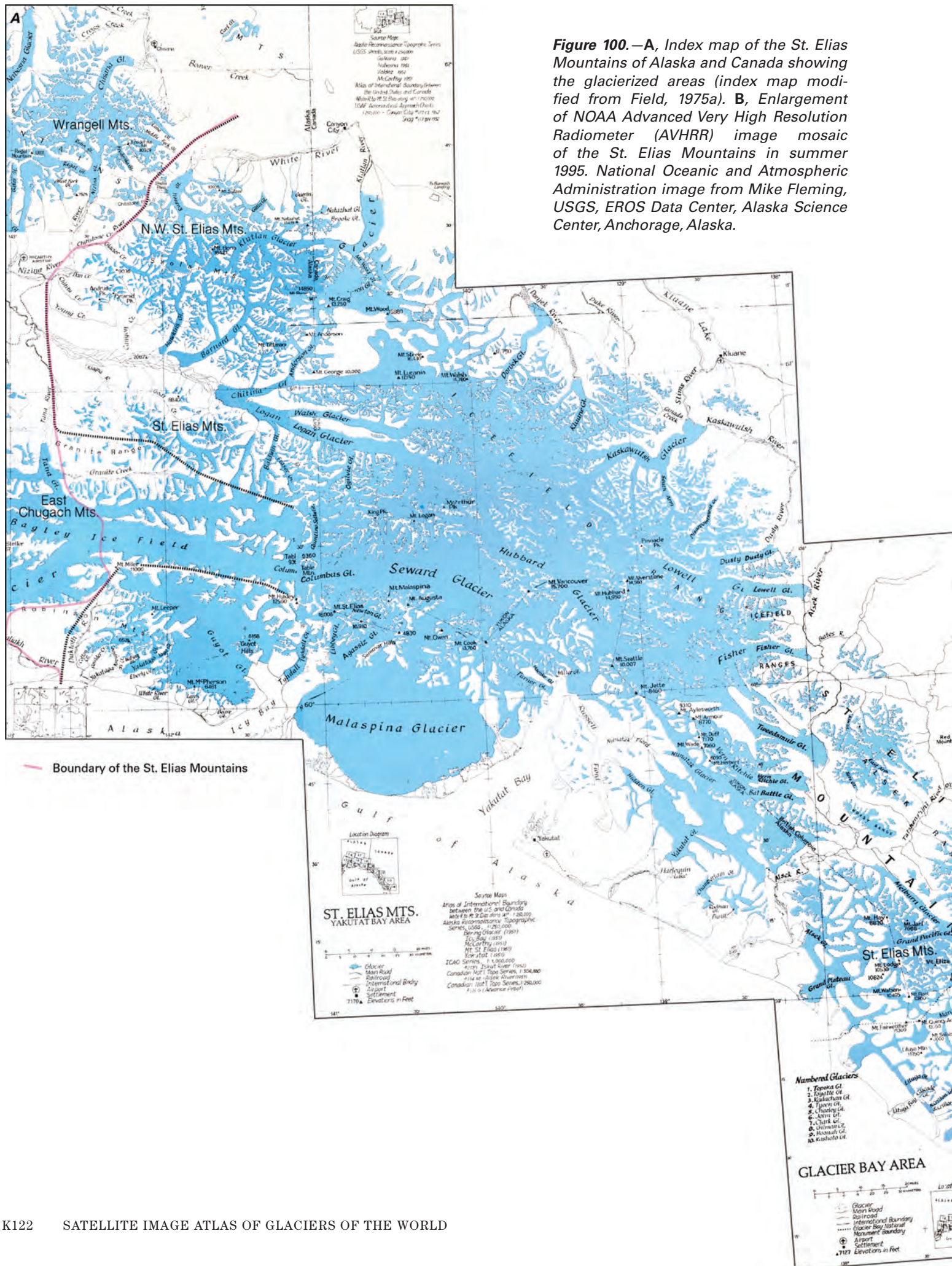
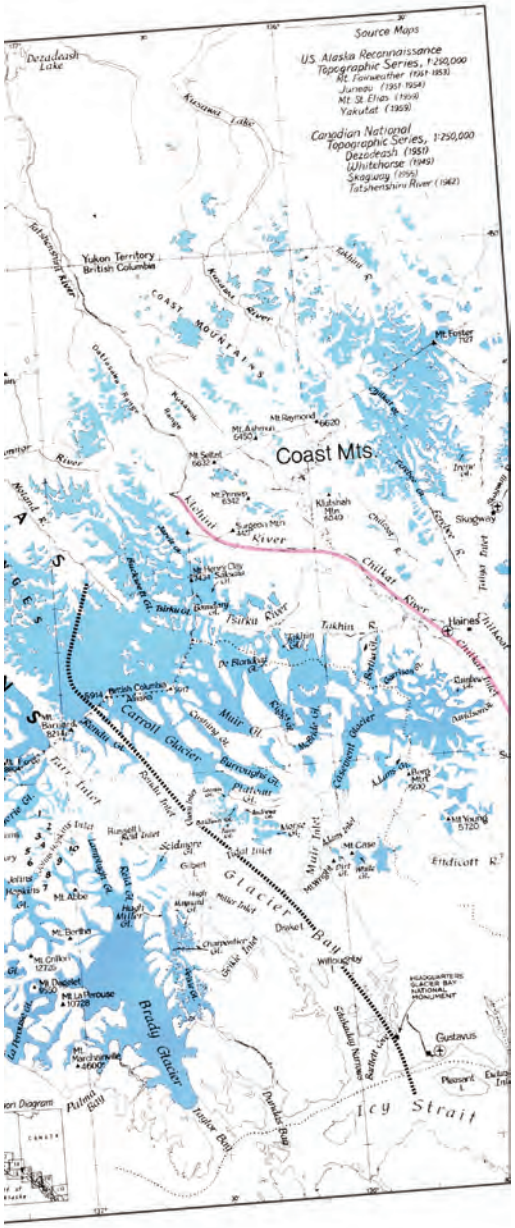
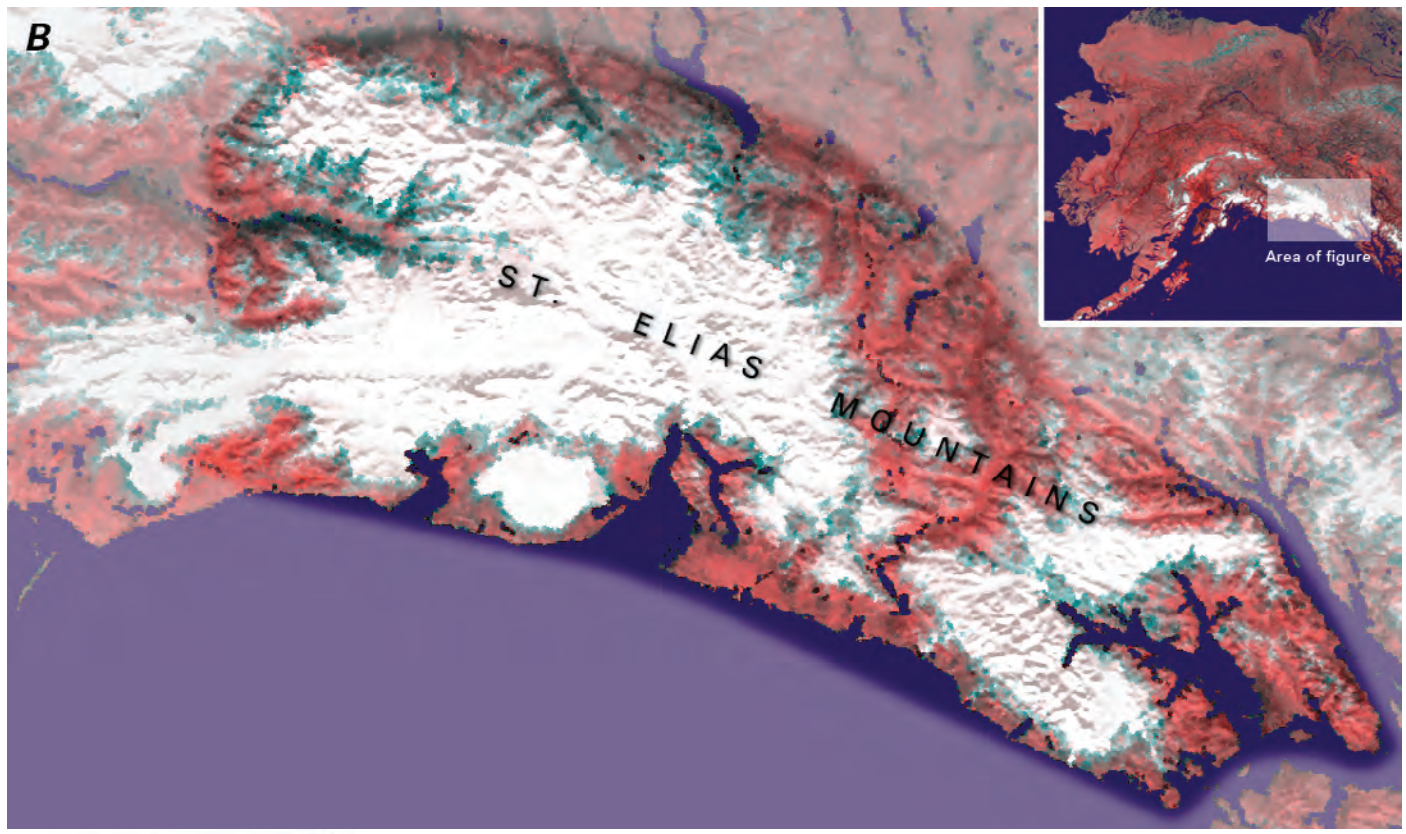


**Figure 100.**—**A**, Index map of the St. Elias Mountains of Alaska and Canada showing the glacierized areas (index map modified from Field, 1975a). **B**, Enlargement of NOAA Advanced Very High Resolution Radiometer (AVHRR) image mosaic of the St. Elias Mountains in summer 1995. National Oceanic and Atmospheric Administration image from Mike Fleming, USGS, EROS Data Center, Alaska Science Center, Anchorage, Alaska.



## St. Elias Mountains

### Introduction

Much of the St. Elias Mountains, a 750×180-km mountain system, straddles the Alaskan-Canadian border, paralleling the coastline of the northern Gulf of Alaska; about two-thirds of the mountain system is located within Alaska (figs. 1, 100). In both Alaska and Canada, this complex system of mountain ranges along their common border is sometimes referred to as the Icefield Ranges. In Canada, the Icefield Ranges extend from the Province of British Columbia into the Yukon Territory. The Alaskan St. Elias Mountains extend northwest from Lynn Canal, Chilkat Inlet, and Chilkat River on the east; to Cross Sound and Icy Strait on the southeast; to the divide between Waxell Ridge and Barkley Ridge and the western end of the Robinson Mountains on the southwest; to Juniper Island, the central Bagley Icefield, the eastern wall of the valley of Tana Glacier, and Tana River on the west; and to Chitistone River and White River on the north and northwest. The boundaries presented here are different from Orth's (1967) description. Several of Orth's descriptions of the limits of adjacent features and the descriptions of the St. Elias Mountains and the Chugach Mountains are contradictory. For instance, he places the Granite Range in the Chugach Mountains yet has its eastern and western sides bounded by St. Elias Mountains features. In this description, the Granite Range is included in the St. Elias Mountains.

The highest peak in the Alaskan St. Elias Mountains is Mount St. Elias (fig. 101). Its 5,489-m-high summit, which lies on the U.S.-Canadian border, is located only about 12 km from sea level as of 2004, measured from the now-stable terminus of the tidewater Tyndall Glacier. During most of the 20th century, as Tyndall Glacier retreated, the distance from the summit to sea level has decreased from nearly 60 km to the present 12 km. This ongoing retreat has produced one of the steepest topographic gradients anywhere on Earth. Elsewhere in the Alaskan St. Elias Mountains, Mount Bona (5,005 m), Mount Vancouver (4,785 m), Mount Fairweather (4,663 m), and Mount Hubbard (4,557 m) all exceed 4,500 m. More than two dozen other peaks have

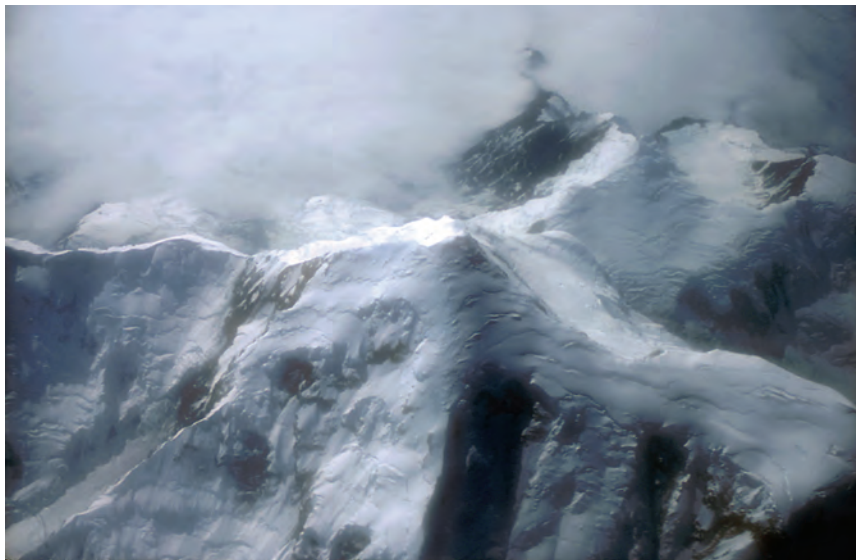


**Figure 101.**—Aerial photograph of the summit of Mount St. Elias and environs on 28 July 2001. At 5,489 m, Mount St. Elias is the highest peak in Alaska's St. Elias Mountains. Photograph by Bruce F. Molnia, U.S. Geological Survey.

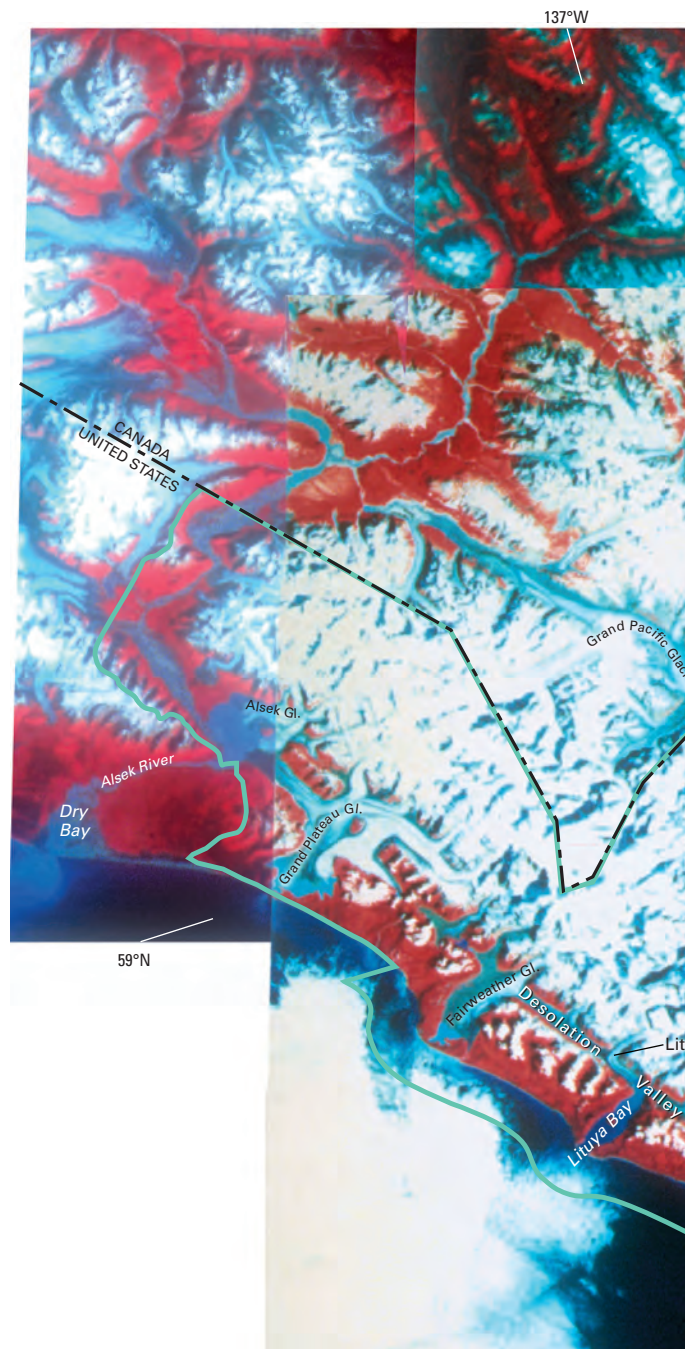
elevations greater than 3,300 m. The highest peak, Mount Logan (6,050 m) is located entirely within Canada (see Ommanney, 2002a, fig. 20).

Glaciers cover about 11,800 km<sup>2</sup> of the Alaskan part of the St. Elias Mountains (Post and Meier, 1980, p. 45). Included are parts of the three largest temperate glaciers in North America: two piedmont outlet glaciers (Bering and Malaspina Glaciers) and one tidewater glacier (Hubbard Glacier). More than 50 glaciers in the St. Elias Mountains have lengths greater than 8 km. Many mountainous areas and ranges of the Alaskan St. Elias Mountains have been given unique names (from east to west): Chilkat Range, Takhinsha Mountains, Fairweather Range, Brabazon Range, Granite Range, Robinson Mountains, and Icefield Ranges. For ease of description, the St. Elias Mountains are divided into segments: (1) southeastern St. Elias Mountains (from the Lynn Canal and Chilkat Inlet and River to the eastern side of the Alsek River); (2) the south-central St. Elias Mountains (from the western side of the Alsek River to the western side of Yakutat Bay); (3) southwestern St. Elias Mountains (from the western side of Yakutat Bay to the western Bagley Ice Valley, the western Robinson Mountains, and the Bering Lobe); and (4) the northwestern St. Elias Mountains (from the Canadian border at long 141°W. to White River, Chitistone River, Tana River, the eastern wall of the valley of Tana Glacier, and the southern side of the Bagley Ice Valley).

### **Southeastern St. Elias Mountains Segment: From the Lynn Canal and Chilkat Inlet and River to the Eastern Side of the Alsek River**

Landsat MSS images that cover the southeastern St. Elias Mountain region from Lynn Canal and Chilkat Inlet and River to the eastern side of the Alsek River have the following Path/Row coordinates: 63/19, 64/18, 64/19, 65/19, and 66/18 (fig. 102). These areas are mapped on the USGS Juneau (Alaska-Canada), Skagway (Alaska-Canada), Mount Fairweather (Alaska-Canada), and Yakutat (Alaska-Canada) 1:250,000-scale topographic maps (appendix A).

East of the Glacier Bay drainage, the area between the Chilkat River and the Canadian border supports more than 100 small glaciers and several larger ones, some with lengths approaching 15 km. The largest glacier in this region is the 20-km-long Davidson Glacier, located in the Chilkat Range, which has an area of 115 km<sup>2</sup> (Field and Collins, 1975, p. 251). Many of these glaciers were photographed by the IBC early in the 20th century (IBC, 1952) and revisited by an AGS expedition led by Field in 1967 (Field and Collins, 1975). Except for subsequent coverage provided by aerial photography and satellite imagery, these investigations were the last detailed documentation for

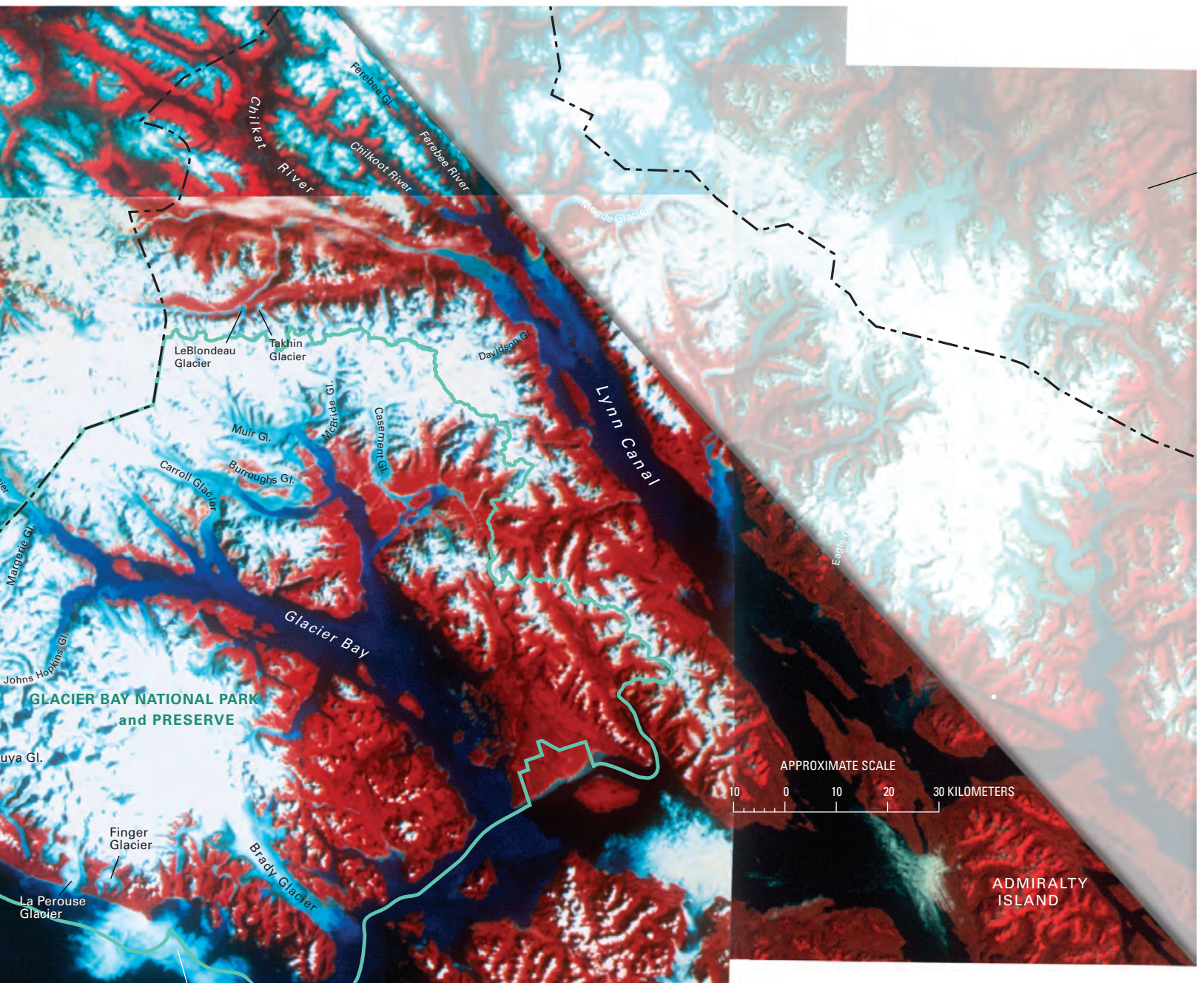




most glaciers in the area. North of the Klehini River, about a dozen unnamed glaciers, all shorter than 3 km, exist on Hiteshitak Mountain, Mount Prinsep, Four Winds Mountain, and Chilkat Peak.

The mountains between the Klehini and Tsirku Rivers also support a number of small glaciers, several of which have been named. With the exception of the Little Jarvis Glacier, very limited recent observations have been made of these glaciers. Named glaciers are Jarvis, Little Jarvis, Boundary, and Saksaiia Glaciers. Unstudied Jarvis Glacier, with a length of more than 15 km, flows from Canada into Alaska. The terminus region of the glacier appears to be stagnant, and the lowermost few kilometers are covered by moraine. The debris-covered terminus lies about a kilometer from a moraine, which represents a former maximum position, perhaps its "Little Ice Age" maximum. Little Jarvis Glacier, with a length of 3.2 km, is one of the glaciers surveyed by the AGS in 1957–58 (see fig. 35) and resurveyed by a University of Alaska Fairbanks team in 1995 (Sapiano and others, 1998). In the 38 years between surveys, the terminus retreated about 190 m, an average of about

**Figure 102.**—Annotated Landsat 2 and 3 MSS false-color composite image mosaic of the St. Elias Mountains from Lynn Canal to the Alsek River, including the glaciers in Glacier Bay and environs and those of the Fairweather Range. Landsat 2 and 3 MSS images (21670–19195; 19 August 1979; Path 62, Row 19; 30147–19373; 30 July 1978; Path 64, Row 18; 2952–19124; 31 August 1977; Path 64, Row 19; 21314–19295; 28 August 1978; Path 66, Row 18) are from U.S. Geological Survey, EROS Data Center, Sioux Falls, S. Dak.



5 m a<sup>-1</sup>. During the 38-year interval, Little Jarvis Glacier experienced a small loss in area (2.45 km<sup>2</sup> in 1995 as opposed to 2.5 km<sup>2</sup> in 1958) but no apparent change in volume.

Boundary Glacier originates in the United States and flows into Canada, where it merges with the Tsirku Glacier. When photographed on 11 August 1979 during the AHAP Program (fig. 103), its terminus was stable, and only a small amount of bedrock was exposed along its valley walls. All but the lower 3 km of 20-km-long Tsirku Glacier is in Canada. As was the case with Boundary Glacier, exposed bedrock along its valley walls was the only evidence of thinning. The glaciers in this area have a long history of photographic coverage. When Tsirku Glacier was photographed in 1910, it had a proglacial lake at its terminus. By 1948, a 300- to 400-m advance of the glacier had filled the lake basin; Field and Collins (1975) reported that the advance continued between 1948 and 1967. In 1979, it appeared that the advance had ended; however, the terminus still maintained its recent maximum position. By the early 21st Century, the terminus had retreated several hundred meters.

South of Tsirku River, along the crest of the Takhinsha Mountains, a number of north- and east-flowing glaciers drain into the Tsirku and Takhin

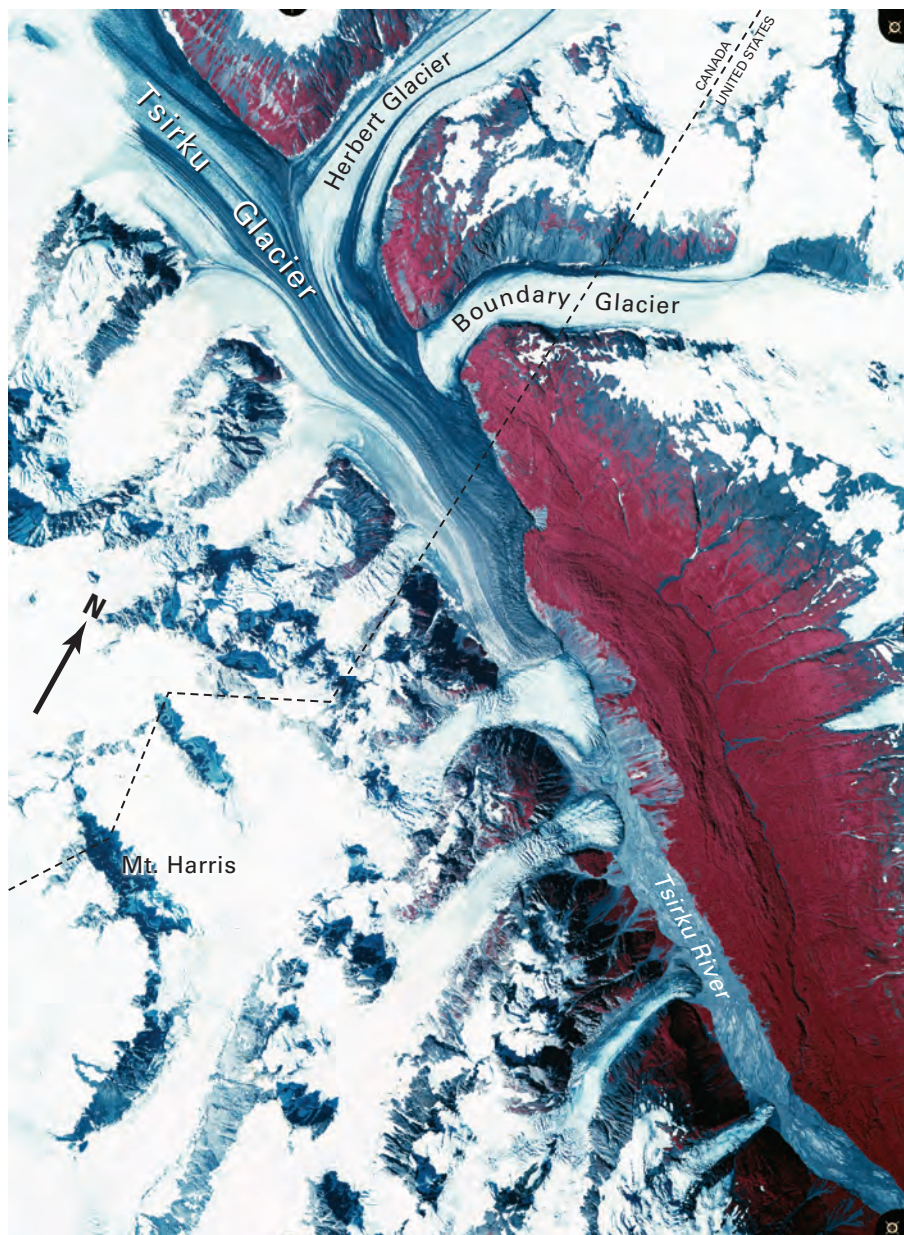


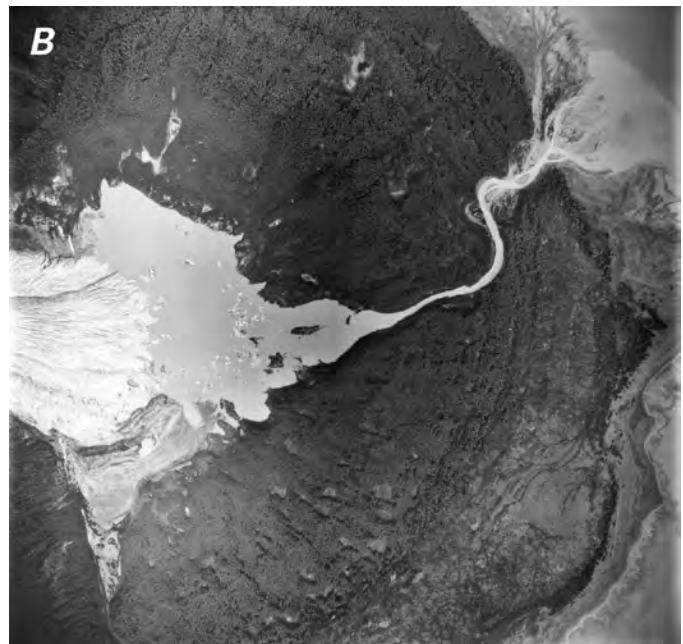
**Figure 103.** — 11 August 1979 AHAP false-color infrared vertical aerial photograph of the area around the Tsirku River. All of the glacier termini shown are at elevations of less than 500 m, and all appear to be relatively stable. Exposed bedrock in some valley walls and vegetation-free areas marking former terminus positions and heights are the only evidence of small variations from recent maximum ice positions. AHAP photograph no. L194F4169 from the GeoData Center, Geophysical Institute, University of Alaska, Fairbanks, Alaska.

Rivers. These glaciers include Le Blondeau, Takhin, Dickinson, Willard, Bertha, and Garrison Glaciers, many of which were described by Arthur and Aural Krause in 1881–82 (Krause, 1883) and photographed by the IBC between 1894 and 1910. Takhin Glacier had retreated several hundred meters from its “Little Ice Age” maximum position when it was first photographed in 1910. Between 1910 and 1967, Le Blondeau Glacier retreated more than 1 km. All were retreating when observed in 2004.

When the Krauses first observed it in 1881, the terminus of Bertha Glacier had advanced into an evergreen forest and was shedding rocks into the trees. According to them, this advance was in marked contrast to all of the other glaciers in the area, which were then in significant retreat. By 1894, the advance had ended. Through 1967, the retreat of the terminus amounted to about 300 m.

Because of its location along the western side of Lynn Canal, Davidson Glacier has been seen by many travelers. In spite of this prominent position, it suffers from a lack of detailed observations. One of its earliest visitors was I.C. Russell in 1889, who observed several signs of recent continuing retreat. He described the terminus as being surrounded by a “mile-and-one half-wide accumulation of ice-marginal sediment deposits, so as to form an encircling girdle now covered on its outer margin with a dense spruce forest.” The inner half-mile he described as “a barren, desolate tract of boulders and gravel of fresh appearance, and evidently but recently abandoned by the glacier” (Russell, 1897, p. 103). A series of arcuate recessional moraines encircles the terminus of Davidson Glacier and documents an advance between the 12th and 14th centuries, a retreat during the 15th century, and a significant readvance in the middle 18th century (Egan and others, 1968), followed by the retreat observed by Russell in 1889. By the time it was photographed 57 years later, in August 1946 (fig. 104A), the terminus of Davidson Glacier had retreated more than 1.5 km from its “Little Ice Age” maximum position and about 0.4 km from the 1889 position observed by Russell. A proglacial lake had also developed. When it was photographed 32 years later on 31 August 1978 (fig. 104B), the lake had expanded in size, encircling two-thirds of the terminus, and the glacier had retreated another 0.7 km. Twenty-six years later, when observed by the author on 18 June 2004, the terminus had retreated an additional 0.7 km.

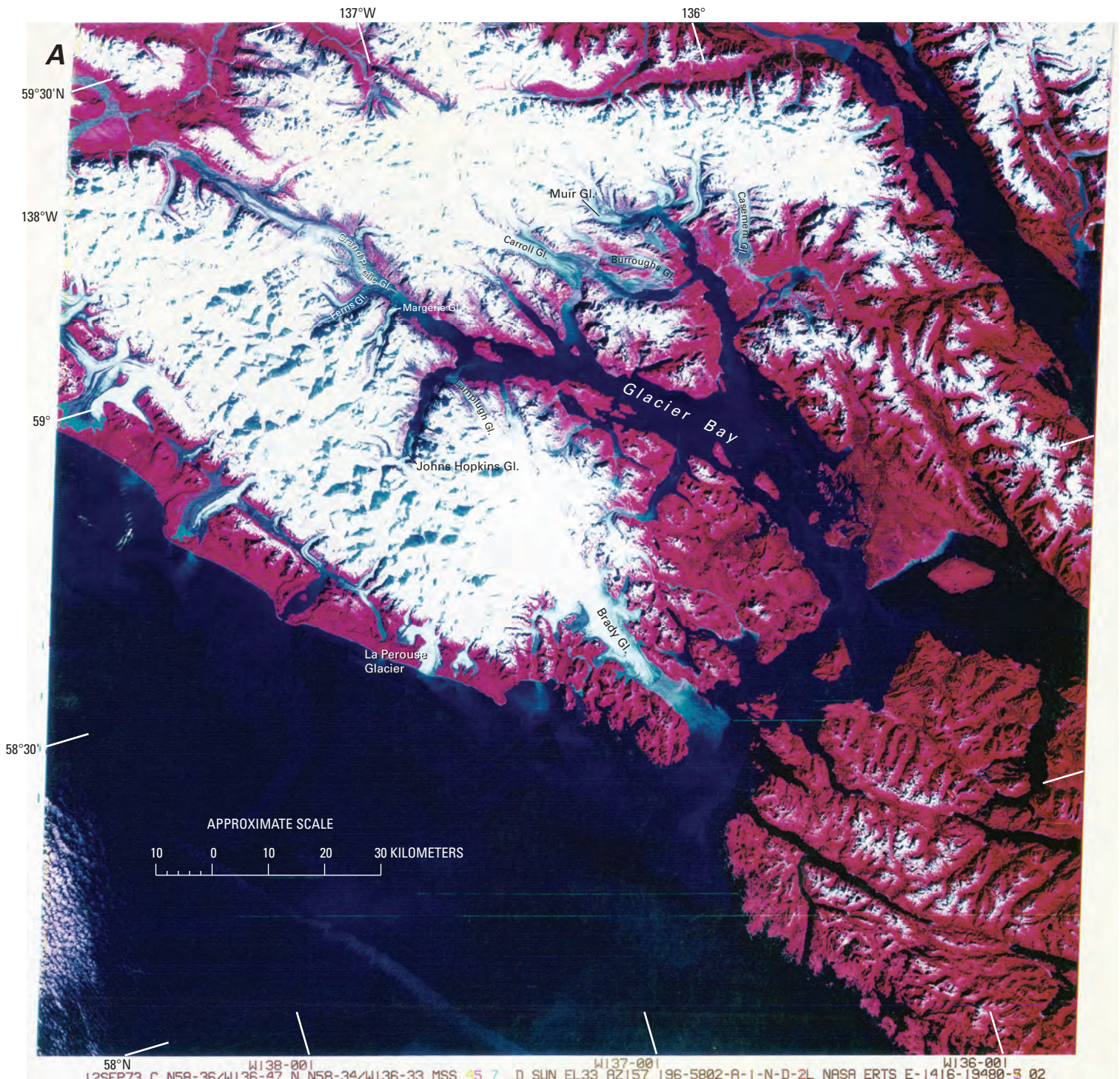
**Figure 104.**—**A**, August 1946 black-and-white vertical aerial photograph of Davidson Glacier showing the series of arcuate recessional moraines that encircles the terminus of Davidson Glacier and documents its “Little Ice Age” history and post-“Little Ice Age” retreat. Photograph SEA-140-100 from the U.S. Army Air Force, Southeast Alaska Project. **B**, 31 August 1978 photograph showing a lake significantly larger than the one that existed in 1946. During the 32 years between the date of this photograph and figure 104A, Davidson Glacier retreated about 0.7 km. Iceberg calving into the ice-marginal lake is contributing to the glacier’s retreat. USGS photograph 78-V2-25 by Austin Post, U.S. Geological Survey.



## Glacier Bay National Park and Preserve

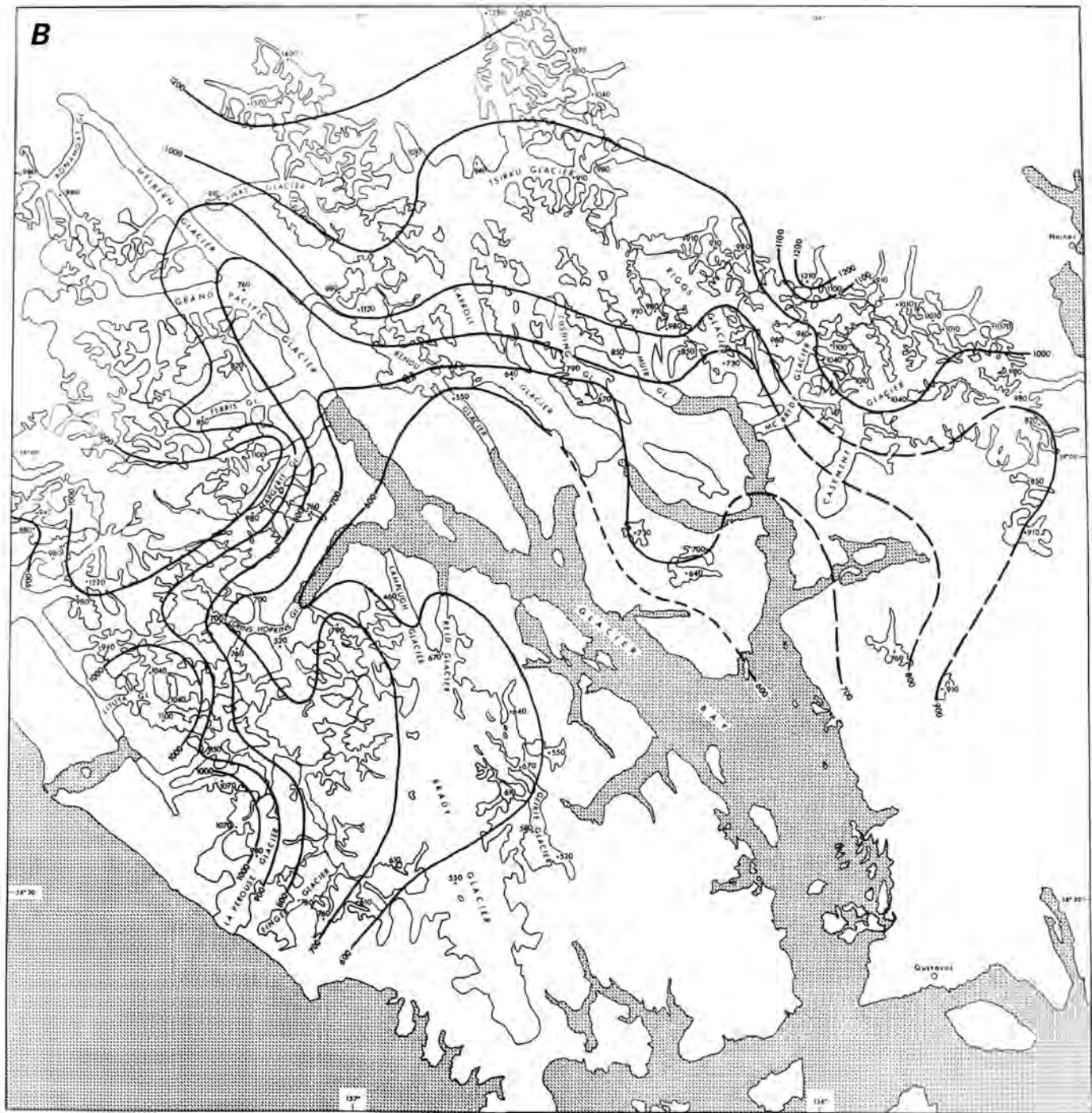
Glacier Bay National Park and Preserve contains more than 50 named glaciers and one of the most spectacular fjords in Alaska (fig. 105). Its glaciers head in the Takhinsha Mountains, the Alsek Ranges of Canada, the St. Elias Mountains, and the Fairweather Range. Many glaciers originate at elevations that exceed 2,000 m. About a dozen glaciers have lengths exceeding 15 km, the longest and largest being Grand Pacific Glacier, which is about 60 km long and has an area of about 650 km<sup>2</sup>. This glacier originates in Alaska, flows through British Columbia, and terminates in Alaska. Both Brady and Carroll Glaciers have areas that exceed 500 km<sup>2</sup>.

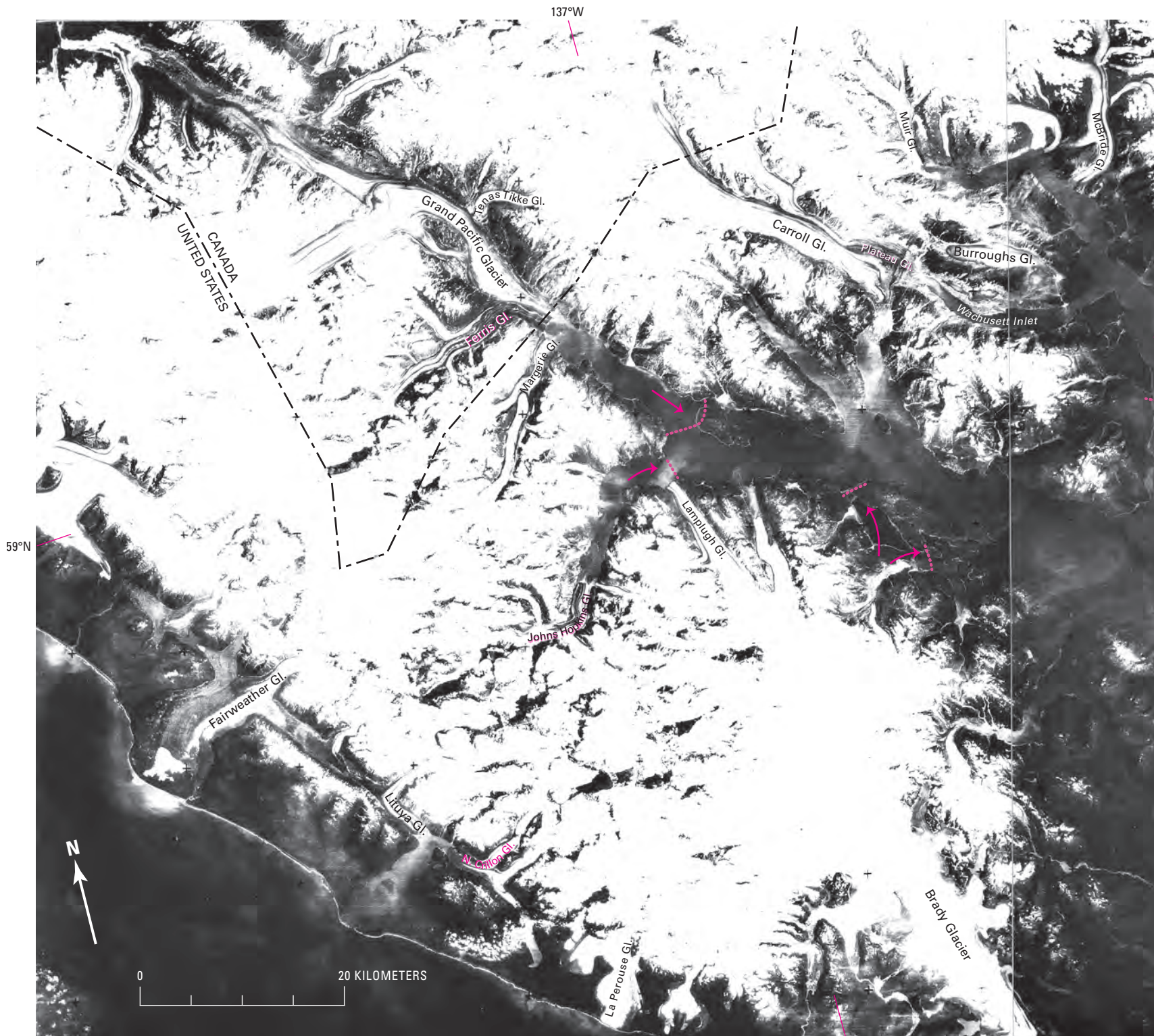
**Figure 105.**—A, Annotated Landsat 1 MSS false-color composite image of Glacier Bay and environs, Alaska. This 1:250,000-scale image, combined with maps, was used to determine the accumulation area ratios (AARs) of individual glaciers and the snow-line altitude throughout Glacier Bay (Robert M. Krimmel, written commun., 1987) (see table 4, p. K132). Landsat 1 MSS image (1416–19480, bands 4, 5, 7; 12 September 1973; Path 64, Row 19) is from the U.S. Geological Survey, EROS Data Center, Sioux Falls, S. Dak.



Many of the glaciers of this area can be seen on two Landsat images acquired on 12 September 1973 (fig. 105A) and on 12 August 1979 (fig. 106); the two images provide clear views of the majority of glaciers within Glacier Bay National Park and Preserve. Table 4, which is based on the work of Robert M. Krimmel (USGS), provides data on AARs of glaciers in Glacier Bay and environs. He based his analysis on a 30 September 1973 Landsat 1 MSS image (1434-19473) of the area. Glacier Bay extends for more than 100 km from its mouth at Icy Strait to the termini of both Grand Pacific Glacier at the head of Tarr Inlet and Johns Hopkins Glacier at the head of John Hopkins Inlet. About 250 years ago, Glacier Bay did not exist. Its basin was filled by a single large ice mass that reached into Icy Strait. The terminus position that

**Figure 105.—B, Contours (in meters) of equal snowline altitude are depressed in the inland portion of Glacier Bay because of late summer storms in that area. Landsat image, AAR table, snowline-altitude map, and caption courtesy of Robert M. Krimmel, U.S. Geological Survey**





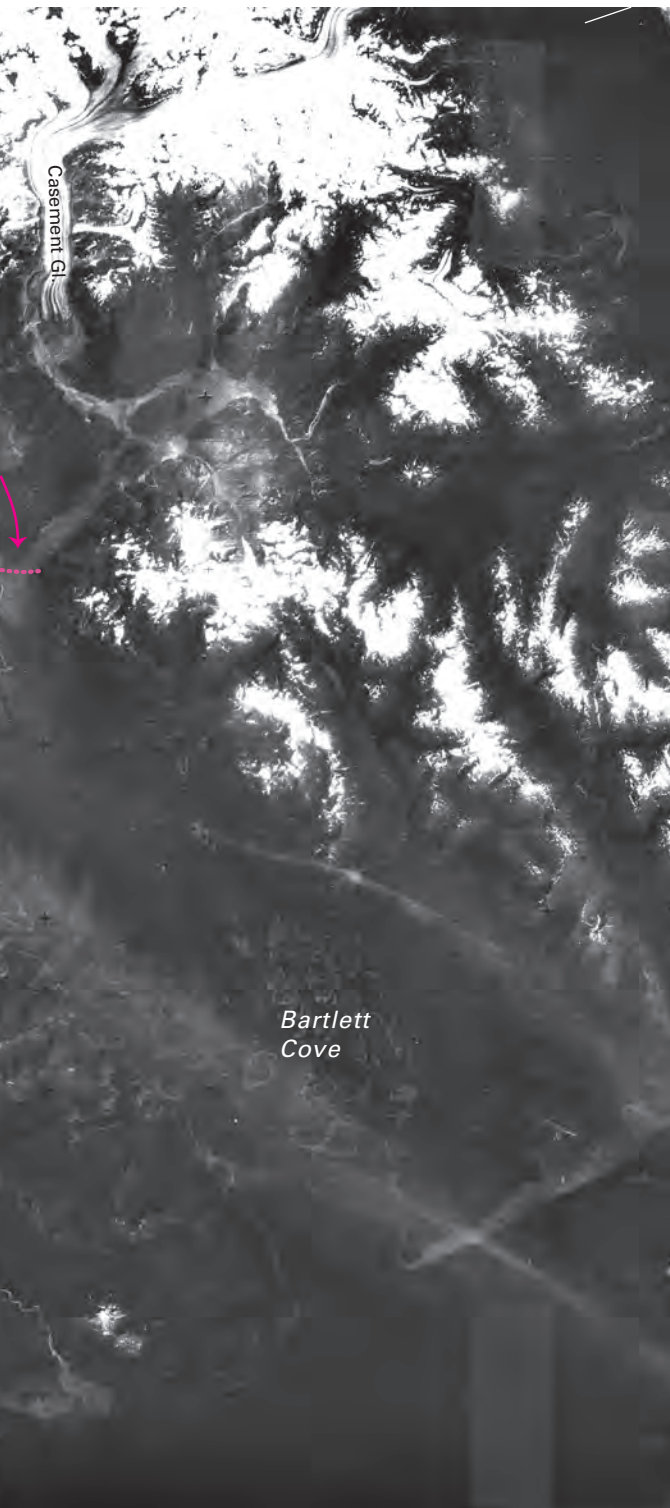


**Figure 106.**—Most of Glacier Bay National Park and Preserve is included in this excellent A and B quadrant composite of a Landsat 3 RBV image acquired on 12 August 1979. There are some high cirrus clouds degrading parts of the image. The clouds are difficult to distinguish from sediment in the water in this broad-band image. The Glacier Bay area is outstanding in its accessibility to tourism, its long record of observation, and its rapidly changing and diverse glaciers (fig. 107). The first record of glacier position is Vancouver's observation in 1794 (Vancouver, 1798), at which time the glacier that filled the bay terminated near Bartlett Cove (Field, 1975a, p. 161). H.F. Reid's map of Glacier Bay, 1890–92 (fig. 108B), indicated recession by that time of about 75 km, shown on this image with dots and arrows to give approximate ice flow direction (Reid, 1896). Muir Glacier continued to recede, although there were occasional periods during which recession slowed in reaches where the fjord narrows (Field, 1975a, p. 167–8). By 1984, Muir Glacier was located at the head of the fjord. In 1991, Muir Glacier receded onto land, and retreat continued more slowly. Casement Glacier became independent of the Muir Glacier about 1911 and had retreated about 6 km by 1975 (Field, 1975a, p. 168). Burroughs Glacier (figs. 109, 112) is a remnant of the Muir complex of decades past and is presently nearly stagnant with no accumulation zone. Carroll Glacier has receded only slightly since it was first observed by Reid (Field, 1975a, p. 171). This glacier was also the source of the nearly disappeared Plateau Glacier, which is shown to have nearly filled Wachusett Inlet on the USGS Mount Fairweather 1:250,000 topographic map dated 1961. Grand Pacific Glacier, mostly in Canada, had receded from the 1892 position some 18.5 km by 1925 (Field, 1975a, p. 173) and, by the time of this image, had readvanced by 1.5 km. This advance has been due primarily to the influence of the Ferris Glacier, which on this image can be seen to account for 60 percent of the width of its active terminus. Margerie Glacier has been fairly stable since its early 20th century retreat ended. Johns Hopkins Glacier has slowly advanced from its minimum position in 1929 (Field, 1975a, p. 176). Lamplugh Glacier retreated, advanced, and retreated and is now stable since it separated from the receding Johns Hopkins Glacier at the beginning of the 20th century. Brady Glacier was nearly stable for most of the 20th century, although in the last few years it has been retreating. La Perouse Glacier is presently separated from the open ocean only by a narrow beach; at times in the recent decades it has advanced across the beach. North Crillon and Lituya Glaciers have had a long history of advance (Field, 1975a, p. 188–190). Fairweather Glacier is in slow retreat (Field, 1975a, p. 192). Many of the glaciers in this area may have responded to nonclimatic factors. The Fairweather Range is notable for large landslides, the debris from which often comes to rest on glaciers and may cause advance by protecting ice from ablation with an insulation layer (Post, 1967a). Ferris, Johns Hopkins, North Crillon, and Fairweather Glaciers all have rock-slide debris partially covering the ablation area. Surges of glaciers are also common in this area. Glaciers known to surge are the Carroll, La Perouse, and Tenas Tikke; the last of which surged in 1972–1973 with a 3-km advance easily seen on repeated Landsat images (Krimmel and Meier, 1975). Landsat 3 RBV image (30525–19370, A and B; 12 August 1979; Path 64, Row 19) is from the U.S. Geological Survey, EROS Data Center, Sioux Falls, S. Dak. Landsat image and caption courtesy of Robert M. Krimmel, U.S. Geological Survey.

the ice occupied from about 1750 to 1780 (fig. 107) marks the maximum areal extent of the ice mass in Glacier Bay during the “Little Ice Age.” By 1794, when Joseph Whidbey and William LeMesurier, two of George Vancouver’s lieutenants, explored Icy Strait, the ice had retreated about 8 km and a small bay had formed. At the time of their observations (Vancouver, 1798), the retreating glacier terminated near Bartlett Cove. By the time the bay was entered by Lt. C.E.S. Wood in 1877 and explored by John Muir in 1879, the ice retreat exceeded 60 km.

Much of the retreat may have been owing to iceberg calving. When Carlson and others (2001) profiled lower Glacier Bay between Sitakaday Narrows and the fjord entrance with a multibeam imaging system, they found an extensive area covered by complex iceberg gouge patterns in the glacial marine sediment of the fjord’s floor in water depths ranging from 50 to 100 m. Individual gouges were as much as 5 km long and a few tens of meters wide and had several meters of relief. They concluded that these gouges were likely formed by massive icebergs with drafts up to 100 m no more than 160 years ago. The large icebergs calved as the glacier retreated up the bay. They reported that the dominant gouge orientation, roughly parallel to the fjord axis, suggests that the strong tidal currents of up to 7 knots through Sitakaday Narrows were responsible for driving the iceberg keels across the seabed. Even though the glaciers have retreated more than 80 km up fjord from Sitakaday Narrows, the gouges remain unburied in this environment of high sedimentation because sediment presently reaching the ice gouges is largely restricted to local runoff and plankton debris. In addition, the strong tidal currents through Sitakaday Narrows effectively keep the ice-gouged fjord floor scoured clean of fine sediment.

By the end of the 19th century, as the ice mass continued to thin and retreat, individual inlets began to become ice free, each with its own unique retreating glacier. Each inlet has its own history and timing of ice movement. For instance, Muir Glacier, located in the eastern arm of the bay, separated from the main ice mass in the early 1860s.

Reid (1892, 1895, 1896) carried out important scientific work on Muir Glacier and other glaciers in Glacier Bay. The scientific significance of his work has been discussed previously in the “Early Observations of Alaska and Its Glaciers” section earlier in this chapter.

Israel C. Russell visited Glacier Bay in 1890 (Russell, 1897, p. 82). He described the massive Muir Glacier as follows:

On nearing the head of Glacier Bay and approaching Muir inlet, one beholds a palisade of ice nearly two miles long and from 130 to 210 feet high, rising from the water and uniting the mountain with mountain and forming a wall across the head of the inlet so as to hold back the waters of the ocean. This wall of ice is the extremity of the justly famed Muir Glacier. As one draws near, the surface of the glacier can be seen above and beyond the line of precipices in which it terminates. ... Soundings made in the central portion of the inlet as near to the ice front as vessels can safely venture, by estimate a thousand yards from the base of the cliffs, give a depth of 720 feet. The glacier extended south of the present limit a few years since and occupied the site where this sounding was taken, and was then certainly fully one thousand feet thick.

John Burroughs (1902, p. 35–36) participated in the Harriman Expedition’s visit to Glacier Bay. He described their arrival at Muir Glacier in June 1899, as follows:

At five o’clock we drop anchor about two miles from its front. In eighty fathoms of water (480 feet), abreast of the little cabin on the east shore built by John Muir some years ago. Not til after repeated soundings did we find bottom within reach of our anchor cables. Could the inlet have been emptied of its water for a moment we should have seen before us a palisade of ice nearly 1,000 feet higher and over two miles long.... Could we have been here many centuries ago, we should have seen, much further down the valley, a palisade of ice two or three thousand feet high. Many of these Alaska glaciers are rapidly melting and are now but the fragments of their former selves. From observations made here twenty years ago by John Muir, it is known that the position of the front of Muir Glacier at that time was about two miles below its present position, which would indicate a rate of recession of about one mile in ten years.

TABLE 4.— *Accumulation area ratios (AARs) for glaciers in Glacier Bay and environs*

[Data courtesy of Robert M. Kimmel, U.S. Geological Survey]

Glacier name	AAR
AAR Analysis from Landsat 1399–19540; 26 August 1973; Path 65, Row 19	
Grand Pacific	0.59
Konamox	.55
AAR Analysis from Landsat image 1434–19473; 30 September 1973; Path 64, Row 19	
Sea Otter	0.64
Fairweather	.52
Lituya	.64
Crillon	.70
La Perouse	.65
Finger	.66
Brady	.64
Geikie	.62
Reid-Lamplugh	.87
Johns Hopkins	.91
Margerie	.83
Ferris	.79
Grand Pacific	.72
Konamox	.61
Tenas Tikke	.76
Rendu	.85
Carroll	.87
Cushing	.80
Riggs	.83
McBride	.63
Casement	.68
Davidson	.87
Tikke	.72





**Figure 107.—A,** Map of the Glacier Bay region showing the chronology of the retreat of the Glacier Bay ice cover between 1750 and the end of the 20th century and the dates of the opening of the individual inlets. Modified from 1997 U.S. National Park Service map. **B,** Oblique orbital view of Glacier Bay and environs based on Landsat 7 ETM+ image combined with digital elevation model from the USGS National Elevation Dataset (NED). Landsat 7 ETM+ image (7059019009921350, 1 August 1999; Path 59, Row 19) is from the National Aeronautics and Space Administration. [<http://earthobservatory.nasa.gov>]



John Muir also participated in the Harriman Expedition, returning to Glacier Bay after an absence of about a decade. This was his seventh and last trip to Alaska. He commented on the differences he observed and presented a description of the changes that occurred in the bay between 1879 and 1899:

In Glacier Bay we remained nearly a week, so that we were able to note the changes which had taken place since my first visit in the fall of 1879. I then sailed around the bay, exploring all its branches and sketching the glaciers which occupied them, sailing up to their discharging fronts and landing on those which were not rendered inaccessible by the freezing together of their crowded bergs. Then (1879) there were only six berg-discharging glaciers in the bay; now (1899) there are nine...the three new ones being formed by one of the tributaries of the Hugh Miller and two of the Grand Pacific, separated from the main glacier and rendered independent by the recession of the trunks beyond their points of confluence. The Hugh Miller and Muir have receded about two miles in the last twenty years, the Grand Pacific about four and the Geike, Rendu, and Carroll perhaps from seven to ten miles. By the recession of the Grand Pacific and corresponding extension of Reid Inlet an island two and a half or three miles long, and over a thousand feet high, has been added to the landscape. Only the end of this island was visible in 1879. New islands have been born in some of the other fiords also, and some still enveloped in the glaciers show only their heads as they bide their time to take their place in the young landscape. Here, then, we have the work of glacial earth-sculpture going on before our eyes, teaching lessons so plain that he who runs may read. Evidently, all the glaciers hereabouts were no great time ago united, and with the multitude of glaciers which loaded the mountains to the south, once formed a grand continuous ice-sheet that flowed over all the island region of the coast and extended at least as far down as the Strait of Juan de Fuca (Muir, 1902, p. 127–128).

Muir also described the glacial origin of the submerged lands in southeastern Alaska that he explored:

The network of so called canals, passages, straits, channels, fiords, and so on, between the islands manifest in their forms and trends and general characteristics the same subordination to the grinding action of a continuous ice-sheet, being simply the margins of the continent eroded below the sea level and therefore covered with the ocean waters which flowed into them as the ice was melted out. And as we have seen, this action is still going on and new islands and new channels are being added to the famous archipelago. The steamer trip to the fronts of the glaciers of Glacier Bay is now from two to eight miles longer than it was only twenty years ago. That the domain of the sea is being extended over the land by the wearing away of its shores is well known, but in this region the coast rocks have been so short a time exposed to wave action that the most resistant of them are scarcely at all wasted. Even as far south as Victoria (British Columbia) the superficial glacial scoring and polish may still be seen on the hardest of the harbor rocks below the tideline. The extension hereabouts of the sea by its own action in post-glacial time is probably less than a millionth part as much as that effected by recent glacial action (Muir, 1902, p. 128–129).

[Editors' note: According to Mark F. Meier (written commun., 2004), 20th and 21st century research addresses the importance of changes in relative sea level caused by uplift of the region, the result of isostatic adjustment of the Earth's crust to loss of glacier ice (glacial rebound) and tectonic processes.]

Grand Pacific Glacier and Johns Hopkins Glacier, located in the western part of the bay, separated from each other about 1890. Each glacier independently continued to retreat for the next 35 to 40 years, and each has since fluctuated around the head of its respective inlet. Muir Inlet, Queen Inlet, Rendu Inlet, Reid Inlet, and Geikie Inlet are all side branches of the main bay. In a similar fashion, Adams Inlet, Wachusett Inlet, and the inlets in front of McBride and Riggs Glaciers are branches of Muir Inlet. Figure 107 shows the position of Glacier Bay's glaciers near the end of the 20th century. Figure 108A is a Landsat 1 MSS image of most of Glacier Bay on 12 September 1973.

Annual field observations made by the author during 1974–82, including much of the Landsat baseline period, indicate that 13 tidewater glaciers (McBride, Riggs, Muir, Carroll, Grand Pacific, Margerie, Toyatte, Johns Hopkins, Gilman, Hoonah, Kashoto, Lamplugh, and Reid Glaciers) were actively calving icebergs into Glacier Bay. Since then, the termini of several, such as Muir, Toyatte, Hoonah, and Kashoto Glaciers, have retreated above sea level. About 90 years earlier (fig. 108B), when Glacier Bay was mapped by Reid in

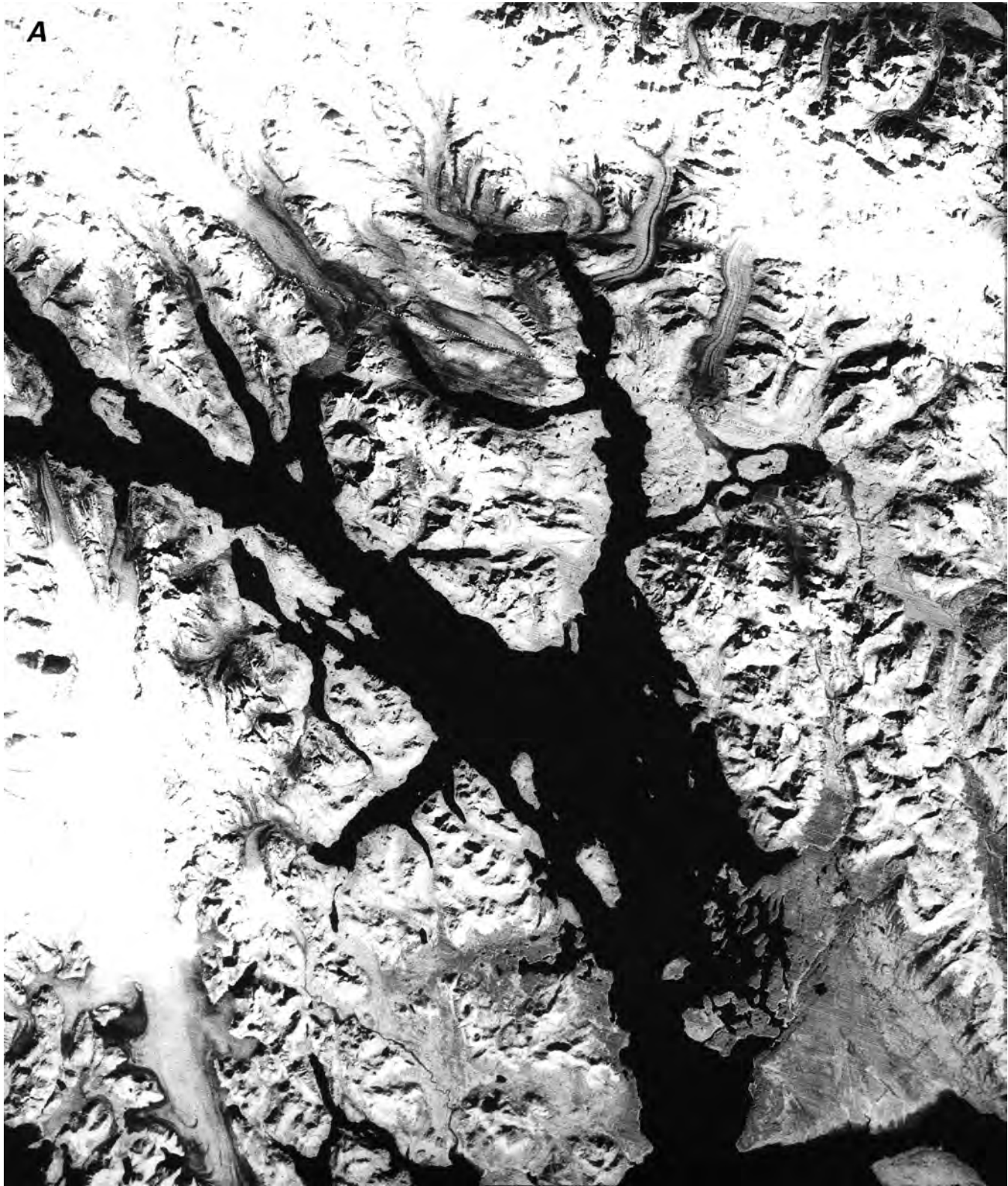


**Figure 108.**—**A**, Part of a 1973 Landsat 1 MSS image of the Glacier Bay region that covers approximately the same area as **B** (see following page).

1890 and 1892 (Reid, 1896), it had only 10 tidewater calving termini (Muir, Carroll, Rendu, Grand Pacific, Johns Hopkins, Reid, Hugh Miller, Charpentier, Geikie, and Wood Glaciers); many of today's glaciers were still part of the much larger late-19th century ice mass.

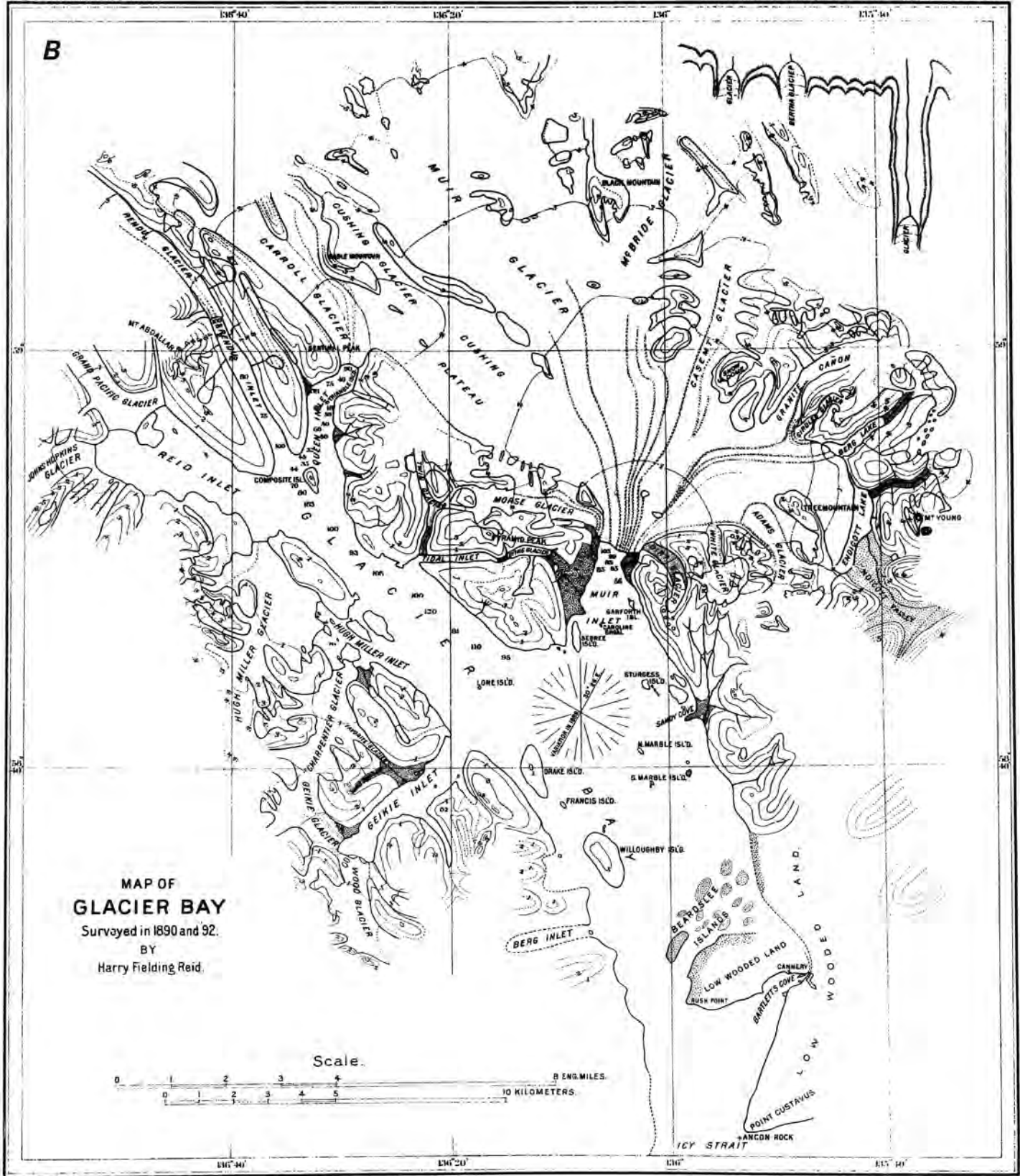


**Figure 108.—B,** Map of the Glacier Bay region made by H.F. Reid based on surveys conducted in 1890 and 1892 (Reid, 1896). At the time this map was made, recession amounted to 75 km. The present-day Muir Glacier is a small remnant of the glacier-ice cover in Glacier Bay that existed at the end of the 19th century. Major recession has affected virtually

all of the glaciers in the Glacier Bay region; however, some glaciers have readvanced. Landsat image, map, and caption courtesy of Robert M. Krimmel, U.S. Geological Survey. Landsat 1 MSS image (1416–19480, band 7; 12 September 1973; Path 64, Row 19) is from the U.S. Geological Survey, EROS Data Center, Sioux Falls, S. Dak.

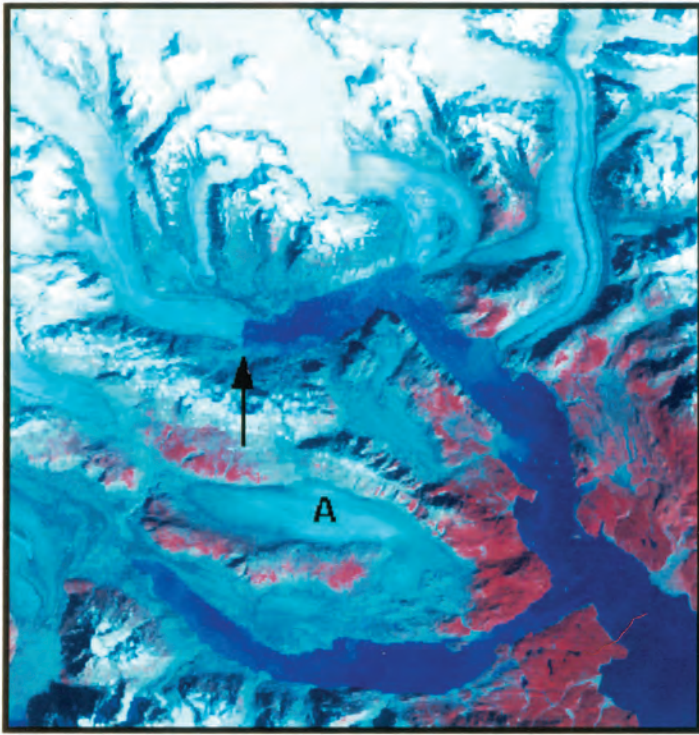
## Muir Inlet

By the early 1880s, the retreat of Muir Glacier began to expose Muir Inlet. By the early 21st century, retreat was more than 40 km. From south to north, Muir's side inlets — Adams Inlet (ca. 1905), Wachusett Inlet (ca. 1927), McBride inlet (ca. 1966), and Riggs inlet (ca. 1966) — began to appear. Field and Collins (1975) reported that, during the 82 years between 1886 and 1968, the average rate of retreat of the Muir Glacier was  $400 \text{ m a}^{-1}$ . Between 1926 and 1982, retreat totaled 30 km, and the ice thickness had decreased more than 650 m at the location of the 1982 terminus (Krimmel and Meier, 1989). By the middle 1990s, the terminus of Muir Glacier ended on land, and its length had decreased to less than 30 km.

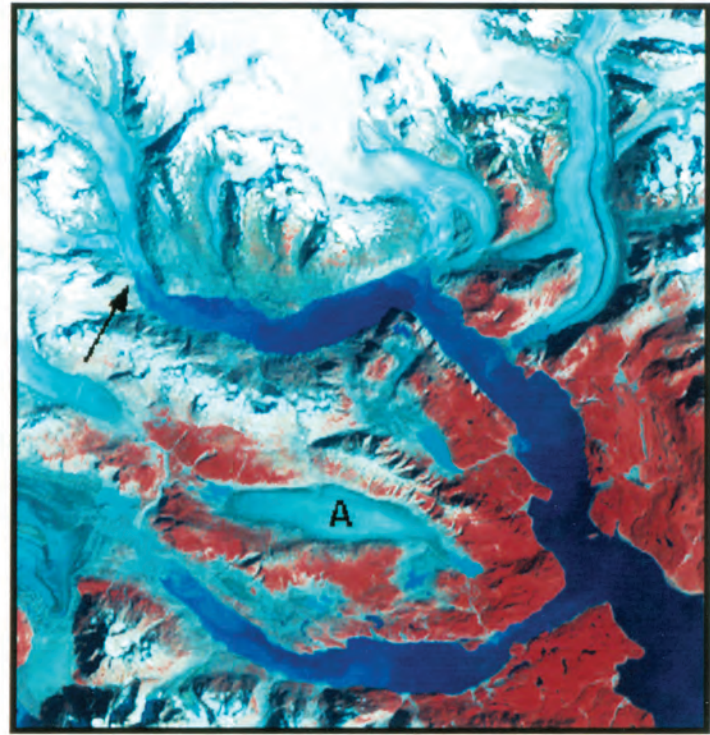
In the late 19th century, the retreat of Muir Glacier exhumed a series of "ancient buried forests," one of the most unusual and scientifically significant features of Glacier Bay. In 1890, Russell (1897) observed these forest beds being exposed by the retreat of the glacier. He presented a photograph of this deposit and reported that:

On landing on either side of the inlet, the first fact that attracts the attention of the geologist is the presence of a heavy deposit of cross-stratified sand and gravel below the extremity of the glacier. This gravel passes beneath the glacier and is plainly of more ancient date than the advance of the ice over it. In this deposit are many trunks and branches of trees; and on the west side of the inlet there are a score or more trunks of spruce trees, still standing as they grew, which have been exposed by the removal of the strata in which they were formerly buried.... The history of this deposit of sand and gravel and of the forest entombed in it is in brief as follows: The glacier was formerly not so extensive as now, having undergone a retreat after a preceding period of marked extension, and a dense forest grew at least on its sides, if not in the center, of the valley left exposed below its terminus. Coincident with the retreat of the glacier and the growth of the forest there must have been an elevation of the land which excluded the water from a portion of the inlet now submerged. While the forest was still standing, the streams from the glacier, then terminating in the valley to the north, brought down large quantities of gravel and sand and built up an alluvial cone about the extremity of the ice. As this alluvial cone, which probably ended in the sea and in fact was in part a delta, increased in size, it invaded the adjacent forest and buried the still upright trees. A subsequent advance of the glacier caused the ice to override the gravel with its entombed forest. When the glacier once more retreated the deposits were uncovered and cut away by streams flowing from the ice, so as to expose the trees buried within their mass. This last step in the history of the inlet is unfinished. The terminus of the glacier is still receding, and as the streams flowing from it are still excavating channels through the gravel, it is to be expected that additional portions of the buried forest will be uncovered....

Hall and others (1995) presented several excellent examples of how Landsat imagery has been used to document changes in Glacier Bay. Figure 109 shows a pair of Landsat multispectral scanner (MSS) images of upper Muir Inlet, acquired on 12 September 1973 and 6 September 1986 (Hall and others, 1995). In the 13 years between images, Muir Glacier retreated more than 7 km. A supervised computer classification comparison of features on this pair of MSS images indicates that the increase in vegetation cover (from 5–9 percent) and open water (from 8–9 percent) was accompanied by a loss in area of glacier ice of more than 5 percent during the 13-year period (Hall and others, 1995).



12 September 1973



6 September 1986

**Figure 109.**— The reduction in glacierized area and volume is documented by these two annotated Landsat MSS false-color composite images of upper Muir Inlet acquired on 12 September 1973 and 6 September 1986. In the 13 years between images, the terminus of Muir Glacier (marked by the arrows) retreated more than 7 km. Burroughs Glacier (A) also suffered a significant loss in area. The increase in both the density and the quantity of red surfaces (color of vegetation in false-color infrared) is another line of evidence that documents the decrease in glacier cover. Figure from Hall and others (1995). Landsat 1 MSS image (1416–19480, bands 4, 5, 7; 12 September 1973; Path 64, Row 19) and Landsat 5 MSS image (5059019008624990, bands 4, 5, 7; 6 September 1986; Path 59, Row 19) are from the U.S. Geological Survey, EROS Data Center, Sioux Falls, S. Dak.

### Adams Inlet

Adams Glacier was named by Reid (1896) for a member of his 1892 field party; the *Southeast Tributary* to Muir Glacier was also a name applied by Reid to the southeastern part of Muir Glacier. By the middle 1890s, the retreat of Adams Glacier had begun to open an inlet to the southeast of the newly forming Muir Inlet. By 1962, the inlet was more than 10 km long, and the terminus of Adams Glacier was in a side valley, about 3 km from the inlet. By 1979, Adams Glacier had retreated another 4 km, leaving a large ice-cored moraine along its former western margin (AHAP photograph L194F4179 acquired on 11 August 1979). Stagnation and retreat have continued into the 21st century.

Casement Glacier (fig. 110), which has a terminus located on the northern side of the inlet, began to separate from the retreating Muir Glacier early in the 20th century. By 1911, it had become completely separated and had retreated onto land (Field and Collins, 1975). By the middle 1960s, retreat had approached 3 km, and the terminus was surrounded by a large, pitted, ice-cored moraine. Stagnation and retreat have continued into the 21st century, with sediment-free ice occurring more than 5 km from the shore of Adams Inlet (fig. 107). Since the 1960s, Casement Glacier has received substantial attention from the glacial geology community as a natural laboratory for understanding the dynamics of ice retreat and stagnation. More than a dozen

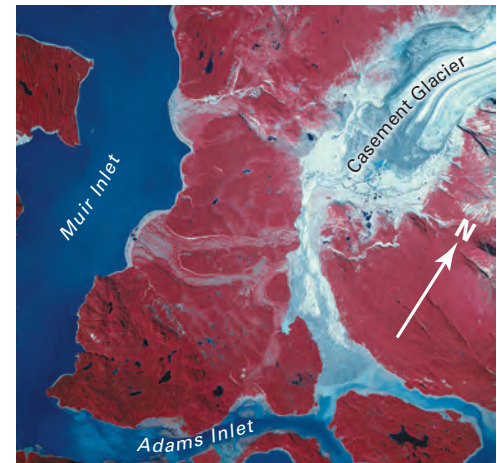


**Figure 110.**— 11 August 1979 AHAP false-color infrared vertical aerial photograph of central Adams Inlet, Glacier Bay, St. Elias Mountains, and the area to the north. The terminus of Casement Glacier is surrounded by a large pitted ice-cored moraine and a number of other ice retreat and stagnation features, including eskers, an ice-marginal lake, and a pitted outwash plain. AHAP photograph no. L194F4177 from the GeoData Center, Geophysical Institute, University of Alaska, Fairbanks, Alaska. A larger version of this figure is available online.

journal articles have documented various aspects of esker formation (Price, 1966), lake dynamics (Lindsay, 1966; Moravek, 1973), and the evolution of collapsed glacial topography (McKenzie and Goodwin, 1987).

### Wachusett Inlet

Various names have been used to describe the land area located on the western side of Muir Inlet, about 20 km north of its mouth. Reid (1896) named the area the Cushing Plateau after Henry Cushing, a professor of geology at Western Reserve University and a member of Reid's 1890 expedition. Reid called the glacier, which drained the plateau, the *Northwest Tributary* of Muir Glacier (Reid, 1892). After the visit of the Harriman Expedition in 1899, Reid's Cushing Plateau was renamed Burroughs Glacier, after John Burroughs, a naturalist who was part of the Harriman Expedition. According to Field and Collins (1975), the name Burroughs Glacier was assigned to the higher part of the Plateau Glacier in 1941. As this large ice mass has thinned and parts of it have become better defined, other names have been proposed. Reid's *Northwest Tributary* was renamed Cushing Glacier by the IBC in 1923 (IBC, 1951), and Cooper named the ice covering the Cushing Plateau as Plateau Glacier in 1937 (Cooper, 1937).

Beginning about 1915, rapid ice retreat began to expose Wachusett Inlet. Between then and about 1985, the very rapid disintegration and retreat of Plateau Glacier, its separation from Carroll and Burroughs Glaciers, and the continuing retreat of Carroll Glacier exposed Wachusett Inlet (fig. 111) (see also AHAP photograph L195F4155 acquired on 11 August 1979). At the beginning of the 21st century, Burroughs Glacier was a melting, stagnant ice mass located completely below its accumulation area (figs. 109, 112).

Plateau Glacier became independent of Muir Glacier around 1915. Between 1929 and the middle 1980s, when the last of the ice that comprised the

**Figure 111.**— 11 August 1979 AHAP false-color infrared vertical aerial photograph of upper Wachusett Inlet, Glacier Bay, St. Elias Mountains. Clearly visible are the retreating glaciers that had filled the inlets until a few years prior to the date of the photograph. Ice that originated from the pair of unnamed glaciers (in lower right corner) that descend from the north side of Mount Merriam was in contact with the retreating Plateau Glacier in 1968 (see fig. 113). The unnamed cirque glacier (A) that descends from the north side of Mount Wordie had separated several decades earlier. The terminus of Carroll Glacier is stagnant, and the margin along which Carroll and Plateau Glacier previously joined (B) shows much evidence of recent retreat. The terminus of Carroll Glacier is covered with thick debris. Stagnant-ice remnants of Plateau Glacier can be seen at several locations (C). The retreating edge of the remnant of Burroughs Glacier and the terminus of Cushing Glacier have conspicuous trimlines. The contorted moraine patterns in the terminus of Carroll Glacier indicate that it is a surging glacier. AHAP photograph no. L195F4158 from the GeoData Center, Geophysical Institute, University of Alaska, Fairbanks, Alaska.



northwestern margin of Plateau Glacier melted away from the stagnant and downwasting terminus of Carroll Glacier, Wachusett Inlet increased in length to more than 20 km. AGS Glacier Studies Map No. 64-2-G9 (Field, 1965) documents the rapid disappearance of Plateau Glacier and the exposure of Wachusett Inlet between 1916 and 1964. Figure 113, a 25 August 1968 oblique aerial photograph shows the continued retreat and location of the terminus of Plateau Glacier and the increase in open water in Wachusett Inlet between 1964 and 1988. It is based on an analysis of four aerial photographs: 29 August 1964, 25 August 1968, 5 September 1972, and 25 August 1988.



**Figure 112.**—Oblique aerial photograph of the Burroughs Glacier (fig. 109) on 12 September 1986. The stagnant ice mass is a remnant of the Muir Glacier complex of past decades which is now left with no accumulation area. The Burroughs Glacier Remnant is ablating at the rate of 5–10 m a<sup>-1</sup>. With the exception of the peaks, ridge crests, and distant ranges, all of the area in this photograph was covered by ice in 1892 when H.F. Reid (1896) mapped Glacier Bay (fig. 108B). USGS photograph no. 86-R1-253 and figure caption by Robert M. Krimmel, U.S. Geological Survey.



**Figure 113.**—Oblique aerial photograph of the rapidly retreating Plateau Glacier and the developing Wachusett Inlet, Glacier Bay, St. Elias Mountains acquired on 25 August 1968. Approximate positions of the terminus on 29 August 1964 (USGS photo no. K647-100), 5 September 1972 (USGS photo no. 72-R5-088) and 25 August 1988 (USGS photo no. 88-R1-198) are indicated. During the interval 1964 to 1988, Plateau Glacier retreated more than 5 km. USGS photograph no. 68-R2-238 by Austin Post, U.S. Geological Survey.



## Upper Muir Inlet

According to Field and Collins (1975), the location of the terminus of Muir Glacier (fig. 114) in 1968 corresponded to the location where the surface of the glacier extended 840 m above sea level in 1890. Seismic profiles showing the configuration of the walls and floor of the fjord between Muir Glacier and Riggs Glacier have been presented by Molnia (1983b, 1989b) who showed that the Muir Glacier had been grounded at 250 m below sea level, for a total thickness of about 1,100 m.

As Muir Glacier retreated, McBride Glacier became separated in 1945–46. By 28 June 1980, McBride Glacier had retreated more than 1 km from the mouth of its inlet (fig. 115). Near the beginning of the 1990s, the retreating



**Figure 114.** — 11 August 1979 AHAP false-color infrared vertical aerial photographic mosaic of upper Muir Inlet, Glacier Bay, St. Elias Mountains. The tidewater termini of McBride, Riggs, and Muir Glaciers are clearly seen. When this area was photographed, a few icebergs and very little sediment were being discharged into the inlet. The stagnant Muir Remnant (A) was detached from the retreating Muir Glacier prior to the 1960s. The north arm of McBride Glacier provided

significant quantities of ice to Riggs Glacier prior to losing contact in the early 1970s. Large lateral and medial moraines mark its recent former extent. The unnamed hanging glacier (just east of Muir Glacier) separated from the retreating Muir Glacier about 1973. AHAP photograph nos. L194F4173 and L194F4174 from the GeoData Center, Geophysical Institute, University of Alaska, Fairbanks, Alaska.



**Figure 115.**—28 June 1980 east-looking oblique aerial photograph of the retreating terminus of McBride Glacier. Its terminus displayed two semicircular calving embayments. A falling tide was drawing the bergs into Muir Inlet through a channel in a recent recessional moraine. Both sides of the glacier show significant trimlines. Photograph by Bruce F. Molnia, U.S. Geological Survey.

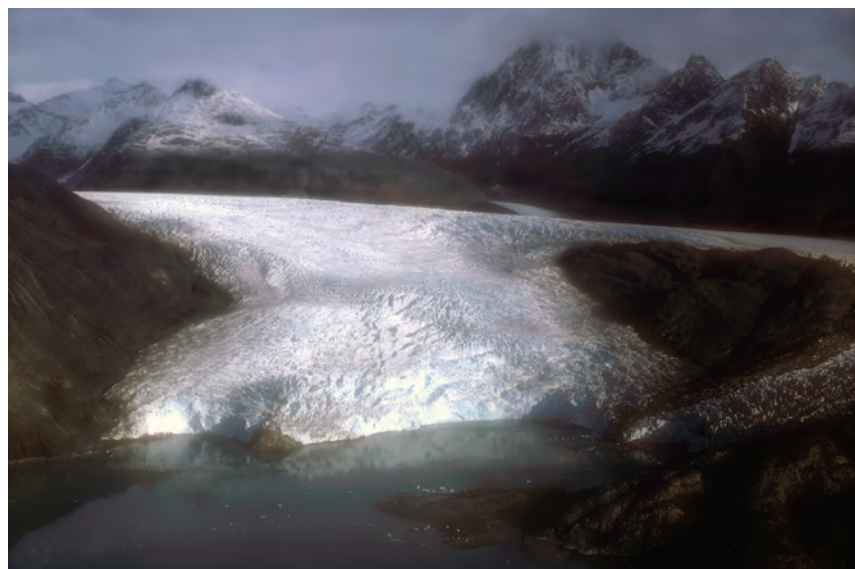


**Figure 116.**—3 October 1979 east-looking oblique aerial photograph of the terminus of Riggs Glacier. In the five years between 1974 and 1979 aerial photographs, the two northern embayments have enlarged, and a bedrock outcrop has begun to be exposed between them. The loss of stagnant ice on the south side of Riggs Glacier has led to the development of a third embayment. Photograph by Bruce F. Molnia, U.S. Geological Survey.

McBride Glacier had a length of about 24 km, a width at its face of 1.2 km, an area of 143 km<sup>2</sup>, and an AAR of 0.59 (table 2) (Viens, 1995). By 2004, McBride had retreated more than 2 km from the mouth of its inlet but continued to be an active tidewater glacier (fig. 115). The retreating Muir Glacier became independent of Riggs Glacier in 1961. During the first half of the 1960s, Muir retreated from Riggs at the rate of ~1 km a<sup>-1</sup>.

Riggs Glacier also thinned and continued to retreat into the 21st century (fig. 116). In the early 1990s, Riggs had a length of about 25 km, a width at its face of 1.5 km, an area of 126 km<sup>2</sup>, and an AAR of 0.72 (table 2) (Viens, 1995). By 2004, Riggs Glacier was about 1.3 km from the mouth of its inlet and had thinned more than 75 m, and its retreat had exposed bedrock along much of its northern margin. Sedimentation had built a delta in front of its eastern terminus.

As Muir Glacier thinned and retreated, upland ice was stranded in bedrock basins. *Muir Remnant* (fig. 117), located on the western side of Muir Inlet, is all that remained by 24 August 1963 to indicate the former majestic thickness of Muir Glacier. During the middle 1970s, the retreat rate of Muir Glacier was more than 1 km a<sup>-1</sup>. Near the beginning of the 1990s (fig. 118), Muir Glacier had decreased in length to 26.5 km. Its area was about 148 km<sup>2</sup>, the width at its face was 0.9 km, and its AAR was 0.75 (table 2) (Viens, 1995).

Muir Glacier retreated onto land in 1991. In 2004, it was continuing to thin and retreat and was more than 15 km from its former confluence with

**Figure 117.**—Oblique aerial photograph of upper Muir Inlet on 24 August 1963. Muir Glacier and Riggs Glacier are separated by about 2.5 km of open water. In the foreground is the shrinking Muir Remnant. Photograph from the U.S. Geological Survey.



**Figure 118.**—12 September 1986 oblique aerial photograph of Muir Glacier. USGS photograph no. 86-R1-263 by Robert M. Kimmel, U.S. Geological Survey.



Riggs Glacier. Not discussed here but relevant to the discussion of tidewater glacier retreat is the sediment accumulation during up-fjord and on-land retreat. Summaries of sediment accumulation in Muir Inlet and other Alaskan fiords have been presented by Molnia (1983b, 1989b).

## Queen Inlet

Carroll Glacier (fig. 111) was a tidewater glacier at the head of 11-km-long Queen Inlet when it was first observed by Reid in 1892 (Reid, 1896). At that time, water depths exceeded 185 m at its terminus. It remained a tidewater glacier until about 1920, by which time an outwash plain had developed in front of its terminus. Surges occurred in 1919 and 1943 (Field, 1964) and from 1966 to 1968 (Field, 1969). The last surge resulted in several hundred meters of terminus advance. The surge pushed ice into part of the area previously occupied by Plateau Glacier. By the mid-1970s, Carroll Glacier was only about 0.5 km from its 1890s position (AGS Glacier Studies Map No. 64-2-G4) (Field, 1965). Stagnation and very slow retreat have characterized the glacier into the 21st century (U.S. Bureau of Land Management [BLM] false-color infrared vertical aerial photograph acquired on 26 May 1997). When the author visited Carroll Glacier in both 2003 and 2004, the lower 1.5 km was covered by thick debris; its terminus had thinned by more than 100 m from its early 20th century thickness, and, where depths had previously exceeded 185 m, sedimentation had filled the upper fjord to above sea level.

## Rendu Inlet

Rendu Glacier was a tidewater glacier at the head of 16-km-long Rendu Inlet when it was first observed and named by Reid in 1892 (Reid, 1896). Since then, a large fan-delta-outwash plain has developed in front of its terminus, and the terminus position has fluctuated by as much as 2 km from its 1911 position (AGS Glacier Studies Map No. 64-2-G2) (Field, 1965). Between 1892 and 1907, the glacier retreated as much as 1.5 km. But a surge from about 1908 to 1909 resulted in the terminus advancing as much as 2.5 km, to its post-“Little Ice Age” maximum areal extent. Rendu Glacier also surged between 1926 and 1929 and in 1965–66. The latter surge resulted in the terminus advancing nearly 0.5 km (Field and Collins, 1975). Stagnation, slow retreat, and the build-up of morainic debris on the glacier’s terminus have characterized Rendu Glacier into the 21st century (fig. 119) (also BLM false-color infrared vertical aerial photographs R1–FL1–FR38 and FR40 acquired on 16 August 1996).

Romer Glacier, located on the western side of Rendu Inlet about 4 km south of Rendu Glacier, also surged during the early 20th century. In 1911, after the 1909 surge, its terminus was tidewater. Since then, it has retreated onto land, and its terminus position has fluctuated by more than 0.5 km.

## Tarr Inlet

At the beginning of the 21st century, Margerie and Grand Pacific Glaciers were located at the head of 16-km-long Tarr Inlet. In 1899, when the Harriman Expedition visited, the inlet did not exist because it was completely filled by an extended Grand Pacific Glacier. Photographs from the Harriman Expedition showing this extent are available in the USGS Photo Library collection (Gilbert 254, 255, 256). Between 1899 and 1912, Grand Pacific Glacier retreated more than 15 km, an average retreat rate of more than 1 km a<sup>-1</sup>. Soon after 1912, the retreating Grand Pacific Glacier separated from Margerie Glacier and retreated into Canada. Grand Pacific Glacier’s terminus remained in Canada until about 1948, when it slowly began to advance, reaching the U.S.-Canadian border in 1961, and advancing more than a kilometer into the United States by 11 August 1979 (fig. 120). The position of Margerie Glacier’s terminus has been fairly stable since its early 20th century retreat ended. However, as figure 121 shows, ice in its principle tributary flowed more than 8 km down glacier during a 6-year period.

In late 1989, Grand Pacific Glacier finally reconnected with Margerie Glacier, primarily because of ice contributed by Ferris Glacier and the surge of the principle tributary of Margerie Glacier. In 1989, the ice from Ferris Glacier comprised 60 percent of the width of the terminus of Grand Pacific Glacier; in 2004, it accounted for the entire width. The glaciers remained connected



**Figure 119.**— 11 August 1979 AHAP false-color infrared vertical aerial photograph of Rendu Glacier, Romer Glacier, and a number of unnamed retreating glaciers. The folded and contorted moraines on the surface of Rendu Glacier are indicative of a recent surge history. Thinning of the glacier has resulted in the development of vegetation and a well-defined trimline along the east side of the main trunk. The unnamed tributary to the left of the Rendu Glacier terminus was surging onto Rendu Glacier on the date of this photograph. Most of the small unnamed glaciers in the photograph show evidence of active thinning and retreat. AHAP photograph no. L197F4109 from the GeoData Center, Geophysical Institute, University of Alaska, Fairbanks, Alaska. A larger version of this figure is available online.

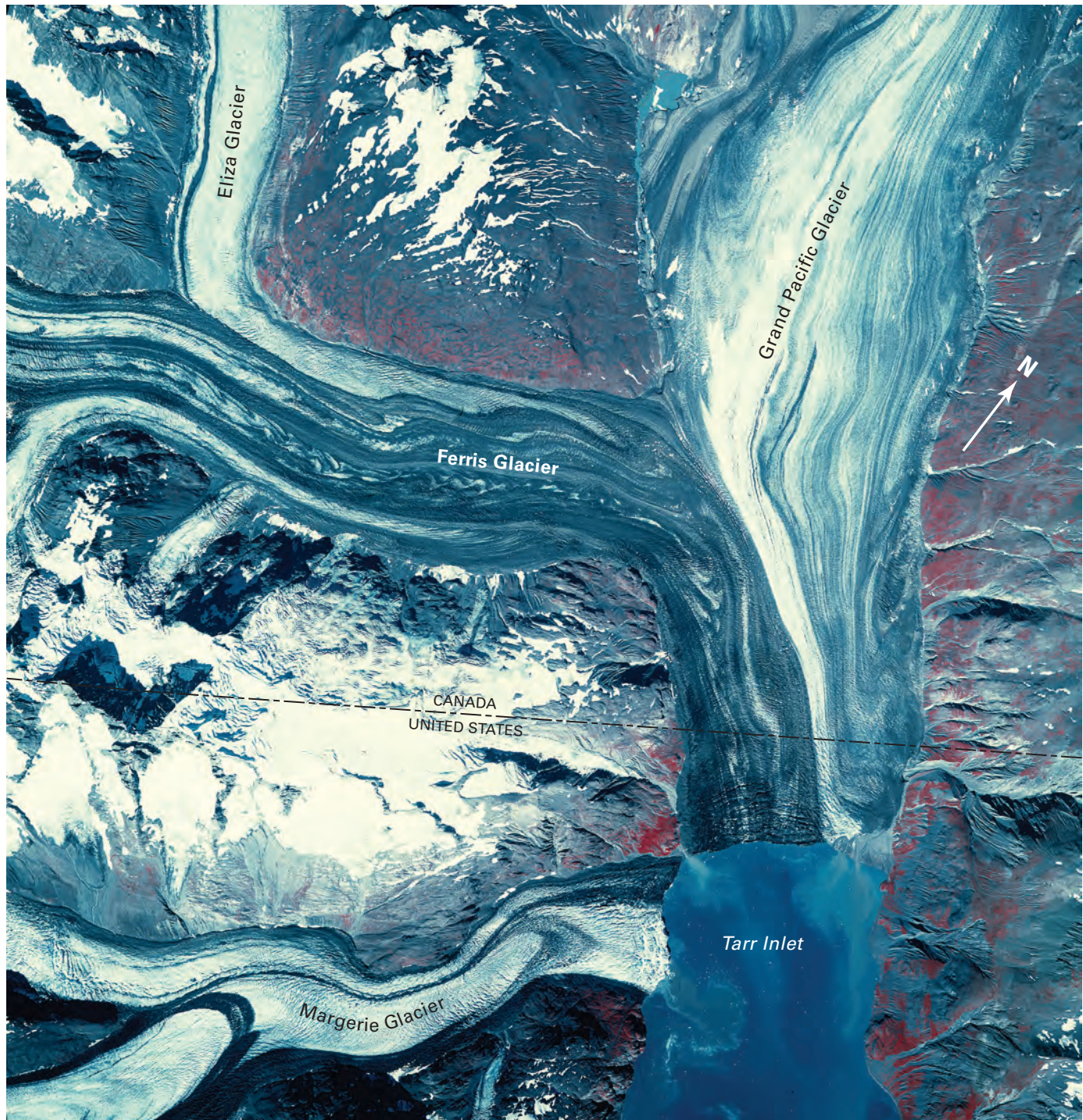
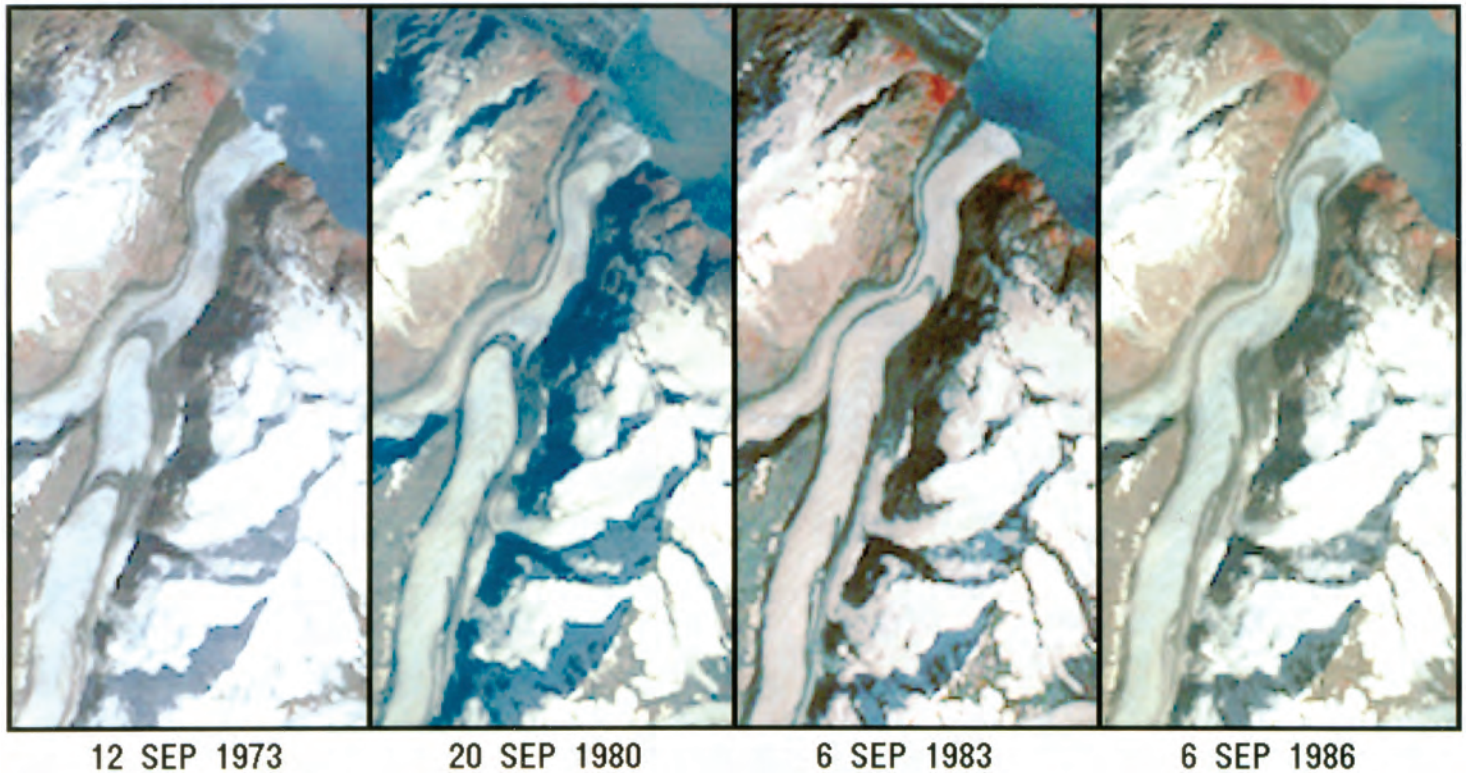


**Figure 120.**—Annotated 11 August 1979 AHAP false-color infrared vertical aerial photograph of the head of Tarr Inlet showing the position of the nearly connected termini of Margerie and Grand Pacific Glaciers. Ferris Glacier provided much of the ice to the then advancing terminus of Grand Pacific Glacier. In 1931, in comparison, Ferris Glacier had only contributed 10 percent of the ice of the terminus. AHAP photograph no. L198F4014 from the GeoData Center, Geophysical Institute, University of Alaska, Fairbanks, Alaska.

(BLM false-color infrared vertical aerial photograph R3-FL6-FR57 acquired on 26 May 1997) until the winter of 1997-98, when the melting of stagnant ice left by the retreat of the terminus of Grand Pacific Glacier resulted in the separation of the two glaciers. When the author visited Grand Pacific Glacier in 2003 and 2004, its terminus was debris covered and retreating and was located several hundred meters north of the point where the two had rejoined.

Near the beginning of the 1990s, Grand Pacific Glacier had a length of about 60 km, a width at its face of 2.7 km, an area of 654 km<sup>2</sup>, and an AAR of 0.70; Margerie Glacier had a length of about 34 km, a width at its face of 1.9 km, an area of 174 km<sup>2</sup>, and an AAR of 0.82 (table 2) (Viens, 1995). Grand Pacific Glacier had an accumulation area of 459 km<sup>2</sup> and an ablation area of

## MARGERIE GLACIER



195 km<sup>2</sup>, whereas Margerie Glacier had an accumulation area of 143 km<sup>2</sup> and an ablation area of 31 km<sup>2</sup> (table 2) (Viens, 1995).

### Johns Hopkins Inlet

At the time of Reid's 1892 visit, Johns Hopkins Inlet was completely filled with glacier ice that extended more than 10 km beyond its late 20th century position (fig. 107). This ice had been a tributary to the massive Grand Pacific Glacier, which, in 1892, covered the northern end of Russell Island and encircled it to the west. Reid applied the name Reid Inlet to the upper end of Glacier Bay southeast of Russell Island and adjacent to Grand Pacific Glacier. This name was adopted by the American Association for the Advancement of Science (AAAS) in 1893 (Orth, 1967, 1971). By 1910, as Grand Pacific Glacier continued to retreat and separate into individual glaciers, an inlet north of Russell Island began to emerge. It was named Tarr Inlet by Lawrence Martin in 1912 for Ralph Tarr, who visited the inlet in 1911. However, the name Reid Inlet continued to be applied to the inlet at the terminus of Johns Hopkins Glacier. In 1931, Cooper proposed the name Johns Hopkins Inlet for this inlet. The name was formally adopted by the BGN in 1954. The name Reid Inlet was then restricted to the inlet formed at the terminus of Reid Glacier.

Between 1892 and 1929, Johns Hopkins Glacier retreated more than 18 km and separated into several dozen individual glaciers (fig. 107). Since then, the terminus position of Johns Hopkins Glacier has experienced numerous fluctuations, but the trend has been dominated by a readvance, which continues into the early 21st century (AGS Glacier Studies Map No. 64-2-G1) (Field, 1965). Near the beginning of the 1990s, Johns Hopkins Glacier (fig. 122) had a length of about 60 km, an area of 654 km<sup>2</sup>, a width at its face of 1.7 km, and an AAR of 0.70 (table 2) (Viens, 1995). In the middle 1990s, the advance of Johns Hopkins Glacier resulted in its briefly joining with Gilman Glacier. At the beginning of the 21st century, Johns Hopkins Glacier was separated from Gilman Glacier and was located about 0.3 km up-fjord. They had rejoined

**Figure 121.**—Segments of four Landsat MSS images of Margerie Glacier, acquired between 12 September 1973 and 6 September 1986, show how a post-September 1980 surge in the principal tributary affected the terminus. Between 1973 and 1980, little change occurred. However, the unnamed tributary advanced more than 3 km between 20 September 1980 and 6 September 1983. It flowed another 5 km downglacier between 6 September 1983 and 6 September 1986. Figure from Hall and others (1995).

**Figure 122.**—Oblique aerial photograph of Johns Hopkins Glacier on 12 September 1986. Another terminus of a tidewater glacier, Gilman Glacier, is in the left foreground. USGS photograph no. 86-R2-292 by Robert M. Krimmel, U.S. Geological Survey.

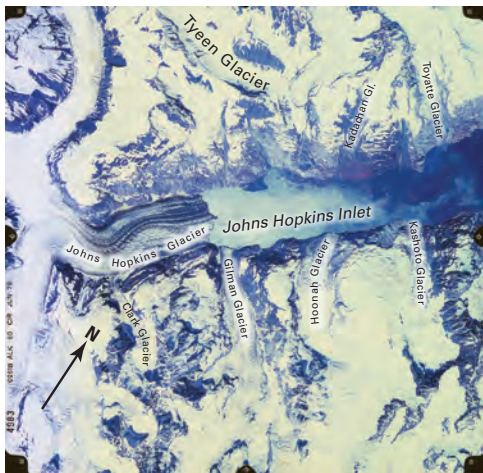


**Figure 123.**—Annotated 14 August 1978 AHAP false-color infrared vertical photograph of the head of Johns Hopkins Inlet showing the position of Johns Hopkins, Toyatte, Kashoto, Hoonah, and Gilman Glaciers and a number of named and unnamed glaciers that descend the inlet's valley walls but did not extend into tidewater, including Clark, Tyee, and Kadachan Glaciers. The fjord depth in front of Gilman Glacier is 350 m. AHAP photograph no. LXXXF4983 from the GeoData Center, Geophysical Institute, University of Alaska, Fairbanks, Alaska. A larger version of this figure is available online.

when the author observed them in late July 2002. In September 2004, the two glaciers were still in contact, although Johns Hopkins Glacier had retreated approximately 200 m from its 2002 position.

During the period of the Landsat baseline, six glaciers in Johns Hopkins Inlet reached tidewater and produced icebergs (fig. 123): Johns Hopkins, Toyatte, Kashoto, Hoonah, Gilman, and Lamplugh Glaciers. Hoonah, Kashoto, and Gilman Glaciers are hanging glaciers that descend to tidewater and are significantly smaller than the other tidewater glaciers in the inlet. Near the beginning of the 1990s, Hoonah Glacier had a length of 7 km, an area of 12 km<sup>2</sup>, a width at its face of 0.2 km, and an AAR of 0.70 (table 2) (Viens, 1995). Kashoto Glacier had a length of 5 km, an area of 5 km<sup>2</sup>, a width at its face of 0.1 km, and an AAR of 0.94 (table 2) (Viens, 1995). Gilman Glacier, the largest of the three, had a length of 12 km, an area of 35 km<sup>2</sup>, a width at its face of 0.45 km, and an AAR of 0.88 (table 2) (Viens, 1995).

Lamplugh Glacier is located just inside the mouth of Johns Hopkins Inlet on its southern side. It separated from the receding Johns Hopkins Glacier sometime before 1906 and has remained a tidewater glacier. Since 1929, its terminus has fluctuated as much as 1.5 km (AGS Glacier Studies Map No. 64-2-G5) (Field, 1965). Field and Collins (1975) reported that Lamplugh Glacier retreated 800 m between 1935 and 1941. Near the beginning of the 1990s, Lamplugh Glacier had a length of about 32 km, an area of 170 km<sup>2</sup>, a width at its face of 0.85 km, and an AAR of 0.85; its accumulation area was 145 km<sup>2</sup>, and its ablation area was 25 km<sup>2</sup> (table 2) (Viens, 1995). When the author observed its terminus in 2003 and 2004, it was more than 0.5 km forward of its 1941 position. However, fresh till located about 200 m forward of the terminus documented an even greater post-1941 advance that occurred in the late 1970s and early 1980s.

Figure 124, an 11 August 1979 AHAP photograph of the northwestern end of Glacier Bay, shows the relationship of Lamplugh Glacier, Reid Glacier and Inlet, and Johns Hopkins Inlet. A BLM photograph (no. R3-FL7-FR75) taken on 26 May 1997 shows the late-20th century location of Lamplugh Glacier.

Many other glaciers descend adjacent mountain slopes, some existing only at higher elevations (fig. 125). Some reach the inlet's walls but remain above tidewater. Named glaciers include Clark, Tyeen, Kadachan, John, Charley, and Topeka Glaciers. John and Charley Glaciers were named for Tlingit guides who helped Muir in 1879. [Editors' note: According to Mark F. Meier (written commun., 2004), some of the glaciers that flow into Johns Hopkins Inlet include some unusual surge-type glaciers noted by Field. For example, the Tyeen Glacier becomes a tidewater glacier during a surge; the surge of a tributary glacier apparently causes a surge of the main stem (see figure in Meier and Post, 1969).]

### Reid Inlet

Reid Glacier, which has a length of about 17 km, an area of 49 km<sup>2</sup>, a width at its face of 0.85 km, and an AAR of 0.64 (table 2) (Viens, 1995), sits at the head of 3-km-long Reid Inlet (fig. 124). A large terminal moraine located at the mouth of the inlet was formed during the first three decades of the 20th century. Between 1929 and 1941, the glacier retreated about 2.5 km (AGS Glacier Studies Map No. 64-2-G3) (Field, 1965). Since then, the terminus has thinned but remained nearly stationary, fluctuating within several hundred meters of its 1941 position. The growth of outwash fans along both margins of the glacier has helped to stabilize the terminus. At the end of the 20th century, a BLM photograph (no. R3-FL6-FR70), taken on 26 May 1997, shows that Reid Glacier was slowly retreating. Retreat continued in 2004.

### Hugh Miller, Charpentier, and Geikie Inlets

Located on the southwestern side of Glacier Bay, the glaciers that filled Hugh Miller, Charpentier, and Geikie Inlets separated from the receding Glacier Bay ice trunk between 1860 and 1880. Muir named the glacier and the inlet in front of it for Scottish geologist Hugh Miller in 1879. By 1892, continued retreat of Hugh Miller Glacier resulted in the formation of two separate ice masses. Reid (1896) called these Hugh Miller Glacier and Charpentier Glacier. By the time Muir revisited Hugh Miller Fiord in June 1899 (fig. 126), it had become an open inlet, as had Queen, Rendu, and Reid Inlets. Between 1892 and 1968, Hugh Miller Glacier retreated about 7 km, an average rate of nearly 100 m a<sup>-1</sup>. As it retreated, it separated from Scidmore Glacier to its north and several unnamed ice masses. By 11 August 1979, it had retreated nearly another kilometer (fig. 127). At the end of the 20th century, Hugh Miller Glacier was continuing to retreat.

Charpentier Glacier has continued to retreat since separating from Hugh Miller Glacier. By the end of the 20th century, it had retreated nearly 10 km. Favorite and Maynard Glaciers separated early in the 20th century; Favorite Glacier disappeared between 1919 and 1926.

Similarly, in 1879, Muir named Geikie Glacier for Scottish geologist James Geikie, author of *The Great Ice Age*, a book that provided Muir with some of his knowledge of glacier processes. By 1892, continued retreat of Geikie Glacier resulted in two separate ice masses. Reid (1896) called these Geikie and Wood Glaciers. Wood Glacier completely disappeared by the early 1940s. Except for a small advance around 1920 (Field and Collins, 1975), Geikie Glacier has continued to retreat since Reid observed it. It retreated above tidewater and onto land about 1911 (AGS Glacier Studies Map No. 64-2-G7) (Field, 1965). By 1968, it had retreated nearly 5 km. By 11 August 1979, it had developed an ice-marginal lake and a large lateral ice-cored stagnant moraine (fig. 127). Retreat and stagnation have continued into the 21st century.

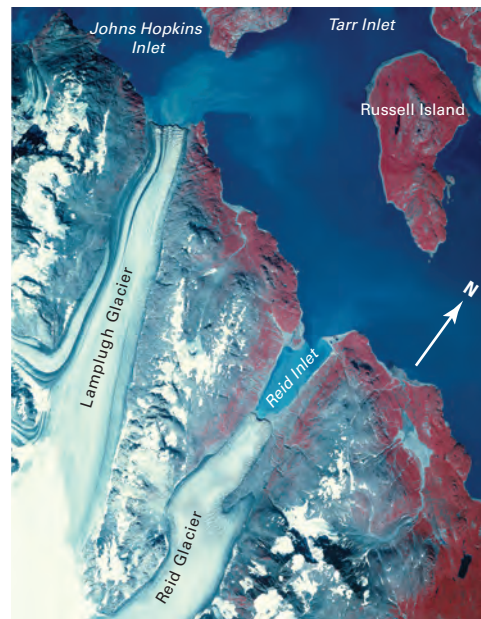


**Figure 124.**—11 August 1979 AHAP false-color infrared vertical aerial photographic mosaic of the lower reaches of Lamplugh and Reid Glaciers. Exposed vegetation-free bedrock along the lateral margins of both glaciers suggests a recent thinning of both glaciers. At the time of the photograph, Lamplugh Glacier was advancing, and Reid Glacier was retreating. AHAP photograph nos. L198F4018 and L198F4019 from the GeoData Center, Geophysical Institute, University of Alaska, Fairbanks, Alaska. A larger version of this figure is available online.



**Figure 125.**—27 July 1980 southeast-looking photograph of the summit of 2,500-m-high Mount Abbe, located adjacent to Johns Hopkins Inlet. Numerous small alpine glaciers are located on its summit and flanks, forming wherever topography permits the accumulation of snow. Most glaciers show evidence of recent thinning and retreat. Photograph by Bruce F. Molnia, U.S. Geological Survey. A larger version of this figure is available online.





**Figure 126.**—June 1899 photograph by USGS geologist Grove Karl Gilbert of part of the West Arm of Glacier Bay, taken from Hugh Miller Inlet. John Muir stands at the lower left. The main West Arm glacier terminus is located nearly 30 km to the north. Carroll Glacier, also nearly 30 km distant, is located at the head of Queen Inlet, located to the left of the photograph. USGS Photo Library photograph Gilbert 284. A larger version of this figure is available online.



**Figure 127.**—11 August 1979 AHAP false-color infrared vertical aerial photographic mosaic of the southwest side of Glacier Bay. The mosaic covers the area from Geikie Inlet to Scidmore Bay. The principal glaciers present are Geikie, Charpentier, Hugh Miller, and Aurora Glaciers. The smaller Maynard Glacier is also visible. At the beginning of the 20th century, this entire area was covered by a large ice mass, with several tidewater termini. All of the glaciers are thinning and retreating. AHAP photograph nos. L198F4022 and L198F4023 are from the GeoData Center, Geophysical Institute, University of Alaska, Fairbanks, Alaska. A larger version of this figure is available online.

## Glaciers of the Glacier Bay National Park and Preserve Region from West of Glacier Bay to the Alsek River

The Fairweather Range stretches more than 120 km along the Gulf of Alaska from Cross Sound to the Alsek River. Eight summits reach elevations exceeding 3,000 m: Mount Fairweather (4,664 m), Mount Quincy Adams (4,134 m), Mount Root (3,920 m), Mount Crillon (3,879 m), Mount Watson (3,815 m), Mount Salisbury (3,710 m), Lituya Mountain (3,635 m) and Mount La Perouse (3,270 m). A dozen large named glaciers flow from the heights of the Fairweather Range to near sea level. One, La Perouse Glacier, frequently fluctuates at the shoreline of the Pacific Ocean, and at times is the only calving glacier in Alaska that discharges icebergs directly into the Pacific Ocean.

Named Fairweather Range glaciers include Brady, Finger, La Perouse, South and North Crillon, Cascade, Lituya, Desolation, Fairweather, Sea Otter, Grand Plateau, and Alsek Glaciers. Several are small piedmont glaciers that almost reach the Pacific Ocean. From the perspective of plate tectonics, several named glaciers and a number of unnamed glaciers flow from a source area on the North American Plate into the Fairweather Fault, a trench that formed along the boundary with the Pacific Plate. Several, including La Perouse, Fairweather, and Grand Plateau Glaciers, flow across the fault and terminate on the Pacific Plate (fig. 128).



**Figure 128.**—24 August 1987 photograph of glaciers flowing into the trench of the Fairweather Fault, looking northwest at the advancing termini of Lituya and North Crillon Glaciers. Both glaciers are building large outwash plain fan deltas in front of their termini. Compare with figures 136 and 137. USGS photograph no. 87-R2-101(B) by Robert M. Krimmel, U.S. Geological Survey.

## Brady Glacier

Brady Glacier, the largest glacier in the Fairweather Range, has a length of 51 km and an area of 590 km<sup>2</sup> (table 2) (Viens, 1995); it heads in the same accumulation area as Reid and Lamplugh Glaciers. It flows southward, ending just above sea level at the head of a 6-km-long outwash-plain–tidal-delta complex (fig. 129). [Editors' note: According to Mark F. Meier (written commun., 2004), the history of the Brady Glacier represents a classic example of the termination of the slow advance phase of a tidewater glacier's instability as described by Post (1975) (see fig. 42).] When Vancouver observed Brady Glacier in 1794, it was a tidewater glacier with its terminus calving icebergs directly into the waters of Taylor Bay. During the 19th century, its terminus advanced as much as 8 km (Klotz, 1899). [Editors' note: According to Austin Post (written commun., 2004), Klotz was mistaken; a close perusal of Vancouver's report (1798) proves that the tidal terminus of Brady Glacier was near where the present-day land-ending terminus is located.] Brady Glacier began building the outwash plain that fronts and separates it from the waters of Taylor Bay in the last quarter of the 19th century (Muir, 1915). Between 1926 and 1977, the sediment plain expanded in length by more than 4 km and increased in area by more than 20 km<sup>2</sup> (Molnia, 1979) (fig. 130). In the early and middle 1970s, its terminus was stable or slowly advancing. However, by the early 1980s, it was thinning and retreating at the terminus and at many locations along its sides, resulting in the formation of many ice-marginal lakes (USGS oblique aerial photograph no. 84–R3–103 acquired on 31 August 1984). This lateral retreat was observed by Bengtson as early as 1950 (Bengtson, 1962). When the author observed the glacier in August 1999, June 2003, and June 2004, its terminus was slowly retreating. In 1999, continued lateral retreat and thinning of the ice margin resulted in the connection of previously separated North and South Trick Lakes into a single Trick Lake, located on the western margin of the glacier about 3 km from the terminus (BLM false-color infrared vertical aerial photograph nos. R7–FL13–FR207–FR209 acquired on 2 August 1999). Near the beginning of the 1990s, Brady Glacier had an AAR of 0.65, along with an accumulation area of 382 km<sup>2</sup> and an ablation area of 208 km<sup>2</sup> (table 2) (Viens, 1995).

Several distributary lobes flow from the main trunk of Brady Glacier to both the east and the west. Three west-side debris-covered lobes supply much of the flow of the Dixon River. During the Landsat baseline period, all three lobes showed significant evidence of retreat and thinning. The terminus of the southernmost of the three is surrounded by North Deception Lake, an ice-marginal lake. Retreat continued into the 21st century (BLM false-color infrared vertical aerial photograph no. R4–FR34 acquired on 26 May 1997).

Brady Glacier has received considerable attention because the Freemont Mining Company discovered abundant massive and disseminated nickel-copper sulfides in three nunataks located near the western edge of the glacier in 1958. This location, at an elevation of about 1,000 m, is about 20 km from the closest Pacific Ocean coastline at Palma Bay. Along the centerline of the glacier, the nunataks are about 30 km from the terminus. The maximum glacier thickness and the ice thickness in the area of the nunataks are not known. There are no immediate plans for mining this deposit.

A number of other unnamed glaciers originate in the mountains north of Palma Bay adjacent to the westernmost Brady Glacier lobe. Several glacier termini (fig. 129) were calving large numbers of icebergs into adjacent ice-



**Figure 129.**—Annotated 12 August 1979 AHAP false-color infrared vertical aerial photographic mosaic of the Brady Glacier, its outwash plain, and Taylor Bay. Although the terminus of Brady Glacier was advancing, numerous lateral margin lakes, such as the Trick Lakes and North Deception Lake, indicate that the glacier was thinning on its sides. Adjacent glaciers, such as the unnamed glacier (A), also showed evidence of thinning and retreat. AHAP photograph nos. L200F4575, L200F4577, and L200F4579 are from the GeoData Center, Geophysical Institute, University of Alaska, Fairbanks, Alaska.

marginal lakes when the author photographed them on 12 August 1979 and in 1997, 2003, and 2004. One of the unnamed glaciers (fig. 131) showed a conspicuous trimline. All of the glaciers show multiple signs of recent retreat. [Editors' note: According to Austin Post (written commun., 2004), the unofficially named *Palma Glacier* formed a 4-km-long proglacial lake during the period between 1970 and 2000.]



**Figure 130.**—16 September 1966 oblique aerial photograph of the advancing terminus of Brady Glacier and the developing outwash plain delta. USGS photograph no. 6610-7 by Austin Post, U.S. Geological Survey.



**Figure 131.**—12 September 1973 oblique aerial photograph of the retreating and thinning unnamed glacier located north of Palma Bay. Iceberg calving into its ice-marginal lake is a significant factor in its rapid retreat. Note the conspicuous trimline. USGS photograph no. 73-L2-120 by Austin Post, U.S. Geological Survey.

### Finger and La Perouse Glaciers

Finger and La Perouse Glaciers (fig. 132) descend from the southernmost part of the Fairweather Range to elevations at or near sea level. Since Guyot Glacier retreated at the end of the first decade of the 20th century, La Perouse Glacier was the only Alaskan glacier to discharge icebergs directly into the Pacific Ocean. Available vertical aerial photography spanning a 34-year period from 1941 to 1975 includes: (1) 1941, nine-lens, vertical aerial photograph no 58716; (2) 25 August 1948, U.S. Air Force (USAF) Southeast Alaska Project vertical aerial photograph no. SEA-138; and (3) 30 August 1975, North Pacific Aerial Surveys vertical aerial photograph no. GLA. BA. 1.76, H-19, 1-8. Along with a 12 August 1979 photograph (fig. 132), these images show that, although the eastern and western lobes of La Perouse Glacier show little change, all five lobes of Finger Glacier show conspicuous retreat. Pre-1941 retreat of three of the lobes of Finger Glacier — the western, central, and east central — created ice-marginal lakes that drain through short sloughs into the Pacific Ocean. Between 1948 and 1975, a small ice-marginal lake began to form at the margin of the eastern lobe as well.

The position of the 3.3-km-wide eastern terminus of La Perouse Glacier (fig. 133) fluctuates around the high tide line, sometimes receding so that it is reached only by storm waves (fig. 134) and sometimes advancing so that



**Figure 132.**—12 August 1979 AHAP false-color infrared vertical aerial photograph of all of the retreating lobes of the terminus of Finger Glacier and all of the terminus of the stable eastern lobe and most of the terminus of the western lobe of La Perouse Glacier. AHAP photograph no. L202F4463 from the GeoData Center, Geophysical Institute, University of Alaska, Fairbanks, Alaska.

**Figure 133.**—12 September 1986 oblique aerial photograph of the 3.3-km-wide eastern terminus of La Perouse Glacier. The glacier originates in the Fairweather Range and is the only Alaskan glacier to occasionally discharge icebergs directly into the Pacific Ocean. Photograph no. 86-R2-022 from Robert M. Krimmel, U.S. Geological Survey.



it extends beyond the surf zone into the Pacific Ocean. Photographs taken by Gilbert (fig. 66) during the Harriman expedition in 1899 show that its terminus was in the surf zone and that its northwestern margin had recently advanced into the adjacent forest. Sixty-seven years later, when it was photographed on 16 September 1966, the eastern lobe terminus extended beyond the surf zone, with a face that was more than 50 m high (fig. 135A). At that time, its small eastern distributary lobe showed evidence of significant thinning and retreat (fig. 135B). At the start of the 1990s, La Perouse Glacier had a length of about 25 km, an area of 147 km<sup>2</sup>, a width at its face of 3.3 km,

**Figure 134.**—18 June 1978 northwest-looking oblique aerial photograph of part of the eastern terminus of La Perouse Glacier. The terminus is located approximately 30 m behind the high-tide line. Photograph by Bruce F. Molnia, U.S. Geological Survey.



**Figure 135.**—Two 16 September 1966 oblique aerial photographs of the eastern lobe terminus of La Perouse Glacier. **A**, View of the eastern terminus extending beyond the surf zone, with an ice face that was more than 50 m high. USGS photograph no. 6610-65 by Austin Post, U.S. Geological Survey.

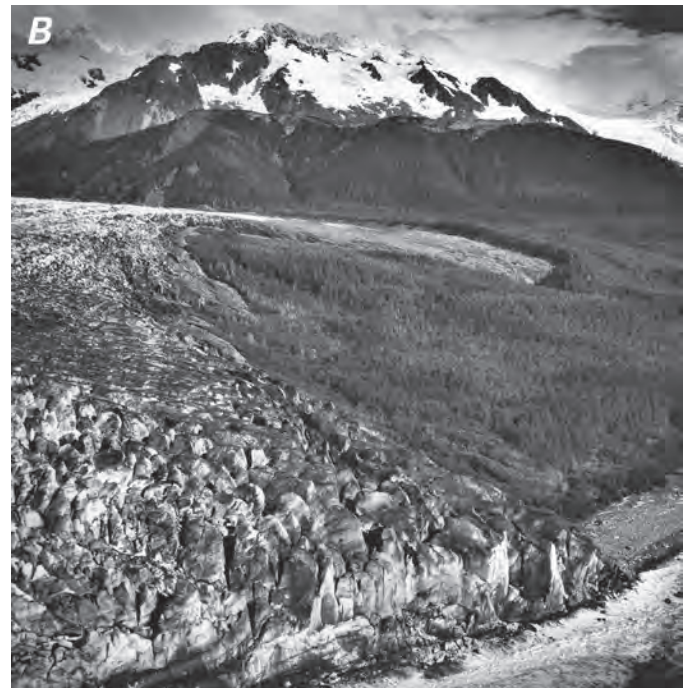


**Figure 135.**—**B**, View of the eastern edge of the extended terminus and a small eastern distributary of the lobe showing evidence of significant thinning and retreat. USGS photograph no. 6610-68 by Austin Post, U.S. Geological Survey.

and an AAR of 0.67 (table 2) (Viens, 1995). When it was observed by the author on 2 August 1999 and 18 June 2004, the terminus was located at the shoreline (BLM false-color infrared vertical aerial photograph no. 7–165).

West of La Perouse Glacier, South and North Crillon Glaciers descend from the southern flank of the Fairweather Range into the plate boundary fault trench, where their adjacent margins have coalesced (fig. 27; see also fig. 128). North Crillon Glacier flows only to the northwest, terminating in Lituya Bay. However, ice from South Crillon Glacier flows in opposite directions; one part of South Crillon Glacier flows to the southeast into Crillon Lake, and one part flows to the southwest, merging with and nearly reaching the terminus of North Crillon Glacier at Lituya Bay. Between 1929 and 1961, South Crillon Glacier advanced more than 300 m into Crillon Lake. Since then, its terminus has fluctuated. When it was observed on 25 June 1998, South Crillon Glacier terminated in the lake but showed no evidence of recent iceberg calving (BLM false-color infrared vertical aerial photograph no. R6–FL19–FR184). In 2003 and 2004, it was advancing and displacing trees along its margins. Goldthwait and others (1963) presented a summary of the Holocene and Pleistocene histories of the Crillon Glaciers.

### Glaciers of Lituya Bay

Lituya Bay, a 15-km-long T-shaped fjord, contains three named glaciers—North Crillon Glacier, Cascade Glacier, and Lituya Glacier—all of which were tidewater at various times during the 20th century (fig. 136). A large terminal moraine at the mouth of the bay and tree-covered stagnant glacier ice located on the western side of the bay are evidence that an expanded glacier filled the fjord during the “Little Ice Age” (Goldthwait and others, 1963). In 1786, when the bay was first mapped by La Pérouse (fig. 9A), it was T shaped, and five glaciers were present. Each glacier in the approximately 10 km-long top of the T, (a segment of the Fairweather Fault) terminated at or near tidewater, a pair in each of the upper ends of the T and one at the head of the fjord. Lituya Glacier, named by J.B. Mertie in 1917 (Orth, 1967, 1971, p. 589), is the westernmost of the five glaciers and descends from the Fairweather Range into Desolation Valley, flowing in both directions; the southeastward-flowing

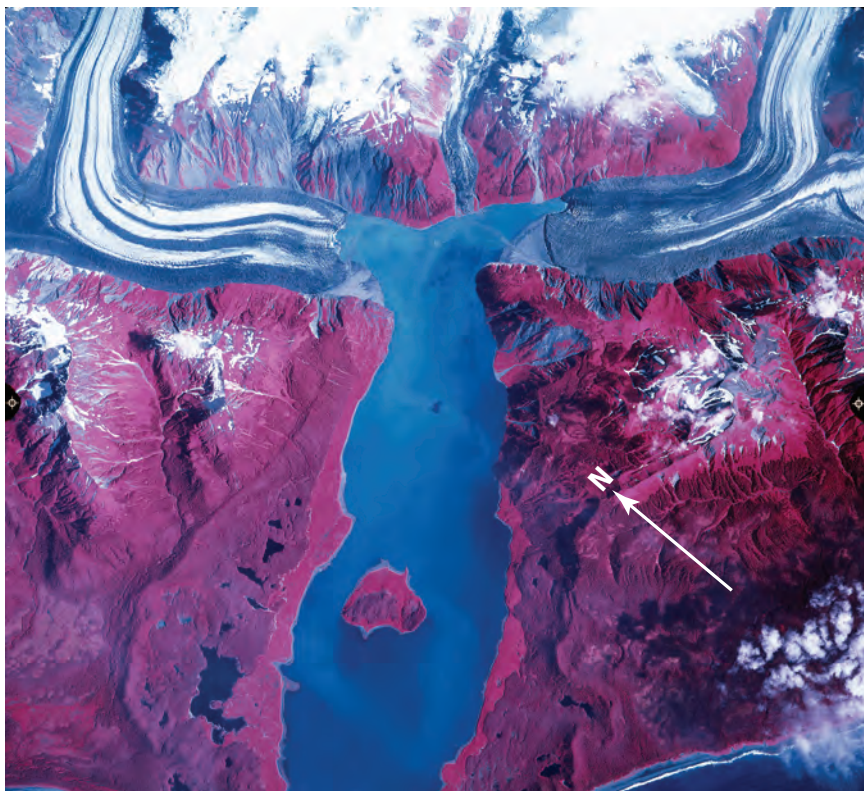


**Figure 136.**—12 August 1979 AHAP false-color infrared vertical aerial photograph of most of Lituya Bay, showing the positions of the then advancing tidewater North Crillon (right) and Lituya Glaciers (left) and the relatively stable terminus of the smaller Cascade Glacier (center). AHAP photograph no. L202F4459 from the GeoData Center, Geophysical Institute, University of Alaska, Fairbanks, Alaska.

**Figure 137.**—2 August 1999 false-color infrared vertical aerial photograph of the head of Lituya Bay showing the positions of North Crillon, Cascade, and Lituya Glaciers. Compare with figure 136. Photograph no. 7-144 is from the U.S. Bureau of Land Management.



lobe ends in Lituya Bay. Nothing was known about the northwestward-flowing lobe until the 1929 USGS-USN Aerial Photographic Expedition, when it was first observed. At that time, it was part of a large ice mass that filled the fault trench. Between the observations of La Pérouse in 1786 and the visits by Klotz in 1894, the Canadian International Boundary Survey in 1895 (USGS Photo Library Gilbert 178 photograph), the Harriman Expedition in 1899, and USGS geologist John Mertie in 1917 (USGS Photo Library Mertie 624 photograph), the tidewater termini of North Crillon Glacier advanced about 3 km into the shortening eastern arm of the T, and Lituya Glacier, located in the shortening western arm, advanced about 5 km into Gilbert Inlet. Both continued to advance through the early 21st century, moving forward about another kilometer and building outwash fan-deltas around each of their termini (fig. 137).

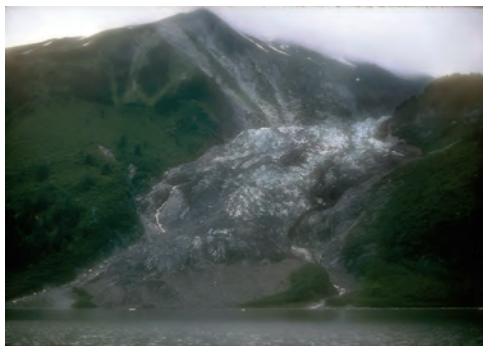


**Figure 138.**—18 July 1979 photograph of the debris-covered, stagnant-ice terminus of Cascade Glacier from Gilbert Inlet. During the last two decades of the 20th century, the terminus of Cascade Glacier has fluctuated by as much as 50 m. Photograph by Bruce F. Molnia, U.S. Geological Survey. A larger version of this figure is available online.

According to Field and Collins (1975), the rate of advance of North Crillon Glacier over its sediment plain between 1926 and 1961 was about twice that of the tidal front — 650 m as opposed to 375 m. During the period of the Landsat baseline, the glacier was slowly advancing. Near the beginning of the 1990s, North Crillon Glacier had a length of about 20 km, an area of 71 km<sup>2</sup>, a width at its face of 500 m, and an AAR of 0.81 (table 2) (Viens, 1995). When it was photographed on 25 June 1998 and 2 August 1999 and observed in June 2003 and June 2004, North Crillon Glacier was fronted by a large outwash plain. With the exception of a small section on its northern side, which was connected to Lituya Bay by a very narrow embayment, its terminus was no longer tidal (fig. 137).

Cascade Glacier, located at the apex of the bay, is a hanging glacier that descends from an elevation above 2,000 m to near sea level. Since it was first photographed by Klotz in 1894, its terminus position has fluctuated within several hundred meters of sea level (fig. 138). Cascade Glacier was named *Glacier du Milieu* by La Pérouse. When it was photographed on 2 August

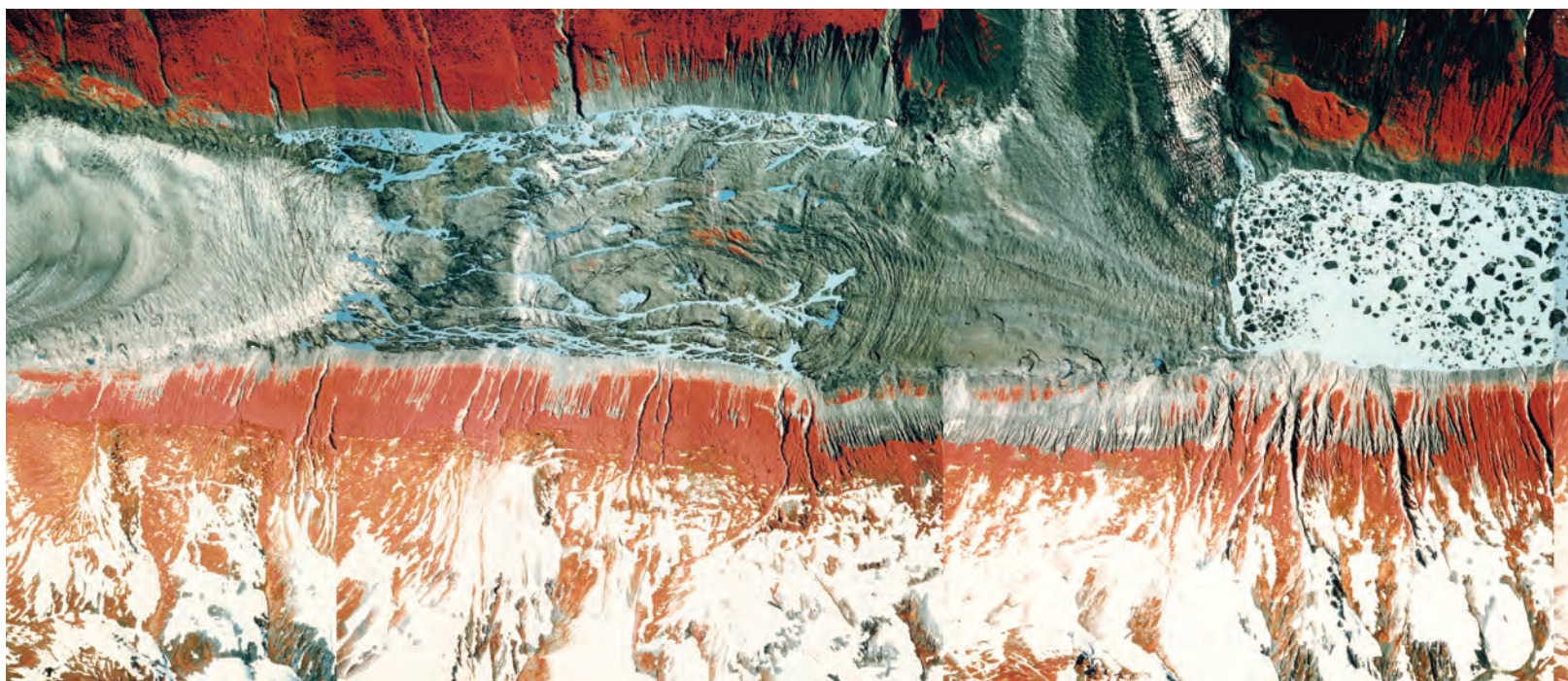
1999 and observed in June 2003 and June 2004, the terminus of Cascade Glacier was more than 100 m above sea level (fig. 137).

Between 1895 and 1958, the eastern terminus of Lituya Glacier advanced 915 m on its northeastern side and 335 m on its southwestern side (Field and Collins, 1975). During the period of the Landsat baseline and when photographed in 1987, it was advancing (figs. 128, 136). When it was photographed on 25 June 1998 (fig. 139) and 2 August 1999 (fig. 137) and observed in June 2003 and June 2004, Lituya Glacier was continuing to advance but no longer had a tidewater terminus. Its entire eastern terminus was surrounded by an outwash-plain-fan delta on 2 August 1999 (fig. 137). Lituya Glacier has a length of about 21 km, an area of 103 km<sup>2</sup>, a width at its face of 700 m, and an AAR of 0.76 (table 2) (Viens, 1995).

An earthquake on 9 July 1958 triggered a 10<sup>6</sup> m<sup>3</sup> rockslide that fell into Gilbert Inlet of Lituya Bay and onto the terminus of Lituya Glacier. Significant shoaling occurred in part of Lituya Bay but the impact on the glaciers varied widely (Miller, 1960). North Crillon Glacier on the opposite end of the bay was not impacted. However, a wave created by the rockslide eroded moraine from the lowest 100 m of Cascade Glacier, and the newly exposed ice rapidly melted away. About 350 m of the Lituya Bay tidewater terminus of Lituya Glacier was almost instantly removed. [Editors' note: According to Mark F. Meier (written commun., 2004), the amplitude of the wave generated may have been the largest ever observed and documented in historic time. The wave runup on the mountainside exceeded 300 m; it lifted a fishing vessel up and over the forested La Chaussee Spit.] [Editors' note: In a review article on the global history of tsunamis (*The Washington Post*, 9 January 2005, p. B2), four tsunamis were described in Alaska. The 1958 earthquake triggered an "avalanche in Lituya Bay...created the highest waves in recorded history; trees were stripped to a height of 1,720 ft (525 m)."]

When it was photographed on 25 June 1998 (fig. 139), the northwest-flowing lobe of Lituya Glacier had a slowly advancing, free-standing, iceberg-calving margin. When it was observed in June 2003 and June 2004, it was actively retreating. Through the last third of the 20th century, melting of a large quantity of the ice in the Fairweather trench between Lituya Glacier and Desolation Glacier resulted in the development of Desolation Lake, a 5-km-long lake that fronts western Lituya Glacier. Formed by the

**Figure 139.**—25 June 1998 false-color infrared vertical aerial photographic mosaic of the then slowly advancing west lobe of Lituya Glacier (on the right), the truncated eastern terminus of Desolation Glacier (top center), and the newly developed proglacial (ice-marginal) Desolation Lake in between. Desolation Lake has formed as the result of late-20th-century stagnation and retreat of the eastern lobe of Desolation Glacier. Also visible are the stagnant western lobe of Desolation Glacier and the stagnant eastern lobe of Fairweather Glacier (left). A number of interconnected ice-marginal lakes are forming at their junction. Photographs nos. GLBA Coastal R6-FL19-FR 169, 170, 172, and 174 are from the U.S. Bureau of Land Management.





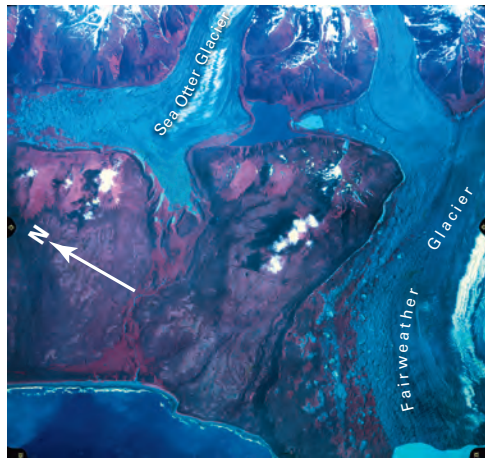


**Figure 140.**—12 August 1979 AHAP false-color infrared vertical aerial photograph of part of the terminus region of Fairweather Glacier and much of the eastern terminus of Sea Otter Glacier. The blue-water lake located between the unnamed western glacier distributary of Fairweather Glacier and the eastern distributary of Sea Otter Glacier, northwest of Fairweather Glacier, has massive lateral moraines at its eastern and western shorelines. The southwestern terminus of Sea Otter Glacier contains stagnant ice and shows the development of a small ice-marginal lake. AHAP photograph no. L202F4454 from the GeoData Center, Geophysical Institute, University of Alaska, Fairbanks, Alaska. A larger version of this figure is available online.



rapid retreat of the eastern lobe of Desolation Glacier (fig. 139), the lake began when two linear ice-marginal lakes formed along the walls of Desolation Valley, the name given to the Fairweather Fault trench in this local area. By 1979, each of the parallel lakes was about  $3.5 \times 0.5$  km (USGS Mount Fairweather 1981 1:250,000-scale map) (appendix A). Between 1979 and 1998, more than  $1.75$  km<sup>2</sup> of ice melted to form the new lake (fig. 139).

### Fairweather and Sea Otter Glaciers

Thirty-three-kilometer-long Fairweather Glacier has an area of about 260 km<sup>2</sup> (Field and Collins, 1975, p. 256) and originates high on the flanks of Mount Fairweather, Mount Quincy Adams, Mount Salisbury, and Lituya Mountain. Field and Collins (1975) reported that the glacier extended about 4 km beyond the former coast sometime in the recent past (probably late “Little Ice Age”). When it was first photographed in 1929, it exhibited a number of signs of retreat, including the development of a large ice-marginal lake that continues to enlarge (fig. 140). The retreat of Fairweather Glacier has continued through the early 21st century (figs. 31, 139) (also North Pacific Aerial Surveys, Inc., vertical aerial photograph GLA.BA., 1:76, H-9, 1-16 acquired on 30 August 1975). Large areas of tree-covered stagnant ice surround the expanding lake.

Sea Otter Glacier (fig. 140), with a length of 19 km and an area of 65 km<sup>2</sup> (Field and Collins, 1975, p. 257), flows into Desolation Valley. It has three separate termini. One flowing to the southeast ends in the expanding ice-marginal lake; one that extends to the southwest flows into the coastal forest; and the largest one to the northwest flows toward Grand Plateau Glacier. All show multiple evidence of recent thinning, stagnation, or retreat. Small unnamed tributary glaciers located between Lituya and Fairweather Glaciers, on the northern side of Desolation Valley, show minor evidence of thinning or retreat.

### Grand Plateau Glacier

Fifty-kilometer-long Grand Plateau Glacier, with an area of 459 km<sup>2</sup> (Field and Collins, 1975, p. 257), originates on the flanks of Mount Fairweather and several other adjacent peaks (NASA space shuttle photograph no. STS-028-097-085 acquired on 3 August 1989 and AHAP false-color infrared vertical aerial photograph no. L171F4972 acquired on 21 June 1978). The glacier has been retreating and thinning through the early 21st century. Its “Little Ice Age” maximum position — at the Gulf of Alaska coastline — was at least 2 km south of its 1906–08 terminus position. At the time it was mapped by the IBC, the terminus of Grand Plateau Glacier was in contact with a large arcuate recessional moraine. By 1941, at least five ice-marginal lakes had developed, the largest being more than 2 km wide. By 1966, the entire southern margin of the glacier was surrounded by a single ice-marginal lake, formed by the enlargement of the original individual lakes. The lake, which was  $7 \times 5$  km in 1975, continued to enlarge through the early 21st century as the glacier calved icebergs, thinned, and retreated (1941 photograph no. 58752 and North Pacific Aerial Surveys, Inc., vertical aerial photograph no. YAKT, 1:76, H-19, 9A-8 acquired on 30 August 1975). Grand Plateau Glacier was one of several experimental test sites for the USGS side-looking airborne radar (SLAR) Program in the late 1980s and was imaged in 1988 with digital X-band radar at frequencies between 8.0 and 12.0 GHz (fig. 141).

### Alsek Glacier

It is uncertain where the terminus of the Alsek Glacier was located when it was first observed in 1894. Field and Collins (1975) stated that members of the Canadian Boundary Survey depicted the terminus fronted by an outwash plain and located from 2.8 to 7.0 km from the Alsek River. In 1906, the glacier was combined with a northwest-flowing distributary of Grand Plateau Glacier and formed the eastern bank of the Alsek River for a distance

of about 6 km (Blackwelder, 1907). The glacier was anchored to a nunatak (Gateway Knob) and had an iceface that was as much as 50 m high. The 320-m-wide river flowed on the western side of Gateway Knob. By 1948, the glacier had retreated 1.5 to 2.5 km. By 25 August 1960 (fig. 142), retreat was as much as 5 km. By 12 August 1978, the retreating and thinning glacier was about to separate into two ice tongues (fig. 143). In the late 1990s, as interpreted on BLM vertical aerial photographs, maximum retreat exceeded 8 km; the retreating terminus, which was separated from the northwest-

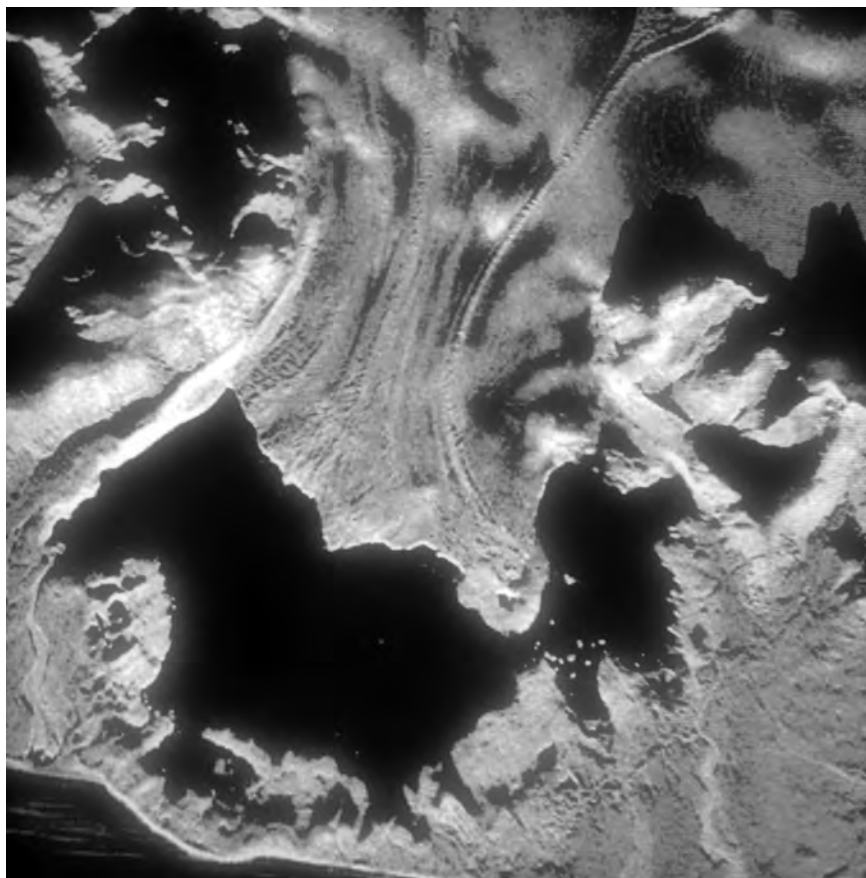


**Figure 141.**—1988 digital X-band (8.0–12.0 GHz) radar image of the terminus of Grand Plateau Glacier. The radar image, which has a picture element (pixel) resolution of about 10 m, documents 1 to 3 km of retreat in comparison with a 21 June 1978 AHAP false-color infrared, vertical aerial photograph no. L171F4972 (not shown; archived at the GeoData Center, Geophysical Institute, University of Alaska, Fairbanks, Alaska).



**Figure 142.**—25 August 1960 east-looking oblique aerial photograph of the retreating, thinning terminus of Alsek Glacier. Note the conspicuous elevated lateral moraine and trimline. USGS photograph no. 60–12 by Austin Post, U.S. Geological Survey.

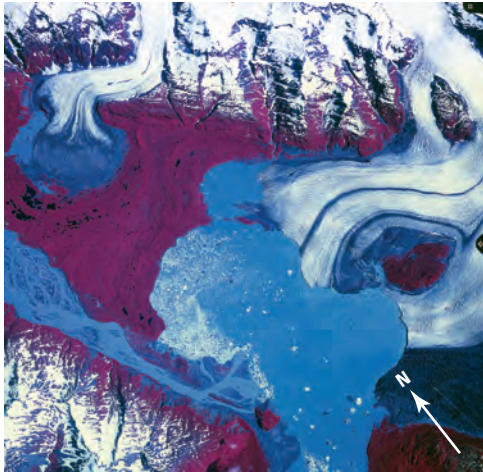


**Figure 143.**—12 August 1978 AHAP false-color infrared vertical aerial photograph of the retreating, thinning terminus of Alsek Glacier. The stagnating margin is on the verge of separating into two ice tongues. AHAP photograph no. L186F4898 is from the GeoData Center, Geophysical Institute, University of Alaska, Fairbanks, Alaska. A larger version of this figure is available online.

flowing distributary of Grand Plateau Glacier, had separated into two distinct ice tongues. By 2003, the terminus separated into three distinct ice tongues. At the beginning of the 21st century, Gateway Knob was an isolated rock outlier, with the river flowing to its east. The closest part of Alsek Glacier was more than 6 km to the east.

All of the other unnamed glaciers on the eastern side of the Alsek River, north of Alsek Glacier, are also retreating. Several have developed nested ice-marginal lakes.

### **South-central St. Elias Mountains Segment: From the Western Side of the Alsek River to the Western Side of Yakutat Bay**

Landsat MSS images that cover the south-central St. Elias Mountains, from the western side of the Alsek River to the western side of Yakutat Bay, have the following Path/Row coordinates: 64/19, 65/18, 66/18, and 67/18 (fig. 144). These areas are mapped on the USGS Yakutat, Alaska-Canada and Mount St. Elias, Alaska-Canada 1:250,000-scale topographic maps (appendix A). Glaciers of this region are located in a 55- to 100-km-wide band bounded on the south by the Gulf of Alaska and on the north by the U.S.-Canadian border. Many of these glaciers originate in Canada and flow into Alaska, including the largest, Hubbard Glacier.

At the start of the 20th century, most of the glaciers in this region were retreating. In 1906, Blackwelder (1907) examined the glaciers on the Alaskan coast between the Alsek River and Yakutat Bay. He concluded that “The fact that each of the glaciers examined is bordered at its end by a terminal moraine, which is separated from the ice itself by a barren space indicates that the lobes have recently retreated through distances varying from one quarter of a mile to one mile.... It is obvious at least that none of these glaciers is now actively forwarding its lower end. In no case did we find glaciers plowing up forested moraines and showing other unmistakable signs of advance” (Blackwelder, 1907, p. 433).

Novatak Glacier and a large unnamed south-flowing glacier to the east were connected when they were mapped in 1906 and 1908 by the IBC (1952). By 1934, when they were photographed by Washburn, the two glaciers were minimally in contact. By the 1950s, they were nearly a kilometer apart (Field and Collins, 1975). In August 1999, they were separated by more than 5 km.

Numerous retreating glaciers descend from the ridge line of the Brabazon Range. Fassett Glacier, with a length of about 16 km and an area of about 58 km<sup>2</sup> (Field and Collins, 1975, p. 265) forms the northern side of Tanis Lake. The 1894–95 Alaska Boundary Tribunal Survey (IBC, 1952) shows no lake. By the 1906 survey, a small lake was developing between the late 19th century end moraine and the ice margin. By 1948, the date of a 1:63,360-scale USGS topographic map (Yakutat B2), the lake was 1.5 km long. A 1968 USGS photograph shows that the lake had lengthened to about 3 km.

In the late 19th century, Rodman and Chamberlain Glaciers were two separate distributary tongues of the same glacier. At the end of the 19th century, Chamberlain Glacier had a terminus that descended more than 300 m from its source plateau to reach the level of the Yakutat Foreland. By 1906, continuing retreat had begun to expose an ice-marginal lake, Akwe Lake. Before 1950, the retreating and thinning terminus of Chamberlain Glacier was well above the 3-km-long lake basin and back up to the level of the plateau. This significant shrinkage has continued into the 21st century. Like Chamberlain Glacier, the retreat of the terminus of Rodman Glacier created Ustay Lake, an ice-marginal lake in the early 20th century. In the early 21st century, the glacier was still in contact with the lake (Ustay Lake), which had a length of more than 3 km.

Yakutat Glacier has a length of 29 km (Field and Collins, 1975, p. 265), an area estimated by the author at 150 km<sup>2</sup>, and a width at its face of 6 km.

Since the beginning of the 20th century, Yakutat Glacier, like its eastern neighbors Fassett and Rodman Glaciers, has developed a large ice-marginal lake (fig. 145). From 1906 to 1980, retreat of Yakutat Glacier resulted in Harlequin Lake growing to a size of 11.5×8.5 km. By the end of the 20th century, continuing retreat of the glacier resulted in the lake's length increasing an additional 5 km.

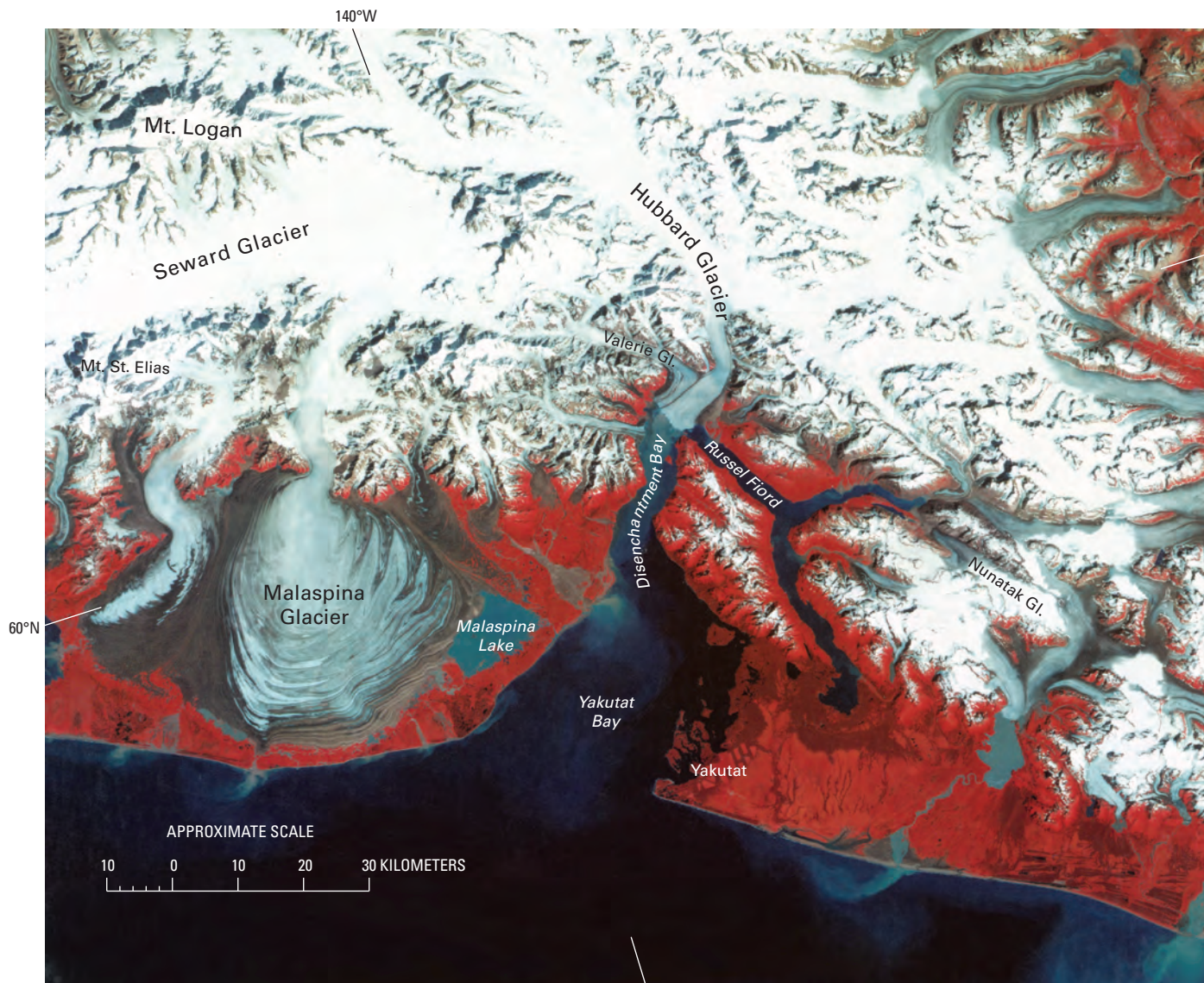


**Figure 144.**—Annotated Landsat 2 MSS false-color composite image of the western St. Elias Mountains. The region has numerous very active glaciers. The Seward Glacier, nourished in part from the upper slopes of Mount Logan (5,951 m), is part of the accumulation zone for the Malaspina Glacier. The folded moraines of Malaspina Glacier (piedmont outlet glacier) are due to differential flow related to surging. Malaspina Lake had been increasing in size, but a 1986–87

surge of the glacier resulted in a loss of two-thirds of the area of the lake. Moraines from advances of the Hubbard Glacier (tidewater glacier) and Nunatak Glacier several centuries ago are evident near Yakutat. Landsat 2 MSS image (21675–19482, bands 4, 5, 7; 24 August 1979; Path 67, Row 18) from the U.S. Geological Survey, EROS Data Center, Sioux Falls, S.Dak. Landsat image and caption courtesy of Robert M. Krimmel, U.S. Geological Survey.

**Figure 145.**—Oblique aerial photograph of Harlequin Lake and the terminus of Yakutat Glacier on 12 September 1986. An ice isthmus connects the glacier terminus to a bedrock peninsula extending into Harlequin Lake. Calving into a lake, this glacier is dynamically similar to a tidewater glacier. The calving rate is lower where the glacier ends in shallow water. Calving is more rapid in the deeper water. Most of the accumulation area of Yakutat Glacier is less than 700 m in elevation and in most years is below the snow line; thus this glacier is undernourished. The combination of rapid calving and a lack of significant ice input suggests that this glacier will continue to retreat. USGS photograph no. 86-R2-091 by Robert M. Krimmel, U.S. Geological Survey. Caption courtesy of Robert M. Krimmel, U.S. Geological Survey.



### **Glaciers of the Eastern Yakutat Bay Region**

Triangular-shaped Yakutat Bay, located on the eastern side of Malaspina Glacier, is about 45 km long and as much as 27 km wide (figs. 53, 144). To the east, Nunatak Fiord joins Russell Fiord, which then enters Disenchantment Bay, the narrow northern neck of upper Yakutat Bay. Early voyages of exploration in search of a Northwest Passage and early climbing and scientific expeditions focused a great deal of attention on the glaciers of the Yakutat Bay region (for example, Russell, 1892, 1894, 1897; Gilbert, 1904; Tarr, 1907; Tarr and Martin, 1906, 1914). This region has a history of advancing glaciers that have blocked tributary fjords and is also well known for its surge-type glaciers. Butler, Art Lewis, and West Nunatak Glaciers (located on the shore of Nunatak Fiord), Hidden Glacier (located between Russell and Nunatak Fiords), Variegated Glacier (at the junction of Disenchantment Bay and Russell Fiord), and Turner Glacier (on the western side of Disenchantment Bay), as well as several other unnamed glaciers in the Yakutat Bay region, have known surge histories (Post, 1969). Interestingly, Variegated and Butler Glaciers both surge, whereas Orange Glacier, located between them, does not.

#### **Southern Russell Fiord**

Southern Russell Fiord has a size and geometry similar to the combined geometry of Yakutat Glacier and Harlequin Lake to the east. The major difference is that Russell Fiord has been deglaciated for several centuries. Fourth Glacier and several unnamed glaciers drain into southern Russell Fiord from the east. All show recent evidences of retreat and thinning.

Fourth Glacier was retreating when Tarr saw it in 1909 (Tarr and Martin, 1914). By the early 1960s, a Y-shaped 3-km-long ice-marginal lake had developed at its terminus. By the end of the 20th century, continuing retreat of the glacier has left the terminus significantly above lake level. The glacier's name was derived from its being the fourth glacier that prospectors tried to traverse to reach the Alsek River gold fields in the late 1890s (Orth, 1967, 1971).



### Hidden Glacier

In 1891, when Russell (1894) observed Hidden Glacier, in June 1899 when the Harriman Expedition visited (fig. 146) (Gilbert, 1904), and in 1905 and 1906 when Tarr visited (Tarr and Martin, 1914), Hidden Glacier was actively retreating, at a rate of about  $50 \text{ m a}^{-1}$ . However, in the 3-year period between Tarr's 1906 visit and 1909, Hidden Glacier advanced 3.2 km. Following the 1909 surge, rapid retreat resumed. Field and Collins (1975) reported that, in the 61 years between 1909 and 1970 (fig. 147), Hidden Glacier retreated 6.4 km. When the author observed it in 1974 and again in 1992, it showed evidence of continued retreat.

### Nunatak Fjord

When Russell visited Nunatak Glacier in 1891, it sat at the head of 15-km-long Nunatak Fjord (fig. 148). It was photographed by Brabazon in 1895 and by Gilbert in 1899. Positions of the glacier's terminus between 1895 and 1909 are shown on three maps prepared by Tarr and Martin, (1914, pl. LXIX, ff p. 160). Between 1895 and 1909, Nunatak Glacier retreated about 4.0 km; a 300-m advance followed between 1909 and 1911. Annual retreat between 1895 and 1905 averaged about  $285 \text{ m a}^{-1}$ . An additional 400 m of retreat occurred through 1913 (Tarr and Martin, 1914). In 1934, following 21 years without observations, Nunatak Glacier was found to have separated into two retreating glaciers, West and East Nunatak Glaciers, and the fjord had nearly doubled in length (see fig. 33).

Tarr and Martin (1914, p. 140) described the geometry of Nunatak Glacier and the fjord on the basis of soundings and surveying: "Soundings in the fjord in 1910 showed that the depth of water about a thousand feet west of the ice front of Nunatak Glacier was 555 feet. A true scale cross-section of Nunatak Glacier when it was at that point (sometime between 1906 and 1909) shows that (a) the glacier was about 750 feet thick; (b) that the portion above sea level was only 200 feet (two-sevenths of the thickness), the glacier could not possibly be afloat; (c) that the slopes of the fjord walls above and below sea level are not significantly different; (d) that the proportion of the glacial valley now occupied by the ice is much less than when the greater glacier overrode and rose high above the nunatak."

#### West Nunatak Glacier

The approximately 20-km-long West Nunatak Glacier (Field and Collins, 1975, p. 265) continued to retreat. Following separation from the East Nunatak Glacier, probably in the middle 1920s, it remained at or near tidewater through about 1934 (Washburn, 1935). By 1959, when it was mapped by the

**Figure 146.**—20 June 1899 photograph by USGS geologist Grove Karl Gilbert of the retreating terminus of Hidden Glacier taken from a hill near the shore of Seal Bay. The gentle, convex profile, the absence of crevassing, and the faint lateral moraines are indicative of a retreating glacier. USGS Photo Library photograph Gilbert 363.

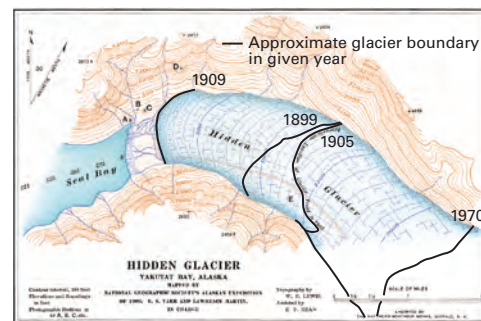


**Figure 147.**—Map showing changes in the position of the terminus of Hidden Glacier ( $59^{\circ}44'N$ ,  $139^{\circ}07'W$ ) between 1905 and 1970. Map No. 5 from Tarr and Martin, 1914, modified by the author. A larger version of this figure is available online.

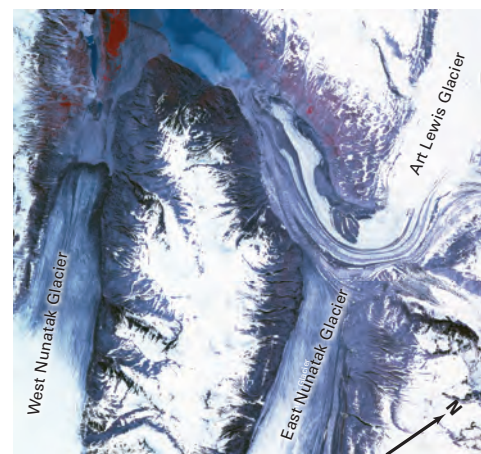


**Figure 148.**—21 June 1978 AHAP false-color or infrared vertical aerial photograph of Art Lewis Glacier flowing into Nunatak Fjord and the termini of East and West Nunatak Glaciers. Both East and West Nunatak Glaciers show multiple evidence of stagnant ice and retreat. AHAP photograph no. LXXXF5013 from the GeoData Center, Geophysical Institute, University of Alaska, Fairbanks, Alaska. A larger version of this figure is available online.

USGS (Yakutat, 1:250,000-scale map) (appendix A), it had retreated about 2.5 km. By 1993, when the author observed it, it had retreated at least another 1.5 km. It was still retreating when the author observed it on 18 June 2004.

#### *East Nunatak Glacier*

Between the late 1890s and 1948, East Nunatak Glacier retreated more than 11.5 km. By 1934, it was about 3.5 km up-fjord from the terminus of West Nunatak Glacier. Maynard Miller reported that it had retreated another 2 km by 1948 (Miller, 1948a, b). However, Field's 1964 (AGS Glacier Studies Map No. 64-2-G8) map (fig. 33) shows only about half that distance. Between 1948 and 1958, an outwash plain began developing in front of the glacier's tidewater terminus; by 1958, the terminus had advanced several hundred meters onto the plain. Since then, continuing slow retreat has occurred (fig. 148). Three ice streams coalesce to make up the face of East Nunatak Glacier. The northern part is supplied by Art Lewis Glacier. A surge of Art Lewis Glacier in the middle 1960s resulted in a temporary advance of the terminus of East Nunatak to tidewater during 1966. Since then, the terminus has retreated more than 300 m.

Hanging, Butler, and Cascading Glaciers are three other former tributary glaciers to Nunatak Glacier. All were studied extensively at the end of the 19th century and the first decade of the 20th. All were probably in contact with an expanded late "Little Ice Age" Nunatak Glacier but separated long before 1890. Each is actively retreating (AHAP false-color infrared vertical aerial photograph no. L121F5094 acquired on 20 June 1978). When it was photographed in 1899, the terminus of Cascading Glacier nearly reached the terminus of Nunatak Glacier (fig. 33; USGS Photo Library Gilbert 302 photograph). Forty-nine years later, when the USGS mapped it, it had retreated more than 1 km. Field evidence suggests that Butler Glacier may have surged several times during the 20th century

#### **Glaciers of Disenchantment Bay**

In 1792, Malaspina gave the name Puerto del Desengano (Bay of Disenchantment) to the 5-km-wide neck at the northern end of Yakutat Bay (figs. 149, 150, 151) (Orth, 1967, 1971). Malaspina, like many early explorers, entered Yakutat Bay seeking a passage to the Atlantic Ocean. Instead, he encountered a sea of floating ice in front of a retreating Hubbard Glacier. Since then, the size of Disenchantment Bay has fluctuated as much as 6 to 8 km as the terminus of the Hubbard Glacier has advanced and retreated (see Tarr and Martin's 1906 map of Disenchantment Bay showing a retracted terminus of the Hubbard Glacier) (Tarr and Martin, 1914, pl. XXXVI, ff p. 112). Hubbard Glacier, the largest glacier in the bay, has steadily shown net advance (fig. 54) through the late 20th century and early 21st century.

Many of the glaciers in the Disenchantment Bay area were the subject of almost annual observations during the last decade of the 19th century and the first decade of the 20th century (1890–1913) by some of the leading names in American glacier science: Israel C. Russell (USGS geologist), Grove Karl Gilbert (USGS geologist), Ralph Stockman Tarr (Professor of Physical Geography, Cornell University), and Lawrence Martin (Professor of Physiography and Geography, University of Wisconsin). Tarr and Martin (1914) summarized their findings on a glacier by glacier basis.

Gilbert (1904, p. 49) described submarine moraines and the bathymetry of the floor of Disenchantment Bay. He related these submarine features in Yakutat Bay to the past advances and retreats of Hubbard Glacier: "the U.S. Coast and Geodetic Survey has published a new chart of Yakutat Bay, giving soundings from the ocean to Point Latouche, six miles below Haenke Island. These soundings give no indication of a moraine in the vicinity of Point Latouche. Not far from this point there is a depth of 1,000 feet and thence southward the channel is shown for five miles. Here, at a distance of twelve miles from Haenke Island, is a submerged bar with a depth of about 300 feet,

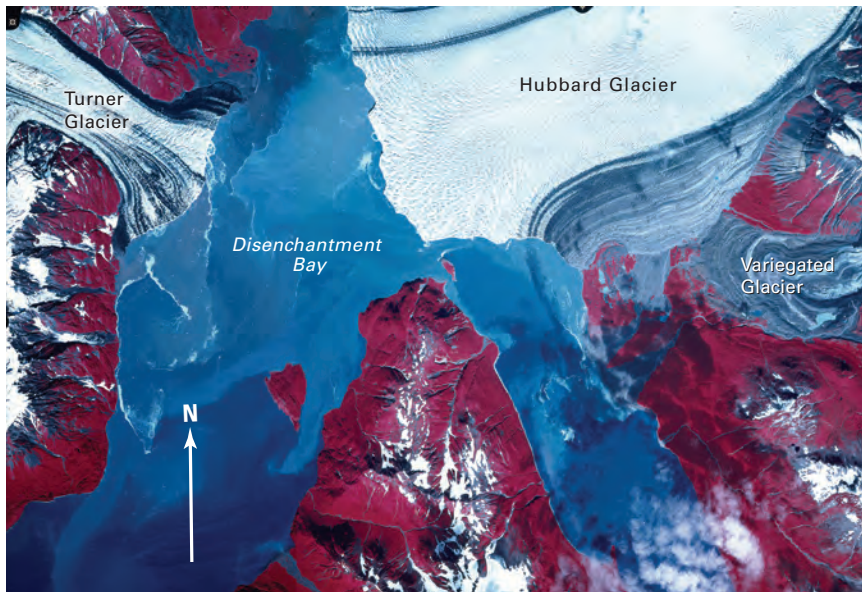


**Figure 149.**— 18 August 1978 AHAP false-color infrared vertical aerial photographic mosaic of Disenchantment Bay and the termini of Hubbard, Turner, and Variegated Glaciers. AHAP photograph nos. L120F6012 and L120F6013 from the GeoData Center, Geophysical Institute, University of Alaska, Fairbanks, Alaska.

and this is probably the last-formed important moraine in the bay. There appears to be another opposite Knight Island, seventeen miles from Haenke Island, the intervening hollow having an extreme depth of about 600 feet.” Haenke Island is located approximately 2 km south of the summer 2004 position of the terminus of Hubbard Glacier.

### **Variegated Glacier**

Variegated Glacier, located adjacent to but independent of Hubbard Glacier, is the most intensively studied surge-type glacier on Earth (figs. 149, 150). Some surges have resulted in more than 6 km of ice advance and chaotic displacement. Twenty-kilometer-long Variegated Glacier has experienced at least six recorded surges during the 20th century: 1906, before 1933, before 1948, 1964–65, 1982–83, and 1995–96. Neither of its tributaries appear to surge. Tarr’s (1907) and Tarr and Martin’s (1914) documentation of the rapid advance in 1906 of Variegated Glacier are the first scientific descriptions of a modern glacier “surge” in the United States, although the term “surge” was not used by glaciologists until 1969 (Post, 1969). Descriptions of the surge history of Variegated Glacier have been presented by Post (1969), Bindschadler and others (1977), and Lawson (1997). The 1964–65 surge produced an advance of almost 6 km (fig. 152), whereas the 1995–96 surge did not affect the lower part of the glacier.

The 1982–83 surge, which had maximum ice velocities reaching  $50 \text{ m d}^{-1}$ , is one of the best documented glacier events. This approximately 20-year surge cycle allowed a group of scientists from the University of Washington, the University of Alaska at Fairbanks, and the California Institute of Technology and a number of international collaborators to begin a program to determine the dynamics of the surge and investigate factors responsible for surge initiation during the winter of 1982–early summer of 1983 event. Kamb and others (1985) described the sequence of events as follows: surging motion began with a compression front in January 1982 that then extended down the glacier. In the spring of 1983, the lower part of the glacier experienced rapid movement. By July 1983, the surge motion had ended, and the glacier had begun to return to pre-surge state. They concluded that the 1982–83 surge resulted from increased basal pore-water pressure and the development of a temporary, stable, linked-cavity system at the interface of the glacier and the underlying terrain. Jacobel and Anderson (1987) used both 4- and 8-MHz radioechosounding as a means of determining the size and location of cavities in the top 200 m of the glacier.



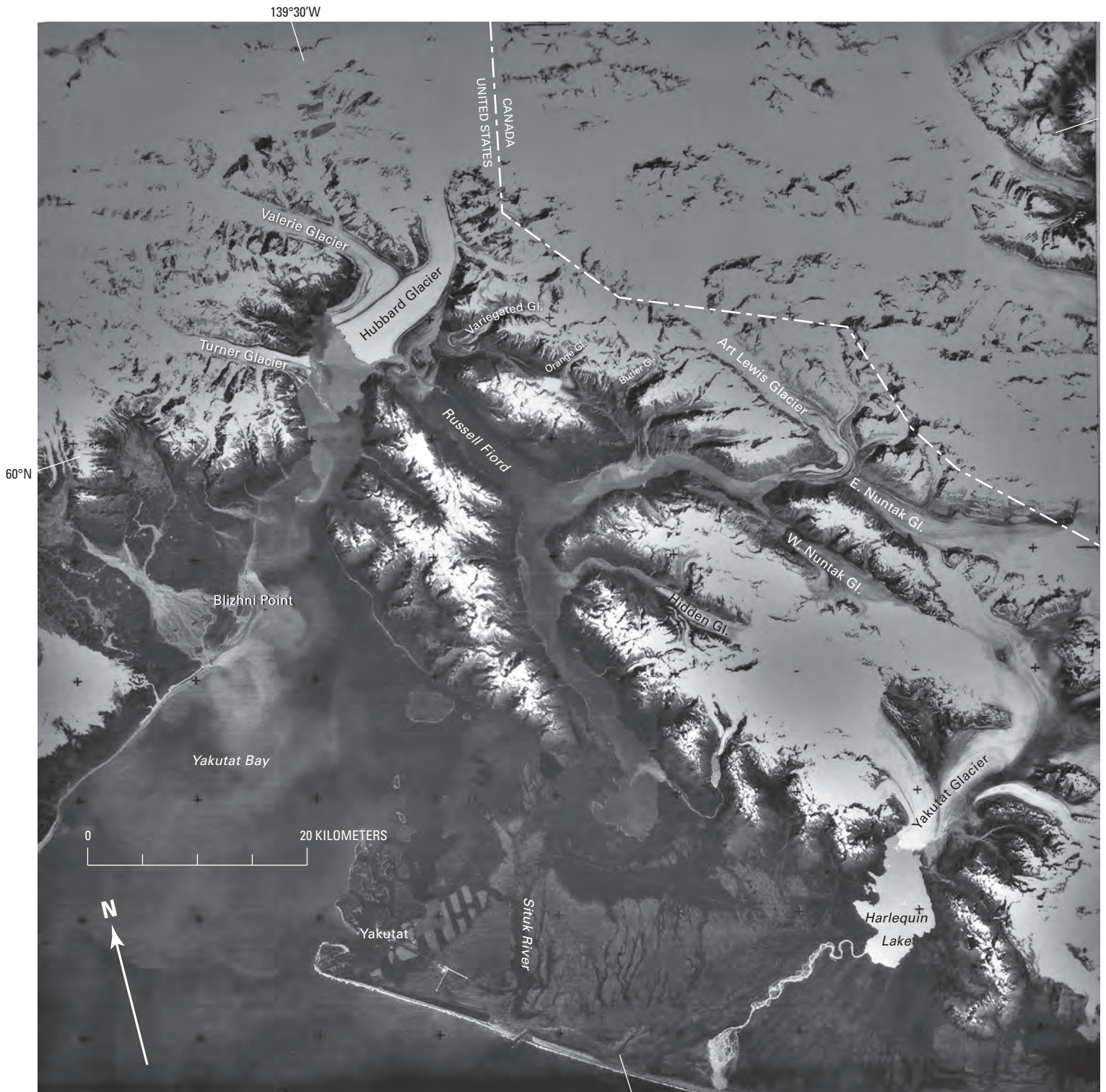


**Figure 150.**—The glaciers north and east of Yakutat are included in this Landsat 3 RBV image. Hubbard Glacier is North America's largest tidewater glacier, more than 114 km long. Only the lower quarter of the glacier is seen here. Hubbard Glacier filled Yakutat Bay for a few hundred years prior to the 14th century, receded, and then readvanced to Blizhni Point during the 18th century (Plafker and Miller, 1958). Evidence of the earlier advance and of a glacier filling Russell Fiord is easily seen as a change in vegetation (a darker gray on this image) about 15 km northeast of the Yakutat airport. Hubbard Glacier has been in a slow advance since at least Isaac Russell's observation in 1891; in 1986 and 2002, it temporarily blocked the tidal entrance to Russell Fiord. Yakutat Glacier has been in recession since 1894, when no proglacial lake existed (Field, 1975a, p. 213). Rapid retreat has recently taken place. This part of the St. Elias Mountains is well known for surging glaciers. The Turner, Variegated, Butler, Art Lewis, West

Nunatak, and Hidden Glaciers, as well as other unnamed glaciers, have a documented history of surging. It is worth noting that Variegated and Butler Glaciers both surge, while Orange Glacier, which is situated between the two, does not. Variegated Glacier has a well-documented surge record of roughly every 20 years since 1906 (Post, 1969). In 1964–1965, Variegated Glacier advanced almost 6 km (fig. 152). The 1982–1983 surge was without doubt one of the best-documented glacier events in North America (Kamb and others, 1985) (fig. 153). The surge began in the winter of 1982 and ended in the early summer of 1983. Kamb and others (1985) concluded that the surge was caused by high basal water pressure, which in turn was the result of a temporary, stable, linked-cavity system at the bed as opposed to the longer term, stable basal tunnel system. Landsat 3 RBV image (30167–19491–C; 19 August 1978; Path 66, Row 18) and caption courtesy of Robert M. Krimmel, U.S. Geological Survey.

Bindschadler (1978) and Raymond and Harrison (1988) provided extensive details about the evolution of progressive changes in geometry and velocity in Variegated Glacier during the decade before the surge. The glacier thickened in its upper 12 km and thinned in its lower 8 km. Changes were as much as 20 percent of total thickness. Pre-surge velocity increased by as much as 500 percent, reaching a maximum of  $0.7 \text{ m d}^{-1}$  in 1981. By 1978, the amplitude of seasonal velocity variation increased as much as  $0.3 \text{ m d}^{-1}$ . Little change occurred in subsequent years. Raymond and Harrison (1988, p. 154) concluded that “a drop in effective normal stress in a zone of decreasing surface slope up-glacier from the largest thickness increase may have been significant in the initiation of surge motion in 1982.”

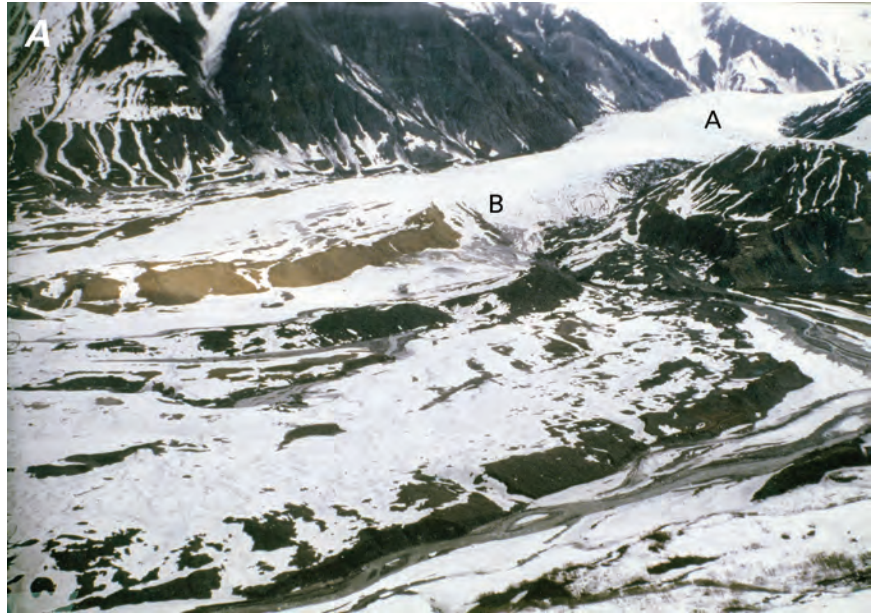
Humphrey and Raymond (1994) provided significant details about the hydrology, erosion, and sediment produced by the 1982–83 surge (fig. 153). They determined that the surging region of the glacier was underlain by a basal hydrologic zone characterized by low water velocity and high water storage. They postulated that flow in this region was distributed and that the volume of water stored in the basal hydrologic zone is the major hydraulic factor that drove the surge. Down-glacier of the surge propagation front, the ice is underlain by a zone of high water velocity and low water storage. They assumed that flow in this region was through a system of conduits. During the surge, basal bedrock erosion was significantly greater than it was at any other time and was “extreme” compared with that of non-surge-type glaciers. Sediment output was directly proportional to the rate of basal sliding. During the 20-year surge cycle, about 0.3 m of bedrock was eroded. About two-thirds of this erosion occurred during the 2-year peak (1982–83) in surge activity. Humphrey and Raymond (1994) concluded that most of this erosion occurred during the 2-month period of peak surge activity. Previously, Humphrey and others (1986) had looked at discharge of turbid water during periods of mini-surges in 1980 and 1981. [Editors’ note: According to Mark F. Meier (written commun., 2004), the relationship of discharge of water before, during, and after surge events was a major scientific finding. Another major finding was the outburst that ended the 1983 surge and the contrast



**Figure 151.**—Sketch map of Disenchantment Bay showing Malaspina’s 1791 survey of an advanced Hubbard Glacier from Davidson (1904). A larger version of this figure is available online.



**Figure 153.**—Two oblique aerial photographs of Variegated Glacier showing changes resulting from the 1982–83 surge. Variegated Glacier is 20 km long. The width of the glacier is 0.8 km at A in figure 153A. The active surge phase lasted from January 1982 until early July 1983, during which period there were several major accelerations. The lower glacier was largely unaffected until May 1983, at which time spectacular changes occurred. By the 4 June 1983 photograph (fig. 153A), the surge front had propagated to approximately B. On 4 July 1983, the surge essentially ended but not before affecting the entire glacier seen in the 7 July 1983 photograph (fig. 153B). The surge front propagated through the lower glacier at  $80 \text{ m d}^{-1}$ . The highest measured ice velocity was in the vicinity of A and was  $65 \text{ m d}^{-1}$  for a period of 2 hours on 9 June 1983. The upper glacier thinned as much as 50 m, and the lower glacier thickened up to 100 m during the surge (Kamb and others, 1985). Photographs and caption courtesy of Robert M. Krimmel, U.S. Geological Survey.



◀ **Figure 152.**—Two oblique aerial photographs of the terminus of Variegated Glacier showing the changes resulting from the 1964–65 surge. In the 358 days between the two photographs, Variegated Glacier advanced almost 6 km. **A**, 29 August 1964 photograph. USGS photograph no. F646–99 by Austin Post, U.S. Geological Survey. **B**, 22 August 1965 photograph. USGS photograph no. 7652–237 by Austin Post, U.S. Geological Survey.

in travel time of water at the base of Variegated Glacier before and after this outburst event (Brugman, 1987).]

The most recent surge was significantly different from previously observed surges of Variegated Glacier. In 1994, anticipating the onset of another surge, Keith Echelmeyer (University of Alaska) overflowed the glacier and noted that surface crevasse and fracture features in the upper glacier suggested that a new surge was imminent. He also obtained aerial photographs of the surface of the glacier (K. Echelmeyer, oral commun., 1997). Center-line elevation profiles made with a geodetic airborne laser altimeter profiler in 1995 and 1996 indicated that surge activity in this event was restricted to the upper part of the glacier, unlike previous surges of Variegated Glacier. An 11 June 1995 sediment-laden jökulhlaup marked the end of initial surge activity, and an anticipated winter rejuvenation of the surge did not occur. The lower reaches of the glacier were not involved in this surge cycle. The geodetic airborne laser altimeter profiler has been described by Echelmeyer and others (1996).



**Figure 154.**—1890 photograph by USGS geologist Israel C. Russell of the terminus of Hubbard Glacier from near Gilbert Point. USGS Photo Library photograph Russell 390.

Variegated Glacier has an extensive photographic history (Lawson, 1996), including 12 sets of vertical aerial photographs taken between 1948 and 1983. It was also photographed as early as 1890 by Israel C. Russell of the USGS (fig. 154), by Bradford Washburn in the 1930s, and by Austin Post repeatedly between 1960 and 1983. Analysis of sequential vertical aerial photographic sets by Lawson (1990) revealed that successive surges and surge cycles produce similar sets and patterns of glacier crevasses and other structures irrespective of the duration and intensity of the individual surges.

### **Hubbard Glacier**

Hubbard Glacier has an area of about 3,900 km<sup>2</sup> and a length more than 114 km (table 2) (Viens, 1995). If it were entirely in Alaska, it would be the third largest glacier in the State (figs. 1, 2). However, more than half of the glacier is in Canada; only the lower part is in Alaska. With the exception of the calving margin of the Bering Lobe, which is located at the head of Vitus Lake (a tidal basin separated from the open ocean by a 5-km-long narrow channel), Hubbard Glacier, which has a 10.5-km-wide calving face, is also Alaska's largest tidewater glacier directly accessible to the Pacific Ocean (through Disenchantment and Yakutat Bays) (figs. 53, 55, 56, 149, 150, 151). Hubbard Glacier has an AAR of 0.96 (table 2) (Viens, 1995). D.C. Trabant (oral commun., August 1990) estimated that 95 percent of the ice lost by Hubbard Glacier is by calving and the remaining 5 percent by melting.

On the basis of a radiocarbon-dated sample, Plafker and Miller (1958) reported that Hubbard Glacier filled Yakutat Bay and extended into the Pacific Ocean 1130±160 yr B.P. Arcuate ridges at Monti Bay and near the city of Yakutat are the terminal and recessional moraines that mark this maximum ice advance. Beginning in the 14th century, Hubbard Glacier underwent a significant retreat of more than 25 km. During the 18th century, it readvanced more than 10 km to Blizhni Point (Plafker and Miller, 1958). A submarine moraine at the lower end of Disenchantment Bay resulted from this advance, which culminated after 1700 A.D. and before Malaspina's visit in 1791. Retreat of more than 5 km occurred in the late 18th century and early 19th century. Before 1890, the glacier again began to advance. Hubbard Glacier was observed to be advancing by Russell in 1890 (fig. 154) and 1891, by Gilbert from 1897 to 1899, by Tarr and Martin several times in the early 1900s (Tarr and Martin, 1914, pl. XLVIII, ff p. 112), by Post on 29 August 1984 (fig. 55) and 12 September 1986 (fig. 56), and by the author on 13 June 2002 and 18 June 2004. Figure 54 compares the positions of Hubbard Glacier's terminus between 1965 and 1997. The continuous advance of Hubbard Glacier during

the 20th century is in accordance with the theory of tidewater glacier stability and cyclicity (fig. 42).

Trabant and others (2003) compared NOAA's 1978 and 1999 bathymetric surveys of Disenchantment Bay to evaluate the displacement of the submarine terminal moraine adjacent to Hubbard Glacier. They integrated the average advance rate of a 2.1-km width of the seaward face of the moraine between the 120- and 170-m isobaths and determined that growth was approximately  $32 \text{ m a}^{-1}$ . This figure is in close agreement with the average rate of terminus advance. For the entire profile area, which spanned depths from about 60 to about 230 m, the average advance rate was approximately  $10 \text{ m a}^{-1}$ .

Trabant and others (2003) also analyzed seven longitudinal profiles collected on the terminal lobe of Hubbard Glacier in 1948, 1959, 1978, 1988, 1992, 1999, and 2000. They determined that the glacier thickened and lengthened in the interval between data sets. Between 1948 and 2000, the glacier thickened by more than 100 m at the location of the 1948 terminus.

Early in the 20th century, a debate existed about the morphology of fjords and about whether glaciers were floating or grounded. Tarr and Martin (1914, p. 224) observed that

The soundings made in 1910 also establish the fact that, deep as the water is, it is practically impossible that any of the glacier fronts of Disenchantment Bay and Russell Fiord are floating now and they do not seem to have been afloat at any stage of their expansion, judging by the depths of water. This means that there was always active glacial grinding on the fiord bottom and the problem arises as to where this eroded material is now. In Russell Fiord the volume, merely from the part of the fiord below sea level would be many cubic miles, and the soundings show that more material was eroded above sea level than below. Some of the material makes up the great moraine south of Russell Fiord, some is in the submerged moraines, and a great deal has gone out to sea. Some, however, doubtless remains in the fiord bottoms, making it impossible to tell how near a given sounding goes to the rock bottom of the fiord. The measures of glacial erosion are, therefore, all minima.

As they do at other large tidewater glaciers, the seasonal development and filling of calving embayments at Hubbard Glacier cause the position of parts of the terminus to undergo fluctuations of up to several hundred meters. Consequently, many historic reports of the position of the terminus of Hubbard Glacier mention that parts of the 10.5-km-long terminus have retreated. In spite of these seasonal fluctuations, the glacier has advanced about 3 km or nearly  $30 \text{ m a}^{-1}$  since the early 1890s, as tidewater glacier theory has predicted. One reason why these types of fluctuations are described here and not at other glaciers is the degree of scrutiny that Hubbard Glacier has received. Similar annual variations are observed at Bering and Columbia Glaciers.

## The 1986 and 2002 Temporary Closures of Russell Fiord by Hubbard Glacier

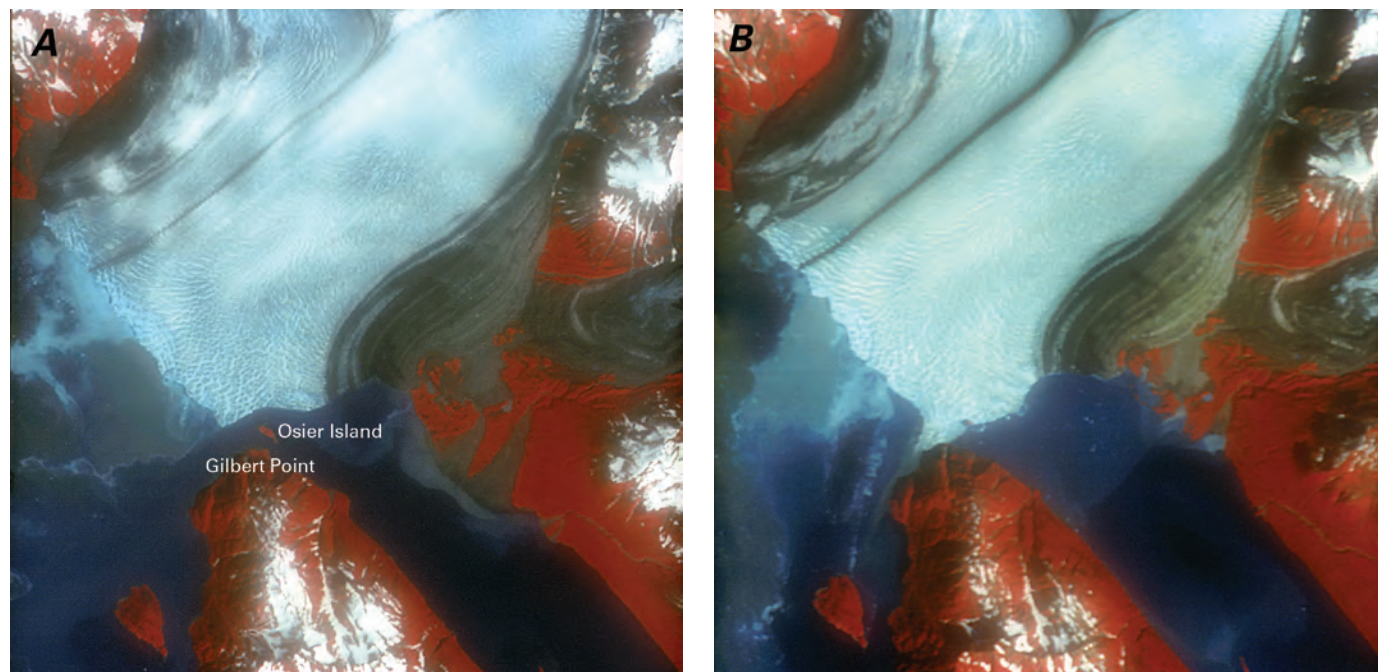
by BRUCE F. MOLNIA,<sup>1</sup> DENNIS C. TRABANT,<sup>2</sup> ROD S. MARCH,<sup>2</sup> and ROBERT M. KRIMMEL<sup>3</sup>

A well-studied closure of Russell Fiord occurred in 1986. By 7 August 1985, the terminus of Hubbard Glacier had advanced into shallow water near Osier Island (fig. 155A). The combination of a decrease in ice loss to calving and a surge at daily flow rates of about 30 m d<sup>-1</sup> of the eastern terminus (North Pacific Aerial Surveys, Inc., vertical aerial photograph no. YAKT, 1:76, H-20, 4-3 acquired on 30 August 1975) resulted in an increase in Hubbard's advance rate, so that its eastern terminus had encroached on Gilbert Point by 11 September 1986 (fig. 155B) and 12 September 1986 (fig. 56). Mayo (1988a, b) stated that, between 7 August 1985 and 12 June 1986, the part of Hubbard Glacier advancing into deep water moved between 48 and 197 m, while the part advancing into shallow water near Russell Fiord moved 300 to 485 m. A 485-m-wide segment advancing toward Gilbert Point moved nearly 788 m. Mayo equated this movement to an advance rate of about 1 km a<sup>-1</sup>.

In early May 1986, the advancing toe of the glacier overrode nearly all of Osier Island and, on 29 May 1986, pushed up and extruded a wedge of glaciomarine sediments against the bedrock wall of the fiord at Gilbert Point. This sedimentary mass blocked the entrance to Russell Fiord, resulting in the transformation of Russell Fiord to the approximately 60-km-long *Russell Lake*. As a result of its long history of 20th century advance and observation, the blockage of Russell Fiord had been predicted by Post and Mayo (1971), Field and Collins (1975), and Reeburgh and others (1976).

The fact that a number of marine mammals were 'trapped' in *Russell Lake* led to international media coverage of the closure. Much concern was focused on whether the marine mammals would be able to find food and how they would be affected as the salinity of *Russell Lake* decreased. During the 132 days between 29 May and 8 October 1986, the sediment dam maintained contact with the bedrock adjacent to Gilbert Point, as a 12 September 1986 aerial photograph (fig. 56) shows. At no time did Hubbard Glacier ice actually make direct contact with Gilbert Point.

**Figure 155.**—A pair of Landsat 5 TM images of the terminus of Hubbard Glacier. **A**, The pre-Russell Lake terminus on 7 August 1985. **B**, The dammed mouth of Russell Fiord on 11 September 1986. Landsat 5 TM image (LT5062018008521910; bands 4, 3, 2; 7 August 1985; Path 62, Row 18) and Landsat 5 TM image (LT5062018008625410; bands 4, 3, 2; 11 September 1986; Path 62, Row 18) from the U.S. Geological Survey, EROS Data Center, Sioux Falls, S.Dak.



<sup>1</sup> USGS, 926A National Center, Reston, VA 20192.

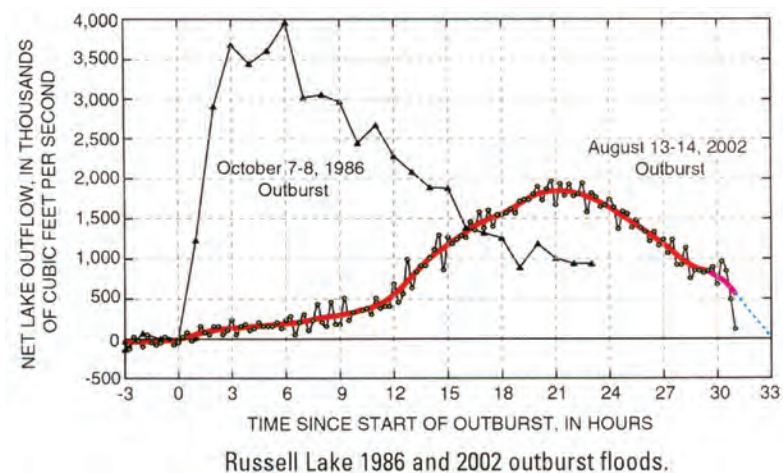
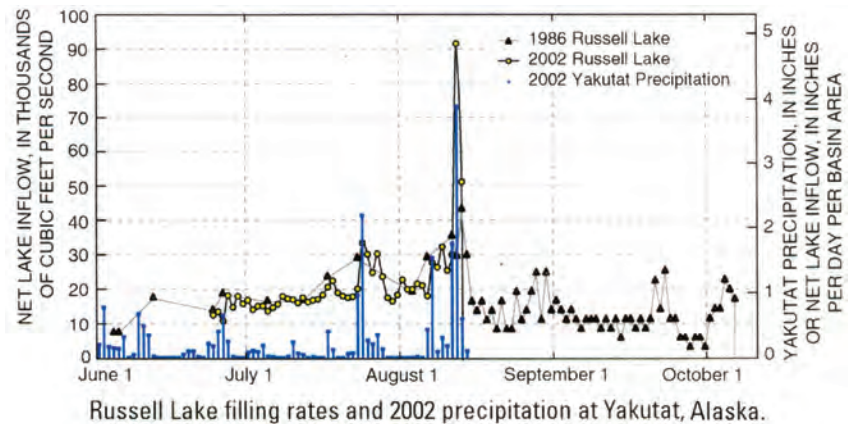
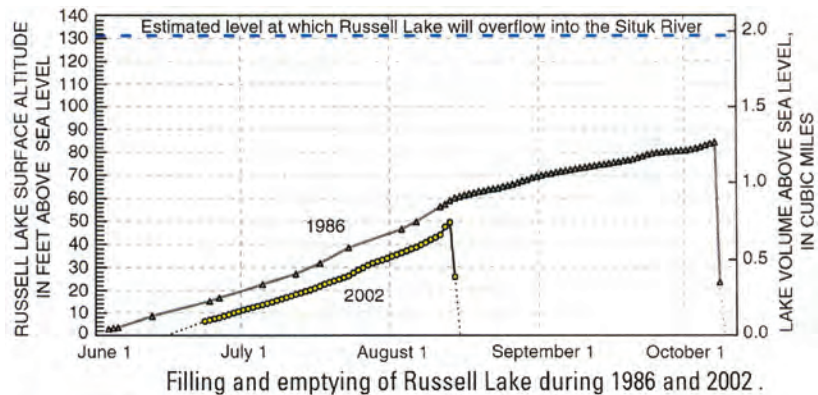
<sup>2</sup> USGS, Geophysical Institute, P.O. Box 757320, Fairbanks, AK 99775-7320

<sup>3</sup> USGS, 1201 Pacific Avenue, Tacoma, WA 98402

As runoff from an approximately 1,800 km<sup>2</sup> drainage area entered the lake, the water level in the lake began to rise quickly. Filling was at times rapid, up to nearly 0.25 m d<sup>-1</sup> following heavy precipitation events. Soon after closure, the USGS began to manually measure the height of the rising water in *Russell Lake*. Twelve stage measurements were made before the installation of an automated stage gage in early August. The volume of water introduced into the lake at its maximum stage was about 5.5 km<sup>3</sup>, an average influx of about 467 m<sup>3</sup> s<sup>-1</sup> (Seitz and others, 1986). Maximum inflow was about 1,200 m<sup>3</sup> s<sup>-1</sup> on 13 August 1986 (figs.156A, B). The water level in *Russell Lake* rose to a maximum of 25.8 m. Filling of the lake to a height of approximately 40 m above mean sea level would have resulted in water flowing out the back (southeastern) end of the lake basin into the Situk River drainage.

Calving of icebergs from both sides of the 400-m-wide ice dam, into both *Russell Lake* and Disenchantment Bay, reduced the width of the ice dam. This narrowing of the ice dam and the increased hydrostatic pressure against

**Figure 156.**—**A**, Filling and emptying of Russell Lake during the 1986 and 2002 closure events. **B**, Russell Lake filling rates in 1986 and 2002 and 2002 precipitation at Yakutat, Alaska. **C**, Hydrographs showing the 1986 and 2002 draining of Russell Lake.



and under the dam further weakened it. Close to midnight on 7 October 1986, the ice dam began to fail. Peak discharge was reached 6 hours after the inception of a jökulhlaup. Within 24 hours, the water level in *Russell Lake* dropped more than 25 m, returning to equilibrium with adjacent Disenchantment Bay (fig. 156C). Emery and Seitz (1987) reported that, between 0200 and 0600 local time on 8 October 1986, the level of the lake decreased as much as  $1.6 \text{ m h}^{-1}$ . Mayo (1988a, b) cited the average discharge from the lake into Disenchantment Bay as about  $1.1 \times 10^5 \text{ m}^3 \text{ s}^{-1}$  and the total volume of water discharged into Disenchantment Bay as  $5.42 \text{ km}^3$ . The peak discharge was  $1.04 \times 10^6 \text{ m}^3 \text{ s}^{-1}$ . Interesting legacies from *Russell Lake* were the presence of ice-rafted dropstones left in the crowns of many trees that had been submerged by the rapidly rising waters; drift logs resting on limbs of other trees, deposited during the rapid draining of the lake; and, years later, a ring of dead trees surrounding the margin of Russell Fiord. [Editors' note: A similar ring of dead trees surrounds the shoreline of Canal de los Tempanos and Brazo Sur, arms of Lago Argentino that are subject to water-level fluctuations caused by the advance and retreat of Glacier Perito Moreno, an outlet glacier from the Southern Patagonia Ice Field, Argentina (see Lliboutry, 1998).]

Ice-velocity measurements made in June 1986 showed that the speed of the ice at the terminus of Hubbard Glacier was  $14 \text{ m d}^{-1}$ . By August 1986, the speed of the ice was  $8 \text{ m d}^{-1}$ , about the same as was measured in August 1978 (Krimmel and Sikonia, 1986). As a result of the jökulhlaup, the erosion of the sediment plug and the adjacent ice dam left the position of the central part of the terminus of Hubbard Glacier nearly 0.5 km north of Osier Island.

Tlingit oral history describes a previous damming of Russell Fiord (de Laguna, 1972), probably early in the 19th century. However, the damming of this lake may have been the result of an ice dam formed by an advance of the terminus of Nunatak Glacier rather than by a Hubbard Glacier ice dam. Whatever the cause, Russell (1893) observed a combination of young vegetation and recent shoreline features in upper Russell Fiord in 1891 that confirmed the recent existence of a 19th century lake.

Through the late 1980s, the 1990s, and into the early 21st century, Hubbard Glacier continued its steady advance south toward Gilbert Point. A comparison of the glacier's terminus position on 7 August 1986 with that on 11 August 2001 showed average advances of 560 m in Disenchantment Bay and 390 m in Russell Fiord.

Trabant and Krimmel (2001) took a close look at annual changes of the terminus of Hubbard Glacier, specifically at when the advance of Hubbard Glacier might next close the entrance of Russell Fiord. By comparing periods of approximately 50 years, they found that the average rate of advance had accelerated from about  $16 \text{ m a}^{-1}$  between 1895 and 1948 to about  $26 \text{ m a}^{-1}$  between 1948 and 1998. During shorter periods, the advance was spatially and temporally erratic. For example, an average advance of 32 m along the 6-km-wide terminus facing Disenchantment Bay between August 1988 and July 1990 contrasts with an advance of 111 m along the 2.8-km-wide terminus of Hubbard Glacier in Russell Fiord during the same period. The terminus of Hubbard Glacier that faced Disenchantment Bay exhibited an extreme temporal rate change during the decade of the 1990s; the rate of advance changed from an average of about  $4 \text{ m a}^{-1}$  between July 1990 and July 1998 to  $149 \text{ m a}^{-1}$  between late July 1998 and early August 1999. The 100-year average advance rate was about  $22 \text{ m a}^{-1}$  for most of the terminus and around  $19 \text{ m a}^{-1}$  toward the closure point.

On 2 August 1999, Hubbard's terminus was about 350 m from Gilbert Point. By the spring of 2002, Hubbard Glacier's advancing terminus had reduced the width of open water between it and Gilbert Point by more than half. On 20 May 2002, a U.S. Forest Service photograph by Bill Lucey showed that the advancing terminus was pushing up and extruding a mass of glaciomarine sediments between it and the bedrock wall of the fiord about 400 m west of



Gilbert Point. No change was noted in the water level of Russell Fiord versus Disenchantment Bay, and tidal exchange between Disenchantment Bay and Russell Fiord appeared to be unimpeded.

The exposed part of this push-moraine sedimentary mass continued to expand and, before 13 June 2002, it made contact with the bedrock wall of Russell Fiord (fig. 157). The surface of the push moraine had four distinct ridges. The areal extent of the 2002 moraine was significantly larger than that of the 1986 moraine, and the location of closure was approximately 500 m west of the 1986 closure. Throughout June 2002, water continuously flowed out of *Russell Lake* through an approximately 90×20-m shallow channel. By early July 2002, the height of the push moraine eliminated the tidal exchange of water with Yakutat Bay (Molnia and others, 2002).

During the ensuing 10 weeks, the area and height of the push moraine continued to increase, again resulting in the transformation of Russell Fiord into *Russell Lake*. Unlike 1986, there was little international media attention, and minimal attention was paid to the presence of marine mammals in *Russell Lake*. By mid-June, the growing push moraine effectively closed the entrance to Russell Fiord. By late-June, the water in *Russell Lake* was more than 7 m above mean sea level. Nearly a kilometer of the terminus was fronted by extruded glacial and glaciomarine sediments as they emerged from the fjord. By mid-July, the sediment mass reached a height of more than 25 m above mean sea level. At Gilbert Point, extruded sediment and moraine were pushed against approximately 250 m of the fjord wall.

By early August, a delicate balance existed between the height of the growing moraine and the volume and height of water in *Russell Lake*. Drainage continued through a narrow channel cut into the top of the push moraine. By 10 August 2002, the maximum height of the growing moraine exceeded 30 m, and the stage of *Russell Lake* reached 12 m above mean sea level (fig. 156A). Part of the terminus of the glacier had advanced to within 15 m of the southern wall of Russell Fiord. At all times, moraine was the only material that made contact with the wall of the fjord.

Within 2 weeks of closure, the USGS had installed an automated stage gage. As was the case in 1986, the water level in the lake had begun to rise immediately. Filling was rapid, averaging 0.22 m d<sup>-1</sup> (fig. 156B). The volume of water introduced into the lake at its maximum stage was about 3.1 km<sup>3</sup>, an average influx of about 530 m<sup>3</sup> sec<sup>-1</sup>. Maximum inflow was about 2,600 m<sup>3</sup> sec<sup>-1</sup> on 12 August 2002.

**Figure 157.**—Northeast-looking oblique aerial photograph of the advancing terminus of Hubbard Glacier on 13 June 2002 taken from over Disenchantment Bay looking across Gilbert Point into Russell Fiord at the push moraine that temporarily blocked the mouth of Russell Fiord. This push moraine is composed of sediment bulldozed from the floor of Russell Fiord by the advancing ice. Part of the Hubbard Glacier that is advancing into Disenchantment Bay can be seen in the center of the photograph. Photograph by Bruce F. Molnia, U.S. Geological Survey.



During the 66 days between 10 June and 14 August 2002, the sediment dam maintained contact with the bedrock wall of Russell Fiord west of Gilbert Point, and the water level in *Russell Lake* rose 15.1 m. At 0300 local time on 14 August 2002, *Russell Lake* began to drain. As much as 15 cm of precipitation had fallen at Yakutat during the two previous days, resulting in an inflow into the lake that was approximately half an order of magnitude greater than the average influx for the previous 60 days (fig. 156B). Unlike the 1986 flood, which resulted from abrupt ice-dam failure, the 2002 flood was the result of prolonged erosion of a deepening and widening channel cut into the push moraine. At noon local time on 14 August 2002, about 9 hours after the onset of the flood, the lake stage had fallen only 0.68 m, and the discharge was approximately  $8,600 \text{ m}^3 \text{ s}^{-1}$ , with super-critical flow and 14-m-high hydraulic jumps. Six hours later, at approximately 1800, and about 15 hours after onset, the lake stage had fallen 2.56 m and the discharge was approximately  $33,000 \text{ m}^3 \text{ s}^{-1}$ . Peak discharge, approximately  $52,000 \text{ m}^3 \text{ s}^{-1}$ , was reached approximately 21 hours into the flood. The flood lasted about 33 hours (fig. 156C). When observed on 15 August 2002, around 12 hours after peak discharge, open exchange was again taking place, and the height of the surface of Russell Fiord had returned to sea level. The newly exposed former lake bed contained numerous trees covered by glacial flour.

As was the case in 1986, the flood removed both the sediment dam and a significant amount of ice from the terminus of the glacier. Following the flood, the width of the channel between Hubbard's terminus and Gilbert Point had widened to approximately 500 m. When observed in early February 2003 and again in June 2004, the terminus again appeared to be advancing and closing the channel. Glacier ice has yet to make contact with the bedrock wall of Russell Fiord at Gilbert Point.

---

### **Southwestern St. Elias Mountains Segment: From the Western Side of Yakutat Bay to the Western Bagley Ice Valley, the Western Robinson Mountains, and the Bering Lobe**

Landsat MSS images that cover the southwestern St. Elias Mountain region from the western side of Yakutat Bay to the Bering Lobe have the following Path/Row coordinates: 66/18, 67/18, 68/18, 69/18, and 70/18 (fig. 3, table 1). These areas are mapped on the USGS Yakutat, Alaska-Canada; Mount St. Elias, Alaska-Canada; and Bering Glacier, Alaska, 1:250,000-scale topographic maps (appendix A). Even though the eastern Bagley Ice Valley (including Quintino Sella, Columbus, and Jefferies Glaciers) is located in the St. Elias Mountains, it is part of the Bering Glacier System. The Bagley Ice Valley will be described in the Chugach Mountains section, so that the Bering Glacier System can be described as a single entity.

Between the southwestern margin of Hubbard Glacier and the northeastern side of the piedmont lobe of Malaspina Glacier, nine east- and south-flowing glaciers descend from the flanks of the St. Elias Mountains to near sea level: Miller, Haenke, Turner, Fallen, Black, Galiano, Atrevida, Lucia, and Hayden Glaciers. In 2000, Haenke and Turner Glaciers reached tidewater. Since then, Haenke's terminus has been stationary.

Miller Glacier is the 5-km-long valley glacier immediately west of Hubbard Glacier. For most of the 20th century, it stagnated in its valley; its 1959 terminus about 1.5 km from shore. Post (1967b) reported that it underwent a small surge in 1966. Since then, its debris-covered terminus has been stagnating and retreating. On 2 August 1999, its terminus was about 2.1 km from the coastline of Disenchantment Bay.

**Figure 158.**—Aerial photographs of the termini of Haenke and Turner Glaciers. **A**, 25 August 1969 oblique aerial photograph shows stagnant ice and downwasting in the terminus area of Haenke Glacier (right) and the tidewater terminus of Turner Glacier (left). The spit on the left (south) side of Turner Glacier marks the position of its recent terminal moraine. The terminus of Turner Glacier appears to have retreated several hundred meters from its recent maximum position. The folded moraines on the left (south) side of Turner Glacier indicate recent surge activity. USGS photograph no. F692-124 by Austin Post, U.S. Geological Survey. **B**, 2 August 1999 black-and-white vertical aerial photograph of the tidewater termini of Turner Glacier (left), and Haenke Glacier (right). The termini of both Turner and Haenke Glaciers extend into tidewater as if both had experienced recent surges. Haenke Glacier has advanced approximately 2 km beyond its 1979 terminus position. Photograph no. 3-6 is from the U.S. Bureau of Land Management.

Haenke Glacier, which is 14 km long (Field and Collins, 1975, p. 266), is another surge-type glacier. Between 1891 and 1905, its terminus was stagnant, downwasting, and located more than a kilometer from Yakutat Bay. Tarr and Martin (1914) reported that it underwent a rapid advance, thickened, became crevassed, and advanced nearly 1.4 km between 1905 and 1906. Retreat followed through 1913. A 1933 Washburn photograph showed that its terminus was located at tidewater. Another period of retreat followed; by 1948, it was again stagnant, with active ice about 3 km from shore (Field and Collins, 1975). By 1959, active ice was about 2 km from shore. By 25 August 1969, after another decade of stagnation, active ice was now more than 3 km from shore (fig. 158A). In 1978, vegetation was growing on the stagnant terminus, and a delta separated the stagnant margin from the adjacent Turner Glacier (AHAP false-color infrared vertical aerial photograph no. L120F6011 acquired on 18 August 1978). At the end of the 20th century, Haenke Glacier had again become a tidewater glacier, with a large bulbous terminus of stagnant ice extending nearly a kilometer into Yakutat Bay (fig. 158B).

When the central part of the terminus of Turner Glacier was observed in August 1891 by Israel C. Russell (fig. 159) and in 1899 by Gilbert (1904), it extended more than 1 km into Disenchantment Bay. Its land-based northern and southern margins, however, were frequently reported as showing signs of minor retreat (Tarr and Martin, 1914). Turner Glacier fluctuated around this position for nearly 60 years until it underwent a catastrophic calving as the result of the 9 July 1958 earthquake, whose epicenter was located near Lituya Bay. As much as 700 m of the terminus calved in a series of seemingly endless events described by Davis and Sanders (1960). Field and Collins (1975)

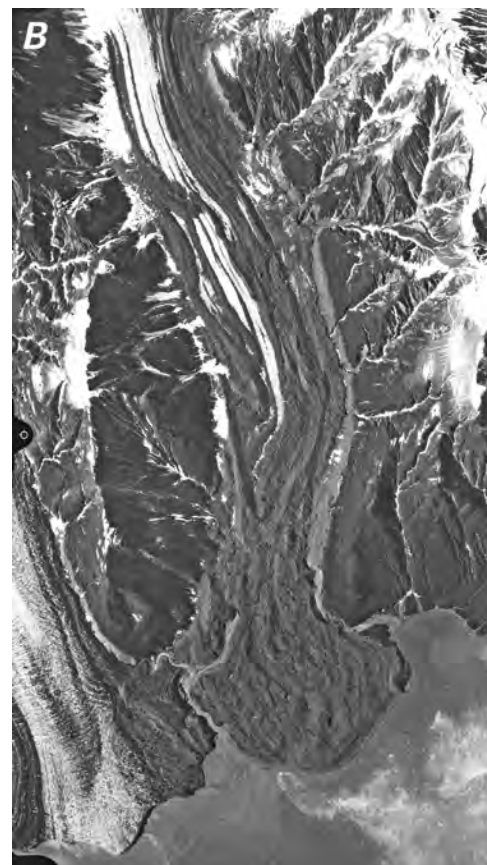




**Figure 159.**—August 1891 photograph by USGS geologist Israel C. Russell of the tidewater terminus of Turner Glacier, which extended about 1 km into Disenchantment Bay. USGS Photo Library photograph Russell 362.

suggested that the massive calving may have resulted from the slumping of unconsolidated sediment beneath the ice mass, which would reduce support and create a very unstable condition. Its 25 August 1969 position (fig. 158A) is as retracted as it has been at any time since it was first observed. By 1978, much of the area lost since 1958 was regained, possibly by a surge-induced advance. By 2 August 1999 (fig. 158B) and through June 2004, the terminus was located at approximately the same location as it was in 1890–99 (fig. 159). Turner Glacier has an area of approximately 186 km<sup>2</sup>, an accumulation area of approximately 150 km<sup>2</sup>, an ablation area of approximately 35 km<sup>2</sup>, and an AAR of 0.81 (table 2) (Viens, 1995). The width of Turner's calving face is about 3.1 km.

All of the glaciers southwest of Turner Glacier and east of the Malaspina Glacier have significantly retreated from the positions that they held when they were mapped in 1909 by the NGS. All are either actively retreating or have stagnant, debris-covered termini. Lucia Glacier, however, is a surge-type glacier and experienced a surge in 1966.

### **Malaspina Glacier System**

Malaspina Glacier (fig. 160), which has a length of 113 km (Field and Collins, 1975, p. 267) and an area of about 5,000 km<sup>2</sup> (table 3) (Viens, 1995), is the second largest and one of the longest glaciers in Alaska and in continental North America (Hubbard Glacier and Bering Glacier are also among the longest). It includes the largest piedmont lobe of any glacier in continental North America. The entire piedmont lobe, which is located between Yakutat Bay and Icy Bay, lies at elevations below 600 m. Alone, it has an area of approximately 2,150 km<sup>2</sup> and a perimeter of about 90 km. Its entire surface is located within the ablation zone. The accumulation area of Malaspina Glacier is only slightly larger than its ablation area (2,575 km<sup>2</sup> as opposed to 2,433 km<sup>2</sup>); consequently, Malaspina Glacier has an AAR of 0.51 (table 2) (Viens, 1995), one of the lowest of any studied glacier in the St. Elias Mountains. Seward and Agassiz Glaciers are the largest of Malaspina Glacier's tributaries. Other large tributaries include Hayden, Marvine, and Libbey Glaciers. Sharp (1951) estimated that Seward and Malaspina Glaciers contain 1,750.6 km<sup>3</sup> of ice jointly. Malaspina Glacier has an extensive photographic record dating from 1890.

Morphologically, the piedmont lobe of Malaspina Glacier consists of three primary components: (1) the eastern *Seward Lobe*, which encompasses about two-thirds of the piedmont lobe, (2) a debris-covered interlobate area, which extends from the Samovar Hills to the glacier's southern margin, and (3) the western *Agassiz Lobe*. The eastern margin of the piedmont lobe abuts the western margin of Marvine Glacier. Similarly, Libbey Glacier flanks the western margin of the lobe. Much of the remaining perimeter of the piedmont lobe is fronted by outwash plains and vegetation-covered stagnant ice,



**Figure 160.**—This Landsat 1 MSS image of the Malaspina Glacier and environs was acquired on 12 February 1973, at a time when glaciers are not best observed generally; snow covers the ice features, and a low Sun angle obscures valleys with shadows. But in this particular region in midwinter, both of these attributes enhance this image of the upper Bering Glacier, Bagley Ice Valley, Seward Glacier, Agassiz Glacier, and the piedmont Malaspina Glacier, allowing other information to be obtained. The uniform snow cover, combined with the low Sun angle, permits subtle slope changes to be seen on the large expanses of relatively flat ice areas. These slope changes are not evident on aerial photos or the

maps made from them. An image such as this one can be stretched in contrast, either photographically or digitally, to further enhance the tonal variations. The surface slope changes give clues as to subglacial topography (Krimmel and Meier, 1975; Molnia and Jones, 1989) and the direction of ice flow in the accumulation areas. The terminus positions of the very active tidewater glaciers in Icy Bay can be easily mapped from an image such as this one. Landsat 1 MSS image (1204–20120, band 7; 12 February 1973; Path 68, Row 18) and caption courtesy of Robert M. Krimmel, U.S. Geological Survey.

pitted with thermokarst features. The largest individual pits are more than 0.5 km in maximum dimension (fig. 161).

At Sitkagi Bluffs, the southern terminus of Malaspina Glacier, the Pacific Ocean washes the base of a 20-m-high stagnant ice cliff. Erosion of a 20th century end moraine now permits high-tide surf and storm waves to reach the glacier ice. What appears to be the advance of a glacier terminus into the ocean is actually an encroachment of the ocean to the base of the ice cliff. As the cliff is undercut and melts, mature trees fall into the surf zone (fig. 162).

The surface of the piedmont lobe is covered by an intricate pattern of folded and convoluted moraines, the result of multiple surges and differential flow between its two primary tributaries (Washburn, 1935). These moraines, referred to by Washburn as “marble cake moraines,” have been repeatedly photographed, not only because of the information that can be learned about the ice dynamics and flow of Malaspina Glacier but also because of their stark beauty (figs. 37, 163). Post (1972) noted that the folding pattern in the Piedmont Lobe defined a 40-year surge cycle.

More than 50 years ago, continued melting of stagnant ice on the glacier’s southeastern side led to the formation of the ice-marginal Malaspina Lake (fig. 164). By the middle 1980s, through the melting and expansion of thermokarst pits, the irregular-shaped lake had increased in size to approximately 25×10 km. A 1986–87 surge reduced its area and width by nearly two-thirds (fig. 7).

The thickness of the piedmont lobe and the morphology of its basin have been investigated by both seismic surveys and ice-penetrating radar (IPR) surveys (Molnia and others, 1990). In 1951, Allen and Smith (1953, p. 755) used seismic reflection and gravity techniques to measure the ice thicknesses and the “configuration of the subglacial floor” of the piedmont lobe along a 16.1-km north-south traverse of the glacier. The range of ice thicknesses that they measured was between 340 and 620 m. They also determined that the basin underlying the glacier extends to at least 250 m below sea level and shallowed both northward toward the mountains and southward toward the ice margin.

In the late 1980s, the author used IPR to measure ice thickness at more than 50 locations and to determine the configuration of the glacier’s bed. The IPR data confirmed that most of the glacier is underlain by a fjord system extending about 50 km inland and about 200 m below sea level. The maximum ice thickness measured with IPR was more than 850 m, whereas the minimum measured thickness was less than 50 m (Molnia and others, 1990).

In spite of its remoteness, Malaspina Glacier was one of the most intensively observed glaciers in Alaska by the first decade of the 20th century. Martin (1907)

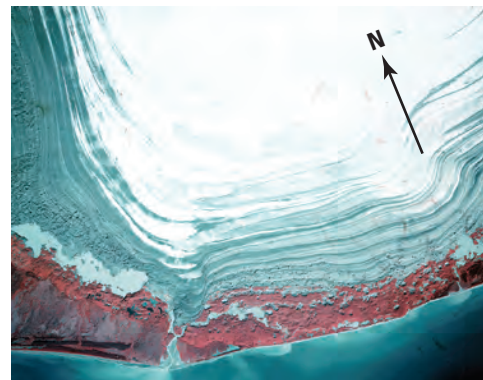


**Figure 161.**—August 1978 AHAP false-color infrared vertical aerial photograph of the southern margin of Malaspina Glacier. Vegetation, growing on the stagnant ice margin, is colored purple in this false-color infrared image. The area to the right of Fountain Stream (largest sediment plume) where the stagnant ice contacts the Gulf of Alaska is Sitkagi Bluffs. AHAP photograph no. LXXXF4931 from the GeoData Center, Geophysical Institute, University of Alaska, Fairbanks, Alaska. A larger version of this figure is available online.



**Figure 162.**—30 July 1999 south-looking oblique aerial photograph of part of the vegetation-covered, stagnant ice terminus of Malaspina Glacier at Sitkagi Bluffs. Pacific Ocean waters wash over the low barrier into the lagoon surrounding the ice margin. The barrier is actually a boulder lag deposit formed by the concentration of coarse sediment during many decades of glacier melting. Photograph by Bruce F. Molnia, U.S. Geological Survey.

described the construction of a 2.1×1.4-m, 1:80,000-scale, exaggeration-free plaster model (relief map) of the glacier and its adjacent area. The model was based on charts, maps, descriptions, and about 625 different photographs. Including himself, Martin credited the following impressive list of people and organizations as having provided these source materials: I.C. Russell, the Alaska Boundary Commission, Lt. Frederick G. Schwatka's *New York Times* Expedition, H.W. Seton Karr, William Libbey, the Topham Expedition, George Broke, the Canadian Boundary Commission, A.J. Brabazon, the Duke of Abruzzi, Vittorio Sella, H.C. Bryant, C.E. Hill, the Harriman Expedition, G.K. Gilbert,

**Figure 163.**—17 September 1972 oblique aerial photograph of the intricately folded medial moraines located on the eastern margin of the Seward Lobe of Malaspina Glacier. The convoluted patterns are the result of multiple surges and differential flow of ice between the Seward and Agassiz Lobes. The Samovar Hills are in the upper center of the photograph, below Mount St. Elias; the Hitchcock Hills are located at the right edge of the photograph. USGS photograph no. 72R8-45 by Austin Post, U.S. Geological Survey.



**Figure 164.**—25 August 1969 southeast-looking oblique aerial photograph of part of the southeastern terminus of Malaspina Glacier showing the developing Malaspina Lake. Within five years, continued melting of thermokarst pits in the buried ice underlying and surrounding the lake led to the joining of the two independent lake basins, here connected by a river. USGS photograph no. 69R2-084 by Austin Post, U.S. Geological Survey.



Henry Gannett, the U.S. Fish Commission, the U.S. Coast and Geodetic Survey, the U.S. Boundary Commission, Fremont Morse, the U.S. Geological Survey, A.G. Maddren, E. Blackwelder, R.S. Tarr, and others.

Sharp (1958a) stated that the latest major advance of Malaspina Glacier culminated 200±50 years ago (A.D. 1708–1808). However, in 1891, Russell photographed part of the eastern terminus of the margin of the Malaspina Glacier advancing into an adjacent forest (USGS Photo Library Russell 396 photograph). During most of the 20th century, the margin of the Malaspina Glacier has been stagnating, downwasting, and retreating. A very thick debris-covered zone 0.75– to 6-km wide surrounds the glacier's margin. In places, the debris is several meters thick and supports mature spruce and hemlock trees, some more than 150 years old. Plafker and Miller (1958) provided a comprehensive summary of the glacial history of the region and a detailed map of the piedmont lobe of Malaspina Glacier. A 1999 survey by the author documented continuing stagnation around the entire margin of the piedmont lobe, including tree- and sediment-covered areas. Unlike the case with a typical valley glacier — where terminus retreat is easily seen and generally characterized by newly exposed lateral moraines, trimlines, and fluted ground moraines — retreat of the terminus of the Malaspina Glacier is generally much harder to document. It is characterized by a decrease in the magnitude of relief of the margin's debris-covered surface and the development of additional vegetation.

Within the Malaspina Glacier system, the eastern two-thirds of Malaspina Glacier, Seward Glacier, Hayden Glacier, Marvine Glacier, and Newton Glacier (a tributary of the Agassiz Glacier) all surge (Post, 1969). The earliest reported surge occurred in 1906 and involved Marvine Glacier and the eastern piedmont lobe (Tarr, 1907). The glacier surged again between 1954 and 1956 (Sharp, 1958b) and again between 1986 and 1987.

Ablation studies conducted in the late 1940s (Sharp, 1951) and again in the late 1990s (Lingle and others, 1999) indicate that the piedmont lobe of Malaspina Glacier is rapidly thinning. Sharp (1951) reported that the annual surplus in the accumulation area was 175 cm of water in 1948–49, 66 cm of water in 1947–48, 43 cm of water in 1946–47, and 76 cm of water in 1945–46. On a daily basis, midsummer gross ablation of firn on upper Seward Glacier ranged from a mean of 7.6 mm to a maximum of 2.2 cm. Variation from year to year was significant; 1948 ablation was 75 percent greater than 1949 ablation. On Malaspina Glacier, daily gross ablation of clean ice in 1949 averaged 5.9 cm, a rate 900 percent greater than on upper Seward Glacier. With respect to mass balance, the glacier in 1947–48 had a negative mass balance of 3.5 km<sup>3</sup> (2.15×10<sup>14</sup> in<sup>3</sup>) of ice (3.19 km<sup>3</sup> water equivalent). In 1948–49, it had a positive mass balance of 1.48 km<sup>3</sup> (0.91×10<sup>14</sup> in<sup>3</sup>) of ice (1.35 km<sup>3</sup> water equivalent), the result of heavy precipitation and reduced ablation. Sharp concluded that, under existing climatological conditions, a “normal” year produces a deficit of about 3.28 km<sup>3</sup> (2.0×10<sup>14</sup> in<sup>3</sup>) of ice (2.98 km<sup>3</sup> water equivalent) and results in “a poor state of health.” Elsewhere, Sharp (1958b) reported that the glacier had experienced marked mass balance deficits in six of the nine budget years studied between 1945 and 1954. Of the other three years, one had a “good surplus,” and the other two were about balanced.

Lingle and others' (1999) numbers are based on laser altimeter profiles of both Seward and Malaspina Glaciers that were obtained by Keith Echelmeyer on 5 June 1995. These profiles were compared with a USGS digital elevation model (DEM) of Alaska at a nominal resolution of 15 m. They concluded that ablation of the Alaskan part of Seward Glacier resulted in a loss of 3.0±1.5 km<sup>3</sup> of water between the early-to-middle-1970s and 1995. The Seward Glacier lobe lost 48.5±5 km<sup>3</sup> of water, and the entire Seward Glacier-Malaspina Glacier system lost 63.0±13 km<sup>3</sup> of water. These amounts are equivalent to an average annual mass balance of -0.97±0.20 m and an annual volume loss of 2.52±0.52 km<sup>3</sup> of water.

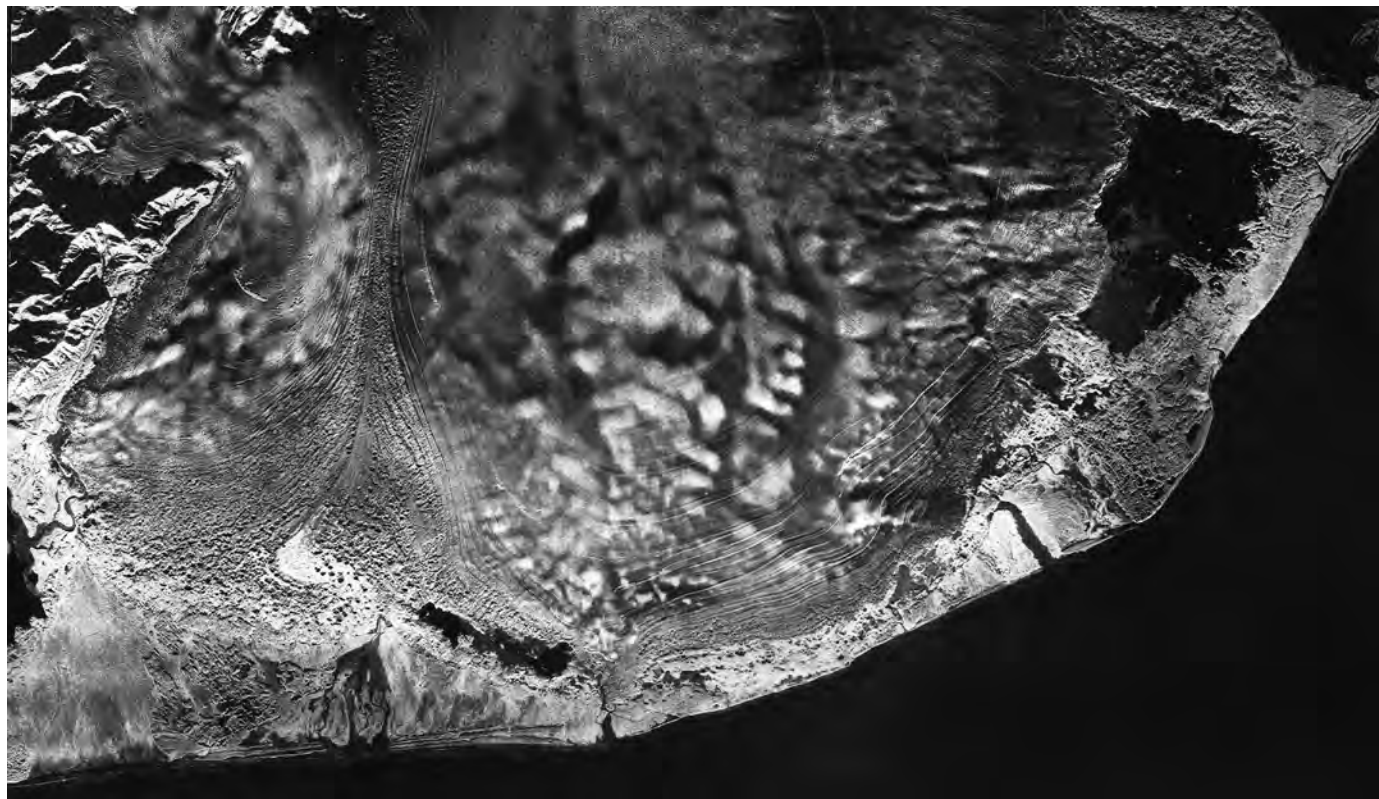


Meteorological records (Lingle and others, 1999) and a mass balance model have been combined by Tangborn (1999) to simulate changes in the Seward Glacier-Malaspina Glacier system for the period 1918–99. Their method generated daily runoff volumes and separated total runoff into two components: runoff produced by glacier melting and runoff contributed by precipitation. For the 82-year period, the annual simulated runoff for these glaciers averaged 3.05 m. Of this 3.05 m, 37 percent (or about 1.12 m of water equivalent per year) is derived from glacier melting.

Comparing these numbers gives the following results. Taking Sharp's (1958b) mean late 1940s summer ice ablation rate of  $-7.6 \text{ mm d}^{-1}$  and assuming a 150-day melt season yields an annual loss of glacier ice from the surface of the piedmont lobe of  $1.14 \text{ m a}^{-1}$  or, when extrapolated for the entire 20th century, a thinning of 114 m. Taking Lingle and others' (1999) average annual mass balance of  $-0.9 \pm 0.20 \text{ m}$  and converting it from water equivalent to ice thickness (assuming an ice density of 0.91) yields an annual loss of glacier ice from the surface of the piedmont lobe of  $1.07 \pm 0.22 \text{ m a}^{-1}$  or, when extrapolated for the entire 20th century, a thinning of  $107 \pm 22 \text{ m}$ . Taking Tangborn's (1999) annual loss of 1.12 m of water equivalent from the surface of the piedmont lobe, yields an annual loss of glacier ice  $1.23 \text{ m a}^{-1}$  or, when extrapolated for the entire 20th century, a thinning of 123 m. In any case, these methods suggest that anywhere from 85 to 129 m of thinning of the piedmont lobe of Malaspina Glacier occurred during the 20th century.

In addition to having been the subject of extensive photographic and satellite imagery coverage, Malaspina Glacier has been imaged on a number of occasions by digital space-borne radar, including missions of SEASAT, ERS-1 and ERS-2, SIR-C, and RADARSAT. It was also imaged with digital synthetic-aperture (SAR), X-band, side-looking airborne radar (SLAR) in November 1986. SLAR data, collected at X-band frequencies between 8.0 and 12.0 GHz at a resolution of about 10 m, revealed a complex pattern of surface features that mimic the configuration of the glacier's bed (fig. 165). Interpretation of these SLAR data provides insights into Malaspina Glacier's neoglacial history (Molnia, 1990a).

**Figure 165.**—November 1986 X-band side-looking airborne radar (SLAR) image of the piedmont lobe of the Malaspina Glacier, Alaska. The surface of the glacier, as seen in this synthetic aperture radar (SAR) image, produces a variety of unusual backscatter responses, including complex, multidirectional fjord- and glacier-like valleys, the margins of which are bounded by numerous cirquelike features; subparallel east-flowing dendritic valleys; and an arcuate lineament extending for about 65 km (Molnia and Jones, 1989). Field investigations have confirmed that these backscatter features correlate to topographic features on the surface of the Malaspina Glacier. The area shown is approximately 70 km by 40 km.



SLAR imagery depicts the surface morphology of the western two-thirds of the glacier as being characterized by broad “glacial valleys” with cirque-like indentations (fig. 165). The eastern one-third of the piedmont lobe is characterized by “dendritic valleys,” which are similar in size and morphology to present-day fluvial discharge channels that are situated along the margin of the glacier. Additionally, an arcuate east-west lineament more than 40 km long was identified cutting across the upper part of the piedmont lobe.

Interpretation of the SLAR data (Molnia and Jones, 1989) and the IPR depths allows a more complete understanding of the relationship between ice surface morphology and the topography and morphology of the underlying bedrock. The valley and lineament features, as well as other features on the glacier’s surface, mimic Malaspina Glacier’s subglacial bedrock morphology. IPR showed that these surface valley features also corresponded to bed morphology.

Some of these features seen on SLAR imagery may also be seen on Landsat imagery of Malaspina Glacier. Krimmel and Meier (1975) examined a conventionally processed, enhanced Landsat image acquired on 12 February 1973, with a Sun angle of 14° and a uniformly reflecting surface of new snow (fig. 160). They observed tonal variations and linear features on the glacier’s surface and noted that many apparent linear features had no positional relationship to known surface features. They stated (Krimmel and Meier, 1975, p. 396) that these tonal variations correspond to “very slight slope changes” and “may be a reflection of the basal features, and perhaps can be interpreted as subglacial stream beds or differential erosion of geologic structures or formations.” They suggested that some “may relate to bedrock roughness elements, and hence subtly reflect the subglacial topographic relief.”

Comparing the 1973 image with the X-band SLAR imagery shows that many of the apparently featureless “wavy patterns and lineaments” seen on the 1973 Landsat image correspond to the glacial valleys and segments of the arcuate lineament. The east-west-trending dendritic valleys, the numerous cirquelike features, and many other significant morphological details seen on the SLAR imagery are not identifiable on the Landsat imagery.

On X-band SLAR imagery, the three types of features have the following characteristics (Molnia, 1990b):

1. The “glacial valleys” are 10 to 25 km in length and about 1.5 km to 2.5 km in width. These valleys are parallel or subparallel to ice-flow directions mapped by Krimmel and Meier (1975). The cirquelike indentations are less than 1 km across, have abrupt changes in backscatter response across their boundaries, and have rounded amphitheater-like geometries. From south to north, the sharpness of the demarcation across the boundary of these cirquelike features decreases, possibly as a function of change in radar depression angle and (or) the thickness of ice cover. Field surveys in 1989 and 1990 confirmed that the glacier-like valleys correspond to topographic lows on the glacier’s surface, whereas the cirquelike features are topographically higher and heavily crevassed. Ice-penetrating radar soundings spaced approximately 100 m apart showed that the ice overlying these valleys is substantially thicker than the ice over adjacent intervalley highs.
2. The “dendritic valleys” are 6 to 12 km in length and 0.5 to 1.0 km in width. At least five distinct, subparallel, generally east-west-trending valleys are discernible on the SLAR imagery (fig. 165). The valleys are oblique to the ice-flow directions mapped by Krimmel and Meier (1975). Marginal cirquelike features are absent. Three of the best expressed examples of these valleys on the X-band imagery terminate adjacent to Malaspina Lake, near a large subglacial stream delta; another terminates near the headwaters of Alder Stream. Field surveys in 1989 and 1990, showed that the valleylike features were as much as 40 m lower than

adjacent highs and were characterized by fewer crevasses, minimal surface relief, a sediment veneer, and both standing and running water.

3. The arcuate lineament is a gently curving linear feature that extends in an east-west direction for more than 40 km. This arcuate lineament may be a trace of one of the boundary faults separating the North American Plate from the Pacific Plate, as is the case with the Fairweather Fault trench located approximately 120 km to the southeast. From west to east, it can be followed from the shoreline of Icy Bay, across outwash sediments and the upper part of Malaspina Glacier, to Malaspina Lake. The lineament crosses a large medial moraine complex characterized by thermokarst features (fig. 165). The trace of the lineament corresponds to the northern shoreline of Malaspina Lake.

The location of the transition between the two types of SLAR valley features corresponds to the inferred location of Hubbard Glacier's neoglacial maximum-advance terminal moraine complex position. Because both Hubbard Glacier and Malaspina Glacier could not have occupied the same space, the piedmont lobe of Malaspina Glacier must have been much smaller or, perhaps, even nonexistent at the time of the Hubbard Glacier maximum. A retracted Malaspina Glacier would open several deepwater embayments, each as much as approximately 50 km inland of the present shoreline. Following the retreat of Hubbard Glacier, expansion of Malaspina Glacier filled the embayments and overtopped the Hubbard Glacier moraine. Subglacial dendritic channels were ice proximal drainages that were overtopped by the advancing glacier. The retreat of Hubbard Glacier is dated at around 600 yr B.P. (Plafker and Miller, 1958); hence, as Sharp (1958a) suggested, the expansion of Malaspina Glacier to its present position could have occurred only during the past few hundred years.

Many of the higher elevation tributaries to Agassiz and Seward Glaciers head in cirques, passes, and valleys on the southern flanks of Mount Owen, Mount Eaton, Mount Augusta, Mount Baird, Mount Malaspina, Mount Bering, Mount Jeannette, Mount Newton, and Mount St. Elias. Dome Pass, at an elevation of approximately 1,300 m, is the divide between Agassiz and Seward Glaciers. Most years, the previous year's snow cover remains through the melt season. With the exception of several cirque glaciers, generally below 1,500 m elevation, no evidence of glacier thinning or retreat could be seen in this region.

### **Glaciers of Icy Bay**

Glaciers have existed in the vicinity of Icy Bay for at least several million years (Armentrout, 1983). The present-day Icy Bay is the result of 20th century retreat of the most recent ice mass to fill the basin (Alpha, 1975; Molnia, 1977, 1979; Porter, 1989). As recently as the middle of the first decade of the 20th century, there was no Icy Bay because the entire basin was filled by an expanded and combined Guyot-Yahtse-Tyndall Glacier System, which extended several kilometers beyond the basin into the Pacific Ocean. Retreat began before 1910 and, in most areas, has continued into the 21st century.

About 200 years earlier, when Vancouver explored the Alaskan coast in 1794, the Icy Bay basin was also filled by an expanded Guyot Glacier. Then, too, Guyot Glacier was connected to the Malaspina Glacier system and extended to the Gulf of Alaska. About 8 km to the east, a small bay, which Vancouver named Icy Bay, was open to the ocean. It had a compound spit on its eastern side, which Vancouver named Point Rioux. In 1852, Teben'kov published an atlas of maps prepared from soundings and topography compiled by Russian trappers, naval officers, and explorers between 1788 and 1807. The late 18th century Icy Bay mapped by Teben'kov (fig. 10A) closely resembles the bay described by Vancouver (AHAP false-color infrared vertical aerial photograph no. L171F4950 acquired on 21 June 1978). As mapped by Teben'kov, the bay is triangular in shape with a length of about 12 km, a

width of about 8 km at its mouth, and a maximum depth of about 27 m. By 1837, when Sir Edward Belcher (1843) sailed along the Gulf of Alaska coast, this second bay had been filled with sediment from the north and had disappeared. Molnia (1977) calculated that about 0.5 km<sup>3</sup> of glacially derived sediment was necessary to fill the bay to sea level. Even after the bay had been filled, its morphology was such that its former location could be discerned easily. The author visited this location several times during the 1970s. The position of the compound spit was easily recognized because of differences in vegetation and elevation.

By 1837, Guyot Glacier had retreated as much as 6 km, resulting in the formation of a small embayment at the mouth of the present Icy Bay. Less than 50 years later, when Seton Karr (1887) visited the area and Topham (1889) mapped it, Guyot Glacier had readvanced and again ended in the Pacific Ocean, seaward of the present coastline (Topham's map is fig. 2 of Tarr and Martin, 1914, p. 50). A large terminal moraine marks this maximum advance (fig. 166). Following the retreat of Guyot Glacier, melting of relict ice in the terminal moraine complex resulted in as much as 30 m of deepening at the mouth of the bay between 1922 and 1976 (Molnia, 1977).

The glaciers of Icy Bay still continue to produce large quantities of sediment. During the summer of 1995, rates of accumulation at the head of the bay, adjacent to Guyot Glacier, averaged 0.3 cm d<sup>-1</sup> and 0.02 cm d<sup>-1</sup> in mid-fjord (Jaeger and Nittrouer, 1999b).

At the beginning of the 20th century, when it was observed by Gilbert (USGS Photo Library Gilbert 332 photograph), the terminus of Guyot Glacier still extended into the Pacific Ocean. Retreat began before 1910, probably as early as 1904; by 1913, the retreating glacier had developed a 12-km-long calving face (USGS Photo Library Maddren 216 and 218–221 photographs). Retreat has continued into the 21st century. By the late 1930s, the glacier had retreated as much as 30 km to a location where its terminus was anchored at the narrow neck of the bay in the general location of present-day Kichyatt and Kageet Points. The terminus stayed close to this position for the next 15 years (USAF for U.S. Army Map Service vertical aerial photograph no. 51-AM-1, AST4, M-233, Roll 66, Frame 8860 acquired on 30 July 1957). Between 1957 and 1963, the terminus retreated another 5 km and separated into three calving termini by 24 August 1963 (fig. 167). In 1965, when the westernmost terminus separated into two distinct termini, Icy Bay was an approximately 40-km-long fjord with four separate fjord arms at its head. Porter (1989) calculated that the mean rate of retreat in Icy Bay was about 1 km a<sup>-1</sup> for the

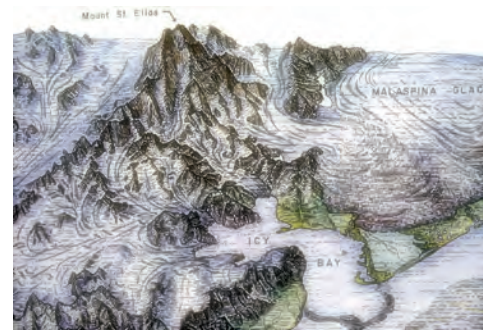


**Figure 166.**— Physiographic diagram modified from Alpha (1975) showing the position of the large terminal moraine that marks the maximum advance of the Guyot Glacier into the Gulf of Alaska prior to 1910 and the location of the glacier termini as they were at the end of 1974. The moraine can be seen at the mouth and following along part of the eastern shore of Icy Bay. A larger version of this figure is available online.

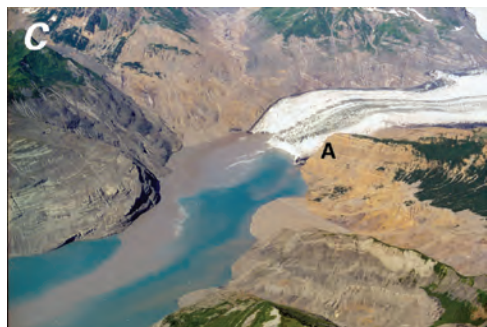


**Figure 167.**— 24 August 1963 oblique aerial photograph showing the retreating glaciers at the head of Icy Bay. In the six years between 1957 [see U.S. Air Force (for U.S. Army Map Service) vertical aerial photograph no. 51-AM-1, AST4, M-233, Roll 66, Frame 8860 acquired on 30 July 1957] and 1963, Tyndall and Yahtse Glaciers have separated from the retreating margin of Guyot Glacier and retreated approximately 5 km. USGS photograph no. K633-52 by Austin Post, U.S. Geological Survey.

period 1904 to 1926 and about  $0.4 \text{ km a}^{-1}$  for the period 1926 to 1989. When the glaciers were observed in 1998, 1999, 2003, and 2004, all were actively calving icebergs, and all of the fjords appeared to be lengthening except for Taan Fiord. Water depths in upper Icy Bay exceed 185 m (Post, 1983).

Tyndall Glacier (fig. 168), which has an accumulation area of around  $130 \text{ km}^2$  and an ablation area of around  $20 \text{ km}^2$ , has a total area of approximately  $150 \text{ km}^2$ . Its length is about 20 km, its AAR is about 0.85 and its calving face is about 1.1-km-long (table 2) (Viens, 1995). By 1960, Tyndall Glacier was separated from Yahtse Glacier and was retreating. Between 1960 and 1999, Tyndall Glacier retreated approximately 17 km. The position of its terminus stabilized after 1990 at the head of its fjord. Between 1981 and 1999, Tyndall Glacier thinned by more than 350 m at the location of the 1999 terminus. As

**Figure 168.**—Three oblique aerial photographs documenting the retreat of Tyndall Glacier from 1963 to 1998. During the 35-year period, Tyndall Glacier retreated more than 14 km. The point labeled A is common to all three photographs. **A**, 24 August 1963 photograph showing the retreating margin of Tyndall Glacier. USGS photograph no. K633-56 by Austin Post, U.S. Geological Survey. **B**, 12 September 1986 photograph showing the retreating margin of Tyndall Glacier. In the 23 years between 1963 and 1986, Tyndall Glacier retreated approximately 12 km. USGS photograph no. 86-R2-168 by Robert M. Krimmel, U.S. Geological Survey. **C**, 13 August 1998 photograph of the retreating margin of Tyndall Glacier. In the 12 years between 1986 and 1998, Tyndall Glacier retreated approximately 3 km, most of its retreat taking place before 1990. Since 1990, the position of the terminus has shown only slight change. The margin of Tyndall Glacier at sea level at this time is located only about 12 km from the summit of Mount St. Elias at an elevation of 5,489 m. This 46-percent gradient is one of the steepest on Earth. Photograph by Bruce F. Molnia, U.S. Geological Survey.



Tyndall Glacier retreated, the distance from sea level to the summit of Mount St. Elias continued to decrease. In 2004, the terminus at sea level was only about 12 km from the summit of Mount St. Elias (at an elevation of 5,489 m). This 46 percent gradient is one of the steepest on Earth.

Yahtse Glacier and the main distributary of Guyot Glacier sit at the head of the unnamed northern arms of Icy Bay and have been receding since 1938 (fig. 169). Their termini are separated by the Guyot Hills. They have a length of about 60 km, an accumulation area of about 1,365 km<sup>2</sup>, an ablation area of



**Figure 169.**—Three oblique aerial photographs showing changes in the slowly retreating Guyot and Yahtse Glaciers and other features at the head of Icy Bay between 1938 and 1986. In 1904, the Guyot-Yahtse Glacier tongue extended out into the Gulf of Alaska. Guyot and Yahtse Glaciers have drastically retreated due to the release of large quantities of icebergs, forming lower Icy Bay and the combined Guyot-Yahtse-Tyndall Glaciers in 1938 (fig. 169A). By 1969 (fig. 169B), much of upper Icy Bay was formed, the Guyot (left and center) and Yahtse (upper right) Glaciers had separated, and recession of the Tyndall had opened up the fjord seen in the lower right. **A**, 1938 oblique aerial photograph of the retreating Guyot-Yahtse Glacier. Icy Bay is in the foreground, and the Guyot Hills are in the right background. Photograph by Bradford Washburn, Museum of Science (Boston). **B**, 25 August 1969 oblique aerial photograph of Guyot and Yahtse Glaciers (left and right of Guyot Hills, respectively). When the photograph is compared with **A**, it is easy to see the separation and substantial retreat of the ice fronts. Photograph no. F693-49 by Austin Post, U.S. Geological Survey. **C**, 12 September 1986 oblique aerial photograph of the retreating margin of Guyot Glacier. The ice front has retreated a considerable distance along the southwestern edge of the Guyot Hills. Photograph no. 86-R2-180 by Robert M. Krimmel, U.S. Geological Survey. Figures 169B and C and caption courtesy of Robert M. Krimmel, U.S. Geological Survey.

about 65 km<sup>2</sup>, and a total area of about 1,430 km<sup>2</sup>. Their AAR is around 0.96; together, their calving face is approximately 5 km long (tables 2, 3) (Viens, 1995). When they were observed in 1998, 1999, 2003, and 2004, both were actively calving icebergs and retreating.

Guyot Glacier and Tsaa Fiord are separated by a peninsula of land named the Kahsteen Hills. A 0.4×0.3-km mass of stranded ice, here called the *Guyot Remnant*, was located on a large plateau on the peninsula. The remnant separated from the retreating Guyot Glacier after 1978. When the remnant was visited in 1998 and on 28 July 1999 (fig. 170), it was melting *in situ*, and an abandoned subglacial stream channel was found to have passed completely through the remnant. The remnant had completely melted by 2004.

*Tsaa Glacier* (fig. 171) is the name that Post (1983) applied to the glacier at the head of Tsaa Fiord. It has a length of about 20 km, an accumulation area of about 145 km<sup>2</sup>, an ablation area of about 6 km<sup>2</sup>, and a total area of about 150 km<sup>2</sup>. Its AAR is about 0.96, and its calving face is approximately 0.6 km long (tables 2, 3) (Viens, 1995). When the glacier was observed in 1998, 2001, 2003, and 2004, a large subglacial stream discharged substantial quantities of sediment-laden turbid water at its face. This water, in turn, cut a large gorge into the surface of the ice. No evidence of the stream was found

**Figure 170.**—28 July 1999 photograph of a part of 0.3-km-long subglacial channel under the Guyot Remnant. The remnant was probably separated from the retreating Guyot Glacier between 1978 and 1986. The location of Guyot Remnant can be seen in the lower left corner of figure 169C. Photograph by Bruce F. Molnia, U.S. Geological Survey.



**Figure 171.**—22 July 1980 oblique aerial photograph of the retreating four distributary-glacier margins at the head of Tsaa Fiord. During the 18-year-period from 1980 to 1998, the margin of Guyot Glacier in Tsaa Fiord retreated less than 1 km. Tsaa Glacier is the name Post (1983) applied to the distributary glacier at the head of the fjord. It is shown as a part of Guyot Glacier on many maps. Photograph by Bruce F. Molnia, U.S. Geological Survey.



in 1999. Several smaller glaciers, including *Grotto Glacier* are located on the western wall of the fjord. In 1999, *Grotto Glacier* was calving icebergs. All of the smaller glaciers showed evidence of thinning and recent retreat. In 2002, an unnamed glacier adjacent to *Grotto Glacier* advanced several hundred meters; it was retreating when observed in June 2003.

A recent study of rates of erosion by tidewater glaciers was conducted by Koppes and others (2001), who examined glaciomarine sediments deposited in fjords. They determined that glacier-erosion rates are recognized to be up to an order of magnitude higher than the highest rates found anywhere else on Earth and that these rates are representative of Alaskan tidewater glaciers during their extensive retreat over the past century. They examined Icy Bay to determine the influence of retreat rate on sediment yields by reconstructing the history of the amount of sediment output from retreating tidewater glaciers that would be necessary to produce the sediment packages observed in seismic profiles of the fjord. Using a numerical model of proglacial sedimentation, seismic profiles of glaciomarine sediments, and a history of terminus retreat, they calculated sediment flux as a function of time for Tyndall Glacier for the period 1961–99. They found that the average sediment flux during the 1961–99 period was  $5.32 \times 10^8 \text{ m}^3 \text{ a}^{-1}$ , corresponding to a basinwide erosion rate of  $35 \text{ mm a}^{-1}$ . During periods of rapid retreat, the erosion rate is up to three times higher, exceeding reported glacial-interglacial rates by more than an order of magnitude.

### Glaciers West of Icy Bay

Located west of Icy Bay, the Robinson Mountains are the southwesternmost extension of the St. Elias Mountains. In August 1913, A.G. Maddren visited the Robinson Mountains area and photographed many of the glaciers. In 1920, Taliaferro (1932, p. 764) also visited the region and commented “There is evidence in both the Yakataga and Katalla Districts that there has been a very recent retreat of the glaciers.” He also mentioned that about 30 m of retreat occurred at the unnamed glacier located at the head of Munday Creek during the period from 1910 to 1920.

In addition to Guyot Glacier, which originates in the eastern Robinson Mountains and flows into Icy Bay, several generally south- and southwest-flowing outlet glaciers descend from its central and western sides. From east to west, named glaciers include: (1) Beare Glacier (AHAP false-color infrared vertical aerial photograph no. L120F5992 acquired on 18 August 1978); (2) Lare Glacier; (3) White River Glacier (fig. 172); (4) Yakataga Glacier (fig. 172) and its three primary tributaries (Eberly, Yaga, and Watson Glaciers); (5) Leeper Glacier; and (6) *Miller Glacier* (fig. 173). Many unnamed cirque and small hanging glaciers also descend from the Robinson Mountains. Regardless of size, all show significant evidence of stagnation or retreat and thinning.

Yakataga Glacier is 21 km long and varies in width from 0.8 to 3.6 km. Located 9 km from the Gulf of Alaska, the stagnant terminus sits at an elevation of approximately 150 m. Miller (1957, p. 126) described the lower 3 km of Yakataga Glacier as being “largely covered by scattered low bushes to dense brush and a spruce forest near the terminus. On the inner face of the terminal moraine and adjacent part of the glacier are 30-cm diameter spruce trees, indicating that the lower end of the glacier has been inactive for at least the past fifty years.” At the end of the 20th century, the glacier margin continued to be characterized by ice stagnation and a cover of vegetation. Using photogrammetric techniques, Miller also determined that the surface velocity of Yakataga Glacier averaged  $114 \text{ m a}^{-1}$  or about  $30 \text{ cm d}^{-1}$  during the 16-year-period between 1938 and 1954. No movement could be detected in the lower 2.3 km of the glacier.

**Figure 172.** — 18 August 1978 AHAP false-color infrared vertical aerial photograph of the southeastern Robinson Mountains with White River, Eberly, and Yakataga Glaciers. All of the valley glaciers show evidence of retreat and stagnant ice. Numerous small north-flowing retreating cirque glaciers descend from the crest of the ridge between Eberly and White River Glaciers. All of the south-facing cirques on this ridge are ice free. Yakataga Glacier has vegetation growing on its debris-covered terminus. Ice from the Eberly Glacier no longer reaches Yakataga Glacier. AHAP photograph no. L119F6051 from the GeoData Center, Geophysical Institute, University of Alaska, Fairbanks, Alaska. A larger version of this figure is available online.

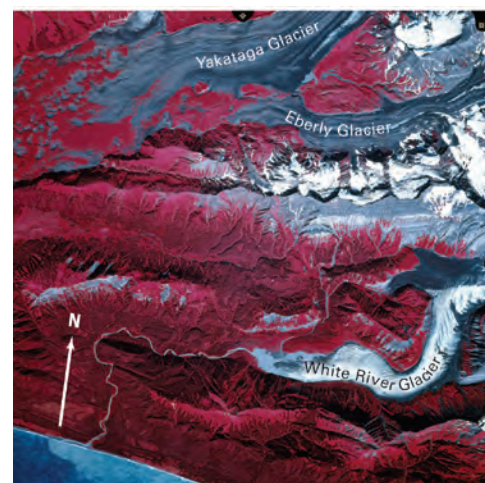




**Figure 173.**—12 September 1986 oblique aerial photograph showing Mount Miller and the numerous thinning and retreating glaciers on its south side. The largest, Miller Glacier, shows multiple evidence of past surges. USGS photograph no. 86-R2-200 by Robert M. Krimmel, U.S. Geological Survey.



**Northwestern St. Elias Mountains Segment:  
From the Canadian Border (long 141° W.) to  
White River, Chitistone River, Tana River,  
the Eastern Wall of the Valley of Tana Glacier,  
and the Southern Side of the Bagley Ice Valley**

Landsat MSS images that cover the northwestern St. Elias Mountains region have the following Path/Row coordinates: 68/17, 68/18, 69/17, 69/18, and 70/17. These areas are mapped on the USGS Bering Glacier, Alaska, and McCarthy, Alaska, 1:250,000-scale topographic maps (appendix A). Even though the easternmost Bering Glacier (including its tributaries Quintino Sella Glacier, Columbus Glacier, and Jefferies Glaciers) is located in the St. Elias Mountains, it will be described in the Chugach Mountains section. The adjacent Granite Range, southwest of the Chitina Glacier and River and placed in the Chugach Mountains by Orth (1967), will be discussed here with the St. Elias Mountains.

Several significant glaciers feed the Chitina River drainage system. North of the eastern Bagley Ice Valley and southeast of the Chitina River, the primary glacier is Logan Glacier; its tributaries include the Fraser, Baldwin, and Walsh Glaciers and an unnamed 23-km-long glacier. The Chitina River emanates from Chitina Glacier (about 70 km long and about 2 km wide), the named tributaries of which include Anderson (about 40 km long and about 2.5 km wide) and Tittmann Glaciers, and Ram Glacier with its tributaries Lamb and Ewe Glaciers. Barnard and Hawkins Glaciers drain into the northern side of the Chitina River.

Northwest-flowing Logan Glacier, which originates in Canada, is about 70 km long (Clarke and Holdsworth, 2002b). About 20 km west of the Canadian Border, it is joined by Walsh Glacier (fig. 174). Another 15 km to the west, Logan Glacier joins Chitina Glacier (fig. 175, 176). All are debris-covered, low-gradient glaciers. All also show significant evidence of recent and long-term stagnation. Before 1920, Moffit (1918) studied the region and documented much evidence of recent glacier retreat and thinning (USGS Photo Library Moffit 618 photograph). Folded moraines on Walsh and Logan



**Figure 174.**—Oblique aerial photograph looking east-southeast at the confluence of the Walsh and Logan Glaciers on 31 August 1984. Their combined flow merges with the terminus of the Chitina Glacier about 10 km to the northwest. USGS photograph no. 84-R3-058 by Robert M. Krimmel, U.S. Geological Survey.

Glaciers and on Baldwin Glacier (a tributary to Logan Glacier) indicate past surge history. Between 1961 and 1966, Walsh Glacier, with an accumulation area of approximately 545 km<sup>2</sup>, underwent a surge (Paige, 1965; Post, 1966, 1967b) that resulted in ice displacement of approximately 11.5 km. In the 13 months between August 1965 and September 1966, displacement in the terminus area totaled 4.0 km, an average daily advance rate of about 10 m d<sup>-1</sup>. This activity rejuvenated the adjacent stagnant terminus of Logan Glacier, causing it to advance about 1.5 km. Post (1967b, p. 765) stated that this surge was the largest for Walsh Glacier “in the past 100 years or more.” A surge of Anderson Glacier in the late 1960s (Horvath and Field, 1969) impacted the central Chitina Glacier in the early 1970s.

Logan, Walsh, and Chitina Glaciers were observed from the air by the author on 10 August 2001. No evidence of current surge activity was noted. All three showed significant evidence of ongoing thinning and stagnation and displayed elevated moraines and trimlines. Logan Glacier was the only one of the three to display white ice within a few kilometers of its terminus. All showed significant numbers of thermokarst pits and downwasting in their terminus regions.

Located west of Logan Glacier, the Granite Range comprises the northwestern part of the St. Elias Mountains. The only published information about the glaciers in this region is a brief series of observations made by D.J. Miller during 1958–59 field studies (Brabb and Miller, 1962). Granite Range glaciers with lengths greater than 6 km and located on the southern side or at the head of Granite Creek include (from west to east): (1) an unnamed glacier adjacent to Ross Green Lake, with a length of approximately 6 km and an area of approximately 8 km<sup>2</sup> (about 142°30'W.); (2) an unnamed glacier with a length of approximately 9 km and an area of approximately 9 km<sup>2</sup>; (3) an unnamed glacier, a distributary of Jefferies Glacier, with a length of approximately 9 km and an area of approximately 9 km<sup>2</sup>; and (4) an unnamed glacier located at the head of Granite Creek, with a length of approximately 21 km and an area of approximately 30 km<sup>2</sup>.

Granite Range glaciers with lengths greater than 6 km located on the northern side of Granite Creek include (from west to east): (1) an unnamed glacier with a length of approximately 10 km and an area of approximately 8 km<sup>2</sup> at the head of the Kiagna River; (2) an unnamed glacier with a length

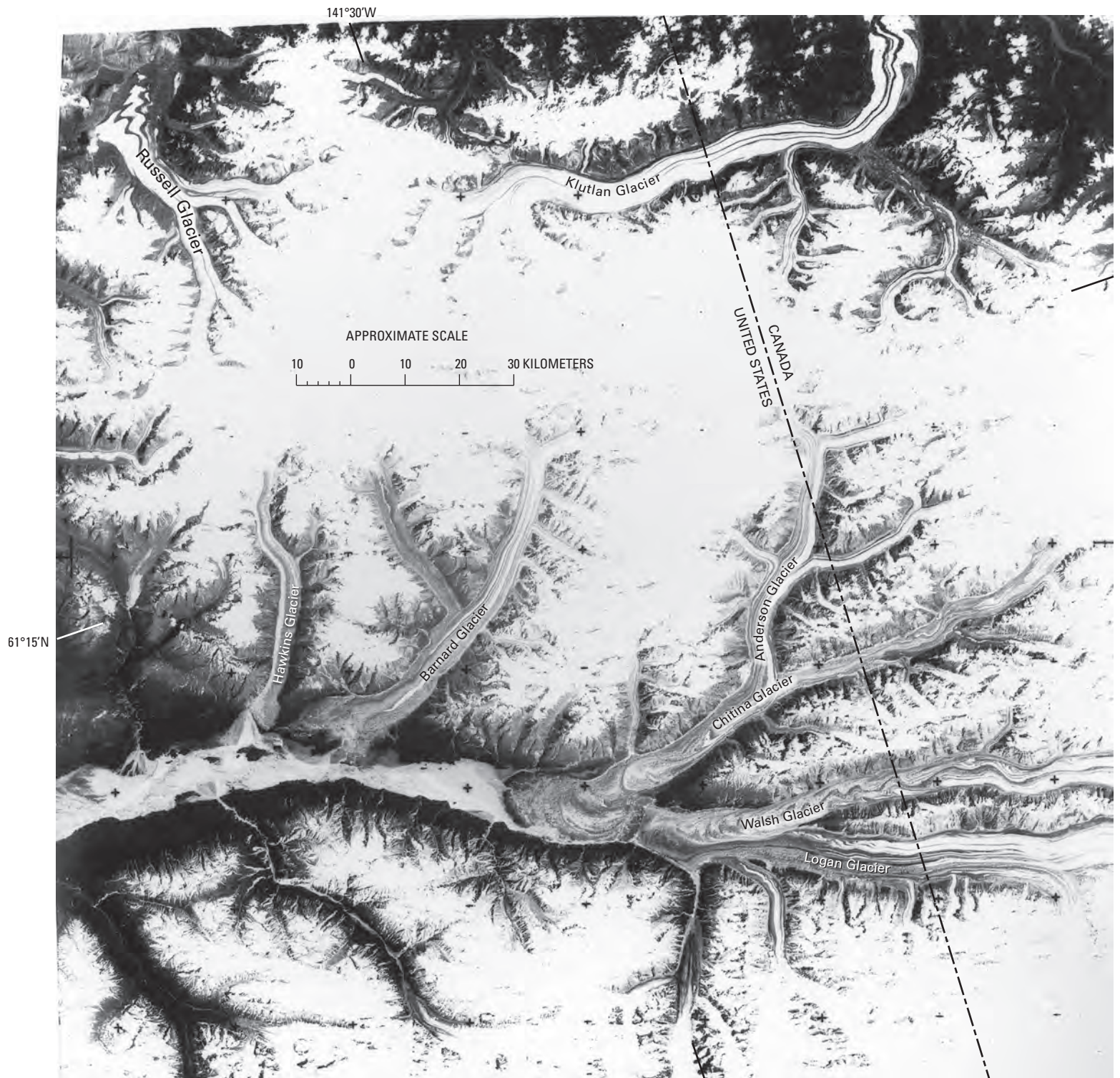


**Figure 175.**—Most of the major glaciers on this annotated Landsat 3 RBV image are known to surge. The Barnard Glacier, with parallel medial moraines delineating the contribution of each of the numerous tributaries, is an exception and does not surge. Walsh Glacier (fig. 174) had a several-year period of surge activity from 1961 to 1966, during which it had ice displacement of more than 10 km (Post, 1966, 1967a). The Chitina, Russell, and Klutlan Glaciers all have contorted medial moraines characteristic of surging glaciers. The Klutlan and Russell Glaciers both began another surge cycle in 1986. Landsat image (30853–19510–C; 5 July 1980; Path 68, Row 17) and caption courtesy of Robert M. Krimmel, U.S. Geological Survey.

of approximately 13 km and an area of approximately 20 km<sup>2</sup> at the head of the East Fork Kiagna River (fig. 177); (3) a 7-km-long unnamed glacier, located north of the previous unnamed glacier, (4) an unnamed glacier located at the head of Goat Creek with a length of approximately 26 km and an area of approximately 35 km<sup>2</sup>; (5) an unnamed glacier forming the western branch of Marble Creek with a length of approximately 6 km and an area of approximately 6 km<sup>2</sup>; (6) an unnamed glacier at the head of Marble Creek with a length of approximately 8 km and an area of approximately 8 km<sup>2</sup>; and (7) an unnamed glacier forming the eastern branch of Marble Creek with a length of approximately 8 km and an area of approximately 9 km<sup>2</sup>.

Miller (Brabb and Miller, 1962) reported on the outermost vegetated moraines of nine glaciers less than 5 miles [8.3 km] in length and located on the northern side of Granite Creek that he believed were formed between A.D. 600 and A.D. 1310. He thought that the moraines represent a greater length of these glaciers (14 to more than 120 percent, with an average of 60 percent) compared to their late 1950s positions. He (Brabb and Miller, 1962) also noted that “a minor glacial advance culminating within the past 300 years, and followed by recession continuing to the present, is recorded by bare or sparsely vegetated moraines bordering nearly all of the glaciers within the map area.” These moraines represent a greater length of the glaciers (6 to 33 percent, with an average of 24 percent) compared to their late 1950s positions. Many of these glaciers were observed by the author on 10 August 2001 (fig. 178). All showed significant evidence of recent thinning and retreat. Many were small remnants confined within parabolic lateral and end moraine complexes that towered above the ice. All were significantly smaller than their 1957 size as depicted on the Bering Glacier, Alaska, 1:250,000-scale topographic map (appendix A) and their size as shown on 1978 AHAP false-color infrared vertical aerial photography.

On the southern side of Granite Creek, on the northern side of Thompson Ridge, numerous valley glaciers have receded from their “Little Ice Age” maximum extent. Virtually all have deposited well-preserved lateral and terminal moraines (fig. 179).

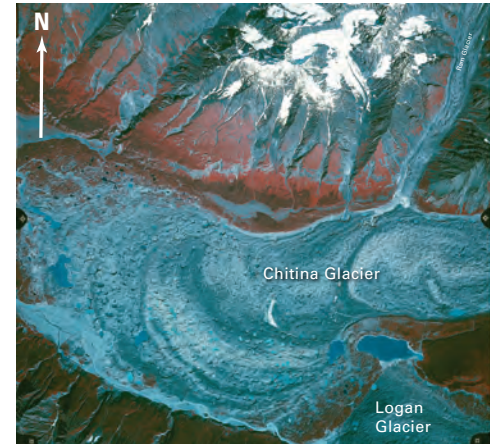
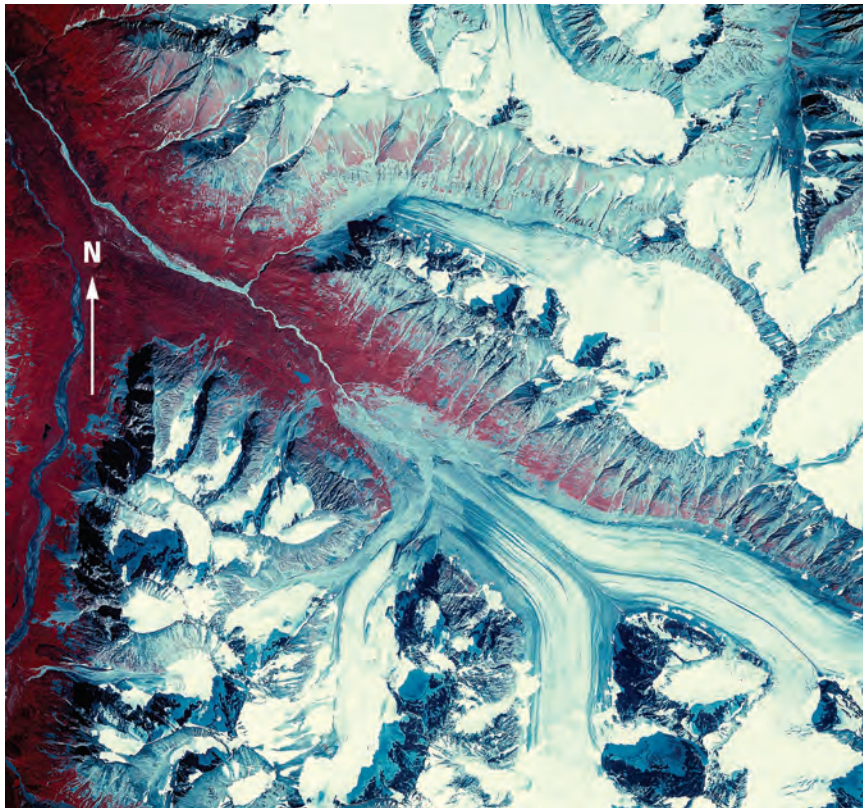


**Figure 176.**—9 July 1978 AHAP false-color infrared vertical aerial photograph of the terminus of Chitina Glacier and the confluence of Logan and Chitina Glaciers. Both glaciers are debris covered and possess numerous water-filled thermokarst pits. The terminus of Logan Glacier does not reach the terminus of Chitina Glacier. The two lakes adjacent to the terminal moraine of Logan Glacier are significantly larger on this photograph than they were when they were mapped by the USGS in 1959. There is no evidence of recent surge activity. Trimlines and ice-marginal lakes are additional evidence of glacier thinning and retreat. Abundant vegetation growing on the terminus of Chitina Glacier is additional evidence that the terminus is comprised of stagnant ice. AHAP photograph no. L110F6252 is from the GeoData Center, Geophysical Institute, University of Alaska, Fairbanks, Alaska. A larger version of this figure is available online.

**Figure 177.**—27 July 1982 AHAP false-color infrared vertical aerial photograph of the northern part of the Granite Range showing many of the glaciers near the headwaters of the East Fork of the Kiagna River. All of the glaciers shown are unnamed, retreating, and thinning. The largest has recently lost contact with its western tributary, which is also rapidly thinning and retreating. AHAP photograph no. L111F9504 from the GeoData Center, Geophysical Institute, University of Alaska, Fairbanks, Alaska.



**Figure 178.** — Two 10 August 2001 oblique aerial photographs showing significant retreat and thinning of small unnamed valley glaciers in the Granite Creek drainage of the Granite Range. Each of these glaciers is confined within a lateral/

terminal moraine complex that marks each glacier's "Little Ice Age" maximum position. **A**, Unnamed retreating glacier terminus located on the north side of Granite Creek, the longest of the glaciers draining south into Granite Creek. The retreat of this glacier started long enough ago that its lower valley is vegetated and its terminal moraine has been eroded away. USGS photograph no. 01-08-3AK-083 by Bruce F. Molnia, U.S. Geological Survey. **B**, Unnamed retreating glacier terminus located on the north side of Granite Creek. The glacier drains south into Granite Creek. In 1957, this glacier was in contact with its encircling moraine. USGS photograph no. 01-08-3AK-086 by Bruce F. Molnia, U.S. Geological Survey.

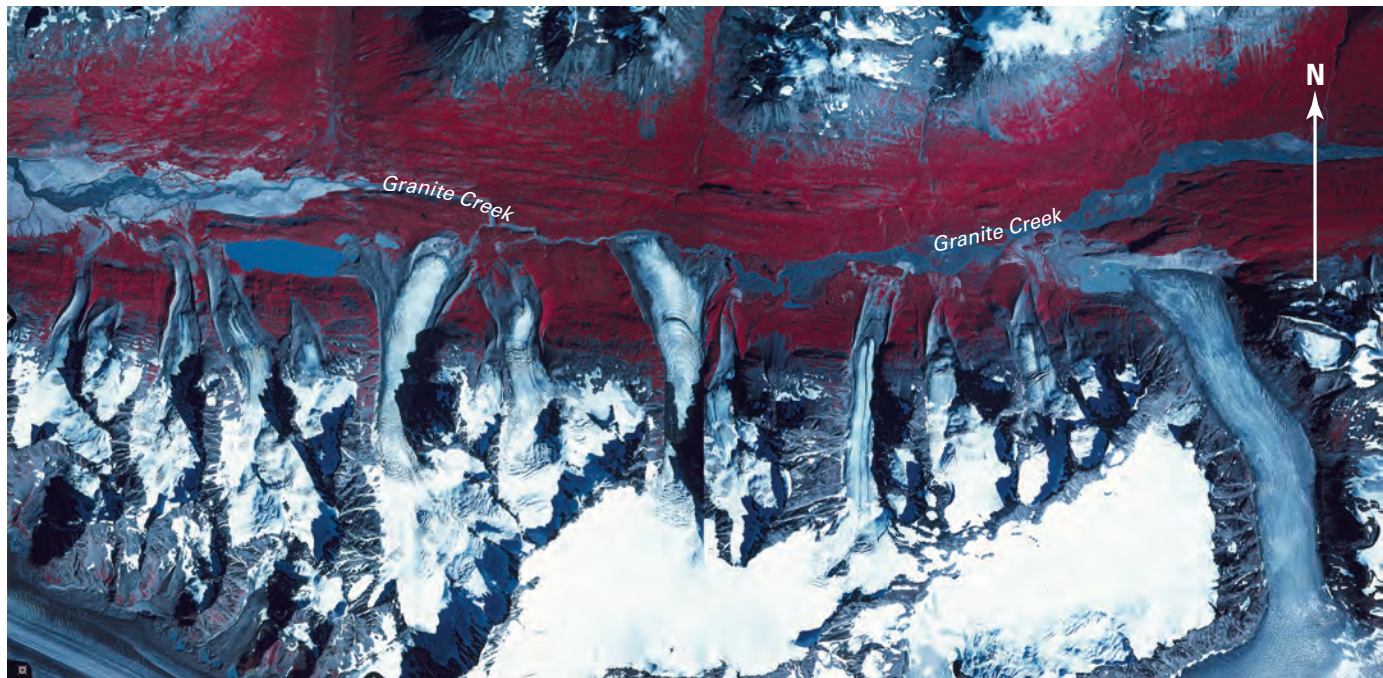


**Figure 179.** — 18 August 1978 AHAP false-color infrared vertical aerial photographic mosaic of numerous unnamed valley glaciers descending from Thompson Ridge toward the east-to-west-flowing Granite Creek, a tributary to the north-flowing Tana River. Virtually all of the glaciers have receded from their "Little Ice Age" maximum extent. Prominent

lateral and terminal moraines are evidence of this recession. Note the well-developed ogives on the valley glacier in the middle of the mosaic. AHAP photograph nos. L112F5840 and L112F5842 from the GeoData Center, Geophysical Institute, University of Alaska, Fairbanks, Alaska.

An unnamed glacier in the Goat Creek drainage on the southern side of the Chitina River, opposite Barnard Glacier, was observed surging by Robert M. Krimmel (USGS) in 1986 (written commun., 1987). The surge, which occurred sometime after midwinter, stranded avalanche cones, some 100 m above the glacier. Displaced ice produced a thick, bulging terminus. The upper glacier was largely unaffected by the surge (fig. 180).

Barnard Glacier, nearly 50-km-long, a non-surge-type glacier, drains into the Chitina River about 20 km west of Chitina Glacier. Located on the southern side of Mount Bona, its 30-km-long main trunk flows in a southwesterly direction with only a gentle bend to the west. When Bradford Washburn first photographed it in 1938 (fig. 37), the upper part of the glacier displayed more than 25 subparallel medial moraines, which were clearly visible on its surface. When Robert M. Krimmel (USGS) photographed it 46 years later on 31 August 1984 (fig. 181), an elevated lateral moraine on its western side and an increased sediment accumulation on its eastern margin (both signs of glacier thinning) were the only signs of change. The debris-covered terminus contains many thermokarst pits and is stagnating in place. In 2004, 20 years later, a continuation of this trend was observed by the author.

Hawkins Glacier is approximately 30 km long and averages about 1.5 km-wide. Minimally observed, the glacier has a debris-covered stagnant terminus and shows no evidence of surge-type activity. Many subparallel moraines are exposed near its head. It drains into the Chitina River approximately 5 km west of Barnard Glacier.

North of the Chitina River and west of Hawkins Glacier, Twaharpies and Chitistone Glaciers and other glaciers of the University Range drain westward into the Chitistone River. Russell Glacier with its numerous unnamed tributaries, Giffin Glacier with its tributary Gooseneck Glacier, and Guerin Glacier all drain north into the White River. The massive Klutlan Glacier, with more than a dozen unnamed tributaries, and the smaller Natazhat Glacier both originate in the United States and cross the border into Canada, where their discharge enters the White River. Because of their remote location, these glaciers have received little recent attention.

Denton and Karlén (1977) examined many of the glaciers in the White River drainage and Skolai Pass area. Specifically, they described the characteristics of Natazhat, Guerin, Giffin, *Sheep*, Russell, and *Moraine Creek* Glaciers and an unnamed glacier between Guerin and Giffin Glaciers. Generally, all have a similar history characterized by "Little Ice Age" advances culminating between the 15th century and the early 20th century. All have vegetated and debris-covered termini and are fronted by older ice-cored moraines. For example, the non-surge-type Guerin Glacier heads on 4,031-m-high Mount Natazhat and terminates in a debris-covered margin at an elevation of 1,500 m. Its firn limit is situated at 2,286 m. Fronting the glacier is a 750-m-wide belt consisting of three nested bands of older hummocky, kettled, ice-cored moraine. The outer moraine terminates at an elevation of 1,173 m. Lichenometry indicates that the outer moraine dates from around A.D. 340 (1,650 lichen yr B.P.). The middle moraine dates between about A.D. 1270 and about 740 (1,230 14C yr B.P. and 800 lichen yr B.P.) and the inner moraine between A.D. 1500 and the 20th century.

Giffin Glacier, a surge-type glacier, is fed by eight tributary glaciers. All head on a ridge that includes 3,330-m-high Mount Sulzer. A ninth tributary, now separated, joined the terminus of an expanded early 20th century Giffin Glacier. In 1970, the glacier terminated in a debris-covered margin at an elevation of 1,250 m. Firn limits of its tributaries are situated between 2,225 and 2,286 m. Like Guerin Glacier, Giffin Glacier is fronted by a ring of several nested bands of ice-cored moraines.

**Figure 180.**—A small, actively surging glacier in Goat Creek drainage south of Barnard Glacier on 14 September 1986. The unnamed glacier is about 6 km long in this view. Previous to this surge, it was separated from the foreground glacier by at least 1 km. The surge occurred sometime after midwinter, because the stranded avalanche cones, some 100 m above the glacier, were formed in the winter while the glacier was still thick in its midglacier section. Ice was transferred from the midglacier section to the now-bulging terminus. The upper glacier was largely unaffected by the surge. USGS photograph no. 86-R3-228 and caption by Robert M. Krimmel, U.S. Geological Survey.



**Figure 181.**—Oblique aerial photograph of Barnard Glacier (figs. 38, 175) on 31 August 1984. It is a major nonsurging glacier in the midst of several major surging glaciers; Walsh and Russell Glaciers are both nearby. The medial moraines are clearly formed at the juncture of the glacier's branches; they are carried downglacier and remain nearly parallel. If there is a disruption in normal flow, as in a surge, the regular pattern of these medial moraines would be altered. Compare the moraines of the Barnard to those of the Muldrow Glacier (figs. 405, 407) and Black Rapids Glacier (fig. 388). It is this difference in moraine patterns that allows sequential images, such as those from Landsat, to distinguish surging from nonsurging glaciers. USGS photograph no. 84-R3-051 and caption by Robert M. Krimmel, U.S. Geological Survey.



*Sheep Glacier* (Denton and Karlén, 1977), a surge-type glacier, also heads on the flank of 3,330-m-high Mount Sulzer and terminates in a debris-covered margin at an elevation of 1,585 m. Fronted by a belt of ice-cored moraine, the upper glacier surged in 1966.

Russell Glacier, a surge-type glacier with a length of 37 km, drains 4,766-m-high Mount Churchill, 5,005 m-high Mount Bona, and many of the higher peaks east of the University Range. Its firn limit is at approximately 2,286 m. Its width ranges from more than 1.5 to approximately 5.5 km. The terminus is a massive ice-cored moraine complex that plugs the head of the White River valley and extends downvalley to an elevation of about 1,219 m (USGS Photo Library Capps 80–83 photographs taken in ca. 1909). Field and Collins (1975) stated that the glacier changed very little through the first half of the 20th century. They describe “progressive wastage” through the 1970s. Denton and Karlén (1977, p. 92) stated that “In the lower region of the glacier, medial moraines become bent and then compressed, until they form a nearly continuous mantle of surficial debris covering the glacier ice and grading into the Holocene moraines.” Robert M. Krimmel (USGS) (oral commun., 1992) stated that the Russell Glacier was beginning to surge in 1986. Some early photographs depict a *Skolai Glacier*, perhaps the westward-flowing distributary from Russell Glacier, that flowed through Skolai Pass into the Skolai Creek drainage.

Denton and Karlén’s (1977) *Moraine Creek Glacier*, a former tributary to the Russell Glacier, is located in the next drainage south of Wiley Creek. Before separating in the early 20th century, it was the ninth tributary to Russell Glacier. It surged just before August 1957. Like all of the other nearby glaciers, its debris-covered terminus grades into a series of Holocene moraines.

Klutlan Glacier also has contorted medial moraines characteristic of a surge-type glacier. Like the Russell Glacier, Robert M. Krimmel (USGS) (oral commun., 1992) observed the Klutlan Glacier beginning to surge in 1986. A previous surge between 1961 and 1963 produced 4 km of ice displacement. Nearly 45 km of Klutlan Glacier are in Alaska. With a length of more than 80 km, it is the longest glacier in the northern St. Elias Mountains. Several of its unnamed tributaries are more than 15 km in length. Like most of the other glaciers in the region, its vegetation-covered, debris-laden terminus is suggestive of ongoing stagnation. Like Klutlan Glacier, the much smaller Natazhat Glacier flows from Alaska into Canada, where it too terminates in a debris-covered margin fronted by several older moraines.

## Summary

During the period of the Landsat baseline, 1972–81, Johns Hopkins, Grand Pacific, Margerie, Brady, North Crillon, Lituya, Hubbard, and Turner Glaciers were advancing. La Perouse and South Crillon Glacier were stable, with the position of their termini fluctuating from year to year. Available evidence suggests that all other valley and outlet glaciers in the St. Elias Mountains were thinning and retreating.

At the beginning of the 21st century, North Crillon, Lituya, Hubbard, and Turner Glaciers were advancing. Johns Hopkins, La Perouse and South Crillon Glacier were stable, with the position of their termini fluctuating from year to year. All other valley and outlet glaciers in the St. Elias Mountains continued to thin and retreat.



# Chugach Mountains

## Introduction

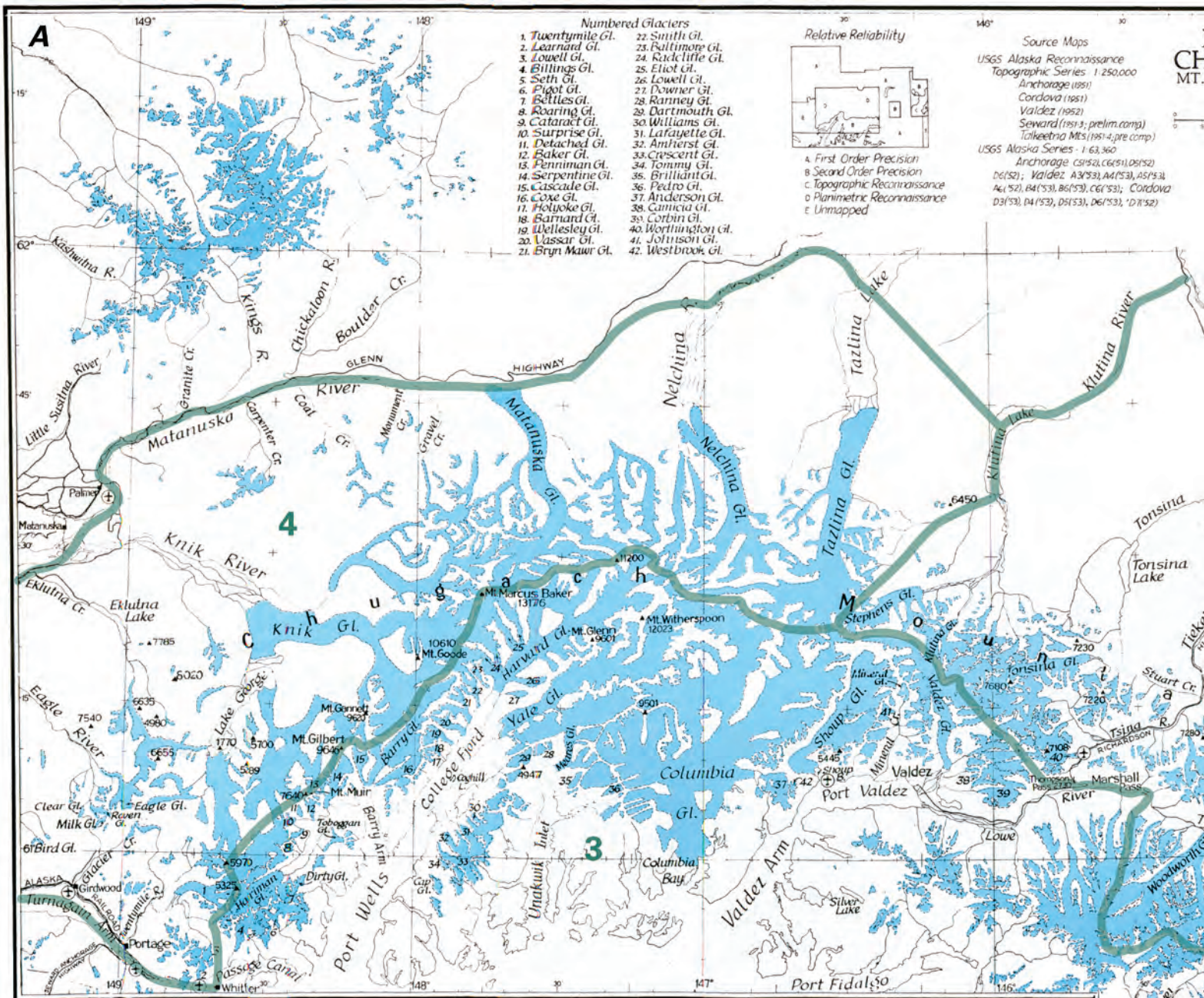
The Chugach Mountains are a 400×95-km-wide mountain range that extends from Turnagain Arm and Knik Arm on the west to the eastern tributaries of Bering Glacier, Tana Glacier, and Tana River on the east. On the north, the Chugach Mountains are bounded by the Chitina, Copper, and Matanuska Rivers. On the south, they are bounded by the northern Gulf of Alaska and Prince William Sound. The Chugach Mountains contain about one-third of the present glacierized area of Alaska (figs. 1, 2, 182) — 21,600 km<sup>2</sup>, according to Post and Meier (1980, p. 45) — and include one of the largest glaciers in continental North America. Bering Glacier is a piedmont outlet glacier with an approximate area of 5,200 km<sup>2</sup> (Viens, 1995; Molnia, 2001, p.73) (table 2).

The eastern part of the Chugach Mountains is covered by a continuous series of connected glaciers and accumulation areas (Field, 1975b). Several studies have characterized this region and adjacent regions as areas experiencing a significant 20th century retreat of its glaciers (Meier, 1984; Molnia and Post, 1995; Arendt and others, 2002; Meier and Dyurgerov, 2002). A study by Sauber and others (2000) examined the effect of this regional ice loss on crustal deformation in the eastern Chugach Mountains. Recognizing that the range of annual thinning of glaciers in this region ranges from 1–6 m a<sup>-1</sup>, they calculated that uplift in ablation regions of these glaciers ranges from 1 to 12 mm a<sup>-1</sup>, the greatest uplift being located just east of the Chugach Mountains, in the Icy Bay region. Sauber and Molnia (2004) hypothesized that continuing loss of glacier ice volume could lead to a future increase in very low magnitude earthquakes.

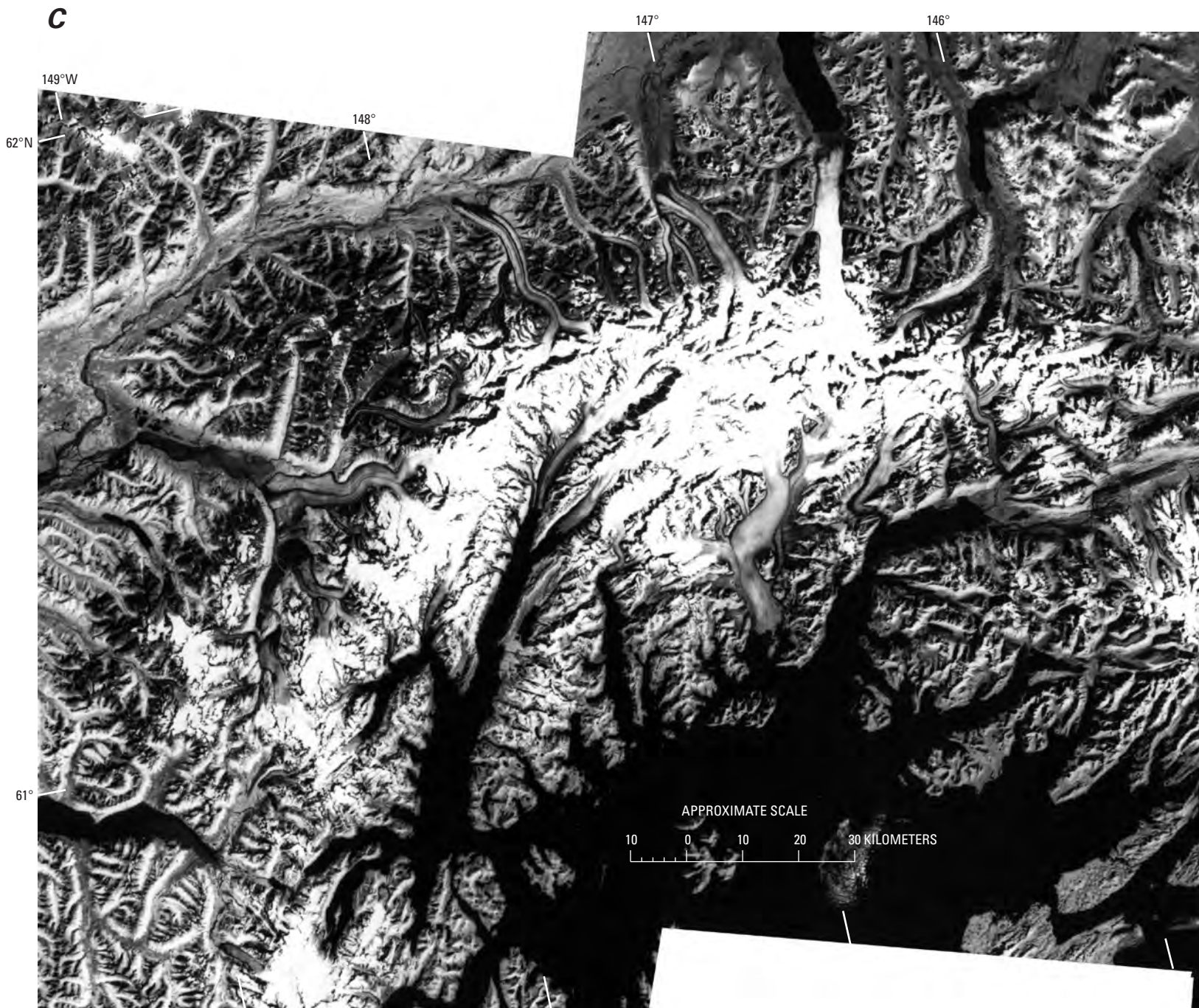
For ease of description, the Chugach Mountains are divided into four segments (fig. 182A): the Bering Glacier System Segment; the Copper River Drainage Segment, which has four subdivisions and includes glaciers that drain directly into the Copper River Delta; the Prince William Sound Segment, which has two subdivisions; and the Northwestern Chugach Mountains Segment, which also has two subdivisions.

The Bering Glacier System is bounded on the east by the St. Elias Mountains; on the south by the Gulf of Alaska; on the west by the Bering River, Canyon Creek, Carbon Mountain, and the Steller Glacier-Martin River Glacier divide; and on the north by an unnamed sinuous ridge that includes the summit of Mount Hawkins, the western Bagley Ice Valley-Tana Glacier divide, and the relatively straight ridge that includes Juniper Island. The eastern part of the Bering Glacier System is located in the western St. Elias Mountains and includes Quintino Sella and Columbus Glaciers, its eastern tributaries, both of which originate in Canada.

The Copper River Drainage Segment is bounded on the east by an irregular border that includes the Bering River, Canyon Creek, Carbon Mountain, the Steller Glacier-Martin River Glacier divide, the northern and eastern sides of Tana Glacier, and the Tana River; on the north by the Chitina River; on the northeast by the upper Copper River; and on the northwest by the Klutina River and Lake, Hallet River, and the divide between Tazlina Glacier and Stephens Glacier. On the southwest, it is bounded by the sinuous ridge that connects Mount Shouplina, Mount Cashman, Mount Mahlo, Mount Schrader, the divide between Valdez Glacier and Tonsina and Tsina Glaciers, Thompson Pass, Marshall Pass, the divide between Marshall Glacier and the unnamed glacier east of Deserted Glacier, the divide between the Gravina River basin and the north-flowing glaciers to its north, the divide between the Scott Glacier and the Rude River, including Cordova Peak, and Heney Range; and on the south by the Gulf of Alaska. This area has four subdivisions: Martin River Glacier–Martin River–lower Copper River–Bremner River–West Fork



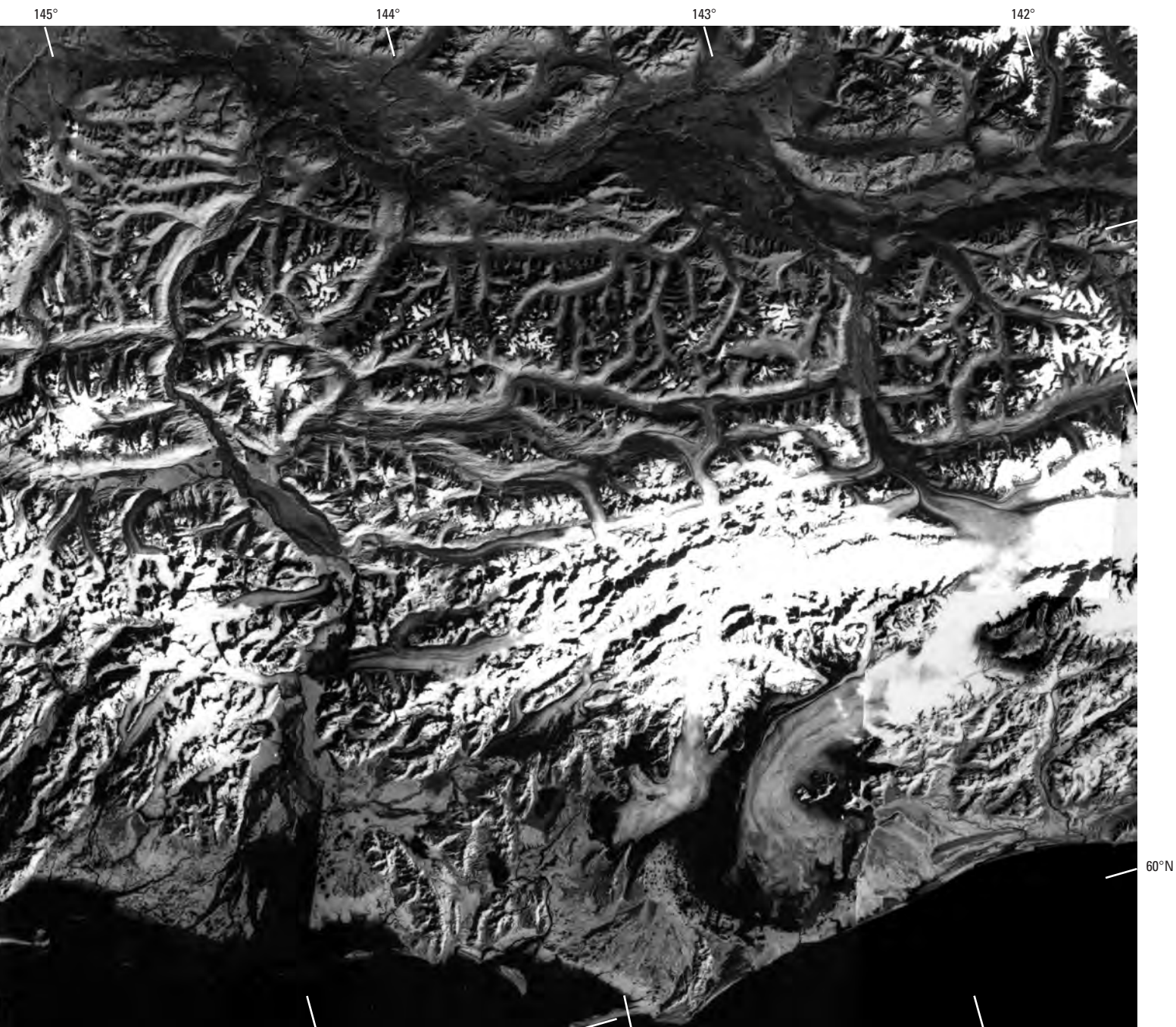




Tana River–Tana Glacier subdivision, located east of the Copper River; the Bremner River–upper Copper River–Chitina River–Tana River subdivision, located east of the Copper River; the western Copper River Delta–lower Copper River–Tasnuna River subdivision on the west side of the Copper River; and the Cleave Creek Glacier–upper Copper River–Stephens Glacier–Tonsina Glacier Northwestern subdivision.

The Prince William Sound Segment is bounded on the east by an irregular border running from Heney Range to the divide between the Scott Glacier and the Rude River, including Cordova Peak, to the divide between the Cordova Glacier and the north-flowing glaciers to its north, to the divide between Marshall Glacier and the unnamed glacier east of Deserted Glacier, to Marshall Pass, to Thompson Pass, to the valley north of Keystone Glacier, to the perimeter of the basin of Camicia Glacier, to Mount Schrader, west of Valdez Glacier in the Chugach Icefield; on the north by the sinuous ridge that connects Mount Schrader, Mount Mahlo, Mount Cashman, Mount Shouplina, Madean Peak, Tazlin Tower, Flat Top Peak, Mount Haley, Mount Fafnir, Mount Thor,

**Figure 182.—C,** Landsat MSS image mosaic of the Chugach Mountains. Landsat images (2956–19350, band 7; 4 September 1977; Path 68, Row 18; 1422–20212, band 7; 18 September 1973; Path 70, Row 17; 2976–19452, band 7; 24 September 1977; Path 70, Row 18; 30209–20233, band 7; 30 September 1978; Path 72, Row 17; and 30175–20345, band 7; 27 August 1978; Path 74, Row 17) are from the U.S. Geological Survey, EROS Data Center, Sioux Falls, S. Dak.



and a number of unnamed peaks between Mount Thor and Mount Marcus Baker; on the west by the sinuous ridge that connects Mount Marcus Baker and Mount Gilbert with Passage Canal, west of Billings Glacier; and on the south by Prince William Sound. This area has two subdivisions: the Heney Range to the eastern side of Valdez Arm subdivision and the Northern Prince William Sound subdivision. Glaciers on Montague Island, the largest island in Prince William Sound, are described in the Kenai Mountains section.

The Northwestern Chugach Mountains Segment of the *Chugach Icefield* is bounded on the east by Hallet River and Klutina Lake and River and on the south by the divide between Stephens and Tazlina Glacier and by the sinuous ridge that extends west of Mount Shouplina and connects Madean Peak, Tazlin Tower, Flat Top Peak, Mount Haley, Mount Fafnir, Mount Thor, and a number of unnamed peaks between Mount Thor and Mount Marcus Baker. Then the boundary continues to the southwest, connecting with Mount Gilbert and Passage Canal, extends along Passage Canal, and continues to the north of Portage Glacier and along Turnagain Arm. The region is bounded on

the west by Knik and Matanuska Rivers and on the north by the Matanuska River, Eureka Creek, and Nelchina River. This segment contains some of the larger valley glaciers of the Chugach Mountains, including Knik, Matanuska, Nelchina, and Tazlina Glaciers. This area has two subdivisions: the north-flowing, large valley glacier subdivision; and the Turnagain Arm–Western Chugach Mountains subdivision.

Landsat MSS images that cover the Chugach Mountains have the following Path/Row coordinates: 68/18, 69/17, 69/18, 70/17, 70/18, 71/17, 71/18, 72/17, 72/18, 73/17, and 74/17 (fig. 3, table 1). The Chugach Mountains contain several thousand glaciers.

## **Bering Glacier System Segment**

### **Introduction**

Bering Glacier is one of the most intensively studied glaciers in Alaska. In addition to historical descriptions, much of what we know about the piedmont outlet glacier is derived from the interpretation of an extensive time series of remotely sensed data sets that include the following: (1) more than 75 vertical and oblique aerial photographic data sets, containing about 10,000 photographs, acquired between 1938 and 2002; (2) more than 50 multispectral scanner (MSS), thematic mapper (TM), and enhanced thematic mapper (ETM+) Landsat images (1972–2002); (3) about 50 digital satellite, space shuttle, and SLR or SLAR images (1978–95); and (4) about 35 hours of airborne video (1989–2000). Additionally, field observations and ice-surface measurements have provided complementary information that enhances the interpretation of remotely sensed data sets, including (1) mapping of glaciological features by the author (1974–2002); (2) time-lapse photography from in place camera systems during the latest surge (1993–96); (3) sequential photography from reoccupation of marked photo stations (1948–2002); (4) discharge measurements and flow information from telemetering stage recorders (1991–95); (5) ice-penetrating radar surveys (1990–93); (6) high-resolution marine seismic-reflection surveys of Vitus Lake, the glacier's principal ice margin lake (1991 and 1993); (7) seismic-refraction surveys of the glacier's outwash plain (1991–93); (8) dendrochronological and tree coring studies (1976–2001); (9) monitoring of movement and erosion stakes at selected terminus sites (1993–96); (10) precision location of features using differential GPS (1992–2001); and (11) sampling for water chemistry and suspended sediment load (1976–80, 1993, 1995). Lastly, a complete topographic and image map base exists for monitoring and recording changes. Topographic mapping by USGS field parties began during the first half decade of the 20th century. Subsequently, the USGS (1959, 1984) prepared 1:250,000-scale (appendix A) and 1:63,360-scale (appendix B) topographic quadrangle maps of the entire glacier using 1957 and 1972 aerial photography. The BLM produced a satellite image base map at 1:100,000-scale and a set of individual 1:63,360-scale quadrangle maps based on a 19 June 1991 Landsat TM acquisition.

The Bering Glacier System (figs. 5, 183) is one of the largest glacier systems in continental North America, with an approximate area of 5,200 km<sup>2</sup> (Viens, 1995; Molnia, 2001, p. 73) (table 2); it is the largest surging glacier known on Earth, outside the Greenland and Antarctic ice sheets. The eastern part of the Bering Glacier System originates in Canada in the St. Elias Mountains, at an elevation above 5,000 m, on the western flanks of the Mount Logan–King Peak massif about 25 km east of the U.S. border [see Clarke and Holdsworth 2002b]. Bering Glacier covers more than 6 percent of the glacierized area of Alaska. The ice flows west-southwestward for more than 120 km through a 7.5- to 12.5-km-wide subglacier valley in the Chugach Mountains. Before turning to the southwest, it flows through a 50-km long by 10-15-km-wide subglacier central valley and then joins the Steller Glacier to form an outlet piedmont

lobe with a diameter of more than 30 km (fig. 183). At 191 km, Bering Glacier is the longest glacier in continental North America. All parts of Bering Glacier lie within 100 km of the Gulf of Alaska. Part of Jefferies Glacier, which is located in the valley north of the Bagley Ice Valley, flows to the south and contributes ice to the eastern Bagley Ice Valley. The remainder of the ice flows to the west and northwest and is the primary source of Tana Glacier.

Bering Glacier has an accumulation area of approximately 3,200 km<sup>2</sup> (Viens, 1995) (table 2), most of which is in the Bagley Ice Valley. The ablation area, which includes the southwestern part of the Bagley Ice Valley, the

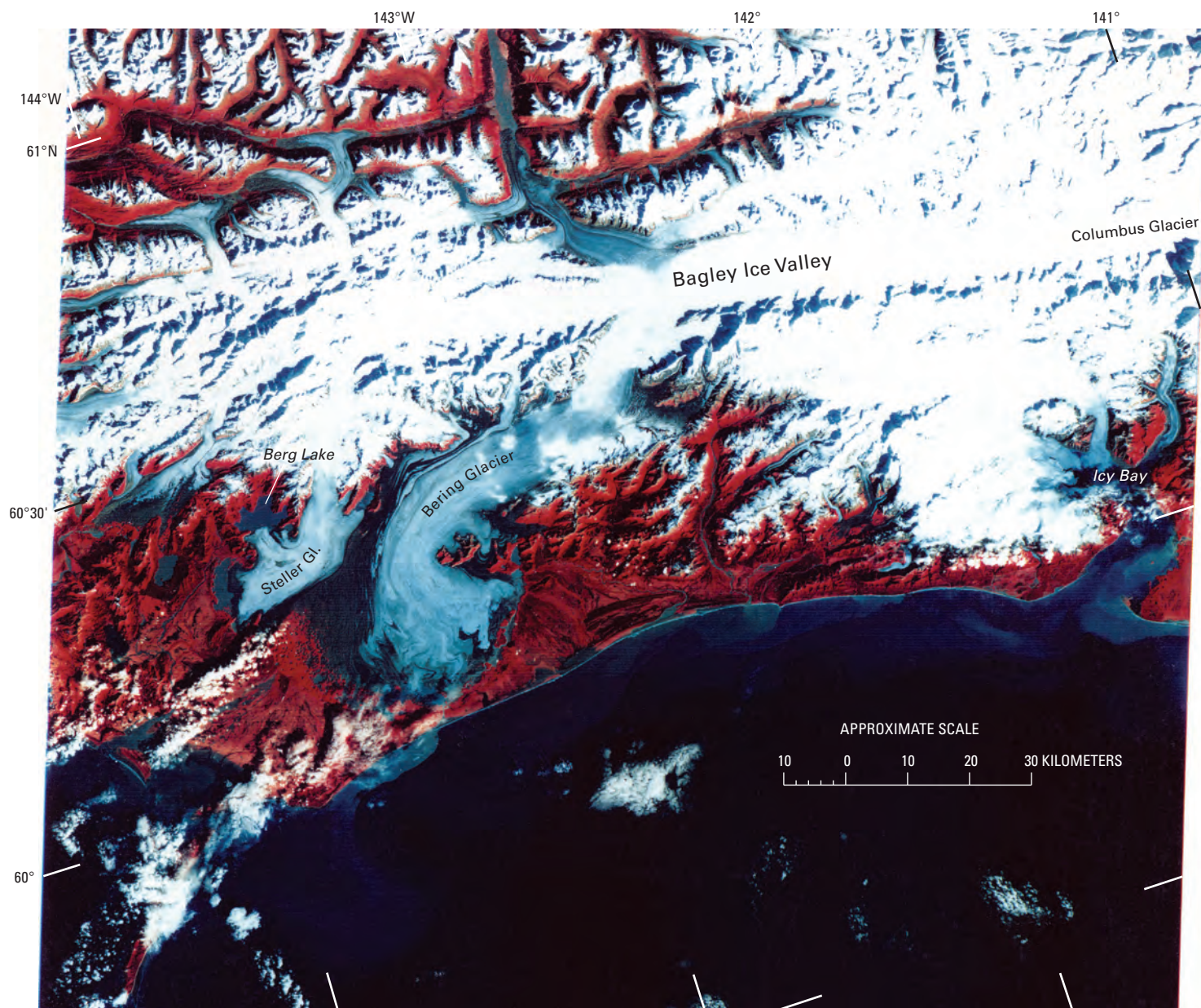


**Figure 183.**—Annotated Landsat 2 MSS image of the Bering Glacier System and Icy Bay on 23 September 1977. Bering Glacier is the largest (~5,200 km<sup>2</sup>) and the longest (~200 km) glacier in continental North America. Its accumulation zone begins north of Mount St. Elias (off the right side of this image; see fig. 109) and includes the Columbus Glacier and Bagley Ice Valley. The Bering Glacier has been thinning in recent decades, and Berg Lake and many other proglacial lakes forming around the Bering Glacier's piedmont perimeter

have increased in size as the thinning progresses. The retreat has been complicated by surges, which occurred in 1957–60, 1965–67, and 1993–95, and displaced parts of the terminal lobe as much as 13 km (Post, 1972). The glaciers of Icy Bay (see St. Elias Mountains section of this volume) began retreating during the first decade of the 20th century. Landsat image (2975–19394, bands 4, 5, 7; 23 September 1977; Path 69, Row 18) and caption courtesy of Robert M. Krimmel, U.S. Geological Survey.

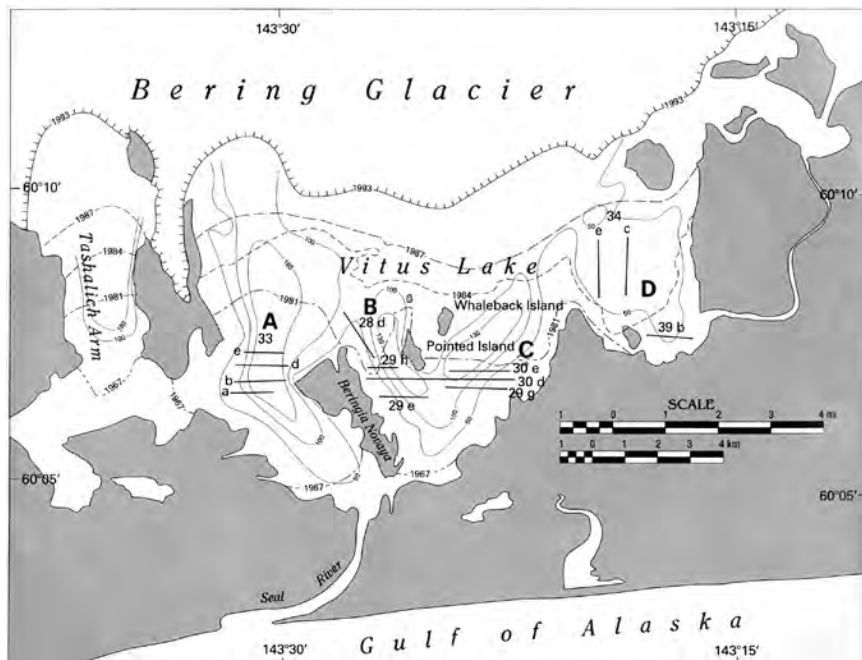


**Figure 184.**—Map of Vitus Lake and the 1993 margin of Bering Glacier (hachured line) showing bathymetry of the lake (in meters), positions of the retreating terminus of the glacier from 1967 to pre-surge-1993 (dashed lines), and the location of 1993 seismic profiles (short straight lines) (Molnia and others, 1996).

Bering Lobe, and a small segment of Steller Lobe and Steller Glacier, has an area of approximately 2,000 km<sup>2</sup>. On the basis of observations made in the late 1980s and early 1990s, the ELA for the glacier ranges between 915 and 1,070 m. The *Piedmont Lobe*, with an approximate area of 900 km<sup>2</sup>, has a maximum elevation of about 550 m and lies completely within the area of ablation. Meier and Post (1962) computed the AAR for Bering Glacier to be 0.63. Viens (1995) (table 2) calculated an AAR of 0.62 for the entire glacier, with an AAR of 0.66 for the Steller Glacier and 0.614 for the remainder of the Bering Glacier.

The highest peaks in the St. Elias Mountains segment of the Bering Glacier System drainage are Mount Logan and Mount St. Elias. Both exceed 5,000 m in elevation. The highest peaks in the Chugach Mountains segment of the Bering Glacier drainage are Mount Miller (3,350 m), Mount Tom White (3,418 m), and Mount Steller (3,237 m).

The valley glacier section, named the Bagley Ice Valley [previously named Bagley Ice Field on maps done by Field (1975a) and Molnia (1982, 1993, 2001)], is more than 150 km in length and occupies a linear trench as much as 12 km wide (fig. 183). The eastern Bagley Ice Valley extends from northeast of the Icy Bay–Mount St. Elias region to southwest of the Tana River. The eastern margin of the Bering Lobe is fronted by Vitus Lake (fig. 184), a 20-km-long ice-marginal lake with an area of about 160 km<sup>2</sup>. Pre-1993–95 surge bathymetric surveys of the lake’s floor revealed a complex bottom morphology with at least four deep basins (informally named A, B, C, and D) having water depths of 165 m (A), 135 m (B), 135 m (C), and 85 m (D). Water depths in Tashalich Arm, the westernmost basin of the Vitus Lake system are deeper than 180 m. Two seismic reflection surveys (Carlson and others, 1993; Molnia and others, 1996) of basins A through D revealed maximum glaciolacustrine sediment-fill thicknesses of more than 110 m; depths to acoustic basement in the basins reached a maximum of 275 m below sea level (Molnia and others, 1996).

Ice Penetrating Radar (IPR) studies (Trabant and others, 1991; Molnia and Trabant, 1992) of the *Piedmont Lobe* and central valley surface conducted to determine ice thickness and morphology (fig. 185), reveal that the bed of the glacier extends as much as 350 m below sea level in places and that maximum glacier ice thicknesses exceed 800 m. These IPR studies suggest that much of the Bering Lobe, *Piedmont Lobe*, and central valley

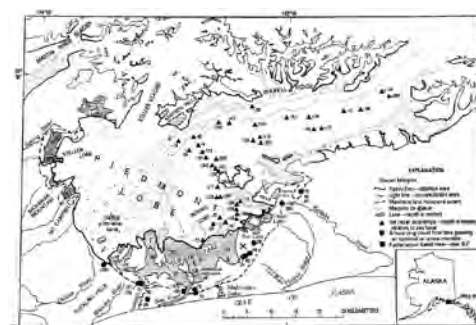


**Figure 185.**—Map of the lower reaches of the Bering Glacier shows geographic features and locations from which data were collected. Triangles identify locations of radio-echosounding- and precision-altimeter surveys. The numbers adjacent to the triangles are basal ice depths relative to sea level expressed in meters. Numbers in Vitus, Tsiu, and Tsviat Lakes are maximum water depths in meters. Tsiu and Tsviat Lake depths are from Fleisher and others (1993). Circles identify positions of trees growing on terminal and lateral moraines from which cores were obtained. The square adjacent to Seal River marks the location of a radiocarbon-dated spruce tree recovered from the sediments comprising the neoglacial terminal moraine. X marks the location of the Giant Log. TA is Tashalich Arm. The glacier margin and Vitus Lake are shown as they appeared in 1991. From Molnia and Post (1995, fig. 2, p. 91). A larger version of this figure is available online.



occupy a deep basin or series of channels, compatible with or even deeper than the depths determined by the high-resolution seismic reflection studies conducted in Vitus Lake. IPR measurements made as much as 60 km upglacier from the Bering Lobe terminus along the centerline of the glacier showed many areas where glacier bed depths were below sea level.

Offshore of Bering Glacier in the Gulf of Alaska is the Bering Trough (fig. 186), a sediment-floored 45-km-long submarine valley (Carlson and others, 1982). The Bering Trough has maximum water depths of 321 m,

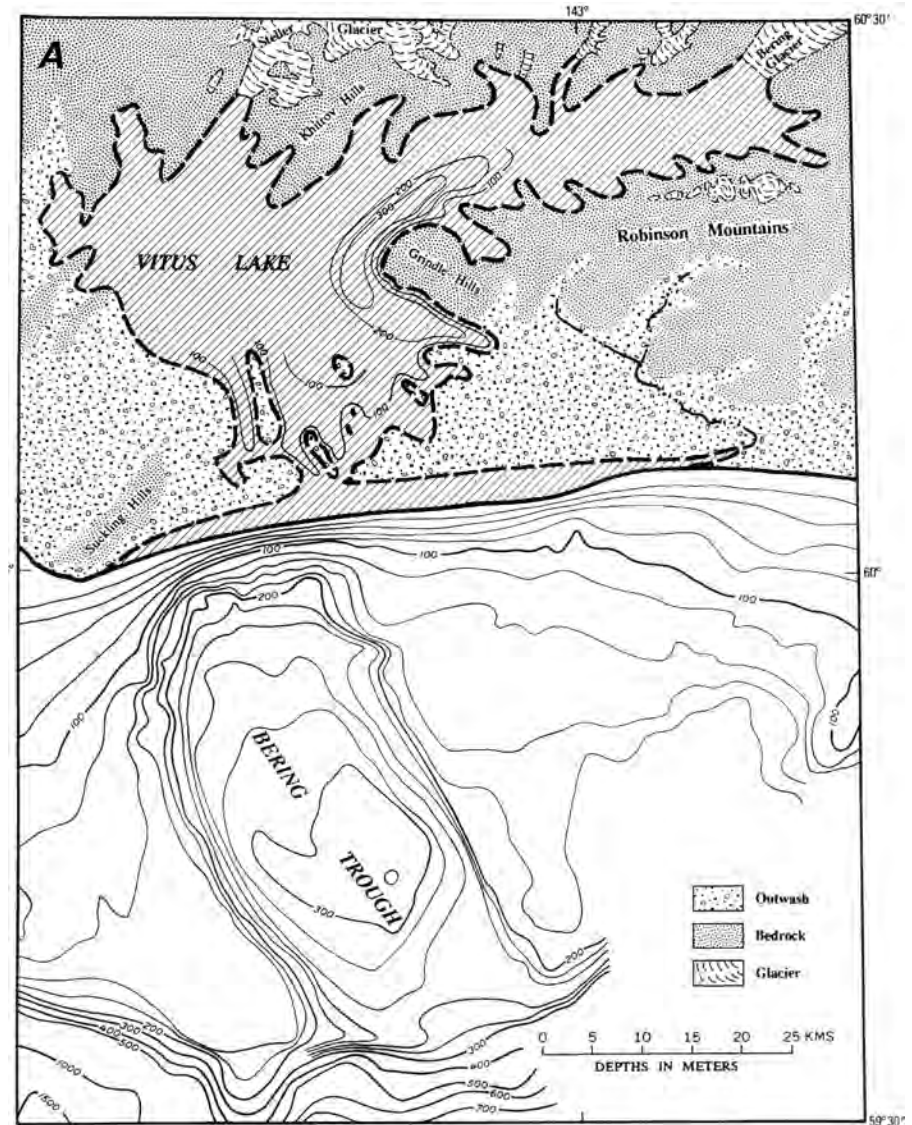


**Figure 186.**—A, Gulf of Alaska bathymetry shows the location, morphology, and depths associated with Bering Trough. Vitus Lake is drawn to show its pre-1993 surge bathymetry (contours adjacent to its southern margin) and the maximum size that it could attain following a catastrophic retreat of the Bering Glacier. Depths adjacent to the Grindley Hills are depths below present sea level to bedrock measured by radio-echosounding traverses. The area depicted by the diagonal pattern is the area where the bed of Bering Glacier is below sea level. B, Glacially eroded morphology of the Gulf of Alaska continental shelf in the vicinity of the Bering Glacier. The trough offshore of the terminus of Bering Glacier is the Bering Trough. The numerous adjacent features attest to both the extent and the erosive power of glaciers that descended from the Chugach Mountains during the Pleistocene Epoch. Diagram by Tau Rho Alpha, U.S. Geological Survey. A larger version of this figure is available online.

maximum bedrock depths of about 500 m, and a maximum width of 25 km. Acoustic-basement depths in Vitus Lake and IPR measurements of glacier-bed depths suggest that the sub-sea-level basins and channels that underlie Bering Glacier and Vitus Lake are landward continuations of the Bering Trough.

Vitus Lake is separated from the Gulf of Alaska by the Bering Glacier foreland, a 3-km-wide beach–outwash plain–moraine complex. The beach is composed of reworked outwash-plain sand and gravel and sand deposited by long-shore transport. The outwash plain and the neoglacial moraine are composed of gravelly sand. With the exception of one small exposure of the Yakataga Formation (fig. 187) exposed along the eastern side of Tashalich Arm in 1992, there are no known bedrock outcrops in the Vitus Lake area, nor was any shallow bedrock identified in seismic-refraction profiling of the beach in 1992.

The *Piedmont Lobe* (fig. 188) consists of three main components, initially described by Post (1972). The *Piedmont Lobe* has an approximate area of 900 km<sup>2</sup> and comprises 17.60 percent of the total glacier system; the Bering Lobe (fig. 189), which consists of relatively debris-free, periodically surging ice, contains 6.76 percent; the Central Medial Moraine Band (CMMB), which Post (1972, p. 219) described as “A very large debris band composed of repeatedly folded medial moraines that extends across the center of the Bering Glacier lobe” (fig. 190), is composed of complexly folded,



**Figure 187.**—13 August 1992 photograph of the only bedrock outcrop found along the southern perimeter of Bering Glacier. The Yakataga Formation series of beds, dipping at approximately N. 45° W., was exposed by the retreat of the Bering Glacier between 1991 and 1992. The margin of Bering Glacier can be seen in the upper left. Photograph by Bruce F. Molnia, U.S. Geological Survey.

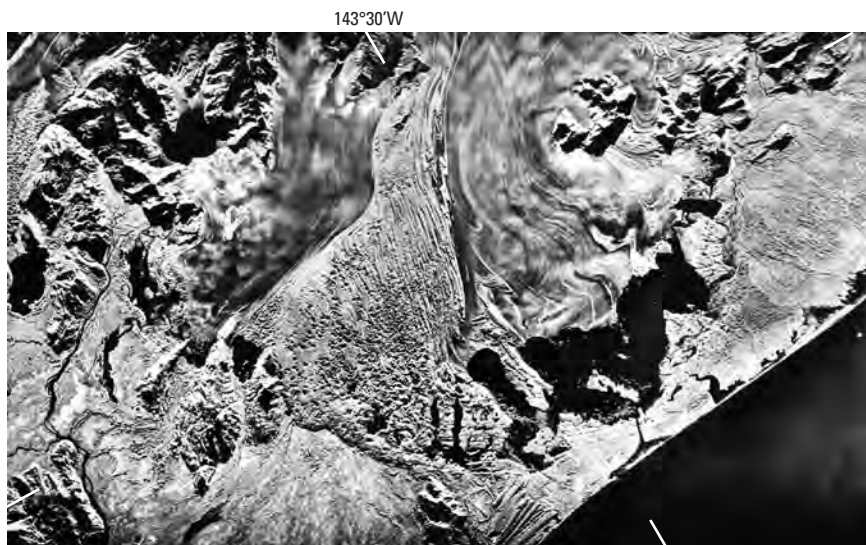


**Figure 188.**—3 August 1990 X-band synthetic aperture, side-looking airborne radar image of the Bering Glacier's Piedmont Lobe. The three components of the Piedmont Lobe, the Bering Lobe, the folded Central Medial Moraine Band, and the Steller Lobe, are visible north of Vitus Lake. About 25 folded medial moraine loops, formed by surges during the past several hundred years, can be seen in the Central Medial Moraine Band. The stagnant-ice-cored medial moraine is characterized by hundreds of thermokarst pits. From Molnia and Post (1995, fig. 3, p. 92).

**Figure 189.**—18 August 1978 AHAP false-color infrared vertical aerial photograph of part of the retreating terminus of the Bering Lobe. Nine years after the end of the 1967 surge, the terminus of Bering Glacier had retreated a maximum of approximately 1.5 km from its surge-maximum position. Two areas of the terminus are producing dozens of large icebergs. This is not a routine calving event in the true sense of the term; it is a disintegration event. Such events occur when the thinning glacier reaches a state of buoyancy and separates from its bed. As it begins to float, large pieces of ice, sometimes about 1 km in maximum dimension, separate from the terminus along old crevasse fracture planes. AHAP photograph no. L119F6063 from the GeoData Center, Geophysical Institute, University of Alaska, Fairbanks, Alaska.

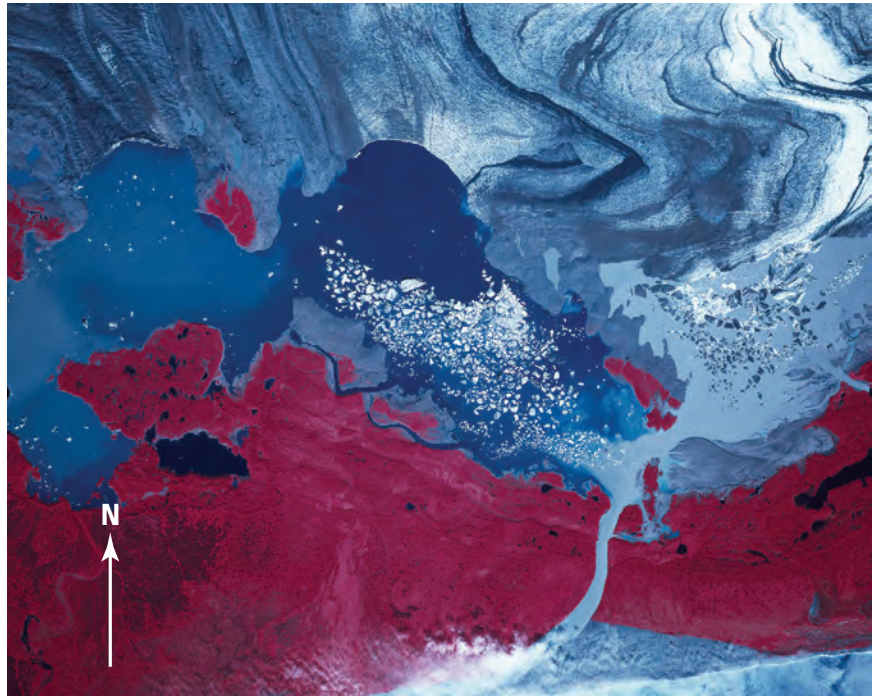


**Figure 190.**—Two views of the Central Medial Moraine Band of Bering Glacier. **A**, Summer 1938, north-looking oblique aerial photograph of most of the northern part of the Central Medial Moraine Band. Individual folded medial moraine loops stand several meters above the bare ice surface of the glacier. Photograph no. 1894 by Bradford Washburn, Museum of Science (Boston). **B**, 12 September 1986 north-looking oblique aerial photograph of the southwestern part of the Central Medial Moraine Band. Vegetation covers much of the southern margin of the moraine band. Most of the Steller Glacier and Steller Lobe can be seen in the background. USGS photograph no. 86-R2-229 by Robert F. Krimmel, U.S. Geological Survey.

moraine-covered, generally stagnant ice and contains 7.36 percent; and the Steller Lobe (fig. 191), which consists of relatively debris free, active ice derived from the 50-km-long Steller Glacier and contains 3.48 percent of the total area. Tributaries of the 180 km<sup>2</sup> Steller Lobe cover an area of 644 km<sup>2</sup> (12.44 percent of the total glacier), whereas tributaries of the 350-km<sup>2</sup> Bering Lobe cover 3,620 km<sup>2</sup>, or 70 percent of the total glacier area (Robert J. Viens, University of Washington, oral commun., 1993). The distance around the perimeter of the *Piedmont Lobe* of Bering Glacier, from the Bering River to the Grindle Hills, is about 75 km. Bering Glacier's *Piedmont Lobe* is about one-third smaller than that of Malaspina Glacier.

On the basis of IPR thickness measurements and bed depths (fig. 185), the CMMB appears to be composed of thin, debris-covered ice overlying a generally shallow bedrock divide between the thicker Bering Lobe and Steller Lobe.



**Figure 191.**—Three oblique aerial photographs of the northwestern terminus of the Steller Lobe of Bering Glacier flowing into Berg Lake. **A**, Summer 1938 north-looking photograph. The ice tongue reaches the north shore of the lake, separating it into two bodies of water. Photograph no. 2274 by Bradford Washburn, Museum of Science (Boston). Martin (1908) reported five smaller lakes here in 1905 with evidence of fluctuations in water level. By about 1940, the Steller Lobe of Bering Glacier had receded and the five lakes coalesced into one. From sometime before 1940 until 1984, there were no jökulhlaups, but Post and Mayo (1971) predicted that continued glacier thinning would allow a new jökulhlaup cycle to begin. **B**, 6 October 1974 northeast-looking photograph of the Steller Lobe damming the southern side of Berg Lake. The Bering Glacier is an effective dam, and the only outlet for the lake is a torrent of water that overtops the low point in the unnamed ridge in the lower right of the photograph. The water runs along the margin as an ice-marginal stream. Thirty-six years earlier, the Bering Glacier covered the eastern part of the ridge. Photograph by Bruce F. Molnia, U.S. Geological Survey. **C**, 12 August 2001 northeast-looking oblique aerial photograph of the northwestern part of the Steller Lobe flowing into the southern side of Berg Lake. In 1984, 1986, and 1994, jökulhlaups occurred and caused major flooding of wildlife habitats. Soon after June 1997, a large mass of ice grounded on the shoreline was separated from the retreating terminus of the Steller Lobe. In early 2000, a small surge began that caused a readvance of the terminus of Steller Glacier and ultimately reconnected the terminus with the grounded ice. The surge continued through the fall of 2001. The level of Berg Lake lowered through the early 21st Century and then stabilized. Photograph by Bruce F. Molnia, U.S. Geological Survey. Larger versions of B and C are available online.

At one location within the CMMB, IPR measurements show that bedrock reaches to about 20 m above sea level and is covered by less than 100 m of ice.

An analysis of historical data includes the following sources: 18th-, 19th-, and early 20th-century exploration maps, description of voyages, and reports of expeditions; 19th century published maps and nautical charts; late 19th and early 20th century geological reports; and early field photography obtained between 1897 and 1905. These sources provide additional information about the history of and changes to Bering Glacier over time and give a much longer term perspective on the glacier's post-“Little Ice Age” history than present-day measurements or remotely sensed data sets do. For example, a description of the physical characteristics of the surface of Bering Glacier from the late 1830s by Belcher (1843) suggests that the glacier was surging at the time of his observation. Similarly, photographs obtained by the Duke of Abruzzi's 1897 climbing expedition and a 1905 USGS geological field party clearly show the characteristics and position of parts of the margin of Bering Glacier. All of these historical data are useful in understanding the behavior of the glacier in the past.

### Pre-20th Century Observations of Bering Glacier

Through the middle of the 1880s, the geography of the southeastern Chugach Mountains was very poorly known. In 1886, Lieutenant H.W. Seton Karr, a member of the New York Times Expedition, applied the name Bering Glacier to the “ice-plain” that he observed west of Icy Bay during an unsuccessful attempt to reach the summit of Mount St. Elias (Seton Karr, 1887). He was knowledgeable about glaciers and realized the significance of his discovery. Seton Karr wrote, “In this direction (west) the ‘foothills’ of Elias stood like islands in the enormous expanse of glacier stretching prairie-like as far as the eye could penetrate through the crystalline air towards the country of the *Atna* [editors' italics] or Copper River” (Seton Karr, 1887, p. 109–110).

Several weeks later, in early August 1886, as he sailed along the Gulf of Alaska coast more than 100 km west of Icy Bay, Seton Karr observed (1887, p. 139–140),

I had understood that with Icy Cape the last ice along the coast was left behind. But looming twenty miles or so to the westward appears another vast ice-plain ... which sweeps down and opens fan-like on the ocean, where the coast range of “foot-hills” comes to an end. It is evidently the opening or outlet of the vast glacier-desert or ice-lake which we saw from the slopes of Mount St. Elias, lying to the northwest of the mountain. Its birthplace is an icy range that forms an enlarged continuation of the great western ridge of Elias. It is not marked or mentioned by the early navigators, all of whom mistook the true nature of these stupendous glaciers. La Perouse describing them as “snow lying upon a barren soil,” and “a plain totally destitute of verdure”

Six years earlier, in 1880, the Coast and Geodetic Survey (C&GS) had named this virtually unknown and unexplored coastal glacier Bering Glacier. The C&GS had chosen the name to commemorate Captain Vitus Bering, a Danish sea captain in the Russian naval service of Czar Peter the Great, who led a voyage of exploration that made a landfall in the vicinity of the glacier's terminus in 1741. As late-19th century C&GS nautical charts (fig. 192) and USGS topographic maps clearly show, nothing was known about the size, shape, or geography of most of Bering Glacier.

In 1890 and again in 1891, USGS expeditions led by Israel C. Russell attempted to climb Mount St. Elias. Although both attempts were unsuccessful, each reached elevations where Russell was able to see the upper parts of Bering Glacier. On the first, Russell observed part of what we now know as the Bagley Ice Valley, which he described as “another vast glacier extending westward to the limits of vision.” (Russell, 1891, p. 141).

On his second expedition in 1891, Russell observed the source area of Bering Glacier to the north of Mount St. Elias. He wrote (Russell, 1893, p. 47):

I was now so near the crest of the divide that only a few yards remained before I should be able to see the country to the north, a vast region which no one had yet beheld. ... I expected to see a comparatively low, forested country, stretching away



**Figure 192.** —Part of a late 19th century U.S. Coast and Geodetic Survey chart of the Gulf of Alaska region showing only the edge of the piedmont lobe of the essentially unknown and unexplored Bering Glacier. A larger version of this figure is available online.

to the north, with lakes and rivers and perhaps some signs of human habitation, but I was entirely mistaken. What met my astonished gaze was a vast snow-covered region, limitless in expanse, through which hundreds and perhaps thousands of barren, angular mountain peaks projected. There was not a stream, not a lake, and not a vestige of vegetation of any kind in sight. A more desolate or more utterly lifeless land one never beheld. Vast, smooth, snow surfaces, without crevasses stretched away to limitless distances, broken only by jagged and angular mountain peaks.

At the beginning of the 20th century, Bering Glacier had nearly a dozen major drainage outlets, arranged in a radial pattern along the piedmont outlet glacier's margin. These included: Kaliakh River, the many branches of the Tsiu and Tsiyat Rivers, Midtimber River, Seal River, Tashalich River, Kiklukh River, Oaklee River, Edwardes River, Campbell River, Nichawak River, Gandil River, and Bering River (Molnia and Post, 1995, p. 104, fig. 9). A significant retreat of Bering Glacier began during the first decade of the 20th century, sometime between 1905 and 1910. Since then, it has lost nearly 100 km<sup>2</sup> of ice from the terminus area of the *Piedmont Lobe* (fig. 193). Loss of ice by melting and calving along the terminus resulted in the development of a series of lakes along much of the glacier's perimeter (figs. 36, 194; see also a 9 June 1948 oblique aerial photograph, USGS photograph no. 119LT-72PL-R-8M-148-72RS-GS6B). Field (1975) reported that, between 1905 and 1957, as the glacier retreated back from its "Little Ice Age" maximum moraine, the percentage of the perimeter of Bering Glacier ending in ice-marginal lakes increased from about 10 percent to about 54 percent. By the early 1920s, with continued melting and retreat, several of these lakes expanded and coalesced to form Vitus Lake.

Retreat along the margin, interrupted by a series of 20th century surges, has resulted in an areal expansion of all the ice-marginal lakes. Along the margin of the Bering Lobe, the result has been an expanded Vitus Lake. To the west, along the eastern margin of the CMMB, a pair of parallel linear lakes began to develop beginning in the 1940s. Formed initially by the coalescence of thermokarst pits, these lakes have continued to lengthen and widen through the early 21st century, with the eastern lake reaching a length of approximately 5 km. These lakes and several other features of Bering Glacier have been used as experimental test sites to compare the use of spaceborne

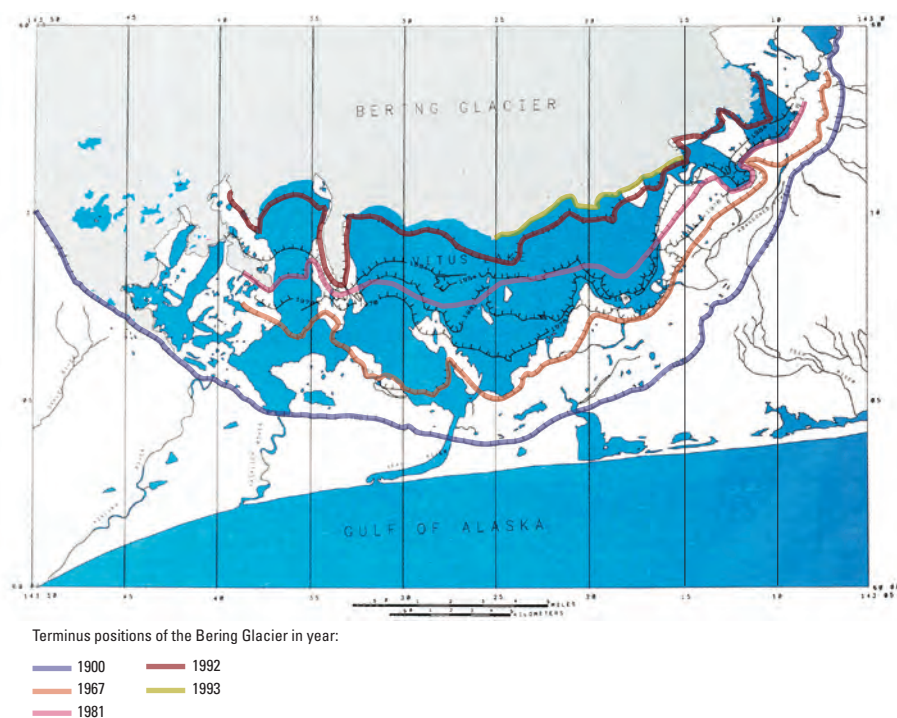


**Figure 193.**—Map showing positions of the terminus of Bering Glacier between 1900 and 1993. The 1993 position shown is the pre-surge (pre-28 August 1993) position of the terminus.

**Figure 194.** — 12 August 1961 oblique aerial photograph of the eastern margin of the Bering Glacier showing development of ice-marginal lakes. Large icebergs can be seen separating from the disintegrating margin of Bering Glacier. View looking westerly across the southeastern part of the terminus shows a continuous ice-marginal lake of variable width fronting Bering Glacier. Photographed a year after a surge, the surging glacier had almost filled the lake northeast of the Seal River. The Seal River is at the center-left edge of the photograph. Photograph by Austin Post, U.S. Geological Survey. A 1938 oblique aerial photograph can be seen in figure 36.



**Figure 195.** — 17 August 1979 oblique aerial photograph showing post-1967 surge retreat of the terminus of Bering Glacier. North-looking view of the southern part of Vitus Lake from offshore, east of the mouth of Seal River. In the 12 years after the end of the surge in 1967, the glacier has retreated about 3 km and thinned significantly. Bering Glacier has a very low gradient and almost no relief at its southern margin. The two large plumes of icebergs are the result of calving from rapidly disintegrating parts of the terminus of the glacier on either side of the island. Photograph by Bruce F. Molnia, U.S. Geological Survey.



ERS-1 and SIR-C synthetic aperture radar (SAR) with airborne SAR in identifying different types of glaciological features (Molnia and Molnia, 1995).

At the beginning of the 21st century, more than 90 percent of the meltwater from the Bering Lobe and the CMMB flows through Vitus Lake, entering the Gulf of Alaska through Seal River. Seal River, a 6-km-long low-gradient tidally dominated stream, flows diagonally across Bering Glacier foreland from east to west (figs. 195, 207). On 28 June 1991, the discharge of the Seal River, measured where it exits Vitus Lake, was approximately  $1.4 \times 10^3 \text{ m}^3 \text{ s}^{-1}$ .

### 20th Century Observations of Bering Glacier

G.C. Martin, a USGS geologist who mapped the Bering River coal field—a large undeveloped coal reserve located on the western side of the glacier—presented the earliest 20th century description of Bering Glacier. Martin (1905, p. 17) described the Bering as:

a large glacier of the piedmont type, and, if considered independently, is second in size, among glaciers of this type, only to the Malaspina Glacier. It is a large field of stagnant ice which has overflowed the eastern extension of the zone of coastal foothills...and it is considered by many as merely the western lobe

of the Malaspina Glacier. It is however, in all probability entirely separate from the latter. A great many valley glaciers coming from the Chugach Range enter it as tributaries. It is fringed along its southwestern border by a wide moraine, while the ice itself is thickly covered by rock debris for a distance of several miles from its front, and, as is in the case of the Malaspina Glacier, this covering is so thick that it is often impossible to determine the margin of the glacier.

Several of his photographs document that retreat of the Steller Lobe was underway before 1905 and that at least one ice-marginal lake had already formed (see USGS Photo Library Martin 245 photograph).

Three years later, Martin (1908) published a second description of the glacier accompanied by a 1:200,000-scale topographic reconnaissance map and a detailed 1:62,500-scale topographic map, both dated 1907, as well as a geologic map of the glacier's western margin (Martin and others, 1907). Martin (1908, p. 16) wrote: "Bering Glacier...is a huge, even-surfaced, stagnant mass of glacial ice, which is fed by many valley glaciers coming from the high mountains north of it. It is a piedmont glacier of the same general character and of about the same size as Malaspina Glacier. Portions of its surface form a good highway to some of the coal camps in the east end of the Bering River coal field, but most of it is so covered by irregular masses of rock and gravel and so much crevassed that travel over its surface is difficult and dangerous." The crevassing described above by Martin (1908) may be the result of a surge that occurred about 1900. The surface elevation of the glacier's margin, inferred from the 1907 topographic map, was quite similar to the Holocene thicknesses of Bering Glacier described by Miller (1958, 1961).

#### *Berg Lake*

On the northwestern margin of Bering Glacier, Berg Lake (also called Berg Lakes on some maps) is the largest (approximate area 30 km<sup>2</sup>) of the ice-marginal lakes formed by the retreat of the Steller Lobe (fig. 191). In 1905, Martin (1908) mapped five separate smaller lakes, many of which showed evidence of fluctuating water levels. He reported maximum water depths of approximately 250 m and noted that the water level had recently been higher. The existence of these five lakes suggests that, by 1905, the Steller Lobe was already in retreat from its "Little Ice Age" maximum position. By the early 1940s, continued retreat of the Steller Lobe resulted in the five lakes coalescing into one. Continued retreat of the Steller Lobe, interrupted by several small pulses or minisurges such as one that occurred in 2000 and 2001, has resulted in the continued expansion of Berg Lake. Post and Mayo (1971) noted that in 1970, the lake was 207 m deep, about 40 m lower than the 1905 level, and that the area of Berg Lake had increased from about 12 km<sup>2</sup> in 1905 to about 28 km<sup>2</sup> in 1970. These changes are the result of the ongoing thinning and retreat of the Steller Lobe.

Berg Lake has a history of at least three late 20th century glacier outburst floods (jökulhlaups). In 1984, 1986, and 1994, jökulhlaups from Berg Lake caused major flooding in the Bering River drainage and severely impacted wildlife habitats. The May 1994 jökulhlaup resulted from the catastrophic draining of partially ice-dammed Berg Lake. The development of an approximately 500-m-long subglacier channel through the northwestern margin of the Steller Glacier resulted in about a 100-m lowering of the lake in a 72-hour period. An estimated  $5.5 \times 10^9$  m<sup>3</sup> of water escaped the 9×6-km Berg Lake and drained through the Bering River during the ensuing 72 hours, completely inundating the floor of the Bering River valley from valley wall to valley wall. Because May is the time of moose calving and prime migratory bird nesting activity, especially Dusky Canada Geese (*Branta canadensis occidentalis*) and Trumpeter Swans (*Olor buccinator*), the flood had a major impact on the local ecosystem. Post and Mayo (1971) predicted that continued thinning of the glacier would result in a cycle of repeated jökulhlaups.

During August 2001, Josberger and others (2001) measured the bathymetry, temperature, and conductivity of Berg Lake. They determined that the



intense vertical convection in the lake is controlled by suspended sediment. The temperature profiles from Berg Lake show a vertical structure that consists of a 10-m thick surface layer, where the temperature drops from near 9°C to approximately 4°C, the temperature of maximum density for fresh water. Below this depth, the temperature decreases to 0°C in the deepest portions of the lake, at a depth of around 75 m. Superimposed on this general unstable temperature profile are spatially variable fine-structure details that include vertical steps and temperature inversions. Although the temperature profiles indicate a highly unstable situation, the subglacier discharge has a suspended sediment load sufficient to marginally stabilize the density structure in the lake. This sediment-laden water flows out from below the glacier and spreads horizontally throughout Berg Lake. As the suspended sediment settles, vertical thermal convection yields the observed fine structure in the temperature profiles.

### **Surges of the Bering Glacier**

The 20th century retreat of Bering Glacier has been interrupted by at least six major episodes of surging. Although rapid retreat and surging may seem incompatible, the results of these two processes have been large-scale fluctuations in the position of the terminus of Bering Glacier and in the continuing drawdown of ice from the accumulation area of the glacier. The surges occurred in: ca. 1900, ca. 1920, ca. 1938–40, 1957–60, 1965–67 (Post, 1972), and 1993–95, an approximate average of 20 years between surges (Post, 1972). The surges that occurred during the second half of the 20th century have been closely monitored. Each surge event resulted in a rapid and significant advance of the terminus of Bering Glacier and was accompanied by the transfer of a significant volume of ice into the expanding terminus area. A rapid retreat of the terminus, significantly enhanced by large-scale calving into Vitus Lake, and disintegration upglacier from the terminus also followed each surge event. The result was a glacier that was much thinner than before the surge. Far more ice was removed from Bering Glacier than melting alone could have done. The two most recent surges (1957–67, 1993–95) consisted of a pair of ice-displacement events separated by periods of stagnant ice. In the earlier surge, ice-displacement occurred from 1957 to 1960 and from 1965 to 1967, and stagnant ice occurred from late 1960 to early 1965. Maximum ice displacement exceeded 10 km (Post, 1972).

Post (1960, 1965, 1967b, 1969, 1972), Meier and Post (1969), and Post and LaChapelle (1971) have shown from direct observations of many surging glaciers that the folding (or contortion) of surface medial and lateral moraines is an expected result of surging. From analysis of vertical aerial photography, Post (1972) determined that individual chevron-folded medial moraines are the product of a separate surge event. He wrote that (Post, 1972, p. 219):

Vertical aerial photography taken before and after surges disclose the direction and magnitude of ice flow in various parts of the piedmont lobe. The ice moved toward the terminus and expanded in a normal, radial pattern with no evidence of unusual shearing that would result in the formation of large folds. Many surging glaciers display repeated lateral displacements in their medial moraines which result from periodic surging of the main glacier past non-surging tributaries. Moraines of the Bering Glacier display small periodic irregularities of this nature. The large “accordion” folds in the moraines in the Bering Lobe are judged to be due to the combined effects of compressive flow and lateral or transverse expansion of those previously formed irregularities. The initially small pre-existing perturbations in the moraines are simply spread laterally and shortened radially into large folds as the ice spreads out.

At Bering Glacier, field observations and analysis of aerial photography and SAR images indicate that at least 25 folded moraines are located in the CMMB. With a 20- to 30-year cycle (Post, 1972), at least 500 to 700 years of periodic surging would be necessary to create the observed number of folded moraines (fig. 190).

## The 1957–60, 1965–67, and 1993–95 Surges of the Bering Glacier

### *1957–60 and 1965–67 Surges*

Following a surge that ended about 1940, Bering Glacier began to retreat. Retreat continued through 1957; Vitus Lake expanded to an approximate size of 14×5 km and an approximate area of 48 km<sup>2</sup>. D.J. Miller's 1958 aerial photograph of a new surge developing in the eastern Bagley Ice Valley showed that the surface of Bering Glacier was lowering and that recent shearing of the glacier's margin had occurred at Waxell Ridge. The surge continued through 1960, probably reaching the terminus in 1959. Much of the margin of Bering Lobe advanced and ice reoccupied much of Vitus Lake. By 1960, the terminus of Bering Lobe had advanced to a position from 0.5 to 3.0 km beyond the 1948 margin, reducing Vitus Lake to a maximum of approximately 3.5×2.5-km and an approximate area of 3 km<sup>2</sup>. Post (1972) reported maximum displacements of as much as 9 km that probably occurred during a 12- to 18-month period. By the fall of 1960, no further terminus activity was observed. The position of the terminus changed little through the spring of 1963 (Molnia and Post, 1995, fig. 13); recession was underway by summer 1963.

A major earthquake occurring on 27 March 1964 produced many rock avalanches that fell on the surface of Bering Glacier. Four had lengths of more than 5 km, all in the Waxell Ridge area. The largest was 6.5 km long and as much as 2.5 km wide. It fell from an elevation of more than 2,000 m and was estimated to have a volume of 10<sup>7</sup> m<sup>3</sup> of rock (Post, 1967a).

Between 1965 and 1967, a smaller surge reactivated much of the terminus and resulted in up to 1.0 km of additional terminus advance. Ice was displaced by as much as 4.0 km (Post, 1972). By 1967, the glacier margin was within 1 to 3 km of its early 20th century maximum position (fig. 193).

Molnia and Post (1995) quantified the post-1967 rate of terminus retreat throughout the eastern margin of Bering Glacier and found that the terminus of Bering Glacier retreated drastically (maximum recession of as much as 10.7 km) between the end of the 1965–67 surge and the 28 August 1993 onset of terminus displacement associated with the 1993–95 surge. Retreat did not occur at a constant velocity because individual years and areas show considerable variability; the average rate of retreat was determined to be 0.43 km a<sup>-1</sup>. Molnia and Post (1995, p. 112, table 1) presented their annual average retreat rates along four approximately north-south transects extending from the 1967 ice limit to the August 1993 pre-surge ice margin (transect locations shown by Molnia and Post, 1995, p. 111, fig. 15).

Annual recession rates were calculated along each of the transects and ranged from 0.04 to 1.0 km a<sup>-1</sup>, except for the times when rapid calving and disintegration occurred. Because ice-margin positions were plotted from available aerial photography, intervals between adjacent dated lines were not necessarily multiples of full years. Except for the times when rapid calving was taking place, the maximum measured recession rates along each transect occurred since 1990. The largest retreat—1.0 km—occurred along transect A in Tashlich Arm between June 1992 and March 1993. The total amount of terminus retreat along each transect is 8.80 km (transect A), 10.70 km (transect B), 8.85 km (transect C), and 7.00 km (transect D). In transects A and D, initial recession rates were low (0.15 km a<sup>-1</sup> or less). In transects B and C, there was an initial rapid loss of what was perhaps a floating, thin extension of ice as retreat began, followed by a much slower rate of terminus retreat.

In 1977 (transect B) and 1984 (transect D) (Molnia and Post, 1995, p. 111), two episodes of very rapid calving and disintegration occurred; each instance resulted in more than 2.0 km of ice-margin recession. These rapid recessions occurred when the thinning, retreating glacier terminus decreased to a minimum thickness, after which buoyancy would not permit it to remain in contact with the bottom. As it floated, it rapidly disintegrated. Many large icebergs separated from the terminus resulting in a very rapid retreat of the



**Figure 196.**—20 July 1993 oblique aerial photograph showing post-1967 surge retreat of the east-central Piedmont Lobe region of Bering Glacier. Northwest-looking view along the terminus of Bering Glacier. The glacier is rapidly calving and disintegrating along old crevasse planes. The height of the shoreline scarp at the northeast edge of Vitus Lake is less than 5 m. Because of their buoyancy, several calved blocks of ice have risen above the elevation of the surface of Bering Glacier. Photograph by Bruce F. Molnia, U.S. Geological Survey. A larger version of this figure is available online.



**Figure 197.**—29 July 1990 east-looking view of part of a 300×600-m mass of debris-covered stagnant Bering Glacier ice located near the head of the Tagglund Peninsula. This remnant had a maximum height of approximately 30 m. When the rapidly advancing ice of the 1993 surge encountered this stagnant ice, it reconnected to the stagnant-ice mass and pushed it forward. Note the person for scale. Photograph by Bruce F. Molnia, U.S. Geological Survey. A larger version of this figure is available online.

margin. This produced substantial short-lived increases in the recession rate. Before the summer of 1991, the retreating margin at the head of Tashlich Arm changed from one with a low rate of iceberg production to one with a much higher rate, and the fjord completely filled with floating calved icebergs. Correspondingly, the 1992–93 retreat rate— $1.0 \text{ km a}^{-1}$ —was nearly twice as high as the next highest rate (1987–90,  $0.53 \text{ km a}^{-1}$ ) and more than six times higher than the initial rate of retreat (1967–69,  $0.15 \text{ km a}^{-1}$ ).

Sequential aerial photography provided additional insights into the characteristics of the post-1967 retreat, as a 17 August 1979 oblique aerial photograph by the author shows (fig. 195). For instance, rates of retreat in the ice-filled basins of Vitus Lake were much greater than they were on the adjacent islands and land areas. Similarly, as the retreat progressed (fig. 196), the surface gradient and elevation of Bering Glacier decreased significantly. On areas adjacent to Vitus Lake, large stagnant masses of glacier ice covered the land surface. Some of these masses were remobilized when they were contacted by surge-displaced land-based ice (fig. 197).

In addition to rapid retreat, Bering Glacier has also thinned significantly during the period of retreat. Between 1967 and 1993, the ablation area of Bering Lobe was virtually stagnant ice, and there was little detectable ice flow. The reduced flow from upglacier contributed to a significant thinning of the ice in the lower 80 km of the glacier. Comparing ice-surface elevations at the terminus of Bering Glacier derived from the 1:63,360-scale USGS Bering Glacier A-7 topographic map (1984), which was based on 1972 aerial photography, with 1991 elevations derived from USGS vertical aerial photography shows a thinning of approximately 150 m at the Bering Lobe terminus, an average of approximately  $7.9 \text{ m a}^{-1}$ . Elsewhere, Trabant and Molnia (1992) compared 1990–92 surface-elevation profiles made by using a precision altimeter with elevations measured from a 1972 Bering Glacier topographic map (USGS, 1972). They determined that a thinning of between 85 and 180 m occurred along the centerline of Bering Lobe. The locations of many of their precision altimeter survey points are shown on figure 185. In some places, ice loss within the subsequent 20-year period represents approximately 20 to 25 percent of the 1972 thickness of Bering Glacier at that location. Molnia and Post (1995) reported that a comparison of 1946 and 1990 vertical aerial photographs shows that almost 200 m of thinning occurred between photographs along the margin of the Bering Glacier at an elevation of 280 m south of the Grindle Hills. Molnia and Post (1995, p. 113, fig. 16) presented surface-elevation profiles of Bering Glacier for 1900, 1957, 1960s, 1972, and 1991 and a mostly below-sea-level profile of the glacier base.

#### *The 1993–95 Surge*

By late August 1993, just before the beginning of the 1993 surge-related terminus advance, approximately  $20 \times 10\text{-km}$  Vitus Lake occupied an area of about  $70 \text{ km}^2$ , an increase in area resulting from late 20th century recession. The 1993–95 surge produced a maximum of around 10 km of advance of the terminus of Bering Lobe. Terminus-ice displacement occurred in two discrete phases—between late August 1993 and 17 September 1994 and between early May 1995 and mid-September 1995. A 7-month period without detectable ice displacement—from 17 September 1994 to early May 1995—separated the two advances. The surge resulted in a substantial increase in iceberg production; significant changes in the size, bathymetry, hydrology, and water chemistry of ice-marginal Vitus Lake; advance over vegetation (fig. 65); and the complete or partial covering of all of the islands within Vitus Lake by advancing ice. Maximum ice-displacement rates and maximum surge-front-displacement velocities approached  $100 \text{ m d}^{-1}$  during the initial period of the surge.

The 1993–95 surge was anticipated and closely monitored. More than a year before the appearance of any evidence that a surge was beginning, the

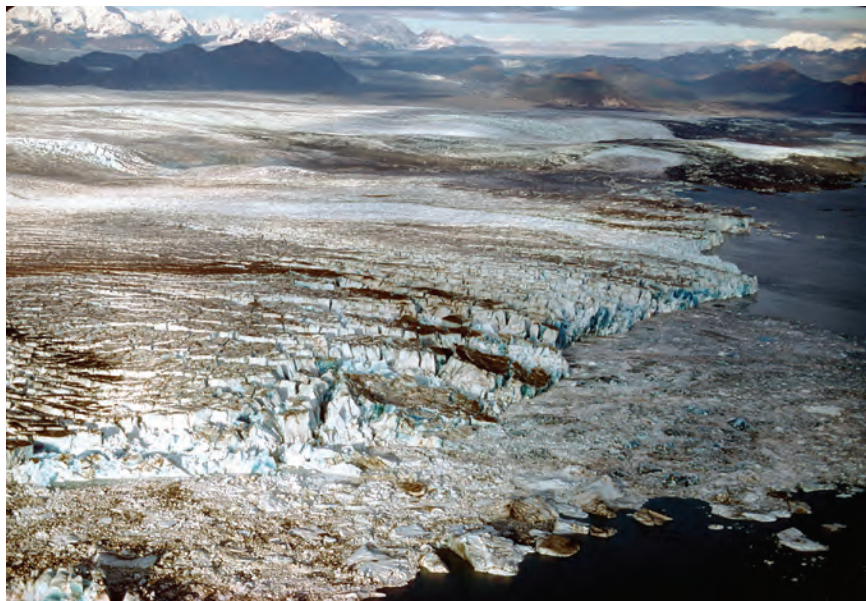


**Figure 198.**—6 October 1993 northeast-looking oblique aerial photograph of the intensively fractured, disintegrating terminus of the Bering Glacier. Fracturing extends many kilometers upglacier. Several large surge-produced pressure ridges can be seen migrating towards the terminus. Photograph by Bruce F. Molnia, U.S. Geological Survey.

tongue of ice that filled the head of Tashalich Arm began to rapidly calve icebergs, and the entire fjord was filled with floating ice within less than 3 months. An analysis of sequential vertical aerial photographs led Robert M. Krimmel (USGS, Tacoma, Washington, oral commun., 1996) to report that, during the 9-month period between 12 June 1992 and 16 March 1993, ice advanced toward Tashalich Arm at a velocity of  $1.3 \text{ m d}^{-1}$ , yet the terminus retreated about 300 m, more than  $1 \text{ m d}^{-1}$ . In the 4 months between 16 March 1993 and 10 July 1993, the velocity increased to 2 to  $3 \text{ m d}^{-1}$ . A similar rapid-calving process was characteristic of changes at several Bering Lobe ice-marginal locations when they were impacted by the arriving surge front, as shown on a 6 October 1993 oblique aerial photograph taken by the author (fig. 198).

#### *The 1993–94 Phase*

In the central Bering Lobe, the first visible evidence of the onset of the surge was the development of a large pressure ridge along the southwestern edge of the Grindle Hills during the spring of 1993, although the ridge probably had been building up for many months before that observation. During the early stages of the surge, this location served as the initiation point for the fracturing and shattering of the surface of Bering Glacier. Within weeks, the upglacier surface of Bering Lobe was fractured for a distance of more than 50 km, and the thickening glacier was overtopping ridges, such as Over-ride Ridge, in the lower Bagley Ice Valley (fig. 199).

A comparison of three sets of mosaicked vertical aerial photographs of the terminus of Bering Glacier in Vitus Lake acquired by the author on 10 July 1993, 10 September 1993, and 25 February 1994 show how various locations along the glacier's terminus responded very differently to the surge process. In some areas, the glacier's terminus rapidly advanced; in other areas, it retreated. During the first 2 months of the surge, the ice in part of the terminus adjacent to the eastern side of the peninsula that separates Vitus Lake from Tashalich Arm shattered and retreated rapidly following the arrival of the surge front, while the front advanced to the east. By November, the entire terminus was advancing rapidly into Vitus Lake.

Comparing two sets of vertical aerial photographs acquired on 17 October 1993 and 16 May 1994 showed that the terminus adjacent to the eastern side of Beringia Novaya advanced about 7.78 km in this 211-day period. The average rate of terminus displacement was about  $36.7 \text{ m d}^{-1}$ . The actual displacement was higher because a significant volume of ice calved daily from the advancing glacier margin. Cross-glacier fracturing proceeded at a much slower rate. But, by July 1994, the CMMB showed fracturing and

**Figure 199.**—6 October 1993 oblique aerial photograph shows surge-thickened ice at the edge of the Bagley Ice Valley expanding over an exposed bedrock ridge. The ridge, named Override Ridge by Austin Post, was also overridden by surge-thickened ice during the 1957–1960 surge. Photograph by Bruce F. Molnia, U.S. Geological Survey.

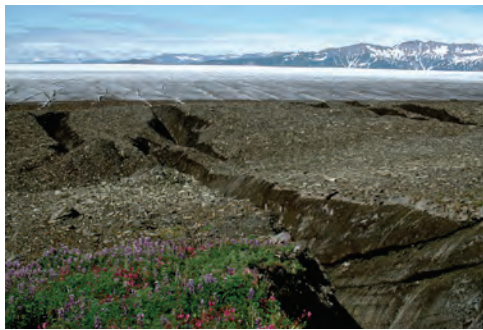
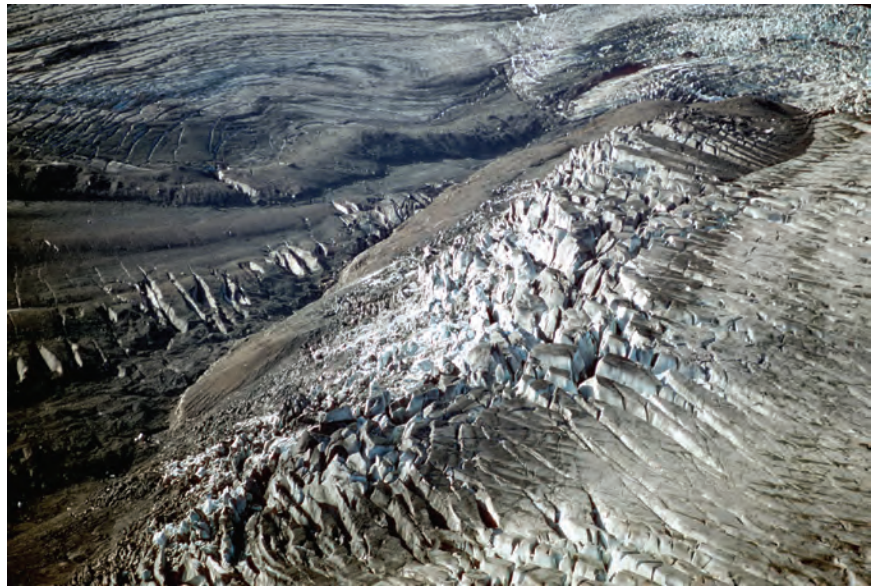


**Figure 200.**—Photograph of several extensional crevasses/faults located on the western side of the Central Medial Moraine Band of the Bering Glacier on 24 July 1994. Before the surge, this area was vegetation-covered stagnant ice. Photograph by Bruce F. Molnia, U.S. Geological Survey. A larger version of this figure is available online.

folding caused by both compressional and extensional stresses (fig. 200). In essence, the fractures were a complex network of parallel and subparallel crevasses that opened in the previously near-stagnant CMMB.

Robert M. Krimmel (USGS, Tacoma, Washington, written commun., 1996) analyzed nine sets of sequential vertical aerial photographs acquired between 12 June 1992 and 7 September 1994 to derive many physical characteristics of the surging Bering Glacier (12 June 1992, 16 March 1993, 10 July 1993, 10 September 1993, 15–17 November 1993, 25 February 1994, 16 May 1994, 13 August 1994, 7 September 1994). He reported velocities lower than those cited above but noted that “the highest speed measured from the successive aerial photographs was 22 m d<sup>-1</sup>. This speed was measured at two locations: in the west terminus area above the entrance to Tashalich Arm and in the area a few kilometers west of Grindle Hills. These speeds were the average speed for a several month period, and it is reasonable to expect that the speed was higher for portions of the measured period.” Krimmel’s plots for seven positions of the terminus of Bering Glacier between 10 July 1993 and 7 September 1994 are shown in figure 201.

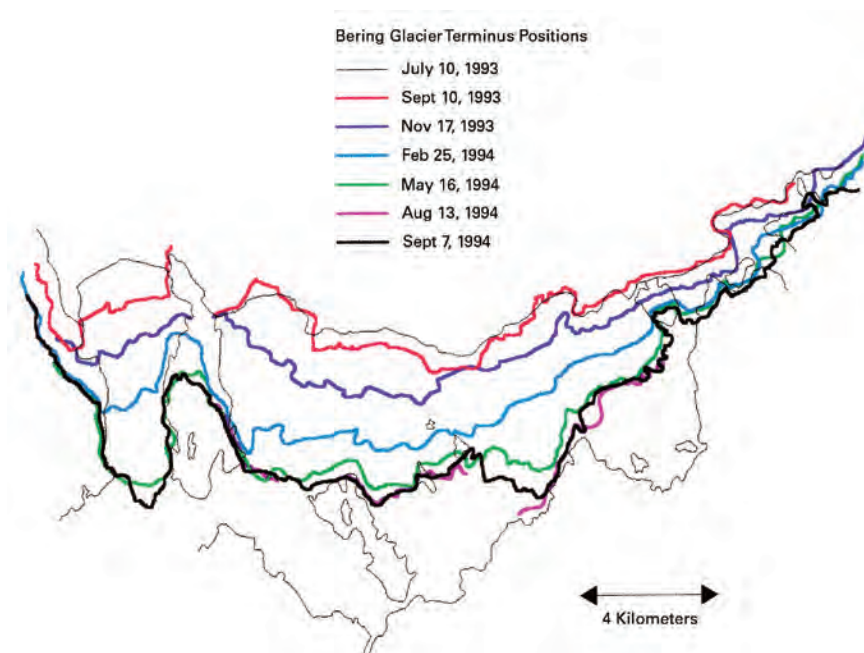


**Figure 201.**—Terminus positions of Bering Glacier are shown between 10 July 1993 and 7 September 1994. The July 1993 shoreline of Vitus Lake is shown as a fine black line. From data compiled by Robert M. Krimmel, U.S. Geological Survey.

Subsequent examination of sequential SAR imagery by Roush (1996) confirmed and enhanced the understanding of many of the events that occurred during the first 8 months of the surge. Roush found that the surge was in progress by 30 April 1993 and may have begun as early as 26 March 1993. Measurements showed that the surge front propagated downglacier at a mean velocity of  $90 \text{ m d}^{-1}$  between 19 May and 25 August 1993, the migrating surge front first reaching the terminus of the glacier in Vitus Lake just before 24 August 1993. Subsequently, the calving terminus advanced rapidly into Vitus Lake. On radar imagery, the advancing surge front consisted of a distributed region of undulations and elongated bulges on the surface of Bering Glacier, having heights estimated from the SAR data of 40 to 110 m and widths varying from about 0.7 to 1.5 km. Roush compared 9 August 1993 and 18 October 1993 radar images and calculated that, during this 71-day period, the average advance rate in its central area was  $19 \text{ m d}^{-1}$  and that the mean rate of advance across the entire width of the terminus was  $11 \text{ m d}^{-1}$ . As previously noted, these rates pertain to the displacement of the ice margin and do not take into account the large volume of ice calved from the end of the advancing margin during the entire period of observation. Additionally, had Roush used 24 August 1993 as a start date, his average rates would have been more than 20 percent higher.

Studies by Fatland and Lingle (1998, 2002) analyzed the surge by using differential SAR interferometry (InSAR) on two pairs of ERS-1 radar images, one pair collected during a 3-day period in January 1992 before the onset of the surge and the second during a 3-day period between 4 and 7 February 1994 at the peak of the surge. Their resulting high-resolution velocity data clearly show that the Bagley Ice Valley—southwest of Tana Glacier and northeast of Steller Glacier—experienced a 2.7-fold increase in velocity during the interval between image pairs, velocity increasing from  $0.36$  to  $0.95 \text{ m d}^{-1}$ . They also reported a drawdown of the surface of Bering Glacier of between 5 and 10 m and speculated that the velocity increase may have been caused by increased longitudinal stress gradients resulting from coupling to the surging main trunk of Bering Glacier. They also reported that InSAR was unsuccessful in determining velocities on the rapidly moving ice of Bering Glacier because there was no image correlation between sequential SAR images.

The advancing ice moved much more rapidly when it filled subglacier and sublacustrine fjord channels than it did when it advanced over land. Average land advance rates rarely exceeded  $4 \text{ m d}^{-1}$ . However, the advancing ice would frequently bulldoze large wedges of sediment in front of its advancing face. Many observed advances were accompanied by upward thrusting. Individual spatulate fingers of ice ranging from a few meters to more than 100 m in width built distinctive push moraines. Several of the islands in Vitus Lake were partially covered during the first phase of the surge. The northern part of 1.7-km-long Tsitus (*Arrowhead*) Island, which had only become free of retreating ice during the summer of 1992, was quickly covered by advancing ice (fig. 202A). By the end of the first phase of the surge, nearly 1 km of the northern end of the island was covered by advancing glacier ice (fig. 202B). The same lobe of ice that overtopped the north end of Tsitus (*Arrowhead*) Island filled the channel east of the island that connected the two eastern ice-marginal lakes with the main body of Vitus Lake. All of the drainage from the eastern part of Bering Glacier that previously flowed through this channel into Vitus Lake was deflected to flow through an abandoned former ice-marginal channel adjacent to the 1967 ice-maximum position, just to the east of the south end of transect D (Molnia and Post, 1995, p. 111, fig. 15).

Advancing ice slowly covered the northern end of Pointed Island. However, a much more rapidly moving tongue of ice, at least 170 m thick, advanced past the island on its western side at a rate that exceeded  $20 \text{ m d}^{-1}$ . Before the first phase of the surge ended, two small islands, named the The Wallypogs

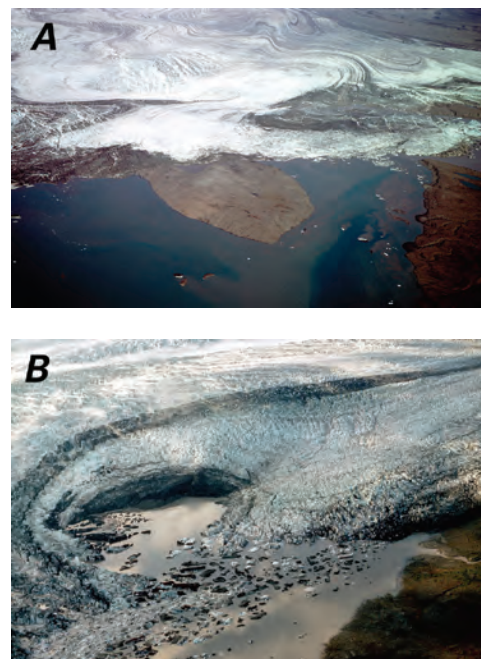


**Figure 202.**—Two oblique aerial photographs of the Tsitus (*Arrowhead*) Island area that show changes that occurred during the first and second phases of the 1993–1995 surge of the Bering Glacier. **A**, 7 October 1993 north-looking oblique aerial photograph shows the advancing margin of the Bering Glacier just as it made contact with the north end of the island. The channel on the east side of the island, which connects to the eastern marginal lakes, is still open. Between the summers of 1992 and 1993, the north end of Tsitus (*Arrowhead*) Island had become ice free. **B**, 9 July 1995 north-looking oblique aerial photograph shows that the advancing margin of Bering Glacier had covered all but the southernmost 45 m of the island. Advancing ice masses in the channels on both sides of the island advanced towards each other but never joined. This photograph depicts the maximum ice advance and ice cover of Tsitus (*Arrowhead*) Island. Photographs by Bruce F. Molnia, U.S. Geological Survey. Larger versions of these figures are available online.

by Austin Post, were completely covered, as were the northern two-thirds of Whaleback Island. The northwestern shoreline of *Taxpayer's Bay*, the area at the southern end of transect D (Molnia and Post, 1995, p. 111, fig. 15) was also overtopped by the advancing glacier.

Robert M. Krimmel (Tacoma, Washington USGS, oral commun., 1996) compared sequential vertical aerial photographs acquired on 16 May 1994, 13 August 1994, and 7 September 1994 to determine when this phase of the surge ended. He reported that ice velocities were high for the period between 16 May 1994 and 13 August 1994. Terminus changes were minor between 13 August 1994 and 7 September 1994. By mid-September 1994, advance of Bering Glacier had ceased. Vitus Lake was so filled with the terminus of Bering Glacier and icebergs that almost no open water remained.

#### *Surge-Produced Changes in Vitus Lake*

Gray and others (1994) documented changes in the physical and sedimentary characteristics of Vitus Lake that occurred during the first year of the surge by comparing pre-surge measurements made during the July 1992 retreat phase with peak surge measurements made in July 1994. In 1992, the lake had an area of approximately 160 km<sup>2</sup>, and about 90 percent of its surface was free of icebergs. The lake was stratified into two distinct layers, the topmost of which extended from the surface to a depth of about 7 m. Generally, specific conductance values increased from about 2,000 to about 5,000  $\mu\text{S cm}^{-1}$  (micro Siemens per centimeter), and water temperature decreased from about 5° to about 3°C. Specific conductance values of approximately 17,000  $\mu\text{S cm}^{-1}$  at a depth of 10 m increased to a maximum of approximately 32,400  $\mu\text{S cm}^{-1}$  at a depth of 142 m. The majority of water temperature measurements made were less than 1°C. The depth of the transition zone between the two layers corresponded to the depth of the thalweg (longitudinal outline of riverbed from source to mouth) of the Seal River. Additionally, the mean Secchi-Disk depth (measurements of water clarity) obtained from measurements made at locations more than 1 km from sediment-rich glacial water inflows was 2.3 m.

When Vitus Lake was measured in mid-July 1994, the surge had reduced its area to approximately 50 km<sup>2</sup>, and more than 90 percent of its surface was covered by floating ice. Specific conductance values ranged from about 2,000 to about 3,200  $\mu\text{S cm}^{-1}$ , and water temperature ranged from about 4° to about 0°C. No evidence of stratification was found. Mean Secchi-Disk depth obtained from measurements made near the head of the Seal River was 0.4 m. Visual observations of water samples collected with a Van Dorn sampling device suggested that suspended sediment concentration increased with depth, unlike it did in 1992 when the lake was essentially sediment free. Lastly, in contrast to the 1992 sediment discharge rate of about 10 kg s<sup>-1</sup>, the suspended sediment discharge in 1994 was around 10<sup>4</sup> kg s<sup>-1</sup>.

#### *The 1995 Phase*

Oblique aerial photographs of the terminus region of Bering Glacier acquired in late November 1994 and again in late January 1995 showed no evidence of surge activity. Following a 7-month period beginning in September 1994 and characterized by minor retreat and near-stagnant ice, parts of the eastern Bering Glacier resumed surging; several areas of the terminus advanced about 750 m in the 13-day period between 19 May and 1 June 1995 (57.7 m d<sup>-1</sup>). The first evidence that new surge activity had begun was noted on 14 April 1995 by pilots Gayle and Steve Ranney of Cordova, Alaska. They observed that a section of the winter-ice cover of Vitus Lake was being compressed into a series of accordionlike folds. They also observed numerous deep fresh cracks and rifts as well as a number of blue-water lakes forming on the surface of Bering Glacier. The lakes, fractures, and rifts were characteristic features of the 1993–94 phase of the surge.

USGS vertical aerial photography of the Bering Lobe terminus and Vitus Lake, acquired on 1 May 1995, confirmed the new fracturing and rifting as well as the numerous lakes. When they were compared with the late November 1994 vertical aerial photographs, the 1 May 1995 photographs showed that the terminus was advancing over the northern end of Beringia Novaya, the largest island in Vitus Lake, and over the north-central part of Pointed Island. The margin showed a significant increase in iceberg production, including several icebergs that were more than 0.5 km long. 19 May 1995 oblique aerial photography confirmed that the terminus was continuing to advance. On the southeastern shoreline of the lake, just west of *Taxpayer's Bay*, the advancing ice margin was redirecting the entire drainage from the eastern part of the glacier to a narrow channel. The result was several tens of meters of shoreline retreat and the development of a high bluff, as two oblique aerial photographs taken on 6 and 9 July 1995 by the author show (fig. 203).

The author's 1 and 2 June 1995 visit to the glacier confirmed that not only was the surge affecting the eastern terminus region but also that it was affecting the northern part of Bering Lobe and the southern part of the Bagley Ice Valley, as much as 30 km north of the terminus (fig. 204). There, the winter 1994–95 snow surface was complexly fractured and rifted, and several large ice-surface (supraglacier) lakes reappeared in the same location where lakes had existed during the January to July 1994 period. On 1 June 1995, only the southernmost 50 m of Pointed Island remained exposed; about 750 m of the island had been covered since 19 May 1995. On Pointed Island, thousands of nesting birds were displaced or killed and their nests destroyed as they were overtopped by the advancing ice margin. On Tsitus (*Arrowhead*) Island, the total ice advance during this phase of the surge was less than 200 m.

This phase of the surge was much shorter lived than the first. However, total terminus advance was as significant as it was in the 1957–67 surge event, and advance speeds into the proglacial Vitus Lake again greatly exceeded flow speeds over islands and adjacent land areas. This advance revitalized the stagnant mass of ice to the north in the Weeping Peat Island area, and the advancing ice reconnected with the toe of the glacier that had been detached by the jökulhlaup in December 1994 (see following section). Here the total amount of advance was about 250 m. As was the case to the west, the last evidence of ice advance disappeared by mid-September 1995.

Muskett and others (2000) reported that, in June 1995, just after the onset of the second phase of the 1993–95 surge, Bering Glacier was profiled by a geodetic airborne laser altimeter according to the methods of Echelmeyer and others (1996). These results were used to compare elevation and volume



**Figure 203.**—Two views show changes occurring on the southeast shoreline of Vitus Lake during July 1995. **A**, 9 July 1995 northeast-looking oblique aerial photograph of the advancing ice margin that forced the entire drainage from the eastern part of the Bering Glacier to flow into a narrow channel. A larger version of this figure is available online. **B**, 6 July 1995 southeast-looking photograph of the shoreline retreat and the development of a high bluff. Photographs by Bruce F. Molnia, U.S. Geological Survey.



**Figure 204.**—Two oblique aerial photographs showing complex fracturing and crevassing that occurred during the later part of phase one and the early part of phase two of the 1993–1995 surge. **A**, 9 May 1994 south-looking view shows a 4-km-wide section of the Bagley Ice Valley, with several types of crevasses, including rectilinear crevasses, and the development of subparallel rifts. **B**, 24 July 1994 north-looking view across the central Piedmont Lobe shows part of a 5-km-long developing rift set in a wide section of rectilinear crevasses. The east-west-trending snow-filled crevasses represent fractures that formed during early fall 1993 and that were subsequently filled with winter 1993–1994 snow. The north-trending fractures and crevasses began forming during the spring of 1994. Photographs by Bruce F. Molnia, U.S. Geological Survey. A larger version of this figure is available online.



changes that occurred between June 1995 and 1972–73. They found that, despite the fact that a significant volume of ice was transported to Bering Lobe by the surge in 1993 and 1994, the surface of the glacier was “generally lower in 1995 than in 1972–1973” (Muskett and others, 2000, p. F404). They estimated that the total volume lost was  $41 \pm 10 \text{ km}^3$  of ice, which they presented as a corresponding area-average mass balance of  $-0.8 \pm 0.2 \text{ m a}^{-1}$  water equivalent. Elevation change was nonuniform; surface lowering was greatest on Bering Lobe near the terminus, where a maximum of 75 to 100 m of lowering had occurred. Although they did not quantify it, Muskett and others (2000) noted an area of the Bering Lobe 13 km upglacier from the terminus where a small thickening occurred. A maximum of 50 m of thickening was seen further upglacier above the equilibrium line. They concluded that “negative mass balance predominated over the massive downglacier transport of ice caused by the 1993–1995 surge” (Muskett and others, 2000, p. F404).

Comparing 1950s map data of the glacier with data obtained during airborne profiling surveys in the middle and late 1990s showed that, on an annual basis, Bering Glacier thinned by  $0.914 \text{ m a}^{-1}$  and that its volume decreased by  $1.78 \text{ km}^3 \text{ a}^{-1}$ . However, between the middle 1990s and 1999, on an annual basis, Bering Glacier thinned by  $3.077 \text{ m a}^{-1}$  and its volume decreased by  $6.0 \text{ km}^3 \text{ a}^{-1}$  (K.A. Echelmeyer, W.D. Harrison, V. B. Valentine, and S. I. Zirnheld, University of Alaska Fairbanks, written commun., March 2001).

### *The 1994–1995 Jökulhlaup*

During the spring of 1994, a number of large blue-water ice-surface (supraglacier) lakes formed at several locations on Bering Lobe and in the Bagley Ice Valley, as a 24 July 1994 oblique aerial photograph by the author shows (fig. 205). The largest of these was more than 1 km long. On 27 July 1994, a large sediment-laden jökulhlaup began at the terminus of Bering Lobe immediately east of Weeping Peat Island. During the first few hours of the jökulhlaup, hundreds of large blocks of ice, many with maximum dimensions estimated to be greater than 30 m, broke off from the glacier face and were jettied into the deep lake adjacent to the ice margin. Within 24 hours, a canyon more than 1 km long was cut into the ice margin as the point of water discharge retreated upglacier. Initial peak discharges were estimated to be greater than  $10^5 \text{ m}^3$ . In early September 1994, the retreating point of the high-volume discharge reached the northern end of Weeping Peat Island. Within days, many of the supraglacier lakes were drained.

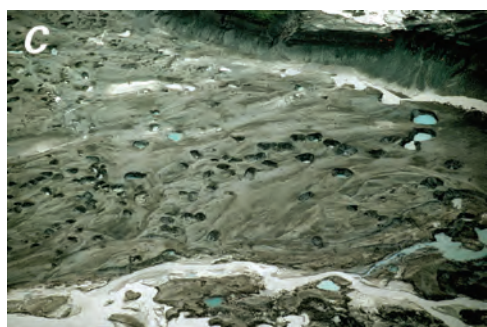
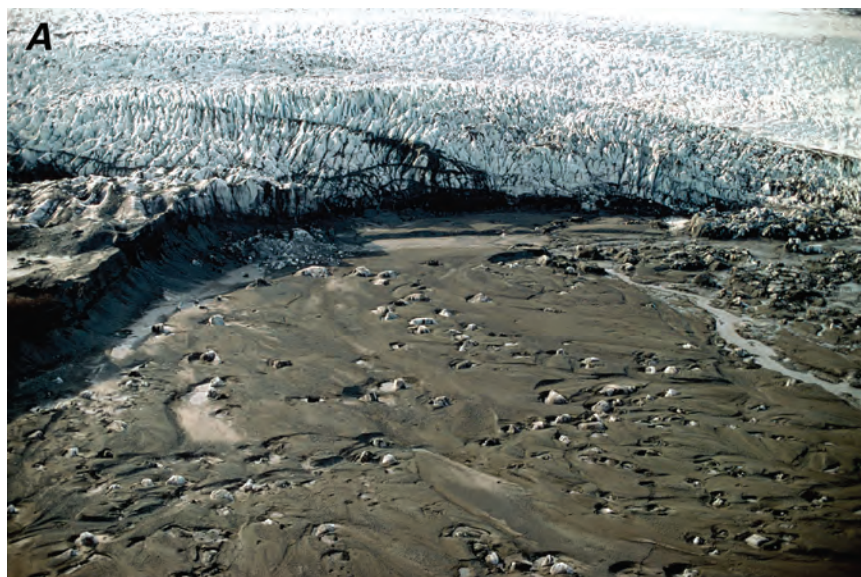
The high-volume discharge of water, which had shifted direction nearly  $90^\circ$ , continued to cut a widening west-trending channel through the stagnant terminus of the glacier during the next few months and dissected the toe from the remainder of the glacier. During the first year of the flood, approximately  $0.3 \text{ km}^3$  of sediment and ice were deposited into the ice-marginal lake system on the southeastern side of the glacier, and a channel was cut through the central area of Weeping Peat Island. The high-volume discharge continued for much of the next year and deposited a large outwash-fan delta, part of which formed in water as deep as 50 m. By late July 1995, following a lowering of the lake's level, the melting of ice blocks buried in the sediment created several dozen near-circular pit pond depressions (kettles) on the surface of the northern end of the outwash-fan delta adjacent to the ice margin. The largest had a diameter of about 20 m and a depth of 5 m. At several lakeshore and riverbank bluffs, blocks of ice buried in the sediment were exposed in profile.

By the spring of 1996, the volume of water discharging from the base of the glacier had decreased to near pre-jökulhlaup levels. As a result, the lake's surface elevation dropped several meters, and more than  $6 \text{ km}^2$  of the outwash plain-fan delta were exposed. The stream discharging at the base of the glacier began to meander across the exposed outwash plain-fan delta. An inversion of topography occurred at many locations where ice blocks were buried in the sediment, and the tops of buried ice blocks were exposed, many reaching more than 3 m above the outwash plain-fan delta's surface (figs. 206A, B). Many blocks were surrounded by moats, some water



**Figure 205.**—24 July 1994 north-looking pre-jökulhlaup oblique aerial photograph of a blue-water lake formed on the surface of Bering Glacier in the Bagley Ice Valley taken less than a week before the onset of the 28 July 1994 jökulhlaup. The photograph shows part of an approximately 350-m-diameter circular lake located approximately 10 km west of Juniper Island. Photograph by Bruce F. Molnia, U.S. Geological Survey.

**Figure 206.**—Three photographs showing the evolution of kettle ponds in the outwash-fan delta formed by sediment deposited during the 1994–1995 jökulhlaup. **A**, 30 April 1996 oblique aerial photograph of the northern end of the outwash-fan delta shows two stages in the development of the kettle ponds. Meandering of the stream located to the right of center has eroded the sediment cover from many large ice boulders to its east. Their rapid melting resulted in the formation of only a few small kettle ponds. To the west of the stream, where only the top part of the ice boulders is exposed, melting over the ensuing 3 months formed many large kettle ponds. **B**, 1 May 1996 ground photograph of a 20-m-long sediment-banded ice boulder present in A. Three months later, a 6-m-deep kettle pond was located at this site. **C**, 20 July 1996 oblique aerial photograph of the same area shown in A. Individual kettle ponds can be correlated with exposed ice blocks in the earlier photograph. Photographs by Bruce F. Molnia, U.S. Geological Survey. Larger versions of B and C are available online.



filled. Erosion and scour resulting from lateral stream-channel migration had removed at least 4 m of sand and gravel and left behind the newly exposed ice boulders. This erosion and downcutting were responsible for the reversal of topography.

All of the exposed ice boulders had melted by 20 July 1996, and the surface of the outwash plain-fan delta was covered with several hundred kettle holes (fig. 206C). Of the 90 kettles the author studied during a 2-week field investigation in mid-August 1996, the largest was about 35 m in diameter and about 5 m deep. More than a dozen had ice exposed in their walls. Most of the studied kettles were continuing to enlarge through slumping and melting of buried ice. Another stream channel migration event was underway on 17 September 1996, the date of the last 1996 site visit. Between 26 August and 17 September 1996, the stream migration had completely removed about 40 of the easternmost kettles and exposed ice boulders at the surface of several of the former kettle locations on the eastern side of the westward-migrating stream. Many other areas showed evidence of surface slumping, an indication that melting of subsurface glacier ice was continuing. When the area was observed in August 2001, there was no evidence of continuing kettle growth, and various types of vegetation were becoming established in the area between the kettles.

It was initially thought that the July 1994 jökulhlaup was a surge-ending flood event because ice velocities decreased following the onset of the jökulhlaup and ice-displacement ceased within 60 days. But it was not, because the ice resumed its advance following a 7-month pause. Perhaps the jökulhlaup was caused by a partial failure of the subglacier “barrier” or “dam” responsible for the initiation of the 1993–94 surge. However, it was the only major jökulhlaup associated with the 1993–95 surge of the glacier.

Following the onset of the July 1994 jökulhlaup, a large suspended-sediment plume began to exit Vitus Lake and entered the Gulf of Alaska through Seal River, as a 7 September 1994 vertical aerial photograph shows (fig. 207). It is likely that the origin of the plume was one or more subglacier channels located on the eastern side of the Bering Lobe. The restriction, if not total blockage, of flow through these sediment-dammed channels may have been responsible for the 1993 surge. The discharge of sediment appears to be closely tied to the mechanics of Bering Glacier’s surge cycle. From the 1970s through the middle-1980s, sediment-laden water flowed from Vitus Lake through Seal River into the Gulf of Alaska. Sometime during 1985, the plume disappeared and remained absent until just after the beginning of the 1994 jökulhlaup. The sediment plume’s reappearance at about the same time



**Figure 207.**—7 September 1994 vertical aerial photograph of Seal River shows the large suspended sediment plume exiting Vitus Lake. At the time of this photograph, the suspended sediment load exceeded  $2 \text{ g L}^{-1}$ . For much of the decade before the onset of the 1994 glacier outburst flood (jökulhlaup), the suspended sediment load dropped by more than an order of magnitude. USGS photograph no. 94-V4-85 by Robert F. Krimmel, U.S. Geological Survey.

as the jökulhlaup's occurrence adds credence to the hypothesis that Bering Glacier's surges are caused by a buildup of subglacier water pressure and water volume resulting from blockage of Bering Glacier's subglacier channels with sediment and that the jökulhlaup resulted from the failure of the subglacier sediment dam.

The Seal River sediment plume is visible on nearly every Landsat image collected during the Landsat baseline period (1972–81) (fig. 208A) (Post, 1976). During that period, it was the second largest and second densest sediment plume entering the Gulf of Alaska. The largest—the Copper River plume—annually transports about  $10^8$  metric tons of sediment into the Gulf of Alaska (Reimnitz, 1966) (fig. 208B). In addition to the Landsat imagery, 1979 aerial photographs of the Seal River also show the sediment plume, but it is absent from 1990 and 1992 photographs. A 22 August 2003 Moderate

► **Figure 208.**—Two 1970s views, a 2003 view, and a 1938 view of the suspended sediment plume from the Seal River. The magnitude of the sediment plume before the middle 1980s suggests that little impediment existed to its flow through subglacial drainage channels of the Bering Glacier. The subsequent closure of the drainage channels, resulting in the middle 1980s decrease in suspended sediment load, may have been a factor in the onset of the 1993 surge. The Seal River sediment plume, west of the terminus of Bering Glacier, separates into two components: part of the plume extends offshore, and part flows along the west side of Kayak Island, merging with the Copper River suspended sediment plume. In the 1970s and early 1980s, the Seal River plume was the second largest sediment plume entering the Gulf of Alaska. For comparison, Reimnitz (1966) calculated that the Copper River plume, largest in Alaska, annually introduced approximately  $10^8$  kg of suspended sediment into the Gulf of Alaska. **A**, Annotated Landsat 3 RBV image of the Copper River Delta area and environs on 24 August 1978. Seal River is to the right off the image, but part of its sediment plume is

visible in the lower right corner. The Steller Lobe dams Berg Lake (fig. 191), which had jökulhlaups in 1984, 1986, and 1994. Martin River Glacier has a large stagnant terminus. Miles Glacier has receded 7.2 km since 1890 (Field, 1975, p. 321). Previously, it coalesced with Childs Glacier on the opposite bank of the Copper River. Childs Glacier surged in 1909, with an advance of several hundred meters, but has not surged since. The Sherman Glacier terminus is covered with the debris from a landslide that occurred during the 1964 earthquake. The Copper River is very turbid; its sediment plume extends far into the Gulf of Alaska. Landsat 3 RBV image (30172–20175–B; 24 August 1978; Path 71, Row 18) and caption courtesy of Robert M. Krimmel, U.S. Geological Survey. **B**, 12 July 1976 photograph taken from the rail of the R.V. Sea Sounder, approximately 3 m above the ocean surface, of the edge of the Seal River plume in the Gulf of Alaska. Photograph by Bruce F. Molnia, U.S. Geological Survey. A larger version of this figure is available online. **C** and **D**, see following page.

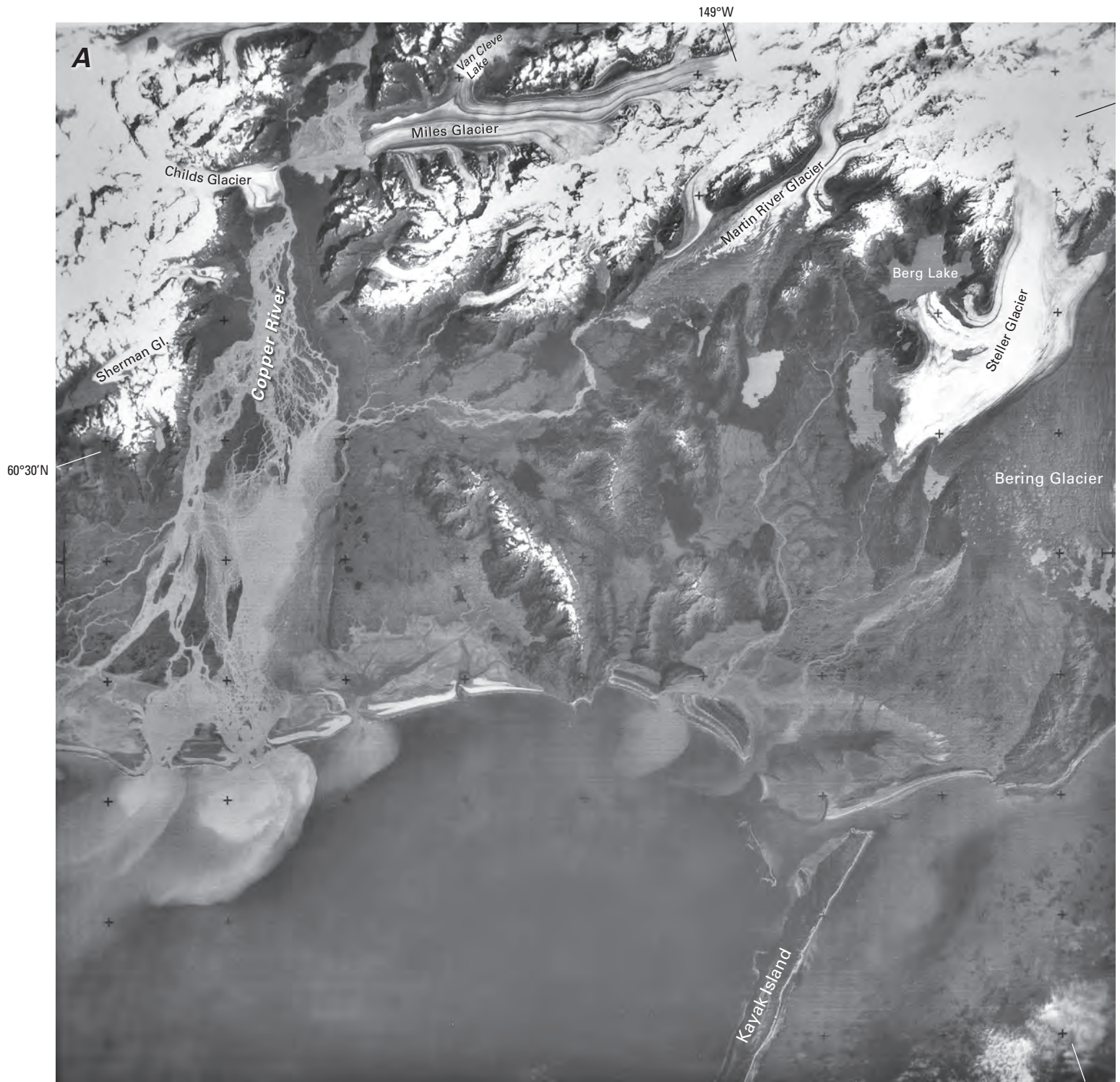




**Figure 208.**—**C**, 22 August 2003 Moderate Resolution Imaging Spectroradiometer (MODIS) image of the Gulf of Alaska coastal area from just east of Prince William Sound (left) to Grand Plateau Glacier (right). The same area shown in A is located on the western third of the MODIS image. MODIS image from the National Aeronautics and Space Administration. **D**, Summer 1938 oblique aerial photograph of the southernmost part of the terminus of Bering Glacier, Vitus Lake, Seal River, and the Gulf of Alaska. In this post-1920s surge photograph, a large sediment plume can be seen entering the Gulf of Alaska and flowing around Kayak Island. A large calving and disintegration event is also taking place at the glacier's terminus. Photograph no. 1000 by Bradford Washburn, Museum of Science (Boston).

Resolution Imaging Spectroradiometer (MODIS) image (fig. 208C) covers approximately the same area encompassed by the 24 August 1978 Landsat 3 RBV image (fig. 208A) and shows multiple plumes. A very large sediment plume is visible on Bradford Washburn's summer 1938 photograph of the mouth of the Seal River (fig. 208D).

#### *Post-Surge Retreat of Bering Glacier*

As it was during the advancing phase, the retreat rate of the terminus from the land areas was significantly less than that of the thicker tongues of ice that filled the deeper basins of Vitus Lake. Before the summer of 1996, little change was noted on the ice-covered islands within Vitus Lake or on the ice-covered part of the mainland east of Vitus Lake. By early summer 1996, the retreat of this land-based ice was underway at an average rate of less than  $0.5 \text{ m d}^{-1}$ . By 1997, multiple recessional moraines indicated hiatuses in the land-based retreat cycle at several locations.

Following the end of terminus advance in mid-September 1995, the parts of Vitus Lake that were not filled by surge-advanced ice were filled with

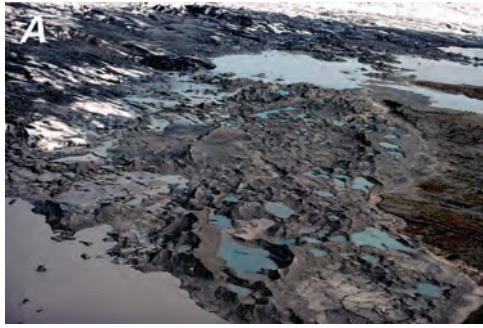


**Figure 209.**—Two oblique aerial photographs of the continued retreat of Bering Glacier from the north end of Beringia Novaya. **A**, 6 June 1997 photograph shows the surge-maximum moraine and several recessional moraines, numerous developing kettles, and the retreating ice margin. **B**, 12 August 2001 photograph taken more than 6 years following the cessation of surge motion within the terminus of the Bering Glacier. The boundary between vegetation and bare ground marks the 1995 maximum advance of the glacier. Continued thinning and retreat have resulted in the rapid disintegration of the terminus of Bering Glacier. Photographs by Bruce F. Molnia, U.S. Geological Survey. Larger versions of these figures are available online.

icebergs. Almost no water was visible between the glacier's margin and the southern shore of Vitus Lake. Calving, which was ongoing during the early rapid advance of the terminus, continued as surge advances waned. The glacier slowly began to actively retreat again (fig. 209A), mostly through the production of many icebergs (fig. 209B). Without the influx of surge-transported ice, rapid retreat of the terminus from the deeper basins of Vitus Lake ensued. Both Vitus Lake and Tashalich Arm quickly developed semicircular calving embayments (fig. 40). Active calving in both areas continued through the summer of 1998. By late 1999, Beringia Novaya and Pointed Island were ice free; Whaleback Island was ice free by early 2001.

The retreat from Tsitus (*Arrowhead*) Island was much slower. Less than 50 m of retreat had occurred by 10 August 1998 (fig. 210); less than 300 m of the southern end of the island had been exposed by August 2001. The ice that had covered Tsitus (*Arrowhead*) Island was the thickest of any island in Vitus Lake. The channel to the east that had connected to the eastern ice-marginal lakes was still filled by a large volume of surge-advanced ice. Similarly, ice that had advanced over the mainland east of Vitus Lake still covered much of the land, as a 12 August 1998 oblique aerial photograph taken by the author shows (fig. 211). Before the summer of 2001, all of the ice that had advanced onto Weeping Peat Island had retreated. The surface of the eastern part of the island displayed at least four recessional moraines.

By late summer 1997, the rate of calving decreased in the Vitus Lake embayment west of Beringia Novaya. Several concentric, arcuate crevasses developed parallel to the perimeter of the terminus in the calving embayment. By 26 September 1997, intensive compressional forces rotated a single large mass of the glacier bounded by two subparallel crevasses and raised it more than 40 m above the surface of the adjacent ice (fig. 212). After about 72 hours, this massive 80×50×10-m pyramidal-shaped piece of ice calved into Vitus Lake.

Calving of the margin continued at a reduced rate from late 1997 through late 1998; however, the physical characteristics of the margin changed significantly. The height of the face of the glacier decreased by more than 50 percent



**Figure 210.**—Oblique aerial photograph of the deglaciated terrain following the post-surge retreat of Bering Glacier from the south end of Tsitus (*Arrowhead*) Island. 10 August 1998 east-looking view of the southern end of Tsitus (*Arrowhead*) Island shows the retreating terminus of Bering Glacier. As was the case on Pointed Island, several recessional moraines mark the post-surge retreat. Many grooves and furrows mark the areas of maximum advance. Photograph by Bruce F. Molnia, U.S. Geological Survey.

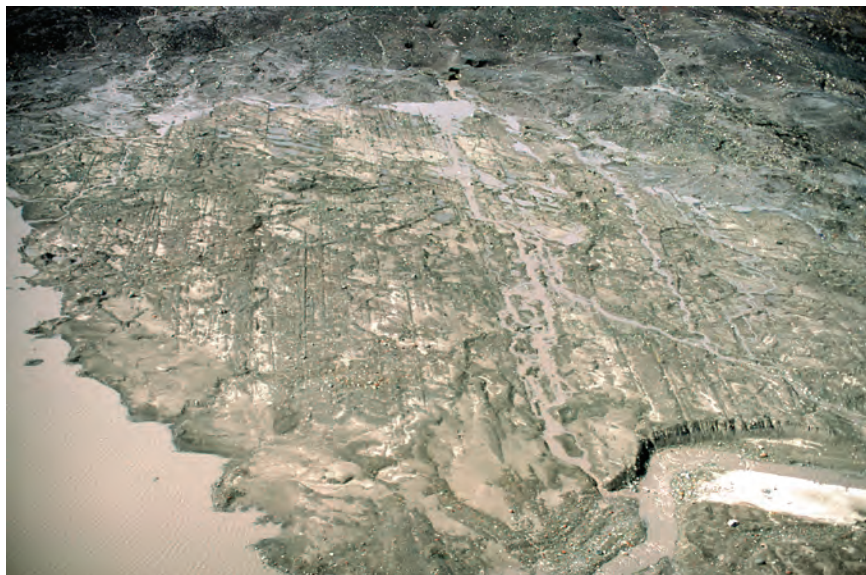


**Figure 211.**—12 August 1998 north-looking oblique aerial photograph of the post-surge retreat of Bering Glacier west of Weeping Peat Island. The most obvious features are the numerous grooves and furrows. Retreat during the 3-year period since the cessation of the surge amounts to approximately 500 m. Photograph by Bruce F. Molnia, U.S. Geological Survey.



**Figure 212.**—Photograph of an uplifted pyramidal-shaped piece of ice, approximately 80×50×10 m, produced by unusual compressional stresses in the calving embayment of Bering Glacier in Vitus Lake on 26 September 1997. Southwest-looking view across the Bering Glacier west of Beringia Novaya. The uplifted triangular block of ice was not observed while being rotated. However, its debris-covered former surface has been rotated towards the west. Note the single-engine aircraft flying behind the ice block. Photograph by Bruce F. Molnia, U.S. Geological Survey.

between 1996 and late 1998. The height of the ice cliff along much of the margin in Vitus Lake continued to decrease in 1999 and 2000. By 1999, part of the terminus had retreated more than 5 km. By 2001, continuing retreat of the glacier had caused much of the terminus to reoccupy positions similar to those held by the ice front in the pre-surge period from 1992 to 1993.

In 2000 and again in 2001, as successions of large icebergs calved from the margin and drifted into Vitus Lake, parts of the terminus were observed retreating as much as 700 m in less than 24 hours. By 12 August 2001, the surface of the glacier in the eastern terminus region closely resembled the pre-1993-surge surface of the glacier (fig. 213).

In the central part of Bering Lobe, several kilometers behind the terminus, dramatic changes occurred during the post-surge period. When the surge ended in September 1995, Bering Lobe's surface was fractured by large rifts, irregular rectangular blocks of crevasse-bounded ice, and many seracs. Local relief was as much as 20 m in places (fig. 204). Rapid melting was accelerated by the large surface area of the numerous surface features. By the end of the summer 1997, the surface of Bering Lobe had little local relief. In August 2001, the time of the last observation made by the author, many areas of the generally flat surface of Bering Lobe showed scars from the intensive deformation that the glacier had undergone during the surge. In addition, extensional fractures (fig. 200) that had opened in the CMMB closed within 24 months. Sauber and others (2000) recognized that substantial quantities of ice were transported from the accumulation area of Bering Glacier to the terminus region during the 1993–95 surge of Bering Glacier. They



**Figure 213.**— 12 August 2001 oblique aerial photograph of the nature of the terminus of Bering Glacier 6 years after the end of the 1995 surge. The north-looking view shows the low-relief terminus of Bering Glacier and the recently emerged Whaleback Island. With the exception of break up of the terminus on the left side of the picture, calving is minimal. The Piedmont Lobe has a very low gradient, and the ice face ranges in height from less than 1 m to approximately 3 m in height. Photograph by Bruce F. Molnia, U.S. Geological Survey.

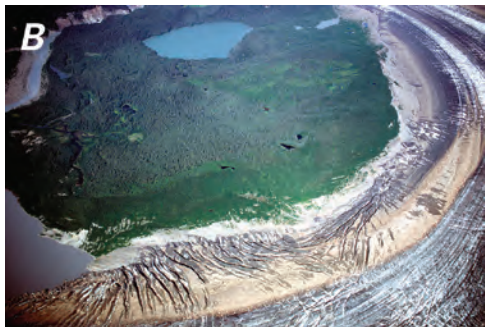


**Figure 214.**— Two oblique aerial photographs of the effects of the surge on the ice-cored lateral moraine of the Steller Lobe, located north of Nichawak Mountain. **A**, 12 August 2000 close-up north-looking view of the distal end of the lateral moraine. In late spring 2000, the ice-cored moraine started to disintegrate. By late summer, the Steller Lobe rapidly advanced into the adjacent lake. **B**, By 12 August 2001, the surge was over. In a higher altitude northeast-looking view, most of the seracs and ice pinnacles visible in 2000 have melted. The rapid advance of the terminus has also ceased. Photographs by Bruce F. Molnia, U.S. Geological Survey. Larger versions of these figures are available online.

noted substantial rates of near-instantaneous uplift in the reservoir region in response. These rates ranged from  $18.2 \pm 6.6$  to  $29.9 \pm 5.7$  mm a<sup>-1</sup>. Sauber and Molnia (2000) also found that seismicity in the region of the dramatic thinning increased during the surge interval relative to the pre-surge period. Following the surge, during the 2-year post-surge period of 1998 to 2000, no earthquakes greater than  $M2.5$  occurred.

Josberger and others (2001) measured the bathymetry, temperature, and conductivity of Vitus Lake during August 2001. They found that intense vertical convection in Vitus Lake was controlled by the salt content of the water and that there was strong saline stratification in the deeper portions of the lake. Thermal diffusion across the pycnocline (zone of change in water density as function of depth) may produce frazil ice growth, whereas melting of the glacier terminus produces convection at the margin of the lake.

### Steller Glacier Activity

Steller Glacier did not actively surge during the 1993–95 Bering Glacier surge. In 1994, it began to develop a series of large subparallel cracks along the southern margin of the Steller Lobe, which were thought to be the result of stresses that were transmitted through the CMMB. By 1998, part of the southwestern terminus of the Steller Lobe experienced a pulse that caused it to advance several hundred meters. By 2000, much of the surface of the Steller Lobe was fractured, and the main trunk of Steller Glacier and the northern lobe of its terminus, which enters (and dams) Berg Lake, began a mini-surge. This surge continued through the late summer of 2001. The ice-cored lateral moraine on the northwestern side of the part of the Steller Lobe that ends in an unnamed lake, north of Nichawak Mountain, became broken up in 2000 and rapidly advanced into the lake (fig. 214). By fall 2001, the surge was over. The southern part of the terminus of the Steller Lobe did not show any evidence of been involved in the surge.

### Glaciers of Waxell Ridge

Waxell Ridge separates the valley glacier section of Bering Glacier from the Bagley Ice Valley. Its high point is the summit of Mount Steller. Several dozen unnamed cirque and small valley glaciers, including Yushin, Betge, and Ovtzyn Glaciers, descend from the southern side of the ridge and the flanks of Mount Steller and flow toward Bering Glacier. During the last half of the 20th century and the early 21st century, every one of these glaciers has thinned and retreated. On the southern flank of Mount Steller, glaciers originate in four cirque basins. Before 1950, a single large glacier flowed out of each cirque basin and de-

scended to the base of the mountain, connecting to one of two debris-covered valley glaciers that flowed into Bering Glacier. When observed from the air on 8 August 2001 (fig. 215), glaciers in each cirque basin had separated into many discontinuous, retreating small ice masses, and cirque glaciers from three of the four basins no longer connected to the valley glaciers.

About a dozen small, unnamed, north-flowing glaciers descend from the northern side of Waxell Ridge into Waxell Glacier to nourish the Bagley Ice Valley. The longest is about 5 km long. Although some show evidence of a little thinning, all reach the Bagley Ice Valley. When observed from the air on 12 August 2001, all were still snow covered.

### **Glaciers of the Southern Side of Juniper Island**

Juniper Island is the 43-km-long east-west-trending ridge that separates the eastern Bagley Ice Valley from Jefferies Glacier. About a half dozen small, unnamed, south-flowing cirque glaciers descend from the ridge. All are rapidly retreating and thinning, and nearly all have lost contact with the Bagley Ice Valley (fig. 216). A conspicuous trimline, with a height of less than 50 to nearly 100 m, extends along the western third of the ridge.



**Figure 215.**—8 August 2001 view of Mount Steller showing the retreat of a number of unnamed glaciers from nearly every cirque basin on the south side of the mountain. When first observed by the author in 1974, each cirque basin was covered by ice and snow, and all of the glaciers descending from Mount Steller were in contact with the Bering Glacier. Photograph by Bruce F. Molnia, U.S. Geological Survey.



**Figure 216.**—12 August 2001 oblique aerial photograph of the Juniper Island area. View of the north side of the Bagley Ice Valley showing several rapidly retreating and thinning cirque glaciers. Photograph by Bruce F. Molnia, U.S. Geological Survey.



**Figure 217.**—Close-up photograph on 13 August 1992 of an in situ mollusk (*Petricola?*) located within the beds of the Yakataga Formation that yielded a  $^{14}\text{C}$ -calibrated age of 4,860 yr B.P. The presence of the bivalve mollusk indicates that, at that time, the Bering Glacier must have been significantly smaller in area than it is at present. Photograph by Bruce F. Molnia, U.S. Geological Survey.

## Holocene History of Bering Glacier

Much of what we know about the Holocene history of Bering Glacier is derived from (1) radiocarbon dating ( $^{14}\text{C}$ ) of subfossil wood, peat, shells, and organic debris recovered from glacial and fluvio-glacial sediment exposed by late 20th century retreat of Bering Glacier (Molnia and Post, 1995) and (2) dendrochronological analysis of subfossil wood by Wiles and others (1999), who developed a floating tree-ring calendar dating to A.D. 1020. Wiles and Calkin (1994) have also shown the benefit of using tree-ring analysis to construct records of past glacial fluctuations in the late Holocene from boreal forest regions of Alaska.

Molnia and Post (1995) constructed a late Pleistocene to present-day history for Bering Glacier. Between 15,000 and 12,000 yr B.P., the large late Pleistocene glacier that covered much of the Gulf of Alaska continental shelf began to retreat (Molnia, 1986). Interpretation of  $^{14}\text{C}$ -dated basal peat samples collected from bogs and fens developed on glacially eroded bedrock basins suggests that, by about 10,000 yr B.P. (if not earlier), the entire Gulf of Alaska continental shelf was ice free, and remnants of the large Pleistocene glacier that filled Bering Trough had retreated into the Chugach Mountains. At this time, the ancestral Bering Glacier did not have a piedmont lobe.

For about the next 5,000 years, the glacier remained in a retracted position.  $^{14}\text{C}$ -dated core samples from bogs and from loose marine shells of about 8,000 yr B.P., all from the Tashalich Arm area, suggest that open-water marine conditions existed in the area of the piedmont lobe. An exposure of the Yakataga Formation containing an in place mollusk (*Petricola?*) emerged from under the pre-1993-surge terminus of the glacier in 1992 (fig. 217). These mollusks lived in abandoned circular borings made by another bivalve mollusk of the family Pholadidae near the limit of low tide. These shells yielded a  $^{14}\text{C}$ -calibrated age of 4,860 yr B.P. Because the clam shells are preserved in perfect condition, it appears that they were buried quickly, possibly in outwash sand and gravel, by an advance of Bering Glacier into marine waters around 5,000 yr B.P. or by rapid sedimentation following a tectonic event. Shortly after the death of the clams, their entombing strata were uplifted above sea level.

$^{14}\text{C}$  dates were also obtained from the top and bottom of a 5-m-thick peat deposit (fig. 218), which was composed of leaves, bark, twigs, and seeds, interbedded with thin (1 mm to 2 cm) silt layers, and located adjacent to the outcrop containing the shells. The peat deposit, which lies just above the level of the Yakataga Formation outcrop, was exposed by glacier recession



**Figure 218.**— 13 August 1992 photograph of part of a 5-m-thick peat deposit located on the northeast side of Tashalich Arm. The  $^{14}\text{C}$  age of the deposit ranges from 2,970 yr B.P. (top) to 4,360 yr B.P. (bottom). Photograph by Bruce F. Molnia, U.S. Geological Survey.

between 1988 and 1993 and occurs about 0.5 km north of the shell-bed exposure described above. The top and bottom of the deposit (elevation of ~3 m) had  $^{14}\text{C}$  ages of 2,970 yr B.P. (top) and 4,360 and 4,130 yrs B.P. (bottom).

Interpretation of the Tashalich Arm deposits and the bog chronology suggests that Bering Glacier was retracted for most, if not all, of the middle Holocene (fig. 219A). It certainly was not in an advanced position between 4,400 and around 3,000 yrs B.P. Molnia and Post (1995) concluded that, following uplift, the Tashalich Arm area was a lowland bog occasionally inundated by marine or fluvial waters. If a glacial advance was responsible for the burial of the Yakataga Formation outcrop, it must have been short lived. The start of the accumulation of peat less than 500 years after the death of the clams indicates that local conditions were favorable for the growth of abundant vegetation.

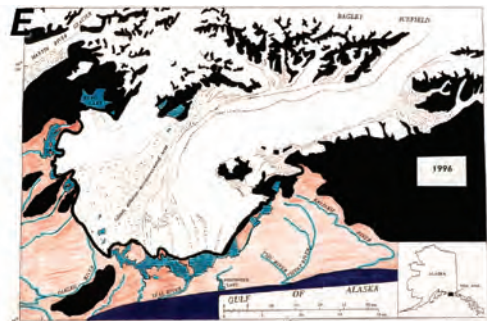
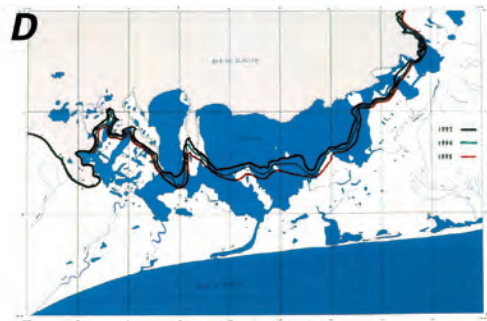
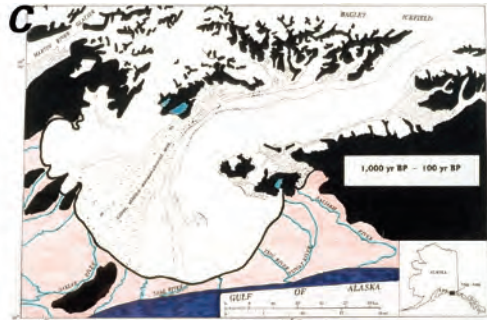
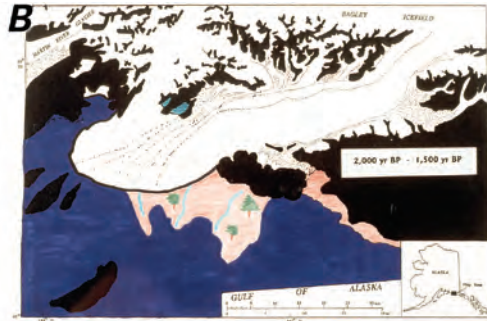
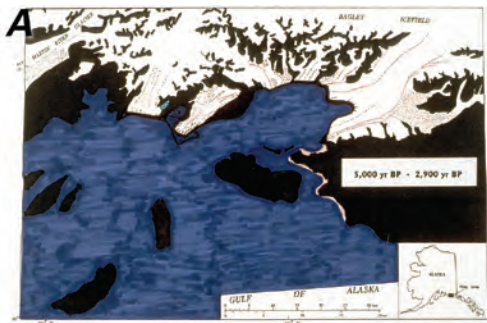
Warm (peat-forming) conditions continued for at least 1,200 years. Sometime after 2,970 yr B.P., the Tashalich Arm peats were buried by outwash sand and gravel deposits, suggestive of the first advance of Bering Glacier in more than 7,000 years. Gravel deposition terminated about 2,000 yr B.P.

Following gravel deposition, a forest, the *Major Forest Bed* (MFB) of Muller and others (1991) grew to near maturity. Although subsequent glacial erosion and overriding by glacier ice have removed much of the forest, enough remains to identify in place trunks of spruce (*Picea* sp.) and hemlock (*Tsuga* sp.), many 200 years old and 40 cm in diameter (Muller and others, 1991). The similarity in both the age and the general level of the trees, usually about 10 m (range of 4–20 m) above the level of Vitus Lake, indicates that most, if not all, of the foreland was stable at the time the forest became established. Many  $^{14}\text{C}$  ages of tree stumps from various locations around eastern Vitus Lake indicate that the trees were growing between approximately 2,000 and approximately 1,500 yr B.P. (A.D. 34 – A.D. 539) In all, 45 tree-ring series from 36 MFB trees indicate that the MFB grew for 299 years from A.D. 277 through A.D. 525 (Wiles and others, 1999). Growth in some places was sustained until about 1,500 yr B.P. (fig. 219B). In some localities, silts up to 2 m thick buried and killed the trees. Floating calendar dating indicates that most or all of these trees then were killed by the deposition of up to 3 m of fine silt around their trunks during a period of 10 years or less (Wiles, written commun., 1994).

Soon thereafter, during the late 5th century through the early 6th century A.D. (around 1,400 yr B.P.), the standing trees were sheared off, presumably at the new ground level, quite probably by an advance of the glacier. As much as 20 m of layered outwash sand and gravel was deposited on top of the sheared forest, suggesting that a nearby glacier was actively advancing. Near Nichawak Mountain, a  $^{14}\text{C}$  age of  $1,250 \pm 60$  yr B.P. obtained from a sheared log suggests that the margin of the Steller Lobe also was advancing at this time.

In several localities around the margin of Bering Glacier, outwash-plain sequences contain at least two more young forest layers. The more prominent, exposed on the western shore of Tashalich Arm where more than 100 stumps have been counted and in canyons on islands in Vitus Lake, grew around 900 to 1,000 years ago (fig. 219C). Nearby, a forest overrun by the glacier's last major advance includes some of the biggest trees exposed by glacier recession in Alaska. The largest, a spruce called *Giant Log*, has more than 375 growth rings 6 m above its roots and is approximately 1.6 m in maximum diameter. Tree-ring chronology indicates this spruce lived during the period A.D. 1256 to 1631 (Wiles and others, 1999). This log and several others nearby appear to have been directly buried by a glacier advance. Trees lived along the eastern margin of Vitus Lake from at least A.D. 1020 until A.D. 1631 The youngest vegetation found in outwash gravels is a small number of in place alder bushes (*Alnus* sp.) that yield  $^{14}\text{C}$  ages of about 400 yr B.P.

► **Figure 219.**—A sequence of five sketch maps that depict positions and events in the Holocene history of the Bering Glacier. **A,** Map showing the retracted position of the terminus of Bering Glacier from approximately 5,000 yr B.P. until approximately 2,900 yr B.P. It is likely that Bering Glacier did not expand beyond the terminus position shown here at any time during the first 7,000 years after its latest Pleistocene retreat into the mountains. **B,** Map showing the first Holocene advance of the terminus of Bering Glacier some time after approximately 2,000 yr B.P. until approximately 1,500 yr B.P. This advance is documented by several forest deposits consisting of numerous rooted trees sheared off by an ice advance. **C,** Map showing the maximum position attained by the terminus of Bering Glacier during the Holocene. Dendrochronological evidence suggests that the Bering Glacier reached this position approximately 1,000 yr B.P. and remained at this maximum position until the first decade of the 20th century. **D,** Sketch map showing the position of Bering Glacier's terminus before and at annual intervals (at the end of each summer) during the 1993–1995 surge. The north shore of Vitus Lake marks the area occupied by the Bering Glacier before the onset of the surge at the end of summer 1992. **E,** Sketch map showing the position of the terminus of Bering Glacier in 1996 following the end of the 1993–1995 surge. With the exception of Arrowhead Island, which was still essentially ice covered, the 2002 position of the Bering Glacier was similar to that of the ice margin at the end of summer 1992 (D). Larger versions of these figures are available online.



During the past 1,500 years, the margin of Bering Glacier has fluctuated, advancing in some places and retreating in others. The net result is that the “Little Ice Age” maximum position, reached at many locations within the past 250 to 1,250 years, represents its greatest advance for at least the last 7,000 years. This advance produced the neoglacial maximum moraine, which rims the glacier. A sheared spruce tree exposed along the western side of the Seal River, where the river cuts through the outer edge of the neoglacial maximum moraine, yields a calibrated  $^{14}\text{C}$  age of  $1,053 \pm 50$  yr B.P., suggesting that the earliest formation of the end moraine occurred no more than about 1,000 years ago.

Elsewhere, growth-ring counts of trees growing on the neoglacial terminal moraine, sampled between 1991 and 1993, yield maximum dendrochronological ages of more than 250 years (near Oaklee River) and more than 180 years (south of Hanna Lake). The oldest living trees growing on the terminal moraine at the edge of the CMMB near Tashlich Arm are around 130 years old. These ages indicate that the active glacier margin may have remained close to the moraine until the middle 18th to early 19th centuries. Recession from the maximum position probably began within the last 200 to 250 years and had reached as much as 12 km before the advent of the 1993 surge.

In most cases, early 20th century positions of the terminus of Bering Glacier are available from early USGS maps and reports. Additional descriptions and maps by D.J. Miller (1958, 1961) provide details about the glacier in the 1940s and 1950s. Oblique aerial photographs taken in 1938, 1946, and 1948 and many vertical aerial photographs acquired since 1950 have been useful for mapping recent end and recessional moraines and for determining positions of the terminus. Comparing terminus positions shown on the early USGS maps with the 1993 pre-surge terminus position (fig. 219D) reveals that parts of the Bering Lobe have retreated as much as 12 km and thinned by more than 200 m, whereas parts of the Steller Lobe have receded a maximum of 4 km. The location of the glacier terminus during the 1993–95 surge (fig. 219D) and at the maximum reached before the latest retreat (fig. 219E) are derived from aerial photography.

### Copper River Drainage Segment (Including Glaciers That Drain Directly into the Copper River Delta)

A number of large glaciers making up part of the eastern shoreline of the lower Copper River drain into it or into the Copper River Delta (see fig. 208). A braided stream, the Copper River is the largest river that drains into the Gulf of Alaska. The Copper River is very turbid and, typically, its sediment plume extends far out into the Gulf of Alaska (see figs. 208A, C). Reimnitz (1966) determined that its typical suspended sediment load exceeds  $1.0 \times 10^8 \text{ kg a}^{-1}$ . Hence, the Copper River transports more sediment than any other river in Alaska, including the Yukon River. About 1905, when large copper deposits were discovered in the Wrangell Mountains, a route to transport the copper ore to the port of Cordova was needed. Much of the route that was selected was within the Copper River valley and had to pass through a reach that contained many large glaciers (Post, 1976). Between 1906 and 1910, the Copper River and Northwest Railway was constructed at a cost of about 20 million dollars. Mining officials were concerned that the railroad could easily be disrupted by advances of other glaciers and by changes in the glaciers on which some of the tracks had been laid. Through the 1930s, work crews continuously struggled to maintain the track and compensate for glacier flow and floods.

## **Martin River Glacier–Martin River–Lower Copper River–Bremner River–West Fork Tana River–Tana Glacier Subdivision**

The Martin River Glacier–Martin River–lower Copper River–Bremner River–West Fork Tana River–Tana Glacier subdivision, located east of the Copper River, is the southeastern part of the Copper River drainage segment. It contains a number of large valley glaciers, including many that drain westward into the lower Copper River and the Copper River Delta. The subdivision has a maximum length of about 95 km and a maximum width of about 95 km. In this subdivision alone, an estimated area of 1,750 km<sup>2</sup> is covered by glaciers, the largest being the combined Jefferies and Tana Glaciers, which feed many unnamed glaciers. Large glaciers in the north-central part of this subdivision not connected to the Bering Glacier System—such as Bremner, Fan, Martin River, Miles, and Wernicke Glaciers—are nourished by a series of interconnected accumulation areas west and north of the Bagley Ice Valley.

All glaciers (named and unnamed) listed have approximate lengths greater than 7 km. The areas of Martin River, Slide, and Johnson Glaciers are according to Field (1975b, p. 461–463). All other glacier areas have been estimated by the author. Glaciers in this subdivision include:

- Martin River Glacier, the source of the Martin River (48 km, 290 km<sup>2</sup>)
- Slide Glacier, named for a large 1964 earthquake-produced rockslide, but previously called *Sioux Glacier* (10 km, 15 km<sup>2</sup>)
- Johnson Glacier (11 km, 26 km<sup>2</sup>)
- An unnamed glacier (9 km, 13.5 km<sup>2</sup>)
- McPherson Glacier (12 km, 15 km<sup>2</sup>)
- Miles Glacier (52 km, 225 km<sup>2</sup>)
- Van Cleve Glacier, which drains into Van Cleve Lake, an ice-dammed lake on the northern side of Miles Glacier (20 km, 30 km<sup>2</sup>)
- Wernicke Glacier, located at the head of the Wernicke River (33 km, 60 km<sup>2</sup>)
- Fan Glacier, which has both an eastern and a western terminus (34 km, 60 km<sup>2</sup>)
- An unnamed glacier (12 km, 14 km<sup>2</sup>)
- An unnamed glacier (7 km, 10 km<sup>2</sup>)
- Bremner Glacier, which has three distinct outlets: Middle Fork Lobe, North Fork Lobe, and Tana Lobe (44 km, 150 km<sup>2</sup>)
- Tana Glacier (68 km, 100 km<sup>2</sup>), including the western part of the Jefferies Glacier (55 km, 300 km<sup>2</sup>), a complex glacier with many outlet glaciers that is contiguous with the Tana Glacier and that is an eastern source of the Bagley Ice Valley.

### **Ragged Mountains**

Less than a dozen small unnamed glaciers exist on the western flank of the Ragged Mountains, heading at elevations between 730 and 1,000 m. The longest is less than 1 km in length. All show conspicuous evidence of thinning and retreat. Several small glaciers, shown with lengths of approximately 400 m on the USGS 1:250,000-scale Cordova topographic quadrangle map (1953) (appendix A), have disappeared.

### **Martin River Glacier**

Martin River Glacier has a length of 48 km and an area of 290 km<sup>2</sup> (Field, 1975b, p. 461) and drains into the Copper River by way of its principal distributary, Martin River (see fig. 213). It has a large stagnant terminus, in places

fronted by a large ice-marginal lake formed by retreat during the 20th century. Elsewhere, the terminus is composed of stagnant ice thermokarst features or supports a mature spruce forest. The terminus of Martin River Glacier has three distinct lobes separated by bedrock ridges. The 7-km-long southeastern lobe, named Kushtaka Glacier, ends on an outwash plain north of Kushtaka Lake. The 3-km-long central lobe, called the *Charlotte Lobe* by Reid and Clayton (1963), is the smallest of the lobes. The unnamed southwestern lobe is more than 7 km wide. Like nearby Bering Glacier, the terminus of Martin River Glacier is presently stagnant, downwasting, and slowly retreating. The lower 11 km of the glacier is covered by an ablation moraine. This morainic debris cover ranges in thickness from 0.3 to 6.0 m, the average thickness being 0.7 m (Reid and Clayton, 1963). Clayton (1964) attributed the ablation till to concentration of subglacial debris brought to the surface by thrusting. The glacier's 4-km-wide marginal zone hosts a number of funnel-shaped sinkholes, most supporting small thermokarst lakes. Reid and Clayton (1963) and Clayton (1964) determined that the sinkholes have an average diameter of 250 to 300 m and depths of 30 to 90 m. Many are connected and partly filled with standing water and significantly increase the discharge of meltwater at the terminus when draining (Reid and Clayton, 1963).

Clayton (1964) described a multitude of thermokarst features that are present on the surface of the glacier, including ice caves, tunnels, sinking streams, dry stream beds, blind valleys, large springs, natural bridges, sinkholes coalescing to form compound sinkholes, thermokarst windows (unroofed parts of englacial or subglacial streams), and glacial uvulas (enlarged thermokarst windows where a stream flows from one side of the uvula across an exposed gravel bed and into another tunnel on its opposite side).

Martin River Glacier was observed many times from the air by the author between 1974 and 2004. During this 30-year interval, parts of the glacier have thinned by at least 30 m, and many of the sinkholes have expanded and connected. Likewise, the ice-marginal lake adjacent to the debris-covered terminus expanded perhaps 250 to 350 m by the melting of stagnant ice.

In a trend first noted by the author in 1974, many small unnamed glaciers—some former tributaries to Martin River Glacier, located adjacent to and along the northern margin of the glacier—have continued to thin and retreat. Some smaller cirque glaciers have disappeared (fig. 220).



**Figure 220.**—North-looking oblique aerial photograph on 31 July 1999 of a pair of small, retreating unnamed glaciers located adjacent to the north side of Martin River Glacier. Many small cirque glaciers in the Chugach Mountains are rapidly retreating. Photograph by Bruce F. Molnia, U.S. Geological Survey.

## Slide Glacier

Slide Glacier, located in a side valley adjacent to and west of Martin River Glacier, has a length of 10 km and an area of 15 km<sup>2</sup> (Field, 1975b, p. 461) (fig. 221). Originally named *Sioux Glacier*, its current name is the result of several large 1964 earthquake-produced rockslides that covered approximately 17 percent of its accumulation area and approximately 90 percent of its ablation area with 2 m or more of debris (Post, 1967a). According to Post, three of the largest slides contained about  $2.4 \times 10^7$  m<sup>3</sup> of rock. Reid (1969) found that, before the earthquake, the glacier had been shrinking. From the beginning of the 20th century until 1964, the glacier had thinned by as much as 35 m. One and one-half years after the slides occurred, differential melting had caused the slide-debris-covered portion of the glacier to be 13 m higher than the adjacent bare ice. The next year, the elevation difference was 18 m. Hence, over three summer ablation cycles (1964, 1965, 1966), the average difference in ablation rate exceeded 5 m a<sup>-1</sup>. When the author observed the glacier from the air on 16 August 2000, he noted a small amount of retreat along the debris-covered terminus; a fresh trimline along the margin of the bare ice portion of the glacier suggested that it was continuing to thin.



**Figure 221.**—Two north-looking oblique aerial photographs of Slide Glacier, with 1964 earthquake-produced rock avalanches covering much of its terminus area. **A**, 6 October 1974 view shows the debris-covered terminus region standing higher than the bare ice to its north. Photograph by Bruce F. Molnia, U.S. Geological Survey. **B**, 13 August 1990 view shows a second 1964 rockslide moving into the terminus region. Photograph by Larry Mayo, U.S. Geological Survey.





### **Johnson Glacier**

Johnson Glacier has a length of 11 km and an area of 26 km<sup>2</sup> (Field, 1975b, p. 461). An unnamed glacier located to its north has a length of 9 km (Field, 1975b, p. 462) and an area estimated by the author at around 13 km<sup>2</sup>. Both Johnson Glacier and the unnamed glacier showed signs of thinning and retreat when the author observed them from the air on 16 August 2000. Both were fronted by ice-marginal lakes and outwash plains indicative of significant retreat during the later half of the 20th century. Johnson Glacier was actively calving large icebergs into its proglacial lake. The size of its ice-marginal lake suggests at least 2.5 km of retreat from its late 1950s terminus position.

### **McPherson Glacier**

When Martin photographed McPherson Glacier in 1910, it had a length of 12 km (Field, 1975b, p. 462) and an area estimated by the author at approximately 15 km<sup>2</sup>; it extended to the floor of the Sheep Creek valley. By the 1960s, retreat of more than 2 km resulted in the disappearance of its terminal tongue and the exposure of an approximately 2.4×1.0-km lake basin that served as the reservoir for an ice-dammed proglacial lake. Several times during the operation of the Copper River and Northwestern Railroad, jökulhlaups washed out part of the railroad. Similarly, one or more jökulhlaups in 1962 or 1963 washed out 1.5 km of the Copper River Highway (Post and Mayo, 1971). An additional jökulhlaup occurred in 1965 (Post, 1967a). When it was observed by the author from the air in 2000, McPherson Glacier had so significantly thinned and retreated that it could no longer impound water. Much of the floor of its former proglacial lake bed was covered with vegetation.

### **Miles Glacier**

Miles Glacier has a length of 52 km (Field, 1975b, p. 462) and an area estimated by the author at about 225 km<sup>2</sup>. It retreated a maximum of 7.2 km between the 1880s and the late 1960s (Field, 1975b) and approximately another 2.9 km through 2004. Late 19th and early 20th century retreat produced Miles Lake, originally an elliptical ice-marginal lake along the southwestern margin of the glacier and now a near-circular body of water approximately 8 km in diameter that fronts the entire terminus of Miles Glacier. Large numbers of icebergs calve off the terminus of the glacier and float across the lake, passing under Million Dollar Bridge as they drift downstream. To protect the bridge from Miles Glacier's icebergs, massive steel and concrete iceberg deflectors were installed upstream of the bridge's main supports when it was built in 1909.

Before 1840, an advance of Miles Glacier resulted in its merging with Childs Glacier. This merger displaced the Copper River to the western side of its valley. Tarr and Martin (1914) suggested that, at that time, the river probably flowed in a tunnel or in a gorge that it cut through the glacier ice. A relict part of this expanded terminus is currently located on the western side of the river, a result of the Copper River's cutting a new channel through this stagnant moraine during the 1940s. Between 1885 and 1888, the terminus of Miles Glacier advanced to a position about 125 m from the site where Million Dollar Bridge would eventually be built. From 1888 to 1908, a 20-year-period of rapid retreat ensued. Miles Glacier's terminus retreated as much as 4 km, an average retreat rate of 200 m a<sup>-1</sup>. A 2-year advance began in 1908; by 1910, the terminus had advanced approximately 1.25 km, an average advance rate of 610 m a<sup>-1</sup>. This advance occurred in spite of a calving event in July 1909 in which an approximately 1-km<sup>2</sup> section of Miles Glacier broke from the terminus and produced icebergs that completely filled Miles Lake (Tarr and Martin, 1914). When Miles Glacier was next described in 1931 by Wentworth and Ray (1936), it had retreated at least 1 km. Field (1975b) reported that, by 1957, the glacier had retreated an additional 800 to 1,800 m (see also AGS

Glacier Studies Map No. 64-3-G6) (Field, 1965) and that, between 1957 and 1968, maximum retreat was an additional 2 km.

Since 1991, the author has observed Miles Glacier from the air annually, most recently on 16 October 2002. During that period, the glacier has continued to retreat (fig. 222) and thin along its margins, losing contact with several tributaries and thinning to the point that former small ice-marginal lakes located along the glacier's northern margin no longer fill with water.

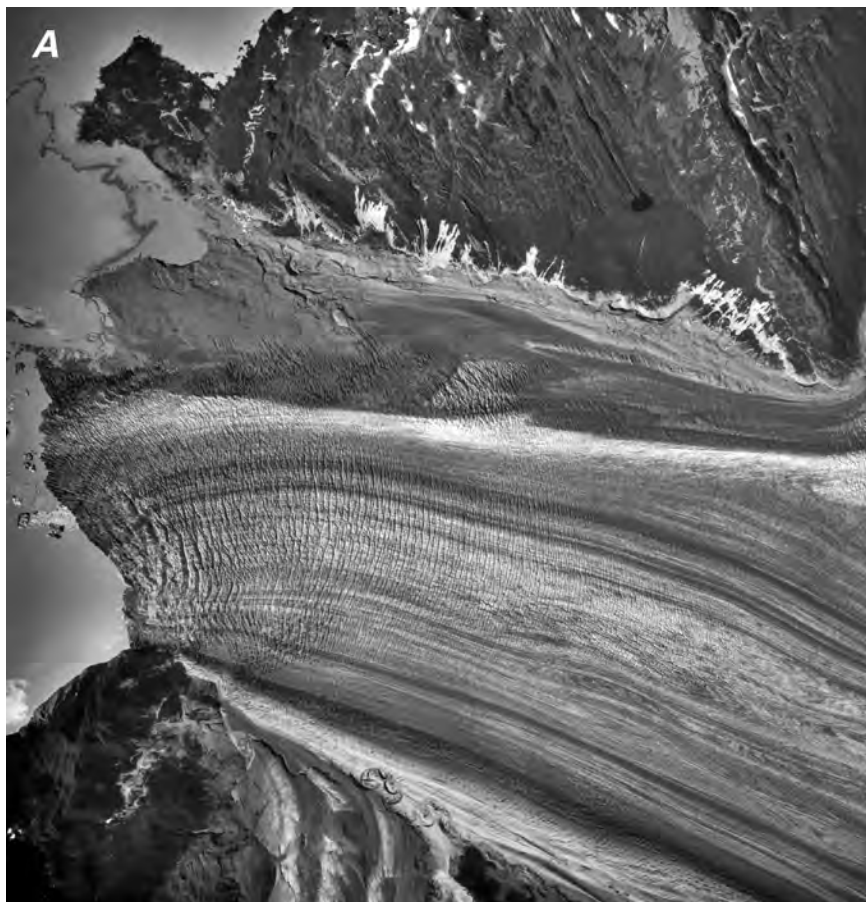


**Figure 222.**—Two photographs of the terminus area of Miles Glacier in Miles Lake in the late 20th and early 21st centuries. **A**, 13 August 1994 vertical aerial photograph of the lower 6 km of Miles Glacier shows multiple evidence of thinning and retreat. An unnamed north-flowing tributary barely reaches the margin of Miles Glacier. USGS photograph no. 94V3-175 by Austin Post, U.S. Geological Survey. **B**, 12 August 2001 east-looking oblique aerial photograph shows that the northern part of the terminus of Miles Glacier is characterized by stagnant, debris-covered ice, whereas the southern side is dominated by an active calving margin. Photograph by Bruce F. Molnia, U.S. Geological Survey.

### Van Cleve Glacier

Van Cleve Glacier has a length of 20 km (Field, 1975b, p. 462) and an area estimated by the author at about 30 km<sup>2</sup>; it drains into Van Cleve Lake, an ice-dammed lake located adjacent to the northern side of Miles Glacier, approximately 7 km east of its terminus (fig. 223). The proglacial lake of Van Cleve Glacier was the source of several early 20th century jökulhlaups that significantly impacted the railroad (Post and Mayo, 1971) and, more recently, the Copper River Highway. Tarr and Martin (1914) thought that calving of Miles Glacier's terminus was influenced by flooding from the lake. Twentieth century retreat of Van Cleve Glacier has lengthened the basin, but lowering the surface of both Miles and Van Cleve Glaciers has reduced the proglacial lake's capacity; it continues, however, to be a source of jökulhlaups.

### Large Glaciers North of Miles Glacier

Four large glaciers — Wernicke, Fan, Bremner, and Tana — flow down the northern side of the mountains and ridges west and north of the Bagley Ice Valley. All four glaciers show evidence of continuing thinning and retreat and the presence of stagnant ice.

#### *Wernicke Glacier*

Wernicke Glacier, the source of the Wernicke River, is located at the head of an approximately 12-km-long outwash plain that ends at the Copper River. It is located in the next large valley north of Miles Glacier and has a length of 52 km (Field, 1975b, p. 462) and an area estimated by the author at about 60 km<sup>2</sup>. Along with Fan Glacier and the three lobes of the Bremner Glacier, it drains the northern side of the unnamed mountain ridge that contains the summits of Mount Tom White (3,419 m) and Mount Hawkins (3,140 m). Although its terminus positions have been compared on oblique aerial photographs taken

**Figure 223.**—7 September 1994 vertical aerial photograph of the southern part of Van Cleve Lake where it is dammed by an unnamed distributary of Miles Glacier. This ice tongue, composed of ice flowing from both upglacier and downglacier, regulates both the depth and volume of Van Cleve Lake. In the 15 years between a photograph taken by Austin Post in 1969 (USGS photograph no. 69-R2-214) and this photograph, little change has occurred in the position of the terminus of the distributary glacier, but a 25-m-high strand zone along the shoreline of the lake indicates a thinning of the ice dam. The numerous folds in the medial moraines indicate the complex flow interaction between the western and adjacent eastern parts of the ice tongue. Note the right-angle bend made by the Miles Glacier medial moraine on the western side of the ice that flows into the unnamed distributary. USGS photograph no. 94-V4-236 by Robert M. Krimmel, U.S. Geological Survey.



by Bradford Washburn in 1938, the U.S. Army Air Forces in 1941, the USAF in 1957, and the USGS in 1964 (Field, 1975b), Wernicke Glacier has not been the subject of scientific investigations (nor have most of the glaciers in this part of the Chugach Mountains). Although Field (1975b) did not quantify the amount of change that he observed, he reported that the end of the lower limit of ice has receded upglacier as the area covered by moraine has been extended. When the author observed it from the air on 16 August 2000, the terminus region of Wernicke Glacier showed significant evidence of recession and thinning and the presence of stagnant ice. Many former tributaries have retreated to the upper reaches of their cirques or have disappeared altogether.

#### *Fan Glacier*

Fan Glacier bifurcates and has both an eastern and a western terminus; it has an approximate length of 34 km (Field, 1975b). The western terminus is located at the head of the South Fork of the Bremner River; the eastern terminus drains into the Middle Fork of the Bremner River. Fan Glacier has received little scientific investigation. However, a comparison by Field (1975b, p. 323) of terminus positions as depicted on oblique aerial photographs taken by Bradford Washburn in 1938, the U.S. Army Air Forces in 1941, the USAF in 1957, and the USGS in 1964 found a “recession from outer moraines, appreciable lowering of the ice surface, and progressive stagnation in the terminal area.” Field (1975b, p. 323) also reported that “all the smaller glaciers, some of which were formerly tributaries, also show evidence of marked recession.” A similar comparison by the author of the USGS Bering Glacier 1:250,000-scale topographic quadrangle map (1959) (appendix A), an AHAP false-color infrared vertical aerial photograph acquired on 18 August 1978 (fig. 224A), and oblique aerial photography of the terminus area of the glacier obtained by the author on 16 August 2000 shows significant evidence of recession and thinning and the presence of stagnant ice (fig. 224B).

East of the eastern terminus of Fan Glacier are several unnamed glaciers that formerly were tributaries to a connected Fan Glacier–Middle Fork Lobe of the Bremner Glacier ice mass (fig. 225). The western unnamed glacier

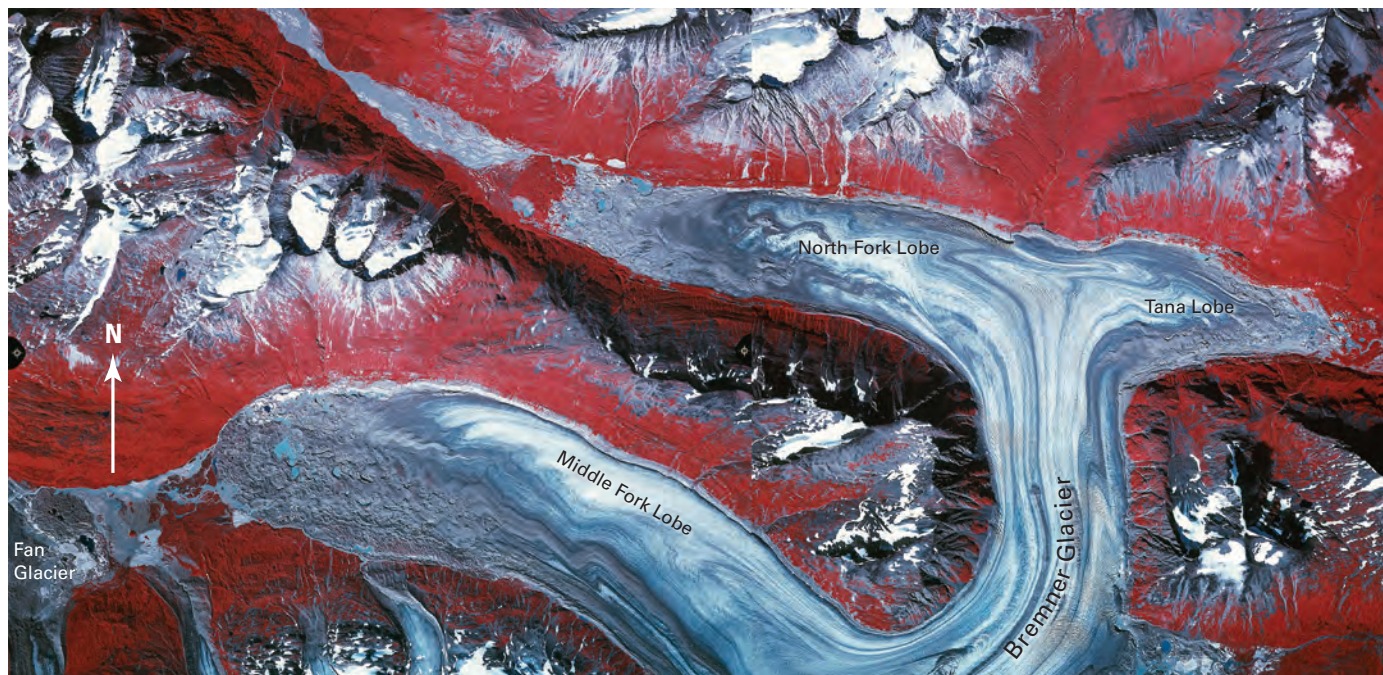


**Figure 224.**—Two aerial photographs of Fan Glacier showing evidence of ongoing retreat, thinning, and stagnation. **A**, 18 August 1978 AHAP false-color infrared vertical aerial photograph of the debris-covered western terminus of Fan Glacier. All of the north-flowing glaciers in the photograph, including those that are former tributaries of Fan Glacier located on the south side of the glacier and those in the unnamed mountain ridge to the north, are actively retreating. Note the trimline and area of stagnation on the north side of Fan Glacier. AHAP photograph no. L111F6217 from the GeoData Center, Geophysical Institute, University of Alaska, Fairbanks, Alaska. **B**, see facing page.

**Figure 224B.**— 16 August 2000 east-looking oblique aerial photograph of the debris-covered western terminus of Fan Glacier. The northern and southern margins show evidence of recent thinning. Numerous thermokarst features characterize the stagnant-ice terminus. Photograph by Bruce F. Molnia, U.S. Geological Survey.



▼ **Figure 225.**— 18 August 1978 AHAP false-color infrared vertical aerial photographic mosaic of the debris-covered Bremner Glacier with its three distinct outlets: Middle Fork Lobe, North Fork Lobe, and Tana Lobe. All of the termini of Bremner Glacier show evidence of stagnation, thinning, and active retreat. Four former tributaries to the Middle Fork Lobe are shown to its south. Note the elevated lateral moraine and trimline north of the North Fork Lobe. AHAP photograph nos. L111F6212 and L111F6214 from the GeoData Center, Geophysical Institute, University of Alaska, Fairbanks, Alaska.



previously flowed into the eastern Fan Glacier terminus; it has a length of 13 km (Field, 1975b, p. 462) and an area estimated by the author of about 14 km<sup>2</sup>. Adjacent to it on the east is another unnamed glacier that terminates between the glaciers; it has a length of 9 km (Field, 1975b, p. 463) and an area estimated by the author at about 10 km<sup>2</sup>. To the east of this latter unnamed glacier are two smaller unnamed glaciers. When the author observed them from the air on 16 August 2000, all showed significant evidence of recession and thinning and the presence of stagnant ice.

#### *Bremner Glacier*

Bremner Glacier has three distinct distributaries (Middle Fork Lobe, North Fork Lobe, and Tana Lobe); it has a length of 44 km (Field, 1975b, p. 463) and an area estimated by the author at about 150 km<sup>2</sup>. Like adjacent Fan Glacier, it has received little scientific investigation. A similar comparison by Field (1975b, p. 323) of terminus positions depicted on oblique aerial photographs taken by Bradford Washburn in 1938, the U.S. Army Air Forces in 1941, the USAF in 1957, and the USGS in 1964 found a “recession from outer moraines, appreciable lowering of the ice surface, and progressive stagnation in the terminal area.” Field (1975b, p. 323) also reported that “all the smaller glaciers, some of which were formerly tributaries, also show evidence of marked recession.” Likewise, a similar comparison by the author of the USGS Bering Glacier 1:250,000-scale topographic quadrangle map (1959) (appendix A), an AHAP false-color infrared photograph acquired on 18 August 1978 (fig. 225), vertical aerial photographs, and oblique aerial photographs of the terminus area of the glacier obtained by the author on 16 August 2000 shows significant evidence of recession and thinning and the presence of stagnant ice.

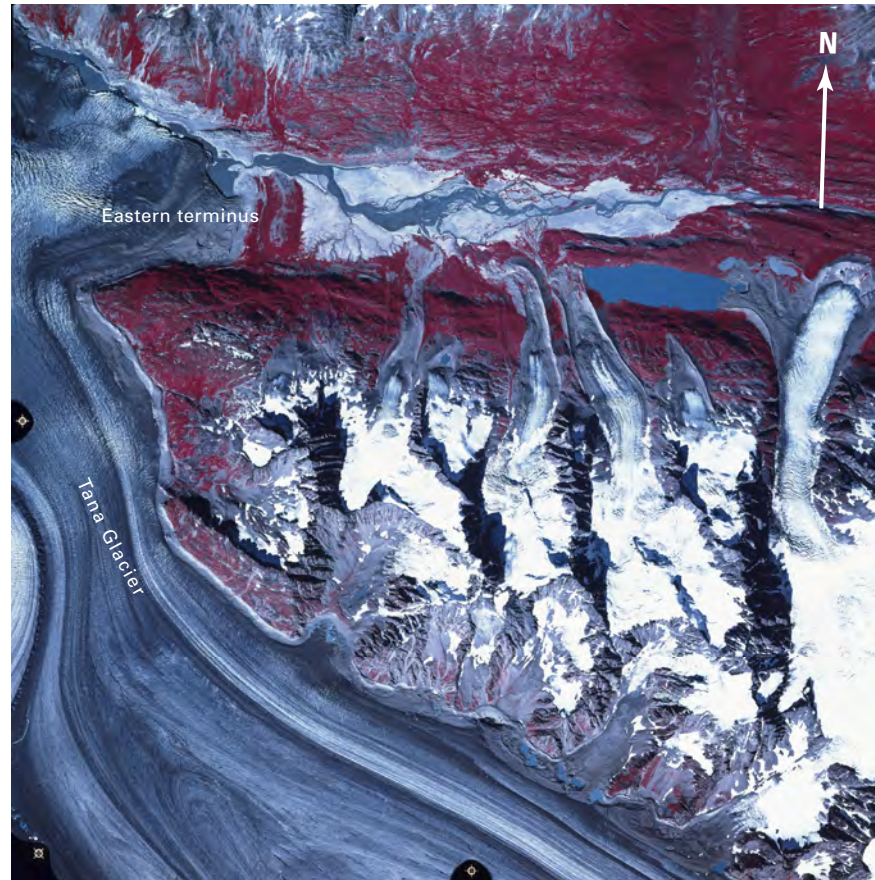
#### *Tana Glacier*

Tana Glacier has a length of 68 km (Field, 1975b, p. 463) and an area estimated by the author at about 100 km<sup>2</sup>, including the western part of Jeffries Glacier. Its primary sources are the valley north and east of Juniper Island, including the western end of an accumulation area of the Jefferies Glacier; the western Bagley Ice Valley; and an unnamed east-flowing tributary that drains the eastern part of the accumulation area that feeds the Bremner Glacier. Much of the lower glacier is flanked by prominent trimlines and freshly exposed lateral moraine. Brabb and Miller (1962) reported that, during the late Wisconsinan, Tana Glacier may have been more than 200 m thicker than it was in the late 1950s.

The glacier has two distributaries. The primary northern terminus is stagnant and is characterized by a network of debris-covered thermokarst pits and open water. The eastern terminus is similar, showing multiple evidence of stagnant ice, thinning, and retreat, as an 18 August 1978 AHAP photograph shows (fig. 226). In 1975, Field (1975b, p. 324) reported that aerial photographs of the glacier obtained in 1938, 1957, and 1960 “show no appreciable change in the position of the terminus, but there appears to have been some surface lowering and progressive stagnation.” Things changed significantly during the later 20th century. Observations of the terminus area made by the author from the air between 1995 and 2001 confirm continued thinning and the presence of stagnant ice in both termini and an increase in the volume of water associated with the two stagnant lobate termini. Behind the termini, the lower 6 km of the glacier is covered by moraine, and the glacier ice appears virtually stagnant. Much of the margin of Tana Glacier shows significant elevated moraines and trimlines, indicative of substantial late 20th century thinning.

Through the first one-third to one-half of the 20th century, the eastern terminus of the glacier dammed the flow of water from Granite Creek, forming Barkley Lake, an ice-dammed lake (Moffitt, 1918) that occupied the lower part of the Granite Creek valley. Annual draining of the lake was through

**Figure 226.**—18 August 1978 AHAP false-color infrared vertical aerial photograph of the retreating, partially debris-covered terminus of the eastern distributary of Tana Glacier. The former bed of Barkley Lake is visible just east of the distributary terminus, as are a number of former tributaries. AHAP photograph no. L113F6174 from the GeoData Center, Geophysical Institute, University of Alaska, Fairbanks, Alaska.



an ice-marginal channel. By the late 1940s, thinning and narrowing of the glacier resulted in unimpeded flow of Glacier Creek. Stone (1955) reported that, before 1951, the lake was “continuously empty for a minimum of three to five years.” A significant jökulhlaup occurred in July 2003.

### **The Bremner River–Upper Copper River–Chitina River–Tana River Subdivision (Located East of the Copper River)**

Every glacier in this subdivision is unnamed. All are less than 7 km long, with the exception of an unnamed glacier located at the head of the Little Bremner River (fig. 227), with a length of 17 km (Field, 1975b, p. 463) and an area estimated by the author at approximately 40 km<sup>2</sup>. Many of the glaciers in this area were observed from the air during several overflights made by the author in August 2000; all showed evidence of thinning and retreat.

Glaciers in this area exist in several locations. About two dozen small unnamed glaciers are located west of Tana River and north of North Fork Lobe and Tana Lobe of Bremner Glacier. There are also about 100 small unnamed glaciers from west of Hanagita Peak to the eastern side of Little Bremner River and Tebay River. The largest glacier between Little Bremner River and Tebay River is the previously mentioned 17 km unnamed glacier. It was actively retreating when observed in 2000. There are several other medium sized glaciers, including an unnamed glacier located at the head of Dewey Creek. The earliest photographs of glaciers in this area were made during the first half of the second decade of the 20th century and show that retreat was underway (USGS Photo Library Moffitt photograph 517). In the northwestern part of this subdivision, about 40 small unnamed glaciers drain into Canyon Creek and its tributaries or Copper River. All glaciers observed have been retreating for most, if not all, of the 20th century and showed significant evidence of thinning and retreat.



**Figure 227.**—Photograph by F.H. Moffitt, taken between 1910 and 1915, showing early 20th century evidence of thinning and retreat of an unnamed glacier located at the head of the Little Bremner River. USGS Photo Library photograph Moffitt 515.

## The Western Copper River Delta–Lower Copper River–Tasnuna River Subdivision (Located on the West Side of the Copper River)

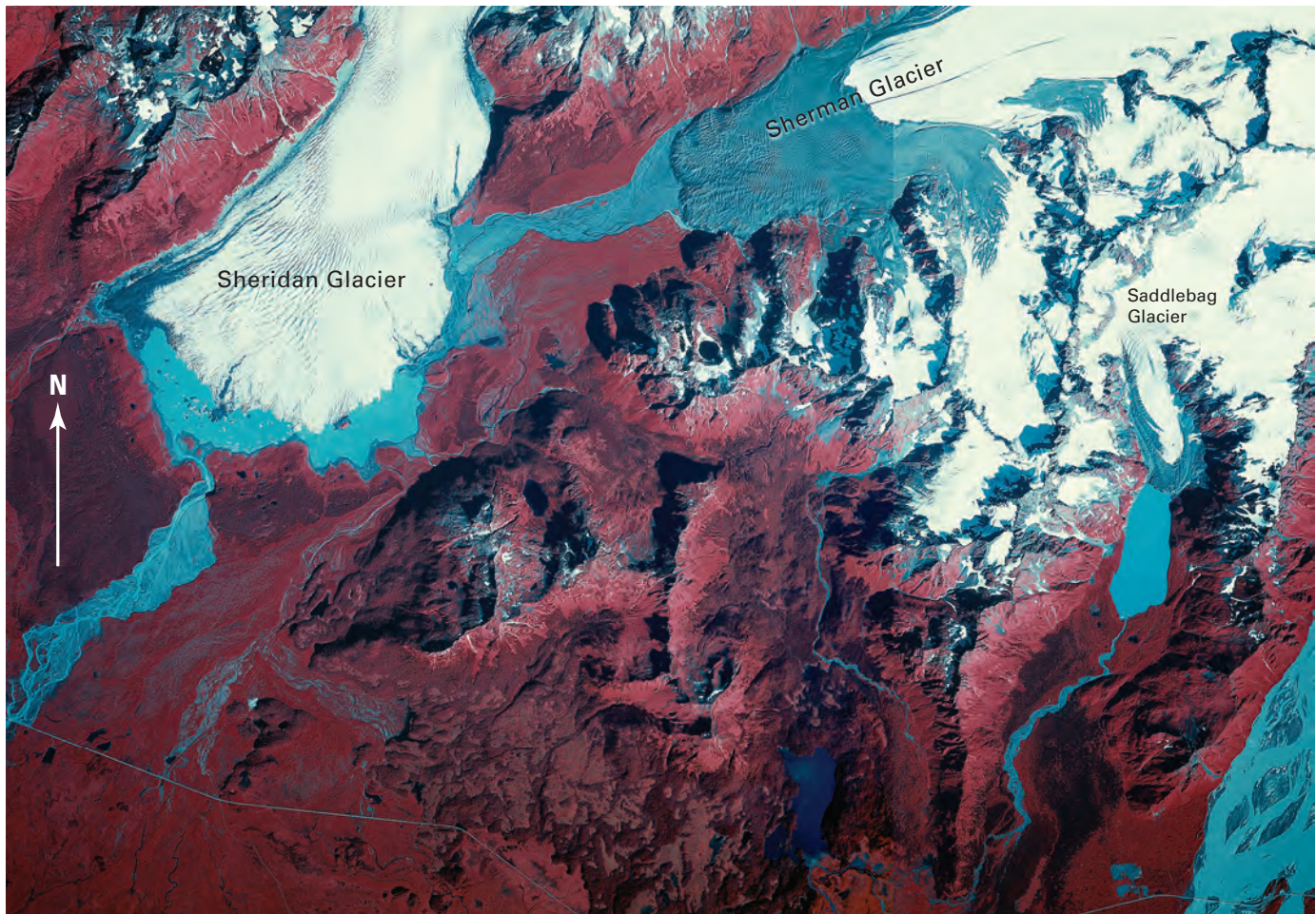
This subdivision contains a number of south-, east-, and north-flowing valley glaciers. Several have played a significant role in the early 20th century history of mineral development and extraction of ore. The Copper River and Northwest Railway was constructed on approximately 9 km of Allen Glacier, about 0.5 km of moraine-covered ice of Grinnell Glacier, and about 0.75 km of the terminal moraine of Heney Glacier. Many jökulhlaups from more than a dozen glaciers in this subdivision disrupted railroad operations. As recently as the summer of 2001, a flood of unknown origin washed out a segment of the Copper River Highway.

In this subdivision, the lengths (>8 km) and areas of glaciers are from measurements made by Field (1975b, p. 467–468) and include: Sherman Glacier (13 km, 55 km<sup>2</sup>), Sheridan Glacier (24 km, 101 km<sup>2</sup>), Scott Glacier (24 km, 160 km<sup>2</sup>), Marshall Glacier (8 km, 8 km<sup>2</sup>), Tasnuna Glacier (13 km, 28 km<sup>2</sup>), Woodworth Glacier (23 km, 185 km<sup>2</sup>), Schwan Glacier (23 km, 131 km<sup>2</sup>), Heney Glacier (19 km, 72 km<sup>2</sup>), Allen Glacier (31 km, 230 km<sup>2</sup>), Childs Glacier (19 km, 100 km<sup>2</sup>), and Goodwin Glacier (9 km, 13 km<sup>2</sup>).

### Saddlebag Glacier

Saddlebag Glacier is the southeasternmost glacier in this subdivision. Figure 228, a 13 August 1982 Alaska AHAP photomosaic of this area, shows the geographic relationship of Saddlebag Glacier and adjacent Sherman and Sheridan Glaciers. When it was photographed by the author on 12 August 2001, the glacier was located at the head of an approximately 3.5-km-long ice-marginal lake, dammed by a large end moraine that was probably deposited

**Figure 228.**—13 August 1982 AHAP false-color infrared vertical aerial photographic mosaic of the area between the Copper River (east) and the Glacier River (west) that flows from the Sheridan Glacier. Shown are Saddlebag Glacier (the southeasternmost glacier in this subdivision), Sherman Glacier, and Sheridan Glacier. All show evidence of thinning and retreat. A large 1964 earthquake-generated rock avalanche covers the terminus of Sherman Glacier. AHAP photograph nos. L115F1516 and L115F1517 from the GeoData Center, Geophysical Institute, University of Alaska, Fairbanks, Alaska.





during the “Little Ice Age” maximum. Field (1975b, p. 345) reported that, in 1899, the terminus of the glacier occupied the lake basin but was “already beginning to withdraw from the end moraine.” Retreat was slow, and an ice tongue filled much of the basin through the late 1950s. Between 12 June 1959, when it was photographed by the USFS, and 25 August 1960, when it was photographed by Post, “a massive break-up of the tongue” occurred and the glacier retreated about 1.5 km. Between 1960 and 2001, approximately 2.0 km of additional retreat occurred, accompanied by significant thinning.

### **Sherman Glacier**

Sherman Glacier (figs. 58, 228, 229) has a length of 13 km and an area of 55 km<sup>2</sup> (Field, 1975b, p. 468). It and adjacent Sheridan Glacier (fig. 228) both drain into the delta of the Copper River through the Glacier River. The surface of the lower 5 to 6 km of Sherman Glacier is covered with rock debris deposited from a massive landslide that occurred during the 27 March 1964 Alaska “Good Friday” Earthquake (figs. 58, 228). The powerful earthquake triggered many large rock and debris avalanches that were deposited on the surfaces of more than 50 glaciers in the Chugach Mountains. The Sherman Glacier landslide was among the largest of all, covering an area of about 8.5 km<sup>2</sup>, about one-third of the glacier’s ablation area (Post, 1967b). The volume of debris that was deposited on the glacier surface was about  $1 \times 10^7$  m<sup>3</sup> (Bull, 1969) (fig. 229A). When the author visited on 12 August 2000, the debris-covered ice stood about 35 m higher than the bare ice immediately upglacier from it. In the 36 years since the landslide, the 1.3- to 8-m-thick debris layer had insulated the ice beneath it and thus retarded its ablation.

Before the landslide, Sherman Glacier had been retreating. Tuthill and others (1968) described both an outer moraine, dating from about 1880, and an inner moraine, dating from about 1910, within 1.2 km of the 1964 terminus position. In the years between 1910 and 1959, the glacier retreated 970 m, yielding an average retreat rate of about 20 m a<sup>-1</sup>. During the 5-year period before the earthquake (1959–64), the glacier retreated approximately 230 m, yielding an average retreat rate of approximately 46 m a<sup>-1</sup>.

Bull (1969) speculated that a surge of this previously receding glacier would occur during the 1970s. He expected rates of advance of 50 to 100 m a<sup>-1</sup> that would persist for perhaps a decade. As of the author’s last observation from the air in August 2004, the predicted surge had not occurred. Bull and Marangunic (1967, 1968) noted that, in the year following the slide, the ice surface below the slide was lowered between 8 and 10 m. They attributed much of this loss to anomalously high air temperatures resulting from the heating of downglacier air as it passed over the surface of the debris slide. Thus, the heat reflected by the slide contributed to increased melting in the bare ice in the ablation area. By 29 August 1984, 20 years after the landslide, almost all of the bare ice below the slide had melted away, and the debris cover had been carried downvalley about 2 km (fig. 229C). The terminus was in nearly the same position in 1984 as it was in 1964, but the debris-covered ice was significantly thicker. All of the landslide debris was derived from one mountain, Shattered Peak. Shreve (1966, 1968) examined the mechanics of the slide and concluded that the debris had moved downglacier on a cushion of air at velocities of up to 75 km h<sup>-1</sup>. Part of the debris glided over a ridge about 130 m high.

Since 1984, the position of the terminus has changed only minimally, with stream erosion and melting of stagnant ice resulting in a few meters of annual retreat. However, many of the tributaries of Sherman Glacier are actively retreating. By 2002, one unnamed tributary on its northern side had separated into seven smaller glaciers.

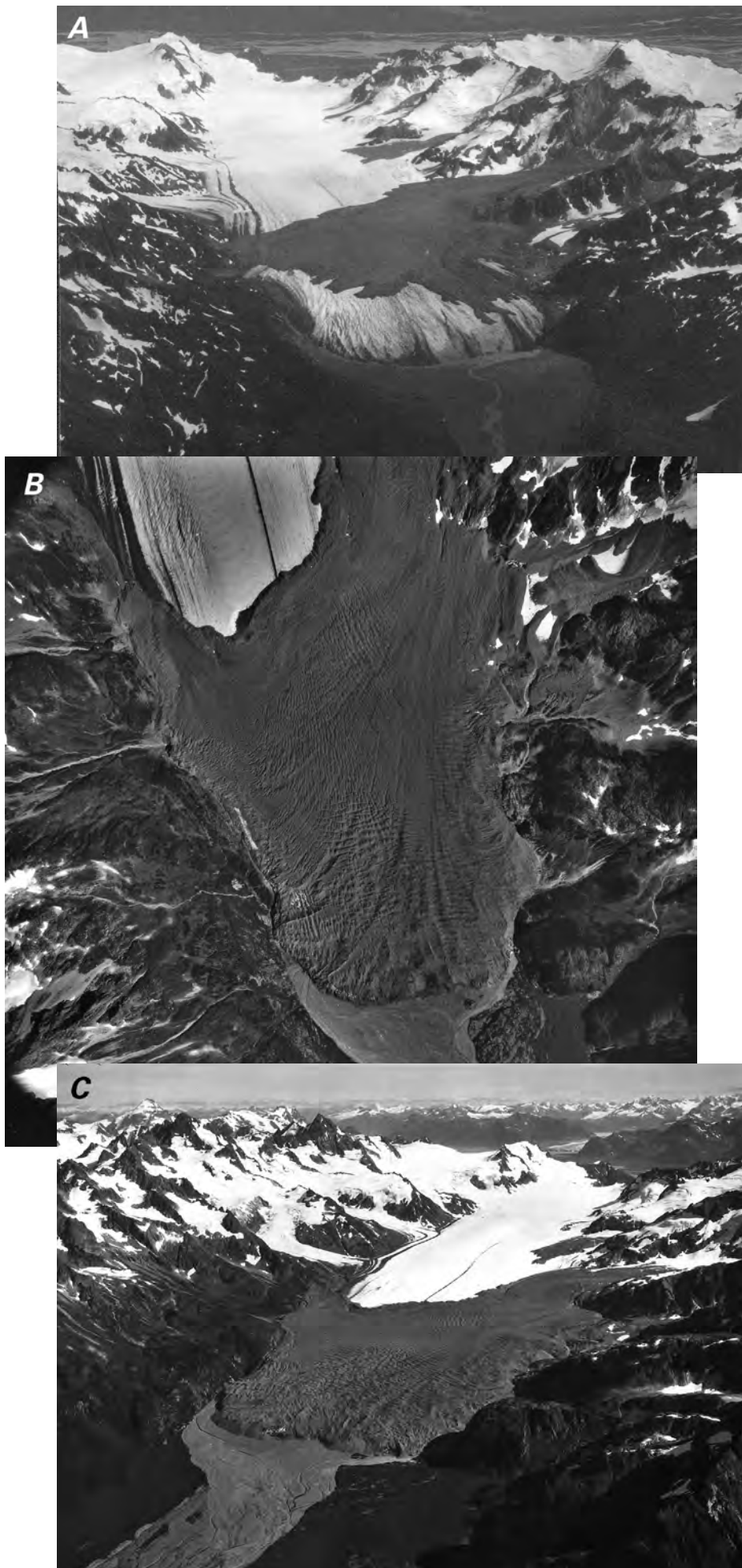


**Figure 229.**—Three aerial photographs of the Sherman Glacier. **A**, Oblique aerial photograph taken 24 August 1964 of a major rock avalanche that occurred during the 1964 Alaska earthquake and covered about 35 percent of the ablation area (Post, 1967b). The volume of the 1.3 to 8-m-thick debris was about  $1 \times 10^7 \text{ m}^3$  (Bull, 1969). The debris layer acted to insulate the buried ice and thus retard ablation, and Bull (1969) speculated that an advance of this previously receding glacier (Field, 1975, p. 347) would occur during the 1970s. Photograph no. K642-108 by Austin Post, University of Washington. **B**, 22 August 1979 vertical aerial photograph of the expanse of the terminus of Sherman Glacier. In the 15 years since the earthquake, all of the bare ice between the rockslide and the terminus melted away. USGS photograph no. 79-V2-186 by Austin Post, U.S. Geological Survey. **C**, By 29 August 1984, the debris cover had been carried down valley by the moving ice about 2 km. Although the terminus was in nearly the same position in 1984 as in 1964, the debris-covered ice was much thicker in 1984. USGS photograph no. 84-R1-222 taken on 29 August 1984 by Austin Post, U.S. Geological Survey. Photographs and caption courtesy of Robert M. Krimmel, U.S. Geological Survey. Photographs taken by the author in August 2000 show little change in the position of the terminus. A lowering of the base level in nearby Sherman Lake has lowered the surface of the outwash plain in front of the glacier. The elevation difference between the covered and bare ice is currently about 35 m.

## Sheridan Glacier

The terminus of Sheridan Glacier is only about 2.5 km to the west of Sherman Glacier. However, Sheridan Glacier, with a length of 24 km and an area of 101 km<sup>2</sup> (Field, 1975b, p. 468), is a much larger glacier. The terminus of Sheridan Glacier is a small retreating piedmont lobe with a width of more than 5 km (fig. 58). At the beginning of the 21st century, nearly all of the margin of the retreating and thinning glacier was fronted by a single large ice-marginal lake (figs. 228, 230).

In 1965, Tuthill and others (1968) examined a series of concentric recessional moraines and related deposits located as much as 2.5 km beyond the present margin of the glacier; by analyzing these deposits, they were able to construct a late Pleistocene-Holocene history for Sheridan Glacier and adjacent Sherman Glacier. Tuthill and others (1968) determined that, at the end of the Pleistocene Epoch, the two glaciers were joined and terminated about 5 km south of the 1965 position of the terminus of Sheridan Glacier. Subsequently, but at an unknown date, Sheridan Glacier retreated to a point north of its present margin. Sheridan Glacier remained in a retracted position until less than about 2,000 years ago, when it readvanced. Sheridan Glacier remained at this location until about A.D. 300, after which it underwent a series of fluctuations in position, culminating in an advance that produced a moraine in about A.D. 1700 (300 years ago). This moraine is the outermost of the concentric recessional moraines that they examined. At least four younger moraines exist between the A.D. 1700 moraine and the present-day margin of Sheridan Glacier.

Tarr and Martin (1914) reported that Seton Karr visited the glacier in 1886 and noted a fresh moraine resulting from a recent advance or stillstand. In 1910, Tarr and Martin (1914, p. 390) observed the glacier and noted that "The presence of thick mature forest up to the very edge of the bulb [bulb-shaped terminus] indicates that the glacier has not been more extensive for a score of years, perhaps for a century." When observed twenty-one years later, Wentworth and Ray (1936) described the margin as having retreated between 100 and 125 m and noted that the surface of Sheridan Glacier was showing signs of thinning produced by ablation. An average retreat rate for this interval would be about 5 to 6 m a<sup>-1</sup>.

Field (1975b, p. 350), on the basis of his own observations and on the analysis of aerial photographs collected by Bradford Washburn in 1938, the U.S. Army Air Forces in 1941, and the USAF in 1950, concluded that "the massive moraine nearest the present terminus was formed in the early or middle 1930's." In the approximately 30 years between the date of the formation of the moraine and the middle 1960s, Field (1975b, p. 350) reported that "recession has varied from around 200 m on the ridges to perhaps 500 m. in the lake basins." Hence, during this period, retreat rates averaged between 7 and 17 m a<sup>-1</sup>. Without quantifying the amount of change, Field (1975, p. 351) reported that, through 1971, the glacier "showed considerable further lowering of the ice surface and some recession of the terminus since 1965 and 1968."

Field (1975b, p. 351) described the evolution of the ice-marginal lakes fronting Sheridan Glacier through 1971. He stated that "The lakes were only beginning to form by the recession of the terminus in 1931." Through examination of the USGS 1:63,300-scale Cordova C-4 topographic quadrangle map (1953) (appendix B), he determined that, by 1950, five lakes had formed: one at the western end of the glacier, draining into the Glacier River; two 1-km-wide lakes along the front of the middle part of the terminus; and two small lakes along the eastern margin of the glacier. All had separate outlets. On the basis of his 1965 observations, Field (1975b) noted that the five lakes still maintained their unique existence but that the level of one of the eastern lakes had dropped when an ice dam was removed. By 1971, the drainage of all of the lakes entered the two middle lakes, generally englacially, and all of Sheridan and Sherman Glaciers' drainage flowed through the middle lake's outlet to the Gulf of Alaska.

Recent changes in the evolution of the ice-marginal lake system were studied by Bailey and others (2000). They found that, by 1981, the ice front in the center of the glacier had receded and allowed the two middle lakes and the western lake to combine. This merging was accompanied by about 10 m of downcutting of the outlet through the A.D. 1700 moraine. By 22 August 1979 (fig. 230), the basins of the eastern lakes had filled with sediment, and they had completely disappeared. When photographed by the author in October 1974, an isolated, small eastern lake still remained. Increased availability of sediment after 1964 from Sherman Glacier may have been a factor in the subsequent infilling of the basin.

Unlike any other part of Sheridan Glacier, the southwesternmost margin is debris covered, possibly from a 1964 earthquake-generated landslide. This debris mantle has protected the terminus in this area from retreat. Repeated visits by the author to this part of the glacier between 1974 and 2002 have documented that the rate of thinning is reduced and the rate of retreat is slower than that of the bare ice to the east. Before 1974, a small lake had formed at the western margin of the debris-covered ice. By 2002, it had a maximum length of around 600 m.

On 17 August 2000 (fig. 231), the author observed from the air that a significant amount of calving was occurring along the eastern margin of the glacier. Continued thinning of the glacier may have resulted in a floating ice tongue that was rapidly disintegrating.

A comparison of 1950s map data of the glacier with data obtained during annual airborne profiling surveys in the middle 1990s indicates that Sheridan Glacier thinned by  $0.725 \text{ m a}^{-1}$  and had a volume decrease of  $0.0729 \text{ km}^3 \text{ a}^{-1}$  (K.A. Echelmeyer, W.D. Harrison, V.B. Valentine, and S.I. Zirnheld, University of Alaska Fairbanks, written commun., March 2001).

### Scott Glacier

Scott Glacier (fig. 232) has a length of 24 km and an area of  $160 \text{ km}^2$  (Field, 1975b, p. 468). Its approximately 2-km-wide terminus is fronted by a braided outwash plain that stretches from valley wall to valley wall. Part of the outwash plain is incised, probably a result of tectonic uplift caused by the 1964 earthquake. When Field (1975b) compared aerial photographs of the terminus area made by Bradford Washburn in 1938 and by Austin Post in the 1960s, he noted that the terminus had retreated about 200 m (a rate of  $\sim 7 \text{ m a}^{-1}$ ) and that a wider marginal zone had developed. When the author photographed the terminus area on 17 August 2000 (fig. 232B), the entire ice margin was covered by sediment, the result of in place melting of at least

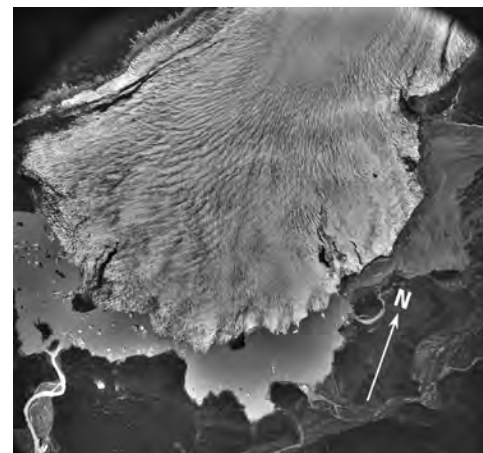


**Figure 230.**—22 August 1979 vertical aerial photograph shows the terminus of the Sheridan Glacier. The large trimline on the west side of Sheridan Glacier documents more than 50 m of 20th century thinning. USGS photograph no. 79-V2-190 by Austin Post, U.S. Geological Survey. A larger version of this figure is available online.



**Figure 231.**—17 August 2000 oblique aerial photograph of the ice-marginal lakes developed in front of Sheridan Glacier. East-looking view across the terminus of Sheridan Glacier shows the lake bounded by an early 20th century recessional moraine to the south and the ice margin to the north. A large amount of calving is occurring. The small basin located on the southwest corner of the Sheridan Glacier has yet to connect with the main lake. Photograph by Bruce F. Molnia, U.S. Geological Survey.

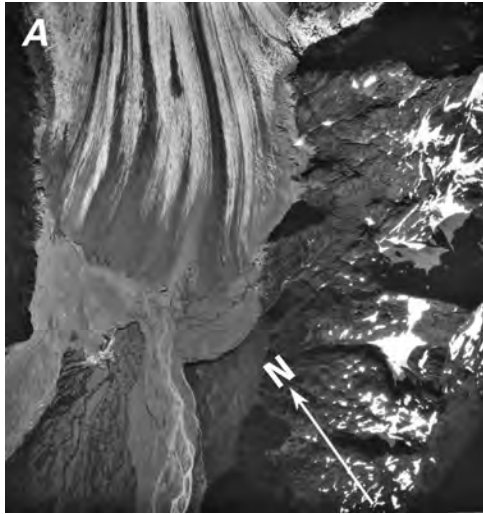


**Figure 232.**—Two aerial photographs of Scott Glacier. **A**, 24 July 1987 vertical aerial photograph of the retreating and thinning terminus of Scott Glacier and the proximal part of its braided outwash plain. Trimlines and several thermokarst pits developing in the terminus region are indicators of the declining health of the glacier. As with Sherman Glacier, the elevation of the surface of the outwash plain of Scott Glacier is being lowered to compensate for 1964 earthquake uplift. USGS photograph no. 87-V2-083 by Robert M. Krimmel, U.S. Geological Survey. A larger version of this figure is available online. **B**, 17 August 2000 north-looking oblique aerial photograph shows the terminus of the Scott Glacier and its adjacent outwash plain. The looping medial moraines that have developed since 1987 are a result of variations in flow between Scott Glacier and its unnamed tributary on the left. Elevated medial moraines, projecting beyond the leading edge of the terminus, are indicators of the continued retreat and thinning of Scott Glacier. Photograph by Bruce F. Molnia, U.S. Geological Survey.

**Figure 233.**—August 1938 near-vertical aerial photograph of an esker, several recessional moraines, and fluted topography on the outwash deposits in front of the retreating terminus of the Woodworth Glacier. Photograph by Bradford Washburn, Museum of Science (Boston), negative no. 1825.

15 medial moraines, all of which stood above the bare ice surface. The height of the marginal zone had more than doubled since the 1960s.

A comparison of 1950s map data of the glacier with data obtained during annual airborne profiling surveys in the middle 1990s indicated that Scott Glacier thinned by  $0.672 \text{ m a}^{-1}$  and had a  $0.0112\text{-km}^3 \text{ a}^{-1}$  volume decrease (K. A. Echelmeyer, W. D. Harrison, V.B. Valentine, and S.I. Zirnheld, University of Alaska Fairbanks, written commun., March 2001).

#### Glaciers Draining into the Tasnuna River

South and east of Marshall Pass, six north-flowing valley glaciers drain into the Tasnuna River (from west to east): Marshall Glacier, Tasnuna Glacier, two unnamed glaciers, Woodworth Glacier, and Schwan Glacier. All rapidly retreated during the second half of the 20th century. Several were documented to be retreating at even earlier dates.

##### Woodworth Glacier

When Schrader (1900) photographed Woodworth Glacier (length 23 km, area  $185 \text{ km}^2$ ) (Field, 1975b, p. 467) in 1898, its terminus was located in the Tasnuna River. By August 1938, when it was photographed again by Bradford Washburn (fig. 233), the glacier had retreated 800 to 900 m. By 1950, the



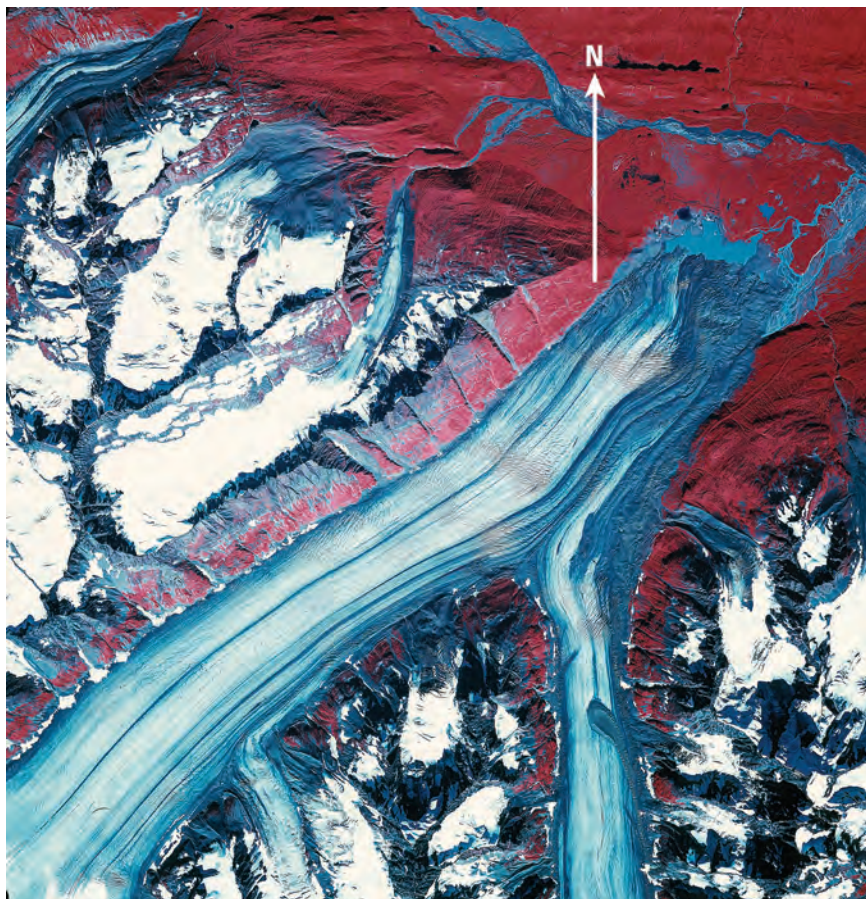


**Figure 234.**—25 August 1978 AHAP false-color infrared vertical aerial photograph of the lower reaches of Woodward Glacier, including the glacier's retreating terminus and the developing ice-marginal lake along its western terminus. Also shown are the retreating and thinning Tasnuna Glacier (upper left) and Tasnuna River (upper right). The area photographed by Bradford Washburn (fig. 233) is located north of the ice-marginal lake and is covered by vegetation. Many of the north- and west-facing tributaries on the eastern side of the Tasnuna Glacier no longer make contact with the trunk glacier. AHAP photograph no. L110F7219 from the GeoData Center, Geophysical Institute, University of Alaska, Fairbanks, Alaska.

date of the photography used to prepare the USGS Valdez A-3 1:63,360-scale topographic quadrangle map (appendix B), the glacier had retreated another 500 m; Field (1975b) reported that there was little change from this position through 1964. By 25 August 1978, approximately 300 m of additional retreat occurred, and an ice-marginal lake had begun to form (fig. 234). When the author observed the glacier from the air on 3 September 2002, it had retreated approximately an additional 800 m.

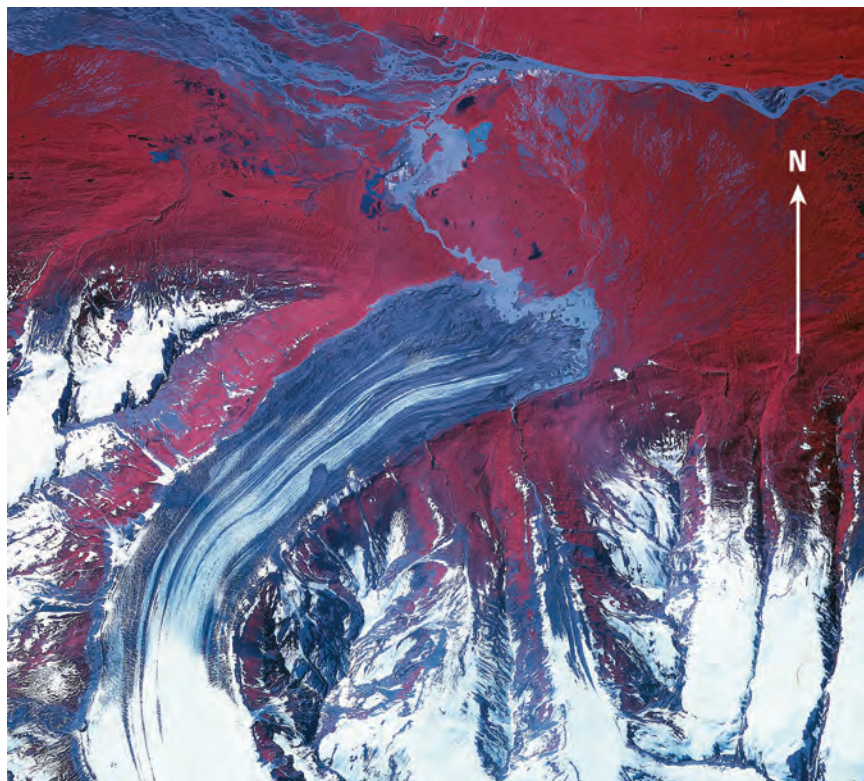
#### *Schwan Glacier*

Schwan Glacier has a length of 23 km and an area of 131 km<sup>2</sup> (Field, 1975b, p. 467). Its 1950 position was approximately 2.5 km behind a 19th century end moraine that marks its most recent maximum position, probably achieved during the "Little Ice Age." Through the late 1930s, retreat totaled about 2 km, but a small moraine visible in Bradford Washburn's 1937 and 1938 aerial photographs suggests that the glacier margin was stable or perhaps even slightly advancing (Field, 1975b). By 1941, the terminus had retreated about 50 m. When the glacier was next photographed in 1950, approximately 350 m of additional retreat had occurred. Through 1964, the glacier retreated an additional 300 m. By 9 July 1978, approximately 250 m of additional retreat had occurred, and an ice-marginal lake had begun to form (fig. 235). When the author observed the glacier from the air on 3 September 2002, it had retreated an estimated additional 600 m, and the ice-marginal lake fronted the entire terminus.

#### **Small Glaciers Between Schwan and Heney Glaciers**

East of Schwan Glacier and just west of the confluence of the Tasnuna and Copper Rivers, about six small, unnamed, north-facing retreating glaciers occur in steep U-shaped valleys separated by distinctive arête ridges. Most have retreated so much that the lower half of their valleys are ice free.

**Figure 235.**—9 July 1978 AHAP false-color infrared vertical aerial photograph of the lower reaches of the Schwan Glacier, including the glacier's retreating terminus and the developing ice-marginal lake. Also shown are several unnamed retreating and thinning glaciers to its east and west. As with the adjacent Woodworth Glacier, many of its tributaries no longer make contact with the Schwan Glacier. Tasnuna River can be seen flowing across the upper part of the photograph. AHAP photograph no. L110F6220 from the GeoData Center, Geophysical Institute, University of Alaska, Fairbanks, Alaska.



### **Heney Glacier**

Heney Glacier has a length of 19 km and an area of 72 km<sup>2</sup> (Field, 1975b, p. 467). In 1910, Lawrence Martin visited the glacier and observed that a large part of the terminus was covered by a thick forest and fronted by a terminal moraine. He determined “that the last expansion of the bulb of Heney Glacier was about a century ago and that for over 76 years there has been no period of activity capable of breaking up the outer portion of the bulb” (Tarr and Martin, 1914, p. 449). He also observed that the central part of the terminus showed no recession from this moraine but that the flanks showed 800 to 1,400 m of retreat (Tarr and Martin, 1914).

In 1910, the Copper River and Northwest Railroad was constructed on the surface of this moraine (Tarr and Martin, 1914, pl. CLXXVIII, ff p. 464). Before Martin's next visit in 1911, a pulse or minor surge event shattered much of the stagnant ice in the terminus region, rendering it impassable. However, it did not cause terminus advance and did not disrupt the railroad track. Field (1975b) reported that little change occurred through 1937. Between 1937 and 1950, about 200 m of retreat occurred; approximately 300 to 350 m of additional retreat occurred through 1964. When the author observed the glacier from the air in 2002, it was estimated to have retreated more than 1.4 km, and an ice-marginal lake fronted the entire terminus.

### **Allen Glacier**

Allen Glacier, located about 11 km north of Childs Glacier, has a length of 31 km and an area of 230 km<sup>2</sup> (Field, 1975b, p. 468). Unlike Childs and Miles Glaciers, which presently calve icebergs directly into the Copper River, the retreating terminus of Allen Glacier is as much as 3 km from the river and is fringed by an estimated 15-km-long arcuate end moraine that separates the river from a broad area of vegetation- and moraine-covered stagnant ice. The first map showing the position of the terminus of Allen Glacier was made by D.C. Witherspoon for the USGS in 1900. It was revised in 1906 and published by Tarr and Martin in 1914. When Lawrence Martin visited and mapped the glacier in 1910 (Tarr and Martin, 1914, pl. CLXXIV, ff p. 448), he found alders

(*Alnus* sp.) as old as 67 years growing on this moraine. About 9 km of the bed of the Copper River and Northwest Railroad was constructed on stagnant ice along the river's edge, which Tarr and Martin described as "the end of a living glacier" (Tarr and Martin, 1914, p. 445). During construction, Tarr and Martin observed that "The ballast beneath the ties and rails of the railway actually rests upon the ice, not upon an abandoned moraine as at Heney Glacier" (Tarr and Martin, 1914, p. 445). In 1912, the northeastern part of the terminus began to advance; by 1913, as much as 800 m of advance had occurred (Wentworth and Ray, 1936). In 1931, Wentworth and Ray (1936, p. 923) visited the glacier and noted that "A more marked stagnation had set in, and the area of active ice movement had been thrown back, perhaps several thousand feet, from the northeast margin of 1910." This advance had only a minimal impact on the railroad; for more than 20 years, trains crossed the glacier margin daily in both directions.

The glacier was photographed by Bradford Washburn in 1938 and by the USN in 1957. In the 47 years between Martin's 1910 map and the 1957 photograph, the northern part of the terminus retreated between 400 m and 1 km, while the middle and southern part of the terminus retreated more than 2 km. Additionally, the glacier had thinned more than 100 m over most of the lobate terminus and at the head of the piedmont lobe, where the main trunk flows from its valley (Field, 1975b). Post (1967a) reported that, beginning in the early 1960s, the glacier again began to advance. Between 1963 and 1964, he noted that the glacier advanced 300 m. Similarly, between 1964 and 1965, the glacier advanced an additional 300 m. This advance reactivated much of the distal part of the stagnant ice area.

The 1964 earthquake caused three large rock avalanches that fell onto the surface of Allen Glacier. The largest, termed "Allen I," had an area of about 2 km<sup>2</sup> and a length of about 3 km. Before 29 July 1965, another rockslide—larger and longer than any that took place during the earthquake—occurred. This slide had an area of about 7.5 km<sup>2</sup> and a length of about 7.5 km and consisted of material that was probably loosened by the 1964 earthquake (Post, 1967a).

In the 36 years between Post's 1966 observations, 17 August 2000 (fig. 236), and 17 October 2002 (the author's most recent visit), the glacier is estimated to have retreated more than 3 km and thinned at least 125 m. Even the upper reaches of the glacier showed significant thinning.

### Grinnell Glacier

According to Tarr and Martin (1914, p. 437), the "last great expansion" of Grinnell Glacier occurred before 1892, with little change occurring between 1891 and 1900. Minor advances occurred in 1907 and between 1909 and 1911. In 1910, the terminus of Grinnell Glacier was located about 500 m from the Copper River and about 600 m from the northern margin of Miles Glacier's stagnant northern lobe, which is located on the eastern side of the Copper River. Railroad track that had been laid over 400 m of stagnant ice was not affected by the early 20th century advances.

The next visitors to the glacier were Wentworth and Ray in 1931. They reported that, "Between 1911 and 1931, there was a general retreat of the active portion of the glacier and continued reduction and melting of the stagnant ice" (Wentworth and Ray, 1936, p. 921). They also noted that trees up to 25 cm in diameter were growing on the ice-cored moraine.

Field (1975b) reported that several hundred meters of retreat occurred in the 28-year interval between photographs by Bradford Washburn in 1938 and an AGS field party's visit in 1966. In the 36 years between Austin Post's 1966 observations and the author's 17 October 2002 aerial observations, Grinnell Glacier is estimated to have retreated 1 km and thinned at least 100 m. The southeastern tributary also separated from the main trunk. Fresh bedrock



**Figure 236.**—Two 17 August 2000 oblique aerial photographs of Allen Glacier show several lines of evidence confirming the rapid thinning and retreat of the glacier. **A**, Northeast-looking view across part of the terminus of Allen Glacier shows the debris-covered southern part of the terminus and the bare ice northern part. The large trimline documents more than 100 m of recent thinning. **B**, View of the northern part of the ice-marginal lake fronting Allen Glacier. The ongoing thinning of the glacier appears to have resulted in flotation of part of the terminus, accompanied by the production of large icebergs. Photographs by Bruce F. Molnia, U.S. Geological Survey. Larger versions of these figures are available online.





**Figure 237.**—17 August 2000 northwest-looking oblique aerial photograph of much of Grinnell Glacier. Several areas of freshly exposed bedrock around the perimeter of each distributary lobe of the terminus of Grinnell Glacier and a fresh trimline along the margin of the glacier are evidence of the rapid thinning and retreat of the glacier. Photograph by Bruce F. Molnia, U.S. Geological Survey. A larger version of this figure is available online.

around the terminus, seen in a 17 August 2000 oblique aerial photograph taken by the author, suggests a recent rapid retreat (fig. 237).

### Childs Glacier

Childs Glacier, located immediately west of Million Dollar Bridge, has a length of 19 km and an area of 100 km<sup>2</sup> (Field, 1975b, p. 468), and makes up the western bank of the Copper River for a distance of about 6 km. U.S. military expeditions led by W.R. Abercrombie in 1884 and H.T. Allen in 1885 provided the first descriptions and photographs (Allen, 1887) of Childs Glacier (Abercrombie, 1900; Allen, 1900).

Most of the early information concerning Childs Glacier, however, resulted from Tarr and Martin's expeditions between 1909 and 1911 (Tarr and Martin, 1914). Although the glacier's "Little Ice Age" chronology is not well dated, several moraines as high as 100 m and located as much as 1.5 km beyond the present margin may represent late 18th century or early 19th century maxima.

Aside from a small advance between 1905 and 1906, the glacier's retreat was slow between 1884 and 1909. A surge that began in the spring of 1909 and lasted through the summer of 1910 was carefully documented by railway engineers, who were concerned about the potential impact of the advancing glacier terminus on the construction of the Million Dollar Bridge across the Copper River. The surge produced a terminus advance of about 600 m that reduced the distance between the ice margin and the bridge by more than 50 percent. A conspicuous moraine formed by this advance is visible approximately 450 m from the bridge. Tarr and Martin (1914) cited maximum flow rates of at least 40 m d<sup>-1</sup> between 29 July and 6 August 1910 and 9 to 12 m d<sup>-1</sup> between May and October. Much ice was lost to calving and river erosion.

Wentworth and Ray (1936) visited the glacier in 1931 and reported that it had retreated between 150 m and 200 m. Field (1975b) summarized the results of more than a dozen visits and photographic observations between 1938 and 1971. In the mid-1930s, an advance of the glacier built "a massive moraine...on the land front at the northern end of the terminus" (Field, 1975b, p. 343). By 1950, however, a retreat of about 60 m occurred; between 1950 and 1959, an additional 200 m of retreat occurred. These retreats were accompanied by a reduction in flow rate and a reduction in the height of the ice margin.

By 1961, Childs Glacier was advancing, and its ice face had thickened to approximately 65 m. Between 1959 and 1961, the glacier advanced as much as 100 m. In the 7 years between 1961 and 1968, the glacier advanced approximately 150 m further. Little change was noted in 1971, although the terminus was within approximately 10 m of the mid-1930s moraine.

Since then, the glacier has thinned and retreated. This ongoing trend was noted by the author in multiple observations made between 1981 and 2004. Aerial photographs taken on 22 August 1979 (see oblique aerial photograph no. 79V2-179 by Austin Post, U.S. Geological Survey), 13 August 1994 (fig. 238A), 17 August 2000 (fig. 238B), and 17 October 2002 show a large arcuate calving embayment forming along the Copper River. The maximum amount of retreat that occurred between 1971 and 2004 was approximately 300 m. Field (1965) provided a map showing terminus positions between 1912 and 1961 (AGS Glacier Studies Map No. 64-3-G1).



**Figure 238.**— **A**, 13 August 1994 vertical aerial photograph showing the terminus of Childs Glacier. Between 22 August 1979 (USGS photograph no. 79V2-179 by Austin Post, U.S. Geological Survey) and 13 August 1994, the calving embayment on the west side of the Copper River deepened by approximately 150 m. Note the elongated mass of landslide debris that is moving down the center of the glacier. USGS photograph no. 94-V3-179 by Robert M. Krimmel, U.S. Geological Survey. **B**, 17 August 2000 northwest-looking oblique aerial photographic mosaic showing the full terminus of Childs Glacier. In addition to a deepening of the calving embayment, the moraines on the southern half of the terminus have become more convoluted and offset. Photograph by Bruce F. Molnia, U.S. Geological Survey. A larger version of this figure is available online.

### Goodwin Glacier

When Tarr and Martin (1914) observed the terminus of Goodwin Glacier, it was located immediately adjacent to a forest. This observation led them to conclude that the glacier had not been more advanced from its current position for a significant period of time. Field (1975b) noted that there were no reports of any advance of Goodwin Glacier during the 20th century. Additionally, Field (1975b, p. 344) compared aerial photographs made in 1938, 1950, and 1961 and stated that “the lower one kilometer of the glacier is moraine-covered which effectively masks most of the ice edge.” His analysis showed that “no appreciable change [had occurred] in recent decades, except extension of the alders on the ice-free and ice-cored parts of the moraines. Slow recession marked by progressive stagnation of the terminus is thus indicated.” Aerial observations by the author between 1990 and 2001 documented continued downwasting of the glacier, separation of the debris-covered stagnant ice part of the terminus from older vegetation-covered ice-cored moraine, and the formation of several ice-marginal lakes.

### Cleave Creek Glacier–Upper Copper River–Stephens Glacier–Tonsina Glacier Northwestern Subdivision

Glaciers in this subdivision that have lengths greater than 8 km and areas determined by Field (1975b, p. 465–467), include Cleave Creek (11 km, 31 km<sup>2</sup>), two unnamed glaciers (9 km, 20 km<sup>2</sup>; 10 km, 22 km<sup>2</sup>), Tsina (10 km, 37 km<sup>2</sup>), Tonsina (17 km, 47 km<sup>2</sup>), two more unnamed glaciers (11 km, 19 km<sup>2</sup>; 8 km, 16 km<sup>2</sup>), Klutina (11 km, 45 km<sup>2</sup>), and Stephens (16 km, 56 km<sup>2</sup>). Worthington Glacier, a popular tourist destination, is also located in this subdivision.

### **Cleave Creek Glacier**

Cleave Creek Glacier is the largest and only named glacier in an upland area located between the Copper, Tasnuna, Tiekel, and Tsina Rivers. All of the glaciers in the complex are actively retreating, and some have completely disappeared since being mapped in the 1950s. At the southeastern end of the area, about a half-dozen small, north-flowing, unnamed, steeply entrenched former tributaries to a previously expanded Cleave Creek Glacier are rapidly thinning and retreating as shown on an 8 August 1996 oblique aerial photograph by the author (fig. 239). The terminus of Cleave Creek Glacier has narrowed to approximately one-third of its 1950s width and exposed a surface of grooved sediment and bedrock.

### **Worthington Glacier**

Worthington Glacier is a small mountain glacier about 6 km long. Its bifurcated terminus, located about 2 km from the Richardson Highway, shows conspicuous evidence of recent retreat. A large lateral and terminal moraine complex surrounds the glacier. A large ice-marginal lake dammed by this moraine is located between the moraine and the southern lobe of the glacier. When the author visited on 3 September 2002, the retreating ice margin no longer reached the shore of the lake. During the later part of the 20th century, the distal end of the northern terminus separated into three separate distributaries. The site of a State of Alaska glacier interpretive center, the glacier has thinned so much that visitors need to walk downhill from a 1960s parking lot to reach the terminus.

A surveying party under the leadership of Austin Post mapped Worthington Glacier at 1:10,000 scale with a 5-m contour interval during the IGY in



**Figure 239.**—8 August 1996 south-looking oblique aerial photograph of several of the former tributaries of the retreating Cleave Creek Glacier. All are rapidly thinning and retreating. The lower reaches of the middle glacier of the three unnamed, steeply entrenched former tributaries have lost contact with the upper accumulation area. Currently, ice and snow reach the lower area through avalanching. Photograph by Bruce F. Molnia, U.S. Geological Survey.

1957. Part of the AGS's Nine Glacier Maps Project, the accompanying text (American Geographical Society, 1960, p.19, 21) described Worthington as "descending eastward from a broad névé field between peaks rising to more than 2,010 meters (6,600 feet) to a bifurcated terminus, one lobe of which extends a short distance into the broad valley of Ptarmigan Creek at an elevation of 660 meters (2,165 feet).... This glacier was receding in 1957, continuing a recession which evidently had been in progress for many years, as evidenced by a large bare area, terminal and recessional moraines. Moderately crevassed and almost completely free of ablation moraine, this glacier is rather typical of the heavy accumulation, rapid velocity, and high ablation glaciers typical of the region. The greatest snow depth noted on the glacier in the first half of July 1957, was less than 3 meters (10 feet)...."

Viereck (1967) visited the glacier in 1957 and identified a major moraine located about 600 m beyond the 1957 ice margin and a set of inner moraines about 200 m from the 1957 terminus. He concluded that the glacier occupied the outer moraine sometime between 1837 and 1857 and the inner moraines sometime beginning in the 1930s.

The glacier was revisited in 1961, 1964, and 1966 by AGS parties that included William Field and was photographed by Austin Post for the USGS in 1968 and 1971. Analysis of these data by Field (1975b) show that the glacier retreated approximately 400 m between the middle 19th century and the middle 1930s ( $\sim 4\text{--}5\text{ m a}^{-1}$ ); approximately 150 m between the middle 1930s and 1957 ( $\sim 7\text{ m a}^{-1}$ ); approximately 50 m between 1957 and 1961 ( $\sim 12\text{ m a}^{-1}$ ); at least 35 m between 1961 and 1964 ( $\sim 12\text{ m a}^{-1}$ ); and at least 35 m between 1964 and 1966 ( $\sim 17\text{ m a}^{-1}$ ). Retreat rates were similar through 1971.

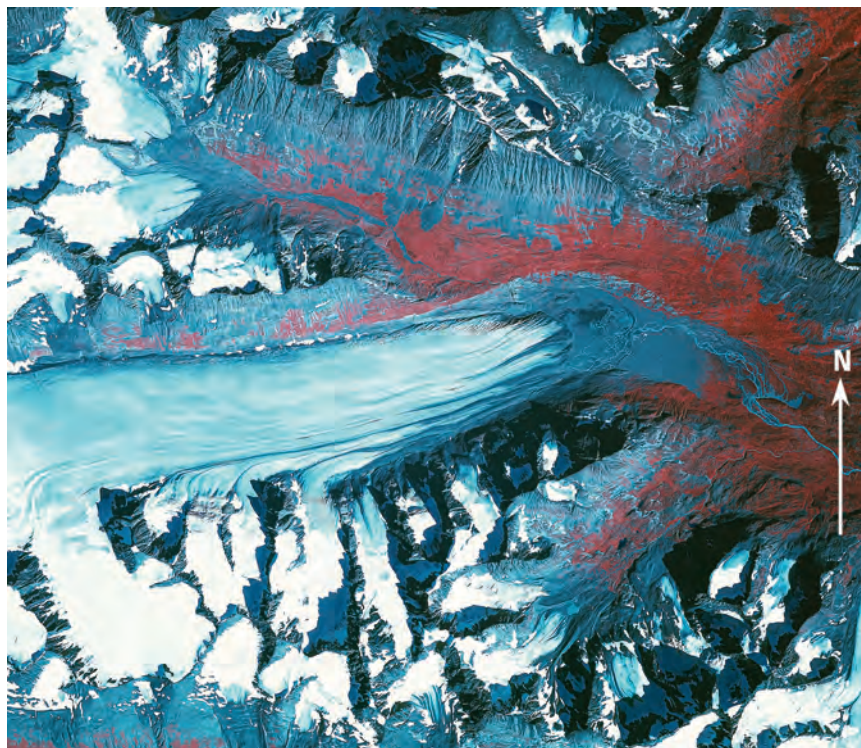
On the basis of a comparison of the USGS map of the glacier based on 1949 and 1950 aerial photography and data obtained during an airborne profiling survey conducted on 31 May 1994, Echelmeyer and others (1996) determined that the terminus of the north lobe of Worthington Glacier retreated about 250 m, and the terminus of the south lobe had retreated about 380 m, an average of about 310 m during the 44 to 45 years between data sets; the average annual retreat rate was about  $7\text{ m a}^{-1}$ . The area of Worthington Glacier decreased from 8.8 to 8.6 km<sup>2</sup> in 1994, a decrease of around 2.3 percent; however, its thickness increased an average of 11.1 m, and its volume increased  $0.97 \times 10^8\text{ m}^3$ . The details of the thickening are actually more complicated than these values suggest. According to Sapiano and others (1998), during the 37 years from 1957 to 1994, the glacier thinned by more than 40 m at elevations of less than 800 m, thinned at all elevations below 1,200 m, and thickened at most locations above 1,200 m.

Between the middle 1990s and 1999, Worthington Glacier thinned by  $0.948\text{ m a}^{-1}$  annually, and its volume decreased by  $0.00856\text{ km}^3\text{ a}^{-1}$  (K.A. Echelmeyer, W.D. Harrison, V.B. Valentine, and S.I. Zirnheld, University of Alaska Fairbanks, written commun., March 2001). In the 1990s, Harper and others (1998) conducted studies of crevasses patterns and longitudinal strain rate. Between 1975 and 2001, the author estimates that the individual termini have retreated about 300 m, and the lower part of the glacier has thinned at least 25 m.

### **Tonsina Glacier**

Little is known about Tonsina Glacier, which has a length of 17 km and an area of 47 km<sup>2</sup> (Field, 1975b, p. 466). A comparison of the position of the glacier's terminus as shown on the USGS Valdez 1:250,000-scale topographic quadrangle map (1960) (appendix A), which is based on early 1950s surveys; a 25 August 1978 AHAP false-color infrared vertical aerial photograph (fig. 240), and observations from the air by the author on 31 August 2000 and 3 September 2002 show that the glacier has retreated about 2 km, and thinned by more than 100 m in the 50 years since the 1950s surveys. All of the other glaciers in the area have also retreated significantly, including Tsina Glacier

**Figure 240.**—25 August 1978 AHAP false-color infrared vertical aerial photograph of the terminus of Tonsina Glacier and a number of adjacent small, unnamed cirque glaciers. All glaciers show evidence of ongoing thinning and retreat. AHAP photograph no. L107F7055 is from the GeoData Center, Geophysical Institute, University of Alaska, Fairbanks, Alaska.



approximately 5 km to the south, many small unnamed cirque glaciers, and an unnamed glacier located about 2.5 km to the north.

Two unnamed glaciers, each having a length of about 4 km and an area of about 7 km<sup>2</sup>, are located between Tonsina and Klutina Glaciers. As are so many other glaciers in the north-central part of the Chugach Mountains, these two are actively thinning and retreating. Both have retreated as much as 2.5 km during the approximately 50-year interval between the time when they were mapped in the early 1950s and when they were observed from the air and photographed by the author in August 1993, on 31 August 2000, and on 2 September 2002.

#### **Klutina and Stephens Glaciers**

Field (1975b, p. 466) reported that Klutina Glacier (fig. 241) has a length of 11 km and an area of 45 km<sup>2</sup>; Stephens Glacier has a length of 16 km and an area of 56 km<sup>2</sup>. Both glaciers were photographed by Bradford Washburn in 1937 and Austin Post in 1964. Comparison shows that both glaciers retreated between 300 and 500 m in the 27-year interval between the two sets of photographs. Individual comparisons of the positions of each glacier's terminus as shown on the USGS Valdez 1:250,000-scale topographic quadrangle map (1960) (appendix A), which is based on early 1950s surveys, and observations made by the author from the air on 30 August 2000 (fig. 241) and 3 September 2002 show that each glacier has thinned significantly and retreated between 2 and 5.5 km in the ensuing 50 years, although little evidence of change is visible in the accumulation areas. When the author observed the glaciers from the air on 3 September 2002, both were actively retreating and thinning. Each had elevated lateral and medial moraines, and each had separated from former tributaries. The terminus of Klutina Glacier was about 4 km upvalley from a conspicuous end moraine, perhaps marking its "Little Ice Age" maximum.

Glaciers draining into the Uranatina River and Haley Creek are also retreating and thinning. Many ice-free cirques suggest that a significant number of glaciers completely disappeared during the 20th century. When the author observed the glaciers from the air on 31 August 2000, less than 30 percent of the cirques examined still had glacier ice.



**Figure 241.**—30 August 2000 oblique aerial photograph of Klutina Glacier, looking north; the former western tributary is now more than 800 m from Klutina Glacier and nearly 200 m above it. Photograph by Bruce F. Molnia, U.S. Geological Survey. A larger version of this figure is available online.

## Prince William Sound Segment—Heney Range to the East Side of Valdez Arm Subdivision

Glaciers in this subdivision that have lengths of 8 km or more and areas determined by Field (1975b, p. 469–470) include two unnamed glaciers (9 km, 26 km<sup>2</sup>; 9 km, 22 km<sup>2</sup>), Cordova (13 km, 45 km<sup>2</sup>), an unnamed glacier (9 km, 13 km<sup>2</sup>), Bench (8 km, 8 km<sup>2</sup>), Deserted (17 km, 36 km<sup>2</sup>), Wortmanns (14 km, 55 km<sup>2</sup>), Keystone (9 km, 20 km<sup>2</sup>), an unnamed glacier (15 km, 30 km<sup>2</sup>), and Valdez (34 km, 158 km<sup>2</sup>).

### Shepherd Glacier

Shepherd Glacier is a small unstudied glacier located at the head of Power Creek northeast of Cordova. Although it was snow covered to within about 200 m of its terminus when the author observed it from the air on 8 August 2000, the terminus was fronted by a barren zone about 1 km in width. The bedrock became deglaciated following the mapping of the glacier in the early 1950s.

### Glaciers of the Rude River Drainage

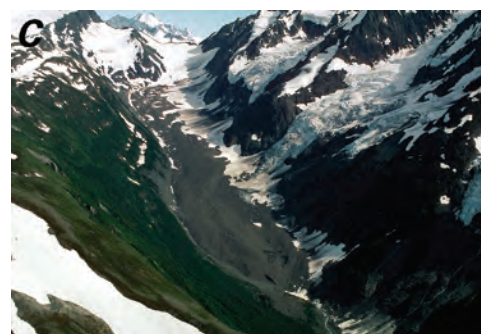
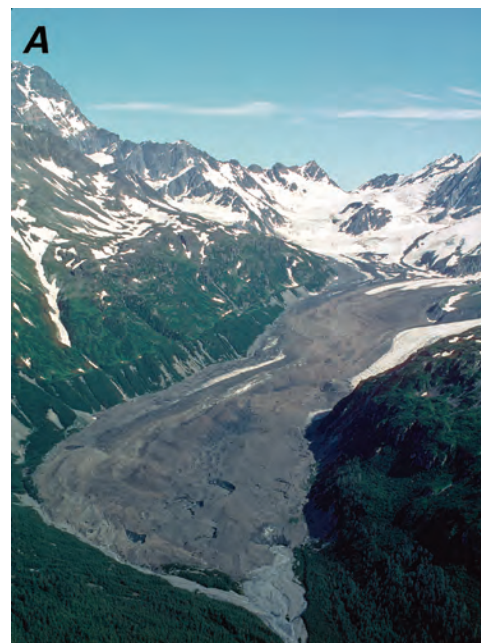
South of 2,350-m-high Cordova Peak, several unnamed debris-covered valley glaciers show signs of thinning, retreat, and stagnation. The largest, an unnamed glacier located at the head of the eastern fork of the Rude River (fig. 242A), has a length estimated by the author of approximately 8 km. More than half its length is mantled by a debris cover that is estimated to be as much as 1 m in thickness. Another unnamed glacier (fig. 242B) is located approximately 3 km to the northwest. Unlike its neighbor, its terminus is debris free. It is surrounded by an apron of abandoned moraine and freshly exposed bedrock, the result of late 20th century thinning and retreat. An unnamed west-flowing glacier located at the head of a northeastern fork of the Rude River has more than 80 percent of its length covered by debris. What is unusual about this glacier (fig. 242C) is that three of its four southern tributaries are in rapid retreat and terminate hundreds of meters above the surface of the glacier; the fourth descends all the way to the valley floor and connects with the thinning main trunk.

#### *Cordova Glacier*

Field (1975b) reported that the terminus of Cordova Glacier, which has a length of 13 km and an area of 45 km<sup>2</sup> (Field, 1975b, p. 469) and is located at the head of the western fork of the Rude River, dammed a lake that was 1.8 km long and an average of 600 m wide in 1950. The distal end of the lake was adjacent to the terminus of an unnamed glacier that has an approximate length of 8 km. The unnamed lake has been described by both Stone (1963b) and Post and Mayo (1971). Field (1975b, p. 353) speculated—correctly—that, “Since all the glaciers in this part of the central Chugach appear to be shrinking, it is likely that some year the ice-dam will not form and this lake will disappear.” Although the date of the last formation of the lake is unknown, much of its former bed was covered by vegetation when the author observed the former area of the lake from the air on 8 August 2000. The terminus of Cordova Glacier had thinned and retreated so much that it was entrenched behind a large terminal and several large recessional moraines at least 1.5 km from the eastern wall of the former lake.

### Glaciers South of Lowe River

To the north and northwest of Cordova Glacier, more than a dozen glaciers flow northward and drain into the Lowe River. An unnamed glacier located at the head of a northeast-flowing creek west of Browns Creek and another unnamed glacier located in the Browns Creek drainage both show evidence of ongoing retreat. Like so many other glaciers in this subdivision, they have large areas of freshly deglaciated bedrock exposed around their margins.



◀ **Figure 242.**—Three 8 August 2000 oblique aerial photographs of unnamed glaciers within the Rude River drainage. **A**, East-looking view of the debris-covered lower portion of an unnamed glacier at the head of the east fork of the Rude River. Note the vegetated, elevated lateral moraine along the north side of the glacier. Thermokarst pits and many other stagnation features are visible. **B**, North-looking view of an unnamed glacier on the southwest flank of Cordova Peak, with its debris-free retreating terminus. Note the apron of abandoned moraine and freshly exposed bedrock. **C**, East-looking view of an unnamed glacier. Of its four southern tributaries, three are in rapid retreat and terminate hundreds of meters above the surface of the glacier, whereas the fourth descends all the way to the valley floor and connects with the thinning main trunk. Photographs by Bruce F. Molnia, U.S. Geological Survey. Larger versions of these figures are available online.

Four of the larger glaciers to the east of Browns Creek—Wortmanns, Bench, Heiden, and Deserted Glaciers—were photographed by Bradford Washburn in 1938 and again by Post in 1960. Field (1975b, p.353) characterized all four glaciers as having “terminal and marginal barren zones in the 1950s and 1960 which indicate recent net recession.”

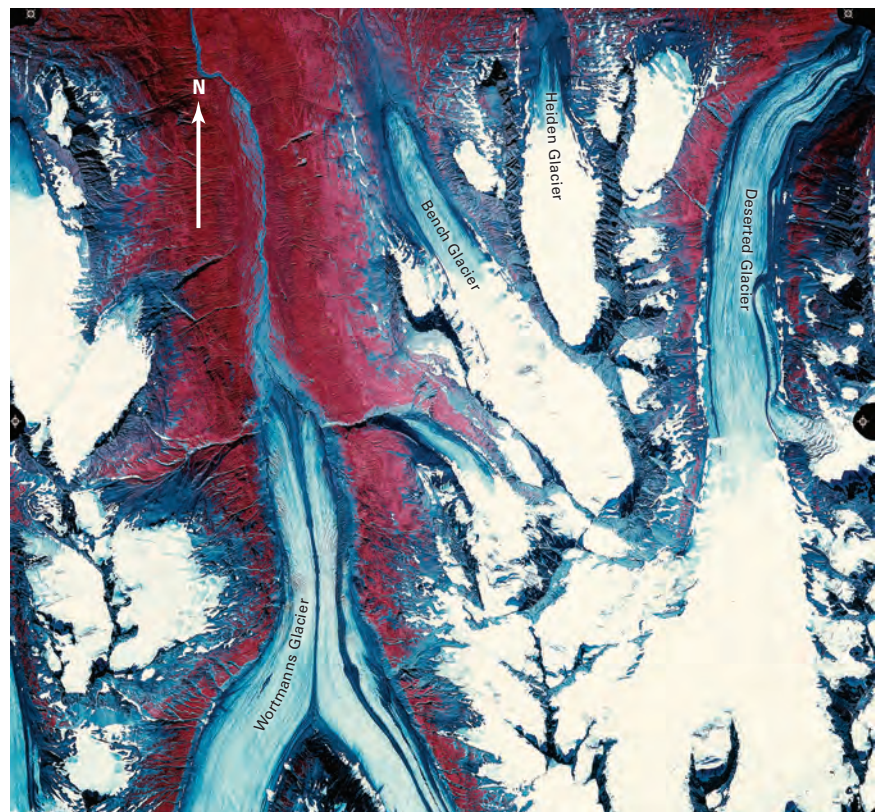
#### *Wortmanns Glacier*

The largest of the four glaciers is Wortmanns Glacier (fig. 243), a retreating wishbone-shaped glacier that is 14 km long and has an area of 55 km<sup>2</sup> (Field, 1975b, p. 469). Field (1975b) reported that, in 1950, its terminus was about 1.5 km behind an outer moraine of unknown age. When the terminus was photographed by the AHAP Program on 25 August 1978 (fig. 243), it had retreated another 250 m. When the author observed it from the air, it had retreated approximately an additional 300 m (August 1996), 350 m (8 August 2000), and 400 m (3 September 2002). A comparison of 1950 map data of the glacier and data obtained during an airborne profiling survey in the middle 1990s, showed that Wortmanns Glacier thinned by an average of 0.5228 m a<sup>-1</sup> and decreased in volume by 0.0305 km<sup>3</sup> a<sup>-1</sup> (K.A. Echelmeyer, W.D. Harrison, V.B. Valentine, and S.I. Zirnheld, University of Alaska Fairbanks, written commun., March 2001).

#### *Bench Glacier*

Bench Glacier, which has a length of 8 km and an area of 8 km<sup>2</sup> (Field, 1975b, p. 469), is located immediately to the east of Wortmanns Glacier. It was photographed by the AHAP Program on 25 August 1978 (fig. 243) and observed from the air by the author in August 1996, on 8 August 2000, and on 3 September 2002. Characterized by Field (1975b) as retreating, its terminus had retreated an additional 50 m by 1978. When the author observed it from the air and photographed it in 2000 and 2002, the terminus had retreated at least another 275 m. Comparison of 1950 map data of the glacier with data obtained during an airborne profiling survey in the middle 1990s showed that Bench Glacier thinned by an average of 1.168 m a<sup>-1</sup> and decreased in volume by 0.0138 km<sup>3</sup> a<sup>-1</sup> (K.A. Echelmeyer, W.D. Harrison, V.B. Valentine, and S.I. Zirnheld, University

**Figure 243.**—25 August 1978 AHAP false-color infrared vertical aerial photograph of the thinning and slowly retreating terminus of Wortmanns Glacier, Bench Glacier, Heiden Glacier, all but the terminus of Deserted Glacier, and several small retreating cirque and valley glaciers. AHAP photograph no. L110F7288 from the GeoData Center, Geophysical Institute, University of Alaska, Fairbanks, Alaska. Every glacier shown presents evidence of thinning and retreat.



of Alaska Fairbanks, written commun., March 2001). Glacier hydrology studies of Bench Glacier, including jökulhlaups associated with the glacier, have been carried out by Howard and others (1996) and Anderson (2003).

#### *Heiden Glacier*

Heiden Glacier, the smallest of the four glaciers south of Lowe River, was photographed by the AHAP Program on 25 August 1978 (fig. 243) and was observed from the air by the author in August 1996, on 8 August 2000, and on 3 September 2002. Between 1978 and September 2002, the terminus retreated at least 400 m.

#### *Deserted Glacier*

The longest glacier of the four is Deserted Glacier, which is 17 km long and 36 km<sup>2</sup> in area (Field, 1975b, p. 469). A comparison of its position on the USGS Cordova D-5, 1:63,360-scale topographic quadrangle map (1953) (appendix B), which is based on 1950 photography, with observations made by the author from the air, including oblique aerial photographs of the glacier taken on 8 August 2000 and on 3 September 2002, indicates that the terminus of the glacier retreated by at least 1.6 km. Similarly, a comparison of 1950 map data of the glacier with data obtained during an airborne profiling survey in the middle 1990s shows that Deserted Glacier thinned by an average of 0.816 m a<sup>-1</sup> and had a volume decrease of 0.03 km<sup>3</sup> a<sup>-1</sup> (K.A. Echelmeyer, W.D. Harrison, V.B. Valentine, and S.I. Zirnheld, University of Alaska Fairbanks, written commun., March 2001).

### **Glaciers North of Lowe River and West of Keystone Canyon**

Three named glaciers—Corbin, Rubin, and Camicia Glaciers—and about 10 unnamed glaciers are all west-flowing glaciers and ultimately drain into Valdez Arm. All of these glaciers and the adjacent Valdez and Hogback Glaciers have been remapped by the USGS in a revision of the USGS 1:63,360-scale Valdez A-6 topographic quadrangle map (1953) (appendix B). Although it was printed in 2002, the revised map has a 1993 date because it was based on 1993 imagery. Since the 1953 edition of the map was compiled, every one of these glaciers has undergone conspicuous thinning and retreating. Aerial observations made on 8 August 2000 and 3 September 2002 show that every glacier was characterized by trimlines well above the ice surface and that there was an apron of vegetation-free bedrock adjacent to the terminus of each glacier.

#### *Valdez Glacier*

Valdez Glacier (fig. 244), which is 34 km long and 158 km<sup>2</sup> in area (Field, 1975b, p. 470), is located 6 km northeast of the pre-1964 Alaska earthquake location of the town of Valdez. Before Valdez was relocated about 4 km to the west, the glacier presented a significant flood threat to the town's inhabitants (Field, 1975b). At the end of the 19th century, when Schrader (1900) first described the glacier, it was thinning and retreating. This was further documented by a series of measurements made by L.S. Camicia, a local optician, between 1901 and 1905 and again in 1908. Reid (1909) and Tarr and Martin (1914) provide summaries of Camicia's measurements. Reid (1909, p. 670) stated that "Dr. L.S. Camicia has been keeping a record since 1901 of the position of the Valdez Glacier, Prince William Sound, Alaska. A stone monument was made on the moraine in front of glacier and the distance to the ice determined. He found the following variations, measurements having been made in June of each year: 1901-2, a retreat of 39 feet; 1902-1904, 165 feet; 1904-1905, 138 feet. The next observation was made in October 1908; as the monument had been destroyed, he estimated its position as well as he could, and found a retreat since the last observation of 244 feet, making a total retreat from 1901 to 1908 of 568 feet." Tarr and Martin (1914) also commented on Camicia's measurements.

These early observations, along with Moffit's 1905 photograph (fig. 244A), documented that, with the exception of a short-lived advance in 1906, the





**Figure 244.**— Two photographs showing changes at Valdez and Camicia Glaciers during the 20th century. **A**, 1905, north-east-looking photograph by F.H. Moffit across the terminus of Valdez Glacier toward Camicia Glacier. Bare bedrock on the west side of the glacier and a trimline on the east side document 19th century thinning of the glacier. Prospectors Peak can be seen above Camicia Glacier. USGS Photo Library photograph, Moffit 344. **B**, 8 August 2000 oblique aerial photograph of the termini of Valdez and Camicia Glaciers. Valdez Glacier is fronted by an ice-marginal lake approximately 2 km in diameter. Camicia Glacier retreated approximately 5 km during the 20th century. Photograph by Bruce F. Molnia, U.S. Geological Survey. Larger versions of these figures are available online.

glacier was in retreat at the beginning of the 20th century. Camicia's measurements continued until 1911, during which time the glacier retreated 179 m (average retreat of  $18 \text{ m a}^{-1}$ ). According to Grant and Higgins (1913), the 1906 advance was as much as 76 to 91 m. Field (1932) visited the glacier in 1931 and determined that an additional 390 m of retreat had occurred in the 20 years since 1911 (average retreat of  $19.5 \text{ m a}^{-1}$ ). Field (1937) again visited the glacier in 1935 and determined that an additional 45 m of retreat had occurred between 1931 and 1935 (average retreat of  $11 \text{ m a}^{-1}$ ). Therefore, in the 34-year-period from 1901 to 1935, the terminus of Valdez Glacier retreated 614 m (average retreat of  $18 \text{ m a}^{-1}$ ).

Field (1975b) reported that, in the 25 years between 1935 and 1961, the terminus retreated an additional 325 m (average retreat of  $13 \text{ m a}^{-1}$ ). He stated that "Since there was a great quantity of stagnant ice in the terminal part of the glacier during the 1950s and 1960s, it was difficult to identify the actual terminus and the position of the lower end of the active ice" (Field, 1975b, p. 363). This active ice edge was 150 to 175 m further back from the terminus. By 1971, when Austin Post photographed the edge of the retreating active ice for the USGS, it was about 175 m from Field's 1964 position. When the author photographed the terminus from the air on 8 August 2000 (fig. 244B) and on 3 September 2002, it had retreated north of the valley of its former eastern tributary, Camicia Glacier. Valdez Glacier was fronted by an ice-marginal lake about 2 km in diameter and was calving, producing large tabular icebergs.

The history of Valdez Glacier is closely tied to the gold rush at the turn of the 20th century. Between 1898 and 1900, the glacier served as a major highway for prospectors traveling from the port of Valdez to the gold fields of the interior (Tarr and Martin, 1914, pl. XCV, ff p. 240). The Valdez Glacier route bypassed the rugged and dangerous route through Keystone Canyon and Thompson Pass (Schrader, 1900) and provided a relatively easy 29-km-long route to the head of Klutina Glacier and from there to Klutina Lake. About 1910, mining began in the bedrock exposed on both walls of the valley of Valdez Glacier. 20th century thinning of the glacier left these mining claims more than 100 m above the present ice surface. Hence, during the 20th century, Valdez Glacier retreated more than 2 km and thinned by more than 100 m.

A comparison of 1950s map data of the glacier with data obtained during a geodetic airborne laser altimeter profiling survey in the middle 1990s, shows that Valdez Glacier thinned by an average of  $1.23 \text{ m a}^{-1}$  and decreased in volume by  $0.201 \text{ km}^3 \text{ a}^{-1}$  (K.A. Echelmeyer, W.D. Harrison, V.B. Valentine, and S.I. Zirnheld, University of Alaska Fairbanks, written commun., March 2001).

An unnamed glacier located north of Prospectors Peak (1975 length estimated by the author of about 12 km, area of about  $42 \text{ km}^2$ ) and Camicia Glacier were both connected to Valdez Glacier in the early 20th century. By the beginning of the 21st century, Camicia Glacier had retreated about 4.2 km, and the unnamed glacier had retreated about 2.5 km. Both are incorrectly mapped on the 1993 revision of the USGS Valdez A-4 topographic quadrangle map (appendix B).

Camicia Glacier separated from Valdez Glacier soon after the beginning of the 20th century. By 1909 (Tarr and Martin, 1914), an ice-marginal lake dammed by the flank of Valdez Glacier separated the two glaciers. In 1931, when Wentworth and Roy (1936) observed the glaciers, the lake still was present. Field (1975b) reported that, by 1950, Valdez Glacier had narrowed to the point where no lake was evident. Field also reported that a comparison of two maps—the first surveyed in 1911 and 1912 and the second based on 1950 photography—showed that, between 1912 and 1950, the terminus of Camicia Glacier retreated 2.75 km and thinned by 335 m (average retreat of  $72 \text{ m a}^{-1}$ , average thinning of  $9 \text{ m a}^{-1}$ ). Thinning and retreat were continuing when both the unnamed glacier and Camicia Glacier were observed from the air by the author on 3 September 2002.

## Prince William Sound Segment—The Northern Prince William Sound Subdivision

Northern Prince William Sound contains one of the greatest concentrations of calving tidewater glaciers in Alaska (figs. 41, 245, tables 2, 3). The Chugach Mountains fjords that have tidewater glaciers are located on the northern and

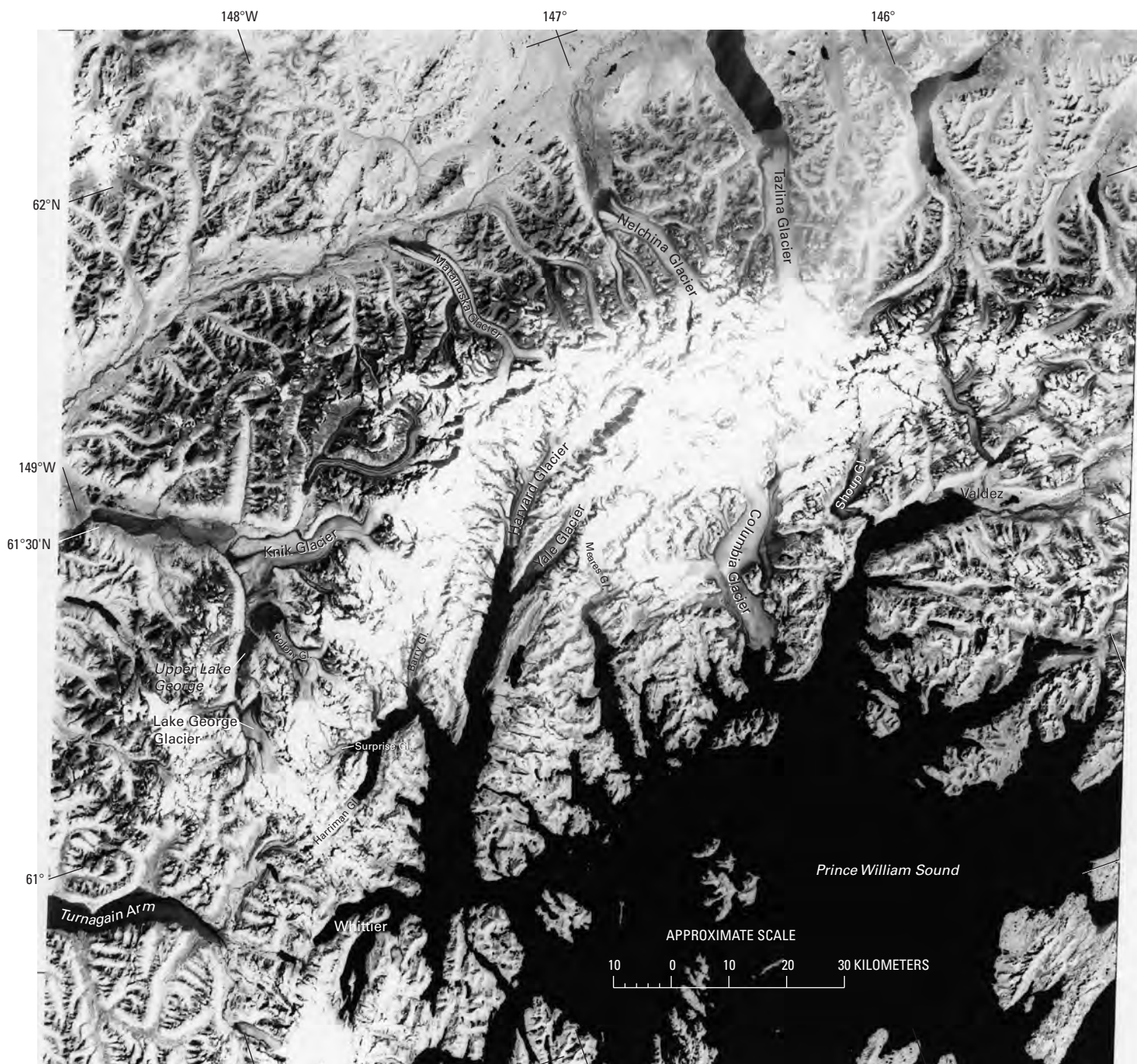


**Figure 245.**—Annotated Landsat 3 MSS image of the western Chugach Mountains on 26 August 1978 showing the location of many of the tidewater and valley glaciers in the region. Of the tidewater glaciers, Surprise and Barry Glaciers were slowly retreating; Harriman, Harvard, and Meares Glaciers were advancing slowly; and Yale and Columbia Glaciers were retreating rapidly (Meier and others, 1980). Shipping lanes used by tankers transporting oil from Valdez are within 20 km of Columbia Bay at the terminus of Columbia Glacier.

Numerous small icebergs enter these lanes, creating a possible hazard to shipping. Knik Glacier dammed the outflow from the Lake George basin annually from 1918 to 1962 and in 1964 and 1965, resulting in annual glacier-outburst floods (jökulhlaups). Since 1966, no ice dam has formed (Post and Mayo, 1971). Matanuska and Nelchina Glaciers are both slowly retreating. Landsat image (30174–20290, band 7; 26 August 1978; Path 73, Row 17) and caption courtesy of Robert M. Krimmel, U.S. Geological Survey.

northwestern sides of Prince William Sound and include the following bays, inlets, and fjords: Shoup Bay, Columbia Bay, Unakwik Inlet, Harvard Arm and Yale Arm of College Fiord, Barry Arm, Harriman Fiord, and Port Wells. Glaciers in this subdivision that have lengths of 8 km or more and areas determined by Field (1975b, p. 470–472) [lengths and areas calculated later by Viens (1995) (table 2) are shown in brackets] include: Shoup (30 km, 146 km<sup>2</sup> [29 km, 156 km<sup>2</sup>]), Columbia (66 km, 1,370 km<sup>2</sup> [59.5 km, 1,121 km<sup>2</sup>]), Meares (25 km, 130 km<sup>2</sup> [25.7 km, 142 km<sup>2</sup>]), Amherst (8 km, ~10 km<sup>2</sup>, estimated by the author), Yale (35 km, 220 km<sup>2</sup> [32.2 km, 194 km<sup>2</sup>]), Harvard (39 km, 500 km<sup>2</sup> [39.4 km, 524 km<sup>2</sup>]), Smith [10 km, 20 km<sup>2</sup>], Bryn Mawr [8 km, 26 km<sup>2</sup>], Coxe (11 km, 19 km<sup>2</sup> [11.3 km, 20 km<sup>2</sup>]), Barry (24 km 75 km<sup>2</sup> [26.5 km, 95 km<sup>2</sup>]), Cascade (9 km, 15 km<sup>2</sup> [8 km, 15 km<sup>2</sup>]), Serpentine (10 km, 23 km<sup>2</sup> [10 km, 30 km<sup>2</sup>]), Surprise (13 km, 66 km<sup>2</sup> [12.1 km, 80 km<sup>2</sup>]), Harriman (13 km, 49 km<sup>2</sup> [12.9 km, 60 km<sup>2</sup>]), and Billings (8 km, 12 km<sup>2</sup>). Information about many of the glaciers in the Prince William Sound region has been presented by Lethcoe (1987).

### Shoup Glacier



**Figure 246.**—Two photographs of Shoup Glacier showing the position of its terminus near the start (A) and at the end of the 20th century (B). Note the position of the triangular snow accumulation just behind the terminus in A. This feature is common to both photographs. **A**, 13 July 1908 photograph by U.S. Grant of the terminus of Shoup Glacier (Grant and Higgins, 1911). A push moraine is located along much of the terminus, suggesting that Shoup Glacier was advancing when it was photographed. The terminus is fronted by an outwash fan delta. **B**, 8 August 2000 north-looking oblique aerial photographic mosaic showing most of the area exposed by 20th century retreat. Note the large barren area around the margin. The proximal edge of the 1908 outwash fan delta is located on the right edge of the photograph. Photograph by Bruce F. Molnia, U.S. Geological Survey. Larger versions of these figures are available online.

At the end of the 20th century, Shoup Glacier (Post and Viens, 2000, pl. 2) was located approximately 6 km from the mouth of Shoup Bay, a sinuous embayment located on the northwestern shore of Valdez Arm. At its “Little Ice Age” maximum position, approximately 250 years ago, its terminus was astride the Valdez Arm shoreline, where it deposited a terminal moraine (Post and Viens, 2000). Hence, in the 250-year period between 1750 and 2000, Shoup Glacier retreated about 6 km, an average annual retreat of 24 m a<sup>-1</sup>.

Originally named Canyon Creek Glacier by Abercrombie in 1898 (Orth, 1971), Shoup Glacier was first photographed the same year by Schrader (1900). At that time, it was located at the head of a shallow 2.5-km-long bay where it discharged into tidewater (2.5 km of retreat in 148 years, an average retreat of ~17 m a<sup>-1</sup>). Tarr and Martin (1914) commented that, before Schrader’s visit in 1898, there were no known previous observations of the glacier by either the Russians or by Whidbey, who visited Valdez Arm in 1794. Tarr and Martin (1914) further stated that the glacier also was photographed by the C&GS in 1901, by Grant in 1905 and 1908 (fig. 246), by the NGS in 1909 and 1910, and by Bradford Washburn on 14 June 1937. The area containing the glacier was surveyed in 1911, 1912, and 1916 by J.W. Bagley, C.E. Giffin, and R.H. Sargent for the USGS topographic quadrangle mapping program. Grant and Higgins (1913, p. 15), commented that Shoup glacier is “of economic importance in that it furnishes ice for Valdez and Fort Lisicum, the detached bergs being lifted upon barges and being taken to these towns.”

Field (1975b) stated that, from 1898 through 1957, there was relatively little change in the position of the glacier’s terminus; the largest change was a recession of less than 200 m. The most significant change was more than 100 m of downwasting of the stagnant terminus. To complicate matters, small advances occurred between 1898 and 1901 (Tarr and Martin, 1914), between 1910 and 1914 (Keen, 1915a), and between 1935 and 1942 (Field, 1975b).

By 1961, the glacier had begun to retreat. Field (1975b) stated that, during the next 7 years, the glacier retreated between 500 and 600 m. In an unpublished map of the terminus of Shoup Glacier based on 1957 aerial photography and 1961 and 1964 field observations (American Geographical Society Glacier Studies Map No. 64–3–G5), Field showed that, at that time, the terminus of Shoup Glacier was separated from Shoup Bay by the terminal moraine, an outwash plain, and a tidal flat. He also showed that a 250-m-diameter tidal lake, the precursor to the present lake, had already formed.

A bathymetric map (Post and Viens, 2000, pl. 2) shows the position of the terminus of Shoup Glacier in 1916, 1966, 1978, 1982, and 1990. In 1990, the terminus sat at the western end of a 1.9-km-long lake named *Shoup Basin* by Post and Viens (2000). The eastern end was bounded by the moraine deposited by the glacier between 1957 and the early 1960s. When the author

photographed the glacier from the air in August 1996, on 8 August 2000 (fig. 246B), and on 3 September 2002, he noted evidence of continued thinning and retreat. The terminus of Shoup Glacier was located a maximum of about 850 m behind its 1990 position, and the southwestern one-third of the margin of the terminus was fringed by a large area of bare bedrock and stagnant, debris-covered ice. In the 34 years between 1968 and 2002, the glacier retreated approximately another 2.85 to 3.15 km. During the 20th century, the glacier retreated a maximum of approximately 3.6 km.

In the early 1990s (Viens, 1995) (tables 2, 3), Shoup Glacier had a length of about 29 km, an area of 156 km<sup>2</sup>, a width at its face of 1.3 km, and an AAR of 0.61. Its accumulation area was about 95 km<sup>2</sup>, and its ablation area was about 62 km<sup>2</sup>.

### Columbia Glacier

The largest glacier in Prince William Sound, Columbia Glacier is located at the head of Columbia Bay (figs. 43, 44, 45, 46), a fjord with depths greater than 300 m. Previously called *Fremantle Glacier*, *Live Glacier*, and *Root Glacier*, Columbia Glacier had a pre-retreat length of 66 km and an area of 1,370 km<sup>2</sup> (Field, 1975b, p. 470). The ice speed at the terminus ranged between 5 and 6 m d<sup>-1</sup>. Named in 1899 by the Harriman Alaska Expedition for Columbia University, it has been rapidly retreating and calving large quantities of icebergs since 1979. Until early 1979, part of the terminus of Columbia Glacier was grounded on Heather Island and an adjacent submarine moraine that protected the terminus from significant loss of ice through calving, as a 24 August 1978 AHAP photograph (fig. 247) shows. But, in January 1979, the glacier retreated from Heather Island and lost contact with its submarine terminal moraine. Thus, Columbia Glacier began a “drastic irreversible, retreat” (Meier and others, 1980, p. 10) that is well documented in this volume in the section authored by Robert M. Krimmel, “Columbia and Hubbard Tidewater Glaciers.” Columbia Glacier has since retreated more than 12 km and thinned as much as 400 m. By 2001, the length had decreased to about 54 km, and, according to Meier and others (2001), the velocity at the terminus in-



**Figure 247.**—24 August 1978 AHAP false-color infrared vertical aerial photograph of the terminus of Columbia Glacier. Note that although part of the terminus of the glacier is in contact with Heather Island (at center of terminus), some retreat is underway along the southeastern margin. AHAP photograph no. L110F6623 from the GeoData Center, Geophysical Institute, University of Alaska, Fairbanks, Alaska.

creased nearly fivefold to  $25 \text{ m d}^{-1}$  (more than  $9 \text{ km a}^{-1}$ ). Columbia Glacier has its source on the southern side of the Chugach Mountains at maximum elevations that exceed 3,500 m. Four principal tributaries combine to form a south-flowing main trunk nearly 5 km wide.

Because of Columbia Glacier's proximity to the port of Valdez, which is the southern terminus of the Trans-Alaska Pipeline, icebergs produced by its retreat pose a real threat, especially to oil tankers transiting shipping lanes in Prince William Sound. These concerns resulted in a USGS comprehensive, multi-year investigation into the glacier's dynamics and an attempt to quantify the potential impacts of increased iceberg production. In addition to the summary provided by Krimmel in this volume, many of these data were released by the USGS in September 2001 (Krimmel, 2001). [Editors' note: According to Mark F. Meier (written commun., 2004), Columbia Glacier—a tidewater glacier in the retreat phase of the cycle of tidewater glacier stability (fig. 42)—is the best-documented and most thoroughly studied glacier in Alaska. Studies done on Columbia Glacier are comparable to studies of the surge-type Variegated Glacier. More than 120 aerial photogrammetric survey missions provided the data to compile an accurate record of its changing velocity and strain-rate fields. Studies of Columbia Glacier provide much of the scientific knowledge about calving of icebergs from a grounded glacier terminus.] Because Krimmel's section of this volume describes the late 20th century retreat of the tidewater glacier, the remainder of this discussion will focus on the early history of Columbia Glacier, which was the subject of much attention at the beginning of the 20th century.

Vancouver's 1794 voyage provided the first mention of the glacier as well as the first map showing its location (Vancouver, 1798). Tarr and Martin (1914) mentioned three other early maps—Applegate's in 1887 (Davidson, 1904), Mahlo's in 1898 (USGS, 1899), and Schrader's in 1900 (Schrader, 1900)—that also show the location of the terminus. All show the glacier at about the same location, leading Tarr and Martin (1914, p. 257) to conclude that "The only fact indicated by these maps is that the glacier was not strikingly different in the years of observation between 1794 and 1900." It must be kept in mind, however, that none of these earlier (pre-1970s) observations were made in the context of tidewater glacier stability (fig. 42), a theory first set forth by Post (1975).

Tarr and Martin (1914, p. 259) reported that, in 1898, the first water depth sounding of approximately 90 m (50 fathoms) near the face of Columbia Glacier was made by the steamship *SS Dora*, captained by A.O. Johansen. In 1899, the Harriman Alaska Expedition arrived in Columbia Bay and named and studied the glacier. From 25 to 28 June 1899, USGS geologist Grove Karl Gilbert (Gilbert, 1904) photographed and mapped the lower 15 km of the glacier (figs. 248, 249, 250), documenting an advance that occurred about 1892 and a retreat underway in 1899.

Grant visited and photographed the glacier in 1905. He was joined by Higgins in both 1908 and 1909 (Grant and Higgins, 1910, 1913). Their collaboration on 23 and 24 June 1909 produced a map of the terminus that compares the 1899 and 1909 terminus positions. They concluded that the glacier retreated between 1899 and 1905, advanced between 1905 and 1908, and advanced even more through June 1909. Tarr and Martin (1914) visited the glacier for the NGS in 1909, twice in 1910, and again in 1911 and observed that the glacier continued to advance through their 1911 visit. Their topographic map shows the terminus of an unnamed eastern branch, most of whose length is separated from the main trunk of the glacier by the Nunatak, making contact with the glacier just below the 1,000-ft contour line (Tarr and Martin, 1914). Gilbert (1904) showed that the two were in only minimal contact on his 1899 map. Tarr and Martin quantified the changes that they and Gilbert observed: (1) 1892–July 1899, retreat of 243 m (800 ft), an average retreat of about  $35 \text{ m a}^{-1}$ ; (2) July 1899–24 June 1909, advance of about 150 m

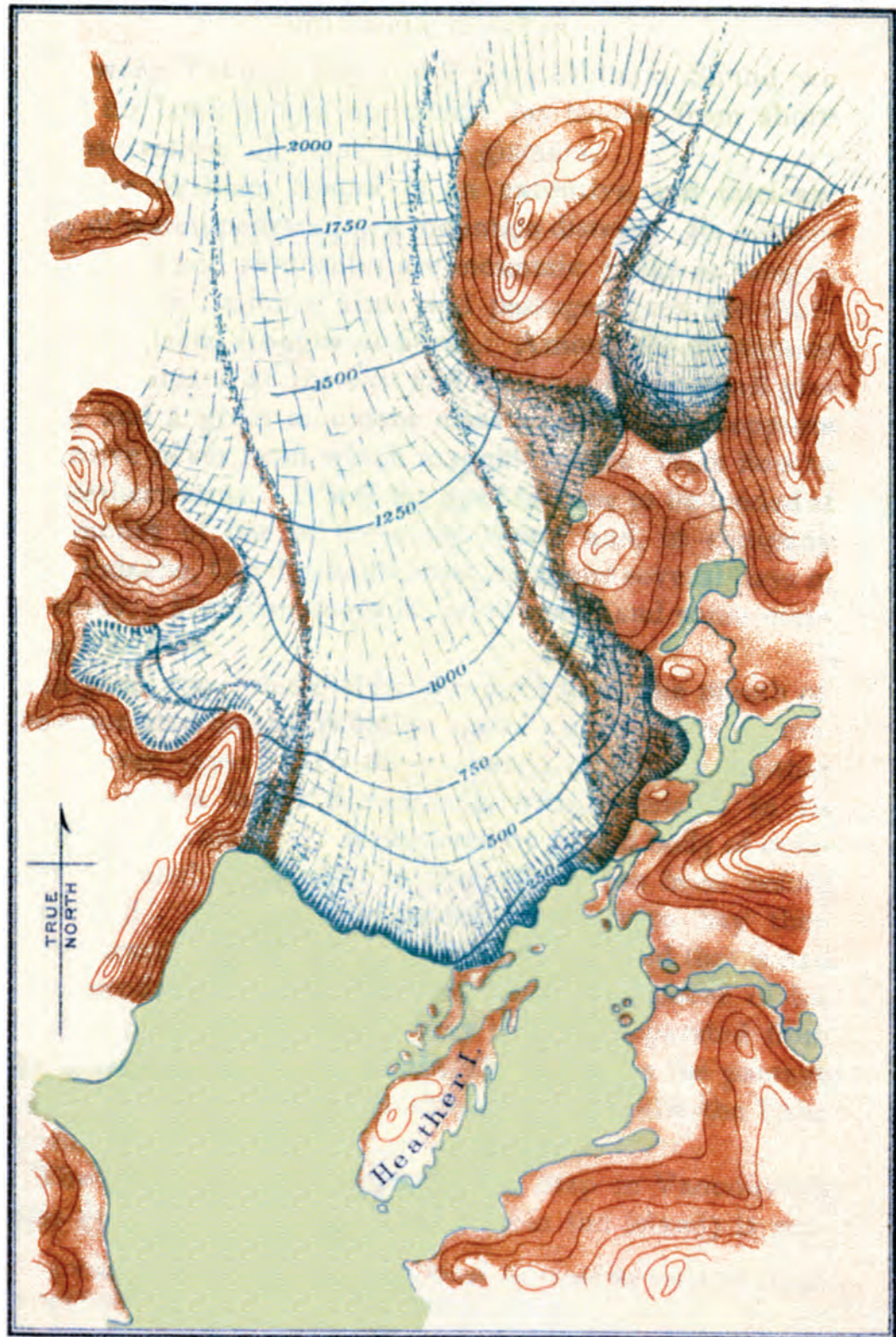


**Figure 248.**—Photographs by USGS geologist Grove Karl Gilbert of the lower Columbia Glacier. **A**, 25 June 1899 photograph of the Harriman Alaska Expedition's vessel S.S. George W. Elder in Columbia Bay, with the grounded terminus (on submarine moraine) of Columbia Glacier in the background. USGS Photo Library photograph Gilbert 339. **B**, 26 June 1899 photograph from the highest point on Heather Island, a 107-m-high hill, of the lower reaches of Columbia Glacier. Note the debris-covered eastern margin. USGS Photo Library photograph Gilbert 343.



(500+ ft), an average advance of about  $15 \text{ m a}^{-1}$ ; (3) 23 August 1909–5 July 1910, advance of 213 m (700 ft), an average advance of about  $245 \text{ m a}^{-1}$ ; (4) 5 July 1910–5 September 1910, advance of 33 m (~110 ft), an average advance of about  $200 \text{ m a}^{-1}$ ; and (5) 5 September 1910–21 June 1911, advance of less than 30 m (<100 ft), an average advance of about  $38 \text{ m a}^{-1}$ . Hence, during the 19-year period from 1892 thru 1911, Columbia Glacier advanced approximately 290 m, an average advance of about  $15 \text{ m a}^{-1}$ .

In 1910, Bean (1911) investigated the “submerged lands” of Prince William Sound. He described his study as follows: “The aim of this thesis is to study the soundings of this embayment (Prince William Sound) and from this study outline the history of the fiords, and determine as far as possible the extent of former glaciers and their influence upon preglacial valleys. Especial attention will be paid to that part of the fiord which is now submerged” (Bean, 1911, p. 2). Working in July and August 1910 as part of an NGS Expedition under the direction of Lawrence Martin, Bean took about 300 soundings in about 150 miles of Prince William Sound using a 20-lb lead weight obtained from the C&GS. He took soundings for his cross sections every 1/8 to 1/2 mi. Along the long axes of the fjord, he spaced soundings at 1- or 2-mi intervals. A sounding taken approximately 400 m in front of Columbia Glacier showed 182 m (600 ft) of water (Tarr and Martin, 1914). Bean found that depths increased with distance from the ice margin—275 m at a point 5.6 km from the glacier and 310 m at a point 8 km from the glacier—and that water depths



MAP OF COLUMBIA GLACIER

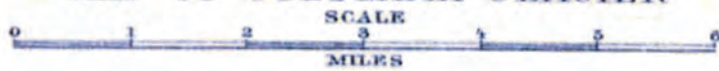


Figure 249.—25–28 June 1899 map by USGS geologist Grove Karl Gilbert of the lower 15 km of Columbia Glacier. Contours are in feet. Published as Plate XI in Gilbert (1904).



**Figure 250.**—Three 26 June 1899 ground photographs by USGS geologist Grove Karl Gilbert, with Professor Charles Palache (Harvard University geologist) for scale, showing late 19th century features at the terminus of Columbia Glacier. **A**, An arcuate lobe of a push moraine formed by an advance of Columbia Glacier before 1892. Immediately adjacent to the moraine are a number of trees that were killed by the advance. USGS Photo Library photograph Gilbert 356. **B**, A recessional moraine formed after 1892. Note the trees that were killed by the advance of the glacier. Between the moraine and Columbia Glacier are numerous flutes exposed by the retreating ice. USGS Photo Library photograph Gilbert 354. **C**, The retreating margin of Columbia Glacier and an approximately 0.75-m-high flute exposed by the retreating ice. USGS Photo Library photograph Gilbert 352.



increased uniformly by about 30 m with every 1,600-m increment away from the face of the glacier. A complete bathymetric survey of Columbia Glacier's margin and approaches was published by Post (1978).

According to Field (1975b), no additional observations were made of the glacier until 1931. In 1931, Field (1932) attempted to reoccupy many of the earlier photographic stations of Gilbert, Grant and Higgins, and Tarr and Martin. He reported that "All the earlier moraines and trimlines had been destroyed by an advance which was then tentatively assigned to the early 1920s and which was later determined by vegetation studies to have occurred at various points along the terminus between 1917 and 1922..." (Field, 1975b, p. 369). He did not specify the magnitude of the advance. Following the 1917 to 1922 advance, the glacier began to retreat. By 1931, Field (1932) measured 275 m of recession at the western margin of the glacier, about 60 m of recession on Heather Island, and from 120 to 250 m of recession along the land-based eastern margin.

This retreat was quickly followed by another advance. Field (1937) revisited Columbia Glacier in 1935 and measured 1,045 m of advance at the western margin of the glacier, 72 m of advance on Heather Island, and 25 m of advance on the land-based eastern margin. Field (1937) described a massive moraine deposited by this advance on Heather Island as a prominent feature that protrudes through the 1920 moraine.

Maynard M. Miller visited Columbia Glacier in 1947 and described a recession of several hundred feet since the 1935 advance (Miller, 1948a). Field (1975b) reported that an advance of 100 m or more was underway between 1947 and 1949. Eight years later, he observed that the glacier was slowly retreating from the moraine formed by the late 1940s advance.

Field (1975b) reported that observations of Columbia Glacier were made by a variety of individuals in 1960, 1961, 1963, 1964, 1965, 1966, 1967, 1968, 1969, 1970, and 1971. During this period, Columbia Glacier experienced several small advances between 1957 and 1961, recession or minimal change between 1961 and 1968, a slight advance of a few tens of meters on land between 1968 and 1969, and an advance on Heather Island and on the eastern land-based terminus between 1969 and 1971. Field (1975b, p. 369) remarked that "Each of the advances since the maximum of 1920 have in most places not extended as far as the previous one, so that their end-moraines have been preserved." Most of the fluctuations in terminus position described here are for the land-based part of Columbia's terminus where the moraine records serve as near-permanent markers to document change. Field (1975b, p. 370) noted that the marine-based termini on either side of Heather Island "have tended to fluctuate with the land termini, but on the whole have remained remarkably stable, in so far as appreciable net change is concerned. Their general appearance in the 1960s was essentially the same as in 1899."

Post (1975), Field (1975b), and Sikonia and Post (1979) described observed changes in the tidal ice-cliff termini of Columbia Glacier and suggested that the increasing size and frequency of seasonal embayments in the terminus might be a precursor to a rapid retreat. Retreat from the terminal moraine shoal, over which water depths are about 20 m or less, formed deep embayments in the ice margin during the summer and fall. Until 1979, winter and spring readvances were normally sufficient to refill the embayment and recover stability on the submarine moraine. Field (1975b) noted that, in a 1938 Washburn photograph, deep embayments existed on both sides of Heather Island. He speculated that, if they had joined north of Heather Island, "they would have probably caused a wide retreat of the whole terminus" (Field, 1975b, p. 370–71). A complete inventory of years in which embayments formed does not exist. However, they were observed in 1938, 1939, 1940, 1941, 1960, 1961, 1964, 1965, 1968, and throughout the 1970s. The lack of embayments between the middle 1940s and 1960 is more likely owing to an absence of observation rather than to an absence of embayments.

The 1964 embayment was 900 m deep and 1,300 m wide, whereas the 1971 embayment was 1,200 m deep and 800 m wide (Field, 1975b). Sequential changes at the terminus of Columbia Glacier from 1966 to 2000 are shown in figure 251. Figure 252 shows different views of the margin of the Columbia Glacier on 8 August 2000. The author began observations from the air in 1974 and has continued them into the 21st century (fig. 252).



**Figure 251.**—Four aerial photographs show changes in the terminus region of Columbia Glacier between 1966 and 2000. **A**, 3 September 1966 oblique aerial photograph of the lower reaches of Columbia Glacier. Note that part of the terminus of Columbia Glacier is in contact with Heather Island. USGS photograph no. 664-18 by Austin Post, U.S. Geological Survey. **B**, 15 August 1981 north-looking oblique aerial photograph of the lower reaches of Columbia Glacier. Note that the terminus of the glacier is retreating and has lost contact with Heather Island and the mainland to the east. Note also the calving embayment. Photograph by Bruce F. Molnia, U.S. Geological Survey. A larger version of this figure is available online.

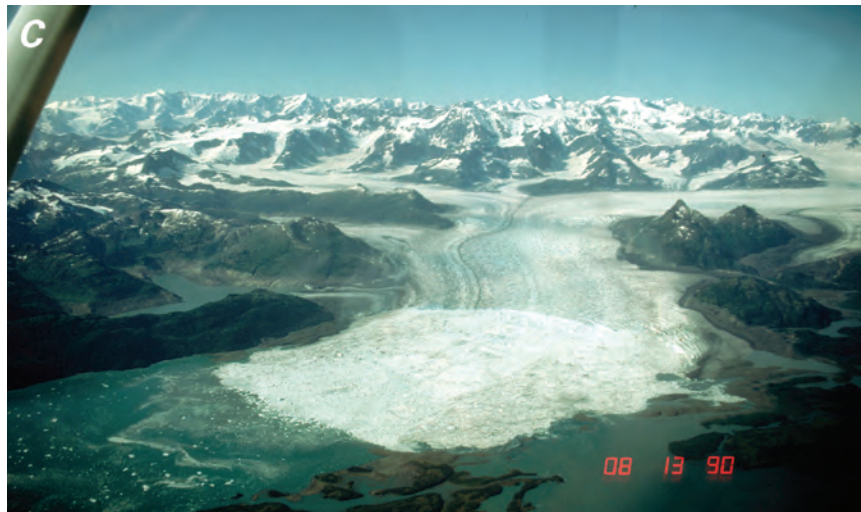


**Figure 251.**—**C**, 13 August 1990 north-looking oblique aerial photograph of the lower reaches of Columbia Glacier. Note that the terminus of the glacier is actively retreating and that the newly exposed part of Columbia Bay bounded on the south by Heather Island is filled by approximately 5 km of icebergs that are contained by the Heather Island terminal moraine. Photograph by Larry Mayo, U.S. Geological

Survey. **D**, 8 August 2000 north-looking oblique aerial photograph of the lower reaches of Columbia Glacier. Note that the terminus has retreated approximately 12 km and that the newly exposed part of Columbia Bay is filled with icebergs. Photograph by Bruce F. Molnia, U.S. Geological Survey. A larger version of D is available online.

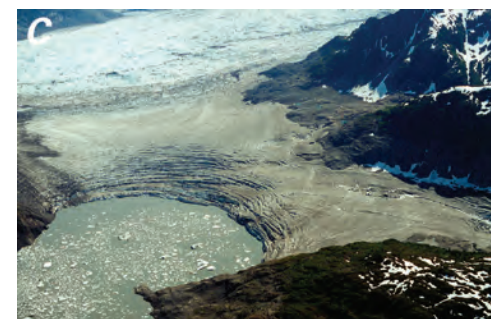


**Figure 252.**—Three 8 August 2000 oblique aerial photographs of features along the margin of Columbia Glacier. **A**, Northwest-looking view of the retreating and thinning eastern Land Lobe of Columbia Glacier. **B**, North-looking view of a lake and an unnamed ice remnant left behind by the rapidly retreating main trunk. The lake at the upper right separates the remnant of ice from the southern margin of the retreating Land Lobe that can be seen on A. Iceberg-filled Columbia Bay is to the left. **C**, Southeast-looking view of Kadin Lake, an ice-dammed lake on the west side of the Columbia Glacier, currently dammed by an unnamed remnant of ice left behind by the rapidly retreating main trunk. The remnant is actively calving icebergs into Kadin Lake and Columbia Bay. The ice remnant of B can be barely seen at the top left of the photograph. Photographs by Bruce F. Molnia, U.S. Geological Survey. Larger versions of these figures are available online.

A comparison of 1950s map data of the glacier with data obtained during geodetic airborne laser altimeter profiling surveys in the middle and late 1990s showed that, on an annual basis, Columbia Glacier thinned by  $1.44 \text{ m a}^{-1}$  and decreased in volume by  $1.54 \text{ km}^3 \text{ a}^{-1}$ . However between the middle 1990s and 1999, Columbia Glacier thinned by an average of  $7.42 \text{ m a}^{-1}$  and decreased in volume by  $7.64 \text{ km}^3 \text{ a}^{-1}$  (K.A. Echelmeyer, W.D. Harrison, V.B. Valentine, and S.I. Zirnheld, University of Alaska Fairbanks, written commun., March 2001). In the early 1990s (Viens, 1995) (tables 2, 3), Columbia Glacier had a length of about 60 km, an area of about  $1,120 \text{ km}^2$ , a width at its calving terminus of 8 km, and an AAR of 0.67. Its accumulation area was about  $753 \text{ km}^2$ , and its ablation area was about  $368 \text{ km}^2$ .

### Meares Glacier

Meares Glacier is located at the head of Unakwik Inlet, a 32-km-long northward-trending fjord between College Fiord and Columbia Bay. The first European explorer to visit the inlet was Whidbey on 4 June 1794 (Vancouver, 1798). Although he did not sail close enough to observe the glacier and determine its position, floating pieces of ice that he noted in the fjord suggested that Meares Glacier was a tidewater glacier at that time. Meares Glacier was first investigated by Grant and Higgins (1910, 1911a, b, 1913) in 1905 and 1909 and again by Lawrence Martin in 1910 (Martin, 1913). At the beginning of the 21st century, Meares Glacier was an advancing, iceberg-calving, tide-water glacier (fig. 253).



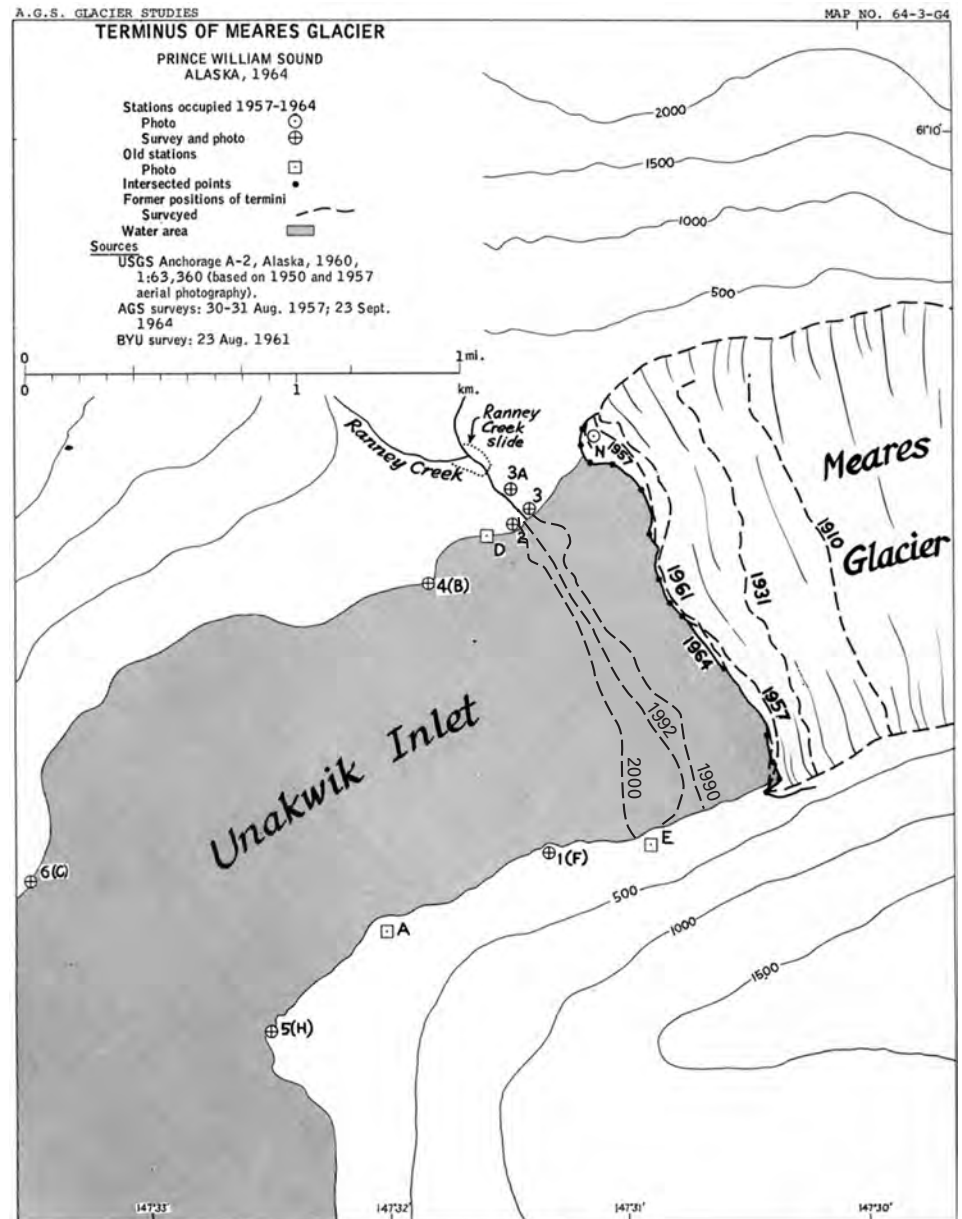
**Figure 253.**—17 August 1999 vertical aerial photograph of the terminus of Meares Glacier. Before the date of the photograph, Meares Glacier advanced into Ranney Creek (to the left of the terminus), diverting its waters to the south. Subsequent calving and retreat of the ice at the western margin resulted in the stranding of a block of ice along the edge of Ranney Creek. Subsequently, the ice was incorporated into the advancing terminus of the glacier. Photograph no. R3-FL7-FR119 from the U.S. Bureau of Land Management.

Meares Glacier has been advancing since it was first observed in 1905. Field (1975b) summarized the reported changes of the terminus of Meares Glacier as follows: 1910–31, advance of 250 to 300 m, annual advance of 12 to 14 m a<sup>-1</sup>; 1931–66, advance of 200 to 425 m, an annual advance of 6–12 m a<sup>-1</sup>. Hence, in the 56 years between 1910 and 1966, the terminus of Meares Glacier advanced between 500 and 675 m, an average advance of 9 to 12 m a<sup>-1</sup>. When the author visited by boat on 3 September 2000, the terminus of Meares Glacier was slowly advancing and pushing down trees. However, the author's observations from the air in 1999, 2000, and 2002 showed some evidence of thinning along the margins of the terminus, especially on its eastern side. Between 1910 and 2000, the terminus advanced about 1.1 km, an average advance of 12.2 m a<sup>-1</sup> (fig. 254). In the 36-year-period between 1966 and 2002, the glacier advanced a maximum of about 550 m, for an average annual advance of about 15 m a<sup>-1</sup>. A large terminal moraine about halfway between the glacier and the mouth of the fjord represents the maximum neoglacial advance of Meares Glacier and presents a significant hazard to navigation.

In 1910, Bean (1911) determined that much evidence of former glacial erosion existed in the submerged lands downfjord from the glacier margins. At Meares Glacier he found that “The depth of water ranges from 534 feet about a half mile south of the glacier to over 1,000 feet near the entrance of the inlet. There is much topographic evidence of former glaciation. The fiord walls are straight and steep, with all spurs truncated, there are numerous hanging valleys from which streams cascade to the sea, and there is abundant rounding of knobs, grooving, plucking and striation. The soundings prove quite conclusively that the Meares Glacier formerly extended much farther, and eroded this great valley.”

Bean (1911, p. 19–20) also determined that Meares Glacier was not floating but was grounded on its bed: “On the assumption that the water does not shallow from the nearest sounding to the glacier, it seems certain that the Meares is not afloat even now, but has great erosive power. Since the height of the ice front is at least 200 feet and the depth of the water is 534 feet, there is a total thickness of 734 feet. If glacier ice floats in sea water with one-sixth of its volume above water, the total thickness of the glacier would have to be 1,200 feet or 456 feet more than it is, in order to be afloat. Five hundred and thirty-four

**Figure 254.**—Map of the terminus of Meares Glacier showing fluctuations in the position of its terminus from 1910 to 2000. Base map is derived from AGS Glacier Studies Map no. 64-3-G4 (Field, 1965). Year 1990, 1992, and 2000 positions (approximate) are based on observations made by the author.



feet of water is sufficient to float a mass of ice with but 107 feet above water. Hence the Meares Glacier is at present resting on the valley floor with the weight of 93 cubic feet of ice or about 4,650 pounds per square foot....”

In the early 1990s (Viens, 1995) (tables 2, 3), Meares Glacier had a length of 26 km, an area of 142 km<sup>2</sup>, a width at its face of 1.2 km, and an AAR of 0.86. Its accumulation area was 121 km<sup>2</sup>, and its ablation area was 20 km<sup>2</sup>.

### **Pedro and Brilliant Glaciers**

Pedro Glacier and Brilliant Glacier, both located on the eastern side of Unakwik Inlet, are two small retreating valley glaciers that were tributaries to a much larger Meares Glacier at the time when it was extended to the position where it deposited its middle fjord moraine. Tarr and Martin (1914) described Brilliant Glacier as descending to an elevation near sea level and being separated from the inlet by a 2.2-km-long outwash plain and delta. By the 1950s (Field, 1975b) observed that its terminus had retreated to an elevation of between 200 and 250 m and that the outwash plain complex had extended to be about 2.5 km long. When the author observed it from the air in 1999, 2000, and 2002, the terminus was located at an elevation of about

350 m, and the margin of Brilliant Glacier showed much evidence of continuing retreat.

### Ranney and Baby Glaciers

Ranney Glacier, a hanging glacier located on the northwestern wall of the Unakwik Inlet, is also retreating. The 1964 earthquake generated a large rockslide that covered much of the lower part of the glacier as it continued down below the terminus to the delta of Ranney Creek (Post, 1967a), the stream that heads at the glacier's terminus. Ranney Glacier has been retreating since it was first observed. Similarly, Baby Glacier—a 2-km-long valley glacier—drains into the western side of the inlet. Like Ranney Glacier, it has been retreating throughout the 20th and early 21st centuries.

### Glaciers of College Fjord

College Fjord (figs. 255, 256), located at the northern end of Port Wells, is about 40 km long and 5 km wide at most. At the beginning of the 21st century, it contained five calving tidewater glaciers: Harvard Glacier and Yale Glacier (fig. 34) (AGS Glacier Studies Map No. 64-3-G10) (Field, 1965), in two arms (Harvard Arm and Yale Arm) at the fjord's head, and Smith, Bryn Mawr, and Wellesley Glaciers on its western wall. Named non-tidewater glaciers in the fjord and in the eastern side valleys include Cap, Tommy, Crescent, Amherst, Lafayette, Williams, Muth, Dartmouth, Downer, Lowell, Eliot, Radcliffe,

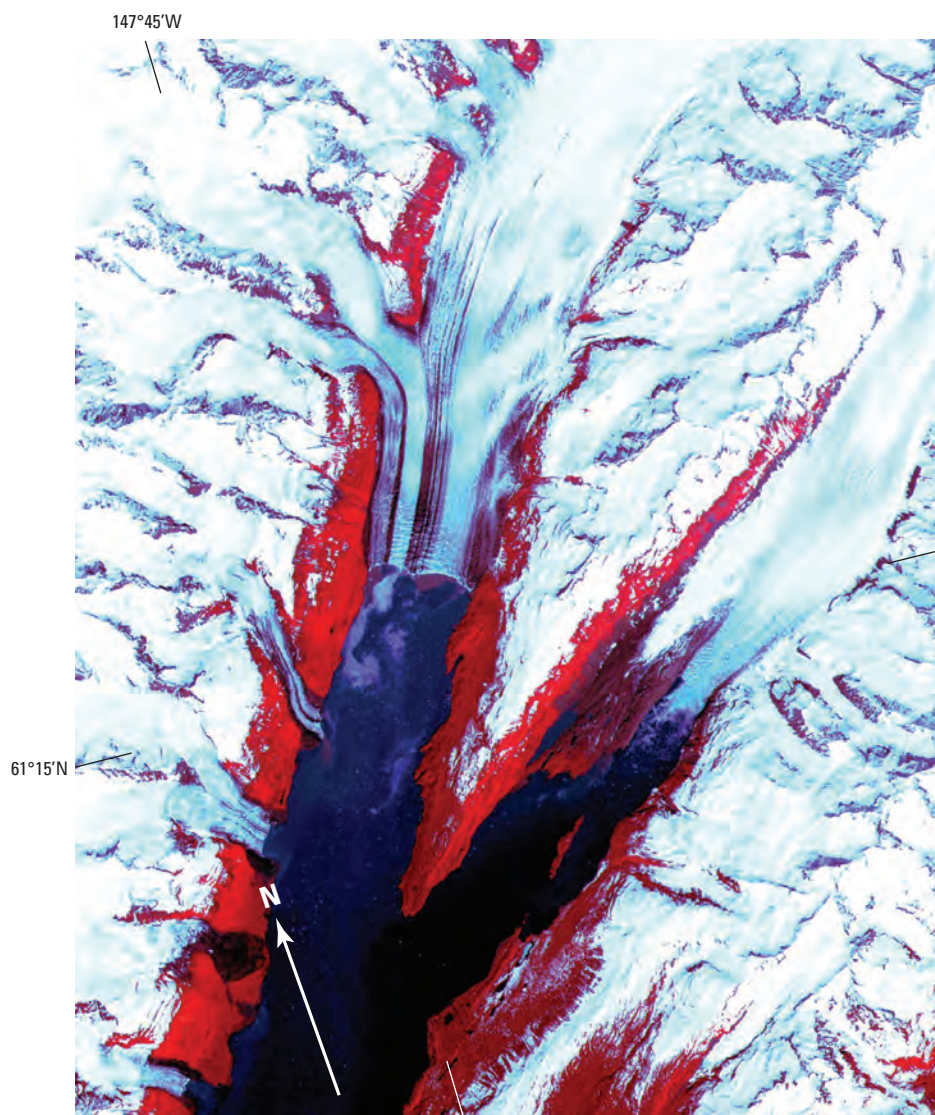


**Figure 255.**—24 June 2000 Advanced Spaceborne Thermal Emission and Reflection Radiometer (ASTER) image of upper College Fjord. The ASTER multispectral sensor on the Terra spacecraft has 15-m-pixel multispectral resolution and is another type of satellite image used to monitor changes in Alaskan glaciers. ASTER image (AST\_LIB.003:2012687866) from the U.S. Geological Survey, EROS Data Center, Sioux Falls, S. Dak.

**Figure 256.**—8 August 2000 north-looking view of College Fiord shows all five of the tidewater glaciers located on the west side. Photograph by Bruce F. Molnia, U.S. Geological Survey.



Baltimore, Vassar, Barnard, and Holyoke Glaciers. With the exception of previously named Cap and Tommy Glaciers, nearly all of these glaciers were named by the geologists of the Harriman Alaska Expedition of 1899, by Grant and Higgins between 1908 and 1912, and by Lawrence Martin in 1910 for Ivy League colleges and eastern universities with which they had affiliations. Included are all seven of the “Seven Sisters” colleges at that time, women’s colleges associated with what were then all-male Ivy League colleges, about half of the Ivy League colleges, two other woman’s colleges, and two past presidents of Harvard University. Baltimore Glacier was named by Grant and Higgins in 1908 for the Woman’s College of Baltimore, now Goucher College; Eliot Glacier was named by Martin in 1910 for Charles William Eliot, former president of Harvard (Tarr and Martin, 1914). Downer Glacier was named for the Milwaukee-Downer College for Women by Martin in 1910; Lowell Glacier, first reported by the USGS in 1915, took its name from the first non-native settler in the Seward area (Orth, 1967).

Most of College Fiord’s glaciers have shown a general trend of slow recession since first being mapped at the beginning of the 20th century. Harvard Glacier, however, has been slowly advancing for nearly 100 years. Yale Glacier retreated rapidly with more than 6 km of recession during the 20th century. The 1964 earthquake caused rockslides and avalanches on Smith, Vassar, Harvard, and Yale Glaciers.

### *Cap and Tommy Glaciers*

Cap Glacier, an unnamed glacier, and Tommy Glacier are the three southernmost glaciers that ultimately drain into College Fiord. Cap Glacier, located on the northern wall of its valley, is a retreating hanging glacier surrounded by exposed bedrock. Its outlet stream enters Davis Lake. The unnamed glacier, located at the head of the Avery River, is a small retreating valley glacier. Tommy Glacier, located on the northern wall of the Avery River valley, is a retreating hanging glacier surrounded by exposed bedrock. When the author observed them from the air on 8 August 2000, all showed evidence of continued retreat.

### *Crescent and Amherst Glaciers*

In 1957, Crescent and Amherst Glaciers were visited by an AGS field party (AGS Glacier Studies Map No. 64-3-G3) (Field, 1965) that included Field and Viereck (Field, 1975b). This party established photographic stations and mapped the glacier termini. The termini of both glaciers had been photographed previously from the deck of the Harriman Alaska Expedition vessel *SS George W. Elder* by Merriam in June 1899. Viereck's 1957 investigation found an end moraine that was 800 m beyond the 1957 margin of Crescent Glacier and a trimline about 60 m above the 1957 ice surface. On the basis of dendrochronology, Viereck concluded that the moraine had formed about 125 years earlier, or ca. 1830. A second moraine 125 m from the 1957 terminus was dated to the middle 1930s. The author has photographed the glacier several times from the air between 1975 and 2002. When he observed it on 5 September 2000, the terminus of Crescent Glacier had retreated about 1.5 km from its 1957 position. Hence, in the 170 years since abandoning its probable "Little Ice Age" maximum position, the glacier has retreated almost 2.3 km, yielding an average retreat rate of  $13.5 \text{ m a}^{-1}$ . Between 1830 and 1957, the glacier retreated at an average rate of  $6.3 \text{ m a}^{-1}$  and thinned an average of  $0.47 \text{ m a}^{-1}$ . Between 1957 and 2000, the average rate of retreat was  $34.9 \text{ m a}^{-1}$ .

The 1957 AGS visit to Amherst Glacier was the first on record. Other than subsequent aerial reconnaissance, it is still the only recorded visit to date. Field (1975b) summarized the 1914-71 history of the glacier by analyzing maps and aerial photography. He reported that, when the glacier was first mapped, it ended on an outwash plain. By 1935, when Bradford Washburn photographed it, the terminus had retreated and caused the formation of an ice-marginal lake. Aerial photographs taken in 1941 by the U.S. Army Air Forces, in 1950 and 1957 by the USAF, in 1964 by the C&GS, in 1965 by the USGS, and in 1966 and 1971 by the AGS all showed continuing retreat and expansion of the lake. This trend was continuing when the author observed Amherst Glacier on 14 July 1978 (fig. 257).

Field (1975b) noted that an end moraine is located on the outwash plain about 1.5 km in front of the 1957 terminus. Unlike the terminal moraine of Crescent Glacier, it could not be dated. The distance between the position of the terminus when it was first surveyed in 1914-16 and again in 1950 is between 500 and 600 m, suggesting a retreat at an average rate of about  $15 \text{ m a}^{-1}$ . Between 1935 and 1950, the glacier retreated about 200 m, suggesting a retreat at an average rate of about  $13 \text{ m a}^{-1}$ . Between 1950 and 1957, the glacier retreated about 100 m, suggesting a retreat at an average rate of about  $14 \text{ m a}^{-1}$ . Field (1975b) speculated that the undated end moraine could be contemporary with the moraine at adjacent Crescent Glacier. When the author observed the terminus of Amherst Glacier from the air on 4 August 2000 and 3 September 2002 and from a boat on 3 September 2000, it had retreated about 1.4 km from its 1957 position. Therefore, since first being mapped in 1914-16, the glacier has retreated about 2.0 km, with an average retreat rate of approximately  $24 \text{ m a}^{-1}$ . Because the glacier margin is ringed by an ice-marginal lake, part of this retreat may have been caused by calving.



**Figure 257.**—14 July 1978 east-looking photograph of Amherst Glacier. A trimline flanks each lateral margin, and an apron of bedrock surrounds the terminus, which has been retreating at a rate of approximately  $15 \text{ m a}^{-1}$  for most of the 20th century. Photograph by Bruce F. Molnia, U.S. Geological Survey. A larger version of this figure is available online.



### *Lafayette Glacier*

Lafayette Glacier is another small west-flowing valley glacier that has received minimal scientific attention. Baird and Field (1951) reported that, during the 2-year period between observations in 1947 and 1949, the glacier's terminus retreated 85 m. Similarly, Field (1975b) reported that a comparison of Bradford Washburn's 1935 photograph and a vertical aerial photograph taken in 1957 by the USAF shows a retreat of 600 to 700 m. When the author observed the glacier from a boat on 3 September 2000 and from the air on 3 September 2002, it had retreated about another 1.2 km from its 1957 position. Hence, in the 67 years between 1935 and 2002, the glacier retreated about 1.85 km, yielding an average retreat rate of about 28 m a<sup>-1</sup>.

### *Glaciers Draining into Coghill Lake*

Coghill Lake, which drains into College Fiord through the Coghill River, is a 5-km-long lake that is a part of the sediment-filled eastern arm of College Fiord. The Coghill Lake and Coghill River basin are separated from College Fiord by a ridge with maximum elevations exceeding 710 m. A number of small west-flowing glaciers descend from the ridge that separates College Fiord and Unakwik Inlet. The named glaciers are Williams, Muth, and Dartmouth Glaciers.

*Williams Glacier.*—Williams Glacier is an approximately 2-km-long unstudied glacier that is sheltered from sunlight by the ridge that separates College Fiord from Unakwik Inlet. When the author observed it from the air on 8 August 2000, it showed evidence of retreat.

*Muth Glacier.*—In 1908, Grant and Higgins gave the name Muth Glacier to a previously unnamed glacier located on the ridge between Unakwik Inlet and College Fiord. However, it is uncertain which glacier they actually named. The USGS Anchorage A-2 1:63,360-scale topographic quadrangle map (1960) (appendix B) shows Muth Glacier as a westward-flowing glacier that drains into Coghill Lake. However, Bean (1911), who mapped the bathymetry of Port Wells and College Fiord in 1910, showed Muth Glacier as being on the eastern side of this divide, approximately 7.5 km to the south. Bean's Muth Glacier is an eastward-flowing glacier within the Unakwik Inlet drainage, draining into Jonah Bay. Both glaciers show signs of continuing retreat and thinning.

*Dartmouth Glacier.*—Dartmouth Glacier is a 3.5-km-long southwest-flowing unstudied valley glacier that has been retreating since it was first photographed in 1941. The 1941 terminus sits nearly 800 m behind a trimline that marks a major previous undated expansion of the glacier. Field (1975b) stated that, between 1941 and 1966, the terminus retreated about 750 m, an annual average rate of 30 m a<sup>-1</sup>. When the author photographed the terminus from the air in August 2000, it was approximately 1.3 km behind the 1966 terminus. During this 34-year interval, the average rate of retreat was around 38 m a<sup>-1</sup>. Between 1941 and 2000, the glacier retreated about 2.1 km, an average rate of retreat of about 35 m a<sup>-1</sup>.

### *Bathymetry of College Fiord*

Bean (1911) performed the first bathymetric survey of College Fiord in 1910. He found that the fjord walls were very steep both above and below the water line, that all spurs were truncated, and that water depths in the fjord ranged from 38 to 245 m, being approximately 194 m deep about 300 m from the 1910 face of Harvard Glacier, and 86 m deep about 540 m from Yale Glacier (Tarr and Martin, 1914, pl. CXXVI, ff p. 320). This shallowing of the water is now known to be the result of a submarine moraine at the grounded terminus of an advancing tidewater glacier, in conformance with the theory of tidewater glacier stability (Post, 1975) (fig. 42).

### *Glaciers of Yale Arm*

*Yale Glacier*.—Yale Glacier, an active calving tidewater glacier, sits at the head of Yale Arm. It originates in snowfields around Mount Witherspoon, which has a summit elevation of more than 3,500 m. In 2002, the terminus of Yale Glacier consisted of two parts—a southeastern tidewater calving terminus with an estimated 15- to 20-m-high ice face and an approximate width of 1 km and a land-based northwestern terminus about 1.2 km wide that lies within a basin of bedrock bosses and knobs that it previously covered. Yale Glacier has retreated nearly 8 km from its “Little Ice Age” maximum position adjacent to College Point at the southern end of Dora Keen Ridge, which separates Yale Arm from Harvard Arm.

In 1887, Yale Glacier was first mapped by Applegate (Davidson, 1904) from a location adjacent to Coghill Point. In late April 1898, it was visited and photographed by Mendenhall (see USGS Photo Library photograph Brooks 1114) and visited by Castner (Glenn, 1899). Castner walked over much of the terminus on snowshoes. That summer, the glacier was mapped again by Glenn (1899). In 1899, it was also observed by the Harriman Alaska Expedition (Tarr and Martin, 1914, pl. CXXI, ff p. 320) and mapped again by Gannett (Gannett, 1899; Gilbert, 1904). Detailed investigations were performed in 1905 and 1909 by Grant and Higgins (1910, 1911a, b, 1913) and by Martin (1913) and Bean (1911) in 1910. In 1910, field surveys were conducted under the direction of Martin for the NGS, with topography by W.B. Lewis and F.E. Williams and soundings by E.F. Bean (Tarr and Martin, 1914, pl. CXXII, ff p. 320). The resulting contour map, published by Tarr and Martin (1914), depicted the lower reaches of Yale, Downer, Lowell, Harvard, Eliot, Radcliffe, Baltimore, Smith, Bryn Mawr, Vassar, and Wellesley Glaciers. Not only did Martin's observations serve as the basis for his doctoral dissertation, but the map produced by his field party is also the first precise map made of the upper College Fjord region.

Glenn (1899, p. 19–20) described Yale Glacier and adjacent Harvard Glacier as follows:

The day was dry and clear. Directly in our front was the most imposing sight we had yet seen—I might add more imposing than any we saw during the season. Glistening in the sun were two large glaciers, which we named the “Twin Glaciers,” the pair being separated by a short ridge of hogback that runs down to salt water. In front of the one on our right (Yale) the sea ice extended for over three miles, while in front of the other (Harvard) this sea ice extended at least twice that distance. The ice was covered with snow several feet in depth. We soon discovered that it would bear up the weight of a man and that we could make no headway against it with the boat. Each of these glaciers is what is termed “live” or “working” glaciers. The front of each was an almost perpendicular mass of ice, from which immense pieces were constantly breaking off and falling into the sea with a great roaring noise, due principally to the action of the tides.

Cooper's (1942) observations of the area around the glacier in 1935 led him to conclude that Yale Glacier had been both thicker and longer quite recently. Development of alder (*Alnus* sp.) thickets about 200 m above the southeastern side of the glacier led Cooper to conclude that the terminus of Yale Glacier had previously reached the mouth of Yale Arm, about 3.2 km in front of its 1935 terminus. Twenty-two years later, Field (1975b) reported that Viereck, a member of the 1957 AGS field party, examined a trimline that he found on the northeastern side of the glacier. On the basis of dendrochronological information that he collected, he concluded that Yale Glacier had reached its most recent maximum position sometime 130 to 150 years before his study (between 1807 and 1827). He also concluded that no larger glacier advance had occurred since at least 1650.

The distance between this 1807–27 limit and the 1910 position of the terminus ranges from 3.5 to 5.0 km. The average rate of retreat during this interval ranges from a minimum of 34 m a<sup>-1</sup> to a maximum of 60 m a<sup>-1</sup>. Vegetative evidence indicates most of the 19th century retreat occurred before 1860. Grant and Higgins (1913, p. 29) stated that “The presence of a mature

alder thicket close to the ice front indicates that the glacier is now very near its maximum advance in a period of perhaps 50 or more years.”

Tarr and Martin (1914) presented evidence that the position of the terminus was relatively unchanged between 1899 and 1910. In 1910, Martin observed as much as 230 m of change in the position of the terminus, an indication that a strong advance was underway. In one location, Tarr and Martin (1914) reported that trees at least 33 years old were being overtopped. When Field (1932) visited Yale Glacier in 1931, he found evidence of a pre-1931 advance of as much as 400 m. Following a short period of retreat, Field (1937) noted that, by 1935, a maximum advance of about 60 m had occurred. On the basis of 1949 photography, Baird and Field (1951) concluded that, aside from thinning, the position of the terminus at most locations was similar to its 1935 position. The major exception was a recession of several hundred meters along the southeastern margin of the terminus.

In addition to using the 1949 photography, Field (1975b) compared aerial photographs of Yale Glacier made by the USAF in 1950, 1954, and 1957 and by the AGS in 1957 with field observations and photographs made by a group from Brigham Young University in 1961 and by the AGS in 1964, 1966, and 1971. He concluded that, between 1950 and 1957, the southern part of the glacier's terminus advanced from 50 to 150 m, so that “At the southeastern end, the 1957 terminus was within 50 m of its 1899 position” (Field, 1975b, p. 385). Retreat began quickly; between 200 and 450 m of retreat occurred between 1957 and 1961. By 1966, the terminus had retreated about 1,350 m, yielding an average annual retreat rate of about  $150 \text{ m a}^{-1}$ . Rapid retreat continued, and, by 1971, the terminus had retreated approximately 2.5 km from its 1957 location. By 1964, retreat had exposed a 2-km-long bedrock island, parts of which had been exposed previously as bedrock ledges in the 1899–1910 period.

Field (1975b) commented that, in 1964, the height of the iceface was measured at 112 m. In all of his observations, which at that time spanned a period approaching 40 years, he had not seen as high an ice face (nor has the author in more than 35 years of observations).

From an analysis of the same photographs and field observations, Field (1975b) reported that the recession of the northwestern part of the terminus was significantly slower than that of the active tidewater southeastern part; between 0.5 and 1.0 km of retreat occurred between 1910 and 1961. This part of the terminus entered tidewater until the 1940s. Between the 1940s and 1957, much of this margin retreated onto land. However, the USGS Anchorage A-2, 1:63,360-scale topographic quadrangle map (1960) (appendix B), which was based on 1957 photography, still shows the presence of a tidewater embayment on the northwestern margin of Yale Glacier.

Sturm and others (1991) summarized historic data on the retreat of Yale Glacier and provided new information about its retreat between 1974 and 1990. Their findings are based on aerial photography acquired in 1987, 1989, and 1990 and on a Landsat image acquired in 1985. They determined that, between 1974 and 1990, the southern side of the glacier retreated 2,070 m, and the northern side retreated 1,640 m. Hence, maximum retreat rates ranged from 103 to  $129 \text{ m a}^{-1}$ . Specifically, for the southern side, they measured 1,380 m of retreat between 1974 and 1978 (an average retreat of  $345 \text{ m a}^{-1}$ ), 260 m of retreat between 1978 and 1985 (an average retreat of  $37 \text{ m a}^{-1}$ ), 320 m of retreat between 1985 and 1987 (an average retreat of  $160 \text{ m a}^{-1}$ ), and 120 m of retreat between 1987 and 1990 (an average retreat of  $40 \text{ m a}^{-1}$ ). For the northern side, they measured 920 m of retreat between 1974 and 1978 (an average retreat of  $230 \text{ m a}^{-1}$ ), 280 m of retreat between 1978 and 1985 (an average retreat of  $40 \text{ m a}^{-1}$ ), 440 m of retreat between 1985 and 1987 (an average retreat of  $220 \text{ m a}^{-1}$ ), and no retreat between 1987 and 1990. Hence, at times, the retreat of the land-based northern part of the terminus exceeded the rate of retreat of the tidewater southern terminus.

The author has observed and photographed the glacier more than a dozen times between 1974 and 2004. During that period, the southeastern tidewater terminus has retreated between 2.7 and 3.1 km, and the northwestern grounded part of the terminus has retreated a maximum of about 2 km. This retreat has been accompanied by significant thinning of the entire terminus area. During the 26-year period between 1974 and 2000, including observations on 15 August 1978 (fig. 258), 13 August 1994 (oblique aerial photograph no. 94VE-88 by Austin Post, USGS), and 17 August 1999 (BLM photograph no. Yale GL.R3, FR-186), Yale Glacier retreated at an average annual rate that ranged between 74 m a<sup>-1</sup> (western side) and 110 m a<sup>-1</sup> (eastern side).

In the early 1990s (Viens, 1995) (table 2), Yale Glacier had a length of 32.2 km, an area of 194 km<sup>2</sup>, a width at its face of 1.0 km, and an AAR of 0.79. Its accumulation area was approximately 153 km<sup>2</sup>, and its ablation area was approximately 41 km<sup>2</sup>.

*Unnamed Glaciers of Yale Arm.*—On the southern side of Yale Arm opposite Dora Keen Ridge, several unnamed west- to north-flowing retreating hanging glaciers descend from the flanks of 1,687-m-high Mount Castner. Two unnamed glaciers were pre-20th century tributaries to Yale Glacier. A third unnamed glacier was still connected to Yale Glacier in 2001. A fourth unnamed glacier has retreated more than 1 km since being photographed in 1957.

#### *Glaciers of Harvard Arm*

*Harvard Glacier.*—Harvard Glacier, located at the head of Harvard Arm, is the second largest and second longest glacier in Prince William Sound. It is an active calving tidewater glacier with a face that is approximately 2.5 km wide. It is fed by more than 20 major tributaries that originate in snow- and ice fields on the flanks of some of the highest peaks of the Chugach Mountains, including 4,017-m-high Mount Marcus Baker, many unnamed summits, Mount Thor, Mount Gilbert Lewis, and Mount Elusive, all having summits higher than 3,500 m. In 2004, the terminus of Harvard Glacier, which has advanced nearly 3 km since first being photographed in the late 19th century, was advancing. Harvard Glacier has four present or former named tributaries: Downer and Lowell Glaciers on its eastern side and Radcliffe and Elliot Glaciers on its western side.

Like Yale Glacier, Harvard Glacier was first mapped from a distance by Applegate in 1887 (Davidson, 1904). Martin (1913) stated that this map and earlier maps are not detailed enough to determine pre-1887 changes. During July 1899, the glacier was observed by the Harriman Alaska Expedition and mapped again by Gannett (Gannett, 1899; Gilbert, 1904). Detailed investigations were performed in 1905 and 1909 by Grant and Higgins (1910, 1911a, b, 1913), and by Martin (1913), and Bean (1911) in 1910. Between 1899 and 1905, the glacier changed very little. However, during the next 4 years, an advance occurred that Grant and Higgins (1911a) reported as being from 400 to 800 m but that Martin (1913) reported as being only about 200 m. Between 1909 and 1910, the glacier advanced another 30 to 45 m. The contour map of upper College Fiord published by Tarr and Martin (1914) shows the relationship of Harvard Glacier and its southern tributaries (Downer, Lowell, Eliot, and Radcliffe Glaciers) and Baltimore Glacier.

Dora Keen visited and mapped the glacier's terminus position in 1914 and reported that the eastern side of the margin showed some recession, although the western side continued to advance (Keen, 1915a). Her observations were made as she attempted to be the first woman to traverse the western Chugach Mountains from south to north. Her route over the lower 26 km of Harvard Glacier (Keen, 1915b) permitted her to map and observe Harvard Glacier and many of its larger tributaries.

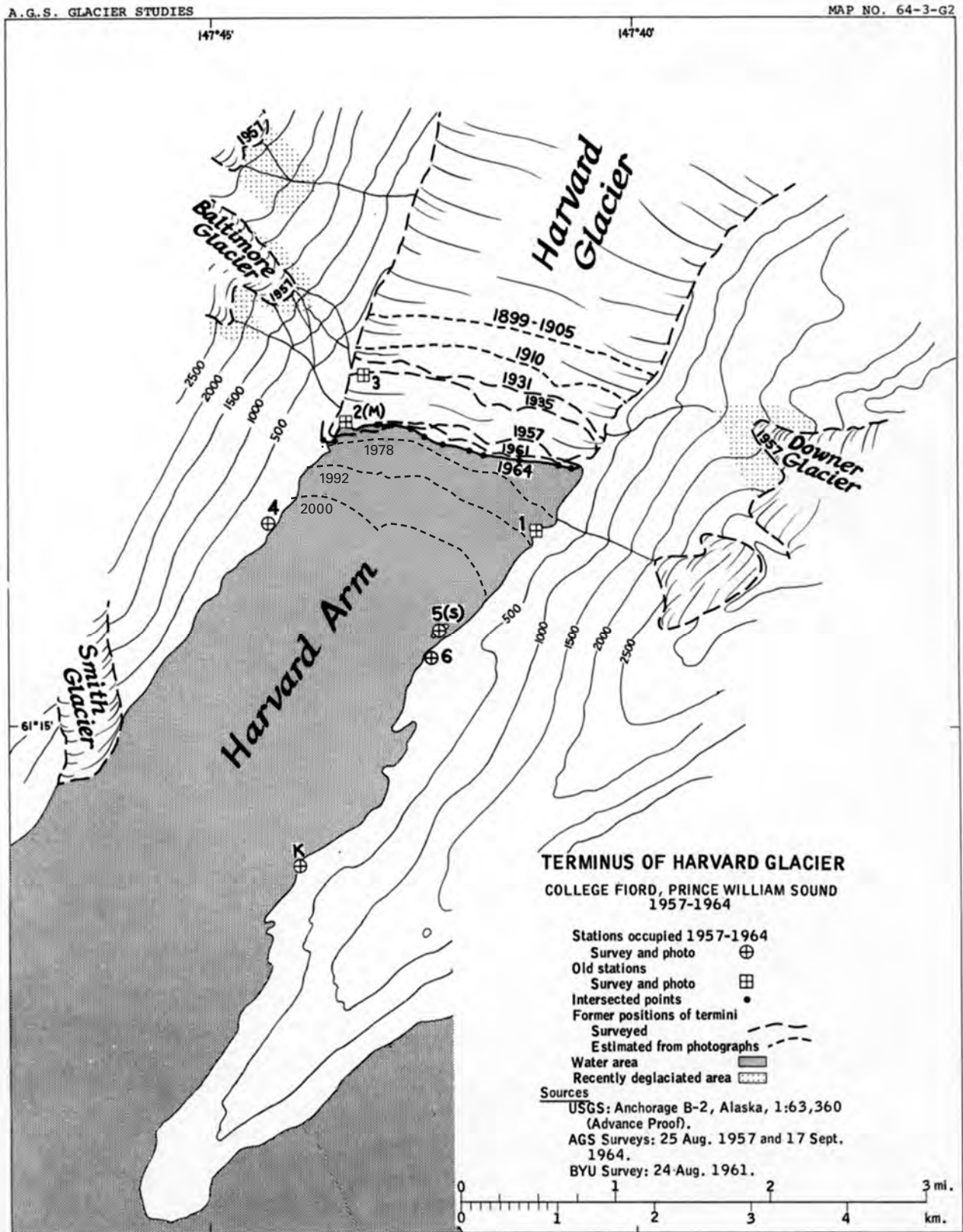
Field monitored changes in Harvard Glacier for more than 50 years. A map that he prepared showing positions of its terminus between 1899 and 1964 has been updated by the author to 2000 (fig. 259). Field first visited Harvard



**Figure 258.**—View of the retreating Yale Glacier on 15 August 1978. Northeast-looking view of ice extending to the right (east) edge of the photograph and newly emergent bedrock to the left of center. Photograph by Bruce F. Molnia, U.S. Geological Survey. A larger version of this figure is available online.

► **Figure 259.**—Map of Harvard Glacier showing fluctuations in the position of its terminus from 1899 to 2000. Base map is derived from AGS Glacier Studies Map no. 64-3-G2 (Field, 1965). Year 1978, 1992, and 2000 positions (approximate) are based on observations made by the author. Positions of the termini of Smith Glacier and several other glaciers are also shown.

Glacier in 1931 (Field, 1932, p. 378-379) and determined that, in comparison with its 1905 position, the terminus had advanced "at least 2000 feet (~610 m) at the eastern margin and somewhat less on the western." Field (1937) visited the glacier again in 1937 and determined that, between 1931 and 1937, the glacier had advanced another 30 to 60 m. A decade later and again in 1949, D.M. Brown (1952) visited the glacier and documented a continuing advance, although he did not quantify the amount of change.



Field (1975b) compared aerial photographs of the glacier made by the USAF in 1950, 1954, and 1957, and the USN in 1957, the C&GS in 1964, and Austin Post between 1960 and 1971 with field observations and photographs made by a group from Brigham Young University in 1961 and the AGS in 1957, 1964, 1966, and 1971. He concluded that, between 1899 and 1971, the terminus of Harvard Glacier advanced about 1.4 km and stated that this location is “its most advanced position since at least the seventeenth century” (Field, 1975b, v. 2, p. 388). Field based this conclusion on Cooper’s (1942) observation that, in 1935, the advancing terminus of the glacier was pushing into a forest of spruce trees (*Picea* sp.) having as many as 246 growth rings. Since then, the glacier has continued to advance. Additional aerial photographs have been acquired by many agencies, including the AHAP Program on 25 August 1978 (fig. 260) and the BLM in 1999 (see BLM vertical aerial photograph no. Harvard GL.R3, FR–208 acquired on 17 August 1999).

**Figure 260.**—25 August 1978 AHAP false-color infrared vertical aerial photograph of upper Harvard Arm and the Harvard Glacier. AHAP photograph no. L107F7037 from the GeoData Center, Geophysical Institute, University of Alaska, Fairbanks, Alaska.



Sturm and others (1991) summarized historical data on the changes in Harvard Glacier and provided new information about its advance during the second half of the 20th century. These new findings are based on data presented by Brown and others (1982) and Meier and Post (1987). Sturm and others (1991) determined that, between 1899 and 1989, the western side of the glacier advanced 1,520 m; the eastern side advanced 2,056 m. Hence, maximum long-term advance rates ranged from 16.9 to 22.9 m a<sup>-1</sup>. Specifically, for the western side, there was no change between 1899 and 1905, 270 m of advance between 1905 and 1910 (an average advance of 54 m a<sup>-1</sup>), 300 m of advance between 1910 and 1931 (an average advance of 14 m a<sup>-1</sup>), 100 m of advance between 1931 and 1935 (an average advance of 25 m a<sup>-1</sup>), 490 m of advance between 1935 and 1957 (an average advance of 22 m a<sup>-1</sup>), 170 m of advance between 1957 and 1961 (an average advance of 43 m a<sup>-1</sup>), 40 m of retreat between 1961 and 1964 (an average retreat of 13 m a<sup>-1</sup>), 80 m of advance between 1964 and 1976 (an average advance of 7 m a<sup>-1</sup>), no change between 1976 and 1978, and 150 m of advance between 1978 and 1989 (an average advance of 14 m a<sup>-1</sup>). For the eastern side, there was no change between 1899 and 1905, 370 m of advance between 1905 and 1910 (an average advance of 74 m a<sup>-1</sup>), 240 m of advance between 1910 and 1931 (an average advance of 11 m a<sup>-1</sup>), 160 m of advance between 1931 and 1935 (an average advance of 40 m a<sup>-1</sup>), 130 m of advance between 1935 and 1957 (an average advance of 6 m a<sup>-1</sup>), 320 m of advance between 1957 and 1961 (an average advance of 80 m a<sup>-1</sup>), 140 m of advance between 1961 and 1964 (an average retreat of 47 m a<sup>-1</sup>), 250 m of advance between 1964 and 1976 (an average advance of 21 m a<sup>-1</sup>), no change between 1976 and 1978, and 446 m of advance between 1978 and 1989 (an average advance of 41 m a<sup>-1</sup>).

The author has observed and photographed Harvard Glacier more than a dozen times between 1974, 14 August 1978 (fig. 261A), 31 August 2002 (fig. 261B), and 2004. During that period, the tidewater terminus has advanced about 1.0 km. This advance has been accompanied by some thinning along the entire margin of the terminus area. Hence, during the 27-year



**Figure 261.**—Two photographs showing details of the advancing Harvard Glacier. **A**, 14 August 1978 north-looking view shows the advancing terminus of Harvard Glacier and its two primary northwestern tributaries, Radcliffe and Elliot Glaciers. **B**, 31 August 2000 south-looking view from a point approximately 10 km north of the terminus of Harvard Glacier shows that the volume of ice delivered by the entering Radcliffe Glacier is sufficient to deflect the central medial moraine complex of Harvard Glacier to the east. Photographs by Bruce F. Molnia, U.S. Geological Survey. A larger version of B is available online.



period between 1974 and 2001, the glacier has advanced at an average annual rate of approximately  $37 \text{ m a}^{-1}$ . In the early 1990s (Viens, 1995) (tables 2, 3), Harvard Glacier had a length of 40 km, an area of  $524 \text{ km}^2$ , a width at its face of 2.4 km, and an AAR of 0.81. Its accumulation area was  $423 \text{ km}^2$ , and its ablation area was  $101 \text{ km}^2$ .

*Radcliffe Glacier.*—Radcliffe Glacier (fig. 260) is a primary tributary of Harvard Glacier that joins it from the west about 6 km above its terminus. It is composed of two principle east-flowing tributaries that coalesce about 2 km above its juncture with Harvard Glacier. When its ice was combined with the main trunk of Harvard Glacier, it made up approximately one-third of the width of the terminus in 2000. Since first being observed in the later part of the 19th century, Radcliffe Glacier has always been connected to Harvard Glacier.

Gilbert (1904, p. 84) described the 1899 relationship of Radcliffe Glacier to Harvard Glacier as follows: “The Radcliffe joins the Harvard so close to the water front that it does not become fully merged with the greater stream, but merely coalesces at one edge on its way to the sea. A conspicuous medial moraine of the Radcliffe maintains its high declivity quite to the water’s edge, and the cliff where the Radcliffe ends is notably lower than the confluent cliff along the front of the Harvard.”

The 1910 position of Radcliffe Glacier and its relationship to Harvard Glacier are shown on Tarr and Martin’s (1914, pl. CXXVI, ff p. 320) topographic map of glaciers in College Fiord. When Martin observed Radcliffe in 1910, it occupied a larger part of the face of Harvard Glacier than it did at the beginning of the 21st century. Tarr and Martin (1914, p. 298) stated that, “The position of the medial moraine formed by the north lateral moraine of the Radcliffe Glacier, indicates that in 1910 the Radcliffe was almost as strong as the main Harvard Glacier above the junction; for this medial moraine reaches the terminal cliff of Harvard Glacier nearly in the middle, showing that at least in the upper layers the ice from Radcliffe Glacier compresses the Harvard stream to half of its normal width.” When the author observed the glacier in September 2000, a recently exposed bare area along its northern margin was evidence of minor thinning. Otherwise, Radcliffe Glacier appeared to be an active and healthy glacier.

*Baltimore Glacier.*—Baltimore Glacier (fig. 260), a small retreating hanging glacier on the western side of Harvard Arm, just south of Radcliffe Glacier, was named by Grant and Higgins in 1908 for the Woman’s College of Baltimore, now Goucher College. Its 1910 position is shown on Tarr and Martin’s (1914, pl. CXXVI, ff p. 320) topographic map of glaciers in College Fiord. When Tarr and Martin observed it in July 1910, they described it as “a clean white ice mass, with no moraine except small medials near the terminus. Half a mile from the end it bifurcates, the north lobe being larger and ending lower (1,004 feet) than the south lobe. A barren zone about its terminus indicates that the glacier is less extensive than it was a few years ago....” (Tarr and Martin, 1914, p. 300).

Field (1975b) reported that a significant amount of retreat occurred during the period through 1931. However, between 1931 and 1935 (Field, 1937), the glacier advanced. From 1935 through 1938, it retreated. This retreat was followed by an advance between 1938 and 1941. Little change occurred through 1954. The glacier resumed its retreat through 1964. Field (1975b) reported no appreciable change between 1964 and 1971 and concluded that, during the 47-year-period 1910 through 1957, the glacier retreated between 500 and 600 m and thinned between 120 and 150 m. The average annual rate of retreat ranged from  $10.6$  to  $12.7 \text{ m a}^{-1}$ , whereas the average rate of thinning ranged from  $2.6$ – $3.2 \text{ m a}^{-1}$ .

Observations by the author were initiated in 1974 and have continued through 2004. During that 30-year-period, the terminus separated into a



number of fingerlike projections, retreated as much as 600 m, and thinned appreciably.

*Smith Glacier.*—Smith Glacier, an iceberg-calving tidewater glacier located about 2.5 km south of Harvard Glacier, has a length of 10 km (Field, 1975b, p. 471) (fig. 260). It was first described by the Harriman Alaska Expedition in 1899 (Gannett, 1899; Gilbert, 1904, p. 86), as follows: “Smith Glacier reaches the fiord three or four miles from the Radcliffe, and is of the same order of magnitude. Fed by several tributaries among the crests of the range, it gathers in a high mountain valley and then descends in magnificent cascades down the mountain front to the sea. In the last part of its course it has scarcely any valley, the outer surface of the ice being flush with the face of the mountain; and there is no flattening of its profile as it reaches the water.”

Through 1909, each margin of the glacier was marked by a narrow barren zone (Tarr and Martin, 1914). However, between 1909 and 1910, the glacier began to advance and widen. By July 1910, the barren zones had been overridden by advancing ice, which was pushing into the adjacent alders (*Alnus* sp.). The 1910 position is shown on Tarr and Martin’s (1914, pl. CXXVI, ff p. 320) topographic map of glaciers in College Fiord. Tarr and Martin described this advance as follows: “Along the advancing margin the alders were being destroyed in three ways, — by actual overriding of the spreading glacier, by stream encroachment, and by ice-block avalanches which rolled some distance out into the forest knocking down and breaking off shrubs and removing their bark 6 or 8 feet above the ground (Tarr and Martin, 1914, pl. CXVI, ff p. 320) [Editors’ note: a ground photograph taken on 22 July 1910]. It was impossible to tell exactly how much the tidal terminus of the glacier had moved forward since 1909 but there was undoubtedly several hundred feet of advance, accompanying the spreading on the north and south margins...” Tarr and Martin (1914, p. 301–302) observed “a flat tidal terminus extending a short distance out into the fiord, where Gilbert says there was none in 1899. The extreme southern edge of ice cliff was a black, crevassed precipice, the lateral moraine of 1899 having been pushed forward into the sea.”

Smith Glacier was next observed by Keen (1915a) in 1914. She reported no change from 1910. Field (1932) visited the glacier in 1931, and noted a significant amount of retreat. Upon his return in 1935, Field (1937) noted an increase in terminus activity. He later reported that, except for several minor fluctuations in the position of the terminus, “the glacier did not change appreciably from 1931 to 1971” (Field, 1975b, v. 2, p. 392). Observations by the author were made first in 1974, repeated on 15 August 1978 (fig. 262A) and 8 August 2000 (fig. 262B), and have continued through 2004. During that 30-year-period (1974–2004), the terminus has maintained a calving face in the fjord, but the barren zone along the margins of the glacier has increased significantly in width. The extent of the terminus in 2004 was larger than that of the terminus in 1910 and was at least 150 m more advanced than the terminus in 1899.

In the early 1990s (Viens, 1995) (tables 2, 3), Smith Glacier had a length of 9.7 km, an area of 20 km<sup>2</sup>, a width at its face of 400 m, and an AAR of 0.81. Its accumulation area was 16 km<sup>2</sup>, and its ablation area was 4 km<sup>2</sup>.

*Bryn Mawr Glacier.*—Bryn Mawr Glacier, an iceberg-calving tidewater glacier located about 2.5 km south of Smith Glacier, is 8 km long (Field, 1975b, p. 471) (fig. 260); it is formed by the joining of two eastward-flowing tributaries about equal in size. When the Harriman Alaska Expedition visited it in 1899, Bryn Mawr’s terminus reached tidewater. Gilbert (1904, p. 88) noted that it is somewhat larger than Smith Glacier. He described its tidewater terminus as follows: “As tide is reached, there is a tendency to flatten the profile, and the central portion of the stream becomes nearly or quite horizontal for a few hundred feet before breaking off in the terminal cliff.”

According to Grant and Higgins (1910, 1911a, b), little change occurred through 1905. By 1909, they noted that the glacier had advanced as much as



**Figure 262.**—Two photographs show changes of Smith Glacier during the last quarter of the 20th century and the beginning of the 21st century. Although Smith Glacier continues to maintain its tidewater terminus, it is clearly thinning and retreating. **A**, 15 August 1978 northwest-looking view of most of Smith Glacier. A trimline on the left and newly emergent bedrock at several locations document the recent thinning of the glacier. Its tidewater calving terminus is located close to its 20th century maximum position. **B**, 8 August 2000 northwest-looking oblique aerial photograph shows nearly all of Smith Glacier (left half of photograph). Emergent bedrock lies along much of the lower lateral margins of both sides of the glacier and at the southern side of its terminus. Note the difference in the position of the southern versus the northern part of the terminus. The northern part of the terminus has retreated several hundred meters since the 1970s; the southern part shows little change. The tidewater terminus of Harvard Glacier is on the right; Radcliffe Glacier is the large tributary glacier that merges with Harvard Glacier. Photographs by Bruce F. Molnia, U.S. Geological Survey. A larger version of B is available online.

150 m. Tarr and Martin (1914, p. 302–303) reported that, when they visited in 1910, the glacier was advancing: “On each side of the glacier a small stream emerges from the ice, and at the time of our visit the borders of the glacier were encroaching on these stream courses. All along its northern margin the Bryn Mawr Glacier was advancing into the forest, where it was killing spruces up to 5 inches in diameter, suggesting that the glacier had not been so large for a half century or thereabouts.” Bryn Mawr’s 1910 position is shown on Tarr and Martin’s (1914) topographic map of glaciers in College Fiord.

By 1931, Field (1932) reported that the glacier had retreated more than 450 m. Upon his return in 1935, he noted that the glacier had advanced and had spread laterally as much as 60 m (Field, 1937). Brown (1952, p. 43) reported that, by 1949, the glacier had readvanced and recovered the area lost before 1931: “Laterally, the tongue has elongated southward over six hundred feet and is tearing up trees with greater than fifty annual rings.” Field (1975b) again visited the glacier in 1957 as part of an AGS field party and measured about 100 m of retreat from the late 1940s maximum position. According to Field (1975b, v. 2, p. 393), the late 1940s advance “was the greatest on the southern margin since at least the 1860s.” Retreat continued until sometime between 1961 and 1964 (AGS Glacier Studies Map No. 64–3–G8) (Field, 1965). Between 1964 and 1971, the last observation reported by Field (1975b), the glacier underwent a small readvance. In summary, during the 72-year period between the observations of the Harriman Alaska Expedition in 1899 and 1971, the position of the terminus of Bryn Mawr Glacier



**Figure 263.**—8 August 2000 oblique aerial photograph shows bare bedrock along each lateral margin and the retreated central part of the terminus of Bryn Mawr Glacier. Photograph by Bruce F. Molnia, U.S. Geological Survey. A larger version of this figure is available online.



**Figure 264.**—15 June 1978 photograph shows the debris-covered terminus of Vassar Glacier and a large area of exposed bedrock in the middle of the glacier. Vassar Glacier shows evidence that it has thinned along each lateral margin and retreated, especially along the south side of its terminus. Photograph by Bruce F. Molnia, U.S. Geological Survey. A larger version of this figure is available online.

fluctuated as much as 575 m, reaching maxima in 1910–14 and again in 1949. By 1971, the glacier was again retreating, although it was still less than 50 m from its 1949 position.

Observations by the author were made first in 1974 and repeated on 8 August 2000 (fig. 263) and have continued through 2004. During the 30-year-period between 1974 and 2004, the terminus first advanced and then retreated. It has continued to maintain a calving face in the fjord, although bedrock is beginning to crop out at sea level along the face of the glacier. The position of the terminus in 2004 is less advanced than in 1978, and at least 250 m more retreated than that of the glacier in 1910. The position of the 1978 terminus is approximately the same as it was in 1949.

In the early 1990s (Viens, 1995) ( tables 2, 3), Bryn Mawr Glacier had a length of 7.6 km, an area of 26 km<sup>2</sup>, a width at its face of 900 m, and an AAR of 0.84; its accumulation area was 22 km<sup>2</sup>, and its ablation area was 4 km<sup>2</sup>.

*Vassar Glacier.*—Vassar Glacier was a tidewater glacier when it was first visited by the Harriman Alaska Expedition in 1899, but it is no longer. Gilbert (1904, p. 88) described it as a cascading glacier similar to Smith and Bryn Mawr Glaciers “but of smaller size and less direct in its course. It is cumbered, especially in its lower part, by rock debris, and close inspection was necessary to determine that it was actually tidal.” Early 20th century observations were made in 1905 and 1909 by Grant and Higgins (1910, 1911a, b, 1913) and by Martin in 1910 (Martin, 1913). Between 1899 and the summer of 1909, the glacier was ringed by a barren zone and showed very little change. However, by 21 July 1910, an advance was underway. Tarr and Martin (1914, p. 304) reported that, “At the time of our visit the glacier touched tidewater along the whole portion of the front between the flanking alluvial fans, but with a low, sloping moraine-veneered margin along the southern half, and with a low, dirty, nearly vertical cliff in the northern half... portions of the barren zone were covered. That on the north side near sea level was not completely overridden by July 21, 1910, but higher on the fiord wall it was almost covered... The southern edge of the glacier at sea level was also obviously advancing... Near sea level the glacier extended right up to the forest which included mature spruces.” The amount of the 1910 advance and its duration are unknown but the advance is estimated to be about 30 to 45 m. The contour map of upper College Fiord, published by Tarr and Martin (1914, pl. CXXVI, ff p. 320), shows the 1910 position and extent of Vassar Glacier.

Vassar Glacier was next observed by Keen (1915a) in 1914. She reported that the glacier was continuing to advance but did not quantify the amount of change from its 1910 position. Field (1932, 1937) visited the glacier in 1931 and again in 1935. He stated that changes from 1910 were not appreciable, but he was unable to make any quantitative comparison of change. However, he noted that between 1931 to 1935, there was evidence of shrinkage in the terminus area and of lateral expansion above the terminus.

Field (1975b) stated that the glacier was photographed in 1941 by the U.S. Army Air Forces and numerous additional times through 1968. He reported that during this period, “the moraine-covered terminal lobe has slowly diminished in volume and has shrunk in height and area since the turn of the century. This shrinkage is especially noticeable in a comparison of vertical aerial photographs taken between 1941 and 1968. Alders are steadily encroaching along the margins and on the moraine-covered, apparently stagnant, ice of the terminal lobe” (Field, 1975b, v. 2, p. 396).

Observations by the author were begun in 1974 and have continued through 2004. When the author observed Vassar Glacier on 15 June 1978 (fig. 264), vegetation was well established near the shoreline on the stagnant debris-covered terminus. It was impossible to tell if any ice remained in the terminus area. During the next 26 years, the width of the cascading lower portion of the glacier diminished by about 30 percent. In 2004, retreat and thinning were apparent along all of the bare-ice margins of the glacier.

*Wellesley Glacier.*—Wellesley Glacier, a tidewater glacier (fig. 41) situated at the head of a small inlet, has a terminus that is about 1 km wide. The inlet has water depths of 6 to 39 m. The shores of the inlet are composed of an undated older breached terminal moraine. Wellesley Glacier, then surrounded by a large barren zone, was first described by the Harriman Alaska Expedition in 1899 (Harriman, 1902). Gilbert (1904, p. 88) characterized it as flowing “with gentle grade through a mountain trough joining the fiord at right angles, and then cascades to the sea, into which it plunges without notable modification of profile. Beyond it are small glaciers occupying alcoves on the mountain front but ending far above the water.”

When Martin next visited in 1910 (Tarr and Martin, 1914), the position of the terminus was essentially unchanged from 1899. Its location is shown on their contour map of upper College Fiord. However, Tarr and Martin (1914, p. 305) presented several lines of evidence that an advance was underway: “Although at the time of our visit there was a very much larger barren zone around the glacier terminus than around any other ice tongue in College Fiord, it was then actively advancing, and the northern and southern margins had partly covered the lateral barren zone previously exposed.”

The glacier was next observed by Keen (1915a) in 1914, who reported that a slight recession had occurred from its 1910 position. Field (1932) visited the glacier in 1931 and found that the 1931 terminus position was advanced beyond the 1910 position. However, he described evidence suggesting that the glacier had first retreated before its advance. Between 1931 and 1935 (Field, 1937), there was evidence of lateral expansion above the terminus, but no evidence of change in the terminus region. Between 1935 and 1968, the glacier changed very little; it experienced a small advance between 1968 and 1971 (Field, 1975b).

The author began his observations in 1974 and continued them through 2004. When he first observed the southern margin of the glacier, it was surrounded by a large vegetation-free, barren bedrock area; the northern margin was composed of a broad area of stagnant, debris-covered ice. By 8 August 2000 (fig. 265), retreat and thinning were apparent along all margins of the glacier, and bedrock was exposed at several locations along its face.

In the early 1990s (Viens, 1995) (tables 2, 3), Wellesley Glacier had a length of 7.2 km, an area of 16 km<sup>2</sup>, a width at its face of 550 m, and an AAR of 0.78; its accumulation area was 12 km<sup>2</sup>, and its ablation area was 4 km<sup>2</sup>.

*Barnard Glacier.*—Barnard Glacier is one of the “small glaciers occupying alcoves on the mountain front but ending far above the water” mentioned by Gilbert (1904, p. 88). This hanging glacier had an extensive barren zone around its margin when first described, but an advance that began after 1899 and before 1910 reduced the size of the zone. Tarr and Martin (1914, p. 306) stated that Barnard Glacier, with two ice tongues, “has not descended much farther toward the fiord for a century or more; but a barren zone between the ice and forest, present in 1899 as well as in 1910, proves that it has been retreating in recent years. Between 1899 and 1910 there was an advance of the south lobe down the lip of the hanging valley, and a slight advance of the north lobe.... We are inclined to believe that the advance was still going on in 1910.” Keen (1915a) noted no change of the margin’s position in 1914. Between 1914 and 1937, when the glacier was photographed by Bradford Washburn, it had retreated. Retreat continued through Field’s (1975b) last data set, which was based on 1971 aerial photography. Field (1975b, p. 397) described this retreat as a “very considerable net recession of the terminus during that interval.”

The author began his observations in 1974 and continued them through 2004. During this 30-year period, the glacier has retreated and thinned significantly. The author’s initial observation of the perimeter of the glacier indicated that it was surrounded by a large vegetation-free, barren bedrock area and that an abandoned lateral moraine was developing a dense vegetative cover. In 2004, retreat and thinning were continuing along all margins of the glacier.



**Figure 265.**—8 August 2000 west-looking oblique aerial photograph shows the calving, retreating terminus of Wellesley Glacier. The debris-covered northern part of the terminus projects beyond the bare ice. Barren zones are visible along both sides of the glacier. Photograph by Bruce F. Molnia, U.S. Geological Survey. A larger version of this figure is available online.

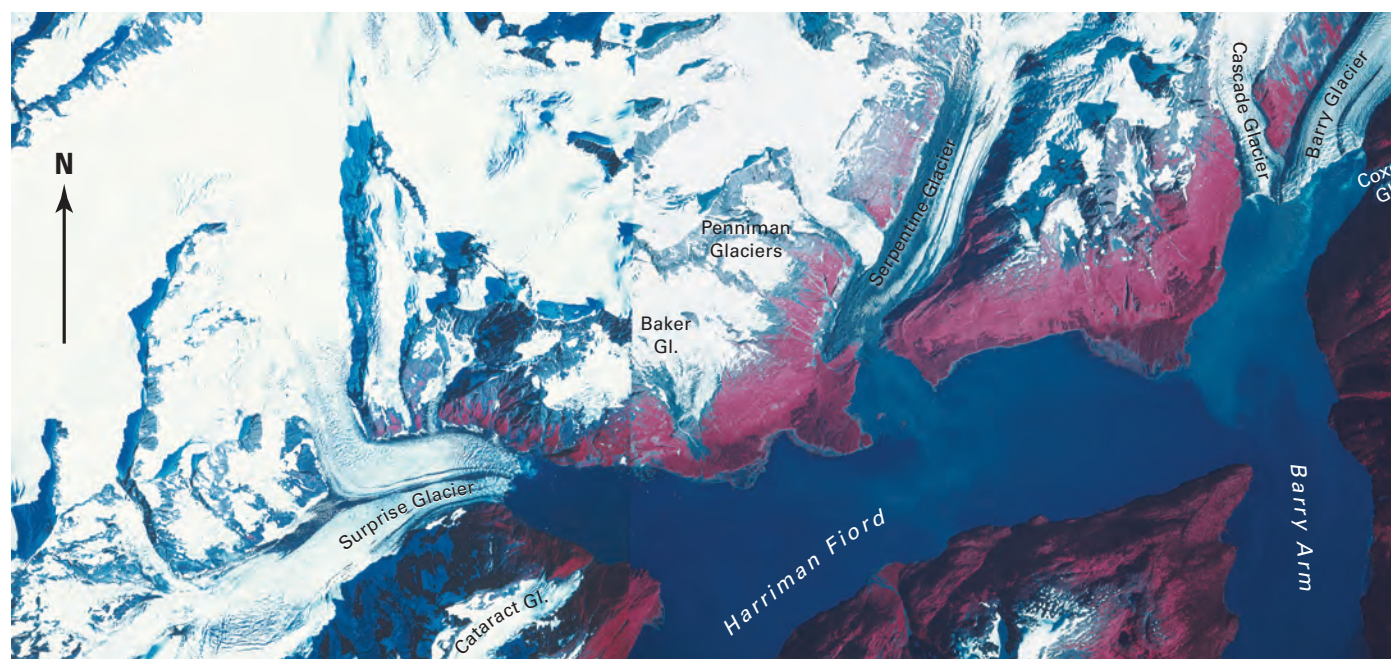
*Holyoke Glacier.*—Holyoke Glacier heads in a large cirque. In 1910, when the glacier was first described by Tarr and Martin (1914), it was fed by two tributaries and surrounded by a large barren zone. At that time, Tarr and Martin (1914, p. 306) reported that “No distinct signs of recent advance were seen.” By 1914, Keen (1915a) noted that an advance was underway. Field (1975b) reported that recession was underway in 1935 and that observations in 1957 and again in 1966 indicated that it was continuing. He reported that the glacier advanced more between 1966 and 1971. The author’s observations were initiated in 1974 and continued through 2004. During this 30-year period of observation, the glacier has retreated and thinned significantly. When the author first observed it, he noted no evidence of the advance underway in 1971. By 2001, the perimeter of the glacier was surrounded by a large vegetation-free, barren bedrock area and the glacier had separated into two distinct ice masses. Retreat and thinning were apparent along all margins of the glacier.

*Barry Arm and Harriman Fiord*

Barry Arm and Harriman Fiord (fig. 266) are connected fjords that comprise the northwestern extension of Port Wells. Between them, they host five tidewater glaciers—Barry, Coxe, Cascade, Surprise, and Harriman Glaciers (fig. 41)—and several former tidewater glaciers, including Serpentine (tables 2, 3) (Viens, 1995) and Cataract Glaciers. With the exception of Harriman Glacier, all of the glaciers in this area have long histories of 20th and early 21st century retreat. Before and including the 1899 visit by the Harriman Alaska Expedition, Barry Arm and the glaciers at its head were mapped with varying degrees of accuracy by Vancouver in 1794 (Vancouver, 1798), Applegate in 1887 (Davidson, 1904), Glenn (1899) in 1898, Castner (1899) in 1898, Mendenhall (1900) in 1898, and the Harriman Alaska Expedition in 1899 (Gannett, 1899; Gilbert, 1904; Tarr and Martin, 1914). Formally named Barry Arm Port Wells by Glenn in 1898 for Col. Thomas Barry, Assistant Adjutant General of the U.S. Army, Barry Arm is a 15-km-long fjord that extends from Barry Glacier at its northern end to Pakenham Point at its mouth.

When they were mapped at the end of the 19th century, three connected glaciers (from west to east)—Cascade, Barry, and Coxe Glaciers—were located at the head of Barry Arm. In 1899, when the Harriman Alaska Expedition explored Barry Arm, Barry Glacier was retreating from a recent, although undated, maximum position. At that time, its terminus extended

**Figure 266.**—24 August 1978 AHAP false-color infrared vertical aerial photographic mosaic of lower Harriman Fiord and Barry Arm. The positions of the termini of Cascade, Barry, Coxe, Surprise, Serpentine, Penniman, Baker, and Cataract Glaciers and several unnamed glaciers indicate that all have retreated since first observed in 1899. AHAP photograph nos. L109F6595 and L109F6597 from the GeoData Center, Geophysical Institute, University of Alaska, Fairbanks, Alaska.



a significant distance down the fjord, nearly completely closing what then was the unknown entrance to Harriman Fiord. When the *SS Elder* reached a location just to the south of the point now known as Point Doran, which juts into Barry Arm from the southwest, the local pilot felt it was no longer safe to pass and returned control of the ship to its captain, Peter Doran. The following description, presented by Muir in 1911 (Lethcoe, 1987, p. 86) summarized what followed:

Then Mr. Harriman asked me if I was satisfied with what I had seen and was ready to turn back, to which I replied: "Judging from the trends of this fiord and glacier, there must be a corresponding fiord or glacier to the southward, and although the ship has probably gone as far as it is safe to go, I wish you would have a boat lowered and let me take a look around that headland into the hidden half of the landscape." "We can perhaps run the ship there," he said and immediately ordered the captain to "go ahead and try to pass between the ice wall and the headland." The passage was dangerously narrow and threatening, but gradually opened into a magnificent icy fiord about twelve miles long, stretching away to the southward. The water continuing deep, as the soundline showed, Mr. Harriman quietly ordered the captain to go right ahead up the middle of the new fiord. "Full speed, sir?" inquired the captain. "Yes, full speed ahead," The sail up this majestic fiord in the evening sunshine, picturesquely varied glaciers coming successively to view, sweeping from high snowy foundations and discharging their thundering wave-raising icebergs, was, I think, the most exciting experience of the whole trip.

The result was the discovery that would become Harriman Fiord, an inlet previously unknown to all but possibly indigenous seal hunters.

#### *Glaciers of Barry Arm*

*Barry Glacier.*—Tarr and Martin (1914, p. 321–322) presented the following compilation of early descriptions of Barry Glacier:

Mendenhall relates that in 1898 Barry Glacier was more extensive than either Harvard or Yale Glaciers. Glenn ... said that it was "one of the most formidable as well as the most interesting" of the glaciers that they saw. Coming from it they saw "immense icebergs that had evidently broken off from the glacier. Many of these were from ten to twenty times as large as our boat." When they were near Yale Glacier ... a "noise caused by the falling of the immense ice floes from Barry Glacier, could be heard like the rumbling of distant thunder and which seemed to shake the mountains on either side of us." In May 1898, Castner went up Barry Arm to "within a half mile of the sea end of the great glacier." Photographs were taken and the interesting manufacture of icebergs watched. The later consisted of a breaking off and tumbling into the sea of tons of blue ice from the face of the glacier, accompanied by the roar of a Niagara, as the berg started on its ocean voyage, eventually to melt and become a part of the tides which now carried it away.

Some confusion exists about where the terminus of Barry Glacier was located during the later part of the 19th century and about its behavior. Applegate's 1887 sketch map of Port Wells shows a glacier with two tributaries filling the entire width of the fjord at a location about 10 km north of Pakenham Point but no evidence of an entrance to Harriman Fiord.

The NGS's expedition to Alaska mapped Barry Glacier in 1910 (fig. 267). An arcuate shallow moraine located north of and within 250 m of Point Doran was mapped by Grant and Higgins (1911a, fig. 7) and by Bean (1911) in 1910. It has shoaling depths as shallow as 5.5 m and spans the width of the fjord. Although its age is unknown, it is probably the "Little Ice Age" maximum terminal moraine of an expanded Barry Glacier. Whether Applegate's mapped terminus position for Barry Glacier and the location of this submarine moraine are coincident is unknown. However, given the geometry of the fjord and the distance from which he observed its head, he could have easily erred in depicting the length of the fjord and the actual 1887 location of the terminus of Barry Glacier.

When the Harriman Alaska Expedition visited Barry Glacier on 26 June 1899, it did not observe the discharge of large icebergs or hear the thunderous noises described the previous year. Gannett's 1899 map of Barry Glacier shows its terminus about 1 km north of Point Doran. Gannett (1899) used the name *Washington Glacier*, although it was not officially adopted. At the same time, C. Hart Merriam of the U.S. Biological Survey photographed the glacier, and Gilbert (1904) described a barren zone on the eastern margin of



**BARRY GLACIER**  
**AND ADJACENT ICE TONGUES IN HARRIMAN FIORD**  
**PRINCE WILLIAM SOUND, ALASKA**

MAPPED BY  
**NATIONAL GEOGRAPHIC SOCIETY'S ALASKAN EXPEDITION**  
**OF 1910. LAWRENCE MARTIN, IN CHARGE**

Contour interval, 100 feet  
 Elevations in feet  
 Soundings in fathoms  
 Photographic Stations □ or A, B, etc.  
 Boundaries of barren zone  
 dotted -----

Topography by  
**W. B. LEWIS**  
 Assisted by  
**F. E. WILLIAMS**  
 Soundings by  
**E. F. BEAN**

**Figure 267.**—Map of Harriman Fiord and Barry Arm showing the position of the combined termini of Cascade, Barry, and Coxe Glaciers as mapped by the National Geographic Society's 1910 Expedition (Martin, 1911; Tarr and Martin 1914). Soundings (in fathoms) were performed by E.F. Bean.

Barry Glacier that he suggested was evidence that retreat from a recent, earlier maximum position was already underway. Grant and Paige visited Barry Glacier in 1905; Grant and Higgins (1913) visited in 1910. All noted that Barry Glacier was still connected to Coxe and Cascade Glaciers but that, in the decade between 1899 and 1909, it had retreated approximately 2.6 km. The face of the combined glacier was about 75 m high in 1905 and in 1908 but had diminished to only about 37.5 m in 1909. The height of the exposed barren zone along the margin of the glacier was approximately 120 m, indicative of

an average rate of retreat of about 260 m a<sup>-1</sup> and an average rate of thinning of about 12 m a<sup>-1</sup>. Tarr and Martin (1914) described a large ice mass that had detached from the retreating glacier and was left stranded on the eastern wall of the fjord in 1910. They described its size as being 400×200 m and extending to elevations of 75 to 85 m. The detached ice mass was located more than 3 km from the face of Barry Glacier in 1910.

A summary of Barry Glacier's behavior through 25 July 1910 was presented by Tarr and Martin (1914): (1) Before Whidbey's 8 June 1794 visit, unknown; (2) 8 June 1794 until Applegate's visit in June 1887, unknown; (3) June 1887 until Castner's visit on 6 May 1898, unknown amount of advance; (4) 6 May 1898 until the Harriman Alaska Expedition on 26 June 1899, retreat of approximately 805 to 1,210 m; (5) 26 June 1899 until Grant and Paige's visit on 20 August 1905, retreat of about 1,930 m; (6) 5 August 1905 until Grant's visit of 20 August 1908, retreat of about 650 m; (7) 11 August 1908 until Grant and Higgins' 29 June 1909 visit, retreat of about 805 m; and (8) 29 June 1909 until Martin's 25 July 1910 visit, retreat of about 150 to 300 m. Hence, in the 3,733 days (10.2 years) between 6 May 1898 and 25 July 1910, Barry Glacier retreated between 4,304 and 4,895 m (as much as 1.3 m d<sup>-1</sup> or nearly 480 m a<sup>-1</sup>).

Bertrand Johnson, a USGS geologist, visited Barry Arm in 1913 and again in 1914 (Johnson, 1917). He noted the continuing retreat of Barry Glacier and the separation of Coxe Glacier from Barry in 1913. Between 1910 and 1913, ongoing retreat of the eastern side of Barry Glacier amounted to about 2 km; on the western side, it was about 750 m. Along the retreating western margin, bedrock was exposed at the base of the ice for the first time. By 1914, the eastern part of the terminus had retreated another 500 m.

In the ensuing 90 years, the glacier has been observed, monitored, and photographed many times. Individuals providing information about Barry Glacier include Keen in 1914 (Keen, 1915a) and again in 1925; Field in 1931 (Field, 1932); Field and Cooper in 1935 (Field, 1937; Cooper, 1942); Robert E. Fellows of the USGS in 1943 (Field, 1975b); and Brown in 1947 and again in 1949 (Brown, 1952). Barry Glacier was photographed by Bradford Washburn in 1937 and 1938, the U.S. Army Air Forces in 1941 and 1942, the USAF in 1950 and 1957, the USN in 1957, Austin Post between 1960 and 1983, and Robert M. Krimmel between 1984 and 1990, among others. These observations document that Barry Glacier had a small advance between 1925 and 1931, advanced more in 1935 and 1937, retreated between 1938 and 1943, and changed little through 1947. A slight recession occurred during the 1950s, followed by an advance beginning about 1961. Since then, the location of the western part of Barry's terminus has remained within a few hundred meters of its 1914 location; the eastern part of the margin has retreated several hundred meters, as two oblique aerial photographs taken by the author on 8 August 1981 (fig. 268A) and 8 August 2000 (fig. 268B) show; the entire glacier has continued to thin.

Although the amount of exposed bedrock has fluctuated substantially (Lethcoe, 1987), at no time has it been reported that the glacier has retreated above sea level. The author has noted substantial exposures of bedrock along the base of the glacier several times. In September 2000, two small bedrock outcrops were noted near the central face of the terminus.

In the early 1990s (Viens, 1995) (tables 2, 3), Barry Glacier had a length of 26.5 km, an area of 95 km<sup>2</sup>, a width at its face of 2.2 km, and an AAR of 0.74; its accumulation area was 70 km<sup>2</sup>, and its ablation area was 25 km<sup>2</sup>.

*Coxe Glacier.*—Coxe Glacier separated from the retreating Barry Glacier in 1913. Between 1913 and the late 1930s, it retreated about 2.5 km; its terminus retreated into its fjord, where it maintained a tidewater terminus (figs. 41, 266). Since then, its terminus has fluctuated: a small advance in the 1941–49 period (Brown, 1952), a period of retreat between 1952 and 1957 (Field, 1975b), and a small advance between 1979 and the late 1980s

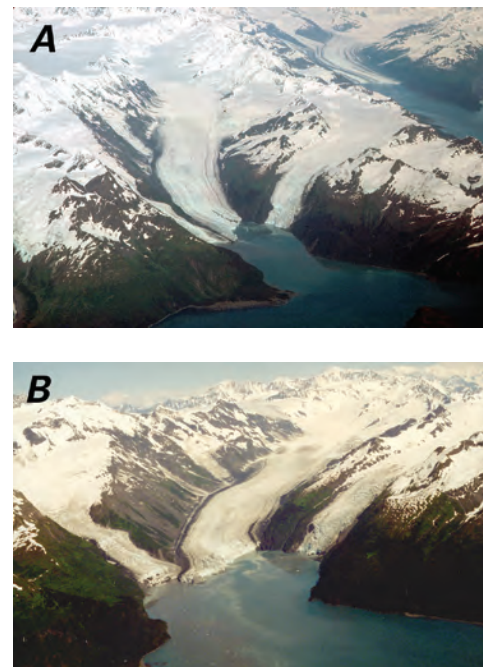


**Figure 268.**—Two north-looking oblique aerial photographs showing changes in Cascade (left), Barry (center), and Coxe (right) Glaciers between 1981 and 2000. **A**, 8 August 1981 photograph shows the tidewater calving termini of all three glaciers and much of their accumulation areas. The most extended part of the combined Barry and Cascade Glaciers is the central part of their combined termini. Harvard Glacier can be seen in the distance. **B**, 8 August 2000 photograph shows the tidewater calving termini of all three glaciers and much of their areas of accumulation. The continued retreat and thinning of Cascade Glacier has exposed bedrock along the western part of its terminus. It is thinner than Barry Glacier at their junction. The east side of Barry Glacier retreated several hundred meters since an earlier visit by the author in 1992. Coxe Glacier also thinned and retreated. Photographs by Bruce F. Molnia, U.S. Geological Survey. Larger versions of these figures are available online.



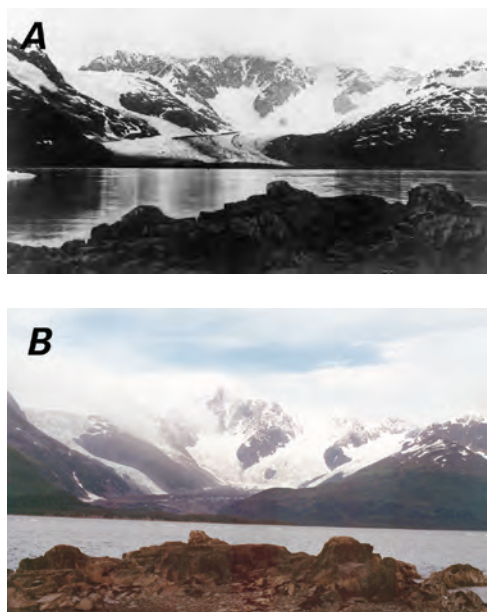


**Figure 269.**—A pair of photographs taken from the east shore of Harriman Fiord show changes in Serpentine Glacier between 1899 and 2000. **A**, 1899 Harriman Alaska Expedition photograph (Harriman, 1902) by Edward Curtis from the east shore of Harriman Fiord shows most of the terminus and source area of Serpentine Glacier. The dark area at the foot of the glacier is an older terminal moraine, dating from circa 1800, that forms much of the entrance to the inlet in front of Serpentine Glacier. **B**, 6 September 2000 photograph from the same vantage point shows that Serpentine Glacier has thinned by approximately 70 to 100 m and has retreated approximately 2.5 km. The terminus is now debris covered and barely visible above the terminal moraine. Photograph by Bruce F. Molnia, U.S. Geological Survey. Larger versions of these figures are available online.

(Lethcoe, 1987). During the past 17 years, the terminus has retreated slightly but maintained some contact with tidewater. During the second half of the 20th century, Coxe Glacier has thinned significantly and narrowed appreciably, producing wide bedrock exposures along both lateral margins of the glacier. When the author visited the glacier on 5 September 2000, bedrock was exposed along the base of the entire southern half of the terminus and at the northernmost edge of the terminus at the base of the glacier. In the early 1990s (Viens, 1995) (tables 2, 3), Coxe Glacier had a length of 11 km, an area of 20 km<sup>2</sup>, a width at its face of 1.1 km, and an AAR of 0.74. Its accumulation area was 15 km<sup>2</sup>, and its ablation area was 5 km<sup>2</sup>.

**Cascade Glacier.**—Cascade Glacier is a steep south-flowing valley glacier that joins the western edge of Barry Glacier at tidewater (figs. 41, 266, 267, 268). During the last few years of the 20th century the two glaciers barely touched. At the beginning of the 20th century, Cascade Glacier was the westernmost tributary to the extended Barry Glacier. By 1913 (Johnson, 1917), Cascade Glacier had become independent from the rapidly shrinking Barry Glacier, although it still made contact with its western margin. At times, retreat of the terminus of Cascade Glacier exposes a large bedrock area just above sea level. During much of the 20th century, fluctuations in the glacier's margin have covered and uncovered this bedrock. Field (1975b) reported that bedrock exposed in the middle 1930s was covered by a minor advance that continued through about 1950 and was followed by recession through 1957. An advance that began in 1968 resulted in the tidewater terminus of Cascade Glacier pushing into Barry Glacier in 1971. In both 1981 (fig. 268) and 1992, when the author visited the eastern margin of Cascade Glacier at its junction with Barry Glacier, it was the most extended part of the terminus. At the start of the 21st century, Barry and Cascade Glaciers remained barely connected. In the early 1990s (Viens, 1995) (tables 2, 3), Cascade Glacier had a length of 8 km, an area of 15 km<sup>2</sup>, a width at its face of 600 m, and an AAR of 0.89; its accumulation area was 14 km<sup>2</sup>, and its ablation area was 2 km<sup>2</sup>.

#### *Glaciers of Harriman Fiord*

Harriman Fiord contains more than a dozen glaciers. The largest and longest is Harriman Glacier at its head. With the exception of Harriman Glacier, all of the glaciers in the fjord have retreated since first being observed.

**Serpentine Glacier.**—In the early 1990s, Serpentine Glacier had a length of 10 km, an area of 30 km<sup>2</sup>, and an AAR of 0.70; its accumulation area was 21 km<sup>2</sup> and its ablation area was 9 km<sup>2</sup> (Viens, 1995) (tables 2, 3). In 1899, when the glacier was first photographed by Curtis (fig. 269A) and described by Gilbert (1904), it was tidal, although much of its margin was fronted by a developing moraine. Gilbert (1904, p. 93) described the glacier as follows: "It is a broad stream, of low grade, fed by four or five tributaries descending steeply from amphitheaters in the encircling mountains. Though it reaches the sea, it yields few bergs, but is building a moraine barrier along most of its front...." When the author visited on 6 September 2000 (fig. 269B), the northern part of the terminus was surrounded by a subcircular-shaped outwash plain about 500 m in diameter; the southern part of the terminus was fronted by a vegetated ridge composed of ablation till and moraine.

Following the Harriman Alaska Expedition's visit in 1899 (Harriman, 1902), Serpentine Glacier was observed in 1905 and again in 1909 by Grant and Higgins (1910, 1911a, b, 1913), and by Martin and the NGS party, who produced a map of its terminus in 1910 (Tarr and Martin, 1914, fig. 45, p. 327). Their studies showed that, in 1910, the terminus of Serpentine Glacier was situated at the head of a 1.6-km-long inlet bounded at its junction with the main part of Harriman Fiord by a breached lobate terminal moraine approximately 2.5 km long. On the basis of dendrochronological evidence, Martin recognized that this terminal moraine consisted of two separate nested moraines that

he concluded were formed by advances in the early 1800s and again in about 1870. Grant and Higgins (1913) observed little change in the terminus position from 1899 until their first visit in 1905 and about 400 m of terminus retreat between 1905 and 1909. Piecing this information together suggests that the glacier reached a maximum—perhaps its “Little Ice Age” maximum—about 1800. For the next 70 years, its position may have fluctuated, but, in 1870, its terminus was near the 1800 maximum. By 1900, the glacier had retreated about 1.2 km, with an average retreat rate of about 40 m a<sup>-1</sup>. From 1900 until 1905, the position of the terminus of Serpentine Glacier was stable. Approximately 400 m of retreat followed between 1905 and 1909, with an average retreat rate of about 100 m a<sup>-1</sup>. Little change was observed in 1910.

Keen (1915a) visited the glacier in 1914 and found no changes from Martin’s 1910 position. Field (1932) observed the glacier in 1931 and noted a recession of about 400 m from its 1910–14 position. Field and Cooper visited in 1935 (Field, 1937) and noted a slight advance since 1931. Bradford Washburn’s 1938 photograph of the terminus showed a continuation of this advance. U.S. Army Air Forces photographs taken in 1941 show the glacier retreating but close to its 1931 position. When Brown visited in 1947 and again in 1949 (Brown, 1952), Serpentine Glacier was advancing. A comparison of an aerial photograph acquired by the USAF in 1950 with the 1941 photograph shows that the terminus was between 200 and 300 m forward of the 1941 position. Between 1957, when it was photographed by the USN, and 1971, when it was photographed by the USGS, the glacier had retreated, although it was less than 50 m. A comparison of the USGS 1960 Anchorage A-4 1:63,360-scale topographic quadrangle map (appendix B), which was based on the 1957 photography, with oblique aerial photographs taken by the author on 8 August 2000 (fig. 270) shows that the lower part of the glacier has retreated approximately 400 m and is now covered by a thick brown-and-black debris cover. The northern perimeter of the glacier consists of stagnant ice-cored moraine.

Compilation and analysis of this information suggests that, between 1910 and 2000, Serpentine Glacier retreated and thinned significantly and that its stagnating debris-covered terminus was located about 2.1 km behind the moraine marking the “Little Ice Age” maximum position. From 1900 until 1914, there was no change in the position of the terminus of Serpentine Glacier. This period of stability was followed by about 400 m of retreat, beginning after 1914 and lasting until 1931, with a minimum average retreat rate of about 23.5 m a<sup>-1</sup>. Little change was observed between 1931 and 1941. By 1950, the



**Figure 270.**—8 August 2000 oblique aerial photograph of Serpentine Glacier. The lower 4 km of the glacier is mantled by thick debris. Note that the terminus of Serpentine Glacier is fronted by a outwash plain fan delta and is no longer at tidewater. Note also that, of the glaciers visible above the terminus, only the northernmost on the right, an unnamed tributary glacier, makes contact with Serpentine Glacier. Photograph by Bruce F. Molnia, U.S. Geological Survey.



**Figure 271.**—Two northwest-looking views showing changes in Baker and Detached Glaciers between 1909 and 2000. **A**, 1909 photograph by Grant and Higgins shows Baker Glacier (right) and Detached Glacier (left). Baker Glacier descends to near sea level, but Detached Glacier terminates at approximately 300 m above sea level. (Published as Plate XXI A, Grant and Higgins, 1913.) **B**, 6 September 2000 photographic mosaic from nearly the same vantage point as A shows the changes that occurred in both glaciers during the 91 years between photographs. Baker Glacier thinned everywhere and retreated a maximum of more than 1 km. Although Detached Glacier has not retreated as much, it also thinned significantly. Photographic mosaic by Bruce F. Molnia, U.S. Geological Survey. Larger versions of these figures are available online.

terminus of Serpentine Glacier had advanced between 200 and 300 m, yielding an average advance rate of between about 22 and 33 m a<sup>-1</sup>. Little change was observed between 1950 and 1957. From 1957 until 1971, the glacier's terminus position retreated minimally, with an average retreat rate of about 7 m a<sup>-1</sup> (AGS Glacier Studies Map No. 64-3-G9) (Field, 1965). From 1971 until 2000, the terminus of Serpentine Glacier retreated about 400 m, and ice became stagnant along most of its terminus area. The average rate of retreat during the latter part of the 20th century was about 14 m a<sup>-1</sup>.

*Penniman Glaciers, Baker Glacier, and Detached Glacier.*—The Penniman Glaciers, Baker Glacier, and Detached Glacier are all small cirque and hanging glaciers on the eastern and southern flanks of Mount Muir. All have retreated significantly during the 20th century. Baker and Detached Glaciers were investigated and photographed by many scientists, including the Harriman Alaska Expedition in 1899 and Grant and Higgins in 1905 and 1909 (fig. 271A) (Grant and Higgins, 1910, 1911a, b, 1913, pl. XXIA), described and mapped by Martin and the NGS party in 1910 (Tarr and Martin, 1914), and photographed by the author on 6 September 2000 (fig. 271B).

The two Penniman Glaciers were named and described in 1914 by Keen (1915a). Since 1914, both have retreated as much as 700 m, with most of the retreat coming at the end of the 20th century. Field (1975b) reported that, between 1914 and 1931, the glaciers experienced a small retreat. Between 1931 and 1935, they advanced slightly. A significant, although not quantified, retreat occurred through 1961, with little change through 1971. During the 30 years since being first observed by the author in 1974, the glaciers have retreated about 500 m.

Martin investigated a large end moraine located adjacent to the shoreline below Baker Glacier (Tarr and Martin, 1914, fig. 47, p. 332). He discovered that some time between the end of the 18th century and the early part of the 19th century, an expanded Baker Glacier reached the shore of Harriman Fiord with a bulb-shaped terminus that was approximately 800 m in diameter. Between the time of the early 18th century maximum and 1910, the glacier had retreated about 400 to 500 m. Since then, Baker Glacier has retreated as much as 1.2 km. However, there have been several intervals of significant advance. Between 1910 and 1914 (Keen, 1915a), Baker Glacier advanced about 300 m to the foreland at the base of Mount Muir. By 1925, when Keen again visited the glacier, a substantial retreat was underway. When the glacier was next observed in 1931 and 1935 by Field (1932, 1937), it was again advancing. Between 1931 and 1935, this advance was as much as 50 to 60 m. Between 1935 and 1949, there was minimal change (Field, 1948; Baird and Field, 1951). Field (1975b) reported that, between 1949 and 1964, there was some recession, followed by a period of no appreciable change through 1971. During the author's 30-year period of observation from 1974 to 2004, Baker Glacier has retreated about 700 m.

Similarly, at the end of the 20th century, Detached Glacier was rapidly retreating. Grant and Higgins (1913) described a barren zone present in 1905 and 1909 below the hanging terminus of the glacier, which they interpreted to indicate that Detached Glacier was recently much larger and was connected to an extended and larger Surprise Glacier. Martin, who visited the glacier in 1910, found no evidence of change since the 1899 visit of the Harriman Alaska Expedition (Tarr and Martin, 1914). Similarly, Keen (1915a) saw no evidence of change through 1914. A significant amount of retreat occurred through 1931, followed by about 30 m of advance between 1931 and 1935 (Field, 1937). By 1957, the glacier was approximately 1.5 km long, and about 200 m of the lower hanging tongue of the glacier had disappeared. Field (1975b) reported that, between 1957 and 1961, there was some recession, followed by a decade of no appreciable change through 1971. During the author's 30 years of observation, from 1974 to 2004, Detached Glacier has retreated about 500 m.

*Surprise Glacier.*—Surprise Glacier, located at the head of Surprise Inlet, is so named because it was the first glacier the Harriman Alaska Expedition saw when it entered Harriman Fiord. The Harriman Alaska Expedition photographed the glacier's tidewater terminus and much of its lower reaches from a distance, and Gannett (Gilbert, 1904) prepared a map showing its terminus position but did not conduct any detailed examination of its margin. A detailed analysis, however, was first accomplished in 1905 and again in 1909 by Grant and Higgins (1913). They noted a large barren zone extending about 160 m beyond Surprise Glacier's 1899 terminus position, suggesting that the glacier was in retreat when Gannett had mapped it. Grant and Higgins (1913) noted that the retreat was continuing in 1905 and that, by 1909, the total recession was about 1.8 km. Bedrock began to appear at the base of the southern part of the margin at that time.

By the time Martin visited the glacier in 1909 (Tarr and Martin, 1914), retreat totaled 2 km. Martin also noted vegetation-free marginal zones up to 90 m wide above the location of the 1909 terminus. Field (1932) reported that little change had occurred in the terminus position through 1931. But when Field (1937) observed the glacier in 1935, a slight advance had taken place. Minor fluctuations occurred, with both short periods of advance and retreat noted through 1971.

The author made several observations of the glacier between 1974 and 2004. During this 30-year period, the terminus retreated about 300 m, thinned, and narrowed, as an 8 August 2000 oblique aerial photograph taken by the author shows (fig. 272). A small bedrock outcrop began to become visible at the base of Surprise Glacier along its southern side, and several tributaries thinned, retreated, and even lost contact with the main glacier. In the early 1990s, Surprise Glacier had a length of 12.1 km, an area of 80 km<sup>2</sup>, a width at its face of 1.2 km, and an AAR of 0.80; its accumulation area was 64 km<sup>2</sup>, and its ablation area was 16 km<sup>2</sup> (Viens, 1995) (tables 2, 3). Stairway Glacier is the name that the Harriman Alaska Expedition gave to the large southeast-flowing tributary that contributes a substantial amount of ice to the northern side of the trunk of Surprise Glacier. Part of Surprise Glacier and all of the glaciers in the northern half of Harriman Fiord are shown in figure 266, a 24 August 1978 AHAP false-color infrared vertical aerial photograph.

*Cataract Glacier.*—Cataract Glacier, a 2.5-km-long northeast-flowing hanging glacier that drains into the southern side of Surprise Inlet, had a tidewater terminus that was in contact with Surprise Glacier when it was first observed by the Harriman Alaska Expedition in 1899. Grant and Higgins (1913) visited the glacier in 1905 and 1909, photographing it in 1909



**Figure 272.**—8 August 2000 northwest-looking oblique aerial photograph shows Surprise Inlet and Surprise and Cataract Glaciers. Cataract Glacier (far left), which had a tidewater terminus in 1910, retreated approximately 600 m. Photograph by Bruce F. Molnia, U.S. Geological Survey.



**Figure 273.**—Two southwest-looking photographs showing changes at Cataract Glacier during the 91-year period from 1909 to 2000. **A**, 1909 photograph by Grant and Higgins shows the terminus of Cataract Glacier reaching tidewater, although some bedrock is exposed at sea level (Grant and Higgins, 1913). **B**, 6 September 2000 view of Cataract Glacier shows that its terminus retreated approximately 700 m and is now located more than 200 m above sea level. Exposed bedrock completely surrounds the ice margin. Photograph by Bruce F. Molnia, U.S. Geological Survey. Larger versions of these figures are available online.

(fig. 273A). They noted that it experienced no appreciable change through 1909. They described “a narrow bare zone along the west side of the glacier, but the extent to which the shrubs have encroached upon this zone indicates that the ice stream has not in recent years (perhaps 25 years) been much larger than at present” (Grant and Higgins, 1913, p. 37).

Cataract Glacier was advancing and overriding shrubs and willows (*Salix* sp.) along the margin when Martin visited the glacier in 1910 (Tarr and Martin, 1914). In 1914, Keen (1915a) visited the glacier and observed that the terminus of the glacier had not changed its position since Martin’s visit. Eleven years later, in 1925, she observed that the glacier had experienced a small recession since 1914 but that its terminus was still at tidewater. In 1931, Field (1932) noted that the terminus had retreated from tidewater but that it was thickening at higher elevations. By 1935 (Field, 1937), the glacier had readvanced to tidewater but was showing signs of narrowing along its margins. Retreat was underway again when Bradford Washburn photographed it in 1938. This retreat, greater than 500 m, continued through Field’s last reported observation of the glacier in 1968 (Field, 1975b). The author made several observations of the glacier between 1974 and 2004, and photographed it on 6 September 2000 (fig. 273B). During this 30-year-period, the terminus retreated about 300 m, thinned, and narrowed.

*Roaring Glacier.*—Roaring Glacier, a hanging glacier with a reconstituted glacier at its base, has retreated since 1899. Gilbert (1904, p. 96) described why it was named Roaring Glacier as follows: “Roaring Glacier, between the Cataract and the Harriman, owes the peculiarity suggesting its name to an abrupt change of grade. From a comparatively gentle slope it passes to one so steep that loose masses find no lodgement, and as its movement steadily projects its end beyond the point of inflection, fragments of ice break away and tumble down the steep incline, to gather in a heap far below, where they lie until melted.” On the basis of the size of the ice and snow accumulation at its base, Grant and Higgins (1913) concluded that the glacier was less active in 1905 than it was in 1899 and more active in 1909. In August 1910, the terminus of Roaring Glacier was between 200 and 300 m above the fjord. By 1957, it was approximately 500 m above the beach. During that 47-year period from 1910–1957 (Field, 1975b), the glacier retreated an additional 300 m. Field also reported that little additional change occurred through 1971. Between 1974 and 2004, the interval of the author’s observations, the glacier thinned and retreated another 50 to 100 m up the face of its steep bed. A 12 July 1978 photograph shows the glacier in retreat (fig. 274).

*Harriman Glacier.*—As was the case with all of the other glaciers in Harriman Fiord, Harriman Glacier was first described by scientists of the Harriman Alaska Expedition in 1899. Gilbert (1904, p. 94–95) described Harriman Glacier as follows: “The valley containing Harriman Glacier is a continuation of the main trough of the fiord and holds the same general southwest trend. The glacier curves toward the west and then toward the south, disappearing from view at a distance of nearly ten miles. As the most distant portion seen has a gentle slope and lies far below the bordering mountains, it is probable that the sources are still several miles beyond. Its general width is about a mile and a half, but its high-grade tributaries are so thick-set as practically to coalesce, especially on the south-east side, giving a broad expanse of nearly continuous ice and snow. This expanse, fully commanded from the water, makes the view of the glacier a most impressive spectacle.”

Gilbert (1904, p. 95) described a “detrital bank,” probably an outwash fan, delta, or moraine along the “eastern” (southern) side of the terminus. He stated: “Above this bank the frontal cliff is low and irregular, but elsewhere it is lofty, ranging in height from 200 to 300 feet. From such a cliff an active discharge of bergs might be assumed, but our parties encountered only a moderate quantity of floating ice near the head of the fiord.” According to tidewater glacier cycle theory (fig. 42), the absence of bergs indicates that



**Figure 274.**—12 July 1978 photograph shows the retreating terminus of Roaring Glacier. Avalanching built a small reconstituted glacier at the base of the near-vertical rock face. Photograph by Bruce F. Molnia, U.S. Geological Survey.

the terminus of the glacier was grounded and sitting on the back side of its submarine moraine. Gilbert (1904, p. 95) could not determine if the glacier was advancing or retreating: “The glacier is not closely approached by forest growth, but shrubs were seen on the shore of the fiord within a few hundred yards of the ice. If the ice is diminishing, the recent retreat of the glacier front would appear not to have been rapid.” In 1899, Gilbert and Curtis made several photographs of the terminus.

In 1905 and again in 1909, Grant and Higgins (1913) visited Harriman Glacier and determined that the southern part of the terminus had retreated about 105 m between 1899 and 1905 and another approximately 210 m through 1909. They noted no change in the position of the northern part of the terminus during the same decade. Martin visited the glacier in 1910 (Tarr and Martin, 1914, p. 335) and reported that, on 10 August 1910, the western margin had advanced about 210 m beyond its 1909 position: “The eastern [southern] margin also advanced, coming forward the whole distance that it had retreated from 1899 to 1909. In 1910 it seemed to be slightly beyond the 1899 position and there was much thickening of the eastern terminus....” Gilbert’s detrital bank was not visible, and iceberg production was much greater than in 1899.

Martin (Tarr and Martin, 1910) also noted that, in addition to the advance and thickening of the part of the eastern margin on the shores of the bay, the glacier was advancing on the land. Annual plants in the barren zone were being buried, and a ridge of push moraine a foot or two high lay at the base of a lofty, uncrevassed ice cliff. On 1 August 1910, the cliff was about 48 m from an older terminal moraine that marked the maximum of a former advance, doubtless before 1899. An analysis of vegetation in the fjord led Cooper (1942) to conclude that Harriman Glacier had not advanced beyond the moraine that it was approaching in 1910 for at least 500 years.

Keen (1915a) noted that Harriman Glacier was continuing to advance in 1914. By 1931 (Field, 1932), the terminus on the southern side of the glacier had advanced approximately 975 m from its 1909 position, an average annual advance of about 44 m a<sup>-1</sup>. Four years later, Field (1937) returned and measured another 47 m of advance, for a total of about 1,022 m between 1909 and 1935. Field measured 470 m of advance on the northern side of the terminus during this 25-year period.

Field (1975b) reported that, by 1957, the terminus of Harriman Glacier had advanced about another 100 m. The southern side had advanced about 150 m by 1961. By 1964, when it was next observed, the southern margin had retreated about 25 m, and the fjord-based ice cliff had retreated about 100 m. Field (1975b) attributed this retreat to the 2.4 m of regional subsidence caused by the 1964 Alaska earthquake. By 1966, most of the terminus had resumed advancing. By 1971, the year of Field's last recorded observation, the terminus on the north had advanced 30 to 50 m, and the ice cliff on the southern side had increased in height.

Field (1975b) summarized the changes of Harriman Glacier's southern margin between 1899 and 1971 as follows: (1) From the unknown date of its pre-20th century maximum to 1899, a recession of about 350 m; (2) from 1899 to 1905, a recession of about 100 m, yielding an average rate of retreat of about 17 m a<sup>-1</sup>; (3) from 1905 to 1909, a recession of about 200 m, yielding an average rate of retreat of about 50 m a<sup>-1</sup>; (4) from 1909 to 1910, an advance of about 300 m, yielding an average rate of advance of about 300 m a<sup>-1</sup>; (5) from 1910 to 1931, an advance of about 675 m, yielding an average rate of advance of about 32 m a<sup>-1</sup>; (6) from 1931 to 1935, an advance of about 47 m, yielding an average rate of advance of about 12 m a<sup>-1</sup>; (7) from 1935 to 1957, an advance of about 97 m, yielding an average rate of advance of about 4 m a<sup>-1</sup>; (8) from 1957 to 1961, an advance of about 151 m, yielding an average rate of advance of about 38 m a<sup>-1</sup>; (9) from 1961 to 1964, a retreat of about 28 m, yielding an average rate of retreat of about 9 m a<sup>-1</sup>; (10) from 1964 to 1966, an advance of about 26 m, yielding an average rate of advance of about 13 m a<sup>-1</sup>; and (11) no change between 1966 and 1971. Hence, between 1899 and 1971, the net change on the southern margin of the glacier was an advance of 1,268 m. For the northern margin, Field reported an advance of 750 to 850 m.

The author observed Harriman Glacier more than a dozen times between 1974 and 2004. Between 1974 and 1984, the glacier was advancing. With the exception of the extreme southern margin of the terminus, which was fronted by a delta, the entire terminus was tidewater in 1976 (fig. 41) and consisted of a vertical face with three semicircular calving embayments, as an 8 June 1976 oblique aerial photograph taken by the author (fig. 275A) shows. On 15 July 1978, a push moraine adjacent to the southern margin indicated that the glacier was recently advancing (figs. 64, 275B), while the northern half of the terminus still maintained a vertical iceberg-calving face. Lethcoe (1987)



◀ **Figure 275.**— Three photographs show characteristics of Harriman Glacier during its late-20th century advance. **A**, 8 June 1976 north-looking oblique aerial photograph shows the width of the terminus of Harriman Glacier. Note the near-vertical character of the ice face, except along the southern edge of the terminus, and the three calving embayments cut into the margin. **B**, 15 July 1978 photograph shows a push moraine formed by a small advance of the terminus earlier in the year. Similar push moraines were seen in both 1998 and 2000 in front of the central part of the terminus, indicating that, even with a cessation of annual advance, winter flow may result in seasonal advances of the terminus. **C**, In this 6 September 2000 photograph, the terminus of Harriman Glacier is more than 750 m more advanced than in 1899 and approximately 50 m forward of its 1978 position and is beginning to change its profile from subrounded to more vertical. By 2002, the northern terminus was near vertical in profile. Photographs by Bruce F. Molnia, U.S. Geological Survey. Larger versions of these figures are available online.

reported that, in 1979 and 1981, two large calving embayments developed in the terminus, with radii of more than 150 m. Similar embayments developed at Bering and Columbia Glaciers before their recent rapid retreats. In 1984, the northern margin of the glacier was adjacent to a triangular-shaped vegetation-free area that served as a major accumulation area for snow sliding off the northern wall of the valley. Lethcoe (1987) stated that, by 1986, both embayments had refilled, and the margins of the glacier advanced about 15 m, causing the abandonment of a kittiwake (*Rissa* sp.) rookery.

By 6 September 2000, the profile of nearly the entire terminus of Harriman Glacier had changed from vertical to subrounded (fig. 275C). With the exception of one calving embayment located adjacent to the delta along the southern margin of the glacier, the entire face of the terminus is fronted by an exposed sediment plain. In 1999, the embayment had a radius of more than 120 m. Since 1984, the position of the northern part of the terminus of the glacier had receded slightly from the snow chute, and a barren zone was developing along the northern margin. Several aerial and ground observations made by the author between 1999 and 2004 confirm that no recent advance of the terminus has occurred. Although the elevation of the terminus has continued to decrease, no evidence of significant retreat along the southern margin or the face of the glacier has been observed. In August 1999, a push moraine was observed about 5 m in front of the glacier along part of the face fronted by the sediment plain. In the early 1990s, Harriman Glacier had a length of 12 km, an area of 60 km<sup>2</sup>, a width at its face of 1.9 km, and an AAR of 0.79. Its accumulation area was 48 km<sup>2</sup>, and its ablation area was 13 km<sup>2</sup> (Viens, 1995) (tables 2, 3).

*Dirty and Wedge Glaciers.*—Dirty and Wedge Glaciers are two small northwest-flowing ice tongues that descend the southern wall of Harriman Fiord. Both have retreated more than 1 km since they were first observed. In 1899, Dirty Glacier terminated close to the shoreline. By 1909, the terminus was about 400 m upvalley from the beach (Grant and Higgins, 1913). By 1935 (Field, 1937), the glacier's debris-covered terminus was about 600 m from the beach, with bare ice about 200 m further upglacier. Field (1975b) reported that an additional 425 m of retreat had occurred by 1961. Hence, between 1899 and 1961, the terminus of Dirty Glacier retreated about 1.25 km, yielding an average annual retreat rate of about 20 m a<sup>-1</sup>. Between 1961 and 2000, the terminus retreated about an additional 250 m. When the author observed the glacier from the air in 2000, it was continuing to thin and retreat and was on the verge of separating into two distinct ice tongues.

In 1899, Wedge Glacier had a steep upper section and a low-relief section terminating close to sea level. The terminus area changed little through 1935 (Field, 1937). By 1961 (Field, 1975b), the low-relief lower part of the glacier had melted away. Between 1950 and the middle 1960s, Field estimated that the glacier had retreated about 500 m (Field, 1975b). Through the end of the 20th century, the terminus retreated an additional 750 to 800 m. When the author observed it from the air in August 2000, all that remained of the glacier was a small ice mass hanging on the valley wall below the divide between Harriman Fiord and Bettles Bay.

*Toboggan Glacier.*—Toboggan Glacier, a small retreating valley glacier flowing from Mount Doran toward the southern side of Harriman Fiord was visited and photographed by Grant and Paige in 1905 and was visited by Grant and Higgins in 1909 and by Martin in 1910. Martin (Tarr and Martin, 1914) mapped both moraine segments and a trimline that was formed by a 19th century advance of the glacier that reached to the shore of the fjord, a distance of about 400 to 500 m beyond the 1910 terminus. He speculated that this advance had occurred in the 1830s. A second moraine located within the outer moraine represents an advance dating to ca. 1880. The 1905 terminus position was about 325 m behind the outer moraine (Grant and Higgins, 1913). Between 1905 and 1909, the glacier fluctuated, advancing about



120 m and then retreating about 195 m. When Toboggan Glacier was photographed in 1909, a trimline was located more than 80 m above the glacier on both sides of its valley. Between 1909 and 1910, the glacier retreated an additional 23 m. Between 1910 and 1931 (Field, 1932), the glacier retreated an additional 282 m, for an average annual rate of about  $13.5 \text{ m a}^{-1}$ . By 1935 (Field, 1937), the glacier had retreated another 22 m.

During the next 22 years, Toboggan Glacier continued to retreat. It had lost an additional 416 m when it was observed by an AGS party that included Field (1975b) in 1957 at the start of the IGY. Four years later, in 1961, a Brigham Young University field party measured an additional 64 m of retreat, which placed the terminus more than 775 m behind its 1910 position (Field, 1975b). When the author observed the glacier in 1978, 2000, and 2004, it was continuing to retreat, losing at least 325 m of its length through 2000. Hence, in the 90-year period between 1910 and 2000, the terminus of Toboggan Glacier retreated about 1.1 km, for an average rate of  $12.2 \text{ m a}^{-1}$ .

#### *Glaciers of Port Wells*

*Bettles and Pigot Glaciers.*—Bettles and Pigot Glaciers are two small retreating glaciers that drain into Port Wells. Field (1975b), reported that Bettles Glacier retreated about 1 km between 1910 and 1950. Since then, it has retreated at least 1 km.

Pigot Glacier has a similar history, retreating about 1.5 km in the 40-year period between 1910 and 1950. Since 1950, it also has retreated at least 1 km. Debris from a large landslide (Post, 1967a) covers the terminus, as an 8 August 2000 oblique aerial photograph made by the author (fig. 276) shows. This debris could be the product of slides that occurred during earthquakes in the 1940s and 1964.



**Figure 276.**—8 August 2000 oblique aerial photograph, looking northwest, of Pigot Glacier, which has retreated more than 2 km since the beginning of the 20th century. Debris from a large landslide covers the terminus. Photograph by Bruce F. Molnia, U.S. Geological Survey.

### *Glaciers of Passage Canal*

*Seth and Billings Glaciers.*—Seth and Billings Glaciers are two small, poorly studied but actively retreating glaciers that drain into Passage Canal. Field (1975b) noted that Seth Glacier retreated about 1.6 to 1.8 km between 1910 and 1950. Since then, it has retreated about an additional 1.5 km.

Field (1975b) reported that Billings Glacier retreated about 1.5 km between 1910 and 1971. At that time, the glacier was separating into a pair of termini, located on either side of an emerging bedrock ledge. Continued retreat through the author's last observation on 8 August 2000 (fig. 277) has accentuated the separation and has also revealed a light-colored bedrock apron, exposed around the margin of the glacier. This light-colored bedrock, possibly aplite, is unlike any other rock unit in the immediate area. Since 1910, the glacier has retreated approximately 1.8 km.



**Figure 277.**—8 August 2000 north-looking oblique aerial photograph of the retreating and thinning Billings Glacier. Note the elevated lateral moraine and the light-colored outcrop of bedrock, possibly aplite, around the retreating terminus of the glacier. Photograph by Bruce F. Molnia, U.S. Geological Survey.

### **Northwestern Chugach Mountains Segment— North-Flowing Large Valley Glacier Subdivision**

The western part of this subdivision, which is the northwesternmost part of the Chugach Mountains (fig. 278), includes a number of small unnamed retreating glaciers located at the heads of Wolverine, Carpenter, Coal, and Monument Creeks and several unnamed creeks, all draining into the westward-flowing Matanuska River. All glaciers showed evidence of significant retreat and thinning when the author observed them from the air in September 2000 and again in September 2002. Some have extensive debris-covered termini, and some have newly vegetated, formerly barren zones around their margins. In this subdivision, glaciers lengthen to the east.

Glaciers that have lengths greater than 8 km and areas determined by Field (1975b, p. 465, 475) include (from west to east): an unnamed glacier (16 km, 74 km<sup>2</sup>), an unnamed glacier (12 km, 21 km<sup>2</sup>), Matanuska Glacier (46 km, 324 km<sup>2</sup>), Powell Glacier (26 km [author's estimate]), Nelchina Glacier (39 km, 328 km<sup>2</sup>), an unnamed glacier (9 km, 16 km<sup>2</sup>), an unnamed glacier (8 km, 16 km<sup>2</sup>), and Tazlina Glacier (47 km, 398 km<sup>2</sup>). Each glacier shows significant evidence of thinning and retreat.

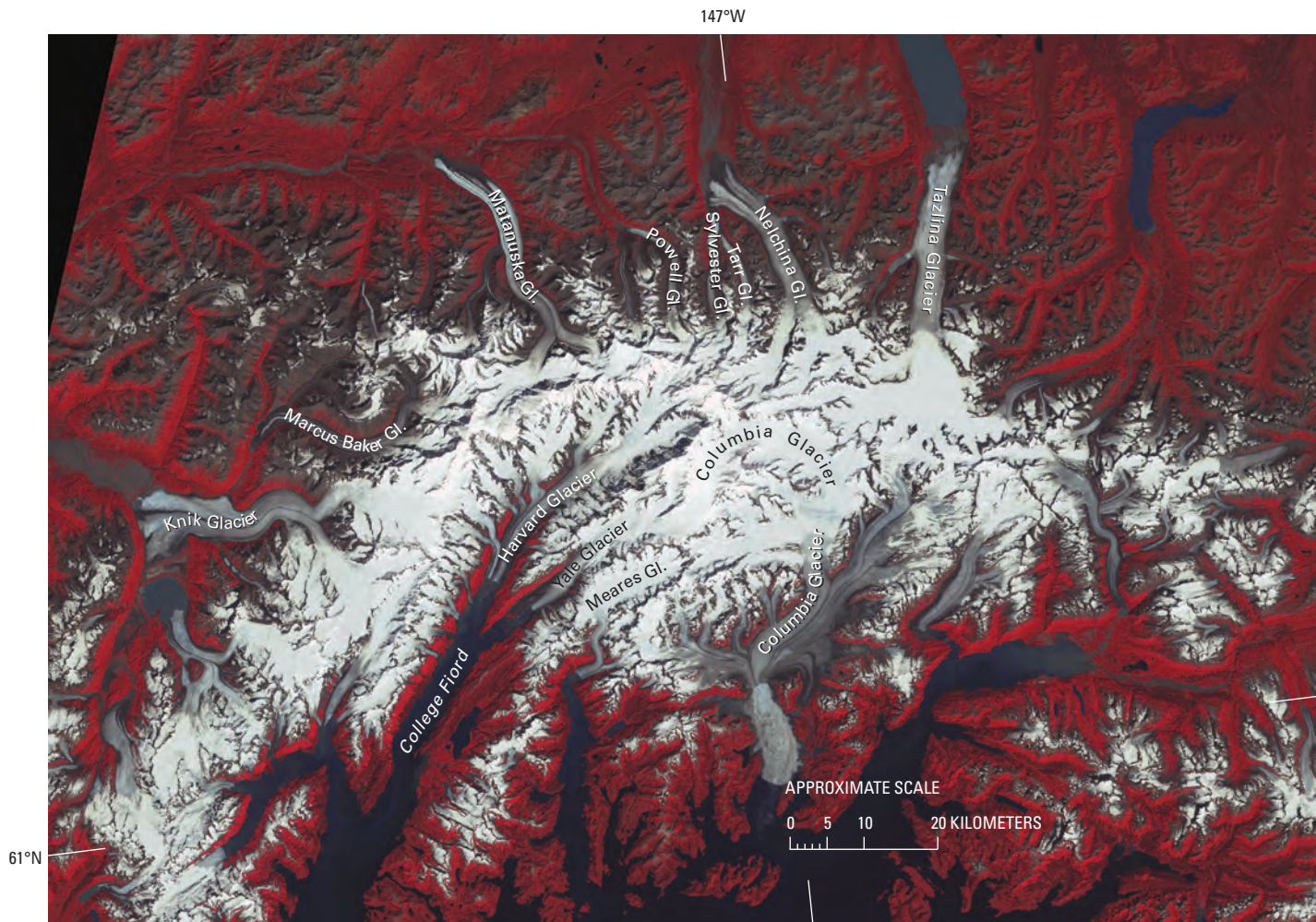


**Figure 278.**—1 August 2002 Landsat 7 ETM+ image of the northwestern part of the Chugach Mountains. Shown is the area that includes the large glaciers on the northwest side of the Chugach Mountains and northwestern College Fiord, including Columbia, Mearnes, Yale, Harvard, Knik, Marcus Baker, Matanuska, Powell, Sylvester, Tarr, Nelchina, and Tazlina Glaciers. Landsat 7 ETM+ image (7067017000221350; 1 August 2002; Path 67, Row 17) from the U.S. Geological Survey, EROS Data Center, Sioux Falls, S. Dak.

### Matanuska Glacier

Matanuska Glacier, which is 46 km long and visible from the Glenn Highway (fig. 279), drains more than 600 km<sup>2</sup> of the central Chugach Mountains between Mount Marcus Baker and Mount Thor. The glacier ranges in width from about 2.2 km near its source to about 5 km near its terminus. Most of the terminus area consists of debris-covered ice, the outer part of which is stagnant. On the western side of the glacier is a zone of active ice with a debris-free surface. Several times during the 20th century, the terminus of Matanuska Glacier has advanced and overridden stagnant ice and ablation moraine.

Nineteenth and early 20th century information about changes in Matanuska Glacier is very limited. In 1898, Mendenhall (1900) observed and photographed the terminus of the glacier and noted that a forest was growing on the surface of the debris-covered, stagnant eastern margin. Reid (1909) noted that the glacier was retreating in 1905. In 1954, Williams and Ferriars (1961) duplicated photographs taken by Mendenhall from Glacier Point. They determined that, in the ensuing 56 years, little horizontal retreat had occurred but noted that enlargement of areas of ablation moraine indicated considerable thinning of the ice. They also determined that a small advance had recently occurred over a till ridge on the west side of the glacier. Stone (1955) dated this advance at about 1945. Williams and Ferriars (1961) described a moraine located about 400 m in front of the terminus that is less than 200 years old. They also mapped earlier Holocene advances about 4,000 and 8,000 years ago that had left conspicuous moraines about 1.4 km and about 8 km, respectively, beyond the present terminus.



**Figure 279.**—30 August 2000 south-looking oblique aerial photograph shows that much of the terminus of Matanuska Glacier is debris covered. Both the east and west margins of the glacier show evidence of recent thinning and narrowing. Photograph by Bruce F. Molnia, U.S. Geological Survey.

Field (1975b) examined aerial photography of the terminus acquired in 1938, 1941, 1948, 1957, and 1964. He reported that, in the 19 years between Bradford Washburn's 1938 photograph and a 1957 USAF photograph, the terminus "is without significant change" (Field, 1975b, v. 2, p. 453). However, between 1957 and 1964, "slight recession can be seen" (Field, 1975b, v. 2, p. 453). Recession continued through the late 1970s. Between 1969 and 1974, Lawson (1979) reported but did not quantify ongoing retreat. During the summer of 1979, this retreat was interrupted, as the terminus advanced more than 30 m in 60 days. A comparison of Lawson's 1969 photograph and a BLM vertical photograph acquired on 17 August 1999 (BLM vertical aerial photograph No. R3-FL6-FR-15) shows about 1 km of terminus retreat during the 30-year period of coverage. When the author observed the glacier from the air on 30 August 2000 (fig. 279), the glacier showed multiple signs of continued thinning and retreat.

Since the 1970s, research has been conducted at the western terminus of the Matanuska Glacier by scientists from the Cold Regions Research and Engineering Laboratory of the U. S. Army Corps of Engineers and by the academic community. Topics include sediment transport and deposition (Lawson, 1979), present-day formation of basal ice (Strasser and others, 1996), and short-pulse radar analysis of subglacier structure (Arcone and others, 1995).

### **Nelchina Glacier**

Although it has been photographed from the air since 1938, Nelchina Glacier, which is 39 km long and 328 km<sup>2</sup> in area (Field, 1975b, p. 465), has not been the subject of any published field investigations. Field (1975b, v. 2, p. 357) reported that, in the 28 years between Bradford Washburn's 1938 photograph and a 1964 photograph of the glacier by Austin Post, "there was no conspicuous change in the position of the terminus. However, the lateral barren zone on the eastern side of the lower part of the glacier appears to have widened, indicating a lowering of the ice surface. Above this barren zone a conspicuous lateral moraine appears to mark the limit of a recent maximum in which the terminus was more advanced, perhaps as much as 500 m."

Between 1964 and 2000, Nelchina Glacier continued to thin and retreat. When the author observed it from the air on 30 August 2000 (fig. 280), several small ice-marginal lakes had developed adjacent to the eastern and central terminus regions of the glacier. Elevated lateral moraines and distinctive trimlines were clearly visible. As much as 2 km of retreat had occurred in



**Figure 280.** — 30 August 2000 south-looking oblique aerial photograph of the thinning and retreating terminus of Nelchina Glacier and its western tributaries, Sylvester and Tarr Glaciers. The absence of any deflection of the moraine where Sylvester and Tarr Glaciers join the Nelchina Glacier suggests that they no longer contribute ice to the Nelchina Glacier. Much of the central part of the terminus of Nelchina Glacier is debris covered and extends beyond the bare ice lobes on either side. Both the east and west margins of Nelchina Glacier show evidence of recent thinning. Photograph by Bruce F. Molnia, U.S. Geological Survey.

the 36 years since the 1964 photograph by Austin Post. Sylvester and Tarr Glaciers, the two western tributaries to Nelchina Glacier, both have thinned significantly as well. At their junction with Nelchina Glacier, their flow has decreased so much that they no longer deflect the medial moraine that separates them from the western side of Nelchina Glacier.

#### **Tazlina Glacier**

Tazlina Glacier, another glacier that was not studied before the IGY, was visited in 1957 by an AGS field party that included Field and Viereck. Viereck (1967) examined the vegetation and confirmed that the terminus had not been more than 2.5 km further advanced since at least 1450 A.D. A terminal moraine located about 1.5 km from the 1957 terminus was formed between 1800 and 1820. Viereck (1967) estimated recession during the first half of the 20th century to be at a rate of 15 to 21 m a<sup>-1</sup> and to be between 24 to 28 m a<sup>-1</sup> since the middle 1940s. The author compared the USGS 1960 Valdez C-7 1:63,360-scale topographic quadrangle map, compiled in 1950, with a 1993 Landsat image. The comparison showed that an ice-marginal lake filling the area of post-1950s retreat formed along much of the terminus of Tazlina Glacier, leaving most of its former outwash plain as a sandflat at the head of Tazlina Lake. When the author observed the glacier from the air on 30 August 2000, continued retreat had all but separated it from its outwash plain (fig. 281). However, the upper part of the glacier, at an elevation of about 1,500 m, showed no evidence of thinning or retreat. Observations on the same day to the east of Tazlina Glacier showed large glacial cirques occupied only by small ice patches, another sign of ongoing glacier retreat.

Comparing 1950s map data of Tazlina Glacier with data obtained during geodetic airborne laser altimeter profiling surveys in the middle 1990s showed that, on an annual basis, Tazlina Glacier thinned by 0.687 m a<sup>-1</sup>, had a volume decrease of 0.252 km<sup>3</sup> a<sup>-1</sup>, and retreated 17 m a<sup>-1</sup> (K. A. Echelmeyer, W. D. Harrison, V. B. Valentine, and S. I. Zirnheld, University of Alaska Fairbanks, written commun., March 2001).



**Figure 281.**—30 August 2000 oblique aerial photograph of Tazlina Glacier. The south-looking view of the terminus region shows that continued retreat had all but separated the glacier from its middle 20th century outwash plain. Note the 1950s end moraine. Photograph by Bruce F. Molnia, U.S. Geological Survey.

### Northeastern Chugach Mountain Segment—The Turnagain Arm—Western Chugach Mountains Subdivision

In this subdivision, glaciers that have lengths greater than 8 km and areas determined by Field (1975b, p. 473–475) include Marcus Baker Glacier (39 km), an unnamed glacier (9 km), Knik Glacier (49 km, 380 km<sup>2</sup>), Gannett Glacier (14 km, 24 km<sup>2</sup>), Colony Glacier (29 km, 237 km<sup>2</sup>), Lake George Glacier (24 km, 88 km<sup>2</sup>), an unnamed glacier (8 km, 15 km<sup>2</sup>), another unnamed glacier (12 km, 43 km<sup>2</sup>), Whiteout Glacier (15 km [author’s estimate]), an unnamed glacier at the head of Troublesome Creek (11 km, 20 km<sup>2</sup>), Twentymile Glacier (15 km, 32 km<sup>2</sup>), Eagle Glacier (14 km, 49 km<sup>2</sup>), Eklutna Glacier (13 km, 31 km<sup>2</sup>), Hunter Creek Glacier (9 km, 14 km<sup>2</sup>), and Metal Creek Glacier (9 km, 12 km<sup>2</sup>).

#### Marcus Baker Glacier

Marcus Baker Glacier, which is 39 km long (Field, 1975b, p. 475) and has an area estimated by the author of about 20 km<sup>2</sup>, is located at the head of Grasshopper Valley and may have been a “Little Ice Age” tributary glacier to Knik Glacier, joining it from the north. Today, its terminus is more than 6 km from Knik Glacier. Marcus Baker Glacier originates on the western flank of Mount Marcus Baker (4,107 m), one of the highest peaks in the Chugach Mountains. Although it has not been the subject of any scientific investigations, its terminus was photographed by Bradford Washburn in 1938 and the U.S. Army Air Forces in 1941. At that time, the lower 1.75 km of the glacier was covered by debris and showed little evidence of retreat (Field, 1975b). When it was mapped in the 1950s, the terminus of Marcus Baker Glacier had begun to retreat. By 1996, an outwash plain about 2 km in length fronted the terminus. When the author photographed the glacier from the air on 30 August 2000, it had retreated about 2.5 km from its 1950s terminus position and showed conspicuous evidence of thinning along both margins (fig. 282).

#### Knik Glacier

Knik Glacier (fig. 6), which is 49 km long and 380 km<sup>2</sup> in area (Field, 1975b, p. 474), terminates in a small piedmont lobe, the perimeter of which is more than 16 km, as a 30 August 2000 oblique aerial photograph taken by the author shows (fig. 283). Several moraines located up to 1 km from the terminus document the fact that Knik Glacier was larger in the early 20th century. At various times during the past, the southern part of the terminus, which flows

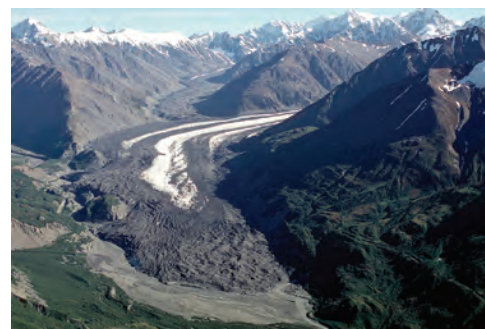


**Figure 282.**—30 August 2000 north-looking oblique aerial photograph of the debris-covered terminus area of Marcus Baker Glacier. The unnamed tributary that enters from the north has separated from Marcus Baker Glacier. Note the difference in elevation between the ice surface and the vegetation on the bedrock knob on the west side of Marcus Baker Glacier, evidence of recent thinning. Photograph by Bruce F. Molnia, U.S. Geological Survey. A larger version of this figure is available online.



**Figure 283.**—30 August 2000 east-looking oblique aerial photograph of the northern part of the terminus of Knik Glacier. The perimeter of this small piedmont lobe is more than 16 km. Thinning and retreat of the terminus have reduced the chance that the volume of water in the glacier-dammed Inner Lake George (off the photograph to the right) would reach a critical level and trigger a jökulhlaup. Photograph by Bruce F. Molnia, U.S. Geological Survey. A larger version of this figure is available online.

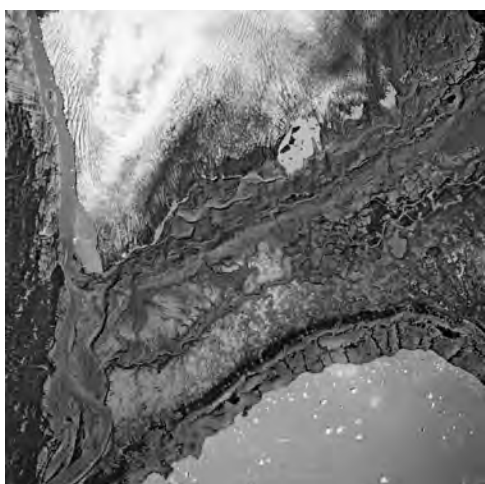


**Figure 284.**—17 August 1999 vertical aerial photograph of the southwestern part of the terminus of Knik Glacier. North is at the top of the photograph. The Gorge is visible on the west side of the photograph. Inner Lake George is at the bottom. Photograph no. R3-FL2- FR-224 from the U.S. Bureau of Land Management. A larger version of this figure is available online.

towards the eastern flank of Mount Palmer, would occasionally make contact with the mountain, blocking meltwater flow, forming a lake, and creating flood potential. Hulsing (1981, p. 10) reported that, before 1900, one flood destroyed three Native villages: “No previous damage along the Knik River had been recorded although, according to the Indians living in the area, the lake emptied once every 15 or 20 years.”

In 1915, Capps (1916, p. 169) visited Knik Glacier and described the terminus: “No facts were observed that would indicate any great amount of recent retreat of Knik Glacier. ... The presence of ... bushes and trees so near the ice front shows conclusively that the glacier is now almost as far advanced as it has been for many years.” He also provided some details about the lake formed by Knik Glacier: “Natives and prospectors report a lake many miles long that occupies a valley along the east side of the southwest fork of Knik Glacier. This lake fills gradually and at intervals of six or seven years breaks out through Knik Glacier and sends great floods of water down Knik River and Knik Arm” (Capps, 1916, p. 169). Capps reported that such a flood occurred in September 1915, causing significant damage to a railroad being constructed across Knik Arm.

After 1915, the lake formed and emptied more regularly. Every winter between 1915 and 1966, with the exception of 1963, the southwestern terminus of Knik Glacier (fig. 284) advanced against the eastern side of Mount Palmer, closing the 10-km-long ice-marginal drainage channel known as The Gorge. This blockage impounded meltwater flowing from Lake George Glacier, Colony Glacier, and the southeastern part of the terminus of Knik Glacier and prevented it from entering the Knik River. Meltwater would pond behind the ice dam each spring and form a large lake (Lake George) that covered an area of as much as 75 km<sup>2</sup>. By late June or early July, the lake would overtop its ice dam and begin a flood that would last for about 2 weeks. During the peak of the jökulhlaup, discharge could be as much as  $9.45 \times 10^6 \text{ l s}^{-1}$  ( $1.5 \times 10^8 \text{ gal min}^{-1}$ ), as predicted by Meier in an unpublished report submitted to the U.S. Department of the Interior in the late 1950s (Mark F. Meier, written commun., 2004). Since 1966, owing to late 20th century thinning and retreat (fig. 285), Knik Glacier has failed to seal the flood channel (Trabant and Mayo, 1980; Mayo and Trabant, 1982). During the early 1970s, the channel had a width of about 300 m (Post and Mayo, 1971). When the author observed it from the air on 12 April 2002, the width was less than 100 m, but the height of the ice wall was significantly smaller.

In 1951, Stone (1955) visited the glacier and studied evidence of higher lake levels. He found evidence of an undated maximum lake level as much as 45 m higher than the 1951 level and a 1940s level as much as 2 m higher. Stone (1955, p. 43–44) concluded that “Knik Glacier’s two ice faces appear to have been in about the same position for at least the past 50 years and the lake probably has existed for as much as 75 years.”

Photographs of the glacier obtained between 1938 and 1968 (Field, 1975b) document that, between 1938 and 1957, the terminus retreated between 150 and 200 m and that its location was 600 to 1,000 m from its most advanced position. An additional 200 m of retreat had occurred by 1964, with 100 m more by 1968. Hence, in the 30 years between 1938 and 1968, the terminus of Knik Glacier retreated between 450 and 500 m, an average retreat of about 15 m a<sup>-1</sup>, the greatest retreat being at the end of the interval. Since 1968, the glacier has continued to thin and retreat. By 2000, when the author photographed it from the air, the terminus had retreated about 600 m from its 1968 position.



**Figure 285.**—30 August 2000 south-looking oblique aerial photograph of the westernmost part of Knik Glacier and the entire length of The Gorge. The Lake Fork of the Knik River flows through The Gorge. Inner Lake George is in the background with Colony Glacier behind it. Although Knik Glacier is closer to the bedrock wall of Mount Palmer now than it has been in the past few decades, the height of the terminus is too low to impound much water because the terminus is fractured and may even be floating, permitting water to drain through the Lake Fork of the Knik River. Photograph by Bruce F. Molnia, U.S. Geological Survey.

### **Gannett Glacier**

Gannett Glacier, named because of its proximity to Mount Gannett, has a length of 14 km and an area of 24 km<sup>2</sup> (Field, 1975b, p. 475). It flows in a northwestwardly direction toward Knik Glacier but ends more than 2 km short of merging with it. According to Field (1975b), relatively fresh trimlines seen in the valley of Gannett Glacier on Bradford Washburn's 1938 photograph of these two glaciers suggests that they were formerly connected. On the USGS Anchorage B-7 1:63,360-scale topographic quadrangle map (1960) (appendix B), which was based on mid-1950s photography, the terminus of Gannett Glacier was about 500 m from the margin of Knik Glacier. By 17 August 1999, the closest point of the debris-covered terminus of Gannett Glacier was about 2.0 km from Knik Glacier, and exposed ice was about 3.9 km from Knik Glacier (fig. 286).

### **Colony Glacier**

Colony Glacier, which has a length of 29 km and an area of 237 km<sup>2</sup> (Field, 1975b, p. 474), fronts on and calves into ice-marginal Inner Lake George. The northern side of the lake, which has an approximate diameter of 6 km, is dammed by Low Ridge, a subcircular terminal moraine that formed around the bulbous terminus of a formerly extended Colony Glacier. Bradley and others (1972) stated that this moraine has an age of less than 200 radiocarbon years. The location of the northern part of Low Ridge is about 1.2 km south of the southernmost terminal moraine previously deposited by Knik Glacier. This interglacier area between moraines is the bed of Lower Lake George, which has been essentially dry since at least the middle 1950s, at which time the terminus of Colony Glacier had retreated approximately 5 km from Low Ridge and had thinned about 150 m. In 1951, Stone (1955) examined the moraine area and concluded that the last 3.5 km of retreat had occurred in the previous 35 years (since 1916).

The termini of Colony and Knik Glaciers were photographed by the AHAP Program on 25 August 1978 (fig. 287A). By that time, the terminus of Colony Glacier had retreated a maximum of 2 km from its middle 1950s position. The author visited Colony Glacier in 1998 and 1999 and photographed it from the air on 15 August 2000 (fig. 287B) and in July 2001. Between August 1978 and July 2001, the glacier retreated at least 1.5 km.



**Figure 286.**— 17 August 1999 vertical aerial photograph of the retreating and thinning terminus of Gannett Glacier, a former tributary to the Knik Glacier. Landslide debris covers much of the terminus. North is at the top of the photograph. Photograph no. R3-FL1-FR-219 from the U.S. Bureau of Land Management.

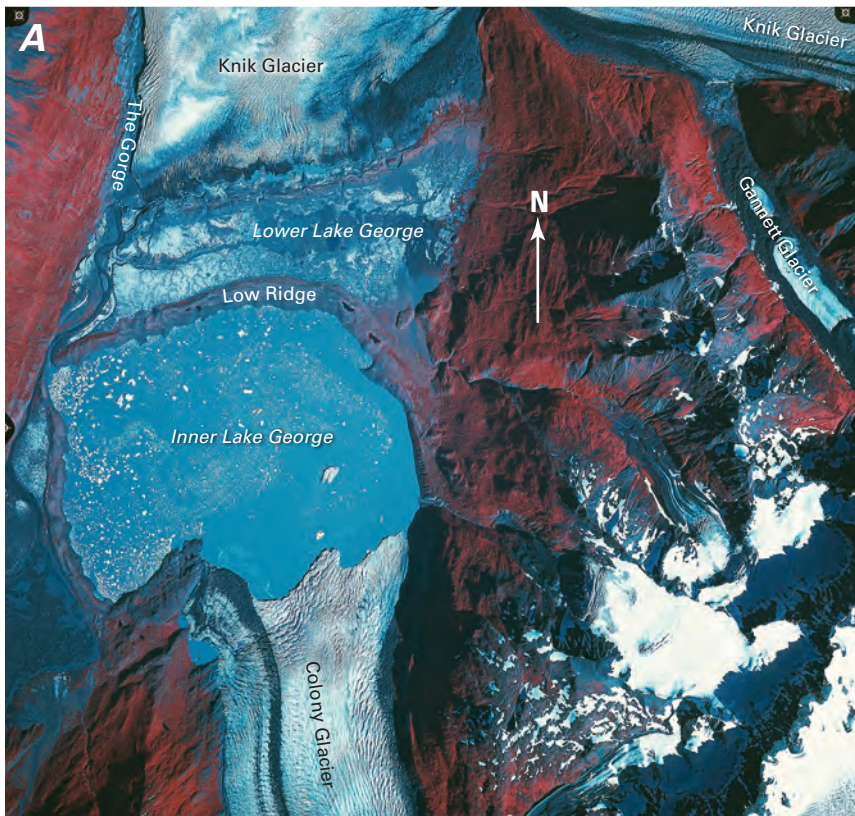
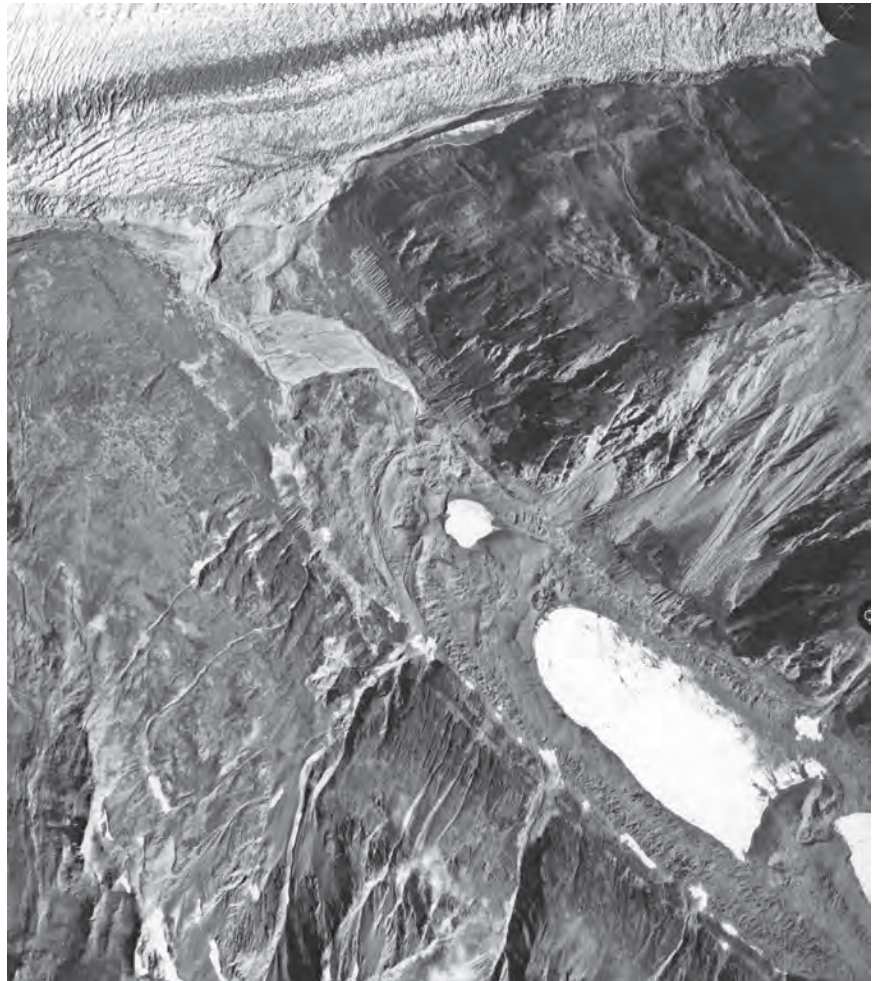


**Figure 287.**— Two aerial photographs of Colony Glacier and the surrounding area. **A**, 25 August 1978 AHAP false-color infrared, vertical aerial photograph of the terminus of Colony Glacier, Inner Lake George, the dry bed of Lower Lake George, the southwestern part of Knik Glacier, The Gorge, and the terminus of Gannett Glacier. The bedrock projection that is in contact with the debris-covered western terminus of Colony Glacier is Colony Point. AHAP photograph no. L107F7031 from the GeoData Center, Geophysical Institute, University of Alaska, Fairbanks, Alaska. **B**, 15 August 2000 high-altitude north-looking oblique aerial photograph of the terminus of Colony Glacier and Inner Lake George. In the 22 years between photographs, Colony Glacier retreated at least 1.5 km. Photograph by Bruce F. Molnia, U.S. Geological Survey. A larger version of B is available online.

## Lake George Glacier

The western part of Low Ridge serves as the dam of the presently dry Upper Lake George, a former proglacial lake bed that is approximately 15 km long and extends from near the terminus of the retreating Lake George Glacier to the western side of Inner Lake George. Lake George Glacier has a length of 24 km and an area of 88 km<sup>2</sup> (Field, 1975b, p. 474). Field (1975b) reported that, in 1957, the terminus of Lake George Glacier was located about 800 m behind a moraine representing an undated recent maximum. When the author observed the terminus in 1998 and 1999, it had retreated another 2.5 km from its 1957 location, and a triangular-shaped ice-marginal lake had formed in front of the terminus.

## Glaciers West of Knik Glacier, Upper Lake George, and Lake George Glacier

West of a line connecting Knik Glacier, Upper Lake George, and Lake George Glacier are a number of small unnamed glaciers and a dozen more with names, including Hunter Creek Glacier (fig. 288). All are retreating, and all were observed from the air by the author in August 2000. An unnamed glacier at the head of Troublesome Creek and Whiteout Glacier are two

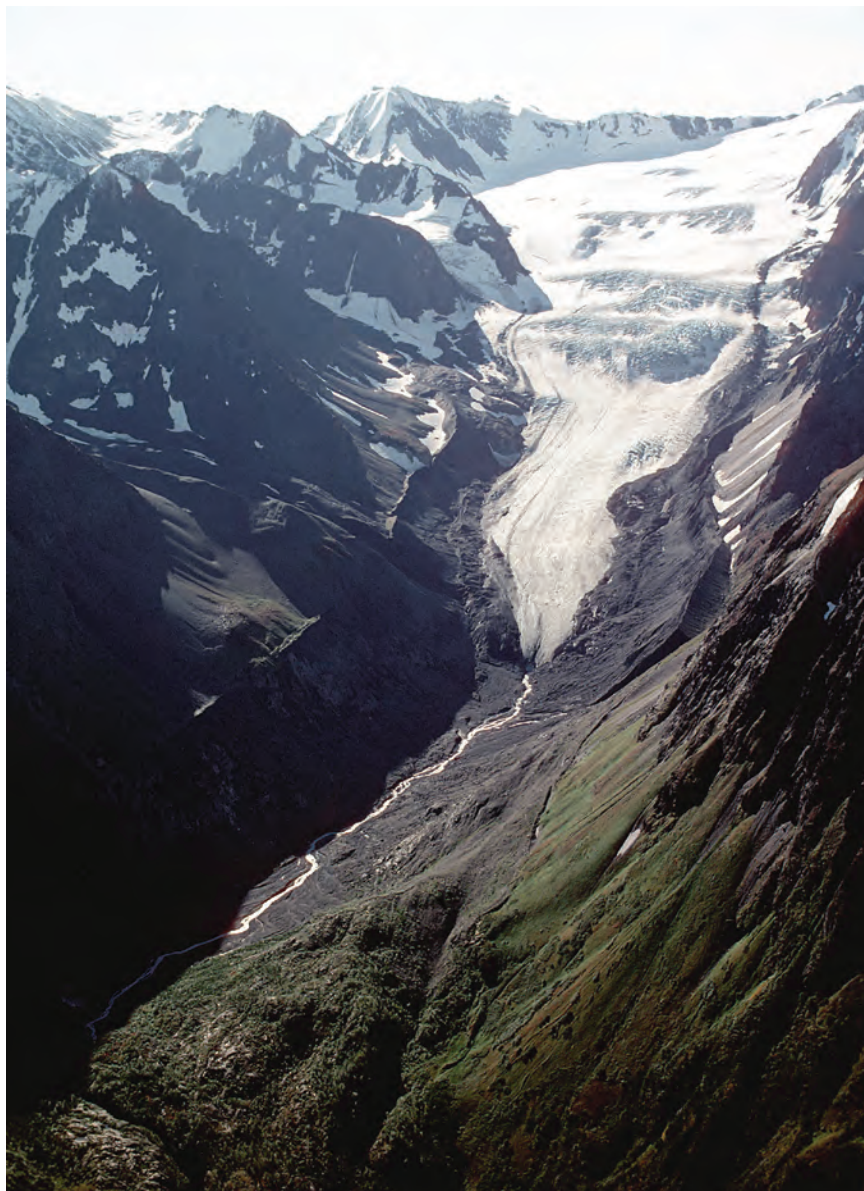


**Figure 288.**—30 August 2000 oblique aerial photograph of Hunter Creek Glacier made during an aerial survey of the western Chugach Mountains area west of a line connecting Lake George Glacier and Knik Glacier. All of the glaciers observed were retreating. The south-looking view of Hunter Creek Glacier shows its terminus is approximately 2 km from the terminal moraines that mark its most recent, undated advances. Elevated lateral moraines and trimlines document that this glacier was recently much thicker. Photograph by Bruce F. Molnia, U.S. Geological Survey.

eastward-flowing glaciers that drain into the bed of Upper Lake George. In 1957, both the unnamed glacier and Hunter Creek Glacier were about 1.5 km from terminal moraines that marked their most recent undated advances. By 30 August 2000 (fig. 288), both glaciers had retreated approximately another 1.0 to 1.5 km upvalley.

### Glaciers of the Eagle River and Crow Creek Drainages

Milk, Crow, Raven, Clear, Flute, Icicle, and Organ Glaciers are located along the drainage of Eagle River or Crow Creek.

#### *Eagle Glacier*

Eagle Glacier at the head of the Eagle River is the largest glacier in the drainage. Its retreating terminus continues to expose bedrock as it thins and narrows. At the foot of its valley is a former ice-marginal lake with an outwash fan delta at its head. The lake is the product of post-1915 retreat. In 1915, Capps (1916) photographed (see USGS Photo Library photograph Capps 732) and described the terminus area of Eagle Glacier. He reported that several crescentic lines of terminal moraines were located in the valley

below the glacier and that the glacier had retreated more than 1 km in the recent past. His photograph shows that an ice-marginal lake of unknown size was located adjacent to the terminus. According to Field (1975b), the location of the terminus in 1915 corresponds to the distal end of the present lake. The most distal moraine, probably corresponding to the “Little Ice Age” maximum position of Eagle Glacier is about 1.5 km beyond the 1915 moraine. A second younger large undated moraine is located about 400 m closer to the glacier. A 1957 photograph shows the terminus position at that time to be about 2.9 km from the outermost moraine. Between 1915 and 1931, Eagle Glacier retreated about 225 m. By 1938, when Bradford Washburn photographed the glacier, another 175 m of retreat had occurred, placing the terminus of the glacier in the emerging lake basin. Another 750 m of retreat occurred in the 12 years between 1938 and 1950. By 1957, Eagle Glacier had retreated another 250 m and receded above the proximal end of the lake, ending on an outwash plain. When the author photographed it from the air on 30 August 2000 (fig. 289), the retreating and thinning terminus was more than 2 km from the distal end of the lake.



**Figure 289.**—30 August 2000 oblique aerial photograph shows the location of the retreating terminus of Eagle Glacier with a delta at the end of the 2-km-long lake. The terminus is more than 2 km from the end of the lake where it was located in 1915. Photograph by Bruce F. Molnia, U.S. Geological Survey.

### *Eklutna Glacier*

Eklutna Glacier, which covers about 50 percent of the West Fork of the Eklutna Lake drainage basin, is 13 km long and has an area of 13 km<sup>2</sup> (Field, 1975b, p. 473). When it was mapped by the USGS in 1957 (Anchorage B-6 1:63,360-scale) (appendix B), the terminus was located at an elevation of about 350 m. Thirty-one years later, during field observations made in 1988 by Brabets (1993), the terminus had retreated to an elevation of about 700 m. The East Fork Eklutna Creek basin has an area of about 100 km<sup>2</sup>, of which 20 percent is glacierized. The West Fork Eklutna Creek basin has an area of approximately 67 km<sup>2</sup>, about 50 percent of which is glacierized. As with Eagle Glacier, Eklutna Glacier was visited and photographed by Capps in 1915 (see USGS Photo Library photograph Capps 698). At that time, its terminus was situated at the head of an outwash plain about 2 km above the proximal end of Eklutna Lake. The lake occupies an elongated, glacially steepened depression dammed by a older terminal moraine of Eklutna Glacier, produced by a pre-19th century advance of the glacier. Field (1975b) stated that the glacier retreated about 1 km between 1915 and 1957, for an average rate of about 24 m a<sup>-1</sup>. Eklutna Glacier was photographed by the BLM on 17 August 1999 (BLM vertical aerial photograph nos. R3-FR-272 and R3-FR-274). When the author observed it from the air in August 1996 and again on 30 August 2000 (fig. 290), the retreating and thinning terminus was about 7 km from the head of Eklutna Lake.

### *Twentymile Glacier*

Twentymile Glacier is a southwest-flowing retreating glacier that is the primary source of the Glacier River, which is the eastern source of Twentymile River. At the end of the 20th century, the terminus of Twentymile Glacier calved icebergs into a large ice-marginal lake. Its southeastern side and its northwestern side—each the product of different tributaries—have retreated at different speeds throughout its observed history. Twentymile Glacier has received little scientific attention, but it has been photographed and observed from the air since 1938. Field (1975b) examined photographs collected at six different times (1938, 1941, 1950, 1957, 1964, 1971) and derived a history of recent changes in Twentymile Glacier. When Bradford Washburn photographed it in 1938, the terminus of Twentymile Glacier was about 1.2 km from a prominent undated terminal moraine. This moraine was about 2.5 km upvalley from an even older terminal moraine, located adjacent to the south side of Carmen Valley, which Field (1975b) speculated dates from approximately 1870 or earlier. The 1938 position of the terminus of Twentymile Glacier is separated from dense vegetation by a 200-m-wide barren zone. This zone suggests that, sometime after 1920, the glacier resumed retreat after a period of perhaps several decades of stability. An ice-marginal lake was also beginning to form adjacent to the southeastern part of the terminus. By 1941, the lake fronted the entire ice face, and the terminus continued to retreat.

Between 1938 and 1941, the southeastern side of Twentymile Glacier retreated 150 m, while the northwestern side of the glacier retreated 100 m. The average annual rates of retreat were 50 m a<sup>-1</sup> and 33 m a<sup>-1</sup>, respectively. Between 1941 and 1950, the southeastern side retreated 550 m, while the northwestern side retreated 100 m. The average annual rates of retreat were 61 m a<sup>-1</sup> and 11 m a<sup>-1</sup>, respectively. Between 1950 and 1957, the southeastern side retreated 350 m, while the northwestern side retreated 400 m. The average annual rates of retreat were 50 m a<sup>-1</sup> and 57 m a<sup>-1</sup>, respectively. Between 1957 and 1964, the southeastern side retreated 300 m, while the northwestern side retreated 100 m. The average rates of retreat were 43 m a<sup>-1</sup> and 14 m a<sup>-1</sup>, respectively. Between 1964 and 1971, the southeastern side retreated 300 m, while the northwestern side retreated 200 m. The average rates of retreat were 43 m a<sup>-1</sup> and 28 m a<sup>-1</sup>, respectively. For the entire 33-year-period



**Figure 290.**—30 August 2000 oblique aerial photograph of the location of the retreating terminus of Eklutna Glacier. The glacier has retreated approximately 5 km since photographed in 1915. Photograph by Bruce F. Molnia, U.S. Geological Survey. A larger version of this figure is available online.

**Figure 291.**—18 July 1978 north-looking oblique aerial photograph of the thinning and retreating terminus of Twentymile Glacier. Note that the proglacial lake has a length of approximately 2.5 km and that the northwestern side of the glacier extends several hundred meters beyond the southeastern side. Photograph by Bruce F. Molnia, U.S. Geological Survey.



from 1938 to 1971, the southeastern side of the glacier retreated 1,650 m, while the northwestern side retreated 900 m. The average rates of retreat were  $50 \text{ m a}^{-1}$  and  $27 \text{ m a}^{-1}$ , respectively. By 18 July 1978, the lake was about 2.5 km long (fig. 291). By 2000, when it was last observed from the air by the author, the lake had a maximum length of about 4 km.

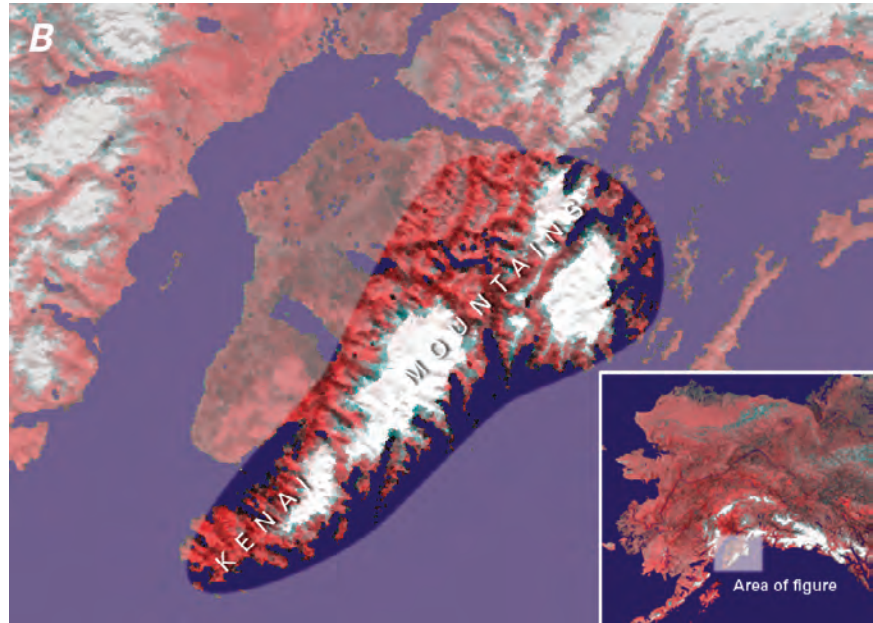
### **Summary**

During the entire period of the Landsat baseline (1972–1981), Meares and Harvard Glaciers were advancing. Bryn Mawr, Harriman, and Columbia Glaciers advanced during the early part of the baseline. Smith Glacier was stable for most of the baseline period, with the position of its termini fluctuating from year to year. Available evidence suggests that all other valley and outlet glaciers in the Chugach Mountains were thinning and retreating.

At the end of the 20th century, Meares and Harvard Glaciers were still advancing. The terminus of Harriman Glacier was stable. All other valley and outlet glaciers in the Chugach Mountains were thinning or retreating or had become stagnant.



**Figure 292.—B,** Enlargement of NOAA Advanced Very High Resolution Radiometer (AVHRR) image mosaic of the Kenai Mountains in summer 1995. National Oceanic and Atmospheric Administration image mosaic from Michael Fleming, Alaska Science Center, U.S. Geological Survey, Anchorage, Alaska.



between Nuka Bay and Kachemak Bay. A number of other generally smaller glaciers descend from other isolated accumulation areas along the crests of many ridges and mountains. The total area of glaciers in the Kenai Mountains is 4,600 km<sup>2</sup> (Post and Meier, 1980, p. 45).

The Sargent and the Harding Icefields have many outlet glaciers that descend toward or into Prince William Sound, Cook Inlet, and the Gulf of Alaska. Many of these outlet glaciers reach to near sea level, and more than a dozen have calving termini, 11 directly into tidewater (fig. 41; tables 2, 3). The region contains several hundred glaciers; almost all of the larger ones have names. Seven have lengths of about 20 km, and 2 exceed 30 km. Unless otherwise noted, lengths and areas given are by Field (1975d) from USGS 1:250,000-scale topographic maps (appendix A), generally compiled from aerial photographic and other surveys performed between 1950 and 1963 and supplemented by the author. Landsat 1–3 MSS images that cover the Kenai Mountains have the following Path/Row numbers: 72/18, 73/17, 73/18, 74/18, 75/17, and 75/18 (fig. 3; table 1).

Wiles and others (1999a) and Barclay and others (1999) performed dendrochronological studies at a number of Kenai Mountain tidewater and former tidewater glaciers. Their work involved both living trees, some more than 680 years old, and a 1,119-year tree-ring-width chronology derived from more than 100 logs recovered from about a dozen glaciers in the western Prince William Sound area. Each of these logs had been sheared or uprooted by a past glacier advance. Their work showed that glacier fluctuations during the “Little Ice Age” were strongly synchronous on decadal time scales at many glaciers (fig. 294). Studies at eight locations indicated that advances occurred during the late 12th through 13th centuries and from the middle 17th to early 18th centuries. Nine glaciers showed evidence of a late 19th century advance. Glaciers studied include Tebenkof, Cotterell, Taylor, Wolverine, Langdon, Kings, Nellie Juan, Ultramarine, Princeton, Excelsior, and Ellsworth Glaciers. They also investigated Billings Glacier in the southern Chugach Mountains.

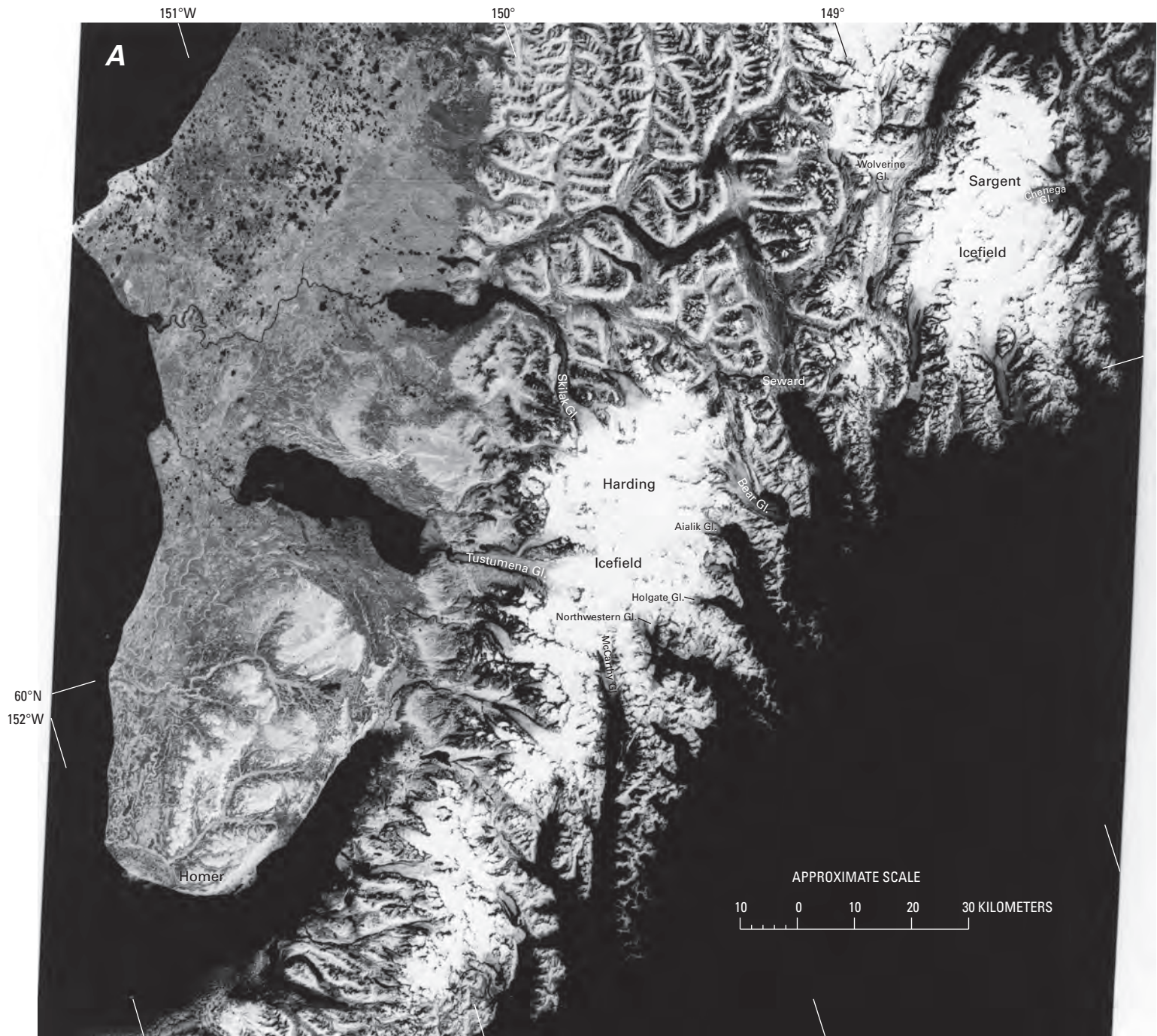


**Figure 293.**—**A**, Annotated Landsat 1 MSS image of the Harding and Sargent Icefields and numerous tidewater glaciers on the Kenai Peninsula. McCarthy, Northwestern, Holgate, Aialik, and Chenega Glaciers are all retreating tidewater glaciers at the head of their fjords (Meier and others, 1980) (see fig. 41 and tables 2 and 3). Wolverine Glacier has been studied by the U.S. Geological Survey since 1966 and was nearly stable from 1966 to 1976, but from 1977 to 1982 thickened more than 8 m (Mayo and Trabant, 1984). It has since thinned and retreated. Landsat image and caption courtesy of Robert M. Krimmel, U.S. Geological Survey. Landsat 1 image (1390–20452, band 7; 17 August 1973; Path 74, Row 18) is from the U.S. Geological Survey, EROS Data Center, Sioux Falls, S. Dak. **B**, see opposite page.



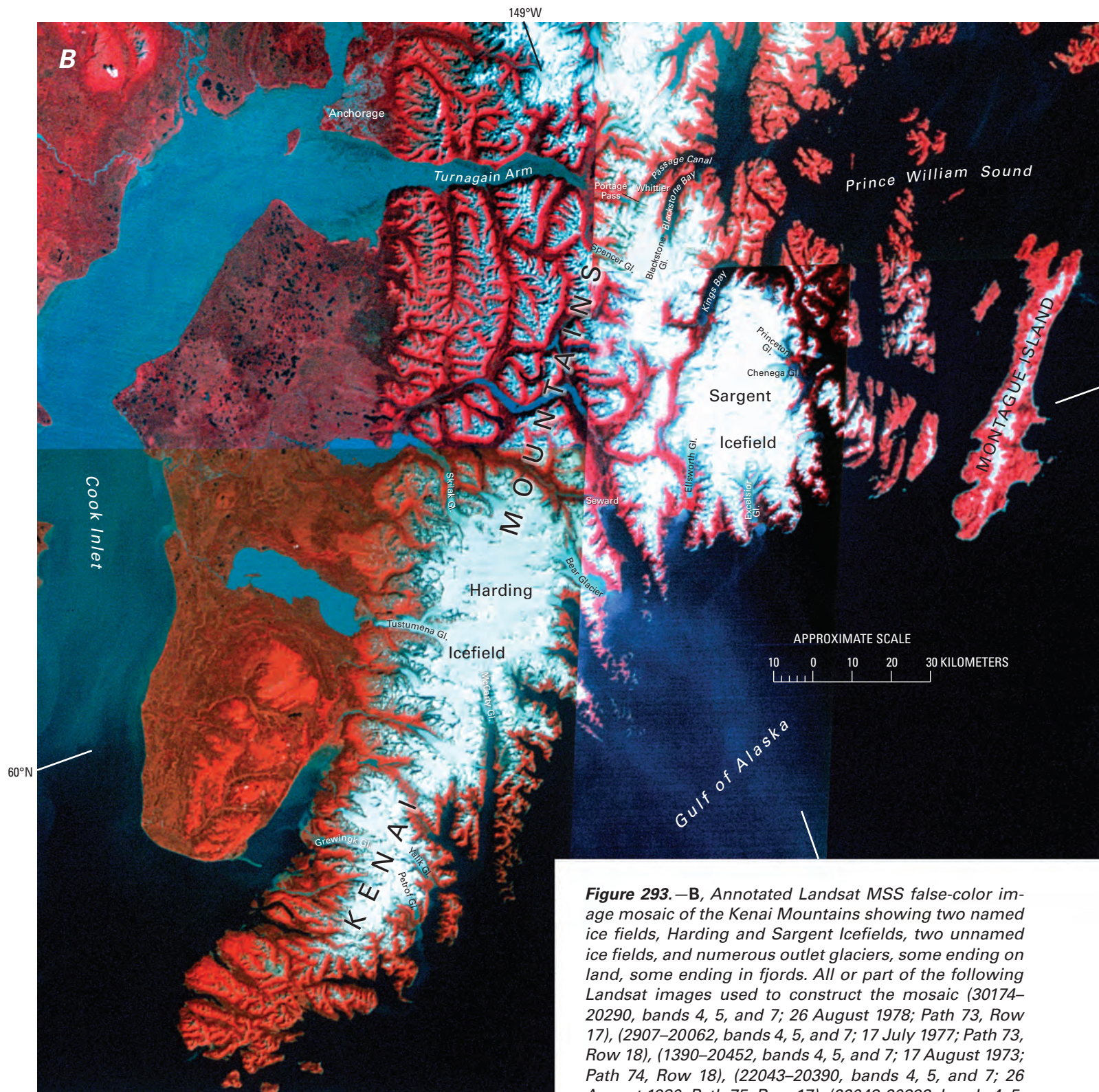


**Figure 293.—B,** Annotated Landsat MSS false-color image mosaic of the Kenai Mountains showing two named ice fields, Harding and Sargent Icefields, two unnamed ice fields, and numerous outlet glaciers, some ending on land, some ending in fjords. All or part of the following Landsat images used to construct the mosaic (30174–20290, bands 4, 5, and 7; 26 August 1978; Path 73, Row 17), (2907–20062, bands 4, 5, and 7; 17 July 1977; Path 73, Row 18), (1390–20452, bands 4, 5, and 7; 17 August 1973; Path 74, Row 18), (22043–20390, bands 4, 5, and 7; 26 August 1980; Path 75, Row 17), (22043–20393, bands 4, 5, and 7; 26 August 1980; Path 75, Row 18) are from the U.S. Geological Survey, EROS Data Center, Sioux Falls, S.Dak.

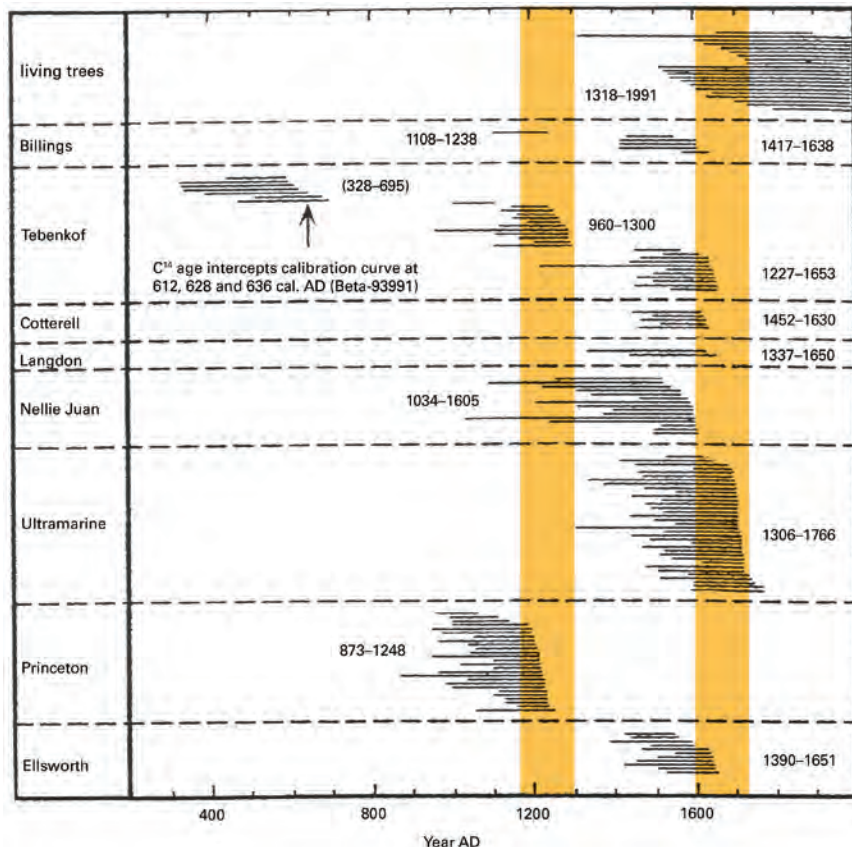


**Figure 294.**—Lifespans of cross-dated, glacially overridden subfossil trees collected from areas adjacent to the termini of seven glaciers in the Kenai Mountains and one glacier in the Chugach Mountains, western Prince William Sound. Dates indicate the timespan for each population of logs. General times of glacier advance in the western Prince William Sound area are colored orange. Figure modified from Wiles and others (1999).

### Unnamed Ice Field North of the Sargent Icefield

The northernmost of the Kenai Mountains ice fields, the unnamed ice field north of the Sargent Icefield, covers an area of about 500 km<sup>2</sup> (fig. 295A). It consists of a series of connected accumulation areas that support several dozen outlet glaciers. It is bounded on the west by Trail Creek and Placer River and on the east by Kings Bay and Nellie Juan River. Aside from the glaciers of Blackstone Bay—Concordia, Northland, Blackstone, Beloit, Marquette, Lawrence, and Ripon Glaciers—other major named glaciers that drain from this ice field include Portage, Burns, Whittier, Tebenkof, Rainey, Cotterell, Taylor, Claremont, Wolverine, Trail, Bartlett, Spencer, and Skookum Glaciers. Blackstone and Beloit Glaciers have tidewater termini (fig. 41; tables 2, 3). All of these glaciers have retreated significant distances since they were first observed. Wolverine Glacier has been monitored annually since 1966 by USGS glaciologists.

#### Portage Glacier

During the 1990s, Portage Glacier retreated around a bend in its valley and was no longer visible from a USFS Visitors Center constructed at the position of its late 19th century “Little Ice Age” maximum advance. Prior to 1794, the glacier was at a position several kilometers to the southeast, permitting an ice-free passage (a portage) between Turnagain Arm and Prince William Sound. After 1794, Portage Glacier advanced and, according to Tarr and Martin (1914), reached its most recent maximum position about 1880. [Editors’ note: According to Austin Post (written commun., 2004), the start of the advance of Portage Glacier occurred considerably earlier than the late 18th century. Crossen’s (1990) recent fieldwork confirmed the early advance.] Viereck (1967) dated its maximum forward position at about 1895 on the basis of botanical evidence. A portage was still possible but required an overice journey of more than 7 km (Mendenhall, 1900). During the advance, the terminus bifurcated, and a limb of the much thicker glacier extended

about 1.5 km into a side valley flowing toward the head of Passage Canal. Much of the ice was contributed by Burns Glacier, then a tributary of Portage Glacier that merged with it from the east. Retreat and thinning led to the limb's disappearance early in the 20th century. The maximum advance of the western lobe of the glacier is marked by a late 19th century end moraine that serves as the topographic high, damming the western end of Portage Lake. Portage Glacier was near this position when it was first photographed in 1914, but the presence of a small ice-marginal lake may indicate that the terminus has retreated somewhat on its southwestern side. By 1950, the date of the first USGS map of the area (Seward D-5, 1:63,360-scale topographic map) (appendix B), the terminus had retreated about 2.5 km from the moraine for an average rate of about  $70 \text{ m a}^{-1}$ . By 8 August 2000, the glacier had retreated almost another 2 km, creating a lake about 4 km long (fig. 295B) (see also 3 September 1966 oblique aerial photograph by Austin Post, USGS photograph no. 644-58). Burns Glacier maintained contact with Portage Glacier until the early 1980s, when its continued thinning caused it to lose contact.

The maximum advance, which ended in the late 1800s, caused a major change in the basin now occupied by Portage Lake. Before the advance, the sediment-filled basin created a land passage to Prince William Sound. During the advance, the basin sediments were overridden, eroded, and replaced by advancing ice to the limit of the end moraine. Eroded sediment was transported toward Turnagain Arm by Portage Creek. When Portage

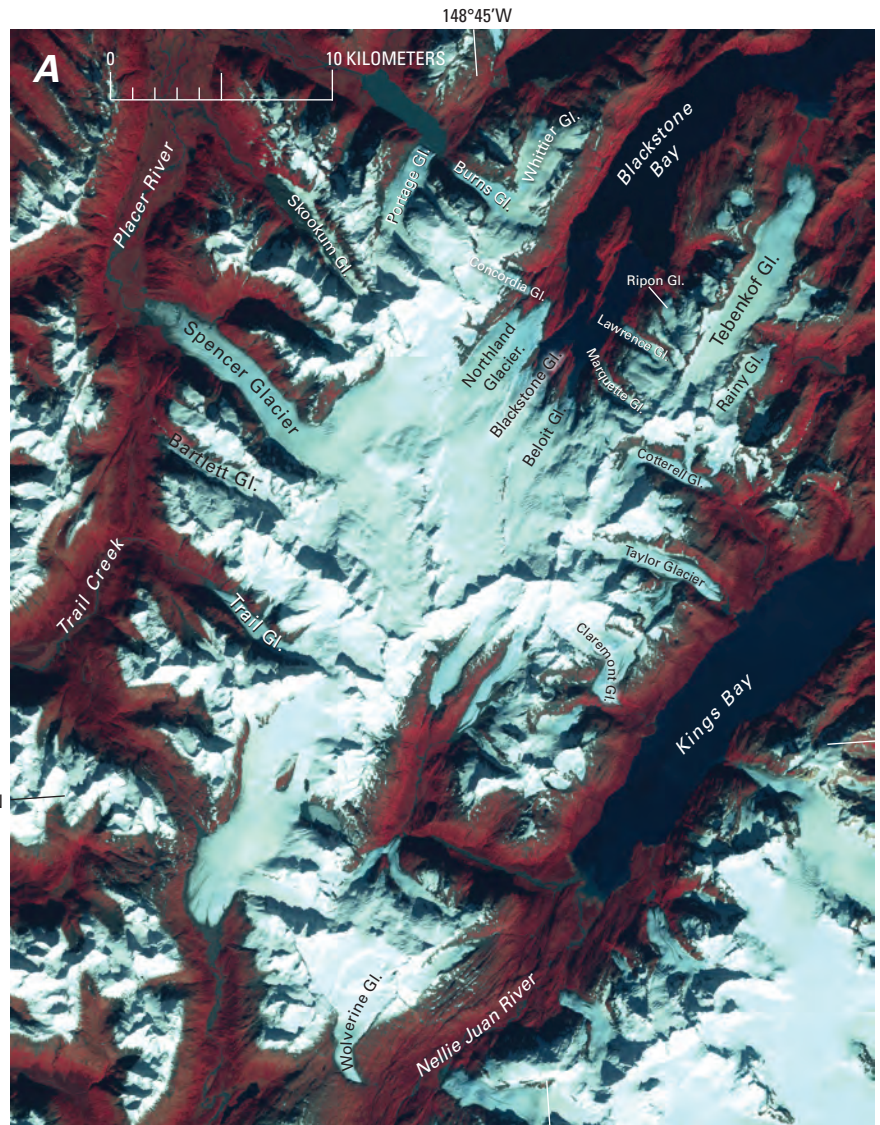


**Figure 295.**—A Landsat image and an oblique aerial photograph of an unnamed ice field north of Sargent Icefield, and Portage Glacier one of its major outlet glaciers. **A**, Annotated digital enlargement of a Landsat 7 ETM+ image (7067018009926950; 26 September 1999; Path 67, Row 18) from the U.S. Geological Survey, EROS Data Center, Sioux Falls, S. Dak. Burns Glacier, the tributary that joined Portage Glacier from the east is closest to its terminus. **B**, see following page.



**Figure 295.**—**B**, 8 August 2000 southwest-looking oblique aerial photograph showing Portage Glacier and the entire length of the lake formed by its retreat. Also barely visible are fuel storage tanks at Whittier in the lower right corner of the photograph. Photograph by Bruce F. Molnia, U.S. Geological Survey.

Glacier subsequently retreated, the basin did not refill with sediment but remained relatively sediment free. R.A.M. Schmidt (reported by Field, 1975d) determined that the basin had a maximum depth of 181 m at a location about 300 m in front of the 1964 terminus position.

### Whittier Glacier

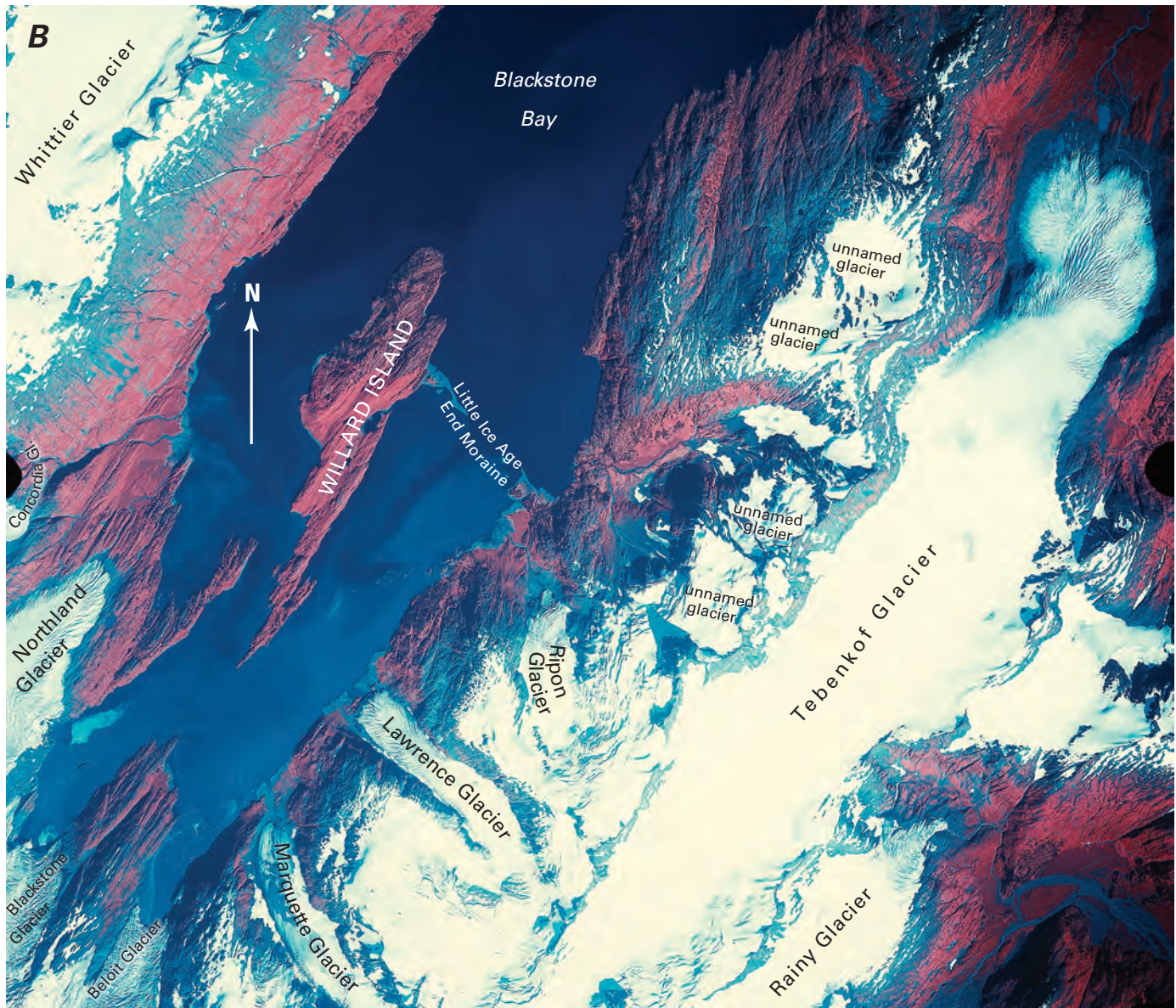
Whittier Glacier was investigated by Barnes (1943), who reported that, between 1913 and 1939, the terminus of Whittier Glacier had retreated “several hundred feet” and that the elevation of the terminus had increased from 180 to about 300 m. The terminus was in this position when it was mapped in 1950 (USGS, 1950) (Seward topographic quadrangle maps, appendix B) and when it was photographed by Post in 1964 (Field, 1975d). When the author flew over the glacier in 2000 and again in 2002, it showed evidence of recent thinning and retreat.

### Glaciers of Blackstone Bay

Blackstone Bay (fig. 296) and Blackstone Glacier were named in 1899 for a miner who lost his life on the glacier in 1896 (Mendenhall, 1900). The glaciers of the bay were first mapped by Grant and Higgins (1913, fig. 5) on 5 July 1909. Nearly a dozen glaciers descend to near sea level; Blackstone and Beloit Glaciers, both located at the head of the bay, reach tidewater. Blackstone Glacier had a length of 12.1 km, an area of 32 km<sup>2</sup>, an accumulation area of 29 km<sup>2</sup>, an ablation area of 2 km<sup>2</sup>, a width at its face of 0.5 km, and an AAR of 0.92 (Viens, 1995) (table 2). Beloit Glacier had a length of 10.1 km, an area of 25 km<sup>2</sup>, an accumulation area of 24 km<sup>2</sup>, an ablation area of 1 km<sup>2</sup>, a width at its terminus of 0.44 km, and an AAR of 0.95 (Viens, 1995) (table 2). Although both glaciers were still tidewater glaciers when the author visited them in September 2000 and observed them from the air on 3 September 2002 and in 2004, they showed exposed bedrock along their margins and evidence of recent thinning.

As in nearby College Fiord [Editors’ note: Fjord is used throughout the text in its geological, glaciological, and geomorphological sense as it applies to the glaciated and glacierized coast of Alaska (Jackson, 1997, p. 237). Its anglicized variant, fiord, is used in geographic place-names of Alaska and is used in the identical sense as fjord.], many of the glaciers here were named for colleges. Northland, Ripon, Lawrence, Marquette, and Beloit Glaciers were all named in 1910 by Martin (1913) for schools in Wisconsin. Northland Glacier, named for Northland College in Ashland, Wisc., is about 9 km long and previously reached tidewater, probably in the middle 19th century.

► **Figure 296.**—Two aerial photographs of Blackstone Bay. **A**, 8 August 1981 south-looking oblique aerial photograph showing the southern half of Blackstone Bay including Willard Island. Most of the glaciers that drain into or near the bay can be seen (left to right): Ripon, Lawrence, Marquette, Beloit, Blackstone, Northland, and Concordia. All are retreating and thinning. Photograph by Bruce F. Molnia, U.S. Geological Survey. **B**, 12 August 1984 AHAP false-color vertical photograph (L113F7087) of the upper two-thirds of Blackstone Bay, including Willard Island and its “Little Ice Age” end moraine. All of the glaciers that drain into or near the bay can be seen. These include Tebenkof Glacier, which flows into the north end of the bay; Ripon, Lawrence, Marquette, Beloit, Blackstone, Northland, and Concordia Glaciers and four unnamed glaciers on the northeast side of the bay. Also visible are Rainy and Whittier Glaciers, located in basins to the east and west. All of the valley glaciers shown on this image, located in the southeastern part of the unnamed ice field north of the Sargent Icefield, show evidence of thinning and retreat. AHAP photograph from the GeoData Center, Geophysical Institute, University of Alaska, Fairbanks, Alaska.



Lawrence Glacier (fig. 297), named for Lawrence College in Appleton, Wisc., is about 4 km long. As have all the valley glaciers on the eastern side of Blackstone Bay, it has thinned and retreated during the 20th century. Between the author's visits in 1978 and 2000, Lawrence Glacier retreated more than 100 m and thinned as much as 40 m.

A conspicuous submarine terminal moraine, part of which is exposed under most tidal conditions, connects Willard Island in the middle of Blackstone Bay with its eastern shore. Grant and Higgins (1913), who first studied the bay in 1909, suggested that the moraine predates the early 18th century.

Tebenkof Glacier (fig. 298), which drains into Blackstone Bay near its mouth and was named for the last Governor General of Russian America, is 13 km long and has an area of about 28 km<sup>2</sup> (Field, 1975d, p. 527; Tarr and Martin, 1914, pl. CXII, ff p. 352.) Until the 19th century, it had a small piedmont lobe and probably had a terminus ending in the tidewater (see map by Wiles and others, 1999a). Today, it is fronted by several large ice-marginal lakes and a large glacial outwash plain. Through the early 21st century, Tebenkof Glacier retreated more than 3.0 km and thinned by several hundred meters. As do all the other glaciers in Blackstone Bay, it continues to retreat and thin.

Wiles and others (1999a), found evidence that Tebenkof Glacier has advanced several times during the past 1,500 years (fig. 294). Seven logs that grew between A.D. 328 and A.D. 695 were found about 1.5 km in front of the 1992 ice margin, suggesting an early glacier advance at approximately A.D. 700 (approximately 1300 years B.P.). Twelve logs that grew between A.D. 960 and A.D. 1300, were found between 0.7 and about 1.5 km in front of the 1992 ice margin, suggesting a second glacier advance beginning between A.D. 1289 and A.D. 1300 (approximately 700 years B.P.). Another group of 11 logs represent trees felled by the advancing glacier between A.D. 1633 and A.D. 1653 and suggest a third advance approximately 350 years B.P. Wiles and others' (1999a) analysis of recent moraines suggested that ice retreat from this approximately 350-year-old maximum position of the glacier began before 1891. They stated (Wiles and others, 1999a, p. 167) that "the 1891 maximum was the greatest extent of Tebenkof Glacier since at least A.D. 1189." They also documented an 1891 to 1992 retreat of 2.7 km, with 1 km of retreat between 1983 and 1992.

### Glaciers of the Western Side and South of Kings Bay

Kings Bay is the western extension of the bay called Port Nellie Juan. Taylor Glacier (fig. 299) (see also 13 August 1982 AHAP photograph L115F1490) has a length of 8 km and an area of 23 km<sup>2</sup> (Field, 1975d, p. 527) and has been retreating since it was first observed in the latter part of the 19th century. About 1870, it had a tidewater terminus; in 1887, when it was first mapped by Applegate, its terminus failed to reach tidewater (Grant and Higgins, 1913). About 25 year later, when Grant and Higgins (1913) mapped it on 8 and 9 August 1909, its terminus again reached tidewater. The 1909 terminus position was about 400 m behind a trimline, probably related to the 1870 maximum (Field, 1975d) (AGS Glacier Studies Map No. 64-4-G6; Field, 1965). By 1924, Taylor Glacier had retreated another 200 m, and its terminus was adjacent to the inland side of a tidewater-influenced lake. When it was photographed in 1966, it had retreated another 600 m and barely made contact with the back edge of the lake basin. During the Landsat baseline period, retreat and thinning continued at an even more rapid rate. When the author observed the glacier from the air in July and August 2000, it had retreated about 2.2 km from its late 19th century position.

Cotterell Glacier, now 4 km long [8 km long, 18 km<sup>2</sup> in area, according to Field (1975d, p. 527)], is another glacier that has experienced a significant amount of recent retreat. Aerial photographs taken in 1966, 1977, and 2000

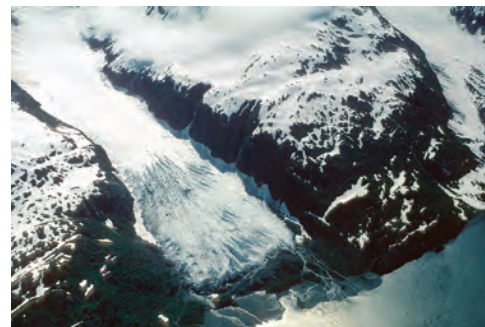


**Figure 297.**—15 July 2000 southeast-looking oblique aerial photograph of the terminus of the Lawrence Glacier showing ice-marginal lakes formed by terminus retreat and thinning of the margin. Photograph by Bruce F. Molnia, U.S. Geological Survey. A larger version of this figure is available online.



**Figure 298.**—15 July 2000 south-looking oblique aerial photograph of the terminus of Tebenkof Glacier showing ice-marginal lakes formed by terminus retreat and the expanding outwash plain. Former positions of its terminus are marked by lakes, trimlines, and moraines. Since 1891, the glacier has thinned by more than 100 m, and parts of its terminus have retreated by more than 3 km. Photograph by Bruce F. Molnia, U.S. Geological Survey. A larger version of this figure is available online.



**Figure 299.**—3 September 1966 oblique aerial photograph of much of Taylor Glacier. Also visible is the adjacent Cotterell Glacier. USGS photograph no. 664–62 by Austin Post, U.S. Geological Survey.

show that the glacier has retreated more than 1.5 km and thinned by more than 50 m during that period of time.

Wiles and others (1999a) found five transported logs that represent trees felled between A.D. 1611 and A.D. 1630, suggesting an advance of the glacier approximately 370 to 390 years B.P. (fig. 294). Their analysis of recent moraines suggested that the “Little Ice Age” maximum position—3.1 km inland from Kings Bay—was reached in 1891.

Claremont Glacier, 6 km long, was named in 1910 by U.S. Grant, who intended to name it for Robert Fulton’s steamboat *Clarmont*, but he misspelled the name. When Grant and Higgins (1913) first observed Claremont Glacier in 1909, it was located about 300 m behind a moraine that marked its late 19th century position. Subsequent retreat has caused the glacier to separate into two retreating tributaries, as a 3 September 1966 oblique aerial photograph (fig. 300A) shows. The southern tributary is now located 2.5 km behind the 1909 moraine; the northern one is 3.5 km behind it. When the author observed them from the air on 15 July 2000 (fig. 300B), both tributary glaciers showed evidence of continued retreat and thinning; the southern tributary showed significantly more retreat than the northern tributary.



**Figure 300.**—Two aerial photographs showing changes of the Claremont Glacier between 1966 and 2000. **A**, 3 September 1966 oblique aerial photograph of the terminus of Claremont Glacier showing the two separated former tributaries of the glacier. At the end of the 19th century, they were connected and reached close to the location of the large right-angle bend in the river, near the mouth of the valley. USGS photograph no. 664-63 by Austin Post, U.S. Geological Survey. **B**, 15 July 2000 northwest-looking oblique aerial photograph of Claremont Glacier showing the two retreating, formerly joined tributaries. The northern lobe shows only a small amount of retreat, but the southern lobe appears to have lost an icefall to melting and has retreated about 800 m. Photograph by Bruce F. Molnia, U.S. Geological Survey. A larger version of B is available online.





## Glaciers of Upper Kings River

Several large unnamed glaciers serve as the source of the upper Kings River. All, including the two largest, show multiple signs of thinning and retreat. During the last quarter of the 20th century, each retreated about 500 m.

### Wolverine Glacier

Wolverine Glacier, as shown on a 3 September 1966 oblique aerial photograph (fig. 301A) (see also 14 August 1984 AHAP photograph L116F0251), has retreated nearly 3 km since the early 18th century (Wiles and others, 1999a). Three moraines dated at A.D. 1713, A.D. 1777, and A.D. 1807, located between 2 and 3 km downvalley from the glacier's terminus in the year 2000, document Wolverine Glacier's "Little Ice Age" maximum position and the location of two recessional moraines (fig. 301B). Wolverine Glacier is one of

three long-term glacier-monitoring sites operated by the USGS. The other two are Gulkana Glacier in the Alaska Range and South Cascade Glacier in the State of Washington. Climate, weather, glacier-motion, mass-balance, terminus position, and stream-flow data are recorded at the three monitoring sites to develop a better understanding of glacier-related hydrologic processes. Wolverine Glacier, which has a terminus elevation of about 400 m, has been studied by the USGS since 1966 (Tangborn and others, 1977) and was nearly stable from 1966 to 1976 but thickened more than 8 m from 1977 to 1982 (Mayo and Trabant, 1984; Mayo and others, 1985). It has since thinned more than 20 m. In the 29 years of measurements from 1966 to 1995, negative mass balances have occurred in 19 of those years. The annual range has varied from a low of -2.37 m in

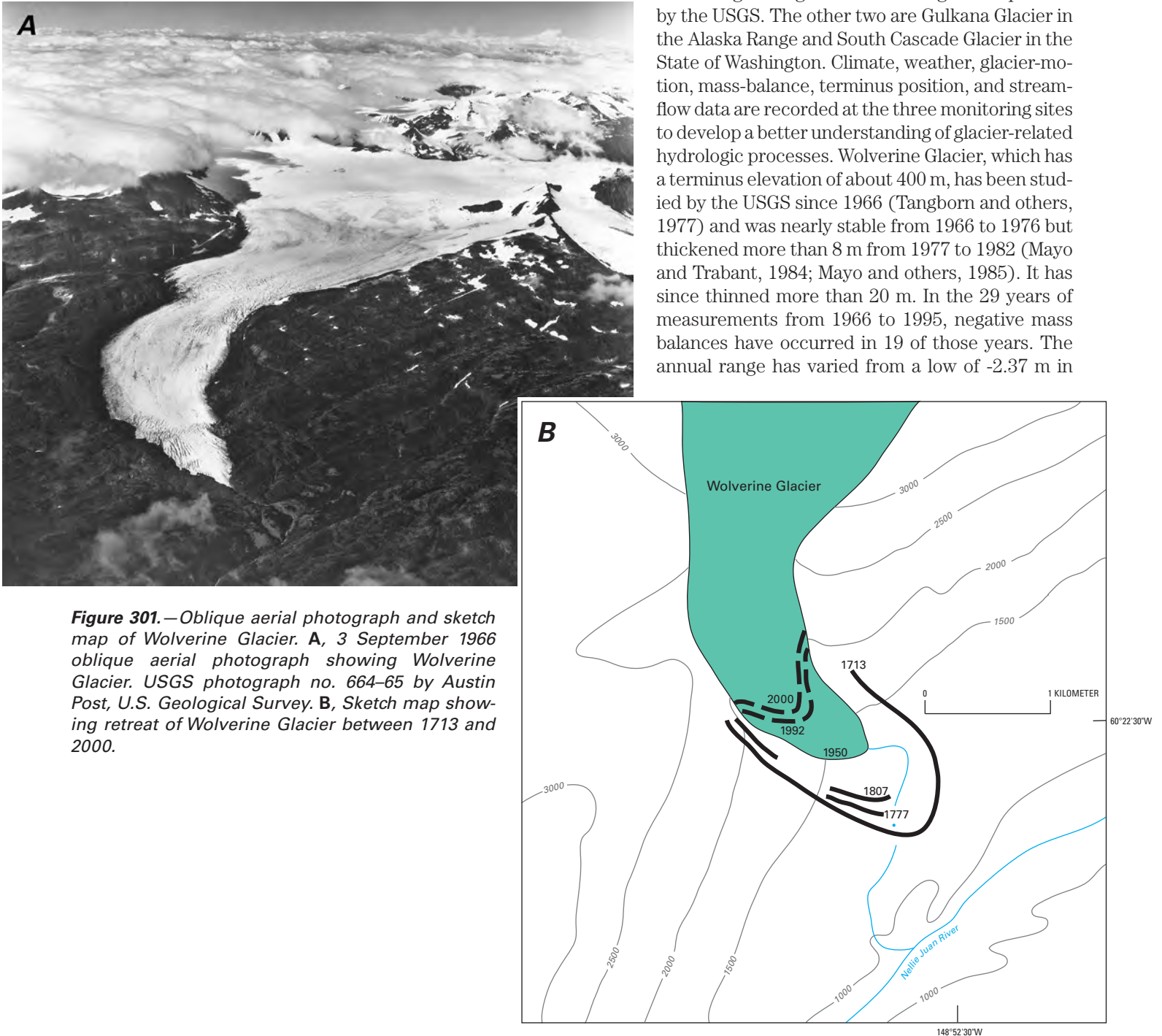


**Figure 301.**—Oblique aerial photograph and sketch map of Wolverine Glacier. **A**, 3 September 1966 oblique aerial photograph showing Wolverine Glacier. USGS photograph no. 664-65 by Austin Post, U.S. Geological Survey. **B**, Sketch map showing retreat of Wolverine Glacier between 1713 and 2000.

1991 to a high of +2.33 m in 1980. Mass balance has been positive every winter, ranging from a high of 4.21 m in 1977 to a low of 0.84 m in 1972. Mass balance has been negative every summer, ranging from a low of -4.23 m in 1981 to a high of -1.34 m in 1973 (Meier and others, 1971; Trabant and March, 1999). Between the 1950s and the middle 1990s, on an annual basis, Wolverine Glacier thinned by 0.519 m, had a volume decrease of 0.00957 km<sup>3</sup>, and had its length shortened by 6 m a<sup>-1</sup>. Between the middle 1990s and 1999, on an annual basis, the glacier thinned by 1.025 m and had a volume decrease of 0.0188 km<sup>3</sup> (K.A. Echelmeyer and others, University of Alaska Fairbanks, written commun., March 2001). A 30-year record of surface mass balance and shorter records of motion and surface altitude were recently published by the USGS (Mayo and others, 2004).

The Wolverine climate station is located at an altitude of 990 m on the crest of a tundra-covered glacial moraine along the western boundary of the basin. The station is slightly lower than the glacier's average ELA and about 500 m from the western edge of the glacier. The average annual air temperature at the recorder site is about -1°C, and the average annual precipitation gage total is about 1,100 mm. Snow is the dominant form of precipitation and usually accumulates on the glacier from September through mid-June. Daily average temperatures range from a low of -25°C to a high of +15°C. Daily precipitation totals range from a low of 0 to a high of approximately 110 mm (Kennedy, 1995; Mayo and others, 1992).

### **Glaciers of Snow River**

Several unnamed glaciers on the western side of the ice field serve as the source of the Snow River. The largest is about 13 km long and has an area of about 75 km<sup>2</sup>. When it was photographed in 1941 and again in 1950 (Field, 1975d), it was "at or close to" its "Little Ice Age" maximum position. Since then, it has retreated more than 0.5 km.

### **Trail Glacier**

Trail Glacier, previously named *Notch Creek Glacier*, was first studied during the construction of the Alaska Railroad, near the beginning of the 20th century (Tarr and Martin, 1914). The part of the glacier photographed by Capps (USGS Photo Library photograph Capps, S.R.12), sometime before 1910, had a large mass of morainic debris covering much of its surface. It was also photographed on 21 September 1911 by the USGS (Martin and others, 1915), but its terminus was obscured by trees. Wentworth and Ray (1936) reported that it had retreated about 1.2 km by 1931. By 1957, it had retreated another 500 m (Field, 1975d). When the author observed it from the air in 2000, the glacier was estimated to have retreated at least another 750 m.

### **Glaciers of Placer River**

Bartlett, Spencer, Deadman, and Skookum Glaciers and several unnamed glaciers, all located on the northwestern part of the ice field north of the Sargent Icefield, all drain into the Placer River. At the beginning of the 20th century, the terminus of Bartlett Glacier was located on the floor of the Placer River valley (21 September 1911 USGS photograph presented by Martin and others, 1915, pl. IXB). Because the terminus covered the only feasible railroad route through the valley, a 2-km-long looping elevated trestle had to be constructed to bypass it. By 1931, the glacier had retreated between 150 and 300 m from its maximum position (Wentworth and Ray, 1936). In the early 1940s, the glacier had retreated enough that the track could be lain over the preferred route, so the trestle was dismantled. Retreat has continued at a slow rate, so that, at the beginning of the 21st century, the terminus was a little more than 1 km from its maximum position.

A similar railroad construction problem was encountered at Spencer Glacier (20 September 1911 photograph presented by Martin and others, 1915,

pl. VIII; 12 August 1984 AHAP photograph L113F7084). At the beginning of the 20th century, the terminus of Spencer Glacier (19 km long and 82 km<sup>2</sup> in area) (Field, 1975d, p. 528) was within 60 m of its 19th century “Little Ice Age” maximum terminal moraine (Viereck, 1967), a position that the glacier reached about 1880. When track was laid on the surface of this moraine, drainage channels were blasted and constructed in the glacier ice and on the adjacent outwash plain to prevent washouts (Tarr and Martin, 1914). By 1931, the glacier had retreated about 640 m (Wentworth and Ray, 1936). By 1964, retreat totaled about 1.2 km (Field, 1975d). When the author observed it from the air in 2000, he estimated that the glacier had retreated at least another 800 m.

### Sargent Icefield

More than 25 outlet glaciers descend from the central accumulation area of the 60×40-km Sargent Icefield (fig. 302). Many of the glaciers draining the

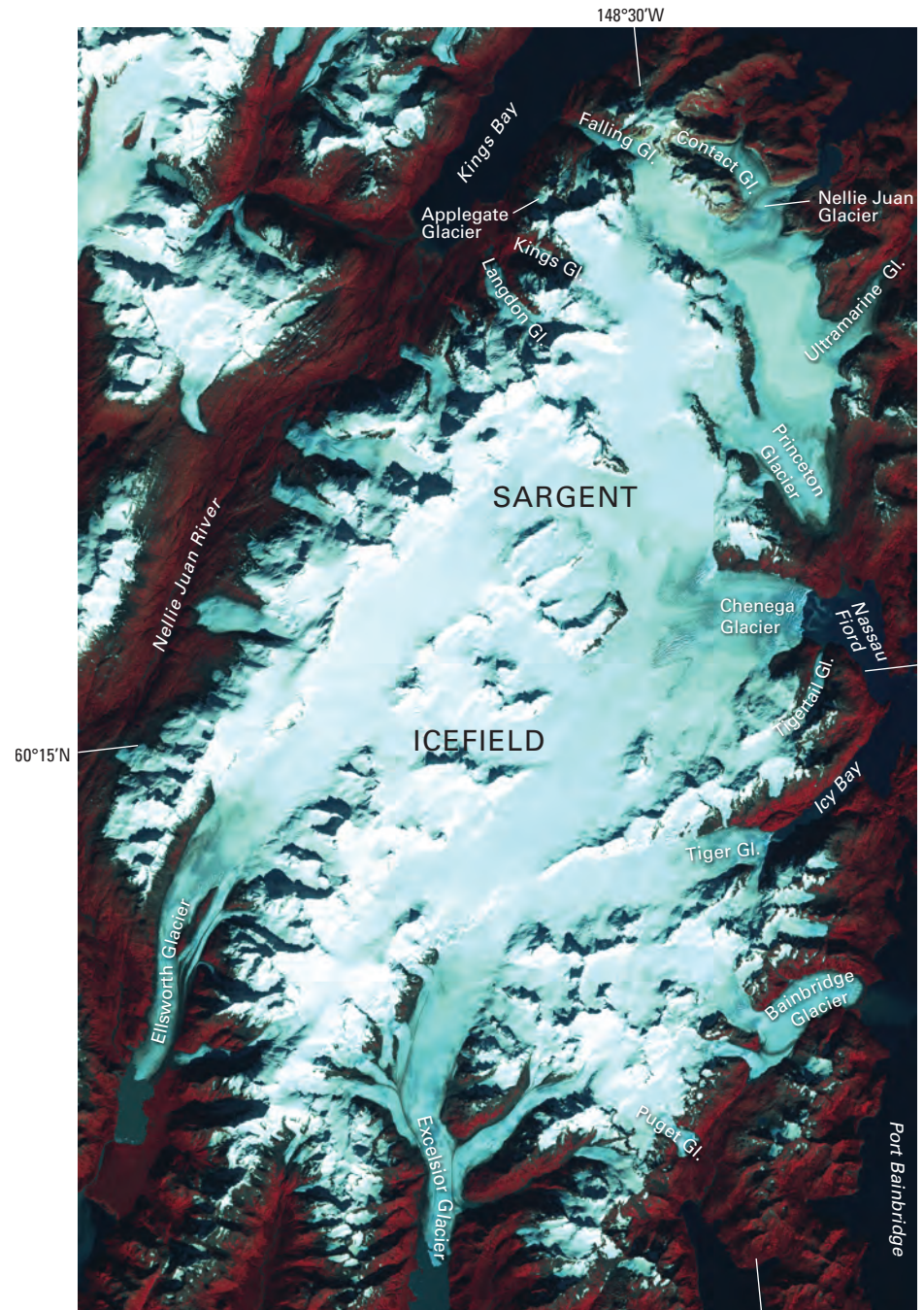


**Figure 302.**—Digital enlargement of a Landsat 7 ETM+ (Enhanced Thematic Mapper Plus) false-color composite image showing the Sargent Icefield. Landsat 7 ETM+ image (7067018009926950; 26 September 1999; Path 67, Row 18) from the U.S. Geological Survey, EROS Data Center, Sioux Falls, S.Dak.

northern, eastern, and southern margins of the ice field end at or near sea level in Kings Bay, Port Nellie Juan, Nassau Fiord, Icy Bay, Port Bainbridge, Puget Bay, Johnstone Bay, and Whidbey Bay. Glaciers flowing from the western side of the ice field all end on land and drain into the Nellie Juan River. Only a few of these have official names. The largest glaciers draining the ice field are 27-km-long Ellsworth and 24-km-long Excelsior Glaciers (Field, 1975d, p. 529–530) and the 24.1-km-long Chenega Glacier (Viens, 1995) (table 2). Three glaciers—Nellie Juan, Chenega, and Tiger—have tidewater termini. All the outlet glaciers of the Sargent Icefield show significant evidence of retreat and thinning.

### Glaciers on the Eastern Side of Kings Bay

Several named and unnamed glaciers drain into the southeastern side of Kings Bay, the western extension of Port Nellie Juan. The largest, Falling Glacier (11 km long, 35 km<sup>2</sup> in area, according to Field, 1975d, p. 528) was first observed and its terminus position mapped on 8 and 9 August 1908 by Grant and Higgins (1913). At that time, “a small tongue from the ice just reached the sea” (Grant and Higgins, 191, p. 46). Based on vegetative evidence, Viereck (1967) dated the formation of its “Little Ice Age” maximum terminal moraine at about 1875 to 1885. As late as 1950, although part of the terminus was adjacent to the end moraine and may have been in contact with Kings Bay, the margins of the glacier were in retreat (Field, 1975d). By 1982, the terminus had retreated more than 1 km from its 1950 position. Since then, the glacier has retreated at least 600 m and thinned significantly (fig. 303). When they were photographed from the air in 1966 and again on 15 July 2000, Applegate, Kings, and Langdon Glaciers and an unnamed glacier, all located near the head of the fjord, showed evidence of continuing thinning and retreat (fig. 304).

According to Wiles and others (1999a), Kings Glacier was a former tributary to Langdon Glacier, and together they produced a “Little Ice Age” maximum moraine located about 2.3 km downvalley from their individual late 20th century positions. Two logs found about 1.8 km in front of the 1992 ice margin were from trees overridden in A.D. 1624 and A.D. 1650, suggesting a



**Figure 303.**—Three photographs, dating from 1924 to 2000, showing changes in the terminus of Falling Glacier. **A**, 1924 photograph by Fred Moffit of the lower reaches of Falling Glacier from the west side of Kings Bay. At the time of this photograph, the central part of the glacier’s terminus still reached tidewater. USGS Photo Library photograph Moffit 1014. **B**, 3 September 1966 southeast-looking oblique aerial photograph of the terminus of Falling Glacier, which is located about 350 m from the shore of Kings Bay. The glacier has thinned appreciably along its western margin. USGS photograph no. 664–71 by Austin Post, U.S. Geological Survey. **C**, 15 July 2000 east-looking oblique aerial photograph of the lower third of Falling Glacier showing its retreating terminus and newly formed ice-marginal lake. Total retreat from its early 20th century position approaches 3.5 km. Photograph by Bruce F. Molnia, U.S. Geological Survey. Larger versions of A and C are available online.





**Figure 304.**—3 September 1966 oblique aerial photograph looking southeast shows the termini of Applegate Glacier (left) and Langdon Glacier (right). Both show evidence of significant recent thinning and retreat. Langdon Glacier has several elevated medial moraines, whereas Applegate Glacier has a very large elevated lateral moraine on its southeast side. USGS photograph no. 664-72 by Austin Post, U.S. Geological Survey.

significant advance approximately 350 years B.P. Between 1889 and the end of the 20th century, Langdon Glacier retreated more than 2 km. However, Wiles and others (1999a) reported that, in 1992, the glacier was advancing and overriding alders that were estimated to be 10 to 20 years old. The author observed no evidence of a continued advance from the air in 2000.

### **Glaciers of Port Nellie Juan**

The glaciers of Port Nellie Juan were first mapped on 8 and 9 August 1908 by Grant and Higgins (1913). Deepwater Bay, Derickson Bay, and Blue Fiord are embayments at the head of Port Nellie Juan. The westernmost of the three named glaciers is Contact Glacier (fig. 302), located about 2 km from the head of Deepwater Bay. When it was observed in 2000, the terminus of Contact Glacier showed multiple evidence of continuing rapid thinning and retreat. Between 1909 and 2000, the terminus of Contact Glacier retreated about 1 km.

Adjacent Nellie Juan Glacier has changed as dramatically as any glacier in the Sargent Icefield. Viereck (1967) stated that Nellie Juan Glacier had

reached its late “Little Ice Age” maximum position between 1860 and 1880. Wiles and others (1999a) identified an advance of the glacier that felled trees between A.D. 1594 and A.D. 1605. They stated that Nellie Juan Glacier had reached its “Little Ice Age” maximum by 1842 and oscillated at this position until general retreat began around 1893. By 1908, retreat was minimal, ranging from 30 to 150 m (Grant and Higgins, 1913). When Moffit photographed the terminus position in 1924, little had changed; one area had actually advanced beyond the 1908 position. By 1935, the glacier had retreated 470 m on its eastern side and 580 m on its western side (Field, 1937) and had deposited a large moraine that blocked much of the head of Derickson Bay. By 3 September 1966, the glacier had retreated another 950 to 1500 m (fig. 305). A tidal river flowing through the 1935 moraine connected the ice-marginal basin, which expanded in area as the glacier continued to retreat, with Derickson Bay. When the author observed it from the air in 2000, the glacier was about 3 km from its 1935 position. It had a length of about 14.5 km, an area of 56 km<sup>2</sup>, an accumulation area of 51 km<sup>2</sup>, an ablation area of 5 km<sup>2</sup>, a width at

**Figure 305.**—3 September 1966 oblique aerial photograph showing the terminus and most of the accumulation area of Nellie Juan Glacier. Fresh bedrock and trimlines near the terminus document ongoing thinning and retreat. USGS photograph no. 664-75 by Austin Post, U.S. Geological Survey.



its face of 0.5 km, and an AAR of 0.91 (Viens, 1995) (table 2). The terminus is now located in a vegetation-free granite fjord.

Wiles and others (1999a) described a sequence of logs dated between A.D. 1692 and A.D. 1715 that represent trees killed by an advance of 8-km-long Ultramarine Glacier. Other stumps were overridden about A.D. 1766 (fig. 294). Viereck (1967) determined that Ultramarine Glacier, which had a length of 9 km and an area of 30 km<sup>2</sup> (Field, 1975d, p. 529), sat at its “Little Ice Age” maximum position from about 1880 to 1890. Wiles and others (1999a) dated the stabilization of the glacier’s terminus at 1889. By 1908, when Grant and Higgins (1913) observed the glacier, it had retreated about 400 m; it retreated another 300 m through 1935 and another 300 m through 1964 (Field, 1975d). Because the end moraine is nearly 3 km from the present margin, the glacier retreated nearly 2 km between 1964 and 2000. In 2000, the terminus of Ultramarine Glacier was surrounded by an apron of morainic-debris-covered stagnant ice and was located at the head of a 2.25-km-long proglacial lake about 4 km from Blue Fiord. The terminus was surrounded by a halo of fresh vegetation-free deglaciated bedrock.

### Glaciers of Icy Bay

The glaciers of Icy Bay and Nassau Fiord, its northwestern arm, were mapped on 5 August 1908 by Grant and Higgins (1913). Chenega, Princeton, and Tiger Glaciers are the three largest glaciers. Chenega Glacier (fig. 306), a tidewater glacier and the largest of the three, has a length of 24.1 km and an area of 369 km<sup>2</sup> (AGS Glacier Studies Map. No. 64-4-G5; Field, 1965) (see also 1924 photograph by Fred Moffit, USGS Photo Library Moffit 974; 3 September 1966 oblique aerial photograph by Austin Post, USGS Photograph no. 664-79). Chenega Glacier has an accumulation area of 346 km<sup>2</sup>, an ablation area of 23 km<sup>2</sup>, a width at its terminus of 0.2 km, and an AAR of 0.94 (Viens, 1995) (table 2). From vegetative evidence, Viereck (1967) determined that Chenega Glacier sat at its “Little Ice Age” maximum position during the second half of the 19th century (about 1857-72). At that time, Chenega, Princeton, and Tigertail Glaciers were joined and reached to the head of Nassau Fiord. Wiles and others (1999a) described several dozen detrital logs from around the perimeter of Princeton Glacier that confirm that the glacier was advancing towards its “Little Ice Age” maximum position before A.D. 1250 (fig. 294).

By 1908, when it was observed by Grant and Higgins (1913), Chenega Glacier had retreated about 5.5 km and had separated from Tigertail and Princeton Glaciers. Since 1908, Chenega Glacier’s terminus has stayed within 1 km of this position (fig. 307). When the author observed the glacier from the air in 2000, freshly exposed bedrock and evidence of minor thinning suggested that it had recently retreated several hundred meters.

When Grant and Higgins (1913) viewed Princeton Glacier in August 1908, it had a massive moraine along its front, but its western side reached tidewater. Between 1908 and 1950, Princeton Glacier retreated about 1.5 km from shore and thinned by at least 60 m. Since then, it has retreated an additional 2.5 km. Similarly, Tigertail Glacier (fig. 306) retreated from the shore in the first decades of the 20th century and now sits a few hundred meters from the fjord. Field (1975d) reported that two small moraines dating from 1950 and 1960 mark brief mid-20th century advances. When the author observed the glacier from the air in 2000, freshly exposed bedrock and evidence of thinning suggested that it is continuing its retreat.

Tiger Glacier (fig. 308) is located at the head of Icy Bay (see 13 August 1984 AHAP photograph L118F1580). The glacier has a length of 11.3 km, an area of 56 km<sup>2</sup>, an accumulation area of 50 km<sup>2</sup>, an ablation area of 6 km<sup>2</sup>, a width at its face of 0.8 km, and an AAR of 0.89 (Viens, 1995) (table 2). Tiger Glacier slowly advanced during the first third of the 20th century. Field (1975d, p. 513) reported that, in 1935, it was “slightly” in advance of its 1908



**Figure 306.**—15 July 2000 southwest-looking oblique aerial photograph of the terminus of Chenega Glacier. Tigertail Glacier can be seen on the left side of the photograph. An apron of freshly exposed bedrock documents recent thinning of the glacier. Several calving embayments mark the front of the glacier. Photograph by Bruce F. Molnia, U.S. Geological Survey. A larger version of this figure is available online.



**Figure 307.**—Two photographs showing late 20th century changes in Nassau Fjord between 1966 and 2000. **A**, 3 September 1966 oblique aerial photograph showing part of the terminus of Chenega Glacier and nearly all of Princeton Glacier. Chenega Glacier is little changed since 1908. Princeton, however, is retreating and thinning significantly. USGS photograph no. 664-78 by Austin Post, U.S. Geological Survey. **B**, 15 July 2000 northwest-looking oblique aerial photograph of the termini of Chenega and Princeton Glaciers. Although Chenega Glacier shows a retreat of only several hundred meters, the terminus of the retreating and thinning Princeton Glacier has retreated more than 1 km since the 1966 photograph. Photograph by Bruce F. Molnia, U.S. Geological Survey.



**Figure 308.**—Two photographs showing the late 20th century position of Tiger Glacier between 1966 and 2000. **A**, 3 September 1966 oblique aerial photograph of the terminus of Tiger Glacier. USGS photograph no. 664–80 by Austin Post, U.S. Geological Survey. **B**, 15 July 2000 southwest-looking oblique aerial photograph of the terminus of Tiger Glacier. Little evidence of change in Tiger Glacier can be seen in this photograph. Photograph by Bruce F. Molnia, U.S. Geological Survey. A larger version of B is available online.



position, but that, by the 1960s (fig. 308A), “considerable recession” had occurred. When it was observed on 15 July 2000 (fig. 308B), Tiger Glacier’s margins were very close to those displayed in a 1908 photograph made by Grant and Higgins (1913). Many small glaciers on the walls of the fjord have almost completely melted away.

### Glaciers of Port Bainbridge

At the beginning of the 21st century, the terminus of 16-km-long Bainbridge Glacier (Viens, 1995) (table 2) sat about 300 m from the head of a short western arm of the Port Bainbridge fjord. According to Grant and Higgins (1913), who mapped the position of the glacier on 3 August 1908, the glacier was located on an outwash plain that was covered by normal high tides (3 August 1908 photograph by Grant and Higgins, 1913, pl. XXIXB). They observed fresh push moraines along the glacier’s margin, some with fresh tree material incorporated into them. They stated (p. 51), “In 1908, the ice was practically, if not absolutely, at its limit of maximum advance since the growth of the present forest.” Viereck (1967) determined that the glacier experienced a small advance about 1934 and overrode its 1908 moraine. The glacier had an area of 56 km<sup>2</sup>, an accumulation area of 39 km<sup>2</sup>, an ablation area of 17 km<sup>2</sup>, and an AAR of 0.70 (Viens, 1995) (table 2); it had retreated several hundred meters by 2000 and had most of its terminus fronted by an arcuate ice-marginal lake. A braided outwash plain was located on the southern side of the glacier’s terminus, as a 15 July 2000 oblique aerial photograph taken by the author shows (fig. 309). Small glaciers also exist south of Claw Peak on the western side of Port Bainbridge (13 August 1982 AHAP photograph L118F1582).



**Figure 309.**—15 July 2000 west-looking oblique aerial photograph of the lower part of Bainbridge Glacier showing its retreating terminus and ice-marginal lake. Total retreat from its early 20th century position is about 300 to 400 m. Photograph by Bruce F. Molnia, U.S. Geological Survey. A larger version of this figure is available online.

### Glaciers of the Puget Bay Region

Puget Glacier, located about 2.5 km north of the head of the bay, is the only named glacier among the half-dozen or so that drain into Puget Bay (3 September 1966 oblique aerial photograph by Austin Post, USGS photograph

no. 664–83). This glacier was depicted on 19th century maps made by the Russian-America Company (Teben'kov, 1852) and was first investigated and mapped on 11 July 1909 by Grant and Higgins (1913). Investigations in 1966 determined that the valley below the glacier contained several moraines dating from before 1750, 1830, 1930, and 1950. The pre-1750 moraine was located about 1 km from the 1966 terminus. The distance between the 1950 moraine and the 1966 moraine was about 90 m. When the author photographed the glacier from the air in 2000, it showed continued thinning around its margins and retreat of its terminus. The 2000 terminus position was 250 to 400 m from its 1966 position.

### Glaciers of Johnstone Bay

When Grant and Higgins (1913) sailed past the terminus of 19-km-long Excelsior Glacier (fig. 310) in 1909, it was located on an outwash plain about 1 km from the head of Johnstone Bay. They commented that a very large bare area surrounding the glacier indicated that it had been much larger in the recent past and that it might have had a marine terminus.

Wiles and others (1999a) identified a late 19th century moraine seaward of and close to the 1908 location of the glacier but found no evidence of a marine terminus. By 1950, the distance from the head of Johnstone Bay to the retreating terminus had increased to about 3 km; a large ice-marginal lake occupied the 2 km adjacent to the glacier's margin. By 3 September 1966, the glacier had retreated an additional kilometer (fig. 310A). Between 1966 and 1991, the lake lengthened by an additional 2 km, with a maximum length of 5 km. Field (1975d, p. 529) stated that Excelsior Glacier was 24 km long and 170 km<sup>2</sup> in area. When the author photographed it from the air on 15 July 2000, Excelsior Glacier showed continued thinning and retreat of its terminus (fig. 310B). The area in 2000 was about 160 km<sup>2</sup>, and the terminus position was more than 3.5 km from its 1966 location. Both the 1966 and 2000 aerial photographs show that Excelsior Glacier calves large tabular icebergs.



**Figure 310.**—Three aerial photographs of Excelsior Glacier showing changes between 1966 and 2000. **A**, 3 September 1966 oblique aerial photograph showing the terminus and much of the accumulation area of Excelsior Glacier. The fractures that cut across the entire terminus suggest that it was actively calving, retreating, and disintegrating when photographed. USGS photograph no. 664–86 by Austin Post, U.S. Geological Survey. **B** and **C**, see opposite page.

Excelsior Glacier's southeasternmost unnamed tributary separated from the main glacier and experienced about 4 km of retreat, resulting in a conspicuous ice-free valley on the eastern side of Excelsior Glacier's valley. Thinning and retreat of this former tributary, probably in the 1950s, resulted in a reversal of flow direction, the creation of a distributary glacier, and the formation of a 4-km-long ice-marginal lake, as a 3 September 1966 oblique aerial photograph shows (fig. 310C).

**Figure 310.**—**B**, 15 July 2000 north-looking oblique aerial photograph of most of Excelsior Glacier, its ice-marginal lake, and the head of Johnstone Bay. In the 34 years between photographs, the glacier significantly thinned and retreated as much as 5 km. Note the large tabular icebergs, evidence of continued calving and disintegration. Photograph by Bruce F. Molnia, U.S. Geological Survey. **C**, 3 September 1966 oblique aerial photograph showing a distributary of the Excelsior Glacier. The pre-1966 retreat of the tributary glacier, probably in the 1940's and 1950's, which was previously joined with the Excelsior Glacier on its eastern margin, resulted in a reversal of flow direction (from tributary to distributary glacier) and the formation of a 4-km-long ice-marginal lake. USGS photograph no. 664-84 by Austin Post, U.S. Geological Survey.



## Glaciers of Day Harbor

Ellsworth Glacier (fig. 311), 27 km long and 137 km<sup>2</sup> in area (Field, 1975d, p. 530), empties into a moraine-dammed lake above the head of Day Harbor. When Grant and Higgins (1913) visited and mapped it on 12 July 1909, the terminus of Ellsworth Glacier was retreating and was located about 2.5 km from the head of Day Harbor. This location was close to Ellsworth's "Little Ice Age" maximum position, which was reached before 1855 (Wiles and others, 1999a).



**Figure 311.**—Two aerial photographs of Ellsworth Glacier showing changes between 1966 and 2000. **A**, 3 September 1966 oblique aerial photograph showing the lower part of Ellsworth Glacier. The glacier retreated about 3 km from its position on the 1909 sketch map by Grant and Higgins (1913). USGS photograph no. 664–87 by Austin Post, U.S. Geological Survey. **B**, 15 July 2000 north-looking oblique aerial photograph of most of Ellsworth Glacier. Compared to its 1966 position, the glacier shows significant thinning of its surface and margins and retreat of its terminus, especially on the west side. The 2000 terminus position was from 2.5 to 3 km from the 1966 position. Note the large tabular icebergs produced by calving. Photograph by Bruce F. Molnia, U.S. Geological Survey. A larger version of B is available online.



By 1950, this distance had increased to a maximum of about 5 km; a large U-shaped ice-marginal lake, which began forming after 1918, occupied the 2 km adjacent to the glacier's margin. By 3 September 1966, the glacier had retreated an additional kilometer and had lost more than a third of its width (fig. 311A). When the author photographed the glacier from the air on 15 July 2000, it showed significant thinning of its surface and margins and retreat of its terminus, especially on the western side (fig. 311B). The 2000 terminus position was from 3.5 to 4.5 km from the 1908 position. Both the 1966 and 2000 aerial photographs document that Ellsworth Glacier, like its eastern neighbor Excelsior Glacier, calves large tabular icebergs into its proglacial lake.

Although not part of the Sargent Icefield, several small glaciers (both named and unnamed) flow into the western side of Day Harbor from Resurrection Peninsula. They are discussed below, in the Glaciers of Resurrection Peninsula section.

### **Glaciers of Nellie Juan River**

More than a dozen unnamed glaciers drain in a westerly direction into the Nellie Juan River and eventually into Kings Bay. All show evidence of retreat and thinning (see two 3 September 1966 oblique aerial photographs by Austin Post, USGS photograph nos. 664-68 and 664-69). Retreat ranges from about 400 m to more than 1 km.

### **Glaciers of Resurrection Peninsula**

Not connected to either the ice field north of the Sargent Icefield or the Sargent Icefield itself are a number of glaciers, mostly unnamed, that drain into Nellie Juan River, Day Harbor, Resurrection Bay, or Resurrection River. Named glaciers include Spoon, Prospect, Porcupine, Godwin, Bear Lake, and Mother Goose Glaciers. According to Field (1975d), the termini of Spoon, Prospect, and Porcupine Glaciers have all retreated, so that their elevations in 1950, as shown on the USGS 1950 Seward A-7 1:63,360-scale topographic map (appendix B), were 60 to 150 m higher than they were on Grant and Higgins (1913) map, which was based on their 1909 observations. All the Resurrection Peninsula glaciers have received minimal attention since their early 20th century studies.

Wentworth and Ray (1936) reported that the surface of Bear Lake Glacier—an IGY AGS glacier—lowered between 45 and 60 m during the 20- to 25-year period before their 1931 visit. When the AGS mapped the 6.3-km-long glacier in 1957 at 1:10,000 scale, it had a large elevated moraine on its southern side. Surface elevation profiling surveys (Sapiano and others, 1998) showed that, between 1957 and 1996, the terminus retreated a total of 515 m (an average retreat of  $13 \text{ m a}^{-1}$ ) and that the elevation of the glacier surface decreased an average of 9.7 m, with a maximum of more than 60 m at an elevation of about 520 m near the terminus. Total volume lost was  $6.5 \times 10^7 \text{ m}^3$  of ice. Between the 1950s and the middle 1990s, on an annual basis, Bear Lake Glacier thinned by  $0.277 \text{ m a}^{-1}$ , its volume decreased by  $0.00192 \text{ km}^3 \text{ a}^{-1}$ , and its terminus receded by  $10 \text{ m a}^{-1}$ . From the middle 1990s to 1999, on an annual basis, the glacier thinned by  $0.953 \text{ m a}^{-1}$  and had its volume decrease by  $0.00652192 \text{ km}^3 \text{ a}^{-1}$  (K.A. Echelmeyer, W.D. Harrison, V.B. Valentine, and S.I. Zirnheld, University of Alaska Fairbanks, written commun., March 2001). The long-term mass balance between 1957 and 1996 averaged  $-0.30 \text{ m a}^{-1}$ .

### **Harding Icefield**

The Harding Icefield (fig. 312) has a maximum length of 80 km, a maximum width of about 50 km (Field, 1975d, p. 497), and an area of about  $1,800 \text{ km}^2$ . It is the largest of the ice fields in the Kenai Mountains and the largest single ice field located entirely in the United States. The ice field has nearly 40 outlet glaciers, 16 of which have lengths greater than 8 km. Alone,

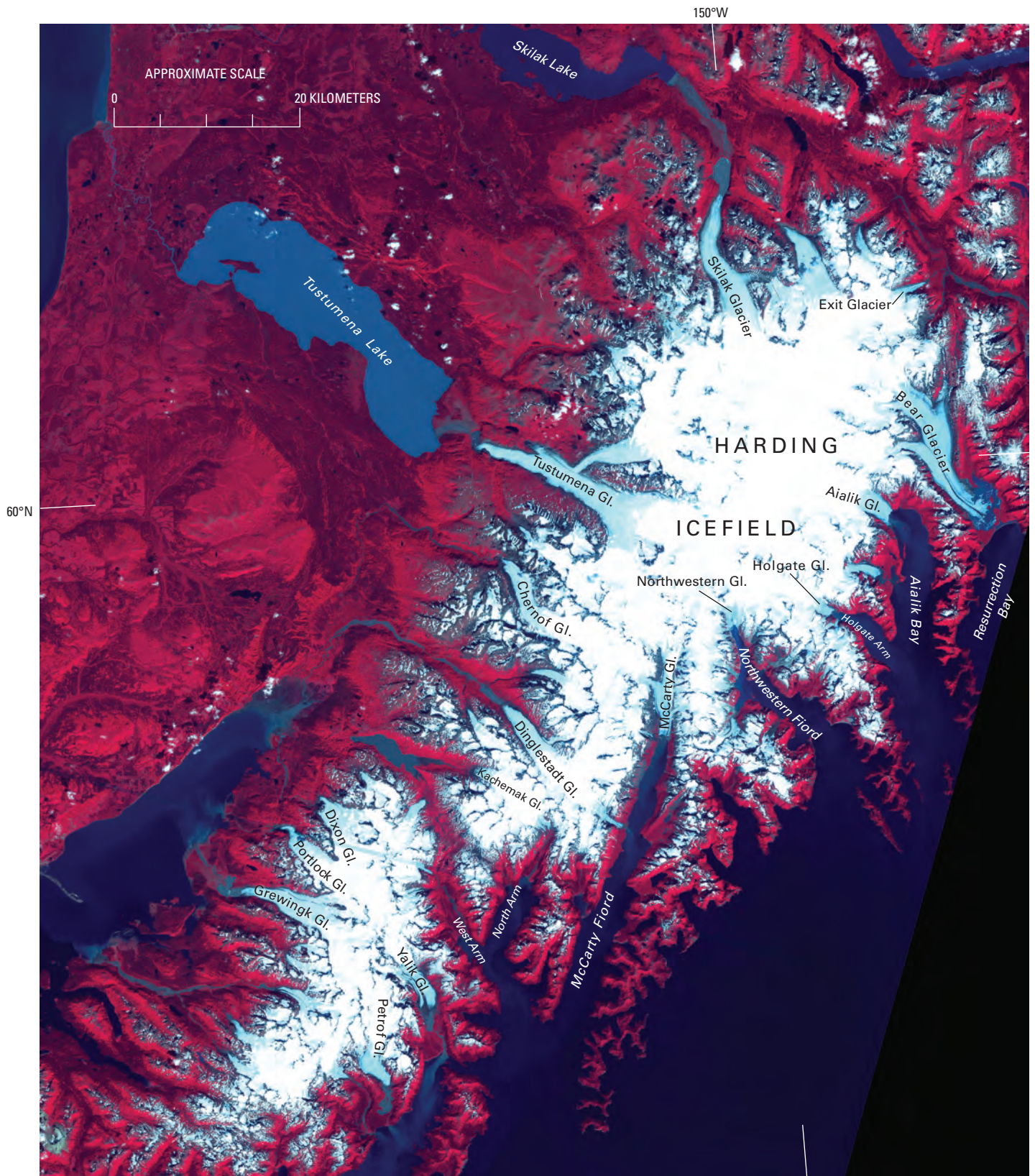


**Figure 312.**—Digital enlargement of a Landsat 7 ETM+ (Enhanced Thematic Mapper Plus) image showing the Harding Icefield and the unnamed ice field to the southwest of the Harding Icefield. Landsat 7 ETM+ image (7069018000022250; 9 August 2000; Path 69, Row 18) from the U.S. Geological Survey, EROS Data Center, Sioux Falls, S. Dak.

these glaciers have an area of about 1,380 km<sup>2</sup>. Four of these glaciers exceed 25 km in length. According to Field (1975d, p. 530–533), Bear Glacier (fig. 313) is 27 km long and has an area of 178 km<sup>2</sup>; an unnamed glacier is 29 km long and has an area of 183 km<sup>2</sup>; Tustumena Glacier is 32 km long and has an area of 390 km<sup>2</sup>; and Skilak Glacier is 34 km long and has an area of 160 km<sup>2</sup>. Meier and Post (1962) estimated the ice field's ELA to be about 600 m and determined that the AAR was 0.68.

Most of the northward-draining glaciers are unnamed and drain into the Resurrection River or Skilak Lake. Southward-draining glaciers generally reach sea level or near to it. Many others—including Aialik Glacier at the head of Aialik Bay, Holgate Glacier in Holgate Arm of Aialik Bay, Northwestern Glacier and two unnamed glaciers in Northwestern Fiord, and McCarty Glacier in McCarty Fiord—have tidewater termini. An unnamed glacier in Holgate Arm had a tidewater terminus in the late 1990s but retreated from tidewater by 2001.

Rice (1987) made planimetric measurements of all of the ice field's glaciers, using 1:63,360-scale topographic maps prepared between 1950 and 1951 (appendix B), and compared them with 1980s aerial photography. He calculated that the ice field had decreased in area as much as 5 percent during the intervening 34 years. The greatest changes were near sea level along the Gulf of Alaska and at the 300- to 600-m elevations on the northern and western sides of the ice field. Many smaller glaciers located at elevations below 1,000 m had disappeared.

Aðalgeirsdóttir and others (1998) obtained airborne surface elevation profiles of 13 Harding Icefield glaciers and the upper accumulation area of the ice field in 1994 and 1996 (table 5). These profiles were compared with 1:63,360-scale topographic maps (appendix B) and the aerial photographs used in their preparation (2 August 1950 and 15 August 1952). They concluded that the ice field has been thinning and shrinking since the 1950s and estimated that it has lost about 34 km<sup>3</sup> of ice in the more than 40-year period between being mapped in the early 1950s and profiled in the middle 1990s.

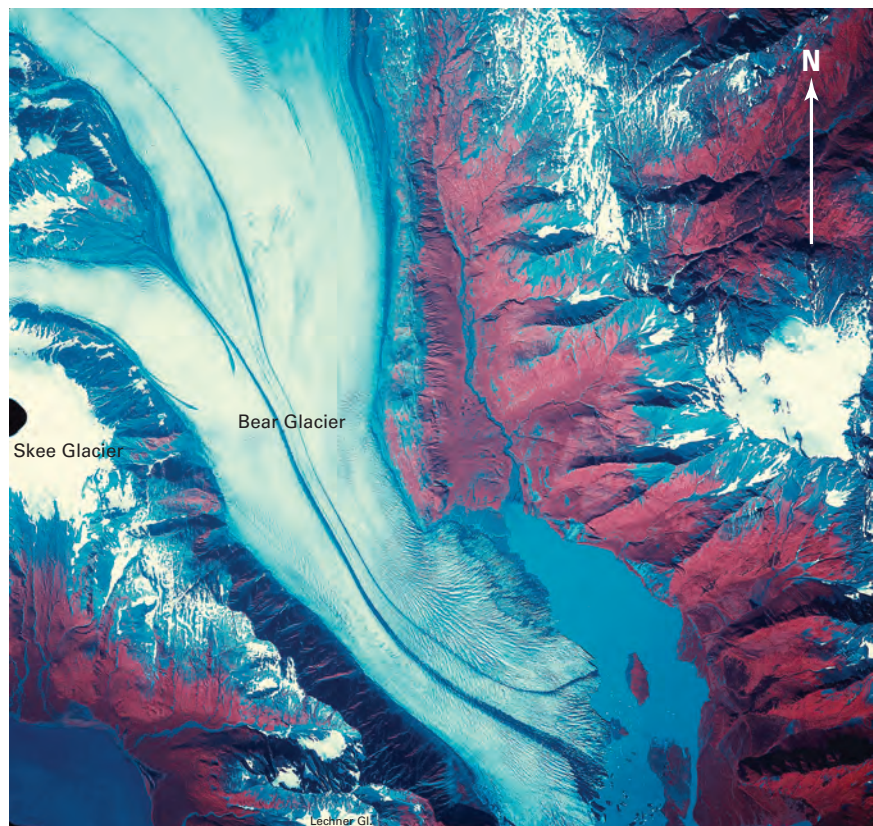


**Figure 313.**—14 August 1984 AHAP false-color vertical aerial photograph (L120F0313) of much of Bear Glacier, a Harding Icefield outlet glacier. The glacier has retreated from its position on its outwash plain and is now surrounded by a large ice-marginal lake. During the early 21st century, it retreated 2 km through calving of its floating terminus.

TABLE 5. — *Changes in outlet glaciers of the Harding Icefield: 1950s to middle 1990s*

Glacier	1950	Mid 1990s <sup>1</sup>					On annual basis <sup>2</sup>		
	Area (km <sup>2</sup> )	Terminus change (m)	Area change (km <sup>2</sup> )	Ice volume change (km <sup>3</sup> )	Average elevation change (m)	Mean annual mass balance (m)	Thickness change (m a <sup>-1</sup> )	Volume change (km <sup>3</sup> a <sup>-1</sup> )	Length change (m a <sup>-1</sup> )
Aialik	118	+540	0	-2.6	-11.0	-0.2	-0.25	-0.0295	+13
Bear	228.5	-1550	-8.75	-9.7	-38.4	-0.7	-0.872	-0.195	-36
Chernof	95.3	-750	-1.0	-2.3	-22.6	-0.4	-0.493	-0.0467	-17
Dinglestadt	79.4	-2300	-4.25	-2.7	-32.4	-0.6	-0.717	-0.0554	-50
Exit	42.8	-490	-0.25	-0.1	-2.6	-0.1	-0.063	-0.00267	-12
Holgate	64.3	-260	-0.25	-1.3	-16.3	-0.3	-0.364	-0.0233	-6
Kachemak	54.9	-900	-0.75	-0.9	-16.3	-0.3	-0.375	-0.0205	-21
<i>Little Dinglestadt</i>	31.5	-370	-0.5	-0.6	-18.6	-0.4	-0.4	-0.0125	-9
McCarty	108.6	-690	-1.38	+1.5	+6.2	+0.1	+0.131	+0.141	-16
<i>Northeastern</i>	15.4	-1350	-1.63	-1.4	-97.1	-1.8	-2.087	-0.0304	-30
<i>Northwestern</i>	66.25	-4200	-8.0	-5.0	-80.2	-1.5	-1.746	-0.109	-92
Skilak	217	-3200	-5.63	-0.9	-4.5	-0.1	-0.104	-0.0222	-74
Tustumena	296.7	-690	-1.75	-8.9	-25.1	-0.5	-0.572	-0.169	-17

<sup>1</sup> Aðalgeirsdóttir and others (1998).

<sup>2</sup> K.A. Echelmeyer, W.D. Harrison, V.B. Valentine, and S.I. Zirnfeld, University of Alaska Fairbanks (written commun., March 2001).

This corresponds to an ice field-wide lowering of about 21 m, the equivalent of an average mass balance of  $-0.4 \text{ m a}^{-1}$  of water. They also concluded that the rate of change of surface elevation between 1994 and 1996 is significantly greater than the long-term average. The glaciers that they profiled were Aialik, Bear, Exit, Holgate, Skilak, Tustumena, Chernof, Dinglestadt, and Kachemak Glaciers, *Little Dinglestadt Glacier* (informally named by Aðalgeirsdóttir and others, 1998), McCarty Glacier, *Northeastern Glacier*, and *Northwestern Glacier*.

The northeastern part of the Harding Icefield supports about a dozen glaciers that drain into Resurrection Bay or Resurrection River. Two have names—Exit and Lowell Glaciers. Aðalgeirsdóttir and others (1998) reported retreat of almost 500 m and other changes between the 1950s and middle 1990s of 7-km-long Exit Glacier (table 5). Lowell Glacier's terminus retreated a similar amount.

## Glaciers of Lower Resurrection Bay

When the 26-km-long Bear Glacier was mapped on 20 and 21 July 1909, it sat at the head of a tidal-flat outwash plain a maximum of about 300 m from the shore of Resurrection Bay (Grant and Higgins, 1913, fig. 11; two 21 July 1909 photographs—pl. XXXIIA, pl. XXXIB). At that time, the central part of the terminus was much closer to the bay. Grant and Higgins stated (p. 56) that “Along the center of the ice front high tide reaches the glacier.” An earlier trimline seaward of the 1909 position was dated by Viereck (1967) as having formed between 1835 and 1845. Trees beyond it were as much as 350 years old. By 1950, the glacier had retreated an additional 400 m, and a small ice-marginal lake had developed along its eastern margin. During the second half of the 20th century, the glacier retreated about 1.5 km.

Aðalgeirsdóttir and others (1998) reported on changes between the 1950s and the middle 1990s of Bear Glacier (table 5). In 2000, the retreating terminus of Bear Glacier was actively calving large numbers of tabular icebergs. By 2004, Bear Glacier had retreated more than 2 km farther.

## Glaciers of Aialik Bay

Named glaciers in Aialik Bay include Aialik, Addison, Pedersen, and Holgate Glaciers. The 12.9-km-long Aialik Glacier (Viens, 1995) (table 2; fig. 314) is a tidewater glacier located at the head of Aialik Bay. Between 22–24 July 1909, when Grant and Higgins (1913, pl. XXXIII) first investigated





**Figure 314.**—15 July 2000 west-looking oblique aerial photograph of the terminus of Aialik Glacier. During the 91 years since it was first photographed, the glacier retreated slightly. When observed by the author on 13 August 2004, the glacier showed signs of recent thinning and retreat. Photograph by Bruce F. Molnia, U.S. Geological Survey. A larger version of this figure is available online.



**Figure 315.**— 15 July 2000 west-looking oblique aerial photograph of the terminus of Pedersen Glacier. During the 91 years since it was first photographed, the glacier has retreated as much as 1.5 km. Photograph by Bruce F. Molnia, U.S. Geological Survey. A larger version of this figure is available online.



and mapped it, and 1950, the terminus position changed very little. In 1909, Aialik Glacier was a tidewater calving glacier and showed a large area of exposed bedrock along its margin (fig. 314) (21 July 1909 photograph by Grant and Higgins, 1913, pl. XXXIVA). Grant and Higgins stated that the glacier may have retreated as much as 400 m in the decade before 1909. Two gravel bars in Aialik Bay indicate significant recessions in the past (Post, 1980a). Aðalgeirsdóttir and others (1998) reported on changes in Aialik Glacier between the 1950s and the middle 1990s (table 5). The glacier both retreated and advanced in that time period; about 300 m of the 540 m of post-1950s retreat occurred between 1950 and 1964 (Field, 1975d). Aialik Glacier has an area of 70 km<sup>2</sup>, an accumulation area of 62 km<sup>2</sup>, an ablation area of 8 km<sup>2</sup>, and an AAR of 0.88 (Viens, 1995) (table 2); the width of its terminus is 0.6 km. When the author visited on 13 August 2004, it was slowly retreating.

Pedersen Glacier (fig. 315) has been retreating since before it was first mapped on 22–24 July 1909 by Grant and Higgins (1913). Its 1909 terminus position was from 400 to 500 m behind its most recent maximum position. Even then, part of the terminus was reached by high tide. Grant and Higgins speculated that the glacier may have been at its maximum position as recently as 15 years earlier. By 1950, the glacier had retreated an additional 400 to 1,200 m. A 600- to 800-m-wide tidal embayment fronted part of the glacier. According to Field (1975d, p. 531), Pedersen Glacier has a length of 9 km and an area of 23 km<sup>2</sup>. By 1964, another 250 of retreat had occurred. At the start of the 21st century, retreat and thinning were continuing. Aðalgeirsdóttir and others (1998) stated that Pedersen Glacier thinned an average of 5 m between the 1950s and the middle 1990s.

Holgate Glacier is a tidewater glacier at the head of Holgate Arm (fig. 316). An unnamed former tributary glacier, located to its southeast, retreated from tidewater before 2001. During the first decade of the 20th century, just before it was mapped on 22–24 July 1909 by Grant and Higgins (1913), the terminus of 8.5-km-long Holgate Glacier retreated about 1.5 km. When they visited it in 1909, the glacier terminus flowed on both sides of a bedrock outcrop that formerly had been a nunatak in the middle of the terminus. By 1950, the southern side of the glacier retreated another 400 m, while the northern side showed no change (Field, 1975d). Aðalgeirsdóttir and others (1998) reported on changes between the 1950s and the 1990s of Holgate Glacier (table 5), which has a length of 12.9 km, an area of 69 km<sup>2</sup>, an accumulation area of 63 km<sup>2</sup>, an ablation area of 6 km<sup>2</sup>, a width at its terminus of 0.6 km, and an AAR of 0.92 (Viens, 1995) (table 2). When the author visited and photographed part of the terminus of Holgate Glacier on 13 August 2004, it had retreated more than 1 km from its 1909 position.

**Figure 316.**— 15 July 2000 northwest-looking oblique aerial photograph of the terminus of Holgate Glacier. Since 30 May 1964, when it was photographed by the U.S. Coast and Geodetic Survey (photograph no. W9372), Holgate Glacier has retreated as much as 300 m. Photograph by Bruce F. Molnia, U.S. Geological Survey. A larger version of this figure is available online.

## Glaciers of Harris Bay

The 12-km-long Northwestern Glacier (fig. 317), which extends from the southeastern side of the Harding Icefield to tidewater in Northwestern Fiord at the head of Harris Bay, was named by U.S. Grant for Northwestern University in Evanston, Ill. The glacier, which had its terminus position mapped for the first time on 23 July 1909 by Grant and Higgins (1913, fig. 12), has been retreating since the beginning of the 20th century, with a total 20th century retreat of about 27 km. A 385-m-high rock knob located in the middle of Northwestern Fiord was completely icecovered in 1909. By 1950, it was a nunatak at the margin of the retreating Northwestern Glacier. Aðalgeirsdóttir and others (1998) reported on its changes between the 1950s and the middle 1990s (table 5). When the author observed the glacier on 15 July 2000 (fig. 317B) and visited it on 11 August 2004, he noted that a ridge of bedrock had separated its terminus into two adjacent ice tongues. Much of the margin of the eastern tongue was located above tidewater. Exposed bedrock along the margins of both tongues documents recent thinning. Northwestern Glacier has a length of 12.1 km, an area of 60 km<sup>2</sup>, an accumulation area of 54 km<sup>2</sup>, an ablation area of 6.0 km<sup>2</sup>, a width at its terminus of 0.9 km, and an AAR of 0.89 (Viens, 1995) (table 2).

A 6-km-long glacier, named *Northeastern Glacier* by Post (1980c), is located on the eastern side of the fjord, about 5 km south of Northwestern Glacier. Aðalgeirsdóttir and others (1998) reported on its changes between the 1950s and the middle 1990s (table 5). When the author flew over the terminus on 3 September 2002, it had retreated nearly 2 km from its position in the early 20th century.

**Figure 317.**—**A**, Part of a mosaic of the USGS Seldovia (1963, limited revision 1985) and Blying Sound (1953, limited revision 1982) 1:250,000-scale topographic maps (appendix A) of Northwestern Glacier and environs, showing the position of its terminus at that time. **B**, 15 July 2000 northwest-looking oblique aerial photograph of the terminus of Northwestern Glacier and the head of Northwestern Fiord. The glacier has retreated more than 25 km since 1909 and substantially since the maps were printed. Continuing retreat has exposed a ridge of bedrock that separates the terminus into two adjacent ice tongues. Much of the margin of the eastern tongue is above tidewater. Exposed bedrock along the margins of both tongues documents recent thinning. Photograph by Bruce F. Molnia, U.S. Geological Survey.

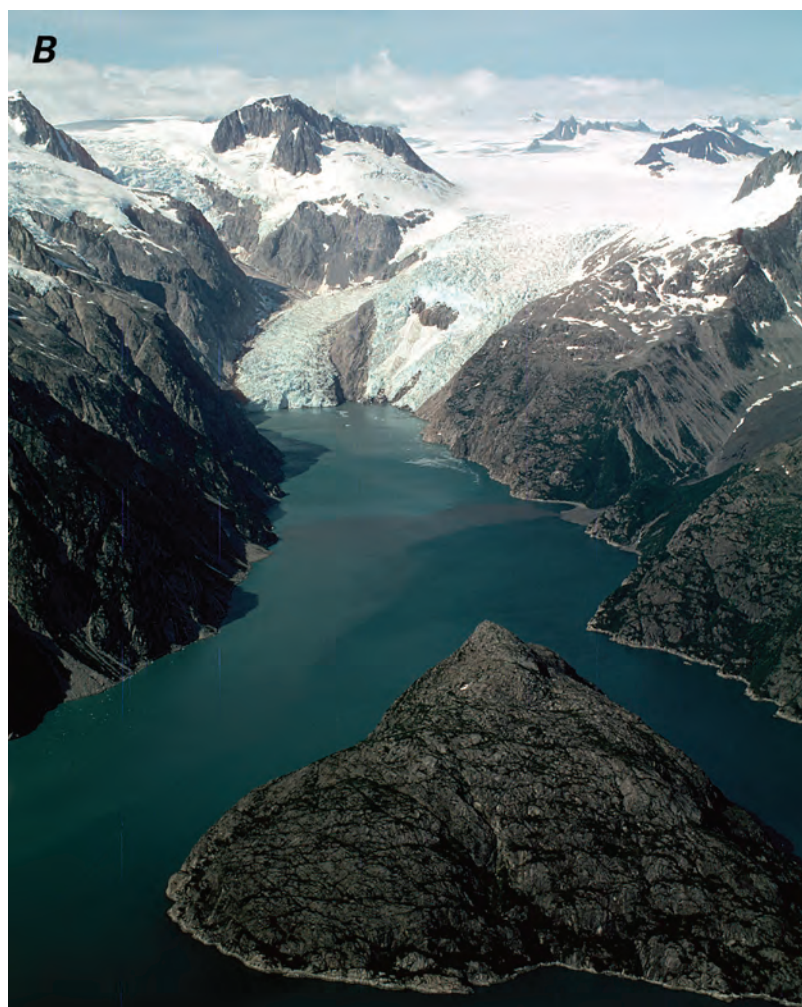




**Figure 318.**—15 July 2000 northwest-looking oblique aerial photograph showing the terminus of Ogive Glacier. Continued retreat and thinning of the glacier has all but separated the terminus from its upper source area. Photograph by Bruce F. Molnia, U.S. Geological Survey. A larger version of this figure is available online.

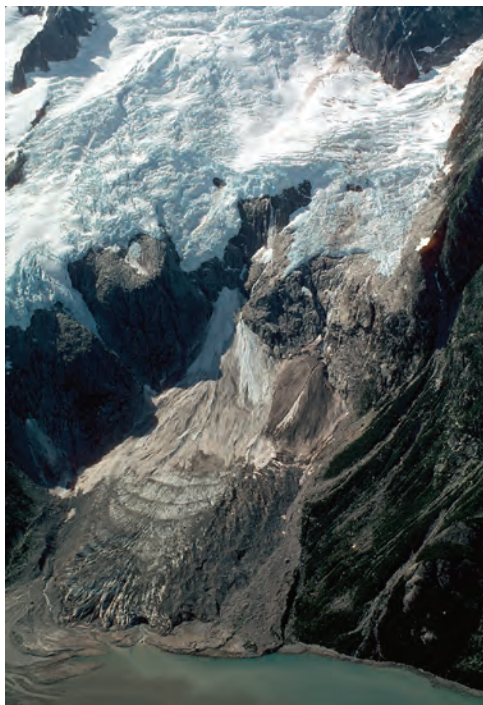


**Figure 319.**—15 July 2000 west-looking oblique aerial photograph showing an unnamed glacier southwest of Anchor Glacier. Continued retreat and thinning of the glacier have separated the terminus from its upper source area, producing a relict and reconstituted glacier. Photograph by Bruce F. Molnia, U.S. Geological Survey. A larger version of this figure is available online.

Two previously unnamed glaciers named *Anchor Glacier* and *Ogive Glacier* (fig. 318) by Post (1980c) [see Viens (1995) (table 2)], reach tidewater southwest of Northwestern Glacier. At each glacier, recent retreat has all but separated the terminus from its upper source area. *Anchor Glacier* had a length of 4.8 km, an area of 7 km<sup>2</sup>, an accumulation area of 5 km<sup>2</sup>, an ablation area of 2 km<sup>2</sup>, a width at its terminus of 0.3 km, and an AAR of 0.77 (Viens, 1995) (table 2). *Ogive Glacier* had a length of 6.8 km, an area of 9 km<sup>2</sup>, an accumulation area of 6 km<sup>2</sup>, an ablation area of 2 km<sup>2</sup>, a width at its terminus of 0.4 km, and an AAR of 0.73 (Viens, 1995) (table 2). An unnamed glacier (fig. 319) just southwest of *Anchor Glacier* is located a few meters above tidewater. Its terminus is completely separated from its upper source area. *Southwestern Glacier* (fig. 320) is located south of *Anchor Glacier* at the head of an outwash plain about 1.5 km from the fjord. Elevated trimlines and medial moraines indicate a significant amount of recent thinning and retreat. Many other glaciers that were tributary to the lower part of Northwestern Glacier at the turn of the 20th century are now small relict ice patches stranded high above Harris Bay.

### Glaciers of Nuka Bay

McCarty Glacier, a tidewater glacier located at the head of the fjord, and *Little Dinglestadt Glacier* are the dominant glaciers in McCarty Fjord, the eastern Arm of Nuka Bay. McCarty Glacier, which was first studied and mapped on 30 July 1909 by Grant and Higgins (1913, fig. 13), retreated about 3.2 km between 1909 and 1927, another 19 km between 1927 and 1950 (Mercer, 1961b), and another 1.4 km through 1978 (Post, 1980b). Between 1978 and the middle 1990s, the terminus advanced about 700 m. When the author visited McCarty Glacier on 9 August 2004, it had retreated about 400 m from the position of its terminus in the middle 1990s. Aðalgeirsdóttir and others (1998) reported on changes between the 1950s and middle 1990s (fig. 321, table 5). McCarty Glacier has a length of 19.3 km, an area of 111 km<sup>2</sup>, an accumulation area of 88 km<sup>2</sup>, an ablation area of about 23 km<sup>2</sup>, a width at its terminus of 1.3 km, and an AAR of 0.79 (Viens, 1995) (table 2). Aðalgeirsdóttir



**Figure 320.**—View of Southwestern Glacier, a former tributary to Northwestern Glacier. 15 July 2000 northwest-looking oblique aerial photograph showing the glacier's terminus with adjacent exposed bedrock, several elevated lateral moraines, and a large abandoned trimline. Parts of the adjacent unnamed glacier and Ogive Glacier can be seen on the west wall of the fjord. Photograph by Bruce F. Molnia, U.S. Geological Survey.



**Figure 321.**—**A**, Part of the USGS Seldovia 1:250,000-scale topographic map (1963, limited revision 1985) of McCartney Glacier and environs, showing the position of its terminus at that time. **B**, 15 July 2000 north-looking oblique aerial photograph of the terminus of McCartney Glacier, located at the head of McCartney Fiord. The glacier retreated, more than 3 km between 1909 and 1928 and 20 km since 1928. An advance in the 1980s and early 1990s was followed by retreat beginning at the end of the 20th century. A fan delta is developing on the east side of the terminus. The central margin has a well-formed calving embayment. Photograph by Bruce F. Molnia, U.S. Geological Survey.

and others (1998) reported on changes between the 1950s and the middle 1990s of 7-km-long *Little Dinglestadt Glacier* (table 5).

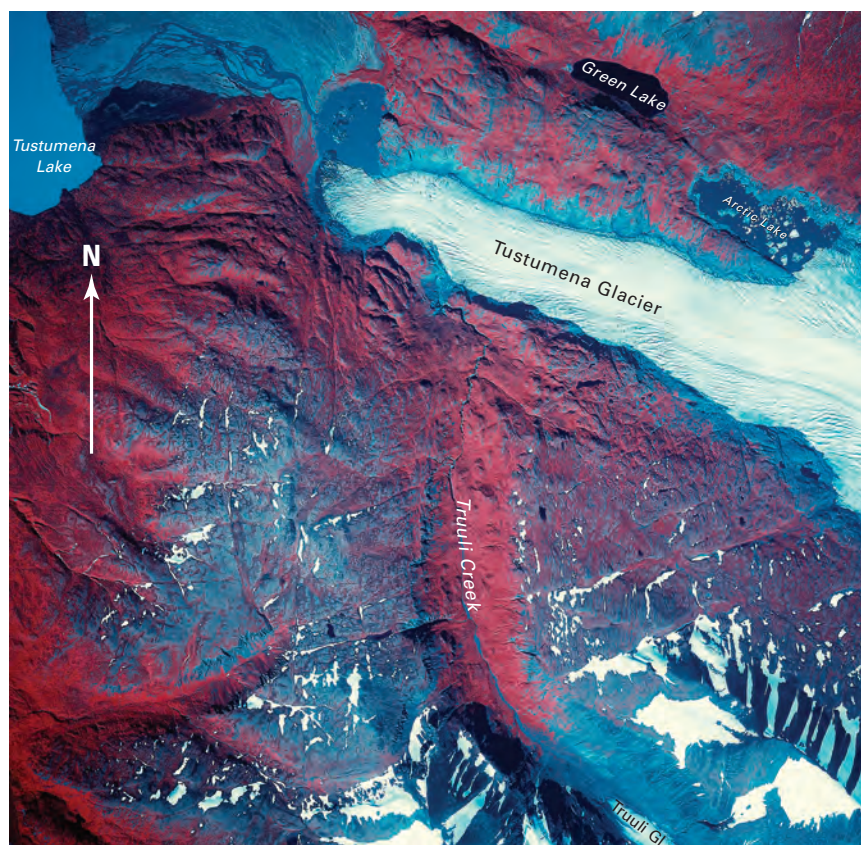
### Glaciers of the Western Harding Icefield

According to Field (1975d, p. 531–532), who measured lengths and areas, Kachemak (8 km, 23 km<sup>2</sup>), Dinglestadt (19 km, 69 km<sup>2</sup>), Chernof (17 km, 61 km<sup>2</sup>), Tustumena (32 km, 390 km<sup>2</sup>), and Skilak Glaciers (34 km, 160 km<sup>2</sup>) are the major named glaciers of the western Harding Icefield. All have terrestrial or lacustrine termini. Aðalgeirsdóttir and others (1998) reported on changes between the 1950s and the middle 1990s of Kachemak Glacier (table 5).

Field (1975d) stated that aerial photographs of Dinglestadt Glacier show evidence of 1.5 km of retreat between 1942 and 1965, including formation and enlargement of the proglacial lake at its terminus. Aðalgeirsdóttir and others (1998) reported on changes between the 1950s and the middle 1990s in 15.5-km-long Dinglestadt Glacier (table 5).

Field (1975d) stated that aerial photographs of Chernof Glacier show evidence of retreat as early as 1942. Aðalgeirsdóttir and others (1998) reported on changes between the 1950s and the middle 1990s in 24-km-long Chernof Glacier (table 5).

**Figure 322.**—14 August 1984 AHAP false-color vertical photograph (L120F0304) of much of the lower Tustumena Glacier and the retreating terminus of Truuli Glacier. Exposed bedrock around the entire perimeter of the Tustumena Glacier documents recent rapid thinning and retreat. When it was mapped in 1958, the glacier filled the entire basin at its terminus with ice. Since the 1990s, an ice-marginal lake has developed around the terminus. AHAP photograph from the GeoData Center, Geophysical Institute, University of Alaska, Fairbanks, Alaska.



Aðalgeirsdóttir and others (1998) reported on changes between the 1950s and the middle 1990s in 35-km-long Tustumena Glacier (fig. 322, table 5). Aðalgeirsdóttir and others (1998) reported on changes between the 1950s and the middle 1990s in 26-km-long Skilak Glacier (table 5). With the exception of the 1978 to the middle 1990s advance of McCarty Glacier, all Harding Icefield glaciers show evidence of ongoing thinning and retreat.

### Unnamed Ice Field Southwest of Harding Icefield

Southwest of Harding Icefield and east of Kachemak Bay is another unnamed ice field (fig. 312). The ice field has a maximum width of about 35 km from east to west and 25 km from north to south. The four largest glaciers have lengths of between 14 and 19 km (Field, 1975d, p. 533). None reach tidewater. According to Field (1975d, p. 533–534) who measured lengths and areas, Yalik (16 km, 151 km<sup>2</sup>) and Petrof (14 km, 46 km<sup>2</sup>) Glaciers are the major glaciers draining the eastern side of the complex, whereas Doroshin (13 km, 28 km<sup>2</sup>), Wosnesenski (11 km, 33 km<sup>2</sup>), Grewingk (19 km, 72 km<sup>2</sup>), Portlock (14 km, 41, km<sup>2</sup>), and Dixon (11 km, 41 km<sup>2</sup>) Glaciers are the major outlet glaciers that drain the western side. None reach tidewater, but several terminate at elevations below 100 m. Comparison of recent aerial photography with maps and early observations shows that each of these glaciers substantially retreated during the 20th century.

In 1909, Grant and Higgins (1913) examined Yalik Glacier. At that time, the terminus was separated from the forest by a deglaciated zone of unspecified length. During the next 41 years, part of the glacier's terminus retreated as much as 400 m. However, the middle of the terminus showed little change. The author visited Yalik Glacier on 10 August 2004 and observed that about 1.5 km of retreat had occurred since the 1950s.

On 8 August 1909, Grant and Higgins (1913) mapped and examined Petrof Glacier [see 8 August 1909 map (fig. 18) and two 8 August 1909 photographs presented by Grant and Higgins (1913, pls. XLA, XXXIXB)]. At that time, the

terminus was separated from the forest by a 300- to 400-m-wide deglaciated zone. During the next 42 years, the glacier's terminus retreated as much as 1.5 km, and an ice-marginal lake developed. When the AHAP program photographed the lake in 1978, it had a length of nearly 3 km.

Dall (1896) visited Grewingk Glacier as early as 1880 and produced its first map. Grove Karl Gilbert, accompanied by Dall and other scientists of the Harriman Expedition, visited the glacier in 1899 (21 July 1899 photograph by G.K. Gilbert, USGS Photo Library photograph Gilbert 456). Gilbert (1904), reported that, between 1880 to 1895, the glacier retreated 75 m; between 1895 and 1899, it retreated another 100 m. During the next half century, no new information was available. By 1951, the date of the USGS Seldovia 1951 1:63,360-scale C-3 topographic map (appendix B), a lake between 1.0 and 1.5 km in width had developed around the northern margin of its terminus. By 1978, the lake surrounded the entire terminus and was as much as 2.5 km wide.

### Glaciers of the Islands of Prince William Sound

Of all of the islands of Prince William Sound, Montague Island (fig. 323) is the only one that supports small glaciers. More than 20 are mapped along a 20-km-long part of the crest of the island at elevations of 600 to 800 m. All are confined to relatively small cirques; when the author observed them from the air in July 2000, all showed significant evidence of thinning and retreat.



**Figure 323.**—13 August 1982 AHAP false-color vertical photograph of central Montague Island. In the approximately 20 years between the production of the USGS Seward A-1 and A-2 and Blying Sound D-1 and D-2, 1:63,360-scale topographic maps in the 1950s and 1960s and the date of this photograph, many glaciers shown at lower elevations on Montague Island disappeared. A likely explanation is that a cartographer incorrectly mapped the unmelted previous winter snow pack as glacier ice. AHAP photograph no. L118F1591 from the GeoData Center, Geophysical Institute, University of Alaska Fairbanks, Fairbanks, Alaska.

### Summary

During the period of the Landsat baseline (1972–81), with the exception of Aialik and McCarty Glaciers, all of the valley and tidewater glaciers in the Kenai Mountains were stagnant, thinning, and (or) retreating. Into the early 21st century, all of the outlet glaciers in the Kenai Mountains continued to thin, stagnate, and retreat. Aialik and McCarty Glaciers each advanced more than 500 m during the second half of the 20th century but were both retreating by 2004. When Tiger Glacier was observed in 2000, it was at about the

same location as it was in 1908. Having retreated during much of the 20th century, Tiger Glacier must have experienced a late 20th century advance to regain its former position.

## Kodiak Island

**Figure 324.**—**A**, Index map of Kodiak Island showing the glacierized areas on the island. **B**, Enlargement of NOAA Advanced Very High Resolution Radiometer (AVHRR) image mosaic of Kodiak Island in summer 1995; National Oceanic and Atmospheric Administration image mosaic from Mike Fleming, EROS Data Center, Alaska Geographic Science Center, U.S. Geological Survey, Anchorage, Alaska.

Kodiak Island is located in the western Gulf of Alaska, south of Cook Inlet and east of Shelikof Strait (figs. 1, 324). At a length of about 160 km and a maximum width of nearly 100 km, Kodiak is the largest island in Alaska. Landsat 1–3 MSS images that cover Kodiak Island have the following Path/Row coordinates: 74/19, 75/19, 76/19, 74/20, 75/20, and 76/20 (fig. 3, table 1). Figure 325 is an annotated Landsat MSS false-color composite image mosaic (2908–20125, bands 4, 5, 7; 18 July 1977; Path 74, Row 20; 2909–20183, bands 4, 5, 7; 19 July 1977; Path 75, Row 20) of Kodiak Island showing all of the glacierized mountainous regions. Numerous fjords, several of which



nearly bisect the island, are evidence of the extent of Pleistocene glacier erosion on Kodiak Island.

The USGS Kodiak, Alaska (1952), 1:250,000-scale topographic quadrangle map (appendix A) which is based on 1948–52 observations and aerial photography, depicts more than 40 cirque glaciers (Denton, 1975b, p. 630; Wahrhaftig, 1965, p. 40), mostly in a narrow upland region located on the mountainous backbone of the island between Koniag Peak (1,362 m) to the south and Mount Glottof (1,343 m) to the north and in adjacent drainages (fig. 325). Koniag Glacier, the only named glacier on the island, is also the largest; it is about 2.5 km long and descends to elevations below 500 m. One cluster of five glaciers occurs approximately 12 km southwest of Koniag Peak at the head of an unnamed tributary to Uyak Bay. An isolated unnamed 1-km-long-glacier, the southernmost and westernmost glacier on the island, can be seen on the western side of an unnamed 1,040-m-high peak about 32 km southwest of Koniag Peak and 6 km north of Deadman Bay on a 25 July 1979 AHAP false-color infrared vertical aerial photograph (fig. 326). In all, the author estimates that the area of glaciers on Kodiak Island is less than 15 km<sup>2</sup>.

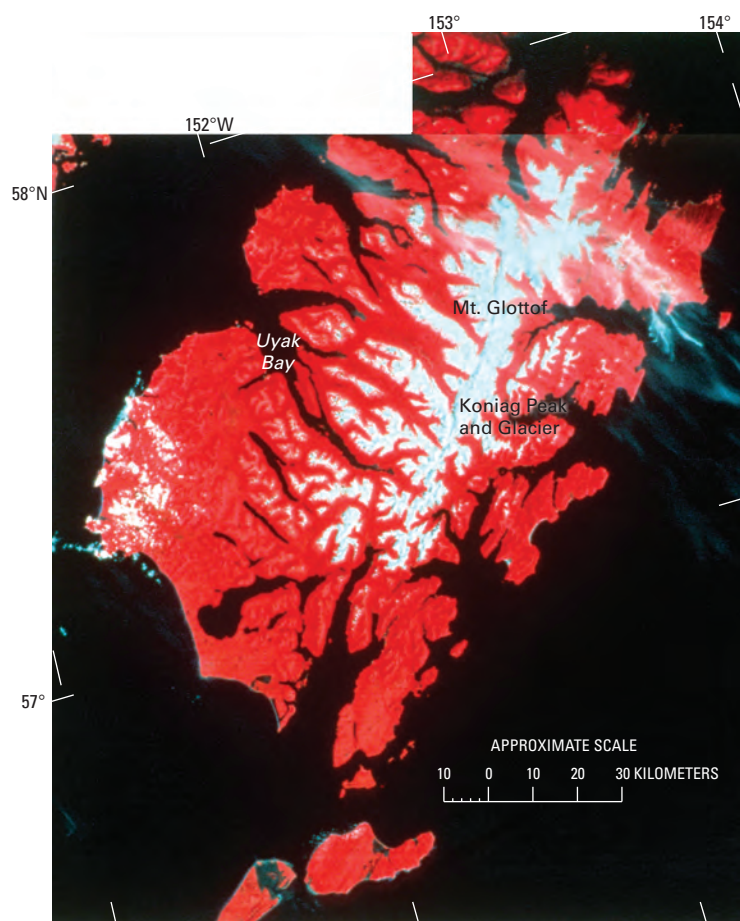


**Figure 325.**—Annotated Landsat 2 MSS false-color composite image mosaic of Kodiak Island. The locations of Mount Glottof, Koniag Peak, and Koniag Glacier are indicated. Landsat images (2908–20125, bands 4, 5, 7; 18 July 1977; Path 74, Row 20; and 2909–20183, bands 4, 5, 7; 19 July 1977; Path 75, Row 20) from the U.S. Geological Survey, EROS Data Center, Sioux Falls, S. Dak.



**Figure 326.**—25 July 1979 AHAP false-color infrared, vertical aerial photograph of south-central Kodiak Island showing part of the glacierized mountains that make up the backbone of the island. An unnamed 1.5-km-long snow-covered glacier is located at the head of a valley near the center of the photograph (A). Its valley is fringed by vegetation-free exposed bedrock. Other than the crevasses that can be seen in an unnamed 1.0-km-long glacier (B), all glacier features were snow covered at the time of acquisition of the photograph. AHAP photograph no. L147F61 from the GeoData Center, Geophysical Institute, University of Alaska, Fairbanks, Alaska.



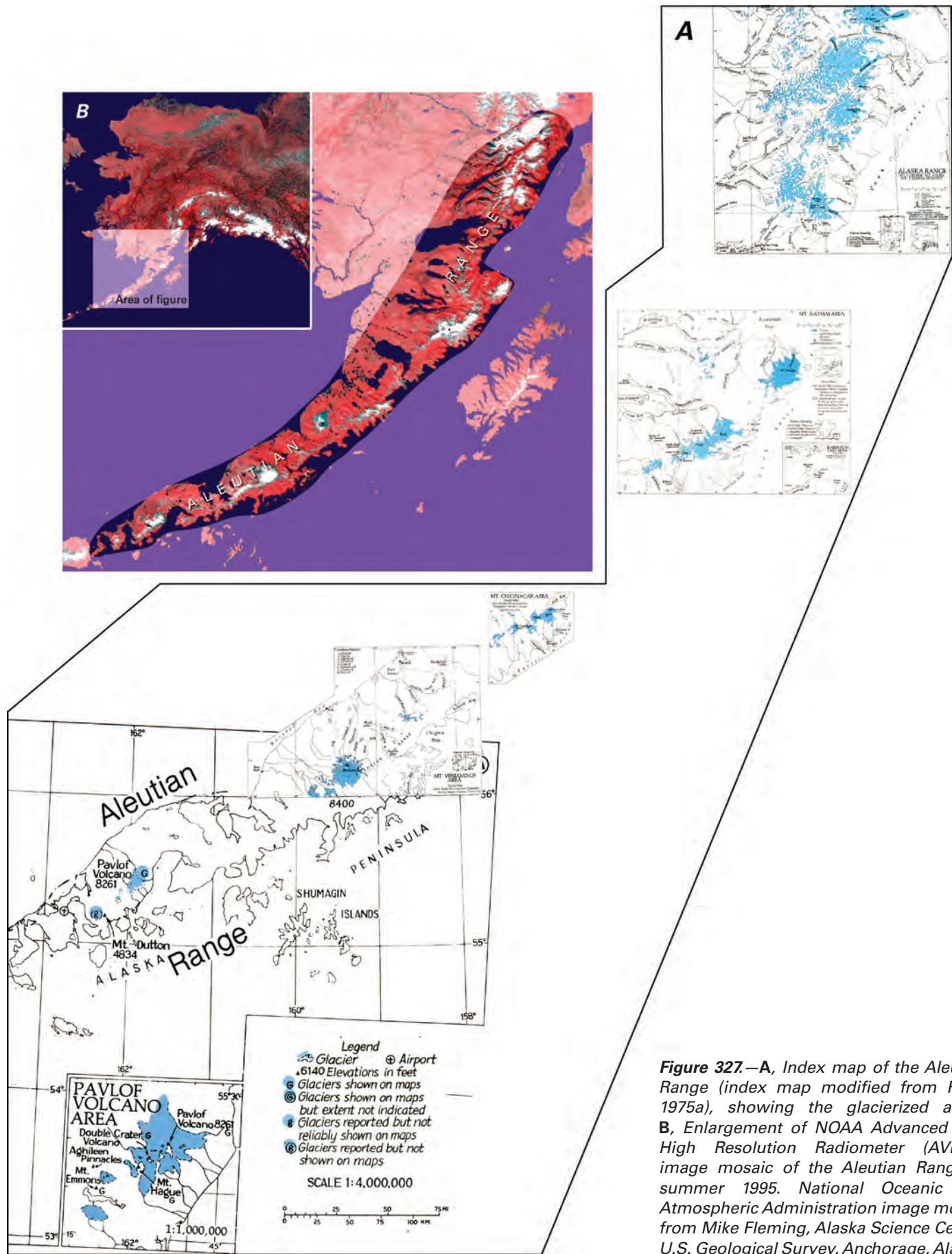
## Summary

During the period of the Landsat baseline (1972–81), all available evidence suggests that the glaciers of Kodiak Island were thinning and retreating. These conclusions are based on a comparison of the size and number of glaciers shown on Kodiak's topographic maps made from 1948–52 data and AHAP photography from the middle of the baseline period (1977–79). No information exists about the status of these glaciers at the end of the 20th century and into the early 21st century. However, given their small size, low elevation, and location on an island experiencing a significant late 20th century temperature increase and surrounded by temperate ocean water, it is likely that they have continued to thin and retreat.

## Aleutian Range

### Introduction

The Aleutian Range (figs. 1, 327), which extends northeast-southwest along the spine and southeastern side of the Alaska Peninsula for nearly 1,000 km, is bounded on the north by the Neacola River, Chakachamna Lake, and Chakachatna River and on the south by Isanotski Strait and False Pass. The range contains more than 30 glaciers having lengths of 8 km or more; Blockade Glacier is 44 km long (Denton and Field, 1975b, p. 601). Most glaciers, large and small, are unnamed. Seven areas support glaciers, including the Neacola and Chigmit Mountains of the northern Aleutian Range; the Kamishak Bay–Big River area; the Ninagiak River–Puale Bay area; the Mount Kialagvik, Icy Peak, and Mount Chiginagak area southwest of Wide Bay; the Aniakchak Crater area (see Landsat 2, MSS image 2534–20511, 9 July 1976, Path 78, Row 20); the Mount Veniaminof–Stepovak Bay area; and the Pavlof Volcano–Frosty Peak area. The area covered by glaciers in the Aleutian



Range is 1,250 km<sup>2</sup> (Post and Meier, 1980, p. 45). Landsat 1–3 MSS images that cover the Aleutian Range have the following Path/Row coordinates: 76/17; 77/17; 76/18; 77/18; 75/19; 76/19; 77/19; 78/19; 76/20; 77/20; 78/20; 79/20; 78/21; 79/21; 80/21; 81/21; and 81/22 (fig. 3, table 1).

## **Glaciers of the Neacola and Chigmit Mountains**

Together, the Neacola and Chigmit Mountains contain more than a thousand glaciers ranging in size from cirque glaciers to some of the largest valley glaciers in the Aleutian Range. Fleming (2000) compiled a 1:250,000-scale Landsat 7 ETM+ satellite image mosaic map of Lake Clark National Park and environs that shows glaciers of the Neacola and Chigmit Mountains and glaciers of the southern Alaska Range. Figure 328 is a modification of part of the Landsat 7 image mosaic. “Little Ice Age” advances of several of the larger valley glaciers resulted in the damming of rivers and the formation of large ice-dammed lakes in both ranges.

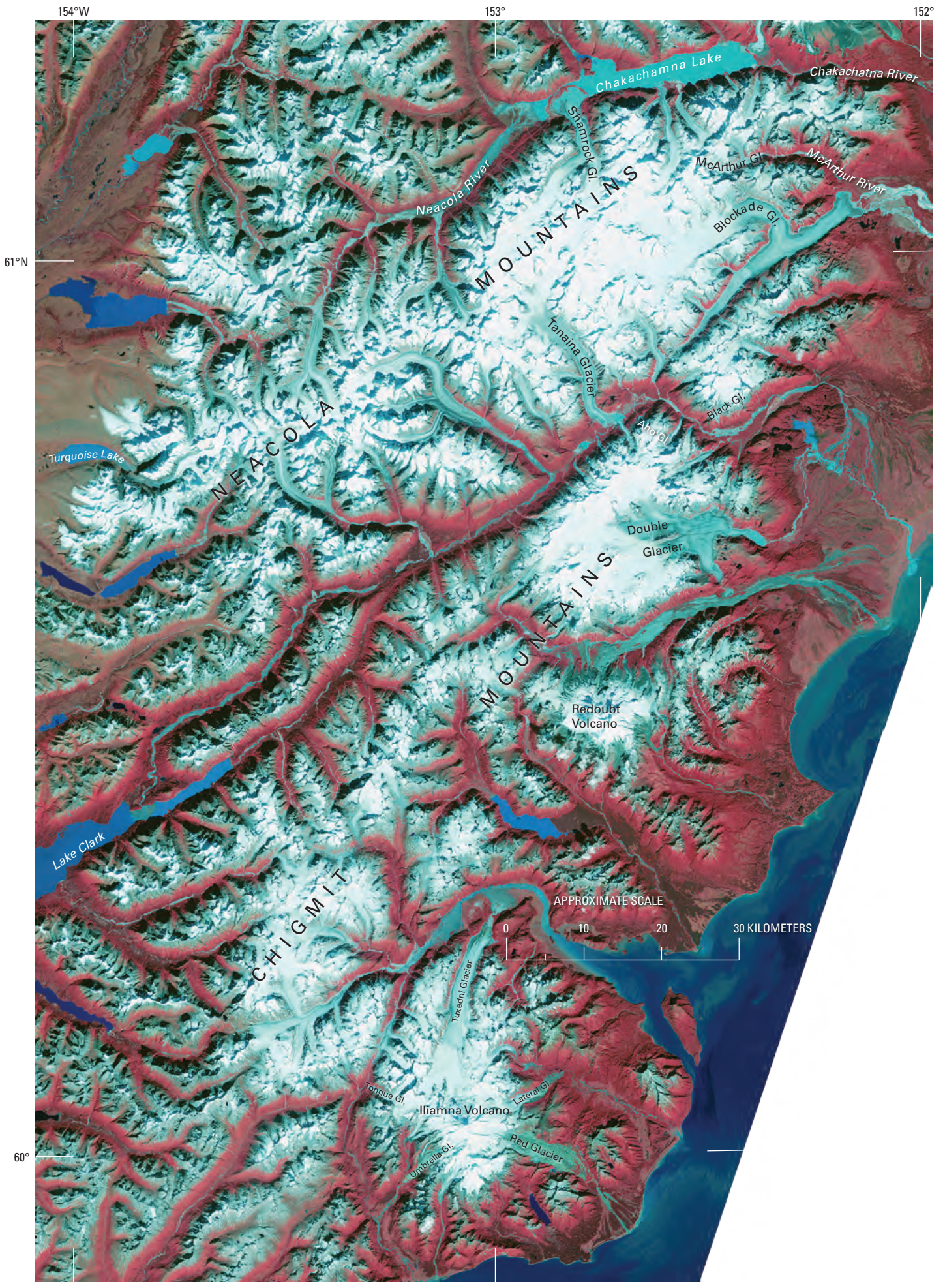
### **Glaciers of the Neacola Mountains**

The 120×30-km Neacola Mountains (fig. 329), the northernmost range in the Aleutian Range, support more than 500 km<sup>2</sup> of glacier ice, including the longest valley glaciers in the Aleutian Range. One, 26-km-long Shamrock Glacier (Denton and Field, 1975b, p. 600) (figs. 59, 330), flows north and reaches into Chakachamna Lake. In the late 19th or early 20th century, its large lobate terminus advanced across the lake and blocked it, forming Kenibuna Lake. In recent years, the glacier has retreated as much as 2.5 km, but the moraine still constrains the width of the lake to just a narrow channel. Between the 1950s and the middle 1990s, on an annual basis, Shamrock Glacier thinned by 0.379 m a<sup>-1</sup> and had its volume decrease by 0.0503 km<sup>3</sup> (K. A. Echelmeyer, W. D. Harrison, V. B. Valentine, and S. I. Zirnheld, University of Alaska Fairbanks, written commun., March 2001).

About 15 km east of Shamrock Glacier, a pair of unnamed glaciers also extended into Chakachamna Lake (20 July 1980 AHAP false-color infrared vertical aerial photograph no. L108F6636), although only a small distance. They too are actively retreating.

Thirty kilometers to the south, 44-km-long Blockade Glacier (fig. 331), with an area of 254 km<sup>2</sup> (Denton and Field, 1975b, p. 601), bifurcates. The lobe of its eastern terminus flows about 10 km to the northeast, where it drains into the McArthur River, and the lobe of its western terminus flows about 5 km to the southwest, where it dams Blockade Lake. Both termini are actively retreating and thinning. About 25 km to the southwest of the western tongue of Blockade Glacier, Tanaina Glacier (fig. 332), which has a length estimated by the author of approximately 30 km, and an area of approximately 150 km<sup>2</sup>, flows into Lake Clark Pass and at times has completely filled its valley with ice, damming Summit Lake. Its retreat during the second half of the 20th century has left the pass ice free and the lake greatly reduced in size. Between the 1950s and the middle 1990s, on an annual basis, Tanaina Glacier thinned by 1.051 m a<sup>-1</sup> and had its volume decrease by 0.173 km<sup>3</sup> (K. A. Echelmeyer, W. D. Harrison, V. B. Valentine, and S. I. Zirnheld, University of Alaska Fairbanks, written commun., March 2001).

When they were observed on 8 August 2000, a number of unnamed south-flowing southern Neacola Mountains glaciers, located in and adjacent to the through valley southwest of Blockade Glacier, were thinning, retreating, and losing contact with their former tributaries (20 June 1978 AHAP false-color infrared vertical aerial photograph no. L112F4732). Examples are the unnamed glacier at the head of the Glacier Fork of the Tlikakila River, another unnamed glacier located immediately west of Tanaina Glacier, two unnamed glaciers that are the western source of the Telaquana River, and an unnamed glacier that is the southwesternmost valley glacier in the Neacola Mountains. Between the 1950s and the middle 1990s, on an annual basis, this



◀ **Figure 328.**—Part of an annotated Landsat 7 ETM+ false-color composite image mosaic of Lake Clark National Park and environs showing the glaciers of the Neacola and Chigmit Mountains. Landsat 7 ETM+ images (7071017009924950 and 707101800924950; bands 2, 3, 4; 6 September 1999; Path 71, Rows 17, 18) courtesy of Mike Fleming, Alaska Science Center, U.S. Geological Survey, Anchorage Alaska.

glacier thinned by  $0.4 \text{ m a}^{-1}$  and had its volume decrease by  $0.0179 \text{ km}^3$  (K. A. Echelmeyer, W. D. Harrison, V. B. Valentine, and S. I. Zirnheld, University of Alaska Fairbanks, written commun., March 2001 ).



**Figure 329.**—4 September 1966 oblique aerial photograph of the Neacola Mountains showing a number of unnamed cirque glaciers located in the remote central part of the range. Photograph No. 666-26 by Austin Post, U.S. Geological Survey.



**Figure 330.**—8 September 2000 south-looking oblique aerial photograph of the terminus of Shamrock Glacier showing the elevated end and lateral moraine complex, which dates from the first half of the 20th century, the retreating terminus, and the lower one-third of the glacier. Photograph by William R. Reckert, Volunteer for Science, U.S. Geological Survey. This photograph should be compared with figure 59, a 20 July 1980 AHAP false-color infrared vertical aerial photograph (L108F6633) of Shamrock Glacier, Chigmit Mountains, Aleutian Range, to determine changes during the 20 years between the photographs.

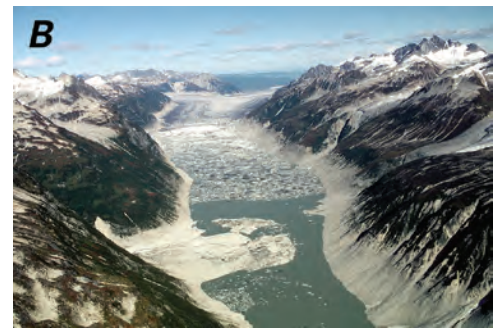


**Figure 331.**—Two 8 September 2000 oblique aerial photographs of the two retreating termini of Blockade Glacier. **A**, West-looking photograph showing the two lobes of the splayed eastern terminus of Blockade Glacier. Both lobes show evidence of recent retreat, especially the northern lobe. An elevated trimline parallels much of the northern margin of the glacier. **B**, Northeast-looking photograph showing the thinning western terminus of Blockade Glacier at the head of Blockade Lake. Elevated shorelines document the recently much thicker character of the glacier. An elevated trimline parallels much of the northern margin of the glacier. A copious discharge of icebergs documents that calving from the retreating margin is a significant factor in its retreat. On the south side of the valley, a pair of retreating former tributaries to a previously larger West Blockade Glacier can be seen. On the north side, lowering of the lake's surface has exposed the formerly submerged fan-delta top of an unnamed and unseen glacier. Just to its east side, at the top of the valley wall, is the exposed bedrock threshold of an unseen retreating cirque glacier. Photographs by William R. Reckert, Volunteer for Science, U.S. Geological Survey. A larger version of B is available online.

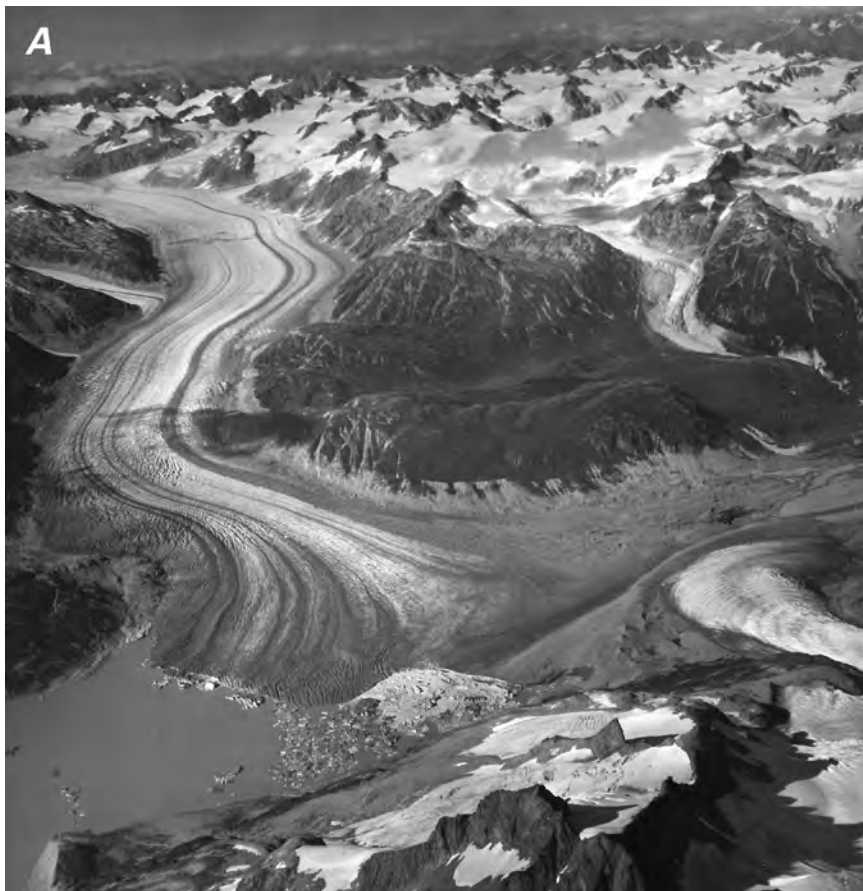


**Figure 332.**—Three oblique aerial photographs of Lake Clark Pass showing changes of Tanaina Glacier, an unnamed glacier, and Summit Lake from 1963 to 2000. **A**, 25 August 1963 north-looking oblique aerial photograph of the terminus of Tanaina Glacier (left) and the terminus of the unnamed glacier (right). The adjacent termini are both in contact with an elevated former terminal moraine ridge of the unnamed glacier and fill the valley floor. Summit Lake is dammed by the iceberg-calving terminus of Tanaina Glacier. The exposed, elevated trimline on the north side of the terminus of Tanaina Glacier documents that the glacier was more than 50 m thicker in the recent past. Photograph no. F632-127 by Austin Post, U.S. Geological Survey. **B** and **C**, see following page.

**Figure 332.**—**B**, August 1970 north-looking oblique aerial photograph of the terminus of Tanaina Glacier (left) and the terminus of the unnamed glacier (right). The termini are no longer in contact, and the draining of Summit Lake has exposed its bed. Both sides of the terminus of Tanaina Glacier have thinned. Retreat along the west side has exposed a significant amount of bedrock and sediment. Little change can be seen at the terminus of the unnamed glacier. Photograph No. 70–N2–55 by Austin Post, U.S. Geological Survey. **C**, 8 September 2000 north-looking oblique aerial photograph of the retreating terminus of Tanaina Glacier and the recently re-formed Summit Lake. The lake, now at a much lower level, is dammed by sediment and an ice-cored moraine left by the retreat of Tanaina Glacier. A recessional moraine wraps around the west side of the retreating terminus of Tanaina Glacier. Photograph by William R. Reckert, Volunteer for Science, U.S. Geological Survey. A larger version of C is available online.



### Glaciers of the Chigmit Mountains

The 195-km-long Chigmit Mountains contain more than 750 km<sup>2</sup> of ice located within a rugged upland area. There are hundreds of cirque glaciers and dozens of outlet valley glaciers, including Double Glacier, the two lobes of which have lengths of 26 and 25 km (Denton and Field, 1975b, p. 602). Additionally, the Chigmit Mountains contain two of the largest glacier-covered volcanoes in the Aleutian Range—Redoubt Volcano (3,099 m) and Iliamna Volcano (3,044 m).

In the northeasternmost Chigmit Mountains, a number of small glaciers drain from an ice-covered upland topped by 1,940-m-high Black Peak. When they were observed on 8 August 2000, the termini of the two largest—8-km-long Black Glacier and a 10-km-long unnamed glacier—showed evidence of recent thinning and retreat. Just to the south, Double Glacier (fig. 333), which has an area of 209 km<sup>2</sup> (Denton and Field, 1975b, p. 602), drains to the east from the largest ice field in the northern Chigmit Mountains. Located between the Tlikakila and Drift Rivers, the unnamed ice field covers an area estimated by the author to be approximately 400 km<sup>2</sup>. Topped by 2,072-m-high Double Peak, more than 30 outlet glaciers flow radially from this ice field. Every outlet glacier shows evidence of recent thinning and retreat. Between the 1950s and the middle 1990s, on an annual basis, Double Glacier thinned by 1.067 m a<sup>-1</sup> and had its volume decrease by 0.243 km<sup>3</sup> (K. A. Echelmeyer, W. D. Harrison, V. B. Valentine, and S. I. Zirnheld, University of Alaska Fairbanks, written commun., March 2001).

Several hundred small unnamed glaciers are located adjacent to the southern side of the eastern end of Lake Clark, Little Lake Clark, and Chokotok River. When they were observed on 8 August 2000, every one showed evidence of thinning and retreat.

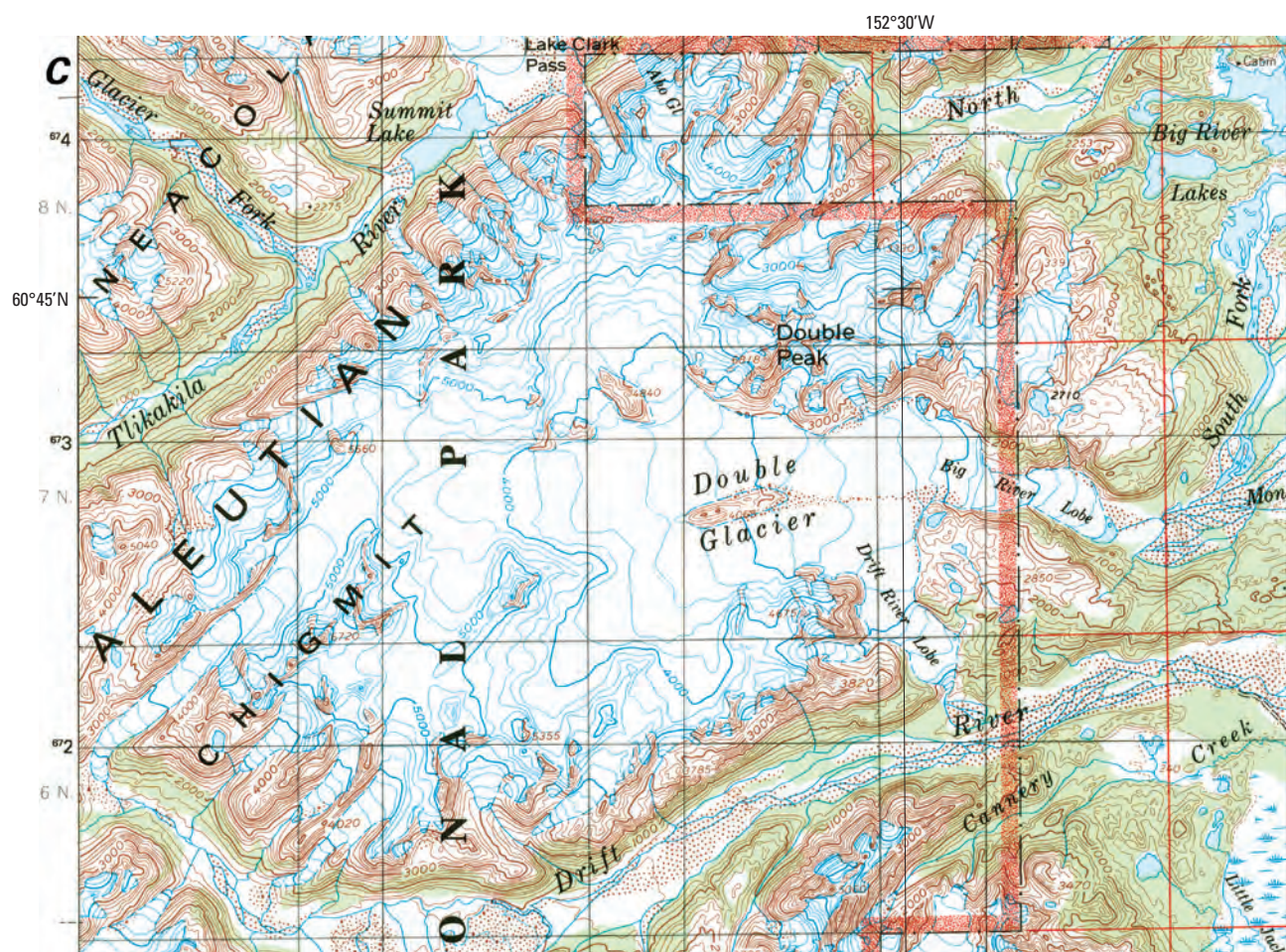
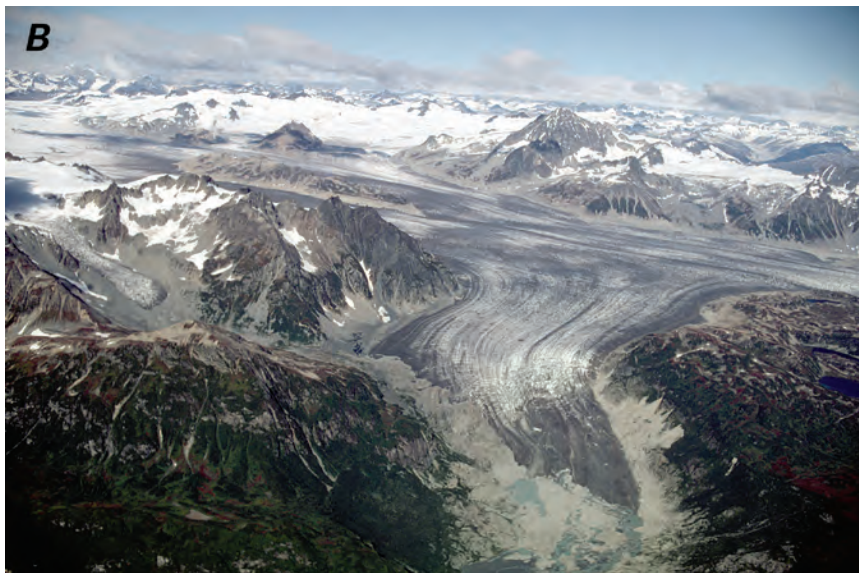
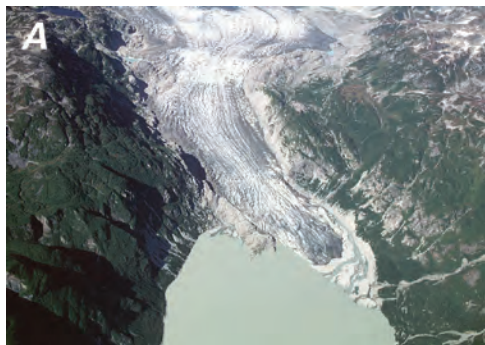


**Figure 333.**—Map and two 8 September 2000 west-looking oblique aerial photographs of the northeastern Chigmit Mountains showing Double Glacier. **A**, Photograph of the terminus of the retreating Big River Lobe, the northern of Double Glacier's two termini. An elevated lateral moraine on its south side and an elevated trimline on its north side document recent retreat and thinning. During the 20th century, the glacier may have thinned by more than 100 m. **B**, Terminus of the retreating Drift River Lobe (right), and

an unnamed former tributary (far left). The Drift River Lobe has retreated about 3 km since it was mapped in the mid-1950s, retreating an average of approximately  $65 \text{ m a}^{-1}$ . The unnamed former tributary has retreated more than 5 km. Photographs by William R. Reckert, Volunteer for Science, U.S. Geological Survey. **C**, Part of the USGS Kenai (1958, revised 1986) 1:250,000-scale map showing Double Glacier and other glaciers in the southeastern Chigmit Mountains. A larger version of A is available online.



### Glaciers of Redoubt Volcano

Redoubt Volcano, a steep-sided cone about 10 km in diameter at its base and with a volume of 30 to 35 km<sup>3</sup>, has been moderately dissected by the action of numerous alpine glaciers. More than a dozen unnamed glaciers descend from Redoubt Volcano's summit. A 1.8-km-wide ice-filled summit crater is breached on the northern side by a northward-flowing glacier, which spreads out and forms a small piedmont lobe in the upper Drift River Valley (fig. 334). When the mountain last erupted in 1989 and 1990, significant melting of the summit glaciers took place, followed by jökulhlaups (glacier-outburst floods) on Drift River. Previously, jökulhlaups in 1966 covered the lower 3 km of Redoubt's northernmost glacier with up to 2 m of volcanic debris. The unnamed glacier's debris-covered terminus is currently about 100 m from Drift River Valley.

Eruptions between 14 December 1989 and 14 March 1990 melted snow and glacier ice and caused winter floods along Drift River that threatened an oil-processing facility at the valley mouth. Trabant and others (1994) reported that pyroclastic flows entrained snow and glacier ice and melted canyons into the unnamed glacier, resulting in the loss of much of the ice in the upper reach of the glacier. The eruption produced an unusual ice diamict consisting of fragments of glacier ice and rock debris in a matrix of snow grains and new volcanic tephra (Waitt and others, 1994). The diamict, which contained rounded fragments of glacier ice as large as 2.5 m, fragments of andesite and other crystalline rocks as large as a meter, and slabs of entrained snow pack as long as 10 m, was deposited on the northern and southern flanks of the mountain. On the northern flank, a northern flow traveled as much as 14 km and covered an area of about 5.7 km<sup>2</sup>. On one unnamed glacier located on Redoubt Volcano's southern side, the diamict was as thick as 20 m, even after traveling 4.3 km. Before the end of the eruption, newly erupted lava created flows that entrained additional snow-and-ice blocks from the crevassed glacier and transported them 35 km down valley to Cook Inlet.

When Trabant and Hawkins (1997) investigated Redoubt Volcano, they developed a model for evaluating glacier volumes. Their model determined that the 1989–90 eruptions removed 0.29 km<sup>3</sup> of perennial snow and glacier ice from a 4.5-km segment of the unnamed summit outlet glacier, providing a unique opportunity for verification of their volume model. In a single 2.5-km reach of denuded glacier valley, the volume of ice removed was  $9.9 \times 10^7$  m<sup>3</sup>, about 1 percent less than the model had estimated. The total volume of perennial snow and glacier ice on Redoubt Volcano was estimated to be  $4.1 \pm 0.8$  km<sup>3</sup>, about 23 times the volume present on Mount St. Helens, Wash., before its 1980 eruption. Since the 1989–90 eruption, new snow and ice has accumulated in Redoubt's summit crater, replacing much of the snow and ice melted during the volcanic activity (McGimsey, 2001).

**Figure 334.**—Oblique aerial photograph of the summit and upper 1,500 m of Redoubt Volcano on 29 July 1978. The valley of the unnamed glacier, which has a conspicuous elevated lateral moraine along its south margin, documents recent thinning of the glacier. Photograph by Bruce F. Molnia, U.S. Geological Survey.



## Glaciers of Iliamna Volcano

Iliamna Volcano is a broad, deeply dissected and highly altered, roughly cone-shaped mountain at the north end of a 5-km-long ridge. Most of the volcano is covered by perennial snow and glacier ice, and more than a dozen large glaciers radiate from the summit area (fig. 335). Large avalanche deposits occur on the flanks of the volcano at several locations.

The northernmost and largest glacier is Tuxedni Glacier, which has a length of 25 km and an area of 106 km<sup>2</sup> (Denton and Field, 1975b, p. 603) (fig. 336) and extends from Iliamna Volcano's summit to nearly sea level. Between the 1950s and the middle 1990s, on an annual basis, Tuxedni Glacier thinned by 0.793 m a<sup>-1</sup> and had a volume decrease of 0.0693 km<sup>3</sup> (K. A. Echelmeyer, W. D. Harrison, V. B. Valentine, and S. I. Zirnheld, University of Alaska Fairbanks, written commun., March 2001).

Red Glacier (figs. 335, 337), named for the iron-rich red-colored moraines that cover much of the glacier, has a length of 17 km and an area of 51 km<sup>2</sup> (Denton and Field, 1975b, p. 603). It terminates at an elevation estimated by the author at approximately 65 m above mean sea level (amsl). Other named Iliamna glaciers include Umbrella (fig. 338) (26 August 1978 AHAP false-color infrared vertical aerial photograph no. L120F7552), Lateral (fig. 339), and Johnson Glaciers. All of these glaciers and all of Iliamna Volcano's unnamed outlet glaciers show multiple evidence of terminus retreat and thinning in

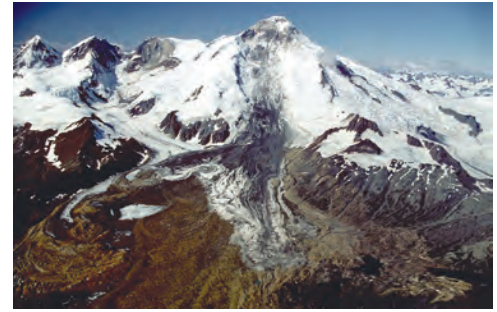


**Figure 335.**—Oblique aerial photograph of Iliamna Volcano. 8 August 2000 west-looking view of the summit showing a large volcanic-debris-rich avalanche that descended onto the surface of Red Glacier below. The glacier-dissected topography of the summit ridge can be seen on the south side of the summit. Photograph by Bruce F. Molnia, U.S. Geological Survey. A larger version of this figure is available online.

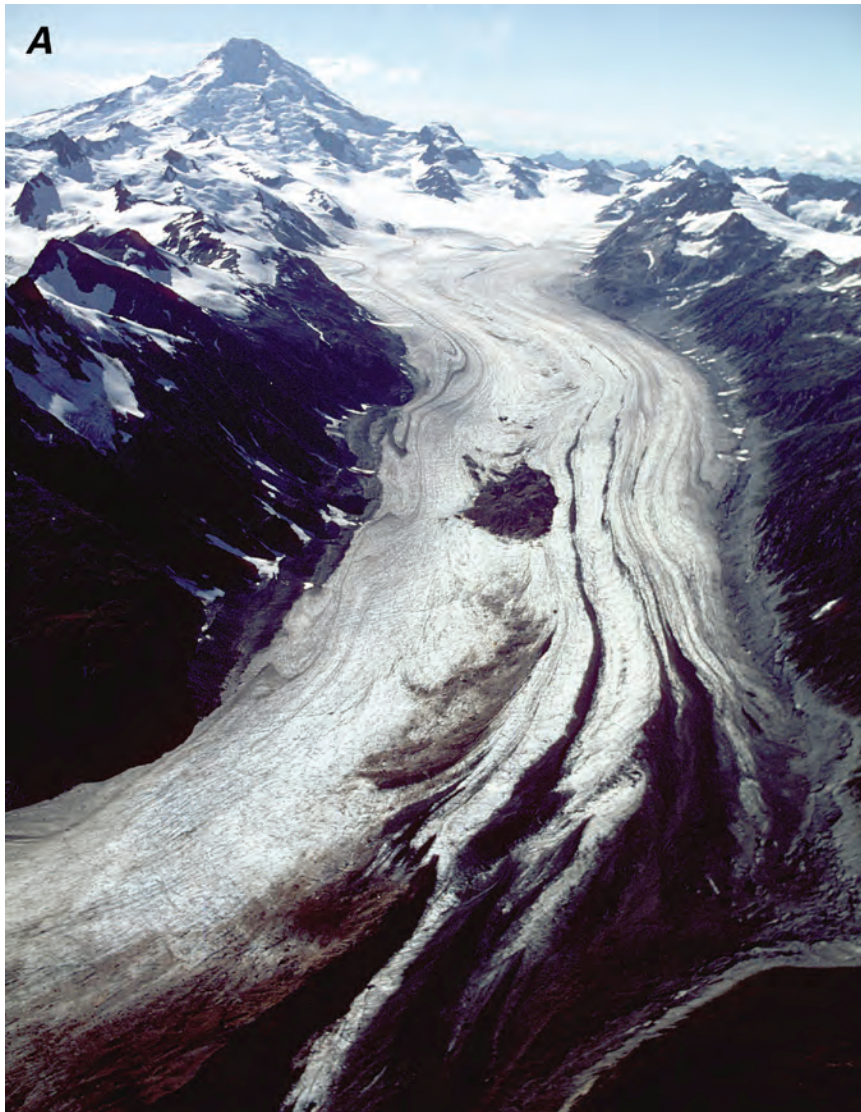


**Figure 336.**—Two 8 August 2000 oblique aerial photographs of Tuxedni Glacier, the largest and longest glacier to head on Iliamna Volcano. **A**, South-looking view up the length of Tuxedni Glacier to its source area on the flanks of Iliamna Volcano. An elevated lateral moraine on its east side and a large elevated trimline and thermokarst-pockmarked stagnant ice area on its west side document recent thinning of the glacier. **B**, East-looking view across the generally retreating and thinning terminus of Tuxedni Glacier. The trimline on the slope in front of the glacier in the upper center of the photograph suggests that the glacier was recently both thicker and more advanced. However, the push moraine on the glacier's surface where the two lobes meet suggests that a tongue of ice had recently advanced from the western tributary of the terminus (lower lobe in the photograph), bulldozing sediment in its path. At the terminus of the western tributary, ice is in contact with a push moraine, suggesting that the western terminus had recently advanced. Its rounded terminus stands several meters higher than the eastern tributary. Many retreating glaciers experience short-lived advances, generally in winter. Photographs by Bruce F. Molnia, U.S. Geological Survey.

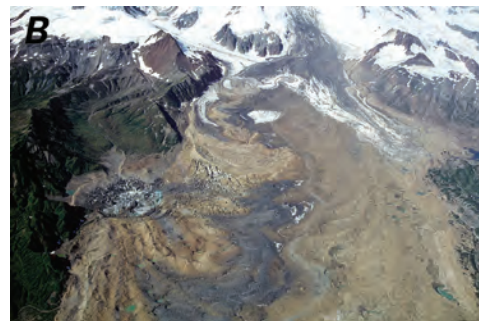
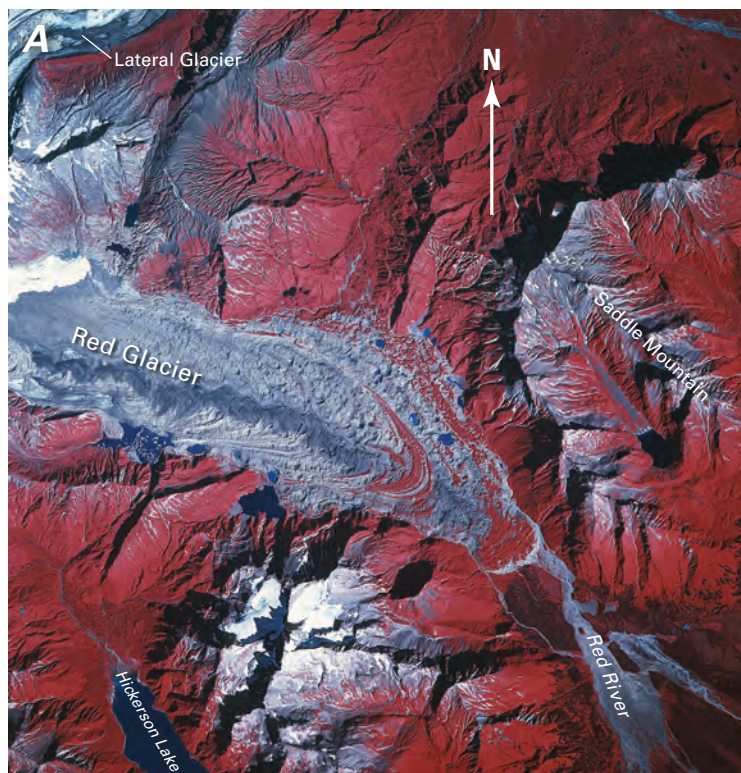


**Figure 337.**—Two aerial photographs of the terminus and lower reaches of Red Glacier, a large east-flowing glacier covered by iron-rich sediment. **A**, 26 August 1978 AHAP false-color infrared, vertical aerial photograph of the terminus of Red Glacier. Several recessional moraine ridges are covered with vegetation. Circular thermokarst melt pits filled with blue water along much of both margins suggest melting of stagnant ice and ice-cored moraines. AHAP photograph no. L120F7549 from GeoData Center, Geophysical Institute, University of Alaska, Fairbanks, Alaska. **B**, 8 August 2000 west-looking oblique aerial photograph of the upper region of Red Glacier showing a complex surface consisting of multiple-nested moraines, avalanche debris, a recently drained supraglacial lake, stagnant ice, an ice-cored moraine, and an elevated lateral moraine on the glacier's north margin. Photograph by Bruce F. Molnia, U.S. Geological Survey. A larger version of B is available online.



**Figure 338.**—8 August 2000 northeast-looking oblique aerial photograph of the summit and southwestern quadrant of the Iliamna Volcano showing Umbrella Glacier, the largest glacier on the southwestern flank. Its white-ice northwestern tributary stands more than 20 m above the iron-rich-sediment-covered surface of the main glacier and does not appear to extend beyond its elevated end moraine. Its former eastern tributaries no longer make contact with the glacier. Photograph by Bruce F. Molnia, U.S. Geological Survey. A larger version of this figure is available online.



**Figure 339.**—8 August 2000 southwest-looking oblique aerial photograph of the summit and eastern quadrant of the Iliamna Volcano showing Lateral Glacier (left), Double Glacier (middle), and Johnson Glacier (right). Lateral Glacier's iron-rich-sediment-covered terminus appears to be stagnant. Elevated moraines on the south side and exposed bedrock on the north document thinning of the glacier. Photograph by Bruce F. Molnia, U.S. Geological Survey.

their lower reaches. Iliamna Volcano's glaciers cover about four times the area of Redoubt Volcano's glaciers.

On the basis of radio-echo-sounding measurements made in July 1988 and volume modeling, Trabant (1999) estimated perennial snow and glacier ice volumes on Iliamna Volcano to be 8.6 km<sup>3</sup> for Tuxedni Glacier, 0.85 km<sup>3</sup> for Lateral Glacier, 4.7 km<sup>3</sup> for Red Glacier, and 0.60 km<sup>3</sup> for Umbrella Glacier. The estimated volume of perennial snow and glacier ice on the upper 1,000 m of the volcano is about 1 km<sup>3</sup>. Errors are thought to be no more than ±25 percent. The volume estimated for the four largest glaciers is more than three times the total volume of perennial snow and glacier ice on Mount Rainier, Wash., and about 82 times the total volume of perennial snow and glacier ice on Mount St. Helens, Wash., before its 18 May 1980 eruption.

### Glaciers West and South of Redoubt and Iliamna Volcanoes

As of an 8 August 2000 observation, all of the outlet glaciers and many of the cirque glaciers located west and south of Redoubt and Iliamna Volcanos were thinning and retreating (fig. 340) (26 August 1978 false-color infrared vertical aerial photograph no. L120F7555). Many of the cirques located on the northern side of the Tuxedni River and in the Pile River and Iliamna River areas in the southernmost Chigmit Mountains appeared to have recently become ice free (26 August 1978 false-color infrared vertical aerial photograph no. L120F7599). In addition to other evidence of glacier thinning and retreat, numerous tarn lakes and ice-free cirques are evidence of recent glacier change and disappearance of some glaciers.

### Glaciers of the Kamishak Bay–Big River Area

It is nearly 80 km from the southernmost glacier in the Chigmit Mountains, located just west of Iliamna Bay, to the summit of Mount Douglas (2,153 m), the highest point on an unnamed ice field, that has an area of more than 300 km<sup>2</sup> and supports more than 20 outlet glaciers (fig. 341). Fourpeaked Mountain (2,104 m) is the highest point on the southern part of the ice field. Seven glaciers have lengths of 8 to 14 km and termini more than 3 km wide. Two of the largest (and the only named) glaciers—Spotted Glacier (12 August 1982 AHAP false-color infrared vertical aerial photograph no. L131F1827) and Fourpeaked Glacier—have debris-covered termini and show evidence of recent retreat. In 1904, Spotted Glacier's terminus was about 1.5 km from Kamishak Bay, ending at an elevation of about 45 m amsl (Tarr and Martin, 1914). By the time of compilation of the Afognak, Alaska, 1:250,000-scale 1952 USGS topographic map (appendix A), the glacier had retreated several hundred meters and terminated at an elevation closer to 90 m amsl. An unnamed glacier just to the west of Spotted Glacier had a barren zone halo a kilometer wide around its margin in 1982. Since then, its western terminus has separated from the main ice tongue. A number of smaller unnamed glaciers occur on ridges immediately west and southwest of the ice field. The largest is about 4 km long.

Fifty-five kilometers to the west of Mount Douglas is another small concentration of upland glaciers that were last surveyed in 1951. Bounded by Pirate Lake and McNeil River to the north, Strike Creek to the east, and Kilik Lake to the west, about 25 small unnamed glaciers occupy cirques or ridge crests at elevations ranging from about 1,200 to 1,670 m on the USGS 1:250,000-scale Mt. Katmai, Alaska, topographic map (appendix A).

In July 1923, USGS geologist K.F. Mather photographed cliff and cirque glaciers at several locations north of the McNeil River and west of Kamishak Bay. His photographs show small retreating and thinning glaciers at locations that no longer support glacier ice (fig. 342)

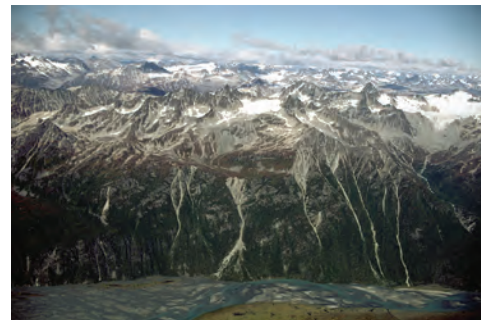
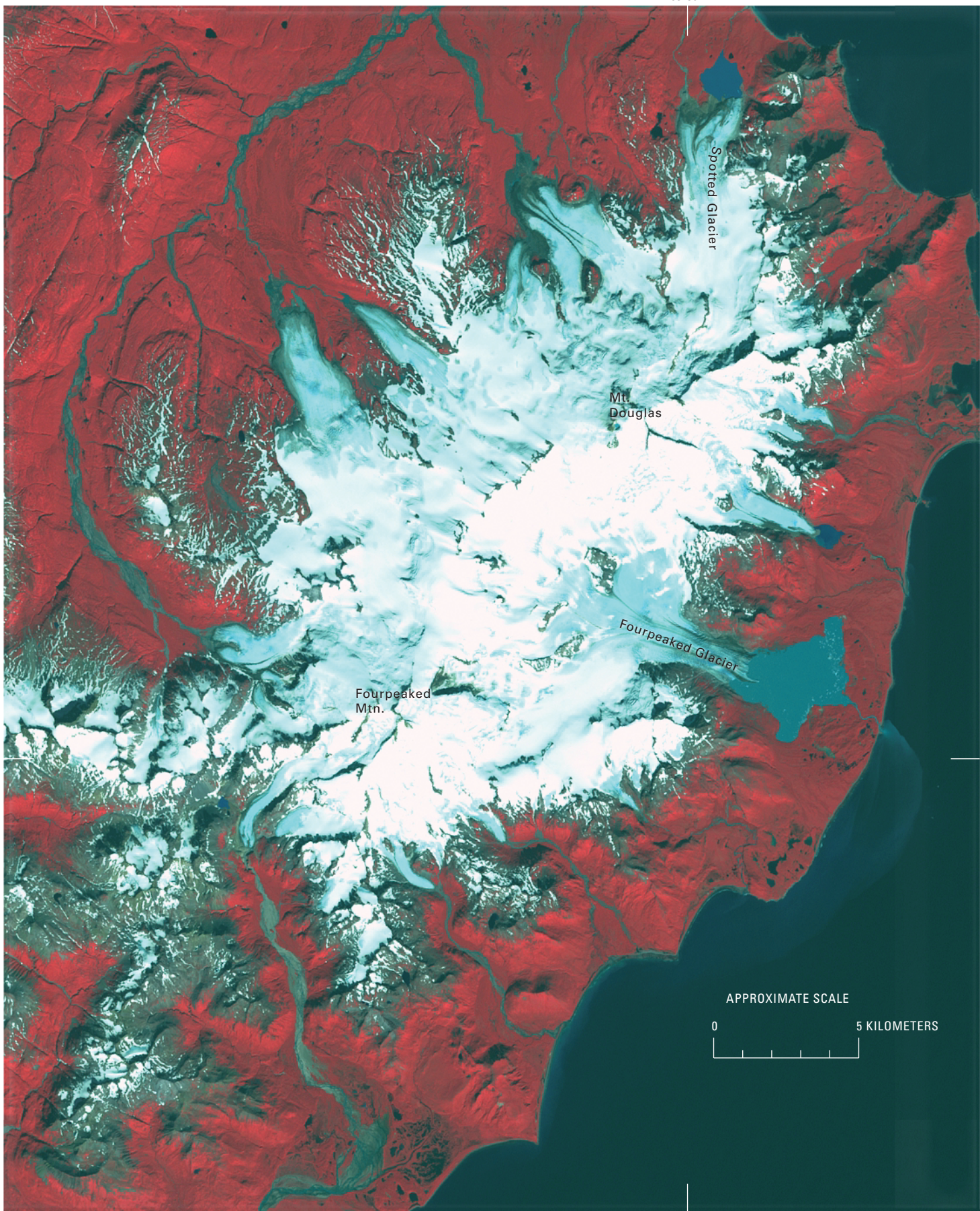


**Figure 340.**—8 August 2000 north-looking oblique aerial photograph of the southwestern Chigmit Mountains north of the Tuxedni River showing shrinkage and disappearance of cirque glaciers, including a number of recently ice-free cirques, several with tarn lakes. All of these abandoned cirques are located above an elevation of 1,000 m. Photograph by Bruce F. Molnia, U.S. Geological Survey. A larger version of this figure is available online.

► **Figure 341.**—Annotated Landsat 7 ETM+ false-color composite image of the Kamishak Bay–Big River area showing an unnamed ice field in the Mount Douglas–Fourpeaked Mountain area and numerous unnamed and several named outlet glaciers. Approximate scale 1:175,000. Landsat 7 ETM+ image (7070019000022950, bands 2, 3, 4; 16 August 2000; Path 70, Row 19) from USGS, EROS Data Center, Sioux Falls, S. Dak.

153°30'W

58°45'N



APPROXIMATE SCALE

0

5 KILOMETERS



**Figure 342.**—A July 1923 photograph by K.F. Mather of small cirque and cliff glaciers located west of Kamishak Bay showing a complex of retreating unnamed cirque glaciers in a large north-facing basin of a 1,230-m-high mountain, just south of the Paint River. The 1957 USGS topographic map of this area shows no glacier at this location. Photograph Alaska 207 from the USGS Photo Library, Denver, Colo.

### Glaciers of the Ninaiak River–Puale Bay Area

More than a hundred glaciers, at least 20 of which have lengths of 5 km or greater, are located in central and southwestern Katmai National Park and Preserve (fig. 343) and immediately to its southwest. Most descend from a 80-km-long area of ice-covered volcanoes and mountains extending from Devils Desk (1,954 m) on the northeast to Mount Martin (1,844 m) on the southeast. Peaks that support glaciers include Kukak Volcano (2,042 m), Mount Steller (2,225 m), Mount Denison (2,318 m), Snowy Mountain (2,161 m), Mount Katmai (2,047 m), Trident Volcano (1,832 m), Mount Griggs (2,316 m), and Mount Mageik (2,210 m). More than a dozen glaciers are more than 8 km long. The longest is east flowing Hallo Glacier, which is 19 km long and 88 km<sup>2</sup> in area (Denton and Field, 1975b, p. 631) (see Landsat 7 ETM+ browse image 7070019000022950; 16 August 2000, Path 70, Row 19) and originates on the flanks of Kukak Volcano, Mount Steller, and Mount Denison. North-flowing Hook Glacier and a western tributary glacier informally known as *West Hook* also originate on these same peaks. Both are known to surge, the latter as recently as 1984. Other named glaciers include Serpent Tongue Glacier and The Knife Creek Glaciers. There are also many unnamed glaciers in the area, such as the six that descend from the summit of Mount Griggs.

Mount Katmai is a large stratovolcano that is about 10 km in diameter and has a central lake-filled caldera about 4.5×3 km in size. The caldera that contains Crater Lake has a maximum wall elevation of 2,047 m, a floor elevation of about 1,036 m, and relief of more than 1 km. The volcano is one of five explosive eruption vents and calderas that encircle Novarupta Dome. Much of the volcano is mantled by perennial snow and glacier ice, and several valley glaciers radiate down its flanks. Three glaciers also originate from the upper caldera walls and descend into the crater to Crater Lake (Motyka and others, 1977). Before its 1912 eruption, Mount Katmai's summit was similar to the summits of Redoubt and Iliamna Volcanoes, which were completely encircled by active glaciers. As a result of the eruption, about 600 m of the mountain's summit (including snow fields and glaciers) disappeared, leaving many beheaded glaciers. Most lost major parts of their accumulation areas (Muller and Coulter, 1957a). Following the eruption, two small glaciers formed on the talus beneath the crater rim (Muller and Coulter, 1957b).

Because more than 30 km<sup>3</sup> of volcanic material was ejected by the 1912 eruption of Mount Katmai (Denton and Field, 1975b; Griggs, 1922), many glaciers on the mountain and on adjacent peaks are covered by tephra (including light-colored pumice) deposits; in places, the airfall deposits are many meters thick. At Knife Creek on nearby Trident Volcano, Muller and Coulter (1957b) described how one of the five Knife Creek Glaciers (which they referred to as *First Knife Creek Glacier* through *Fifth Knife Creek Glacier*),

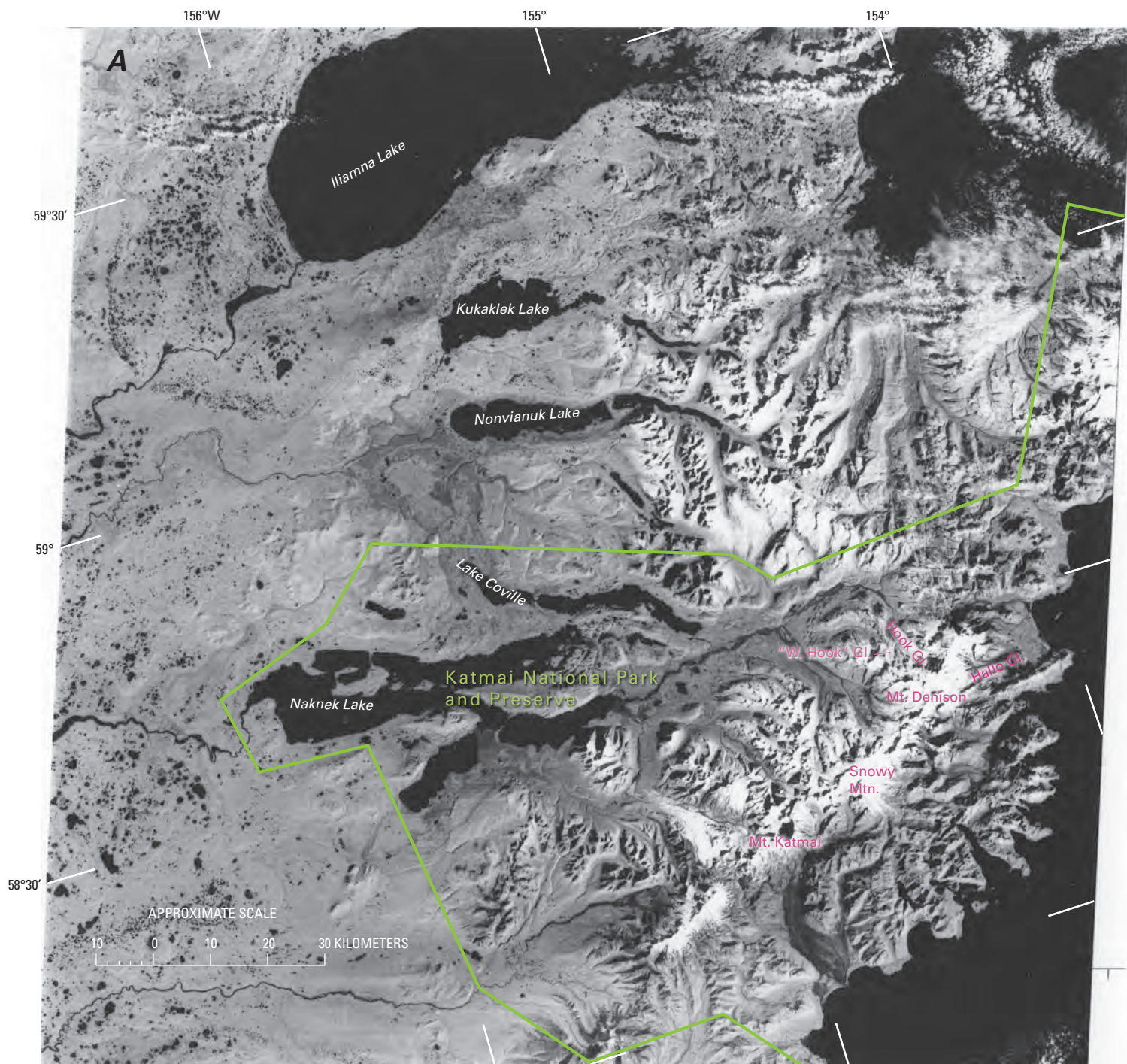
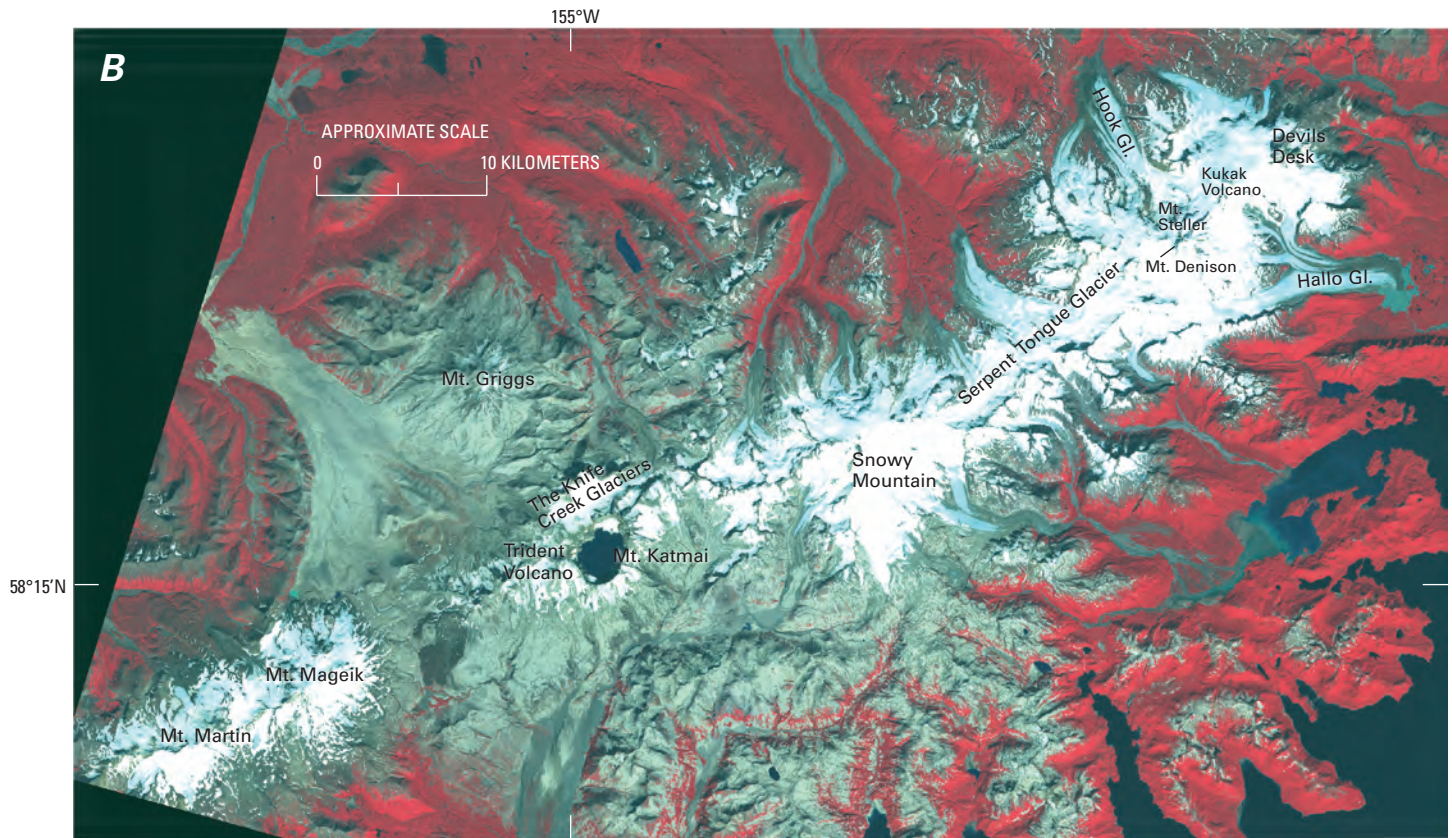


**Figure 343.**—A, Annotated Landsat 2 MSS image of Katmai National Park and Preserve and environs. Mount Katmai (2,047 m), Snowy Mountain (2,161 m), Mount Denison (2,301 m), and Mount Douglas (2,153 m) (just off the upper right edge of the image) all support large glaciers. The glaciers on Mount Katmai, barely visible on this image, lost major portions of their accumulation areas when Mount Katmai erupted in 1912 (Muller and Coulter, 1957b). The West Hook Glacier and Hook Glacier are known to surge; the latter glacier surged in 1984. The glaciers in this area have lengths of up to about 15 km. Evidence of past glaciation is striking. The basin of Iliamna Lake was once glacier filled, and the limit of ice is indicated by an arcuate line of small lakes 35 km west of the present west shore. Other notable moraines occur west of Naknek Lake, Lake Colville, Nonvianuk Lake, and Kukaklek Lake. Landsat image and caption courtesy of Robert M. Krimmel, U.S. Geological Survey. Landsat 2 image (2983–20253, band 7; 10 October 1977; Path 77, Row 19) is from the USGS, EROS Data Center, Sioux Falls, S. Dak. B, see following page.



was covered by pyroclastic debris that protected it from subsequent ablation despite the loss of most of its accumulation area during the eruption. The 18 May 1980 eruption of Mount St. Helens, Wash., also beheaded and destroyed glaciers on its northern side.

More than a dozen glaciers descend from the flanks of Mount Mageik and Mount Martin (27 August 1983 AHAP false-color infrared vertical aerial photograph no. L138F6708). Mount Mageik was visited in the early 1920s by Smith (1925) and Hubbard (1935), who described a small crevassed tephra-covered glacier that was located on its northern flank. Mount Martin is a largely ice-covered stratovolcano at the southern end of the Katmai group. Recent volcanic activity has deposited yellow sulfur on its snow- and ice-covered crater walls (6 October 1994 space shuttle photograph no. STS-068-244-010). Several isolated unnamed glaciers located about 25 km southwest of Mount Martin near Kejulik Pass form the headwaters of Takayofu Creek.

The glaciers of the Ninagiak River–Puale Bay area were first described by Spurr (1900), who briefly noted that glaciers were common on mountain axes and also descended down the flanks of the volcanoes into the valleys. Beginning in 1915, Griggs (1922) led five expeditions to the Mount Katmai area to document the impacts of the 1912 eruption. He (Griggs, 1922, p. 171) described the accumulation of volcanic deposits on the surface of glaciers that he traversed in 1916:

“The appearance of these ice fields was curious in the extreme. Where a glacier was moving rapidly, the variously colored layers of ash were dumped about promiscuously among the glacial seracs, making a bizarre and highly colored picture, the reds, browns, blacks, yellows in vivid contrast to the pure blue ice. Where the glacial motion was slower and steadier the ash deposit still lay as it fell.... Glaciers of this peculiar type extended clear up to the very rim of the crater, above whose depths the loose blocks of ice hung with such a precarious hold that we dared not approach.”

Several days later, Griggs (1922, p. 173–4) described the glaciers of the crater rim:

...we could see another notch in the rim at about the same altitude as the one where we stood, But this one was occupied by a wall of ice which rose vertically, flush with the crater walls, as though sheared off by the explosion. It was surprising at first sight to find that a glacier could have persisted on the crater rim, unmelted by the heat of

**Figure 343.—B, Annotated Landsat 7 ETM+ false-color composite image of the Ninagiak River–Puale Bay area, providing coverage similar to A but 23 years later. Approximate scale 1:330,000. Landsat 7 ETM+ image (7070019000022950, bands 2, 3, 4; 16 August 2000; Path 70, Row 19) from USGS, EROS Data Center, Sioux Falls, S. Dak.**



the eruption. ... Ice cliffs, the exposed ends of beheaded glaciers, stretch for several miles along the crater rim. The glaciers bear little if any indication of having dwindled during the eruption. The parts preserved on the outer slope were outside the blast of the explosions, which must have been directed skyward. ... The crater wall has caved in considerably since the eruption and is still slumping away at short intervals. It is such an unstable condition that it is no infrequent experience, while standing on the crater rim, to be startled by a roar as something lets go, and on searching for the cause to find a mass of ice and rock bouncing down the half-mile precipices into the abyss.

### Glaciers of the Icy Peak–Mount Kialagvik–Mount Chiginagak Area



**Figure 344.**—Summer 1919 southwest-looking panorama of the unnamed cirque and mountain glaciers that descend from the north side of Icy Peak. Kialagvik Creek is in the foreground and the head of Wide Bay is to the east (left). Several cirques show significant evidence of recent glacier thinning and retreat. Photographs Capps 993–995 from the USGS Photo Library, Denver, Colo. A larger version of this figure is available online.

The distance from Mount Martin to the eastern end of an unnamed ice field that includes as its highest points Mount Kialagvik (~1,596 m) and Icy Peak (1,370 m) is about 100 km. This small ice field, which has an area of about 40 km<sup>2</sup>, supports more than a dozen small unnamed glaciers that combine for an area of approximately 15 km<sup>2</sup>. They descend from an upland more than 12 km in length to elevations below 300 m. The glacier that forms the headwater of Glacier Creek is more than 8 km long and terminates at an elevation of less than 200 m amsl. A number of unnamed cirque and mountain glaciers are situated on Icy Peak; figure 344 shows some of them on the northern flank of Icy Peak in 1919.

More than a dozen outlet glaciers drain the summit and flanks of Mount Kialagvik. Three unnamed glaciers that form the headwaters of the eastern fork of the Dog Salmon River range in length from about 3 to about 4.5 km. The largest unnamed glacier, which is about 6 km in length, descends from Mount Kialagvik to an elevation of about 300 m and forms the headwaters of the central fork of the Dog Salmon River.

Mount Chiginagak (2,067 m) is a symmetric composite cone about 8 km in diameter. Glaciers cover about 20 to 25 km<sup>2</sup> of its summit and slopes (fig. 345)



**Figure 345.**—August 1960 oblique aerial photograph of the glacier-covered summit of Mount Chiginagak. Fresh crevasses are indicative of bergschrund development in individual glacier basins. Photograph No. 12–50 by Austin Post, U.S. Geological Survey.

at elevations above about 500 m. The earliest description of the glaciers of Mount Chiginagak was provided by Smith and Baker (1924.) From about 10 to 25 km west of the summit of Mount Chiginagak, several ridges are covered by accumulations of ice. The largest, which is nearly 10 km long, forms the headwaters of Painter Creek.

### Glaciers of the Aniakchak Crater Area

Denton and Field (1975a) reported that several unnamed glaciers with a combined area of about 0.6 km<sup>2</sup> are located inside the southern wall of 1,340 m-high Aniakchak Crater (fig. 346). Formed during a catastrophic ash-flow eruption about 3,400 years ago, Aniakchak caldera is about 10 km

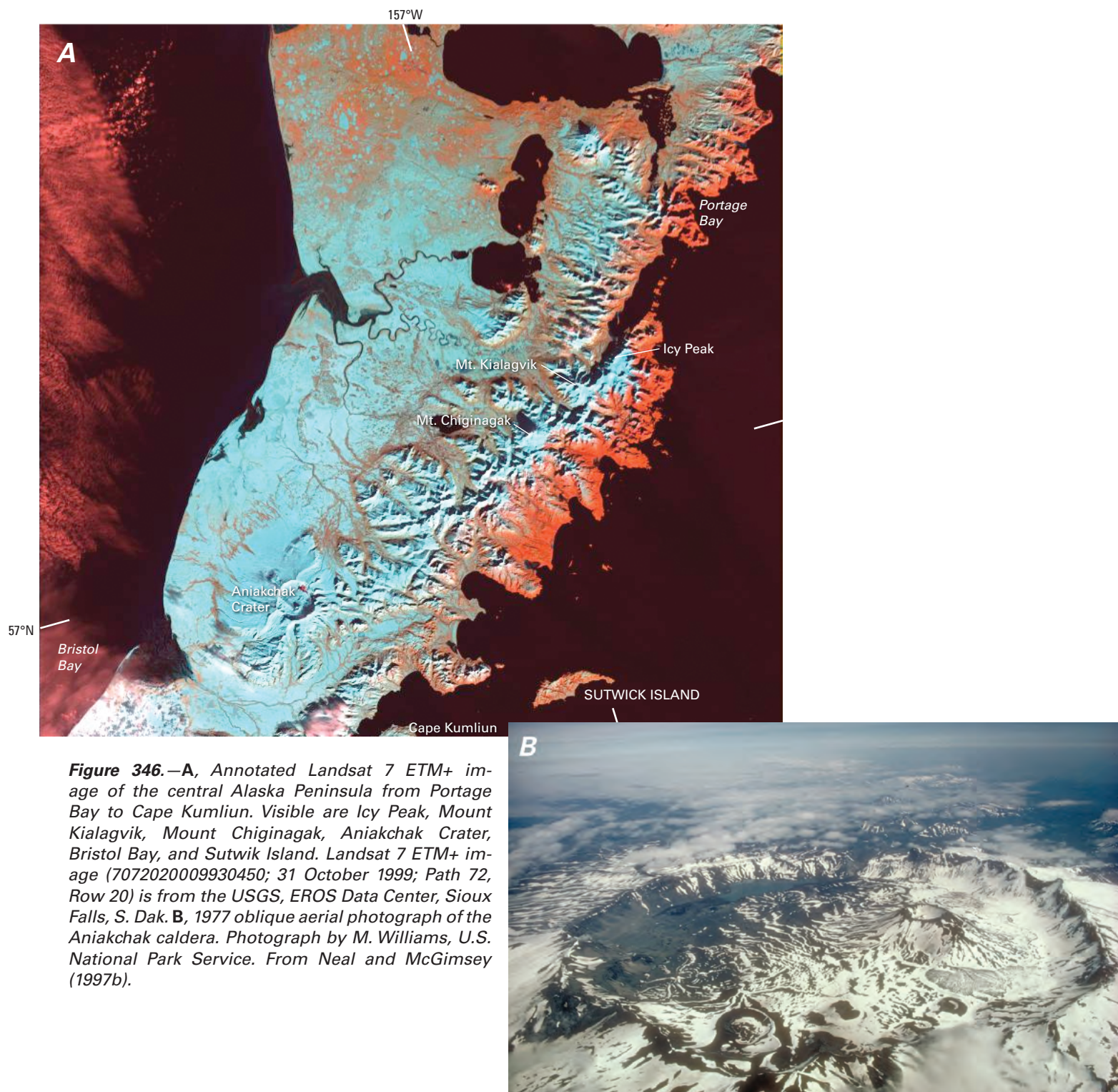


**Figure 346.**—**A**, Annotated Landsat 7 ETM+ image of the central Alaska Peninsula from Portage Bay to Cape Kumliun. Visible are Icy Peak, Mount Kialagvik, Mount Chiginagak, Aniakchak Crater, Bristol Bay, and Sutwick Island. Landsat 7 ETM+ image (7072020009930450; 31 October 1999; Path 72, Row 20) is from the USGS, EROS Data Center, Sioux Falls, S. Dak. **B**, 1977 oblique aerial photograph of the Aniakchak caldera. Photograph by M. Williams, U.S. National Park Service. From Neal and McGimsey (1997b).

across and averages 500 m in depth (fig. 346). Glacier ice also fills the crater of 1,018-m-high Vent Mountain, a large cinder cone within the crater on the southern side (Knappen, 1929). Glaciers on the crater floor are covered by a thick deposit of pumice.

### **Glaciers of the Mount Veniaminof–Stepovak Bay Area**

Mount Veniaminof (fig. 347) is a broad cone-shaped volcano 2,507 m high and about 35 km across at its base. The size of its steep-walled summit caldera is approximately 8×11 km. The caldera is filled by a large ice accumulation ranging in elevation from about 1,750 to 2,000 m. Ice overflows the southern rim of the caldera and covers more than 200 km<sup>2</sup> of the upper slopes on the southern side of the volcano. Knappen (1929) described the crater's glaciers as follows: "The crater of Mount Veniaminof is filled with a great circular glacier, 8 to 10 km in diameter, which overflows in three directions. To the northeast it flows through small cols, spilling down the mountain and forming Crab Glacier outside the crater; to the south the ice overtops the crater for a length of 3 km or more, but probably this ice stream is relatively shallow; to the west, the ice flows through a canyon estimated as 600 m deep, forming Cone Glacier. The western outlet is fully 300 m lower than either of the others, and a great river of crevassed and shattered ice, perhaps 200 m wide, grinds through the passageway and greatly depresses the level of the ice on that side of the crater."

In the western part of the caldera, a 570-m-high active cone with a small summit crater reaches an elevation of 2,156 m, approximately 330 m above the surrounding glacier ice. In 1983, eruptive activity from this cinder cone melted about 0.15 km<sup>3</sup> of the summit ice cap (fig. 347). The rim of a larger but lower cone protrudes just above the ice surface in the northwestern part of the caldera.

Eight named valley glaciers having a combined area of approximately 15 km<sup>2</sup> descend from the caldera through gaps on the western and northern sides of the rim, and other alpine glaciers occupy valleys on the north-, east-, and west-facing slopes of the mountain. Named glaciers include Cone, Fog, Island, Outlet, Crab, Harpoon, Finger, and Slim Glaciers. An unnamed glacier is located between Fog and Island Glaciers. The terminus of Slim Glacier extends to an elevation 275 m amsl and is 14 km from the summit crater (Denton and Field, 1975b, p. 633). A number of other unnamed glaciers are present to the southwest, east, and northeast. All of Mount Veniaminof's outlet glaciers are tephra covered, so that it is difficult to assess their mass balance. Telltale signs indicate evidence of recent retreat, however.

From about 10 to about 75 km west of the summit of Mount Veniaminof, several ridges are covered by significant accumulations of ice, many with small unnamed outlet glaciers. The largest ridge, which is nearly 20 km long, is located north of Stepovak Bay (26 August 1983 AHAP false-color infrared vertical aerial photograph no. L161F6197) and supports several outlet glaciers up to 4 km long.

### **Glaciers of Pavlof Volcano–Frosty Peak Area**

Located about 120 km southwest of Stepovak Bay, the Pavlof Sister (2,122 m)–Pavlof Volcano (2,507 m)–Little Pavlof (2,038 m)–Mount Hague (~1,450 m) complex hosts an ice accumulation about 20 km long that has more than a dozen outlet glaciers. The glaciers of the Pavlof Volcano area cover an area of more than 130 km<sup>2</sup> (Denton and Field, 1975b, p. 629). Much of the upper slopes of Pavlof Volcano, Little Pavlof Volcano, Double Crater, Pavlof Sister, Mount Hague, and Mount Emmons are also covered by snowfields and glacier ice at elevations above 300 m (fig. 348). Pavlof Volcano is the most active volcano in the Aleutian Range with about 40 documented eruptions since 1790 (McGimsey and Miller, 1995).

The glaciers of this area were mapped by Kennedy and Waldron (1955), who described Mount Hague as having several individual glaciers in its crater

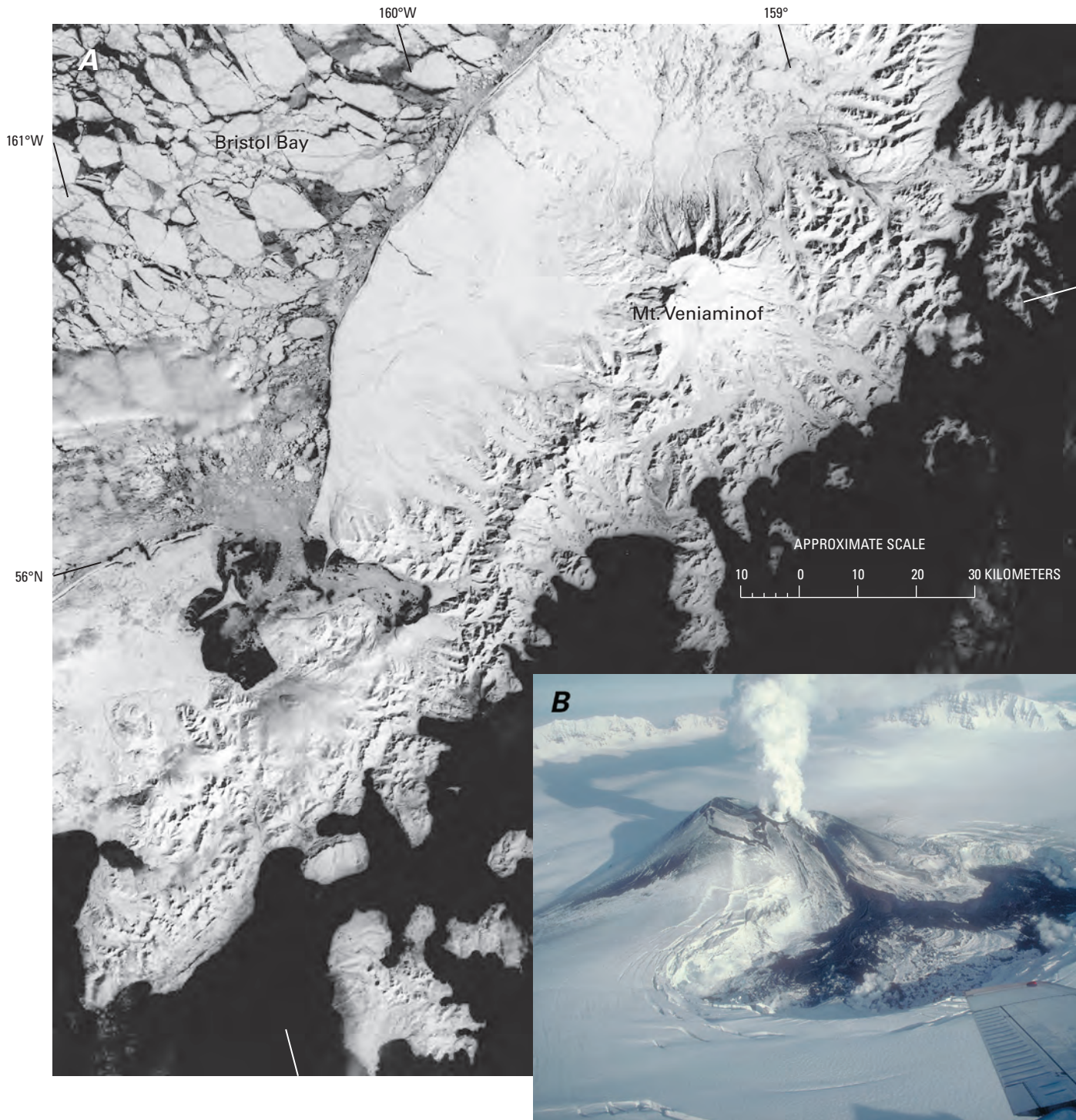


**Figure 347.**—The glaciers of the Western Aleutian Range and Aleutian Islands are difficult to observe using Landsat because they are relatively small and because the weather is notoriously poor. Most of these glaciers lie on volcanoes. **A**, Landsat 2 MSS image of Mount Veniaminof (2,507 m); the volcano was active in 1983 and 1984. Several eruptions have flowed from a cone within the ice-filled caldera, melting a large amount of ice. This March scene is of little value for delineating present-day glaciers because of the snow cover. However, the ice-filled summit caldera and glacier-carved valleys radiating to the north from Mount Veniaminof are visible. Bristol Bay is

covered with broken sea ice. Landsat image and caption courtesy of Robert M. Krimmel, U.S. Geological Survey. Landsat 2 image (2427–21001, band 7; 24 March 1976; Path 79, Row 21) is from the USGS, EROS Data Center, Sioux Falls, S. Dak. **B**, Oblique aerial photograph showing “Steam rising from the intracaldera cinder cone at Mount Veniaminof on 23 January 1984 in the waning stages of the 1983–1984 eruption. Cooling lava flows fill a pit about 2.3×1.0 km that has been melted in the summit ice cap” (Neal and McGimsey, 1997b). Photograph by M.E. Yount, U.S. Geological Survey.

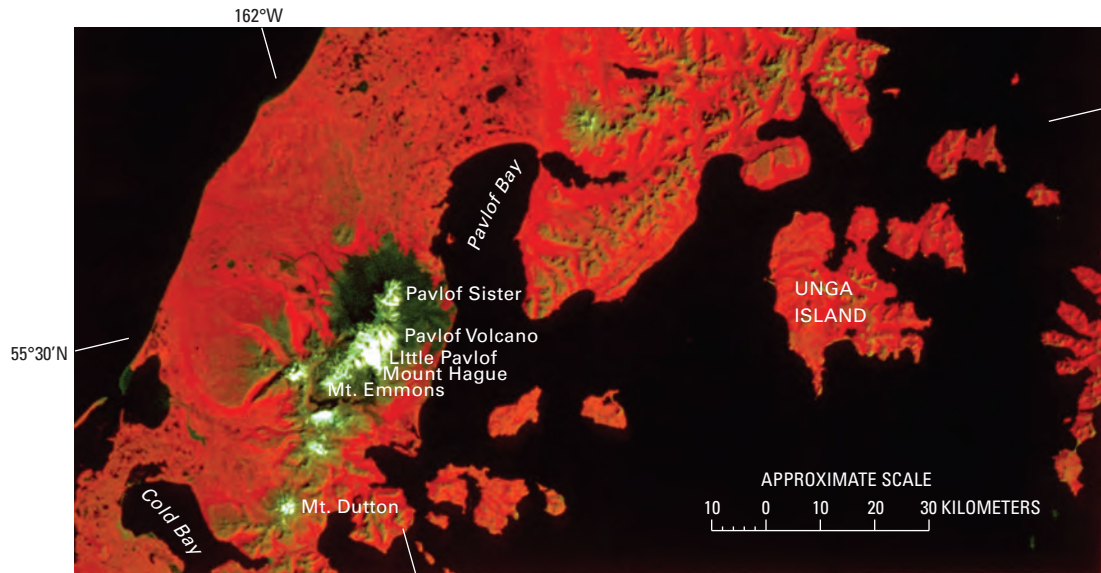


**Figure 348.**—Part of an annotated Landsat 2 MSS false-color composite image of the southern Aleutian Range. The image shows part of the southern Alaska Peninsula from Pavlof Bay to Cold Bay. Visible are Pavlof Volcano, Pavlof Sister, Mount Emmons, Mount Dutton, and Unga Island. Landsat image (2168–821044, bands 4, 5, 7; 6 August 1979; Path 80, Row 21) is from the USGS, EROS Data Center, Sioux Falls, S. Dak.

and several more on its slopes. Mount Emmons supports a small glacier with an area of a few square kilometers; a glacier with an elliptical shape occurs on the highland immediately adjacent to the southern side of Emmons Lake. The Aghileen Pinnacles also support several small glaciers. Although none of these glaciers have been studied in recent years, Neal and McGimsey (1997a) noted that the most recent eruptive episode at Pavlof Volcano, which began about 11 September 1996 and continued into early 1997, melted a narrow channel through the snow and glacier-ice cover of the volcano.

Frosty Peak (1,746 m) hosts the westernmost and southernmost glaciers in the Aleutian Range. About a dozen descend from its summit ridge and slopes (fig. 349). The largest is an unnamed glacier about 4 km long and as much as 2.4 km wide. The northeastern side of the mountain contains several large Pleistocene and early Holocene cirques that extend as much as 6 km from its summit. Holocene moraines reach as far as 10 km from the peak. The age of the latest advance is unknown but is probably between 3,000 and 10,000 yr B.P. (Funk, 1973; Black, 1976).

## Summary

During the period of the Landsat baseline (1972–81), all of the surge-type and non-surge-type valley glaciers in the Aleutian Range were stagnant, thinning, and (or) retreating. Some surge-type glaciers were reported to have surged during the baseline period, but no terminus advances were reported. At the end of the 20th century, all of the observed valley and outlet glaciers in the Aleutian Range continued to thin, stagnate, and retreat. Some glaciers showed evidence of surging near the end of the 20th century, including Capps Glacier, which surged in 2000. However, no reported surge events resulted in terminus advance.

When the terminus of Tuxedni Glacier was observed in 2000, it showed evidence of a recent small advance. However, trimlines and abandoned moraines document a previous long-term history of retreat and thinning. Following the 1989–90 eruptions of Mount Redoubt, new snow and ice has accumulated in its summit crater, essentially replacing all of the glacier ice and snow that was lost during the eruptions. This situation is similar to that of a pair of glaciers that formed in the summit crater of Mount Katmai in the years following its 1912 eruption.

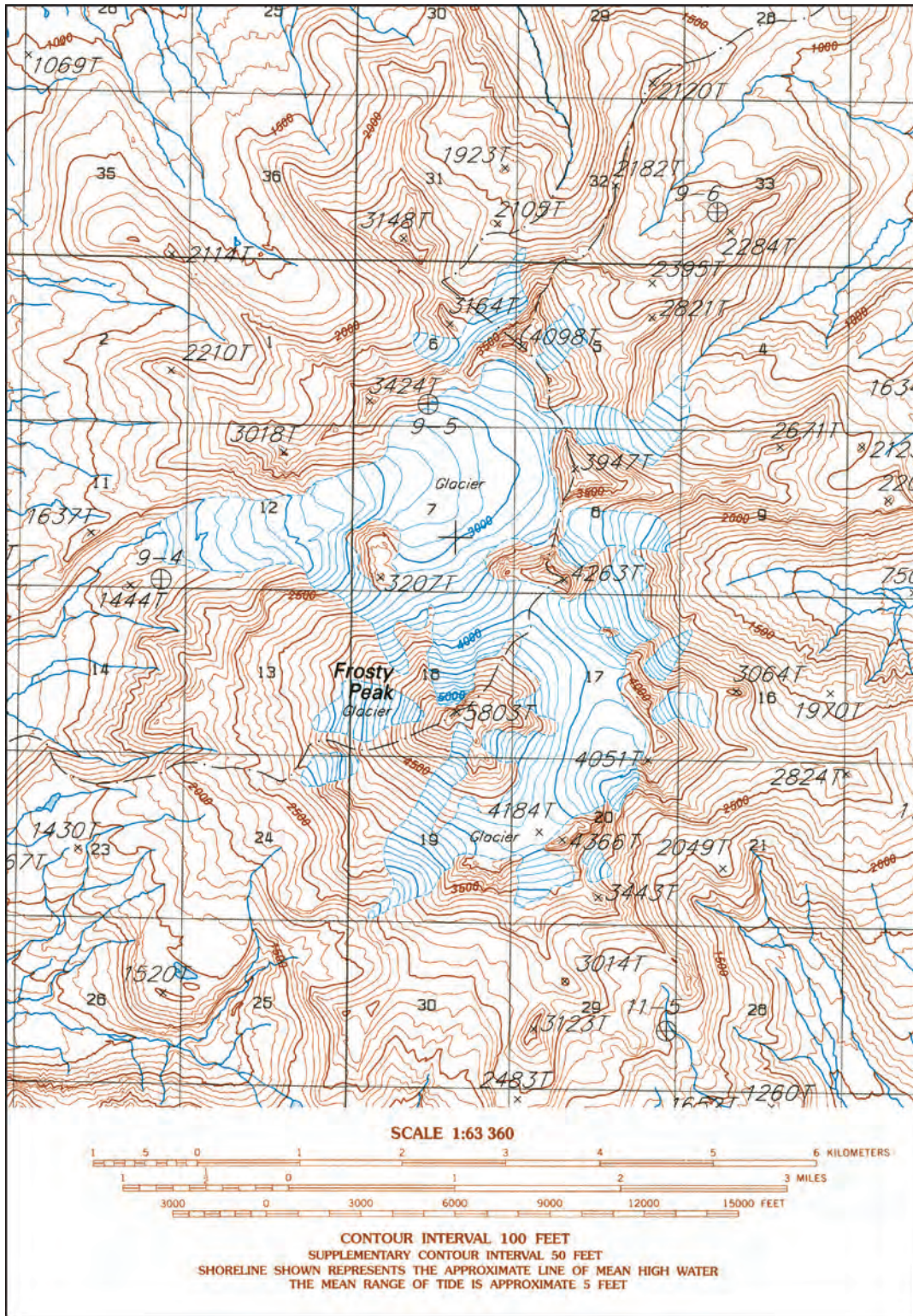


**Figure 349.**—Part of the provisional 1:63,360-scale topographic map of the Cold Bay, Alaska A-3 quadrangle. At the end of the 1990s, when the provisional 1:63,360-scale topographic maps of parts of the Cold Bay, Alaska quadrangle based on 1987 aerial photography were released, they showed extensive glacierization of Frosty Peak. No glaciers were shown on the 1943 Cold Bay, Alaska 1:250,000-scale USGS topographic map (appendix A). Because many glaciers are either completely or partially covered by tephra (airborne volcanic ejecta), cartographers, working only with aerial photographs for such areas, where there were no field surveys or very limited data, may have been unable to determine the presence and locations of glaciers. Snow cover would have made this task even more difficult.

# Aleutian Islands

## Introduction

The Aleutian Islands volcanic archipelago, the 1,900-km-long island arc that separates the Pacific Ocean from the Bering Sea, extends westward from False Pass at the western end of the Alaska Peninsula to about long 172°E., north of eastern Russia (figs. 1, 350). Wahrhaftig (1965) stated that the islands contain 57 volcanoes, 27 of which are active. “Most high volcanoes bear icecaps or small glaciers and there are a few cirque glaciers on the mountainous islands” (Wahrhaftig, 1965, p. 25). A recent summary of active Alaskan volcanoes by Wallace and others (2000) identified 24 that have been active since the middle 1700s.

At least 10 islands in the eastern and central part of the arc have been reported to have glaciers. From east to west, islands where glaciers have been reported are Unimak, Akutan, Unalaska, Umnak, Herbert, Atka, Great Sitkin, Tanaga, Gareloi, and Kiska (figs. 1, 350). All of the mapped glaciers of the Aleutian Islands descend from the summits of active or dormant volcanoes, extending either into calderas or down their flanks. All head at elevations greater than 1,200 m. Descriptions of the glaciers of the Aleutian Islands have been presented by Westdahl (1903), Tarr and Martin (1914), Finch (1934), Collins (1945), Sharp (1956), Denton (1975a), Molnia (1982, 1993, 2001), and Field (1990). The total area of glaciers is 960 km<sup>2</sup> (Post and Meier, 1980, p. 45).

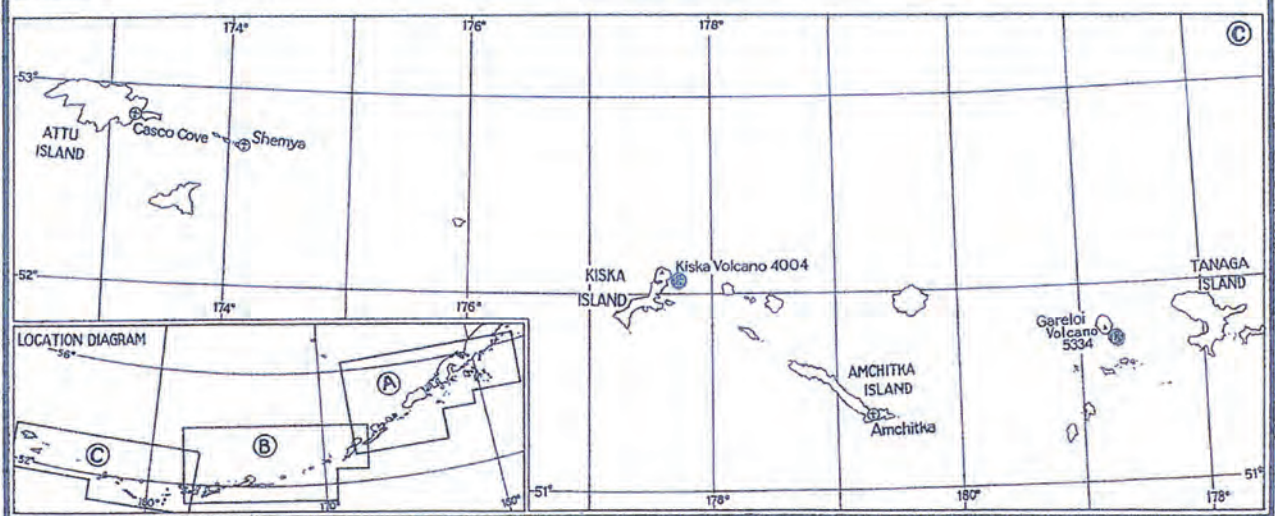
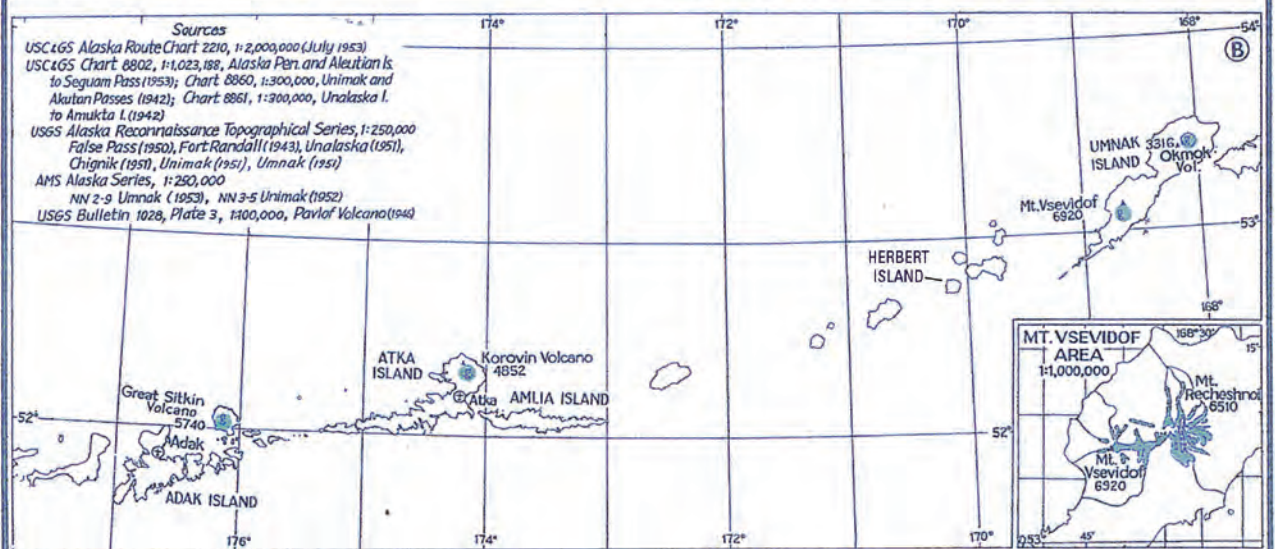
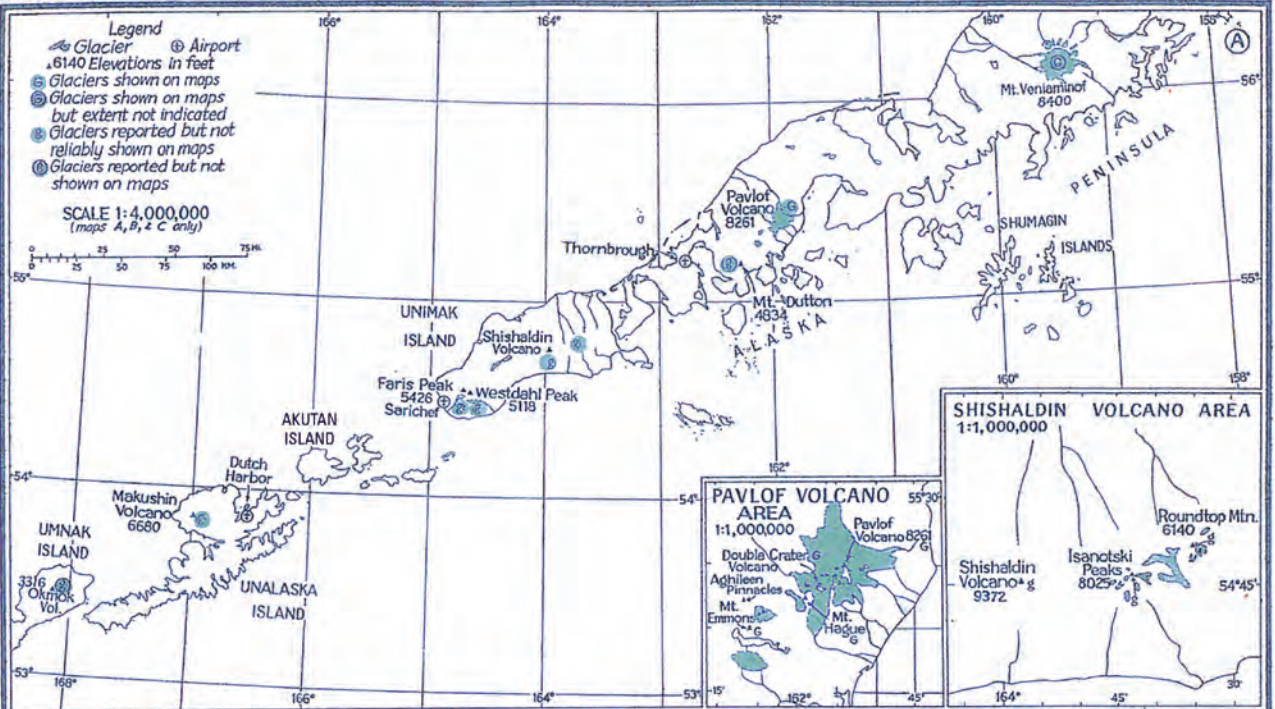
It is possible that glaciers may exist on other islands within the Aleutians because there is a lack of basic information on the physical geography of many of them. For instance, Mount Cleveland— a stratovolcano on Chuginadak Island, one of the Islands of the Four Mountains— has a summit elevation of about 1,730 m, higher than many peaks in the Aleutian Islands that support glaciers. Although no information could be found about glaciers on Mount Cleveland, Chuginadak Island shows evidence of recent glacial erosion.

Landsat MSS images that cover the glacierized Aleutian Islands have the following Path/Row coordinates: 81/22, 82/22, 83/22, 83/23, 84/23, 85/23, 86/23, 87/24, 88/24, 89/24, 90/24, 91/24, 93/24, and 94/24 (fig. 3, table 1). These areas are mapped (from east to west) on the False Pass (1949), Unimak (1951), Unalaska (1951), Umnak (1951), Samalga Island (1951), Amukta (1951), Atka (1959), Adak (1957), Gareloi Island (1954), and Kiska (1951) USGS 1:250,000-scale topographic quadrangle maps of Alaska (appendix A). Regardless of the printed publication date for a specific map, the date of the source material used for map compilation is older.

Many of the 10 USGS 1:250,000-scale topographic quadrangle maps (appendix A) are based on old surveys and maps produced by the AMS (later DMA, then NIMA, now the NGA) between 1947 and 1958; on NOAA topographic manuscripts surveyed between 1953 and 1959; and on NOAA nautical charts. Two of the quadrangle maps state that plane-table surveys were the basis for mapping: the first was carried out in 1928 (False Pass map sheet) and the second between 1940 and 1944 (Unalaska map sheet). Only 4 of 10 topographic quadrangle maps state that the topographic contours are based on aerial photography collected between 1934 and 1948: False Pass (1942–43 aerial photography), Unimak (“culture and drainage in part compiled from 1942 trimetrogon aerial photography”), Unalaska (1934, 1943 aerial photography), and Umnak (1942–48 aerial photography). Very few topographic quadrangle maps have been field checked, a process generally restricted to islands where there are military facilities. Some of the maps, especially at higher elevations, are incomplete, showing only form lines for “elevation” and no contour lines. The lack of accurate, modern maps of the Aleutian Islands is the result of the remoteness of the area, nearly perpetual cloud cover on the highest peaks, and the absence of high-resolution, cloud-free photographs and/or images.

A

# GLACIERS OF THE ALEUTIAN ISLANDS





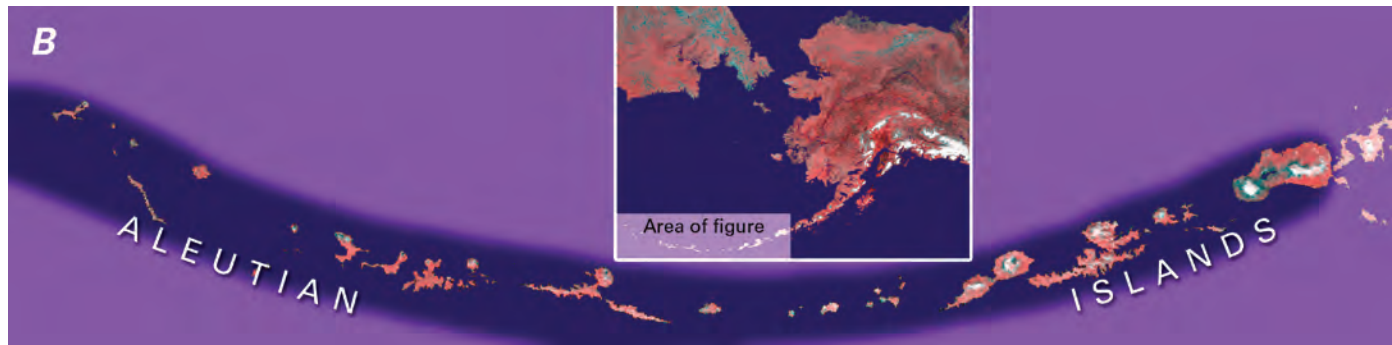


**Figure 350.**—**A**, Index map of glacierized Aleutian Islands (modified from Field, 1975a). **B**, Enlargement of NOAA Advanced Very High Resolution Radiometer (AVHRR) image mosaic of the glacierized islands of the Aleutian Islands in summer 1995. National Oceanic and Atmospheric Administration image mosaic from Mike Fleming, Alaska Science Center, U.S. Geological Survey, Anchorage, Alaska.

Consequently, during the last 50+ years, the glaciers of the Aleutian Islands have received minimal scientific attention. As a result, little new information has been produced. Therefore, much of the information in the following descriptions of the individual glacierized islands is significantly outdated, and some of the glaciers described in earlier publications probably no longer exist because of regional climate warming in the 20th and early 21st centuries.

### Unimak Island

At a length of about 120 km, Unimak Island is the easternmost and largest of the Aleutian Islands. Glacier ice and snow cover is concentrated on 2,857-m-high Shishaldin Volcano, the Isanotski Peaks (2,446 m) (figs. 351, 352), and Roundtop Mountain (1,872 m) on the eastern part of the island (Denton, 1975a). Field (1975a) stated that these three peaks support a continuous snow and ice cover for nearly 40 km and cover an area greater than 50 km<sup>2</sup>. An end-of-summer 1972 Landsat 1 MSS image acquired on 17 September 1972 (see Landsat image 10562–13315; 17 September 1972; Path 82, Row 22), shows a snow-free view of the glacier cover on that date. On the southwestern end of the island, Pogromni Volcano (2,002 m), Faris Peak (1,628 m), and Westdahl Peak (1,560-m-high pyroclastic cone) host an unnamed ice cap, which Field (1990) described as having an area of 26 km<sup>2</sup> from which at least two outlet glaciers flow. As delineated on the Unimak, Alaska, 1:250,000-scale USGS topographic quadrangle map (1951) (appendix A), which is based on 1942 aerial photography, these two outlet glaciers have lengths of about 9 and about 12 km and retreated between 1942 and 1972. An eruption occurred through Westdahl Peak's part of the ice cap in 1992.

### Akutan Island

Akutan Volcano, located in the west-central part of Akutan Island and largest of the Krenitzin Island group, is a 1,303-m-high composite stratovolcano having a circular summit caldera about 2 km wide and 60 to 365 m deep and an active intra-caldera cinder cone. A small section of the floor of Akutan's summit caldera is covered with glacier ice. No information could be found about the status of the caldera's glacier.

### Unalaska Island

The greatest concentration of glaciers in the Aleutian Islands is on Makushin Volcano (2,004 m) on 107-km-long Unalaska Island. The summit is covered by a small ice cap, which feeds several small unnamed outlet glaciers (fig. 353) descending to elevations below 500 m. A map of the island by Drewes and others (1961) also depicts several small unnamed valley glaciers on the flanks of the Shaler Mountains, which are located in the south-central part of the island. The earliest descriptions of the glaciers on Unalaska Island in the scientific literature date back to the 1880s (Davidson, 1886). Other descriptions are presented by Tarr and Martin (1914), Collins (1945), and Bradley (1948). Sharp (1956) suggested that Unalaska Island has the largest ice cover of any island in the Aleutian chain. Although little new information exists about Unalaska's glaciers, recent observations and maps suggest that all are retreating.

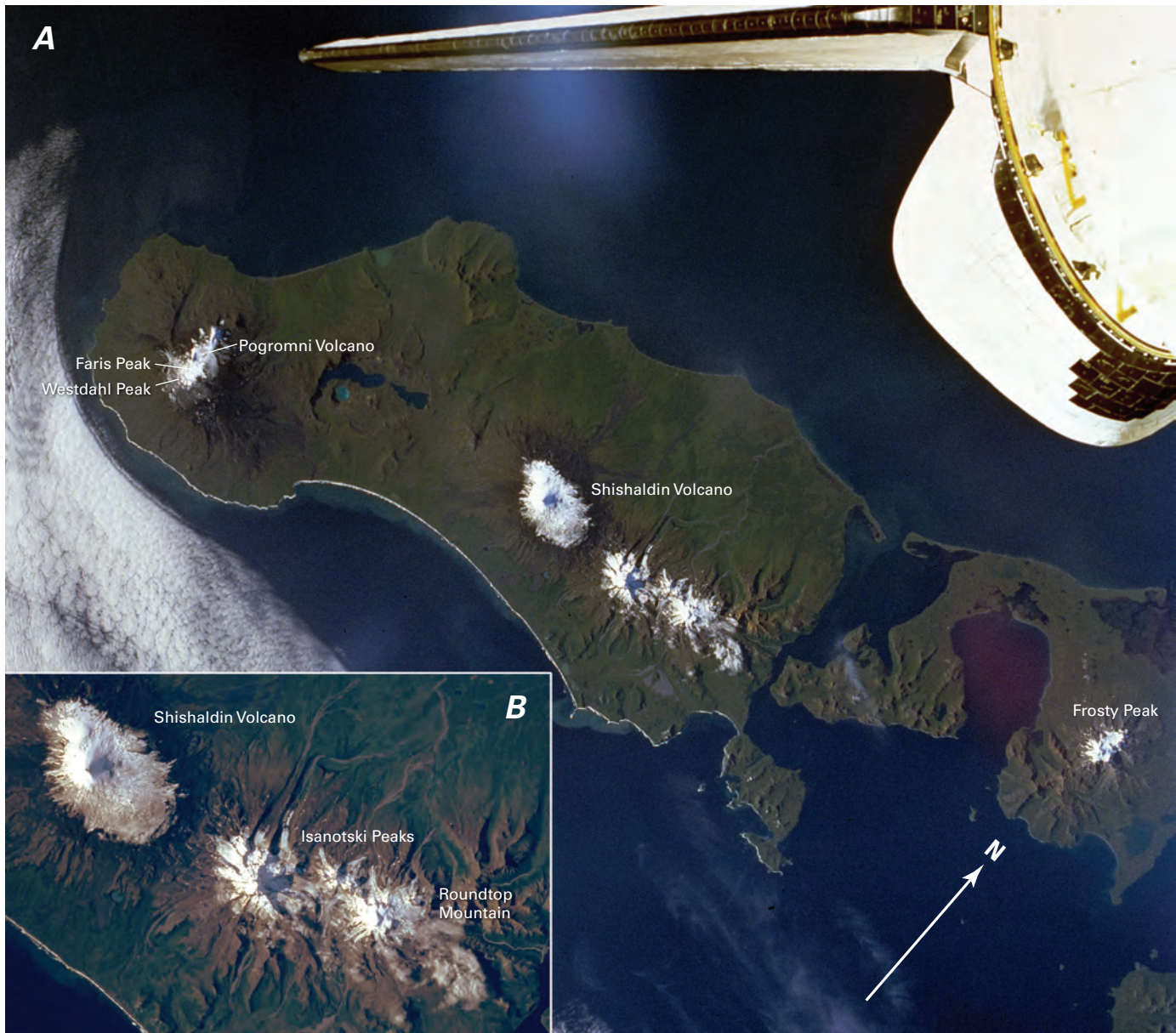


**Figure 351.**—Annotated Space Shuttle photographs of the glacierized volcanoes of Unimak Island in September 1992. **A**, Space Shuttle photograph of all of Unimak Island and the western end of the Alaska Peninsula. Many glacier-covered stratovolcanoes and pyroclastic cones can be seen. From west to east, these include Pogromni Volcano (2,002 m), Faris Peak (1,628 m), Westdahl Peak (1,560 m), Shishaldin Volcano (2,857 m), the Isanotski Peaks (2,446 m), Roundtop Mountain (1,872 m), and Frosty Peak (1,746 m) at the western end of the Peninsula. National Aeronautics and Space Administration photograph no. STS047-77-034. **B**, Enlargement of Space Shuttle photograph of the eastern end of Unimak Island. From west to east, Shishaldin Volcano (2,857 m), the Isanotski Peaks (2,446 m), and Roundtop Mountain (1,872 m), all glacier-covered stratovolcanoes, can be seen. Several large, north-trending valleys, evidence of significant recent glacial erosion can be seen on the north sides of the Isanotski Peaks and Roundtop Mountain. Vegetation-free areas around each peak indicate the recent extent of snow and ice cover. Photograph No. STS047-081-025 from the National Aeronautics and Space Administration .



**Figure 352.**—Oblique aerial photographs of Shishaldin Volcano and environs, Unimak Island, Aleutian Islands. **A**, View from the southeast of retreating, tephra- or debris-covered glaciers on southeast flank of Shishaldin Volcano taken in 1932. Two fingers of ice labeled A and B extend to the north margin of the nearly circular, water-filled depression. The 1-km-diameter depression is mapped as being approximately 3 km from the closest ice margin on the False Pass 1:250,000-scale topographic map of the area, which is based on 1942 and 1943 aerial photography. Photograph Capps 1544a from the USGS Photo Library, Denver, Colo. **B**, High-angle oblique, color aerial photograph from east of Isanotski Peaks and Shishaldin Volcano, Unimak Island, Aleutian Islands, taken 21 September 1990. Photograph frame no. CF008 from AeroMap U.S. Used with permission. A larger version of A is available online.

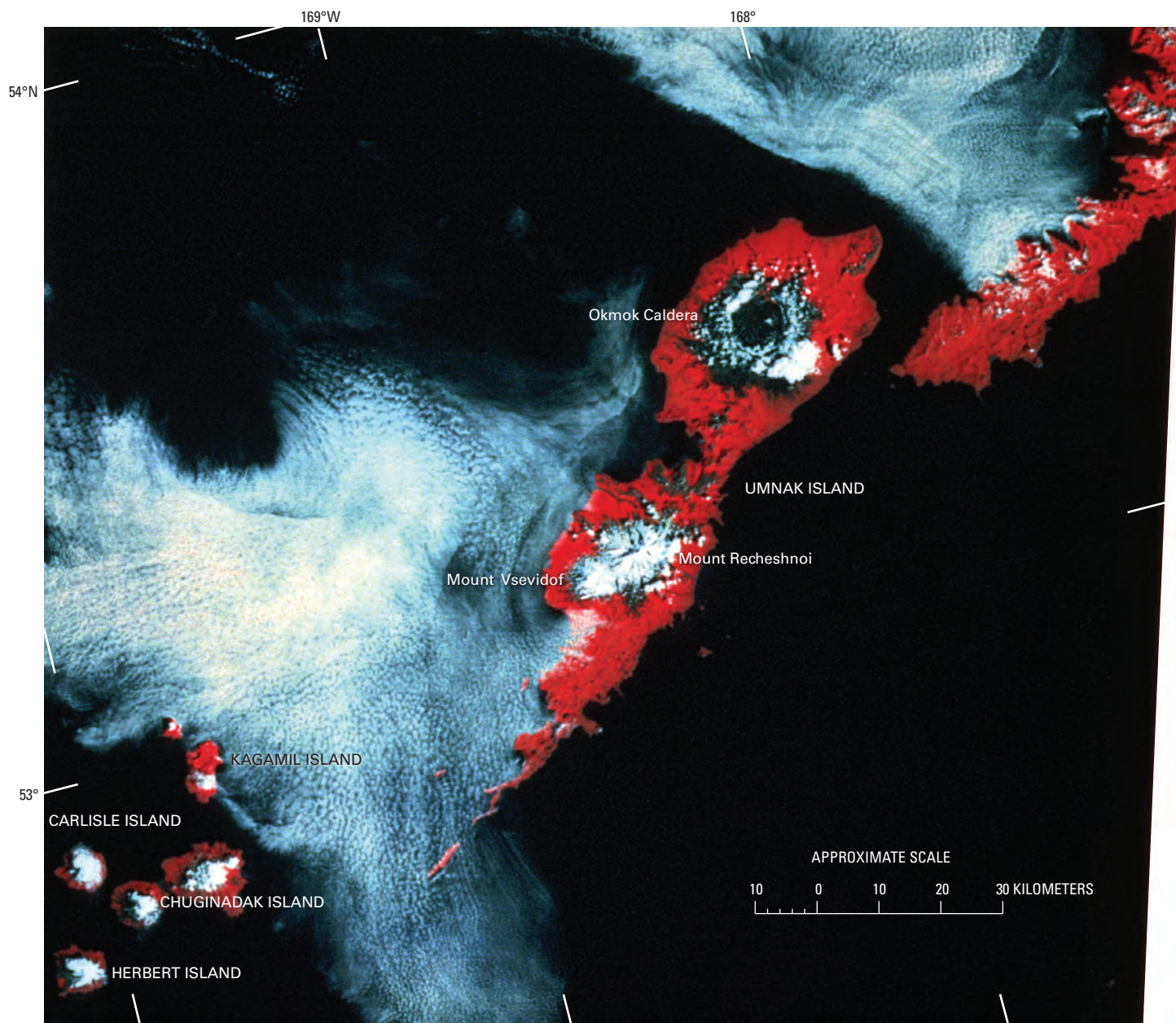


**Figure 353.**—Oblique aerial photograph of the summit region of Makushin Volcano, Unalaska Island, in August 1982. The glacier-capped stratovolcano has several outlet glaciers flowing from its ice cap. A steaming volcanic crater in an ice cauldron can be seen in the middle background. Photograph by C. Nye, Alaska Division of Geological and Geophysical Surveys (Neal and McGimsey, 1997b).

## Umnak Island

A late summer Landsat 2 MSS image acquired on 2 September 1977 (fig. 354) shows the glaciers of Umnak Island. Byers (1959) described nine unnamed valley glaciers descending from Mount Vsevidof (2,149 m) and Mount Recheshnoi (1,953 m) (21 August 1983 AHAP false-color infrared vertical aerial photograph no. L155F5808). Mount Vsevidof supports two valley glaciers, whereas Mount Recheshnoi supports at least seven glaciers. At least one small summit glacier and several hanging glaciers, all unnamed, also exist inside the southern rim of 1,073-m-high Okmok Caldera (21 August 1983 AHAP false-color infrared vertical aerial photograph no. L155F5816). A 1945 eruption melted a large area of the caldera's glacier. Okmok Caldera and the eastern part of Mount Recheshnoi are also depicted on a winter Landsat MSS image acquired on 10 March 1976 (Path 83, Row 23). As of 1999, little, if any, glacier ice remained on Umnak's peaks (USGS Alaska Volcano Observatory, oral commun., 2001).

**Figure 354.**—Annotated Landsat 2 MSS false-color composite image of glaciers on Umnak Island, Aleutian Islands. Byers (1959) described two valley glaciers on Mount Vsevidof and seven valley glaciers on Mount Recheshnoi. Glaciers have also been described in Okmok Caldera. However, little glacier ice may remain now. Landsat image (29542-10905, bands 4, 5, 7; 2 September 1977; Path 84, Row 23) from the USGS, EROS Data Center, Sioux Falls, S. Dak.



## Herbert Island

On 1 January 2001, NASA's International Space Station acquired a photograph of Chuginadak, Carlisle, and Herbert Islands (fig. 355A). A 27 September 1996 oblique color aerial photograph of the more than 900-m-high summit caldera of Herbert Island (fig. 355B) depicts at least two tongues of ice that descend to the crater floor and at least one hanging glacier. Acquired by AeroMap U.S., this photograph is not only perhaps the first cloud-free photograph of Herbert Island ever obtained, it is also the first documentation

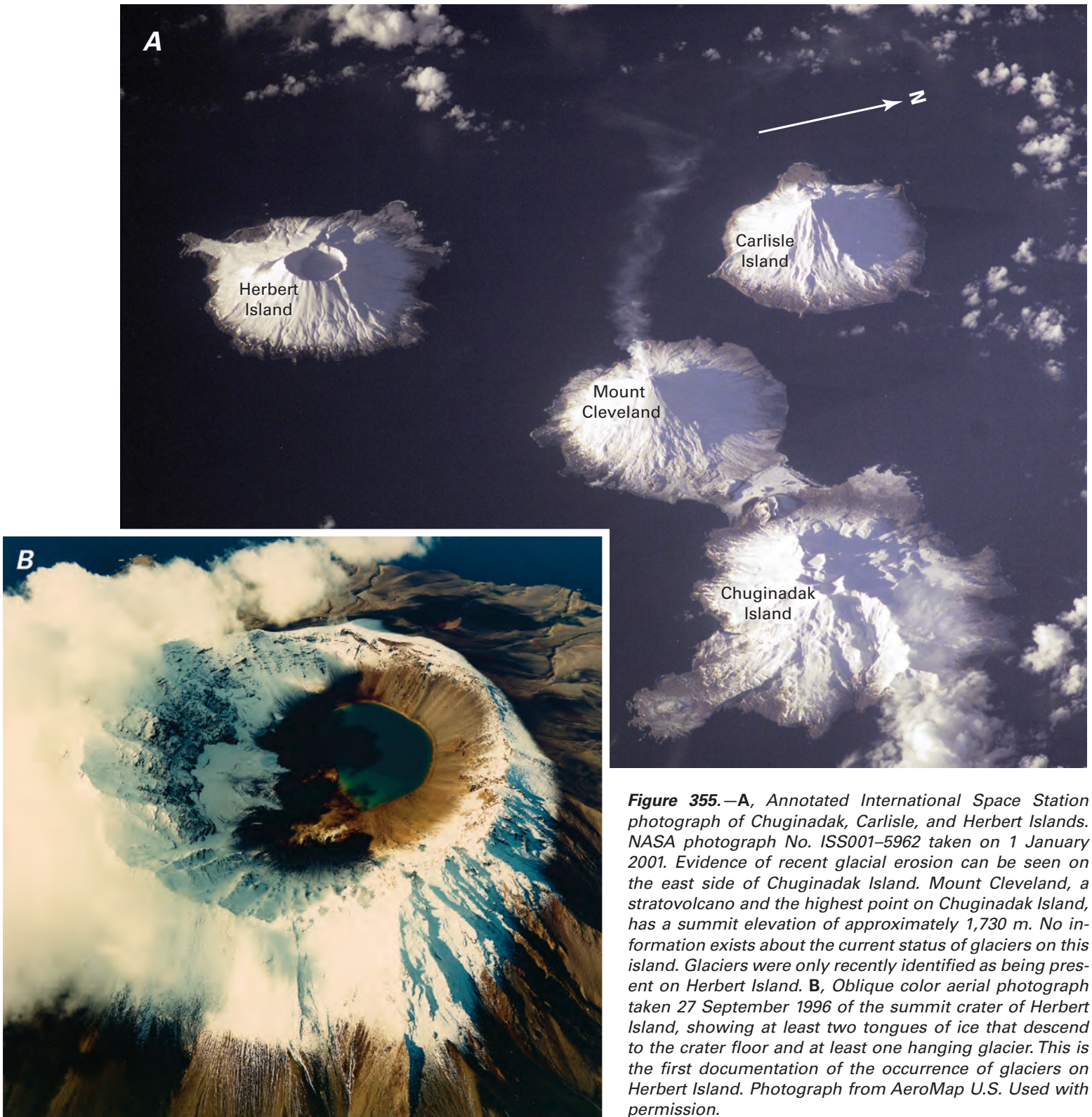


**Figure 355.**—**A**, Annotated International Space Station photograph of Chuginadak, Carlisle, and Herbert Islands. NASA photograph No. ISS001-5962 taken on 1 January 2001. Evidence of recent glacial erosion can be seen on the east side of Chuginadak Island. Mount Cleveland, a stratovolcano and the highest point on Chuginadak Island, has a summit elevation of approximately 1,730 m. No information exists about the current status of glaciers on this island. Glaciers were only recently identified as being present on Herbert Island. **B**, Oblique color aerial photograph taken 27 September 1996 of the summit crater of Herbert Island, showing at least two tongues of ice that descend to the crater floor and at least one hanging glacier. This is the first documentation of the occurrence of glaciers on Herbert Island. Photograph from AeroMap U.S. Used with permission.

of any glaciers on the Islands of Four Mountains. No information exists about the past or current status of these glaciers.

### Atka Island

The USGS topographic map of Atka (appendix A) shows two volcanoes on Atka Island that support unnamed summit glaciers. Korovin Volcano, a 1,533-m-high stratovolcano that was last active in June 1998, and Mount Kliuchef (1,450 m) have a total glacier-covered area of about 20 km<sup>2</sup> (fig. 356). Several unnamed ice tongues descend from the summit of Mount Kliuchef; one flowing to the northeast terminates at an elevation of about 525 m. No information exists about the past or current status of these glaciers.

### Great Sitkin Island

Great Sitkin Island, located northeast of Adak, was mapped in 1957 on USGS 1:250,000-scale Adak map, which was based on 1954–56 surveys (appendix A). The map shows that Great Sitkin Volcano, a 1,740-m-high stratovolcano with caldera and dome that was last active in September 1974, has an unnamed ring glacier on the eastern side of its crater and nine small unnamed glaciers of varying length descending from its summit. The largest of these glaciers was about 3 km in length. No information exists about the past or current status of these glaciers.

### Tanaga Island

Tanaga Island is a semi-circular island with a length of about 40 km and a maximum width of about 15 km. The AMS (1957) 1:25,000-scale map of Tanaga Island shows a few unnamed glaciers about 1.6 km in length on 1,806-m-high Tanaga Volcano, a stratovolcano flanked by two stratocones that were last active in 1914. Several unnamed smaller glaciers are also shown on an unnamed 1,449-m-high stratovolcano to the east. The largest glacier shown on this volcano headed at about 1,295 m and descended to about 875 m. No glaciers are shown on the most recent USGS 1:250,000-scale topographic quadrangle maps of the island (Adak, 1957; Gareloi Island, 1954) (appendix A). No information exists about the past or current status of these glaciers.

### Gareloi Island

The Gareloi Island 1954 USGS 1:250,000-scale topographic map (appendix A) shows a small glacier-covered area on Mount Gareloi, a 1,573-m-high stratovolcano last active in August 1989. At least two small glaciers were situated on the northern side of its cone (Coats, 1956). A single, very small glacier (<0.04 km<sup>2</sup>) is also shown on the southeastern side of the summit of Mount Gareloi, according to the USGS 1:250,000-scale topographic quadrangle map (appendix A). No information exists about the past or current status of these glaciers.

### Kiska Island

In 1943, Kiska Island possessed a small glacier on Kiska Volcano, a 1,220-m-high stratovolcano last active in June 1990. Henderson and Putnam (1947) visited the glacier at least once in 1943 and described it (p. 32) as being a “small, decadent, dirty piece of ice, but it still merited the name glacier.” However, no evidence of this or any glacier is shown on Kiska Volcano on the most recent 1951 USGS 1:250,000-scale topographic quadrangle map of the area (appendix A). No additional information exists about this glacier.

### Summary

Less information exists about the glaciers of the Aleutian Islands than for any other area in Alaska. The extremely limited information that is available is generally four to six decades old. Glaciers for which information exists are retreating and (or) thinning.

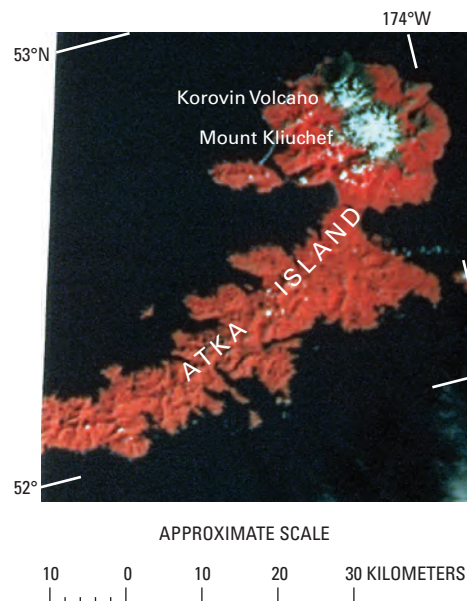


**Figure 356.**—Part of an annotated Landsat 2 MSS false-color composite image of Korovin Volcano and Mount Kliuchef, Atka Island, Aleutian Islands. Both volcanoes have summit glaciers totaling about 20 km<sup>2</sup> in area. Landsat image (2975–21252, bands 4, 5, 7; 23 September 1977; Path 87, Row 24) is from the USGS, EROS Data Center, Sioux Falls, S. Dak.

# Wrangell Mountains

## Introduction

The Wrangell Mountains (figs. 1, 357), a large young volcanic massif having a maximum length of about 155 km and width of 85 km, are located between Nabesna (to the north), Skolai Pass and the Chitistone River (to the east), the Chitina River (to the south), and the Copper River (to the west). They are included in the Wrangell-St. Elias National Park and Preserve, Alaska,

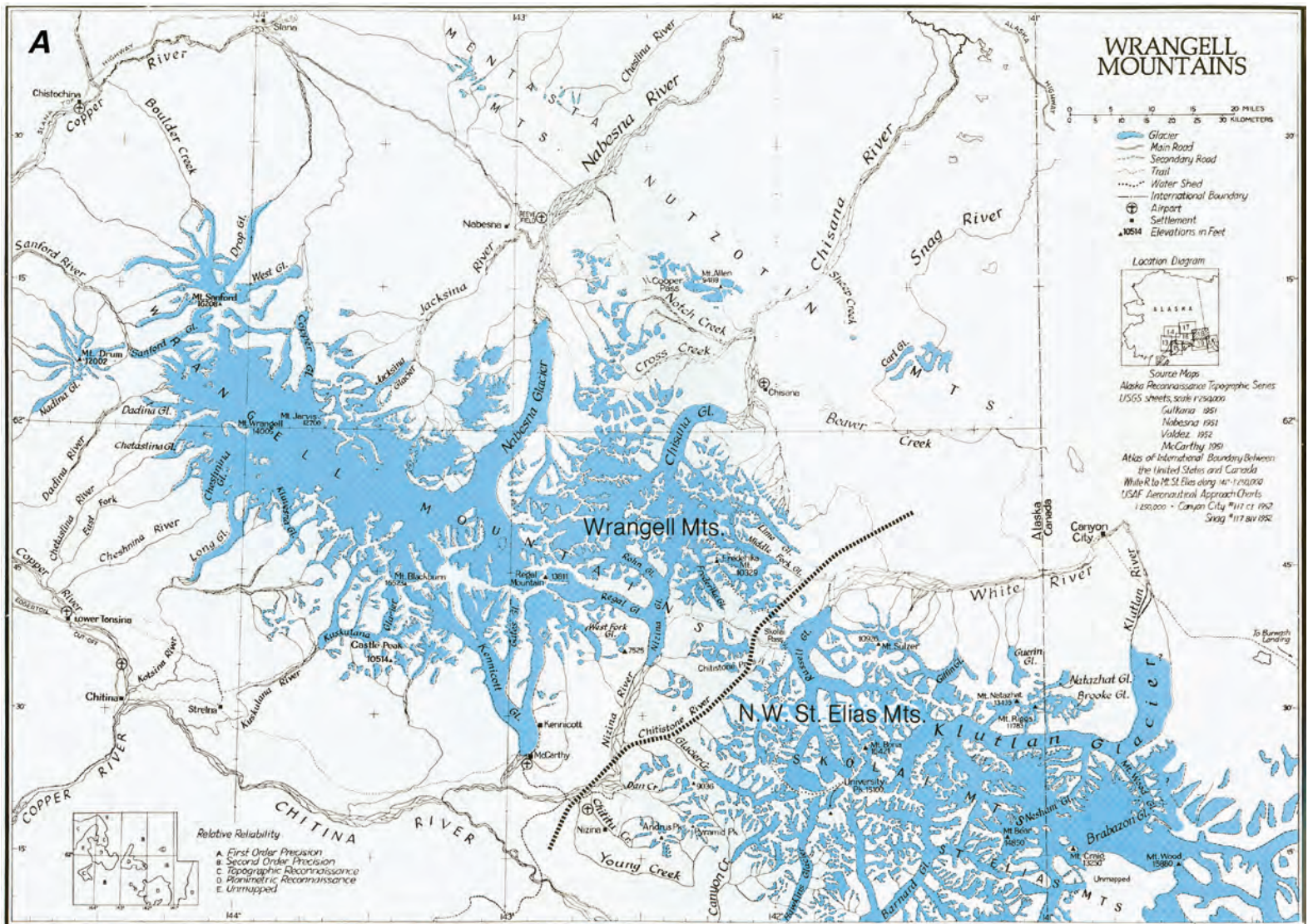
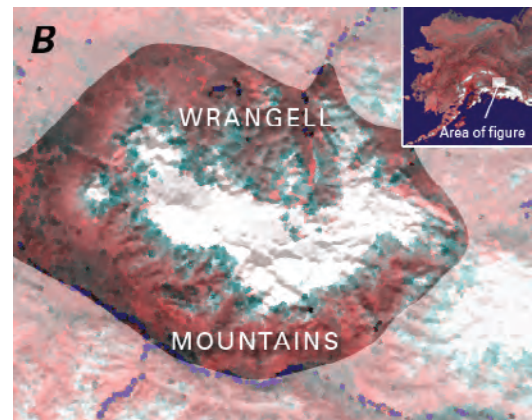


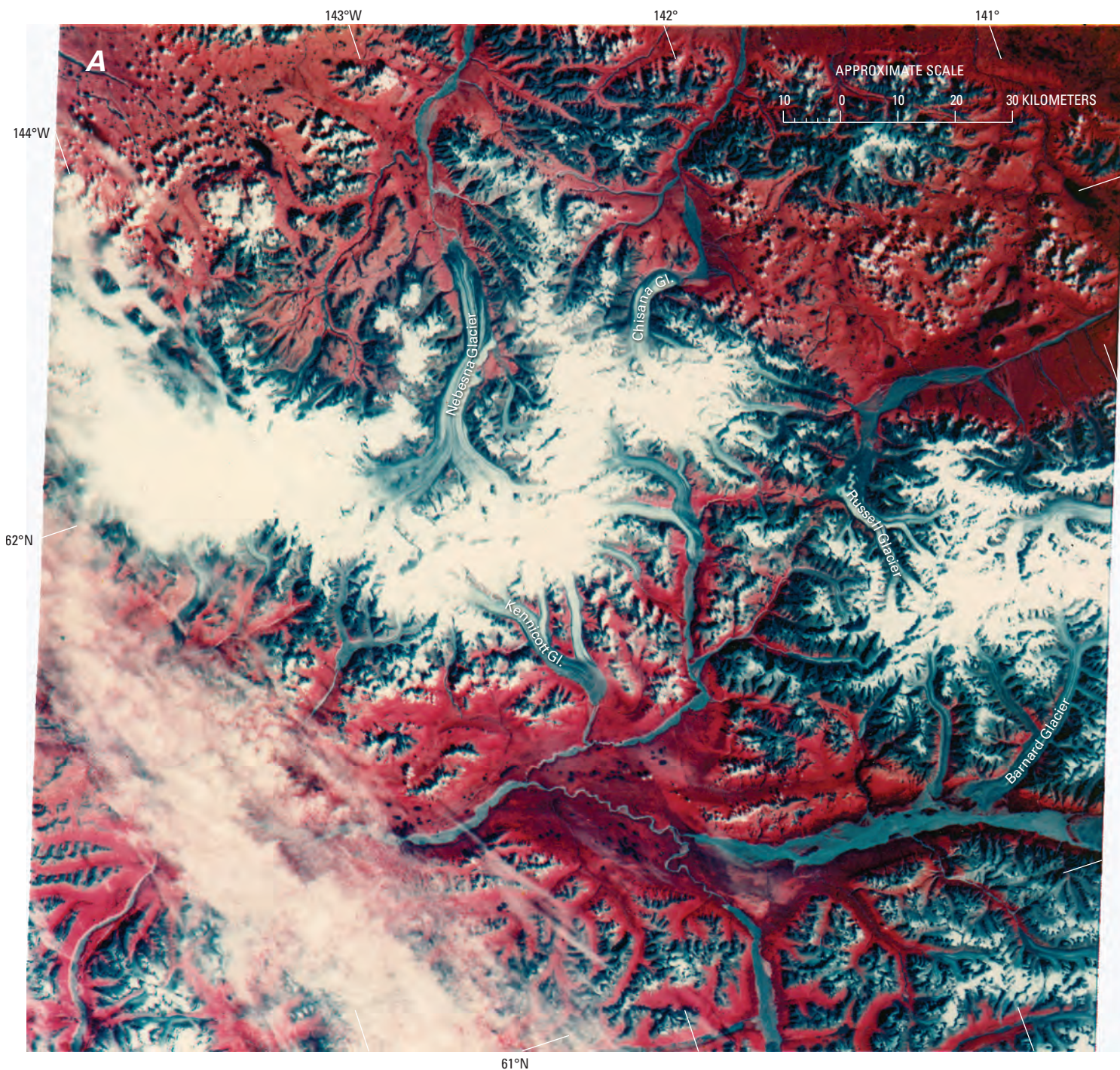
**Figure 357.—A**, Index map of the glacierized Wrangell Mountains (modified from Field, 1975a). **B**, Enlargement of NOAA Advanced Very High Resolution Radiometer (AVHRR) image mosaic of the glacierized Wrangell Mountains in summer 1995. National Oceanic and Atmospheric Administration image mosaic from Mike Fleming, Alaska Science Center, U.S. Geological Survey, Anchorage, Alaska.



which is contiguous with Kluane National Park, Yukon Territory, Canada, on the east. The highest peaks are Mount Blackburn (4,996 m), Mount Sanford (4,949 m), Mount Wrangell (4,317 m—an active volcano with a summit caldera), Regal Mountain (4,220 m), Mount Jarvis (4,091 m), Mount Zanetti (3,965 m), Rime Peak (3,883 m), and Mount Drum (3,661 m). The peaks are either Quaternary volcanoes or are composed of layered volcanic material. Mount Drum and Mount Sanford are free-standing mountains that support a number of glaciers radiating from their summits.

In total, the Wrangell Mountains support about 50 outlet glaciers that have lengths of 8 km or more and have a glacier-covered area of 8,300 km<sup>2</sup> (Post and Meier, 1980, p. 45) (fig. 358). Table 6, which is based on Krimmel's analysis of an 18 August 1972 Landsat 1 MSS image (1026–20220) of the area, provides data on the AARs of 14 glaciers in the Wrangell Mountains. Many are surge-type glaciers. At the center of the west-central Wrangell Mountains

**Figure 358.**—**A**, Annotated Landsat 1 MSS false-color composite image of the Wrangell Mountains and northwestern part of the St. Elias Mountains. An enlargement of this image, combined with topographic maps, was used to determine the accumulation area ratios (AARs) (see table 6) and snowline altitudes on 14 glaciers in this area. **► B**, Contour map of equal snowline altitude (in meters) showing that snowline altitudes are higher to the northeast of the mountains and thus indicating less snow accumulation there. Landsat image and caption courtesy of Robert M. Krimmel, U.S. Geological Survey. Landsat image (1026–20220; bands 4, 5, 7; 18 August 1972; Path 70, Row 17) is from the USGS, EROS Data Center, Sioux Falls, S. Dak.





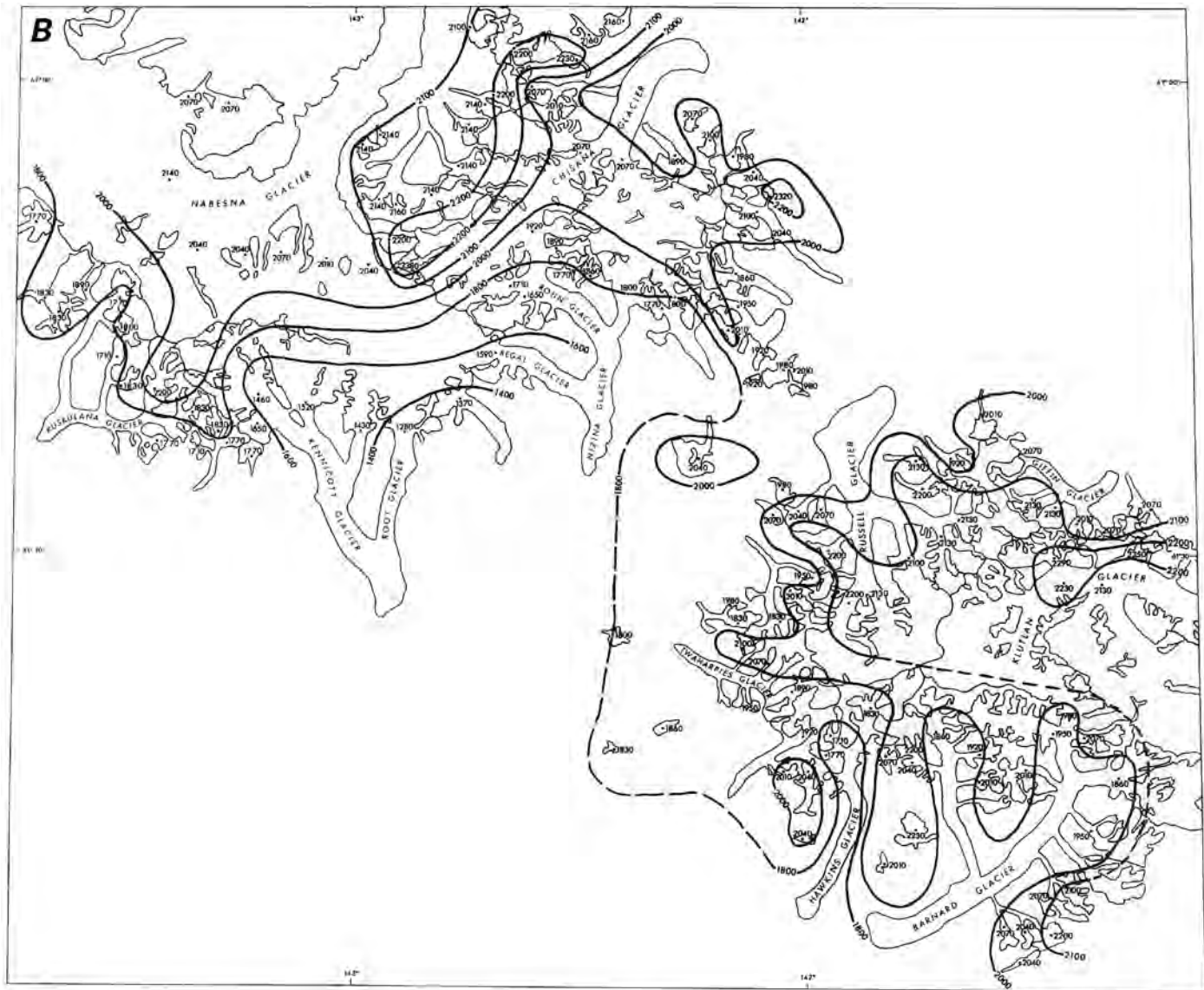


TABLE 6.—Wrangell Mountains accumulation area ratios (AAR)

[Data courtesy of Robert M. Krimmel, USGS, derived from Landsat 1 MSS image 1026–20220, 18 August 1972]

Glacier name	AAR
Hawkins	0.39
Barnard	0.67
Russell	0.64
Chisana	0.73
Nabesna	0.64
Kuskulana	0.55
Kennicott	0.60
Nizina	0.67
Lakina	0.65
Kluvesna	0.64
Giffin	0.56
Twaharpies	0.55
Chitistone	0.63
Lime	0.62

is a broad upland ice field covering an area of about 750 km<sup>2</sup> and extending eastward from the crater of Mount Wrangell to the head of Nabesna Glacier, a distance of about 35 km. It is bounded on the north by Mount Sanford and Mount Jarvis. Nabesna Glacier, which is 87 km long, and has an area of 819 km<sup>2</sup> (Denton and Field, 1975c, p. 566), is the largest of the outlet glaciers in the Wrangell Mountains as well as the largest inland glacier in North America. In the eastern part of the mountains, a series of interconnected unnamed ice fields are drained by Chisana, Lime, Middle Fork, and Frederika Glaciers, and Nizina Glacier and its tributaries.

Landsat 1–3 MSS images that cover the Wrangell Mountains have the following Path/Row coordinates: 69/17, 70/16, 70/17, 71/16, 71/17, and 72/16 (fig. 3, table 1). These areas are mapped on the USGS Gulkana, Alaska (1959), McCarthy, Alaska (1960), Nabesna, Alaska (1960), and Valdez, Alaska (1960) 1:250,000-scale topographic maps (appendix A). Landsat 7 ETM+ images of the Wrangell Mountains also have been acquired, and several are included in this section.

Topographic information, including information about glaciers of this area, was collected as early as 1885 (Allen, 1887); the first sketch maps appeared as early as 1892 (Rohn, 1900). A 1:750,000-scale map (fig. 359) depicting the location of many of the glaciers of the Wrangell Mountains and 1:250,000-scale topographic maps showing details of individual glacier

termini appeared in 1902 and were printed in USGS Professional Paper 41 (Mendenhall, 1905). Much of these early topographic data were collected by T.G. Gerdine, W.J. Peters, and D.C. Witherspoon, all of the USGS. Gerdine was often assisted by W.C. Mendenhall, who was mapping the geology of the region (Mendenhall, 1905). Remarkably, the map, made in a remote, unknown region and using late 19th century planetable and telescopic-alidade methods, remains accurate. A 1908 topographic survey by Witherspoon and H.M. Lafollette produced a 1:62,250-scale topographic map that included the eastern margin of Kennicott Glacier and was published in USGS Bulletin 448 (Moffit and Capps, 1911).

Rock glaciers are abundant throughout the Wrangell Mountains (fig. 360), as 1905 photographs by Moffit (USGS Photo Library photographs Moffit 384 and 390) and 1908 photographs by Capps (USGS Photo Library photographs Capps 141 and 142) show. Capps (1910b) mapped more than 30 rock glaciers in the area to the south and east of Kennicott Glacier, describing features common to rock glaciers in the Wrangell Mountains as follows: "They vary greatly in size, but are usually many times longer than wide, occupying, as they do, the bottoms of cirque-like valleys. Some have wide, fan-shaped heads and narrow down to a tongue below. Others are narrow above, and deploy into spatulate lobes below.....but the greater number are narrow bodies of nearly uniform width, from one-tenth to one-fourth of a mile wide and from one-half to 2½ miles long. The surface slopes vary in different cases from 9° to 18° for the whole course of the rock glacier." (Capps. 1910b, p. 360). Capps thought there was a resemblance to true glaciers. In many of the rock glaciers, fragmental rocks extend all the way to the head of the cirque; no ice



**Figure 359.**—Part of a map of the Mount Wrangell District, Alaska, a 1:750,000-scale map based on data collected between 1885 and 1902, depicting the location of many of the glaciers of the Wrangell Mountains. From Mendenhall (1905, plate number XI). A larger version of this figure is available online.



**Figure 360.**—1961 northeast-looking oblique aerial photograph of a rock glacier on the west side of Bonanza Peak, east of Kennicott Glacier. A road is shown on this rock glacier on the 1911 topographic map. The buildings constructed on the northwest side of the rock glacier, below the snowline, and the roads on its surface suggest that the surface of this rock glacier is stationary and stable and has been for many years. University of Washington photograph No. F7-61 by Austin Post, U.S. Geological Survey.

is visible, and there is little or no snow on the surface. In several cases, however, the rock glaciers grade into true glaciers at their upper ends, without any sharp line of demarcation, so that gradation between the two is complete (fig. 360).

### **Glaciers of the Regal Mountain – Frederika Mountain Area and the Eastern Wrangell Mountains**

Outlet glaciers of the eastern Wrangell Mountains (Chisana, Lime, Middle Fork, Frederika, Shelter Valley, and Whiskey Hill Glaciers) originate from a 20×10-km unnamed upland ice field surrounded by several isolated peaks with elevations higher than 2,500 m. The highest of these is 3,150-m-high Mount Frederika. Glaciers of the southeastern Wrangell Mountains (Rohn, Regal, West Fork, Root, and Gates Glaciers) originate mainly on the southern flanks of Regal Mountain. Rohn and Regal Glaciers descend from the eastern flank of Regal Mountain as well, and Rohn Glacier is also fed from the northern flank of Regal Mountain and the unnamed upland ice field. Other, generally smaller glaciers, flow from isolated accumulation areas located on upland ridges and isolated peaks.

Chisana Glacier (fig. 361), which is 39 km long and 440 km<sup>2</sup> in area (Denton and Field, 1975c, p. 567), is the northeasternmost and third largest glacier in the Wrangell Mountains. It drains several large interconnected accumulation areas north of Regal Mountain and Frederika Mountain. Chisana Glacier has been also named *Tanana Glacier* (Rohn, 1900) and was locally called *Shushana Glacier* (Orth, 1967).

The terminus of Chisana Glacier was visited independently in 1899 by Brooks and then by Rohn and again in 1908 by Capps, who stated that “a comparison of the photographs taken by Rohn in 1899 with those taken by the writer nine years later show surprisingly little change in the aspect of the glacier.....” (Capps, 1910a, p. 45). At one place, a slight recession had occurred in the edge of the glacier. Although there was little change, Capps’ 1908 photograph (USGS Photo Library photograph S.R.15) clearly shows an arcuate ridge located more than 500 m downvalley of the terminus that was deposited by the glacier some time in the recent past.

Denton and Field (1975c) reported that little change can be seen when the 1908 terminus position is compared with the one shown in Washburn’s 1938 photograph. Denton and Field (1975c) stated that the glacier had retreated about 600 m and showed a pronounced lateral recession and a shrinkage of its first tributary by 1957, the date of the photography used to produce the first



**Figure 361.**—30 August 2000 northwest-looking oblique aerial photograph of the retreating terminus of Chisana Glacier. The exposed bedrock along its margin appeared after 1957. Its appearance suggests thinning of as much as 50 m during the second half of the 20th century. Photograph by Bruce F. Molnia, U.S. Geological Survey.

1:63,360-scale topographic map of the glacier (USGS, Nabesna A-3, Alaska, 1960) (appendix B). After 1957, the terminus of Chisana Glacier fluctuated; even though the glacier experienced a number of small surges, it continued to thin and retreat. In August 1978, Austin Post (written commun., 1978) reported that three or four recent moraines were located adjacent to the active ice margin. When the author observed it from the air on 30 August 2000, the terminus of Chisana Glacier showed much evidence of active thinning and retreat (fig. 361).

To the southeast of Chisana Glacier, in the area west of Bow Pass, a number of small glaciers originate from isolated accumulation areas that are independent of the larger interconnected accumulation area. Several drain into Boomerang Creek. All show evidence of thinning and retreat. The only Wrangell Mountains' glacier observed surging on 30 August 2000 is also located near Bow Pass (fig. 362).

Middle Fork Glacier, a surge-type glacier that is 13 km long and 38 km<sup>2</sup> in area (Denton and Field, 1975c, p. 567), is located to the northeast of Frederika Peak. It was last reported surging between 1964 and 1966 (Post, 1967a). When the author observed it from the air on 30 August 2000 (fig. 363), its upper part showed evidence of thinning.

Frederika Glacier, another surge-type glacier, is 19 km long and 58 km<sup>2</sup> in area (Denton and Field, 1975c, p. 562) (1905 Moffit photograph, USGS Photo Library photograph Moffit 338); 1908 Capps photograph, USGS Photo Library Capps 104). The earliest description of the glacier was made by Hayes (1892, p. 133) in 1891 during a surge: "The glacier terminates in a nearly vertical ice cliff stretching across the lateral valley a mile in length and about 250 feet high. Its surface is free from moraine, but is extremely rough and broken, wholly unlike the surface of stagnant ice at the end of a retreating glacier. At the foot of the cliff is a small accumulation of gravel and ice fragments being pushed along by the advancing mass."

When Capps (1910a) visited in 1908, melting and erosion had removed all signs of the former surge. He described the glacier's surface as being remarkably smooth and sloping evenly to a thin edge, stating that "It was easier to take a pack train across this low ice-tongue than to ford the torrential

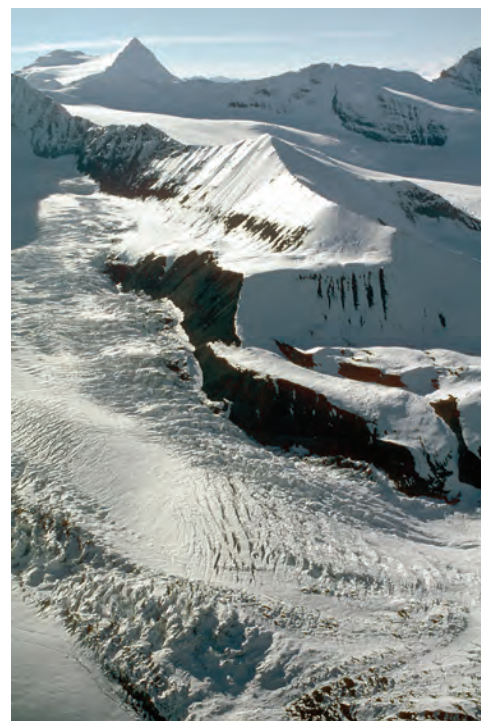


**Figure 362.**—30 August 2000 northwest-looking oblique aerial photograph of an unnamed surging glacier in the Bow Pass area, northeastern Wrangell Mountains. This glacier was the only one in the Wrangell Mountains observed to be surging in 2000. Photograph by Bruce F. Molnia, U.S. Geological Survey. A larger version of this figure is available online.

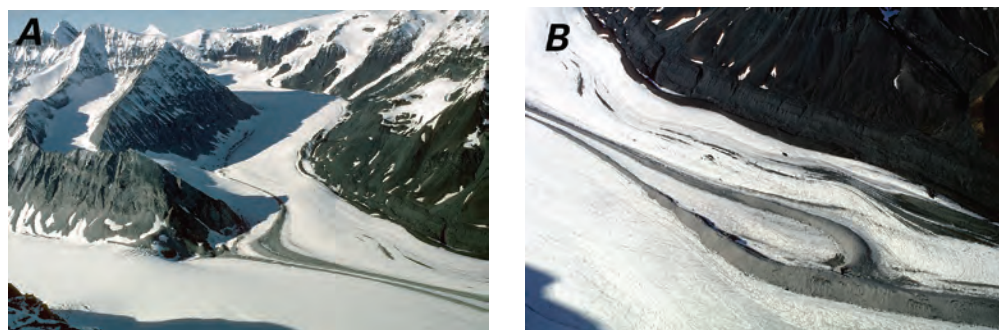


**Figure 363.**—Two 30 August 2000 northwest-looking oblique aerial photographs of parts of Middle Fork Glacier showing much evidence of thinning and retreat of upper reach tributaries. **A**, View of the junction area of the two primary tributaries of Middle Fork Glacier. The northern tributary has an elevated trimline on its north margin, at the right edge of the photograph. The glacier, which enters the northern tributary from the cirque to the left of center, has retreated into the cirque, leaving an elevated loop moraine that extends several kilometers downglacier. The southern tributary also has an elevated trimline on its north margin, and its height suggests more than 50 m of recent thinning. **B**, Slightly overlapping view of the width of Middle Fork Glacier just downglacier from A, showing an elevated trimline on its north margin, the elevated loop moraine, and many other elevated moraines. Although the terminus of the glacier was not observed, upglacier evidence suggests significant thinning. Photographs by Bruce F. Molnia, U.S. Geological Survey. Larger versions of these figures are available online.

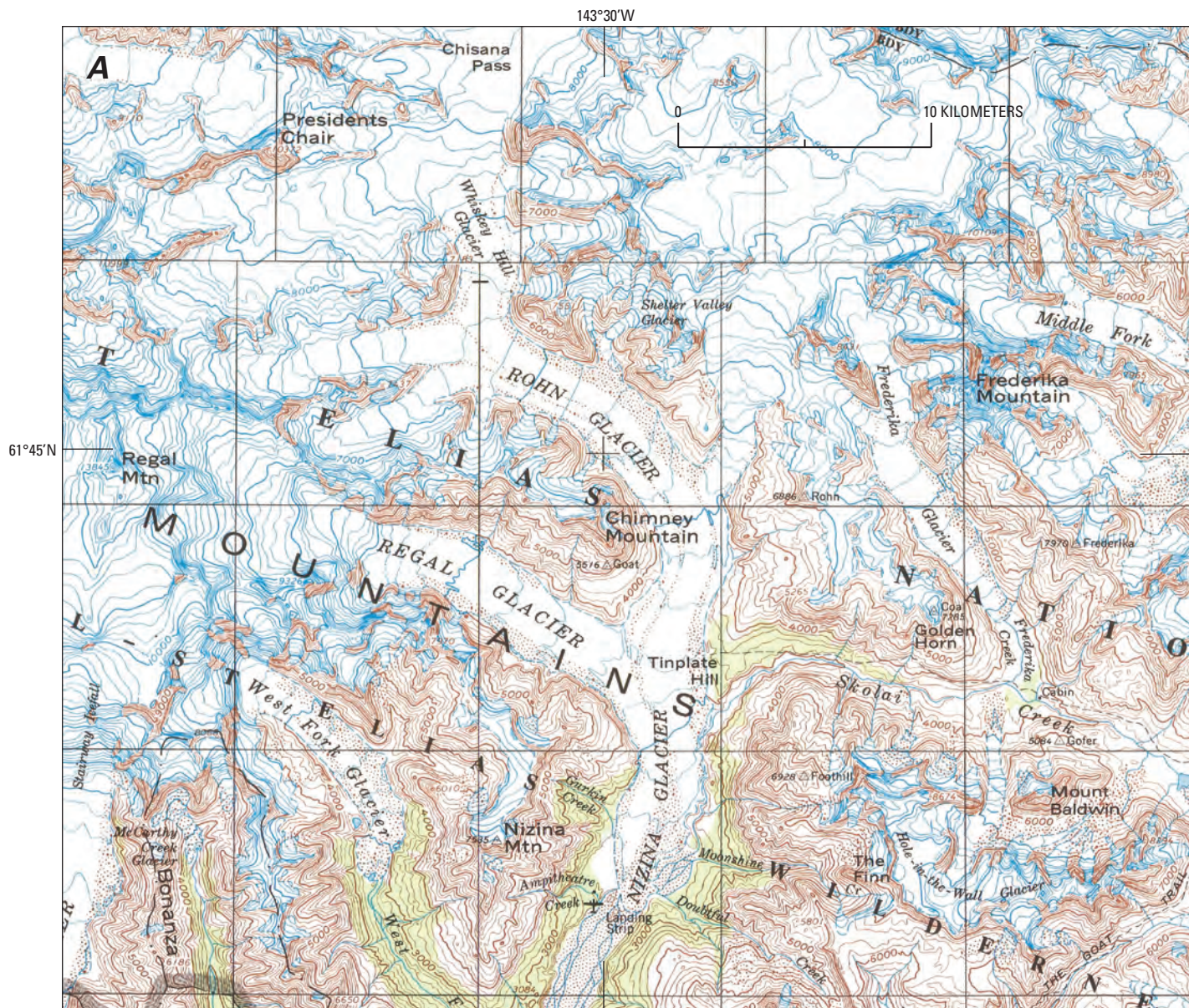


**Figure 364.** — Two 20th century views of the Hole-in-the-Wall Glacier. **A**, 1905 view from the north, looking south at the edge of the then-surging margin of Hole-in-the-Wall Glacier. The duration and displacement of the surge are unknown. Photograph Moffit 339 from the USGS Photo Library, Denver, Colo. **B**, A 1966 photograph showing that Hole-in-the-Wall Glacier has retreated and thinned since the 1905 surge. Elevated lateral moraines are present along both margins of the glacier. Shortly after this photograph was taken the glacier surged again. U.S. Geological Survey photograph by E.M. MacKevett, Jr. From Winkler (2000, fig 39). A larger version of A is available online.

stream below.” (Capps, 1910a, p. 56). This gently sloping terminus was photographed by Moffit in 1905.

North-flowing Hole-in-the-Wall Glacier, which is 9 km long and 19 km<sup>2</sup> in area (Denton and Field, 1975c, p. 562), is a surge-type glacier that originates from an isolated accumulation area west of Chitistone Pass. Its terminus is within a few kilometers of the terminus of Frederika Glacier. Capps (1910a) saw its terminus in 1908 when it was surging (1908 Capps photograph, USGS Photo Library photograph Capps 105) and described it (p. 56) as “a beautiful cascade glacier [that] tumbles out from between castellated peaks and pushes northward to Skolai Creek.” Hole-in-the-Wall was the only advancing glacier that Capps observed during the field season, and he concluded that he was “...unable to account for the singular change in conditions which has caused Frederika Glacier, which 17 years ago was advancing, to retreat, and at the same time has brought about the advance of a glacier just to the south, which in 1891 was retreating.” (Capps, 1910a, p. 56). The dates of the onset and completion of the surge are unknown, but a 1905 photograph by Moffit (fig. 364A) shows that the glacier was surging at that time. Several years of retreat followed (fig. 364B). Hole-in-the-Wall Glacier surged again late in 1966 (Meier and Post, 1967). Winkler (2000) stated that the glacier has recently retreated 0.7 to 1.4 km and thinned by as much as 80 m.

Nizina Glacier (fig. 365A–C) is the name given to the ice tongue formed by the joining of Rohn and Regal Glaciers. Both its principal tributaries descend from the eastern slopes of Regal Mountain, although Rohn Glacier also receives ice from the northern flank of Regal Mountain and the unnamed upland ice field to the north. Nizina Glacier, which is 51 km long and 429 km<sup>2</sup> in area (Denton and Field, 1975c, p. 562), is the southeasternmost large valley glacier in the Wrangell Mountains. When a gold rush began at Chisana in 1913, the shortest route from the Chitina Valley was a 60-km-trek over the Nizina, Rohn, and Chisana Glaciers. The surface of the Nizina Glacier became a popular highway. When it was photographed in 1905 by Moffit and again in 1913 by Capps (1905 Moffit photograph, USGS Photo Library photograph Moffit 341; 1913 Capps photographs, USGS Photo Library photographs Capps 519, 520, and 521), its eastern margin blocked the valley of Skolai Creek and formed a lake at least 3 km long. By 1937, when Bradford Washburn photographed it, the glacier thinned enough to permit the lake to drain and a stream channel to develop along the eastern margin of Nizina Glacier (Denton and Field, 1975c). Little net change had occurred when it was next photographed in 1964 by Post (Denton and Field, 1975c). When the author

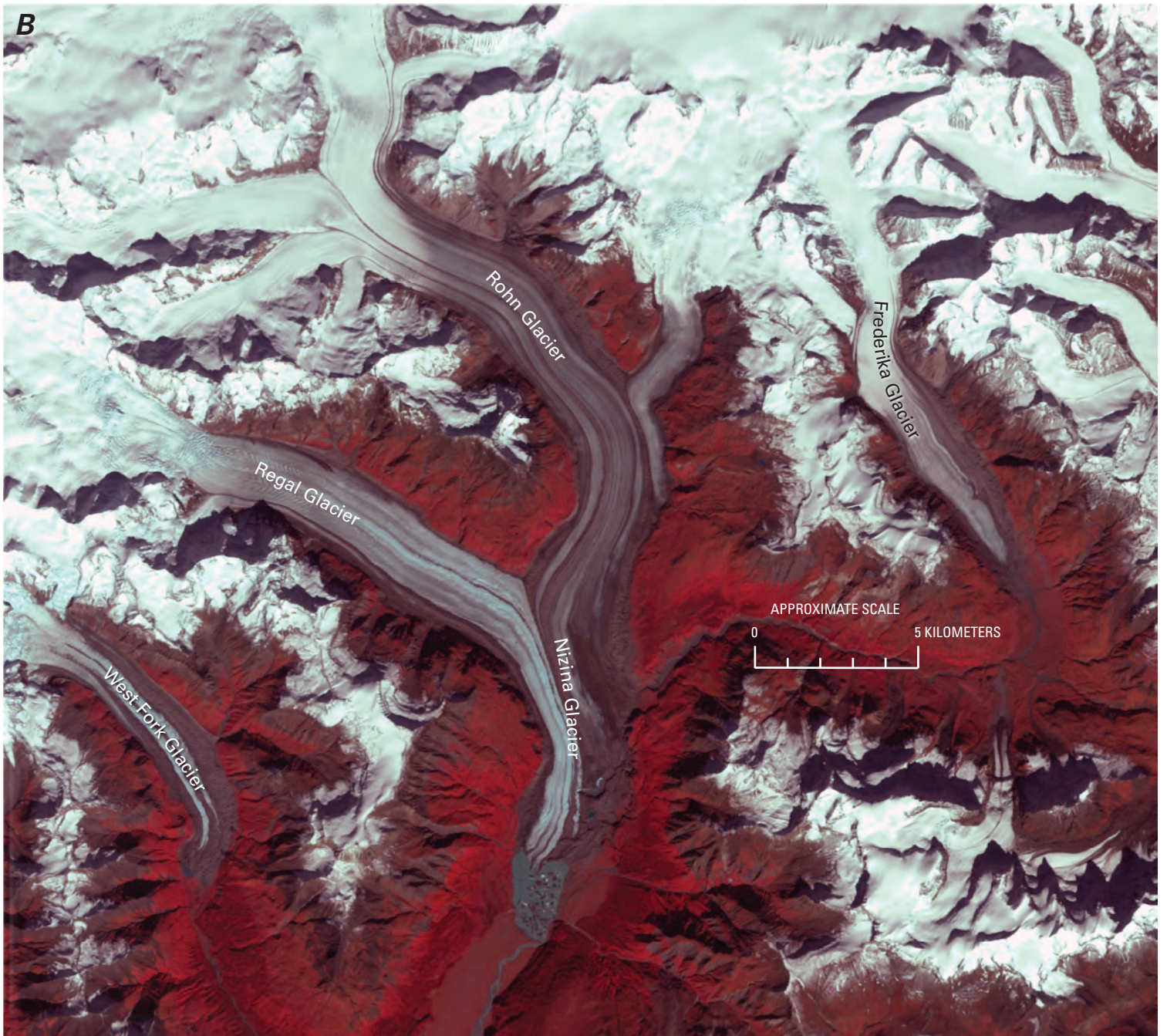


observed it from the air on 30 August 2000 (fig. 365C), a 3-km-long ice marginal lake had developed at its terminus, and large tabular icebergs were calving into the lake. Compared to 1957 aerial photographs, the terminus has retreated at a rate of approximately  $90 \text{ m a}^{-1}$ . The author also observed the upper regions of both Rohn and Regal Glaciers from the air on 30 August 2000 (fig. 366) and noted that both showed much evidence of thinning.

West Fork Glacier, which is 18 km long and about  $49 \text{ km}^2$  in area, (Denton and Field, 1975c, p. 562), originates from several small interconnected accumulation areas on the southern side of Mount Regal. When the author observed it from the air on 30 August 2000, its upper part showed evidence of thinning.

Between West Fork and Root Glaciers, several small glaciers flow from isolated accumulation areas located on upland ridges at the head of McCarthy Creek. Moffit photographed two of these glaciers—McCarthy Creek Glacier and an unnamed glacier—in 1919 and 1922 (1919 Moffit photographs, USGS Photo Library photographs Moffit 849 and 850; 1922 Moffit photograph, USGS Photo Library photograph Moffit 844), and the author photographed them from the air on 30 August 2000. In 1919, little could be said about the status of McCarthy Creek Glacier, but the unnamed glacier was thinning and retreating. Eighty-one years later, both showed evidence of thinning, and the unnamed glacier was retreating.

**Figure 365.**—Map, Landsat image, and photograph of the Nizina Glacier. **A**, Section of USGS McCarthy, Alaska (1960, revised 1981) 1:250,000-scale map showing the Nizina Glacier and its tributaries. **B**, Enlarged section of annotated Landsat 7 ETM+ false-color composite image of Nizina Glacier. Landsat 7 image (LE7064017000125350; 10 September 2001; Path 64, Row 17) from the USGS, EROS Data Center, Sioux Falls, S. Dak. **C**, 30 August 2000 south-looking oblique aerial photograph of the terminus of Nizina Glacier. Since 1957, a 3-km long ice-marginal lake has developed due to the retreat of the glacier. Photograph by Bruce F. Molnia, U.S. Geological Survey.



Root and Gates Glaciers are the principal eastern tributaries of Kennicott Glacier (1919 Moffit photograph, USGS Photo Library photograph Moffit 832). Both descend from the southern flank of Regal Mountain. The western side of Kennicott Glacier dams the mouth of Hidden Creek Valley, located approximately 16 km north of Kennicott Glacier's stagnant terminus. Annually, 3-km-long Hidden Creek Lake forms, dammed by the margin of Kennicott Glacier. Between July and September, the lake drains subglacially, releasing as much as  $4$  to  $5 \times 10^7$  m<sup>3</sup> of water (Cunico and others, 2001), causing a jökulhlaup on the Kennicott River. In 2000, a year in which the lake drained completely in approximately 75 hours, Cunico and others (2001) studied the mechanics of the glacier to understand the evolution of the flood. They placed 22 survey targets on the glacier's surface over an area about equal in width to the lake, from near the glacier/lake margin to a distance of about 1 km from the margin. They surveyed the targets over a 24-day period as the lake filled and then drained. Independent monitoring of changes in the lake's level revealed that, as the lake filled, targets 300 to 400 m away from the lake rose at nearly the same rate as the lake, typically about 0.5 m d<sup>-1</sup>. Several rose faster than the lake. The rate of vertical movement fell off rapidly with distance from the lake. At a distance of about 1 km, vertical movement of the targets seemed to be uncorrelated with lake stage. Cunico and others (2001) concluded that the general pattern of observed displacement is consistent with a wedge of water extending beneath the glacier to a distance of perhaps 300 to 400 m from the visible margin of the lake and exerting buoyant stresses on the ice that were then transmitted into the main body of the glacier and caused flexure. For a given value of lake stage, target elevations were invariably higher as the lake drained than they were as the lake filled. Moreover, survey targets at a distance of about 400 m or more from the lake continued to rise for some time even after the lake began to drain. The lag time between the beginning of lake drainage and the beginning of target dropping increased with distance from the lake, the lag being about 14 hours 400 m from the lake. They concluded that movement of water from the lake into temporary storage—a sort of hydraulic jacking—was responsible for the observed ice displacements. Using the vertical dropdown of the ice as a guide, they calculated that the volume of the subglacial water “wedge” plus the water released from distributed storage is about  $7.0 \times 10^6$  to  $1.1 \times 10^7$  m<sup>3</sup> (Cunico and others, 2001).

The surfaces of both Root and Gates Glaciers possess multiple ogive-like undulations; a USGS photograph from the early 1980s shows that the surface of Root Glacier features many pits (Winkler, 2000, fig. 71). When the author observed them from the air on 30 August 2000, the upper regions of both glaciers showed much evidence of thinning, and the terminus of Kennicott Glacier was stagnant.

With only a few exceptions, almost every glacier in the Wrangell Mountains that descends below 2,000 m shows evidence of thinning, retreat, or stagnation. However, at higher elevations such as the Frederika Peak area, temperatures remain cold enough and precipitation is sufficient to nourish existing ice accumulations in spite of changing climate. Hence, in the eastern Wrangell Mountain, glaciers at elevations above 2,500–3,000 m show no evidence of ice loss.

### **Glaciers of Mount Blackburn and the Southeastern Wrangell Mountains**

Mount Blackburn, the highest peak in the Wrangell Mountains, is an erosional remnant of a large shield volcano. The mountain is covered with ice and gives rise to several large glaciers: Kennicott Glacier (fig. 367) which flows to the southeast; part of Nabesna Glacier which flows to the northeast; and Kuskulana Glacier, which flows to the south and west. Other, generally



**Figure 366.**—30 August 2000 oblique aerial photograph of the central Rohn Glacier adjacent to Chimney Mountain, looking to the northwest. In the 88 years since Rohn Glacier was photographed by S.R. Capps, the glacier has thinned as much as 30 m. The trimlines and the barren zone adjacent to the eastern tributary are evidence of this change. Photograph by Bruce F. Molnia, U.S. Geological Survey. A larger version of this figure is available online.



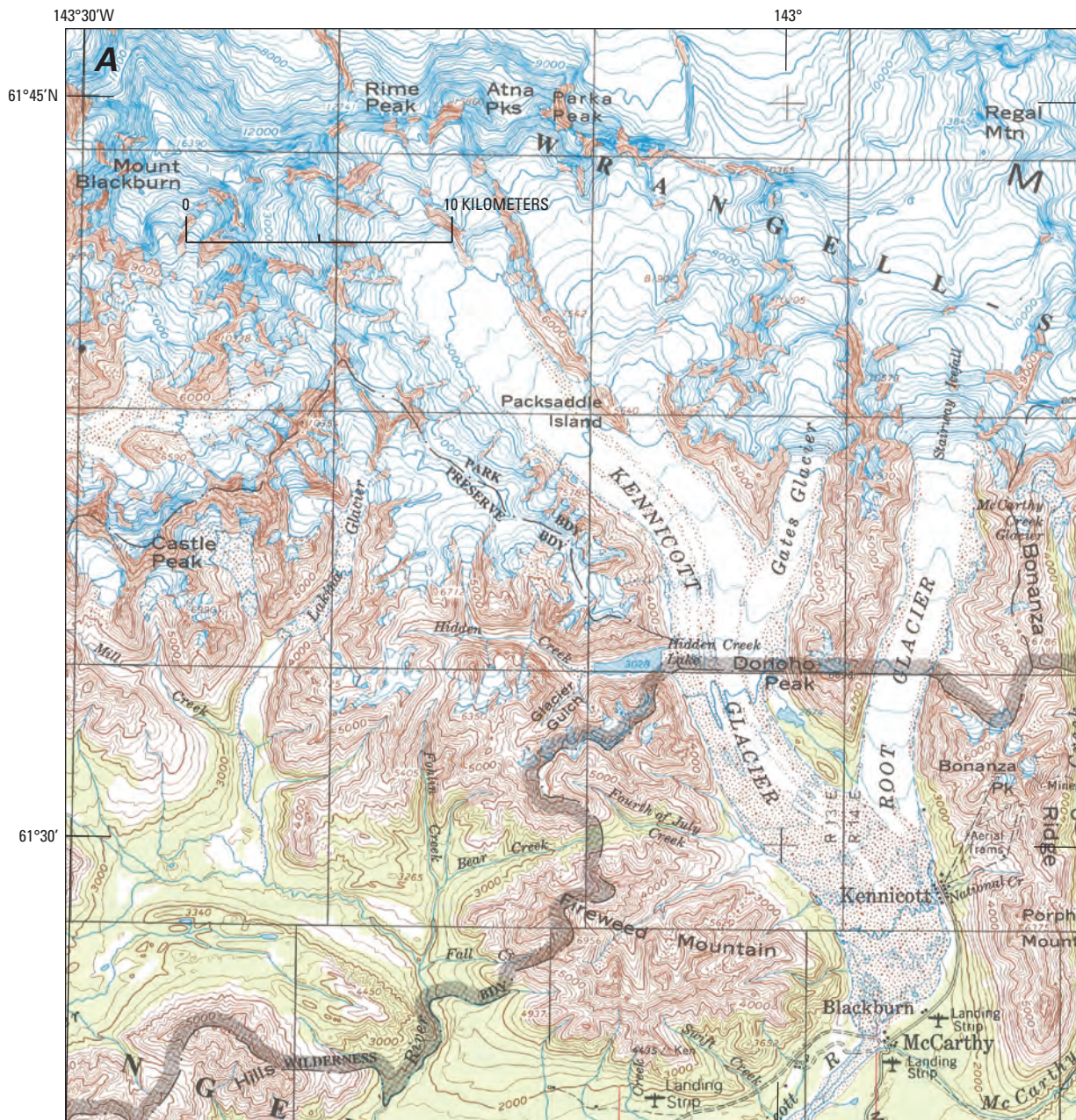
smaller glaciers, flow from isolated accumulation areas located on upland ridges and isolated peaks (fig. 368).

### Kennicott Glacier

Kennicott Glacier (figs. 367A–D), which is 44 km long and 551 km<sup>2</sup> in area (Denton and Field, 1975c, p. 562), is the second largest in the Wrangell Mountains. It heads on the eastern side of Mount Blackburn but also receives ice from a 10-km-long ridge capped with Rime Peak, the Atna Peaks, and Parka Peak. Its primary eastern tributaries, Root Glacier and Gates Glacier, descend from the southern flanks of Regal Mountain. Much of the glacier's surface is debris-covered and has been since at least 1900 (1905 Capps photographs, USGS Photo Library photograph Capps 123, 124, and 125; 1919 Moffit photograph, USGS Photo Library photograph Moffit 826).

As early as the end of the first decade of the 20th century, questions were being asked about whether the glacier was stagnant. After visiting the glacier in 1910, Reid (1913a) wrote that the glacier was stagnant and inactive, as it had been since before 1899. Two years later, he repeated his assertion, stating

**Figure 367.**—Map, Landsat image, and aerial photographs of the Kennicott Glacier. **A**, Section of the USGS McCarthy, Alaska (1960, revised 1981) 1:250,000-scale map showing the Kennicott Glacier and its tributaries. **B–D**, see following page.



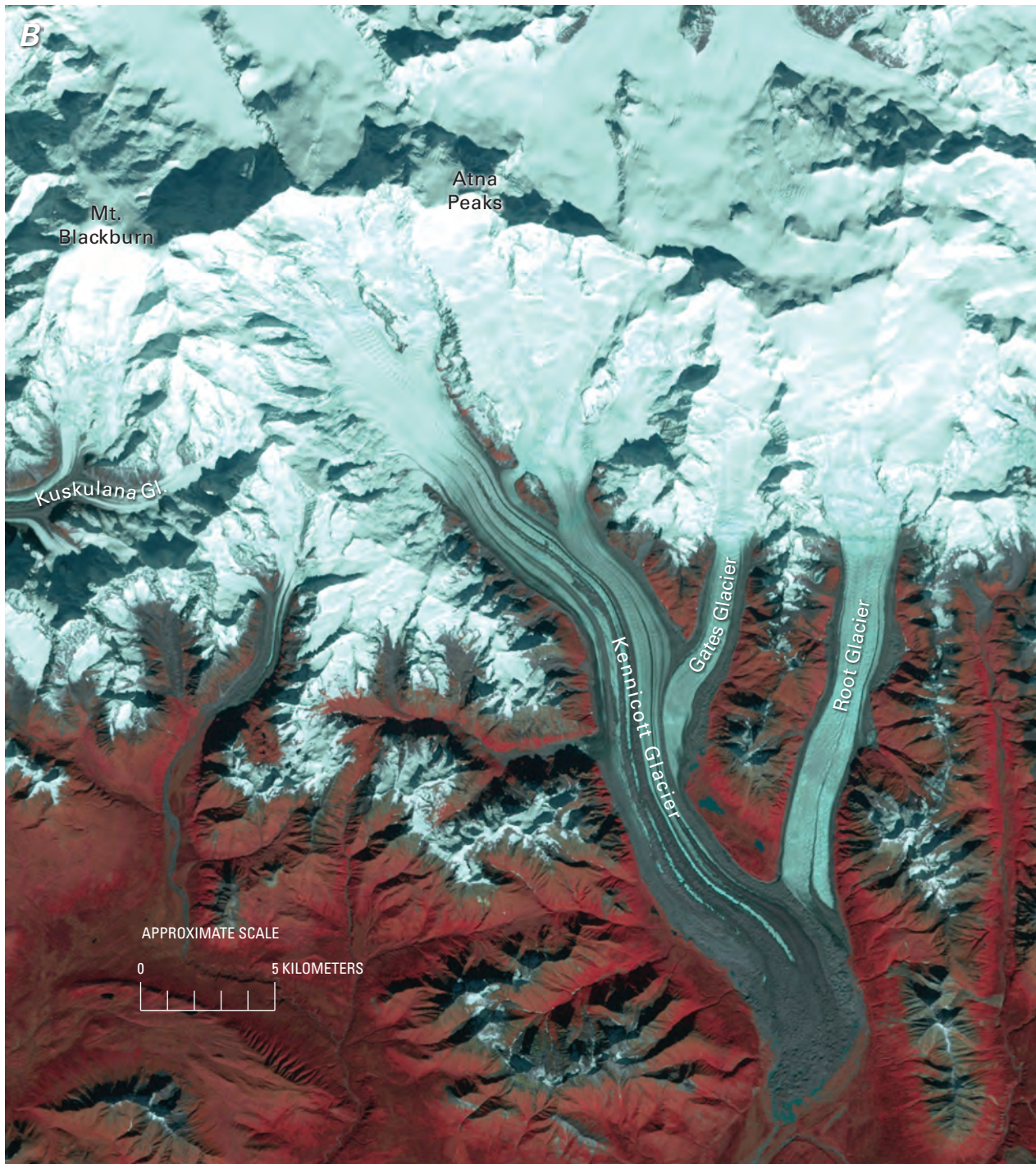
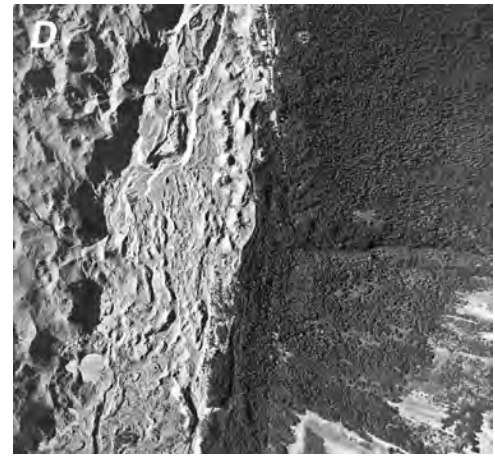


**Figure 367.—B,** Enlarged section of annotated Landsat 7 ETM+ false-color composite image of the Kennicott Glacier area. Landsat 7 image (LE7064017000125350; 10 September 2001; Path 64, Row 17) from the USGS, EROS Data Center, Sioux Falls, S. Dak. **C** and **D,** see opposite page.



▲ **Figure 367.**—**C**, 30 August 2000 north-looking oblique aerial photograph of the head of Kennicott Glacier with Rime Peak, the Atna Peaks, and Parka Peak. Elevated lateral moraines and vegetation growing on the eastern margin document continued thinning of the glacier. Photograph by Bruce F. Molnia, U.S. Geological Survey. **D**, 30 August 1999 black-and-white vertical aerial photograph of part of the eastern margin of Kennicott Glacier showing a marginal sediment zone, possibly with some ice-core remaining and a pitted, hummocky ice-cored moraine zone with several water-filled thermokarst pits. Photograph from U.S. Bureau of Land Management, roll 3, frame 14. A larger version of D is available online.



**Figure 368.**—A 1919 photograph by F.H. Moffit of a small unnamed glacier located at the head of Rock Creek, a tributary to the Kotsina River. Located on the flanks of an unnamed 2,332-m peak, this glacier, the southwesternmost glacier in the Wrangell Mountains, shows several signs of thinning and retreat. The glacier is typical of small cirque and mountain glaciers that originate from isolated accumulation areas southwest of Mount Blackburn. Photograph Moffit 644 from the USGS Photo Library, Denver, Colo.

that Kennicott Glacier was unchanged from 1911 to 1912 (Reid, 1913b). In September 1918, Bateman (1922) placed a line of stakes on the surface of the glacier at a location about 6.5 km above the terminus. Upon returning the following year, he determined that the stakes had moved as much as 25 m in the ensuing 374 days, a confirmation that very slow motion was taking place.

When Bradford Washburn photographed Kennicott Glacier in 1937 and 1938, the terminus had retreated several hundred meters (Denton and Field, 1975c). Little net change had occurred when it was next photographed by Post in 1964 (Denton and Field, 1975c). When the author observed it from the air on 30 August 2000 (fig. 367C), its upper region showed evidence of thinning.



The apparently stagnant Kuskulana Glacier, its southern half covered by moraine, is 25 km long and has an area of 156 km<sup>2</sup> (Denton and Field, 1975c, p. 563) (fig. 369). Little information could be found about changes in Kuskulana Glacier. Denton and Field (1975c) stated that the glacier changed little from the late 1930s to the late 1950s. They attributed a lateral barren zone, seen in photographs made by Bradford Washburn in 1937 and 1938, to recent surface lowering. It is very apparent in several early 1980s photographs of the junction of the eastern and northeastern tributaries of the glacier that the surface lowering of the stagnant terminus continued during the Landsat baseline period. When the author observed it from the air on 30 August 2000, no evidence of terminus advance or glacier thickening could be seen. Kuskulana Glacier is difficult to discern in its entirety on Landsat 7 ETM+ false-color composite images because supraglacial morainic debris masks the underlying ice.

**Figure 369.**—31 August 1984 oblique aerial photograph of the junction of the northeast tributary of the Kuskulana Glacier and the main trunk of the glacier. Elevated lateral moraines and thinning tributaries document recent thinning of the glacier. Photograph 84-R3-032 by Robert M. Krimmel, U.S. Geological Survey.

## Glaciers of Mount Wrangell

Mount Wrangell, the youngest and only currently active volcano in the Wrangell Mountains, is a large andesitic shield volcano with a volume of about  $900 \text{ km}^3$  (Nye, 1983) (fig. 370A) (1902 Brooks photograph, USGS Photo Library photograph Brooks 1111). Nearly all of the mountain is covered by glacier ice and perennial snow. Its glaciers drain into both the Copper River and Yukon River drainages. Its top is capped by a  $4 \times 6 \text{ km}$  ice-filled summit caldera (fig. 370B), the depth of which approaches  $1 \text{ km}$  (Benson and Motyka, 1978; Clarke and others, 1989). Three craters are located along its northern rim, (from west to east): Mount Wrangell Crater, North Crater, and East Crater. Studies by Benson and others (1975), Benson and Motyka (1975, 1978), Benson and others (1985), and Benson and Follett (1986) showed that the volume of ice in the North Crater has decreased significantly since studies began during the IGY. Between 1957 and 1984, the crater's ice thinned significantly, and its surface elevation decreased by nearly  $200 \text{ m}$ . Between 1965 and 1976, about  $3.2 \times 10^7 \text{ m}^3$  of ice was lost to melting and evaporation. In the 20 years between 1965 and 1984, about 85 percent of the crater's ice disappeared. An increase in heat flux, a result of the 27 March 1964 Alaskan earthquake, is thought to be responsible for the crater's ice loss. To account for the ice lost between 1965 and 1976, an average volcanic heat flux of  $62 \text{ W m}^{-2}$ —approximately 1,400 times Earth's average heat flux—is required. Elsewhere in the summit caldera, little change has been noted in the surface elevation of the caldera's ice cover.

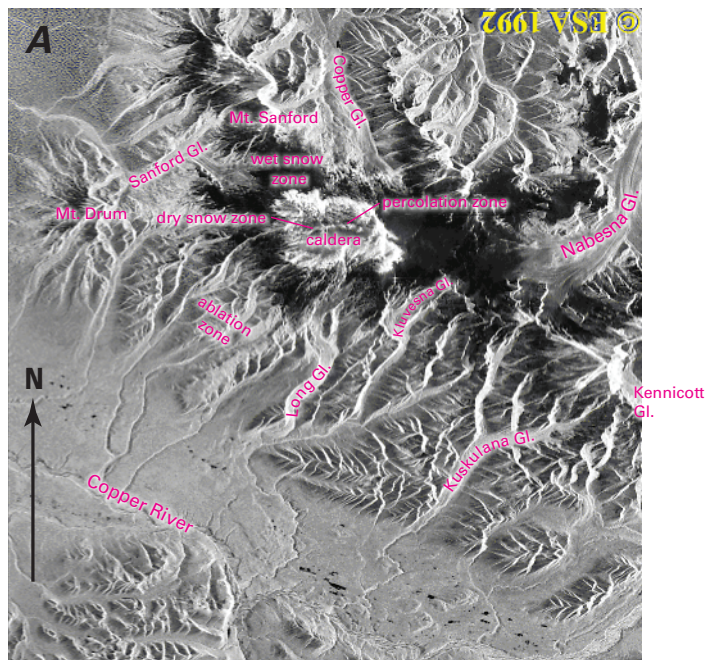


**Figure 370.**— Two views of Mount Wrangell. **A**, Digital radar image of part of the Wrangell Mountains and Copper River Valley showing the caldera of Mount Wrangell ( $4,317 \text{ m}$ ), Mount Drum ( $3,660 \text{ m}$ ) and Mount Sanford ( $4,950 \text{ m}$ ). Mount Wrangell's  $4 \times 6 \text{ km}$  summit caldera holds approximately  $10 \text{ km}^2$  of ice. There are approximately  $150 \text{ km}^2$  of ice on its flanks. This scene also illustrates the concept of glacier facies (Williams and others, 1991). The ice in the summit caldera is in the dry snow zone. The surrounding area of bright tone is probably the percolation zone, where melt features such as ice lenses, layers, and pipes contribute to the stronger backscatter. Beyond the percolation zone is the wet snow zone with a dark tone caused by low backscatter from the wet surface. Below the wet snow zone is the ablation zone, illustrated by the many glaciers flowing away from Mount Wrangell, particularly Nabesna Glacier at the upper right of the scene. Copyright for this image rests with the European Space Agency (ESA). Printed with permission. Caption modified from the Alaska Science Facility (ASF). **B**, 1981 oblique aerial photograph of a part of Mount Wrangell's ice-filled caldera. Photograph by Roman Motyka, Alaska Division of Geological and Geophysical Surveys. From Neal and McGimsey (1996). A larger version of B is available online.

## Glaciers Descending from Mount Wrangell's Summit Caldera

More than a dozen glaciers radiate from Mount Wrangell's summit. Starting from the southeasternmost and moving in a clockwise direction, Denton and Field (1975c, p. 563–564, 566) determined the following lengths and areas: Kluvesina Glacier (22 km, 71 km<sup>2</sup>); Long Glacier, which originates within the caldera of Mount Wrangell (fig. 371) (39 km, 121 km<sup>2</sup>); Cheshnina Glacier (14 km, 28 km<sup>2</sup>); *East Chetaslina Glacier*; Chetaslina Glacier (17 km, 60 km<sup>2</sup>); *East Fork Glacier* (16 km, 43 km<sup>2</sup>); Chichokna Glacier; Dadina Glacier (18 km, 32 km<sup>2</sup>); *Betseli Glacier*; *North Mackeith Glacier*; *Center Mackeith Glacier*; *South Mackeith Glacier*; *Athna Glacier* (26 August 1981 AHAP false-color infrared vertical aerial photograph no. L99F4733); and Copper Glacier (29 km, 172 km<sup>2</sup>).

Seasonal studies (Sturm, 1995) and photogrammetric investigations (Sturm and others, 1991) show that the 30-km-long *Athna Glacier* and the smaller *South* and *Center Mackeith Glaciers* have been advancing from 5 to 18 m a<sup>-1</sup> since the onset of increased heat flux following the 1964 earthquake. All of Mount Wrangell's other outlet glaciers have remained stationary or retreated. Sturm stated that the advancing glaciers display little seasonal variation in surface velocity, whereas other glaciers, such as *East Chetaslina Glacier* and *West Chetaslina Glacier*, experience a 50-percent increase in surface velocity in spring and summer. These glaciers have a common accumulation zone located around North Crater.

Analysis of 1957 photography of Copper Glacier (Denton and Field, 1975c) show that it is fronted by two sets of moraines that are located about 5 and 7 km in front of the terminus. Identified as not more than a few hundred years old, the more distant of the two moraines may represent Copper Glacier's "Little Ice Age" maximum position.

Northward-flowing Nabesna Glacier (fig. 372A–E) (1916 Capps photograph, USGS Photo Library photograph Capps 5) originates high on the southeastern slopes of the ice field that covers the summit area of Mount Wrangell and also receives ice from the northwestern slopes of Mount Regal. Nabesna is the largest of Mount Wrangell's outlet glaciers and the largest in the Wrangell Mountains. It is about 87 km long and 819 km<sup>2</sup> in area (Denton and Field, 1975c, p. 566) and has as many as 40 tributaries. Capps first visited Nabesna's terminus in 1908, at which time the first 3 km of the glacier were covered by thick debris. Capps (1910a, p. 40) stated that "The extent of the terminal moraine shows that the glacier is at present retreating. It has been deposited so recently that over most of it no vegetation has as yet obtained a foothold....."

Denton and Field (1975c) analyzed available photography to determine the mass balance of Nabesna Glacier. They stated that a 1938 photograph by Bradford Washburn indicated slow shrinkage of the lower part of the glacier and some withdrawal from the terminal moraine. They also indicated that other photographs obtained in 1957 and 1964 showed a continuation of this trend. An early 1980s photograph by D.H. Richter (Winkler, 2000, fig. 4) showed that thinning of the glacier at elevations above 2,250 m had exposed several nunataks. When the author observed the terminus from the air on 30 August 2000 (fig. 372E), he noted a number of characteristics suggesting that it is actively retreating and thinning.

East of Nabesna Glacier and northwest of the terminus of Chisana Glacier in the drainage of Cross Creek is an area of small named and unnamed retreating glaciers (26 August 1981 AHAP false-color infrared vertical aerial photograph no. L99F4720). One unnamed glacier located at the head of Ramshole Creek has retreated more than 3 km from its "Little Ice Age" maximum position. The next glacier to the west, another unnamed glacier, has retreated approximately 1.7 km from its "Little Ice Age" maximum position. Many smaller glaciers in the vicinity have completely disappeared.



**Figure 371.**—30 August 2000 oblique aerial photograph of the pitted, partially vegetation-covered, hummocky terminus of Long Glacier. The terminus has retreated several kilometers during the second half of the 20th century. Photograph by Bruce F. Molnia, U.S. Geological Survey. A larger version of this figure is available online.

**Figure 372.**—Views of Nabesna Glacier. **A**, Sections of USGS 1:250,000-scale maps of Nabesna, Alaska (1960, revised 1982) and McCarthy, Alaska (1960, revised 1981) mosaicked to show Nabesna Glacier, the Icefields Plateau, and Mount Gordon. **B–E**, see following pages.

143°30'W

143°

62°N

61°45'



**Figure 372.**—**B**, Part of the topographic reconnaissance map of the central Copper River region, Alaska, a 1:250,000-scale map based on field topographic surveys conducted prior to 1902 showing the larger outlet glaciers of the eastern Wrangell Mountains. Published as Plate Number XX in USGS Professional Paper 41 (Mendenhall, 1905). **C**, Landsat 7 ETM+ (EnhancedThematic Mapper Plus) false-color composite image showing the same general area. It is remarkable that the 1902 map of such a remote area, using ground-based surveying techniques compares favorably to the depiction of the glaciers on the Landsat 7 ETM+ image. Landsat image (7064017000125350; 10 September 2001; Path 64, Row 17) from the USGS, EROS Data Center, Sioux Falls, S. Dak. A larger version of B is available online.





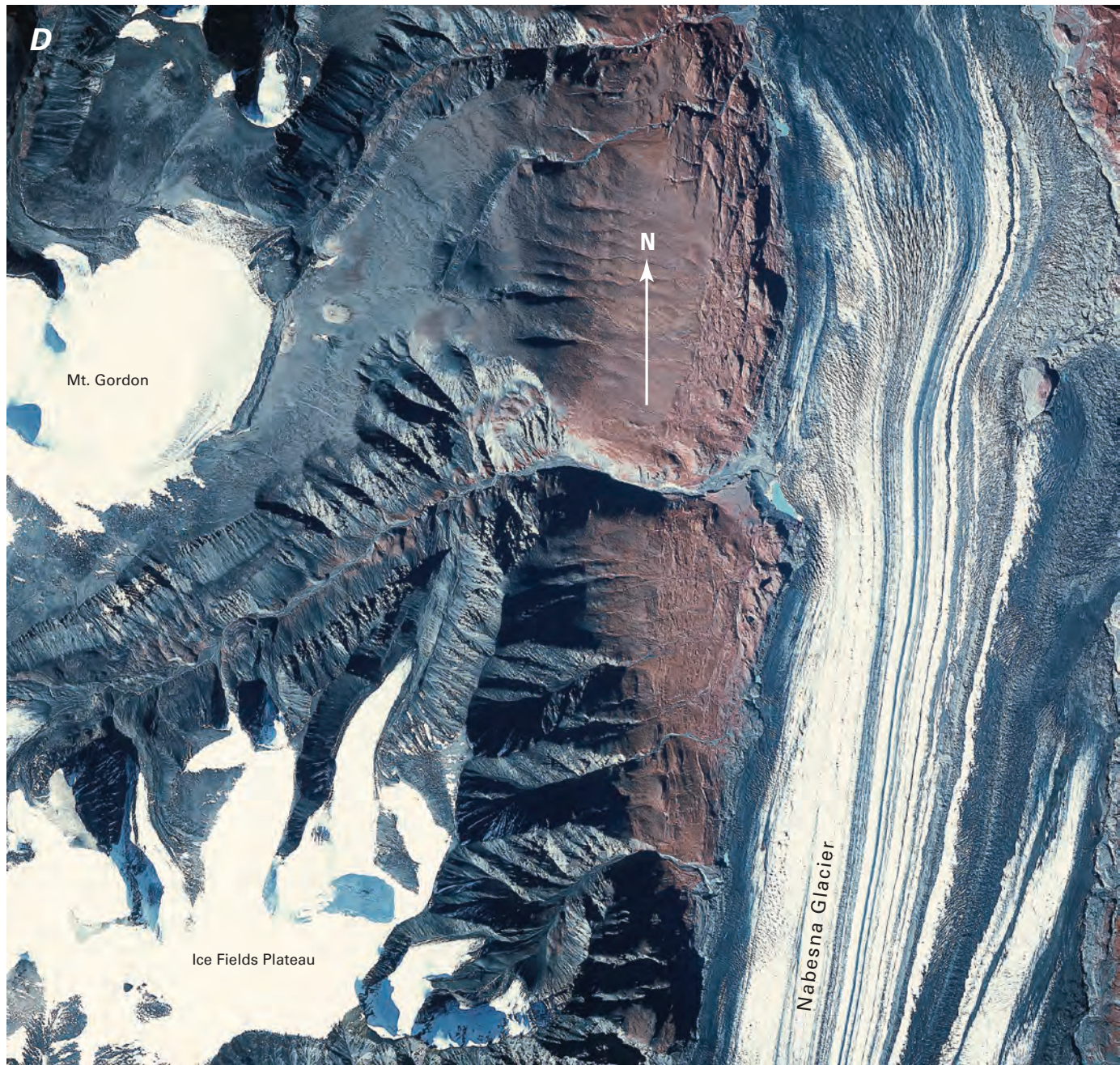
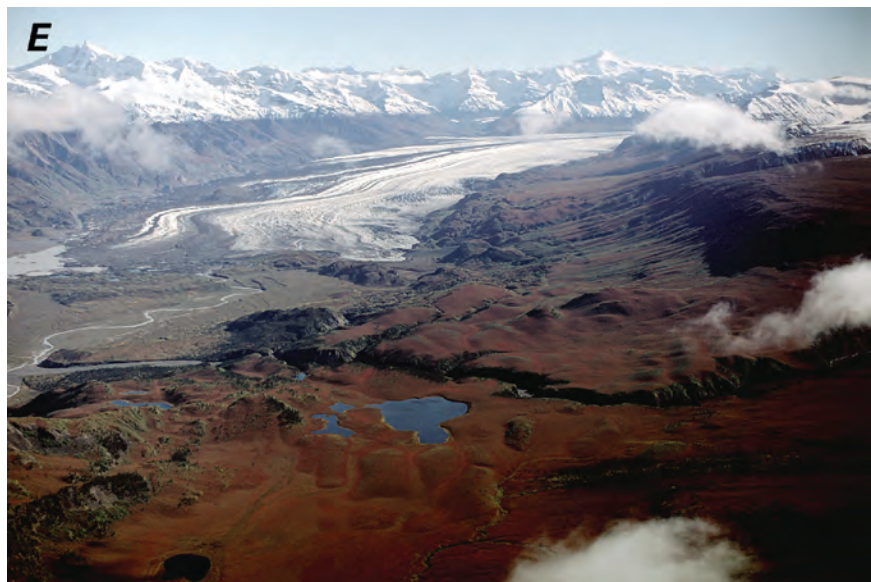


**Figure 372.** —**D**, 26 August 1981 AHAP vertical, false-color aerial photograph of part of the northern Nabesna Glacier, just south of its terminus. Evidence of thinning exists along both margins. Also visible are the Icefields Plateau and Mount Gordon; both show evidence of recent retreat. AHAP photograph no. L99F4725 from the GeoData Center, Geophysical Institute, University of Alaska, Fairbanks, Alaska. **E**, 30 August 2000 southeast-looking oblique aerial photograph showing the retreating and thinning terminus of Nabesna Glacier. An ice-marginal lake has developed on the eastern side of the margin through the retreat of the terminus. Photograph by Bruce F. Molnia, U.S. Geological Survey.



## Mount Drum

Mount Drum (fig. 373A, B) (26 August 1981 AHAP false-color infrared vertical aerial photograph no. L99F4740), a glacier-capped stratovolcano, is the westernmost volcano in the Wrangell Mountains. Its last eruption was between 125,000 and 150,000 years ago (Richter and others, 1995). Eleven outlet glaciers with lengths of 3 to 16 km descend from the perennial ice field that covers the mountain at elevations above 2,400 m. Nadina Glacier, the only named glacier, is the largest, having a length of 16 km and an area of 25 km<sup>2</sup> (Denton and Field, 1975c, p. 564). At elevations below about 1,000 m, its stagnant terminus is covered by vegetation, including mature spruce trees. When observed from the air by the author on 9 July 1999 and 31 August 2000 (fig. 373B), all of the outlet glaciers showed signs of stagnation, thinning, or retreat.

## Mount Sanford

A complex shield volcano, Mount Sanford is the second highest peak in the Wrangell Mountains and is covered by a perennial ice and snow cover at elevations above 2,400 m. Last active at least 100,000 years ago, it possesses some of the steepest topography in North America. The upper reaches of Sanford Glacier descend about 2.5 km in a distance of only about 1.5 km. On its southern side, ice flowing from Mount Sanford merges with ice descending from the northern side of Mount Wrangell.

Ten glaciers (4 formally named) having lengths of 8 to 27 km descend from the summit of Mount Sanford. The largest, Sanford Glacier, is debris-covered and has a length of 27 km and an area of 199 km<sup>2</sup> (Denton and Field, 1975c, p. 564) (fig. 374) (26 August 1981 AHAP false-color infrared vertical aerial photograph no. L99F4737). A comparison of the position of the glacier as mapped in 1902 by Mendenhall and Gerdine (Mendenhall, 1905) and the position seen on Bradford Washburn's 1938 photograph, shows Sanford Glacier extending about 3 km further to the north on the earlier map and connected to two tributaries originating on Mount Drum. Denton and Field (1975b) questioned the reliability of the earlier map.

The three other named glaciers include Sheep Glacier (1908 Capps photograph, USGS Photo Library photograph Capps 544), with a length of 9 km and an area of 9 km<sup>2</sup> (Denton and Field, 1975c, p. 565); Drop Glacier, with a length of 24 km and an area of 55 km<sup>2</sup> (Denton and Field, 1975c, p. 565); and West Glacier with a length of 18 km and an area of 39 km<sup>2</sup> (Denton and Field, 1975c, p. 565). These glaciers and all of the other unnamed glaciers that descend from Mount Sanford showed signs of stagnation, thinning, or retreat when the author observed them from the air on 31 August 2000.

## Glaciers of Mount Jarvis and Mount Gordon and the Ice Fields Plateau

Mount Jarvis, a shield volcano, is the 2,852-m-high summit of an 8-km-long ice-covered ridge located east of Copper Glacier. Three large glaciers and several smaller ones flow eastward from the ridge. The largest, Jacksina Glacier, has a length of 19 km and an area of 72 km<sup>2</sup> (Denton and Field, 1975c, p. 566). When the author observed them from the air on 31 August 2000, all of the Jarvis ridge glaciers showed signs of stagnation, thinning, or retreat.

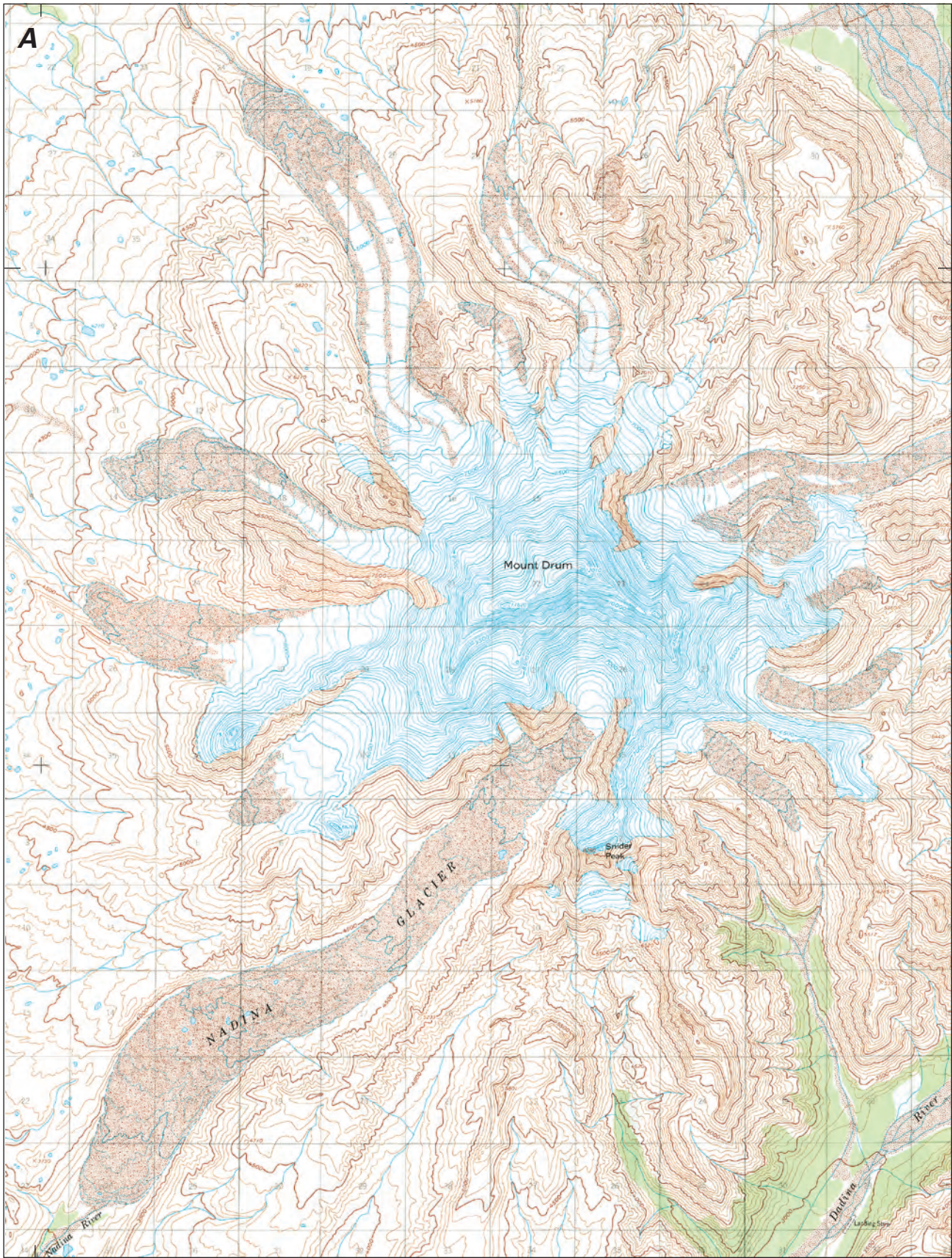
Less than a million years old, Mount Gordon is a 2,755-m-high cinder cone with its summit almost completely covered by ice. When it was photographed by the AHAP Program on 26 August 1981, a few very small outlet glaciers descended from the crater. An ice-free cirque on its northern flank suggests that there has been a recent loss of glacier ice from the mountain's flanks.

The Icefields Plateau is a 13.5×7.5-km ice-covered upland located south of Mount Gordon, between Jacksina Glacier and Nabesna Glacier. With a surface elevation of about 2,500 m, it supports about 10 small outlet glaciers. When they were photographed by the AHAP Program on 26 August 1981, all of the glaciers showed signs of stagnation, thinning, or retreat.

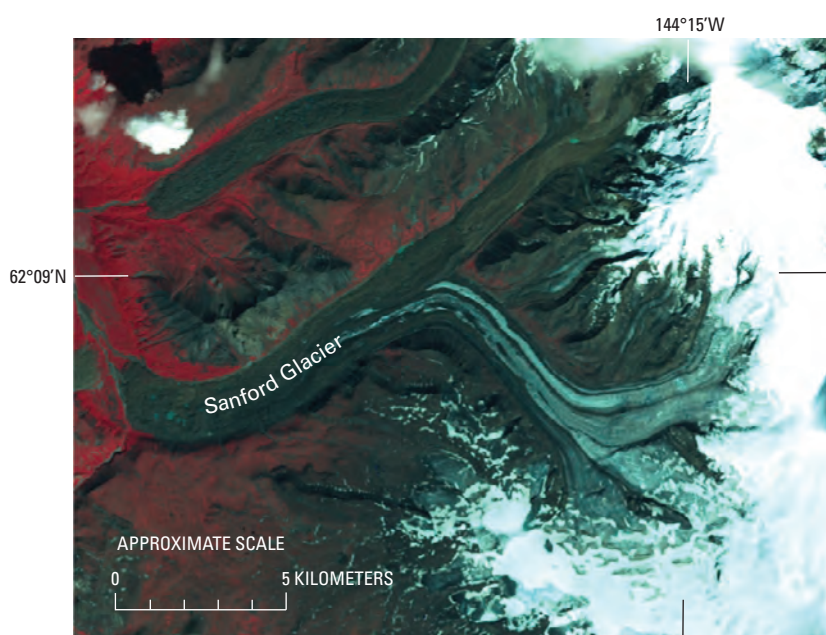
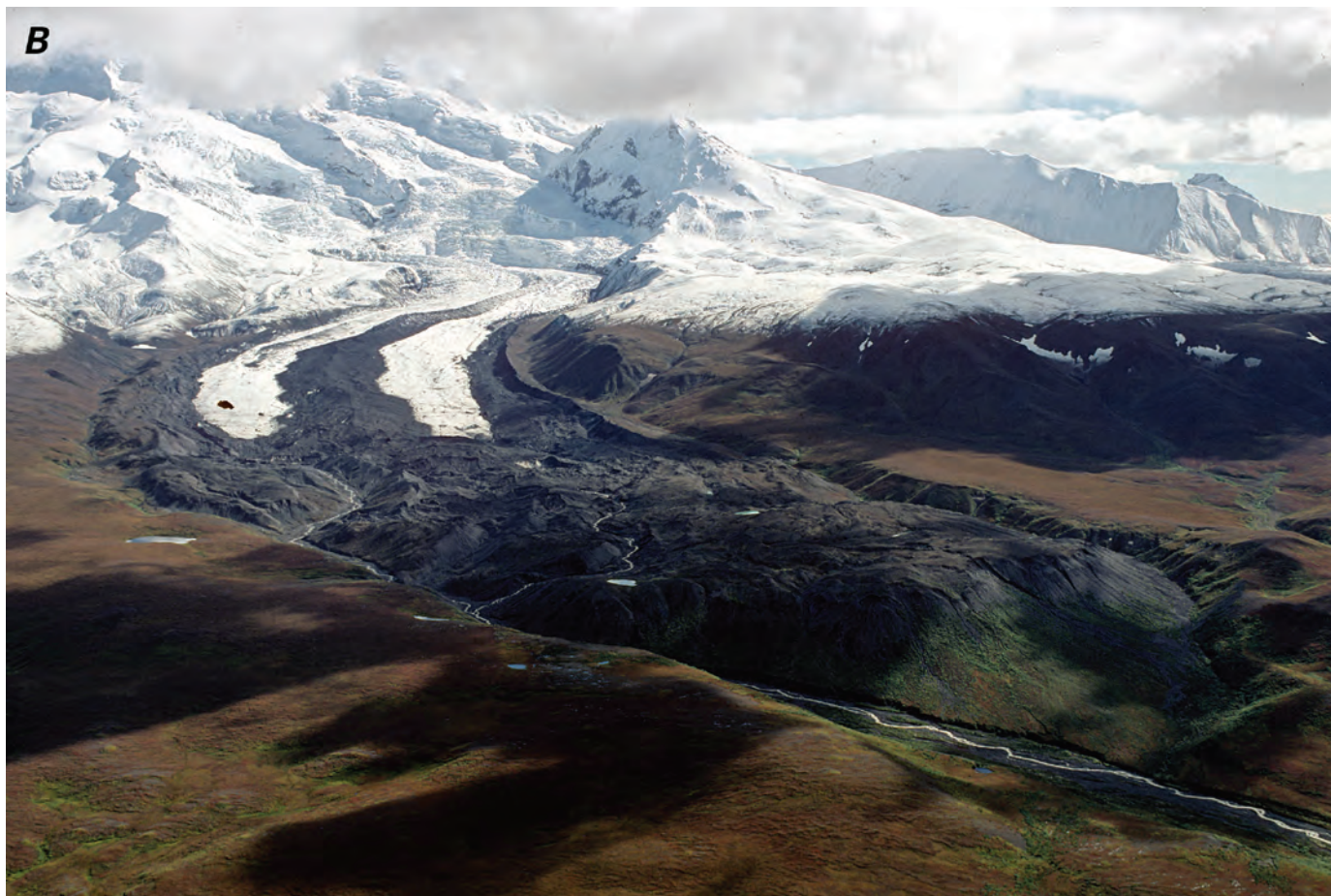
► **Figure 373.**—Map and aerial photograph of the glaciers of Mount Drum. **A**, Section of the USGS Gulkana, Alaska A-2, 1:63,360 topographic map (1959), based on 1955 and 1957 photography, showing all of the glaciers that descend from Mount Drum. **B**, see following page.

144°50'W

62°10'N



CONTOUR INTERVAL 100 FEET  
DOTTED LINES REPRESENT 50 FOOT CONTOURS  
DATUM IS MEAN SEA LEVEL



▲ **Figure 373.**—**B**, 30 August 2000 south-east-looking oblique aerial photograph showing the terminus of one of Mount Drum's unnamed outlet glaciers and Mount Drum. The glacier's surface is significantly lower than that of the elevated lateral moraines on both of its margins. It also has an elevated medial moraine and vegetation growing on the distal end of its end moraine, all evidence of recent thinning, stagnation, and retreat. Photograph by Bruce F. Molnia, U.S. Geological Survey.

**Figure 374.**—Landsat 7 ETM+ (Enhanced Thematic Mapper Plus) false-color composite image of Sanford Glacier. The glacier descends from Mount Sanford on the northeast and Mount Wrangell on the southeast. Landsat image (7064017000125350; 10 September 2001; Path 64, Row 17) from the USGS, EROS Data Center, Sioux Falls, S. Dak.

## Summary

During the period of the Landsat baseline (1972–81), all of the valley and outlet glaciers within the Wrangell Mountains were retreating, thinning, or stagnant, with the exception of *Athna Glacier* and *South and Center MacKeith Glaciers*, which were advancing.

Through the end of the 20th century and into the 21st century, no additional information was available about the continued advance of *Athna Glacier* and *South and Center MacKeith Glaciers*. All other valley and outlet glaciers in the Wrangell Mountains continued to thin, retreat, or stagnate.

## Talkeetna Mountains

The Talkeetna Mountains are named for the Talkeetna River, which means “river of plenty” in the language of the Tanaina Indians (Collins, 1975, p. 543). The long axis of the 160×130-km Talkeetna Mountains is oriented north-south (figs. 1, 375). The mountains are bounded on the north by the Nenana River and Broad Pass, on the east by the Susitna and Tyone Rivers, on the west by the Chulitna and Susitna Rivers, and on the south by the Matanuska River. Many peaks have summit elevations greater than 2,000 m; the highest, an unnamed peak, reaches an elevation of 2,550 m.

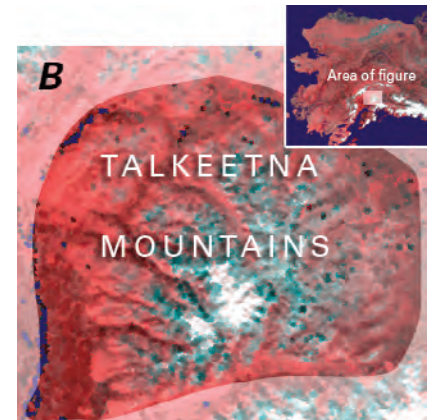
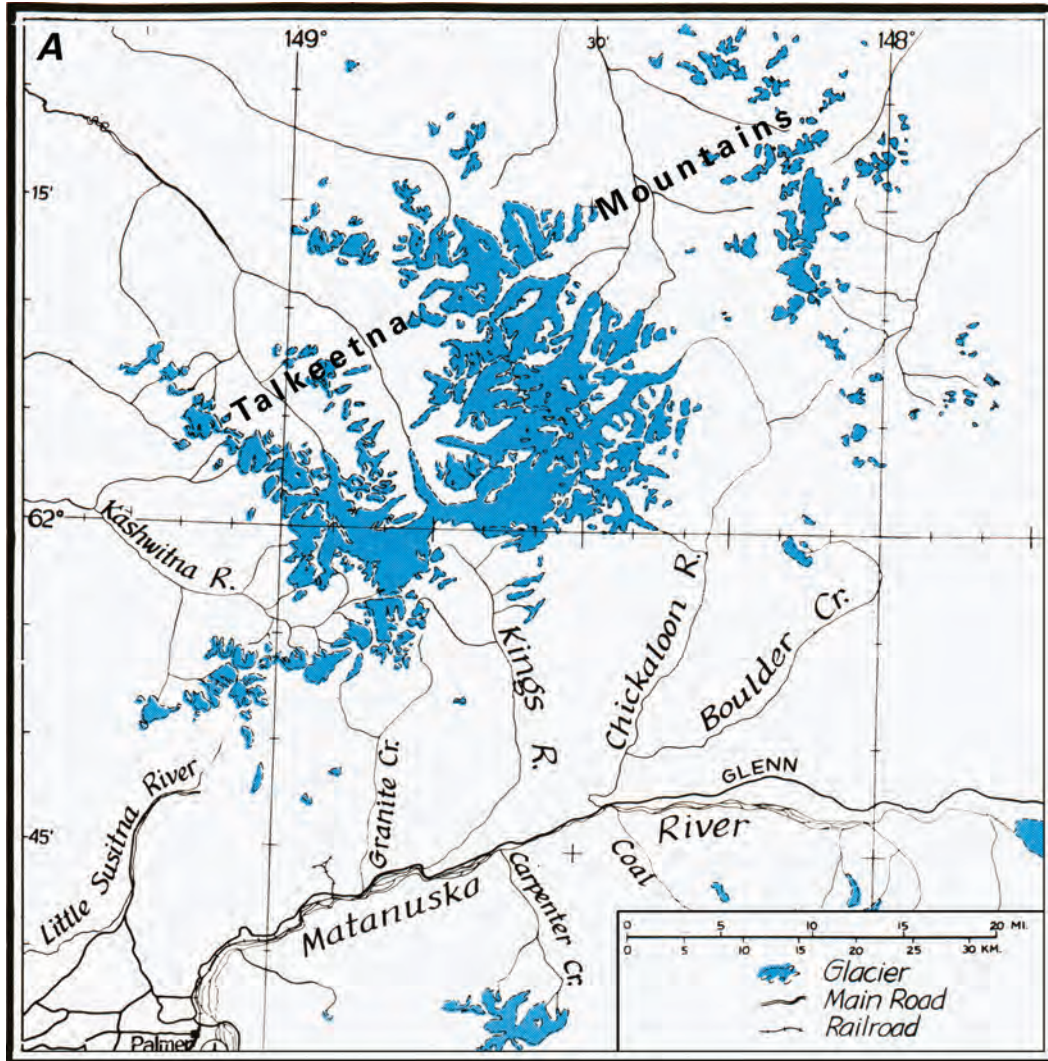
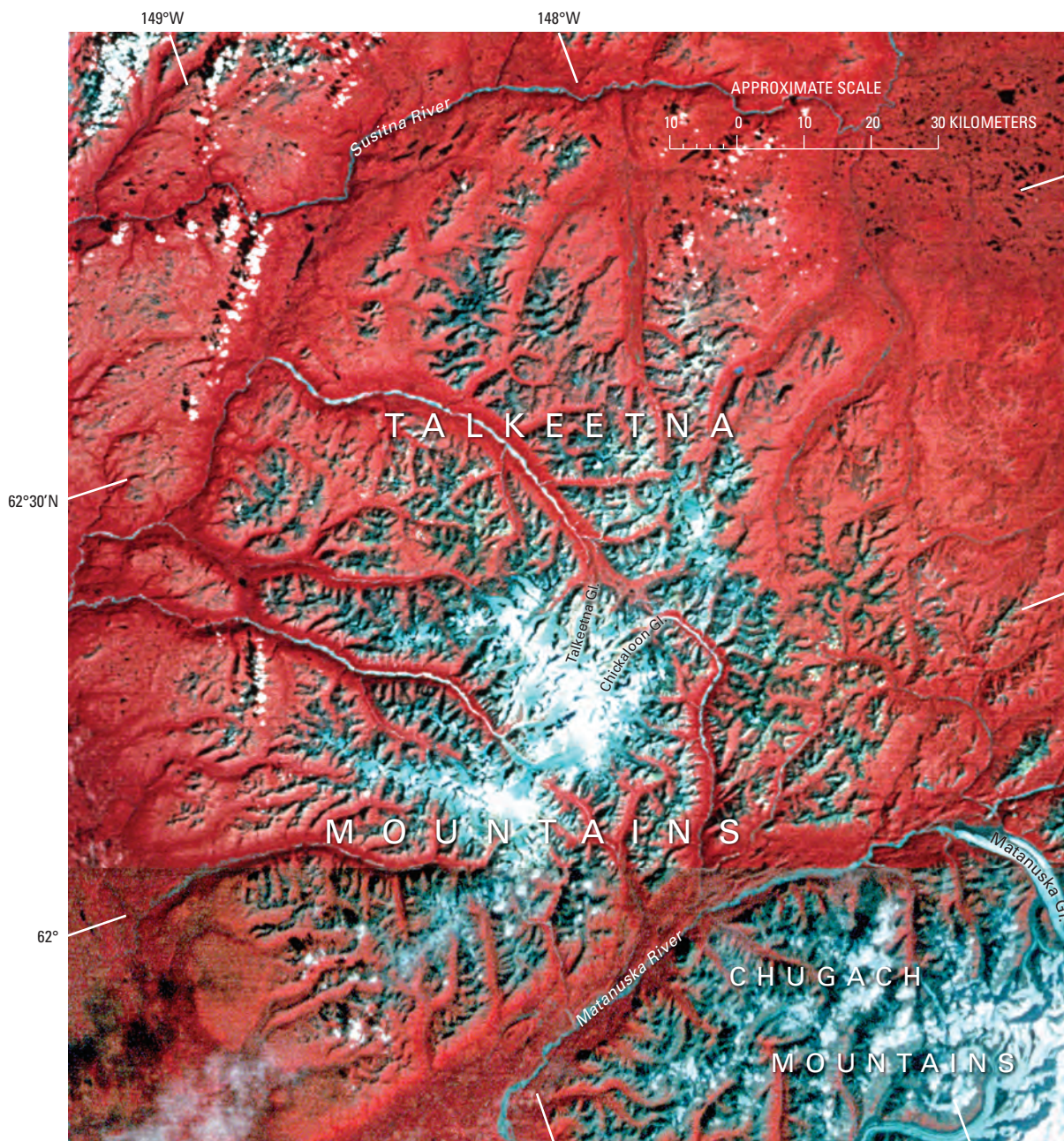


**Figure 375.**—**A**, Index map of the Talkeetna Mountains showing the glacierized areas (index map modified from Field, 1975a). **B**, Enlargement of NOAA Advanced Very High Resolution Radiometer (AVHRR) image mosaic of the Talkeetna Mountains in summer 1995. National Oceanic and Atmospheric Administration image mosaic from Mike Fleming, Alaska Science Center, U.S. Geological Survey, Anchorage, Alaska.

Landsat MSS images that include the glacier-covered Talkeetna Mountains have the following Path/Row coordinates: 74/16, 74/17, and 75/16 (figs. 3, 376; table 1). The southwestern part of the Talkeetna Mountains is shown on a 1:250,000-scale satellite image map of the Anchorage quadrangle made from 4 September 1980 Landsat 3 MSS data (USGS, 1980). The glacier-covered part of the Talkeetna Mountains is mapped on the Anchorage (1962) and Talkeetna Mountains (1954) USGS 1:250,000-scale topographic maps of Alaska (appendix A).

Photographs of glaciers in the Talkeetna Mountains taken by Capps between 1913 and 1917 show many retreating glaciers (9 August 1917 Capps photograph, USGS Photo Library photograph Capps 435; summer 1913 Capps photograph, USGS Photo Library photograph Capps 876). This trend has continued through the early 21st century. Comparing Capps' photographs with aerial observations, shows that one unnamed glacier at the head of Iron Creek retreated approximately 4 km between August 1917 and August 2000. Collins (1945, p. 544) stated that "It can reasonably be deduced that general recession has been the rule here in recent decades, and that

**Figure 376.**—Annotated Landsat 3 MSS false-color composite image mosaic showing the Talkeetna Mountains and part of the northern Chugach Mountains. Shown are the locations of Chickaloon and Talkeetna Glaciers in the Talkeetna Mountains; and Matanuska Glacier in the Chugach Mountains. Landsat images (30175–20342, bands 4, 5, 7; 27 August 1978; Path 74, Row 16 and 2531–20322, bands 4, 5, 7; 9 September 1979; Path 74, Row 17) are from the USGS, EROS Data Center, Sioux Falls, S. Dak.



climatic changes have caused a significant rise in the lower limit at which accumulation can take place. At present this lower limit of accumulation seems to be generally higher than 1850 m.”

When the area was mapped between 1951 and 1954, more than 100 glaciers were located on the southwestern flank of the mountains, generally heading at elevations above 1,800 m. Seven had lengths of more than 8 km. The longest, an unnamed glacier located above the headwaters of the north-west-flowing Sheep River, had a length of 17.7 km, and an area of 77 km<sup>2</sup> (Collins, 1975, p. 546); it has retreated since it was last mapped (fig. 377). Both Chickaloon Glacier, which is 14.5 km long and 33 km<sup>2</sup> in area (Collins, 1975, p. 546) (fig. 378), and Talkeetna Glacier, which is 11.6 km long and

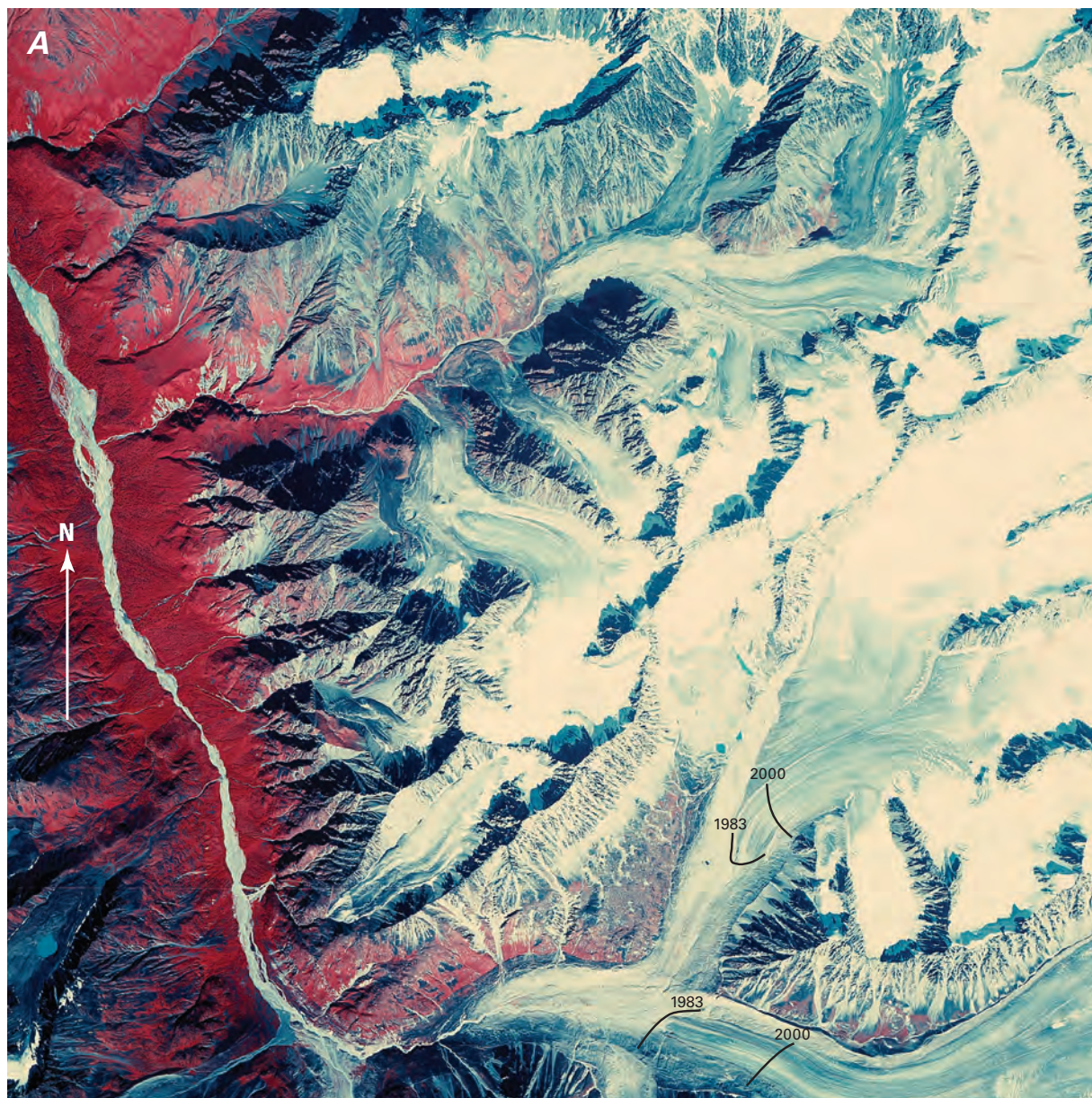


**Figure 377.**—Two photographs of glaciers at the head of the Sheep River. This area contains the largest concentration of glacier ice in the Talkeetna Mountains. **A**, 3 August 1983 AHAP false-color infrared vertical aerial photograph of the area showing a number of retreating glaciers. All of the unnamed glaciers have their margins surrounded by combinations of stagnant ice, unvegetated ground moraine, elevated trimlines, or relict lateral and medial moraines, all evidence of retreat, thinning, or stagnation. When mapped

in 1954, the ice margin of the unnamed glacier at the southern edge of the photograph, longest in the area, sat about 2 km further downvalley. The area between the two terminus positions is covered by stagnant ice and ice-cored moraine. The locations of the debris-free ice margin in 1983 and 2000 are shown. The 2000 termini positions are based on photographs by the author. AHAP photograph no. L99F5175 from the GeoData Center, Geophysical Institute, University of Alaska, Fairbanks, Alaska. **B**, see following page.



**Figure 377.—B**, 31 August 2000 east-looking oblique aerial photograph of the long unnamed glacier described in A. Now separated into two distinct ice tongues, the glacier retreated more than 3 km during the 20th century. Photograph by Bruce F. Molnia, U.S. Geological Survey.

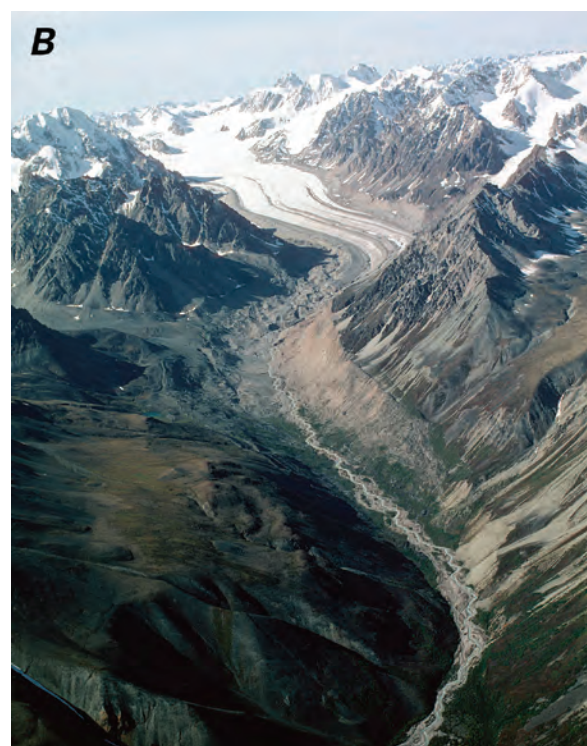
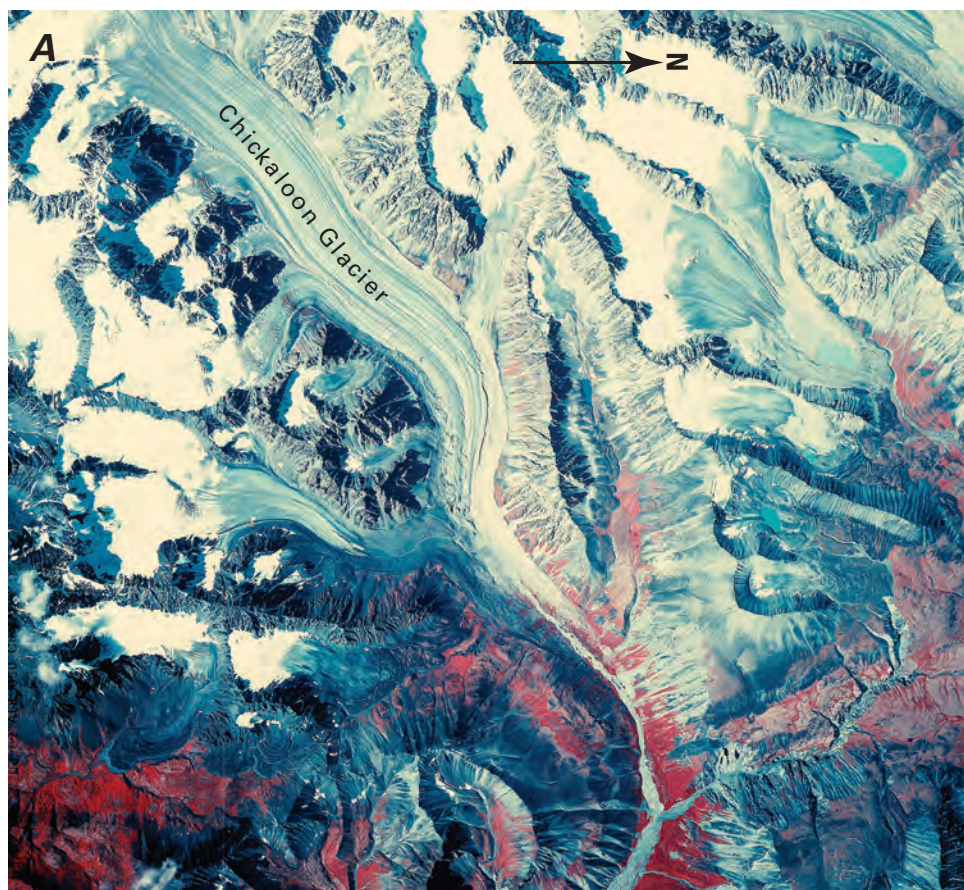


**Figure 378.** — Two photographs of Chickaloon Glacier and its surrounding area. **A**, Annotated 3 August 1983 AHAP false-color infrared vertical aerial photograph of the area showing the retreating Chickaloon Glacier and a number of retreating glaciers located in a small drainage basin to the north. All of the unnamed glaciers in the photograph north of Chickaloon Glacier have their margins surrounded by combinations of stagnant ice, unvegetated ground moraine, elevated trimlines, or relict lateral and medial moraines, all evidence of retreat, thinning, or stagnation. When mapped in 1954, the

ice margin of Chickaloon Glacier was located approximately 3 km downvalley from its 1983 position. The tributary glaciers south of Chickaloon Glacier also show evidence of retreat, thinning, or stagnation. AHAP photograph no. L99F5172 from the GeoData Center, Geophysical Institute, University of Alaska, Fairbanks, Alaska. **B**, 31 August 2000 west-looking oblique aerial photograph of Chickaloon Glacier and its valley. Chickaloon Glacier retreated more than 5 km during the 20th century. Photograph by Bruce F. Molnia, U.S. Geological Survey.





▲ **Figure 379.**—A 31 August 2000 oblique aerial photograph of Talkeetna Glacier and its surrounding area. The view is northeast, downglacier, of the lower approximately 5 km of the glacier. Elevated trimlines, relict lateral and medial moraines, the low gradient, and generally featureless surface are all evidence of rapid retreat and thinning. Photograph by Bruce F. Molnia, U.S. Geological Survey. A larger version of this figure is available online.

**Figure 380.**—31 August 2000 oblique aerial photograph of several large rock glaciers located south of Talkeetna Glacier. Many are located at the foot of cirques or on the flanks of glacier valleys. Also note the thick end-and-ground-moraine complex left by the retreat of the unnamed valley glacier in the valley to the left of the cirque. Photograph by Bruce F. Molnia, U.S. Geological Survey.



32 km<sup>2</sup> in area (Collins, 1975, p. 546) (fig. 379), had retreating termini that were covered with thick ablation moraines. Recent observations made by the author suggest that these long glaciers have lost as much as 5 km of their lengths since 1951–54.

McCauley (1958) made planimetric measurements of all of the glaciers in the Talkeetna Mountains, using USGS 1:63,360-scale topographic maps prepared between 1948 and 1958. She calculated that the total glacierized area was about 300 km<sup>2</sup>. The seven largest glaciers had a cumulative area of 212 km<sup>2</sup>, accounting for approximately two-thirds of the total area. These seven glaciers had termini elevations at between 1,460 and 885 m. Recent observations made by the author show that every one of these glaciers has retreated, some more than 3 km; it is estimated that the Talkeetna Mountains have lost as much as 15 percent of its glacier cover since 1948–58. However, Post and Meier (1980, p. 45) reported the total area of glaciers in the Talkeetna Mountains at 800 km<sup>2</sup>.

Limited revisions made in 1983 by the USGS to the 1954 Talkeetna Mountains 1:250,000-scale topographic map (appendix A) were based on aerial photography obtained in 1978, 1980, and 1981. These revisions showed that at least 50 glaciers east of the Talkeetna and Chickaloon Rivers either decreased significantly in area or melted completely away. Similarly, almost all of the large glaciers west of the two rivers show retreat and shrinkage.

A survey of the glacierized Talkeetna Mountains made by the author from the air on 31 August 2000 documented that glaciers descending below an elevation of about 1,500 m were conspicuously thinning and retreating. Several large glaciers had retreated to the point that primary lobes had separated into several distinct tributary glaciers. On the southern and southwestern sides of the mountains, many of the cirques and valleys were ice free. Many glacier-free cirques and valleys hosted large lobate rock glaciers (fig. 380).

## Summary

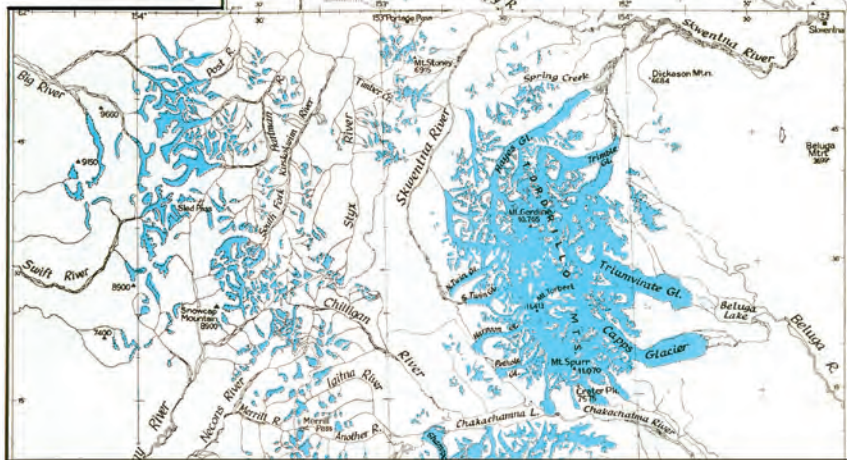
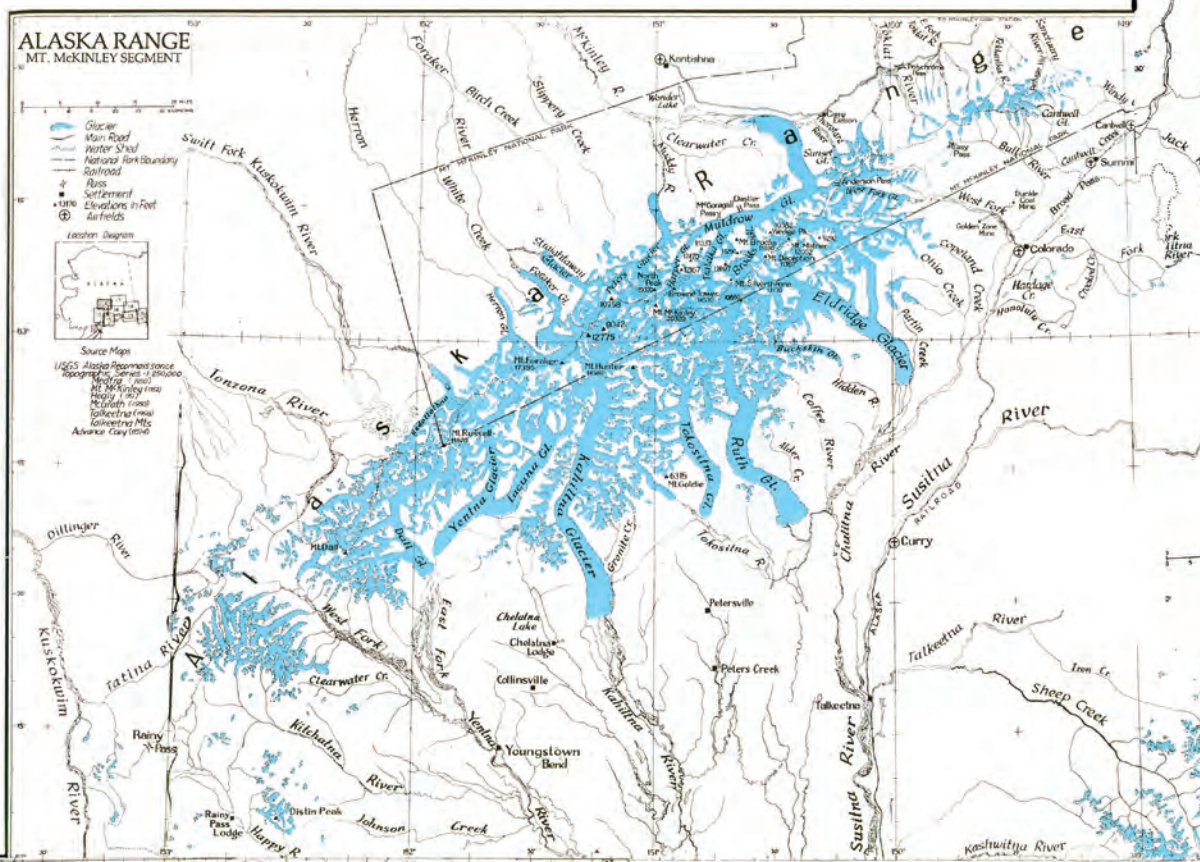
During the period of the Landsat baseline (1972–81), all available evidence suggests that the glaciers of the Talkeetna Mountains were thinning and retreating. These conclusions are based on a comparison of the size and number of glaciers shown on topographic maps made from data acquired between 1948 and 1952 with AHAP photography from the middle of the baseline period (1977) and just after the baseline interval (1983). When they were observed at the end of the 20th century, every glacier examined showed significant evidence of thinning and retreat, and many smaller glaciers had completely disappeared.

# Alaska Range

## Introduction

The heavily glacierized Alaska Range consists of a number of adjacent and discrete mountain ranges that extend in an arc more than 750 km long (figs. 1, 381). From east to west, named ranges include the Nutzotin, Mentasta, Amphitheater, Clearwater, Tokosha, Kichatna, Teocalli, Tordrillo, Terra Cotta, and Revelation Mountains. This arcuate mountain massif spans the area from the White River, just east of the Canadian Border, to Merrill Pass on the western side of Cook Inlet southwest of Anchorage. Many of the individual ranges support glaciers. The total glacier area of the Alaska Range is approximately 13,900 km<sup>2</sup> (Post and Meier, 1980, p. 45). Its several thousand glaciers range in size from tiny unnamed cirque glaciers with areas of less than 1 km<sup>2</sup> to very large valley glaciers with lengths up to 76 km (Denton

**Figure 381.**—Index map of the Alaska Range showing the glacierized areas. Index map modified from Field (1975a).

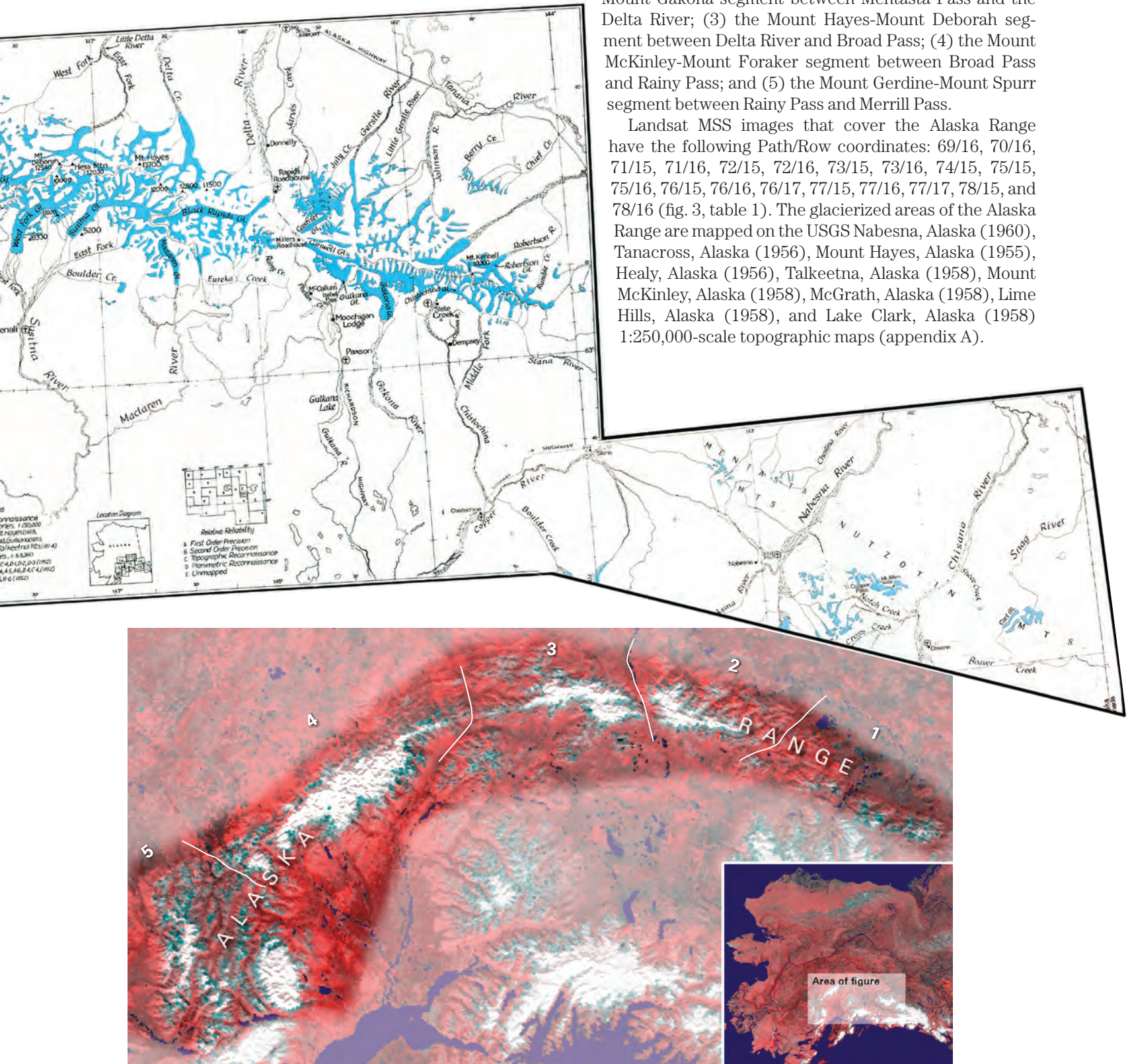


► **Figure 382.**—Enlargement of NOAA Advanced Very High Resolution Radiometer (AVHRR) image mosaic of the Alaska Range in summer 1995. National Oceanic and Atmospheric Administration image mosaic from Mike Fleming, Alaska Science Center, U.S. Geological Survey, Anchorage, Alaska. The numbers 1–5 indicate the segments of the Alaska Range discussed in the text.

and Field, 1975a, p. 575) and areas of greater than 500 km<sup>2</sup>. Alaska Range glaciers extend in elevation from above 6,000 m, near the summit of Mount McKinley, to slightly more than 100 m above sea level at Capps and Triumvirate Glaciers in the southwestern part of the range.

From east to west, the Alaska Range can be divided into five principal segments (fig. 382): (1) the Mentasta and Nutzotin Mountains segment between the Canadian border and Mentasta Pass; (2) the Mount Kimball-Mount Gakona segment between Mentasta Pass and the Delta River; (3) the Mount Hayes-Mount Deborah segment between Delta River and Broad Pass; (4) the Mount McKinley-Mount Foraker segment between Broad Pass and Rainy Pass; and (5) the Mount Gerdine-Mount Spurr segment between Rainy Pass and Merrill Pass.

Landsat MSS images that cover the Alaska Range have the following Path/Row coordinates: 69/16, 70/16, 71/15, 71/16, 72/15, 72/16, 73/15, 73/16, 74/15, 75/15, 75/16, 76/15, 76/16, 76/17, 77/15, 77/16, 77/17, 78/15, and 78/16 (fig. 3, table 1). The glacierized areas of the Alaska Range are mapped on the USGS Nabesna, Alaska (1960), Tanacross, Alaska (1956), Mount Hayes, Alaska (1955), Healy, Alaska (1956), Talkeetna, Alaska (1958), Mount McKinley, Alaska (1958), McGrath, Alaska (1958), Lime Hills, Alaska (1958), and Lake Clark, Alaska (1958) 1:250,000-scale topographic maps (appendix A).



## The Mentasta and Nutzotin Mountains Segment between the Canadian Border and Mentasta Pass

The Nutzotin Mountains extend for nearly 100 km from east of the Canadian border to the Nabesna River. Aside from several isolated glaciers, two areas support small concentrations of glaciers. Collectively, they contain as many as 100 small glaciers having a combined area of about 14.3 km<sup>2</sup> (Denton and Field, 1975a, p. 575). The first area, approximately 20 km west of the Canadian border, is located on the flanks of an unnamed ridge (fig. 383). Glaciers drain into Snag, Klein, Crescent, Baultoff, and Carl Creeks. Only one of the two largest glaciers is named (Carl Glacier, which is approximately 5 km long). When the area was photographed by the AHAP Program on 26 August 1981, all of its glacier termini, including the terminus of the large unnamed glacier that drains into Crescent Creek, showed multiple evidence of recent thinning and retreat.

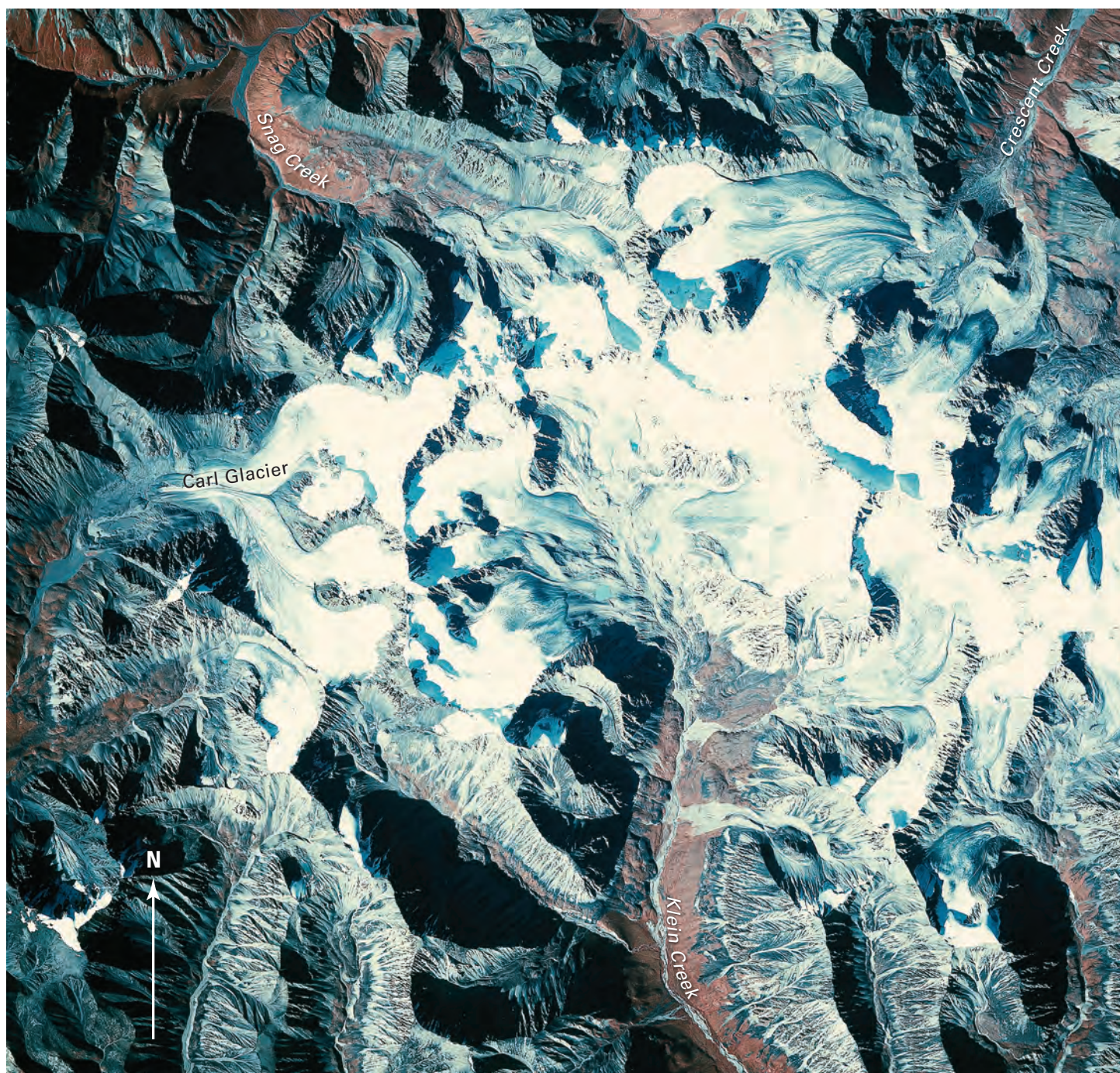




**Figure 384.**—Two oblique aerial photographs of unnamed peaks in the Nutzotin Mountains and valleys showing the presence of small glaciers, rock glaciers, or both on 30 August 2000. **A**, The northern (left) of two cirques, located between the Nabesna River and Pickerel Lake, hosts a small glacier in a valley mantled by rock-glacier debris. **B**, Located southeast of Alder Creek, this unnamed tributary to Stuver Creek has several rock-glacier lobes in its valley and either a small glacier or rock glacier at its head. Photographs by Bruce F. Molnia, U.S. Geological Survey. Larger versions of these figures are available online.



◀ **Figure 383.**—26 August 1981 AHAP false-color infrared vertical aerial photograph of the concentration of glaciers located southeast of Needle Peak in the eastern Nutzotin Mountains. All of the glacier termini, including the largest (Carl Glacier) and an unnamed glacier draining into Crescent Creek show multiple evidence of recent retreat and thinning, including elevated moraines, trimlines, abandoned moraines, and bare bedrock aprons. The unnamed glacier originates on the flank of an unnamed 2,606-m peak, the highest in the area. Four unnamed glaciers located in the upper reaches of Klein Creek appear to be the separated remnants of a single larger glacier that filled the head of Klein Creek within the last 100 years. Two other unnamed glaciers were also recently joined and probably were connected to the other Klein Creek glaciers during the “Little Ice Age.” AHAP photograph no. L99F4712 from the GeoData Center, Geophysical Institute, University of Alaska, Fairbanks, Alaska.

The second concentration of glaciers is located on the slopes of 2,591-m-high Mount Allen and on a west-trending ridge north of Cooper Pass and west of Chisana River. When the author observed the area from the air on 30 August 2000 (fig. 384), most cirques were ice free, whereas others supported small glaciers, rock glaciers, or both. Many of the glaciers of this area were observed at the beginning of the 20th century by Brooks (1900, 1906a, b, 1914), Moffit and Knopf (1909), and Capps (1910a, b) but have not received much attention since.

The Mentasta Mountains extend for more than 60 km from the Nabesna River to the Slana River. Because the elevations of the highest peaks are significantly lower than 3,000 m, the glaciers of this region all exist at relatively low elevations along a 30-km-long ridge. The largest concentration is located on the western flanks of a ridge between 2,511-m-high Noyes Mountain (see 24 August 1981 AHAP false-color infrared vertical aerial photograph no. L94F4128) and an unnamed 2,527 m-high-peak to its southeast. Approximately 5.5 km<sup>2</sup> of glacier ice exists in the western Mentasta Mountains (Denton and Field, 1975a, p. 575).

### **The Mount Kimball-Mount Gakona Segment between Mentasta Pass and the Delta River**

The 100×60-km Mount Kimball-Mount Gakona segment supports a glacier-covered area of approximately 1,036 km<sup>2</sup> (Denton and Field, 1975a, p. 578–581). Most of the glaciers in this area descend from an 85-km-long southeast-to-northwest interconnected unnamed ice field. This unnamed ice field—topped in the east by Mount Kimball (3,140 m), in the center by Mount Gakona (2,875 m), and on the west by Mount Silvertip (~2,980 m)—is as much as 55 km wide from glacier terminus to glacier terminus. About 20 outlet valley glaciers that head in this ice field have lengths of 6 km or more, and most are named. The largest—the 33-km-long Johnson Glacier—has an area of 183 km<sup>2</sup> (Denton and Field, 1975a, p. 580) and forms the headwaters of the Johnson River. In 1902, a topographic map of part of this area made by Mendenhall and Gerdin (Mendenhall, 1905) showed the location and size of several of the area’s larger south-flowing glaciers.

Outlet glaciers that drain the northern side of the unnamed ice field from east to west include (lengths and areas measured by Denton and Field, 1975a, p. 579–581, from USGS maps): (1) an unnamed glacier at the head of Rumble Creek (8 km, 18 km<sup>2</sup>), the easternmost outlet of the ice field (see 24 August 1981 AHAP false-color infrared vertical aerial photograph no. L88F3863); (2) Robertson Glacier (22 km, 85 km<sup>2</sup>), located at the head of Robertson

River; (3) Kimball Glacier, the western tributary of Robertson Glacier, which has a length of more than 10 km; (4) an unnamed glacier (24 km, 108 km<sup>2</sup>) that forms the headwaters of the West Fork of Robertson River; (5) another unnamed glacier (10 km, 18 km<sup>2</sup>) that forms the headwaters of an unnamed eastern tributary of the Johnson River; (6) Johnson Glacier; (7) Spur Glacier, so named because of the shape of its arcuate tributaries and straight terminus (12 km, 51 km<sup>2</sup>); (8) Gerstle Glacier (fig. 385) (24 km, 80 km<sup>2</sup>), which forms the headwaters of the Gerstle River; (9) an unnamed glacier at

**Figure 385.**—South-looking oblique aerial photograph of the icefall of the Gerstle Glacier at an elevation of approximately 1,600 m on 22 August 1960. Both sides of the glacier show several trimlines, suggesting that the glacier has experienced significant thinning. University of Washington photograph no. 6-42 taken by Austin Post, U.S. Geological Survey.



the head of July Creek (9 km, 25 km<sup>2</sup>), which drains from the northern side of Mount Silvertip (~2,980 m); and (10) *Jarvis Glacier* (9 km, 19 km<sup>2</sup>), the northwesternmost outlet glacier.

North of the unnamed ice field, a number of small unnamed glaciers drain in all directions from Mount Hajdukovich (2,698 m), located between Spur and Gerstle Glaciers, and from an unnamed isolated 2,383-m-high peak, located between the West Fork of the Robertson River and Johnson River. Riley Creek Glacier and several other small unnamed glaciers drain from an unnamed 2,520-m-high peak at the northwestern end of the ice field.

Outlet glaciers that drain the southern side of the unnamed ice field from east to west are (lengths and areas measured by Denton and Field, 1975a, p. 578–579, from USGS maps): (1) Tok Glacier, the easternmost outlet of the ice field, which forms the headwaters of the Tok River; (2) an unnamed glacier (9 km, 17 km<sup>2</sup>), the largest of three glaciers that drain into the Slana River; (3) two unnamed glaciers (10 km, 15 km<sup>2</sup>; 8 km, 9 km<sup>2</sup>), both contributing their meltwater to the Middle Fork of the Chistochina River; (4) another unnamed glacier (6 km, 13 km<sup>2</sup>), an eastern distributary of Chistochina Glacier; (5) Chistochina Glacier (13 km, 21 km<sup>2</sup>) (see 24 August 1981 AHAP false-color infrared vertical aerial photograph no. L88F3868); (6) an unnamed glacier (17 km, 52 km<sup>2</sup>) that forms the headwaters of the West Fork of the Chistochina River and was photographed by Moffit in 1910 (see USGS Photo Library photograph Moffit 418); (7) Gakona Glacier (32 km, 112 km<sup>2</sup>), the largest south-flowing outlet glacier of the unnamed ice field; (8) Gulkana Glacier (10 km, 21 km<sup>2</sup>), a glacier with a long history of 20th century scientific investigations (figs. 386, 387A); (9) West Gulkana Glacier, mapped during the IGY (AGS, 1960) and again in the late 1980s (figs. 386, 387A); (10) Canwell Glacier (24 km, 89 km<sup>2</sup>); (11) Fels Glacier, mislabeled as Eel Glacier on the Mount Hayes, Alaska (1955), 1:250,000-scale (appendix A) and the

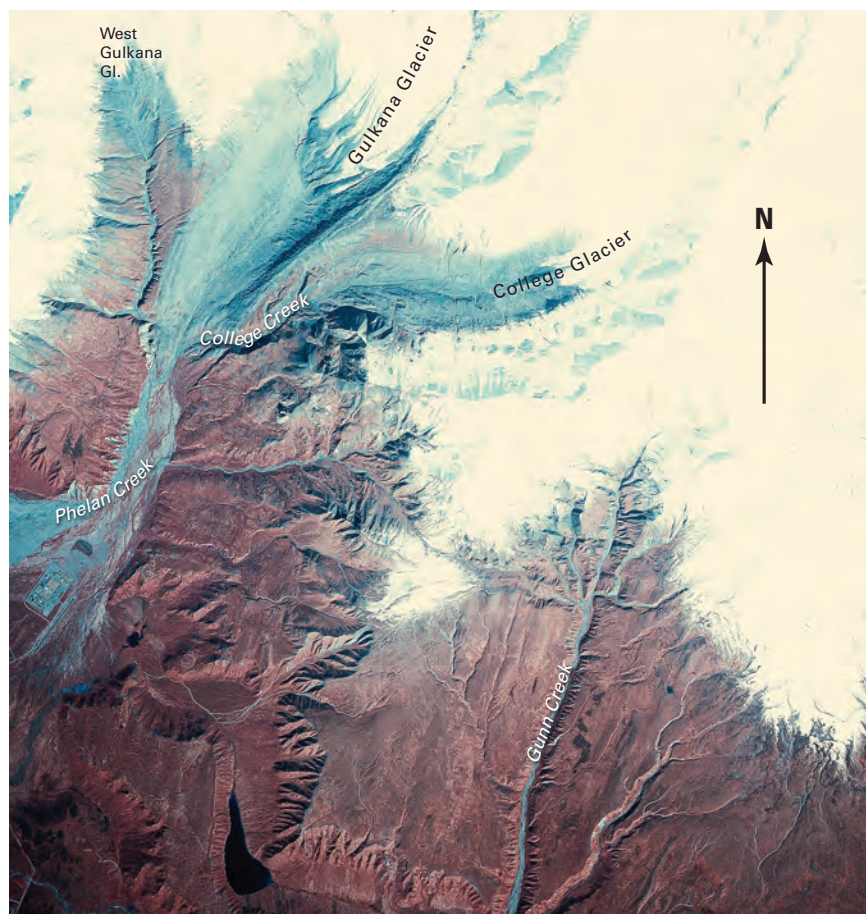


**Figure 386.**—24 August 1981 AHAP false-color infrared vertical aerial photograph of the termini of Gulkana, West Gulkana, and College Glaciers. All three glaciers show evidence of ongoing recession and thinning. AHAP photograph no. L88F3873 from the GeoData Center, Geophysical Institute, University of Alaska, Fairbanks, Alaska.

Mount Hayes B-4, Alaska (1955), 1:63,000-scale (appendix B) USGS topographic maps (15 km, 22 km<sup>2</sup>); and (12) Castner Glacier (20 km, 79 km<sup>2</sup>). The last three are west-flowing glaciers that drain into the Delta River.

Studies of Canwell and Castner Glaciers by Péwé (1957) found that both glaciers had advanced about 1.5 km during the early part of the “Little Ice Age” and that Canwell Glacier experienced a second smaller advance within the past 200 years. Canwell’s advance was then followed by a retreat of nearly 2 km. During the first half of the 20th century, between 1902 and 1941, Canwell Glacier advanced again, a distance of approximately 1.5 km. Since then, its terminus has stagnated, thinned, and retreated.

### Gulkana Glacier

The post-Pleistocene history of Gulkana Glacier has been described by a number of researchers. Calkin (1988) reported that the glacier occupied its Holocene maximum position about 5,700 yr B.P. at a location about 2.5 km forward of the 1962 ice margin. Péwé and Reger (1983) reported that cycles of retreat and advance followed; the glacier readvanced about 4,700 yr B.P., again at about 4,030 yr B.P., and again at about 800 yr B.P. Calkin (1988) used lichenometry to determine that Gulkana Glacier advanced about 560 yr B.P. and again at about 390 yr B.P. He stated that “historic evidence and lichen

**Figure 387.**—Four photographs showing changes in Gulkana Glacier during the 20th century. **A**, North-looking oblique aerial photograph of the terminus of Gulkana Glacier and parts of the termini of West Gulkana (west) and College (east) Glaciers on 31 August 1967. The trimlines along the Gulkana Glacier and in the former terminus region confirm that the glacier has experienced more than 4 km of retreat since photographed in July 1910 by F.H. Moffit (Photograph Moffit 427 from the USGS Photo Library, Denver, Colo.). Photograph 67-R4-87 by Austin Post, U.S. Geological Survey. **B–D**, see following pages.





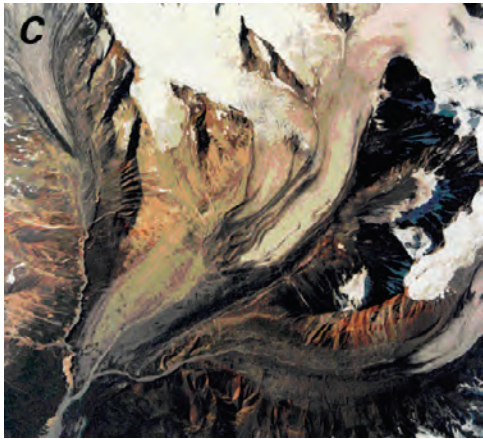
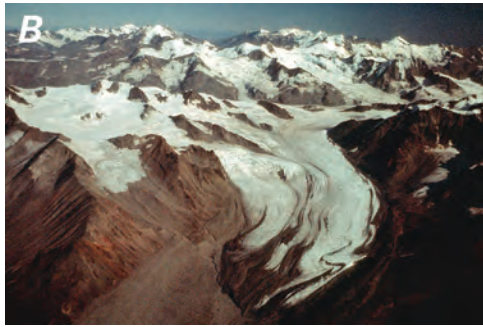


**Figure 387.**—**B**, Oblique color aerial photograph of the terminus of Gulkana Glacier around 1975. The terminus has retreated about 30 m from its 1967 position. Undated photograph by Dennis C. Trabant, U.S. Geological Survey. **C**, Color vertical aerial photograph of the retreating termini of Gulkana and West Gulkana Glaciers on 11 July 1993. Since 1967, Gulkana Glacier has retreated more than 100 m. Photograph 1 No. 4 by AeroMap US, Inc. **D**, see following page. Larger versions of B and C are available online.

data substantiate” an advance of the glacier after A.D. 1875. Mercer (1961a) determined that the rise in the firm limit of Gulkana Glacier may have been as much as 380 m since the “Little Ice Age” maxima.

Gulkana Glacier was photographed by Moffit on 15 July 1910 (see USGS Photographic Library photographs Moffit 423, 424, 427) and by Péwé on 12 July 1952. In the 42 years between photographs, the terminus of Gulkana Glacier retreated more than 4 km. Two oblique aerial photographs were acquired on 31 August 1967 (fig. 387A) and in 1975(?) (fig. 387B). General thinning occurred until 1976, but the glacier gained mass from 1976 to the early 1980s, and recession probably stopped (Mayo and Trabant, 1986). More recently, a comparison of a 1957 map of the glacier with data obtained during a geodetic airborne laser altimeter profiling survey carried out on 12 June 1993 allowed Echelmeyer and others (1996) to determine that Gulkana Glacier had retreated by about 1.75 km during the 36 years between data sets (an average annual retreat rate of  $48.6 \text{ m a}^{-1}$ ) and that the glacier’s area had decreased from  $18.5 \text{ km}^2$  in 1957 to  $17.0 \text{ km}^2$  in 1993 (a decrease of approximately 8 percent). The glacier also thinned an average of 10.9 m, and its volume decreased by  $1.94 \times 10^8 \text{ m}^3$ . Between the 1950s and middle 1990s, on an annual basis, Gulkana Glacier thinned by  $0.434 \text{ m a}^{-1}$  and had a volume decrease of  $0.00822 \text{ km}^3 \text{ a}^{-1}$ ; between the middle 1990s and 1999, on an annual basis, Gulkana Glacier thinned by  $0.748 \text{ m a}^{-1}$  and had a volume decrease of  $0.0136 \text{ km}^3 \text{ a}^{-1}$  (K.A. Echelmeyer, W.D. Harrison, V.B. Valentine, and S.I. Zirnheld, University of Alaska Fairbanks, written commun., March 2001). Figure 387C is a vertical aerial photograph acquired on 11 July 1993, one month after the geodetic airborne laser altimeter profiling survey. Figure 387A–D presents a photographic summary of changes in Gulkana Glacier during the 20th century.

Ostenso and others (1965) determined the configuration of the valley in which Gulkana Glacier flows by a gravimetric survey acquired by traverses across the glacier’s surface. They determined that the subglacier valley of Gulkana Glacier consists of two parallel bedrock channels separated by a medial ridge. Ice in the eastern channel was about 225 m thick, whereas ice in the shallower western valley was only about 125 m thick. A recent study combining SAR and 50-MHz monostatic short-pulse radar data (Moran and others, 2000) determined that Gulkana Glacier’s ice thickness in the upper 2 km of the eastern channel, above the juncture with the western tributary, was no thicker than 140 m and that the glacier’s bed was steeply dipping, both parallel and transverse to the direction of ice flow. Because the locations of the gravity and radar surveys were not identical, no absolute change in thickness can be determined between the two. However, the maximum ice thickness measured by the radar survey is a third thinner than that measured by the earlier gravimetric survey.

In the early 1960s, the University of Alaska and the USGS began studies at Gulkana Glacier focused on characterizing its geophysical and glaciological parameters, including foliation patterns, structure, flow patterns, and ablation (Mayo and Péwé, 1963; Tangborn and others, 1977). Kennedy and others (1997) analyzed air temperature and precipitation data recorded at Gulkana Glacier basin between October 1967 and September 1996. The data set is important because it provides long-term climate information from the highest year-round climatological recording site in Alaska. Annual data summaries were calculated for each hydrologic year, from 1 October through 30 September, for years that have 12 months of data. Monthly precipitation-catch and average air temperature summaries were calculated for months with nine or fewer daily records missing. The average annual air temperature recorded at the site from hydrologic years 1968 through 1996 was  $-4.1^\circ\text{C}$ . The coldest recorded year was 1972, which had an average annual temperature of  $-6.7^\circ\text{C}$ . The warmest year was 1981, which had an average annual temperature of  $+2.6^\circ\text{C}$ . The coldest month was January 1971, which had an



average temperature of  $-20.8^{\circ}\text{C}$ . The warmest month was July 1989, which had an average temperature of  $+8.7^{\circ}\text{C}$ . The coldest day was 17 January 1971, which had an average temperature of  $-35.0^{\circ}\text{C}$ . The warmest day was 15 June 1969, which had an average temperature of  $+16.4^{\circ}\text{C}$ .

The average annual precipitation gage catch recorded at the site from hydrologic years 1968 through 1992 was 1.02 m. The highest annual precipitation gage catch recorded was 1.572 m in 1981; the lowest was 0.555 m in 1969. The highest recorded monthly precipitation catch was 0.448 m in July 1981. In several different months, no precipitation was recorded. The highest daily precipitation gage catch was 9.9 cm on 12 September 1972. On

**Figure 387.—D,** Black-and-white 1:24,000-scale vertical aerial photograph of the retreating terminus of Gulkana Glacier on 18 August 1999. The response to changing climate has caused Gulkana Glacier to retreat more than 40 m and to thin by more than 5 m since the 1993 photograph. Photograph from U.S. Bureau of Land Management, roll 3, frame 333.

many different dates, no precipitation was recorded. Because of low precipitation gage-catch efficiency, the reported annual precipitation gage-catch data are estimated to represent about 62 percent of the actual annual basin precipitation. Snowfall is the dominant form of precipitation on the glacier from September through mid-June. In 1976, glacier ice thickness from a single site near the highest measurement site was 180 m; two glacier cross profiles near midglacier indicated that the thickness was 270 m on the centerline; glacier ice was determined to be 150 m thick on the centerline at a downglacier measurement site.

The 1992 measured winter-snow, maximum winter-snow, net, and annual balances in the Gulkana Glacier basin were evaluated by March and Trabant (1996). Averaged over the glacier, the measured winter-snow balance was 0.97 m on 26 March 1992; the maximum winter-snow balance was 1.05 m on 19 May 1992; the net balance (from 8 September 1991 to 17 August 1992) was -0.29 m; and the annual balance (1 October 1991 to 30 September 1992) was -0.38 m. Annual stream runoff was 1.24 m averaged over the basin.

For 1993, March and Trabant (1997) found that the 1993 measured winter-snow balance was 0.81 m on 31 March 1993, 1.2 standard deviations below the long-term average; the maximum winter-snow balance, 0.84 m, was recorded on 10 May and 11 May 1993; the net balance (from 18 August 1992 to 8 September 1993) was -1.80 m, the most negative balance year on record at 2.8 standard deviations below the long-term average. The annual balance (1 October 1992 to 30 September 1993) was -1.64 m. Annual stream runoff was 1.996 m averaged over the basin, 0.2 standard deviations above the long-term average.

For 1994, March (1998) found that the measured winter-snow balance was 1.34 m on 29 April 1994, 0.9 standard deviation above the long-term average; the maximum winter-snow balance, 1.43 m, was recorded on 18 April 1994; the net balance (from 8 September 1993 to 17 September 1994) was -0.72 m, 0.7 standard deviation below the long-term average. The annual balance (1 October 1992, to 30 September 1993) was -0.88 m. Annual stream runoff was 1.93 m averaged over the basin.

For 1995, March (2000) found that the measured winter-snow balance was 0.94 m on 19 April 1995, 0.6 standard deviation below the long-term average; the maximum winter-snow balance, 0.94 m, was recorded on 25 April 1995; the net balance (from 18 September 1994 to 29 August 1995) was -0.70 m, 0.76 standard deviation below the long-term average. The annual balance (1 October 1994, to 30 September 1995) was -0.86 m. Annual stream runoff was 2.05 m averaged over the basin, approximately equal to the long-term average.

During the four-year period from 1992 through 1995, Gulkana Glacier's average measured winter-snow balance was +1.015 meters; its average maximum winter-snow balance was +1.0625 m; its average net balance was -0.88 m; and its average annual balance was -0.94 m. Average annual stream runoff was 1.804 m averaged over the basin. Retreat was continuing at the end of the 20th century, as shown on an 18 August 1999 vertical aerial photograph (fig. 387D).

### **West Gulkana Glacier**

West Gulkana Glacier, a small valley glacier approximately 4 km long was mapped in 1957 (AGS, 1960) (figs. 386, 387A). Austin Post, who was a leader of the IGY team that mapped the glacier, reported it to be "virtually stagnant" and receding; almost no snow remained from the previous winter. The IGY map of West Gulkana Glacier shows a retreating glacier with a significant trimline on its eastern side (AGS, 1960). In 1987, a team from Arizona State University and the U. S. Military Academy at West Point, led by Melvin Marcus and L.S. Thompson remapped the glacier (Thompson and Smith, 1988).

A comparison of the two maps shows that the glacier retreated about 520 m and thinned and narrowed in the 30 years between maps.

West Gulkana Glacier was resurveyed in 1993 by a geodetic airborne laser altimeter profiler (Sapiano and others, 1998). Interpretation of a single profile acquired on 12 June 1993, field observations made in 1995, and a 1957 map showed that the terminus of West Gulkana Glacier had retreated by approximately 480 m during the 38 years between surveys, an average annual retreat rate of 12.6 m a<sup>-1</sup>, and that the glacier's area had decreased from 4.2 km<sup>2</sup> in 1957 to 3.59 km<sup>2</sup> in 1993, a decrease of around 15 percent. During the 38 years of observation, the glacier thinned an average of 24 m, its volume decreased by 9.3×10<sup>7</sup> m<sup>3</sup>, and its average annual mass balance was -0.61 m. Retreat was continuing at the end of the 20th century (fig. 387C) (see 18 August 1999 BLM vertical aerial photograph—Roll 3, Frame 323).

### **Jarvis Glacier**

In 1955, Ostenso and Holmes (1962) used gravimetric techniques to study *Jarvis Glacier*. They found that it lies in a deep U-shaped valley with a cirque at its head. The cirque, which has a sill at its downglacier end, had ice thicknesses of as much as 321 m.

## **The Mount Hayes-Mount Deborah Segment between Delta River and Broad Pass**

The 160-km-long Mount Hayes section, which includes Mount Hayes (4,216 m), Mount Moffit (3,957 m), and Mount Deborah (3,750 m), has a glacier-covered area of about 1,900 km<sup>2</sup> (Denton and Field, 1975a, p. 583–586). Most glaciers originate from an ice-covered interconnected upland accumulation area, an unnamed ice field that has a maximum width of more than 60 km. A number of isolated, generally small glaciers descend from individual peaks and ridges to the south, including several shown on the USGS Mount Hayes, Alaska (1955), 1:250,000-scale topographic map (appendix A) of the northern side of the Amphitheater Mountains named by Troy Péwé for the numerous cirques that are present (see 24 August 1981 AHAP false-color infrared vertical aerial photograph no. L88F3880). Most of the glaciers in this area are named and more than 15 glaciers have lengths of more than 7 km. According to Denton and Field (1975a, p. 583–586), who measured the following lengths and areas of glaciers, the longest are Black Rapids Glacier (fig. 388) (40 km, 341 km<sup>2</sup>), West Fork Glacier (41 km, 311 km<sup>2</sup>), and Susitna Glacier (36 km, 323 km<sup>2</sup>). There are many surging glaciers in this section. The surge dynamics of glaciers in the Susitna River Basin were summarized by Clarke (1991).

Beginning on the northern side of the unnamed ice field (counter-clockwise, from east to west, starting west of Black Rapids Glacier) glaciers (lengths and areas measured by Denton and Field, 1975a, p. 583–586) include (1) two unnamed glaciers draining into the Delta River, the western one with a length of 10 km and an area of 13 km<sup>2</sup>; (2) McGinnis Glacier (13 km, 33 km<sup>2</sup>); (3) Trident Glacier (28 km, 222 km<sup>2</sup>); (4) Hayes Glacier; (5) an unnamed glacier (7 km, 8 km<sup>2</sup>), which descends from Mount Giddings and Mount Skarland; (6) Gillam Glacier (25 km, 144 km<sup>2</sup>); (7) an unnamed glacier west of Gillam Glacier (8 km, 12 km<sup>2</sup>); (8) an unnamed glacier draining into the Wood River; (9) Yanert Glacier (35 km, 183 km<sup>2</sup>), which advanced about 5 km in a 1942 surge, stagnated for more than 57 years, and surged again in 2000 and 2001; (10) an unnamed glacier (8 km, 12 km<sup>2</sup>), which descends from the western flank of Nenana Mountain; (11) Nenana Glacier, (16 km, 29 km<sup>2</sup>); (12) West Fork Glacier (41 km, 311 km<sup>2</sup>); (13) Susitna Glacier (fig. 389) (36 km, 323 km<sup>2</sup>), which surged about 5 km in 1952 or 1953; (14) an unnamed glacier draining into the East Fork Susitna River (fig. 390) (17 km, 46 km<sup>2</sup>), which has thinned more than 50 m and retreated several kilometers since being mapped in the 1950s; (15) Maclaren Glacier (17 km, 68 km<sup>2</sup>); (16) Eureka Glacier, which is around 10 km long (estimated

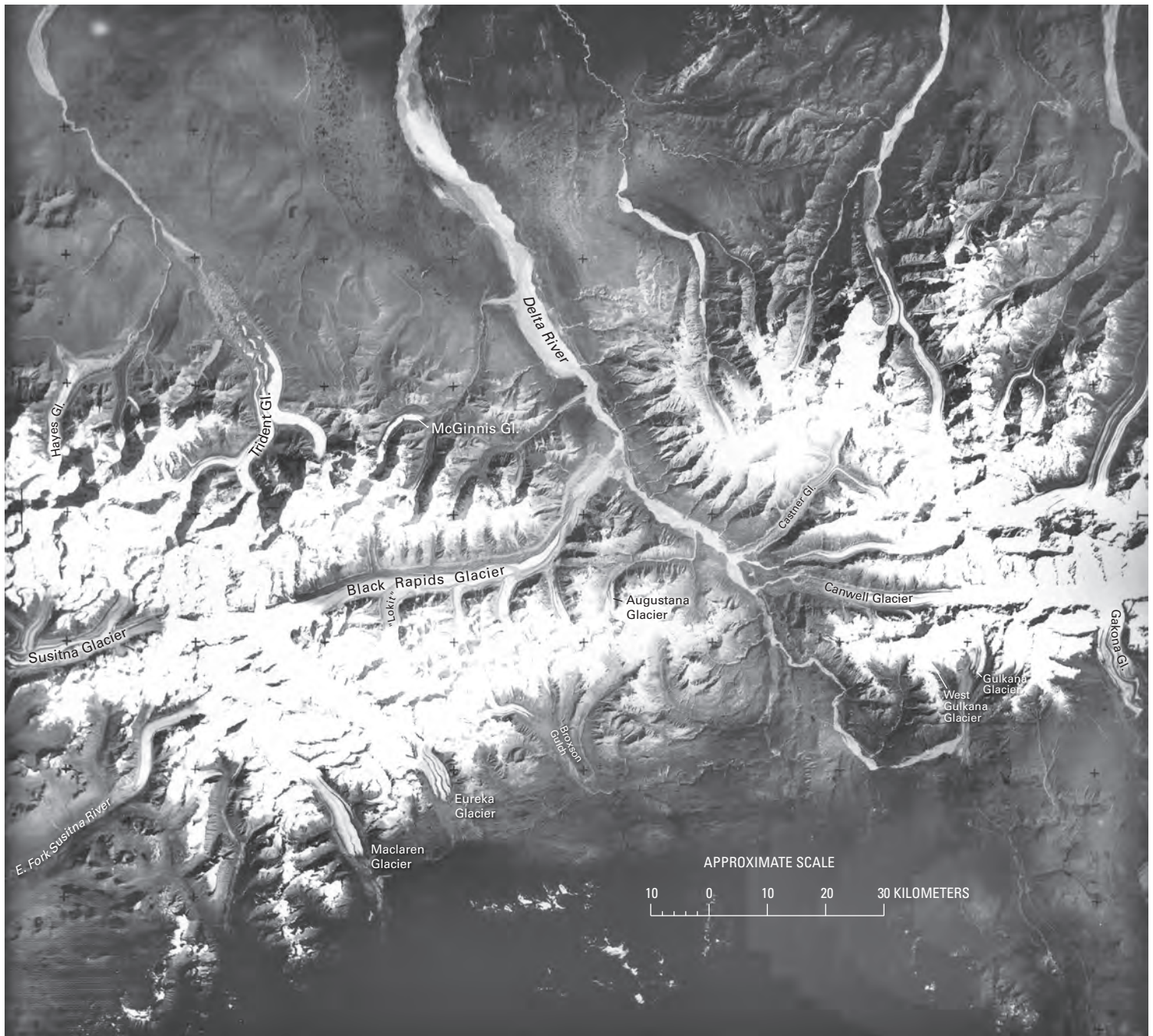


**Figure 388.**—Annotated Landsat 3 return beam vidicon (RBV) image of Black Rapids Glacier, Susitna Glacier, Gulkana Glacier, West Gulkana Glacier, Canwell Glacier, Castner Glacier, and other glaciers in the Alaska Range. The Black Rapids Glacier has been long known to have unusual flow characteristics. During a surge in the winter of 1936–1937, the terminus advanced 4.8 km in about 3 months (Post, 1960). There are two indications of the cyclic nature of surges visible on this RBV image. The large tributary glacier, informally known as “Lokit,” entering from the south near the mid-point of the Black Rapids Glacier is forcing a medial moraine across the main glacier; two other similar moraine loops from the same tributary are displaced about 8 and 16 km downglacier. These displacements occurred during 1936–1937 and an earlier surge. Also, the terminal moraine that formed in 1936–1937 is clearly visible about 2 km from the Delta River; a terminal moraine, an additional 2 km downvalley, was from a previous surge, which probably temporarily blocked the Delta River. The medial moraine patterns

can also be used as an indicator of how the surge cycle is progressing; in 1981, the “Lokit” moraine loop was pushed nearly as far across the Black Rapids Glacier as the 1936–1937 “Lokit” loop had been at the time of that surge. This evidence suggests that the surge cycle was near completion; however, through 2004, no new major surge had begun. It is unlikely that a near-future surge of the Black Rapids Glacier would disrupt the Trans-Alaska Pipeline or Richardson Highway, both of which follow the Delta River. There are many other surging glaciers in this area (notably the Susitna and Gakona Glaciers). Mass balance has been measured at the Gulkana Glacier since 1965. There is evidence of more extensive past glaciation in the form of a moraine area covered with small lakes extending far to the north. It is not known if this larger glacier complex was affected by surges. Landsat 3 RBV image (31273–20304–D; 8 August 1981; Path 71, Row 15) from the USGS, EROS Data Center, Sioux Falls, S. Dak. Landsat image and caption courtesy of Robert M. Krimmel, U.S. Geological Survey.

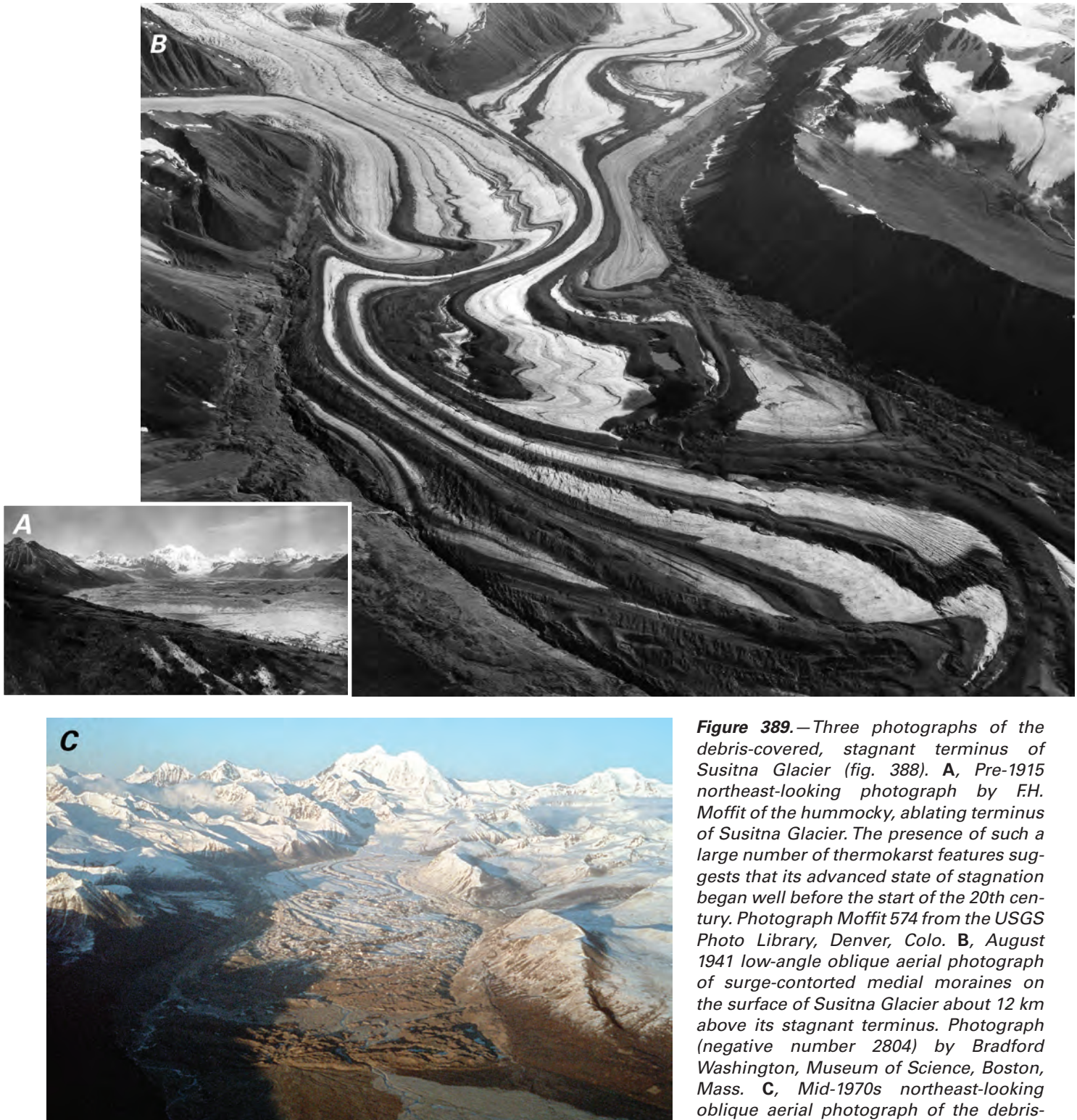


**Figure 389.**—Three photographs of the debris-covered, stagnant terminus of Susitna Glacier (fig. 388). **A**, Pre-1915 northeast-looking photograph by F.H. Moffit of the hummocky, ablating terminus of Susitna Glacier. The presence of such a large number of thermokarst features suggests that its advanced state of stagnation began well before the start of the 20th century. Photograph Moffit 574 from the USGS Photo Library, Denver, Colo. **B**, August 1941 low-angle oblique aerial photograph of surge-contorted medial moraines on the surface of Susitna Glacier about 12 km above its stagnant terminus. Photograph (negative number 2804) by Bradford Washington, Museum of Science, Boston, Mass. **C**, Mid-1970s northeast-looking oblique aerial photograph of the debris-covered, stagnant terminus of Susitna Glacier. Folded loop moraines from a 1950s surge can be seen several kilometers above the terminus. The snow cover enhances the features. Mount Hayes is in the background. Photograph by Dennis C. Trabant, U.S. Geological Survey. A larger version of A is available online.

**Figure 390.**—14 September 1999 east-looking oblique aerial photograph of the terminus of an unnamed glacier that drains to the East Fork of the Susitna River. The western end of the lake corresponds to the 1955 position of the terminus. The large trimline suggests that the glacier has recently thinned significantly more than 50 m and retreated more than 2 km. Photograph by Bruce F. Molnia, U.S. Geological Survey.



**Figure 391.**—North-looking oblique aerial photograph of the terminus area of an unnamed rock glacier on the south side of Nenana Mountain on 14 September 1999. The rock glacier, which is more than 4 km long, heads in a cirque. Photograph by Bruce F. Molnia, U.S. Geological Survey. A larger version of this figure is available online.

by the author); (17) an unnamed glacier approximately 8 km long (estimated by the author) draining into Broxson Gulch; (18) Augustana Glacier, which is about 6 km long (estimated by the author); and (19) Black Rapids Glacier (fig. 388) (40 km, 341 km<sup>2</sup>).

Rock glaciers exist on many mountains, including Nenana Mountain (fig. 391). Some occur at the mouths of valleys that were glacier filled during the “Little Ice Age,” whereas others are isolated bodies on the flanks of mountains and ridges.

As are the majority of glaciers in the Alaska Range, the glaciers in this area are stagnant, thinning, and (or) retreating. Aside from an occasional surge-produced thickening or advance, no glaciers below 2,000 m were observed to be either thickening or advancing. No late 20th or early 21st century surge events have resulted in terminus displacements.

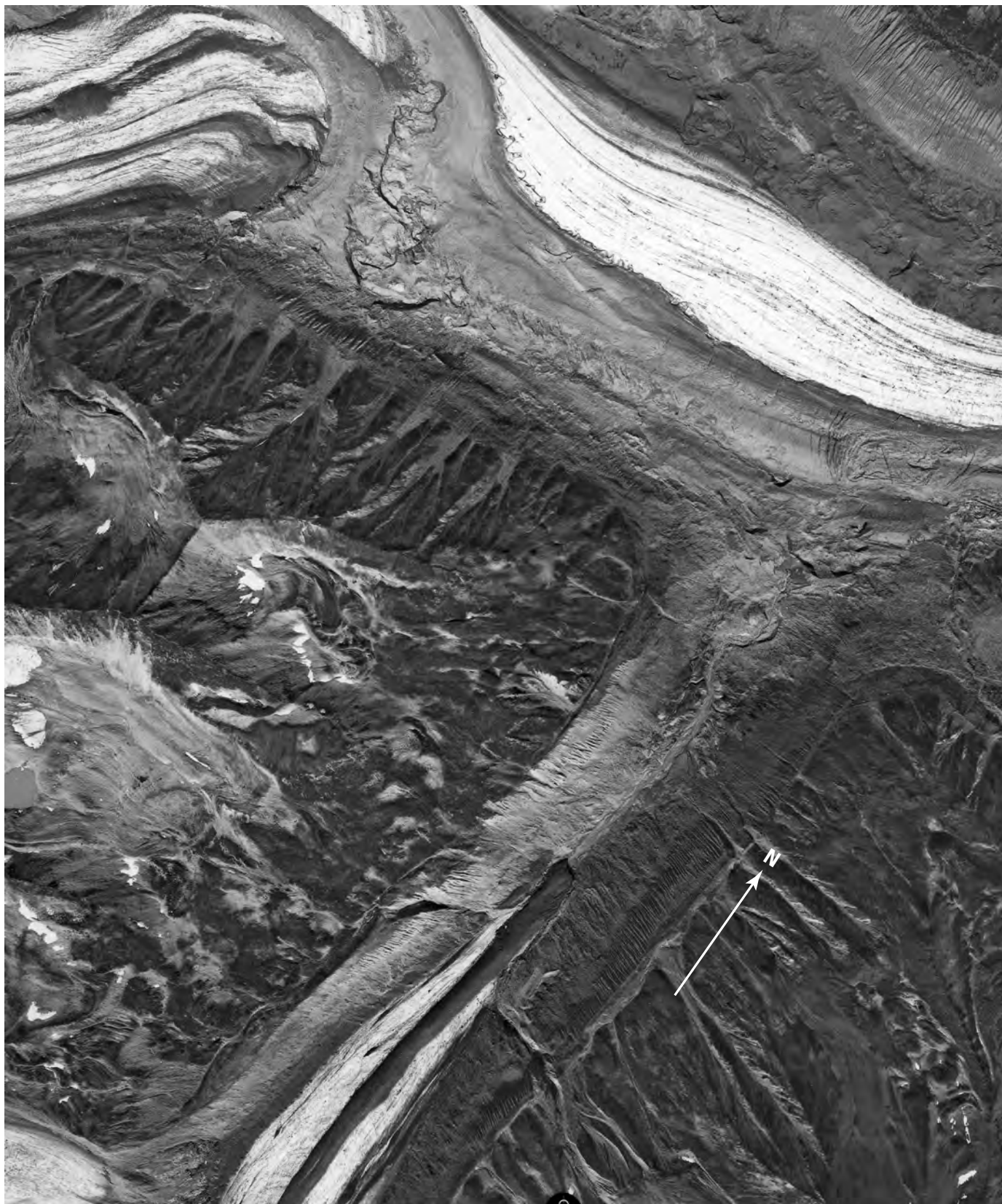
### **Black Rapids Glacier**

Between 1912 and 1936, Black Rapids Glacier retreated about 5 km. In 1936, the stagnation and retreat of Black Rapids Glacier were interrupted by a catastrophic surge that began in September or October (Moffit, 1942) and was the first to receive attention from the popular media. The 1 March 1937 issue of *Time Magazine* described the surge: “The Black Rapids Glacier, long dying in its valley 125 miles south of Fairbanks, has come to life. Its mile-and-a-quarter face was shoving toward the Delta River and the Richardson Highway (sole motor road from Fairbanks to the coast), rearing ice crests to 500 ft., breaking off great land icebergs which tumbled thunderously ahead onto the mossy valley floor” (*Time Magazine*, 1937). O.W. Geist, a geologist at the then Alaska Territorial School of Mines (now the University of Alaska Fairbanks), observed the surge and reported that “The glacier is bifurcated. One fork is moving into the other, grinding and crunching at a point five miles back. The intersection is the scene of a giant upheaval.... Three days ago we could walk to the face of the glacier. Now so much water is flowing that we could not walk to the front” (*Time Magazine*, 1937).

During a three-month period during the winter of 1936–37, Black Rapids Glacier advanced 4.8 km (Post, 1960). By February 1937, the glacier had reached a position that threatened the Richardson Highway adjacent to the Delta River. This location, fortunately, was close to the point of maximum advance. Retreat and downwasting began in the summer of 1937 and continues to the present. During the period of maximum surge, Black Rapids Glacier advanced as much as 30 to 65 m d<sup>-1</sup>. Since then, the glacier has been stagnant, has become thinner, and has had several of its tributaries undergo

significant retreat, as an 18 August 1999 vertical aerial photograph shows (fig. 392). As a result of the surge, the media nicknamed Black Rapids Glacier “Galloping Glacier” and “Runaway Glacier.”

Since 1971, the USGS and the University of Alaska Fairbanks (Heinrichs and others, 1995, 1996) have measured systematic mass balances,





equilibrium line elevations (ELA), surface elevations, ice thicknesses, near-surface temperatures, and ice velocities. Heinrichs and others (1995) summarized the behavior of Black Rapids Glacier during a quiescent period from 1970 to 1992. Typically, they made semi-annual measurements of surface velocity, surface elevation, and mass balance at 10 sites along the centerline of the glacier. Their measurements show “synchronous interannual fluctuations” with a variability of about 20 percent and a period of 4 to 9 years. A winter-summer oscillation of about the same magnitude also exists. They also found large seasonal changes in surface speed of as much as 400 percent, caused primarily by changes in basal motion. During May through July 1993, the velocity of several surface markers along the glacier was measured twice daily; seismic-reflection measurements of the bed and ice-radar measurements were made daily. A subglacier stream originating at the terminus was monitored continually throughout the summer to investigate the glacier’s basal hydrology. Measurements included stage, dye tracing, electrical conductivity, and turbidity. Acquiring the data simultaneously permitted direct measurement of changes at the bed that were correlated with changes in the velocity on the glacier’s surface. Subglacier draining of several ice marginal lakes produced large increases in surface speed.

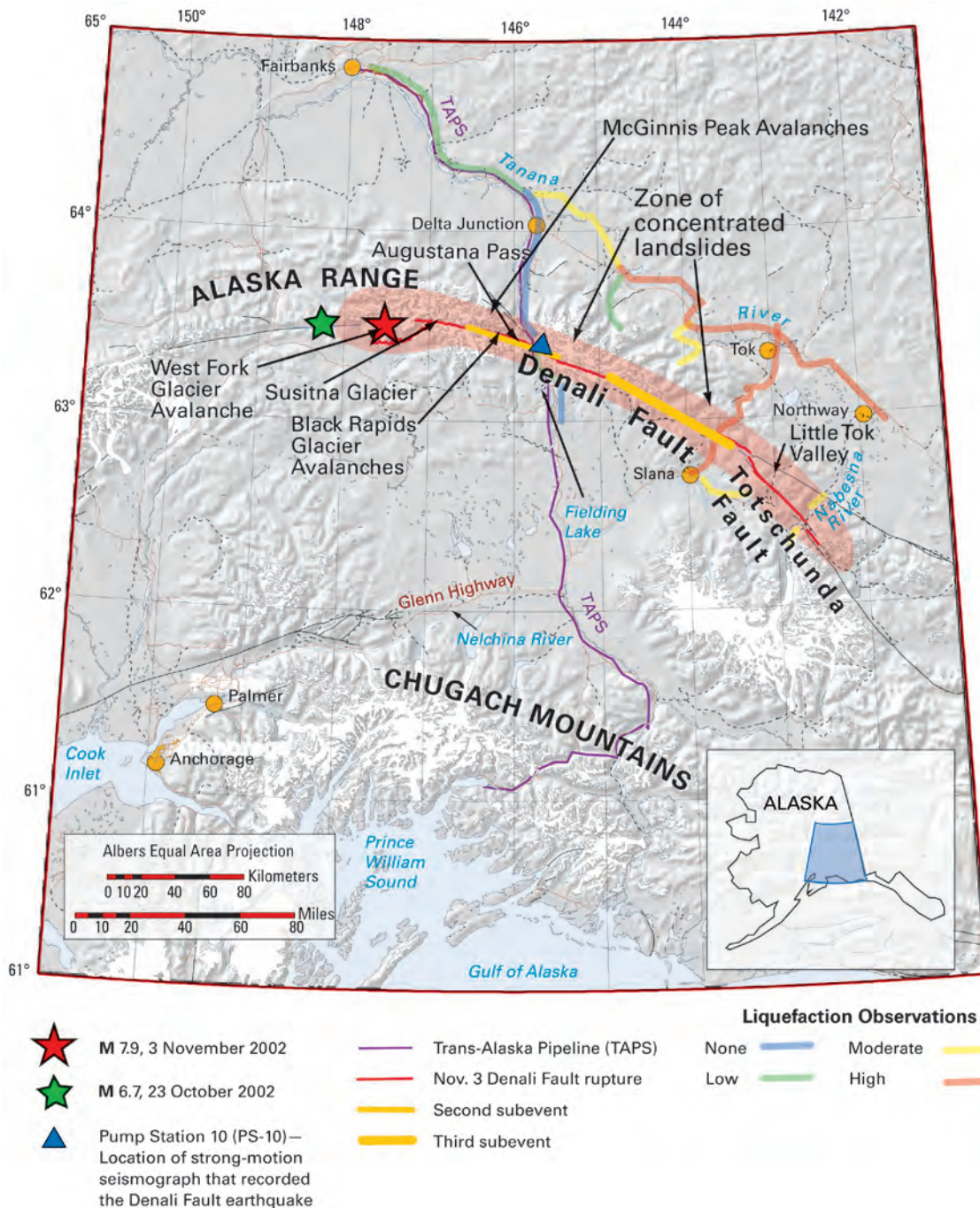
Raybus and Fatland (2000) compared SAR-interferometric techniques with conventional surface-velocity measurements to test whether the interferometric data are “quantitatively consistent with terrestrial velocity measurements.” (p. 119). They compared velocities derived from two ERS-1 SAR images collected on 22 and 25 January 1992 with surface measurements made in 1987, 1990, and 1996 and concluded that the “interferometric and terrestrial datasets are mutually consistent.” (Raybus and Fatland, 2000, p. 127).

Between the 1950s and the middle 1990s, on an annual basis, Black Rapids Glacier thickened by  $0.343 \text{ m a}^{-1}$ , and its volume increased by  $0.099 \text{ km}^3 \text{ a}^{-1}$ . Much of this increase was in the form of replenishment in the accumulation area of the ice mass displaced during the 1936–37 surge. Between the middle 1990s and 1999, on an annual basis, Black Rapids Glacier thinned by  $0.655 \text{ m a}^{-1}$ , and its volume decreased by  $0.189 \text{ km}^3 \text{ a}^{-1}$  (K.A. Echelmeyer, W.D. Harrison, V.B. Valentine, and S.I. Zirnheld, University of Alaska Fairbanks, written commun., March 2001).

### **Rock Avalanches onto Glaciers Resulting from the 3 November 2002 Earthquake ( $M$ 7.9) on the Denali Fault**

A large-magnitude ( $M$  7.9) earthquake on 3 November 2002 generated three large surface ruptures, which had a cumulative length of approximately 320 km. The largest was a 225-km-long rupture of the Denali Fault (fig. 393), which had a maximum right-lateral slip displacement of almost 9 m (Harp and others, 2003). The earthquake epicenter was located near an icefall in a tributary of West Fork Glacier. The westernmost surface rupture (first subevent of  $M$  7.2) was a thrust fault that offset the surface of Susitna Glacier (fig. 389). Truffer and others (2002) presented a summary of the impact of the earthquake on glaciers within the Alaska Range. They reported that glaciers are located in many valleys aligned with the Denali Fault; consequently, more than 40 percent of the surface rupture resulting from the event can be seen on glaciers. Surface rupture was observed not only on Susitna Glacier but also on Black Rapids, Canwell, Gakona, and Chistochina Glaciers (fig. 388). In addition, offset glacier ice was observed near the terminus of West Fork Glacier where Susitna Glacier fault intersects it. Truffer and others (2002) reported that offsets in glacier ice have variable morphologies. Almost all seracs in the icefall toppled during the quake. The Denali Fault laterally offset preexisting crevasses on the northern side of Canwell Glacier, and vertical offset was observed at many localities. At some locations, one or more long linear cracks appeared along the glacier surface, often following medial moraines. Truffer and others (2002) suggested that

◀ **Figure 392.** — 18 August 1999 black-and-white 1:24,000-scale vertical aerial photograph of the part of Black Rapids Glacier west of its terminus. The tributary entering from the south has retreated more than 2 km in the 44 years since it was mapped. The small unnamed glaciers have either completely disappeared or have retreated and lost contact with their main trunks. Photograph from U.S. Bureau of Land Management, roll 3, frame 322.



moraines represent areas of weakness. The Susitna Glacier fault appears to make a sharp turn to the west where it follows a looped moraine across the glacier. At some locations along the Denali Fault, cracks in the ice are oriented perpendicular to the fault trace. Their observations suggest that careful examination of glacier morphology must be considered when delineating the trace of a fault across a glacier.

The earthquake also produced thousands of rock avalanches, many of which covered parts of glaciers in the Alaska Range. Most of the rock avalanches were located in a zone approximately 30 km wide that straddled fault-rupture zones along the Totschunda and Denali Faults. McGinnis, Black Rapids, and West Fork Glaciers were affected by large rock avalanches, many of which consisted of a mixture of rock, snow, and glacier ice.

According to Harp and others (2003) the largest rock avalanche on McGinnis Glacier (fig. 394A) had a volume of greater than  $30 \times 10^6 \text{ m}^3$ . They reported that two large rock avalanches originated at two different sites on the flanks of McGinnis Peak, the largest part resulting from the collapse of

**Figure 393.**—Map showing mainshock, foreshock, zone of fault rupture, concentrated landslides, individual landslides on glaciers in the Alaska Range, and observations of liquefaction effects triggered by the Denali Fault earthquake of 3 November 2002. Modified from Harp and others (2003, fig. 1, p. 5).

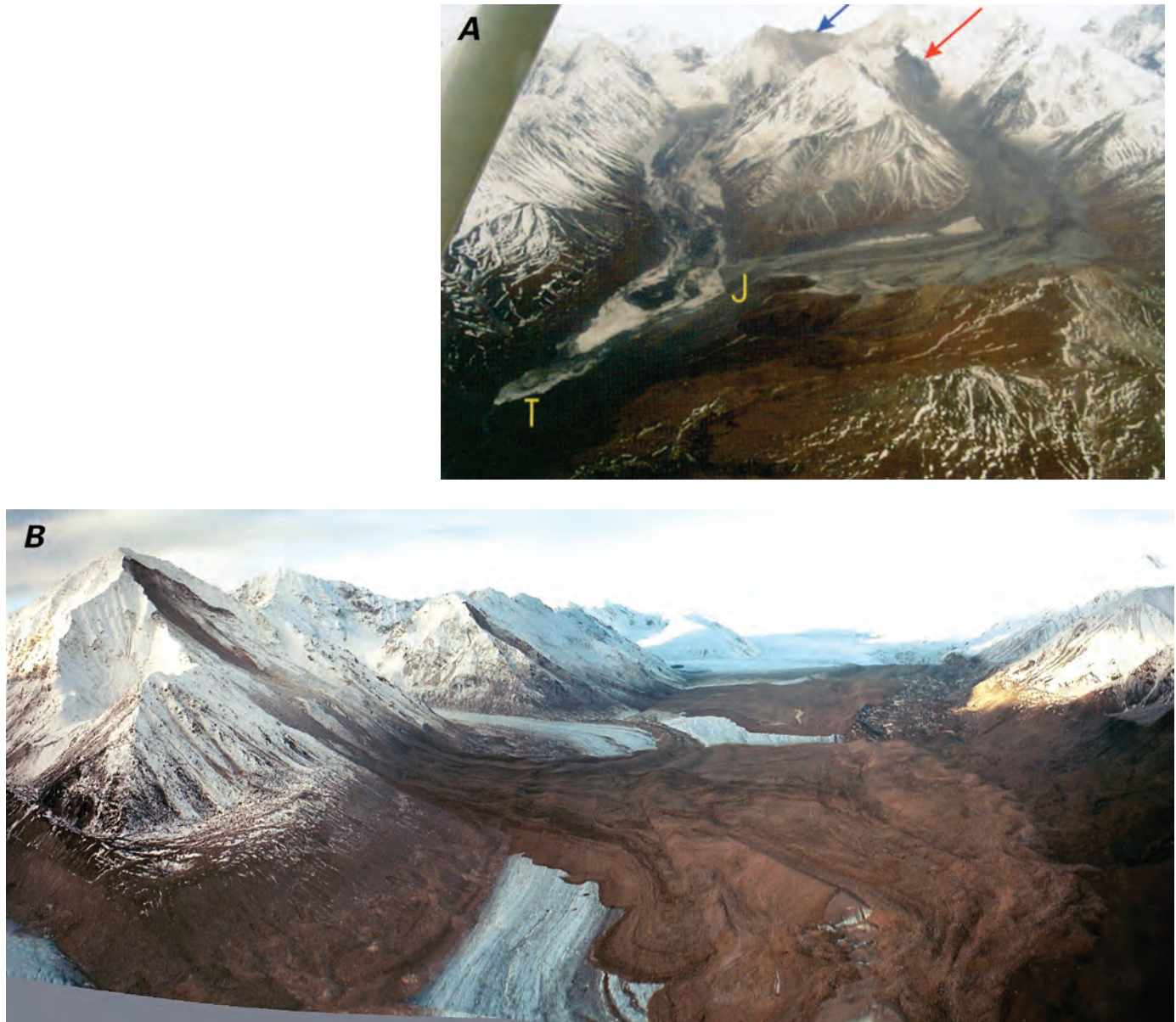


**Figure 394.**—**A**, Oblique aerial photograph of landslides from McGinnis Peak onto McGinnis Glacier modified from Harp and others (2003, fig. 2, p. 6). Two huge rock avalanches originated from different flanks of McGinnis Peak. The rock avalanche to the right (red arrow denoting head scarp) is composed mainly of rock and is approximately  $30 \times 10^6 \text{ m}^3$  in volume. The runout path of the rock avalanche is approximately 10 km. The avalanche to the left (blue arrow denoting head scarp) has more ice and snow included within the avalanche debris. The landslides converged in the center part of the photo (J), and the avalanche on the left continued down to the toe of McGinnis Glacier (T). **B**, Oblique aerial photographic mosaic, taken on 7 November 2002, of multiple rock avalanches on Black Rapids Glacier. On 3 November 2002, a moment magnitude (M)7.9 earthquake occurred along the Denali Fault in central Alaska (fig. 393). It was the largest earthquake in the United States since 1987 and ties for the 9th largest earthquake in the United States in the last 100 years (comes from USGS list of top 10 largest earthquakes in the United States). The earthquake ruptured 225 km of the

Denali Fault with measured offsets as much as 8 m. The fault is of interest to glaciologists because 130 km, or about half, of the rupture lies under glaciers. The fault rupture crosses the West Fork, Susitna, Black Rapids, Canwell, Gakona, and Chistochina Glaciers, and numerous smaller glaciers. In this oblique aerial photographic mosaic, the composite of three rockfall avalanches from the south wall of the Black Rapids Glacier can be seen blanketing about  $13 \text{ km}^2$  of the ablation area or about 5 percent of the total glacier area. The blanketing effect of these rockfalls is expected to increase the glacier's mass balance by about  $+0.2 \text{ m a}^{-1}$  by reducing the melting of glacier ice during subsequent summer melt periods. The Denali Fault underlies this reach of Black Rapids Glacier. The 3 November 2002 earthquake fractured the glacier surface from its confluence with the Susitna Glacier (upper center of the photo) to just below the bottom of the photo, along a 30-km-long path near the northern margin (right margin in this photo) of Black Rapids Glacier. Caption and photograph courtesy of Dennis C. Trabant and Rod S. March, U.S. Geological Survey.

a 750-m-high rock wall. Debris flowed down each of the glacier's two major tributaries on relatively low-angle slopes before converging and flowing to the toe of the 10-km-long glacier.

Harp and others (2003) also reported that large rock avalanches occurred at Black Rapids Glacier (fig. 394B) when granite slopes on the southern side of the glacier failed. The three largest rock avalanches each had volumes of several million cubic meters of debris that together covered about 13 km<sup>2</sup> of the ablation area or about 5 percent of the total glacier area. Truffer and others (2002) suggested that the blanketing effect of the rock avalanches will increase the glacier's mass balance by about 0.2 m a<sup>-1</sup> by insulating the ice from warm summer temperatures. The rock avalanches, which descended from elevations of several thousand meters, completely crossed the glaciers and flowed up the opposite valley walls, similar to the Shattered Peak rock avalanche, which flowed onto the Sherman Glacier during the March 1964 Great Alaskan earthquake (fig. 229). The rock-avalanche deposits were generally 2 to 3-m thick and relatively uniform in their distribution. Lateral margins of the flows were quite sharp. Harp and others (2003) described the rock-avalanche debris flowing up and over a 5 to 6-m-high medial moraine and blanketing it and the surrounding glacier with a uniform thickness.

Harp and others (2003) also described large rock avalanches that were triggered onto the surface of West Fork Glacier above a thrust fault that ruptured during the 2002 earthquake.

Metamorphic rock debris that fell from the valley walls encountered the adjacent medial moraine and became airborne before it landed on the surface of the glacier and fanned out. The largest rock block that they observed was more than 20 m on its largest side. The thickness of the deposit ranged from 3 to 15 m.

A large rock and ice fall also occurred on upper Gakona Glacier. Truffer and others (2002) postulated that this rock and ice fall will not affect the glacier's mass balance immediately because it was deposited onto its accumulation area. They concluded that these rock falls will be a readily visible surface feature for the next 200 to 400 years or more. Before the 3 November 2002 earthquake, large rock and ice-fall debris cover was not evident on the glaciers of the region, suggesting that an earthquake event of similar magnitude has not occurred in at least 200 years and perhaps longer.

---

## **Geospatial Inventory and Analysis of Glaciers: A Case Study for the Eastern Alaska Range**

*By* William F. Manley<sup>1</sup>

### **Abstract**

Recent advances in Geographic Information Systems (GIS) make it possible to assemble large empirical multiparameter datasets that provide important information on environmental variation, process, and change. Such a GIS-based application is presented here for glaciers in the eastern Alaska Range. Data sources include USGS Digital Line Graphic (DLG), Digital Raster Graphic (DRG), and Digital Elevation Model (DEM) files, which were derived from USGS topographic quadrangle maps representing glacier and landscape conditions from 1948 to 1954. Information from 10 USGS 1:63,360-scale topographic quadrangle maps was combined and processed in the GIS to summarize parameters and to analyze spatial relationships. The 279 glaciers shown on the 10 maps occupy a total area of 1,229 km<sup>2</sup>. Data trends are dominated by a disproportionate decrease in the frequency distribution of glaciers by area.

---

<sup>1</sup> Institute of Arctic and Alpine Research (INSTAAR), University of Colorado Boulder, CO 80309-0450; william.manley@colorado.edu; 303-735-1300

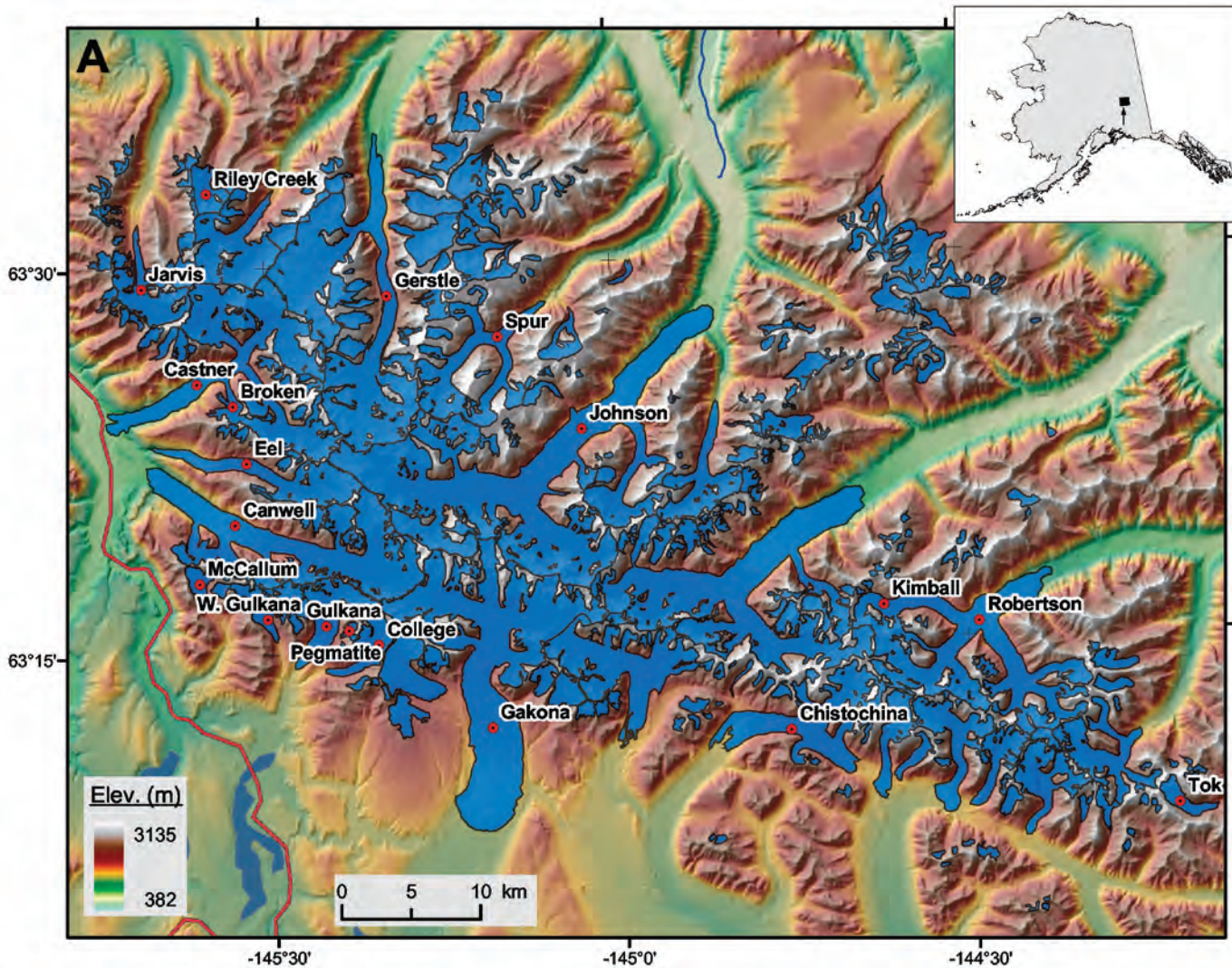
A “typical” glacier in the region measures only 0.6 km<sup>2</sup> in area, is as wide as it is long, and occupies a basin only slightly larger than the glacier itself (for example, a cirque glacier). In contrast, the relatively few named or previously measured glaciers yield median values of 19.5 km<sup>2</sup> for area, 4.0 for the ratio of length to width, and 1.7 for the ratio of basin area to glacier area (large valley glaciers). Other parameters are not found to be strongly related to glacier area, including median elevation and the shape of hypsometric curves. The GIS layers of glacier extent form a comprehensive digital inventory revealing a range of morphologic relationships that quantitatively define feedbacks between glacier dynamics and mountainous terrain. The geospatial data are also useful for mapping and visualization, selection or analysis of “representative” glaciers, deriving or applying scaling relationships, modeling of ice dynamics and retreat, and as a decades-old baseline for comparison with recent airborne and satellite remote-sensing measurements. As a complement to field measurements, maps, geodetic airborne laser-altimetry, aerial photographs, and satellite imagery, the GIS approach takes advantage of spatial variation to better understand environmental controls on glacier distribution and geometry.

### **Introduction**

Inventories of glaciers and glacier systems in Alaska and elsewhere are important in the assessment of water resources, glacier hazards, the response of glaciers to climate change, and, under negative mass-balance conditions, their excess meltwater contribution to sea-level rise (for example, Fountain and others, 1997; Käab and others, 2002; Paul, 2003; Meier and Wahr, 2002; Meier and others, 2003). Recent studies have shown that Alaska’s glaciers are undergoing pronounced thinning and retreat and that mass balances are consistently negative (Echelmeyer and others, 1996; Hodge and others, 1998; Arendt and others, 2002) as a result of historically unprecedented Arctic warming (cf. Serreze and others, 2000). However, less than 1 percent of Alaska’s glaciers by area has been included in a global inventory (for example, the World Glacier Monitoring Service’s World Glacier Inventory) (National Snow and Ice Data Center, 1999, 2003), and existing tabular databases are limited in their capability to spatially represent the three-dimensional context of glaciers within mountain environments.

This section provides a new approach to documenting and investigating glaciers by means of GIS. The study takes advantage of detailed and extensive aerial photographic interpretation and glacier mapping done by the USGS in the early 1950s. Goals of the study are to (1) develop, test, and apply a series of procedures to create a glacier atlas in the form of a geospatial database; (2) in addition to mapping and visualization, use spatial analysis to investigate geomorphic relationships resulting from the interplay of climate, topography, and ice dynamics; and (3) make a glacier inventory – and the specific GIS algorithms used to create it – available for further research. This study is part of a broader project using GIS to document and analyze glaciers, environments, and climate across the State of Alaska.

The study area, in the eastern Alaska Range, lies in the east-central interior of Alaska (fig. 395) and spans approximately 100 km from the Delta River valley on the west to Mentasta Pass on the east. The mountainous terrain and its glaciers are further described and illustrated in the section on the Mount Kimball-Mount Gakona Segment between Mentasta Pass and the Delta River. The region includes the relatively well studied Gulkana Glacier (cf. Mayo and Trabant, 1986; March and Trabant, 1996; Hodge and others, 1998). This “benchmark” glacier and the adjacent West Gulkana Glacier were included in recent studies of volumetric change determined from laser altimetry (Echelmeyer and others, 1996; Sapiano and others, 1998; Arendt and others, 2002). Glaciers in the area are not yet a part of the World Glacier Inventory (National Snow and Ice Data Center, 1999, 2003), but 19 of them were cataloged in a preliminary inventory by Denton and Field (1975a; see also



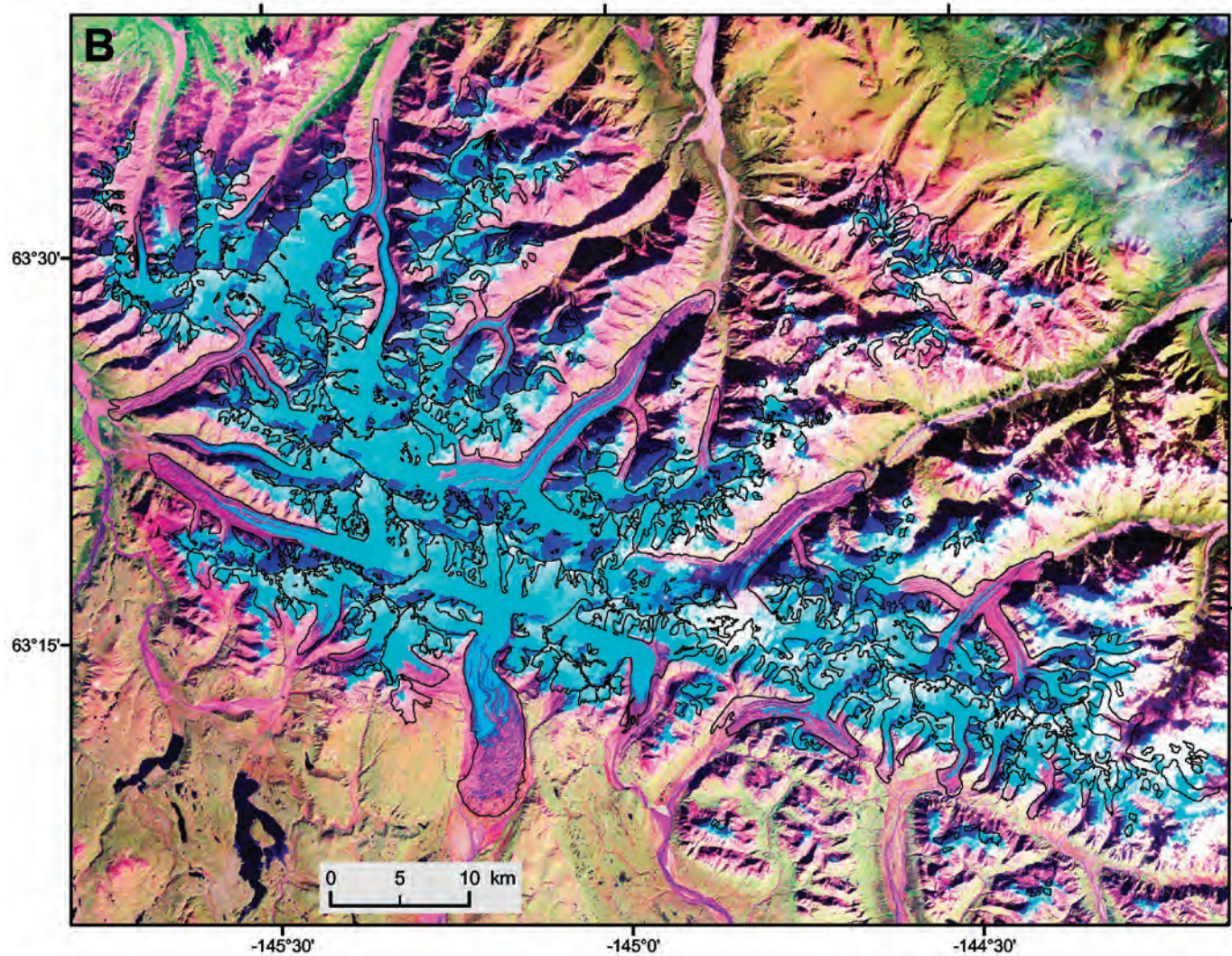
Field, 1958). The region has a continental climate, partially shielded from transport of moisture from the Gulf of Alaska by the Wrangell, Talkeetna, and Chugach Mountains, and the St. Elias Mountains to the south.

### Methods

Three types of data from the USGS were used as the foundation of this study (fig. 396). Hydrographic DLG files are vector representations of water features as digitized from the USGS 1:63,360-scale 15-minute topographic quadrangle maps that include polygons having “Minor1” values of 103 or 411 encode features, originally mapped as a “Glacier or permanent snowfield” (USGS, 1998a, b). DRG files are images scanned from the topographic quadrangle maps. The DEM used in this study was derived from the USGS National Elevation Dataset (NED) files, which were compiled from the 15-minute DEMs for Alaska, which, in turn, are based on contours, spot heights, and other terrain features on the topographic quadrangle maps. Thus, all three datasets used here were derived from the same source: 10 15-minute topographic quadrangle maps for the eastern Alaska Range (Mount Hayes A1-A3, B1-B4, and C2-C4). The maps were originally compiled by using stereophotogrammetric mapping technology and 1948–54 vertical aerial photographs acquired by the USAF for the AMS. Because the datasets share a common origin, they have the advantage of sharing the same spatial registration and temporal basis (for example, a maximum of 6 years from oldest to youngest aerial photographic coverage).

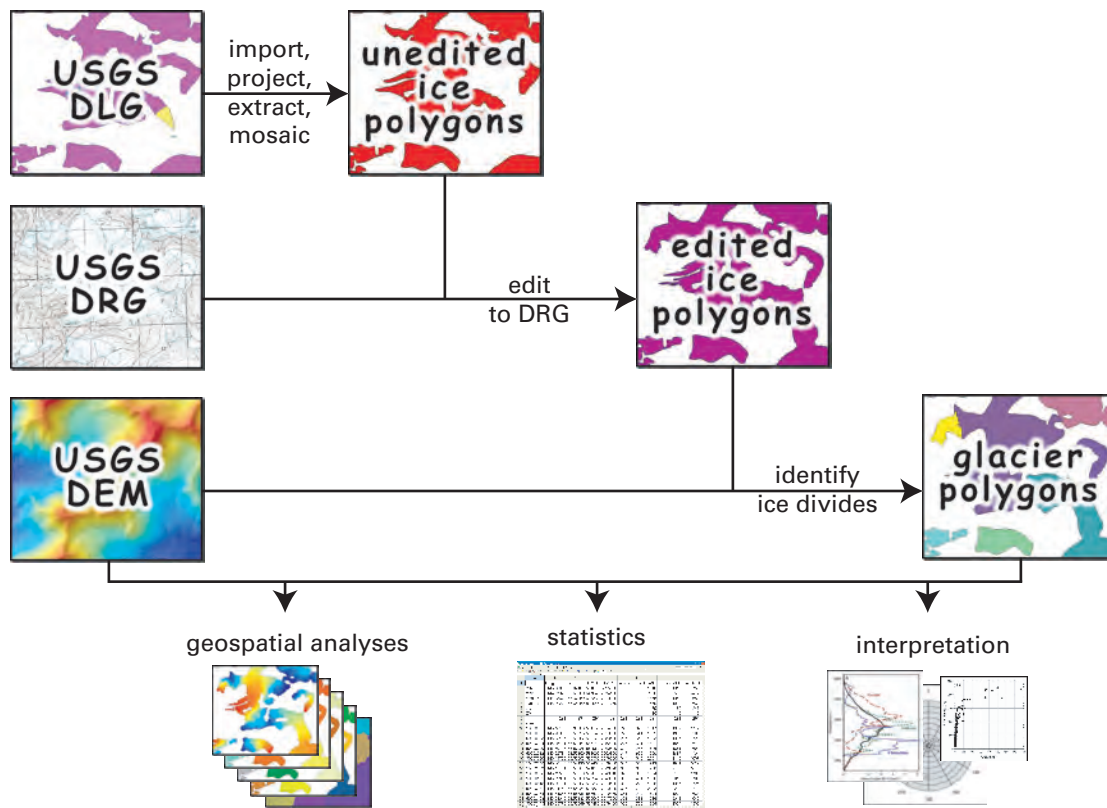
To process and analyze the GIS data, more than 90 individual “scripts” were written, tested, and applied, where each “script” is a stepwise semiautomated

**Figure 395.** — Maps of glaciers and terrain in the eastern Alaska Range. **A**, Glacier polygons in the digital inventory are overlain on color-coded topography and shaded relief. Three small glaciers in the database, northeast of Tok Glacier, are not shown. Tick marks display the boundaries of 1:63,360-scale, 15-minute topographic maps for the area. **B**, The glacier polygons, representing the areal extent of glacier ice during 1948–1954, are shown as black lines over a GeoCover Landsat mosaic. This orthorectified false-color composite displays TM bands 7, 4, and 3 from imagery acquired in approximately 1990. Although glacier termini are obscured by debris-covered ice, the mosaic reveals in detail some evidence for thinning and ice-marginal retreat.



procedure that may include macros (prerecorded series of actions executed with a single command) or programming code for direct GIS processing. For example, five scripts were used to import the NED DEM, project it from an original map projection, datum, and resolution (Geographic NAD 27 with 2-arc-second spacing) to UTM zone 6 with 60-m spacing, and clip it (trim to eliminate data outside the study area). GIS processing was handled by ArcGIS Desktop (ArcInfo), as well as MFWorks, a simple raster program used for some of the final geometric calculations. Error assessment is presented in the next section.

Major processing steps (fig. 396) began with database preparation and quality editing. An extensive review of metadata was undertaken to assure that the three types of data sources were temporally compatible, all derived from the original 1950s topographic quadrangle maps, which are compiled from 1948–54 vertical aerial photographs. Ten DLG files were imported and projected to Universal Transverse Mercator (UTM). Glacier polygons were extracted and mosaicked to yield “unedited ice polygons.” These features were compared directly with the DRG files (fig. 397A). In most cases, the unedited ice polygons very closely matched the glacier outlines as shown on the topographic quadrangle maps (within a 60-m grid-cell tolerance commensurate with the DEM). However, some of the ice polygons displayed digitization and other unexplainable errors that required intensive manual editing. Thus, “edited ice polygons” were created that more closely depict the complex glaciers and contiguous ice masses in the study area, as the topographic quadrangle maps show.



The next major step addresses the fundamental “geospatial definition” of a glacier. The ice masses shown on topographic maps are rarely simple, isolated cirque or separate valley glaciers. They commonly are complex features joined at drainage divides from which separate glacier ice bodies flow downslope. To “cut” the “ice polygons” into “glacier polygons” along ice divides, an algorithm was developed that takes advantage of watershed functions in ArcInfo. This script identifies glacier “toes” as parts of each ice polygon that lie below the median elevation of the polygon and uses the toes as “pour points” for the watershed function. The resulting, often contiguous glacier polygons (fig. 397) then can be analyzed separately. Automated processing avoids subjective and time-intensive manual editing. A byproduct is a GIS layer of separate glacier basins, each enclosing a glacier and the upslope area that sheds snow or meltwater onto its surface.

Finally, a variety of raster commands were used to measure a variety of parameters for each glacier on the basis of the glacier outlines and the co-registered DEM (table 7). This approach builds upon that of Allen (1998) (see also Paul and others, 2002; Paul, 2003) and relies on zonal functions acting on each glacier’s 60×60-m grid cells. The DEM has sufficient resolution for this task: 26 grid cells for the smallest glacier, a median glacier area of 160 grid cells, and more than 42,000 grid cells for the largest glacier.

Parameters were measured for the purposes of compiling a digital inventory as well as for geospatial and glaciologic analysis. Location is described by the **latitude** and **longitude** of the centroid grid cell. The GIS readily calculates **minimum**, **maximum**, **median**, and **average elevation** as well as the **range in elevation** for each glacier. Basic geometric parameters for each glacier include **area**, **perimeter**, average **slope angle**, and average **aspect** (following directional statistics presented by Davis, 1986). **Compactness**, a nondimensional measure of shape, was calculated as  $4\pi$  multiplied by area, divided by perimeter squared (cf. Davis, 1986; Allen, 1998). This parameter varies from 0.0 for infinitely narrow or convoluted shapes to 1.0 for a circle. Glacier **length** is difficult to quantify objectively with an automated script owing to the constraints imposed by raster processing but was estimated

**Figure 396.**—Flow diagram for processing of the original cartographic source material to create and analyze the glacier spatial database. DLG, Digital Line Graph; DRG, Digital Raster Graphic; DEM, Digital Elevation Model. See text for additional details.



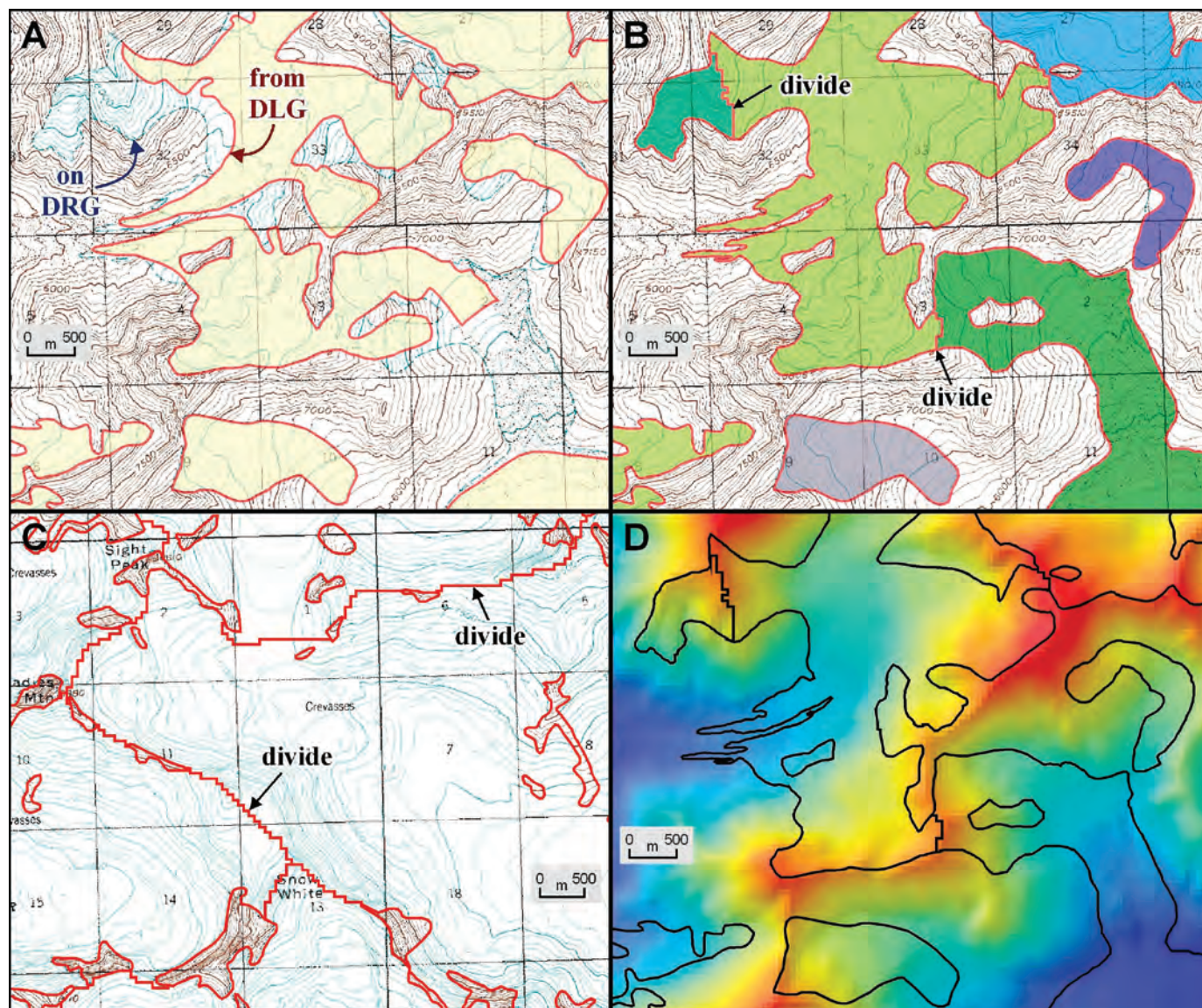


**Figure 397.**—Close-ups of selected GIS processing steps and results. **A**, Close-up of DLG polygons shown over the DRG for a small area northeast of Gerstle Glacier. Glacier extents in the DLG files did not everywhere match those depicted on the DRGs owing to digitization and other errors. **B**, The glacier features were edited to agree with the DRGs, and the “ice polygons” were cut along automatically identified drainage divides to form separate “glacier polygons.” **C**, Example of ice divides at the upper limits of the Johnson, Canwell, Fels, and Gerstle Glaciers. The jagged nature of ice divides is inherited from the processing of 60-m DEM grid cells. **D**, Glacier polygons as black outlines over the DEM for the area shown in A and B.

as the longest flowline using a downhill FLOWLENGTH command. Glacier **width** is similarly difficult to process consistently as a human would measure and is simply calculated here as area divided by length, yielding also the **length/width ratio** as a second metric for shape. The **basin coefficient** is defined as **basin area** divided by glacier area, a relative measure of the up-slope area available for avalanching and snowdrift onto the glacier surface. A few other parameters, including backwall height, were estimated as part of a broader study related to estimated ELAs but are not presented here.

The spatial variables extracted from the GIS for each glacier are based on all 60×60-m cells that make up the glacier. Thus, mean elevation is the true mean, not simply the average of minimum and maximum elevations. Similarly, slope angle is averaged across the entire glacier, not simply derived from elevation range and length. As an aside, calculation of average aspect for each glacier involves complex statistics to avoid the problems resulting from geometric means of azimuthal data.

Also, with each glacier’s surface geometry represented in the GIS, it is possible to quantify **area-altitude distribution**. A script was developed that determines the cumulative area for each glacier grid cell as the percent of that glacier’s area lying above the elevation of that grid cell. The area-altitude grid can then be used to plot hypsometric curves related to mass balance for individual glaciers or entire ranges.

TABLE 7. Results of the spatial analysis of 279 glaciers in the eastern Alaska Range.<sup>1</sup>

	Longitude DD	Latitude DD	Minimum Elevation (m)	Maximum Elevation (m)	Median Elevation (m)	Average Elevation (m)	Elevation Range (m)	Area (km <sup>2</sup> )	Perimeter (km)	Compactness	Aspect (degrees)	Slope (degrees)	Length (km)	Width (km)	Length/width ratio	Basin area (km <sup>2</sup> )	Basin coefficient
<b>All glaciers</b>																	
Minimum			756	1424	1237	1216	90	0.09	1.6	0.01	0	8	0.1	0.2	0.1	0.13	1.0
Maximum			2472	3135	2599	2590	2276	154.52	360.5	0.65	359	37	34.4	6.1	11.1	277.92	8.2
Median						459	0.57	5.4	0.26				0.7	0.8	1.0	1.12	1.8
Average			1638	2241	1910	1913					6	18					
Sum							1229										
<b>Selected glaciers</b>																	
																950	
Canwell	-145.45884	63.32222	808	2721	1639	1630	1913	70.76	176.9	0.03	307	10	24.4	2.9	8.4	117.03	1.7
Castner/Broken	-145.52845	63.43713	766	2935	1818	1758	2169	70.58	208.2	0.02	260	13	20.8	3.4	6.1	114.57	1.6
Chistochina	-144.72919	63.20041	1139	2974	1518	1666	1835	35.09	108.1	0.04	214	9	11.0	3.2	3.5	72.46	2.1
College	-145.35955	63.25648	1257	2420	1754	1729	1163	8.54	31.6	0.11	214	11	6.8	1.3	5.4	15.67	1.8
Eel/Fels	-145.47815	63.36497	863	2718	1865	1803	1855	21.52	65.9	0.06	278	12	15.4	1.4	11.1	43.76	2.0
Gakona	-145.18597	63.24145	1059	2944	1644	1642	1885	108.72	203.4	0.03	184	8	17.9	6.1	2.9	155.16	1.4
Gerslie	-145.32490	63.46235	821	2993	2091	2040	2172	86.84	204.2	0.03	41	12	23.4	3.7	6.3	136.33	1.6
Gulkana	-145.42431	63.27445	1141	2431	1834	1786	1290	19.45	60.7	0.07	182	10	8.5	2.3	3.7	27.38	1.4
Jarvis	-145.66714	63.48103	1283	2794	1763	1792	1511	14.76	64.1	0.05	325	13	9.3	1.6	5.9	23.85	1.6
Johnson	-145.13283	63.36141	756	2963	1758	1766	2207	154.52	360.5	0.01	36	11	34.4	4.5	7.7	277.92	1.8
McCallum	-145.60371	63.29947	1415	1826	1670	1649	411	3.14	10.7	0.35	146	10	2.3	1.4	1.7	5.05	1.6
Pegmatite	-145.38774	63.26542	1549	2008	1783	1777	459	0.89	7.3	0.21	265	17	1.0	0.9	1.2	1.62	1.8
Riley Creek	-145.58049	63.55183	1540	2483	2023	2013	943	6.01	17.8	0.24	35	20	2.7	2.3	1.2	6.46	1.1
Robertson/Kimball	-144.51903	63.24377	912	3135	1664	1731	2223	72.41	219.1	0.02	28	12	17.0	4.3	4.0	158.60	2.2
Spur	-145.22050	63.43740	1105	2928	1958	1999	1823	29.12	110.5	0.03	42	15	13.0	2.2	5.8	70.86	2.4
Tok	-144.20409	63.13876	1401	2206	1788	1800	805	4.27	15.1	0.23	105	10	4.7	0.9	5.1	9.10	2.1
W. Gulkana	-145.51717	63.28298	1296	2435	1723	1734	1139	6.34	25.4	0.12	178	15	3.7	1.7	2.2	9.33	1.5
AL-6308/14424	-144.39882	63.15864	1161	2767	1857	1845	1606	15.36	57.7	0.06	197	14	4.4	3.5	1.3	25.86	1.7
AL-6310.5/14417	-144.31543	63.17109	1135	2708	1750	1764	1633	18.35	73.7	0.04	70	14	6.8	2.7	2.5	33.16	1.8
AL-6310/14431	-144.53144	63.18256	1117	2603	1755	1722	1486	16.27	55.7	0.07	193	13	9.9	1.6	6.1	39.39	2.4
AL-6310/14437.5	-144.61454	63.18722	1111	2648	2031	1861	1537	9.13	31.1	0.12	200	12	5.8	1.6	3.7	13.87	1.5
AL-6313-14459	-145.00096	63.23897	1161	2612	1685	1698	1451	38.83	118.9	0.03	157	9	12.2	3.2	3.8	52.95	1.4
AL-6317/14450	-144.81841	63.28315	850	3126	1586	1630	2276	100.14	262.6	0.02	31	11	24.7	4.0	6.1	185.73	1.9
AL-6322/14453	-144.87769	63.35569	1073	2867	1850	1846	1794	16.37	56.9	0.06	5	17	10.4	1.6	6.6	38.83	2.4
AL-6331.5/14532	-145.54385	63.51268	1215	2720	1950	1939	1505	23.07	60.6	0.08	27	16	8.8	2.6	3.3	32.53	1.4

<sup>1</sup> Median values shown in summary sections at top for parameters that are not normally distributed. Named glaciers (below) include those identified by Denton and Field (1975) with alphanumeric codes.

## Error Analysis

A thorough analysis of error is difficult to accomplish because of the lack of independent, detailed measurements related to these glaciers for the time period of acquisition of the aerial photographs (1948–54) used for map compilation. Some of the potential sources of error are not significant. Changes in glacier area over the 6-year span of aerial photography are probably negligible, and photographs for 8 of the 10 quadrangle maps were taken during the same year (1954). Co-registration errors among the DEM, DLGs, and DRGs are also negligible. Most of the GIS processing to estimate glacier parameters (such as **area**, **elevation**, and **aspect**) adds negligent numerical error due to GIS processing alone. More important are errors associated with the source data.

The primary elevation datasets (the 15-minute DEMs) are probably a source of error. USGS national map-accuracy standards (USGS, 1998b) state that root mean square errors (RMSEs) for Level 2 DEMs are less than one half of the contour interval [15 m (50 ft) or 30 m (100 ft) for these quadrangles; for example, RMSE < 15 m]. The average vertical RMSE for the 10 topographic quadrangle maps used in this analysis, as reported in DEM metadata and based on 300 geodetic control points, is 3.6 m. However, other glacier studies utilizing 15-minute DEMs (Aðalgeirsdóttir and others, 1998; Arendt and others, 2002) have documented vertical errors of about 45 m (standard deviation of random error with negligible systematic offset) for upper accumulation areas on glaciers. The lack of contrast on vertical aerial photographs of snow-covered glaciers precludes the use of stereophotogrammetric plotters to determine accurate surface-elevation data (for example, a “floating” white dot in the plotters cannot be accurately positioned on a “white” surface by the photogrammetrist). All elevations of the snow-covered areas of glaciers (accumulation area) depicted on topographic maps are unreliable. This error affects calculation of average elevation and — to a lesser extent — of median elevation. It probably also adds error to the identification of ice divides.

For the glacier polygons, this study relies on the original USGS mapping by cartographers during the late 1940s and early 1950s, among which were included (as best as can be determined) glaciologists specifically tasked with glacier delineation. The original USAF vertical aerial photographs acquired for the AMS are generally of high quality. By definition, the polygons include “permanent snowfields,” although polygons less than 0.1 km<sup>2</sup> (a commonly accepted lower limit for glaciers) were excluded from analysis. A related conceptual “error” reflects how to quantitatively and objectively define a glacier (see “Methods” and “Discussion”). But the greatest source of uncertainty for this study is probably associated with the subjective nature of glacier mapping by cartographers from stereoscopic pairs of vertical aerial photographs — a process that is not exactly reproducible because of variation in the skills of the cartographers.

In general, the possible errors are random rather than systematic in nature. On the basis of the discussion above, the glacier-elevation measurements (**min.**, **max.**, **median**, and **average elevations** and **elevation range**) are probably accurate within approximately 50 m. The error for glacier area is roughly 5 percent for small glaciers and approaches about 1 percent for large glaciers. Derived parameters such as average slope angle and aspect probably carry a very small uncertainty, with the exception of length and width, which are difficult to objectively measure in automated fashion, and may vary about 15 percent from how a glaciologist would manually measure such values on a map. Errors for any single glacier or grid cell may be significant but are minimized with mean or median calculations for individual glaciers and for relationships among glaciers with a large sample size ( $n=279$ ).

It is instructive to compare this GIS analysis with previously published information for Gulkana Glacier. The GIS analyses are based on the USGS-

mapped extent as interpreted from aerial photographs taken in 1954 (most of the glacier) and 1949 (the lower kilometer). The geospatial results include an area of 19.45 km<sup>2</sup>, a length of 8.5 km, a minimum elevation of 1,141 m, and an average slope angle of 10°. These values compare with (1) an estimate of area (18.5 km<sup>2</sup>) using the same maps (Echelmeyer and others, 1996); (2) estimates of length (8 km), terminus elevation (1,180 m), and slope angle (7°) based on a 1993 geodetic airborne laser altimeter profiling survey (Echelmeyer and others, 1996); (3) a description of area (19.3 km<sup>2</sup>) and length (8.5 km) by Hodge and others (1998); and (4) a listing of area (20 km<sup>2</sup>) that apparently used the same maps (Arendt and others, 2002). The GIS results appear comparable, and other methodologies may carry uncertainties in detail.

Another “test” is a comparison with previously published data for 19 glaciers (fig. 398). Denton and Field (1975a) presented a summary of glaciers in the area, based on the USGS 1955 1:250,000-scale topographic quadrangle map for Mount Hayes. The Mount Hayes map was compiled by the AMS from USAF aerial photographs acquired between 1948 and 1955, using the same source materials that were used for the 10 15-minute topographic quadrangle maps used in the GIS analyses of glaciers. Their estimates of area and length are thus associated with a smaller scale Level 1 (equivalent in DEM terms to a 90-m grid cell) data source and manual map measurements. Discrepancies for area are minor, probably related to the smaller scale mapping. Discrepancies for length are more significant and probably reflect differences between manual and GIS-based approaches (see “Methods” section). In general, the regressions – only for the largest glaciers in this region – affirm the reliability of the geospatial approach.

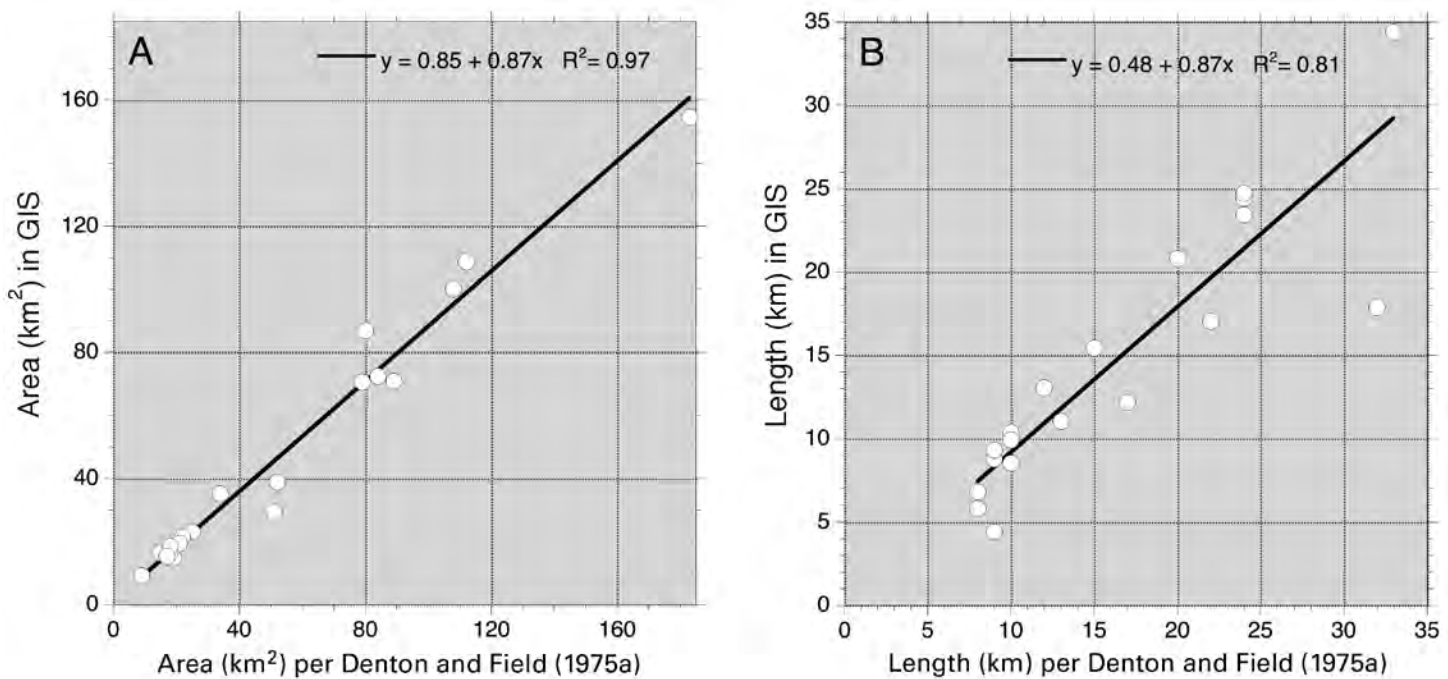


**Figure 398.** — Comparison of GIS results for **A** (area) and **B** (length) with the 19-glacier inventory of Denton and Field (1975a).

## Results

The geospatial analysis yields details for 279 glaciers thus identified for the eastern Alaska Range. Summary statistics are given in table 1 for all glacier polygons, along with summary results and individual measurements for the 19 previously measured or named glaciers. Selected parameters are shown in map form in figure 399. Relationships among glacier parameters were also explored through correlation analysis. Log-normal transformations were applied to elevation range, area, perimeter, length, width, length/width ratio, basin area, and basin coefficient.

The cirque, valley, and complex mountain glaciers range in size from 0.1 km<sup>2</sup> (the minimum threshold for inclusion in the GIS processing) to 154.5 km<sup>2</sup> (Johnson Glacier); the average area is 4.4 km<sup>2</sup>, and the median area is 0.6 km<sup>2</sup>. Total glacier area is 1,229 km<sup>2</sup>. The total comprises about 8 percent of the glacierized area of the entire Alaska Range and less than 2 percent of the glacier area for the entire State (Post and Meier, 1980) but more than twice the area of glaciers in the lower 48 States (about 513 km<sup>2</sup>, cf. Meier, 1961; about 580 km<sup>2</sup>, Krimmel, 2002). The largest glaciers flow from the central divide of the range; smaller glaciers are clustered around nunataks, on ridges standing above valley glaciers and their tributary glaciers, and on isolated massifs mainly north of the range divide (fig. 399A). Taken as a whole, the glacierized area extends from a minimum elevation of 756 m at the toe of Johnson Glacier to a maximum of 3,135 m at the upper limit of Robertson Glacier.

The results for the calculation of glacier area, illustrated in figures 399A and 400, highlight a dominant trend: small glaciers are much more common than large ones. The frequency distribution by area is similar in form to the combined exponential and power relationships noted for other detailed regional inventories (including the Brooks Range) and as applied through geometrical scaling to a global scale (Meier and Bahr, 1996; Bahr, 1997; Bahr and Meier, 2000). It is not surprising, therefore, that the number of small glaciers is disproportionately higher than the number of large ones. The results here document a systematic area-scaling relationship empirically for a relatively small region. The results also exemplify the ability of semiautomated GIS analysis to comprehensively examine relationships among all glaciers in a region, including small glaciers that are not commonly inventoried or studied.

Some of the fundamental parameters of glacier geometry are not strongly related to glacier area. For example, glacier aspect varies throughout the cardinal directions of the compass. North-facing glaciers are concentrated on the northern side of the range (fig. 399B), and there is a weak but marginally preferred aspect of 6° ( $p = 0.10$ , with a mean resultant vector length of 0.09) (Davis, 1986). However, aspect is not significantly related to glacier area (fig. 401) ( $r = 0.06$ ;  $p = 0.29$ ). [Editors' note:  $r$  is a correlation coefficient where 1 indicates perfect correlation between variables and 0 indicates no correlation;  $p$  is a probability ranking where higher values show higher relation between variables.] Median glacier elevation ranges from 1,237 m (a north-facing cirque glacier 11 km north-northeast of Robertson Glacier) to 2,599 m (for a small southwest-facing glacier 9 km east of Johnson Glacier); the average for the region is 1,910 m. Higher values exist for the northern and western glacierized areas of the region (fig. 399C), with a trend surface dipping 10.9 m km<sup>-1</sup> at an azimuth of 186°; RMSE = 134 m;  $r^2 = 0.46$ ;  $p < 0.0001$ . The median elevation of glaciers may be closely related to the regional long-term ELA (cf. Braithwaite and Müller, 1980). However, for this region, median elevation is not convincingly related to glacier area ( $r = -0.12$ ;  $p = 0.05$ ). A closely related parameter, average glacier elevation, exhibits similar spatial and statistical relationships.

A few geometric parameters are significantly but weakly related to glacier area. Slope angles range from 8° (for Gulkana Glacier) to 37° (for a small

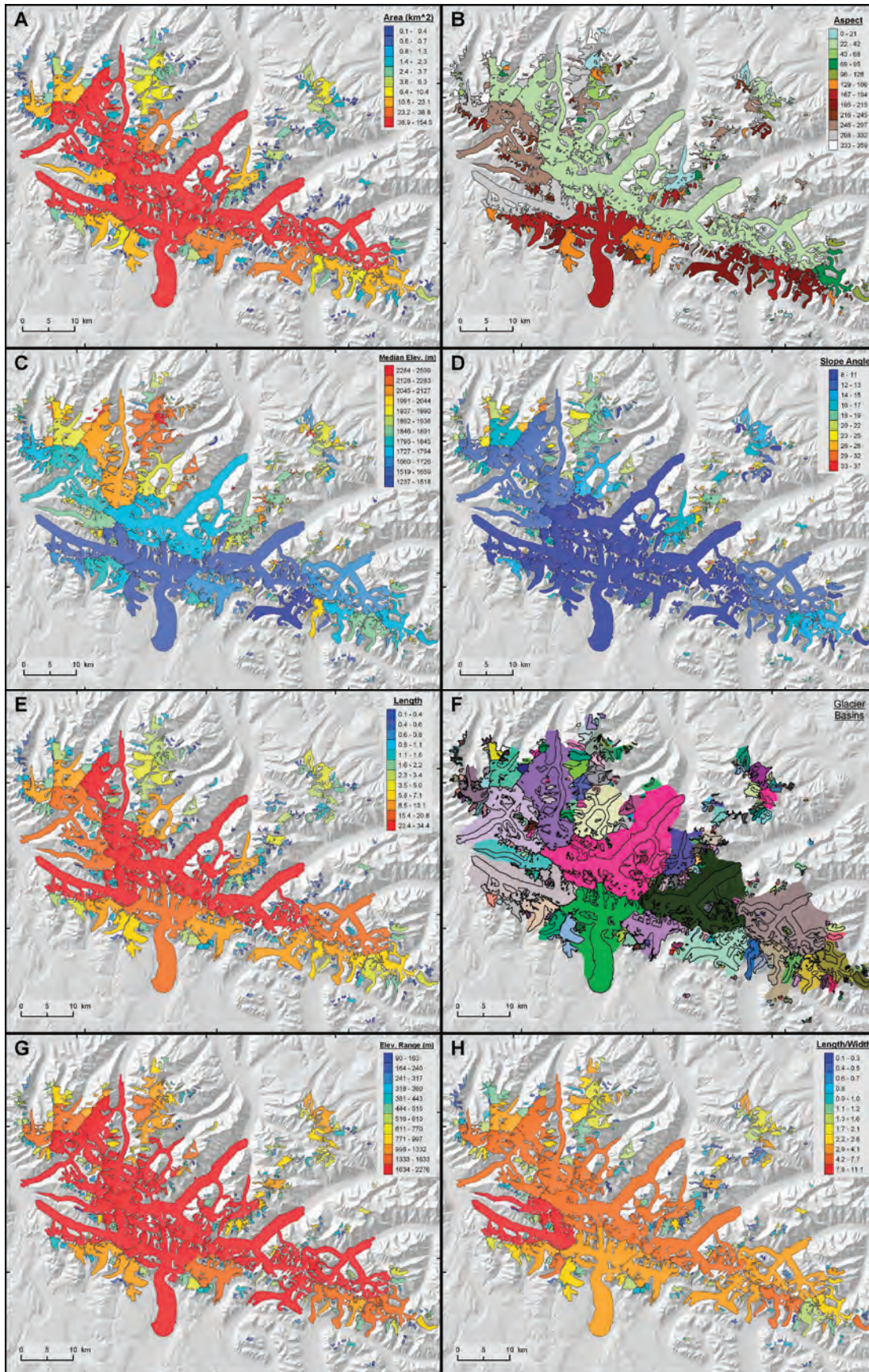


**Figure 399.**— Shaded-relief maps of the glaciers color-coded for selected GIS results: **A**, area; **B**, aspect; **C**, median elevation; **D**, slope angle; **E**, length; **F**, glacier basins randomly colored; **G**, elevation range; and **H**, length-to-width ratio.

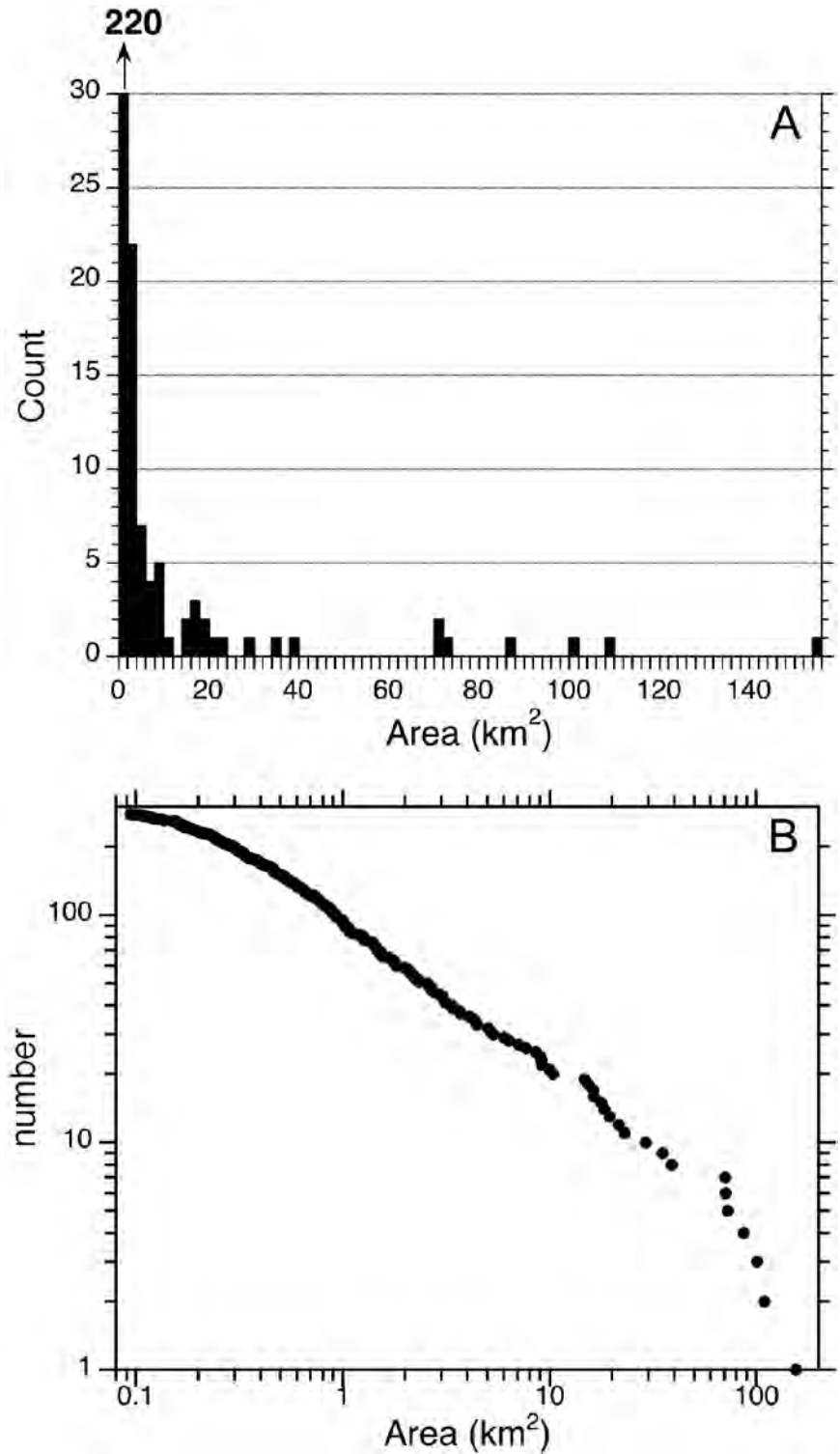


**Figure 400.**—Frequency distribution of glaciers by area. **A**, Shown as a histogram. The leftmost column extends beyond the Y-axis limit of the graph. **B**, Log-log plot of cumulative number of glaciers greater than a given area. Compare with Meier and Bahr (1996) and Bahr (1997).

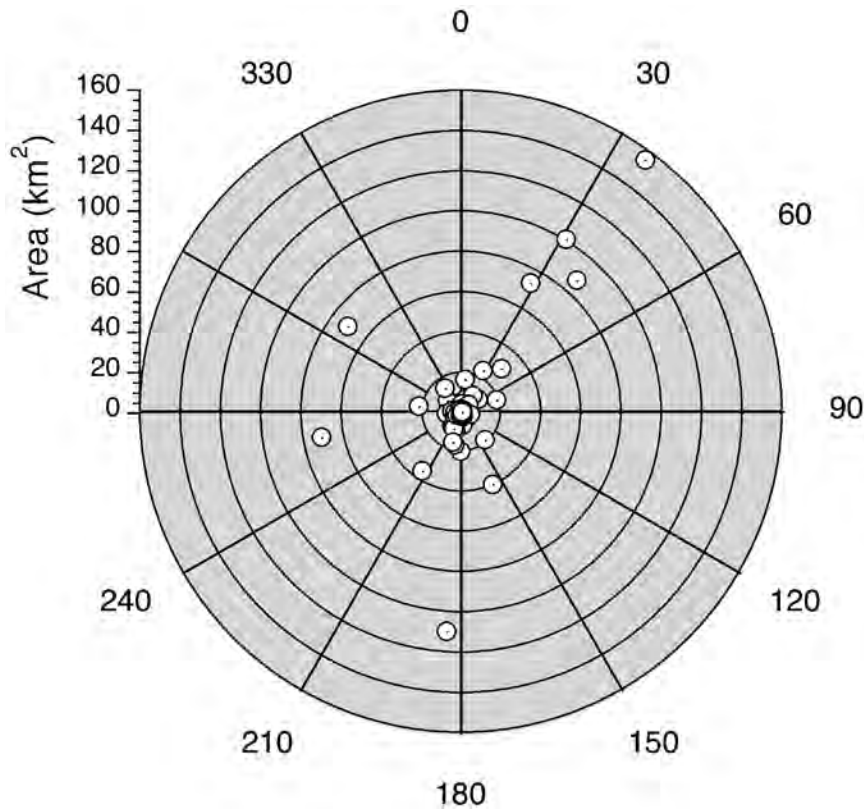


**Figure 401.**—Polar diagram of glacier area versus aspect. Most glaciers fall close to the central origin, with the largest glaciers facing northeast, south, and west.

glacier 8 km west of Kimball Glacier); the regional average is  $18^\circ$  (fig. 399D). Not surprisingly, the smallest glaciers tend to have steep surfaces (fig. 402A). However, correlation with area is weak ( $r = -0.40$ ;  $p < 0.0001$ ). Similarly, the basin coefficient varies from 1.0 (for example, the glacier completely occupies its basin) to 8.2 (for example, the basin is eight times larger than the glacier area); the median value is 1.8. This proportional metric is highest for small glaciers (fig. 402B), but correlation with area is weak ( $r = -0.26$ ;  $p < 0.0001$ ). To summarize, many of the glaciers are typical cirque glaciers that have steep surfaces and are bounded by ice-free headwall areas, whereas large valley glaciers typically have low slopes and relatively small ice-free catchments. However, not all of the glaciers analyzed fall within this spectrum.

Other morphologic parameters are strongly related to glacier area. Not surprisingly, strong relationships exist between area and length (figs. 399E, 402C) ( $r = 0.96$ ), width ( $r = 0.85$ ), perimeter ( $r = 0.98$ ), and basin area (cf. fig. 399F) ( $r = 0.96$ ). Larger glaciers tend to have a greater range in elevation from head to toe (figs. 399G, 402D) ( $r = 0.85$ ). They also tend to be more elongate, having high length-to-width ratios (fig. 399H) ( $r = 0.66$ ), whereas smaller glaciers are more circular in shape (for example, compactness) ( $r = 0.66$ ). These parameters strongly express, in a quantitative sense, a range in morphology normally described qualitatively – from niche and cirque glaciers to simple valley glaciers or those with numerous tributaries and compound accumulation basins. They similarly characterize morphologic changes for alpine glaciers as they advance and retreat in mountainous terrain.

Another parameter relates strongly to area. Only the largest glaciers in the region have been studied previously. Glaciers given names on the USGS topographic quadrangle maps and included in the inventory by Denton and Field (1975a) comprise only 7 percent of the glaciers in the eastern Alaska Range. Not surprisingly, these 19 glaciers have morphologies that differ greatly from the “typical” values for the range (table 7). For example, they are much larger ( $19.5 \text{ km}^2$  versus  $0.6 \text{ km}^2$ ), longer (9.9 km versus 0.7 km), and elongate (length-width ratio of 4.0 versus 1.0) and have a greater range in elevation (1,606 m as opposed to 459 m), than could be considered “representative”



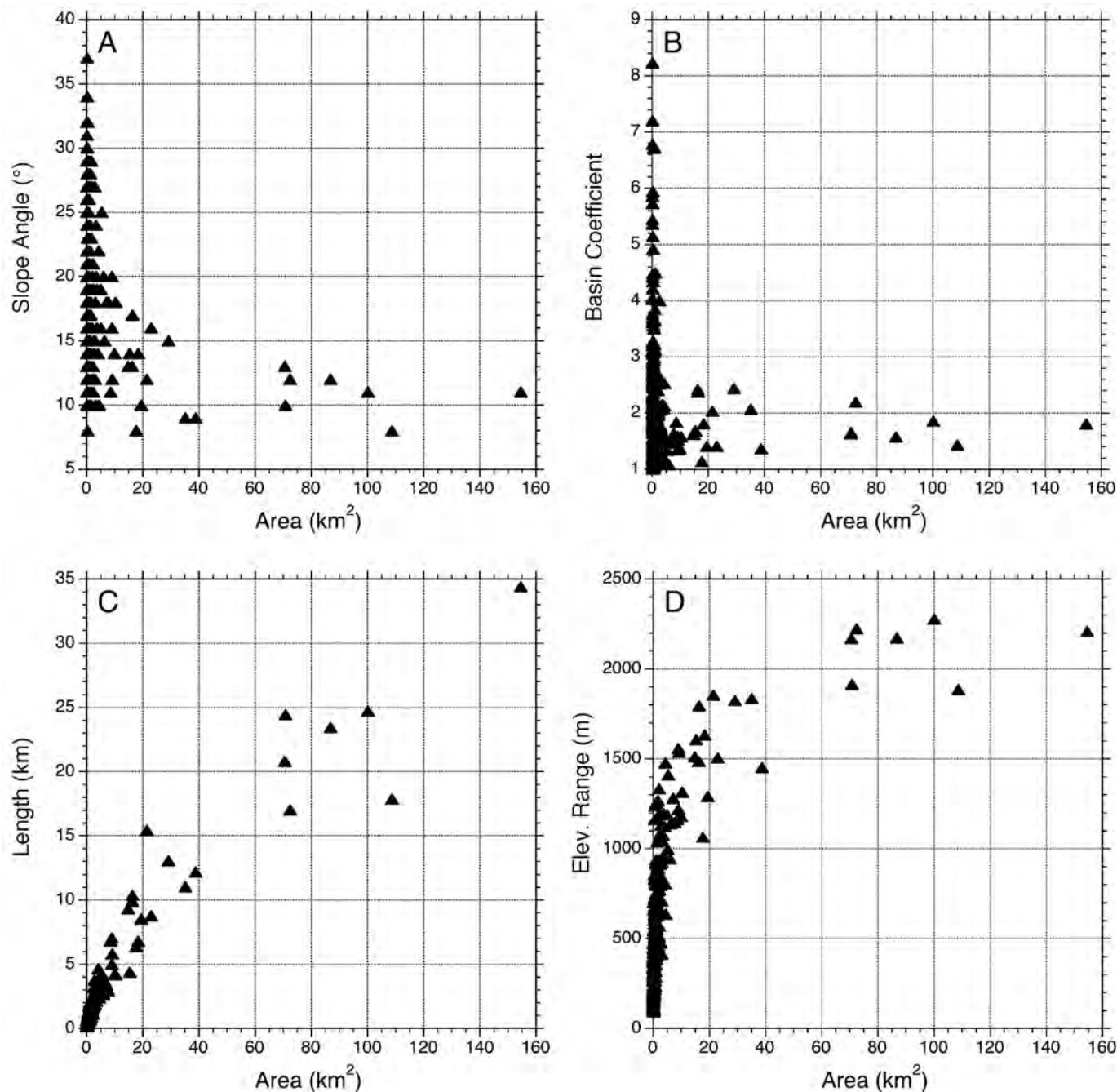
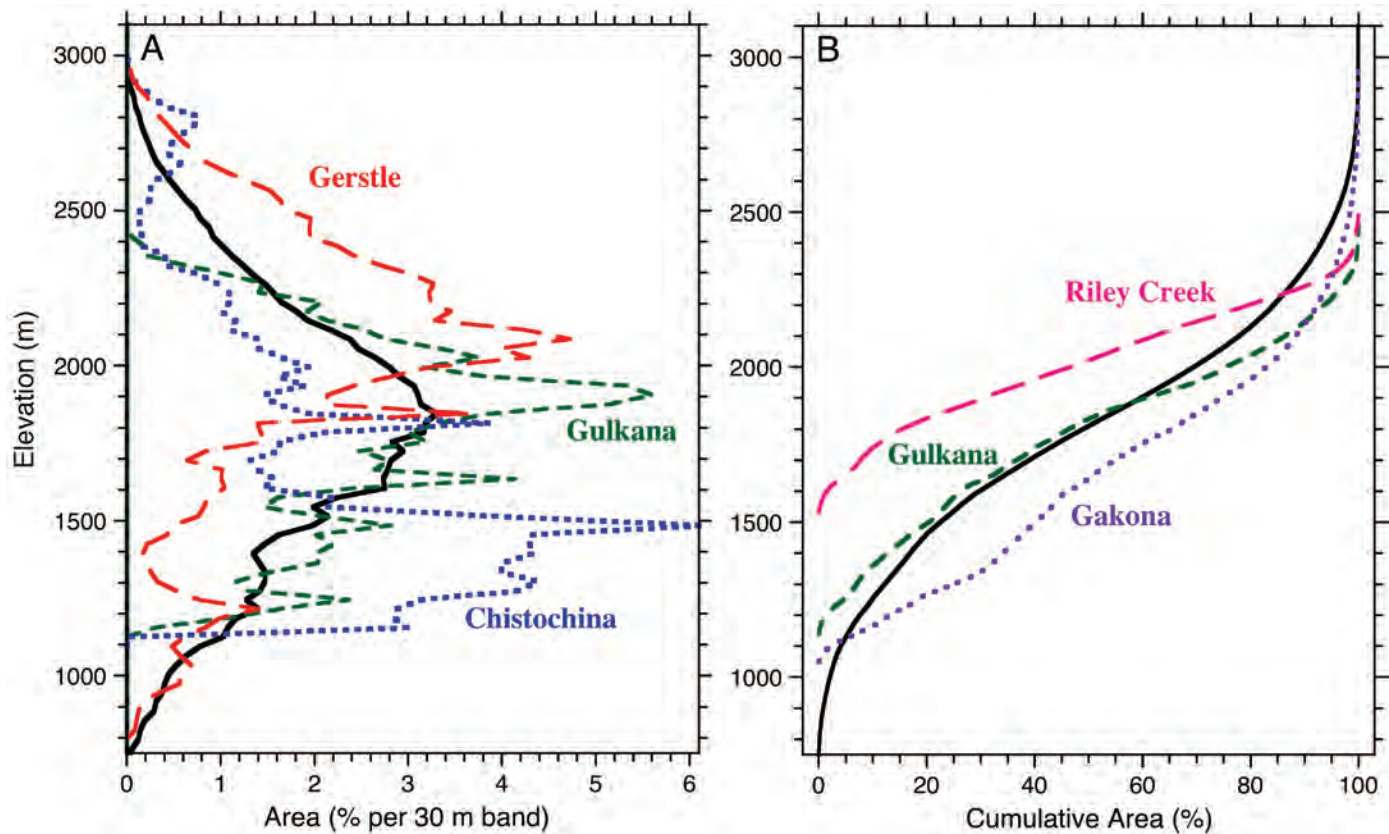


**Figure 402.**—Plots of four geospatial measurements versus glacier area. **A**, Slope angle; **B**, basin coefficient; **C**, length; and **D**, elevation range.

(see “Discussion”). Conversely, the 19 glaciers together cover 950 km<sup>2</sup> or 77 percent of the total glacierized area in the region.

Finally, the area-altitude distribution, or hypsometry, can be plotted and evaluated for selected glaciers and for the region as a whole (fig. 403). Glacier ice integrated across the range displays a normal distribution with elevation and yields a characteristic sigmoidal curve when plotted as cumulative area versus elevation (cf. Arendt and others, 2002). Some glaciers show skewed concentrations of surface area in their higher (for example, Gerstle Glacier) or lower (for example, Chistochina and Gakona Glaciers) reaches. Others such as Gulkana Glacier, do not fully encompass the vertical range of ice in the region but display bell-shaped distributions that mirror the distribution for the range as a whole. Still others yield normal distributions that are shifted above (for example, Riley Creek Glacier) or below the regional curve. Together with climate and flow dynamics, glacier hypsometry is closely linked to mass balance.



### Discussion

Presented here is a new digital inventory of glaciers in the eastern Alaska Range as they existed during the 1948–54 period. Nineteen glaciers were previously detailed by area, length, width, and other parameters (Denton and Field, 1975a). None of the glaciers are currently in the World Glacier Inventory (National Snow and Ice Data Center, 1999, 2003). The region includes Gulkana Glacier, a well-studied “benchmark” glacier (cf. Echelmeyer and others, 1996; Hodge and others, 1998; Molnia, this volume). The geospatial database of glacier extent builds upon extensive mapping and GIS layers produced by the USGS. A total of 279 glaciers (only 19 have formal names) cover an area of 1,229 km<sup>2</sup>. Beyond mapping and visualization, the advantages of using GIS to study these glaciers include the capability of investigating all of the glaciers in the region, statistically analyzing glaciological properties, and sharing the digital inventory for other uses.

Quantitative geospatial analysis is a relatively new approach to studying glacier systems. Studies to date include objective glacier classification, digital inventory, and analysis of change (for example, Allen, 1998; Paul and others, 2002; Kääb and others, 2002; Ommanney, 2002b; Paul, 2003). The technique used here relies on spatial rather than temporal variability. As such, it is complementary to time-series studies of glacier change based on field measurements and (or) remote sensing (cf. Arendt and others, 2002; Paul, 2002, 2003), which are commonly limited to only a limited number of “selected” glaciers in any given glacierized region.

This study takes advantage of a large, comprehensive, empirical dataset. Created from glacier extents shown on 1:63,360-scale USGS topographic quadrangle maps, the spatial dataset includes all glaciers in the eastern Alaska Range at moderately high resolution, including very small ones. The glacier polygons include debris-covered areas, which are problematic for automated processing of satellite imagery. Measurement error for individual glaciers may be higher than that which exists with intensive manual editing. However, semiautomated GIS processing yields a large sample size that reveals coherent patterns among morphologic parameters.

**Figure 403.**—Area-altitude distribution integrated for all glacier ice in the region (black lines) compared with curves for selected glaciers. **A**, Plotted as percent area per 30-m elevation band. **B**, Cumulative area, in percent, versus elevation.

Most of the 15 parameters of glacier morphology are strongly linked to a prominent trend: large glaciers are much less common than small ones. The area of the largest glacier measures 154 km<sup>2</sup>, whereas the median glacier area is only 0.6 km<sup>2</sup>. Glaciers ranging from 0.1 to 1.0 km<sup>2</sup> in size account for 6 percent of the glaciers by area and 67 percent by number. Properties that are correlated with glacier area yield average or median values that are characteristic of small cirque or niche glaciers: the “typical” glacier is almost as long (0.7 km) as it is wide (0.8 km), occupies a small basin (1.1 km<sup>2</sup>), slopes 18° on average, and spans 460 m in elevation. Glaciers in the region have only a weak statistical preference to form north-facing surfaces. The glaciers commonly have “normal” bell-shaped distributions of area versus elevation.

Geospatial data help to address the question “Is Gulkana Glacier generally ‘representative’ of all the glaciers in the region?” In other words, are studies to date on this “benchmark” glacier regionally significant (cf. Echelmeyer and others, 1996; Hodge and others, 1998)? On the one hand, Gulkana Glacier is much larger, longer, wider, elongate, and more gently sloped than the typical glacier and has a greater elevation range and basin size. However, other metrics imply that Gulkana Glacier is indeed “representative” in terms of mass balance. Its median and mean elevations are close to “typical”; more importantly, its elevational distribution (hypsometric curve) is closely similar to that for glacier ice integrated across the region as a whole. At any rate, the issue depends largely on the specific question at hand, and the digital inventory can help to identify additional glaciers for study that are—in various ways—“representative.”

As geospatial analysis of glaciers becomes more common, it will be important to reduce redundant effort and to assure comparability among datasets. In this regard, the digital inventory is available as an attributed vector GIS layer from the Quaternary GIS Laboratory at the Institute of Arctic and Alpine Research (INSTARR), University of Colorado [<http://instaar.colorado.edu/QGISL/>]. The stepwise algorithms are also available and can be applied to other glacierized regions. Among other methodologic issues, the “scripts” help address a fundamental concern: an objective, quantitative, geospatial definition of a “glacier.” The definition is inherently linked to how drainage areas and ice divides are identified. Similarly, parameters such as length and width are dependent in detail on the chosen analytical approach. Hopefully a community consensus or protocol for standardized geospatial processing will emerge, perhaps as part of the Global Land Ice Measurements from Space (GLIMS) Program (Keiffer and others, 2000; Bishop and others, 2004) or as presented in the important Ph.D. dissertation by Paul (2003). The digital inventory is valuable for other studies. Though limited in extent, the database would assist in the regional analysis of the following glacier parameters: (1) derivation of, or application of, scaling relationships to estimate such quantities as thickness, volume, activity index, response times, and so on; (2) analysis and modeling of mass balance, ELAs, and local to regional controls on glacier-climate relationships; (3) analysis and modeling of glacier hazards, meltwater runoff, and contribution to sea-level rise; and (4) studies of glacier change as a decades-old baseline for comparison with recent satellite imagery and other remotely sensed measurements of glacier response to climate change.

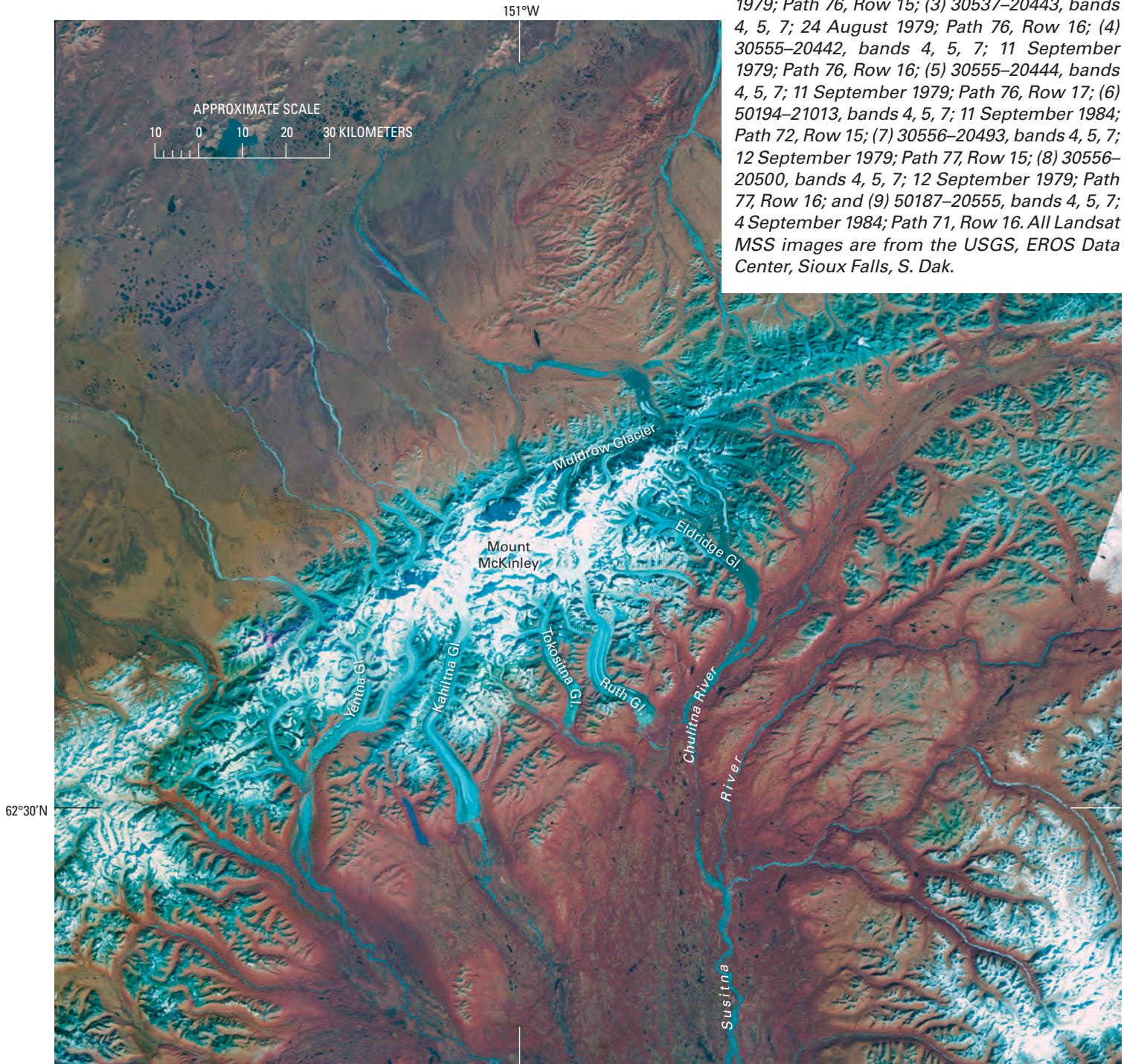
### **Acknowledgments**

Extensive GIS editing and processing were done by Denise Dundon and Evan Burgess (University of Colorado). Thanks also go to Mark F. Meier and Mark B. Dyurgerov (University of Colorado) for guidance and discussions. Most important, this study would not have been possible without the considerable efforts and skills of USGS cartographers and earth scientists involved in the compilation and publication of the topographic quadrangle maps and derived GIS layers.

## The Mount McKinley-Mount Foraker Segment between Broad Pass and Rainy Pass

The Mount McKinley-Mount Foraker segment, which is about 275 km long and almost 80 km wide, contains the highest mountain in North America, Mount McKinley (6,195 m) (Brooks, 1911). Two views of this segment and its glaciers are presented (figs. 404, 405). Although it is officially named Mount McKinley (fig. 406), this mountain is popularly called *Denali*, meaning the *Great* or *High One* in the Athapaskan language. Other high peaks in this region include Mount Foraker (5,303 m), the third highest summit in Alaska; Mount Hunter (4,443 m); Mount Brooks (3,640 m); and Mount Russell (3,558 m). This segment also includes the Kichatna Mountains.

**Figure 404.**—Landsat 3 and 5 MSS false-color infrared composite image mosaic of Mount McKinley area and environs, Alaska Range, Alaska, used for the 1:250,000-scale, experimental satellite image map of Denali National Park and Preserve, Alaska, published by the USGS in 1984. Numerous glaciers are visible on the flanks of the massif. Yentna Glacier (center) shows contorted medial moraines characteristic of a surging glacier. Reddish hues represent various types of vegetation. The following 9 Landsat 3 and 5 MSS images were used to compile the mosaic: (1) 30914–20281, bands 4, 5, 7; 4 September 1980; Path 75, Row 16; (2) 30537–20441, bands 4, 5, 7; 24 August 1979; Path 76, Row 15; (3) 30537–20443, bands 4, 5, 7; 24 August 1979; Path 76, Row 16; (4) 30555–20442, bands 4, 5, 7; 11 September 1979; Path 76, Row 16; (5) 30555–20444, bands 4, 5, 7; 11 September 1979; Path 76, Row 17; (6) 50194–21013, bands 4, 5, 7; 11 September 1984; Path 72, Row 15; (7) 30556–20493, bands 4, 5, 7; 12 September 1979; Path 77, Row 15; (8) 30556–20500, bands 4, 5, 7; 12 September 1979; Path 77, Row 16; and (9) 50187–20555, bands 4, 5, 7; 4 September 1984; Path 71, Row 16. All Landsat MSS images are from the USGS, EROS Data Center, Sioux Falls, S. Dak.



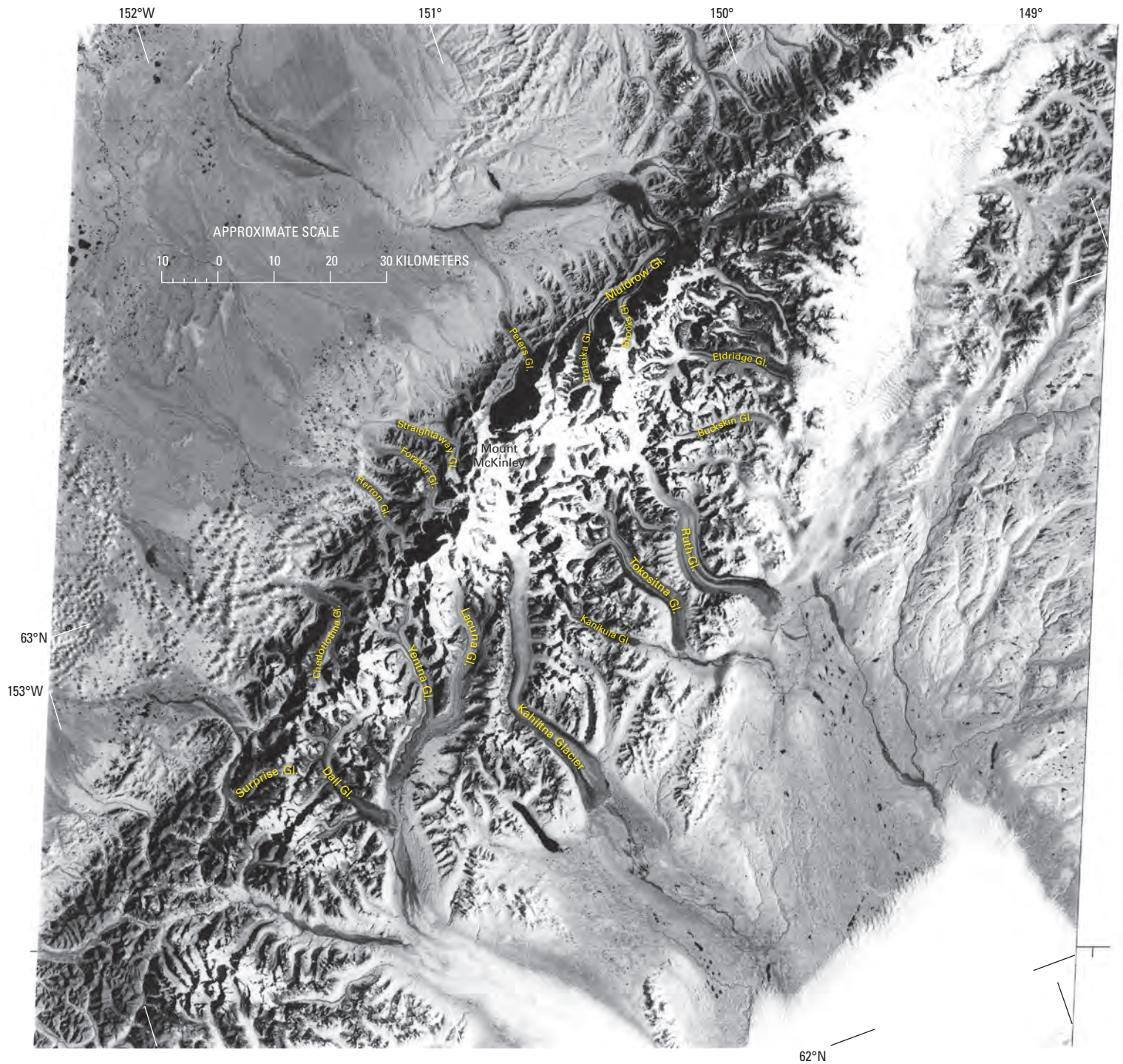


**Figure 405.**—Annotated Landsat 1 MSS image of Mount McKinley and Denali National Park and Preserve. Mount McKinley (6,195 m) supports numerous large glaciers. Many of the glaciers on the northwest side of the McKinley massif, including the Straightaway, Peters, and Muldrow Glaciers. Muldrow Glacier had a strong surge that began in the winter of 1956–1957. During the course of the surge, which lasted less than 1 year, the terminus advanced 6.6 km, and surface levels dropped up to 100 m in the upper glacier area and increased 200 m in the lower glacier (Post, 1960).

The contorted medial moraines of the Muldrow Glacier can be clearly seen on this image. Peters Glacier had a strong surge in 1986. The large glaciers on the south side of the massif — the Kahiltna, Ruth, and Eldridge Glaciers — do not show evidence of surging. The Tokositna Glacier surged in 1971–72 and in 2002–02. Landsat 1 MSS image (5865–19312, band 7; 31 August 1977; Path 77, Row 16) from the USGS, EROS Data Center, Sioux Falls, S. Dak. Landsat image and caption courtesy of Robert M. Krimmel, U.S. Geological Survey.

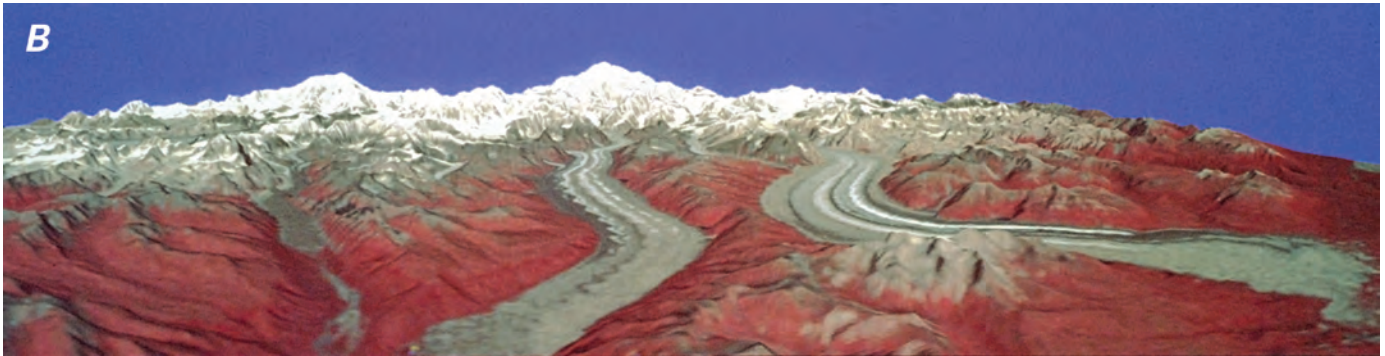


**Figure 406.**—Three views of Mount McKinley. **A**, 1923 photograph by Blanchard of Mount McKinley from the north side of the hummocky stagnant ice terminus of Muldrow Glacier. Photograph Alaska 100 from the USGS Photo Library, Denver, Colo. **B**, A computer-generated north-looking view of the central Alaska Range including Mount McKinley and Mount Foraker produced by combining part of the Landsat image mosaic used in figure 404 with corresponding digital elevation data. The point of view is located about 4,500 m above the Tokositna River. From east to west, key foreground features are: Ruth Glacier, the Tokosha Mountains, Tokositna Glacier, and Kanikula Glacier. Produced by the USGS, EROS Data Center, Sioux Falls, S. Dak., courtesy of the author. **C**, Oblique aerial photograph taken in October 1965 looking towards the summit of Mount McKinley across the snow-covered upper part of the Traleika Glacier (including its West Fork) a major tributary of the Muldrow Glacier. U.S. Air Force Cambridge Research Laboratories photograph taken by T/Sgt. Roland E. Hudson, courtesy of Richard S. Williams, Jr., U.S. Geological Survey.

More than 20 glaciers with lengths of greater than 8 km descend from many isolated peaks to the east and a broad interconnected accumulation area to the west. The unnamed ice field is more than 115 km in length. Six glaciers have lengths of greater than 40 km. From east to west, in a counter-clockwise direction, these are (according to lengths and areas measured by Denton and Field, 1975a, p. 588–590 and p. 593 from USGS maps): Muldrow Glacier (fig. 407) (61 km, 516 km<sup>2</sup>); Yentna Glacier (51 km, 487 km<sup>2</sup>); Kahiltna Glacier (76 km, 580 km<sup>2</sup>); Tokositna Glacier (fig. 408) (44 km, 240 km<sup>2</sup>); Ruth Glacier (63 km, 449 km<sup>2</sup>); and Eldridge Glacier (48 km, 485 km<sup>2</sup>). Many of the glaciers in this segment surge, including Tokositna, Lacuna, Yentna, Straightaway, Peters, and Muldrow Glaciers. These glaciers and many others show multiple evidence of surging. Tokositna, Lacuna, and Yentna Glaciers have large looped and folded moraines (Meier, 1976) that result from long periods of near stagnation alternating with brief periods of extremely high surge flow.

Beginning on the northern side of the unnamed ice field, moving counter-clockwise from east to west, the major glaciers are listed with approximate lengths and approximate areas measured by Denton and Field (1975a, p. 588–593) from USGS maps: (1) an unnamed glacier draining to the East Fork Toklat River; (2) Polychrome Glacier; (3) an unnamed glacier draining to the Toklat River (8 km, 15 km<sup>2</sup>), which, on an annual basis between the middle 1950s and the middle 1990s, thinned by 1.82 m a<sup>-1</sup> and decreased in volume by 0.016 km<sup>3</sup> a<sup>-1</sup> (K.A. Echelmeyer, W.D. Harrison, V.B. Valentine, and S.I. Zirnheld, University of Alaska Fairbanks, written commun. March 2001); (4) Sunset Glacier (9 km, 9 km<sup>2</sup>); (5) Muldrow Glacier (61 km, 516 km<sup>2</sup>); (6) Peters Glacier (27 km, 123 km<sup>2</sup>), which surged in 1986; (7) an unnamed glacier draining into Slippery Creek (8 km, 11 km<sup>2</sup>); (8) Straightaway Glacier (fig. 409) (22 km, 71 km<sup>2</sup>); (9) Foraker Glacier (fig. 410) (25 km, 74 km<sup>2</sup>); (10) Herron Glacier (25 km, 79 km<sup>2</sup>); (11) an unnamed glacier draining into Swift Fork (8 km, 27 km<sup>2</sup>); (12) Chedotlothna Glacier (see 1925 Capps photograph, USGS Photo Library photograph Capps 1103) (27 km, 97 km<sup>2</sup>); (13) an unnamed glacier draining into Ripsnorter Creek (7 km, 8 km<sup>2</sup>); (14) Surprise Glacier (15 km, 47 km<sup>2</sup>), which has retreated more than 2 km since 1958, opening an ice-marginal lake adjacent to

**Figure 407.**—13 September 1986 oblique aerial photograph of Muldrow Glacier, the largest glacier on the north side of Mount McKinley; it had a major surge from 1956 to 1957. The aerial photograph shows only the middle part of the glacier; the lower glacier extends another 15 to 20 km beyond the photograph to the right. The large, arcuate moraine loop in the foreground was displaced to its present position from in front of the major left tributary in the middle of the photograph by the 1957 surge (Post, 1960). Presumably, the foreground loop will be displaced downglacier and replaced by the loop now forming in front of the major left tributary during the next surge. Photograph no. 86-R3-182 and caption courtesy of Robert M. Krimmel, U.S. Geological Survey.





**Figure 408.**—Oblique aerial photograph of Tokositna Glacier on 30 August 1984; the glacier is located on the south side of Mount McKinley and has frequent minor surges. This view, looking down the glacier, shows well the characteristic contorted medial moraines of surging glaciers. These features on the Tokositna Glacier are barely large enough to be seen on the Landsat MSS image mosaic (fig. 404) and image (fig. 405). Photograph no. 84–R2–248, 30 August 1984, by Robert M. Krimmel, U.S. Geological Survey.



▲ **Figure 409.**—14 September 1999 north-looking oblique aerial photograph of the terminus area of Straightaway Glacier showing its hummocky, debris-covered surface and the development of thermokarst features. A vegetation-covered lateral moraine has developed on the east side of the glacier. Photograph by Bruce F. Molnia, U.S. Geological Survey. A larger version of this figure is available online.



◀ **Figure 410.**—14 September 1999 northwest-looking oblique aerial photograph of the terminus area of Foraker Glacier showing its hummocky, debris-covered surface and the development of thermokarst features. Of all the large glaciers observed in 1999 flowing out of the Alaska Range, Foraker Glacier appeared to have experienced the greatest amount of recent thinning and retreat, thinning by as much as 75 m. Photograph by Bruce F. Molnia, U.S. Geological Survey.

its terminus; (15) an unnamed glacier draining from Mount Dall (16 km, 55 km<sup>2</sup>); (16) Dall Glacier (36 km, 243 km<sup>2</sup>); (17) Yentna Glacier (fig. 411) (51 km, 487 km<sup>2</sup>), which surged in 1972 and again in 2000, while its major tributary, Lacuna Glacier (fig. 412), which had been stagnant for about 60 years, surged in 2001; (18) an unnamed glacier (10 km, 25 km<sup>2</sup>); (19) an unnamed glacier (10 km, 14 km<sup>2</sup>); (20) the stagnant Kahiltna Glacier (76 km, 580 km<sup>2</sup>) (see 1910 Capps photograph, USGS Photographic Library photograph Capps 312), some of whose unnamed tributaries were studied and photographed by Capps in 1910 (fig. 413); (21) Kanikula Glacier (18 km, 48 km<sup>2</sup>); (22) Tokositna Glacier (44 km, 240 km<sup>2</sup>), which surges about every 25 to 30 years; (23) Ruth Glacier (fig. 414) (63 km, 449 km<sup>2</sup>); (24) an unnamed glacier at the head of the Coffee River (11 km, 11 km<sup>2</sup>); (25) Buckskin Glacier (23 km,



47 km<sup>2</sup>), which retreated more than 2 km between 1958 and 1999; (26) Eldridge Glacier (48 km, 485 km<sup>2</sup>); and (27) two unnamed glaciers draining into Ohio Creek, one having a length of 8 km and an area of 12 km<sup>2</sup> and the other having a length of 14 km and an area of 17 km<sup>2</sup>. Other glaciers, the lengths and (or) areas of which have been estimated by the author, are the 6-km-long West Fork Glacier (one of three glaciers with that name in Alaska) and an unnamed glacier that drains into Boulder Creek that has a length of about 8 km and an area of about 10 km<sup>2</sup> and originates from an isolated unnamed peak west of Chedotlothna Glacier.



**Figure 411.**—31 August 1967 north-looking oblique aerial photograph of the upper part of Yentna Glacier at an elevation of approximately 1,600 m. Although trimlines are close to the ice surface, elevated lateral and medial moraines and a thick marginal sediment zone on many tributaries suggest that the Yentna Glacier has undergone some recent thinning. Because the date of this aerial photograph is 5 years prior to the 1972 surge, it is doubtful that any of the thinning seen here is related to surge drawdown. Photograph no. 67-R3-67 by Austin Post, U.S. Geological Survey.



**Figure 412.**—31 August 1967 north-looking oblique aerial photograph of the upper part of Lacuna Glacier at an elevation of approximately 1,500 m. Folded loop moraines provide evidence of a past surge. Trimlines and elevated lateral and medial moraines suggest that the glacier has experienced recent thinning. Few glaciers have the number of potholes that are seen on the surface of this glacier. Photograph 67-R3-60 by Austin Post, U.S. Geological Survey.



**Figure 413.**—Two 1910 photographs by S.R. Capps mosaicked to show two unnamed retreating glaciers located at the head of Hidden Creek, a 9-km-long eastern tributary to the valley of the Kahiltna Glacier. Both glaciers have elevated lateral moraines and are fronted by large debris aprons. Photographs Capps 306 and 307 from the USGS Photo Library, Denver, Colo.



**Figure 414.**—**A**, 4 September 1966 north-looking oblique aerial photograph of The Great Gorge of Ruth Glacier, with Mount McKinley in the background. Elevated lateral moraines located on both sides of the valley suggest that here, more than 30 km above the terminus, at an elevation of approximately 1,000 m, recent thinning has occurred. Photograph no. 665–82 by Austin Post, U.S. Geological Survey. **B**, 14 September 1999 south-looking oblique aerial photograph of a large thermokarst lake in the central terminus area of Ruth Glacier. This lake is the result of the coalescence of many individual thermokarst pits. Photograph by Bruce F. Molnia, U.S. Geological Survey.



## **Tokositna Glacier**

Tokositna Glacier surged in 1970 and in 1972. Neither surge resulted in the displacement of the terminus. Essentially stagnant since the end of the surge in 1972, Tokositna suddenly began surging in late February 2001, moving forward at a rate of approximately  $2 \text{ m d}^{-1}$ . The 1971–72 surge resulted in about 2 km of displacement. The 2001 surge produced significantly less displacement and did not impact the terminus. Before the early 1970s surge, Post (1969) had identified Tokositna Glacier as a surge-type glacier on the basis of contorted moraines that resulted from a pre-1957 surge.

## **Polychrome Glacier**

Polychrome Glacier, a north-flowing 4-km-long valley glacier at the eastern end of this group of glaciers, discharges into an unnamed eastern fork of the Toklat River; it was mapped by the AGS during the IGY (AGS, 1960). In the notes accompanying the map, Post (AGS, 1960, p. 21) described an ablation moraine covering the lower 1.5 km of the glacier that effectively protected the covered ice so that “little or no retreat was evident.” Post (AGS, 1960, p. 21) also noted that almost no snow remained from the previous winter and that he doubted if “the glacier had experienced a positive snow budget for many years at any point in the basin.” In 1995, Polychrome Glacier was re-surveyed by a geodetic airborne laser altimeter profiler (Sapiano and others, 1998). A comparison of two profiles collected on 28 June 1995 with profiles constructed from a 1957 map showed that the 1995 terminus of Polychrome Glacier was very close to its 1957 position, a change of  $10 \pm 5 \text{ m}$  during the 38 years between surveys. The glacier’s area, however, had decreased from  $1.84 \text{ km}^2$  in 1957 to  $1.7 \text{ km}^2$  in 1995, a decrease of about 9 percent. The glacier had thinned an average of 8.5 m, its volume had decreased by  $1.5 \times 10^7 \text{ m}^3$ , and its average annual mass balance was  $-0.2 \text{ m}$ .

## **Muldrow Glacier**

Muldrow Glacier (figs. 405, 406, 407) flows to the northeast from high on the slopes of Mount McKinley, ending at a moraine-covered terminus near the Eielson Visitors Center in Denali National Park. Two named tributary glaciers, Brooks and Traleika Glaciers (fig. 406C), are the primary sources of ice for Muldrow Glacier. From May of 1956 through the summer of 1957, Muldrow Glacier surged a distance of about 6.6 km (Post, 1960). The maximum observed velocity during the peak of movement was about  $350 \text{ m d}^{-1}$  or about  $24 \text{ cm min}^{-1}$ . The glacier surface elevation decreased up to 100 m in the upper glacier area and increased 200 m in the lower glacier. For almost a decade before the surge, a wave of thickening ice moved down the upper part of the glacier at a rate of approximately  $0.75 \text{ m d}^{-1}$ . Post (1960), who described the 1956–57 surge, reported that an analysis of moraine patterns on the surface of Muldrow Glacier suggests that at least four prior surges have occurred within the past several hundred years, the most recent pre-1956 surge occurring between 1906 and 1912. A large moraine visible from the Eielson Visitors Center was formed by a late 16th or early 17th century advance that represents the “Little Ice Age” maximum position of Muldrow Glacier. Ice stagnation and retreat followed, but, about 150 years ago, the recession was interrupted by a new surge that deposited a second set of moraines approximately 1.5 to 4.5 km behind the 16th or 17th century moraines. The 1957 surge overrode much of the second set of moraines and reached to within 5 km of the park road. In 1976 and 1977, Bradford Washburn, acting on the recommendation of the Swiss glaciologist Fritz Müller and working jointly with the Museum of Science (Boston, Massachusetts) and the Swiss Foundation for Alpine Research, mapped the lower 37 km of the Muldrow Glacier from vertical aerial photographs acquired on 21 August 1976 by Air Photo Tech of Anchorage, Alaska (Field, 1990). The orthophoto contour map, which has a 10-m contour interval on the glacier (20-m contours on steep off-glacier topography), was published as five 1:10,000-scale sheets, each covering about  $8 \times 10 \text{ km}$  (Washburn, 1983).

When the author observed it from the air in 1978, in September 1999, and on 3 September 2002, vegetation covered the ablating, stagnant, ice-cored moraine for a distance of 2 km or more from the glacier's terminus. For the next 15 km further upglacier, this continuous morainic cover graded into areas of debris-covered stagnant ice and bare ice. More than 25 km further upglacier, the glacier's surface was a mixture of bare ice and contorted moraines.

### Kichatna Mountains

The Kichatna Mountains (fig. 415A, B) support several dozen glaciers, seven of which are more than 8 km long. Many of the smaller glaciers, which sit in cirques or small valleys, were retreating when they were first observed at the start of the 20th century (fig. 415A). The largest radiate like claws from the northern flanks of Augustin Peak, Gurney Peak, Cathedral Spires, and Lewis Peak. The glaciers, whose lengths and areas have been measured by Denton and Field (1975a, p. 590–591), include four unnamed glaciers (8 km, 9 km<sup>2</sup>; 10 km, 21 km<sup>2</sup>; 15 km, 26 km<sup>2</sup>; about 6 km, about 5 km<sup>2</sup>, estimated by the author); Shadows Glacier (14 km, 24 km<sup>2</sup>); Cul-de-sac Glacier (12 km, 14 km<sup>2</sup>); and Tatina Glacier (10 km, 11 km<sup>2</sup>).

Glaciers of this area were used to compare the capabilities of two of the first satellite remote sensing systems and their ability to resolve glaciological



**Figure 415.** — Two views of cirque and small valley glaciers in the Kichatna Mountains. **A**, 1902 panoramic photographs by A.H. Brooks of several glaciers in the south-central Kichatna Mountains, probably east of Caldwell Glacier. The unnamed glaciers show multiple evidence of retreat and thinning. Photographs Capps 878 and 879 from the USGS Photo Library, Denver, Colo. **B**, 24 August 1979 east-looking oblique aerial photograph of the summits of several unnamed, approximately 2,000-m-high Kichatna Mountains peaks adjacent to Augustin Peak. Because only the snow-covered heads of these glaciers can be seen, the status of their terminus regions cannot be determined. Photograph no.79-R2-233 by Austin Post, U.S. Geological Survey.



features from space. Hall and Ormsby (1983) compared a Landsat image (30177–20455, 29 August 1978) of the Alaska Range and a SEASAT SAR image (03800083, 23 July 1978) that was also analyzed by Ford and others (1980). Both images show glaciers in the area. They concluded that Landsat and SEASAT SAR images were equally useful in determining the position of glacier termini, delineating medial moraines, and depicting terminal moraine areas. Landsat images can be used to determine the snowline; SEASAT SAR images cannot. Ford (1984) was also able to delineate glacial lakes, fluted ridges, and drumlinized topography along the valleys of the Chulitna and Tokositna Rivers.

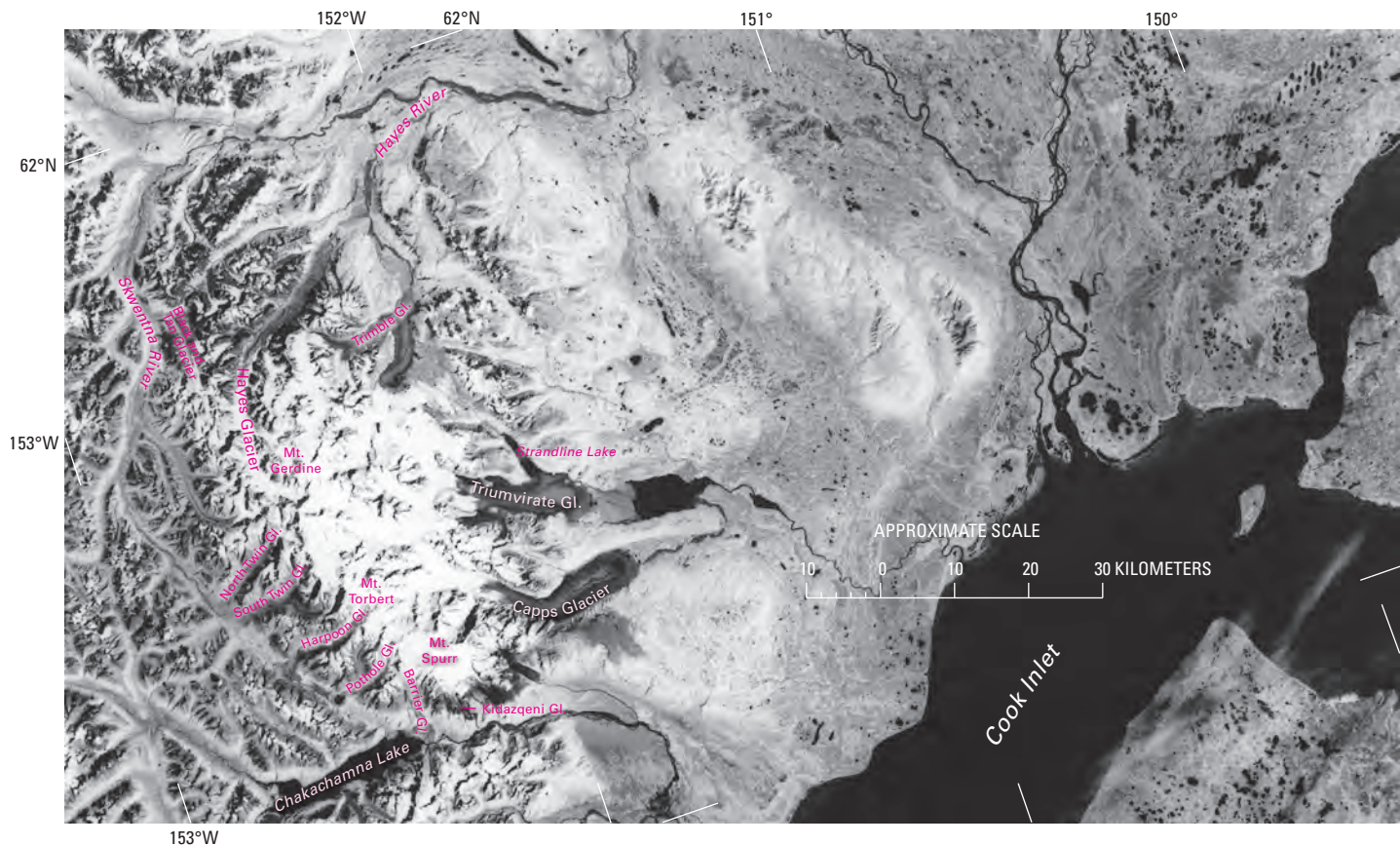
### The Mount Gerdine-Mount Spurr Segment between Rainy Pass and Merrill Pass

This segment, which has a maximum length of approximately 140 km, includes the Tordrillo Mountains, which hosts both the largest concentrations of glacier ice and the largest glaciers; the Terra Cotta Mountains; the Revelation Mountains; and some isolated accumulation areas from which a number of small glaciers descend.

Peaks of the Tordrillo Mountains that support large glaciers include Mount Torbert (3,480 m), Mount Gerdine (3,432 m) and Mount Spurr (3,374 m) (fig. 416), the only active volcano in the Alaska Range. More than 15 glaciers longer than 8 km descend from a broad interconnected accumulation area more than 45 km long and located between Hayes River and Chakachamna Lake. The three longest—Hayes, Triumvirate, and Capps Glaciers—all drain eastward and are longer than 40 km (Denton and Field, 1975a, p. 595–596).

The named glaciers of the Tordrillo Mountains, whose lengths and areas have been measured by Denton and Field, 1975a, p. 595–597, are (from the north in a clockwise direction): Hayes Glacier (48 km, 207 km<sup>2</sup>), which is known to surge (fig. 417A) and originates on the western side of Mount Gerdine; Trimble Glacier (33 km, 286 km<sup>2</sup>) (fig. 417B), which originates on the eastern side of Mount Gerdine, Triumvirate Glacier (45 km, 402 km<sup>2</sup>)

**Figure 416.**—Annotated Landsat 2 image of the Tordrillo Mountains, southwestern Alaska Range. There are numerous ice-dammed lakes, surge-type glaciers, and glaciers on volcanoes in this area. Chakachamna Lake has not been ice-dammed in recent years; however, an advance of the Barrier Glacier or a debris flow from Mount Spurr, which had major eruptive activity in 1953 and was becoming active again in 2004, could easily dam the lake again. Strandline Lake has a history of repeated jökulhlaups (Juhle and Coulter, 1955; Post and Mayo, 1971; Sturm and Benson, 1985). The Hayes Glacier is known to surge (Post, 1969), as does the Harpoon Glacier, which was actively surging in 1984. This Landsat image barely shows the characteristic contorted medial moraines of surge-type glaciers on the Hayes, Harpoon, and Capps Glaciers. Landsat 2 MSS image (21288–20253, band 7; 2 August 1978; Path 76, Row 17) from the USGS, EROS Data Center, Sioux Falls, S. Dak. Landsat image and caption courtesy of Robert M. Krimmel, U.S. Geological Survey.



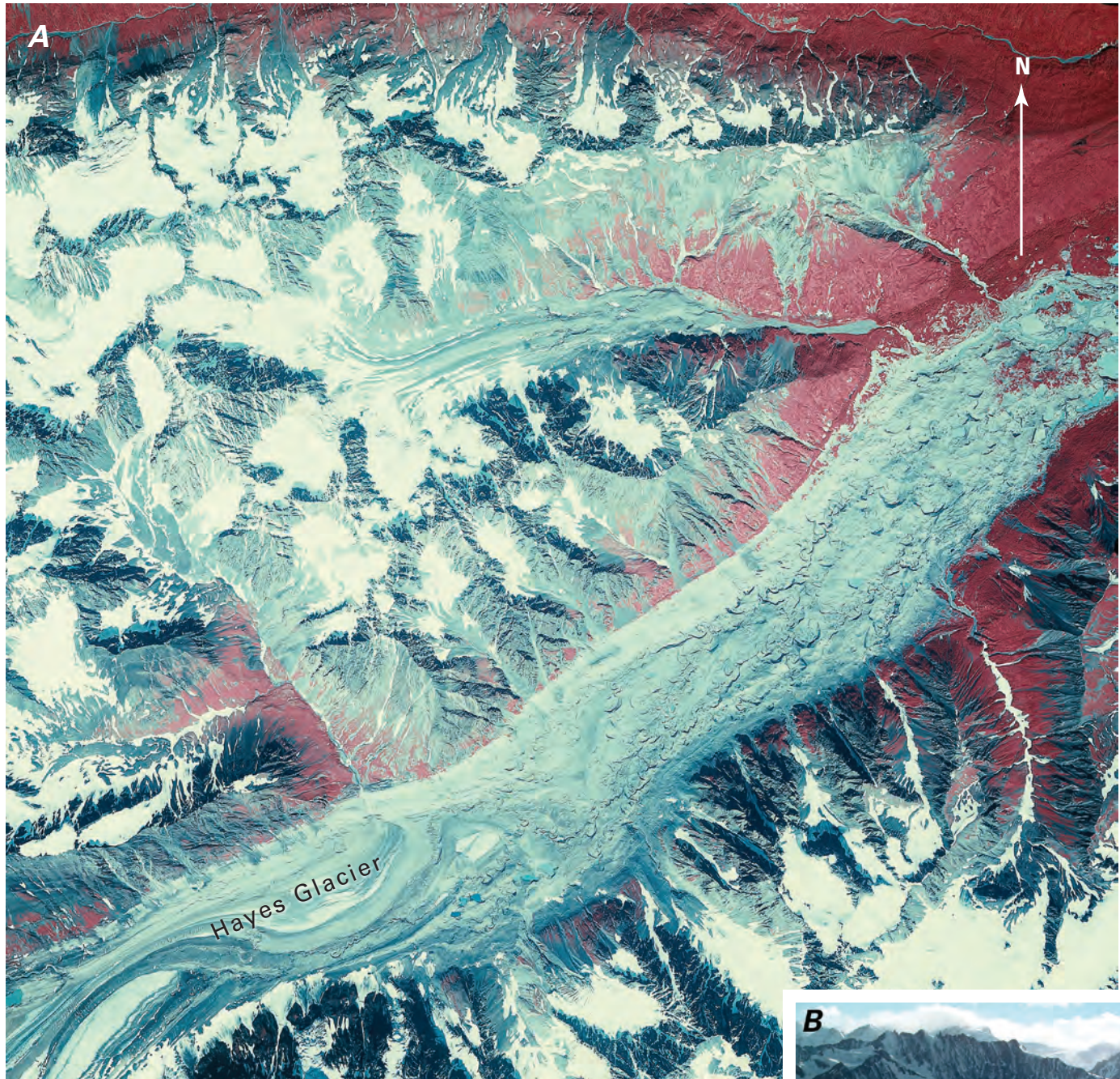


**Figure 417.**—**A**, 20 July 1982 annotated AHAP false-color infrared vertical aerial photograph of the lower part and terminus of the Hayes Glacier, an unnamed glacier to the north, and a number of cirques containing small glaciers. Hayes Glacier shows multiple evidence of stagnant ice, retreat, and thinning, including the growth of vegetation on its terminus. The surface of its lower 15 km is mantled by ablation debris and is covered by hundreds of thermokarst pits and lakes. Trimlines rim the two glaciers. The cirques are either deglaciated or the glaciers have retreated so much that they no longer make contact with Hayes Glacier or the unnamed glacier. AHAP photograph no. L102F9235 from the GeoData Center, Geophysical Institute, University of Alaska, Fairbanks, Alaska. **B**, 8 September 2000 west-looking oblique aerial photograph of the upper part (North Branch) of the Trimble Glacier showing a distinct trimline and sediment accumulation on the southern margin of the glacier. Photograph by William R. Reckert, Volunteer for Science, U.S. Geological Survey. A larger version of B is available online.



(fig. 418), which originates on the southern side of Mount Gerdine and from the flanks of a number of unnamed peaks. It has a small northern distributary that dams Strandline Lake, which has a history of repeated glacier outburst floods (jökulhlaups) (Juhle and Coulter, 1955; Post and Mayo, 1971; Sturm and Benson, 1985). Continuing clockwise is (1) Capps Glacier (fig. 419) (42 km, 293 km<sup>2</sup>), originating on the eastern side of Mount Torbert and the northern side of Mount Spurr [Capps Glacier was reported to be surging during September 2000 by Austin Post (oral commun., 8 September 2000), but the surge was not affecting the terminus region]; (2) an unnamed glacier

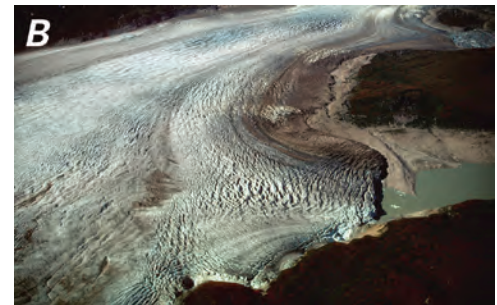


**Figure 418.**—Two 8 September 2000 oblique aerial photographs of the terminus of Triumvirate Glacier showing multiple evidence of stagnant ice, retreat, and thinning. **A**, West view upglacier from above the outwash plain that fronts the glacier and its sequence of multiple, recessional moraines, many with interlobe lakes. Other features include the development of a hummocky pitted surface, large trimlines, a large ice-marginal lake, Strandline Lake, and significant accumulations of glacio-fluvial sediments along the margins of the glacier. **B**, View of the retreating ice margin adjacent to Strandline Lake and to a second lake to the west. Continued thinning of Triumvirate Glacier results in a lowering of the surface level of both lakes. The water level in both lakes is low enough that water is no longer flowing along the northern margin of the glacier. In the past, a thicker glacier would block the outflow from both lakes resulting in a period of glacier outburst floods (jökulhlaups). Photographs by William R. Reckert, Volunteer for Science, U.S. Geological Survey. A larger version of B is available online.

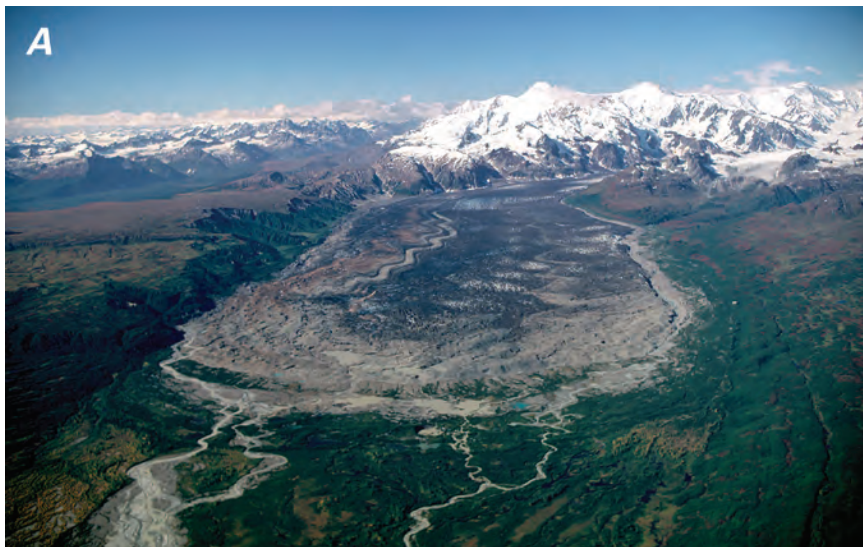


**Figure 419.**—Two 8 September 2000 oblique aerial photographs of Capps Glacier. **A**, View looking west across the terminus of Capps Glacier showing evidence of stagnant ice, retreat, and thinning, including the development of a hummocky pitted surface with thermokarst lakes, trimlines, an ice-marginal lake, and large volumes of sediment accumulating along the margins of the glacier. The folded medial moraines are indicative of past surge behavior. Photograph by William R. Reckert, Volunteer for Science, U.S. Geological Survey. **B**, Oblique aerial photograph looking southwest across the central part of the glacier showing the fractured vertical margin and shattered surface indicative of a surge in the middle part of the glacier. Photograph no. C-26 by Austin Post, U.S. Geological Survey. A larger version of B is available online.





**Figure 420.**—Three photographs of Kidazqeni Glacier. **A**, September 1966 northwest-looking oblique aerial photograph of the summits of Mount Spurr and Crater Peak showing two glaciers on the south side of Mount Spurr. The eastern one, incorrectly mapped as Kidazgeni (with a g) Glacier in 1958 is actually unnamed. The western glacier is Kidazqeni Glacier (with a q). The unnamed glacier has a heavily tephra-covered piedmont lobe. Aside from exposed bedrock in its bed, an elevated lateral moraine on its west side, a small barren halo around the terminus of Kidazqeni Glacier, and an elevated lateral moraine on the east side of the unnamed glacier, neither glacier shows significant evidence of thinning or retreat. In the 8 years between the 1958 map and the photograph, no change could be detected in either glacier. Photograph no. 666-6 by Austin Post, U.S. Geological Survey. **B**, 2 September 1970 north-looking oblique aerial photograph of the summit of Crater Peak and Kidazqeni Glacier. Steam is rising from Crater Peak. In the 4 years between photographs, no significant change could be detected in Kidazqeni Glacier. Photograph no. 7OR2-252 by Austin Post, U.S. Geological Survey. **C**, 22 September 1992 oblique aerial photograph of the summit of Mount Spurr and Kidazqeni Glacier. In the 22 years since the 1970 photograph, the debris-covered, ice-marginal zone has retreated slightly from an end moraine that has developed adjacent to the terminus of the glacier and the individual ogive ridges have become muted. Photograph no. 92-V4-130 by Austin Post, U.S. Geological Survey. Larger versions of A and C are available online.

(14 km, 33 km<sup>2</sup>) originating on the southeastern side of Mount Spurr and forming the headwaters of Straight Creek; (3) a tephra-covered unnamed glacier draining from Crater Peak (fig. 420) (10 km, 27 km<sup>2</sup>), incorrectly labeled as Kidazgeni (with a 'g') Glacier on the USGS 1:63,000-scale Tyonek A-6, Alaska (1958) topographic map, originating on the southern side of Mount Spurr; (4) Kidazqeni Glacier (fig. 420) (9 km, 10 km<sup>2</sup>), correctly labeled on the USGS 1:250,000-scale Tyonek, Alaska (1958) topographic map; (5) Barrier Glacier (fig. 421) (see 22 September 1992 vertical aerial photograph by Austin Post, USGS photograph no. 92V4-98), (15 km, 49 km<sup>2</sup>), which originates on the western and northern sides of Mount Spurr, so named because it obstructs the flow of water in the Neacola River–Chakachatna River drainage system, forming Chakachamna Lake; (6) stagnant Pothole Glacier (14 km, 56 km<sup>2</sup>), which originates on the unnamed accumulation area located between Mount Spurr and Mount Torbert; (7) Harpoon Glacier (13 km, 21 km<sup>2</sup>), which heads

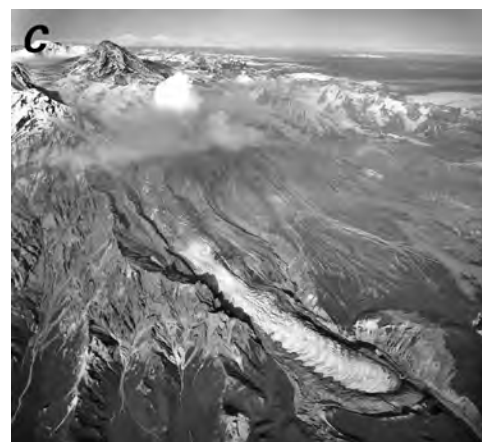
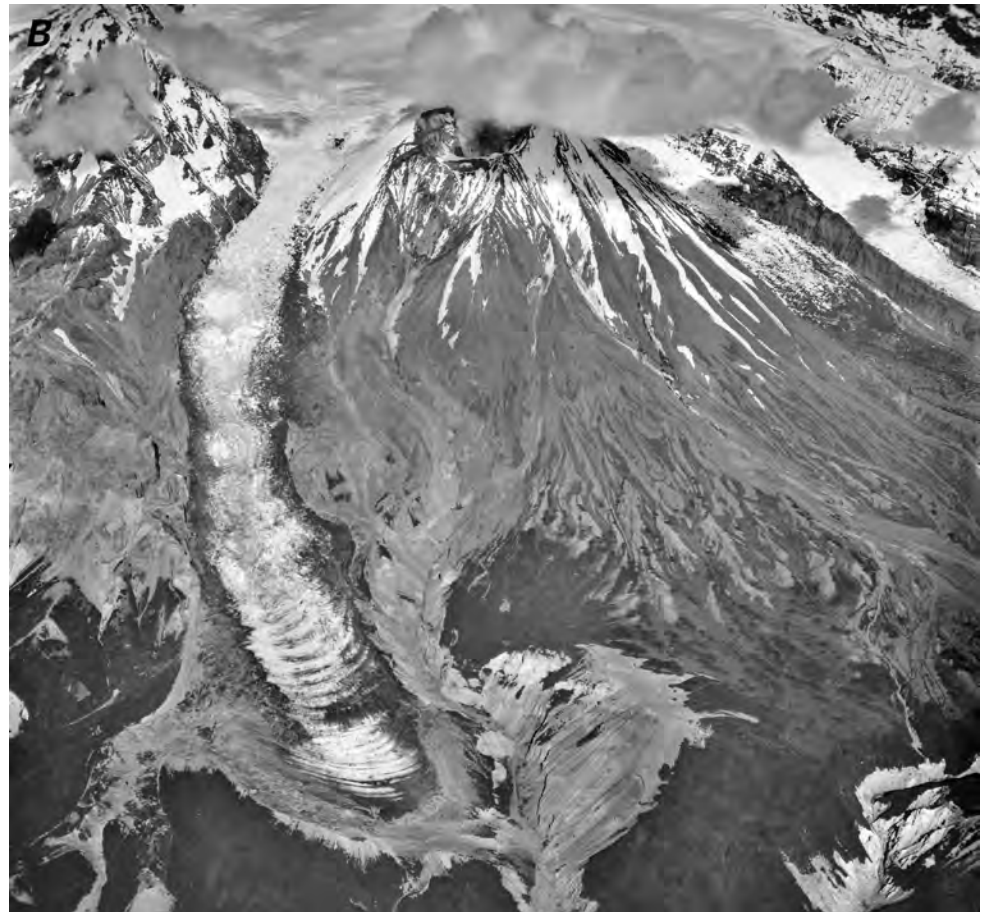




**Figure 421.** — Two photographs of Barrier Glacier. **A**, 4 September 1966 north-west-looking oblique aerial photograph of the summit of Mount Spurr and Barrier Glacier. The southern debris-covered part of the glacier's terminus is the barrier at the head of the Chakachatna River, creating Chakachamna Lake. A trimline on the west side of the glacier, a lobate ice-margin separated by as much as 75 m from its end moraine, and the development of a hummocky, pitted surface on its southern lobe are signs that Barrier Glacier has experienced recent thinning and retreat. In the 8 years between a USGS map (1958; Tyonek A-7) and the photograph, no change could be detected in the glacier. Photograph no. 666-9 by Austin Post, U.S. Geological Survey. **B**, 8 September 2000 oblique aerial photograph looking northeast across the terminus of Barrier Glacier. Although there has been no change in the position of the debris-covered terminus of the glacier, its surface has been lowered and its bare ice, finger-like lobes continue to retreat. Photograph by William R. Reckert, Volunteer for Science, U.S. Geological Survey. A larger version of B is available online.



on the western side of Mount Torbert and was surging in 1984 (see 4 August 1925 Capps photographs, USGS Photographic Library photographs Capps 1172 and 1173); (8) South Twin Glacier (15 km, 33 km<sup>2</sup>); which heads in several cirques located on the western margin of an unnamed accumulation area between Mount Torbert and Mount Gerdine; (9) North Twin Glacier (see 4 August 1925 Capps photograph, USGS Photographic Library photograph Capps 1169) (16 km, 34 km<sup>2</sup>), which heads in several cirques located on the southwestern flank of Mount Gerdine; (10) a debris-covered unnamed glacier (19 km, 62 km<sup>2</sup>), which drains into the Skwentna River and heads in several isolated cirques west of Mount Gerdine; and (11) Black and Tan Glacier (see 20 July Capps photographs, USGS Photographic Library photographs Capps 1142 and 1143, and 20 July 1982 AHAP false-color infrared vertical aerial photograph no. L102F9238) (17 km, 20 km<sup>2</sup>), which drains into the Skwentna River, and heads in several isolated cirques northwest of Mount Gerdine.

In August 1925, Capps photographed several small valley glaciers at a location that he called the head of *Tumbling Creek*, a tributary to the Skwentna River. All showed significant evidence of recent thinning and retreat (see August 1925 Capps photograph, USGS Photographic Library photograph Capps 1149). Because the name *Tumbling Creek* was never formally adopted, the exact location of these glaciers is not known. Photograph numbers indicate that they are probably located between North Twin Glacier and Black and Tan Glacier on the eastern side of the Skwentna River.

Mount Spurr is an active glacier-covered Quaternary stratovolcano located at the southern end of the Alaska Range and the northeastern end of the Aleutian volcanic arc (figs. 1, 420A, C). Crater Peak (2,309 m) (fig. 420A, B), a parasitic spatter cone, was the source of recent activity (Riehle, 1985) in 1953 and 1992, when eruptions deposited tephra on glaciers to the east and generated lahars that affected the glaciers on the southern side of the mountain. The eruption that began on 9 July 1953 produced a glacier-covering tephra blanket about 4 mm thick at Anchorage and detectable up to 350 km to the east (Wilcox, 1953). Lahars, including entrained snow and glacier ice, swept down valleys on the southern flank and dammed the Chakachatna River, which raised the level of Chakachamna Lake at least 3 m (Juhle and Coulter, 1955). The 1992 eruption began on 27 June 1992 and lasted more than 3 months. Westerly winds carried tephra to the east and deposited a tephra layer on glaciers as far east as Yakutat. Up to 3 mm of sand-sized tephra fell in Anchorage, while coastal communities more than 1,000 km away reported dustings of fine-grained tephra (Neal and others, 1992). On 16 September 1992, pyroclastic flows entrained snow and other surface debris and formed lahars that again temporarily dammed the Chakachatna River. Beginning in the summer of 2004, Mount Spurr began a new period of activity, including an increase in seismicity and the melting of glacier ice that covered its summit.

In the Tordrillo Mountains, many of the smaller valley glaciers and small cirque glaciers show multiple evidence of recent thinning and retreat (see 20 July 1980 AHAP false-color infrared vertical aerial photograph no. L108F6629). In some cases, retreat predates the 20th century. This continuing trend was documented by Brooks as early as 1902 (see USGS Photographic Library photograph Brooks 847).

Similarly, many upland areas of glacier ice show evidence of rapid thinning. Newly exposed bedrock can be seen in the upper reaches of many glacierized drainage basins in the Tordrillo Mountains, such as on the eastern side of Mount Gerdine (fig. 422).

To the west, in the Revelation Mountains and in isolated accumulation areas on peaks between the Tordrillo and Revelation Mountains, such as Mount Stoney and Mount Estelle, more than 15 glaciers longer than 8 km are located. The lengths and areas of some of these glaciers have been measured by Denton and Field (1975a, p. 597–598) and the others are estimated by



**Figure 422.**—8 September 2000 oblique aerial photograph looking northwest across an unnamed ridge west of the South Branch of Trimble Glacier and showing newly exposed bedrock, several detached former tributary glaciers, and several cirques that have recently become deglaciated. Photograph no. C-2 by Austin Post, U.S. Geological Survey.

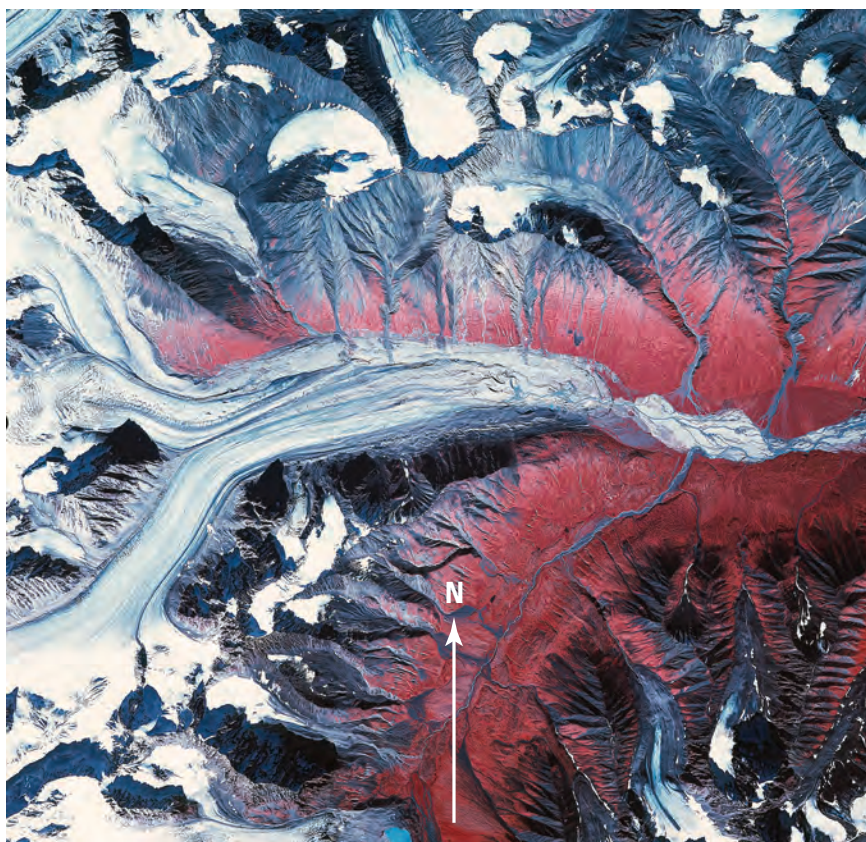


**Figure 423.**—26 August 1978 AHAP false-color infrared vertical aerial photograph of the lower part of an unnamed glacier at the head of Hartman River and many small cirque glaciers. In the 20 years since being mapped by the USGS in 1958 (Lime Hills C-2, Alaska), the unnamed glacier has retreated about 1 km and begun to separate into at least four unique tributaries. Of the dozen or so cirque glaciers mapped in 1958, about two-thirds exhibit significant reductions in area, and the other third have completely melted, leaving numerous deglaciated cirques. AHAP photograph no. L103F7860 from the GeoData Center, Geophysical Institute, University of Alaska, Fairbanks, Alaska.

the author: (1) an unnamed glacier (8 km, 9 km<sup>2</sup>) that forms the head of Chilligan River; (2) an unnamed glacier (13 km, 25 km<sup>2</sup>) located at the head of the eastern tributary of Stony River; (3) an unnamed south-flowing glacier on the eastern side of 2,540-m-high Mount Snowcap (~14 km, ~18 km<sup>2</sup>; estimated by the author); (4) two other unnamed glaciers originating on Mount Snowcap, an east-flowing glacier (~10 km, ~20 km<sup>2</sup>, estimated by the author) and a north-flowing glacier (~9 km, ~15 km<sup>2</sup>, estimated by the author); (5) an unnamed glacier (~8 km, ~7 km<sup>2</sup>, estimated by the author) that drains into Stony River; (6) an unnamed glacier (13 km, 40 km<sup>2</sup>) that is located at the head of Hartman River (fig. 423); (7) Tired Pup Glacier, named by Orth in 1956 (Orth, 1967) (9 km, 15 km<sup>2</sup>); (8) three unnamed glaciers (10 km, 18 km<sup>2</sup>; 9 km, 12 km<sup>2</sup>; ~10 km, ~10 km<sup>2</sup>, estimated by the author), all eastern tributaries to the Swift River; (9) Stony Glacier (~8 km, ~12 km<sup>2</sup>, estimated

by the author), a primary source of the Stony River; (10) an unnamed glacier (15 km, 44 km<sup>2</sup>), the source of Fish Creek; (11) an unnamed glacier (14 km, 38 km<sup>2</sup>) located at the head of Big River; (12) Revelation Glacier (16 km, 36 km<sup>2</sup>) the westernmost named glacier in the Revelation Mountains; (13) an unnamed glacier (~8 km, ~7 km<sup>2</sup>); (14) an unnamed glacier (10 km, 22 km<sup>2</sup>) located at the head of the Post River; and (15) two unnamed glaciers (11 km, 18 km<sup>2</sup>; ~9 km, ~17 km<sup>2</sup>, estimated by the author), both sources of meltwater for the Lyman Fork of the Big River.

A number of smaller glaciers lie on the summits and flanks of the Revelation Mountains (see 26 August 1978 AHAP false-color infrared vertical aerial photograph no. L103F7865) and on a number of peaks between the Skwetna, Stoney, and Styx Rivers. These glaciers are generally valley glaciers less than 8 km long and less than 1.5 km wide.

## Summary

During the period of the Landsat baseline (1972–81), all of the non-actively surging valley glaciers in the Alaska Range were stagnant, thinning, and (or) retreating. Several glaciers surged early during the baseline period, but no terminus advances were reported. At the end of the 20th century and during the first few years of the 21st century, all of the valley and outlet glaciers in the Alaska Range continued to thin, stagnate, and retreat.

## Wood River Mountains

The Wood River Mountains of southwestern Alaska (figs. 1, 424) have maximum elevations of approximately 1,500 m. They are northeast- to southwest-trending mountain ranges that are about 160 km long and about 50 km wide and extend from Bristol Bay to Chikuminuk Lake. They are bounded on the west by Togiak River and Togiak Lake, on the north and northwest by Trail Creek and Milk Creek, on the east by the Tikchik Lakes and the lowlands of the Nuyakuk and Nushagak Rivers, and on the south by Bristol Bay. The total area of glaciers in the Wood River Mountains was estimated at 230 km<sup>2</sup> by Post and Meier (1980, p. 45).

Landsat MSS images that cover the Wood River Mountains area have the following Path/Row coordinates: 80/18 (fig. 425) and 81/18 (fig. 3, table 1). The area is covered by two USGS 1:250,000-scale topographic maps: Bethel (1980) and Goodnews Bay (1979) (appendix A). The maps are based on data collected between 1954 and 1979. The area was photographed from the space shuttle in 1992 (see 26 January 1992 photograph no. STS042–96–071, NASA). A GIS analysis of USGS 1:63,360-scale topographic maps of the Wood River Mountains by William F. Manley determined that 106 glaciers exist at several locations along the crest of the west-central part of the mountains: on the summit and flanks of Mount Waskey, on the ridge crests west of the head of Nuyakuk Lake, on the summit and flanks of Konarut Mountain (1,533 m) west of Lake Chauekuktuli, and along a 25-km-long ridge southwest of Chikuminuk Lake and north and west of Konarut Mountain (figs. 425, 426) (William F. Manley, written commun., 1999, 2000).

Manley (1999, 2000) quantified 32 different parameters of these 106 glaciers. He also determined that the total glacier-covered area was approximately 60 km<sup>2</sup> and that individual glaciers ranged in area from 0.05 to 6.4 km<sup>2</sup> (median area 0.26 km<sup>2</sup>). They ranged in average elevation from 581 to 1,176 m (median elevation 937 m), in length from 0.25 to 4.38 km (median length 0.61 km), in width from 0.17 to 2.97 km (median width 0.72 km), and in perimeter from 1.0 to 23.8 km (median perimeter 2.6 km). The ELAs ranged from 545 to 1,155 m (average 929 m) and displayed high local variability.

More than 20 glaciers head along the summit ridge and slopes of 1,532-m-high Mount Waskey, the second highest peak in the Wood River Mountains, and on the nearby peaks and ridges (figs. 427, 428). Another group of more

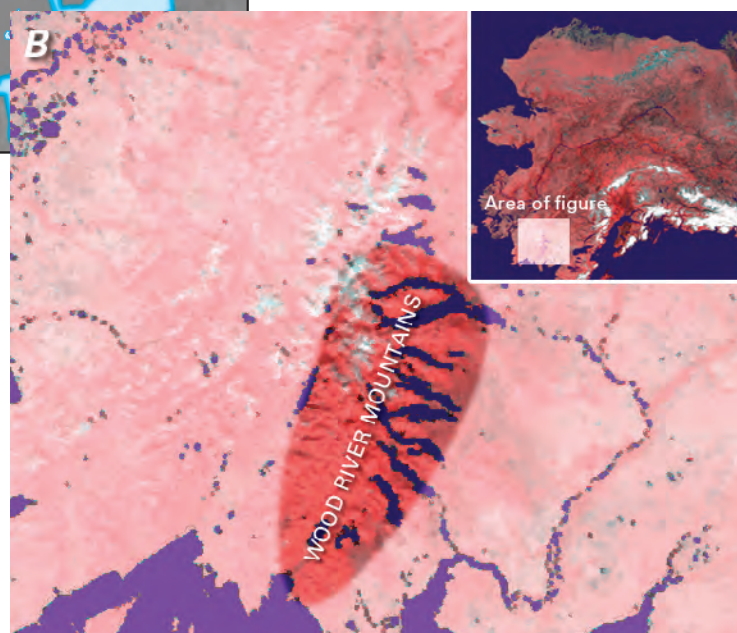
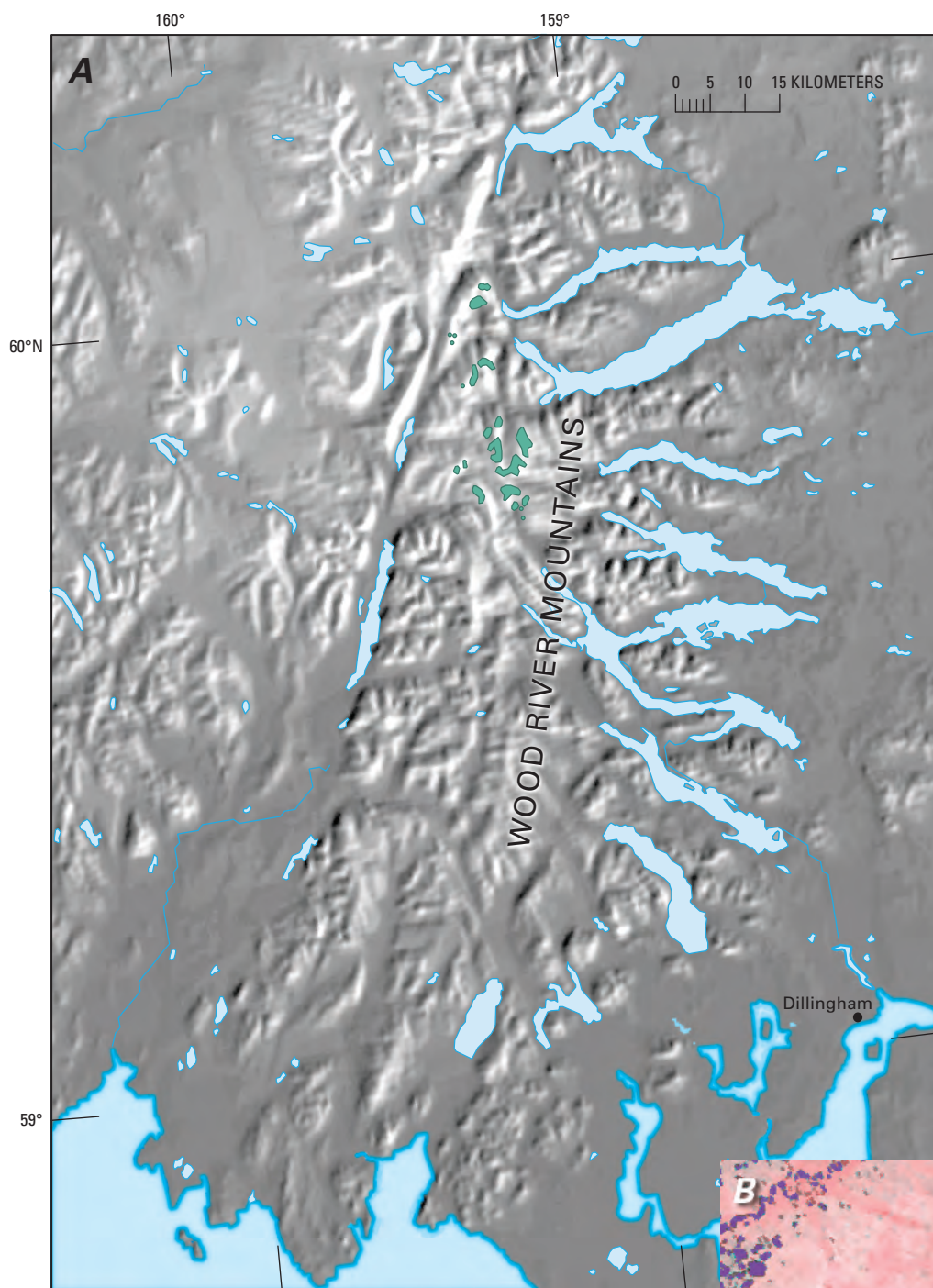


**Figure 424.** — **A**, Index map of the Wood River Mountains showing the location of glaciers in green. **B**, Enlargement of NOAA Advanced Very High Resolution Radiometer (AVHRR) image mosaic of the Wood River Mountains in summer 1995. National Oceanic and Atmospheric Administration image mosaic from Mike Fleming, Alaska Science Center, U.S. Geological Survey, Anchorage, Alaska.

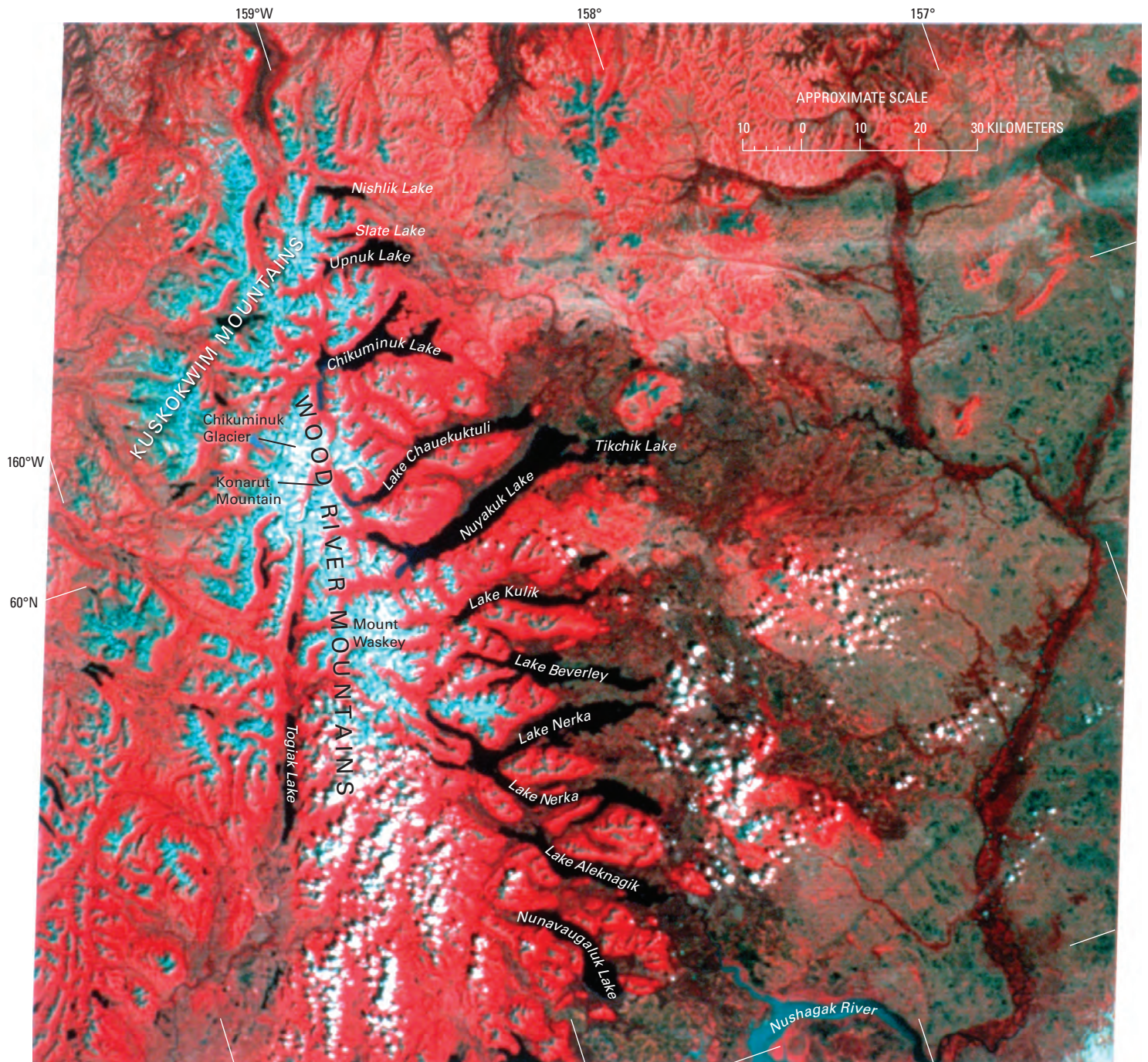


**Figure 425.** — Annotated Landsat MSS false-color composite image showing the northern Wood River Mountains and the adjacent Kuskokwim Mountains. East of the mountains are the Tikchik Lakes, a group of more than a dozen finger lakes formed by glacier erosion during the Pleistocene. Also shown are the locations of Togiak Lake, Chikuminuk Glacier, Konarut Mountain, and Mount Waskey. Landsat image (30145–21091, bands 4, 5, 7; 28 July 1978, Path 80, Row 18) is from the USGS, EROS Data Center, Sioux Falls, S. Dak.

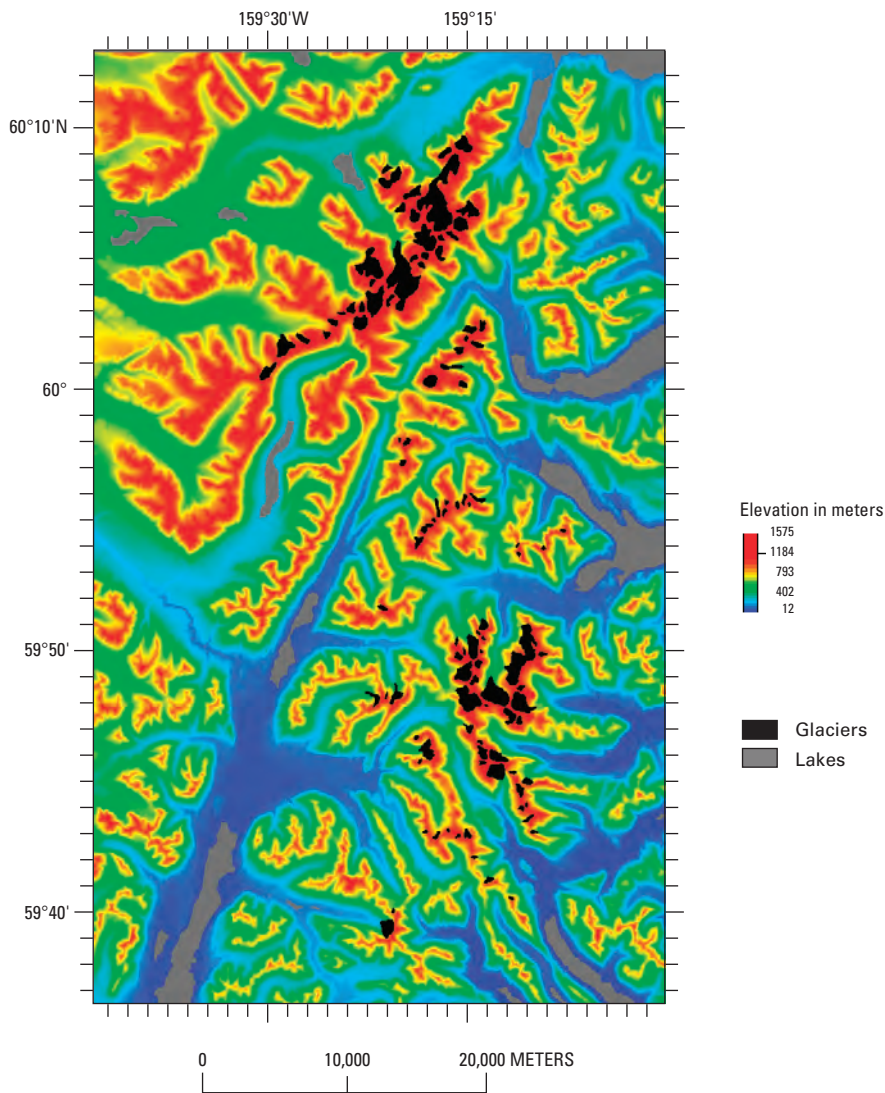


**Figure 426.**— Map showing elevations and locations of glaciers in the central Wood River Mountains. Source: unpublished data provided by William F. Manley, University of Colorado, December 2001.

than a dozen small unnamed glaciers lie along two ridges 8 to 15 km north-northwest of Mount Waskey and drain west into the Izavieknik River and east into Nuyakuk Lake (see 15 August 1984 AHAP false-color infrared vertical aerial photograph no. L121F0066). The area is referred to by some as the Ahklun Mountains, although, on USGS maps, the Ahklun Mountains are an independent parallel mountain range that lies about 60 km northwest of the Wood River Mountains. When they were photographed on 15 August 1984 by the AHAP Program (fig. 427) and in 1999 and 2000 by a University of Northern Arizona field party, all showed evidence of appreciable retreat and thinning. Additional glacial geology research by the University of Northern Arizona and other institutions was directed at Holocene glacier fluctuations (Levy and others, 2004). Another group of more than a dozen glaciers, all less than 2 km long, lies east and northeast of the summit of 1,533 m-high Konarut Mountain, the highest peak in the Wood River Mountains. Most drain eastward into Lake Chauekuktuli.

More than 20 glaciers lie along a 1350- to 1400-m-high, 25-km-long ridge southwest of Chikuminuk Lake and north and west of Konarut Mountain. This group is the greatest concentration of glaciers in the Wood River Mountains area. Their size increases to the north. The largest, the compound Chikuminuk Glacier is located almost at the northeastern end of the ridge. Chikuminuk Glacier, also called Kilbuck Glacier, was mapped at a scale of 1:10,000 during the IGY by the AGS (1960) (see sheet 8, AGS Glacier Mapping Project: Nine Glacier Maps, Northwestern North America). At that time, it was 5.5 km long and 1.0 km wide, had an area of 5.77 km<sup>2</sup>, and was



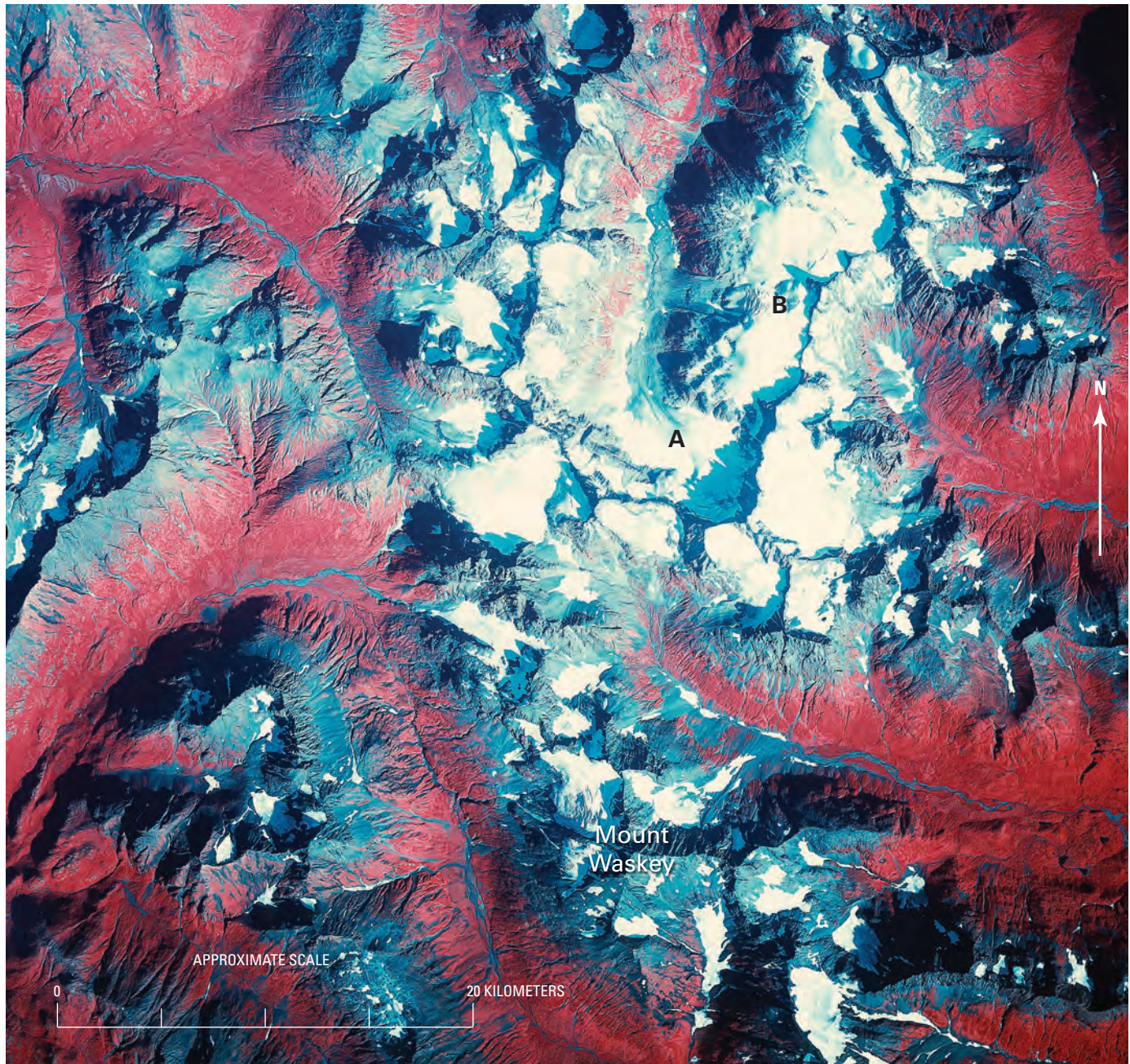


**Figure 427.**—15 August 1984 annotated AHAP false-color infrared vertical aerial photograph of Mount Waskey and the adjacent glacier-covered ridges in the central Wood River Mountains. At least seven small glaciers can be seen. In each case, a bare-ice terminus is visible below a snow-covered upper glacier. At least one valley with an unnamed glacier at its head (A) shows evidence of recently hosting a 3- to 4-km-long valley glacier. A former tributary glacier (B) has two well-preserved elevated lateral moraines and an end moraine on the floor of its valley. It has recently retreated more than 1 km. Even in August, many other adjacent cirques are snowfilled, making the identification of glaciers in those cirques difficult. AHAP photograph no. L122F0166 from the GeoData Center, Geophysical Institute, University of Alaska, Fairbanks, Alaska.



**Figure 428.**—July 1999 ground photograph of the glacier-covered summit of the Mount Waskey massif from Waskey Lake. Several recently deglaciated hanging valleys can be seen below the snowline. Photograph by Darrell S. Kaufman, Northern Arizona University.



**Figure 429.**—6 September 1957 east-looking oblique aerial photograph of most of the northern tributary and part of the southern tributary glaciers that form the Chikuminuk Glacier. Most of the larger southern tributary lies off the right edge of the aerial photograph. The terminus shows evidence of recent retreat and thinning. Photograph from the U.S. Navy. Facsimile of photograph published by the American Geographical Society (1960).

retreating. More than 75 percent of the glacier was located at elevations above approximately 1,000 m. When it was photographed in 1957, the terminus region exhibited much evidence of rapid retreat (fig. 429). Almost the entire surface of the glacier was bare ice, and the accumulation area was very small. Elevated trimline positions indicated that Chikuminuk Glacier was retreating. Other glaciers in the area also show signs of retreat, and areas mapped as glaciers on the USGS 1:63,360-scale topographic maps of this area—Bethel A1 (1979) and Bethel A2 (1979)—are now deglaciated.

Chikuminuk Glacier was one of nine glaciers mapped during the IGY that was resurveyed with a geodetic airborne laser altimeter system to obtain accurate profiles (Sapiano and others, 1998). Interpretation of six profiles collected on 11 May 1996 showed that the terminus of Chikuminuk Glacier had retreated 830 m during the 39 years between surveys, an average annual retreat rate of 21.2 m a<sup>-1</sup>. The glacier's area had decreased by approximately 9 percent (from 5.77 km<sup>2</sup> in 1957 to 5.33 km<sup>2</sup> in 1996) (Sapiano and others, 1998). Of the nine glaciers mapped during the IGY, the terminus of Chikuminuk Glacier had retreated the most. Between surveys, at an elevation of about 480 m, the glacier thinned as much as about 42 m. Above an elevation of approximately 1,075 m the glacier thickened by an average of about 10 m. Sapiano and others (1998) stated that a comparison of the 1957 and 1996 volumes suggests that the total volume of the glacier increased by 8×10<sup>6</sup> m<sup>3</sup>; however, because of 1957 survey errors, there is a large uncertainty in this number.

With the exception of Chikuminuk Glacier, lack of recent information makes it difficult to determine the status of the Wood River Mountains glaciers through the end of the 20th century. However, all of the glaciers show evidence of thinning and retreat. The 1984 AHAP photography indicated that the glaciers near Mount Waskey had actively thinned and retreated during the Landsat baseline period (1972–81).

## Summary

The Wood River Mountains is an area in which no glacier observations were reported during the period of the Landsat baseline 1972–81. However, comparing pre-Landsat topographic maps and photographs with AHAP photographs collected during 1984 shows that every glacier depicted in the AHAP photographs had lost length and area during the interval between data sets. Observations by William H. Manley of the University of Colorado suggest that every glacier continued to lose area and volume through the end of the 20th century. The terminus region of Chikuminuk Glacier, the most studied glacier in the region, has been retreating and thinning since it was mapped during the IGY in the middle 1950s.

## Kigluaik Mountains

The only glaciers on the Seward Peninsula are located in the 65 km-long east-west trending Kigluaik Mountains (figs. 1, 430). The total glacier area was estimated at about 3 km<sup>2</sup> by Post and Meier (1980, p. 45). Three glaciers exist in drainages on the flanks of 1,437-m-high Mount Osborn and adjacent peaks about 50 km north of Nome. Twentieth century investigations by Brooks in 1900 (Brooks and others, 1901), Henshaw and Parker in 1909 (Henshaw and Parker, 1913), Moffit (1913), Hopkins in 1973 (Hopkins and others, 1983), Kaufman and Calkin (1988), Kaufman and others (1989), and Calkin and others (1998) confirm that (1) from the start of the 20th century through the late 1980s, glaciers existed in the Kigluaik Mountains; (2) during the 20th century, several glaciers have completely disappeared; and (3) the remaining Kigluaik Mountain glaciers, according to the last field observation in 1986, had continued to decrease in area and length. The Kigluaik Mountains can be seen on Landsat MSS Path 88, Row 14 (fig. 3, table 1). Figure 431 is a Landsat 2 MSS false-color composite image acquired on 26 June 1977.

Brooks and others (1901) described two small glaciers that he observed in the vicinity of Mount Osborn in 1900. One was located at the head of the eastern fork of Grand Union Creek and the other near the head of the north fork of the Grand Central River (fig. 432). When they visited the area in 1909, nine years later, Henshaw and Parker (1913) observed a third small glacier, which they described as being located at the head of Pass Creek. David M. Hopkins (personal commun. to Camilla McCauley in correspondence to the



**Figure 430.**—**A**, Index map of the Kigluaik Mountains, the only glacierized part of the Seward Peninsula. **B**, Enlargement of NOAA Advanced Very High Resolution Radiometer (AVHRR) image mosaic of the Kigluaik Mountains in summer 1995. National Oceanic and Atmospheric Administration image mosaic from Mike Fleming, Alaska Science Center, U.S. Geological Survey, Anchorage, Alaska.

AGS, 1956; cited by McCauley, 1975, p. 668) determined that this glacier was actually located in the eastern fork of Smith Creek. His examination of 1949 and 1950 aerial photographs of these locations determined that all three glaciers had completely melted and no longer existed.

Using the same 1949–50 photography, Hopkins discovered three previously “unknown” glaciers elsewhere in the area with a total area of less than 5 km<sup>2</sup>. He described the largest of these, *Grand Union Glacier*, “being about a mile long” and having a “prominent vegetation-free moraine a few hundred feet down-valley from the front; presumably the moraine is between a few decades and a century in age” (McCauley, 1975, p. 668). According to Calkin and others (1998), the glacier lies sheltered in a cirque below

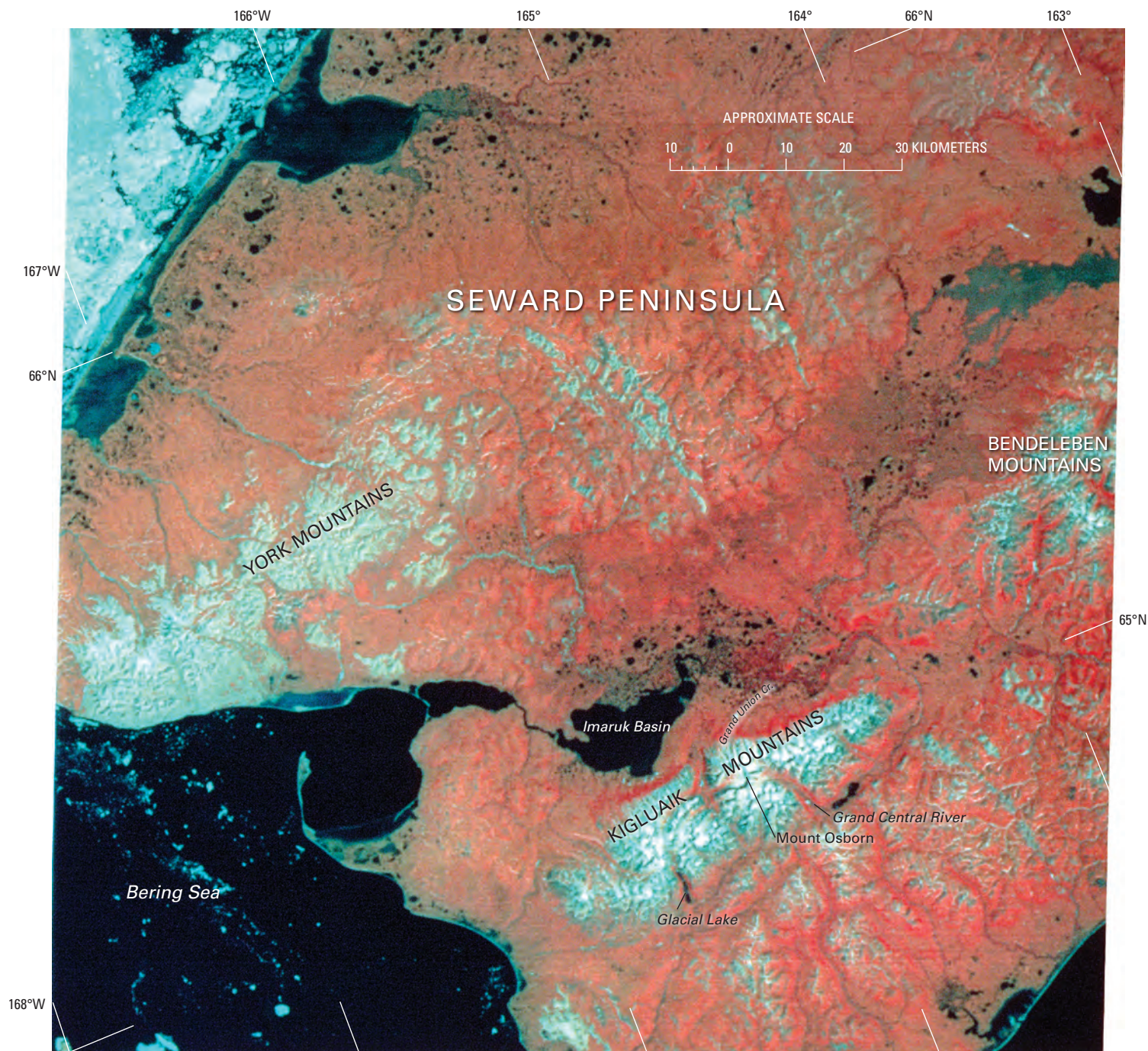


**Figure 431.**—Annotated Landsat 2 MSS false-color composite image of much of the Seward Peninsula, including all of the Kigluaik Mountains. The locations of Mount Osborn, Grand Union Creek, Grand Central River, and Glacial Lake are indicated. Landsat 2 image (2886–213155; bands 4, 5, 7; 26 June 1977; Path 88, Row 14) is from the USGS, EROS Data Center, Sioux Falls, S. Dak.

the northeastern margin of Mount Osborn at the head of the middle fork of Grand Union Creek. Hopkins also identified two other small cirque glaciers, one in the Glacial Lake valley about 12 km southwest of Mount Osborn and one at the head of an unnamed tributary of the Pilgrim River adjacent to Grand Union Creek. When Hopkins visited *Grand Union Glacier* in 1973, he observed that the length of the glacier had decreased to only about 800 m. In the 23 years between the 1950 aerial photography and Hopkins' 1973 field observations, *Grand Union Glacier's* length had decreased approximately 800 m or about  $35 \text{ m a}^{-1}$ .

Péwé and Reger (1972) and McCauley (1975) also studied the glaciers of the Kigluaik Mountains by using the 1949–50 photography. They reported the length of *Grand Union Glacier*, the westernmost active Alaskan glacier located north of the Aleutian Islands, to be about 1 km. Calkin and others (1998) reported that its length had decreased about 30 percent to about 700 m by 1986. Figure 433 is an AHAP photograph acquired on 1 August

1985 that shows *Grand Union Glacier* and numerous ice-free cirques. In 1986, its area was 0.28 km<sup>2</sup>, and its mean altitude was 700 m. Evidence of its recent larger extent is a broad looped terminal moraine that reached 410 m beyond the glacier terminus in a summer 1983 photograph (fig. 434). Local lichen chronology led Calkin and others (1998) to place the date of its Holocene maximum advance at 1645 A.D.

Mass-balance studies were performed in 1985 and 1986 (Przybyl, 1988). Winter balances were 1.5 m (1984–85) and 2.3 m (1985–86); summer balances were -2.3 m (1984–85) and -3.1 m (1985–86). The net mass balance was a loss of about 0.8 m annually. The other two smaller stagnant cirque glaciers, informally called *Thrush Glacier* and *Phalarope Glacier* by Calkin and others (1998), occur in north-facing canyon-like cirques whose mean surface elevations are 630 and 820 m, respectively. *Thrush Glacier* is located at the head of the main northeastern tributary of Glacial Lake in a northwest-facing cirque. In 1986, its area was 0.10 km<sup>2</sup>, and its length was 350 m (Calkin and others, 1998). Its Holocene maximum length was 400 m. Calkin and others (1998) based the 1675 A.D. date of its Holocene maximum advance on local lichen chronology.

*Phalarope Glacier*, located 7.6 km northwest of *Thrush Glacier* is the smallest of the three. In 1986, its area was 0.06 km<sup>2</sup>, and its length was 150 m (Calkin and others, 1998). Its Holocene maximum length was only 160 m. On the basis of local lichen chronology, Calkin and others (1998) dated its Holocene maximum advance at 1825 A.D.



**Figure 432.**—Summer 1900 photograph by A.H. Brooks of a small retreating cirque glacier located at the head of the North Fork of the Grand Central River. Photograph Brooks 360 from the USGS Photo Library, Denver, Colo. A larger version of this figure is available online.

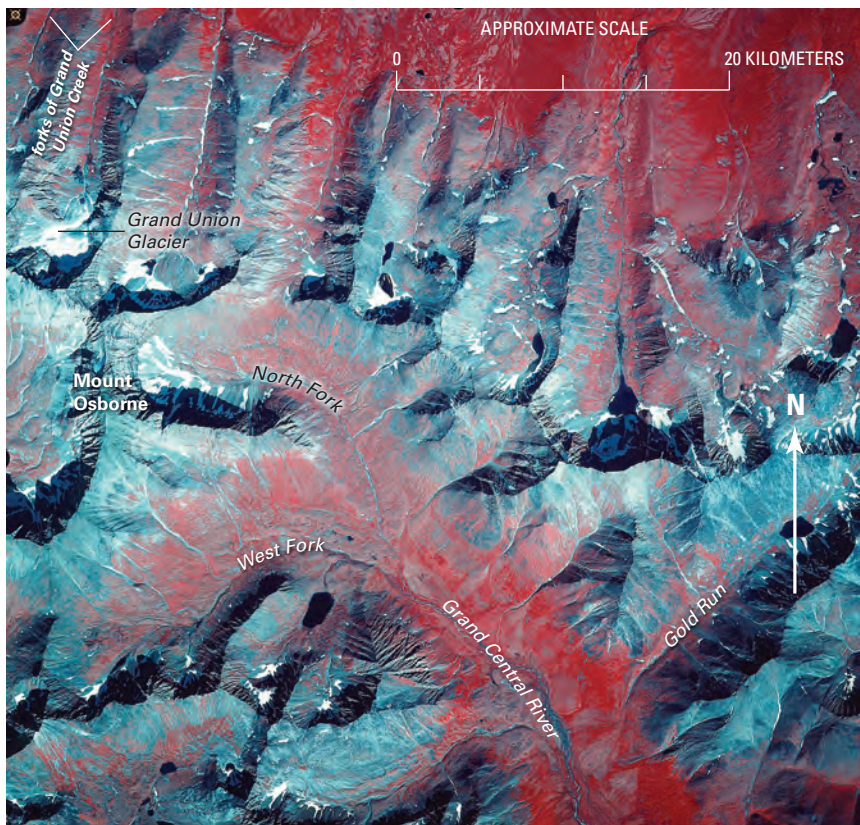


**Figure 433.**—1 August 1985 annotated AHAP false-color infrared vertical aerial photograph of the Mount Osborn area showing Grand Union Glacier and numerous ice-free cirques. The valley of the North Fork of the Grand Central River where one of Brooks' 1900 glaciers was located is east of Mount Osborn's summit. AHAP photograph no. L168F8277 from the GeoData Center, Geophysical Institute, University of Alaska, Fairbanks, Alaska.

**Figure 434.**—Summer 1983 photograph of the Grand Union Glacier, located north-east of Mount Osborn. The retreating glacier is surrounded by a broad, looped terminal moraine that dates from 1645 A.D. Photograph by Darrell Kaufman, University of Northern Arizona.



## Summary

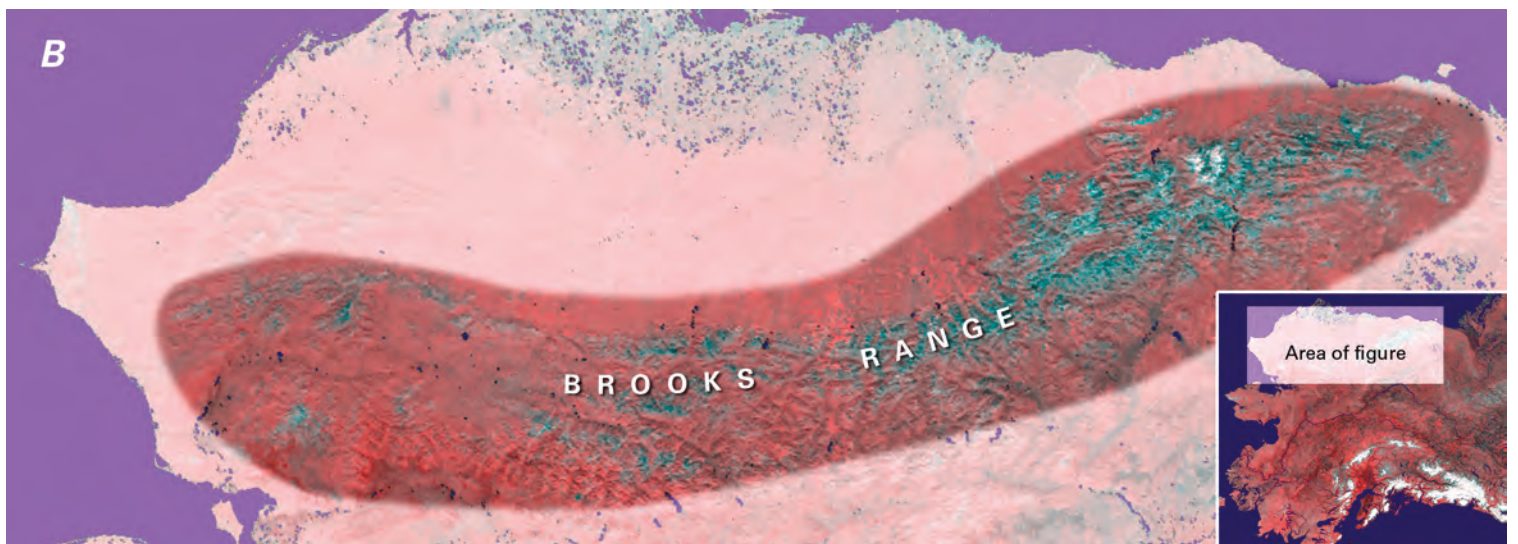
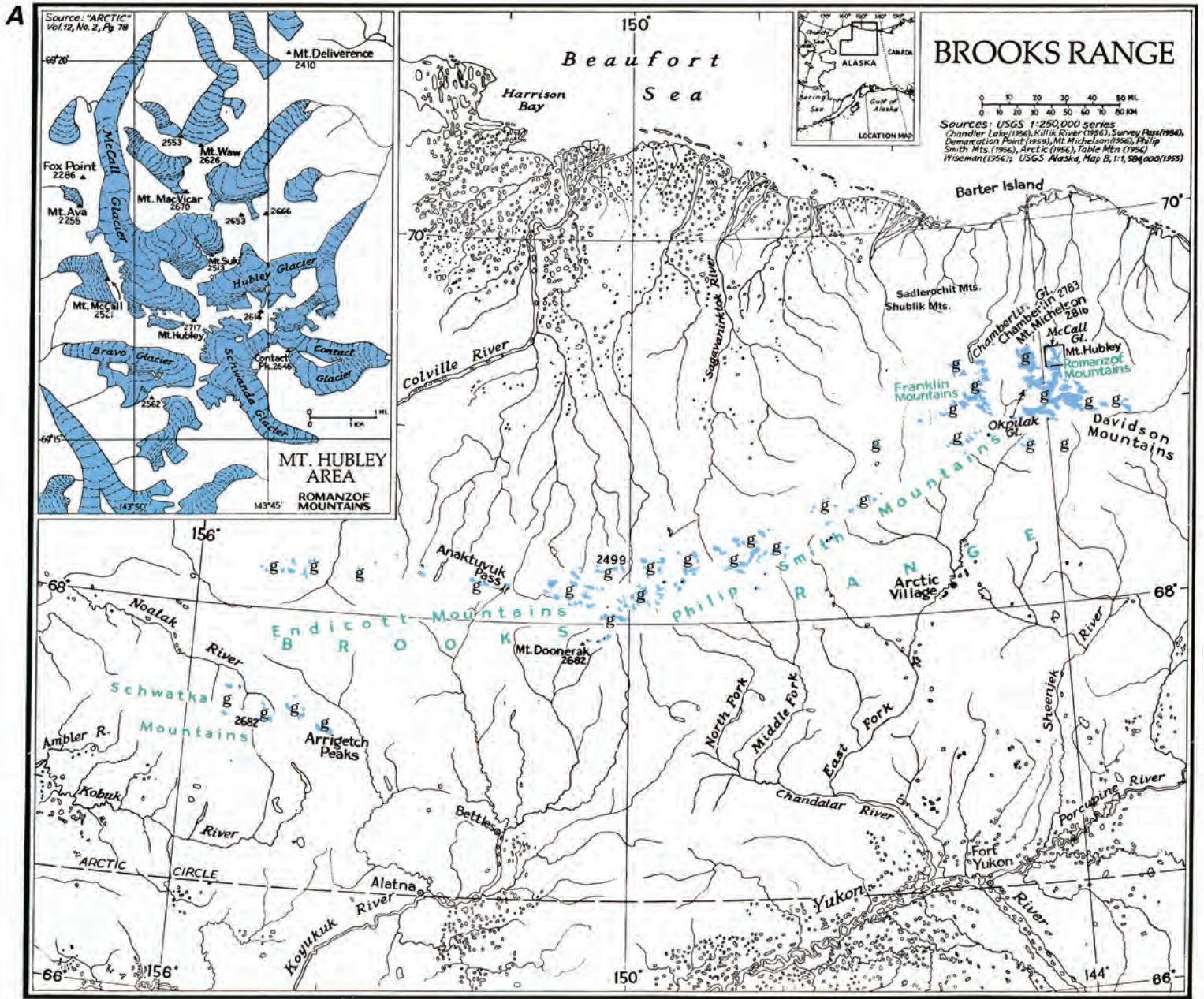
The glaciers of the Kigluaik Mountains have received little recent attention. During the Landsat baseline period (1972–81), three glaciers—*Grand Union Glacier*, *Thrush Glacier*, and *Phalarope Glacier*—existed in the Kigluaik Mountains. Field investigations performed in 1986, 5 years after the end of the Landsat baseline period, confirm that several glaciers had completely disappeared during the first eight decades of the 20th century and document that the remaining three Kigluaik Mountain glaciers were continuing to decrease in area and length. At the rate that these three glaciers were retreating and thinning, it is possible that one or more of them may have disappeared by the beginning of the 21st century.

## Brooks Range

### Introduction

The Brooks Range (figs. 1, 435), the northernmost mountain group in Alaska, extends for nearly 1,000 km in an east-west direction from the Yukon Territory, Canada-Alaska border, on the east to the Chukchi Sea on the west. It forms the drainage divide between the Arctic Slope to the north and the Kobuk and Yukon Rivers to the south. The Brooks Range contains about a dozen named generally east-west-trending contiguous mountain ranges (from east to west): British, Davidson, Romanzof, Franklin, Sadlerochit, Shublik, Philip Smith, Endicott, Schwatka, Baird, and DeLong Mountains. Glaciers within the eastern and central Brooks Range are found over a distance of about 650 km in the Romanzof, Franklin, Philip Smith, Endicott, and Schwatka Mountains (figs. 1, 435). Because the Brooks Range lies wholly north of the Arctic Circle, glaciers in the region are generally classified as polythermal; most of them are located in steep cirques and have a northern exposure (Denton, 1975b). The largest glaciers and the greatest concentration of ice are located in the eastern ranges. Two of the three highest peaks in the Brooks Range—Mount Isto (2,761 m) and Mount Michelson (2,699 m)—are in the Romanzof Mountains. Mount Chamberlin (2,750 m), the second highest peak, is in the Franklin Mountains. The glaciers of the Brooks Range cover an area of 723 km<sup>2</sup> (C Suzanne Brown, oral commun., 1992; Post and Meier, 1980, p. 45).

Present-day glacierization is significantly less than it was during the late Wisconsinan (Hamilton and Porter, 1975), when individual ice streams and piedmont lobes flowed as much as 50 km beyond the northern and southern





◀ **Figure 435.**—**A**, Index map of the central and eastern Brooks Range showing major secondary mountain ranges and general location of glaciers (g) (index map modified from Field, 1975a). Names of glacierized ranges shown in green, unglacierized ranges in black. **B**, Enlargement of NOAA Advanced Very High Resolution Radiometer (AVHRR) image mosaic of the Brooks Range in summer 1995. National Oceanic and Atmospheric Administration image mosaic from Mike Fleming, Alaska Science Center, U.S. Geological Survey, Anchorage, Alaska.

margins of the Brooks Range. At least five neoglacial advances occurred in the central Brooks Range, dated at 4,400 yr B.P., 3,500 yr B.P., 2,900 yr B.P., 1,800±500 yr B.P., and 1,120±180 yr B.P. (Ellis and Calkin, 1979, 1984).

Landsat MSS images that cover the Brooks Range have the following Path/Row coordinates: 75/11, 75/12, 76/11, 76/12, 77/11, 77/12, 78/11, 78/12, 79/11, 79/12, 80/11, 80/12, 81/12, 82/12, 83/12, and 84/12 (fig. 3, table 1). Individually, most of the glaciers in the Brooks Range are too small to be delineated on Landsat MSS images; however, many of the glacier tongues in the Romanzof and Franklin Mountains can be discerned. Glacierized areas are mapped on the following 1:250,000-scale USGS topographic quadrangle maps of Alaska: Demarcation Point (1955), Table Mountain (1956), Mount Michelson (1956), Arctic (1956), Philip Smith Mountains (1956), Chandler Lake (1956), Killik River (1956), and Survey Pass (1956) (appendix A).

Very little was known about the glaciers of the Brooks Range until the second half of the 20th century. Writing about northern Alaska glaciers in the first third of the 20th century, Smith and Mertie (1930) described only three. Because USGS reconnaissance surveys made before World War I included photographs of more than a dozen glaciers, Smith and Mertie's work needs to be viewed as applicable only to the larger valley glaciers in the Brooks Range. In June 1907, Leffingwell (1919) mapped in the Romanzof Mountains and took a number of photographs of Okpilak Glacier and adjacent areas (fig. 436). Four years later, in July 1911, Smith photographed several glaciers in the Arrigetch Peaks area in the central Brooks Range. Significant new information began to be collected beginning in the late 1950s, mostly as a direct result of research carried out during the IGY. By the late 20th century, aerial photography and systematic mapping of the Brooks Range revealed that significantly more glaciers existed than previously expected. An inventory of Brooks Range glaciers by the USGS (C Suzanne Brown, oral commun., 1992) identified 1,001 glaciers having a total area of 723 km<sup>2</sup>.

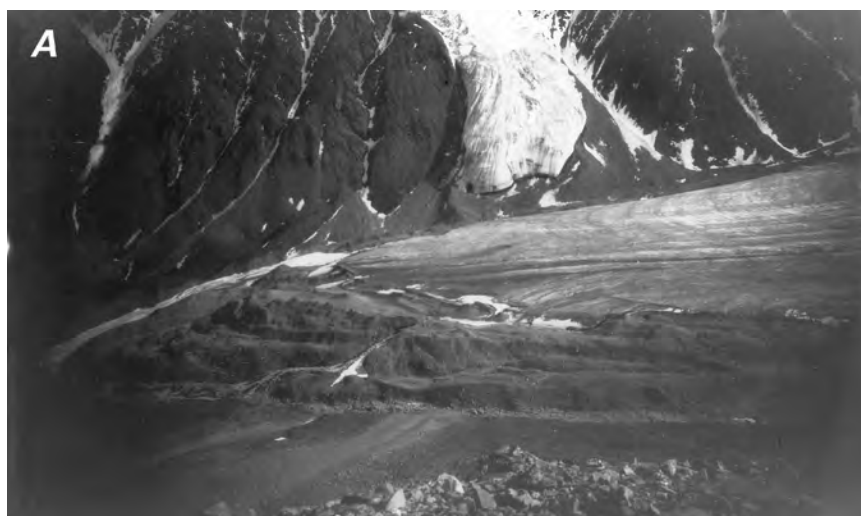


**Figure 436.**—Three June 1907 photographs of Okpilak Glacier, Romanzof Mountains. **A**, The terminus of Okpilak Glacier and an unnamed hanging glacier. Abandoned lateral moraines on both sides of the hanging glacier and an elevated multiple-lobe terminal-recessional moraine complex at the terminus of Okpilak Glacier suggest that the glaciers had thinned significantly before 1907. The moraine complex may mark Okpilak Glacier's "Little Ice Age" maximum extent. The proximity of the terminus of Okpilak Glacier to the moraine complex suggests that retreat pre-1907 was less than 100 m. **B** and **C**, see following page.



**Figure 436.**—**B**, View upglacier toward the glacier's source. The low-relief rounded right margin of the glacier and the elevated lateral moraine are all evidence for previous thinning of Okpilak Glacier. **C**, View downglacier toward the glacier's terminus. The emergent medial moraine and the three tributary glaciers that enter from the left, all separated from the main ice trunk and mantled by debris, are evidence for previous thinning and retreat of the Okpilak Glacier and its tributaries. Photographs by Ernest de K. Leffingwell. Photographs Leffingwell 84 (A), 63 (B), and 64f (C) are from the USGS Photo Library, Denver, Colo.



## Romanzof Mountains

The 105-km-long Romanzof Mountains (figs. 1, 435, 437), located between the Hulahula and Kongakut Rivers, have a glacier area of about 260 km<sup>2</sup> (Denton, 1975b, p. 653) and contain at least 188 glaciers (Evans, 1977), 4 of which have lengths of 5 km or more. Wendler (1969) determined that no glacier ice was exposed at elevations of less than 1,500 m and that at least 66 percent of the glaciers are located on north-facing slopes (fig. 438); only about 15 percent have south-facing exposures. Studies of two glaciers—8.3-km-long Okpilak Glacier (figs. 436, 439) and 7.6-km-long McCall Glacier (figs. 440, 441)—have provided significant information about 20th century glacier fluctuations and related changes. McCall Glacier was intensively investigated during the IGY, and the International Hydrological Decade (IHD), which ran from 1965 to 1974. Investigations continue to the present.

Okpilak Glacier (figs. 436, 439), which Leffingwell visited in 1907 (Leffingwell, 1919), descends from an unnamed 2,435-m-high mountain about 18 km south of Mount Michelson. In 1958, Sable (1960) examined a number of glaciers in the Romanzof Mountains and revisited several photographic sites occupied by Leffingwell at Okpilak Glacier. A comparison of photographs documents that the Okpilak Glacier retreated more than 300 m in the intervening 51 years. Sable (1960) reported that Okpilak's lateral moraines were 45±6 to 63.5±6 m above the margins of the glacier in 1956–58. In 1907, they ranged from being level to 6 m above the ice (fig. 436). Sable stated (p. 185) that “The average amount of thinning in the lower 1.2 miles (2.3 km) is estimated to be 150 feet (45.3 m), and the mean rate from 1907 to 1958 to be about 3 feet per year (0.9 m).” Hence, the Okpilak Glacier had thinned

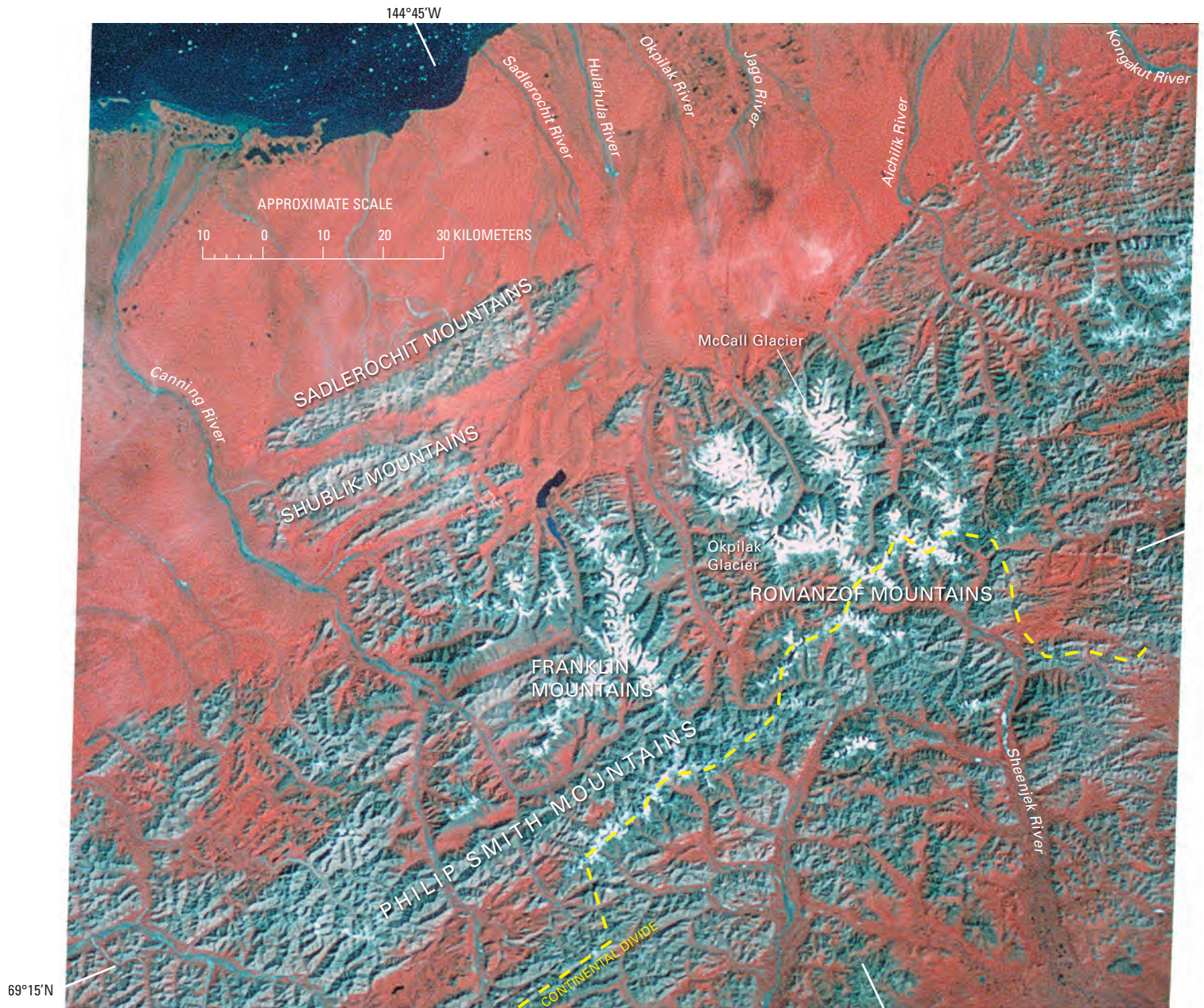


**Figure 437.**—Annotated Landsat 2 MSS false-color composite image of the Brooks Range from just west of Canning River to west of the Kongakut River. Shown are the Romanzof, Franklin, Sadlerochit, and Shublik Mountains, and part of the Phillip Smith Mountains. The location of the largest concentration of glaciers in the Brooks Range occurs north of the Continental Divide in the center of this image. Landsat image (22387–20443, bands 4, 5, 7; 5 August 1981; Path 77, Row 11) is from the USGS, EROS Data Center, Sioux Falls, S. Dak.

from 33 to 69.5 m ( $0.65\text{--}1.35\text{ m a}^{-1}$ ) between 1907 and 1958. Sable also commented that, the ratio of ice lost to thinning versus the ice lost by recession of the Okpilak Glacier terminus is roughly estimated to be at least 25:1. Sable (1960, p. 185) further stated that “All the smaller glaciers in the vicinity of Okpilak Glacier, for which photographic information from 1907 and 1958 can be compared, show evidence of marked recent recession and thinning.” Figure 439 is an AHAP false-color infrared vertical aerial photograph of Okpilak Glacier taken on 24 August 1982, 75 years after Leffingwell’s ground photographs (fig. 436).

Located about 15 km northeast of Okpilak Glacier, 7.6-km-long McCall Glacier (figs. 440, 441), which has an area of 6.0 km<sup>2</sup>, heads on 2,693-m-high Mount Hubley. Its terminus is located at an elevation of about 1,350 m. In August 1956, Walter A. Wood and Richard C. Hubley, accompanied by Robert W. Mason (Mason, 1959), traveled to northern Alaska hoping to find “a valley glacier in the highest area of the Brooks Range... that would lend itself to a micrometeorological and glacier-movement survey program that could be undertaken during the International Geophysical Year” (Mason, 1959, p. 77). They quickly located “a slender valley glacier with a gentle gradient,

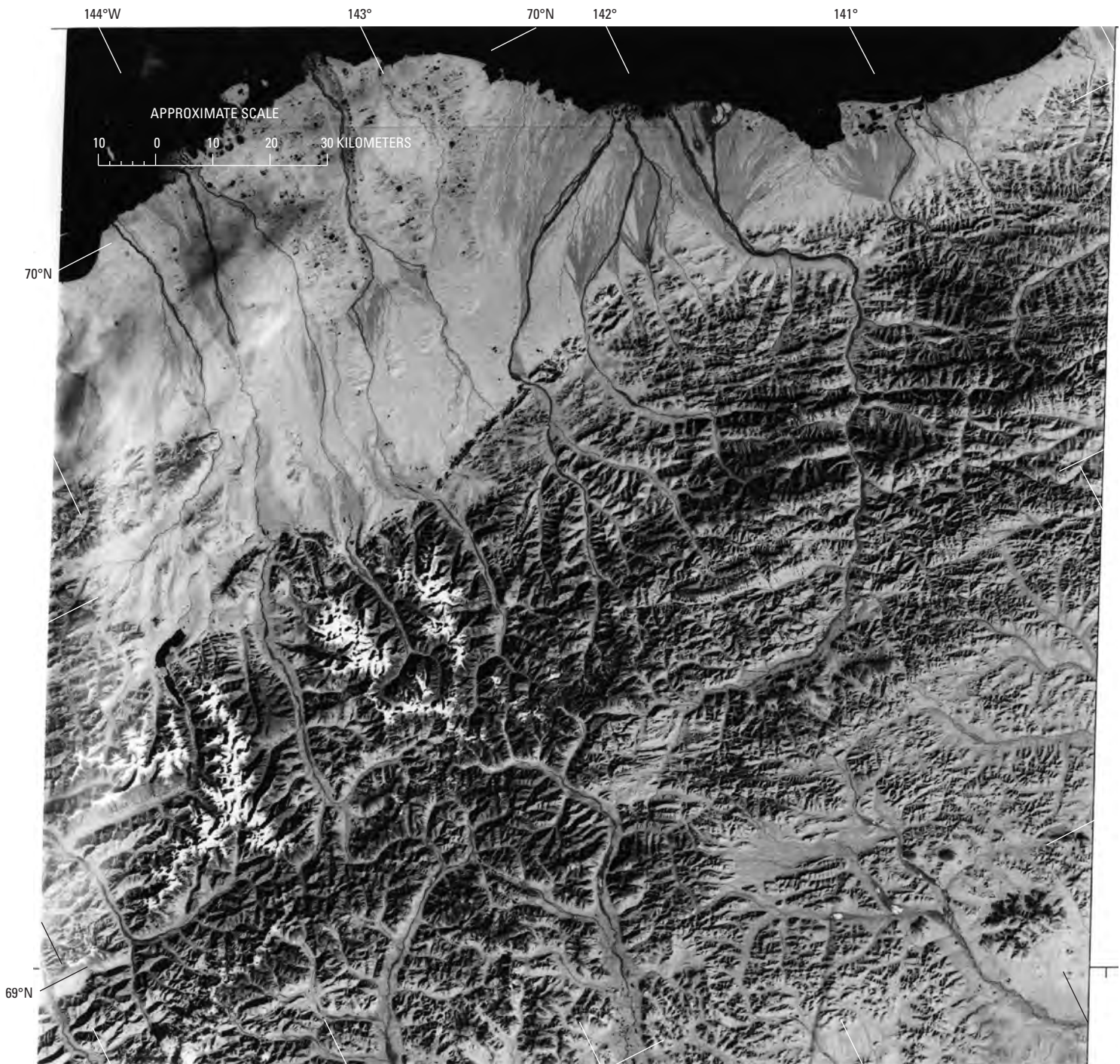
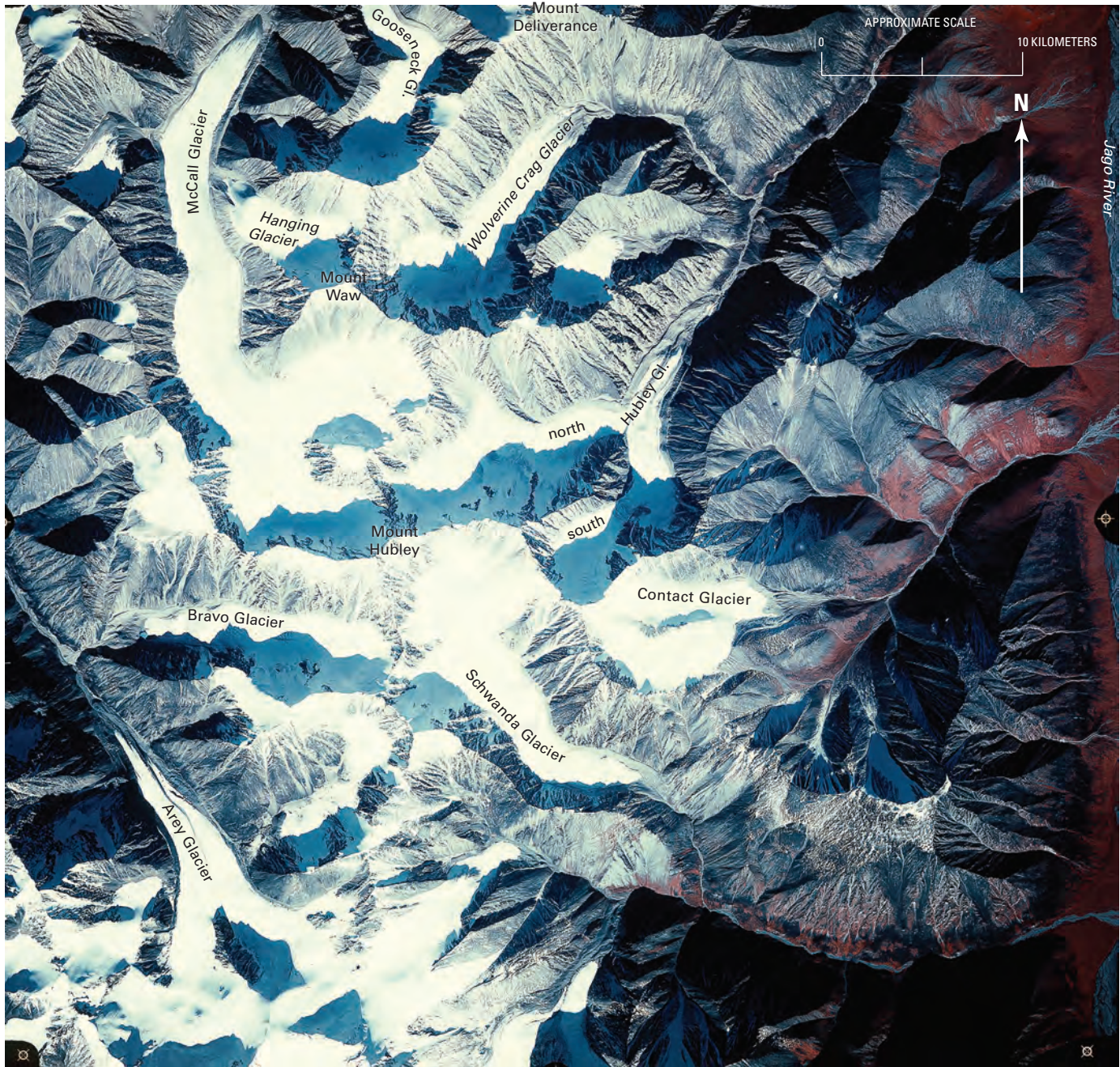


**Figure 438.**—Landsat 3 MSS image of the eastern part of the Brooks Range showing glaciers in the Franklin Mountains and Romanzof Mountains (left side of image). The largest glacier in the Brooks Range is less than 10 km long. Most of the glaciers are in steep cirques with northern exposures. The most detailed glacier inventory to date (C Suzanne Brown, oral commun., 1992) counted 1,001 glaciers, with a total area of 723 km<sup>2</sup> in the Brooks Range. Most of these glaciers are too small to be discernible on Landsat MSS images. Many of these glaciers were already retreating before observations by E. de K. Leffingwell in 1907 (Hamilton, 1965). Patches of river ice (aufeis) deposits from the previous winter (1977–1978) remain and can be seen in the lower right corner of the image. Landsat image and caption courtesy of Robert M. Krimmel, U.S. Geological Survey. Landsat image (30177–20435; band 7; 29 August 1978; Path 76, Row 11) is from the USGS, EROS Data Center, Sioux Falls, S. Dak.



**Figure 439.**—24 August 1982 annotated AHAP false-color infrared vertical aerial photograph of the eastern Romanzof Mountains showing Okpilak Glacier, East Okpilak Glacier, and more than a dozen other unnamed glaciers. The location of E. de K. Leffingwell's photograph of the position of the terminus of Okpilak Glacier in 1907 is shown, as well as the view directions of the two other E. de K. Leffingwell photographs (figs. 436B, C). The debris-mantled, stagnant termini

of many of the glaciers can be seen in this photograph. Five glaciers, labeled A through E and one, informally called East Okpilak Glacier by Raybus and Echelmeyer (1998), show either conspicuous retreat of the terminus or elevated lateral and (or) terminal moraines, clear evidence of glacier thinning and retreat. AHAP photograph no. L28F2321 from GeoData Center, Geophysical Institute, University of Alaska, Fairbanks, Alaska.



no ice falls, limited crevassing, and no tributary cirque glaciers. The glacier terminus lay almost at the frontal scarp of the mountains. This meant that the glacier could, if necessary, be approached on foot from a low camp on the tundra, that a light plane on skis could probably land on the glacier without difficulty, and that perhaps vehicles could be driven up the valley to transport fragile supplies to a glacier camp site” (Mason, 1959, p. 77–78). Hubley named the glacier for John McCall, an Alaskan geologist who died in 1954. Ironically, Hubley himself died in an accident on McCall Glacier in October 1957. Work started in May 1957 and continued through the end of the summer of 1958. A detailed topographic map (fig. 441) was made by the AGS from geodetic ground control collected in 1957 and aerial photography acquired by the USAF in 1958. Summaries of the results of IGY glaciological and geological investigations of McCall Glacier were presented by Sater (1959) and Keeler (1959).

**Figure 440.**—Annotated 24 August 1982 AHAP false-color infrared vertical aerial photograph of the eastern Romanzof Mountains showing Mount Hubley, Mount Waw, Mount Deliverance, McCall Glacier, Gooseneck Glacier, Bravo Glacier, Wolverine Crag Glacier, north Hubley Glacier, south Hubley Glacier, Arey Glacier, and Hanging Glacier. All of the named glaciers show evidence of retreat and thinning. AHAP photograph no. L27F2369 from the GeoData Center, Geophysical Institute, University of Alaska, Fairbanks, Alaska.



**Figure 441.**—Topographic map of McCall Glacier produced by the American Geographical Society (1960) based on 1958 vertical aerial photography and 1957 geodetic ground control. More than 75 percent of the glacier exists at an elevation of greater than 1,750 m. A larger version of this figure is available online.

Between 1969 and 1975, research continued on the following attributes of McCall Glacier: heat balance (Wendler and Weller, 1974); a comparison of monitoring methods (stake measurements versus controlled run-off site measurements versus calculated heat balance) for determining ice melt (Wendler and Ishikawa, 1973); the heat, ice, and water balance of the glacier (Wendler and Ishikawa, 1974a); the effect of slope, exposure, and mountain screening on solar radiation reaching the glacier (Wendler and Ishikawa, 1974b); and climatological change (Dorrer and Wendler, 1976). All work was done as part of the IHD. During four years of observation (1969–72), McCall Glacier’s mass balance was consistently negative. Ninety-eight percent of ice loss was owing to melting and 2 percent to evaporation.

During 1993 and 1994, a University of Alaska Fairbanks scientific team returned to the glacier to investigate how it had changed since the IHD. Continuous measurements of temperature, precipitation, short-wave radiation, and snow depth began in June 1993. The ice surface and the outline of the terminus were surveyed using optical and GPS methods, and ice thickness was determined by radio-echo-sounding methods. The survey determined that the maximum ice thickness was 250 m in McCall’s overdeepened lower cirque; the average thickness along the glacier’s centerline was 140 m (Raybus and Echelmeyer, 1997). A contour map of the bed of McCall Glacier was made from the ice-thickness measurements. The present velocity field, the elevation, the volume change from 1972 to 1993, and the average mass balance during this period were determined from the surveys. Annual velocities measured during 1993 and 1994 were found to be similar to those measured in the 1970s. However, velocities measured in the ablation area during the summer of 1993 were about 30 percent greater than the annual velocities for the same area. This discovery indicated to Raybus and Echelmeyer (1997) that McCall Glacier slides in summer and led them to suggest that it is a polythermal glacier containing a mixture of temperate and polar ice. Ice temperatures in the accumulation area range between  $-1$  and  $-1.5^{\circ}\text{C}$ ; basal ice is temperate in the accumulation area.

Geodetic airborne laser altimeter surveys (profiles of surface elevation) (Sapiano and others, 1998) show that, since 1958, the elevation of the glacier surface has decreased everywhere, from a few meters in the accumulation zone to more than 70 m at an elevation of about 1,425 m near the terminus. Total volume of ice lost was  $6.4 \times 10^7 \text{ m}^3$ . The long-term mass balance between 1972 and 1993 was  $-0.33 \text{ m a}^{-1}$  (Raybus and Echelmeyer, 1998). The average mass balance from 1993 to 1996 was  $-0.60 \text{ m a}^{-1}$ . These results document a significant thinning of the glacier during the second half of the 20th century. Because the average mass balance of McCall Glacier between 1958 and 1972 was  $-0.15 \text{ m a}^{-1}$ , the 1993–96 mass balance represents a 400 percent increase in the already negative mass balance and also documents an increase in the rate of volumetric loss since the early 1970s. Individual hydrologic year (HY) annual balances are  $-42 \text{ cm}$  in HY 1969,  $-8 \text{ cm}$  in HY 1970,  $-14 \text{ cm}$  in HY 1971,  $-19 \text{ cm}$  in HY 1972,  $-48 \text{ cm}$  in HY 1993,  $-74 \text{ cm}$  in HY 1994, and  $-55 \text{ cm}$  in HY 1995 (Bernhard Raybus, oral commun., 1996). Repeated surveys of detailed profiles across the lower ablation area from 1969 to 1994 show that a three-fold increase in the rate of surface lowering occurred after 1975 (Raybus and Echelmeyer, 1998).

In the 37 years between 1956 and 1993, the area of McCall Glacier decreased from about  $6.2$  to  $6.0 \text{ km}^2$ , its length decreased by  $353 \text{ m}$ , and it thinned an average of  $10.5 \text{ m}$ . In the 14 years between 1958 and 1972, the terminus retreated  $68 \text{ m}$ , an average recession rate of  $5.7 \text{ m a}^{-1}$ . In the 21 years between 1972 and 1993, the terminus retreated  $285 \text{ m}$ , more than doubling its rate, for an average recession rate of  $13.6 \text{ m a}^{-1}$ .

Raybus and Echelmeyer (1998) also compared surface-elevation and terminus profiles of 10 other glaciers (fig. 440) located within a 30-km radius of McCall Glacier, collected between 1993 and 1995, with topographic maps

made in 1956 or 1973. Their comparisons showed that nine glaciers had average mass balances of between -20 and -54 cm a<sup>-1</sup>: 3.1-km-long Gooseneck Glacier (area 1.1 km<sup>2</sup>), 3.2-km-long Bravo Glacier (area 1.6 km<sup>2</sup>), 3.0-km-long *Wolverine Crag Glacier* (area 1.9 km<sup>2</sup>), 3.1-km-long north Hubley Glacier (area 1.8 km<sup>2</sup>), 3.0-km-long south Hubley Glacier (area 1.2 km<sup>2</sup>), 4.2-km-long Arey Glacier (area 4.6 km<sup>2</sup>), 8.3-km-long Okpilak Glacier (called *West Okpilak Glacier* by Raybus and Echelmeyer, 1998) (area 11.0 km<sup>2</sup>), 6.0-km-long *East Okpilak Glacier* (area 8.8 km<sup>2</sup>), and 7.7-km-long Esetuk Glacier (area 7.1 km<sup>2</sup>). A tenth—1.8-km-long *Hanging Glacier*, which has an area of 0.8 km<sup>2</sup>—had an average mass balance of -1 cm a<sup>-1</sup>.

Raybus and Echelmeyer's (1998) data also showed that all 10 glaciers retreated during the period of comparison. They calculated changes in length, changes in ice volume, average changes in elevation, and mean annual mass balances for: Gooseneck Glacier (-16 m, -1.4×10<sup>7</sup> m<sup>3</sup>, -12.3 m, -28 cm a<sup>-1</sup>), Bravo Glacier (-300 m, -1.8×10<sup>7</sup> m<sup>3</sup>, -10.2 m, -27 cm a<sup>-1</sup>), *Wolverine Crag Glacier* (-265 m, -4.6 ×10<sup>7</sup> m<sup>3</sup>, -23.3 m, -27 cm a<sup>-1</sup>), north Hubley Glacier (-1,030 m, -4.2×10<sup>7</sup> m<sup>3</sup>, -22.0 m, -54 cm a<sup>-1</sup>), south Hubley Glacier (-890 m, -134×10<sup>7</sup> m<sup>3</sup>, -10.5 m, -25 cm a<sup>-1</sup>), Arey Glacier (-570 m, -5.2×10<sup>7</sup> m<sup>3</sup>, -11.4 m, -27 cm a<sup>-1</sup>), *West Okpilak Glacier* (-420 m, -17×10<sup>7</sup> m<sup>3</sup>, -15.2 m, -37 cm a<sup>-1</sup>), *East Okpilak Glacier* (-1,020 m, -7.2×10<sup>7</sup> m<sup>3</sup>, -8.1 m, -20 cm a<sup>-1</sup>), Esetuk Glacier (-814 m, -9.2 ×10<sup>7</sup> m<sup>3</sup>, -12.9 m, -30 cm a<sup>-1</sup>) [see 24 August 1982 AHAP false-color infrared vertical aerial photograph no. L27F2372], and *Hanging Glacier* (-260 m, -4.0×10<sup>5</sup> m<sup>3</sup>, -0.5 m, -1 cm a<sup>-1</sup>).

Combining Sable's (1960) observations with those of Raybus and Echelmeyer (1998) indicates that Okpilak Glacier underwent a maximum thinning of as much as 84.7 m and retreated more than 750 m during an 85-year observational period during the 20th century. The annual average change is 1.0 m a<sup>-1</sup> of thinning and 8.8 m a<sup>-1</sup> of terminus retreat.

A concentration of small cirque and valley glaciers straddles the continental divide on either side of the Sheenjek River (figs. 435, 437). Many glaciers there show multiple evidence of recent retreat and stagnation, and some cirques have recently become ice free (see 24 August 1982 AHAP false-color infrared vertical aerial photograph no. L30F1444).

## Franklin Mountains

The Franklin Mountains (figs. 1, 435, 437, 438, 442) support several dozen cirque and small valley glaciers between the Sadlerochit and Hulahula Rivers. The greatest concentrations of glacier ice and the largest glaciers are located along a 25-km-long ridge and upland between the summit of Mount Chamberlin and the head of the Canning River. Two named and two unnamed glaciers descend from 2,739-m-high Mount Chamberlin's summit and flanks. Chamberlin Glacier on the northwest and Peters Glacier on the southwest are the named glaciers (fig. 442). Chamberlin Glacier, which is 2.4 km long and as much as 800 m wide (Denton, 1975b, p. 654), terminates at an elevation above 2,000 m. During the IGY in 1958, meteorological investigations of the glacier were conducted by the USAF Cambridge Research Center (later USAF Cambridge Research Laboratories; now Air Force Phillips Laboratory). Larsson (1960) concluded that the current meteorological regime measured at the glacier was incompatible with the continuing existence of the glacier. A glacier hydrology and hydrochemistry study was carried out on the Chamberlin Glacier by Rainwater and Guy (1961). Several longer unnamed glaciers flow into Carnivore Creek and West Patuk Creek to the south (fig. 442). All of the glaciers examined in the Franklin Mountains show evidence of thinning and retreat.



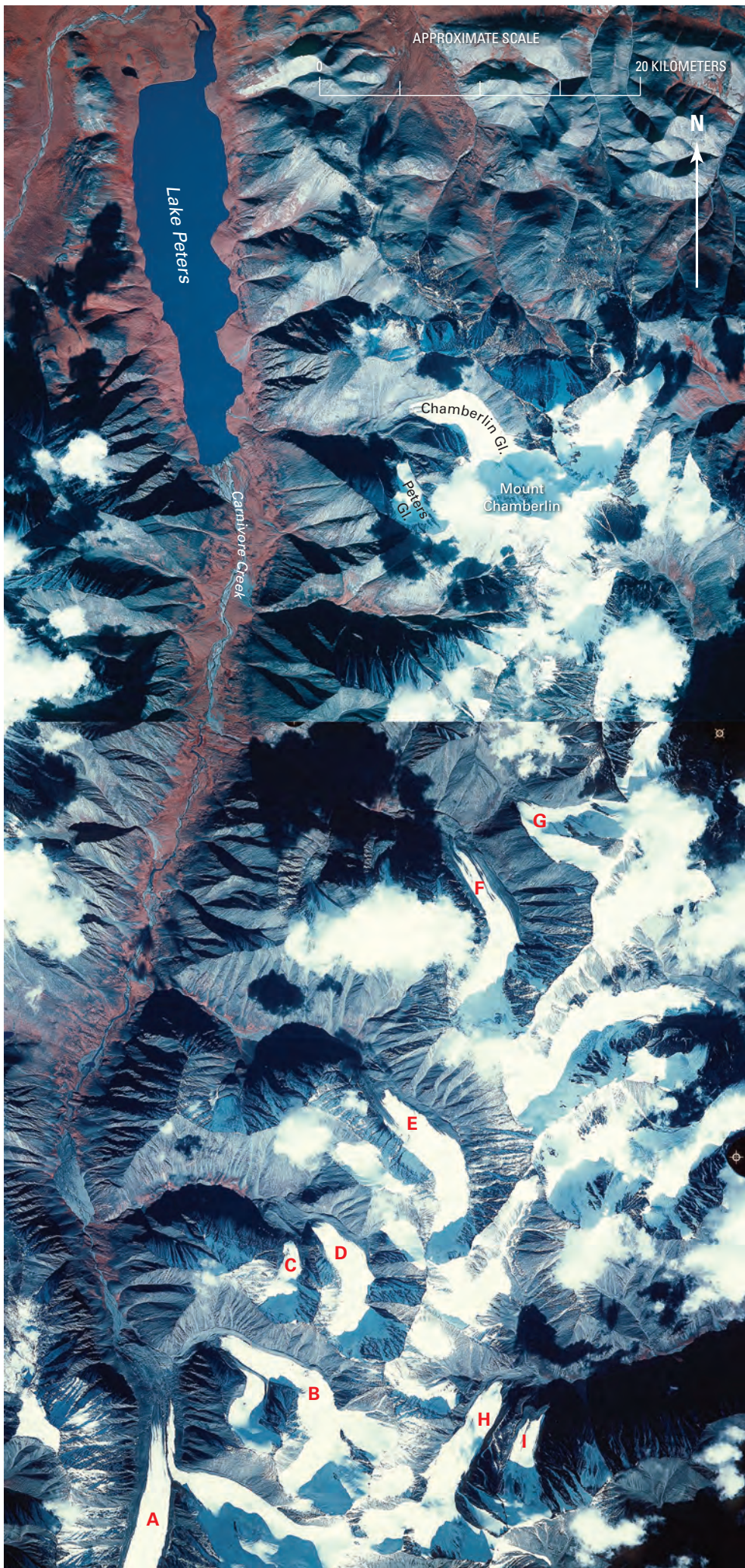


**Figure 442.**—24 August 1982 annotated AHAP false-color infrared vertical aerial photographic mosaic of the central Franklin Mountains showing Mount Chamberlin, Lake Peters, Carnivore Creek, Chamberlin Glacier, Peters Glacier, and several unnamed glaciers. Shadows and clouds obscure several of the termini, but Chamberlin Glacier shows a conspicuous, fresh-looking elevated end moraine — lateral moraine complex, several kilometers downvalley from the exposed-ice terminus, evidence of recent glacier thinning, and retreat. On the southern part of the mosaic, two unnamed glaciers, A and B, have separated and retreated into their individual valleys, as have two others labeled C and D. Five other unnamed glaciers, labeled E through I, show multiple evidence of recent retreat and stagnation. Recent end moraine positions are shown for several of the glaciers. AHAP photograph no. L27F2377 (north) and L28F2316 (south) from GeoData Center, Geophysical Institute, University of Alaska, Fairbanks, Alaska.

## Philip Smith and Endicott Mountains

Ellis and Calkin (1979) studied 133 mostly unnamed glaciers in a 4,000-km<sup>2</sup> area of the Philip Smith and Endicott Mountains (fig. 435). The area is centered around Atigun Pass (lat 68°08'N., long 149°29'W.), a rugged area where relief exceeds 1,000 m and peaks rise to 2,300 m. All of the active glaciers occurred at elevations above 1,500 m; 97 percent were located north of the Continental Divide. Glaciers that were fronted by stable moraines varied uniformly in elevation by latitude. Glacier terminus elevations were at about 1,600 m south of the Continental Divide. The further north the glacier, the higher the terminus, maximum elevations being about 2,000 m 25 km to the north. Typically, the glaciers had 220 m of relief, ranged in length from less than 100 m to about 2.5 km, and had areas of 2 km<sup>2</sup> or less. Ellis and Calkin (1979, p. 406) stated that "Under the present climate, the cirque glaciers of the area are wasting away." During July and August of 1977, they observed the complete loss of the previous year's snow accumulation plus the loss of an additional 1 to 2 m of glacier ice at three cirque glaciers near Atigun Pass.

Ellis and Calkin (1979) evaluated glacial deposits adjacent to the ice margins of 102 glaciers. Of these, 55 extended into ice-cored or ice-cemented moraines; 23 extended into ice-cored looping rock glacier ridges located on older rock glacier deposits; 19 extended into ice-cored rock glaciers; and 5 had no associated deposits. They also mapped 113 tongue- and 502 lobate-shaped rock glaciers in the area. Of the 83 tongue-shaped rock glaciers that occur north of the Continental Divide, 76 percent are active, and 46 percent have exposed ice cores. South of the divide, only 30 percent of the tongue-shaped rock glaciers are active, and 9 percent have exposed ice cores. On both sides of the divide, rock glaciers with exposed ice cores have active termini.

Lobate rock glaciers occur in a 500-m-thick altitudinal zone from lat 68°N. to the foothills of the Brooks Range. South of the Continental Divide, only 50 percent of the lobate-shaped rock glaciers are active; north of the Continental Divide, 70 percent of the lobate-shaped rock glaciers are active. Active lobes occur 150 m higher than inactive lobes.

In a later study, Ellis and Calkin (1984) discussed Neoglacial glacier fluctuations in the central Brooks Range, stating that (p. 897) "for the past ~1,100 yr, cirque glaciers have been continuously in more extended positions than they are today... the last two major advances occurred at 800 ±150 (A.D.) and 390 ±90 yr B.P. (A.D. 1410–1600). Glaciers across the central Brooks Range stayed close to their maxima until A.D. 1640–1750. Historical photographs and lichenometry show that retreat was most rapid after A.D. 1870 and decelerated after the mid-1900s. Recession from this most recent Neoglacial maximum has amounted to 150–700 m and continues at present." Results from the eastern Brooks Range suggest that the rate of retreat is again accelerating into the early 21st century.

Elsewhere in this region, Porter's (1966) study of glaciers in the Anaktuvuk Pass area (lat 68°09'N., long 151°43'W.) showed that many lie in deep north-facing cirques and are located at elevations below the present regional snowline. He noted that the snowline was at about 2,070 m, well above the cirque glaciers in the area, and concluded that they are in a state of disequilibrium with present climatic conditions.

In the Arrigetch Peaks area (lat 67°25'N., long 154°13'W.), active glaciers head at elevations of approximately 1,800 m and flow to elevations below 1,500 m. Many stagnant ice bodies lie between 1,200 and 1,500 m. In 1962, Hamilton (1965) reoccupied photographic stations established in 1911 by Philip Smith (1912) and made photographic comparisons of glacier position and glacier mass balance. In the 51 years between studies, Hamilton noted both a recession and a thinning of the glaciers. In one instance, he stated that an ice-cored moraine had thinned by roughly 20 m. In another, he noted "the

ice in the head-wall gully... has thinned appreciably, leaving a pronounced trimline where none was visible in 1911” (Hamilton, 1965, p. 483). In a third observation, he stated that “Present terminal positions are roughly 200 m further up-valley and lie at elevations nearly 100 m higher than in 1911.”

### **Schwatka Mountains**

At least four peaks support valley glaciers in the Schwatka Mountains (fig. 435) south of the Noatak River. The largest glaciers descend from the slopes of 2,571-m-high Mount Igikpak and 2,208-m-high Oyukak Mountain. The largest glacier on Mount Igikpak is about 3 km long and unnamed and terminates at an elevation of about 1,150 m. Glaciers also exist on the flanks of Mount Chitiok and Shulakpak Peak.

### **Summary**

During the period of the Landsat baseline (1972–81), all available evidence suggests that the glaciers of the Brooks Range were thinning and retreating. These conclusions are based on published field descriptions, the author’s comparison of the size and number of glaciers shown on pre-Landsat baseline USGS topographic maps (ca. 1950s) (appendix A), and 1982 AHAP photography from the end of the Landsat baseline period. Limited information is available about behavior at the end of the 20th and into the early 21st century. However, every glacier described showed significant evidence of thinning and retreat.

## Summary and Conclusions

During the period of the Landsat Baseline Decade (1972–1981), glaciers covered about 75,000 km<sup>2</sup> of Alaska (Post and Meier, 1980, p. 45), representing about 5 percent of Alaska's land area. Glacierized regions include 11 mountain ranges (Coast Mountains; Saint Elias Mountains; Chugach Mountains; Kenai Mountains, including Montague Island; Aleutian Range; Wrangell Mountains; Talkeetna Mountains; Alaska Range; Wood River Mountains; Kigluaik Mountains; and Brooks Range), one large island (Kodiak Island), one island archipelago (Alexander Archipelago), and one island chain (Aleutian Islands). Glaciers in Alaska extend over an area from the southeast at lat 55°19'N., long 130°05'W., about 100 km east of Ketchikan to the southwest at Kiska Island at lat 52°05'N., long 177°35'E., in the Aleutian Islands and to the north at lat 69°20'N., long 143°45'W., in the Brooks Range. Because the actual number of glaciers has never been systematically inventoried, it is unknown but probably exceeds 100,000. Alaskan glaciers range in elevation from more than 6,000 m to below sea level. Most of Alaska's glaciers are unnamed; less than 700 have been officially named by the BGN (appendix C) (<http://geonames.usgs.gov/>).

During the “Little Ice Age,” the total glacier-covered area and the number of mountain ranges and islands having glacier cover were significantly larger than they were during the “baseline” period. Since the end of the “Little Ice Age,” there has been a decrease in the glacier area and the thickness of most of the Earth's glacierized areas in the middle and low latitudes, along with advances of individual glaciers in some areas including about a dozen in Alaska. However, the timing, magnitude, and complexity of this post-“Little Ice Age” glacier change have been different in each of Alaska's 14 glacierized areas. Although there is almost total thinning of glaciers in lower elevations and a retreat of glacier termini, the details presented in this volume demonstrate that the current status of Alaska's glaciers varies significantly from area to area and with elevation.

Although most Alaskan glaciers at lower elevations are retreating, not all are doing so. At elevations below about 1,500 m, about a dozen glaciers, including Hubbard, Harvard, Meares, Taku, and Lituya Glaciers (all tidewater or former tidewater glaciers), are currently thickening and advancing. Many glaciers at higher elevations are thickening or exhibit no change. Several volcanoes, including Redoubt Volcano, have had 20th century eruptions that melted summit glaciers, but new glaciers have formed in their craters.

The following region-by-region summary details the observed changes in glaciers described in this volume.

*Coast Mountains.* — During the period of the Landsat Baseline Decade, the glacierized area of the Coast Mountains was approximately 10,500 km<sup>2</sup> (Post and Meier, 1980, p. 45). Taku, Hole-in-the-Wall, and Mead Glaciers were advancing. All other valley and outlet glaciers in the Coast Mountains were thinning and retreating. At the end of the 20th century and early in the 21st century, Taku Glacier was advancing, and Hole-in-the-Wall Glacier was stable. Mead Glacier was advancing in the 1990s and continues in the early 21st century; all other observed valley and outlet glaciers in the Coast Mountains continued to thin and retreat.

*Alexander Archipelago.* — Glaciers are mapped in mountainous areas on middle 20th century USGS 1:250,000-scale topographic maps on six of the islands in the Alexander Archipelago: Revillagigedo, Prince of Wales, Kupreanof, Baranof, Chichagof, and Admiralty Islands. During the period of the Landsat Baseline Decade, the Alexander Archipelago had a glacierized area of less than 150 km<sup>2</sup>. No recent information exists about the status of these glaciers at the beginning of the 21st century. However, their small size, low elevation, and southerly location in an area with late 20th century

temperature increases indicate that they have probably continued to thin and retreat. Some glaciers may have melted completely and no longer exist.

*St. Elias Mountains.* —During the period of the Landsat Baseline Decade, the glacierized area of the Alaskan St. Elias Mountains was approximately 11,800 km<sup>2</sup> (Post and Meier, 1980, p. 45). Throughout the decade, Johns Hopkins, Grand Pacific, Margerie, Brady, North Crillon, Lituya, Hubbard, and Turner Glaciers were advancing. La Perouse and South Crillon Glacier were stable, although the positions of their termini fluctuated from year to year. All other valley and outlet glaciers in the St. Elias Mountains were thinning and retreating. At the beginning of the 21st century, North Crillon, Lituya, Hubbard, and Turner Glaciers were advancing. Johns Hopkins, La Perouse, and South Crillon Glacier were stable, although the positions of their termini fluctuated from year to year. All other observed valley and outlet glaciers in the St. Elias Mountains continued to thin and retreat.

*Chugach Mountains.* —During the period of the Landsat Baseline Decade, the glacierized area of the Chugach Mountains was approximately 21,600 km<sup>2</sup> (Post and Meier, 1980, p. 45). Two tidewater glaciers, Meares and Harvard Glaciers, were advancing throughout the decade; Bryn Mawr, Harriman, and Columbia Glaciers advanced during the early part of the “baseline” period. Smith Glacier was stable for most of the period, although the position of its termini fluctuated from year to year. All other valley and outlet glaciers in the Chugach Mountains were thinning and retreating. At the end of the 20th century and during the early 21st century, Meares, Harriman, and Harvard Glaciers were still advancing. All other valley and outlet glaciers in the Chugach Mountains were thinning, retreating, or stagnant.

*Kenai Mountains.* —During the period of the Landsat Baseline Decade, the glacierized area of the Kenai Mountains was approximately 4,600 km<sup>2</sup> (Post and Meier, 1980, p. 45). With the exception of Aialik and McCarty Glaciers, both of which advanced more than 500 m during the second half of the 20th century, all of the valley and tidewater glaciers in the Kenai Mountains continued to stagnate, thin, and (or) retreat. By the end of the 20th century, all of the valley and outlet glaciers in the Kenai Mountains continued to stagnate, thin, and (or) retreat. When Tiger Glacier was observed in 2000, it was at about the same location as it was in 1908. Because it had been retreating during much of the 20th century, Tiger Glacier must have undergone a late-20th century advance to regain its former position.

*Kodiak Island.* —During the Landsat Baseline Decade, the glacierized area of Kodiak Island was less than 15 km<sup>2</sup>. A comparison of the sizes and numbers of glaciers shown on USGS topographic maps made from 1948 to 1952 aerial photographs with AHAP photography from the middle of the “baseline” period (1977–78) show that the glaciers of Kodiak Island were thinning and retreating. No information exists about the status of Kodiak Island’s glaciers at the end of the 20th century and the beginning of the 21st century. However, their small size, low elevation, and location on an island that has undergone a temperature increase and is surrounded by temperate ocean water suggest that its glaciers likely have continued to thin and retreat. Some may have melted completely away and no longer exist.

*Aleutian Range.* —During the period of the Landsat Baseline Decade, the glacierized area of the Aleutian Range was approximately 1,250 km<sup>2</sup> (Post and Meier, 1980, p. 45). All of the nonactive surge-type valley glaciers in the Aleutian Range were stagnant, thinning, and (or) retreating. Several glaciers surged during the “baseline” period, but no termini advances were reported. At the end of the 20th century and into the early 21st century, all of the valley and outlet glaciers in the Aleutian Range continued to thin, stagnate, and retreat. When Tuxedni Glacier was observed in 2000, it showed some evidence of a recent terminus advance. However, trimlines and abandoned moraines document a long-term history of retreat and thinning. The 1912 eruption of Mount Katmai melted and beheaded a number of summit and flank glaciers.

Following the eruption, two small glaciers formed on the talus beneath the crater rim. They continued to exist throughout the “baseline” period and into the early 21st century. Similarly, following the 1989-90 eruption of Mount Redoubt, snow and glacier ice accumulating in the crater have replaced snow and ice melted during the eruption.

*Aleutian Islands.* — During the period of the Landsat Baseline Decade, the glacierized area of the Aleutian Islands was approximately 960 km<sup>2</sup> (Post and Meier, 1980, p. 45). Glaciers are shown in mountainous areas on mid-20th century USGS 1:250,000-scale topographic maps on at least 10 islands in the eastern and central part of the Aleutian Islands. From east to west, islands where glaciers have been reported are Unimak, Akutan, Unalaska, Umnak, Herbert, Atka, Great Sitkin, Tanaga, Gareloi, and Kiska Islands. All of the mapped glaciers of the Aleutian Islands descend from the summits of active or dormant volcanoes, extending into either calderas or down their flanks. All head at elevations of greater than 1,200 m. No information exists about the status of glaciers in the Aleutian Islands during the “baseline” period or at the end of the 20th century and into the early 21st century. However, their small size, low elevation, and southerly latitudinal location in an area of late-20th century temperature increases indicates that the glaciers likely have continued to thin and retreat. Some may have melted completely and no longer exist.

*Wrangell Mountains.* — During the period of the Landsat Baseline Decade, the glacierized area of the Wrangell Mountains was approximately 8,300 km<sup>2</sup> (Post and Meier, 1980, p. 45). With the exception of *Athna Glacier* and *South* and *Center Mackeith Glaciers*, which were advancing, apparently in response to heat-flow-related nonclimatic forcing, all of the valley and outlet glaciers in the Wrangell Mountains were retreating, thinning, or stagnant. At the end of the 20th century and into the early 21st century, no additional information was available about *Athna Glacier* and *South* and *Center Mackeith Glaciers*. All other valley and outlet glaciers in the Wrangell Mountains continued to thin, stagnate, and retreat.

*Talkeetna Mountains.* — During the period of the Landsat Baseline Decade, the glacierized area of the Talkeetna Mountains was approximately 800 km<sup>2</sup> (Post and Meier, 1980, p. 45). Analyzing the comparative sizes and numbers of glaciers shown on topographic maps made from 1948 to 1952 aerial photography and on AHAP photography from the middle of the “baseline” period (1977) and just after the “baseline” period (1983) shows that the glaciers of the Talkeetna Mountains were thinning, retreating, and (or) stagnant. Every glacier observed from the air at the beginning of the 21st century (31 August 2000) showed evidence of thinning and retreat, and many smaller glaciers had completely disappeared.

*Alaska Range.* — During the period of the Landsat Baseline Decade, the glacierized area of the Alaska Range was approximately 13,900 km<sup>2</sup> (Post and Meier, 1980, p. 45). All of the nonactive, surge-type valley glaciers in the Alaska Range were stagnant, thinning, and (or) retreating. Several glaciers surged early during the “baseline” period, but no terminus advances were reported at the time or documented subsequently. At the end of the 20th century and into the early 21st century, all of the valley and outlet glaciers in the Alaska Range continued to thin, stagnate, and (or) retreat.

*Wood River Mountains.* — During the period of the Landsat Baseline Decade, the glacierized area of the Wood River Mountains was less than 230 km<sup>2</sup> (Post and Meier, 1980, p. 45; Kilbuk-Wood River Mountains). No reported observations were made of any Wood River Glaciers during the “baseline” period. However, a comparison of pre-“baseline” period topographic maps and photographs with 1984 AHAP photography shows that every glacier visible on the aerial photographs had lost length and area during the interval between the data sets. Every glacier continued to lose area and length through the late 20th century. No early 21st century information exists. Chikuminuk

Glacier was mapped in 1957 and 1958 during the IGY. Since then, its terminus region has thinned and retreated. However, at elevations above 1,000 m, it has thickened by an average of about 10 m.

*Kigluaik Mountains.* — During the period of the Landsat Baseline Decade, three glaciers—*Grand Union*, *Thrush*, and *Phalarope* Glaciers, which have a collective glacierized area of less than 3 km<sup>2</sup> (Post and Meier, 1980, p. 45; Seward Peninsula)—existed in the Kigluaik Mountains. Since then, they have received little attention. Field investigations performed in 1986, confirmed that other glaciers that existed during the early 20th century have completely disappeared and documented that the remaining three Kigluaik Mountain glaciers were continuing to decrease in area and length. Given the rate at which these three glaciers were retreating and thinning, it is possible that one or more of them may have subsequently disappeared. The absence of recent field observations, including recent aerial photography of the area, renders the continued existence of Kigluaik Mountains glaciers at the end of the 20th century and into the early 21st century a matter of speculation.

*Brooks Range.* — During the period of the Landsat Baseline Decade, the glacierized area of the Brooks Range was less than 723 km<sup>2</sup> (Post and Meier, 1980, p. 45). Analysis of published field descriptions and a comparison by the author of the sizes and numbers of glaciers shown on pre-Landsat baseline USGS topographic maps and 1982 AHAP photography from the end of the “baseline” period suggest that the glaciers of the Brooks Range are continuing to thin and retreat. Limited information is available about the status of the glaciers at the end of the 20th century and into the early 21st century. However, every glacier described showed evidence of thinning and retreat.

As was noted above, the general thinning and retreat of lower elevation temperate glaciers is one of the most visible manifestations of the post-“Little Ice Age” response of Alaska’s glaciers to the changing regional climate. As the regional summaries of the status of Alaska’s glaciers presented here document, most Alaskan mountain glaciers at lower elevations are stagnant and (or) retreating and thinning in response to a post-“Little Ice Age” regional warming. In fact, of the more than 1,000 glaciers described in this chapter, more than 98 percent are currently thinning, retreating, or stagnant. As has also been shown, local and regional variability has given every glacier in Alaska its own complex and unique history of change. For example, many glaciers in southeastern Alaska—such as most of the glaciers of the Glacier Bay and the Lynn Canal areas—began to retreat as early as the mid-18th century, some more than 100 years before the advent of systematic meteorological measurements of air temperatures; others in the same area advanced during that entire period. Today most of Alaska’s glaciers continue to retreat. Others, such as the tidewater Harvard and Hubbard Glaciers, have been advancing for more than a century.

Nearly all mountain glaciers in Alaska are temperate; that is, meltwater exists in, on, or under the glacier for part, if not all, of the year. Globally, temperate and tropical mountain glaciers are shrinking on all continents and are thus excellent indicators of climate change. Small changes in temperature and precipitation can have an impact on the status of these glaciers. Ongoing glacier melting does, and will continue to substantially reduce the lengths, areas, thicknesses, and volumes of Earth’s temperate mountain glaciers. As the glaciers of Alaska melt, their meltwaters flow into the Gulf of Alaska and into the Bering, Chukchi, and Beaufort Seas, contributing to global (eustatic) sea-level rise.

Many investigations have examined the role that temperate glaciers play in present and future sea-level changes; most of the attention has been directed toward the last five decades of the 20th century (National Research Council, 1977, 1983, 1984, 1990; Meier, 1984; 1990 1998; Dyurgerov and Meier, 1997a, 1997b, 1999, 2000; Bahr and Meier, 2000; Dyurgerov and Dwyer, 2000;

Arendt and others, 2002; Meier and Wahr, 2002). Almost all of these reports state that, if all the remaining nonpolar glacier ice were to melt, a sea-level rise of less than 1 m would result. Complete melting of the glacier ice in the Antarctic and Greenland ice sheets would lead to a potential global sea-level rise of about 80 m—73.4 m from Antarctica, and 6.5 m from Greenland (Williams and Hall, 1993). Several of the studies state that glacier melting and meltwater production have increased significantly during the later part of the 20th century (Arendt and others, 2002; Meier and Dyurgerov, 2002). Of the approximately 4 percent of the glacierized area on Earth that is covered by mountain glaciers, less than one-tenth (<0.4 percent) is Alaskan glaciers. However, as Meier (1984) first showed, the glaciers of the Alaskan coastal region, most of which are melting rapidly under present climatic conditions, may contribute more than one-third of the total annual glacier meltwater entering the global ocean. Because current climate models predict future temperature increases, these glaciers may make even larger contributions to future rising sea level.

Arendt and others (2002), synthesized the result of more than a decade of geodetic airborne laser profiling of 67 glaciers in Alaska and adjacent Canada. The glaciers that they studied represent about 20 percent of the glacierized area of Alaska and adjacent Canada, including glaciers that have all or part of their termini calving into tidewater or into ice-marginal lakes and glaciers that terminate on land. They estimate the total annual volume change of Alaska glaciers, expressed as water equivalent, to be  $-52 \pm 15 \text{ km}^3 \text{ a}^{-1}$  for the period from the 1950s to the early 1990s and  $-96 \pm 35 \text{ km}^3 \text{ a}^{-1}$  for the period from the middle 1990s to the late 1990s. These volumes are equivalent to a rise in sea level of  $0.14 \pm 0.04 \text{ mm a}^{-1}$  during the early period and  $0.27 \pm 0.10 \text{ mm a}^{-1}$  during the more recent period.

With respect to thickness change, they report that most glaciers thinned during both periods, an indication of surface lowering. They stated that measurements for both early- and recent-period glaciers indicate that thinning during the recent period was more than twice as much ( $-1.8 \text{ m a}^{-1}$ ) as what they calculated for the early period ( $-0.7 \text{ m a}^{-1}$ ).

With respect to area, Arendt and others (2002) also reported that most (but not all) of the glaciers that they investigated had retreated. The total area of measured glaciers decreased 0.8 percent ( $131 \text{ km}^2$ ) during the early period and 0.4 percent during the recent period. They observed that approximately 10 percent of the sampled glaciers either advanced while simultaneously thinning or (during the early period) retreated while thickening. During the recent period, the 10 largest meltwater contributions came from Columbia ( $7.1 \text{ km}^3 \text{ a}^{-1}$ ), Bering ( $6.0 \text{ km}^3 \text{ a}^{-1}$ ), Malaspina ( $2.8 \text{ km}^3 \text{ a}^{-1}$ ), LeConte ( $1.0 \text{ km}^3 \text{ a}^{-1}$ ), Tazlina ( $0.56 \text{ km}^3 \text{ a}^{-1}$ ), Brady ( $0.54 \text{ km}^3 \text{ a}^{-1}$ ), Baird ( $0.42 \text{ km}^3 \text{ a}^{-1}$ ), Black Rapids ( $0.19 \text{ km}^3 \text{ a}^{-1}$ ), Mendenhall ( $0.14 \text{ km}^3 \text{ a}^{-1}$ ), and Susitna ( $0.11 \text{ km}^3 \text{ a}^{-1}$ ) Glaciers.

The two largest contributors of meltwater during the recent period—Columbia and Bering Glaciers, which together contributed  $13.1 \text{ km}^3 \text{ a}^{-1}$  of water to the global ocean (nearly 15 percent of the annual total)—are not simply responding to changing climate. The significant increase in Columbia Glacier's meltwater production resulted from the onset of its catastrophic calving retreat, which began in the early 1980s (Krimmel, this volume), whereas much of the ice lost at Bering Glacier is the result of rapid calving of ice from the surge-advanced terminus. Most of this ice was transported from the accumulation area into the ablation area by surge processes between 1993 and 1995 (see the Chugach Mountains section in this volume). Similarly, much of the increased meltwater contribution from Mendenhall Glacier results from the fact that, since 1990, its eastern terminus has ceased to be grounded on a sediment plain and is now calving into Mendenhall Lake (see the Coast Mountains section in this volume).



The significance of the contribution of Alaskan glaciers to global sea level can be seen by comparing similar data from Greenland. Krabill and others (2000) reported that analysis of 1994-99 aircraft laser altimeter surveys over Greenland indicates a net loss of approximately  $51 \text{ km}^3 \text{ a}^{-1}$  of ice from the entire Greenland ice sheet. They stated that this amount is sufficient to raise sea level by  $0.13 \text{ mm a}^{-1}$ , approximately 7 percent of the observed rise. The estimated annual volume loss from Alaska during the recent period,  $96 \pm 35 \text{ km}^3 \text{ a}^{-1}$  (Arendt, and others, 2002), is nearly twice that estimated for the entire Greenland ice sheet during the same period.

This chapter has summarized the areal extent and distribution of Alaska's glaciers during the Landsat Baseline Decade (1972–1981) and, where possible, drawn inferences about the past and speculated about the future. This “baseline” period can be used by both present and future researchers to document changes in the numbers, lengths, and areas of Alaskan glaciers. The diverse data contained herein document that many Alaskan glaciers are rapidly changing, with most glaciers at lower elevations thinning, retreating, and (or) stagnant. The chapter also presents examples of the dynamic behavior of some glaciers, ranging from calving glaciers that have receded a kilometer or more in a year to surge-type glaciers that have advanced more than 10 km during a surge event. These larger scale changes are easily seen at the pixel resolution of Landsat images; in a few instances, Landsat has been the only record of these changes.

Through the use of retrospective and prospective data, this chapter has also shown many examples of the natural variability displayed by glaciers throughout Alaska. For instance, in less than a century, major coastal bays such as Glacier Bay and Icy Bay have formed or expanded in area owing to glacier recession; the catastrophic retreat of Columbia Glacier resulted in the production of icebergs that are a hazard to maritime navigation; the retreat of major glaciers such as Tazlina Glacier resulted in the formation of ice-dammed and ice-marginal lakes that can produce jökulhlaups when the ice dam fails; and, twice since the end of the “baseline” period, the ongoing advance of Hubbard Glacier has blocked Russell Fiord and produced two of the largest jökulhlaups ever witnessed in North America during modern times. Finally, this chapter has reviewed how changing climate has affected the areas (and volumes) of nearly all of Alaska's valley and piedmont glaciers, impacting the storage and release of freshwater and contributing in part to the observed increase in global sea level.

## Acknowledgments

Special thanks are offered to Maynard M. Miller, University of Idaho, Moscow, Idaho; Austin Post, U.S. Geological Survey (ret.); and the late William O. “Bill” Field, American Geographical Society. More than 35 years ago, Maynard gave me my first opportunity to become familiar with Alaskan glaciers; Bill gladly shared his data and his experiences in the 20 years that I knew him; and Austin was a good friend who, in addition to providing dozens of photographs included in this volume, accompanied me on many adventures to some of the most spectacular glaciers and fjords in the world—the glaciers and fjords of Alaska. Also, thanks to Darrell S. Kaufman, Department of Geology, Northern Arizona University, Flagstaff, Arizona; Robert M. Krimmel, USGS (ret.); Lawrence C. Mayo, USGS (ret.); and Dennis C. Trabant, USGS (ret.), for providing some of the images and (or) photographs and captions used in this volume. I especially want to recognize series editors Jane G. Ferrigno and Richard S. Williams, Jr., for their thorough technical reviews and comprehensive technical editing of the text and illustrations, Janice G. Goodell for typing multiple revisions and the final preparation of the manuscript, and Kirsten C. Healey for her outstanding work in the preparation of graphics throughout the volume, in both the printed and web versions. I also appreciate Kathie Rankin’s fine work in editing the text, graphics, and figure captions.

I also want to acknowledge the assistance provided by Rose Watabe, GeoData Center, Geophysical Institute, University of Alaska, in the correct identification of all of the AHAP false-color infrared vertical aerial photographs used throughout the chapter. I appreciate the efforts of John Pojeta, Jr., USGS (ret.), and Thomas R. Waller, National Museum of Natural History, Smithsonian Institution, to identify the bivalve mollusk *Petricola* sp. shown in figure 217. I am particularly grateful to the following technical reviewers, who freely gave of their time to review all or part of the text and illustrations: Anthony A. Arendt, Keith Echelmeyer, and William D. Harrison, Geophysical Institute, University of Alaska; Austin Post, USGS (ret.); Vashon, Washington; Mark F. Meier, University of Colorado, Institute for Arctic and Alpine Research, Boulder, Colo.; C Suzanne Brown, Tacoma, Wash.; and Parker E. Calkin, University of Colorado, Boulder, Colo.

## References Cited

- Abercrombie, W.R., 1900, Supplementary expedition into the Copper River Valley, Alaska, *in* Compilation of narratives of explorations in Alaska, part A: Washington, D.C., Government Printing Office, 169 p.
- Aðalgeirsdóttir, G., Echelmeyer, K.A., and Harrison, W.D., 1998, Elevation and volume changes on the Harding Icefield, Alaska: *Journal of Glaciology*, v. 44, 148, p. 570–582.
- Allen, C.R., and Smith, G.I., 1953, Seismic and gravity investigations on the Malaspina Glacier, Alaska: *Transactions, American Geophysical Union*, v. 34, no. 5, p. 755–760.
- Allen, H.T., 1887, Report of an expedition to the Copper, Tanana, and Koyukuk Rivers, in the Territory of Alaska, in the year 1885, for the purpose of obtaining all information which will be valuable and important, especially to the military branch of the government: Washington, D.C., Government Printing Office, 172 p.
- Allen, H.T., 1900, Military reconnaissance in Alaska, *in* Compilation of narratives of explorations in Alaska, part B: Washington, D.C., U.S. Government Printing Office, p. 411–488.
- Allen, T.R., 1998, Topographic context of glaciers and perennial snowfields, Glacier National Park, Montana: *Geomorphology*, v. 21, p. 207–216.
- Alpha DVD, 2003, *Glaciers. Alaska's rivers of ice: DVD International Learning Series, DVDI0736; in cooperation with the U.S. Geological Survey and the Alaska Geographic Society, 90-min. Digital Video Disk (DVD).*
- Alpha, T.R., 1975, The evolution of Icy Bay, Alaska, *in* Carlson, P.R., Conomos, T.J., Janda, R.J., and Peterson, D.H., eds., *Principal sources and dispersal patterns of suspended particulate matter in nearshore surface waters of the northeast Pacific Ocean: Final report prepared for NASA Goddard Space Flight Center, National Technical Information Service document no. E75-10266, p. 4–9.*
- American Geographical Society, 1960, *Nine glacier maps, Northwestern North America: American Geographical Society Special Publication no. 34, 37 p., 9 pls.*
- Anderson, S., 2003, Glacier behavior linked to seasonal hydrology: *Witness the Arctic*, v. 10, no. 1, p. 17.
- Anderson, S.P., Walder, J.S., Harris, R.S., Kraal, E.R., Cunico, M., Fountain, A.G., and Trabant, D.C., 2003, Integrated hydrologic and hydrochemical observations of Hidden Creek Lake jökulhlaups, Kennicott Glacier, Alaska: *Journal of Geophysical Research*, v. 108, pt. 1, p. 4.
- Andrews, C.L., and Gilbert, G.K., 1903, Muir Glacier: *National Geographic Magazine*, v. 14, no. 12, p. 441–444.
- Arcone, S.A., Lawson, D.E., and Delaney, A.J., 1995, Short-pulse radar wavelet recovery and resolution of dielectric contrasts within englacial and basal ice of Matanuska Glacier, Alaska, U.S.A.: *Journal of Glaciology*, v. 41, no. 137, p. 68–86.
- Arendt, A.A., Echelmeyer, K.A., Harrison, W.D., Lingle, C.S., and Valentine, V.B., 2002, Rapid wastage of Alaska glaciers and their contribution to rising sea level: *Science*, v. 297, no. 5580, p. 382–386. [Figs. S1, S2, and Table S1 at [<http://www.sciencemag.org/cgi/content/full/297/5580/382/DC1>]]
- Armentrout, J.M., 1983, Glacial lithofacies of the Neogene Yakataga Formation, Robinson Mountains, southern Alaska, Coast Range, *in* Molnia, B.F., ed., 1981, *Glacial-marine sedimentation: New York, Plenum Press, p. 629–665.*
- Bagley, J.W., 1917, The use of the panoramic camera in topographic surveying: *U.S. Geological Survey Bulletin* 657, 88 p.
- Bahr, D.B., 1997, Global distributions of glacier properties: A stochastic scaling paradigm: *Water Resources Research*, v. 33, no. 7, p. 1669–1679.
- Bahr, D.B. and Meier, M.F., 2000, Snow patch and glacier size distribution: *Water Resources Research*, v. 36, no. 2, p. 495–501.
- Bailey, Palmer, Fleisher, P.J., Mankoff, Evan, and Senglaub, Michael, 2000, An evolving ice-contact proglacial lake, Sheridan Glacier, Alaska [abs.]: *Geological Society of America, Abstracts with Programs*, v. 32, no. 7, p. 117.
- Baird, P.D., and Field, W.O., 1951, Report on the northern American glaciers, *in* General Assembly of Brussels, International Association of Scientific Hydrology: IASH Publication No. 32, v. 1, p. 120–128.
- Baker, Marcus, 1902, *Geographic dictionary of Alaska: U.S. Geological Survey Bulletin* 187, 446 p.
- Baker, Marcus (prepared by McCormick, James), 1906, *Geographic dictionary of Alaska: U.S. Geological Survey Bulletin* 299, 690 p.
- Balise, M.J., and Raymond, C.F., 1985, Transfer of basal sliding variations to the surface of a linearly viscous glacier: *Journal of Glaciology*, v. 31, no. 109, p. 308–318.
- Barclay, D.J., Calkin, P.E., and Wiles, G.C., 1999, A 1,119-year tree-ring-width chronology from western Prince William Sound, southern Alaska: *The Holocene*, v. 9, no. 1, p. 79–84.
- Barnes, F.F., 1943, *Geology of the Portage Pass area, Alaska: U.S. Geological Survey Bulletin* 926D, p. 211–235, with map.
- Bateman, A.M., 1922, *Kennecott Glacier of Alaska: Geological Society of America Bulletin*, v. 33, no. 3, p. 527–539.
- Bates, R.L., and Jackson, J.A., eds., 1987, *Glossary of geology (3d ed.): Alexandria, Virginia, American Geological Institute, 788 p.*
- Bean, E.F., 1911, *Fiords of Prince William Sound, Alaska: University of Wisconsin, M.A. dissertation, 63 p.*
- Beddall, B.G., 1979, *Scientific books and instruments for an eighteenth-century voyage around the world: Antonio Peneda and the Malaspina Expedition: Journal of the Society for the Bibliography of Natural History*, v. 9, part 2, p. 95–107.
- Belcher, E.B., 1843, *Narrative of a voyage around the world performed in Her Majesty's Ship Sulphur during the years 1836–1842: London, Henry Colburn Publisher, v. 1, p. 75–79.*
- Belcher, E.B., 1862, *Remarks on the glacial movements noticed in the vicinity of Mount St. Elias on the northwest coast of America: London, British Association for the Advancement of Science, Report of the 31st Meeting, Manchester, 1861, Notices and Abstracts of Miscellaneous Communications to the Sections, p. 186–187.*

- Bendavid-Val, Leah, Sobieszek, Robert, Naggar, Carole, Hoy, A.H., Protzman, Ferdinand, and Ritchin, Fred, 1999, National Geographic photographs. The milestones: Washington, D.C., National Geographic Society, 336 p. [The 1910 Von Engeln photograph is on p. 5; the caption is on p. 4.]
- Bengston, K.B., 1962, Recent history of the Brady Glacier, Glacier Bay National Monument, Alaska, U.S.A., *in* Symposium of Obergurgl, Variations in the regime of existing glaciers: International Association of Hydrological Sciences-Association Internationale des Sciences Hydrologiques (IAHS-AISH) Publication No. 58, p. 78–87.
- Benson, C.S., and Follett, A.B., 1986, Application of photogrammetry to the study of volcano-glacier interactions on Mount Wrangell, Alaska: *Photogrammetric Engineering and Remote Sensing*, v. 52, no. 6, p. 813–827.
- Benson, C.S., and Motyka, R.J., 1975, Recent glaciological and volcanological studies at the summit of Mt. Wrangell, Alaska [abs.]: *EOS (Transactions, American Geophysical Union)*, v. 56, no. 12, p. 1,073.
- Benson, C.S., and Motyka, R.J., 1978, Glacier-volcano interactions on Mt. Wrangell, Alaska: University of Alaska Fairbanks, Geophysical Institute, Annual Report 1977–78, p. 1–25.
- Benson, C.S., Bingham, D.K., and Wharton, G.B., 1975, Glaciological and volcanological studies at the summit of Mt. Wrangell, *in* Snow and Ice Symposium, Moscow, 9–13 August 1971: International Association of Hydrological Sciences-Association Internationale de Sciences Hydrologiques (IAHS-AISH) Publication No. 104, p. 95–98.
- Benson, C.S., Motyka, R.J., Bingham, D.K., Wharton, G., MacKeith, P., and Sturm, M., 1985, Glaciological and volcanological studies on Mt. Wrangell, Alaska, *in* Kotlyakov, V.M., Vinogradov, V.N., and Glazovsky, A.F., eds., Interaction between volcanism and glaciology: Moscow, Academy of Sciences of the USSR, Soviet Geophysical Committee, Glaciological Research No. 27, p. 114–133.
- Bindschadler, R.A., 1978, A time dependent model of temperate glacier flow and its application to predict changes in the surge-type Variegated Glacier during its quiescent phase: Ph.D. dissertation, University of Washington.
- Bindschadler, R.A., and Rasmussen, L.A., 1983, Finite-difference model predictions of the drastic retreat of Columbia Glacier, Alaska: U.S. Geological Survey Professional Paper 1258–D, 17 p.
- Bindschadler, R., Harrison, W.D., Raymond, C.F., and Crosson, R., 1977, Geometry and dynamics of a surge-type glacier: *Journal of Glaciology*, v. 18, no. 79, p. 181–194.
- Bishop, M.P., Olsenholler, J.A., Shroder, J.F., Barry, R.G., Raup, B.H., Bush, A.B.G., Coplan, L., Dwyer, J.L., Fountain, A.G., Haeberli, W., Käab, A., Paul, F., Hall, D.K., Kargel, J.S., Molnia, B.F., Trabant, D.C., and Wessels, R., 2004, Global land ice measurements from space (GLIMS): Remote sensing and GIS investigations of the Earth's cryosphere: *Geocarto International*, v. 19, no. 2, p. 57–84.
- Björnsson, Helgi, 1976, Subglacial water reservoirs, jökulhlaups, and volcanic eruptions: *Jökull*, v. 25 [1975], p. 1–14.
- Björnsson, Helgi, 1977, Marginal and supraglacial lakes in Iceland: *Jökull*, v. 26 [1976], p. 40–51.
- Black, Robert F., 1976, Late Quaternary glacial events, Aleutian Islands, Alaska, *in* Easterbrook, D.J., and Sibrava, V., eds., Quaternary glaciations in the Northern Hemisphere: IUGS-UNESCO, International Geological Correlation Programme, Project 73–1–24, Report 3, p. 285–301.
- Blackwelder, Eliot, 1907, Glacial features of the Alaskan coast between Yakutat Bay and the Alsek River: *Journal of Geology*, v. 15, no. 5, p. 415–433.
- Blake, W.P., 1867, The glaciers of Alaska, Russian America: *American Journal of Science*, v. 44, no. 130, p. 96–101.
- Blake, W.P., 1868, Geographical notes upon Russian America and the Stickeen River, being a report addressed to the Hon. W.H. Seward, Secretary of State: Washington, D.C., Government Printing Office, 19 p., 1 map.
- Brabb, E.E., and Miller, D.J., 1962, Reconnaissance traverse across the eastern Chugach Mountains, Alaska: U.S. Geological Survey Miscellaneous Geological Investigations Map I–341, 1 sheet, scale 1:96,000.
- Brabets, T.P., 1993, Glacier runoff and sediment transport and deposition, Eklutna Lake basin, Alaska: U.S. Geological Survey Water-Resources Investigations Report 92–4132, 47 p.
- Bradley, C.C., 1948, Geologic notes on Adak Island and the Aleutian Chain, Alaska: *American Journal of Science*, v. 246, no. 4, p. 214–240.
- Bradley, W.C., Fahnestock, R.K., and Rowekamp, E.T., 1972, Coarse sediment transport by flood flows on Knik River, Alaska: *Geological Society of America Bulletin*, v. 83, no. 5, p. 1,261–1,284.
- Braithwaite, R.J., and Müller, F., 1980, On the parameterization of glacier equilibrium line altitude, *in* World Glacier Inventory, Proceedings of the Workshop, 17–22 September 1987, Reideralp, Switzerland: International Association of Hydrological Sciences/Association Internationale des Sciences Hydrologiques (IAHS-AISH) Publication No. 126, p. 263–271.
- Brooks, A.H., 1900, A reconnaissance in the White and Tanana River basins, Alaska, in 1898: U.S. Geological Survey Annual Report 20 (1898–99), pt. vii, Explorations in Alaska in 1898, p. 425–494.
- Brooks, A.H., 1902, Proposed surveys of Alaska in 1902: *National Geographic Magazine*, v. 13, p. 133–135.
- Brooks, A.H., 1904, Geography of Alaska: *National Geographic Magazine*, v. 15, p. 213–219.
- Brooks, A.H., 1906a, How much is known of Alaska?: *National Geographic Magazine*, v. 17, p. 112–114.
- Brooks, A.H., 1906b, The geography and geology of Alaska: USGS Professional Paper 45, 327p.
- Brooks, A.H., 1911, The Mount McKinley region, Alaska: USGS Professional Paper 70, 234 p.
- Brooks, A.H., 1914, Mountain exploration in Alaska: *Alpina America*, v. 3, 22 p.
- Brooks, A.H., and Raeburn, D.L., 1903, Plan for climbing Mt. McKinley: *National Geographic Magazine*, v. 9, p. 30–35.
- Brooks, A.H., Richardson, G.B., Collier, A.J., and Mendenhall, W.C., 1901, Reconnaissances in the Cape Nome and Norton Bay regions, Alaska, in 1900: U.S. Geological Survey Special Publication, 222 p.

- Brooks, P.D., 1988, The Alaska High-Altitude Aerial Photography (AHAP) Program: A state/federal cooperative program: Anchorage, AHAP Program Office, 8 p.
- Brown, C.S., Meier, M.F., and Post, Austin, 1982, Calving speed of Alaska tidewater glaciers, with application to Columbia Glacier: U.S. Geological Survey Professional Paper 1258-C, 13 p.
- Brown, C.S., Rasmussen, L.A., and Meier, M.F., 1986, Bed topography inferred from airborne radio-echosounding of Columbia Glacier, Alaska: U.S. Geological Survey Professional Paper 1258-G, 26 p.
- Brown, D.M., 1952, Glaciers advance: *Appalachia*, v. 29, no. 114, p. 41-44.
- Brugman, M.M., 1987, Water flow at the base of a surging glacier: Ph.D. dissertation, California Institute of Technology.
- Buddington, A.F., and Chapin, Theodore, 1929, Geology and mineral deposits of southeastern Alaska: U.S. Geological Survey Bulletin 800, 398 p.
- Bull, Colin, 1969, The 1978-1980 surge of the Sherman Glacier, south-central Alaska: *Canadian Journal of Earth Sciences*, v. 6, no. 4, p. 841-843.
- Bull, Colin, and Marangunic, Cedomir, 1967, The earthquake-induced slide on the Sherman Glacier, south-central, Alaska and its glaciological effects, *in* Hirobumi, Oura, ed., *Physics of snow and ice*, Proceedings of the International Conference on Low Temperature Science, Sapporo, Japan, 1966: Sapporo, Institute of Low Temperature Science, v. 1, pt. 1, p. 395-408.
- Bull, Colin, and Marangunic, Cedomir, 1968, Glaciological effects of debris slide on Sherman Glacier, *in* The great Alaska earthquake of 1964, v. 1, Hydrology, pt. A: Washington, D.C., National Academy of Sciences, Publication 1603, p. 309-317.
- Burroughs, John, 1902, Narrative of the Expedition, *in* Burroughs, John, Muir, John, and Grinnel, G.B., *Alaska—narrative, glaciers, natives: Volume I of the Harriman Alaska Expedition with cooperation of the Washington Academy of Sciences*: New York, Doubleday, Page, and Company, p. 1-118.
- Burroughs, John, Muir, John, and Grinnel, G.B., 1902, *Alaska—narrative, glaciers, natives: Volume I of the Harriman Alaska Expedition with cooperation of the Washington Academy of Sciences*: New York, Doubleday, Page, and Company, 183 p.
- Byers, F.M., Jr., 1959, Geology of Umnak and Bogoslof Islands, Aleutian Islands, Alaska: U.S. Geological Survey Bulletin 1028-L, p. 267-369, maps.
- Calkin, P.E., 1988, Holocene glaciation of Alaska (and adjoining Yukon Territory, Canada): *Quaternary Science Reviews*, v. 7, no. 2, p. 159-184.
- Calkin, P.E., Kaufman, D.S., Przybyl, B.J., Whitford, W.B., and Peck, B.J., 1998, Glacier regimes, periglacial landforms, and Holocene climate change in the Kigluaik Mountains, Seward Peninsula, Alaska, U.S.A.: *Arctic and Alpine Research*, v. 30, no. 2, p. 154-165.
- Capps, S.R., 1910a, Glaciation on the north side of the Wrangell Mountains, Alaska: *Journal of Geology*, v. 18, no. 1, p. 33-57.
- Capps, S.R., 1910b, Rock glaciers in Alaska: *Journal of Geology*, v. 18, no. 4, p. 359-375.
- Capps, S.R., 1916, The Turnagain-Knik region: U.S. Geological Survey Bulletin 642, p. 147-194.
- Carlson, P.R., Bruns, T.R., Molnia, B.F., and Schwab, W.C., 1982, Submarine valleys in the northeastern Gulf of Alaska: characteristics and probable origin: *Marine Geology*, v. 47, no. 3/4, p. 217-242.
- Carlson, P.R., Tagg, R.A., and Molnia, B.F., 1993, Acoustic profiles of sediment in a melt-water lake adjacent to the Bering Glacier, Alaska, *RV Kartuk* cruise K2-91-YB, July 1-7, 1991: U.S. Geological Survey Open-File Report 93-266, 26 p.
- Carlson, P.R., Hooge, P.N., and Stevenson, Andrew, 2001, Multi-beam imagery shows extensive iceberg reworking of the lower Glacier Bay, Alaska fjord [abs.]: *EOS (Transactions, American Geophysical Union)*, v. 82, no. 47, Fall Meeting Supplement, Abstract B12C-0145, p. F165.
- Castner, J.C., 1899, Report of Lieutenant J.C. Castner, *in* Glenn, E.F., and Abercrombie, W.R., 1899, Reports of explorations in the Territory of Alaska, made under the direction of the Secretary of War: U.S. War Department, Adjunct General's Office, Publication XXV, p. 189-265.
- Clarke, G.K.C., 1991, Length, width and slope influences on glacier surging: *Journal of Glaciology*, v. 37, no. 126, p. 236-246.
- Clarke, G.K.C., and Holdsworth, Gerald, 2002a, Glaciers of the Coast Mountains, *in* Williams, R.S., Jr., and Ferrigno J.G., eds, *Satellite image atlas of glaciers of the world: U.S. Geological Survey Professional Paper 1386-J (Glaciers of North America)*, p. J291-J300. [<http://pubs.usgs.gov/prof/p1386j>]
- Clarke, G.K.C., and Holdsworth, Gerald, 2002b, Glaciers of the St. Elias Mountains, *in* Williams, R.S., Jr., and Ferrigno, J.G., eds, *Satellite image atlas of glaciers of the world: U.S. Geological Survey Professional Paper 1386-J (Glaciers of North America)*, p. J301-J328. [<http://pubs.usgs.gov/prof/p1386j>].
- Clarke, G.K.C., and Mathews, W.H., 1981, Estimates of the magnitude of glacier outburst floods from Lake Donjek, Yukon Territory, Canada: *Canadian Journal of Earth Sciences*, v. 18, no. 9, p. 1,452-1,463.
- Clarke, G.K.C., and Waldron, D.A., 1984, Simulation of the August 1979 sudden discharge of glacier-dammed Flood Lake, British Columbia: *Canadian Journal of Earth Sciences*, v. 21, no. 4, p. 502-504.
- Clarke, G.K.C., Schmok, J.P., Ommanney, C.S.L., and Collins, S.G., 1986, Characteristics of surge-type glaciers: *Journal of Geophysical Research*, v. 91, no. 7, p. 7,165-7,180.
- Clarke, G.K.C., Cross, G.M., and Benson, C.S., 1989, Radar imaging of glaciovolcanic stratigraphy, Mount Wrangell caldera, Alaska: Interpretation model and results: *Journal of Geophysical Research*, v. 94, no. B6, p. 7,237-7,249.
- Clarke, T.S., 1991, Glacier dynamics in the Susitna River basin, Alaska: *Journal of Glaciology*, v. 37, no. 125, p. 97-106.
- Clayton, Lee, 1964, Karst topography on stagnant glaciers: *Journal of Glaciology*, v. 5, no. 37, p. 107-112.
- Coats, R.R., 1956, Reconnaissance geology of some western Aleutian Islands, Alaska: U.S. Geological Survey Bulletin 1028-E, p. 83-97.
- Collins, H.B., Jr., 1945, The islands and their people, *in* The Aleutian Islands: their people and natural history: Washington, D.C., Smithsonian Institution, War Background Studies Number 21, Smithsonian Institution Publication 3775, p. 1-30.

- Collins, S.G., 1975, Glaciers of the Talkeetna Mountains, Alaska, *in* Field, W.O., ed., Mountain glaciers of the Northern Hemisphere: Hanover, New Hampshire, U.S. Army Corps of Engineers, Cold Regions Research and Engineering Laboratory, v. 2, p. 543–548.
- Collins, S.G., and Clarke, G.K.C., 1977, History and bathymetry of a surge-dammed lake: Arctic, v. 30, no. 4, p. 217–224.
- Connor, C.L., Seifert, S.L., Matlocks, K., Graves, A.J., Tabor, L.F., Motyka, R.J., and O'Neel, S., 1999, Undergraduates study calving retreat at Le Conte Glacier, southeast Alaska [abs.]: *in* Abstracts with Programs (Geological Society of America), v. 31, no. 4, p. 8.
- Cooper, W.S., 1937, The problem of Glacier Bay, Alaska — A study of glacier variations: Geographical Review, v. 27, no. 1, p. 37–62.
- Cooper, W.S., 1942, Vegetation of the Prince William Sound region, Alaska, with a brief excursion into post-Pleistocene climatic history: Ecological Monographs, v. 12, no. 1, p. 1–22.
- Crossen, K.J., 1990, Neoglacial history of Portage Glacier, Kenai Mountains, Alaska [abs.]: *in* Abstracts with Programs, Geological Society of America 1990 Annual Meeting, v. 22, no. 7, p. 177.
- Cunico, M.L., Walder, J.S., Fountain, A.G., and Trabant, D.C., 2001, Localized glacier deformation associated with filling and draining of a glacier-dammed lake and implications for outburst flood hydraulics [abs.]: EOS (Transactions, American Geophysical Union), v. 82, no. 47, Fall Meeting Supplement, Abstract IP11A–0650, p. F522.
- Cushing, H.P., 1896, Notes on the areal geology of Glacier Bay, Alaska: New York Academy of Sciences Transactions, v. 15, p. 24–34.
- Dall, W.H., 1870, Alaska and its resources: London, Sampson Low, Son and Marston, 627 p.
- Dall, W.H., 1884, Glaciation in Alaska: Philosophical Society of Washington Bulletin, v. 6, p. 33–36.
- Dall, W.H., 1896, Report on coal and lignite of Alaska: U.S. Geological Survey Annual Report, v. 17, pt. 1, p. 763–875.
- Davidson, George, 1886, The first ascent of the volcano Makushin: Appalachia, v. 4, no. 1, p. 1–11.
- Davidson, George, 1901, The tracks and landfalls of Bering and Chirikof on the northwest coast of America. From the point of their separation in latitude 49°10', longitude 176°40' West, to their return to the same meridian, June, July, August, September 1741: San Francisco, John Partridge, Stationer and Printer, Private Publication, 44 p., 1 map.
- Davidson, George, 1903, The Alaska boundary: San Francisco, Alaska Packers Association, 234 p., 2 pls.
- Davidson, George, 1904, The glaciers of Alaska that are shown on Russian charts or mentioned in older narratives: Geographical Society of the Pacific Transactions and Proceedings, Series 2, v. 3, p. 1–98.
- Davis, J.C., 1986, Statistics and data analysis in Geology, 2nd ed.: New York, Wiley and Sons, 646 p.
- Davis, T.N., and Sanders, N.K., 1960, Alaska earthquake of July 10, 1958: Intensity distribution and field investigation of northern epicentral region: Seismological Society of America Bulletin, v. 50, no. 2, p. 221–252.
- de Fillippi, Fillippo, 1899, The Ascent of Mount St. Elias [Alaska] by H.R.H. Prince Luigi Amedeo Di Savoia, Duke of the Abruzzi: New York, Frederick A. Stokes, Co. Publishers, 242 p., 4 mosaic pls., 2 maps.
- de Laguna, Frederica, 1972, Under Mount Saint Elias: The history and culture of the Yakutat Tlingit: Washington, D.C., Smithsonian Institution Press, Smithsonian Contributions to Anthropology, v. 7, pt. 1, 547 p.
- DeLorme Mapping, 1992, Alaska atlas and gazetteer (1st ed.): Freeport, Maine, 156 p.
- DeLorme Mapping, 1998, Alaska atlas and gazetteer (2d ed.): Yarmouth, Maine, 156 p.
- DeLorme Mapping, 2001, Alaska atlas and gazetteer (4th ed.): Yarmouth, Maine, 156 p.
- Denton, G.H., 1975a, Glaciers of the Aleutian Islands, *in* Field, W.O., ed., Mountain glaciers of the Northern Hemisphere: Hanover, New Hampshire, U.S. Army Corps of Engineers, Cold Regions Research and Engineering Laboratory, v. 2, p. 641–650.
- Denton, G.H., 1975b, Glaciers of the Brooks Range, *in* Field, W.O., ed., Mountain glaciers of the Northern Hemisphere: Hanover, New Hampshire, U.S. Army Corps of Engineers, Cold Regions Research and Engineering Laboratory, v. 2, p. 651–662.
- Denton, G.H., and Field, W.O., 1975a, Glaciers of the Alaska Range, *in* Field, W.O., ed., Mountain glaciers of the Northern Hemisphere: Hanover, New Hampshire, U.S. Army Corps of Engineers, Cold Regions Research and Engineering Laboratory, v. 2, p. 573–620.
- Denton, G.H., and Field, W.O., 1975b, Glaciers of the Aleutian Range and Kodiak Island, *in* Field, W.O., ed., 1975, Mountain glaciers of the Northern Hemisphere: Hanover, New Hampshire, U.S. Army Corps of Engineers, Cold Regions Research and Engineering Laboratory, v. 2, p. 621–639.
- Denton, G.H., and Field, W.O., 1975c, Glaciers of the Wrangell Mountains, *in* Field, W.O., ed., 1975, Mountain glaciers of the Northern Hemisphere: Hanover, New Hampshire, U.S. Army Corps of Engineers, Cold Regions Research and Engineering Laboratory, v. 2, p. 549–571.
- Denton, G.H., and Karlén, Wibjorn, 1977, Holocene glacial and tree-line variations in the White River valley and Skolai Pass, Alaska and Yukon Territory: Quaternary Research, v. 7, no. 1, p. 63–111.
- Dickey, W.A., 1897, The Susitna River, Alaska: National Geographic Magazine, v. 8, p. 322–327.
- Dorrer, Egon, and Wendler, Gerd, 1976, Climatological and photogrammetric speculations on mass-balance changes of McCall Glacier, Brooks Range, Alaska: Journal of Glaciology, v. 17, no. 77, p. 479–490.
- Drewes, Harold, Fraser, G.D., Snyder, G.L., and Barnett, H.F., Jr., 1961, Geology of Unalaska Island and adjacent insular shelf, Aleutian Islands, Alaska: U.S. Geological Survey Bulletin 1028, p. 583–676.
- Driedger, C.L., 1981, Effect of ash thickness on snow ablation; *in* Lipman, P.W., and Mullineaux, D.R., eds., The 1980 eruptions of Mount St. Helens, Washington: U.S. Geological Survey Professional Paper 1250, p. 757–760.

- Dyurgerov, M.B., and Dwyer, Jerry, 2000, The steepening of glacier mass balance gradients with Northern Hemisphere warming: *Zeitschrift für Gletscherkunde und Glazialgeologie*, v. 36, p. 107–118.
- Dyurgerov, M.B., and Meier, M.F., 1997a, Mass balance of mountain and subpolar glaciers: a new assessment for 1961–1990: *Arctic and Alpine Research*, v. 29, no. 4, p. 379–391.
- Dyurgerov, M.B., and Meier, M.F., 1997b, Year-to-year fluctuations of global mass balance of small glaciers and their contribution to sea level changes: *Arctic and Alpine Research*, v. 29, no. 4, p. 392–402.
- Dyurgerov, M.B., and Meier, M.F., 1999, Analysis of winter and summer mass balances: *Geografiska Annaler*, v. 81A, no. 4, p. 541–554.
- Dyurgerov, M.B., and Meier, M.F., 2000, Twentieth century climate change: Evidence from small glaciers: *Proceedings, National Academy of Sciences*, v. 97, no. 4, p. 1,406–1,411.
- Echelmeyer, Keith, and Motyka, R.J., 1997, LeConte Glacier, Alaska—Surface elevation changes and calving retreat, *in* Van der Veen, C.J., ed., *Calving glaciers; Report of a Workshop February 28–March 2, 1997*: Columbus, Ohio, The Ohio State University, Byrd Polar Research Center, BPRC Report No. 15, p. 67–70.
- Echelmeyer, K.A., Harrison, W.D., Larsen, C.F., Sapiano, J., Mitchell, J.E., DeMallie, J., Rabus, B., Adalgeirsdóttir, G., and Sombardier, L., 1996, Airborne surface profiling of glaciers: a case-study in Alaska: *Journal of Glaciology*, v. 42, no. 142, p. 538–547.
- Egan, C.P., Miller, M.M., and Loken, K., 1968, The Davidson Glacier buried forest [abs.]: *Alaskan Science Conference, 19th, Science in the North, Whitehorse, Yukon Territory, 26–30 August 1968, Abstracts of Papers*, p. 24.
- Ellis, J.M., and Calkin, P.E., 1979, Nature and distribution of glaciers, Neoglacial moraines, and rock glaciers, east-central Brooks Range, Alaska: *Arctic and Alpine Research*, v. 11, no. 4, p. 409–420.
- Ellis, J.M., and Calkin, P.E., 1984, Chronology of Holocene glaciation, central Brooks Range, Alaska: *Geological Society of America Bulletin*, v. 95, no. 8, p. 897–912.
- Emery, P.A., and Seitz, H.R., 1987, In the St. Elias Mountains, Hubbard Glacier is still on the move: *Geotimes*, v. 32, no. 5, p. 8–9.
- Evans, I.S., 1977, World-wide variations in the direction and concentration of cirque and glacier aspects: *Geografiska Annaler*, v. 59A, no. 3–4, p. 151–175.
- Fatland, D.R., and Lingle, C.S., 1998, Analysis of the 1993–95 Bering Glacier (Alaska) surge using differential SAR interferometry: *Journal of Glaciology*, v. 44, no. 148, p. 532–546.
- Fatland, D.R., and Lingle, C.S., 2002, InSAR observations of the 1993–95 Bering Glacier (Alaska, U.S.A.) surge and a surge hypothesis: *Journal of Glaciology*, v. 48, no. 162, p. 439–451.
- Field, W.O., 1926, The Fairweather Range: *Mountaineering and Glacier Studies: Appalachia*, v. 16, no. 4, p. 460–472.
- Field, W.O., 1932, The glaciers of the northern part of Prince William Sound, Alaska: *Geographical Review*, v. 22, no. 3, p. 361–388.
- Field, W.O., 1937, Observations on Alaskan coastal glaciers in 1935: *Geographical Review*, v. 27, no. 1, p. 63–81.
- Field, W.O., 1942, Glacier studies in Alaska: *Geographical Review*, v. 32, no. 1, p. 154–155.
- Field, W.O., 1948, The variations of Alaskan glaciers, 1935–1947: *International Geodetic and Geophysical Union, Association of Scientific Hydrology, Assemblée Générale d'Oslo, 19–28 August 1948*, v. 2, p. 277–282.
- Field, W.O., 1958, *Glaciers of the Alaska Range, geographic study of mountain glaciation in the Northern Hemisphere, Part 2a, Chapter 7*: New York, American Geographical Society, p. 2a.7.1–2a.7.6.
- Field, W.O., 1964, Observations of glacier variations in Glacier Bay, southeastern Alaska, 1958 and 1961, *Glacier Bay National Monument—Preliminary Report*: American Geographical Society, unpublished report, 35 p.
- Field, W.O., 1965, Maps of glacier termini in southern Alaska: *American Geographical Society, unpublished report*, 2 p., 25 maps.
- Field, W.O., 1969, Current observations on three surges in Glacier Bay, Alaska, 1965–1968: *Canadian Journal of Earth Sciences*, v. 6, no. 4, p. 831–839.
- Field, W.O., ed., 1975a, *Mountain glaciers of the Northern Hemisphere*: Hanover, New Hampshire, U.S. Army Corps of Engineers, Cold Regions Research and Engineering Laboratory, 2 vols., v. 1, 698 p., v. 2, 932 p. includes Atlas containing index maps of each glacierized region.
- Field, W.O., 1975b, *Glaciers of the Chugach Mountains*, *in* Field, W.O., ed., *Mountain glaciers of the Northern Hemisphere*: Hanover, New Hampshire, U.S. Army Corps of Engineers, Cold Regions Research and Engineering Laboratory, v. 2, p. 299–492.
- Field, W.O., 1975c, *Glaciers of the Coast Mountains, Boundary Ranges*, *in* Field, W.O., ed., *Mountain glaciers of the Northern Hemisphere*: Hanover, New Hampshire, U.S. Army Corps of Engineers, Cold Regions Research and Engineering Laboratory, v. 2, p. 11–141.
- Field, W.O., 1975d, *Glaciers of the Kenai Mountains, Alaska*, *in* Field, W.O., ed., *Mountain glaciers of the Northern Hemisphere*: Hanover, New Hampshire, U.S. Army Corps of Engineers, Cold Regions Research and Engineering Laboratory, v. 2, p. 493–541.
- Field, W.O., 1990, *Glaciers of Alaska and adjacent Yukon Territory and British Columbia: The American Alpine Journal*, v. 32, Issue 64, p. 79–149.
- Field, W.O., 2004, *With a camera in my hands: William O. Field, pioneer glaciologist [A life history as told to C Suzanne Brown]*: Fairbanks, University of Alaska Press, 184 p. + xxiv.
- Field, W.O., and Collins, S.G., 1975, *Glaciers of the St. Elias Mountains*, *in* Field, W.O., ed., *Mountain glaciers of the Northern Hemisphere*: Hanover, New Hampshire, U.S. Army Corps of Engineers, Cold Regions Research and Engineering Laboratory, v. 2, p. 143–297.
- Finch, R.H., 1934, *Shishaldin Volcano*, *in* *Fifth Pacific Science Congress, Canada, 1933, Record of the Proceedings*: Toronto, University of Toronto Press, v. 3, p. 2,369–2,376.
- Fleisher, P.J., Franz, J.M., Gardiner, J.A., 1993, Bathymetry and sedimentary environments in proglacial lakes at the eastern Bering Piedmont Glacier of Alaska: *Journal of Geological Education*, v. 41, no. 3, p. 267–274.

- Fleming, M.D., 2000, Satellite image map of Lake Clark National Park: U.S. Geological Survey satellite image map, 1 sheet, scale 1:250,000.
- Ford, J.P., 1984, Mapping of glacial land forms from Seasat radar images: *Quaternary Research*, v. 22, no. 3, p. 314–327.
- Fountain, A.G., Krimmel, R.M., and Trabant, D.C., 1997, A strategy for monitoring glaciers: U.S. Geological Survey Circular 1132, 19 p.
- Funk, J.M., 1973, Late Quaternary geology of Cold Bay, Alaska and vicinity: University of Connecticut, M.S. dissertation, unpublished, 45 p.
- Gannett, Henry, 1899, The Harriman Alaska Expedition: *National Geographic Magazine*, v. 10, no. 12, p. 507–512.
- Gilbert, G.K., 1903, *Glaciers of Alaska*: National Geographic Magazine, v. 14, p. 449–450.
- Gilbert, G.K., 1904, *Alaska-glaciers and glaciation*, Volume 3 of the Harriman Alaska Expedition with Cooperation of the Washington Academy of Sciences: New York, Doubleday, Page, and Company, 231 p.
- Glen, J.W., 1954, The stability of ice-dammed lakes and other water-filled holes in glaciers: *Journal of Glaciology*, v. 2, no. 15, p. 316–318.
- Glenn, E.F., 1899, Report of Captain Edwin F. Glenn, *in* Glenn, E.F., and Abercrombie, W.R., 1899, Reports of explorations in the Territory of Alaska, made under the direction of the Secretary of War: U.S. War Department, Adjunct General's Office, Publication 25, p. 5–123.
- Goldthwait, R.P., McKellar, I.C., and Crank, Casper, 1963, Fluctuations of the Crillon Glacier system, southeastern Alaska: *IASH Bulletin*, v. 8, no. 1, p. 62–74.
- Grant, U.S., and Higgins, D.F., 1910, *Glaciers of Prince William Sound and the southern part of the Kenai Peninsula, Alaska, part 1, Glaciers of the northern part of Prince William Sound*: American Geographical Society Bulletin, v. 42, no. 10, p. 721–738.
- Grant, U.S., and Higgins, D.F., 1911a, *Glaciers of Prince William Sound and the southern part of the Kenai Peninsula, Alaska, part 2, Glaciers of Port Wells, Prince William Sound*: American Geographical Society Bulletin, v. 43, no. 5, p. 321–338.
- Grant, U.S., and Higgins, D.F., 1911b, *Glaciers of Prince William Sound and the southern part of the Kenai Peninsula, Alaska, part 3, Glaciers of the West Coast of Prince William Sound*: American Geographical Society Bulletin, v. 43, no. 6, p. 401–417.
- Grant, U.S., and Higgins, D.F., 1913, *Coastal glaciers of Prince William Sound and Kenai Peninsula, Alaska*: U.S. Geological Survey Bulletin 526, 75 p., 2 pls.
- Gray, J.R., Hart, R.J., and Molnia, B.F., 1994, 1994 changes in physical and sedimentary characteristics of proglacial Vitus Lake resulting from the surge of Bering Glacier, Alaska [abs.]: EOS (Transactions, American Geophysical Union), 1994 Fall Meeting Supplement, v. 75, no. 44, p. 63.
- Griggs, R.F., 1922, The Valley of the Ten Thousand Smokes: Washington, D.C., The National Geographic Society, 341 p.
- Hall, D.K., and Ormsby, J.P., 1983, Use of SEASAT synthetic aperture radar and LANDSAT multispectral scanner subsystem data for Alaskan glaciology studies: *Journal of Geophysical Research*, v. 88, no. C3, p. 1,597–1,607.
- Hall, D.K., Benson, C.S., and Field, W.O., 1995, Changes in glaciers in Glacier Bay, Alaska, using ground and satellite measurements: *Physical Geography*, v. 16, no. 1, p. 27–41.
- Hamilton, T.D., 1965, Comparative glacier photographs from northern Alaska: *Journal of Glaciology*, v. 5, no. 40, p. 479–487.
- Hamilton, T.D., and Porter, S.C., 1975, Itkillik glaciation in the Brooks Range, northern Alaska: *Quaternary Research*, v. 5, no. 4, p. 471–497.
- Harp, E.L., Jibson, R.W., Kayen, R.E., Keefer, D.K., Sherrod, B.L., Carver, G.A., Collins, B.D., Moss, R.E.S., and Sitar, N., 2003, Landslides and liquefaction triggered by the M7.9 Denali Fault earthquake of 3 November 2002: *GSA Today*, v. 13, no. 8, p. 4–10.
- Harper, J.T., Humphrey, N.F., and Pfeffer, W.T., 1998, Crevasse patterns and the strain-rate tensor; a high-resolution comparison: *Journal of Glaciology*, v. 44, no. 146, p. 68–76.
- Harriman, E.H., 1902, Preface, *in* Burroughs, John, Muir, John, and Grinnell, G.B., 1902, *Alaska—narrative, glaciers, natives*, Volume 1 of the Harriman Alaska Expedition with Cooperation of the Washington Academy of Sciences: New York, Doubleday, Page, and Company, 183 p.
- Harrison, W.D., and Post, A.S., 2003, How much do we really know about glacier surging?: *Annals of Glaciology*, v. 36, p. 1–6.
- Harrison, W.D., Raymond, C.F., and MacKeith, P., 1986, Short period motion events on Variegated Glacier as observed by automatic photography and seismic methods: *Annals of Glaciology*, v. 8, p. 82–89.
- Hayes, C.W., 1892, An expedition through the Yukon District: *National Geographic Magazine*, v. 4, p. 117–159.
- Heinrichs, T.A., Mayo, L.R., Trabant, D.C., and March, R.S., 1995, Observations of the surge-type Black Rapids Glacier, Alaska, during a quiescent period, 1970–92: U.S. Geological Survey Open-File Report 94–512, 98 p., appendixes and diskette.
- Heinrichs, T.A., Mayo, L.R., Echelmeyer, K.A., and Harrison, W.D., 1996, Quiescent-phase evolution of a surge-type Black Rapids Glacier, Alaska, U.S.A.: *Journal of Glaciology*, v. 42, no. 140, p. 110–122.
- Henderson, K.A., and Putnam, W.L., 1947, Aleutian mountaineering: *Harvard Mountaineering*, no. 8, p. 27–32.
- Henry, J.F., 1984, Early maritime artists of the Pacific Northwest coast, 1741–1841: Seattle, University of Washington Press, 240 p.
- Henshaw, F.F., and Parker, G.L., 1913, Surface water supply of Seward Peninsula, Alaska: U.S. Geological Survey Water-Supply Paper 314, 317 p.
- Heusser, C.J., and Marcus, M.G., 1964, Historical variations of Lemon Creek Glacier, Alaska, and their relationship to the climatic record: *Journal of Glaciology*, v. 5, no. 37, p. 77–86.
- Hodge, S.M., Trabant, D.C., Krimmel, R.M., Heinrichs, T.A., March, R.S., Josberger, E.G., 1998, Climate variations and changes in mass of three glaciers in western North America: *Journal of Climate*, v. 11, no. 9, p. 2,161–2,179.
- Hopkins, D.M., Pratt, Richard, Nelso, R.E., and Powell, C.L., II, 1983, Glacial sequence, southwestern Seward Peninsula [abs.], *in* Thorson, R.M., and Hamilton, T.D., eds., *Glaciation in Alaska*. Extended abstracts from a workshop: Fairbanks, Alaska, Alaskan Quaternary Center, University of Alaska Museum, Occasional Paper No. 2, p. 45–50.



- Horvath, E.V., and Field, W.O., 1969, References to glacier surges in North America: *Canadian Journal of Earth Science*, v. 6, no. 4, p. 845–851.
- Howard, K.M., Anderson, R.S., and Anderson, S.P., 1996, Ice motion and water and sediment fluxes through a spring flood event, Bench Glacier, Alaska [abs.]: *EOS (Transactions, American Geophysical Union)*, v. 77, no. 46, supplement, p. 217.
- Hubbard, B.R., 1935, *Cradle of the storms*: New York, Dodd, Mead, and Company, 285 p.
- Hulley, C.C., 1953, *Alaska 1741–1953*: Portland, Ore., Binforde and Mort, Publishers, 406 p.
- Hulsing, Harry, 1981, *The breakout of Alaska's Lake George*: U.S. Geological Survey General Interest Publication, 15 p.
- Humphrey, N.F., and Raymond, C.F., 1994, Hydrology, erosion and sediment production in a surging glacier: *Variogated Glacier, Alaska, 1982–83*: *Journal of Glaciology*, v. 40, no. 136, p. 539–552.
- Humphrey, Neil, Raymond, Charles, and Harrison, Will, 1986, Discharges of turbid water during mini-surges of *Variogated Glacier, Alaska, U.S.A.*: *Journal of Glaciology*, v. 32, no. 111, p. 195–207.
- Hunter, L.E., Motyka, R.J., and Echelmeyer, Keith, 2001, Sedimentation and denudation rates of a tidewater glacier eroding batholithic bedrock, LeConte Glacier, Alaska [abs.]: *EOS (Transactions, American Geophysical Union)*, v. 82, no. 47, Fall Meeting Supplement, Abstract IP52A-0747, p. 556.
- International Boundary Commission, 1951, *Joint maps of the international boundary between the United States and Canada, from Cape Munzon to Mount St. Elias*: Washington, D.C., Department of State, 13 sheets (all published individually at earlier dates).
- International Boundary Commission, 1952, *Establishment of the boundary between Canada and the United States, Tongas Passage to Mount St. Elias*: Washington, D.C., U.S. Department of State, 365 p.
- Jackson, J.A., ed., 1997, *Glossary of geology (4th ed.)*: Alexandria, Va., American Geological Institute, 769 p.
- Jacobel, R.W., and Anderson, S.K., 1987, Interpretation of radio-echo returns from internal water bodies in *Variogated Glacier, Alaska, U.S.A.*: *Journal of Glaciology*, v. 33, no. 115, p. 319–323.
- Jaeger, J.M., and Nittrouer, C.A., 1999a, Marine record of surge-induced outburst floods from the Bering Glacier, Alaska: *Geology*, v. 27, no. 9, p. 847–850.
- Jaeger, J.M., and Nittrouer, C.A., 1999b, Sediment deposition in an Alaskan fjord: controls on the formation and preservation of sediment structures in Icy Bay: *Journal of Sedimentary Research*, v. 69, no. 5, p. 1,011–1,026.
- Johnson, B.L., 1917, *Retreat of Barry Glacier, Port Wells, Prince William Sound, Alaska, between 1910 and 1914*: U.S. Geological Survey Professional Paper 98, p. 35–36.
- Jordan, G.F., 1962, Redistribution of sediments in Alaskan bays and inlets: *The Geographical Review*, v. 52, no. 4, p. 548–558.
- Josberger, E.G., Meadows, G.A., Shuchman, R.A., and Payne, J.R., 2001, Sediment control of convection in glacier dammed lakes [abs.]: *EOS (Transactions, American Geophysical Union)*, v. 82, no. 47, Fall Meeting Supplement, Abstract IP52A-0743, p. F556.
- Juhle, R.W., and Coulter, H.W., 1955, The Mt. Spurr eruption, July 9, 1953: *EOS (Transactions, American Geophysical Union)*, v. 36, no. 2, p. 199–202.
- Kääb, Andreas, Paul, Frank, Maisch, Max, Hoelzle, Martin, and Haerberli, Wilfried, 2002, The new remote-sensing-derived Swiss glacier inventory: II. First results: *Annals of Glaciology*, v. 34, p. 362–366.
- Kamb, Barclay, 1987, Glacier surge mechanism based on linked cavity configuration on the basal water conduit system: *Journal of Geophysical Research*, v. 92, no. 9, p. 9,083–9,100.
- Kamb, Barclay, Raymond, C.F., Harrison, W.D., Englehardt, Hermann, Echelmeyer, K.A., Humphrey, N., Brugman, M.M., and Pfeffer, T., 1985, Glacier surge mechanism — 1982–1983 surge of *Variogated Glacier, Alaska*: *Science*, v. 227, no. 4686, p. 469–479.
- Kamb, Barclay, Englehardt, Hermann, Fahnestock, M.A., Humphrey, N., Meier, M.F., and Stone, D., 1994, Mechanical and hydrological basis for the rapid motion of a large tidewater glacier, Part 2, Interpretation: *Journal of Geophysical Research*, v. 99B, no. 8, p. 15,231–15,244.
- Kaufman, D.S., and Calkin, P.E., 1988, Morphometric analysis of Pleistocene moraines in the Kigluaik Mountains, northwestern Alaska, U.S.A.: *Arctic and Alpine Research*, v. 20, no. 3, p. 273–284.
- Kaufman, D.S., Calkin, P.E., Whitford, W.B., Przybyl, B.J., Hopkins, D.M., Peck, B.J., and Nelson, R.E., 1989, *Surficial geologic map of the Kigluaik Mountains area, Seward Peninsula, Alaska*: U.S. Geological Survey Miscellaneous Field Studies Map, MF-2074, 1:63,360 scale.
- Kayastha, R.B., Takeuchi, Yukari, Nakawo, Masayoshi, and Ageta, Yutaka, 2000, Practical prediction of ice melting beneath various thickness of debris cover on Khumbu Glacier, Nepal, using a positive degree-day factor, *in* Nakawo, M., Raymond, C.F., and Fountain, A, eds., 2000, *Debris-covered glaciers*: Oxfordshire, UK, IAHS Press, IAHS Series of Proceedings and Reports No. 264, p. 71–82.
- Keeler, C.M., 1959, Notes on the geology of the McCall Valley area: *Arctic*, v. 12, no. 1, p. 87–97.
- Keen, Dora, 1915a, Studying the Alaskan glaciers: *Geographical Society of Philadelphia Bulletin*, v. 13, no. 2, p. 25–32.
- Keen, Dora, 1915b, Exploring the Harvard Glacier: *Harper's Magazine*, v. 132, p. 113–125.
- Kennedy, B.W., 1995, Air temperature and precipitation data, Wolverine Glacier basin, Alaska, 1967–94: U.S. Geological Survey Open-File Report 95-444, 79 p., diskette.
- Kennedy, B.W., Mayo, L.R., Trabant, D.C., and March, R.S., 1997, Air temperature and precipitation data, Gulkana Glacier, Alaska, 1968–96: U.S. Geological Survey Open-File Report 97-358, 144 p.
- Kennedy, G.C., and Waldron, H.H., 1955, *Geology of Pavlof Volcano and vicinity, Alaska*: U.S. Geological Survey Bulletin 1028-A, 19 p., map.
- Kieffer, Hugh, and 41 others, 2000, New eyes in the sky measure glaciers and ice sheets: *EOS (Transactions of the American Geophysical Union)*, v. 81, no. 24, p. 265, and p. 270–271.
- Klotz, O.J., 1895, Experimental application of the photo-topographical method of surveying to the Baird Glacier, Alaska: *Journal of Geology*, v. 3, no. 5, p. 512–518.

- Klotz, O.J., 1899, Notes on the glaciers of southeastern Alaska and adjoining territory: *Geographical Journal*, v. 14, no. 5, p. 523–534.
- Knappen, R.S., 1929, Geology and mineral resources of the Aniakchak district: U.S. Geological Survey Bulletin 797-F, p. 161–227.
- Knopf, Adolph, 1912, The Eagle River region, southeastern Alaska: U.S. Geological Survey Bulletin 502, p. 7–58.
- Koppes, M.N., Hallet, Bernard, and Merrand, Yves, 2001, Influence of rapid glacial retreat on erosion rates in southeastern Alaska [abs.]: EOS (Transactions, American Geophysical Union), v. 82, no. 47, Fall Meeting Supplement, Abstract IP52A-0749, p. F557.
- Krabill, W., Abdalati, W., Frederick, E., Manizade, S., Martin, C., Sonntag, J., Swift, R., Thomas, R., Wright, W., and Yungel, J., 2000, Greenland ice sheet: high-elevation balance and peripheral thinning: *Science*, v. 289, no. 5478, p. 428–430.
- Krause, A., 1883, Das Chilcat-Gebiet in Alaska [The Chilkat region in Alaska]: *Zeitschrift Gesellschaft für Erdkunde*, v. 18, no. 4–5, p. 344–368.
- Krimmel, R.M., 1987, Columbia Glacier, Alaska: Photogrammetry data set 1981–82 and 1984–85: U.S. Geological Survey Open-File Report 87–219, 104 p.
- Krimmel, R.M., 2001, Photogrammetric data set, 1957–2000, and bathymetric measurements for Columbia Glacier, Alaska: U.S. Geological Survey Water-Resources Investigation Report 01–4089, 40 p., 1 CD-ROM.
- Krimmel, R.M., 2002, Glaciers of the Western United States, *in* Williams, R.S., Jr., and Ferrigno J.G., eds., *Satellite image atlas of glaciers of the world*: U.S. Geological Survey Professional Paper 1386-J (Glaciers of North America), p. J329–J381. [<http://pubs.usgs.gov/prof/p1386j>]
- Krimmel, R.M., and Meier, M.F., 1975, Glacier applications of ERTS images, *in* Proceedings of Symposium on Remote Sensing in Glaciology, Cambridge, England, 1974: *Journal of Glaciology*, v. 15, no. 73, p. 391–402.
- Krimmel, R.M., and Meier, M.F., 1989, Glaciers and glaciology of Alaska, v. 1 *in* Glacial geology and geomorphology of North America, *in* Hanshaw, P.M., ed., *Field trips for the 28th International Geological Congress*, Washington, D.C., July 9–19, 1989: American Geophysical Union, Field Trip T301, 61 p.
- Krimmel, R.M., and Sikonia, W.G., 1986, Velocity and surface altitude of the lower part of Hubbard Glacier, Alaska, August 1978: U.S. Geological Survey Open-File Report 86–549, 13 p.
- Krimmel, R.M., and Trabant, D.C., 1992, The terminus of Hubbard Glacier, Alaska: *Annals of Glaciology*, v.16, p. 151–157.
- Krimmel, R.M., and Vaughn, B.H., 1987, Columbia Glacier, Alaska—Changes in velocity 1977–1986: *Journal of Geophysical Research*, v. 92, no. B9, p. 8,961–8,968.
- Krimmel, R.M., Post, Austin, and Meier, M.F., 1976, Surging and nonsurging glaciers in the Pamir Mountains, U.S.S.R., *in* Williams, R.S., Jr., and Carter, W.D., eds., ERTS–1, a new window on our planet: U.S. Geological Survey Professional Paper 929, p. 178–179.
- Lamke, R.L., 1991, Alaska floods and droughts, *in* U.S. Geological Survey, 1991, National Water Summary 1988–89, State Summaries: U.S. Geological Survey Water-Supply Paper 2375, p. 171–180.
- La Pérouse, J.-F.deG., 1798–1799, A voyage round the world, performed in the years 1785, 1786, 1787, and 1788, by the *Boussole* and *Astrolabe*, under the command of J.-F.deG. de La Pérouse; pub. by order of the National Assembly under the Superintendence of L.A. Milet-Mureau...Tr. from the French: London, G.G. and J. Robinson, 2 v. and atlas.
- Larson, Peter, 1960, A preliminary investigation of the meteorological conditions on the Chamberlain Glacier, 1958: Washington, D.C., Arctic Institute of North America, Research Paper No. 2, 89 p.
- Lawrence, D.B., 1950, Glacier fluctuations for six centuries in southeastern Alaska and its relation to solar activity: *Geographical Review*, v. 40, no. 2, p. 191–223.
- Lawson, D.E., 1979, Sedimentological analysis of the western terminus region of the Matanuska Glacier, Alaska: Hanover, New Hampshire, U.S. Army Corps of Engineers, Cold Regions Research and Engineering Laboratory, CRREL Report 79–9, 112 p.
- Lawson, W.J., 1990, The structural evolution of Variegated Glacier, Alaska: University of Cambridge, Ph.D. dissertation, unpublished, 240 p.
- Lawson, Wendy [W.J.], 1996, Structural evolution of Variegated Glacier, Alaska, U.S.A., since 1948: *Journal of Glaciology*, v. 42, no. 141, p. 261–270.
- Lawson, Wendy [W.J.], 1997, Spatial, temporal and kinematic characteristics of surges of Variegated Glacier, Alaska: *Annals of Glaciology*, v. 24, p. 95–101.
- Leffingwell, E. de K., 1919, The Canning River region, northern Alaska: U.S. Geological Survey Professional Paper 109, 251 p.
- Lethcoe, N.R., 1987, An observer's guide to the glaciers of Prince William Sound, Alaska: Valdez, Alaska, Prince William Sound Books, 151 p.
- Levy, L.B., Kaufman, D.S., and Werner, A., 2004, Holocene glacier fluctuations, Waskey Lake, northeastern Ahklun Mountains, southwestern Alaska: *The Holocene*, v. 14, no. 2, p. 185–193.
- Lewis, Oscar, 1954, George Davidson, pioneer west coast scientist: University of California Press, 146 p.
- Libbey, William, Jr., 1886, Some of the geographical features of south-eastern Alaska: *American Geographical Society Bulletin*, v. 18, no. 4, p. 279–300.
- Liestøl, Olav, 1956, Glacier dammed lakes in Norway: *Norsk Geografisk Tidsskrift*, v. 15, no. 3–4, p. 122–149.
- Liestøl, Olav, 1993, Glaciers of Svalbard, Norway, *in* Williams, R.S., Jr., and Ferrigno, J.G., eds., *Satellite image atlas of glaciers of the world*: U.S. Geological Survey Professional Paper 1386-E (Glaciers of Europe), p. E127–E151. [<http://pubs.usgs.gov/prof/p1386e/>]
- Lindsay, J.F., 1966, Observations on the level of a self-draining lake on the Casement Glacier, Alaska: *Journal of Glaciology*, v. 6, no. 45, p. 443–445.
- Lingle, C.S., Echelmeyer, K.A., Seider, W.A., Li, H., and Valentine, V.B., 1999, A new estimate of elevation and volume changes on Seward and Malaspina Glaciers, southcentral Alaska and Yukon, from small-aircraft laser altimetry, ERS SAR imagery, and the 15 min. DEM of Alaska [abs.]: EOS (Transactions, American Geophysical Union), v. 80, no. 46, Fall Meeting Supplement, p. F355.

- Lliboutry, Louis, 1998, Glaciers of the Wet Andes, *in* Williams, R.S., Jr., and Ferrigno J.G., eds., *Satellite image atlas of glaciers of the world: U.S. Geological Survey Professional Paper 1386-I (Glaciers of South America)*, p. 1148–1206. [<http://pubs.usgs.gov/prof/p1386i/>]
- Manley, W.F., 1999, GIS assessment of glaciers, equilibrium line altitudes and climate sensitivity—An example from southwestern Alaska [abs.]: *Geological Society of America Annual Meeting, Programs and Abstracts*, v. 31, no. 7, p. 366.
- Manley, W.F., 2000, Demonstration of GIS applications in paleoglaciology, glaciology, and bathymetry, Alaska [abs.]: *International Arctic Workshop, 30th, March 15–18, 2000, Boulder, Colorado, University of Colorado, Institute of Arctic and Alpine Research, Program and abstracts*, p. 120–121.
- March, R.S., 1998, Mass balance, meteorological, ice motion, surface altitude, and runoff data at Gulkana Glacier, Alaska, 1994 balance year: *U.S. Geological Survey Water-Resources Investigations Report 97–4251*, 31 p.
- March, R.S., 2000, Mass balance, meteorological, ice motion, surface altitude, runoff and ice thickness data at Gulkana Glacier, Alaska, 1995 balance year: *U.S. Geological Survey Water-Resources Investigations Report 00–4074*, 33 p.
- March, R.S., and Trabant, D.C., 1996, Mass balance, meteorological, ice motion, surface altitude, and runoff data at Gulkana Glacier, Alaska, 1992 balance year: *U.S. Geological Survey Water-Resources Investigations Report 95–4277*, 32 p.
- March, R.S., and Trabant, D.C., 1997, Mass balance, meteorological, ice motion, surface altitude, and runoff data at Gulkana Glacier, Alaska, 1993 balance year: *U.S. Geological Survey Water-Resources Investigations Report 96–4299*, 30 p.
- Marcus, M.G., and Reynolds, W.J., eds., 1988, *Glacier and climate studies, West Gulkana Glacier and environs, Alaska: Arizona State University, Department of Geography, Research Paper No. 4*, 142 p., 1 map sheet.
- Marcus, M.G., Chambers, F.B., Miller, M.M., and Lang, M., 1995, Recent trends in the Lemon Creek Glacier, Alaska: *Physical Geography*, v. 16, no. 2, p. 150–161, 1 map sheet.
- Martin, G.C., 1905, The petroleum fields of the Pacific Coast of Alaska with an account of the Bering River coal deposits: *U.S. Geological Survey Bulletin 250*, 64 p.
- Martin, G.C., 1907, Topographic reconnaissance map of the Pacific Coast from Yakutat Bay to Prince William Sound, Alaska, Plate 1 *in* *Geology and Mineral Resources of the Controller Bay Region, Alaska [1908]: U.S. Geological Survey Bulletin 335*, 1 sheet, scale 1:1,200,000.
- Martin, G.C., 1908, *Geology and mineral resources of the Controller Bay region, Alaska: U.S. Geological Survey Bulletin 335*, 141 p., maps.
- Martin, G.C., Maddren, A.G., Paige, Sidney, and Weaver, C.E., 1907, *Geologic map and sections of Controller Bay region, Alaska: U.S. Geological Survey Bulletin 335, Plate V*, scale 1:62,500.
- Martin, G.C., Johnson, B.L., and Grant, U.S., 1915, *Geology and mineral resources of Kenai Peninsula, Alaska: U.S. Geological Survey Bulletin 587*, 243 p.
- Martin, Lawrence, 1909, The Malaspina Glacier region of Alaska: *Journal of Geology*, v. 17, no. 7, p. 664–666.
- Martin, Lawrence, 1911, The National Geographic Society researches in Alaska: *The National Geographic Magazine*, v. 22, no. 6, p. 537–561.
- Martin, Lawrence, 1913, Some features of glaciers and glaciation in College Fiord, Prince William Sound, Alaska: *Zeitschrift für Gletscherkunde*, v. 7, no. 5, p. 289–333.
- Mason, R.W., 1959, The McCall Glacier Project and its logistics: *Arctic*, v. 12, no. 1, p. 77–86.
- Mayo, L.R., 1978, Identification of unstable glaciers intermediate between normal and surging glaciers: Moscow, Academy of Sciences of the U.S.S.R., Section of Glaciology of the Soviet Geophysical Committee and Institute of Geography, Data of Glaciological Studies, Publication No. 33, [Proceedings, Alma-Ata, 1976], p. 47–55 and p. 133–135.
- Mayo, L.R., 1988a, Advance of Hubbard Glacier and closure of Russell Fiord, Alaska; Environmental effects and hazards in the Yakutat area, *in* Galloway, J.P., and Hamilton, T.D., eds., *Geologic studies in Alaska by the U.S. Geological Survey during 1987: U.S. Geological Survey Circular 1016*, p. 4–16.
- Mayo, L.R., 1988b, Hubbard Glacier near Yakutat, Alaska — The ice damming and breakout of Russell Fiord/Lake, 1986, *in* Moody, D.W., and others, compilers, *National Water Summary, 1986 — Hydrologic events and ground-water quality: U.S. Geological Survey Water Supply Paper 2325*, p. 42–49.
- Mayo, L.R., and Péwé, T.L. 1963, Ablation and net total radiation, Gulkana Glacier, Alaska, chap. 43 *in* *Ice and snow, Properties, Processes, and Applications Conference, Massachusetts Institute of Technology, 1962, Proceedings: Cambridge, Mass., M.I.T. Press*, p. 633–643.
- Mayo, L.R., and Trabant, D.C., 1982, Geodetic trisection, altitude, and ice-radar surveying techniques used at Knik Glacier, Alaska, and summary of 1979, 1980, and 1981 data: *U.S. Geological Survey Open-File Report 82–685*, 26 p.
- Mayo, L.R., and Trabant, D.C., 1984, Observed and predicted effects of climate change on Wolverine Glacier, southern Alaska, *in* McBeath, J.H., Juday, G.P., Weller, Gunter, and Murray, Mayo, eds., *The potential effects of carbon dioxide-induced climate change in Alaska: Fairbanks, University of Alaska Miscellaneous Publication 83–1*, p. 114–123.
- Mayo, L.R., and Trabant, D.C., 1986, Recent growth of Gulkana Glacier, Alaska Range, and its relation to glacier-fed river runoff, *in* Subitzky, Seymour, ed., *Selected papers in the hydrologic sciences 1986: U.S. Geological Survey Water-Supply Paper 2290*, p. 91–99.
- Mayo, L.R., March, R.S., and Trabant, D.C., 1992, Air temperature and precipitation data, 1967–88, Wolverine Glacier basin, Alaska: *U.S. Geological Survey Open-File Report 91–246*, 80 p.
- Mayo, L.R., Trabant, D.C., and March, R.S., 2004, A 30-year record of surface mass balance (1966–95), and motion and surface altitude (1975–95) at Wolverine Glacier, Alaska: *U.S. Geological Survey Open-File Report 2004-1969*, 105 p. [CD-ROM]
- McCauley, Camilla, 1958, *Glaciers of the Talkeetna Mountains, Alaska, in* Field, W.O. ed., 1958, *Geographic study of mountain glaciation in the Northern Hemisphere, pt. 2a: American Geographic Society*, p. 2a.5.1–2a.5.4.

- McCauley, Camilla, 1975, Glaciers of the Kigluaik Mountains, *in* Field, W.O., ed., 1975, Mountain glaciers of the Northern Hemisphere: Hanover, New Hampshire, U.S. Army Corps of Engineers, Cold Regions Research and Engineering Laboratory, v. 2, p. 668–670.
- McGimsey, Game, 2001, Redoubt Volcano and the Alaska Volcano Observatory, 10 years later, *in* Gough, L.P., and Wilson, F.H., eds., Geologic Studies in Alaska by the U.S. Geological Survey, 1999: U.S. Geological Survey Professional Paper 1633, p. 5–12.
- McGimsey, R.G., and Miller, T.P., 1995, Quick reference to Alaska's active volcanoes and listing of historical eruptions, 1760–1994: U.S. Geological Survey Open-File Report 95–520, 13 p.
- McKenzie, G.D., and Goodwin, R.G., 1987, Development of collapsed glacial topography in the Adams Inlet area, Alaska, U.S.A.: *Journal of Glaciology*, v. 33, no. 113, p. 55–59.
- McMeeking, R.M., and Johnson, R.E., 1986, On the mechanics of surging glaciers: *Journal of Glaciology*, v. 32, no. 110, p. 120–132.
- Meier, M.F., 1961, Distribution and variations of glaciers in the United States exclusive of Alaska, *in* General Assembly of Helsinki, July 25–August 6, 1960: Association Internationale d'Hydrologie Scientifique/International Association of Scientific Hydrology, Publication No. 54, p. 420–429.
- Meier, M.F., 1976, Monitoring the motion of surging glaciers in the Mount McKinley massif, Alaska, *in* Williams, R.S., Jr., and Carter, W.D., eds., ERTS–1, a New Window on our Planet: U.S. Geological Survey Professional Paper 929, p. 185–187.
- Meier, M.F., 1984, Contributions of small glaciers to global sea level: *Science*, v. 226, no. 4681, p. 1418–1421.
- Meier, M.F., 1990, Role of land ice in present and future sea-level change, *in* Sea-level change: Washington, D.C., National Academy Press, p. 171–184.
- Meier, M.F., 1994, Columbia Glacier during rapid retreat: Interactions between glacier flow and iceberg calving dynamics, *in* Reeh, Nils, ed., Workshop on the Calving Rate of West Greenland Glaciers in Response to Climate Change, Copenhagen, 13–15 September 1993: Denmark, Danish Polar Center, p. 63–83.
- Meier, M.F., 1997, The iceberg discharge process—Observations and inferences drawn from the study of Columbia Glacier, *in* Van der Veen, C.J., ed., Calving Glaciers; Report of a Workshop, February 28–March 2, 1997: Columbus, Ohio, The Ohio State University, Byrd Polar Research Center, BPRC Report No. 15, p. 109–114.
- Meier, M.F., 1998, Monitoring ice sheets, ice caps, and large glaciers, Chap. 13 *in* Haeberli, W., Hoelzle, M., Suter, S., eds., Into the second century of worldwide glacier monitoring: Paris, UNESCO Publishing, Studies and Reports in Hydrology, v. 56, p. 209–214.
- Meier, M.F., and Bahr, D.B., 1996, Counting glaciers: use of scaling methods to estimate the number and size distribution of the glaciers of the world, *in* Colbeck, S.C., ed., Glaciers, Ice Sheets and Volcanoes: A tribute to Mark F. Meier: Hanover, New Hampshire, U.S. Army Corps of Engineers, Cold Regions Research and Engineering Laboratory (CRREL) Special Report no. 96–27, p. 89–94.
- Meier, M.F., and Dyurgerov, M.B., 2002, Sea level changes: How Alaska affects the world: *Science*, v. 297, no. 5580, p. 350–351.
- Meier, M.F., and Post, Austin, 1962, Recent variations in mass net budgets of glaciers in western North America, *in* Symposium of Obergurgl, Variations in the regime of existing glaciers: International Association of Hydrological Sciences-Association Internationale des Sciences Hydrologiques (IAHS-AISH), Publication No. 58, p. 63–77.
- Meier, M.F., and Post, Austin, 1967, Spectacular surges of glaciers reported: Mineral Information Service, v. 20, no. 5, p. 51–53.
- Meier, M.F., and Post, Austin, 1969, What are glacier surges?: *Canadian Journal of Earth Sciences*, v. 6, no. 4, p. 807–817.
- Meier, M.F., and Post, Austin, 1980, The scientific ideas of G.K. Gilbert; an assessment on the occasion of the centennial of the United States Geological Survey (1879–1979): Geological Society of America, Special Paper No. 183, p. 115–123.
- Meier, M.F., and Post, Austin, 1987, Fast tidewater glaciers: *Journal of Geophysical Research*, v. 92B, no. 9, p. 9,051–9,058.
- Meier, M.F. and Wahr, J., 2002, Sea level is rising—do we know why? *Proceedings of the National Academy of Sciences*, v. 99, no. 10, p. 6,524–6,526.
- Meier, M.F., Tangborn, W.V., Mayo, L.R., and Post, Austin, 1971, Combined ice and water balances of Gulkana and Wolverine Glaciers, Alaska, and South Cascade Glacier, Washington, 1965 and 1966 hydrologic years: U.S. Geological Survey Professional Paper 715–A, 23 p.
- Meier, M.F., Post, Austin, Brown, C.S., Frank, David, Hodge, S.M., Mayo, L.R., Rasmussen, L.A., Senear, E.A., Sikonia, W.G., Trabant, D.C., and Watts, R.D., 1978, Columbia Glacier progress report—December 1977: U.S. Geological Survey Open-File Report 78–264, 56 p.
- Meier, M.F., Rasmussen, L.A., Post, Austin, Brown, C.S., Sikonia, W.G., Bindschadler, R.A., Mayo, L.R., and Trabant, D.C., 1980, Predicted timing of the disintegration of the lower reach of Columbia Glacier, Alaska: U.S. Geological Survey Open-File Report 80–582, 47 p.
- Meier, M.F., Rasmussen, L.A., Krimmel, R.M., Olsen, R.W., and Frank, David, 1985, Photogrammetric determination of surface altitude, terminus position, and ice velocity of Columbia Glacier, Alaska, 1974–1981: U.S. Geological Survey Professional Paper 1258-F, 41 p.
- Meier, M.F., Lundstrom, S., Stone, D., Kamb, B., Engelhardt, H., Humphrey, N., Dunlap, W.W., Fahnestock, M.A., Krimmel, R.M., and Walters, R., 1994, Mechanical and hydrologic basis for the rapid motion of a large tidewater glacier: Part 1, Observations: *Journal of Geophysical Research*, v. 99B, no. 8, p. 15,219–15,229.
- Meier, M.F., Cohn, Josh, Krimmel, R.M., and Pfeffer, W.T., 2001, The past and future dynamics of Columbia Glacier, Alaska [abs.]: EOS (Transactions, American Geophysical Union), v. 82, no. 47, Fall Meeting Supplement, Abstract IP22C–02, p. F535.
- Meier, M.F., Dyurgerov, M.B., and McCabe, G.J., 2003, The health of glaciers: Recent changes in glacier regime: *Climate Change*, v. 59, nos. 1–2, p. 123–135.
- Mendenhall, W.C., 1900, A reconnaissance from Resurrection Bay to the Tanana River, Alaska, in 1898: U.S. Geological Survey Annual Report 20, Part 7, p. 265–340.
- Mendenhall, W.C., 1903a, The Wrangell Mountains, Alaska: *National Geographic Magazine*, v. 9, p. 395–407.

- Mendenhall, W.C., 1903b, The Wrangell Mountains, Alaska: National Geographic Magazine, v. 9, Photo Supplement.
- Mendenhall, W.C., 1905, Geology of the central Copper River region, Alaska: U.S. Geological Survey Professional Paper 41, 133 p., 20 pls.
- Mercer, J.H., 1961a, The estimation of the regimen and former firm limit of a glacier: *Journal of Glaciology*, v. 3, no. 30, p. 1,053–1,062.
- Mercer, J.H., 1961b, The response of fjord limits to changes in the firm limit: *Journal of Glaciology*, v. 3, no. 29, p. 850–858.
- Miller, D.J., 1957, The surface velocity of the Yakataga Glacier, Alaska: *Journal of Glaciology*, v. 3, no. 22, p. 125–130.
- Miller, D.J., 1958, Anomalous glacial history of the northeastern Gulf of Alaska region: *Geological Society of America Bulletin*, v. 69, no. 12, part 2, p. 1,613–1,614.
- Miller, D.J., 1960, Giant waves in Lituya Bay, Alaska: U.S. Geological Survey Professional Paper 354-C, 38 p.
- Miller, D.J., 1961, Geology of the Yakataga District, Gulf of Alaska Tertiary Province, Alaska: U.S. Geological Survey Open-File Report, 2 map sheets.
- Miller, L.D., Miller, J.W., and Miller, M.M., 1987, The Juneau Icefield-Alaska: Juneau, The Foundation for Glacier and Environmental Research, color slides and text.
- Miller, M.M., 1948a, Aerial survey of Alaskan glaciers, 1947: *Appalachia*, v. 105, p. 113–115.
- Miller, M.M., 1948b, Observations on the regimen of the glaciers of Icy Bay and Yakutat Bay, Alaska: New York, Columbia University, unpublished Master's thesis, 71 p.
- Miller, M.M., 1963, Taku Glacier evaluation study: Juneau, Alaska Department of Highways, 200 p.
- Miller, M.M., 1964, Inventory of terminal position changes in Alaskan coastal glaciers since the 1750's: *Proceedings of the American Philosophical Society*, v. 108, no. 3, p. 257–273.
- Moffit, F.H., 1913, Geology of the Nome and Grand Central quadrangles, Alaska: U.S. Geological Survey Bulletin 533, 140 p.
- Moffit, F.H., 1918, The upper Chitna Valley, Alaska: U.S. Geological Survey Bulletin 675, 82 p.
- Moffit, F.H., 1942, Geology of the Gerstle River district, Alaska, with a report on the Black Rapids Glacier: U.S. Geological Survey Bulletin 926-B, p. 107–160.
- Moffit, F.H., and Capps, S.R., 1911, Geology and mineral resources of the Nizina District, Alaska: U.S. Geological Survey Bulletin 448, 111 p., 12 pls.
- Moffit, F.H., and Knopf, Adolph, 1909, Mineral resources of the Nabesna-White River district: U.S. Geological Survey Bulletin 379-E, p. 161–180.
- Molnia, B.F., 1977, Rapid shoreline erosion and retreat at Icy Bay Alaska — A staging area for offshore petroleum development, *in* Annual Offshore Technology Conference, 9th, Proceedings: v. 3, p. 115–126.
- Molnia, B.F., 1979, Sedimentation in coastal embayments, in the northern Gulf of Alaska, *in* Annual Offshore Technology Conference, 11th, Proceedings: v. 1, p. 665–676.
- Molnia, B.F., 1982 (rev. 1993), Alaska's glaciers: Anchorage, Alaska Geographic, v. 9, no. 1, 144 p.
- Molnia, B.F., ed., 1983a, Glacial-marine sedimentation: New York, Plenum Press, 844 p.
- Molnia, B.F., 1983b, Subarctic glacial-marine sedimentation: a model, *in* Molnia, B.F., ed., *Glacial-Marine Sedimentation*: New York, Plenum Press, p. 95–144.
- Molnia, B.F., 1986, Glacial history of the northeastern Gulf of Alaska, *in* Hamilton, T.D., Reed, K.M., and Thorson, R.M., eds., *Glaciation in Alaska—the geologic record*: Anchorage, Alaska Geologic Society, p. 219–236.
- Molnia, B.F., 1989a, Advance induced retreat of the Mendenhall Glacier, Alaska [abs.]: *Geological Society of America, Abstracts with Programs*, v. 21, no. 6, p. A54.
- Molnia, B.F., 1989b, Subarctic glacial-marine sedimentation, *in* Anderson, J.B., and Molnia, B.F., *Glacial-marine sedimentation: American Geophysical Union short course in geology, International Geological Congress, 28th, Washington, D.C., v. 9, p. 59–109.*
- Molnia, B.F., 1990a, Neoglacial history of the Malaspina Glacier, Alaska—Inferences from two types of radar analyses [abs.]: *Geological Society of America, Abstracts with Programs*, v. 22, no. 7, p. A177–A178.
- Molnia, B.F., 1990b, Radar remote sensing of glacial features, Malaspina Glacier, Alaska: *AAPG Bulletin*, v. 74, no. 5, p. 723.
- Molnia, B.F., 1991, Mendenhall Glacier retreats: *Anchorage, Alaska Geographic*, v. 17, no. 4, p. 92.
- Molnia, B.F., 1993, Major surge of the Bering Glacier: *EOS (Transactions, American Geophysical Union)*, v. 74, no. 29, p. 322.
- Molnia, B.F., 1998, Environmental impacts of 1994 Bering Glacier outburst floods [abs.]: *EOS (Transactions, American Geophysical Union)*, v. 79, no. 17, Spring Meeting Supplement, p. S–15.
- Molnia, B.F., 2001, *Glaciers of Alaska*: Anchorage, Alaska Geographic, v. 28, no. 2, 112 p.
- Molnia, B.F., and Jones, J.E., 1989, View through ice: Are unusual airborne radar backscatter features from the surface of the Malaspina Glacier, Alaska, expressions of subglacial morphology?: *EOS (Transactions, American Geophysical Union)*, v. 70, no. 28, p. 701–710.
- Molnia, B.F., and Molnia, M.I., 1995, Comparison of spaceborne ERS-1 and SIR-C synthetic aperture radar (SAR) with airborne SAR of the Bering Glacier, Alaska [abs.]: *Geological Society of America, Abstracts with Programs*, v. 27, no. 5, p. 65.
- Molnia, B.F., and Post, Austin, 1995, Holocene history of Bering Glacier, Alaska: a prelude to the 1993–1994 surge: *Physical Geography*, v. 16, no. 2, p. 87–117.
- Molnia, B.F., and Trabant, D.C., 1992, Ice thickness measurements on Bering Glacier, Alaska and their relation to satellite and airborne SAR image patterns [abs.]: *EOS (Transactions, American Geophysical Union)*, v. 73, no. 43, Fall Meeting Supplement, p. 181.
- Molnia, B.F., Jones, J.E., and Schoonmaker, J.W., Jr., 1990, Ice-penetrating radar investigations of the Malaspina Glacier, Alaska: *EOS (Transactions, American Geophysical Union)*, v. 70, no. 43, p. 1,085.
- Molnia, B.F., Post, Austin, and Carlson, P.R., 1996, 20th-century glacial-marine sedimentation in Vitus Lake, Bering Glacier, Alaska, U.S.A.: *Annals of Glaciology*, v. 22, p. 205–210.
- Molnia, B.F., Trabant, D.C., and March, R.S., 2002, The 2002 closure of Russell Fiord, Alaska—June & July 2002 [abs.]: *in* *Geological Society of America, Abstracts with Programs*, v. 34, no. 6, p. 477.

- Moran, M.L., Greenfield, R.J., Arcone, S.A., and Delaney, A.J., 2000, Delineation of a complexly dipping temperate glacier bed using short-pulse radar arrays: *Journal of Glaciology*, v. 46, no. 153, p. 274–286.
- Moravek, J.R., 1973, Some further observations on the behavior of an ice-dammed self-draining lake, Glacier Bay, Alaska, U.S.A.: *Journal of Glaciology*, v. 12, no. 66, p. 505–507.
- Morrison, Marie, 1995, William O. Field and the American Geographical Society—the early years: *Physical Geography*, v. 16, no. 1, p. 9–14.
- Morse, Fremont, 1908, The recession of glaciers of Glacier Bay, Alaska: *National Geographic Magazine*, v. 19, no. 1, p. 76–78.
- Motyka, R.J., Ferrell, V.E., and Benson, C.S., 1977, Glaciological-volcanological investigations in Katmai National Monument [abs.], in Scott, S.A., ed., National Park Service Pacific Northwest Region Science/Management Annual Conference, 4th, Issaquah, Washington, 1–3 May 1977: p. 22.
- Motyka, R.J., Echelmeyer, Keith, and Elsberg, Daniel, 2001, Taku Glacier on the move again: active deformation of proglacial sediments, 2001 [abs.]: *EOS (Transactions, American Geophysical Union)*, v. 82, no. 47, Fall Meeting Supplement, Abstract IP52A–0745, p. F556.
- Motyka, R.J., O’Neel, Shad, Connor, C.L., and Echelmeyer, K.A., 2003, Twentieth century thinning of Mendenhall Glacier, Alaska, and its relationship to climate, lake calving, and glacier run-off: *Global and Planetary Change*, v. 35, no. 1–2, p. 93–112.
- Muir, John, 1893, Alaska: *American Geologist*, v. 11, no. 5, p. 287–299.
- Muir, John, 1895, The discovery of Glacier Bay: *Century*, v. 50, p. 234–247.
- Muir, John, 1902, Notes on the Pacific Coast glaciers, in Burroughs, John, Muir, John, and Grinnel, G.B., 1902, Alaska—Narrative, glaciers, natives, Volume 1 of the Harriman Alaska Expedition with Cooperation of the Washington Academy of Sciences: New York, Doubleday, Page and Company, p. 119–135.
- Muir, John, 1915, *Travels in Alaska*: Boston, Houghton Mifflin Co., 326 p.
- Muldrow, Robert, 1901, Mount McKinley: *National Geographic Magazine*, v. 12, p. 312–313.
- Muller, E.H., and Coulter, H.W., 1957a, The Knife Creek Glaciers of Katmai National Monument, Alaska: *Journal of Glaciology*, v. 3, no. 22, p. 116–122.
- Muller, E.H., and Coulter, H.W., 1957b, Incipient glaciers development within Katmai caldera, Alaska: *Journal of Glaciology*, v. 3, no. 21, p. 13–17.
- Muller, E.H., Post, Austin, Fleisher, P.J., Franzi, D.A., Stuckenrath, R., and Cadwell, D.H., 1991, Buried forest beds exposed by lowering of glacial Lake Tsiu reveal late Holocene history of Bering Glacier, Alaska [abs.]: *Geological Society of America, Abstracts with Programs*, v. 23, no. 1, p. 106.
- Muskett, R.R., Lingle, C.S., Echelmeyer, K.A., and Valentine, V.B., 2000, Mass balance of Bering Glacier-Bagley Icefield during a surge cycle: *EOS (Transactions, American Geophysical Union)*, v. 81, no. 48, Fall Meeting Supplement, p. F 403–404.
- Nakawo, Masayoshi, Raymond, C.F., and Fountain, Andrew, eds., 2000, *Debris-covered glaciers*: Wallingford, Oxfordshire, UK, IAHS Press, International Association of Hydrological Sciences (IAHS) Publication No. 264, 288 p.
- National Research Council, 1977, *Energy and climate*: Washington, DC, National Academy Press, 158 p.
- National Research Council, 1983, *Changing climate, report of the carbon dioxide assessment committee*: Washington, DC, National Academy Press, 496 p.
- National Research Council, 1985, *Glaciers, ice sheets, and sea level—effects of a CO<sub>2</sub>-induced climatic change, report of a workshop held in Seattle, Washington, September 13–15, 1984*: Washington, D.C., National Academy Press, 348 p.
- National Research Council, 1990, *Sea-level change*: Washington, D.C., National Academy Press, 234 p.
- National Snow and Ice Data Center, 1999 (updated in 2003), *World Glacier Inventory: World Glacier Monitoring Service and National Snow and Ice Data Center/World Data Center for Glaciology*, Boulder, CO. Digital media.
- Neal, Christina [C.A.], and McGimsey, R.G., 1996, *Volcanoes of the Wrangell Mountains and Cook Inlet Region, Alaska*: U.S. Geological Survey Digital Data Series DDS–039.
- Neal, C.A., and McGimsey, R.G., 1997a, 1996 volcanic activity in Alaska and Kamchatka: summary of events and response of the Alaska Volcano Observatory: U.S. Geological Survey Open-File Report 97–433, 34 p.
- Neal, Christina [C.A.], and McGimsey, R.G., 1997b, *Volcanoes of the Alaska Peninsula and Aleutian Islands, Alaska*: U.S. Geological Survey Digital Data Series, DDS–40.
- Neal, C.A., McGimsey, R.G., Doukas, M.P., Miller, T.P., Richter, D., Paskievitch, J.F., and Ellersieck, I., 1992, The August 18, 1992 eruption of Mount Spurr volcano, Alaska: Tephra-fall stratigraphy, distribution and impact [abs.]: *EOS (Transactions, American Geophysical Union)*, v. 73, no. 43, Fall Meeting Supplement, p. 342.
- Nichols, R.L., and Miller, M.M., 1952, The Moreno Glacier, Lago Argentino, Patagonia: *Journal of Glaciology*, v. 2, no. 11, p. 41–50.
- Nolan, Matt, Motyka, R.J., Echelmeyer, Keith, and Trabant, D.C., 1995, Ice-thickness measurements of Taku Glacier, Alaska, U.S.A., and their relevance to its recent behavior: *Journal of Glaciology*, v. 41, no. 139, p. 541–553.
- Nye, C.J., 1983, *Petrology and geochemistry of Okmok and Wrangell Volcanoes, Alaska*: Santa Cruz, California, University of California, Ph.D. dissertation, unpublished, 215 p.
- Nye, J.F., 1976, Water flow in glaciers: Jökulhlaups, tunnels and veins: *Journal of Glaciology*, v. 17, no. 76, p. 181–207.
- Ommanney, C.S.L., 2002a, History of glacier investigations in Canada, in Williams, R.S., Jr., and Ferrigno J.G., eds., *Satellite image atlas of glaciers of the world*: U.S. Geological Survey Professional Paper 1386–J (*Glaciers of North America*), p. J27–J82. [<http://pubs.usgs.gov/prof/p1386j>]

- Ommanney, C.S.L., 2002b, Mapping Canada's glaciers, with a section on mapping glaciers in the *Interior Ranges* and Rocky Mountains with Landsat data by Wheate, R.D., Sidjak, R.W., and Whyte, G.T., in Williams, R.S., Jr., and Ferrigno J.G., eds., *Satellite image atlas of glaciers of the world: U.S. Geological Survey Professional Paper 1386-J (Glaciers of North America)*, p. J83–J99. [<http://pubs.usgs.gov/prof/p1386j>]
- O'Neel, Shad, Pfeffer, W.T., Krimmel, R.M., and Meier, M.M., 2005, Evolving force balance at Columbia Glacier, Alaska, during its rapid retreat: *Journal of Geophysical Research*, v. 110, F03012, 18 p. doi:10.1029/2005JF000292.
- Orth, D.J., 1967, *Dictionary of Alaska place names: U.S. Geological Survey Professional Paper 567*, 1,084 p., 12 maps.
- Orth, D.J., 1971, *Dictionary of Alaska place names: U.S. Geological Survey Professional Paper 567*, 1,084 p., 12 maps (Reprint of 1967 edition, with minor revisions).
- Osgood, W.H., 1904, Lake Clark, a little known Alaskan lake: *National Geographic Magazine*, v. 15, p. 326–331.
- Ostenso, N.A., and Holmes, G.W., 1962, Gravimetric determinations of ice thickness of Jarvis Glacier, Alaska, in *Geological Survey Research 1962, Short papers in geology and hydrology*, articles 60–119: U.S. Geological Survey Professional Paper 450–C, p. C93–C96.
- Ostenso, N.A., Sellman, P.V., and Péwé, T.L., 1965, The bottom topography of Gulkana Glacier, Alaska Range, Alaska: *Journal of Glaciology*, v. 5, no. 41, p. 651–660, map.
- Paige, R.A., 1965, Advance of Walsh Glacier: *Journal of Glaciology*, v. 5, no. 42, p. 876–878.
- Paul, Frank, 2002, Combined technologies allow rapid analysis of glacier changes: *EOS (Transactions of the American Geophysical Union)*, v. 83, no. 23, p. 253, 260–261.
- Paul, Frank, 2003, *The new Swiss glacier inventory 2000. Application of remote sensing and GIS: Zürich, Switzerland, Dr. Sc. Nat. (Ph.D.) dissertation, University of Zürich*, 199 p.
- Paul, Frank, Kääb, Andreas, Maisch, Max, Kellenberger, Tobias, and Haeblerli, Wilfried, 2002, The new remote-sensing-derived Swiss glacier inventory: I. Methods: *Annals of Glaciology*, v. 34, p. 355–361.
- Pelto, M.S., 2000, Mass balance of adjacent debris-covered and clean glacier ice in the North Cascades, Washington, in Nakawo, Masayoshi, Raymond, C.F., and Fountain, Andrew, eds., *Debris-covered glaciers: Wallingford, Oxfordshire, UK, IAHS Press, International Association of Hydrological Sciences (IAHS) Publication No. 264*, p. 35–42.
- Péwé, T.L., 1957, Recent history of Canwell and Castner Glaciers, Alaska: *Geological Society of America Bulletin*, v. 68, no. 12, p. 1,779.
- Péwé, T.L., and Reger, R.D., 1972, Modern and Wisconsinan snowlines in Alaska: *International Geological Congress, 24th, Montréal, Proceedings*, p. 187–197.
- Péwé, T.L., and Reger, R.D., 1983, Delta River area, Alaska Range, in Péwé, T.L., and Reger, R.D., eds., *Guidebook to permafrost and Quaternary geology along the Richardson and Glenn Highways between Fairbanks and Anchorage, Alaska: Alaska Division of Geological and Geophysical Surveys, Guidebook*, p. 47–135.
- Pfeffer, W.T., 2007, A simple mechanism for irreversible tidewater glacier retreat: *Journal of Geophysical Research*, v. 112, F03S25, doi:10.1029/2006JF000590.
- Pfeffer, W.T., Cohn, J., Meier, M.F., and Krimmel, R.M., 2000, Alaskan glacier beats a dramatic retreat: *EOS (Transactions, American Geophysical Union)*, v. 81, no. 48, p. 577 and p. 584.
- Plafker, George, and Miller, D.J., 1958, Glacial features and surficial deposits of the Malaspina District, Alaska: U.S. Geological Survey Miscellaneous Geologic Investigations Map I–27, 1 sheet, scale 1:96,000.
- Porter, S.C., 1966, Pleistocene geology of Anaktuvuk Pass, central Brooks Range, Alaska: Arctic Institute of North America, Technical Paper 18, 100 p.
- Porter, S.C., 1989, Late Holocene fluctuations of the fiord glacier system in Icy Bay, Alaska, U.S.A.: *Arctic and Alpine Research*, v. 21, no. 4, p. 364–379.
- Post, Austin, 1960, The exceptional advances of the Muldrow, Black Rapids, and Susitna Glaciers: *Journal of Geophysical Research*, v. 65, no. 11, p. 3,703–3,712.
- Post, Austin, 1965, Alaskan glaciers—Recent observations in respect to the earthquake-advance theory: *Science*, v. 148, no. 3668, p. 366–368.
- Post, Austin, 1966, The recent surge of Walsh Glacier, Yukon and Alaska, 1966: *Journal of Glaciology*, v. 6, no. 45, p. 375–381.
- Post, Austin, 1967a, Effects of the March 1964 Alaska earthquake on glaciers: U.S. Geological Survey Professional Paper 544–D, 42 p.
- Post, Austin, 1967b, Walsh Glacier surge, 1966 observation: *Journal of Glaciology*, v. 6, no. 47, p. 763–765.
- Post, Austin, 1969, Distribution of surging glaciers in western North America: *Journal of Glaciology*, v. 8, no. 53, p. 229–240.
- Post, Austin, 1972, Periodic surge origin of folded medial moraines on Bering Piedmont Glacier, Alaska: *Journal of Glaciology*, v. 11, no. 62, p. 219–226.
- Post, Austin, 1975, Preliminary hydrography and historic terminal changes of Columbia Glacier, Alaska: U.S. Geological Survey Hydrological Investigations Atlas HA–559, 3 sheets, scale 1:10,000.
- Post, Austin, 1976, Environmental geology of the central Gulf of Alaska coast, in Williams, R.S., Jr., and Carter, W.D., eds., *ERTS–1, a new window on our planet: U.S. Geological Survey Professional Paper 929*, p. 117–119.
- Post, Austin, 1978, Interim bathymetry of Columbia Glacier and approaches, Alaska: U.S. Geological Survey Open-File Report 78–449, 1 sheet, scale 1:20,000.
- Post, Austin, 1980a, Preliminary bathymetry of Aialik Bay and neoglacial changes of Aialik and Pederson Glaciers, Alaska: U.S. Geological Survey Open-File Report 80–423, 1 sheet, scale 1:20,000.
- Post, Austin, 1980b, Preliminary bathymetry of McCarty Fiord and neoglacial changes of McCarty Glacier, Alaska: U.S. Geological Survey Open-File Report 80–424, 4 sheets, scale 1:20,000.
- Post, Austin, 1980c, Preliminary bathymetry of Northwestern Fiord and neoglacial changes of Northwestern Glacier, Alaska: U.S. Geological Survey Open-File Report 80–414, 2 sheets, scale 1:20,000.

- Post, Austin, 1983, Preliminary bathymetry of upper Icy Bay, Alaska: U.S. Geological Survey Open-File Report 83-256, 1 sheet, scale 1:20,000.
- Post, Austin, 1995, Annual aerial photography of glaciers in north-west North America: How it all began and its Golden Age: *Physical Geography*, v. 16, no. 1, p. 15-26.
- Post, Austin, 1997, Passive and active iceberg producing glaciers, *in* Van der Veen, C.J., ed., *Calving Glaciers: Report of a Workshop*, February 28-March 2, 1997: Columbus, Ohio, The Ohio State University, Byrd Polar Research Center, BPRC Report No. 15, p. 121-136.
- Post, Austin, and LaChapelle, E.R., 1971, *Glacier ice*: Seattle, University of Washington Press, 110 p.
- Post, Austin, and LaChapelle, E.R., 2000, *Glacier ice*; Revised Edition: Seattle, University of Washington Press, in association with the International Glaciology Society, Cambridge, England, 145 p.
- Post, Austin, and Mayo, L.R., 1971, Glacier-dammed lakes and outburst floods in Alaska: U.S. Geological Survey Hydrological Atlas HA-455, 10 p., 3 pls.
- Post, Austin, and Meier, M.F., 1980, A preliminary inventory of Alaskan glaciers, *in* World Glacier Inventory Workshop, 17-22 September 1987, Reideralp, Switzerland, Proceedings: International Association of Hydrological Sciences (IAHS) Publication No. 126, p. 45-47.
- Post, Austin, and Motyka, R.J., 1995, Taku and Leconte Glaciers, Alaska—Calving-speed control of late-Holocene asynchronous advances and retreats: *Physical Geography*, v. 16, no. 1, p. 59-82.
- Post, Austin, and Viens, R.J., 2000, Preliminary bathymetry of Shoup Glacier Basin and late-Holocene changes of Shoup Glacier, Alaska: U.S. Geological Survey Water-Resources Investigations Report 94-4093, 11 p., 2 pls.
- Price, R.J., 1966, Eskers near the Casement Glacier, Alaska: *Geografiska Annaler*, v. 48A, no. 3, p. 111-125.
- Przybyl, B.J., 1988, The Regimen of Grand Union Glacier and the glacial geology of the northwestern Kigluaik Mountains, Seward Peninsula: State University of New York at Buffalo, unpublished M.S. dissertation, 106 p.
- Rainwater, F.H., and Guy, H.P., 1961, Some observations on the hydrochemistry and sedimentation of the Chamberlin Glacier area: U.S. Geological Survey Professional Paper 414-C, p. C1-C14.
- Rasmussen, L.A., 1989, Surface velocity variations of the lower part of Columbia Glacier, Alaska, 1977-1981: U.S. Geological Survey Professional Paper 1258-H, 52 p.
- Rasmussen, L.A., and Meier, M.F., 1982, Continuity equation model of the predicted drastic retreat of Columbia Glacier, Alaska: U.S. Geological Survey Professional Paper 1258-A, 23 p.
- Rasmussen, L.A., and Meier, M.F., 1985, Surface topography of the lower part of Columbia Glacier, Alaska, 1974-81: U.S. Geological Survey Professional Paper 1258-E, 63 p.
- Raybus, B.T., and Echelmeyer, K.A., 1997, The flow of a polythermal glacier: McCall Glacier, Alaska, U.S.A.: *Journal of Glaciology*, v. 43, no. 145, p. 522-536.
- Raybus, B.T., and Echelmeyer, K.A., 1998, The mass balance of McCall Glacier, Brooks Range, Alaska, U.S.A.; its regional relevance and implications for climate change in the Arctic: *Journal of Glaciology*, v. 44, no. 147, p. 333-351.
- Raybus, B.T., and Fatland, D.R., 2000, Comparison of SAR-interferometric and surveyed velocities on a mountain glacier: Black Rapids Glacier, Alaska, U.S.A.: *Journal of Glaciology*, v. 46, no. 152, p. 119-128.
- Raymond, C.F., 1987, How do glaciers surge? A review: *Journal of Geophysical Research*, v. 92 (B9), p. 9,121-9,134.
- Raymond, C.F., and Harrison, W.D., 1987, Fit of ice motion models to observations from Variegated Glacier, Alaska: International Association of Hydrological Sciences Publication No. 170, p. 153-166.
- Raymond, C.F., and Harrison, W.D., 1988, Evolution of Variegated Glacier, Alaska, U.S.A., prior to its surge: *Journal of Glaciology*, v. 34, no. 117, p. 154-169.
- Raymond, C.F., and Malone, S.D., 1986, Propagating strain anomalies during mini-surges of Variegated Glacier, Alaska: *Journal of Glaciology*, v. 32, no. 111, p. 178-191.
- Raymond, C.F., Johannesson, T., Pfeffer, W.T., and Sharp, M., 1987, Propagation of a glacier surge into stagnant ice: *Journal of Geophysical Research*: v. 92, no. B9, p. 9,037-9,049.
- Reeburgh, W.S., Muench, R.D., and Cooney, R.T., 1976, Oceanographic conditions during 1973 in Russell Fjord, Alaska: *Estuarine and Coastal Marine Science*, v. 4, no. 2, p. 129-145.
- Reid, H.F., 1892, Studies of Muir Glacier, Alaska: *National Geographic Magazine*, v. 4, p. 19-84.
- Reid, H.F., 1895, The variations of glaciers: *Journal of Geology*, v. 3, no. 3, p. 278-288.
- Reid, H.F., 1896, Glacier Bay and its glaciers: U.S. Geological Survey Annual Report 16 (1894-1895), pt. 1, p. 415-461.
- Reid, H.F., 1897, Variations of glaciers II: *Journal of Geology*, v. 5, no. 4, p. 378-383.
- Reid, H.F., 1898, Variations of glaciers III: *Journal of Geology*, v. 6, no. 5, p. 473-476.
- Reid, H.F., 1899, Variations of glaciers IV: *Journal of Geology*, v. 7, no. 3, p. 217-225.
- Reid, H.F., 1900, Variations of glaciers V: *Journal of Geology*, v. 8, no. 2, p. 154-159.
- Reid, H.F., 1904, Variations of glaciers IX: *Journal of Geology*, v. 12, no. 3, p. 252-263.
- Reid, H.F., 1909, Variations of glaciers XIV: *Journal of Geology*, v. 17, no. 7, p. 667-671.
- Reid, H.F., 1913a, Variations of glaciers XVII: *Journal of Geology*, v. 21, no. 5, p. 422-426.
- Reid, H.F., 1913b, Variations of glaciers XVIII, *Journal of Geology*, v. 21, no. 8, p. 748-753.
- Reid, H.F., 1915, Variations of glaciers XIX: *Journal of Geology*, v. 23, no. 6, p. 548-553.
- Reid, J.R., 1969, Effects of a debris slide on "Sioux Glacier," south-central Alaska: *Journal of Glaciology*, v. 8, no. 54, p. 353-367.
- Reid, J.R., and Clayton, Lee, 1963, Observations of rapid water-level fluctuations in ice sink-hole lakes, Martin River Glacier, Alaska: *Journal of Glaciology*, v. 4, no. 35, p. 650-652.
- Reimnitz, Erk, 1966, Late Quaternary history and sedimentation of the Copper River Delta and vicinity, Alaska: University of California, San Diego, Ph.D. dissertation, 188 p.



- Rice, B., 1987, Changes in the Harding Icefield, Kenai Peninsula, Alaska, with management implications for Kenai Fjords National Park: University of Alaska Fairbanks, School of Agriculture and Land Resources, unpublished M.S. dissertation, 142 p.
- Richardson, S.D., and Reynolds, J.M., 2000, Degradation of ice-cored moraine dams: implications for hazard development, *in* Nakawo, Masayoshi, Raymond, C.F., and Fountain, Andrew, eds., Debris-covered glaciers: Wallingford, Oxfordshire, UK, IAHS Press, International Association of Hydrological Sciences (IAHS) Publication No. 264, p.187–196.
- Richter, D.H., Rosenkrans, D.S., and Steigerwald, M.J., 1995, Guide to the volcanoes of the western Wrangell Mountains, Alaska—Wrangell - St. Elias National Park and Preserve: U.S. Geological Survey Bulletin 2072, 31 p.
- Riehle, J.R., 1985, A reconnaissance of the major Holocene tephra deposits in the upper Cook Inlet region, Alaska: *Journal of Volcanology and Geothermal Research*, v. 26, no. 1–2, p. 37–74.
- Rohn, Oscar, 1900, A reconnaissance of the Chitina River and the Skolai Mountains, Alaska: U.S. Geological Survey Annual Report 21, pt. II, Alaska, p. 393–440.
- Roush, J.J., 1996, The 1993–1994 surge of Bering Glacier, Alaska, observed with satellite synthetic aperture radar: University of Alaska Fairbanks, M.S. dissertation, 101 p.
- Russell, I.C., 1891, An expedition to Mount St. Elias, Alaska: *The National Geographic Magazine*, v. 3, p. 53–204.
- Russell, I.C., 1892, Mount St. Elias and its glaciers: *American Journal of Science*, v. 43, no. 255, p. 169–182.
- Russell, I.C., 1893, Second expedition to Mount Saint Elias, *in* Powell, J.W., U.S. Geological Survey Annual Report 13 to the Secretary of Interior (1891–1892), pt. II - geology: Washington, D.C., Government Printing Office, p. 1–91.
- Russell, I.C., 1894, Second expedition to Mount Saint Elias in 1891; Extract from the thirteenth annual report of the director, 1891–92: Washington, D.C., U.S. Government Printing Office, 91 p.
- Russell, I.C., 1897, *Glaciers of North America*: Boston, Ginn and Co., 210 p.
- Sable, E.G., 1960, Recent recession and thinning of Okpilak Glacier, northeastern Alaska: *Arctic*, v. 14, no. 76, p. 176–187.
- Sapiano J.J., Harrison, W.D., and Echelmeyer, K.A., 1998, Elevation, volume, and terminus changes of nine glaciers in North America: *Journal of Glaciology*, v. 44, no. 146, p. 119–135.
- Sargent, R.H., 1930, Photographing Alaska from the air: *The Military Engineer*, v. 22, no. 122, p. 131–145.
- Sargent, R.H., and Moffit, F.H., 1929, Aerial photographic surveys in southeastern Alaska: U.S. Geological Survey Bulletin 797–E, p. 143–160.
- Sater, J.E., 1959, Glacier studies of the McCall Glacier, Alaska: *Arctic*, v. 12, no. 2, p. 82–86.
- Sauber, Jeanne, and Molnia, B.F., 2000, Glacial fluctuations and the rate of deformation in south central coastal Alaska [abs.]: EOS (Transactions, American Geophysical Union), v. 81, no. 48, Fall Meeting Supplement, p. F325.
- Sauber, Jeanne, and Molnia, B.F., 2004, Glacier ice mass fluctuations and fault instability in tectonically active southern Alaska: *Journal of Global and Planetary Change*, v. 42, no. 1–4, p. 279–293.
- Sauber, Jeanne, Plafker, George, Molnia, B.F., and Bryant, M.A., 2000, Crustal deformation associated with glacial fluctuations in the eastern Chugach Mountains, Alaska: *Journal of Geophysical Research*, v. 105B, no. 4, p. 8,055–8,077.
- Scarp Exploration, Inc., 1998–2003, Alaska place-names dictionary and USGS maps: Fairbanks, Alaska, CD-ROM.
- Schorr, A.E., 1991, *Alaska place names (4th ed.)*: Juneau, The Denali Press, 191 p.
- Schrader, F.C., 1900, A reconnaissance of a part of Prince William Sound and the Copper River District, Alaska, in 1898: U.S. Geological Survey Annual Report 20 (1898–99), pt. 7, Explorations in Alaska in 1898, p.341–423.
- Schwatka, Frederick, 1885, *Along Alaska's great river*: New York, Cassell and Company, 360 p.
- Seitz, H.R., Thomas, D.S., and Tomlinson, Bud, 1986, The storage and release of water from a large glacier-dammed lake—Russell Lake near Yakutat, Alaska, 1986: U.S. Geological Survey Open-File Report 86–545, 10 p.
- Serreze, M.C., Walsh, J.E., Chapin, F.S., Osterkamp T., Dyurgerov, M., Romanovsky, V., Oechel, W.C., Morison, J., Zhang, T., and Barry, R.G., 2000, Observational evidence of recent change in the northern high-latitude environment: *Climatic Change*, v. 46, nos. 1–2, p. 159–207.
- Seton Karr, H.W., 1887, *Shores and alps of Alaska*: London, Sampson, Low, Marston, Searle and Rivington, 248 p.
- Sfraga, Michael, 2004, *Bradford Washington — A life of exploration*: Corvallis, OR, Oregon State University Press, 280 p.
- Sharp, R.P., 1951, Accumulation and ablation on the Seward-Malaspina Glacier system, Canada-Alaska: *Geological Society of America Bulletin*, v. 62, no. 7, p. 725–744.
- Sharp, R.P., 1956, *Glaciers in the Arctic*: Arctic, v. 9, nos. 1 and 2, p. 78–117.
- Sharp, R.P., 1958a, The latest major advance of Malaspina Glacier, Alaska: *Geographical Review*, v. 48, no. 1, p. 16–26.
- Sharp, R.P., 1958b, Malaspina Glacier, Alaska: *Geological Society of America Bulletin*, v. 69, no. 6, p. 617–646.
- Sherwood, M.B., 1965, *Exploration of Alaska, 1865–1900*: New Haven, Yale University Press, 207 p.
- Shreve, R.L., 1966, Sherman landslide, Alaska: *Science*, v. 154, no. 3756, p. 1,639–1,643.
- Shreve, R.L., 1968, Sherman landslide, *in* The great Alaska earthquake of 1964, v. 1, Hydrology, pt. A : Washington, D.C., National Academy of Sciences, Publication 1603, p. 395–401.
- Sikonia, W.G., 1982, Finite element glacier dynamics model applied to Columbia Glacier, Alaska: U.S. Geological Survey Professional Paper 1258–B, p. B1–B74.
- Sikonia, W.G., and Post, Austin, 1979, Columbia Glacier, Alaska—Recent ice loss and its relationship to seasonal terminal embayments, thinning, and glacier flow: U.S. Geological Survey Open-File Report 79–1265, 3 sheets. (also printed 1980 as U.S. Geological Survey Hydrological Investigations Atlas HA–619)
- Simpson, George, 1847, *Narrative of a journey round the World, during the years 1841–1842*: London, H. Colburn.
- Skidmore, E.R., 1894, Recent explorations in Alaska: *National Geographic Magazine*, v. 5, p. 173–179.
- Skidmore, E.R., 1896, *Discovery of Glacier Bay*: *National Geographic Magazine*, v. 7, p. 140–146.

- Skidmore, E.R., 1899, The Stikine River in 1898: National Geographic Magazine, v. 10, p. 1–15.
- Smith, P.S., 1912, Glaciation in northwestern Alaska: Geological Society of America Bulletin, v. 23, p. 563–570.
- Smith, P.S., and Mertie, J.B., Jr., 1930, Geology and mineral resources of northwestern Alaska: U.S. Geological Survey Bulletin 815, 351 p.
- Smith, W.R., 1925, The Cold Bay-Katmai District, *in* Mineral resources of Alaska: Report on progress of investigations in 1923: U.S. Geological Survey Bulletin 773, p. 183–207.
- Smith, W.R., and Baker, A.A., 1924, The Cold Bay-Chignik District, *in* Mineral resources of Alaska: Report on progress of investigations in 1922: U.S. Geological Survey Bulletin 755, p. 151–218.
- Spurr, J.E., 1900, A reconnaissance in southwestern Alaska in 1898: U.S. Geological Survey Annual Report 20 (1898–99), pt. VII: Explorations in Alaska in 1898, p. 31–264.
- Stone, K.H., 1955, Alaskan ice-dammed lakes: Arctic Institute of North America Report, unpublished, Project Report ONR-67, 86 p.
- Stone, K.H., 1963a, Alaskan ice-dammed lakes: Association of American Geographers, Annals, v. 53, no. 3, p. 332–349.
- Stone, K.H., 1963b, The annual emptying of Lake George, Alaska: Arctic, v. 16, no. 1, p. 26–40.
- Strasser, J.C., Lawson, D.E., Larson, G.J., Evenson, E.B., and Alley, R.B., 1996, Preliminary results of tritium analyses in basal ice, Matanuska Glacier, Alaska, U.S.A.: evidence for subglacial ice accretion: Annals of Glaciology, v. 22, p. 126–133.
- Sturm, Matthew, 1987, Observations on the distribution and characteristics of potholes on surging glaciers: Journal of Geophysical Research, v. 92B, no. 9, p. 9,015–9,022.
- Sturm, Matthew, 1995, Short-period velocity fluctuations of two glaciers on Mt. Wrangell, Alaska: Physical Geography, v. 16, no. 1, p. 42–58.
- Sturm, Matthew, and Benson, C.S., 1985, A history of jökulhlaups from Strandline Lake, Alaska, U.S.A.: Journal of Glaciology, v. 31, no. 109, p. 272–280.
- Sturm, Matthew, Hall, D.K., Benson, C.S., and Field, W.O., 1991, Non-climatic control of glacier-terminus fluctuations in the Wrangell and Chugach Mountains, Alaska, U.S.A.: Journal of Glaciology, v. 37, no. 127, p. 348–356.
- Swithinbank, Charles, 1988, Antarctica, *in* Williams, R.S., Jr., and Ferrigno J.G., eds., Satellite image atlas of glaciers of the world: U.S. Geological Survey Professional Paper 1386-B, 278 p.
- Takeuchi, Yukari, Kayastha, R.B., and Nakawo, Masayoshi, 2000, Characteristics of ablation and heat balance in debris-free and debris-covered areas on Khumbu Glacier, Nepal Himalayas, in the pre-monsoon season, *in* Nakawo, Masayoshi, Raymond, C.F., and Fountain, Andrew, eds., Debris-covered glaciers: Wallingford, Oxfordshire, UK, IAHS Press, International Association of Hydrological Sciences (IAHS) Publication No. 264, p. 53–62.
- Taliaferro, N.L., 1932, Geology of the Yakataga, Katalla, and Nichawak Districts, Alaska: Geological Society of America Bulletin, v. 43, no. 3, p. 749–782.
- Tangborn, W.V., 1999, A mass balance model that uses low-altitude meteorological observations and the area-altitude distribution of a glacier: Geografiska Annaler, v. 81A, no. 4, p. 753–765.
- Tangborn, W.V., Mayo, L.R., Scully, D.R., and Krimmel, R.M., 1977, Combined ice and water balances of Maclure Glacier, California, South Cascade Glacier, Washington, and Wolverine and Gulkana Glaciers, Alaska, 1967 hydrologic year: U.S. Geological Survey Professional Paper 715-B, 20 p.
- Tarr, R.S., 1907, The advancing Malaspina Glacier: Science, v. 25, no. 627, p. 34–37.
- Tarr, R.S., and Martin, Lawrence, 1906, Glaciers and glaciation of Yakutat Bay, Alaska: American Geographical Society Bulletin, v. 38, no. 3, p. 145–167.
- Tarr, R.S., and Martin, Lawrence, 1910, The National Geographic Society's Alaskan Expedition of 1909: The National Geographic Magazine, v. XXI, no. 1, p. 1–53.
- Tarr, R.S., and Martin, Lawrence, 1914, Alaskan glacier studies of the National Geographic Society in the Yakutat Bay, Prince William Sound and lower Copper River regions: Washington, D.C., National Geographic Society, 498 p.
- Teben'kov, M.D., 1852, Atlas "sieverozapadnykh beregov' Ameriki ot' Bering ova proliva do mysy Korrientes' i ostrovov' Aleutskikh' s" prisovokupleniem' niekotorykh' miest' Sieverovostochnago berega Azii: Sankt-peterburg [An English version exists: Teben'kov, M.D., 1981, Atlas of the northwest coasts of America: from Bering Strait to Cape Corrientes and the Aleutian Islands with several sheets on the northeast coast of Asia: Kingston, Ontario, Limestone Press, 109 p., 20 maps.
- Thompson, L.S., and Smith, S.E., 1988, Constructing a 5-meter contour map and determining volumetric change from digital data, West Gulkana Glacier, Alaska, *in* Marcus, M.G., and Reynolds, W.J., eds., Glacier and climate studies, West Gulkana Glacier and environs, Alaska, v. 1: Arizona State University, Department of Geography Publications Series No. 4 and United States Military Academy, Department of Geography and Computer Science Research Paper No. 1, 142 p. and map.
- Thorarinsson, Sigurdur, 1939, The ice dammed lakes of Iceland with particular reference to their values as indicators of glacier oscillations: Geografiska Annaler, v. 21, no. 3–4, p. 216–242.
- Time Magazine, 1937, Runaway glacier: 1 March 1937, v. 29, no. 9, p. 34.
- Topham, H.W., 1889, An expedition to Mount St. Elias, Alaska: Alpine Journal, v. 14, no. 105, p. 345–371.
- Trabant, D.C., 1999, Perennial snow and ice volumes on Iliamna Volcano Alaska, estimated with ice radar and volume modeling: U.S. Geological Survey Water-Resources Investigations Report 99–4176, 11 p.
- Trabant, D.C., and Hawkins, D.B., 1997, Glacier ice-volume modeling and glacier volumes on Redoubt Volcano, Alaska: U.S. Geological Survey Water-Resources Investigations Report 97–4187, 29 p.
- Trabant, D.C., and Krimmel, R.M., 2001, Hubbard Glacier will block the entrance to Russell Fiord, Alaska [abs.]: EOS (Transactions, American Geophysical Union), v. 82, no. 47, Fall Meeting Supplement, Abstract IP22A-0685, p. F531–532.

- Trabant, D.C., and March, R.S., 1999, Mass-balance measurements in Alaska and suggestions for simplified observation programs: *Geografiska Annaler*, v. 81A, no. 4, p. 777–789.
- Trabant, D.C., and Mayo, L.R., 1980, Knik Glacier, May 1979 monument and glacier survey: U.S. Geological Survey Open-File Report 80–48, 23 p.
- Trabant, D.C., Krimmel, R.M., and Post, Austin, 1990, A preliminary forecast of the advance of Hubbard Glacier and its influence on Russell Fiord, Alaska: U.S. Geological Survey Water-Resources Investigations Report 90–4172, 34 p.
- Trabant, D.C., Molnia, B.F., and Post, Austin, 1991, Bering Glacier, Alaska—bed configuration and potential for calving retreat [abs.]: *EOS (Transactions, American Geophysical Union)*, v. 72, no. 44, Fall Meeting Supplement, p. 159.
- Trabant, D.C., Waitt, R.B., and Major, J.J., 1994, Disruption of Drift Glacier and origin of floods during the 1989–90 eruption of Redoubt Volcano, Alaska: *Journal of Volcanology and Geothermal Research*, v. 62, nos. 1–4, p. 369–385.
- Trabant, D.C., Krimmel, R.M., Echelmeyer, K., Zirnheld, S.L., Elsborg, D.H., 2003, The slow advance of a calving glacier: Hubbard Glacier, Alaska: *Annals of Glaciology*, v. 36, p. 45–50.
- Tryggvason, Eysteinn, 1960, Earthquakes, jökulhlaups, and subglacial eruptions: *Jökull*, v. 10, p. 18–22.
- Truffer, Martin, Craw, Patty, Trabant, Dennis, and March, Rod, 2002, Effects of the M7.9 Denali Fault Earthquake on glaciers in the Alaska Range (abs. & poster): AGU 2002 Fall Meeting, S72F-1334. [available at [http://ak.water.usgs.gov/glaciology/M7.9\\_quake/reports/2002agu\\_poster/](http://ak.water.usgs.gov/glaciology/M7.9_quake/reports/2002agu_poster/)]
- Tuthill, S.J., Field, W.O., and Clayton, Lee, 1968, Postearthquake studies at Sherman and Sheridan Glaciers, *in* The great Alaska earthquake of 1964: v. 1, Hydrology, pt. A, National Academy of Sciences, Publication 1603, p. 318–328.
- U.S. Army Map Service, 1957, Adak C–6 SW, Alaska: United States Army Map Service Topographic Map, Sheet 2524-IV SW, scale 1:25,000.
- United States Coast Survey, 1878, Mount St. Elias and Coast Range to Cape Spencer, Alaska, *in* United States Coast Survey, 1878, The progress of the Survey during the year 1875: Washington, D.C., Government Printing Office, Plate 22, 1:1,500,000 scale.
- United States Coast and Geodetic Survey, 1882, Coast from Lituya Bay to Yakutat Bay, *in* United States Coast and Geodetic Survey, 1883, Pacific Coast Pilot, Alaska, part 1: Washington, D.C., Government Printing Office, Chart 15, Plate 1578, scale 1:510,000.
- United States Coast and Geodetic Survey, 1891, Pacific Coast Pilot, Alaska, part 1, Dixon Entrance to Yakutat Bay, 3d edition: Washington, D.C., Government Printing Office, p. 136.
- United States Geological Survey, 1899, Maps and descriptions of routes of exploration in Alaska in 1898, with general information concerning the territory: USGS Special Publication, 138 p., 10 maps.
- United States Geological Survey, 1929, Mineral resources of Alaska, report on progress of investigations in 1926: Bulletin 797, 227 p.
- United States Geological Survey, 1998a, Standards for Digital Line Graphs: National Mapping Program Technical Instructions, Version 07/98.
- United States Geological Survey, 1998b, Standards for Digital Line Graphs: National Mapping Program Technical Instructions, Version 01/98.
- United States National Park Service, 1997, Glacier Bay, official map and guide: Washington, D.C., Government Printing Office, 1 sheet.
- Vancouver, George, 1798, A voyage of discovery to the North Pacific Ocean, and round the world in the years 1790–1795: printed for G.G. and J. Robinson, London, Paternoster-Row, and J. Edwards, Pall-Mall, v. 4, 1,752 p.
- Van der Veen, C.J., 1995, Controls on calving rate and basal sliding: Observations from Columbia Glacier, Alaska, prior to and during its rapid retreat, 1976–1993: Columbus, Ohio, The Ohio State University, Byrd Polar Research Center, BPRC Report No. 11, 72 p.
- Van der Veen, C.J., 1996, Tidewater calving: *Journal of Glaciology*, v. 42, no. 141, p. 375–385.
- Van der Veen, C.J., ed., 1997a, Calving Glaciers; Report of a Workshop, February 28–March 2, 1997: Columbus, Ohio, The Ohio State University, Byrd Polar Research Center, BPRC Report No.15, 194 p.
- Van der Veen, C.J., 1997b, Controls on the position of iceberg-calving fronts, *in* Van der Veen, C.J., ed., Calving glaciers; Report of a Workshop, February 28–March 2, 1997: Columbus, Ohio, The Ohio State University, Byrd Polar Research Center, BPRC Report No. 15, p. 163–172.
- Viens, R.J., 1995, Dynamics and mass balance of temperate tidewater calving glaciers of southern Alaska: Seattle, University of Washington, M.S. dissertation, 149 p.
- Viereck, L.A., 1967, Botanical dating of recent glacial activity in western North America, *in* Wright, H.E., Jr., and Osburn, W.H., eds., Arctic and Alpine Environment: Indiana University Press, p. 189–204.
- von Engeln, O.D., 1910, Photography in glacial Alaska: *The National Geographic Magazine*, v. 21, no. 1, p. 54–62.
- Wahrhaftig, Clyde, 1965, Physiographic divisions of Alaska: U.S. Geological Survey Professional Paper 482, 52 p., with maps.
- Waitt, R.B., Gardner, C.A., Pierson, T.C., Major, J.J., and Neal, C.A., 1994, Unusual ice diamicts emplaced during 15 December 1989 eruption of Redoubt Volcano, Alaska: *Journal of Volcanology and Geothermal Research*, v. 62, nos. 1–4, p. 409–428.
- Wallace, K.L., McGimsey, R.G., and Miller, T.P., 2000, Historically active volcanoes in Alaska, a quick reference: U.S. Geological Survey Fact Sheet 118–00, online version 1.0 [<http://pubs.usgs.gov/fs/2000/fs118-00/>].
- Walters, R.A., and Dunlap W.W., 1987, Analysis of time series of glacier speed—Columbia Glacier, Alaska: *Journal of Geophysical Research*, B, Solid Earth and Planets, v. 92, no. 9, p. 8,969–8,975.
- Washburn, Bradford, 1935, Morainic banding of Malaspina and other Alaskan glaciers: *Geological Society of America Bulletin*, v. 46, no.12, p. 1,879–1,890.
- Washburn, [H.]B., 1971a, The mapping of Mount Hubbard and Mount Kennedy, *in* Oehser, P.H., ed., National Geographic Society Research Reports, 1966 [v. 7], p. 249–277.

- Washburn, [H.]B., 1971b, Oblique aerial photography of the Mount Hubbard - Mount Kennedy area on the Alaska-Yukon border, *in* Oehser, P.H., ed., National Geographic Society Research Reports, 1966 [v. 8], p. 283–297.
- Washburn, [H.]B., 1983, The Muldrow Glacier, Mount McKinley, Alaska: Boston, The Museum of Science, and Zürich, The Swiss Foundation for Alpine Research; a large-scale (1:10,000) orthophoto map based on field surveys (1977) and vertical aerial photography (21 August 1976) arranged in five sheets which show the glacier from Gunsight Pass to its terminus. [Editors' note: the original map sheets are archived at the Elmer E. Rasmussen Library, University of Alaska, Fairbanks, Alaska.]
- Waxell, Sven, 1952, The American Expedition: London, William Hodge and Company, 236 p. [Author's note: This is the first printing of Waxell's manuscript describing the 1733–1742 expedition; it was translated, with an introduction and note by M.A. Michael. His manuscript, which he probably completed about 1756, was lost for nearly 200 years.]
- Wendler, Gerd, 1969, Characteristics of the glaciation of Brooks Range, Alaska: *Archiv für Meteorologie, Geophysik und Bioklimatologie, Serie B.*, v. 17, no.1, p. 85–92.
- Wendler, Gerd, and Ishikawa, Nobuyoshi, 1973, Experimental study of the amount of ice melt using three different methods: a contribution to the International Hydrological Decade: *Journal of Glaciology*, v. 12, no. 66, p. 399–410.
- Wendler, Gerd, and Ishikawa, Nobuyoshi, 1974a, The combined heat, ice, and water balance of McCall Glacier, Alaska: a contribution to the International Hydrological Decade: *Journal of Glaciology*, v. 13, no. 68, p. 227–241.
- Wendler, Gerd, and Ishikawa, Nobuyoshi, 1974b, The effect of slope, exposure and mountain screening on the solar radiation of McCall Glacier, Alaska: a contribution to the International Hydrological Decade: *Journal of Glaciology*, v. 13, no. 68, p. 213–226.
- Wendler, Gerd, and Weller, Gunter, 1974, A heat balance study on McCall Glacier, Alaska, Brooks Range, Alaska: a contribution to the International Hydrological Decade: *Journal of Glaciology*, v. 13, no. 67, p. 13–26.
- Wentworth, C.K., and Ray, L.L., 1936, Studies of certain Alaskan glaciers in 1931: *Geological Society of America Bulletin*, v. 47, no. 6, p. 879–933.
- Westdahl, Ferdinand, 1903, Mountains on Unimak Island, Alaska: *National Geographic Society Magazine*, v. 14, no. 3, p. 90–99.
- White, B.M., Siefert, S.L., Hitchcock, B.W., O'Neel, S., Motyka, R.J., and Connor, C.L., 1999, 1999 results of student field survey at LeConte tidewater glacier, southeastern Alaska [abs.]: *in* Abstracts with Programs, Geological Society of America, v. 31, no. 7, p. 269.
- Wilcox, R.E., 1953, The eruption of Mount Spurr, Alaska: *The Volcano Letter*, no. 521, p. 8.
- Wiles, G.C., and Calkin, P.C., 1994, Late Holocene, high resolution glacial chronologies and climate, Kenai Mountains, Alaska: *Geological Society of America Bulletin*, v. 106, no. 2, p. 281–303.
- Wiles, G.C., Barclay, D.J., and Calkin, P.C., 1999, Tree-ring dated “Little Ice Age” histories of maritime glaciers from western Prince William Sound, Alaska: *The Holocene*, v. 9, no. 2, p. 163–173.
- Wiles, G.C., Post, Austin, Muller, E.H., and Molnia, B.F., 1999, Dendrochronology and late Holocene history of Bering Piedmont Glacier, Alaska: *Quaternary Research*, v. 52, no.2, p. 185–195.
- Williams, J.R., and Ferrians, O.J., Jr., 1961, Late Wisconsin and Recent history of the Matanuska Glacier, Alaska: *Arctic*, v. 14, no. 2, p. 82–90.
- Williams, R.S., Jr., and Ferrigno J.G., eds., 2002, *Glaciers of North America: U.S. Geological Survey Professional Paper 1386-J, Satellite Image Atlas of Glaciers of the World*, 405 p. [<http://pubs.usgs.gov/prof/p1386j/>]
- Williams, R.S., Jr., and Hall, D.K., 1993, Glaciers, in chapter on the cryosphere, *in* Gurney, R.J., Foster, J.L., and Parkinson, C.L., eds., *Atlas of Earth Observations Related to Global Change*: Cambridge, (U.K.), Cambridge University Press, p. 401–422.
- Williams, R.S., Jr., Hall, D.K., and Benson, C.S., 1991, Analysis of glacier facies using satellite techniques: *Journal of Glaciology*, v. 37, no. 125, p. 120–128.
- Winkler, G.R., 2000, A geologic guide to Wrangell-Saint Elias National Park and Preserve, Alaska: a tectonic collage of north-bound terranes: U.S. Geological Survey Professional Paper 1616, 166 p.
- Wittich, Wilhelm, 1869, *Curiosities of physical geography, comprising avalanches, icebergs, trade winds, earthquakes, volcanoes, etc.*: London, J. Blackwood, 412 p.
- Wood, C.E.S., 1882, Among the Thlinkits in Alaska: *Century Magazine*, v. 24, no. 3, p. 323–339.
- Wright, G.F., 1887, Muir Glacier: *American Journal of Science*, v. 33, no.193, p. 1–18.
- Wright, G.F., 1889, The Ice Age in North America and its bearings upon the antiquity of man: New York, D. Appleton and Co., 622 p.

# Appendix A

## 1:250,000-scale U.S. Geological Survey topographic quadrangle maps of Alaska that show glaciers

[?, date is uncertain]

Quadrangle name	Release date(s) and Data date(s)	Revision and Data date(s)
Adak	1957 (1954–56)	1983 (?)
Afognak	1952 (1951–52)	1982 (1978)
Amutka <sup>1, 2</sup>	1951 (?)	1983 (?)
Anchorage	1962 (1948, 1950, 1952, 1960, 1962)	1985 (1978, 1979)
Arctic	1956 (1955)	1983 (1978 <sup>3</sup> )
Atka	1959 (1953–59)	1983 (?)
Atlin	1960 (1960)	None
Bering Glacier	1959 (1957, 1959)	1983 (1978 <sup>3</sup> )
Bethel	1980 (1954, 1979)	1987 (?)
Blying Sound	1953 (1951, 1952, 1953)	1982 (1978 <sup>3</sup> )
Bradfield Canal	1955 (1955)	None
Chandler Lake	1956 (1955, 1956)	1985 (1979)
Cold Bay <sup>2</sup>	1943 (1929, 1942, 1943)	1975 (?)
Cordova	1959 (1950, 1953, 1959)	1982 (1978 <sup>3</sup> )
Craig	1957 (1950–56)	1972 (?)
Demarcation Point	1955 (1955)	1983 (1978)
False Pass <sup>1</sup>	1949 (1928, 1942, 1943)	1970 (?)
Gareloi Island <sup>2</sup>	1954 (1949, 1952, 1954)	1983 (?)
Goodnews Bay	1979 (1954, 1978)	None
Gulkana	1959 (1949, 1950, 1955, 1959)	1985 (1981)
Healy	1956 (1950–56)	1981 (?)
Icy Bay	1961 (1957, 1961)	1983 (1978)
Iliamna	1957 (1957)	1985 (1978, <sup>3</sup> 1980 <sup>3</sup> )
Juneau	1962 (1948–62)	1985 (1979 <sup>3</sup> )
Kenai	1958 (1951, 1952, 1958)	1986 (1977, 1978)
Ketchikan	1955 (1948, 1952–55)	1976 (?)
Killik River	1956 (1955, 1956)	1983 (1978, 1979)
Kiska <sup>2</sup>	1951 (1947, 1951)	1983 (?)
Kodiak	1952 (1948, 1949, 1952)	1983 (1978, 1979)
Lake Clark	1958 (1953–58)	1983 (1978, <sup>3</sup> 1980 <sup>3</sup> )
Lime Hills	1958 (1953–58)	1983 (1978, <sup>3</sup> 1980 <sup>3</sup> )
McCarthy	1960 (1951–60)	1981 (1978)
McGrath	1958 (1953–55)	1984 (1978, 1980)
Mt. Fairweather	1961 (1948–61)	1982 (1978 <sup>3</sup> )
Mt. Hayes	1955 (1948–55)	1975 (?)
Mt. Katmai	1951 (1951)	1975 (?)
Mt. McKinley	1958 (1952, 1954, 1958)	1982 (?)
Mt. Michelson	1956 (1955, 1956)	1983 (1978)
Mt. St. Elias	1959 (1959, 1961)	1983 (1978 <sup>3</sup> )
Nabesna	1960 (1948–60)	1982 (?)
Nome <sup>2</sup>	1950 (1950)	1985 (1952, 1977, 1980)

<b>Quadrangle name</b>	<b>Release date(s) and Data date(s)</b>	<b>Revision and Data date(s)</b>
Petersburg	1960 (1948–60)	None
Philip Smith Mountains	1956 (1955, 1956)	1983 (1975, 1978, 1982)
Port Alexander	1951 (1951)	1994 (?)
Port Moller	1988 (1963, 1983)	None
Samalga Island <sup>1, 2</sup>	1951 (1944, 1949)	1983 (?)
Seldovia	1963 (1950–63)	1985 (1978 <sup>3</sup> )
Seward	1953 (1950, 1952, 1953)	1985 (1978 <sup>3</sup> )
Sitka	1951 (1949, 1951)	1987 (?)
Skagway	1961 (1949–61)	1982 (1978, <sup>3</sup> 1979 <sup>3</sup> )
Stepovak Bay	1963 (1963)	1981 (?)
Sumdum	1961 (1948–61)	1971 (?)
Survey Pass	1956 (1956)	1982 (1978, 1979)
Sutwik Island	1963 (1943, 1963)	None
Table Mountain	1956 (1955, 1956)	1984 (1979–81)
Taku River	1960 (1951, 1960)	None
Talkeetna	1958 (1954, 1958)	1967 (?)
Talkeetna Mountains	1954 (1951–54)	1983 (1978, <sup>3</sup> 1980, <sup>3</sup> 1981 <sup>3</sup> )
Tanacross	1956 (1948–56)	1981 (?)
Teller <sup>2</sup>	1950 (1950)	1977 (?)
Tyonek	1958 (1952, 1954, 1958)	1985 (1978–80, 1982)
Ugashik	1963 (1951–63)	1975 (?)
Umnak	1951 (1942–48)	1983 (?)
Unalaska <sup>1, 2</sup>	1951 (1937–44)	1984 (?)
Unimak <sup>1</sup>	1951 (1938–45)	1983 (?)
Valdez	1960 (1949–51, 1958–60)	1981 (1978 <sup>3</sup> )
Wiseman	1956 (1955–56)	1983 (1970–78)
Yakutat	1959 (1948–59)	1982 (1978 <sup>3</sup> )

<sup>1</sup> Incomplete map.

<sup>2</sup> Glaciers known to be present but not mapped.

<sup>3</sup> Changes in glacier terminus shown on latest map by purple-pattern overprint.

## Appendix B

### 1:63,360-scale U.S. Geological Survey topographical quadrangle maps of Alaska, cited in the text and that show glaciers discussed in the chapter

<b>Quadrangle name</b>	<b>Map publication date</b>
Anchorage, Alaska A-2	1960
Anchorage, Alaska A-4	1960
Anchorage, Alaska B-7	1960, 1994
Bering Glacier, Alaska A-7	1984
Cordova, Alaska C-4	1953, 2000
Cordova, Alaska D-5	1954, 1950
Gulkana, Alaska A-2	1959
Juneau, Alaska B-2	1962
McCarthy, Alaska C-4	1959, 1993
Nabesna, Alaska A-3	1960
Seldovia, Alaska C-3	1951
Seward, Alaska A-7	1950, 1997
Seward, Alaska D-5	1950, 1995
Valdez, Alaska A-4	1993
Valdez, Alaska A-5	1953
Valdez, Alaska A-6	1953
Valdez, Alaska C-7	1960, 1993
Valdez and vicinity, Alaska sheet number 29	1962

## Appendix C

### Named Alaska glaciers from the U.S. Board on Geographic Names, Geographic Features Names Database,<sup>1</sup> and Alaska Dictionary Database<sup>2</sup> (as of 2004)

Glacier name	Latitude	Longitude	Map name <sup>3</sup>
Adams Glacier	58°46'57"N.	135°50'12"W.	Juneau D-6
Addison Glacier	59°56'07"N.	149°47'20"W.	Blying Sound D-8
Agassiz Glacier	60°11'10"N	140°44'31"W.	Mount Saint Elias A-8
Aho Glacier	60°48'51"N.	152°39'00"W.	Kenai D-8
Aialik Glacier	59°58'05"N.	149°47'59"W.	Blying Sound D-8
Alexander Glacier	59°53'54"N.	139°24'57"W.	Yakutat D-4
Allen Glacier	60°47'00"N.	144°37'00"W.	Cordova D-2
Alsek Glacier	59°12'00"N.	138°08'00"W.	Yakutat A-1
Alverstone Glacier	60°17'56"N.	139°08'33"W.	Mount Saint Elias A-4, B-4
Amherst Glacier	61°00'56"N.	147°51'20"W.	Anchorage A-3
Anderson Glacier	61°05'46"N.	141°05'45"W.	McCarthy A-1
Anderson Glacier	61°07'47"N.	146°44'00"W.	Valdez A-8
Andrews Glacier	58°54'45"N.	136°20'30"W.	Mount Fairweather D-2
Annin Glacier	61°06'28"N.	146°41'11"W.	Valdez A-8
Antler Glacier	58°50'44"N.	134°37'54"W.	Juneau D-2, D-3
Applegate Glacier	60°27'31"N.	148°35'55"W.	Seward B-5
Arey Glacier	69°14'24"N.	143°51'33"W.	Demarcation Point A-5
Art Lewis Glacier	59°53'04"N.	138°52'27"W.	Yakutat D-3
Arthur Glacier	59°14'00"N.	135°50'00"W.	Skagway A-3
Atrevida Glacier	59°57'38"N.	139°47'43"W.	Yakutat D-5
Augusta Glacier	60°15'32"N.	140°25'35"W.	Mount Saint Elias A-7, B-7
Aurel Glacier	59°14'15"N.	135°57'00"W.	Skagway A-3
Aurora Glacier	58°39'58"N.	136°42'12"W.	Mount Fairweather C-3
Baby Glacier	61°09'46"N.	147°35'56"W.	Anchorage A-2
Bacon Glacier	58°38'59"N.	133°48'29"W.	Taku River C-6
Bainbridge Glacier	60°06'31"N.	148°29'08"W.	Seward A-4
Baird Glacier	57°13'32"N.	132°25'36"W.	Sumdum A-2
Baker Glacier	61°04'48"N.	148°21'45"W.	Anchorage A-4
Baldwin Glacier	60°47'51"N.	141°18'22"W.	Bering Glacier D-1
Baldwin Glacier	58°55'30"N	136°23'00"W.	Mount Fairweather D-2
Baltimore Glacier	61°18'06"N.	147°46'14"W.	Anchorage B-2, B-3
Barnard Glacier	61°10'34"N.	147°56'27"W.	Anchorage A-3
Barnard Glacier	61°09'54"N.	141°33'59"W.	McCarthy A-2
Barrier Glacier	61°14'46"N.	152°21'46"W.	Tyonek A-6, A-7
Barry Glacier	61°11'43"N.	148°02'29"W.	Anchorage A-3, A-4
Bartlett Glacier	60°37'30"N.	148°58'29"W.	Seward C-6
Battle Glacier	58°43'38"N.	134°34'09"W.	Juneau C-2, D-2
Battle Glacier	59°38'00"N.	138°16'30"W.	Yakutat C-1
Bear Glacier	59°59'38"N.	149°37'06"W.	Blying Sound D-7
Bear Lake Glacier	60°10'09"N.	149°14'50"W.	Seward A-6, A-7
Beare Glacier	60°01'21"N.	141°40'44"W.	Bering Glacier A-2
Beloit Glacier	60°38'43"N.	148°41'23"W.	Seward C-5



<b>Glacier name</b>	<b>Latitude</b>	<b>Longitude</b>	<b>Map name<sup>3</sup></b>
Bench Glacier	61°01'59"N.	145°41'16"W.	Valdez A-5
Bering Glacier System	60°30'01"N.	142°30'01"W.	Bering Glacier 1:250,000
Bering Glacier	60°18'08"N.	143°25'11"W.	Bering Glacier A-8, B-7
Bertha Glacier	59°11'37"N.	135°48'22"W.	Skagway A-3
Betge Glacier	60°28'05"N.	143°00'05"W.	Bering Glacier B-7
Bettles Glacier	60°55'50"N.	148°24'35"W.	Seward D-4
Billings Glacier	60°52'22"N.	148°35'07"W.	Seward D-5 SE
Bird Glacier	61°00'38"N.	149°16'52"W.	Anchorage A-7 SE
Black Glacier	59°57'42"N.	139°40'23"W.	Yakutat D-5
Black Rapids Glacier	63°27'41"N.	146°11'36"W.	Mount Hayes B-5, C-4
Black and Tan Glacier	61°44'22"N.	152°37'51"W.	Tyonek C-8, D-8
Blackstone Glacier	60°38'26"N.	148°44'01"W.	Seward C-5
Blockade Glacier	61°00'43"N.	152°17'18"W.	Tyonek A-6, A-7
Blossom Glacier	60°01'38"N.	140°03'50"W.	Mount Saint Elias A-6
Boundary Glacier	59°20'29"N.	136°26'08"W.	Skagway B-4
Boundary Glacier	56°06'20"N.	130°07'08"W.	Bradfield Canal A-1
Brady Glacier	58°34'52"N.	136°47'02"W.	Mount Fairweather B-2, C-3
Bravo Glacier	69°16'06"N.	143°50'12"W.	Demarcation Point B-5
Bremner Glacier	60°49'57"N.	143°18'55"W.	Bering Glacier D-7, D-8
Bridge Glacier	58°24'35"N.	133°40'26"W.	Taku River B-6
Brilliant Glacier	61°07'57"N.	147°26'29"W.	Anchorage A-2
Broken Glacier	63°24'42"N.	145°32'57"W.	Mount Hayes B-4
Brooks Glacier	63°09'18"N.	150°36'08"W.	Mount McKinley A-2
Brown Glacier	57°41'47"N.	132°57'48"W.	Sumdum C-3, C-4
Bryn Mawr Glacier	61°15'13"N.	147°49'29"W.	Anchorage A-3, B-3
Bucher Glacier	58°52'48"N.	134°32'10"W.	Juneau D-2
Buckskin Glacier	62°59'09"N.	150°21'50"W.	Talkeetna D-1
Burns Glacier	60°43'59"N.	148°44'41"W.	Seward C-5, D-5 SW
Burroughs Glacier	58°59'27"N.	136°17'23"W.	Mount Fairweather D-1
Butler Glacier	59°57'05"N.	139°03'17"W.	Yakutat D-3
Byron Glacier	60°45'03"N.	148°51'26"W.	Seward D-5 SW
Caldwell Glacier	62°23'36"N.	152°39'51"W.	Talkeetna B-6
Camicia Glacier	61°08'08"N.	146°03'37"W.	Valdez A-6 NW
Cantwell Glacier	63°26'48"N.	149°25'35"W.	Healy B-5
Canwell Glacier	63°20'05"N.	145°32'56"W.	Mount Hayes B-4
Canyon Glacier	59°16'47"N.	138°25'55"W.	Yakutat B-2
Cap Glacier	60°57'03"N.	147°54'33"W.	Seward D-3
Capps Glacier	61°19'43"N.	151°59'24"W.	Tyonek B-5, B-6
Carl Glacier	62°07'09"N.	141°32'14"W.	Nabesna A-2
Carroll Glacier	59°05'03"N.	136°38'42"W.	Skagway A-5
Carroll Glacier	60°42'00"N.	148°43'00"W.	Seward C-5
Cascade Glacier	61°08'45"N.	148°11'06"W.	Anchorage A-4
Cascade Glacier	58°40'39"N.	137°25'53"W.	Mount Fairweather C-5
Cascade Glacier	60°13'03"N.	140°28'47"W.	Mount Saint Elias A-7
Cascading Glacier	59°47'48"N.	139°03'47"W.	Yakutat D-3
Casement Glacier	59°01'18"N.	135°55'49"W.	Skagway A-3, Juneau D-6
Casey Glacier	56°02'23"N.	130°10'34"W.	Bradfield Canal A-1

<b>Glacier name</b>	<b>Latitude</b>	<b>Longitude</b>	<b>Map name<sup>3</sup></b>
Castner Glacier	63°25'35"N.	145°36'00"W.	Mount Hayes B-4
Cataract Glacier	61°01'52"N.	148°24'59"W.	Anchorage A-4
Chamberlain Glacier	59°22'56"N.	138°40'39"W.	Yakutat B-2, B-3
Chamberlin Glacier	69°17'18"N.	144°55'37"W.	Mount Michelson B-2
Charley Glacier	58°51'42"N.	137°09'05"W.	Mount Fairweather D-4
Charpentier Glacier	58°39'58"N.	136°34'30"W.	Mount Fairweather C-2
Chedotlothna Glacier	62°53'22"N.	151°52'17"W.	Talkeetna D-4
Chenega Glacier	60°14'40"N.	148°28'24"W.	Seward A-4, B-4
Chernof Glacier	59°51'01"N.	150°23'25"W.	Seldovia D-1, D-2
Cheshnina Glacier	61°54'45"N.	144°07'05"W.	Valdez D-1
Chetaslina Glacier	62°00'09"N.	144°11'59"W.	Gulkana A-1, Valdez D-1
Chichokna Glacier	62°00'43"N.	144°17'11"W.	Gulkana A-1, Valdez D-1
Chickaloon Glacier	62°06'06"N.	148°26'09"W.	Talkeetna Mountains A-3
Chickamin Glacier	56°03'46"N.	130°17'56"W.	Bradfield Canal A-1
Chikuminuk Glacier	60°06'56"N.	159°17'15"W.	Bethel A-1
Childs Glacier	60°40'44"N.	144°52'04"W.	Cordova C-3
Chilkat Glacier	59°40'49"N.	135°39'48"W.	Skagway C-2, C-3
Chisana Glacier	62°00'44"N.	142°20'45"W.	Nabesna A-3
Chistochina Glacier	63°11'36"N.	144°45'33"W.	Mount Hayes A-2, Gulkana A-2
Chitina Glacier	61°00'15"N.	141°15'27"W.	McCarthy A-1, Bering Glacier D-2
Chitistone Glacier	61°29'46"N.	142°04'49"W.	McCarthy B-3, C-4
Clara Smith Glacier	56°14'17"N.	130°29'44"W.	Bradfield Canal A-2
Claremont Glacier	60°30'37"N.	148°42'38"W.	Seward C-5
Clark Glacier	58°48'41"N.	137°06'28"W.	Mount Fairweather D-4
Clear Glacier	61°03'39"N.	149°09'13"W.	Anchorage A-6
Cleave Creek Glacier	61°08'16"N.	145°12'43"W.	Valdez A-4
Coal Glacier	60°11'53"N.	141°12'16"W.	Bering Glacier A-1
College Glacier	63°15'20"N.	145°20'47"W.	Mount Hayes A-3, B-3
Colony Glacier	61°14'22"N.	148°30'27"W.	Anchorage A-5, B-5
Columbia Glacier	61°13'11"N.	146°53'43"W.	Valdez A-8, Seward D-1
Columbus Glacier	60°24'23"N.	141°05'10"W.	Bering Glacier B-1
Concordia Glacier	60°41'44"N.	148°43'33"W.	Seward C-5
Cone Glacier	56°12'39"N.	159°29'21"W.	Chignik A-5
Contact Glacier	60°28'13"N.	148°26'32"W.	Seward B-4
Contact Glacier	69°15'55"N.	143°42'12"W.	Demarcation Point B-5
Copper Glacier	62°08'57"N.	143°46'13"W.	Nabesna A-6
Corbin Glacier	61°06'51"N.	145°58'20"W.	Valdez A-6 SE
Cordova Glacier	60°49'56"N.	145°36'06"W.	Cordova D-5
Cotterell Glacier	60°36'43"N.	148°35'49"W.	Seward C-5
Coxe Glacier	61°08'23"N.	148°03'09"W.	Anchorage A-3, A-4
Crab Glacier	56°14'35"N.	159°17'59"W.	Chignik A-4, B-4
Crater Glacier	61°13'23"N.	152°13'50"W.	Tyonek A-6, A-7, B-7
Crescent Glacier	60°59'47"N.	147°51'26"W.	Seward D-3, Anchorage A-3
Cross Creek Glacier	62°02'22"N.	142°38'27"W.	Nabesna A-4
Crow Glacier	61°02'56"N.	149°08'45"W.	Anchorage A-6
Cul-de-sac Glacier	62°27'31"N.	152°46'07"W.	Talkeetna B-6, C-6
Cushing Glacier	59°06'05"N.	136°31'38"W.	Skagway A-4, A-5

<b>Glacier name</b>	<b>Latitude</b>	<b>Longitude</b>	<b>Map name<sup>3</sup></b>
Dadina Glacier	62°02'28"N.	144°19'29"W.	Gulkana A-1
Dagelet Glacier	58°34'00"N.	137°12'00"W.	Mount Fairweather C-4
Daisy Glacier	60°10'11"N.	141°14'14"W.	Bering Glacier A-1
Dall Glacier	62°41'27"N.	152°04'08"W.	Talkeetna C-4, C-5
Dartmouth Glacier	61°10'11"N.	147°37'04"W.	Anchorage A-2
Davidson Glacier	59°04'54"N.	135°28'21"W.	Skagway A-2
Dawes Glacier	57°28'31"N.	132°42'12"W.	Sumdum B-3
Deadman Glacier	60°39'01"N.	149°00'32"W.	Seward C-6
Demorest Glacier	58°40'45"N.	134°04'51"W.	Juneau C-1
Denver Glacier	59°25'08"N.	135°05'47"W.	Skagway B-1
Deserted Glacier	60°59'32"N.	145°36'07"W.	Cordova D-5, Valdez A-5
Desolation Glacier	58°47'00"N.	137°32'01"W.	Mount Fairweather D-5
Detached Glacier	61°04'23"N.	148°23'44"W.	Anchorage A-4
Dickinson Glacier	59°12'53"N.	135°56'09"W.	Skagway A-3
Dinglestadt Glacier	59°43'02"N.	150°26'26"W.	Seldovia C-2
Dirt Glacier	58°49'37"N.	136°01'25"W.	Mount Fairweather D-1
Dirty Glacier	60°57'17"N.	148°24'59"W.	Seward D-4
Dixon Glacier	59°40'15"N.	150°53'10"W.	Seldovia C-3
Dogshead Glacier	61°22'18"N.	152°01'42"W.	Tyonek B-6
Doroshin Glacier	59°27'44"N.	151°06'17"W.	Seldovia B-3, B-4
Double Glacier	60°04'24"N.	152°59'46"W.	Kenai A-8
Double Glacier	60°40'34"N.	152°39'50"W.	Kenai C-8
Downer Glacier	61°16'26"N.	147°36'47"W.	Anchorage B-2
Drop Glacier	62°19'17"N.	144°00'34"W.	Gulkana B-1, Nabesna B-6
Dying Glacier	58°49'50"N.	136°15'10"W.	Mount Fairweather D-1
Eagle Glacier	61°06'06"N.	149°00'02"W.	Anchorage A-6
Eagle Glacier	58°38'11"N.	134°40'35"W.	Juneau C-3
Eaglek Glacier	60°56'16"N.	147°48'19"W.	Seward D-3
East Alapah Glacier	68°08'23"N.	150°48'37"W.	Chandler Lake A-2
East Nunatak Glacier	59°45'29"N.	138°44'30"W.	Yakutat D-2, D-3
East Twin Glacier	58°34'57"N.	133°53'08"W.	Taku River C-6
Eberly Glacier	60°07'50"N.	142°03'16"W.	Bering Glacier A-3
Echo Glacier	58°44'50"N.	134°24'04"W.	Juneau C-2, D-2
Eel Glacier	63°22'28"N.	145°31'52"W.	Mount Hayes B-4
Eklutna Glacier	61°15'43"N.	148°59'00"W.	Anchorage B-6
Eldridge Glacier	63°01'24"N.	150°07'26"W.	Mount McKinley A-1, Talkeetna Mountains D-6
Eliot Glacier	61°21'25"N.	147°38'03"W.	Anchorage B-2
Ellsworth Glacier	60°13'40"N.	148°51'38"W.	Seward A-5, A-6
Esetuk Glacier	69°17'54"N.	144°19'22"W.	Mount Michelson B-1
Eureka Glacier	63°20'21"N.	146°21'32"W.	Mount Hayes B-5
Ewe Glacier	61°02'33"N.	141°17'07"W.	McCarthy A-1
Excelsior Glacier	60°02'04"N.	148°45'31"W.	Seward A-5, Blying Sound D-5
Exit Glacier	60°11'00"N.	149°37'32"W.	Seward A-8
Explorer Glacier	60°46'41"N.	148°54'59"W.	Seward D-6 SE
Fairweather Glacier	58°50'33"N.	137°38'54"W.	Mount Fairweather D-5
Falling Glacier	60°29'04"N.	148°32'50"W.	Seward B-5
Fan Glacier	60°50'29"N.	143°43'23"W.	Bering Glacier D-8

<b>Glacier name</b>	<b>Latitude</b>	<b>Longitude</b>	<b>Map name<sup>3</sup></b>
Fassett Glacier	59°18'48"N.	138°32'20"W.	Yakutat B-2
Fels Glacier	63°23'10"N.	145°40'00"W.	Mount Hayes B-4
Ferebee Glacier	59°32'31"N.	135°36'49"W.	Skagway B-2, C-2
Ferguson Glacier	56°01'30"N.	130°13'30"W.	Bradfield Canal A-1
Fickett Glacier	60°33'28"N.	145°00'26"W.	Cordova C-3
Field Glacier	58°55'58"N.	134°47'05"W.	Juneau D-2
Finger Glacier	56°12'25"N.	159°14'54"W.	Chignik A-4
Finger Glacier	58°29'52"N.	137°06'59"W.	Mount Fairweather B-4
Fleischmann Glacier	62°21'13"N.	152°50'21"W.	Talkeetna B-6
Flute Glacier	61°08'40"N.	149°17'05"W.	Anchorage A-7 NE
Fog Glacier	56°14'34"N.	159°27'04"W.	Chignik A-5, B-5
Foraker Glacier	63°08'00"N.	151°35'00"W.	Mount McKinley A-4
Fourpeaked Glacier	58°47'16"N.	153°31'03"W.	Afognak D-5
Fourth Glacier	59°36'47"N.	139°07'49"W.	Yakutat C-4 SE
Fraser Glacier	60°45'17"N.	141°13'33"W.	Bering Glacier D-1
Frederika Glacier	61°44'25"N.	142°16'13"W.	McCarthy C-4
Gakona Glacier	63°12'01"N.	145°11'13"W.	Mount Hayes A-3
Galiano Glacier	59°57'40"N.	139°43'17"W.	Yakutat D-5
Gannett Glacier	61°17'16"N.	148°17'29"W.	Anchorage B-4
Garrison Glacier	59°09'47"N.	135°41'31"W.	Skagway A-2
Gates Glacier	61°37'41"N.	142°59'05"W.	McCarthy C-6
Geikie Glacier	58°35'48"N.	136°36'34"W.	Mount Fairweather C-2
Gerstle Glacier	63°28'51"N.	145°19'22"W.	Mount Hayes B-3, C-3
Giffin Glacier	61°33'50"N.	141°22'00"W.	McCarthy C-1
Gilkey Glacier	58°48'42"N.	134°25'22"W.	Juneau D-2, D-3
Gillam Glacier	63°41'57"N.	147°07'22"W.	Healy C-1
Gilman Glacier	58°48'07"N.	137°02'13"W.	Mount Fairweather D-4
Girdled Glacier	58°56'51"N.	135°43'51"W.	Juneau D-6
Godwin Glacier	60°08'01"N.	149°10'19"W.	Seward A-6, A-7
Goodwin Glacier	60°36'36"N.	144°55'39"W.	Cordova C-3
Gooseneck Glacier	69°19'56"N.	143°46'53"W.	Demarcation Point B-5
Gracey Creek Glacier	56°13'26"N.	130°34'14"W.	Bradfield Canal A-2, B-2
Grand Pacific Glacier	59°03'50"N.	137°03'30"W.	Skagway A-6, A-7
Grand Plateau Glacier	59°02'35"N.	137°53'04"W.	Skagway A-8, Yakutat A-1
Gray Glacier	56°00'35"N.	130°09'59"W.	Bradfield Canal A-1
Great Glacier	56°50'00"N.	131°47'00"W.	Bradfield Canal D-6
Greenpoint Glacier	56°00'42"N.	130°16'56"W.	Bradfield Canal A-1
Grewingk Glacier	59°34'51"N.	150°57'01"W.	Seldovia C-3
Griddlecake Glacier	60°26'49"N.	143°24'11"W.	Bering Glacier B-7
Grinnell Glacier	60°43'09"N.	144°47'09"W.	Cordova C-2, C-3
Guerin Glacier	61°35'36"N.	141°06'18"W.	McCarthy C-1
Gulkana Glacier	63°16'07"N.	145°25'17"W.	Mount Hayes A-3, B-3
Guyot Glacier	60°10'33"N.	141°39'08"W.	Bering Glacier A-1, A-2
Hades Highway	58°39'42"N.	133°55'54"W.	Taku River C-6, Juneau C-1
Haenke Glacier	60°04'05"N.	139°38'51"W.	Mount Saint Elias A-5
Hallo Glacier	58°24'37"N.	154°14'29"W.	Mount Katmai B-1
Hanging Glacier	59°51'11"N.	138°57'27"W.	Yakutat D-3

<b>Glacier name</b>	<b>Latitude</b>	<b>Longitude</b>	<b>Map name<sup>3</sup></b>
Harper Glacier	63°05'22"N.	150°58'37"W.	Mount McKinley A-2
Harpoon Glacier	56°14'09"N.	159°13'27"W.	Chignik A-4
Harpoon Glacier	61°22'10"N.	152°33'56"W.	Tyonek B-7, B-8
Harriman Glacier	60°56'28"N.	148°31'04"W.	Seward D-4, D-5
Harvard Glacier	61°23'20"N.	147°26'11"W.	Anchorage B-2, C-2
Hawkins Glacier	61°13'59"N.	141°53'37"W.	McCarthy A-3
Hayden Glacier	60°02'19"N.	140°01'31"W.	Mount Saint Elias A-6, Yakutat D-6
Hayes Glacier	61°46'31"N.	152°18'37"W.	Tyonek C-7, D-6, D-7
Hayes Glacier	63°42'17"N.	146°41'45"W.	Mount Hayes C-6
Heiden Glacier	61°02'52"N.	145°39'39"W.	Valdez A-5
Hendrickson Glacier	59°49'32"N.	139°25'09"W.	Yakutat D-4
Heney Glacier	60°53'15"N.	144°53'36"W.	Cordova D-2, D-3
Henry Glacier	59°51'42"N.	139°28'38"W.	Yakutat D-4
Herbert Glacier	58°34'09"N.	134°36'30"W.	Juneau C-2, C-3
Herron Glacier	63°03'18"N.	151°36'54"W.	Mount McKinley A-4
Hesselberg Glacier	60°21'30"N.	143°22'01"W.	Bering Glacier C-7
Hidden Glacier	59°44'05"N.	139°06'55"W.	Yakutat C-3, D-4
Hidden Glacier	56°01'45"N.	130°07'57"W.	Bradfield Canal A-1
Hitchcock Glacier	60°05'30"N.	140°22'54"W.	Mount Saint Elias A-7
Hogback Glacier	61°06'19"N.	145°56'53"W.	Valdez A-5, A-6 SE
Hole-in-the-Wall Glacier	58°28'45"N.	133°59'35"W.	Juneau B-1, Taku River B-6
Hole-in-the-Wall Glacier	61°39'30"N.	142°12'31"W.	McCarthy C-4
Holgate Glacier	59°52'16"N.	149°55'07"W.	Blying Sound D-8
Holyoke Glacier	61°09'40"N.	147°57'28"W.	Anchorage A-3
Hook Glacier	58°28'22"N.	154°26'36"W.	Mount Katmai B-2, C-2
Hoonah Glacier	58°50'26"N.	137°03'23"W.	Mount Fairweather D-4
Hubbard Glacier	60°18'50"N.	139°22'15"W.	Mount Saint Elias A-5, B-4
Huble Glacier	69°17'13"N.	143°44'37"W.	Demarcation Point B-5
Hugh Miller Glacier	58°44'29"N.	136°41'12"W.	Mount Fairweather C-3, D-2
Hummel Glacier	56°01'35"N.	130°15'44"W.	Bradfield Canal A-1
Hunter Creek Glacier	61°19'52"N.	148°42'00"W.	Anchorage B-5
Huscroft Glacier	58°37'00"N.	137°23'45"W.	Mount Fairweather C-5
Icicle Glacier	61°12'18"N.	149°06'28"W.	Anchorage A-6
Indian Glacier	60°07'51"N.	150°15'29"W.	Kenai A-1
Irene Glacier	59°34'28"N.	135°24'49"W.	Skagway C-1 SW, C-2
Island Glacier	56°15'16"N.	159°23'43"W.	Chignik B-5
Jacksina Glacier	62°05'21"N.	143°28'27"W.	Nabesna A-5
James Robert Glacier	69°08'00"N.	145°02'00"W.	Mount Michelson A-2
Jarvis Glacier	59°25'59"N.	136°26'59"W.	Skagway B-4 NW
Jefferies Glacier	60°37'08"N.	141°50'55"W.	Bering Glacier C-3, C-4
Jeffery Glacier	63°08'16"N.	151°04'33"W.	Mount McKinley A-3
John Glacier	58°51'17"N.	137°10'32"W.	Mount Fairweather D-4
Johns Hopkins Glacier	58°48'24"N.	137°15'01"W.	Mount Fairweather D-4
Johnson Glacier	61°14'25"N.	146°22'17"W.	Valdez A-7 NE
Johnson Glacier	63°23'30"N.	145°02'49"W.	Mount Hayes B-2, B-3
Johnson Glacier	60°06'13"N.	153°01'54"W.	Lake Clark A-1, Kenai A-8
Johnson Glacier	60°30'47"N.	144°28'31"W.	Cordova C-2

<b>Glacier name</b>	<b>Latitude</b>	<b>Longitude</b>	<b>Map name<sup>3</sup></b>
Jones Glacier	58°55'45"N.	137°08'50"W.	Mount Fairweather D-4
Kachemak Glacier	59°42'42"N.	150°34'56"W.	Seldovia C-2
Kadachan Glacier	58°53'33"N.	137°06'28"W.	Mount Fairweather D-4
Kahiltna Glacier	62°45'57"N.	151°18'12"W.	Talkeetna B-3, D-3
Kanikula Glacier	62°44'39"N.	151°01'11"W.	Talkeetna C-2, C-3
Kashoto Glacier	58°51'31"N.	137°00'22"W.	Mount Fairweather D-4
Kennicott Glacier	61°36'01"N.	143°04'11"W.	McCarthy C-6
Keystone Glacier	61°07'15"N.	145°56'15"W.	Valdez A-6 SE
K'idazq'eni Glacier	61°14'00"N.	152°10'00"W.	Tyonek A-6
Killey Glacier	60°08'57"N.	150°09'32"W.	Kenai A-1
Kimball Glacier	63°16'20"N.	144°37'15"W.	Mount Hayes B-2
Kings Glacier	60°26'06"N.	148°36'17"W.	Seward B-5
Klooch Glacier	58°35'05"N.	137°21'15"W.	Mount Fairweather C-5
Klutina Glacier	61°22'08"N.	146°12'53"W.	Valdez B-6
Klutlan Glacier	61°27'03"N.	141°10'45"W.	McCarthy B-1
Kluvesna Glacier	61°49'28"N.	143°48'55"W.	McCarthy D-8
Knife Creek Glaciers, The	58°16'16"N.	155°02'26"W.	Mount Katmai B-4
Knik Glacier	61°22'03"N.	148°17'55"W.	Anchorage B-4, B-5
Konamoxt Glacier	59°23'00"N.	137°38'00"W.	Skagway B-8
Koniag Glacier	57°22'31"N.	153°18'30"W.	Kodiak B-4
Krishna Glacier	59°12'30"N.	135°49'30"W.	Skagway A-3
Kulavok Glacier	69°12'00"N.	144°52'31"W.	Mount Michelson A-2
Kuleska Glacier	60°22'25"N.	142°31'55"W.	Bering Glacier B-5
Kushtaka Glacier	60°25'59"N.	144°05'17"W.	Cordova B-1
Kuskulana Glacier	61°38'31"N.	143°36'03"W.	McCarthy C-7, C-8
La Perouse Glacier	58°32'28"N.	137°13'27"W.	Mount Fairweather C-4, D-4
LaGorce Glacier	60°44'15"N.	144°27'49"W.	Cordova C-2
Lacuna Glacier	62°44'28"N.	151°32'16"W.	Talkeetna C-4
Lafayette Glacier	61°01'47"N.	147°47'17"W.	Anchorage A-3
Lake George Glacier	61°03'30"N.	148°39'57"W.	Anchorage A-5
Lakina Glacier	61°35'29"N.	143°18'36"W.	McCarthy C-7
Lamb Glacier	61°03'42"N.	141°17'30"W.	McCarthy A-1
Lamplugh Glacier	58°49'56"N.	136°53'43"W.	Mount Fairweather D-3
Langdon Glacier	60°24'55"N.	148°38'01"W.	Seward B-5
Lare Glacier	60°02'46"N.	141°48'27"W.	Bering Glacier A-3
Lateral Glacier	60°03'37"N.	152°56'47"W.	Kenai A-8
Latouche Glacier	59°52'07"N.	139°35'45"W.	Yakutat D-5
Laughton Glacier	59°31'21"N.	135°06'05"W.	Skagway C-1 SE
Lawrence Glacier	60°39'43"N.	148°36'50"W.	Seward C-5
Leaking Glacier	58°26'20"N.	134°25'30"W.	Juneau B-2
Learnard Glacier	60°48'23"N.	148°43'16"W.	Seward D-5 SW
Le Blondeau Glacier	59°16'35"N.	136°13'30"W.	Skagway B-4
Lechner Glacier	59°56'15"N.	149°37'24"W.	Blying Sound D-7, D-8
LeConte Glacier	56°56'46"N.	132°19'46"W.	Petersburg D-1, D-2
Leeper Glacier	60°15'33"N.	142°17'58"W.	Bering Glacier A-4, B-4
Leffingwell Glacier	69°18'00"N.	144°08'00"W.	Mount Michelson B-1
Lemon Creek Glacier	58°23'24"N.	134°20'56"W.	Juneau B-2

<b>Glacier name</b>	<b>Latitude</b>	<b>Longitude</b>	<b>Map name<sup>3</sup></b>
Libbey Glacier	60°10'31"N.	140°56'54"W.	Mount Saint Elias A-8
Lime Glacier	61°51'48"N.	142°04'44"W.	McCarthy D-3
Little Jarvis Glacier	59°24'25"N.	136°25'09"W.	Skagway B-4 NW
Lituya Glacier	58°44'07"N.	137°26'41"W.	Mount Fairweather C-5
Logan Glacier	60°53'22"N.	141°11'43"W.	Bering Glacier D-1, D-2
Long Glacier	61°47'34"N.	144°03'56"W.	Valdez C-1, D-1
Lookout Glacier	58°36'00"N.	137°21'00"W.	Mount Fairweather C-5
Loomis Glacier	58°56'30"N.	136°25'30"W.	Mount Fairweather D-2
Lowell Glacier	60°50'14"N.	148°41'26"W.	Seward D-5 SE, SW
Lowell Glacier	61°18'13"N.	147°34'00"W.	Anchorage B-2
Lowell Glacier	60°13'03"N.	149°45'44"W.	Seward A-8
Lucia Glacier	59°59'38"N.	139°54'42"W.	Yakutat D-6
Maclaren Glacier	63°18'57"N.	146°31'11"W.	Mount Hayes B-6
Malaspina Glacier	59°58'53"N.	140°43'06"W.	Yakutat C-8, D-8
Marcus Baker Glacier	61°26'38"N.	147°59'51"W.	Anchorage B-3, B-4
Margerie Glacier	58°58'04"N.	137°10'33"W.	Mount Fairweather D-4, Skagway A-6
Marquette Glacier	60°38'43"N.	148°38'44"W.	Seward C-5
Marshall Glacier	61°04'45"N.	145°31'30"W.	Valdez A-5
Martin Glacier	59°17'30"N.	138°27'59"W.	Yakutat B-2
Martin River Glacier	60°34'05"N.	143°52'09"W.	Bering Glacier C-8, Cordova B-1
Marvine Glacier	60°06'05"N.	140°08'57"W.	Mount Saint Elias A-6
Matanuska Glacier	61°39'21"N.	147°34'52"W.	Anchorage C-2, D-3
Matthes Glacier	58°44'50"N.	134°11'56"W.	Juneau C-1
Maynard Glacier	58°41'23"N.	136°36'00"W.	Mount Fairweather C-2
McArthur Glacier	61°06'01"N.	152°25'31"W.	Tyonek A-7
McBride Glacier	59°05'46"N.	136°02'49"W.	Skagway A-3, A-4
McCall Glacier	69°18'13"N.	143°50'44"W.	Demarcation Point B-5
McCallum Glacier	63°17'50"N.	145°36'07"W.	Mount Hayes B-4
McCarthy Creek Glacier	61°37'11"N.	142°48'41"W.	McCarthy C-5
McCarty Glacier	59°46'12"N.	150°13'15"W.	Seldovia C-1, D-1
McCarty Glacier	59°52'17"N.	139°24'23"W.	Yakutat D-4
McCune Glacier	60°52'56"N.	144°49'41"W.	Cordova D-3
McGinnis Glacier	63°35'08"N.	146°07'36"W.	Mount Hayes C-5
McPherson Glacier	60°33'01"N.	144°35'37"W.	Cordova C-2
Meade Glacier	59°11'48"N.	134°45'12"W.	Atlin A-8, Skagway A-1
Meares Glacier	61°14'23"N.	147°25'03"W.	Anchorage A-2
Mendenhall Glacier	58°29'45"N.	134°31'56"W.	Juneau B-2 NW
Metal Creek Glacier	61°39'01"N.	148°19'48"W.	Anchorage C-4
Middle Fork Glacier	61°47'49"N.	142°07'17"W.	McCarthy D-3
Miles Glacier	60°37'17"N.	144°07'08"W.	Cordova C-1, C-2
Milk Glacier	61°02'53"N.	149°04'57"W.	Anchorage A-6
Miller Glacier	59°32'21"N.	138°59'27"W.	Yakutat C-3
Miller Glacier	60°04'28"N.	139°34'28"W.	Mount Saint Elias A-5
Milton Glacier	60°41'00"N.	148°44'00"W.	Seward C-5
Mineral Creek Glacier	61°16'41"N.	146°18'25"W.	Valdez B-7
Mint Glacier	61°52'16"N.	149°03'41"W.	Anchorage D-6
Morse Glacier	59°10'16"N.	136°30'54"W.	Skagway A-5

<b>Glacier name</b>	<b>Latitude</b>	<b>Longitude</b>	<b>Map name<sup>3</sup></b>
Morse Glacier	58°52'19"N.	136°16'32"W.	Mount Fairweather D-1
Moser Glacier	59°34'37"N.	139°02'21"W.	Yakutat C-3
Mother Goose Glacier	60°20'34"N.	149°12'11"W.	Seward B-6
Muir Glacier	59°04'42"N.	136°21'38"W.	Skagway A-4, Mount Fairweather D-1
Muldraw Glacier	63°15'38"N.	150°26'14"W.	Mount McKinley B-1, B-2
Muth Glacier	61°06'49"N.	147°40'14"W.	Anchorage A-1, A-2
Nabesna Glacier	61°56'00"N.	143°05'26"W.	McCarthy D-6
Nadina Glacier	62°02'56"N.	144°43'34"W.	Gulkana A-2
Natazhat Glacier	61°31'48"N.	141°01'23"W.	McCarthy C-1
Nelchina Glacier	61°37'43"N.	146°54'37"W.	Valdez C-8, Anchorage C-1
Nellie Juan Glacier	60°27'20"N.	148°22'33"W.	Seward B-4
Nelson Glacier	56°29'40"N.	132°00'52"W.	Petersburg B-1, Bradfield Canal B-6
Nenana Glacier	63°31'23"N.	147°40'13"W.	Healy B-2, C-2
Netland Glacier	59°25'00"N.	137°53'00"W.	Skagway B-8
Nikonda Glacier	62°03'18"N.	142°44'20"W.	Nabesna A-4
Nizina Glacier	61°37'52"N.	142°27'03"W.	McCarthy C-4
Norris Glacier	58°26'20"N.	134°11'03"W.	Juneau B-1
North Baird Glacier	57°13'21"N.	132°44'55"W.	Sumdum A-3
North Crillon Glacier	58°39'18"N.	137°19'53"W.	Mount Fairweather C-4, C-5
North Dawes Glacier	57°37'07"N.	132°57'02"W.	Sumdum C-3, C-4
North Twin Glacier	61°29'30"N.	152°36'27"W.	Tyonek B-7, B-8
Northland Glacier	60°40'17"N.	148°43'35"W.	Seward C-5
Northwestern Glacier	59°49'31"N.	150°03'18"W.	Seldovia D-1
Novatak Glacier	59°28'37"N.	138°28'47"W.	Yakutat B-1, B-2
Nugget Creek Glacier	58°25'49"N.	134°23'28"W.	Juneau B-2
Nuka Glacier	59°38'56"N.	150°45'46"W.	Seldovia C-3 NE
Oasis Glacier	57°14'40"N.	132°37'04"W.	Sumdum A-2
Ogive Glacier	59°03'07"N.	134°47'54"W.	Atlin A-8
Okpilak Glacier	69°09'46"N.	144°11'42"W.	Mount Michelson A-1
Orange Glacier	59°57'42"N.	139°14'37"W.	Yakutat D-4
Organ Glacier	61°08'35"N.	149°15'39"W.	Anchorage A-7 NE
Outlet Glacier	56°15'45"N.	159°20'46"W.	Chignik B-5
Ovtsyn Glacier	60°27'30"N.	142°53'30"W.	Bering Glacier B-6
Pangnik Glacier	69°11'30"N.	144°51'00"W.	Mount Michelson A-2
Patterson Glacier	57°00'35"N.	132°33'14"W.	Sumdum A-2, Petersburg D-3
Patton Glacier	58°54'00"N.	136°18'00"W.	Mount Fairweather D-1
Pedersen Glacier	59°53'34"N.	149°46'50"W.	Blying Sound D-8
Pedro Glacier	61°07'43"N.	147°21'25"W.	Anchorage A-1, A-2
Pegmatite Glacier	63°15'55"N.	145°23'21"W.	Mount Hayes B-3
Penniman Glaciers	61°05'34"N.	148°20'31"W.	Anchorage A-4
Peters Glacier	63°10'52"N.	151°00'09"W.	Mount McKinley A-3, B-2
Peters Glacier	69°16'51"N.	144°57'23"W.	Mount Michelson B-2
Petrof Glacier	59°27'16"N.	150°49'51"W.	Seldovia B-3
Pigot Glacier	60°54'06"N.	148°30'16"W.	Seward D-4, D-5
Pinnacle Glacier	60°08'32"N.	140°19'11"W.	Mount Saint Elias A-7
Plateau Glacier	58°58'32"N.	136°22'17"W.	Mount Fairweather D-1, D-2
Polychrome Glacier	63°27'24"N.	149°50'46"W.	Healy B-6



<b>Glacier name</b>	<b>Latitude</b>	<b>Longitude</b>	<b>Map name<sup>3</sup></b>
Popof Glacier	56°44'47"N.	132°15'48"W.	Petersburg C-1
Porcupine Glacier	60°00'05"N.	149°16'08"W.	Seward A-7 SE
Portage Glacier	60°45'11"N.	148°47'08"W.	Seward D-5 SW
Portlock Glacier	59°38'09"N.	150°56'30"W.	Seldovia C-3 NW
Pothole Glacier	61°18'29"N.	152°26'48"W.	Tyonek B-7
Princeton Glacier	60°19'32"N.	148°23'22"W.	Seward B-4
Prospect Glacier	60°01'44"N.	149°15'14"W.	Seward A-7
Ptarmigan Glacier	58°22'28"N.	134°22'17"W.	Juneau B-2 SE
Puget Glacier	60°04'20"N.	148°34'41"W.	Seward A-5
Quintino Sella Glacier	60°32'39"N.	141°01'15"W.	Bering Glacier B-1, C-1
Radcliffe Glacier	61°19'21"N.	147°43'35"W.	Anchorage B-2
Rainbow Glacier	59°06'52"N.	135°29'55"W.	Skagway A-2
Rainy Glacier	60°38'28"N.	148°32'54"W.	Seward C-5
Ram Glacier	61°05'16"N.	141°21'36"W.	McCarthy A-1, A-2
Ranney Glacier	61°11'04"N.	147°33'46"W.	Anchorage A-2
Rasmuson Glacier	59°47'00"N.	139°23'00"W.	Yakutat C-4, D-4
Raven Glacier	61°03'52"N.	149°05'14"W.	Anchorage A-6
Red Glacier	55°57'28"N.	130°10'06"W.	Ketchikan D-1
Red Glacier	60°00'28"N.	152°55'55"W.	Kenai A-8, Seldovia D-8
Regal Glacier	61°42'21"N.	142°35'47"W.	McCarthy C-4, C-5
Reid Glacier	58°46'27"N.	136°48'23"W.	Mount Fairweather D-3
Rendu Glacier	59°05'29"N.	136°50'52"W.	Skagway A-5
Revelation Glacier	61°45'21"N.	154°09'21"W.	Lime Hills D-4
Rex Glacier	61°17'49"N.	142°25'49"W.	McCarthy B-4
Riggs Glacier	59°10'08"N.	136°14'37"W.	Skagway A-4
Riley Creek Glacier	63°32'57"N.	145°34'50"W.	Mount Hayes C-4
Ripon Glacier	60°40'51"N.	148°35'46"W.	Seward C-5
Roaring Glacier	60°59'47"N.	148°27'30"W.	Seward D-4, Anchorage A-4
Robertson Glacier	63°15'34"N.	144°29'04"W.	Mount Hayes B-1
Rodman Glacier	59°20'27"N.	138°41'47"W.	Yakutat B-2
Rohn Glacier	61°45'14"N.	142°29'27"W.	McCarthy D-4
Romer Glacier	58°59'09"N.	136°44'32"W.	Mount Fairweather D-3
Root Glacier	61°34'36"N.	142°54'07"W.	McCarthy C-6
Roscoe Glacier	59°58'00"N.	153°25'00"W.	Iliamna D-2
Rubin Glacier	61°07'47"N.	146°02'29"W.	Valdez A-6 SW
Russell Glacier	61°36'52"N.	141°53'26"W.	McCarthy C-3
Ruth Glacier	62°45'55"N.	150°37'42"W.	Talkeetna C-1 NW, D-2
Saddlebag Glacier	60°31'42"N.	145°04'53"W.	Cordova B-3, C-3
Saksaia Glacier	59°22'23"N.	136°23'34"W.	Skagway B-4 NW
Sanford Glacier	62°08'30"N.	144°27'30"W.	Gulkana A-1
Sarokin Glacier	60°28'31"N.	142°23'47"W.	Bering Glacier B-4
Saussure Glacier	59°39'18"N.	135°19'49"W.	Skagway C-1 NW
Sawyer Glacier	57°57'20"N.	133°05'24"W.	Sumdum D-4
Schubee Glacier	59°20'57"N.	135°17'43"W.	Skagway B-1 SW
Schwan Glacier	60°58'28"N.	145°08'07"W.	Cordova D-4, Valdez A-3
Schwanda Glacier	69°15'37"N.	143°45'44"W.	Demarcation Point A-5, B-5
Scidmore Glacier	58°48'19"N.	136°43'46"W.	Mount Fairweather D-3

<b>Glacier name</b>	<b>Latitude</b>	<b>Longitude</b>	<b>Map name<sup>3</sup></b>
Scott Glacier	60°41'46"N.	145°10'37"W.	Cordova C-4 SW
Sea Otter Glacier	58°55'21"N.	137°42'07"W.	Mount Fairweather D-6
Seefar Glacier	68°33'40"N.	147°16'30"W.	Philip Smith Mountains C-1
Serpent Tongue Glacier	58°22'09"N.	154°38'12"W.	Mount Katmai B-2
Serpentine Glacier	61°07'12"N.	148°16'15"W.	Anchorage A-4
Seth Glacier	60°52'17"N.	148°32'11"W.	Seward D-5 SE
Seward Glacier	60°12'31"N.	140°22'48"W.	Mount Saint Elias A-7
Shadows Glacier	62°27'57"N.	152°42'08"W.	Talkeetna B-6, C-6
Shakes Glacier	56°48'51"N.	132°10'23"W.	Petersburg D-1
Shakespeare Glacier	60°45'04"N.	148°43'24"W.	Seward D-5 SW
Shamrock Glacier	61°08'54"N.	152°47'16"W.	Tyonek A-8
Sheep Glacier	62°19'55"N.	144°13'37"W.	Gulkana B-1
Shelf Glacier	62°27'33"N.	152°43'58"W.	Talkeetna B-6
Shelter Valley Glacier	61°47'43"N.	142°29'07"W.	McCarthy D-4, D-5
Shephard Glacier	60°41'00"N.	145°21'00"W.	Cordova C-4
Sheridan Glacier	60°37'32"N.	145°09'17"W.	Cordova C-4 SW
Sherman Glacier	60°33'28"N.	145°06'58"W.	Cordova C-3, C-4
Shiels Glacier	60°52'18"N.	144°46'50"W.	Cordova D-2, D-3
Shoup Glacier	61°12'23"N.	146°33'27"W.	Valdez A-7
Silver Glacier	60°53'34"N.	146°24'24"W.	Cordova D-7
Skee Glacier	59°59'34"N.	149°42'04"W.	Blying Sound D-8
Skilak Glacier	60°14'06"N.	150°04'43"W.	Kenai A-1, B-1
Skookum Glacier	60°43'47"N.	148°53'44"W.	Seward C-6
Slide Glacier	60°31'04"N.	144°18'51"W.	Cordova B-1, C-1
Slim Glacier	56°11'10"N.	159°15'08"W.	Chignik A-4
Slope Glacier	60°28'06"N.	143°51'21"W.	Bering Glacier B-8
Smith Glacier	61°16'26"N.	147°46'49"W.	Anchorage A-1, B-3
Soule Glacier	55°53'08"N.	130°15'05"W.	Ketchikan D-1
South Crillon Glacier	58°37'53"N.	137°19'34"W.	Mount Fairweather C-4, C-5
South Glacier	59°28'22"N.	135°03'52"W.	Skagway B-1
South Sawyer Glacier	57°40'51"N.	132°49'02"W.	Sumdum C-3, D-3, D-4
South Twin Glacier	61°26'01"N.	152°39'52"W.	Tyonek B-8
Southern Glacier	59°23'23"N.	151°06'27"W.	Seldovia B-3, B-4
Speel Glacier	58°19'22"N.	133°27'19"W.	Taku River B-5
Spencer Glacier	60°38'00"N.	148°54'10"W.	Seward C-6
Split Glacier	69°15'00"N.	144°07'00"W.	Mount Michelson A-1
Split Glacier	59°39'28"N.	150°28'03"W.	Seldovia C-2
Spoon Glacier	60°01'15"N.	149°16'05"W.	Seward A-7 SE
Spotted Glacier	58°55'36"N.	153°28'58"W.	Afognak D-5
Spur Glacier	63°27'10"N.	145°09'53"W.	Mount Hayes B-3
Stairway Glacier	61°04'37"N.	148°29'15"W.	Anchorage A-4
Steller Glacier	60°28'08"N.	143°33'23"W.	Bering Glacier B-7, B-8
Stephens Glacier	61°25'26"N.	146°21'47"W.	Valdez B-6, B-7
Stoney Glacier	61°55'31"N.	152°53'19"W.	Tyonek D-8
Stony Glacier	61°36'35"N.	153°48'19"W.	Lime Hills C-3
Straightaway Glacier	63°06'46"N.	151°19'55"W.	Mount McKinley A-3, A-4
Sumdum Glacier	57°47'05"N.	133°27'04"W.	Sumdum D-5

<b>Glacier name</b>	<b>Latitude</b>	<b>Longitude</b>	<b>Map name<sup>3</sup></b>
Summit Glacier	56°47'39"N.	132°16'18"W.	Petersburg D-1
Sunrise Glacier	63°22'25"N.	150°10'40"W.	Mount McKinley B-1
Sunset Glacier	63°20'06"N.	150°13'04"W.	Mount McKinley B-1
Surprise Glacier	62°41'55"N.	152°18'27"W.	Talkeetna C-5
Surprise Glacier	61°00'54"N.	148°31'23"W.	Anchorage A-5
Susitna Glacier	63°30'38"N.	147°01'28"W.	Healy B-1, C-1
Takhin Glacier	59°13'56"N.	136°09'02"W.	Skagway A-4, B-4
Taku Glacier	58°35'43"N.	134°10'47"W.	Juneau B-1, C-1
Talkeetna Glacier	62°08'12"N.	148°31'37"W.	Talkeetna Mountains A-3, A-4
Tana Glacier	60°43'53"N.	142°43'51"W.	Bering Glacier C-5
Tanaina Glacier	60°48'30"N.	152°44'00"W.	Kenai D-8
Tasnuna Glacier	60°59'21"N.	145°31'33"W.	Cordova D-5, Valdez A-4
Tatina Glacier	62°27'03"N.	152°48'44"W.	Talkeetna B-6
Taylor Glacier	60°34'36"N.	148°37'42"W.	Seward C-5
Tazlina Glacier	61°28'51"N.	146°35'41"W.	Valdez B-7, C-7
Tebenkof Glacier	60°41'01"N.	148°31'18"W.	Seward C-4, C-5
Texas Glacier	56°05'23"N.	130°10'25"W.	Bradfield Canal A-1
Thiel Glacier	58°43'01"N.	134°39'48"W.	Juneau C-2
Through Glacier	55°59'04"N.	130°22'02"W.	Ketchikan D-2, Bradfield Canal A-1
Thumb Glacier	55°59'13"N.	130°13'00"W.	Ketchikan D-1
Tiger Glacier	60°10'18"N.	148°33'14"W.	Seward A-4, A-5
Tigertail Glacier	60°13'19"N.	148°26'24"W.	Seward A-4, B-4
Tired Pup Glacier	61°29'24"N.	153°56'16"W.	Lime Hills B-3
Tittmann Glacier	61°08'07"N.	141°07'09"W.	McCarthy A-1
Toboggan Glacier	61°01'18"N.	148°16'37"W.	Anchorage A-4
Tok Glacier	63°08'13"N.	144°12'30"W.	Mount Hayes A-1
Tokositna Glacier	62°50'07"N.	150°51'36"W.	Talkeetna C-2, D-2
Tommy Glacier	60°59'13"N.	147°52'49"W.	Seward D-3
Tongue Glacier	60°04'05"N.	153°16'21"W.	Lake Clark A-1
Tonsina Glacier	61°18'50"N.	145°48'50"W.	Valdez B-5
Topeka Glacier	58°56'05"N.	137°05'02"W.	Mount Fairweather D-4
Toyatte Glacier	58°54'29"N.	137°06'18"W.	Mount Fairweather D-4
Trail Glacier	60°33'33"N.	148°57'39"W.	Seward C-6
Traleika Glacier	63°09'30"N.	150°46'26"W.	Mount McKinley A-2
Trident Glacier	63°42'22"N.	146°24'13"W.	Mount Hayes C-5, D-5
Trimble Glacier	61°43'32"N.	152°04'08"W.	Tyonek C-6
Triumvirate Glacier	61°28'01"N.	152°00'09"W.	Tyonek B-5, B-6
Truuli Glacier	59°57'55"N.	150°30'20"W.	Seldovia D-2
Tsina Glacier	61°15'30"N.	145°51'49"W.	Valdez B-5
Tsirku Glacier	59°18'15"N.	136°27'28"W.	Skagway B-4
Turner Glacier	60°02'48"N.	139°42'17"W.	Mount Saint Elias A-3, A-5
Tustumena Glacier	59°59'47"N.	150°21'34"W.	Seldovia D-1, Kenai A-2
Tuxedni Glacier	60°09'42"N.	153°05'29"W.	Lake Clark A-1, B-1
Twaharpies Glacier	61°22'57"N.	142°12'03"W.	McCarthy B-4
Twentymile Glacier	60°57'10"N.	148°38'55"W.	Seward D-5
Twentyseven Mile Glacier	61°09'09"N.	145°46'54"W.	Valdez A-5
Twin Glacier	58°53'47"N.	136°25'10"W.	Mount Fairweather D-2

<b>Glacier name</b>	<b>Latitude</b>	<b>Longitude</b>	<b>Map name<sup>3</sup></b>
Tyeen Glacier	58°52'03"N.	137°10'45"W.	Mount Fairweather D-4
Tyndall Glacier	60°08'52"N.	141°08'50"W.	Bering Glacier A-1
Ultramarine Glacier	60°24'18"N.	148°19'44"W.	Seward B-4
Umbrella Glacier	59°59'45"N.	153°10'10"W.	Iliamna D-1
Unknown Glacier	58°43'47"N.	133°56'56"W.	Taku River C-6
Valdez Glacier	61°17'24"N.	146°12'28"W.	Valdez A-6, B-6
Valerie Glacier	60°08'38"N.	139°35'14"W.	Mount Saint Elias A-4, A-5
Van Cleve Glacier	60°42'00"N.	144°17'00"W.	Cordova C-1
Variiegated Glacier	59°59'54"N.	139°19'54"W.	Yakutat D-4
Vassar Glacier	61°12'55"N.	147°51'56"W.	Anchorage A-3
Vaughan Lewis Glacier	58°49'45"N.	134°15'06"W.	Juneau D-1
Villard Glacier	59°17'30"N.	135°15'30"W.	Skagway B-1 SW
Walsh Glacier	60°55'21"N.	141°06'45"W.	Bering Glacier D-1
Watson Glacier	60°11'21"N.	142°11'59"W.	Bering Glacier A-4
Waxell Glacier	60°36'05"N.	143°00'05"W.	Bering Glacier C-6
Wedge Glacier	60°57'39"N.	148°23'23"W.	Seward D-4
Wellesley Glacier	61°11'55"N.	147°55'12"W.	Anchorage A-3
Wernicke Glacier	60°45'52"N.	143°53'50"W.	Bering Glacier D-8, Cordova D-1
West Alapah Glacier	68°08'36"N.	150°51'45"W.	Chandler Lake A-2
West Fork Glacier	61°39'06"N.	142°42'35"W.	McCarthy C-5
West Fork Glacier	63°17'00"N.	150°05'48"W.	Mount McKinley B-1, Healy B-6
West Fork Glacier	63°30'59"N.	147°21'18"W.	Healy B-2, C-1
West Glacier	62°15'29"N.	143°56'50"W.	Nabesna B-6, Gulkana A-1
West Gulkana Glacier	63°16'25"N.	145°30'20"W.	Mount Hayes B-3, B-4
West Nunatak Glacier	59°41'18"N.	138°48'51"W.	Yakutat C-3, D-3
West Twin Glacier	58°34'45"N.	133°57'18"W.	Taku River C-6
Westbrook Glacier	61°07'10"N.	146°41'01"W.	Valdez A-8
Whiskey Hill Glacier	61°49'13"N.	142°35'16"W.	McCarthy D-5
White Glacier	58°48'04"N.	135°56'03"W.	Juneau D-6
White River Glacier	60°04'18"N.	142°02'04"W.	Bering Glacier A-3
Whiteout Glacier	61°10'35"N.	148°49'06"W.	Anchorage A-5
Whittier Glacier	60°45'15"N.	148°41'00"W.	Seward C-5, D-5 SE
Willard Glacier	59°12'34"N.	135°51'56"W.	Skagway A-3
Williams Glacier	61°03'37"N.	147°45'49"W.	Anchorage A-3
Windy Glacier	68°33'53"N.	147°24'27"W.	Philip Smith Mountains C-1
Witches Cauldron	57°06'46"N.	132°29'09"W.	Sumdum A-2
Wolverine Glacier	60°24'42"N.	148°55'04"W.	Seward B-6
Woodworth Glacier	60°58'22"N.	145°24'19"W.	Cordova D-4, Valdez A-4
Worthington Glacier	61°10'13"N.	145°45'48"W.	Valdez A-5
Wortmanns Glacier	61°01'30"N.	145°44'55"W.	Cordova D-5, Valdez A-5
Wosnesenski Glacier	59°28'57"N.	150°56'00"W.	Seldovia B-3, C-3 SW
Wright Glacier	58°28'12"N.	133°31'20"W.	Taku River B-5
Yaga Glacier	60°10'30"N.	142°00'53"W.	Bering Glacier A-3
Yahrtse Glacier	60°18'20"N.	141°43'37"W.	Bering Glacier A-2, B-2
Yakataga Glacier	60°08'45"N.	142°09'06"W.	Bering Glacier A-4
Yakutat Glacier	59°31'35"N.	138°48'33"W.	Yakutat B-3, C-3
Yale Glacier	61°17'16"N.	147°28'40"W.	Anchorage A-2, B-2

Glacier name	Latitude	Longitude	Map name <sup>3</sup>
Yalik Glacier	59°31'23"N.	150°45'15"W.	Seldovia B-2, C-3
Yanert Glacier	63°36'10"N.	147°37'30"W.	Healy C-2
Yentna Glacier	62°43'07"N.	151°40'57"W.	Talkeetna C-4
Yushin Glacier	60°26'05"N.	143°13'05"W.	Bering Glacier B-6
<b>Named Alaskan icefields</b>			
Bagley Ice Field <sup>4</sup> /Icefield	60°33'00"N.	142°30'00"W.	Bering Glacier 1:250,000
Juneau Icefield	58°37'00"N.	134°30'00"W.	Juneau C-2
Harding Icefield/Ice Field	60°01'05"N.	149°59'10"W.	Seward A-8, Seldovia D-1
Sargent Icefield/Ice Field	60°17'48"N.	148°35'09"W.	Seward A-5, B-4, B-5
<i>Stikine Icefield</i>	57°40'00"N.	132°45'00"W.	Petersburg C-1, D-1, D-2; Sumdum A-1, A-2, A-3, B-2, B-3, C-2, C-3, C-4, D-3, D-4, D-5; Taku River A-4, A-5
<b>Named branches of Alaskan glaciers</b>			
Dead Branch Norris Glacier	58°24'05"N.	134°13'18"W.	Juneau B-1
Death Valley Branch Norris Glacier	58°29'00"N.	134°15'00"W.	Juneau B-1
Middle Branch Norris Glacier	58°28'00"N.	134°15'00"W.	Juneau B-1
North Branch Norris Glacier	58°31'16"N.	134°13'41"W.	Juneau B, C-1
North Branch Trimble Glacier	61°41'41"N.	152°14'22"W.	Tyokek C-6
South Branch Trimble Glacier	61°39'03"N.	152°08'54"W.	Tyokek C-6
Southwest Branch Taku Glacier	58°33'05"N.	134°17'19"W.	Juneau C-1
West Branch Eklutna Glacier	61°13'05"N.	149°00'50"W.	Anchorage A-6, B-6
West Branch Taku Glacier	58°39'52"N.	134°31'49"W.	Juneau C-2
<b>Named forks of Alaskan glaciers</b>			
East Fork Kahiltna Glacier	63°00'18"N.	151°04'45"W.	Mount McKinley A-3, Talkeetna D-3
North Fork Ruth Glacier	63°02'57"N.	150°40'57"W.	Mount McKinley A-2
Northeast Fork Kahiltna Glacier	63°02'39"N.	151°06'20"W.	Mount McKinley A-3
Northwest Fork Ruth Glacier	63°02'01"N.	150°51'54"W.	Mount McKinley A-2
Southeast Fork Kahiltna Glacier	62°58'04"N.	151°07'16"W.	Talkeetna D-3
West Fork Ruth Glacier	62°59'30"N.	150°49'30"W.	Talkeetna D-2
West Fork Traleika Glacier	63°06'54"N.	150°51'04"W.	Mount McKinley A-2
<b>Named lobes of Alaskan glaciers</b>			
Bering Lobe	60°10'00"N.	143°23'00"W.	Bering Glacier A-6, A-7, A-8, B-6, B-7
Big River Lobe Double Glacier	60°41'18"N.	152°25'46"W.	Kenai C-7
Drift River Lobe Double Glacier	60°39'44"N.	152°30'41"W.	Kenai C-7
Kaliakh Lobe Bering Glacier	60°18'10"N.	143°10'10"W.	Bering Glacier B-6
Middle Fork Lobe Bremner Glacier	60°51'40"N.	143°26'43"W.	Bering Glacier D-7
North Fork Lobe Bremner Glacier	60°54'49"N.	143°23'43"W.	Bering Glacier D-7
Steller Lobe	60°21'00"N.	143°45'00"W.	Bering Glacier B-7, B-8
Tana Lobe Bremner Glacier	60°54'17"N.	143°12'53"W.	Bering Glacier D-6

<sup>1</sup> The Geographic Features Names Database is available at <http://geonames.usgs.gov/>.

<sup>2</sup> The Alaska Dictionary Database can be found in Orth (1967).

<sup>3</sup> The map names refer to the 1:250,000-scale USGS map series of Alaska. Each 1:250,000-scale map is subdivided into four east-west strips; lettered A, B, C, and D, south to north. Each letter strip is subdivided into 1, 2, 3, 4, ...from east to west. The alphanumeric map designations are part of the 1:63,360-scale USGS map series. The NE, SW, SE, or SW following some map names identifies a 1:24,000- or 1:25,000-scale map.

<sup>4</sup> At the request of Austin Post (USGS), the Bagley Ice Valley was added as an approved name by the BGN in 1997. Post defines the Bagley Ice Valley as the central part of the Bagley Ice Field; the Bagley Ice Field extends from the head of Steller Glacier on the west to the head of Columbus Glacier on the east. In DeLorme Mapping (2001, p. 76-77) and on the USGS Bering Glacier 1:250,000-scale map, only the Bagley Ice Field is shown. Ice Field and Icefield are BGN-approved variant names.

# Appendix D

## Chronological list of pre-20th century Alaska explorers, cartographers, historians, naturalists, and expeditions

[Compiled from the following sources: Baker (1902, 1906), Davidson (1901, 1904), Henry (1984), Hulley (1953), Molnia and Post (1995), Orth (1967), and Sherwood (1965)]

Name	Country	Date(s) of activities
Vitus Jonassen Bering	Russia	1741
Alexi Ilich Chirikov	Russia	1741–42
Sofron Khitrov	Russia	1741–42
Georg Wilhelm Steller	Russia	1741–42
Sven Waxell	Russia	1741–42
Emilian Bassov	Russia	1745–47
Captain Rybinski	Russia	1748
Nikisor Trapesnikov	Russia	1749–61
Ivan Nikisorov	Russia	1757
Simon Krasilnikov	Russia	1758–61
Captain Pushkarev	Russia	1760–62
Captain Lazerov	Russia	1761
Captain Korovin	Russia	1762–66
Stephen Glotov	Russia	1763–66
Ivan Maximovich Soloviov	Russia	1764–69
Lieutenant Synd	Russia	1767–68
Peter Kuzmich Krenitzin	Russia	1768–70
Mikhail Dmitrievich Levashov	Russia	1768–70
Stephen Zaikov	Russia	1772–83
Juan F. de la Bodega y Quadra	Spain	1775–79
Antonio Maria Bucareli	Spain	1775–79
Francisco Antonio Maurelle	Spain	1775–79
William Bligh	England	1778
James Cook	England	1778
Charles Clerke	England	1778
Captain Nagaiev	Russia	1781
Grigorii Ivanovich Shelikhov	Russia	1783–91
Don Ignacio Arteaga	Spain	1779
William Coxe	England and Russia	1780
Jean F. de Galaup de La Pérouse	France	1786
Lieutenant de fregate Blondela	France	1786
Gaspard Duche de Vancy	France	1786
John Mears	England	1786–89
Nathaniel Portlock	England	1786–87
Gerassim Gavrilovich Pribilov	Russia	1786
William Douglas	England	1788–89
Gonzalo Haro	Spain	1788
Estevan Martinez	Spain	1788
Joseph Billings	Russia	1789–92
Gavrila Andreevich Sarichev	Russia	1790–92
Martin Sauer	Russia	1790–92

<b>Name</b>	<b>Country</b>	<b>Date(s) of activities</b>
Luka Alekseevich Voronin	Russia	1790–92
Alessandro Malaspina	Spain	1791
Antonio Pineda	Spain	1791
Don Jacinto Caamano	Spain	1792
William R. Broughton	England	1793–94
Thomas Heddington	England	1793–94
George Vancouver	England	1793–94
James Whidbey	England	1793–94
Gavril Ivanovitch Davidov	Russia	1803
Nikolai Alexanderovitch Khwostov	Russia	1803
Adam Johann von Krusenstern	Russia	1804–05
Georg Heinrich Langsdor	Russia	1804–05
Yuri Theodorovich Lisianski	Russia	1804–05
Ivan Filippovich Vasiliev	Russia	1808–09
Glieb Semenovich Shishmarev	Russia	1816–21
Otto von Kotzebue	Russia	1816–17
Adolph Karlovich Etolin	Russia	1818–22
Peter Ivanovitch Ilin	Russia	1818–42
Mikhail Nikolaievich Vasiliev	Russia	1819–21
Ioann Veniaminov	Russia	1824–42
Sir John Franklin	England	1826
Feodor Petrovich Litke	Russia	1827–28
Mikhail Nikolaievich Staniukovich	Russia	1827–28
Captain Ingenstrem	Russia	1829–32
Mikhail Dimitrievich Teben'kov	Russia	1831–50
Ensign Vasiliev	Russia	1831–32
Ivan Chernov	Russia	1832–38
Dionysius Federovich Zarembo	Russia	1834–39
Edward Belcher	England	1837
Peter W. Dease	England	1837
Thomas Simpson	England	1837
Captain Lindenberg	Russia	1838
Mikhail Murashev	Russia	1839–40
George Simpson	England	1841
Lieutenant Woronkofski	Russia	1842–43
Laurenti Alexief Zagoskin	Russia	1842–45
Captain Archimandritov	Russia	1848–50
George Dixon	England	1848
Full Pilot Kuritzien	Russia	1849
Constantin Grewingk	Germany	1850
William Gibson	United States	1854–55
North Pacific Exploring Expedition	United States	1854–55
Cadwalder Ringwalder	United States	1854
John Rodgers	United States	1854–55
Robert Kennicott	United States	1860–65
Peter Tikhmeniev	Russia	1861–63
William P. Blake	United States	1863–68

<b>Name</b>	<b>Country</b>	<b>Date(s) of activities</b>
Commander Bassarguine	Russia	1863
William H. Dall	United States	1865–99
Western Union Telegraph Exp.	United States	1865–67
Ivan Petroff	United States	1866–92
George Davidson	United States	1867–69
Noah Brooks	United States	1867
Richard W. Meade	United States	1868–69
David Pender	United States	1868
Charles W. Raymond	United States	1869
Henry W. Elliot	United States	1872–76
Marcus Baker	United States	1873–80
C.E.S. Wood	United States	1877
Sheldon Jackson	United States	1877–05
Edward W. Nelson	United States	1877–81
Lester A. Beardslee	United States	1879–80
John Muir	United States	1879–99
Samuel Hall Young	United States	1879
Calvin L. Hooper	United States	1880–99
Henry Glass	United States	1881
Henry E. Nichols	United States	1881–83
Patrick H. Ray	United States	1881–83
Arthur and Aurel Krause	Germany	1882
Thomas Meehan	United States	1883
George M. Stoney	United States	1883–86
Frederick Schwatka	United States	1883–86
William R. Abercrombie	United States	1884–99
John C. Cantwell	United States	1884–85
Joseph Bullock Coghlan	United States	1884
Henry T. Allen	United States	1885
Richardson Clover	United States	1885
William Libbey, Jr.	United States	1886
Heywood W. Seaton-Karr	England	1886
Albert S. Snow	United States	1886
G. Frederick Wright	United States	1886
Charles M. Thomas	United States	1887–88
Zera L. Tanner	United States	1888–93
Harold W. Topham	England	1888
Otto J. Klotz	Canada	1889–94
Henry B. Mansfield	United States	1889–91
Charles H. Stockton	United States	1889
John H. Turner	United States	1889–91
H. P. Cushing	United States	1890
Leslie Expedition	United States	1890–91
National Geographic Society	United States	1890–present
Henry Fielding Reid	United States	1890–92
Israel C. Russell	United States	1890–91
Charles W. Hayes	United States	1891



<b>Name</b>	<b>Country</b>	<b>Date(s) of activities</b>
Joseph Stanley-Brown	United States	1891
William I. Moore	United States	1892–95
Edward K. Moore	United States	1895–98
Frank C. Schrader	United States	1896–1903
Josiah E. Spurr	United States	1896–98
Luigi Amedeo-Duke of Abruzzi	Italy	1897
Fillippo de Fillippi	Italy	1897
Will W. Duffield	United States	1897
David H. Jarvis	United States	1897–98
Jefferson F. Moser	United States	1897–1901
George R. Putnam	United States	1897–99
William Yanert	United States	1897
Edward C. Barnard	United States	1898–1900
Alfred H. Brooks	United States	1898–1925
George H. Eldridge	United States	1898
Robert L. Faris	United States	1898–1901
John A. Flemer	United States	1898
Edwin F. Glenn	United States	1898–99
Walter C. Mendenhall	United States	1898–1905
William J. Peters	United States	1898–1902
John F. Pratt	United States	1898–1904
Homer P. Ritter	United States	1898–1904
Edmund F. Dickins	United States	1899–1905
Thomas G. Gerdine	United States	1899–1905
Grove Karl Gilbert	United States	1899–1901
Harriman Alaska Expedition	United States	1899
Joseph S. Herron	United States	1899
Wilfred H. Osgood	United States	1899–1902



Williams and Ferrigno, Eds.—SATELLITE IMAGE ATLAS OF GLACIERS: ALASKA—U.S. Geological Survey Professional Paper 1386-K

ISBN 978-0-607-98291-6



9 780607 982916



Printed on recycled paper